VOLUME 27 / NUMBER 12
JUNE 23, 1989
ACC. NOS. N89-19226 TO N89-20085

STAR

AN ABSTRACT JOURNAL

Scientific and Technical Aerospace Reports

PRODUCED BY THE
SCIENTIFIC AND TECHNICAL
INFORMATION
DIVISION

NASA

NATIONAL AERONAUTICS AND SPACE ADMINISTRATION

WHAT YOU CAN DO FOR *STAR*

All users of this abstract service are urged to forward reports to be considered for announcement in *STAR*. This will aid NASA in its efforts to provide the fullest possible coverage of all scientific and technical publications that might support aeronautics and space research and development. If you have prepared relevant reports (other than those that you will transmit to NASA, DoD, or DOE through the usual contract- or grant-reporting channels), please send them for consideration to the NASA Scientific and Technical Information Facility, P.O. Box 8757, BWI Airport, Maryland 21240.

Reprints of journal articles, book chapters, and conference papers are also welcome. These will be considered for announcement in *STAR's* companion journal, *International Aerospace Abstracts*.

You may specify a particular source to be included in a report announcement if you wish; otherwise the report will be placed on public sale at the National Technical Information Service. Copyrighted publications will be announced but not distributed or sold.

PURCHASE OF *STAR*

The semimonthly issues are available to registered users on annual subscription for $99.00 from the NASA Scientific and Technical Information Facility, ATTN: Registration Services, P.O. Box 8757, BWI Airport, MD 21240. *STAR* is publically available on annual subscription for $99.00 from the Superintendent of Documents, U.S. Government Printing Office, Washington, DC 20402.

PUBLISHED BY:

UNITED STATES GOVERNMENT
NATIONAL AERONAUTICS AND SPACE ADMINISTRATION
SCIENTIFIC AND TECHNICAL INFORMATION DIVISION
Scientific and Technical Aerospace Reports, Volume 27, is prepared by the NASA Scientific and Technical Information Facility operated for the National Aeronautics and Space Administration by RMS Associates.

The Administrator of the National Aeronautics and Space Administration has determined that the publication of this periodical is necessary in the transaction of the public business required by law of this Agency. Use of funds for printing this periodical has been approved by the Director of the Office of Management and Budget through March 22, 1989.

US ISSN 0036-8741

INTRODUCTION

Scientific and Technical Aerospace Reports (STAR) is a major component of a comprehensive National Aeronautics and Space Administration information system covering aeronautics, space, and supporting disciplines. *STAR* is issued on the 8th and 23rd of each month and announces current publications of the following types:

- NASA, NASA contractor, and NASA grantee reports
- Reports issued by other U.S. Government Agencies, domestic and foreign institutions, universities, and private firms
- Translations in report form
- NASA-owned patents and patent applications
- Other U.S. Government Agency and foreign patents and patent applications
- Domestic and foreign dissertations and theses

Journal, book, and conference literature, cover-to-cover journal translations, and certain foreign dissertations are announced in a companion journal, *International Aerospace Abstracts (IAA),* available on subscription from the American Institute of Aeronautics and Astronautics, Technical Information Service, 555 West 57th Street, 12th Floor, New York, New York 10019.

SUBJECT SCOPE

Subject scope of *STAR,* and *IAA* includes all aspects of aeronautics and space research and development, supporting basic and applied research, and applications. Aerospace aspects of earth resources, energy development, conservation, oceanography, environmental protection, urban transportation, and other topics of high national priority are also covered.

OTHER NASA PUBLICATIONS

Other NASA publications and information services are described in the publication, *The NASA Scientific and Technical Information System ... and How to Use It,* available without charge from the NASA Scientific and Technical Information Facility, P.O. Box 8757, BWI Airport, Maryland 21240.

HOW TO USE *STAR* SUBJECT CATEGORIES

STAR is categorized by 10 major subject divisions divided into 76 specific subject categories and one general category/division. The major subject divisions are listed in the Table of Contents, together with a note for each that defines its scope and provides any cross-references. For example:

AERONAUTICS

Includes aeronautics (general); aerodynamics; air transportation and safety; aircraft communications and navigation; aircraft design, testing and performance; aircraft instrumentation; aircraft propulsion and power; aircraft stability and control; and research and support facililties (air).

For related information see also *Astronautics.*

Each major division is further divided into as many as nine specific categories, which are identified by category numbers.

Abstracts in *STAR* are grouped by specific category, the categories appearing in sequential order. Category breaks in the abstract section are identified by the category number and title, and a scope note. Cross-references to other categories are provided as appropriate. For example:

02 AERODYNAMICS

Includes aerodynamics of bodies, combinations, wings, rotors, and control surfaces; and internal flow in ducts and turbomachinery.

For related information see also *34 Fluid Mechanics and Heat Transfer.*

CROSS-REFERENCES

Individual *STAR* abstracts are not ordinarily cross-referenced, except for certain conference reports or book translations that have had separate abstracts written for their component papers or chapters. Citations and abstracts of the components follow immediately after those of the parent document. When the subject content of a component differs sufficiently from the general content of the parent, a cross-reference citation also is printed at the end of the category to which it normally would have been assigned if it were independent.

DOCUMENTS ON MICROFICHE

Documents on microfiche[1] are designated by a pound sign (#) following the accession number. The pound sign is used without regard to the source or quality of the microfiche.

AVAILABILITIES

One or more sources from which a document announced in *STAR* is available to the public is given in each citation. The most commonly indicated sources and their acronyms or abbreviations are listed below. If the publication is available from a source other than those listed, the publisher and his address will be displayed on the availability line or in combination with the corporate source line.

Avail: NTIS. Sold by the National Technical Information Service. Prices for hard copy (HC) and microfiche (MF) are indicated by a price code following the letters HC or MF in the *STAR* citation. Current values for the price codes are given in the tables on page vii.

Initially distributed microfiche under the NTIS SRIM (Selected Research in Microfiche) is available at greatly reduced unit prices. For this service and for information concerning subscription to NASA printed reports, consult the NTIS Subscription Section, Springfield, Va. 22161.

NOTE ON ORDERING DOCUMENTS: When ordering NASA publications (those followed by the * symbol), use the N accession number. NASA patent applications (only the specifications are offered) should be ordered by the US-Patent-Appl-SN number. Non-NASA publications (no asterisk) should be ordered by the AD, PB, or other *report number* shown on the last line of the citation, not by the N accession number. It is also advisable to cite the title and other bibliographic identification.

Avail: SOD (or GPO). Sold by the Superintendent of Documents, U.S. Government Printing Office, in hard copy. The current price and order number are given following the availability line. (NTIS will fill microfiche requests, as indicated above, for those documents identified by a # symbol.)

(1) A microfiche is a transparent sheet of film, 105 by 148 mm in size, containing as many as 60 to 98 pages of information reduced to micro images (not to exceed 26:1 reduction).

Avail: BLL (formerly NLL): British Library Lending Division, Boston Spa, Wetherby, Yorkshire, England. Photocopies available from this organization at the price shown. (If none is given, inquiry should be addressed to the BLL.)

Avail: DOE Depository Libraries. Organizations in U.S. cities and abroad that maintain collections of Department of Energy reports, usually in microfiche form, are listed in *Energy Research Abstracts.* Services available from the DOE and its depositories are described in a booklet, *DOE Technical Information Center - Its Functions and Services* (TID-4660), which may be obtained without charge from the DOE Technical Information Center.

Avail: ESDU. Pricing information on specific data, computer programs, and details on ESDU topic categories can be obtained from ESDU International Ltd. Requesters in North America should use the Virginia address while all other requesters should use the London address, both of which are on page vi.

Avail: Fachinformationszentrum, Karlsruhe. Sold by the Fachinformationszentrum Energie, Physik, Mathematik GMBH, Eggenstein Leopoldshafen, Federal Republic of Germany, at the price shown in deutschmarks (DM).

Avail: HMSO. Publications of Her Majesty's Stationery Office are sold in the U.S. by Pendragon House, Inc. (PHI), Redwood City, California. The U.S. price (including a service and mailing charge) is given, or a conversion table may be obtained from PHI.

Avail: NASA Public Document Rooms. Documents so indicated may be examined at or purchased from the National Aeronautics and Space Administration, Public Documents Room (Room 126), 600 Independence Ave., S.W., Washington, D.C. 20546, or public document rooms located at each of the NASA research centers, the NASA Space Technology Laboratories, and the NASA Pasadena Office at the Jet Propulsion Laboratory.

Avail: Univ. Microfilms. Documents so indicated are dissertations selected from *Dissertation Abstracts* and are sold by University Microfilms as xerographic copy (HC) and microfilm. All requests should cite the author and the Order Number as they appear in the citation.

Avail: US Patent and Trademark Office. Sold by Commissioner of Patents and Trademarks, U.S. Patent and Trademark Office, at the standard price of $1.50 each, postage free. (See discussion of NASA patents and patent applications below.)

Avail: (US Sales Only). These foreign documents are available to users within the United States from the National Technical Information Service (NTIS). They are available to users outside the United States through the International Nuclear Information Service (INIS) representative in their country, or by applying directly to the issuing organization.

Avail: USGS. Originals of many reports from the U.S. Geological Survey, which may contain color illustrations, or otherwise may not have the quality of illustrations preserved in the microfiche or facsimile reproduction, may be examined by the public at the libraries of the USGS field offices whose addresses are listed in this Introduction. The libraries may be queried concerning the availability of specific documents and the possible utilization of local copying services, such as color reproduction.

Avail: Issuing Activity, or Corporate Author, or no indication of availability. Inquiries as to the availability of these documents should be addressed to the organization shown in the citation as the corporate author of the document.

NASA PATENTS AND PATENT APPLICATIONS

Patents and patent applications owned by NASA are announced in *STAR* under appropriate subject categories and are referenced in the *STAR* indexes. In the Report/Accession Number Index, patents are indexed by the NASA Case Number (which appears in lieu of the report number in other indexes), the U.S. Patent Number, the U.S. Patent Application Serial Number, and the U.S. Patent Class. Patent applications for which patents have not yet been issued are indexed by the NASA Case Number and the U.S. Patent Application Serial Number.

NASA *patent application specifications* are sold in paper copy by the National Technical Information Service at price code A02. Microfiche are sold at price code A01. The US-Patent-Appl-SN- number should be used in ordering either paper copy or microfiche from NTIS. Printed copies of *patents* (which are not microfiched) are available for purchase at $1.50 per copy from:

Commissioner of Patents and Trademarks
U.S. Patent and Trademark Office
Washington, D.C. 20231

When ordering patents, the U.S. Patent Number should be used, and payment must be remitted in advance, preferably by money order or check payable to the Commissioner of Patents and Trademarks. Prepaid purchase coupons for ordering are also available from the Patent and Trademark Office. The patents and patent applications announced in *STAR* are owned by NASA and are available for royalty-free licensing. Requests for licensing terms and further information should be addressed to:

Associate General Counsel for Intellectual Property/Code GP
National Aeronautics and Space Administration
Washington, D.C. 20546

ELIGIBILITY AND REGISTRATION FOR NASA INFORMATION PRODUCTS AND SERVICES

A variety of services is available to organizations of the following types that have registered with NASA to receive specific services or products:

1. NASA offices, research centers, contractors, subcontractors, grantees, and consultants;
2. Other U.S. Government agencies and their contractors;
3. Libraries in the United States that have arrangements with NASA to maintain collections of NASA documents for public reference;
4. Other organizations in the United States having a need for NASA documents in work related to aeronautics and space research;
5. Organizations abroad that have established reciprocal document exchange arrangements with NASA.

Only the central service points or central points of document acquisition and control within qualified organizations are eligible to register for NASA products and services. Domestic organizations that may be eligible to receive various classes of NASA publications and services should address their requests for registration or for further information to:

NASA Scientific and Technical Information Facility
ATTN: Registration Services
Post Office Box 8757
BWI Airport, Maryland 21240

Organizations abroad should direct requests to Manager, International STI Activities, NTT, NASA Headquarters, Washington, D.C. 20546.

AVAILABILITY OF *STAR* ABSTRACTS ON MICROFICHE

Microfiche of the abstract sections of this issue and other issues of *STAR* are available on annual subscription from NTIS as PB89-911300, Attn: Subscriptions, 5285 Port Royal Road, Springfield, Virginia 22161. Annual subscription rates are $70.00 North America; $140.00 foreign. Abstract sections for previous years retroactive to 1964 are available at the current rates. Microfiche for individual *STAR* issue abstract sections are not available.

PUBLIC COLLECTIONS OF NASA DOCUMENTS

DOMESTIC: NASA and NASA-sponsored documents and a large number of aerospace publications are available to the public for reference purposes at the library maintained by the American Institute of Aeronautics and Astronautics, Technical Information Service, 555 West 57th Street, 12th Floor, New York, New York 10019

EUROPEAN: An extensive collection of NASA and NASA-sponsored publications is maintained by the British Library Lending Division, Boston Spa, Wetherby, Yorkshire, England for public access. The British Library Lending Division also has available many of the non-NASA publications cited in *STAR*. European requesters may purchase facsimile copy or microfiche of NASA and NASA-sponsored documents, those identified by both the symbols # and * from ESA - Information Retrieval Service European Space Agency, 8-10 rue Mario-Nikis, 75738 Paris CEDEX 15, France.

FEDERAL DEPOSITORY LIBRARY PROGRAM

In order to provide the general public with greater access to U.S. Government publications, Congress established the Federal Depository Library Program under the Government Printing Office (GPO), with 50 regional depositories responsible for permanent retention of material, inter-library loan, and reference services. At least one copy of nearly every NASA and NASA-sponsored publication, either in printed or microfiche format, is received and retained by the 50 regional depositories. A list of the regional GPO libraries, arranged alphabetically by state, appears on the inside back cover. These libraries are *not* sales outlets. A local library can contact a Regional Depository to help locate specific reports, or direct contact may be made by an individual.

ADDRESSES OF ORGANIZATIONS

American Institute of Aeronautics and Astronautics
Technical Information Service
555 West 57th Street, 12th Floor
New York, New York 10019

British Library Lending Division,
Boston Spa, Wetherby, Yorkshire,
England

Commissioner of Patents and Trademarks
U.S. Patent and Trademark Office
Washington, D.C. 20231

Department of Energy
Technical Information Center
P.O. Box 62
Oak Ridge, Tennessee 37830

ESA-Information Retrieval Service
ESRIN
Via Galileo Galilei
00044 Frascati (Rome) Italy

ESDU International
P.O. Box 1633
Manassas, Virginia 22110

ESDU International, Ltd.
251-259 Regent Street
London, W1R 7AD, England

Fachinformationszentrum Energie, Physik, Mathematik GMBH
7514 Eggenstein Leopoldshafen
Federal Republic of Germany

Her Majesty's Stationery Office
P.O. Box 569, S.E. 1
London, England

NASA Scientific and Technical Information Facility
P.O. Box 8757
B.W.I. Airport, Maryland 21240

National Aeronautics and Space Administration
Scientific and Technical Information Division (NTT)
Washington, D.C. 20546

National Technical Information Service
5285 Port Royal Road
Springfield, Virginia 22161

Pendragon House, Inc.
899 Broadway Avenue
Redwood City, California 94063

Superintendent of Documents
U.S. Government Printing Office
Washington, D.C. 20402

University Microfilms
A Xerox Company
300 North Zeeb Road
Ann Arbor, Michigan 48106

University Microfilms, Ltd.
Tylers Green
London, England

U.S. Geological Survey Library
National Center - MS 950
12201 Sunrise Valley Drive
Reston, Virginia 22092

U.S. Geological Survey Library
2255 North Gemini Drive
Flagstaff, Arizona 86001

U.S. Geological Survey
345 Middlefield Road
Menlo Park, California 94025

U.S. Geological Survey Library
Box 25046
Denver Federal Center, MS914
Denver, Colorado 80225

NTIS PRICE SCHEDULES

(Effective January 1, 1989)

Schedule A
STANDARD PRICE DOCUMENTS AND MICROFICHE

PRICE CODE	NORTH AMERICAN PRICE	FOREIGN PRICE
A01	$ 6.95	$13.90
A02	10.95	21.90
A03	13.95	27.90
A04-A05	15.95	31.90
A06-A09	21.95	43.90
A10-A13	28.95	57.90
A14-A17	36.95	73.90
A18-A21	42.95	85.90
A22-A25	49.95	99.90
A99	*	*
NO1	55.00	70.00
NO2	55.00	80.00

Schedule E
EXCEPTION PRICE DOCUMENTS AND MICROFICHE

PRICE CODE	NORTH AMERICAN PRICE	FOREIGN PRICE
E01	$ 9.00	18.00
E02	11.50	23.00
E03	13.00	26.00
E04	15.50	31.00
E05	17.50	35.00
E06	20.50	41.00
E07	23.00	46.00
E08	25.50	51.00
E09	28.00	56.00
E10	31.00	62.00
E11	33.50	67.00
E12	36.50	73.00
E13	39.00	78.00
E14	42.50	85.00
E15	46.00	92.00
E16	50.50	101.00
E17	54.50	109.00
E18	59.00	118.00
E19	65.50	131.00
E20	76.00	152.00
E99	*	*

*Contact NTIS for price quote.

IMPORTANT NOTICE

NTIS Shipping and Handling Charges

U.S., Canada, Mexico — ADD $3.00 per TOTAL ORDER

All Other Countries — ADD $4.00 per TOTAL ORDER

Exceptions — Does NOT apply to:

ORDERS REQUESTING NTIS RUSH HANDLING

ORDERS FOR SUBSCRIPTION OR STANDING ORDER PRODUCTS *ONLY*

NOTE: Each additional delivery address on an order requires a separate shipping and handling charge.

VOLUME 27 NUMBER 12/ JUNE 23, 1989

TABLE OF CONTENTS

AERONAUTICS

Includes aeronautics (general); aerodynamics; air transportation and safety; aircraft communications and navigation; aircraft design, testing and performance; aircraft instrumentation; aircraft propulsion and power; aircraft stability and control; and research and support facilities (air).

For related information see also *Astronautics.*

01 AERONAUTICS (GENERAL) 1603

02 AERODYNAMICS 1604

Includes aerodynamics of bodies, combinations, wings, rotors, and control surfaces; and internal flow in ducts and turbomachinery.

For related information see also *34 Fluid Mechanics and Heat Transfer*

03 AIR TRANSPORTATION AND SAFETY 1611

Includes passenger and cargo air transport operations; and aircraft accidents.

For related information see also *16 Space Transportation* and *85 Urban Technology and Transportation.*

04 AIRCRAFT COMMUNICATIONS AND NAVIGATION 1612

Includes digital and voice communication with aircraft; air navigation systems (satellite and ground based); and air traffic control.

For related information see also *17 Space Communications, Spacecraft Communications, Command and Tracking* and *32 Communications and Radar.*

05 AIRCRAFT DESIGN, TESTING AND PERFORMANCE 1613

Includes aircraft simulation technology.

For related information see also *18 Spacecraft Design, Testing and Performance* and *39 Structural Mechanics.* For land transportation vehicles see *85 Urban Technology and Transportation.*

06 AIRCRAFT INSTRUMENTATION 1614

Includes cockpit and cabin display devices; and flight instruments.

For related information see also *19 Spacecraft Instrumentation* and *35 Instrumentation and Photography.*

07 AIRCRAFT PROPULSION AND POWER 1614

Includes prime propulsion systems and systems components, e.g., gas turbine engines and compressors; and onboard auxiliary power plants for aircraft.

For related information see also *20 Spacecraft Propulsion and Power, 28 Propellants and Fuels,* and *44 Energy Production and Conversion.*

08 AIRCRAFT STABILITY AND CONTROL 1617

Includes aircraft handling qualities; piloting; flight controls; and autopilots.

For related information see also *05 Aircraft Design, Testing and Performance.*

09 RESEARCH AND SUPPORT FACILITIES (AIR) 1618

Includes airports, hangars and runways; aircraft repair and overhaul facilities; wind tunnels; shock tubes; and aircraft engine test stands.

For related information see also *14 Ground Support Systems and Facilities (Space).*

ASTRONAUTICS

Includes astronautics (general); astrodynamics; ground support systems and facilities (space); launch vehicles and space vehicles; space transportation; space communications, spacecraft communications, command and tracking; spacecraft design, testing and performance; spacecraft instrumentation; and spacecraft propulsion and power.

For related information see also *Aeronautics*

12 ASTRONAUTICS (GENERAL) 1619

For extraterrestrial exploration see *91 Lunar and Planetary Exploration.*

13 ASTRODYNAMICS 1619

Includes powered and free-flight trajectories; and orbital and launching dynamics.

14 GROUND SUPPORT SYSTEMS AND FACILITIES (SPACE) 1620

Includes launch complexes, research and production facilities; ground support equipment, e.g., mobile transporters; and simulators.

For related information see also *09 Research and Support Facilities (Air).*

15 LAUNCH VEHICLES AND SPACE VEHICLES 1620

Includes boosters; operating problems of launch/space vehicle systems; and reusable vehicles.

For related information see also *20 Spacecraft Propulsion and Power.*

16 SPACE TRANSPORTATION 1620

Includes passenger and cargo space transportation, e.g., shuttle operations; and space rescue techniques.

For related information see also *03 Air Transportation and Safety* and *18 Spacecraft Design, Testing and Performance.* For space suits see *54 Man/System Technology and Life Support.*

17 SPACE COMMUNICATIONS, SPACECRAFT COMMUNICATIONS, COMMAND AND TRACKING N.A.

Includes telemetry; space communications networks; astronavigation and guidance; and radio blackout.

For related information see also *04 Aircraft Communications and Navigation* and *32 Communications and Radar.*

18 SPACECRAFT DESIGN, TESTING AND PERFORMANCE 1621

Includes satellites; space platforms; space stations; spacecraft systems and components such as thermal and environmental controls; and attitude controls.

For life support systems see *54 Man/System Technology and Life Support.* For related information see also *05 Aircraft Design, Testing and Performance, 39 Structural Mechanics,* and *16 Space Transportation.*

19 SPACECRAFT INSTRUMENTATION N.A.

For related information see also *06 Aircraft Instrumentation* and *35 Instrumentation and Photography.*

20 SPACECRAFT PROPULSION AND POWER 1627

Includes main propulsion systems and components, e.g. rocket engines; and spacecraft auxiliary power sources.

For related information see also *07 Aircraft Propulsion and Power, 28 Propellants and Fuels, 44 Energy Production and Conversion,* and *15 Launch Vehicles and Space Vehicles.*

CHEMISTRY AND MATERIALS

Includes chemistry and materials (general); composite materials; inorganic and physical chemistry; metallic materials; nonmetallic materials; propellants and fuels; and materials processing.

23 CHEMISTRY AND MATERIALS (GENERAL) 1628

24 COMPOSITE MATERIALS 1629

Includes physical, chemical, and mechanical properties of laminates and other composite materials.

For ceramic materials see *27 Nonmetallic Materials.*

25 INORGANIC AND PHYSICAL CHEMISTRY 1631

Includes chemical analysis, e.g., chromatography; combustion theory; electrochemistry; and photochemistry.

For related information see also *77 Thermodynamics and Statistical Physics.*

26 METALLIC MATERIALS 1634

Includes physical, chemical, and mechanical properties of metals, e.g., corrosion; and metallurgy.

27 NONMETALLIC MATERIALS 1637

Includes physical, chemical, and mechanical properties of plastics, elastomers, lubricants, polymers, textiles, adhesives, and ceramic materials.

For composite materials see *24 Composite Materials.*

28 PROPELLANTS AND FUELS 1640

Includes rocket propellants, igniters and oxidizers; their storage and handling procedures; and aircraft fuels.

For related information see also *07 Aircraft Propulsion and Power, 20 Spacecraft Propulsion and Power,* and *44 Energy Production and Conversion.*

29 MATERIALS PROCESSING 1640

Includes space-based development of products and processes for commercial application.

For biological materials see *55 Space Biology.*

ENGINEERING

Includes engineering (general); communications and radar; electronics and electrical engineering; fluid mechanics and heat transfer; instrumentation and photography; lasers and masers; mechanical engineering; quality assurance and reliability; and structural mechanics.

For related information see also *Physics.*

31 ENGINEERING (GENERAL) 1641

Includes vacuum technology; control engineering; display engineering; cryogenics; and fire prevention.

32 COMMUNICATIONS AND RADAR 1642

Includes radar; land and global communications; communications theory; and optical communications.

For related information see also *04 Aircraft Communications and Navigation* and *17 Space Communications, Spacecraft Communications, Command and Tracking.* For search and rescue see *03 Air Transportation and Safety,* and *16 Space Transportation.*

33 ELECTRONICS AND ELECTRICAL ENGINEERING 1648

Includes test equipment and maintainability; components, e.g., tunnel diodes and transistors; microminiaturization; and integrated circuitry.

For related information see also *60 Computer Operations and Hardware* and *76 Solid-State Physics.*

34 FLUID MECHANICS AND HEAT TRANSFER 1651

Includes boundary layers; hydrodynamics; fluidics; mass transfer and ablation cooling.

For related information see also *02 Aerodynamics* and *77 Thermodynamics and Statistical Physics.*

35 INSTRUMENTATION AND PHOTOGRAPHY 1656

Includes remote sensors; measuring instruments and gages; detectors; cameras and photographic supplies; and holography.

For aerial photography see *43 Earth Resources and Remote Sensing.* For related information see also *06 Aircraft Instrumentation* and *19 Spacecraft Instrumentation.*

36 LASERS AND MASERS 1657

Includes parametric amplifiers.

For related information see also *76 Solid-State Physics.*

37 MECHANICAL ENGINEERING 1660

Includes auxiliary systems (nonpower); machine elements and processes; and mechanical equipment.

38 QUALITY ASSURANCE AND RELIABILITY 1664

Includes product sampling procedures and techniques; and quality control.

39 STRUCTURAL MECHANICS 1665

Includes structural element design and weight analysis; fatigue; and thermal stress.

For applications see *05 Aircraft Design, Testing and Performance* and *18 Spacecraft Design, Testing and Performance.*

GEOSCIENCES

Includes geosciences (general); earth resources and remote sensing; energy production and conversion; environment pollution; geophysics; meteorology and climatology; and oceanography.

For related information see also *Space Sciences.*

42 GEOSCIENCES (GENERAL) 1669

43 EARTH RESOURCES AND REMOTE SENSING 1690

Includes remote sensing of earth resources by aircraft and spacecraft; photogrammetry; and aerial photography.

For instrumentation see *35 Instrumentation and Photography.*

44 ENERGY PRODUCTION AND CONVERSION 1692

Includes specific energy conversion systems, e.g., fuel cells; global sources of energy; geophysical conversion; and windpower.

For related information see also *07 Aircraft Propulsion and Power, 20 Spacecraft Propulsion and Power,* and *28 Propellants and Fuels.*

45 ENVIRONMENT POLLUTION 1693

Includes atmospheric, noise, thermal, and water pollution.

46 GEOPHYSICS 1695

Includes aeronomy; upper and lower atmosphere studies; ionospheric and magnetospheric physics; and geomagnetism.

For space radiation see *93 Space Radiation.*

47 METEOROLOGY AND CLIMATOLOGY 1700

Includes weather forecasting and modification.

48 OCEANOGRAPHY 1710

Includes biological, dynamic, and physical oceanography; and marine resources.

For related information see also *43 Earth Resources and Remote Sensing.*

LIFE SCIENCES

Includes life sciences (general); aerospace medicine; behavioral sciences; man/system technology and life support; and space biology.

51 LIFE SCIENCES (GENERAL) 1711

52 AEROSPACE MEDICINE 1712

Includes physiological factors; biological effects of radiation; and effects of weightlessness on man and animals.

53 BEHAVIORAL SCIENCES 1714

Includes psychological factors; individual and group behavior; crew training and evaluation; and psychiatric research.

54 MAN/SYSTEM TECHNOLOGY AND LIFE SUPPORT 1714

Includes human engineering; biotechnology; and space suits and protective clothing.

For related information see also *16 Space Transportation.*

55 SPACE BIOLOGY N.A.

Includes exobiology; planetary biology; and extraterrestrial life.

MATHEMATICAL AND COMPUTER SCIENCES

Includes mathematical and computer sciences (general); computer operations and hardware; computer programming and software; computer systems; cybernetics; numerical analysis; statistics and probability; systems analysis; and theoretical mathematics.

59 MATHEMATICAL AND COMPUTER SCIENCES (GENERAL) 1718

60 COMPUTER OPERATIONS AND HARDWARE 1732

Includes hardware for computer graphics, firmware, and data processing.

For components see *33 Electronics and Electrical Engineering.*

61 COMPUTER PROGRAMMING AND SOFTWARE 1733

Includes computer programs, routines, algorithms, and specific applications, e.g., CAD/CAM.

62 COMPUTER SYSTEMS 1738

Includes computer networks and special application computer systems.

63 CYBERNETICS 1738

Includes feedback and control theory, artificial intelligence, robotics and expert systems.

For related information see also *54 Man/System Technology and Life Support.*

64 NUMERICAL ANALYSIS 1741

Includes iteration, difference equations, and numerical approximation.

65 STATISTICS AND PROBABILITY 1743

Includes data sampling and smoothing; Monte Carlo method; and stochastic processes.

66 SYSTEMS ANALYSIS 1745

Includes mathematical modeling; network analysis; and operations research.

67 THEORETICAL MATHEMATICS N.A.

Includes topology and number theory.

PHYSICS

Includes physics (general); acoustics; atomic and molecular physics; nuclear and high-energy physics; optics; plasma physics; solid-state physics; and thermodynamics and statistical physics.

For related information see also *Engineering.*

70 PHYSICS (GENERAL) 1745

For precision time and time interval (PTTI) see *35 Instrumentation and Photography;* for geophysics, astrophysics or solar physics see *46 Geophysics, 90 Astrophysics,* or *92 Solar Physics.*

71 ACOUSTICS 1745
Includes sound generation, transmission, and attenuation.
For noise pollution see *45 Environment Pollution.*

72 ATOMIC AND MOLECULAR PHYSICS 1746
Includes atomic structure, electron properties, and molecular spectra.

73 NUCLEAR AND HIGH-ENERGY PHYSICS 1747
Includes elementary and nuclear particles; and reactor theory.
For space radiation see *93 Space Radiation.*

74 OPTICS 1748
Includes light phenomena and optical devices.
For lasers see *36 Lasers and Masers.*

75 PLASMA PHYSICS 1749
Includes magnetohydrodynamics and plasma fusion.
For ionospheric plasmas see *46 Geophysics.* For space plasmas see *90 Astrophysics.*

76 SOLID-STATE PHYSICS 1751
Includes superconductivity.
For related information see also *33 Electronics and Electrical Engineering* and *36 Lasers and Masers.*

77 THERMODYNAMICS AND STATISTICAL PHYSICS 1754
Includes quantum mechanics; theoretical physics; and Bose and Fermi statistics.
For related information see also *25 Inorganic and Physical Chemistry* and *34 Fluid Mechanics and Heat Transfer.*

SOCIAL SCIENCES

Includes social sciences (general); administration and management; documentation and information science; economics and cost analysis; law, political science, and space policy; and urban technology and transportation.

80 SOCIAL SCIENCES (GENERAL) N.A.
Includes educational matters.

81 ADMINISTRATION AND MANAGEMENT 1755
Includes management planning and research.

82 DOCUMENTATION AND INFORMATION SCIENCE 1756
Includes information management; information storage and retrieval technology; technical writing; graphic arts; and micrography.
For computer documentation see *61 Computer Programming and Software.*

83 ECONOMICS AND COST ANALYSIS N.A.
Includes cost effectiveness studies.

84 LAW, POLITICAL SCIENCE AND SPACE POLICY 1756
Includes NASA appropriation hearings; aviation law; space law and policy; international law; international cooperation; and patent policy.

85 URBAN TECHNOLOGY AND TRANSPORTATION 1757
Includes applications of space technology to urban problems; technology transfer; technology assessment; and surface and mass transportation.
For related information see *03 Air Transportation and Safety, 16 Space Transportation,* and *44 Energy Production and Conversion.*

SPACE SCIENCES

Includes space sciences (general); astronomy; astrophysics; lunar and planetary exploration; solar physics; and space radiation.
For related information see also *Geosciences.*

88 SPACE SCIENCES (GENERAL) N.A.

89 ASTRONOMY 1757
Includes radio, gamma-ray, and infrared astronomy; and astrometry.

90 ASTROPHYSICS 1758
Includes cosmology; celestial mechanics; space plasmas; and interstellar and interplanetary gases and dust.
For related information see also *75 Plasma Physics.*

91 LUNAR AND PLANETARY EXPLORATION 1760
Includes planetology; and manned and unmanned flights.
For spacecraft design or space stations see *18 Spacecraft Design, Testing and Performance.*

92 SOLAR PHYSICS 1760
Includes solar activity, solar flares, solar radiation and sunspots.
For related information see *93 Space Radiation.*

93 SPACE RADIATION 1761
Includes cosmic radiation; and inner and outer earth's radiation belts.
For biological effects of radiation see *52 Aerospace Medicine.* For theory see *73 Nuclear and High-Energy Physics.*

GENERAL

Includes aeronautical, astronautical, and space science related histories, biographies, and pertinent reports too broad for categorization; histories or broad overviews of NASA programs.

99 GENERAL 1761

Note: N.A. means that no abstracts were assigned to this category for this issue.

SUBJECT INDEX I-1
PERSONAL AUTHOR INDEX I-55
CORPORATE SOURCE INDEX I-63
CONTRACT NUMBER INDEX I-75
REPORT/ACCESSION NUMBER INDEX I-77

TYPICAL CITATION AND ABSTRACT

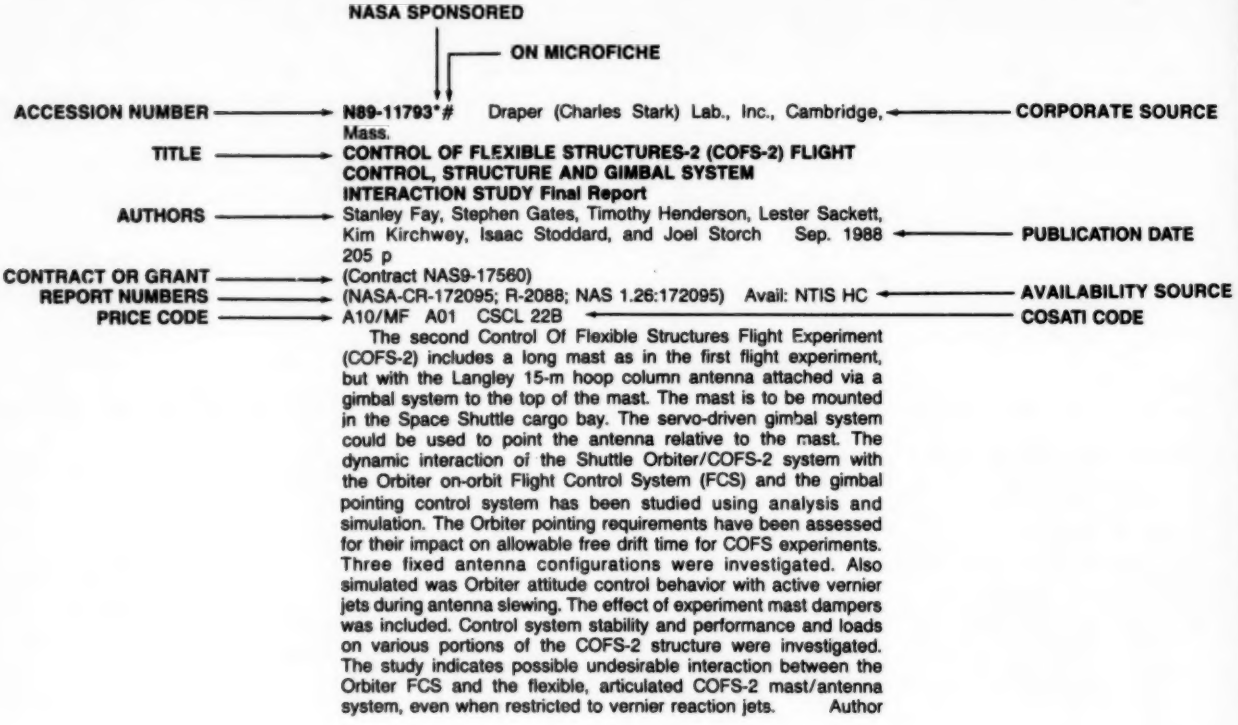
NASA SPONSORED
ON MICROFICHE
ACCESSION NUMBER
N89-11793*# Draper (Charles Stark) Lab., Inc., Cambridge, Mass.
CORPORATE SOURCE
TITLE
CONTROL OF FLEXIBLE STRUCTURES-2 (COFS-2) FLIGHT CONTROL, STRUCTURE AND GIMBAL SYSTEM INTERACTION STUDY Final Report
AUTHORS
Stanley Fay, Stephen Gates, Timothy Henderson, Lester Sackett, Kim Kirchwey, Isaac Stoddard, and Joel Storch Sep. 1988
PUBLICATION DATE
205 p
CONTRACT OR GRANT
(Contract NAS9-17560)
REPORT NUMBERS
(NASA-CR-172095; R-2088; NAS 1.26:172095) Avail: NTIS HC
AVAILABILITY SOURCE
PRICE CODE
A10/MF A01 CSCL 22B
COSATI CODE
The second Control Of Flexible Structures Flight Experiment (COFS-2) includes a long mast as in the first flight experiment, but with the Langley 15-m hoop column antenna attached via a gimbal system to the top of the mast. The mast is to be mounted in the Space Shuttle cargo bay. The servo-driven gimbal system could be used to point the antenna relative to the mast. The dynamic interaction of the Shuttle Orbiter/COFS-2 system with the Orbiter on-orbit Flight Control System (FCS) and the gimbal pointing control system has been studied using analysis and simulation. The Orbiter pointing requirements have been assessed for their impact on allowable free drift time for COFS experiments. Three fixed antenna configurations were investigated. Also simulated was Orbiter attitude control behavior with active vernier jets during antenna slewing. The effect of experiment mast dampers was included. Control system stability and performance and loads on various portions of the COFS-2 structure were investigated. The study indicates possible undesirable interaction between the Orbiter FCS and the flexible, articulated COFS-2 mast/antenna system, even when restricted to vernier reaction jets. Author

VOLUME 27 NUMBER 12 / JUNE 23, 1989

Scientific and Technical Aerospace Reports

A Semimonthly Publication of the National Aeronautics and Space Administration

01 AERONAUTICS (GENERAL)

N89-19226# Air Force Inst. of Tech., Wright-Patterson AFB, OH.
ESTIMATING AIRCRAFT AIRFRAME TOOLING COST: AN ALTERNATIVE TO DAPCA 3 M.S. Thesis
Patricia L. Meyer Sep. 1988 89 p
(AD-A201506; AFIT/GCA/LSQ/88S-6) Avail: NTIS HC A05/MF A01 CSCL 01C

The purpose of this study was to evaluate the tooling cost estimating equation of the DAPCA 3 model and determine if more accurate models can be developed. The five objectives of the research were: (1) Determine the accuracy of the DAPCA 3 model; (2) Determine if the independent variables in DAPCA 3 are logically valid; (3) Determine if the data base which was used to develop DAPCA 3 is appropriate for estimating today's aircraft systems; (4) Determine if the accuracy of the DAPCA 3 model can be improved; and (5) Determine if using a factor of manufacturing is sufficient to estimate tooling costs. When tooling was regressed against manufacturing and engineering, the data without the prototypes indicated that engineering was more significant than manufacturing. Both manufacturing and engineering were significant for the data with the prototypes. GRA

N89-19227# Air Force Inst. of Tech., Wright-Patterson AFB, OH.
ANALYSIS OF COST GROWTH AND COST COMPOSITION IN THE DEFENSE AEROSPACE INDUSTRY M.S. Thesis
Thomas M. Obringer Sep. 1988 132 p
(AD-A201544; AD-E951221; AFIT/GCA/LSY/88S-7) Avail: NTIS HC A07/MF A01 CSCL 05C

The objective of this thesis was to determine if real cost growth occurred in the defense aerospace industry during the period 1980 to 1986 and if the percentage of overhead costs to total cost increased during the same period. Cost data from 16 defense aerospace plants were studied results of the hypothesis tests indicate that there was no real cost growth in the industry during this period and that overhead costs did not increase relative to total cost. However, when contractors in the sample were tested individually, results indicate that eight of the sixteen contractors experienced significant cost growth. The conflicting results may be due to the wide dispersion of the data points used in the statistical tests which, in turn, may be caused by the differing variety of aerospace industry segments. Descriptive statistics computed for the study's sample show that the percentage of direct labor, direct material, other direct charges, and overhead to total cost remained stable over the year period. Although overhead costs were not found to be increasing relative to total cost, they still make up the second largest component of total cost (32 percent) behind direct materials (42 percent). GRA

N89-19228# Air Force Inst. of Tech., Wright-Patterson AFB, OH. School of Systems and Logistics.
R AND M (RELIABILITY AND MAINTAINABILITY) QUALITY TEAM CONCEPT AND C-17 DESIGN AT DOUGLAS AIRCRAFT COMPANY: AN R AND M 2000 INITIATIVE CASE STUDY M.S. Thesis
R. Anthony Phillips Sep. 1988 89 p
(AD-A201574; AFIT/GLM/LSM/88S-56) Avail: NTIS HC A05/MF A01 CSCL 05A

The Aeronautical Systems Divisions's C-17 System Program Office has developed a quality management initiative called the R and M (Reliability and Maintainability) Quality Team Concept. Its purpose is to provide companies with better management of R and M during the full-scale engineering development acquisition phase. Douglas Aircraft Co. (DAC) agreed to implement the R and M Quality Team Concept during design of the C-17. This thesis examined the effect of the R and M Quality Team Concept as instituted by DAC on the quality management of the R and M process during C-17 design. Research assessed the concept's perceived impact on: (1) communication on R and M issues; (2) R and M problem solving; and (3) specific C-17 design changes. A survey was administered to DAC employees and interviews were conducted with management at DAC's Long Beach, CA, facility. Hypothesis testing using z and t-tests assisted in evaluating survey results. Study results revealed overall employee support for the R and M Quality Team Concept. The concept provided a method of R and M management and problem solving not available in a traditional program organization, and a number of C-17 design changes resulted from concept application. GRA

N89-19229# Transportation Systems Center, Cambridge, MA.
GENERAL AVIATION ACTIVITY AND AVIONICS SURVEY Annual Summary Report, CY 1987
Michael A. Rossetti Nov. 1988 289 p
(AD-A201760; DOT-TSC-FAA-88-6; FAA-MS-88-5) Avail: NTIS HC A13/MF A01 CSCL 01D

The results and a description of the 1987 General Aviation Activity and Avionic Survey are presented. The survey was conducted during 1988 by the FAA to obtain information on the activity and avionics of the United States registered general aviation aircraft fleet, the dominant component of civil aviation in the U.S. The survey was based on a statistically selected sample of about 11.1 percent of the general aviation fleet. A response rate of 61.1 percent was obtained. Survey results are based upon responses but are expanded upward to represent the total population. Survey results revealed that during 1987 an estimated 33.4 million hours of flying time were logged and 93.7 million operations were performed by the 217,183 active general aviation aircraft in the U.S. fleet. The mean annual flight time per aircraft was 148.4 hours. The active aircraft represented about 81.2 percent of the registered general aviation fleet. The report contains breakdowns of these and other statistics by manufacturer/model group, aircraft type, state and region of based aircraft, and primary use. Also included are fuel consumption, lifetime airframe hours, avionics, engine hours, and miles flown estimates, tables for detailed analysis of the avionics capabilities of the GA (General Aviation) fleet. GRA

N89-19230*# National Aeronautics and Space Administration. Langley Research Center, Hampton, VA.
JOINT UNIVERSITY PROGRAM FOR AIR TRANSPORTATION RESEARCH, 1987
Frederick R. Morrell, comp. Apr. 1989 118 p Presented at a conference held in Atlantic City, NJ, 14-15 Jan. 1988
(NASA-CP-3028; L-16547; NAS 1.55:3028) Avail: NTIS HC A06/MF A01 CSCL 01B

The research conducted during 1987 under the NASA/FAA sponsored Joint University Program for Air Transportation Research is summarized. The Joint University Program is a coordinated set of 3 grants sponsored by NASA-Langley and the FAA, one each with the MIT, Ohio Univ., and Princeton Univ. Completed works, status reports, and annotated bibliographies are presented for research topics, which include computer science, guidance and control theory and practice, aircraft performance, flight dynamics, and applied experimental psychology. An overview of the year's activities for each university is also presented. Author

02 AERODYNAMICS

Includes aerodynamics of bodies, combinations, wings, rotors, and control surfaces; and internal flow in ducts and turbomachinery.

For related information see also *34 Fluid Mechanics and Heat Transfer.*

N89-19231*# National Aeronautics and Space Administration. Langley Research Center, Hampton, VA.

THE NASA LANGLEY LAMINAR-FLOW-CONTROL EXPERIMENT ON A SWEPT, SUPERCRITICAL AIRFOIL - DRAG EQUATIONS

Cuyler W. Brooks, Jr., Charles D. Harris, and William D. Harvey Mar. 1989 42 p

(NASA-TM-4096; L-16322; NAS 1.15:4096) Avail: NTIS HC A03/MF A01 CSCL 01A

The Langley Research Center has designed a swept, supercritical airfoil incorporating Laminar Flow Control for testing at transonic speeds. Analytical expressions have been developed and an evaluation made of the experimental section drag, composed of suction drag and wake drag, using theoretical design information and experimental data. The analysis shows that, although the sweep-induced boundary-layer crossflow influence on the wake drag is too large to be ignored and there is not a practical method for evaluating these crossflow effects on the experimental wake data, the conventional unswept 2-D wake-drag computation used in the reduction of the experimental data is at worst 10 percent too high. Author

N89-19232*# National Aeronautics and Space Administration. Langley Research Center, Hampton, VA.

DRAG MEASUREMENTS ON A LAMINAR-FLOW BODY OF REVOLUTION IN THE 13-INCH MAGNETIC SUSPENSION AND BALANCE SYSTEM

David A. Dress [1989] 37 p

(NASA-TP-2895; L-16483; NAS 1.60:2895) Avail: NTIS HC A03/MF A01 CSCL 01A

Low speed wind tunnel drag force measurements were taken on a laminar flow body of revolution free of support interference. This body was tested at zero incidence in the NASA Langley 13 in. Magnetic Suspension and Balance System (MSBS). The primary objective of these tests was to substantiate the drag force measuring capabilities of the 13 in. MSBS. The drag force calibrations and wind-on repeatability data provide a means of assessing these capabilities. Additional investigations include: (1) the effects of fixing transition; (2) the effects of fins installed in the tail; and (3) surface flow visualization using both liquid crystals and oil flow. Also two simple drag prediction codes were used to assess their usefulness in estimating overall body drag. Author

N89-19233 Boston Univ., MA.

THE BOUNDARY ELEMENT METHOD FOR THE DIFFUSION EQUATION Ph.D. Thesis

Dorothy Claire Attaway 1988 115 p

Avail: Univ. Microfilms Order No. DA8813631

The Boundary Element Method for solving parabolic partial differential equations, and in particular the diffusion equation, is presented. The Boundary Element Method involves transforming the partial differential equation which holds over a given domain into an integral equation which holds over the boundary of the domain. Two methods are described for obtaining the integral equation. In the classical Green's Function Method, boundary conditions are imposed which result in an explicit expression for the unknown function which is difficult to solve. The Boundary Integral Equation Method imposes no such boundary conditions, which yields an integral equation which must be solved numerically. In the Boundary Integral Equation Method, this solution is obtained by using the finite-element method for the spatial and time discretizations. There are two approaches for the discretization in time. In the step by step approach, the solution is obtained for all control points on the boundary and in the field for each successive time step. In the initial value approach, the solution is first obtained for all control points on the boundary for all time steps, and can then be obtained for any desired interior point. The method has been implemented in a computer program, and numerical results were obtained for different domain geometries in order to validate the method. Dissert. Abstr.

N89-19234*# National Aeronautics and Space Administration. Langley Research Center, Hampton, VA.

TRANSONIC UNSTEADY AERODYNAMICS AND AEROELASTICITY 1987, PART 1

Samuel R. Bland, comp. Washington, DC Feb. 1989 261 p Symposium held in Hampton, VA, 20-22 May 1987

(NASA-CP-3022-Pt-1; L-16532-Pt-1; NAS 1.55:3022-Pt-1) Avail: NTIS HC A12/MF A01 CSCL 01A

Computational fluid dynamics methods have been widely accepted for transonic aeroelastic analysis. Previously, calculations with the TSD methods were used for 2-D airfoils, but now the TSD methods are applied to the aeroelastic analysis of the complete aircraft. The Symposium papers are grouped into five subject areas, two of which are covered in this part: (1) Transonic Small Disturbance (TSD) theory for complete aircraft configurations; and (2) Full potential and Euler equation methods. For individual titles, see N89-19235 through N89-19246.

N89-19235*# Air Force Wright Aeronautical Labs., Wright-Patterson AFB, OH. Structures Div.

UNSTEADY AERODYNAMICS AND AEROELASTIC RESEARCH AT AFWAL

L. J. Huttsell and W. A. Sotomayer *In* NASA, Langley Research Center, Transonic Unsteady Aerodynamics and Aeroelasticity 1987, Part 1 Feb. 1989 p 1-14 (For primary document see N89-19234 12-02)

Avail: NTIS HC A12/MF A01 CSCL 01A

An efficient and accurate transonic unsteady aerodynamic method is needed for predicting flight loads, flutter and aeroelastic stability for advanced aircraft. There have been new developments and many improvements to older codes. XTRAN3S was improved and is a useful code for the near term. However, to predict the unsteady aerodynamics for high performance maneuvering aircraft, the Euler/Navier-Stokes codes must be extended and improved for complex 3-D configurations. The long term goal is development of Euler/Navier-Stokes unsteady aerodynamic methods for aeroelastic analysis. Author

N89-19236*# Boeing Military Airplane Development, Seattle, WA.

EXTENSIONS AND IMPROVEMENTS ON XTRAN3S **c61**

C. J. Borland *In* NASA, Langley Research Center, Transonic Unsteady Aerodynamics and Aeroelasticity 1987, Part 1 Feb. 1989 p 15-45 (For primary document see N89-19234 12-02)

Avail: NTIS HC A12/MF A01 CSCL 09B

Improvements to the XTRAN3S computer program are summarized. Work on this code, for steady and unsteady aerodynamic and aeroelastic analysis in the transonic flow regime has concentrated on the following areas: (1) Maintenance of the XTRAN3S code, including correction of errors, enhancement of operational capability, and installation on the Cray X-MP system; (2) Extension of the vectorization concepts in XTRAN3S to include additional areas of the code for improved execution speed; (3) Modification of the XTRAN3S algorithm for improved numerical

stability for swept, tapered wing cases and improved computational efficiency; and (4) Extension of the wing-only version of XTRAN3S to include pylon and nacelle or external store capability. Author

N89-19237*# National Aeronautics and Space Administration. Ames Research Center, Moffett Field, CA.
ROLE OF COMPUTATIONAL FLUID DYNAMICS IN UNSTEADY AERODYNAMICS FOR AEROELASTICITY c34
Guru P. Guruswamy (Sterling Federal Systems, Moffett Field, CA.) and Peter M. Goorjian *In* NASA, Langley Research Center, Transonic Unsteady Aerodynamics and Aeroelasticity 1987, Part 1 Feb. 1989 p 47-61 (For primary document see N89-19234 12-02)
Avail: NTIS HC A12/MF A01 CSCL 20D

In the last two decades there have been extensive developments in computational unsteady transonic aerodynamics. Such developments are essential since the transonic regime plays an important role in the design of modern aircraft. Therefore, there has been a large effort to develop computational tools with which to accurately perform flutter analysis at transonic speeds. In the area of Computational Fluid Dynamics (CFD), unsteady transonic aerodynamics are characterized by the feature of modeling the motion of shock waves over aerodynamic bodies, such as wings. This modeling requires the solution of nonlinear partial differential equations. Most advanced codes such as XTRAN3S use the transonic small perturbation equation. Currently, XTRAN3S is being used for generic research in unsteady aerodynamics and aeroelasticity of almost full aircraft configurations. Use of Euler/Navier Stokes equations for simple typical sections has just begun. A brief history of the development of CFD for aeroelastic applications is summarized. The development of unsteady transonic aerodynamics and aeroelasticity are also summarized. Author

N89-19238*# National Aeronautics and Space Administration. Langley Research Center, Hampton, VA.
CAP-TSD: A PROGRAM FOR UNSTEADY TRANSONIC ANALYSIS OF REALISTIC AIRCRAFT CONFIGURATIONS c05
John T. Batina, David A. Seidel, Samuel R. Bland, and Robert M. Bennett *In its* Transonic Unsteady Aerodynamics and Aeroelasticity 1987, Part 1 Feb. 1989 p 63-95 (For primary document see N89-19234 12-02)
Avail: NTIS HC A12/MF A01 CSCL 01C

The development of a new transonic code to predict unsteady flows about realistic aircraft configurations are described. An approximate factorization algorithm for solution of the unsteady transonic small disturbance equation is first described. Because of the superior stability characteristics of the AF algorithm, a new transonic aeroelasticity code was developed which is described in some detail. The new code was very easy to modify to include the additional aircraft components, so in a very short period of time the code was developed to treat complete aircraft configurations. Finally, applications are presented which demonstrate many of the geometry capabilities of the new code. Author

N89-19239*# McDonnell Aircraft Co., Saint Louis, MO.
CAP-TSD ANALYSIS OF THE F-15 AIRCRAFT c05
Dale M. Pitt *In* NASA, Langley Research Center, Transonic Unsteady Aerodynamics and Aeroelasticity 1987, Part 1 Feb. 1989 p 97-116 (For primary document see N89-19234 12-02)
Avail: NTIS HC A12/MF A01 CSCL 01C

The F-15 fighter aircraft was modeled using Computational Aeroelasticity Program - Transonic Small Disturbance (CAP-TSD). The complete aircraft was modeled including the wing, stabilator, flow through inlets, and fuselage body. CAP-TSD was used to make static pressure runs for Mach numbers of 0.8, 0.9, 0.95 and 1.2. The angle of attack for these runs ranged from 0 to 5 degs. The CAP-TSD program showed good agreement between the computed fuselage and wing pressures and the measured wind tunnel pressures. Including the fuselage and inlets in the CAP-TSD analysis is important and improves the correlation of wing pressures with test data. Author

N89-19240*# National Aeronautics and Space Administration. Langley Research Center, Hampton, VA.
CALCULATION OF STEADY AND UNSTEADY PRESSURES AT SUPERSONIC SPEEDS WITH CAP-TSD
Robert M. Bennett, Samuel R. Bland, John T. Batina, Michael D. Gibbons, and Dennis G. Mabey (Royal Aircraft Establishment, Bedford, England) *In its* Transonic Unsteady Aerodynamics and Aeroelasticity 1987, Part 1 Feb. 1989 p 117-137 (For primary document see N89-19234 12-02)
Avail: NTIS HC A12/MF A01 CSCL 01A

A finite difference technique is used to solve the transonic small disturbance flow equation making use of shock capturing to treat wave discontinuities. Thus the nonlinear effects of thickness and angle of attack are considered. Such an approach is made feasible by the development of a new code called CAP-TSD (Computational Aeroelasticity Program - Transonic Small Disturbance), and is based on a fully implicit approximate factorization (AF) finite difference method to solve the time dependent transonic small disturbance equation. The application of the CAP-TSD code to the calculation of low to moderate supersonic steady and unsteady flows is presented. In particular, comparisons with exact linear theory solutions are made for steady and unsteady cases to evaluate shock capturing and other features of the current method. In addition, steady solutions obtained from an Euler code are used to evaluate the small disturbance aspects of the code. Steady and unsteady pressure comparisons are made with measurements for an F-15 wing model and for the RAE tailplane model. Author

N89-19241*# Arizona State Univ., Tempe. Dept. of Mechanical and Aerospace Engineering.
AN EFFICIENT METHOD FOR COMPUTING UNSTEADY TRANSONIC AERODYNAMICS OF SWEPT WINGS WITH CONTROL SURFACES
D. D. Liu, Y. F. Kao, and K. Y. Fung (Arizona Univ., Tucson.) *In* NASA, Langley Research Center, Transonic Unsteady Aerodynamics and Aeroelasticity 1987, Part 1 Feb. 1989 p 139-155 Previously announced in IAA as A86-11029 Sponsored in part by NASA, Ames Research Center, Moffett Field, CA (For primary document see N89-19234 12-02)
(AIAA-85-4058) Avail: NTIS HC A12/MF A01 CSCL 01A

A transonic equivalent strip (TES) method was further developed for unsteady flow computations of arbitrary wing planforms. The TES method consists of two consecutive correction steps to a given nonlinear code such as LTRAN2; namely, the chordwise mean flow correction and the spanwise phase correction. The computation procedure requires direct pressure input from other computed or measured data. Otherwise, it does not require airfoil shape or grid generation for given planforms. To validate the computed results, four swept wings of various aspect ratios, including those with control surfaces, are selected as computational examples. Overall trends in unsteady pressures are established with those obtained by XTRAN3S codes, Isogai's full potential code and measured data by NLR and RAE. In comparison with these methods, the TES has achieved considerable saving in computer time and reasonable accuracy which suggests immediate industrial applications. Author

N89-19242*# National Aeronautics and Space Administration. Langley Research Center, Hampton, VA.
APPLICATION OF A FULL POTENTIAL METHOD TO AGARD STANDARD AIRFOILS
Woodrow Whitlow, Jr. *In its* Transonic Unsteady Aerodynamics and Aeroelasticity 1987, Part 1 Feb. 1989 p 157-174 (For primary document see N89-19234 12-02)
Avail: NTIS HC A12/MF A01 CSCL 01A

One of the most important uses of method that calculate unsteady aerodynamic loads is to predict and analyze the aeroelastic responses of flight vehicles. Currently, methods based on transonic small disturbance potential aerodynamics are the primary tools for aeroelastic analysis. Flow solutions obtained using isentropic potential theory can be highly inaccurate and even multivalued, because they do not model the effects of entropy

that is produced when shock waves are in the flow field. From the results that are presented, it is concluded that nonisentropic potential methods more accurately model Euler solutions than do isentropic methods. The primary effects of modeling shock generated entropy are: (1) to eliminate mulitple flow solutions when strong shock waves are in the flow field; and (2) to bring the strengths and locations of computed shock waves into better agreement with those calculated using Euler method and those measured during experiments. E.R.

N89-19243*# Rockwell International Science Center, Thousand Oaks, CA.
FULL POTENTIAL UNSTEADY COMPUTATIONS INCLUDING AEROELASTIC EFFECTS
Vijaya Shankar and Hiroshi Ide (Rockwell International Corp., Los Angeles, CA.) *In* NASA, Langley Research Center, Transonic Unsteady Aerodynamics and Aeroelasticity 1987, Part 1 Feb. 1989 p 175-191 (For primary document see N89-19234 12-02)
Avail: NTIS HC A12/MF A01 CSCL 01A

A unified formulation is presented based on the full potential framework coupled with an appropriate structural model to compute steady and unsteady flows over rigid and flexible configurations across the Mach number range. The unsteady form of the full potential equation in conservation form is solved using an implicit scheme maintaining time accuracy through internal Newton iterations. A flux biasing procedure based on the unsteady sonic reference conditions is implemented to compute hyperbolic regions with moving sonic and shock surfaces. The wake behind a trailing edge is modeled using a mathematical cut across which the pressure is satisfied to be continuous by solving an appropriate vorticity convection equation. An aeroelastic model based on the generalized modal deflection approach interacts with the nonlinear aerodynamics and includes both static as well as dynamic structural analyses capability. Results are presented for rigid and flexible configurations at different Mach numbers ranging from subsonic to supersonic conditions. The dynamic response of a flexible wing below and above its flutter point is demonstrated. Author

N89-19244*# National Aeronautics and Space Administration. Langley Research Center, Hampton, VA.
FLUX-VECTOR SPLITTING FOR UNSTEADY CALCULATIONS ON DYNAMIC MESHES
W. Kyle Anderson, James L. Thomas, and Christopher L. Rumsey *In its* Transonic Unsteady Aerodynamics and Aeroelasticity 1987, Part 1 Feb. 1989 p 193-214 (For primary document see N89-19234 12-02)
Avail: NTIS HC A12/MF A01 CSCL 01A

The method of flux vector splitting used is that of Van Leer. The fluxes split in this manner have the advantage of being continuously differentiable at eigenvalue sign changes and this allows normal shocks to be captured with at most two interior zones, although in practice only one zone is usually observed. The fluxes as originally derived, however did not include the necessary terms appropriate for calculations on a dynamic mesh. The extension of the splitting to include these terms while retaining the advantages of the original splitting is the main purpose of this investigation. In addition, the use of multiple grids to reduce the computer time is investigated. A subiterative procedure to eliminate factorization and linearization error so that larger time steps can be used is also investigated. Author

N89-19245*# Air Force Armament Lab., Eglin AFB, FL.
UNSTEADY TRANSONIC FLOW USING EULER EQUATIONS
Dave M. Belk and L. Bruce Simpson *In* NASA, Langley Research Center, Transonic Unsteady Aerodynamics and Aeroelasticity 1987, Part 1 Feb. 1989 p 215-241 (For primary document see N89-19234 12-02)
Avail: NTIS HC A12/MF A01 CSCL 01A

An implicit, two factor, split flux, finite volume Euler equations solution algorithms is applied to the time accurate solution of transonic flow about an NACA 0012 airfoil and a rectangular planform supercritical wing undergoing pitch oscillations. Accuracy for Courant numbers greater than one is analyzed. Freezing the flux Jacobians can result in significant savings for steady state solutions; the accuracy of freezing flux Jacobians for unsteady results is investigated. The Euler algorithm results are compared with experimental results for an NACA 0012 and a rectangular planform supercritical wing. Author

N89-19246*# National Aeronautics and Space Administration. Langley Research Center, Hampton, VA.
AGARD STANDARD AEROELASTIC CONFIGURATIONS FOR DYNAMIC RESPONSE
E. Carson Yates, Jr. *In its* Transonic Unsteady Aerodynamics and Aeroelasticity 1987, Part 1 Feb. 1989 p 243-259 (For primary document see N89-19234 12-02)
Avail: NTIS HC A12/MF A01 CSCL 01A

Since emphasis is on the transonic speed range, special importance is placed on configurations for which available data are sufficient to define accurately a transonic flutter boundary. Only configurations with clean, smooth surfaces are considered suitable. Segmented models or models with surface-slope discontinuities are inappropriate. Excluded also, in general, are configurations and data sets that involve behavior that is uncertain or not well understood, uncertain model properties, or know sensitivities to small variations in model properties. In order to assess the suitability of configurations already tested and the associated data for designation as standard, a survey of AGARD member countries was conducted to seek candidates for the prospective set. The results of that survey are given and summarized along with the initial selection of a standard configuration. Author

N89-19247*# National Aeronautics and Space Administration. Langley Research Center, Hampton, VA.
TRANSONIC UNSTEADY AERODYNAMICS AND AEROELASTICITY 1987, PART 2
Samuel R. Bland, comp. Washington, DC Feb. 1989 379 p Symposium held in Hampton, VA, 20-22 May 1987
(NASA-CP-3022-Pt-2; L-16532-Pt-2; NAS 1.55:3022-Pt-2) Avail: NTIS HC A17/MF A01 CSCL 01A

This two part document contains copies of the text and figures for the papers presented at the symposium held at NASA Langley on 20 to 22 May, 1987. The papers are grouped in five subject areas. The areas covered by this part includes the following: Methods for vortex and viscous flows; Aeroelastic applications, and Experimental results and cascade flows. For individual titles, see N89-19248 through N89-19264.

N89-19248*# Old Dominion Univ., Norfolk, VA.
SOLUTION OF STEADY AND UNSTEADY TRANSONIC-VORTEX FLOWS USING EULER AND FULL-POTENTIAL EQUATIONS
Osama A. Kandil, Andrew H. Chuang, and Hong Hu *In* NASA, Langley Research Center, Transonic Unsteady Aerodynamics and Aeroelasticity 1987, Part 2 Feb. 1989 p 261-311 (For primary document see N89-19247 12-02)
(Grant NAG1-648)
Avail: NTIS HC A17/MF A01 CSCL 01A

Two methods are presented for inviscid transonic flows: unsteady Euler equations in a rotating frame of reference for transonic-vortex flows and integral solution of full-potential equation with and without embedded Euler domains for transonic airfoil flows. The computational results covered: steady and unsteady conical vortex flows; 3-D steady transonic vortex flow; and transonic airfoil flows. The results are in good agreement with other computational results and experimental data. The rotating frame of reference solution is potentially efficient as compared with the space fixed reference formulation with dynamic gridding. The integral equation solution with embedded Euler domain is computationally efficient and as accurate as the Euler equations. Author

N89-19249*# National Aeronautics and Space Administration. Langley Research Center, Hampton, VA.
VISCOUS FLOW CALCULATIONS FOR THE AGARD STANDARD CONFIGURATION AIRFOILS WITH EXPERIMENTAL COMPARISONS
James T. Howlett *In its* Transonic Unsteady Aerodynamics and Aeroelasticity 1987, Part 2 Feb. 1989 p 313-330 (For primary document see N89-19247 12-02)
Avail: NTIS HC A17/MF A01 CSCL 01A

Recent experience in calculating unsteady transonic flow by means of viscous-inviscid interactions with the XTRAN2L computer code is examined. The boundary layer method for attached flows is based upon the work of Rizzetta. The nonisentropic corrections of Fuglsang and Williams are also incorporated along with the viscous interaction for some cases and initial results are presented. For unsteady flows, the inverse boundary layer equations developed by Vatsa and Carter are used in a quasi-steady manner and preliminary results are presented. Author

N89-19250*# Mississippi State Univ., Mississippi State.
UNSTEADY TRANSONIC VISCOUS-INVISCID INTERACTION USING EULER AND BOUNDARY-LAYER EQUATIONS
Shahyar Pirzadeh and Dave Whitfield *In* NASA, Langley Research Center, Transonic Unsteady Aerodynamics and Aeroelasticity 1987, Part 2 Feb. 1989 p 331-349 (For primary document see N89-19247 12-02)
Avail: NTIS HC A17/MF A01 CSCL 01A

The Euler code is used extensively for computation of transonic unsteady aerodynamics. The boundary layer code solves the 3-D, compressible, unsteady, mean flow kinetic energy integral boundary layer equations in the direct mode. Inviscid-viscous coupling is handled using porosity boundary conditions. Some of the advantages and disadvantages of using the Euler and boundary layer equations for investigating unsteady viscous-inviscid interaction is examined. Author

N89-19251*# Georgia Inst. of Tech., Atlanta.
NUMERICAL SOLUTION OF UNSTEADY ROTATIONAL FLOW PAST FIXED AND ROTARY WING CONFIGURATIONS
N. L. Sankar, B. E. Wake, S. Y. Ruo, and J. B. Malone (Lockheed-Georgia Co., Atlanta.) *In* NASA, Langley Research Center, Transonic Unsteady Aerodynamics and Aeroelasticity 1987, Part 2 Feb. 1989 p 351-374 (For primary document see N89-19247 12-02)
Avail: NTIS HC A17/MF A01 CSCL 01A

The application of unsteady 3-D Euler and Navier-Stokes equations to transonic flow past rotor blades, and wing-alone configurations is described. A promising approach for the numerical solution of these equations is examined. Additional work is needed for improving the efficiency of the present procedure. It is hoped that the techniques presented will find use in fixed and rotary wing aircraft analysis. Author

N89-19252*# National Aeronautics and Space Administration. Langley Research Center, Hampton, VA.
UNSTEADY NAVIER-STOKES COMPUTATIONS OVER AIRFOILS USING BOTH FIXED AND DYNAMIC MESHES
Christopher L. Rumsey and W. Kyle Anderson *In its* Transonic Unsteady Aerodynamics and Aeroelasticity 1987, Part 2 Feb. 1989 p 375-394 (For primary document see N89-19247 12-02)
Avail: NTIS HC A17/MF A01 CSCL 01A

A finite volume implicit approximate factorization method which solves the thin layer Navier-Stokes equations was used to predict unsteady turbulent flow airfoil behavior. At a constant angle of attack of 16 deg, the NACA 0012 airfoil exhibits an unsteady periodic flow field with the lift coefficient oscillating between 0.89 and 1.60. The Strouhal number is 0.028. Results are similar at 18 deg, with a Strouhal number of 0.033. A leading edge vortex is shed periodically near maximum lift. Dynamic mesh solutions for unstalled airfoil flows show general agreement with experimental pressure coefficients. However, moment coefficients and the maximum lift value are underpredicted. The deep stall case shows some agreement with experiment for increasing angle of attack, but is only qualitatively comparable past stall and for decreasing angle of attack. Author

N89-19253*# National Aeronautics and Space Administration. Ames Research Center, Moffett Field, CA.
THE OBLIQUE-WING RESEARCH AIRCRAFT: A TEST BED FOR UNSTEADY AERODYNAMIC AND AEROELASTIC RESEARCH
Glenn B. Gilyard *In* NASA, Langley Research Center, Transonic Unsteady Aerodynamics and Aeroelasticity 1987, Part 2 Feb. 1989 p 395-414 (For primary document see N89-19247 12-02)
Avail: NTIS HC A17/MF A01 CSCL 01A

The advantages of oblique wings have been the subject of numerous theoretical studies, wind tunnel tests, low speed flight models, and finally a low speed manned demonstrator, the AD-1. The specific objectives of the OWRA program are: (1) to establish the necessary technology base required to translate theoretical and experimental results into practical mission oriented designs; (2) to design, fabricate and flight test an oblique wing aircraft throughout a realistic flight envelope, and (3) to develop and validate design and analysis tools for asymmetric aircraft configurations. The preliminary design phase of the project is complete and has resulted in a wing configuration for which construction is ready to be initiated. Author

N89-19254*# Purdue Univ., West Lafayette, IN.
STATIC AEROELASTICITY OF A COMPOSITE OBLIQUE WING IN TRANSONIC FLOWS
Jonathan D. Bohlmann *In* NASA, Langley Research Center, Transonic Unsteady Aerodynamics and Aeroelasticity 1987, Part 2 Feb. 1989 p 415-425 (For primary document see N89-19247 12-02)
Avail: NTIS HC A17/MF A01 CSCL 01A

One aircraft configuration that shows great promise in achieving high performance is that of an asymmetrically swept wing. When compared to conventional swept wings, these advantages include higher lift to drag ratios and reduced takeoff and landing speeds, which translate into greater performance in terms of fuel comsumption, loiter time, and range. However, the oblique wing has a number of disadvantages because of its asymmetric configuration. The question is how to best achieve maximum stability and roll equilibrium without compromising performance. Using aeroelastic tailoring to enhance aeroelastic stability and control has been demonstrated in several analyses, especially for the forward swept wing. The advantages and disadvantages for the oblique wing configuration are discussed. Author

N89-19255*# National Aeronautics and Space Administration. Langley Research Center, Hampton, VA.
INVESTIGATION AND SUPPRESSION OF HIGH DYNAMIC RESPONSE ENCOUNTERED ON AN ELASTIC SUPERCRITICAL WING
David A. Seidel, William M. Adams, Jr., Clinton V. Eckstrom, and Maynard C. Sandford *In its* Transonic Unsteady Aerodynamics and Aeroelasticity 1987, Part 2 Feb. 1989 p 427-448 (For primary document see N89-19247 12-02)
Avail: NTIS HC A17/MF A01 CSCL 01A

The DAST Aeroelastic Research Wing had been previously in the NASA Langley TDT and an unusual instability boundary was predicted based upon supercritical response data. Contrary to the predictions, no instability was found during the present test. Instead a region of high dynamic wing response was observed which reached a maximum value between Mach numbers 0.92 and 0.93. The amplitude of the dynamic response increased directly with dynamic pressure. The reponse appears to be related to chordwise shock movement in conjunction with flow separation and reattachment on the upper and lower wing surfaces. The onset of flow separation coincided with the occurrence of strong shocks on a surface. A controller was designed to suppress the wing response. The control law attenuated the response as compared

with the uncontrolled case and added a small but significant amount of damping for the lower density condition. Author

N89-19256*# General Dynamics Corp., Fort Worth, TX.
THE ROLE OF SHOCK INDUCED TRAILING-EDGE SEPARATION IN LIMIT CYCLE OSCILLATIONS
Atlee M. Cunningham, Jr. *In* NASA, Langley Research Center, Transonic Unsteady Aerodynamics and Aeroelasticity 1987, Part 2 Feb. 1989 p 449-462 (For primary document see N89-19247 12-02)
(Contract NAS4-2577)
Avail: NTIS HC A17/MF A01 CSCL 01A

The potential role of shock induced trailing edge separation (SITES) in limit cycle oscillations (LCO) was established. It was shown that the flip-flop characteristics of transition to and from SITES as well as its hysteresis could couple with wing modes with torsional motion and low damping. This connection led to the formulation of a very simple nonlinear math model using the linear equations of motion with a nonlinear step forcing function with hysteresis. A finite difference solution with time was developed and calculations were made for the F-111 TACT were used to determine the step forcing function due to SITES transition. Since no data were available for the hysteresis, a parameter study was conducted allowing the hysteresis effect to vary. Very small hysteresis effects, which were within expected bounds, were required to obtain reasonable response levels that essentially agreed with flight test results. Also in agreement with wind tunnel tests, LCO calculations for the 1/6 scale F-111 model showed that the model should have not experienced LCO. Author

N89-19257*# National Aeronautics and Space Administration. Langley Research Center, Hampton, VA.
INITIAL APPLICATION OF CAP-TSD TO WING FLUTTER
Herbert J. Cunningham, Robert M. Bennett, and John T. Batina *In its* Transonic Unsteady Aerodynamics and Aeroelasticity 1987, Part 2 Feb. 1989 p 463-475 (For primary document see N89-19247 12-02)
Avail: NTIS HC A17/MF A01 CSCL 01A

The initial application of the CAP-TSD computer program for wing flutter analysis is presented. Computational Aeroelasticity Program - Transonic Small Disturbance (CAP-TSD) is based on an approximate factorization (AF) algorithm that is stable and efficient on supercomputers with vector arithmetic. CAP-TSD was used to calculate steady and unsteady pressures on wings and configurations at subsonic, transonic, and supersonic Mach numbers. However, the CAP-TSD code has been developed primarily for aeroelastic analysis. The initial efforts for validation of the aeroelastic analysis capability is presented. The initial applications include two series of symmetric, planar wing planforms. Well defined modal properties are available for these wings. In addition, transonic flutter boundaries are available for evaluation of the transonic capabilities of CAP-TSD. Author

N89-19258*# Princeton Univ., NJ.
TRANSONIC FLUTTER CALCULATIONS USING THE EULER EQUATIONS
Oddvar O. Bendiksen and Kenneth A. Kousen *In* NASA, Langley Research Center, Transonic Unsteady Aerodynamics and Aeroelasticity 1987, Part 2 Feb. 1989 p 477-491 (For primary document see N89-19247 12-02)
Avail: NTIS HC A17/MF A01 CSCL 01A

In transonic flutter problems where shock motion plays an important part, it is believed that accurate predictions of the flutter boundaries will require the use of codes based on the Euler equations. Only Euler codes can obtain the correct shock location and shock strength, and the crucially important shock excursion amplitude and phase lag. The present study is based on the finite volume scheme developed by Jameson and Venkatakrishnan for the 2-D unsteady Euler equations. The equations are solved in integral form on a moving grid. The variable are pressure, density, Cartesian velocity components, and total energy. Author

N89-19259*# National Aeronautics and Space Administration. Langley Research Center, Hampton, VA.
UNSTEADY PRESSURE MEASUREMENTS ON A SUPERCRITICAL AIRFOIL AT HIGH REYNOLDS NUMBERS
R. W. Hess *In its* Transonic Unsteady Aerodynamics and Aeroelasticity 1987, Part 2 Feb. 1989 p 493-517 (For primary document see N89-19247 12-02)
Avail: NTIS HC A17/MF A01 CSCL 01A

Steady and unsteady pressures were measured on a 14 percent supercritical airfoil at transonic Mach numbers at Reynolds numbers from 6,000,000 to 35,000,000. Instrumentation techniques were developed to measure unsteady pressures in a cryogenic tunnel at flight Reynolds numbers. Experimental steady data, corrected for wall effects show very good agreement with calculations from a full potential code with an interacted boundary layer. The steady and unsteady pressures both show a shock position that is dependent on Reynolds number. For a supercritical pressure distribution at a chord Reynolds number of 35,000,000 laminar flow was observed between the leading edge and the shock wave at 45 percent chord. Author

N89-19260*# United Technologies Research Center, East Hartford, CT.
AIRFOIL STALL PENETRATION AT CONSTANT PITCH RATE AND HIGH REYNOLDS NUMBER
Peter F. Lorber and Franklin O. Carta *In* NASA, Langley Research Center, Transonic Unsteady Aerodynamics and Aeroelasticity 1987, Part 2 Feb. 1989 p 519-542 (For primary document see N89-19247 12-02)
Avail: NTIS HC A17/MF A01 CSCL 01A

The model wing consists of a set of fiberglass panels mounted on a steel spar that spans the 8 ft test section of the UTRC Large Subsonic Wind Tunnel. The first use of this system was to measure surface pressures and flow conditions for a series of constant pitch rate ramps and sinusoidal oscillations a Mach number range, a Reynolds number range, and a pitch angle range. It is concluded that an increased pitch rate causes stall events to be delayed, strengthening of the stall vortex, increase in vortex propagation, and increase in unsteady airloads. The Mach number range causes a supersonic zone near the leading edge, stall vortex to be weaker, and a reduction of unsteady airloads. Author

N89-19261*# National Aeronautics and Space Administration. Langley Research Center, Hampton, VA.
EXPERIMENTAL TRANSONIC STEADY STATE AND UNSTEADY PRESSURE MEASUREMENTS ON A SUPERCRITICAL WING DURING FLUTTER AND FORCED DISCRETE FREQUENCY OSCILLATIONS
Douglas S. Piette (Lockheed-Georgia Co., Atlanta.) and Frank W. Cazier, Jr. *In its* Transonic Unsteady Aerodynamics and Aeroelasticity 1987, Part 2 Feb. 1989 p 543-570 (For primary document see N89-19247 12-02)
Avail: NTIS HC A17/MF A01 CSCL 01A

Present flutter analysis methods do not accurately predict the flutter speeds in the transonic flow region for wings with supercritical airfoils. Aerodynamic programs using computational fluid dynamic (CFD) methods are being developed, but these programs need to be verified before they can be used with confidence. A wind tunnel test was performed to obtain all types of data necessary for correlating with CFD programs to validate them for use on high aspect ratio wings. The data include steady state and unsteady aerodynamic measurements on a nominal stiffness wing and a wing four times that stiffness. There is data during forced oscillations and during flutter at several angles of attack, Mach numbers, and tunnel densities. Author

N89-19262*# National Aeronautics and Space Administration. Lewis Research Center, Cleveland, OH.
TURBOMACHINERY AEROELASTICITY AT NASA LEWIS RESEARCH CENTER **c07**
Krishna Rao V. Kaza *In* NASA, Langley Research Center, Transonic Unsteady Aerodynamics and Aeroelasticity 1987, Part 2

Feb. 1989 p 571-603 (For primary document see N89-19247 12-02)
Avail: NTIS HC A17/MF A01 CSCL 21E

The turbomachinery aeroelastic effort is focused on unstalled and stalled flutter, forced response, and whirl flutter of both single rotation and counter rotation propfans. It also includes forced response of the Space Shuttle Main Engine (SSME) turbopump blades. Because of certain unique features of propfans and the SSME turbopump blades, it is not possible to directly use the existing aeroelastic technology of conventional propellers, turbofans or helicopters. Therefore, reliable aeroelastic stability and response analysis methods for these propulsion systems must be developed. The development of these methods for propfans requires specific basic technology disciplines, such as 2-D and 3-D steady and unsteady aerodynamic theories in subsonic, transonic and supersonic flow regimes; modeling of composite blades; geometric nonlinear effects; and passive and active control of flutter and response. These methods are incorporated in a computer program, ASTROP. The program has flexibility such that new and future models in basic disciplines can be easily implemented. Author

N89-19263*# United Technologies Research Center, East Hartford, CT.
UNSTEADY AERODYNAMICS OF BLADE ROWS **c07**
Joseph M. Verdon *In* NASA, Langley Research Center, Transonic Unsteady Aerodynamics and Aeroelasticity 1987, Part 2 Feb. 1989 p 605-630 (For primary document see N89-19247 12-02)
Avail: NTIS HC A17/MF A01 CSCL 21E

The requirements placed on an unsteady aerodynamic theory intended for turbomachinery aeroelastic or aeroacoustic applications are discussed along with a brief description of the various theoretical models that are available to address these requirements. The major emphasis is placed on the description of a linearized inviscid theory which fully accounts for the affects of a nonuniform mean or steady flow on unsteady aerodynamic response. Although this linearization was developed primarily for blade flutter prediction, more general equations are presented which account for unsteady excitations due to incident external aerodynamic disturbances as well as those due to prescribed blade motions. The motivation for this linearized unsteady aerodynamic theory is focused on, its physical and mathematical formulation is outlined and examples are presented to illustrate the status of numerical solution procedures and several effects of mean flow nonuniformity on unsteady aerodynamic response. Author

N89-19264*# National Aeronautics and Space Administration. Langley Research Center, Hampton, VA.
COMPUTATIONAL AEROELASTICITY CHALLENGES AND RESOURCES
John W. Edwards *In its* Transonic Unsteady Aerodynamics and Aeroelasticity 1987, Part 2 Feb. 1989 p 631-637 (For primary document see N89-19247 12-02)
Avail: NTIS HC A17/MF A01 CSCL 01A

In the past decade, there has been much activity in the development of computational methods for the analysis of unsteady transonic aerodynamics about airfoils and wings. Significant features are illustrated which must be addressed in the treatment of computational transonic unsteady aerodynamics. The flow regimes for an aircraft on a plot of lift coefficient vs. Mach number are indicated. The sequence of events occurring in air combat maneuvers are illustrated. And further features of transonic flutter are illustrated. Also illustrated are several types of aeroelastic response which were encountered and which offer challenges for computational methods. The four cases illustrate problem areas encountered near the boundaries of aircraft envelopes, as operating condition change from high speed, low angle conditions to lower speed, higher angle conditions. Author

N89-19265*# National Aeronautics and Space Administration. Lewis Research Center, Cleveland, OH.
WIND-TUNNEL RESULTS OF ADVANCED HIGH-SPEED PROPELLERS AT TAKEOFF, CLIMB, AND LANDING MACH NUMBERS
George L. Stefko and Robert J. Jeracki Nov. 1985 51 p (NASA-TM-87030; E-2417; NAS 1.15:87030) Avail: NTIS HC A04/MF A01 CSCL 01A

Low-speed wind-tunnel performance tests of two advanced propellers have been completed at the NASA Lewis Research Center as part of the NASA Advanced Turboprop Program. The 62.2 cm (24.5 in.) diameter adjustable-pitch models were tested at Mach numbers typical of takeoff, initial climbout, and landing speeds (i.e., from Mach 0.10 to 0.34) at zero angle of attack in the NASA Lewis 10 by 10 Foot Supersonic Wind Tunnel. Both models had eight blades and a cruise-design-point operating condition of Mach 0.80, and 10.668 km (35,000 ft) I.S.A. altitude, a 243.8 m/s (800 ft/sec) tip speed, and a high power loading of 301 kW/sq m (37.5 shp/sq ft). Each model had its own integrally designed area-ruled spinner, but used the same specially contoured nacelle. These features reduced blade-section Mach numbers and relieved blade-root choking at the cruise condition. No adverse or unusual low-speed operating conditions were found during the test with either the straight blade SR-2 or the 45 deg swept SR-3 propeller. Typical efficiencies of the straight and 45 deg swept propellers were 50.2 and 54.9 percent, respectively, at a takeoff condition of Mach 0.20 and 53.7 and 59.1 percent, respectively, at a climb condition of Mach 0.34. Author

N89-19266*# National Aeronautics and Space Administration. Langley Research Center, Hampton, VA.
TWO EXPERIMENTAL SUPERCRITICAL LAMINAR-FLOW-CONTROL SWEPT-WING AIRFOILS
Dennis O. Allison and J. Ray Dagenhart Feb. 1987 24 p (NASA-TM-89073; NAS 1.15:89073) Avail: NTIS HC A03/MF A01 CSCL 01A

Two supercritical laminar-flow-control airfoils were designed for a large-chord swept-wing experiment in the Langley 8-Foot Transonic Pressure Tunnel where suction was provided through most of the model surface for boundary-layer control. The first airfoil was derived from an existing full-chord laminar airfoil by extending the trailing edge and making changes in the two lower-surface concave regions. The second airfoil differed from the first one in that it was designed for testing without suction in the forward concave region of the lower surface. Differences between the first airfoil and the one from which it was derived as well as between the first and second airfoils are discussed. Airfoil coordinates and predicted pressure distributions for the design normal Mach number of 0.755 and section lift coefficient of 0.55 are given for the three airfoils. Author

N89-19267# National Research Council of Canada, Ottawa (Ontario).
USE OF RIBLETS TO OBTAIN DRAG REDUCTION ON AIRFOILS AT HIGH REYNOLDS NUMBER FLOWS
M. Khalid Aug. 1988 26 p (AD-A201485; NRC-29459; NAE-AN-53) Avail: NTIS HC A03/MF A01 CSCL 01A

An investigation was carried out to study the drag reduction capabilities of riblets (commercially available) when installed on a supercritical airfoil which was aerodynamically tested in the NAE's High Reynolds Number 2 D Test Facility. The flow conditions in this test ranged from M = 0.15 to M = 0.76, and Re/ft = 1.5 million to Re/ft = 8 million. The airfoil with riblets exhibited less drag than a completely turbulent air foil (without riblets) for Mach Number M less than or = 0.5 and Reynolds Numbers Re/ft less than or = 5 million. It was found that the thinner riblets material (0.0013) gave more attractive drag results than the thicker riblets (0.0030). However, at higher Mach numbers Reynolds number no drag reduction was observed. GRA

N89-19268# Naval Postgraduate School, Monterey, CA.
A DATA ANALYSIS SYSTEM FOR UNSTEADY TURBULENCE MEASUREMENTS M.S. Thesis
Donald K. Johnson Sep. 1988 238 p
(AD-A201662) Avail: NTIS HC A11/MF A01 CSCL 20D

A data analysis system has been developed to analyze unsteady turbulence measurements obtained in the boundary layer of an airfoil subjected to periodic turbulent pulse disturbances such as a propeller slipstream. Specific algorithms for analyzing the non-stationary data are identified, developed and implemented. Where alternate algorithms are developed, each is evaluated and the best method is recommended based on specific criteria. The statistical parameters used to characterize the unsteady turbulent boundary layer include the non-stationary mean velocity, turbulence intensity, power spectral density and the autocorrelation and cross correlation functions. Since the data is periodic, both ensemble averaging and special non-stationary empirical model techniques are employed. Each of the algorithms has been implemented in the FORTRAN language and examples are presented using representative test case data. GRA

N89-19269 Virginia Polytechnic Inst. and State Univ., Blacksburg.
A VORTEX PANEL METHOD FOR POTENTIAL FLOWS WITH APPLICATIONS TO DYNAMICS AND CONTROLS Ph.D. Thesis
Curtis Paul Mracek 1988 313 p
Avail: Univ. Microfilms Order No. DA8825335

A general nonlinear, nonplanar unsteady vortex panel method for potential flow is developed. The surface is modeled as a collection of triangular elements on which the vorticity vector is piecewise linearly varying. The wake emanates from the sides and trailing edges of the thin lifting surfaces and is modeled as a progressively formed collection of vortex filaments. This model provides a continuous pressure distribution on the surface while allowing the wake to roll up as tightly as needed. The wake position is determined as part of the solution and no prior knowledge of the position or strength is assumed. An adaptive grid technique is used to redistribute the circulation of the vortex filaments of the wake as the wake sheet spreads. The aerodynamic model is coupled with dynamic equations of motion. Forced oscillation tests are conducted on flat rectangular and delta wings. Dynamic tests are performed to predict wing rock of a slender delta wing restricted to one degree of freedom in roll. The aerodynamic/dynamic model is coupled with control laws that govern the motion of flaperons so that a prescribed pitch motion is executed and wing rock is suppressed. Dissert. Abstr.

N89-19270 Florida Univ., Gainesville.
NUMERICAL SIMULATION OF THE AERODYNAMICS OF TURBULENT TRANSONIC FLOW PAST A PROJECTILE Ph.D. Thesis
Nae-Haur Eric Shiau 1987 144 p
Avail: Univ. Microfilms Order No. DA8817854

Steady, transonic flow over a projectile was numerically investigated to gain insight and understanding of the thin-layer Navier-Stokes approximation and to assess the relative importance of viscous effects on the aerodynamic forces acting on a projectile at transonic speeds. The turbulence model used in the computation is an algebraic two-layer eddy viscosity turbulence model proposed by Baldwin and Lomax. The projectile model considered was a secant ogive-cylinder boattail configuration for which accurate surface pressure measurements are available to assess the numerical results. The sensitivity of the numerical scheme to the grid resolution and added numerical dissipation terms was investigated. The surface shear stress distribution has also been computed to aid in identifying regions of the reversed flow. The computed results, based on a grid system generated by a set of hyperbolic partial differential equations, were verified by comparing with experimental measurements. Good agreement between the numerical results and measured data indicates that the numerical scheme can predict the essential features of the flow field. The calculated results obtained at zero angle of attack and Mach number 0.91 show that the viscous drag is as important as the pressure drag (no base drag). However, the relative importance of viscous drag decreases with increasing Mach number and angle of attack. At 10 and 45 degrees angle of attack, the viscous forces had a negligible effect on both the lift force and the pitching moment. Author

N89-19271 California Inst. of Tech., Pasadena.
TIP VORTICES: SINGLE PHASE AND CAVITATING FLOW PHENOMENA Ph.D. Thesis
Sheldon Isaiah Green 1988 200 p
Avail: Univ. Microfilms Order No. DA8820949

The tip vortex shed by several rectangular planform wings, fitted with three different tips, was studied in a water tunnel. Four techniques were employed to examine the tip vortex: surface flow visualization to reveal the early stages of vortex rollup; double pulsed holography of buoyant, Lagrangian particle tracers for detailed tangential and axial velocity data around the vortex core; holograms were also a source of instantaneous core structure information; tailored air bubble, non-intrusive, measurement of the average and transient vortex core pressure; and direct observation of vortex cavitation. Dissert. Abstr.

N89-19272 Delaware Univ., Newark.
COMPUTATIONAL STUDY OF INCOMPRESSIBLE TURBULENT FLOW OVER A SWEPT REARWARD-FACING STEP Ph.D. Thesis
Robert Marshall Hartman 1988 258 p
Avail: Univ. Microfilms Order No. DA8824209

A computational study of a special case of three-dimensional, subsonic turbulent flow over a swept rearward-facing step is presented. This flow encompases the significant characteristics of separating and reattaching flows. A finite-difference computer code, requiring minimum input information has been developed and is used to investigate the flow. The code utilizes a two-layered eddy viscosity model which has been modified to account for the presence of the vertical wall and for flow reattachment. The wall shear stress used in the turbulent model is calculated by way of a new nonlinear numerical boundary function for wall vorticity. Predicted results are compared to measured results for a flat plate, rearward-facing step, and a swept rearward-facing step, with reasonable results. The effects of sweep angle on reattachment length are presented for two step heights. Additionally, the crossflow velocity profiles (i.e., flow parallel to the vertical wall of the step) are computed and presented for the flow in the recirculation region. The results indicate that reattachment length, in terms of step heights, decreases with sweep angle and step height. The latter finding is in conflict with the limited experimental data available. A brief history of turbulent modeling is included along with an extended review and bibliography of related experimental and computational research. The listing of the computer code with a sample output is included in the appendix. Author

N89-19273 Old Dominion Univ., Norfolk, VA.
A STUDY OF FLOW SEPARATION IN TRANSONIC FLOW USING INVISCID AND VISCOUS CFD SCHEMES Ph.D. Thesis
James Andrew Rhodes 1988 220 p
Avail: Univ. Microfilms Order No. DA8823958

A comparison of flow separation in transonic flows is made using various computational schemes which solve the Euler and the Navier-Stokes equations of fluid mechanics. The flows examined are computed using several simple two-dimensional configurations including a backward facing step and a bump in a channel. Comparison of the results obtained using shock fitting and flux vector splitting methods are presented and the results obtained using the Euler codes are compared to results on the same configurations using a code which solves the Navier-Stokes equations. Dissert. Abstr.

N89-19274# Texas Univ., Arlington.
EXPERIMENTAL SIMULATION OF TRANSONIC VORTEX-AIRFOIL INTERACTIONS Final Report, 1 Aug. 1984 - 31 Aug. 1988

Donald R. Wilson and Donald D. Seath 31 Oct. 1988 50 p
(Contract DAAG29-84-K-0131)
(AD-A201934; ARO-21346.4-EG) Avail: NTIS HC A03/MF A01 CSCL 01A

Results from an experimental investigation of helicopter rotor blade-vortex interaction (BVI) phenomena at transonic Mach numbers and at Reynolds numbers representative of actual helicopter flight operations are presented. The study examined both perpendicular (vortex core perpendicular to the blade leading edge) and parallel (vortex core parallel to blade leading edge) interaction geometries. The significant results are: (1) Perpendicular Interaction: The effect of the vortex causes a large reduction in upper surface pressure distribution (lift increase). This lift increase correlates with strength of the vortex and closeness of the vortex encounter. The interaction is most pronounced near the leading edge of the airfoil. A large spanwise deflection of the vortex is observed as it passes over the airfoil. (2) Parallel Interaction: A similar reduction in upper surface pressure distribution is also observed during the transient passage of the parallel vortex over the airfoil. Like the perpendicular interaction, this effect is also most pronounced near the leading edge, which is in contrast to the general results of numerous CFD simulations. For certain combinations of vortex strength and encounter distance, a class-C shock motion (forward propagation of the airfoil shock wave) was observed. GRA

N89-19275# General Dynamics Corp., Fort Worth, TX.
UNSTEADY LOW-SPEED WIND TUNNEL TEST OF A STRAKED DELTA WING, OSCILLATING IN PITCH. PART 2: PLOTS OF STEADY AND ZEROTH AND FIRST HARMONIC UNSTEADY PRESSURE DISTRIBUTIONS Final Report, Jun. 1985 - Aug. 1987
A. M. Cunningham, Jr., R. G. denBoer, C. S. G. Dogger, E. G. M. Guerts, A. J. Persoon, A. P. Retel, and R. J. Zwaan (National Aerospace Lab., Amsterdam, Netherlands) Apr. 1988 309 p
(Contract F33615-85-C-3013)
(AD-A201936; AFWAL-TR-87-3098-Pt-2) Avail: NTIS HC A14/MF A01 CSCL 01A

Results of a wind tunnel test of an oscillating straked wing are given. The report provides unsteady airloads and pressure distributions for a range of incidences (-8 to 50 deg.) and amplitudes (1 to 16 deg.). The wind speed was 80 meters/second, which provided reduced frequencies up to 0.50 based on root chord. The zeroth and first harmonic as well as the continuous time history of the pressure and overall loads were measured. Flow visualization was performed for flow of 30 meters/second using a pulsating laser light sheet. The plots of the pressure distributions included in this part are presented in the order of the run numbers. Tables 4 and 5 in part 1 provide a convenient cross reference of conditions and run numbers. All steady test cases which were covered in table 4 of part 1 are presented in appendix B for runs up to no. 674. All runs presented in this part relate to the test conditions of 80 m/s windspeed and zero sideslip. GRA

N89-19276# Naval Surface Warfare Center, Dahlgren, VA.
DRAG COEFFICIENTS FOR IRREGULAR FRAGMENTS Final Report
Frank McCleskey Feb. 1988 111 p
(AD-A201943; NSWC-TR-87-89) Avail: NTIS HC A06/MF A01 CSCL 20D

Drag coefficients for irregular fragments were determined for 96 fragments in a vertical wind tunnel at Mach numbers of approximately 0.1. Correlation of drag coefficient with the maximum-to-average presented area ratio is presented. A method for approximating the whole drag curve is also given. Physical characteristics, photos, and wind tunnel test results are given in the appendixes. GRA

N89-19277# Ballistic Research Labs., Aberdeen Proving Ground, MD.
NUMERICAL COMPUTATIONS OF TRANSONIC CRITICAL AERODYNAMIC BEHAVIOR
Jubaraj Sahu Dec. 1988 38 p
(AD-A202412; BRL-TR-2962) Avail: NTIS HC A03/MF A01 CSCL 20D

The determination of aerodynamic coefficients by shell designers is a critical step in the development of any new projectile design. Of particular interest is the determination of the aerodynamic coefficients at transonic speeds. It is in this speed regime that the critical aerodynamic behavior occurs and a rapid change in the aerodynamic coefficients is observed. Three-dimensional transonic flow field computations over projectiles have been made using an implicit, approximately factored, partially flux-split algorithm. A composite grid scheme has been used to provide the increased grid resolution needed for accurate numerical simulation of three-dimensional transonic flows. Details of the asymmetrically located shockwaves on the projectiles have been determined. Computed surface pressures have been compared with experimental data and are found to be in good agreement. The pitching moment coefficient, determined from the computed flow fields, shows the critical aerodynamic behavior observed in free flights. GRA

N89-19278# Royal Inst. of Tech., Stockholm (Sweden). Dept. of Aeronautics.
TWO-DIMENSIONAL TEST SECTION WITH PREADJUSTED ADAPTIVE WALLS FOR LOW SPEED WIND TUNNEL
F. Khadjavi Oct. 1987 17 p
(KTH-Aero-Rept-57; TRITA-FPT-051; ISSN-0280-1078) Avail: NTIS HC A03/MF A01

Some relevant methods for reducing or eliminating the wall interference effects in wind tunnels are mentioned. A calculation method was suggested for a preadjusted adaptive wall test section. Some different arrangements for a contraction - transition - test section - transition - diffuser configuraton were discussed. The effects of test section height and length on the model were investigated. Author

03 AIR TRANSPORTATION AND SAFETY

Includes passenger and cargo air transport operations; and aircraft accidents.

For related information see also *16 Space Transportation* and *85 Urban Technology and Transportation.*

N89-19279# Defence and Civil Inst. of Environmental Medicine, Downsview (Ontario).
POSITIVE FLOTATION HARNESS (PFH) FOR USE BY CANADIAN FORCES SEARCH AND RESCUE TECHNICIANS
James A. Firth and Jean C. Steffler May 1988 40 p
(AD-A200727; DCIEM-88-TR-27) Avail: NTIS HC A03/MF A01 CSCL 23E

At the request of Maritime Air Group Headquarters Halifax, National Defence Headquarters (NDHQ) tasked the Medical Life Support Division (MLSD) of this Institute (DCIEM) to research and develop a flotation system for the Canadian Forces Safety Restraint Harness, Rescue Specialist (Double Lift Harness). The system should provide sufficient independent buoyancy for the wearer to conduct water rescue exercises without relying on the use of a life preserver. Utilizing unicellular foam for buoyancy, MLSD designed four prototype flotation systems over a period of four years, for operational evaluations (OPVAL) by Helicopter Squadrons 406, 423, 443, and the Diving Team of Canadian Forces Base Shearwater, Nova Scotia. Initial test results revealed deficiencies which were rectified by MLSD, based on operator recommendations. The last prototype evaluation concluded that the tested flotation system had sufficient buoyancy to keep two persons afloat, was a suitable replacement for the Double Lift Harness/Jacket Lifesaving Combination and recommended that production models be acquired for the CH124A Helicopter fleet. A Canadian Aerospace Company is now finalizing fabrication of 70 flotation vests with inherent buoyancy and MLSD has submitted a

draft Canadian Forces Modification Instruction detailing the interface of the vest and Double Lift Harness to NDHQ. GRA

N89-19280# Boeing Advanced Systems Co., Seattle, WA.
HYPERVELOCITY TECHNOLOGY ESCAPE SYSTEM CONCEPTS. VOLUME 1: DEVELOPMENT AND EVALUATION Final Report, Oct. 1986 - Jan. 1988
A. K. Trikha, P. C. Chen, and S. F. Sielaff Jul. 1988 283 p
(Contract F33615-86-C-3410)
(AD-A201719; AFWAL-TR-88-3044-Vol-1) Avail: NTIS HC A13/MF A01 CSCL 01C

This report describes the results of a study conducted to develop crew escape system concepts for hypervelocity vehicles capable of transatmospheric missions. These escape system concepts were required to provide survivable escape and recovery throughout all phases of flight, including launch, upper atmospheric hypervelocity flight, orbit, reentry and terminal approach. The effort was divided into three tasks. In task 1, 16 different concepts were studied to evaluate the feasibility of their meeting all the crew escape and protection requirements. The study vehicles included a horizontally launched vehicle with dual place cockpit and a vertically-launched vehicle with a single place cockpit. Only 3 of 16 concepts were determined to be viable options. A preliminary evaluation reduced the possible escape system candidates to two; an encapsulated seat with thermal protection and an escape capsule with thermal protection. In task 2, various advanced technologies were investigated for possible application to the HVT crew escape concepts design development. These technologies included aerodynamics, thermal protection, propulsion, structures, materials, flight controls, sensors, crew station design, and life support. The results from this technology evaluation were used to refine the subsystem designs during task 3, so that the design requirements were satisfied with minimum penalties to the vehicles. Trade studies were then conducted to select the best escape system concepts. GRA

N89-19281# Boeing Advanced Systems Co., Seattle, WA.
HYPERVELOCITY TECHNOLOGY ESCAPE SYSTEM CONCEPTS. VOLUME 2: SOFTWARE MANUAL Final Report, Oct. 1986 - Jan. 1988
A. K. Trikha and P. C. Chen Jul. 1988 114 p
(Contract F33615-86-C-3410)
(AD-A201720; AFWAL-TR-88-3044-Vol-2) Avail: NTIS HC A06/MF A01 CSCL 01C

This report documents the software developed during the Hypervelocity Technology Escape System Concepts program for dynamic simulation and display of various escape system concepts. It contains a description of the new EASY5 component subroutines and the model file used for analysis. The description includes associated mathematical background, flowcharts, input/output variables, and source code listings. The data used to generate the graphic models of the selected escape concepts are also provided. GRA

N89-19282# Deutsche Forschungs- und Versuchsanstalt fuer Luft- und Raumfahrt, Cologne (Germany, F.R.). Hauptabteilung Verkehrforschung.
SIMULTANEOUS THREE-DIMENSIONAL MODELING OF COMMERCIAL FLIGHTS WITHIN THE AIRSPACE OF THE FEDERAL REPUBLIC OF GERMANY
Hanns-Juergen Peters Oct. 1987 307 p In GERMAN; ENGLISH summary
(DFVLR-FB-88-31; ISSN-0171-1342; ETN-89-93970) Avail: NTIS HC A14/MF A01; DFVLR, VB-PL-DO, Postfach 90 60 58, 5000 Cologne, Federal Republic of Germany, 91.50 deutsche marks

A model is set up to simulate commercial flights in 4-D mode. Basic data are standard flight tracks of German domestic flights; altitudes included range up to FL 630. For simulation runs, flight times and profiles are derived both from real flights and departure times, and fly-over times of the Berlin gates. Aircraft movements are simulated with respect to airways, departure and arrival routes, air traffic control areas, starts, and landings. Conflicts arise in the case of too short distances to other aircraft. They are solved depending on flight attitude, e.g., en route state by changing the flight level, or by holding procedures if an aircraft cannot be sequenced for final approach. The simulation is carried out for 465 domestic flights per day. Results are given for defined model segments, for number of conflicts, distribution, and type of solution. ESA

N89-19832*# National Aeronautics and Space Administration. Hugh L. Dryden Flight Research Facility, Edwards, CA.
APPLICATION OF FLIGHT SYSTEMS METHODOLOGIES TO THE VALIDATION OF KNOWLEDGE-BASED SYSTEMS
Eugene L. Duke *In* NASA. Lyndon B. Johnson Space Center, 2nd Annual Workshop on Space Operations Automation and Robotics (SOAR 1988) Nov. 1988 p 107-121 Previously announced as N88-25207 (For primary document see N89-19817 12-59)
Avail: NTIS HC A22/MF A01 CSCL 01C

N89-19858*# Air Force Wright Aeronautical Labs., Wright-Patterson AFB, OH.
LIGHT WEIGHT ESCAPE CAPSULE FOR FIGHTER AIRCRAFT
James A. Robert *In* NASA. Lyndon B. Johnson Space Center, 2nd Annual Workshop on Space Operations Automation and Robotics (SOAR 1988) Nov. 1988 p 303-307 (For primary document see N89-19817 12-59)
Avail: NTIS HC A22/MF A01 CSCL 01C

04 AIRCRAFT COMMUNICATIONS AND NAVIGATION

Includes digital and voice communication with aircraft; air navigation systems (satellite and ground based); and air traffic control.

For related information see also *17 Space Communications, Spacecraft Communications, Command and Tracking* and *Communications and Radar.*

N89-19283# Federal Aviation Administration, Washington, DC. Advanced System Design Service.
MINIMUM REQUIRED HELIPORT AIRSPACE UNDER VISUAL FLIGHT RULES Final Report
Robert D. Smith Oct. 1988 25 p
(AD-A201433; DOT/FAA/DS-88/12; DOT/FAA/AS-89/1) Avail: NTIS HC A03/MF A01 CSCL 01E

Recently, the FAA started a flight measurement project to examine the issue of minimum required VFR airspace. Test data were collected objectively in a manner similar to what is done to define the minimum airspace for a precision approach. Heliport approach and departure flight profiles were recorded using a variety of subject pilots flying several different helicopters. Data were analyzed statistically to determine the mean, standard deviation, and 6 sigma isoprobability curves. Results of this effort are documented in FAA/CT-TN87/40, Heliport Visual Approach and Departure Airspace Tests. An analysis of the statistical distribution of these data is contained in FAA/CT-TN88/44, Analysis of Distributions of VFR Heliport Data. These test reports are not likely to be the last word on this topic but they should serve to focus the discussion on specific issues in a way that is constructive. This report is intended to focus discussion on how the data should be interpreted, some of the historical issues involved, and the direction to be taken in future work. GRA

N89-19284# Naval Ocean Systems Center, San Diego, CA.
THE EFFICACY OF COLOR-CODED SYMBOLS TO ENHANCE AIR-TRAFFIC CONTROL DISPLAYS Final Report
S. V. Bemis, E. A. Winer, and J. L. Leeds Aug. 1988 39 p
(AD-A201594; NOSC-TR-1244) Avail: NTIS HC A03/MF A01 CSCL 17G

This research tested the effect of color-coded air-traffic control displays on working memory and accuracy performance. Color, as a primary code and as a redundant code, was compared with

shape coding under memory and no-memory conditions at varying density levels (5,8,11, and 14 symbols per display). In the shape-coded condition, symbol shapes denoted the altitude, or altitude and speed. All symbols had the same shape when color was used as a primary code. Only color denoted the altitude, or altitude and speed when color was tested redundantly. In the memory condition, subjects were required to remember the altitude and speed on each displayed symbol, and then sequence the planes in approach order to the landing area. Significant differences in recall accuracy occurred in the 8 and 11 symbol density displays. Compared to shape coding, color, either as a primary code or as a redundant code, significantly improved recall accuracy when altitude alone was encoded on each symbol. When both altitude and speed were encoded on each symbol, color as a redundant code significantly improved recall accuracy for the 8 and 11 symbol density levels. GRA

N89-19285# Societe Nationale Industrielle Aerospatiale, Cannes (France). Div. Systemes Strategiques et Spatiaux.
ECONOMIC ANALYSIS OF NAVSAT SYSTEM Final Report
P. Fiorito, F. Giovagnoli, C. Carnebianca, B. Pavesi, M. Britten, and T. Torkildsen Paris, France ESA Jun. 1988 279 p Prepared in cooperation with Italspazio, Rome, Italy; Racal-Decca Advanced Development Ltd., Walton-on-Thames, England; the Continental Shelf and Petroleum Technology Research Institute A/S, Trondheim, Norway; and Norges Teckniske Hoegskole, Trondhei
(Contract ESA-7112/87-S-RD(SC))
(Rept-1013-CA/TS; ESA-CR(P)-2673; IKU-88.068; ETN-89-93913) Avail: NTIS HC A13/MF A01

The relative cost of different regional coverages by NAVSAT versus global coverage was analyzed. The analysis confirms the interest of the NAVSAT system: a worldwide coverage, expensive and long to implement can be established step by step, and quickly provides important regional coverage services with limited cost. The cost of an operational service over the North Atlantic high traffic area is 24 pct of the price of an improved worldwide system. To cover North Atlantic and North Pacific the cost amounts to 26 pct. The proposed system which offers integrated navigation and communication services can provide a variety of services for aeronautical, maritime, and land applications. Wide market possibilities are expected in particular in the aeronautical field. The acceptance of the proposed system assumes international agreement. Launches with Ariane 4 lead to important launch costs and heavy and expensive satellites. Launch with other vehicles (type Delta-2, Atlas, Centaur) reduces launch costs, and allows a smaller and less expensive satellite. With Delta-2 deeper analysis to assess a dual launch possibility is suggested. ESA

N89-19286# Continental Shelf Inst., Trondheim (Norway). Sintef Group.
STUDY OF NAVSAT FOR PRECISE POSITIONING Final Report
Oystein Baltzersen, Kjell Berg (Norges Tekniske Hoegskole, Trondheim.), Borje Forssell, and Torbjorn Hals Paris, France ESA 19 Jul. 1988 81 p
(Contract ESA-7312/87-F-RD(SC))
(IKU-88.068; ESA-CR(P)-2674; ETN-89-93928) Avail: NTIS HC A05/MF A01

The usefulness of NAVSAT for high-accuracy (i.e., sub-meter) positioning, and system parameters to be modified or added to meet the requirements were examined. Measurement methods imply the use of carrier phase differences of different kinds, i.e., between-satellite, between-receiver, and between-epoch differences. The desired resolution and accuracy are given by the wavelength and the signal-to-noise ratio in the receiver, and it turns out that cm, and in some cases mm, accuracies are achievable. The most important change to the navigational version of NAVSAT is the inclusion of a continuous carrier. This is necessary because of the need for a signal without phase jumps in order to make the difference measurements feasible. For several reasons, e.g., available communication signals, a continuous carrier frequency at L-band appears to be optimum. This carrier has to be modulated by an identification signal to enable the receivers to distinguish between the different satellites. The parameters of the proposed CW signal (e.g., power, antenna gain, and frequency stability) are analyzed, and the requirements are given. Verification and test aspects of the high-accuracy system are presented. It is shown that the construction field is by far the most important one economically. ESA

N89-19287# Deutsche Forschungs- und Versuchsanstalt fuer Luft- und Raumfahrt, Brunswick (Germany, F.R.). Abteilung fuer Systemtechnik und Navigation.
EXAMINATIONS ON TERCOM NAVIGATION BY EVALUATION OF TEST FLIGHTS DONE OVER THE TESTING AREAS DEISTER AND HARZ (GERMANY, F.R.)
Franz Knabe Aug. 1988 107 p In GERMAN; ENGLISH summary
(DFVLR-FB-88-37; ISSN-0171-1342; ETN-89-93971) Avail: NTIS HC A06/MF A01; DFVLR, VB-PL-DO, Postfach 90 60 58, 5000 Cologne, Federal Republic of Germany, 29 deutsche marks

The TERCOM (Terrain Contour Matching) navigation principle which uses position information from comparison of the overflown terrain profile with an onboard stored digital terrain elevation model for updates of a basic navigation system was tested. As heading and speed errors of the basic navigation system have a negative influence on computation of model profiles, the qualities of basic navigation and TERCOM position are coupled strongly together. Systematic errors in terrain elevation measuring and the chosen comparison function influence quality of the positions. Data from test flights using a low-performance basic navigation system are assessed. Effects of terrain contour, comparison mode, sample rate, and terrain model on TERCOM position are examined. Incremental computation of trajectories allows use of arbitrary lines of flight. ESA

N89-19288# Deutsche Forschungs- und Versuchsanstalt fuer Luft- und Raumfahrt, Oberpfaffenhofen (West Germany). Inst. fuer Hochfrequenztechnik.
DESIGN OF DIGITAL FILTERS FOR NAVIGATION RECEIVERS
Joachim Willner Sep. 1988 48 p In GERMAN; ENGLISH summary
(DFVLR-Mitt-88-23; ISSN-0176-7739; ETN-89-93976) Avail: NTIS HC A03/MF A01; DFVLR, VB-PL-DO, Postfach 90 60 58, 5000 Cologne, Federal Republic of Germany, 18 deutsche marks

The bilinear transformation was used for the design of Infinite Impulse Response (IIR) filters, and for Finite Impulse Response (FIR) filter Parks/McClellan's Tschebyscheff approximation was used. The computer programs are written in IBM FORTRAN-77 and are executed in the operating system VM mode, for example on the colored graphic screen of an IBM 3278 terminal. ESA

05 AIRCRAFT DESIGN, TESTING AND PERFORMANCE

Includes aircraft simulation technology.

For related information see also *18 Spacecraft Design, Testing and Performance* and *39 Structural Mechanics*.For land transportation vehicles see *85 Urban Technology and Transportation*.

N89-19289*# Lockheed-Georgia Co., Marietta. Advanced Design Div.
MULTIPLE-PURPOSE SUBSONIC NAVAL AIRCRAFT (MPSNA) MULTIPLE APPLICATION PROPFAN STUDY (MAPS) Final Report
D. M. Winkeljohn and C. H. Mayrand Mar. 1986 88 p
(Contract NAS3-24528)
(NASA-CR-175096; NAS 1.26:175096; LG86ER0053) Avail: NTIS HC A05/MF A01 CSCL 01C

A conceptual design study compared a selected propfan-powered aircraft to a turbofan-powered aircraft for multiple Navy carrier-based support missions in the 1995 timeframe. Conventional takeoff and landing (CTOL) propfan and turbofan-powered designs and short takeoff/vertical landing

(STOVL) propfan-powered designs are presented. Ten support mission profiles were defined and the aircraft were sized to be able to perform all ten missions. Emphasis was placed on efficient high altitude loiter for Airborne Early Warning (AEW) and low altitude high speed capability for various offensive and tactical support missions. The results of the study show that the propfan-powered designs have lighter gross weights, lower fuel fractions, and equal or greater performance capability than the turbofan-powered designs. Various sensitives were developed in the study, including the effect of using single-rotation versus counter-rotation propfans and the effect of AEW loiter altitude on vehicle gross weight and empty weight. A propfan technology development plan was presented which illustrates that the development of key components can be achieved without accelerated schedules through the extension of current and planned government and civil propfan programs. Author

N89-19290# Aeronautical Research Labs., Melbourne (Australia).
AN EXAMINATION OF THE FATIGUE METER RECORDS FROM THE RAAF (ROYAL AUSTRALIAN AIR FORCE) CARIBOU FLEET
Douglas J. Sherman Jul. 1988 44 p
(AD-A201074; ARL/STRUC-TM-489; DODA-AR-005-526) Avail: NTIS HC A03/MF A01 CSCL 01C

In the early 1960's the Royal Australian Air Force ordered 25 Caribou I aircraft from the Canadian de Havilland Company. These aircraft came into service in 1964, and at the present time 21 of these aircraft are still on the register. The aircraft were all fitted with M1946 fatigue meters (Mk11), and these meters are, in general, read at the end of each flight. Since the beginning of March 1975 these fatigue meter data have been entered into a computer, and the present report is based on an analysis of the computerized data base extending from 3 March 1975 to 25 August 1984. This period includes data from just over 100 000 hours of flying - a very large data base- so the results have sufficient significance to distinguish between different gust load prediction methods. Of the various types of flying missions, type 4 (Display) is clearly more severe than all other types. At the two highest g levels, the loading frequencies are, respectively, 20 and 30 times the corresponding average frequencies for all types of flying. GRA

N89-19291# Naval Postgraduate School, Monterey, CA.
THE DESIGN AND INITIAL CONSTRUCTION OF A COMPOSITE RPV (REMOTELY PILOTED VEHICLE) FOR FLIGHT RESEARCH APPLICATIONS M.S. Thesis
H. Keith Parker Sep. 1988 100 p
(AD-A201884) Avail: NTIS HC A05/MF A01 CSCL 01C

A remotely piloted vehicle, similar to the U.S. Navy's Pioneer RPV, was designed and initial construction implemented for the purpose of establishing an RPV flight research program at the Naval Postgraduate School. The RPV will be used to investigate the Wortmann FX63-137 airfoil for low Reynolds applications, testing airborne avionic devices, investigate new aerodynamic phenomena of interest to NAVAIR, and serve as a transition trainer for future RPVs. Constructed primarily of composite materials, the vehicle will provide the opportunity to conduct real time/in-flight composite structural analysis. Additionally, the opportunity of using an RPV in their research, will provide the students of the Naval Postgraduate School with a unique capability limited to very few universities throughout the country. GRA

N89-19292# Naval Postgraduate School, Monterey, CA.
THE IMPORTANCE OF AIRCRAFT PERFORMANCE AND SIGNATURE REDUCTION UPON COMBAT SURVIVABILITY M.S. Thesis
John D. Langford, Jr. Sep. 1988 128 p
(AD-A202106) Avail: NTIS HC A07/MF A01 CSCL 17D

An investigation was conducted to estimate the relative impact the six susceptibility reduction concepts of threat warning, tactics, signature reduction, noise jammers and deceivers, expendables, and threat suppression have on aircraft survivability, with particular emphasis given to tactics with increased aircraft performance and signature reduction. An essential elements analysis (EEA) was conducted for three representative scenarios, with and without threat warning available, to identify the essential events and elements in each scenario critical to aircraft survivability. The six concepts were assessed as to their relative impact on the essential events and an estimate of the aircraft's susceptibility and survivability was made. The results of the EEAs are presented in tabular format. The general conclusion is made that both increased aircraft performance, with threat warning available, and signature reduction, with and without threat warning available, play important roles in increasing aircraft survivability through a reduction in an aircraft's susceptibility. GRA

N89-19293# Air War Coll., Maxwell AFB, AL.
RPV (REMOTE PILOTED VEHICLE) APPLICATIONS IN THE US NAVY
Maximo A. Barela and James Jackson May 1988 71 p
(AD-A202151; AU-AWC-88-052) Avail: NTIS HC A04/MF A01 CSCL 01C

This report describes the status of the U.S. Navy's remote piloted vehicle (RPV) program. It also presents numerous possible applications which exploit many of the RPV's capabilities. The author questions the aggressiveness and direction of the program and recommends that the program be modified so that it may fully exploit the RPVs' potentials. Appendices provide: (1) data on vehicle and payload capabilities of RPVs which are in current production or which are under development; and (2) a historical military perspective of the RPV from its birth to the present. GRA

N89-19294# Naval Postgraduate School, Monterey, CA.
A COMPARATIVE ANALYSIS OF TILT ROTOR AIRCRAFT VERSUS HELICOPTERS USING SIMULATOR RESULTS M.S. Thesis
Gregory K. Mislick Sep. 1988 74 p
(AD-A202190) Avail: NTIS HC A04/MF A01 CSCL 01C

This thesis conducts a comparative analysis of the tilt rotor aircraft with conventional helicopters using simulator results from LHX-representative missions. Results regarding inter-aircraft differences using Ordinary Least Squares regression analysis are discussed. Also examined are single versus dual piloted airframe configurations, cockpit designs, varied background inter-pilot differences, those transitions from the helicopter to the tilt rotor causing the most difficulties, those flight missions causing the most operator overloads, and what automated features best help relieve these workloads. Pilot opinions from a questionnaire concerning these subjects are also presented. Results show the tilt rotor superior in hard, maximum effort turns and in firing at elevated and depressed targets, while the helicopter has the advantage in lateral movements and quick hover up/hover down maneuvers. The two-man cockpit configuration is notably safer with significantly less operator overloads. Pilot differences between communities were found to be negligible in this study. GRA

N89-19295# Army Aviation Engineering Flight Activity, Edwards AFB, CA.
COMBINED PRELIMINARY AIRWORTHINESS EVALUATION AND AIRWORTHINESS AND FLIGHT CHARACTERISTICS EVALUATION OF THE UH-1H WITH PREPRODUCTION HUB SPRING AND COMPOSITE MAIN ROTOR BLADES INSTALLED Final Report, 30 Jul. 1986 - 16 Nov. 1987
Gary L. Skinner, Joseph Piotrowski, Michael E. White, Austin R. Omlie, and James D. Brown Jun. 1988 53 p
(AD-A202316; USAAEFA-84-33) Avail: NTIS HC A04/MF A01 CSCL 01C

The Army has incorporated a main rotor hub spring on the UH-1H helicopter designed to reduce large main rotor flapping angles which occur during some flight maneuvers. Composite main rotor blades (CMRB), also incorporated, are intended to increase performance and to improve reliability and survivability of the UH-1H. A preliminary airworthiness evaluation was conducted to determine suitability of the combined preproduction CMRB and

hub spring configuration for compliance with the CMRB Critical Item Development Specification (CIDS). Due to high vibration characteristics and the occurrence of cyclic control feedback contributing to loss of aircraft control associated with CMRB, additional testing was conducted for comparison with standard metal main rotor blades (STD) and composite main rotor blades constructed with production tooling (PROD CMRB). Flight testing was evaluated under a variety of operating conditions from field elevations of 2302 ft to 9980 ft. Some improvement was noted in out-of-ground effect hover performance with PROD CMRB compared to CMRB, while level flight performance of the CMRB and PROD CMRB was not significantly different. Performance improved for the PROD CMRB compared to STD, but did not meet CIDS requirements. GRA

N89-19296# Defence Research Information Centre, Orpington (England).
SHORT-RANGE ANTI-ARMOUR FLIGHT VEHICLES OF THE APACHE/CWS FAMILY
Dieter Weidenhagen Aug. 1988 21 p Transl. into ENGLISH of paper presented at the Annual Conference of the DGLR, 1984 Conference held in Hamburg, Fed. Republic of Germany, 1-3 Oct. 1984 Previously announced in IAA as A85-40338
(DRIC-T-8130; BR107730; ETN-89-93670) Copyright Avail: NTIS

Status and development of the Tornado aircraft MW-1 dispenser and submunitions are discussed. The MW-1 ejection procedure utilizes a central gas generator. The employment of a rocket motor makes it possible to reduce the width of a dispenser significantly. An ejection procedure with ejection velocities up to 75 m/sec involving the employment of MW-1 submunitions is described. Methods of using flight vehicles in anti-armor warfare; mines equipped with acoustic sensors; the modular concept of the Apache/CWS system; and conduct of missions against armored vehicles are reviewed. ESA

N89-19297# Centre d'Essais Aeronautique Toulouse (France).
LIGHTNING CAMPAIGN 85/86 TRANSALL C160 A04: FLYING TESTS Final Report [CAMPAGNE FOUDRE 85/86 TRANSALL C160 A04. ESSAIS EN VOL. PROCES-VERBAL 85/535800]
Itef M. Asselineau 25 Apr. 1988 260 p In FRENCH
(Rept-85/535800; CR-010825; ETN-89-94096) Avail: NTIS HC A12/MF A01

The results of the lightning tests performed onboard a fully equipped aircraft are presented. A total of nine lightning discharges were observed. The data show maximum intensity of 10 kA, a maximum derivative of 100 kA/microsec, an average of 0.5 kA/microsec, and a maximum duration of 320 ms. ESA

N89-19238*# National Aeronautics and Space Administration. Langley Research Center, Hampton, VA.
CAP-TSD: A PROGRAM FOR UNSTEADY TRANSONIC ANALYSIS OF REALISTIC AIRCRAFT CONFIGURATIONS
John T. Batina, David A. Seidel, Samuel R. Bland, and Robert M. Bennett *In its* Transonic Unsteady Aerodynamics and Aeroelasticity 1987, Part 1 Feb. 1989 p 63-95 (For primary document see N89-19234 12-02)
Avail: NTIS HC A12/MF A01 CSCL 01C

N89-19239*# McDonnell Aircraft Co., Saint Louis, MO.
CAP-TSD ANALYSIS OF THE F-15 AIRCRAFT
Dale M. Pitt *In* NASA, Langley Research Center, Transonic Unsteady Aerodynamics and Aeroelasticity 1987, Part 1 Feb. 1989 p 97-116 (For primary document see N89-19234 12-02)
Avail: NTIS HC A12/MF A01 CSCL 01C

N89-19859*# Air Force Wright Aeronautical Labs., Wright-Patterson AFB, OH.
CHEMICAL WARFARE PROTECTION FOR THE COCKPIT OF FUTURE AIRCRAFT
William C. Pickl *In* NASA. Lyndon B. Johnson Space Center, 2nd Annual Workshop on Space Operations Automation and Robotics (SOAR 1988) Nov. 1988 p 309-312 (For primary document see N89-19817 12-59)
Avail: NTIS HC A22/MF A01 CSCL 01C

06 AIRCRAFT INSTRUMENTATION

Includes cockpit and cabin display devices; and flight instruments.

For related information see also *19 Spacecraft Instrumentation* and *35 Instrumentation and Photography.*

N89-19298# Naval Air Test Center, Patuxent River, MD.
DEVELOPMENT OF A LOW-COST HELMET MOUNTED EYE GAZE SENSOR
Richard S. Dunn and Donna L. Haspel 27 Oct. 1988 33 p
(AD-A202303; NATC-TM-88-46-SY) Avail: NTIS HC A03/MF A01 CSCL 06D

This report documents Phase 1 of a Small Business Innovation Research (SBIR) contract for development of a low-cost helmet mounted eye gaze point sensor. The device, in completed form, is for use in laboratory, simulator, and in-flight studies by NAVAIRTESTCEN in aircraft test and evaluation projects. Numerous other potential applications in behavioral research and development would benefit from use of the device throughout the Department of Defense and in commercial and academic settings. The device produces a time history of eye gaze point information along with pupil diameter and eye-blink data. It has flexibility as a sensor system for many different modes of application. Sentient Systems Technology, Incorporated, completed design, testing, prototype hardware and software development, and functional testing of a prototype unit. The effort constituted a full feasibility demonstration in the multistage SBIR contract cycle format. Success in Phase 1 is intended to lead to follow-on contracts for engineering development and applications development or production during Phases 2 and 3. Functional demonstrations of the prototype unit with Sun Microsystems computer equipment were convincing and fully successful. A complete prototype with simplified software for operation with an IBM compatible PC system is now being evaluated for in-house applications in a behavioral test and evaluation laboratory setting. GRA

07 AIRCRAFT PROPULSION AND POWER

Includes prime propulsion systems and systems components, e.g., gas turbine engines and compressors; and onboard auxilliary power plants for aircraft.

For related information see also *20 Spacecraft Propulsion and Power, 28 Propellants and Fuels,* and *44 Energy Production and Conversion.*

N89-19299*# Hamilton Standard Div., United Aircraft Corp., Windsor Locks, CT.
LARGE-SCALE ADVANCED PROP-FAN (LAP) HUB/BLADE RETENTION DESIGN REPORT
Matthew Soule 31 Jan. 1986 77 p
(Contract NAS3-23051)
(NASA-CR-174786; NAS 1.26:174786; HSER-9247) Avail: NTIS HC A05/MF A01 CSCL 21E

The Large-scale Advanced Prop-fan (LAP) hub assembly forms a semi-rigid link between the blades, which provide the thrust, and the engine shaft, which provides the torque. The hub and tailshaft is a one piece partially forged part which is carburized, heat treated and machined. A single row ball bearing restrains each of the eight blades in the hub, while the tailshaft secures the propeller to the engine shaft with two cone seats that are preloaded against each other by the Prop-fan retaining nut. The hub also forms the support for the pitch change actuator system, the control and the spinner. The retention transmits the loads from the blades to the hub while allowing the changes in blade pitch. The single row ball bearing retention provides ease of

maintenance by allowing individual blade replacement without dissassembly of the hub. It has a through hardened inner race which seats against the aluminum blade shank and an outer race which is integral with the barrel. The outer race area is carburized to achieve the hardness necessary to support the ball loads. The balls are kept from contact with each other by a separator. The rotational speed of the propeller keeps the retention submerged in the oil which is contained in the hub by a seal. Stress and strain analysis, material hardness requirements, weight predictions, and stiffness characteristics are discussed. Author

N89-19300*# Douglas Aircraft Co., Inc., Long Beach, CA.
MULTIPLE APPLICATION PROPFAN STUDY (MAPS): ADVANCED TACTICAL TRANSPORT Final Report, Aug. 1984 - Apr. 1985
F. C. Newton, R. H. Liebeck, G. H. Mitchell, A. Mooiweer, M. M. Platte, T. L. Toogood, and R. A. Wright Mar. 1986 105 p
(Contract NAS3-24348)
(NASA-CR-175003; NAS 1.26:175003) Avail: NTIS HC A06/MF A01 CSCL 21E

This study was conducted to ascertain potential benefits of a propfan propulsion system application to a blended wing/body military tactical transport. Based on a design cruise Mach no. of 0.75 for the design mission, the results indicate a significant advantage in various figures of merit for the propfan over those of a comparable technology turbofan. Although the propfan has a 1.6 percent greater takeoff gross weight, its life cycle cost is 5.3 percent smaller, partly because of a 27 percent smaller specific fuel consumption. When employed on alternate missions, the propfan configuration offers significantly improved flexibility and capability: an increase in sea level penetration distance of more than 100 percent, or in time-on-station of 24 percent, or in deployment payload of 38 percent. Author

N89-19301# Detroit Diesel Allison, Indianapolis, IN. Allison Gas Turbine Div.
IN-LINE WEAR MONITOR Interim Report, Nov. 1985 - Jun. 1988
Keith A. Pieper and Ivor J. Taylor Sep. 1988 68 p
(Contract F33615-85-C-2537)
(AD-A201292; DDA-EDR-13632; AFWAL-TR-88-2095) Avail: NTIS HC A04/MF A01 CSCL 21E

This report describes the construction and test results of an in-line monitor for critical ferrous and nonferrous metal debris in turbine engine lubrication systems. The in-line wear monitor (ILWM) is being developed by Allison Gas Turbine Division and a subcontractor, Princeton Gamma-Tech. The system uses the X-ray fluorescence principle for detecting metal debris on a continuous basis while the engine is running. The sensor portion of the system is engine mounted and contains a radioactive X-ray source, a flow cell to direct the oil across an X-ray permeable window, a proportional counter X-ray detector and its associated preamplifier and amplifier electronics. The data acquisition electronics is mounted on the airframe and contains a microprocessor based system for inputting pulses from the sensor, classifying and counting them according to energy bands, and analyzing the data and outputting metal concentration values to the engine monitoring system. GRA

N89-19302# Rolls-Royce Ltd., Derby (England).
PROPULSION
D. J. Pickerell 15 Mar. 1988 30 p Presented at the Royal Aeronautical Society's 45th Oxford Air Transport Course, Oxford, England, Mar. 1988
(PNR90472; ETN-89-93675) Copyright Avail: NTIS HC A03/MF A01

The engine design criteria necessary to minimize direct operating costs for various types of operation are reviewed. Prospects for further reductions in fuel consumption including ultra high bypass ratio propulsion concepts are discussed. Long term prospects for second generation supersonic transport and hypersonic vehicles are described. ESA

N89-19303# Rolls-Royce Ltd., Derby (England).
THE GAS TURBINE ENGINE AND ITS CERTIFICATION
R. Stimpson 1 Jul. 1988 16 p Presented at the United Kingdom Airworthiness Course, Canterbury, England, 1 Jul. 1988
(PNR90496; ETN-89-93690) Copyright Avail: NTIS HC A03/MF A01

The joint European engine requirements, already accepted by the UK and France are described as well as the certification compliance sheet used by the manufacturer to test each requirement. The tests include a 150 hr endurance test based on 6hr cycles at the highest allowed speed and temperature. The considerable effort put into the certification, product assurance and quality control in the production of gas turbine aero engines is shown. ESA

N89-19304# Deutsche Forschungs- und Versuchsanstalt fuer Luft- und Raumfahrt, Cologne (Germany, F.R.). Inst. fuer Antriebstechnik.
THEORETICAL AND EXPERIMENTAL INVESTIGATIONS ON SHOCKS LOSSES IN TRANSONIC AXIAL FLOW COMPRESSORS Ph.D. Thesis - Technische Hochschule, Aachen
Reiner Dunker Sep. 1988 231 p In GERMAN; ENGLISH summary
(DFVLR-FB-88-38; ISSN-0171-1342; ETN-89-93972) Avail: NTIS HC A11/MF A01; DFVLR, VB-PL-DO, Postfach 90 60 58, 5000 Cologne, Federal Republic of Germany, 80 deutsche marks

Shock models to be incorporated in an off-design performance prediction method for transonic axial flow compressor stages for more accurate flow prediction were developed. The improvement of shock models used for evaluating the shock losses, especially at supercritical subsonic, but also at supersonic inflow conditions, is emphasized. The methods were verified by calculating, investigating, and analyzing the losses of compressor cascades, as well as a transonic axial flow compressor. ESA

N89-19305*# National Aeronautics and Space Administration. Lewis Research Center, Cleveland, OH.
ICING RESEARCH TUNNEL TEST OF A MODEL HELICOPTER ROTOR
Thomas L. Miller (Sverdrup Technology, Inc., Cleveland, OH.) and Thomas H. Bond 1989 14 p Proposed for presentation at the 45th Annual Forum and Technology Display, Boston, MA, 22-24 May 1989; sponsored by the American Helicopter Society
(NASA-TM-101978; E-4677; NAS 1.15:101978) Avail: NTIS HC A03/MF A01 CSCL 21E

An experimental program has been conducted in the NASA Lewis Research Center Icing Research Tunnel (IRT) in which an OH-58 tail rotor assembly was operated in a horizontal plane to simulate the action of a typical main rotor. Ice was accreted on the blades in a variety of rotor and tunnel operating conditions and documentation of the resulting shapes was performed. Rotor torque and vibration are presented as functions of time for several representative test runs, and the effects of various parametric variations on the blade ice shapes are shown. This OH-58 test was the first of its kind in the United States and will encourage additional model rotor icing tunnel testing. Although not a scaled representative of any actual full-scale main rotor system, this rig has produced torque and vibration data which will be useful in assessing the quality of existing rotor icing analyses. Author

N89-19306# Rolls-Royce Ltd., Derby (England).
CURRENT DIAGNOSTIC PRACTICE IN GAS TURBINE COMBUSTORS
B. Jones 14 Sep. 1987 16 p Presented at the NATO/Advanced Study Institute on Instrumentation for Combustion and Flow in Engines, Vimeiro, Portugal, 14-25 Sep. 1987
(PNR90530; ETN-89-93702) Copyright Avail: NTIS HC A03/MF A01

Methods and equipment used for gas turbine engine performance assessment and research are illustrated. Internal flow; carbon deposition; film mixing; heat transfer measurement; fuel

spray visualization; and combustion instability are considered. ESA

N89-19307# Rolls-Royce Ltd., Derby (England).
THE RELATIONSHIP BETWEEN MANUFACTURING TECHNOLOGY AND DESIGN
J. D. Alexander and M. Jezioro 6 Jun. 1988 7 p Presented at the 6th International Conference on Titanium: Titanium '88, Cannes, France, 6-9 Jun. 1988
(PNR90537; ETN-89-93704) Copyright Avail: NTIS HC A02/MF A01

It is argued that failures in aero engine components during service or development are frequently caused by a lack of understanding of the total engineering process. This process involves not only design, material selection, and stressing criteria but must include a detailed appreciation of the associated manufacturing processes. Only if the manufacturing constraints and their influence on microstructural development are fully understood can a consistent product be guaranteed to meet the engineering need. The design manufacturing interface is addressed from a processing manufacturing systems point of view. The type of philosophy which needs to be implemented if new titanium alloys and processing routes are to be more rapidly introduced for aero-engine components is identified. ESA

N89-19308# Rolls-Royce Ltd., Derby (England).
THE DIFFUSION BONDING OF AEROENGINE COMPONENTS
G. A. Fitzpatrick and T. Broughton 6 Jun. 1988 7 p Presented at the 6th World Conference on Titanium: Titanium '88, Cannes, France, 6-9 Jun. 1988
(PNR90540; ETN-89-93705) Copyright Avail: NTIS HC A02/MF A01

The process parameters of diffusion bonding are recalled, and diffusion bonding applications for aeroengine components are described. A liquid-phase diffusion bonding process (activated diffusion bonding) for the manufacture of hollow titanium wide chord fan blades is presented. The development of a high integrity bond was fundamental to the design concept of this component. Solid-state diffusion bonding is utilized in the manufacture of hollow vane/blade airfoil constructions mainly in conjunction with superplastic forming and hot-forming techniques. ESA

N89-19262*# National Aeronautics and Space Administration. Lewis Research Center, Cleveland, OH.
TURBOMACHINERY AEROELASTICITY AT NASA LEWIS RESEARCH CENTER
Krishna Rao V. Kaza *In* NASA, Langley Research Center, Transonic Unsteady Aerodynamics and Aeroelasticity 1987, Part 2 Feb. 1989 p 571-603 (For primary document see N89-19247 12-02)
Avail: NTIS HC A17/MF A01 CSCL 21E

N89-19263*# United Technologies Research Center, East Hartford, CT.
UNSTEADY AERODYNAMICS OF BLADE ROWS
Joseph M. Verdon *In* NASA, Langley Research Center, Transonic Unsteady Aerodynamics and Aeroelasticity 1987, Part 2 Feb. 1989 p 605-630 (For primary document see N89-19247 12-02)
Avail: NTIS HC A17/MF A01 CSCL 21E

08 AIRCRAFT STABILITY AND CONTROL

Includes aircraft handling qualities; piloting; flight controls; and autopilots.

For related information see also *05 Aircraft Design, Testing and Performance.*

N89-19309*# National Aeronautics and Space Administration. Langley Research Center, Hampton, VA.
INTEGRATED TOOLS FOR CONTROL-SYSTEM ANALYSIS
Aaron J. Ostroff, Melissa S. Proffitt, and David R. Clark (Planning Research Corp., Hampton, VA.) Washington NASA Mar. 1989 61 p
(NASA-TP-2885; L-16482; NAS 1.60:2885) Avail: NTIS HC A04/MF A01 CSCL 01C

The basic functions embedded within a user friendly software package (MATRIXx) are used to provide a high level systems approach to the analysis of linear control systems. Various control system analysis configurations are assembled automatically to minimize the amount of work by the user. Interactive decision making is incorporated via menu options and at selected points, such as in the plotting section, by inputting data. There are five evaluations such as the singular value robustness test, singular value loop transfer frequency response, Bode frequency response, steady-state covariance analysis, and closed-loop eigenvalues. Another section describes time response simulations. A time response for random white noise disturbance is available. The configurations and key equations used for each type of analysis, the restrictions that apply, the type of data required, and an example problem are described. One approach for integrating the design and analysis tools is also presented. Author

N89-19310 Minnesota Univ., Minneapolis.
CONTROL OF NONLINEAR SYSTEMS USING PARTIAL DYNAMIC INVERSION Ph.D. Thesis
Michael Ray Elgersma 1988 143 p
Avail: Univ. Microfilms Order No. DA8815802

Since linear control theory is well developed, methods for controlling nonlinear systems have focused on how to transform them into equivalent linear systems. Current research has centered on determining which nonlinear systems can be transformed into linear systems, and find methods for making the transformation. Whether or not a nonlinear system can be linearized depends on what class of transformations are allowed and on whether the transformations are required to be exact or only approximate. The class of systems considered is of the form $x=f(x)+g(x)h(x,u)$ where x is the n-dimensional state, us is the m-dimensional control, and g(x) is an n x m matrix. This form allows the inclusion of certain types of nonlinearities in the control, while providing an affine structure in h. The function h can be considered the new control input, subject to constraints. Practical methods for controlling nonlinear systems were determined. The prototype nonlinear system studied here is a 6 degree-of-freedom nonlinear aircraft model. The method used to control this nonlinear aircraft model is called partial dynamic inversion. The generic six degree-of-freedom nonlinear aircraft model used is general enough to apply to almost any aircraft. The model includes nonlinear kinematics and aerodynamics as well as gravity and thrust. The aerodynamic functions can be general tabular functions of angle of attack, side-slip angle, and Mach. A closed form solution is given for the aircraft equilibrium equations. Since the model had four control inputs, the equilibrium set is four dimensional. Dissert. Abstr.

N89-19311 Michigan Univ., Ann Arbor.
MINIMAX AND MAXIMAX OPTIMAL CONTROL PROBLEMS WITH APPLICATIONS IN AEROSPACE ENGINEERING Ph.D. Thesis
Ping Lu 1988 144 p
Avail: Univ. Microfilms Order No. DA8821615

Some previous work on the so-called Chebyshev minimax problem is reviewed. An extended theorem of optimal control is given that is part of the theoretical foundation in the following discussion. A set of practical yet sufficiently general necessary conditions for minimax and maximax problems is derived. Some of the previous work on the minimax problem is shown to be the special cases of our necessary conditions. The effect of the discontinuity of adjoint states on controls is exploited for the first time and the significant difference between the minimax and maximax problems is revealed. Analytical examples are presented to verify all aspects of the results. As an application of the maximax problem in aerospace engineering, the maximization of the flight radius of a hypervelocity aeroglider is discussed thoroughly and

numerical results are given. One of the important applications of the minimax problem is the minimization of the peak heating rate and the peak deceleration of a trans-atmospheric vehicle. Some characteristics of the problem are investigated and the control property is analyzed with the aid of necessary conditions. Numerical experiments are carried out to verify the analysis. Dissert. Abstr.

N89-19312 Air Force Inst. of Tech., Wright-Patterson AFB, OH.
TIME PERIODIC CONTROL OF A MULTIBLADE HELICOPTER Ph.D. Thesis
Steven Garnett Webb 1988 217 p
Avail: Univ. Microfilms Order No. DA8821884

The flap-lag equations of motion of an isolated rotor blade and those for a rigid helicopter containing four blades free to flap and lag are derived. Control techniques are developed which stabilize both systems for a variety of flight conditions. Floquet theory is used to investigate the stability of a rotor blade's flap-lag motion. A modal control technique, based on Floquet theory, is used to eliminate the blade's instabilities using existing collective and cyclic pitch control mechanisms. The technique shifts the unstable roots to desired locations while leaving the other roots unaltered. The control, developed for a single design point, is shown to significantly reduce or eliminate regions of flap-lag instabilities for a variety of off design conditions. Both scalar and vector control are successfully used to stabilize the blade's motion. Dissert. Abstr.

N89-19313 Arizona Univ., Tucson.
ESTIMATING PROJECTED CONTROLLABLE SETS FOR DYNAMICAL CONTROL SYSTEMS Ph.D. Thesis
Zong Yeng Wu 1988 126 p
Avail: Univ. Microfilms Order No. DA8820134

A method is developed to estimate the projection of a higher dimensional (3 or more) controllable set onto a lower dimensional (usually 1 or 2) space. This method requires that an n-dimensional dynamical system subject to a scalar control be transformed into two lower dimensional subsystems by choosing a proper transformation matrix. It is shown that such a transformation can always be determined for an n-dimensional linear I/O system. For some nonlinear dynamical system problems, such as an aircraft missile avoidance problem, a proper transformation matrix still can be determined. From the transformed system, both an overestimate and an underestimate for an actual projected controllable set in the state space of interest can be provided by using the method presented. With this information, the actual projected controllable set can be estimated. Two linear I/O systems subject to a scalar control and an aircraft missile avoidance problem are used to illustrate the method. Dissert. Abstr.

N89-19314# Georgia Inst. of Tech., Atlanta. School of Aerospace Engineering.
A SYSTEMS APPROACH TO ROTORCRAFT STABILITY AND CONTROL RESEARCH Final Report, 1 Sep. 1986 - 31 Oct. 1988
D. P. Schrage, J. V. Prasad, C. M. McKeithan, B. H. Tongue, P. Fitzsimmons, and D. Teare 24 Oct. 1988 26 p
(Contract DAAL03-86-K-0160)
(AD-A201784; ARO-23246.1-EG) Avail: NTIS HC A03/MF A01 CSCL 20D

Helicopters exhibit undesireable dynamic characteristics due to strong coupling that exists between longitudinal and lateral modes. In addition to being unstable at hover and low forward flight speeds, the helicopter has significantly different dynamic modal characterizing in hover and low speeds as compared to forward flight. For example, in hover, the body translational motion and pitching motion are decoupled from the heaving motion. In forward flight, the pitching motion and the vertical motion are strongly coupled. These dissimilar characteristics in hover and forward flight make piloting techniques more difficult and increase pilot workload and degrade handling qualities. This research has attempted a systems approach to rotorcraft stability and control. GRA

N89-19315# Toledo Univ., OH. Dept. of Electrical Engineering.
ROBUST CONTROL FOR LINEAR SYSTEMS WITH STRUCTURED UNCERTAINTY Final Report, 17 Jun. 1986 - 17 Jun. 1988
Rama K. Yedavalli Nov. 1988 113 p
(Contract F33615-86-K-3611)
(AD-A201947; AFWAL-TR-88-3077) Avail: NTIS HC A06/MF A01 CSCL 01D

The main theme of this research is the robust stabilization of linear uncertain control systems with structured uncertainty, from both the time domain and frequency domain perspectives. First, from an analysis point of view, two new results on improved measures of stability robustness are presented, one from the frequency domain (polynomial) perspective, the other from the state space (matrix theory) perspective. Design algorithms are presented that completely utilize the structural information of the uncertainty. The frequency domain based design also considers a class of non-minimum phase systems. Finally the aspect of combined structured and unstructured uncertainty is addressed and design methods are presented that treat these two types of uncertainty in a unifying framework. GRA

N89-19316*# Information and Control Systems, Inc., Hampton, VA.
A VARIABLE-GAIN OUTPUT FEEDBACK CONTROL DESIGN METHODOLOGY Final Report
Nesim Halyo, Daniel D. Moerder, John R. Broussard, and Deborah B. Taylor Washington NASA Mar. 1989 92 p
(Contract NAS1-17493)
(NASA-CR-4226; NAS 1.26:4226; FR-688106) Avail: NTIS HC A05/MF A01 CSCL 01C

A digital control system design technique is developed in which the control system gain matrix varies with the plant operating point parameters. The design technique is obtained by formulating the problem as an optimal stochastic output feedback control law with variable gains. This approach provides a control theory framework within which the operating range of a control law can be significantly extended. Furthermore, the approach avoids the major shortcomings of the conventional gain-scheduling techniques. The optimal variable gain output feedback control problem is solved by embedding the Multi-Configuration Control (MCC) problem, previously solved at ICS. An algorithm to compute the optimal variable gain output feedback control gain matrices is developed. The algorithm is a modified version of the MCC algorithm improved so as to handle the large dimensionality which arises particularly in variable-gain control problems. The design methodology developed is applied to a reconfigurable aircraft control problem. A variable-gain output feedback control problem was formulated to design a flight control law for an AFTI F-16 aircraft which can automatically reconfigure its control strategy to accommodate failures in the horizontal tail control surface. Simulations of the closed-loop reconfigurable system show that the approach produces a control design which can accommodate such failures with relative ease. The technique can be applied to many other problems including sensor failure accommodation, mode switching control laws and super agility. Author

09 RESEARCH AND SUPPORT FACILITIES (AIR)

Includes airports, hangars and runways; aircraft repair and overhaul facilities; wind tunnels; shock tubes; and aircraft engine test stands.

For related information see also *14 Ground Support Systems and Facilities (Space).*

N89-19317# Air Force Occupational and Environmental Health Lab., Brooks AFB, TX.
NOISE ASSESSMENT OF THE ROCKET SLED TEST TRACK OPERATION AT HOLLOMAN AFB, NEW MEXICO Final Report
Winston J. Shaffer, II Oct. 1988 42 p

(AD-A201279; USAFOEHL-88-140EH0087JNA) Avail: NTIS HC A03/MF A01 CSCL 14B

This report presents the results of noise data measurements of the Holloman AFB rocket sled test track operations. Impulse and community noise measurements were made to determine the impact of the rocket sled noise on the surrounding community. A worst case sled run was measured and used to determine that the rocket sled has very little impact on the community for a worst case rocket sled run and little or no impact for the majority of the runs. Recommendations were made to limit the number of people exposed to the rocket sled noise and require test track personnel to wear hearing protection. Sonic boom measurement equipment should be purchased to document all sonic booms created by the rocket sled. GRA

N89-19318# Naval Postgraduate School, Monterey, CA.
AEROTHERMODYNAMICS OF A JET CELL FACILITY M.S. Thesis
Eric A. Nicolaus Sep. 1988 151 p
(AD-A202142; AD-E501048) Avail: NTIS HC A08/MF A01 CSCL 21E

This thesis consists of a three-dimensional numerical analysis of the Jet Aircraft Hush House located at Naval Air Station Jacksonville, Florida. Utilizing the PHOENICS Code allows for the determination of the aerothermal characteristics including velocity, pressure, enthalpy, turbulent kinetic energy and the dissipation rate of turbulent kinetic energy in the facility during testing of the U.S. Navy's F-4 (Phantom II) J-79-GE-8 gas turbine engine with afterburner. How and by what method PHOENICS arrives at this solution is discussed. Of greatest importance is the resulting behavior of the aerothermal system. Problems encountered using the PHOENICS code, resulting numerical solutions to the particular facility, comparison to actual test data and recommendations for further applications of the PHOENICS Code are presented. GRA

N89-19319# Royal Aerospace Establishment, Farnborough (England).
AIRFIELD LIGHTING: FUTURE TRENDS
A. J. Smith Aug. 1988 22 p Presented at the Illuminating Engineering Society of North America/Aviation Lighting Division Conference, DC, 10-13 Oct. 1988
(RAE-TM-FM-6; BR107591; ETN-89-93671) Copyright Avail: Defence Research Information Centre, 65 Brown Street, Glasgow, G2 8EX Scotland

Approach and runway lighting for fixed wing precision approaches is reviewed. The importance of equipment maintenance is emphasized. Requirements for visual aids to support helicopter operations and to enhance surface movement, guidance, and control are considered. ESA

12 ASTRONAUTICS (GENERAL)

For extraterrestrial exploration see *91 Lunar and Planetary Exploration.*

N89-19320# DeLande Long (I. B. and M. A.) Software and Consultancy, Seeheim (Germany, F.R.).
STUDY OF A SOFTWARE SYSTEM CONCEPT FOR MISSION ANALYSIS PRESENTATION Final Report
M. A. deLandeLong Paris, France ESA Jun. 1988 38 p Original contains color illustrations
(Contract ESA-6864/86-D-MD)
(ESA-CR(P)-2661; ETN-89-93923) Avail: NTIS HC A03/MF A01

The Mission Analysis Presentation System (MAPS) which can produce animated graphics sequences illustrating aspects of spacecraft missions (orbits, spacecraft rotations, approach phases) was developed. The user specifies the requirements for an animation via an interactive interface with forms and menus. The mission analysis results to be presented are passed to MAPS in data files; the files contain spacecraft trajectories, for example. The MAPS generates the graphics commands for drawing each frame of the animated sequence on the graphics terminal. The MAPs is not expected to be a static system. Possible further developments include extensions to the MAPS facilities, such as moving light sources, new scenario types, and other central bodies for the central body scenario; extensions to the hardware to enable recording of the animations on film or video tape; and replacement of the Model One/380 with a new graphics terminal. ESA

N89-19321*# National Aeronautics and Space Administration. Goddard Space Flight Center, Greenbelt, MD.
GET AWAY SPECIAL (GAS): EDUCATIONAL APPLICATIONS OF SPACE FLIGHT
George G. Gerondakis [1989] 21 p
(NASA-TM-101287; NAS 1.15:101287) Avail: NTIS HC A03/MF A01 CSCL 22A

The Small Self-Contained Payloads (SCCP) program, commonly known as the Get Away Special (GAS) is discussed. The program allows a person to place a small self-contained experimental payload on the Space Shuttle at a very low cost. The payloads must be of peaceful intent and an engineering and/or science endeavor. The prime objective of the GAS program is to foster enthusiasm in the younger generation in the use of space. The paper presents the history of the program, its interaction with the educational/industrial relationship, some educational objectives, and predictions for the future. NASA

13 ASTRODYNAMICS

Includes powered and free-flight trajectories; and orbital and launching dynamics.

N89-19322# Technische Univ., Delft (Netherlands). Faculty of Technical Mathematics and Informatics.
ORIENTATION OF ORBITS IN FLOWS
J. M. Aarts 1988 17 p
(Rept-88-05; B8809734; ISSN-0920-8577; ETN-89-93842)
Copyright Avail: NTIS HC A03/MF A01

An explicit definition of orientation of an orbit is presented, for orbits of moving points only. It is explained how this can be incorporated into the framework of orientation preserving homeomorphisms. The orientation of orbits is introduced by regarding an orbit as a parametrized curve which in a natural way inherits the orientation of the space of real numbers. ESA

N89-19323# Technische Univ., Berlin (Germany, F.R.). Inst. fuer Luft- und Raumfahrt.
A MODEL FOR THE GEOSTATIONARY ORBITAL INFRASTRUCTURE, SYSTEM ANALYSIS
H. H. Koelle and N. Millin 1 Aug. 1988 35 p
(ILR-Mitt-205; ETN-89-93978) Avail: NTIS HC A03/MF A01

The functions and architecture of an infrastructure in the geostationary orbit (GEO) are discussed. A case study of a typical GEO infrastructure as it may develop during the next century was carried out, emphasizing conceptual design and analysis of a subsystem of this GEO infrastructure: the GEO Regional Transportation Company (GRET) envisaged as a commercial enterprise serving the 39 routes within the GEO complex by 10 different types of robots, taxis, and tugs. Results of simulation runs over a 110 yr life cycle produce timelines of several system performance parameters including prices for services within the market scenario assumed, which includes the acquisition and operation of a solar power system with 500 GW output. ESA

14 GROUND SUPPORT SYSTEMS AND FACILITIES (SPACE)

Includes launch complexes, research and production facilities; ground support equipment, e.g., mobile transporters; and simulators.

For related information see also *09 Research and Support Facilities (Air).*

N89-19324*# North Dakota Univ., Grand Forks. Dept. of Space Studies.
VARIABLE GRAVITY RESEARCH FACILITY
Sean Allan, Stan Ancheta, Donna Beine, Brian Cink, Mark Eagon, Brett Eckstein, Dan Luhman, Daniel McCowan, James Nations, and Todd Nordtvedt et al 13 Jun. 1988 96 p
(Grant NGT-21-002-080)
(NASA-CR-184714; NAS 1.26:184714) Avail: NTIS HC A05/MF A01 CSCL 14B

Spin and despin requirements; sequence of activities required to assemble the Variable Gravity Research Facility (VGRF); power systems technology; life support; thermal control systems; emergencies; communication systems; space station applications; experimental activities; computer modeling and simulation of tether vibration; cost analysis; configuration of the crew compartments; and tether lengths and rotation speeds are discussed. B.G.

15 LAUNCH VEHICLES AND SPACE VEHICLES

Includes boosters; operating problems of launch/space vehicle systems; and reusable vehicles.

For related information see also *20 Spacecraft Propulsion and Power.*

N89-19325# Committee on Commerce, Science, and Transportation (U.S. Senate).
COMMERCIAL EXPENDABLE LAUNCH VEHICLE LIABILITY
1988 82 p Hearing before the Subcommittee on Science, Technology and Space of the Committee on Commerce, Science and Transportation, 100th Congress, 2d Session, 17 May 1988
(S-Hrg-100-750; GPO-87-608) Avail: Subcommittee on Science, Technology and Space, Senate, Washington DC 20510 HC free

Hearings before a subcommittee of the House Committee on Commerce, Science, and Transportation are presented. Cost and availability of insurance for commercial launch providers was discussed. The contribution of the domestic launch industry to the Space Program is examined. All written testimony and submittals for the record are also included. B.G.

N89-19830*# General Dynamics Corp., San Diego, CA.
ARTIFICIAL INTELLIGENT DECISION SUPPORT FOR LOW-COST LAUNCH VEHICLE INTEGRATED MISSION OPERATIONS
Gerard P. Szatkowski and Roger Schultz (Abacus Programming Corp., Van Nuys, CA.) *In* NASA. Lyndon B. Johnson Space Center, 2nd Annual Workshop on Space Operations Automation and Robotics (SOAR 1988) Nov. 1988 p 87-94 Sponsored in part by AF (For primary document see N89-19817 12-59)
Avail: NTIS HC A22/MF A01 CSCL 22B

16 SPACE TRANSPORTATION

Includes passenger and cargo space transportation, e.g., shuttle operations; and space rescue techniques.

For related information see also *03 Air Transportation and Safety* and *18 Spacecraft Design, Testing and Performance.* For space suits see *54 Man/System Technology and Life Support.*

N89-19326*# National Aeronautics and Space Administration. John F. Kennedy Space Center, Cocoa Beach, FL.
ICE/FROST/DEBRIS ASSESSMENT FOR SPACE SHUTTLE MISSION STS-27R, DECEMBER 2, 1988
Gregory N. Katnik and Scott A. Higginbotham Feb. 1989 200 p
(NASA-TM-102144; NAS 1.15:102144) Avail: NTIS HC A09/MF A01 CSCL 22B

An Ice/Frost/Debris assessment was conducted for Space Shuttle Mission STS-27R. Debris inspections of the flight elements and launch pad are performed before and after launch. Ice/frost conditions are assessed by the use of computer programs, nomographs, and infrared scanner data during cryogenic loading of the vehicle followed by an on-pad visual inspection. High speed photography is viewed after launch to identify ice/debris sources and evaluate potential vehicle damage. The Ice/Frost/Debris conditions of Mission STS-27R and their effect on the Space Shuttle Program are documented. Author

N89-19327# Air Force Geophysics Lab., Hanscom AFB, MA.
MEASUREMENTS OF SHUTTLE GLOW ON MISSION STS 41-G
W. F. Denig, S. B. Mende, G. R. Swenson, D. J. Kendall, R. L. Gattinger, and E. J. Llewellyn (Saskatchewan Univ., Saskatoon.) 29 Sep. 1988 14 p
(AD-A201769; AFGL-TR-88-0262) Avail: NTIS HC A03/MF A01 CSCL 22A

The analysis of data from a set of experiments conducted during Mission STS 41-G has shown that the intensity of the shuttle glow measured during this mission was more than an order of magnitude less than the intensity measured under similar conditions on earlier flights. In addition the thruster enhanced glow was found to be spectrally continuous at the 0.4 nm resolution of the optical systems. Two separate activities, namely the Canadian Orbiter Glow (OGLOW) experiment and the USAF Auroral Photography Experiment (APE), were conducted simultaneously during STS 41-G and resulted in similar findings. The goals of both the OGLOW and the APE were to image earth aurora and airglow as well as glows emanating off shuttle surfaces. The experimental apparatus used for each experiment was a separate, hand-held, image intensified camera system with appropriate front-end optics. The interferometry data reported here were obtained using Fabry Perot techniques. GRA

N89-19328# Air War Coll., Maxwell AFB, AL.
A CASE STUDY OF SMALL GROUP DECISION-MAKING AS INFLUENCED BY THE ABILENE PARADOX: THE CHALLENGER MISHAP
James Y. Gaskins May 1988 83 p
(AD-A202102) Avail: NTIS HC A05/MF A01 CSCL 05H

On 27 January 1986 a group of decision-makers representing the public and private sectors of leadership in our national space exploration program evaluated the risk associated with known discrepancies in solid rocket motor seals. The risk assessment that was made led the group to agree that the discrepancies were within an acceptable margin of safety and authorized the launch of the Space Shuttle Challenger. Two phenomena which describe flawed decision-making processes, groupthink and the Abilene Paradox, provide a framework for a study of the agreements which culminated in the launch of Challenger. Analysis of the pitfalls of the decision-making process reveals various phenomena. One of them is known as groupthink or, e.g., a mode of thinking that people engage in when they are deeply involved in cohesive in-groups. They exhibit the desire for unanimity which overrides their motivation to realistically appraise alternative courses of action. Another pitfall in the decision-making process is described

in the Abilene Paradox. It is described as a phenomenon which occurs when decision-making groups take actions in contradiction to available information when dealing with problems. The mismanagement of agreement is central to the issue of understanding dysfunctional organizational behavior. GRA

N89-19329# Technische Univ., Berlin (Germany, F.R.). Inst. fuer Luft- und Raumfahrt.
MODEL OF A GEOSTATIONARY REGIONAL TRANSPORTATION COMPANY (GRET): FLEET COMPOSITION AND FACILITY LAYOUT
U. Wirt, S. Al-Kenany, B. Canpolat, D. Dallmann, A. Eckert, Klaus Heinemann, R. Kleessen, H. W. Renn, R. Schmudlach, and Carel Stuurman 1 Aug. 1988 50 p
(ILR-Mitt-207; ETN-89-93979) Avail: NTIS HC A03/MF A01

A design and layout study of a commercial, geostationary regional transportation company and related fleet of service vehicles, part of a project for modeling the operation of an infrastructure in geostationary orbit, is summarized. Considering potential customers, orbital environmental conditions and operational procedures, facility and fleet elements were characterized and defined. Based on the configuration of near-future space stations, the hardware was selected and two families of transport vehicles as well as a cluster of servicing vehicles were designed. ESA

N89-19330# Technische Univ., Berlin (Germany, F.R.). Inst. fuer Luft- und Raumfahrt.
PRELIMINARY COST MODEL FOR A COMMERCIAL GEOSTATIONARY TRANSPORTATION COMPANY (GRET)
H. H. Koelle, Z. Matijevic, J. Czarnitzki, Klaus Heinemann, Hakan Kayal, Claudia Lotze, Juergen Mayer, Hatto W. Renn, Frank Schneider, and Carel Stuurman et al 1 Aug. 1988 34 p
(ILR-Mitt-208; ETN-89-93980) Avail: NTIS HC A03/MF A01

The cost of one element of the geostationary orbital infrastructure was estimated. This element is a commercial transportation company to serve all other elements of the GEO infrastructure, offering passenger and cargo transportation within the local GEO regime. The estimates result in a figure of 30 billion dollars for the acquisition phase and annual expenses between 3 and 4 billion during the operational phase. Calculations show that it takes 20 yr before a positive cash flow can be expected and up to 40 yr before a (big) profit can be made. ESA

N89-19331# Technische Univ., Berlin (Germany, F.R.). Inst. fuer Luft- und Raumfahrt.
PRELIMINARY PROJECT PLAN FOR A GEO REGIONAL TRANSPORTATION AND SERVICING COMPANY
Fabian Eilingsfeld, Sven Abitzsch, and Michael Mielke 1 Aug. 1988 42 p
(ILR-Mitt-210; ETN-89-93981) Avail: NTIS HC A03/MF A01

Management and financing of a GEO Regional Transportation and Servicing Company (GRET) were studied. The planning, acquisition and operation of such a space system were examined. The GRET system is planned for a life cycle of 105 yr, beginning in the year 2004. The estimated life cycle costs are $ 350 billion ($ 1985), while the costs for a system with initial operating capability are under $ 25 billion. ESA

N89-19829*# National Aeronautics and Space Administration. John F. Kennedy Space Center, Cocoa Beach, FL.
CIRCA 2000 OPERATIONS CRITERIA
Arthur L. Scholz (Boeing Aerospace Co., Kennedy Space Center, FL.) and William J. Dickinson *In* NASA. Lyndon B. Johnson Space Center, 2nd Annual Workshop on Space Operations Automation and Robotics (SOAR 1988) Nov. 1988 p 81-85 (For primary document see N89-19817 12-59)
Avail: NTIS HC A22/MF A01 CSCL 22B

N89-19831*# McDonnell-Douglas Corp., Houston, TX.
A DESIGN AND IMPLEMENTATION METHODOLOGY FOR DIAGNOSTIC SYSTEMS
Linda J. F. Williams *In* NASA. Lyndon B. Johnson Space Center, 2nd Annual Workshop on Space Operations Automation and Robotics (SOAR 1988) Nov. 1988 p 95-103 (For primary document see N89-19817 12-59)
Avail: NTIS HC A22/MF A01 CSCL 22B

N89-19887*# Rockwell International Corp., Downey, CA. Space Transportation Systems Div.
EXPERT SYSTEMS APPLICATIONS FOR SPACE SHUTTLE PAYLOAD INTEGRATION AUTOMATION
Keith Morris *In* NASA. Lyndon B. Johnson Space Center, 2nd Annual Workshop on Space Operations Automation and Robotics (SOAR 1988) Nov. 1988 p 517-523 (For primary document see N89-19817 12-59)
Avail: NTIS HC A22/MF A01 CSCL 22B

17 SPACE COMM., SPACECRAFT COMM., COMMAND & TRACKING

Includes telemetry; space communications networks; astronavigation and guidance; and radio blackout.

For related information see also *04 Aircraft Communications and Navigation* and *32 Communications and Radar.*

No abstracts in this category.

18 SPACECRAFT DESIGN, TESTING AND PERFORMANCE

Includes satellites; space platforms; space stations; spacecraft systems and components such as thermal and environmental controls; and attitude controls.

For life support systems see *54 Man/System Technology and Life Support.* For related information see also *05 Aircraft Design, Testing and Performance, 39 Structural Mechanics,* and *16 Space Transportation.*

N89-19332# Committee on Science, Space and Technology (U.S. House).
THE ATLAS/CENTAUR 67 LAUNCH MISHAP
Washington GPO 1987 111 p Hearing before the Subcommittee on Space Science and Applications of the Committee on Science, Space and Technology, 100th Congress, 1st Session, No. 87, 4 Aug. 1987
(GPO-80-201) Avail: Subcommittee on Space Science and Applications

The findings of an investigation concerning the loss of the Atlas/Centaur-67 launch vehicle are presented. The loss is primarily attributed to a hardover engine yaw command which was caused by an erroneous signal from the digital computer unit. The generation of the erroneous signal was blamed on unfavorable weather conditions which created a lightning hazard. Recommendations for avoiding similar occurrences are submitted. Author

N89-19333# Virginia Univ., Charlottesville. Dept. of Mechanical and Aerospace Engineering.
PROCEEDINGS OF THE FIFTH AFOSR FORUM ON SPACE STRUCTURES
Walter D. Pilkey, ed. and Robert L. Kosut, ed. (Integrated Systems, Inc., Palo Alto, CA.) 11 Dec. 1987 92 p Forum held at Monterey, Calif., 20-21 Aug. 1987
(Contract F49620-86-K-0009; AF Proj. 2302)
(AD-A194761; AFOSR-88-0477TR; UVA/525673/MAE88/102)
Avail: NTIS HC A05/MF A01 CSCL 22E

This is the Proceedings of the Fifth AFOSR Forum on Space Structures. The topics covered include modeling of spacecraft, wave propagation in large space structures, multiflexible body dynamic simulation, adaptive structures, electromechanical

actuators for controlling flexible structures, system identification of suboptimal control parameters, integrated structural analysis and control, active control of elastic wave motion in structural networks, adaptive control of large space structures; analysis of performance degradation, optimal projection equations for fixed-order dynamic compensation, decentralized/relegated control for large space structures, Frobenius-Hankel norm framework for disturbance rejection and low order decentralized controller design, a method for truss structure vibration control, and robust eigenstructure assignment by a projection method. For individual titles, see N89-19334 through N89-19349.

N89-19334# Howard Univ., Washington, DC. Dept. of Mechanical Engineering.
MODELING OF FLEXIBLE SPACECRAFT ACCOUNTING FOR ORBITAL EFFECTS
Peter M. Bainum *In* Virginia Univ., Proceedings of the Fifth AFOSR Forum on Space Structures 11 Dec. 1987 p 3-8 (For primary document see N89-19333 12-18)
Avail: NTIS HC A05/MF A01 CSCL 22E

Many current investigations of the shape and orientation control of proposed flexible orbiting large space structures (LSS) do not incorporate the effects of the gravity-gradient and orbital dynamic coupling into the plant models. This means that for the corresponding linearized unforced, open-loop systems, the poles of the rigid rotational modes are at the origin. The manner in which the orbitally induced coupling effects, due to gravity-gradient and gyroscopic effects, are introduced is clearly indicated in the continuum formulation of Santini for predicting the motion of a general orbiting flexible body in orbit. These coupling terms reflect both coupling between the rigid and flexible motions and also intra-modal coupling effects. Elastic deformations are considered small as compared with characteristic body dimensions. Equations are developed for both the rigid and elastic (generic) motions, based on an a prior knowledge of the frequencies and shape functions of all modes included within the truncated system model. The orbitally induced coupling terms are seen to depend on volume integrals whose integrands are functions of the various components of the different modal shape functions together with the coordinates of the differential mass elements. Author

N89-19335# Massachusetts Inst. of Tech., Cambridge. Dept. of Mechanical Engineering.
WAVE PROPAGATION IN LARGE SPACE STRUCTURES
James H. Williams, Jr. and Raymond J. Nagem *In* Virginia Univ., Proceedings of the Fifth AFOSR Forum on Space Structures 11 Dec. 1987 p 9-11 (For primary document see N89-19333 12-18)
Avail: NTIS HC A05/MF A01 CSCL 22E

The first step in the mathematical analysis of any physical system is the selection of a mathematical model to represent the system. This selection is extremely important, since it not only determines in advance the scope of possible results of the analysis, but also heavily influences the design of auxiliary devices and systems, such as control systems. In the dynamic analysis of large space structures, mathematical models have consisted primarily of a set of vibration modes. The popularity of the modal vibration model of large space structures is due partly to the well-developed analytical techniques which can be applied to such a model, and partly to the success with which modal vibration models have been used to describe structures on earth. However, in view of the unprecedented size of large space structures and their potential technological importance, it is worthwhile to examine the limitations of modal vibration models and to consider the usefulness of other models. A particular concern here is with models which view large space structures as media in which wave propagation provides an accurate dynamic description. Author

N89-19336# Iowa Univ., Iowa City. Center for Computer Aided Design.
A RECURSIVE METHOD FOR PARALLEL PROCESSOR MULTIFLEXIBLE BODY DYNAMIC SIMULATION
Edward J. Haug *In* Virginia Univ., Proceedings of the Fifth AFOSR Forum on Space Structures 11 Dec. 1987 p 13-17 (For primary document see N89-19333 12-18)
Avail: NTIS HC A05/MF A01 CSCL 22E

The purpose of this note is to outline a recently developed method for formulating and solving equations of motion of multibody dynamic systems that is well suited for high speed dynamic simulation using parallel processors. An outline of the approach is given here, with references to papers that develop the mathematical foundations. Examples involving a rigid body vehicle system real-time simulation, a geometrically nonlinear rotating blade, and a space manipulator are used to illustrate application of the method and to indicate computational efficiency that can be gained. Author

N89-19337# Virginia Polytechnic Inst. and State Univ., Blacksburg. Dept. of Engineering Science and Mechanics.
MANEUVERING EQUATIONS IN TERMS OF QUASI-COORDINATE
Leonard Meirovitch *In* Virginia Univ., Proceedings of the Fifth AFOSR Forum on Space Structures 11 Dec. 1987 p 19-21 (For primary document see N89-19333 12-18)
Avail: NTIS HC A05/MF A01 CSCL 22E

The equations for the motion of a flexible spacecraft in space can be described conveniently in terms of quasi-coordinates. The nonlinear equations can be treated by a perturbation approach, resulting in a low-order nonlinear problem for the rigid-body maneuvering and linear time-varying problem for angular perturbations from the rigid-body maneuver and elastic vibration. Author

N89-19338# Jet Propulsion Lab., California Inst. of Tech., Pasadena. Applied Technologies Section.
CONCEPT OF ADAPTIVE STRUCTURES
Michail Zak *In* Virginia Univ., Proceedings of the Fifth AFOSR Forum on Space Structures 11 Dec. 1987 p 23-24 (For primary document see N89-19333 12-18)
Avail: NTIS HC A05/MF A01 CSCL 22E

The concept of adaptive structures is brought up in connection with the need in ultra lightweight structural systems to maintain desired properties and configurations without human intervention when subjected to dynamic, thermal, and other environmental forces. Examples are large antenna structures and flexible robotic structures. In the both cases such adaptivity would allow less massive structural members to be employed under normal loading conditions. During special circumstances when unusually large loads are encountered, temporary stiffening would allow the use of less sturdy structures, resulting in large savings in their cost, and in increasing their mobility and efficiency. Within the framework of a finite-dimensional representation of structural dynamics, the adaptivity can be implemented by the dependence of the stiffness matrix (k) upon the expected load (Q), or expected (programmed) changes in configurations, i.e., (k) = (k(t)) where the dependence upon time is programmed in advance. In order to sustain unexpected loads the adaptive structure can be provided by feedback force control, or by a parametrical stiffness control. Author

N89-19339# State Univ. of New York, Buffalo. Dept. of Mechanical and Aerospace Engineering.
COMMENTS ON ELECTROMECHANICAL ACTUATORS FOR CONTROLLING FLEXIBLE STRUCTURES
D. J. Inman, R. W. Mayne, and D. C. Zimmerman (Florida Univ., Gainesville.) *In* Virginia Univ., Proceedings of the Fifth AFOSR Forum on Space Structures 11 Dec. 1987 p 25-27 (For primary document see N89-19333 12-18)
Avail: NTIS HC A05/MF A01 CSCL 22E

Two types of specific electromechanical actuators are described and discussed. A proof mass actuator and an electric motor are examined in terms of the amount of damping each produces in a specific structural control experiment. Theoretical and experimental values of actuator produced damping are examined. The effects of actuator dynamics on control law implementation are noted. In

addition, a theoretical parameter study of the dynamic response of a dc motor controlling a flexible model of a beam are summarized. Author

N89-19340# Virginia Univ., Charlottesville. Dept. of Mechanical and Aerospace Engineering.
SYSTEM IDENTIFICATION OF SUBOPTIMAL FEEDBACK CONTROL PARAMETERS BASED ON LIMITING-PERFORMANCE/MINIMUM-TIME CHARACTERISTICS
Walter D. Pilkey *In its* Proceedings of the Fifth AFOSR Forum on Space Structures 11 Dec. 1987 p 29-32 (For primary document see N89-19333 12-18)
Avail: NTIS HC A05/MF A01 CSCL 22E

Most active controllers developed to control large structures are subject to constraints. For instance, control characteristics of proof-mass actuators are dominated by the nature of the constraints. To find the optimal or suboptimal control laws for such controllers can be a formidable task. Intuition of a designer plays an important role and the design method may vary dramatically in accordance with the constraints of the system. Therefore, one may wish to have a systematic methodology to solve the control problems subject to control force and state variable constraints. Limiting-performance/minimum-time (LP/MT) control calculates the optimal control force as a function of time for a known system with initial conditions, subject to certain constraints and external excitations while minimizing a given performance index. Although the LP/MT control gives optimal open loop control for the system, it is desirable to develop a closed loop control which has more practical value. Perhaps a system identification technique can be used to establish a suboptimal feedback control law based on the LP/MT control characteristics. Author

N89-19341# Aerospace Corp., Los Angeles, CA.
INTEGRATED STRUCTURAL ANALYSIS AND CONTROL (ISAAC): ISSUES AND PROGRESS
M. Aswani, D. S. Flamm, C. L. Gustafson, A. B. Jenkin, J. D. Kawamoto, and G. T. Tseng *In* Virginia Univ., Proceedings of the Fifth AFOSR Forum on Space Structures 11 Dec. 1987 p 43-47 (For primary document see N89-19333 12-18)
Avail: NTIS HC A05/MF A01 CSCL 22E

The ISAAC program at the Aerospace Corporation has been pursuing issues which arise in the simultaneous design of structures and control systems for large space structures using a mathematical programming code. There are many practical advantages to such integrated design, such as tuning the structure to directly improve the closed loop performance measure. Here, the focus is on key elements in the work, and in particular those elements which distinguish our emphasis from that of other workers in the field. There is obviously more to gain by simultaneously tuning structural and controller designs. Closed loop performance criteria which directly measure desired characteristics are available. The big issues are parametrization of controller and structure, and computational techniques for evaluation of criteria, constraints, and their derivatives. Author

N89-19342# Massachusetts Inst. of Tech., Cambridge. Dept. of Aeronautics and Astronautics.
ACTIVE CONTROL OF ELASTIC WAVE MOTION IN STRUCTURAL NETWORKS
David W. Miller and Andreas H. vonFlotow *In* Virginia Univ., Proceedings of the Fifth AFOSR Forum on Space Structures 11 Dec. 1987 p 49-51 (For primary document see N89-19333 12-18)
Avail: NTIS HC A05/MF A01 CSCL 22E

Recent work performed at the M.I.T. Space Systems Laboratory 1 has dealt with control design based on wave propagation models of flexible structures. Reflection and transmission properties of performance critical locations are actively altered in order to meet mission requirements regarding dynamic isolation, energy shunting, and vibration suppression. Using an input/output relation, the wave scattering characteristics of the location, or structural junction, can be actively altered in order to vary the path of power transmission or reduce power emanating from the junction. Such a technique has several advantages. Wave control approaches the problem as feedforward disturbance rejection of incoming waves. In some applications, this can eliminate resonant behavior by creating matched terminations. Local models are insensitive to all but local modelling errors. Since a wave model is a local description, a guarantee of control stability is not based upon knowledge of global structural behavior. Instead, stability is judged based on the frequency dependent power generation/dissipation properties of the active junction. Global control performance is dependent upon significance of the disturbance path containing the active junction. The control energy expended is of the order of the disturbance energy and only a few actuators and sensors are required to carry out most tasks. Author

N89-19343# Integrated Systems, Inc., Santa Clara, CA.
ADAPTIVE CONTROL OF LARGE SPACE STRUCTURES
Robert L. Kosut *In* Virginia Univ., Proceedings of the Fifth AFOSR Forum on Space Structures 11 Dec. 1987 p 51-55 (For primary document see N89-19333 12-18)
Avail: NTIS HC A05/MF A01 CSCL 22E

Some of the research issues involved in the design and analysis of adaptive control systems for large space structures (LSS) are described. The need for adaptive control arises from many envisioned future LSS missions which impose stringent performance demands on tracking accuracy and structural vibration attenuation. Both active feedback control and passive damping will be a practical necessity, and moreover, their design will require a model of the LSS system whose accuracy is compatible with the performance demands. Structural variations from many sources, such as deployment, material fatigue, and even random variations in materials and manufacturing tolerances, will significantly degrade closed-loop performance. Thus, the on-orbit dynamics of LSS will not be sufficiently like those obtained from either ground-testing or even from sophisticated computer generated modeling techniques, such as finite element modeling. Current structural modeling techniques are just not sufficiently accurate or able to account for all the possible sources of parameter variations. Therefore, under these conditions, it will be necessary to identify the LSS dynamics directly from on-orbit measurements, and simultaneously, tune or redesign the control. Hence, the control design cycle will be an adaptive process. Author

N89-19344# Harris Corp., Melbourne, FL. Government Aerospace Systems Div.
MAJORANT ANALYSIS OF PERFORMANCE DEGRADATION DUE TO UNCERTAINTY
David C. Hyland *In* Virginia Univ., Proceedings of the Fifth AFOSR Forum on Space Structures 11 Dec. 1987 p 57-64 (For primary document see N89-19333 12-18)
Avail: NTIS HC A05/MF A01 CSCL 22E

The problem addressed here is the determination of bounds on the degradation of system performance due to uncertainties and/or unforeseen and imperfectly modelled subsystem interactions. Such bounding techniques represent a fundamental systems analysis tool that is indispensable for further elucidation of decentralized controller architectures and robust design. Author

N89-19345# Harris Corp., Melbourne, FL. Government Aerospace Systems Div.
THE OPTIMAL PROJECTION EQUATIONS FOR FIXED-ORDER DYNAMIC COMPENSATION: EXISTENCE, CONVERGENCE AND GLOBAL OPTIMALITY
David C. Hyland *In* Virginia Univ., Proceedings of the Fifth AFOSR Forum on Space Structures 11 Dec. 1987 p 65-72 (For primary document see N89-19333 12-18)
Avail: NTIS HC A05/MF A01 CSCL 22E

Regardless of how appealing the optimal projection formulation may appear to be, its contribution is vacuous unless certain serious questions can be resolved. These include: (1) Under what conditions can the optimal projection equations be guaranteed a

priori to possess a solution. (2) Given problem data, exactly how many solutions do the equations possess. (3) Of the possible solutions, what are their stability properties, what is their performance, and which is the global optimum. (4) How can numerical algorithms be constructed which can be guaranteed to converge to any desired solution especially the global minimum. It seems clear that any attempt to address the above issues must utilize mathematical methods which are global in nature. To this end we have applied degree theory and associated homotopic continuation methods to analyze the solutions to the optimal projection equations and to construct convergent, implementable algorithms for their computation. The purpose of this presentation is to report significant recent results in this regard. Author

N89-19346# Ohio State Univ., Columbus. Dept. of Electrical Engineering.
DECENTRALIZED/RELEGATED CONTROL FOR LARGE SPACE STRUCTURES
Umit Ozguner and Steve Yurkovich *In* Virginia Univ., Proceedings of the Fifth AFOSR Forum on Space Structures 11 Dec. 1987 p 73-75 (For primary document see N89-19333 12-18)
Avail: NTIS HC A05/MF A01 CSCL 22E

The complexity of present and envisaged space structures dictates the inevitable need for emphasis on control and structure interaction. Moreover, in view of present methodologies, stringent control requirements such as precise pointing and slewing, vibration suppression, and shape control indicate that much work remains to be done in this important area. Recent results in the decentralized, relegated control of large space structures, with concentration on topics of decentralization, relegation, servomechanism design, and multiple mirror system examples are given. Author

N89-19347# Illinois Univ., Urbana. Coordinated Science Lab.
FROBENIUS-HANKEL NORM FRAMEWORK FOR DISTURBANCE REJECTION AND LOW ORDER DECENTRALIZED CONTROLLER DESIGN
J. Medanic and W. R. Perkins *In* Virginia Univ., Proceedings of the Fifth AFOSR Forum on Space Structures 11 Dec. 1987 p 77-79 (For primary document see N89-19333 12-18)
Avail: NTIS HC A05/MF A01 CSCL 22E

There is a desire to design low-order controllers for high order plants. Procedures to solve the low-order controller design problem can broadly be divided into two classes. Direct methods, in which the parameters defining a low order controller are computed by some optimization or other procedure, and indirect methods, in which a high order controller is found first, and then a procedure is used to simplify it. Examples of direct methods are the parametric linear-quadratic (LQ) design and the projective controls procedure developed by the authors. In the case of indirect methods, the linear-quadratic-Gaussian (LQG), the frequency weighted LQG, and the H (infinity)-norm minimization approaches provide the high order controller and, each in its own right, captures many relevant performance/robustness design goals. However, procedures for reducing high order controllers to low order controllers are less well developed. Author

N89-19348# Lawrence Livermore National Lab., CA.
A CONTROLLED COMPONENT SYNTHESIS METHOD FOR TRUSS STRUCTURE VIBRATION CONTROL
K. David Young *In* Virginia Univ., Proceedings of the Fifth AFOSR Forum on Space Structures 11 Dec. 1987 p 81-83 (For primary document see N89-19333 12-18)
(Contract W-7405-eng-48)
Avail: NTIS HC A05/MF A01 CSCL 22E

A new framework for the design of controllers for truss structure vibration control which is closely related to that of the Subsystem Decomposition Approach is introduced. The method developed herein deviates from conventional control system design practice in which a dynamic model of the open loop plant is often the initial data given to the control system designer. Instead, the controlled plant is assembled from the controlled components in the control design process. The development of this controlled component synthesis method is motivated on one hand by the well developed component mode synthesis methods (8 to 10) - a collection of structural analysis methods which has been demonstrated to be effective for solving large complex structural analysis problems for almost three decades, and on the other, stimulated by the subsystem decomposition viewpoint in large scale system theory. Connections between controlled component synthesis and existing large scale system decomposition techniques are established herein to build a control theoretic foundation for the developed method. A simple truss vibration control problem has been employed to illustrate the design procedures, as well as demonstrating the potentials of the developed method for controlling very large dimensional repetitive truss structures. Author

N89-19349*# National Aeronautics and Space Administration. Langley Research Center, Hampton, VA.
ROBUST EIGENSTRUCTURE ASSIGNMENT BY A PROJECTION METHOD: APPLICATION USING MULTIPLE OPTIMIZATION CRITERIA
J. L. Junkins, D. W. Rew, and J. N. Juang *In* Virginia Univ., Proceedings of the Fifth AFOSR Forum on Space Structures 11 Dec. 1987 p 85-88 Sponsored by NASA (For primary document see N89-19333 12-18)
Avail: NTIS HC A05/MF A01 CSCL 22E

New ideas which lead to feedback control laws for large flexible structures which are insensitive to model uncertainty are presented. A pole placement method is presented which leads to near-unitary closed loop eigenvectors, and a new method is introduced to design the control while simultaneously considering three competing measures of optimality. Robustness versus Integral algorithms are applicable to at least moderately high-dimensioned systems. In the present discussion, controls for two coupled flexible bodies are considered. A 6x24 gain matrix is designed to control a 12 modes system using 6 actuators. Researchers also developed control laws for the R2P2 simulator at Martin Marietta; in this case 3 actuators are used to control a 12th order system. Simulation studies indicate that researchers indeed achieved robust designs without significant difficulties associated with spillover into the uncontrolled modes. Here, several key ideas and numerical results are given. In the references, details of the formulation, discussions of salient features, and connection to the availiable literature are given. Author

N89-19350 Virginia Polytechnic Inst. and State Univ., Blacksburg.
DAMAGE DETECTION AND LOCATION IN LARGE SPACE TRUSSES Ph.D. Thesis
Suzanne Weaver Smith 1988 139 p
Avail: Univ. Microfilm Order No. DA8817424

Researchers pursuing the goal to design and construct a large orbiting space structure are directing considerable effort toward many issues, including the ability to maneuver a flexible structure. In particular, basic research is underway into the technologies of control system design and structural modeling to support this effort. The thesis of this research is that structural damage can be detected and located with the control system of a large space structure. A concept for damage location was developed and demonstrated in simulated tests. The control system tests the structure and measures the response. The measurement are then used in a system identification algorithm to produce a model of the damaged structure. The model is compared to one for the undamaged structure to find regions of reduced stiffness which indicate the location of damage. Simulation studies were performed on two truss models. The members of both and the design of the second were borrowed form the concept design for the Space Station. Exact and inexact data simulated tests with the two structures indicated that damage can be located with this approach. Dissert. Abstr.

N89-19351# Instituto de Pesquisas Espaciais, Sao Jose dos Campos (Brazil).
SCD2 SATELLITE SPIN AXIS REORIENTATION AND FEASIBILITY STUDY
Luiz Danilo DamascenoFerreira, Jose Jaime daCruz, and Valdemir Carrara Sep. 1988 27 p In PORTUGUESE; ENGLISH summary
(INPE-4688-NTE/285) Avail: NTIS HC A03/MF A01

The feasibility studies of spin axis reorientation and stabilization of the Data Collecting Satellite 2 (SCD2) are presented. Also contained are analyses of the spin rate decay and simultaneous visibility among Cuiaba (tracking station)/SCD2/PCD's (Data Collecting Platforms). Author

N89-19352*# Colorado Univ., Boulder.
THE DEVELOPMENT OF A CISLUNAR SPACE INFRASTRUCTURE Final Report
C. A. Buck, A. S. Johnson, J. M. McGlinchey, and K. D. Ryan [1989] 59 p
(Grant NGT-21-002-080)
(NASA-CR-184728; NAS 1.26:184728) Avail: NTIS HC A04/MF A01 CSCL 22B

The primary objective of this Advanced Mission Design Program is to define the general characteristics and phased evolution of a near-Earth space infrastructure. The envisioned foundation includes a permanently manned, self-sustaining base on the lunar surface, a space station at the Libration Point between earth and the moon (L1), and a transportation system that anchors these elements to the Low Earth Orbit (LEO) station. The implementation of this conceptual design was carried out with the idea that the infrastructure is an important step in a larger plan to expand man's capabilities in space science and technology. Such expansion depends on low cost, reliable, and frequent access to space for those who wish to use the multiple benefits of this environment. The presence of a cislunar space infrastructure would greatly facilitate the staging of future planetary missions, as well as the full exploration of the lunar potential for science and industry. The rationale for, and a proposed detailed scenario in support of, the cislunar space infrastructure are discussed. Author

N89-19353# Tokyo Univ. (Japan). Inst. of Space and Astronautical Science.
ANALYTICAL INTERPRETATION ON LATERAL/DIRECTIONAL STABILITY AND CONTROLLABILITY OF HIGH ANGLE-OF-ATTACK REENTRY FLIGHT
Koichi Yonemoto and Yoshifumi Inatani Jul. 1988 68 p
(ISAS-630; ISSN-0285-6808) Avail: NTIS HC A04/MF A01

Since winged space vehicles perform unpowered hypersonic reentry flights at very high angle of attack avoiding excessive heat loads, the lateral directional stability and controllability are the critical aerodynamic design subjects to accomplish desired trajectory and to meet cross range requirements. The lateral stability and controllability criteria is reviewed, and analytical considerations are presented on the lateral control divergence mechanism using linear transfer function method. It is shown that the zero loci of the multiloop control transfer function indicate the stability of the bank angle control with rudder coordination and has equivalent meaning to the lateral control divergence parameter. A synthesis of simple lateral multiloop controller is proposed for practical application of the reentry vehicles flying at very high angle of attack. Author

N89-19354# Hughes Research Labs., Malibu, CA.
FLIGHT MODEL DISCHARGE SYSTEM Report, Mar. 1987 - Apr. 1988
R. R. Robson and W. W. Williamson Jun. 1988 85 p
(Contract F19628-83-C-0143)
(AD-A201605; HAC-REF-F4890; AFGL-TR-88-0150; SR-4) Avail: NTIS HC A05/MF A01 CSCL 22A

The Flight Model Discharge System (FMDS) Program has completed its fourth year. The FMDS is a spacecraft charge control system designed to overcome the problem of charge buildup on a space vehicle which occurs during periods of adverse space environmental conditions. An overview of the FMDS system is presented, followed by an in-depth treatment of the significant technical developments that have occurred during the past year. The major areas covered include the plasma generator and electrostatic analyzer testing. GRA

N89-19355# Naval Postgraduate School, Monterey, CA.
EFFECTS OF REDUCED ORDER MODELING ON THE CONTROL OF A LARGE SPACE STRUCTURE M.S. Thesis
William J. Preston Sep. 1988 81 p
(AD-A201674) Avail: NTIS HC A05/MF A01 CSCL 22B

The motion of a large space structure, such as a space station, is described by a large number of coupled, second order differential equations. To effectively control this structure, a mathematical model is required. Both the mathematical model developed directly from the physics of the structure, and the simplified model developed with modal analysis are of extremely high dimension. A reduced order model is therefore required in order to design a control system for the structure. A straightforward approach to the control problem is taken by using linear quadratic optimal control techniques to determine the reduced order control solution for the truncated modal model. The effects of reduced order modeling on the control of the space station will be evaluated by observing the response of the closed loop system to several disturbances. GRA

N89-19356 Virginia Polytechnic Inst. and State Univ., Blacksburg.
NONLINEAR OPTIMAL CONTROL AND NEAR-OPTIMAL GUIDANCE STRATEGIES IN SPACECRAFT GENERAL ATTITUDE MANEUVERS Ph.D. Thesis
Yiing-Yuh Lin 1988 94 p
Avail: Univ. Microfilms Order No. DA8825331

Solving the optimal open-loop control problems for spacecraft large-angle attitude maneuvers generally requires the use of numerical techniques whose reliability is strongly case dependent. The primary goal of this dissertation is to increase the solution reliability of the associated nonlinear two-point boundary-value problems as derived from Pontryagin's Principle. Major emphasis is placed upon the formulation of the best possible starting or nominal solution. Constraint relationships among the state and costate variables are utilized. A hybrid approach which begins with the direct gradient method and ends with the indirect method of particular solutions is proposed. Test case results which indicate improved reliability are presented. The nonlinear optimal control law derived from iterative procedures cannot adjust itself in accordance with state deviations measured during the control period. A real-time near-optimal guidance scheme which takes the perturbed states to the desired manifold by tracking a given optimal trajectory is also presented. Numerical simulations are presented which show that highly accurate tracking results can be achieved. Dissert. Abstr.

N89-19357# Harris Corp., Melbourne, FL. Government Aerospace Systems Div.
EXPERIMENTAL VERIFICATION OF AN INNOVATIVE PERFORMANCE-VALIDATION METHODOLOGY FOR LARGE SPACE SYSTEMS Annual Report, Aug. 1987 - Aug. 1988
David C. Hyland Sep. 1988 53 p
(Contract F49620-87-C-0108)
(AD-A202243; AFOSR-88-1192TR) Avail: NTIS HC A04/MF A01 CSCL 22B

A technology gap exists in verifying performance of large space systems. To fill that gap the proposed program seeks to develop and validate an efficient pre-flight performance verification methodology. The approach involves selective component testing along with analysis of subsystem interactions. The method exploits MEOP (Maximum Entropy/Optimal Projection) Control-System Design and Majorant Robustness Analysis. The approach will be formulated for several representative large space systems and experimentally verified on a 3-meter diameter multi-hex panel ground-based active controls testbed. GRA

N89-19358# Harris Corp., Melbourne, FL. Government Aerospace Systems Div.
MAXIMUM ENTROPY/OPTIMAL PROJECTION DESIGN SYNTHESIS FOR DECENTRALIZED CONTROL OF LARGE SPACE STRUCTURES Final Report, Oct. 1986 - May 1988
David C. Hyland, Dennis S. Bernstein, and Emmanuel G. Collins, Jr. May 1988 281 p
(Contract F49620-86-C-0038)
(AD-A202375; AFOSR-88-1203TR) Avail: NTIS HC A13/MF A01 CSCL 22B

The Maximum Entropy/Optimal Projection (MEOP) Methodology is a novel approach to designing implementable vibration-suppression controllers for large space systems. Two issues, in particular, have been addressed, namely, controller order (i.e., complexity) and system robustness (i.e., sensitivity to plant variations). Extensions developed herein include generalizations to decentralized controller architectures and a new robustness analysis technique known as Majorant Robustness Analysis. This final report also encompasses extensions to hierarchical control as well as the development of numerical algorithms for solving the control design equations. GRA

N89-19359# ANT Nachrichtentechnik, Backnang (Germany, F.R.).
DEFINITION OF THE TRANSMISSION SYSTEM FOR A EUROPEAN DATA RELAY SATELLITE Final Report
F. Diener, W. Heine, S. Rasmussen, W. Schreitmueller, and W. Steinert Paris, France ESA May 1987 640 p
(Contract ESA-CR(P)-6499/85-NL-DG)
(ESA-CR(P)-2632; ETN-89-93647) Avail: NTIS HC A99/MF A01

The transmission system for a European Data Relay Satellite was investigated to define efficient transmission strategies for high data rate transmission with 26 GHz interorbit link and for low and medium rates for the S-band interorbit link. Decoder strategies for control of S-band interference were derived. User terminal aspects were studied, in particular with respect to terminal architecture and implementation of acquisition, synchronization, and tracking functions. Data relay satellite alternatives with different frequency conversion schemes (single or double conversion) and channelization concepts (1 to 4 transponder channels for 500 Mb/s transmission on the return link) were compared. Preliminary system recommendations are presented. ESA

N89-19360# Messerschmitt-Boelkow-Blohm G.m.b.H., Ottobrunn (Germany, F.R.). Space Div.
PSDE/SAT-2 PRELIMINARY SPACECRAFT CONFIGURATION STUDY, EXECUTIVE SUMMARY
H. Kellermeier, W. Rupp, H. Kuhlen, H. Vorbrugg, H. Fetzer, M. Chognot, and N. Limbourg Mar. 1988 40 p Prepared in cooperation with Societe Nationale Industrielle Aerospatiale, Cannes; and Etudes Techniques et Constructions Aerospatiales, Charleroi, Belgium
(Contract ESA-7189/87-NL-DG)
(ESA-CR(P)-2689; ETN-89-93918) Avail: NTIS HC A03/MF A01

The SAT-2 configuration for a 426 to 441 kg payload consisting of a laser single access (LSA), S-band single access (SSA), land mobile access (LAMEX), millimeter wave, and 20/30 GHz feeder link systemes is presented. The system budget shows that this payload can be accommodated by SPACEBUS 100 B (EUTELSAT-2) with a mass margin of 90 kg. The selected (fairly balanced) configuration is characterized by the optical LSA terminal and the large electronically steered offset antenna used for S and L-band communication. The 80 precent transparent reflector is counterbalanced by a solid 2 m reflector for LAMEX. A LOCSTAR payload was also envisaged for SAT-2 but the additional 600 W eclipse power required exceeds the SB 100 B payload capability. Two RITA ion thruster assemblies are envisaged. ESA

N89-19361# Katholieke Universiteit te Leuven (Belgium). Werktuigkunde Mechanische Konstructie en Produktie.
ERROR LOCALIZATION AND UPDATING OF SPACECRAFT STRUCTURES MATHEMATICAL MODELS Final Report
P. Sas, W. Heylen, T. Janter, C. Liefooghe, C. Stavrinidis, and E. Fissette Paris, France ESA Jun. 1988 131 p
(Contract ESTEC-1511/87-NL-PH)
(YMD/EF/0175; ESA-CR(P)-2667; ETN-89-93925) Avail: NTIS HC A07/MF A01

A procedure for updating finite element input data directly was developed. The method is formulated as a minimization problem, that can be approached with a linear, quadratic or nonlinear programming algorithm. For a highly underdetermined problem (far more variables than constraints), the traditional least squares approach is still applicable. The software was evaluated as to error localization, coupling analysis, loads and stress evaluation, and dynamic response computations, using beam, coil, and spacecraft structure examples. For all examples, the updating procedure improves the correlation between experimental and analytical results. The applied updating algorithms seem to be stable, and a limited number of iterations is generally sufficient for improving the finite element model. Although the applied updating technique was not developed especially for error localization, it is possible to draw conclusions from the update results for error localization if enough experimental information is included in the updating process. A substantial improvement for coupling analysis is obtained when using updated models. Dynamic and static response calculations are improved. ESA

N89-19362# Deutsche Forschungs- und Versuchsanstalt fuer Luft- und Raumfahrt, Oberpfaffenhofen (West Germany). Space Flight Dynamics Section.
INVESTIGATION OF FLIGHT SENSORS AND ACTUATORS FOR THE VIBRATION DAMPING AUGMENTATION OF LARGE FLEXIBLE SPACE STRUCTURES Final Report
Th. Lange, comp. Paris, France ESA May 1988 237 p
(Contract ESTEC-6902/86-NL-MAC(SC))
(ESA-CR(P)-2670; ETN-89-93926) Avail: NTIS HC A11/MF A01

Sensor and actuator hardware was analyzed with respect to a two-dimensional generic structural model representing a material processing platform on a large space structure. Two devices based on inertial control for vibration damping are presented. The Rotating Resonance InTegrating Accelerometer (RITA) is based upon a rotating pendulum to be applied for inertial acceleration measurement without any bias or stiction effect associated with ordinary servoed proof-mass accelerometers. The RITA features the suspension of the rotating proof-mass by a spring assembly tuned in resonance with the rotor spin frequency. Thus high measurement sensitivity and a high axial stiffness can be realized. The LInear Stepper Motor Actuator (LISA) is proposed as an alternative with respect to the pivoted proof-mass actuators. In LISA the proof-mass incorporates the motor coils, which are attached to a lightweight carriage by a spring/damper assembly. Thus high stepping rates with low switching times can be realized with relatively low motor power. This kind of proof-mass suspension damps out the high frequency noise level to a large extent. Semiactive hydraulic control methods utilizing the energy dissipation property of viscous fluids flowing through special surface treated pipes to increase the frictional effect are also presented. Due to the high weight penalty they are not suitable for structures represented by the box truss model but could be applied for structures extending over several hundred meters. This is due to the expected high damping forces requiring a smaller number of actuators and reducing the relative weight penalty. ESA

N89-19363# British Aerospace Public Ltd. Co., Stevenage (England). Space and Communications Div.
METEOSAT MILLIMETRE WAVE SOUNDER (MWS) STUDY Final Report
A. R. L. Tatnall and P. Foster Jun. 1988 610 p Prepared in cooperation with Farran Technology Ltd., Ballincolling, Ireland; Laben Space Instrumentation and Systems, Milan, Italy, TICRA

A/S, Lyngby, Denmark; Construcciones Aeronauticas SA, Madrid, Spain; and Alcatel Espace, Toulouse, France
(Contract ESA-7231/87-NL-JS)
(BAe-TP-9119; ESA-CR(P)-2698; ETN-89-93939) Copyright
Avail: NTIS HC A99/MF A01

For the Meteosat millimeter waver sounder (MSW) axisymmetric cassegrain and dual offset configurations were studied, because they were both compatible with the spacecraft constraints and they represent the best mechanical and electrical solutions respectively. An N-S location is most suitable for the dual spinner, but this spacecraft option is very difficult to accommodate. Location of the MSW on the Earth and E-W face of the spacecraft is compared. The major difference between the two options is the beam efficiency particularly at the lower frequency. For the dual offset configuration the most important degradation is due to spillover past the subreflector; whereas the cassegrain solution has degradation produced by spillover and blockage by the subreflector and the structs. Sensitivity of the two configurations is the same and is compatible with the requirements. Options to improve sensitivity include using a dual aperture system to improve RF demultiplexing losses (particularly attractive) and using a polarizing grid rather than a dichroic plate for channel separation. The beamwidth of both configurations can be made to meet the requirements although the dual offset configuration has a large main reflector for the same projected aperture. There is more likely to be a calibration error with the axisymmetric solution with the predicted performance, because more of the antenna pattern is likely to intersect the spacecraft or the Earth during cold calibration. ESA

N89-19364# Selenia Spazio S.p.A., Rome (Italy).
PSDE/SAT-2: PRELIMINARY SPACECRAFT CONFIGURATION STUDY, EXECUTIVE SUMMARY
Perrotta, Levrini, Manoni, Protto, Montedori, and Mazzini Paris, France ESA 1988 135 p
(Contract ESA-7574/88)
(ESA-CR(P)-2704; ETN-89-93942) Avail: NTIS HC A07/MF A01

The SAT-2 configuration for a 426 to 441 kg payload consisting of a laser single access (LSA), S-band single access (SSA), land mobile access (LAMEX), millimeter wave, and 20/30 GHz feeder link systems is presented. The system budget shows that this payload can be accommodated by SPACEBUS 100 B (EUTELSAT-2) with a mass margin of 90 kg. The selected (fairly balanced) configuration is characterized by the optical LSA terminal and the large electronically steered offset antenna used for S and L-band communication. The 80 percent transparent reflector is counter balanced by a solid 2 m reflector for LAMEX. A LOCSTAR payload was also envisaged for SAT-2 but the additional 600 W eclipse power required exceeds the SB 100 B payload capability. Two RITA ion thruster assemblies are envisaged. ESA

N89-19819*# National Aeronautics and Space Administration. Marshall Space Flight Center, Huntsville, AL.
SPACE STATION PAYLOAD OPERATIONS SCHEDULING WITH ESP2
Kenneth L. Stacy and John P. Jaap *In* NASA. Lyndon B. Johnson Space Center, 2nd Annual Workshop on Space Operations Automation and Robotics (SOAR 1988) Nov. 1988 p 7-13 (For primary document see N89-19817 12-59)
Avail: NTIS HC A22/MF A01 CSCL 22B

N89-19822*# National Aeronautics and Space Administration. Marshall Space Flight Center, Huntsville, AL.
AUTOMATION OF THE SPACE STATION CORE MODULE POWER MANAGEMENT AND DISTRIBUTION SYSTEM
David J. Weeks *In* NASA. Lyndon B. Johnson Space Center, 2nd Annual Workshop on Space Operations Automation and Robotics (SOAR 1988) Nov. 1988 p 25-29 (For primary document see N89-19817 12-59)
Avail: NTIS HC A22/MF A01 CSCL 22B

N89-19839*# Rome Air Development Center, Griffiss AFB, NY.
AUTONOMOUS SATELLITE COMMAND AND CONTROL: A COMPARISON WITH OTHER MILITARY SYSTEMS
Robert J. Kruchten and Wayne Todd *In* NASA. Lyndon B. Johnson Space Center, 2nd Annual Workshop on Space Operations Automation and Robotics (SOAR 1988) Nov. 1988 p 161-166 (For primary document see N89-19817 12-59)
Avail: NTIS HC A22/MF A01 CSCL 22B

N89-19852*# RCA Advanced Technology Labs., Moorestown, NJ.
AN INTELLIGENT INTERFACE FOR SATELLITE OPERATIONS: YOUR ORBIT DETERMINATION ASSISTANT (YODA)
Anne Schur *In* NASA. Lyndon B. Johnson Space Center, 2nd Annual Workshop on Space Operations Automation and Robotics (SOAR 1988) Nov. 1988 p 259-265 (For primary document see N89-19817 12-59)
Avail: NTIS HC A22/MF A01 CSCL 22B

N89-20066*# Prairie View Agricultural and Mechanical Coll., TX. Dept. of Mechanical Engineering.
MODEL FORMULATION OF NON-EQUILIBRIUM GAS RADIATION FOR HYPERSONIC FLIGHT VEHICLES Final Report
Ing Chang *In* NASA, Lyndon B. Johnson Space Center, National Aeronautics and Space Administration (NASA)/American Society for Engineering Education (ASEE) Summer Faculty Fellowship Program 1988, Volume 1 Feb. 1989 10 p (For primary document see N89-20058 12-99)
Avail: NTIS HC A09/MF A01 CSCL 22B

N89-20083*# Alabama A & M Univ., Normal. Dept. of Physics.
ESTIMATION OF VELOCITY PERTURBATIONS IN SATELLITE FRAGMENTATION EVENTS Final Report
Arjun Tan *In* NASA, Lyndon B. Johnson Space Center, National Aeronautics and Space Administration (NASA)/American Society for Engineering Education (ASEE) Summer Faculty Fellowship Program 1988, Volume 2 Feb. 1989 15 p (For primary document see N89-20073 12-99)
Avail: NTIS HC A09/MF A01 CSCL 22B

19 SPACECRAFT INSTRUMENTATION

For related information see also *06 Aircraft Instrumentation* and *35 Instrumentation and Photography.*

No abstracts in this category.

20 SPACECRAFT PROPULSION AND POWER

Includes main propulsion systems and components, e.g., rocket engines; and spacecraft auxilliary power sources.

For related information see also *07 Aircraft Propulsion and Power, 28 Propellants and Fuels, 44 Energy Production and Conversion,* and *15 Launch Vehicles and Space Vehicles.*

N89-19365* Battelle Columbus Labs., OH.
STUDIES AND ANALYSES OF THE SPACE SHUTTLE MAIN ENGINE. APPENDIX B: SSME FIPM DRAWINGS Final Report
31 Dec. 1987 142 p
(Contract NASw-3737)
(NASA-CR-183594; NAS 1.26:183594;
BCD-SSME-TR-87-3-App-B) Avail: Issuing Activity CSCL 21H

This appendix contains drawings of Space Shuttle main engine components. The titles of the engineering drawings are: heat exchanger, main injector, main combustion chamber, nozzle, fuel

preburner, oxidizer preburner, high-pressure fuel turbopump, high-pressure oxidizer turbopump, low-pressure fuel turbopump, and low-pressure oxidizer turbopump. NASA

N89-19366*# Boeing Aerospace Co., Seattle, WA.
BOOSTER PROPULSION/VEHICLE IMPACT STUDY Final Report, 1 Sep. 1987 - 30 Mar. 1988
Vincent Weldon, Michael Dunn, Lawrence Fink, Dwight Phillips, and Eric Wetzel Jun. 1988 574 p
(Contract NAS8-36944)
(NASA-CR-183584; NAS 1.26:183584; D180-30083) Avail: NTIS HC A24/MF A01 CSCL 21H

The use of hydrogen RP-1, propane, and methane as fuels for booster engines of launch vehicles is discussed. An automated procedure for integrated launch vehicle, engine sizing, and design optimization was used to define two stage and single stage concepts for minimum dry weight. The two stage vehicles were unmanned and used a flyback booster and partially reusable orbiter. The single stage designs were fully reusable, manned flyback vehicles. Comparisons of these vehicle designs, showing the effects of using different fuels, as well as sensitivity and trending data, are presented. In addition, the automated design technique utilized for the study is described. NASA

N89-19367*# Lockheed Missiles and Space Co., Huntsville, AL. Computational Mechanics Section.
DUCT FLOW NONUNIFORMITIES FOR SPACE SHUTTLE MAIN ENGINE (SSME) Final Report
30 Jun. 1988 155 p
(Contract NAS8-34507)
(NASA-CR-183595; NAS 1.26:183595; LMSC-HEC-TR-F225968) Avail: NTIS HC A08/MF A01 CSCL 21H

Analytical capabilities for modeling hot gas flow on the fuel side of the Space Shuttle Main Engines are developed. Emphasis is placed on construction and documentation of a computational grid code for modeling an elliptical two-duct version of the fuel side hot gas manifold. Computational results for flow past a support strut in an annular channel are also presented. NASA

N89-19368# R and D Associates, Alexandria, VA.
MPD (MAGNETOPLASMADYNAMIC) THRUST CHAMBER FLOW DYNAMICS Annual Technical Report, 1 Oct. 1987 - 30 Sep. 1988
30 Sep. 1988 28 p
(Contract F49620-86-C-0117)
(AD-A201263; RDA-TR-144200-002; AFOSR-88-1183TR) Avail: NTIS HC A03/MF A01 CSCL 21C

Magnetoplasmadynamic (MPD) arcjet thrusters inherently involve close coupling of the electromagnetic discharge structure and the flow field in the thrust chamber. The discharge and internal flow field structures are not simply determined by the arcjet geometry, but depend on the values and partitioning of injected mass flow for each operating current condition. In order to understand the internal flow dynamics of an MPD arcjet, experiments are performed in which electromagnetic fields and flow properties are measured within the thrust chamber. Electric and magnetic field probes are used to obtain the electromagnetic structure, while spectroscopic techniques are used to estimate particle velocities and densities. GRA

N89-19369# Edgerton, Germeshausen and Grier, Inc., Idaho Falls, ID.
SAFE, COMPACT NUCLEAR PROPULSION: SOLID CORE NUCLEAR PROPULSION CONCEPT Final Report, Oct. 1986 - Sep. 1987
Jack H. Ramsthaler, Gerry Farbman, Paul Harris, and Tal Sulmeisters Oct. 1988 310 p Prepared in cooperation with Idaho National Engineering Lab., Westinghouse Electric Corp., Rockwell International, Rocketdyne Div., and Martin Marietta
(Contracts DE-AC07-76ID-01570; AFAL-89-014; AF Proj. 3058)
(AD-A202339; EGG-ES-8093; AFAL-TR-88-033) Avail: NTIS HC A14/MF A01 CSCL 21F

The NERVA nuclear rocket engine was compared to an advanced nuclear electric engine as well as an advanced chemical engine for use in orbital transfer, and lunar and Mars missions. The NERVA stage had advantages over the chemical stage in payload, life cycle cost, and propellant consumption. The NERVA stage also had lower mission time requirements and life cycle cost compared to the nuclear electric stage. Fabrication of the NERVA stage does not require an extensive engine development program and demonstrated engine operating characteristics assure a reliable, flexible stage with a multiple mission capability. THe single propellant used in nuclear engines eliminates the combustion hazards associated with the use of dual propellants in space. Preliminary evaluations also indicated that varying the tankage used according to mission could reduce the cost of operating the nuclear engine. The open air engine tests used to develop the NERVA fuel and engine system are not environmentally acceptable today. A proposed alternate fuel development approach is to screen candidate fuel systems and conduct failure tests in test reactors. Such testing facilities are designed for testing of closed loop systems. Failure tests on full scale core segments could also be conducted closed loop in larger facilities. A full scale engine system qualification could be accomplished but the facility must be designed to shut down immediately at the first detection of fission product release. It is estimated that all non-nuclear components of the NERVA engine system could be qualified for engine testing within four years and depending on the problems encountered, cost could range from $55 to $180 million. GRA

N89-19370# Technische Univ., Hamburg (Germany, F.R.). Measurement Technology Group.
EXPERIMENTAL INVESTIGATION ON PLUME CONTAMINATION AND SURFACE EFFECTS, PHASE 2 Final Report, Jan. 1986 - Apr. 1987
H. Trinks, I. Bindemann, W. Ewering, and A. Girlich Paris, France ESA 15 Apr. 1987 209 p
(Contract ESTEC-6559/85-NL-PH(SC))
(TUHH-TRI-ESA-1987; ESA-CR(P)-2685; ETN-89-93934) Avail: NTIS HC A10/MF A01

Bipropellant and monopropellant thrusters in the range between 5N and 66N were investigated using the standard Exhaust Plume Analysis Procedure (EPAP). From the experimental findings, the procedure is improved leading to EPAP 2. Contamination effects were studied, and a corresponding Plume Surface Effect Analysis Procedure is established and verified by experiment. This procedure makes possible a realistic prediction of contamination effects and surface properties change using experimentally derived data as input to the theoretical code CONTAM SURFACE. ESA

N89-20063*# Louisiana Tech Univ., Ruston. Dept. of Electrical Engineering.
DEVELOPMENT OF PARALLEL ALGORITHMS FOR ELECTRICAL POWER MANAGEMENT IN SPACE APPLICATIONS Final Report
Frederick C. Berry *In* NASA, Lyndon B. Johnson Space Center, National Aeronautics and Space Administration (NASA)/American Society for Engineering Education (ASEE) Summer Faculty Fellowship Program 1988, Volume 1 Feb. 1989 9 p (For primary document see N89-20058 12-99)
Avail: NTIS HC A09/MF A01 CSCL 10B

23 CHEMISTRY AND MATERIALS (GENERAL)

N89-19371*# National Aeronautics and Space Administration. Lewis Research Center, Cleveland, OH.
TENSILE AND CREEP RUPTURE BEHAVIOR OF P/M PROCESSED Nb-BASE ALLOY, WC-3009
Mohan G. Hebsur (Sverdrup Technology, Inc., Cleveland, OH.) and Robert H. Titran Sep. 1988 12 p Presented at the TMS-AIME Fall Meeting, Chicago, IL, 25-28 Sep. 1988

(NASA-TM-101954; E-4311; NAS 1.15:101954) Avail: NTIS HC A03/MF A01 CSCL 20K

Due to its high strength at temperatures up to 1600 K, fabrication of niobium base alloy WC-3009 (Nb30Hf9W) by traditional methods is difficult. Powder metallurgy (P/M) processing offers an attractive fabrication alternative for this high strength alloy. Spherical powders of WC-3009 produced by electron beam atomizing (EBA) process were successfully consolidated into a one inch diameter rod by vacuum hot pressing and swaging techniques. Tensile strength of the fully dense P/M material at 300-1590 K were similar to the arc-melted material. Creep rupture tests in vacuum indicated that WC-3009 exhibits a class 1 solid solution (glide controlled) creep behavior in the 1480 to 1590 K temperature range and stress range of 14 to 70 MPa. The creep behavior was correlated with temperature and stress using a power law relationship. The calculated stress exponent n, was about 3.2 and the apparent activation energy, Q, was about 270 kJ/mol. The large creep ductility exhibited by WC-3009 was attributed to its high strain rate sensitivity. Author

24 COMPOSITE MATERIALS

Includes physical, chemical, and mechanical properties of laminates and other composite materials.

For ceramic materials see *27 Nonmetallic Materials*.

N89-19372# Naval Research Lab., Washington, DC.
COMPOSITE MATERIALS AT HIGH TEMPERATURES M.S. Thesis
Charles R. Bess Sep. 1988 64 p
(AD-A201163) Avail: NTIS HC A04/MF A01 CSCL 11D

An experimental investigation was made to determine the ultimate tensile strength and elastic modulus of IM6-3501-6 graphite epoxy laminated specimens exposed to temperatures from 70F to 600F. Specimens were layered (0), (90, 0), (90, 0, 90). The coupons used are candidate materials for advanced tactical missile airframe design. A Material Testing System (MTS) testing machine with 100,000 lb. maximum load capacity was used to apply the programmed uniaxial tensile loading. A Research Incorporated quad elliptical heating chamber, together with temperature and power controller, were used for maintaining the elevated temperatures. A Measurements Group data acquisition system 4000 was used for data acquisition and data reduction. The ultimate strength of the 12 plied composite specimen was determined at two temperatures, 70F and 138F. The failure of the grips precluded the determination of the modulus at higher temperatures. The overall modulus was obtained for the same type of specimen at several temperatures up to 400F. GRA

N89-19373# Southwest Research Inst., San Antonio, TX.
A NEW APPROACH TO THE EVALUATION OF THE EFFECTS OF STRESS STATE AND INTERFACIAL PROPERTIES ON THE BEHAVIOR OF ADVANCED METAL MATRIX COMPOSITES Final Report, 1 Feb. 1985 - 30 Sep. 1988
K. S. Chan and G. R. Leverant 30 Sep. 1988 6 p
(Contract DAAG29-85-K-0050)
(AD-A201246; ARO-21569.3-MS) Avail: NTIS HC A02/MF A01 CSCL 11D

The processing/microstructure/fracture properties relationships in fiber-reinforced Mg-alloy and Al-alloy composites have been characterized using mechanical testing, fractography, and Auger spectroscopy techniques. Fatigue crack growth mechanisms have also been identified, and the crack tip strain field and crack opening displacements measured using a stereoimaging technique. Local conditions for fiber and interface fracture have been determined as a function of fiber orientation. Relevant information of fracture mechanisms and failure criteria have been used to develop a 2-D fracture-mechanics-based micromechanical fatigue crack growth model. GRA

N89-19374# McDonnell Aircraft Co., Saint Louis, MO.
DURABILITY AND DAMAGE TOLERANCE OF BISMALEIMIDE COMPOSITES, VOLUME 1 Final Technical Report, 13 Sep. 1985 - 15 Jan. 1988
S. T. Tyahla and Paul S. McClellan, Jr. Jun. 1988 168 p
(Contract F33615-85-C-3212)
(AD-A201273; AFWAL-TR-88-3026-Vol-1) Avail: NTIS HC A08/MF A01 CSCL 11D

The evaluation of durability and damage tolerance of bismaleimide (BMI) composites is presented. BMI resins have been developed for structural applications in 350F to 450F environments. This represents an improvement over epoxy resin capability of approximately 100F. In Task 1 of this program, we experimentally evaluated two second generation BMI systems (IM6/3100 and IM6/F650) and compared their performances with those of the baseline systems AS1/3501-6 and T300/V378A. The intermediate modulus fiber IM6 was chosen as the common fiber for both material systems because its high strength and stiffness are properties that are important for future fighter design. In Task 2, basic material properties were determined. The data included moisture absorption, glass transition temperature, thermal spike susceptibility, lamina properties, and interlaminar fracture toughness test results. Lamina properties and fracture toughness test data were used to correlate laminate behavior exhibited in Task 3. GRA

N89-19375 Salford Univ. (England).
HEAT TRANSFER PROPERTIES OF SATELLITE COMPONENT MATERIALS Ph.D. Thesis
Stuart Donald McIvor 1988 150 p
Avail: Univ. Microfilms Order No. BRD-83072

The thermal conductivities of samples of unidirectional fibre reinforced composites were measured both perpendicular to and parallel to the fibres. Two types of samples were measured, Fibredux 914 resin reinforced with R-Glass fibres, and Code 69 resin reinforced with GY80 carbon fibres. A model has been produced which can be used to predict the thermal conductivity of any rectangular unidirectional fibre reinforced composite lamina. The model was constructed using a method of finite difference analysis performed by a computer program written in FORTRAN. Three samples of Code 69 resin reinforced with GY70 carbon fibres were produced with their fibres aligned at 30, 45, and 60 deg to the horizontal and their thermal conductivities measured. In order to examine the accuracy of the model the values of the conductivities of these samples were compared with those calculated using the model. The heat transfer properties of thermal blankets used to insulate satellites were investigated. The heat flow across blankets, placed in a thermal vacuum chamber and subjected to similar temperature differentials as would be found in Earth orbit, was measured and the values for the effective thermal conductance and the effective emissivity of the blankets calculated. Dissert. Abstr.

N89-19376 Cornell Univ., Ithaca, NY.
A MONTE CARLO SIMULATION OF THE SINGLE-FILAMENT-COMPOSITE TEST Ph.D. Thesis
Robert Brown Henstenburg 1988 188 p
Avail: Univ. Microfilms Order No. DA8821222

A Monte Carlo simulation is developed to provide a foundation for interpreting experimental data from the single-filament-composite test. The main focus is on developing an improved procedure for arriving at a realistic value for the shear strength of the fiber/matrix interface, but it is also shown how the test may be used to characterize the strength distribution of fibers at a length scale much shorter than is achievable in standard tension tests. The simulation is based on the widely used Poisson/Weibull probability model for fiber failure which characterizes the strength in terms of the random flaws distributed along the fiber. The primary mechanical model for stress buildup at the fiber end is the same as that assumed by most authors. A bilinear model was also considered which allows for a zone of debonding with a constant shear stress lower than in the primary plastic zone. This second model gives rise to a bilinear tensile

stress buildup in the fiber near a break. Simulation results are cast in terms of nondimensional variables and tabulated to allow for wide applicability. Sample size and confidence issues are also discussed. The Monte Carlo simulation results are then used to determine the interfacial shear strengths from some existing experimental data. These data consisted of the distribution of fiber fragment lengths from several single-filament-composite tests using carbon fiber in an epoxy matrix. Six different blends of epoxy, formulated to yield a wide range of stiffnesses, were used to study their effect on the interface. Dissert. Abstr.

N89-19377 Delaware Univ., Newark.
NONLINEAR VIBRATIONS OF COMPOSITE MATERIAL SHELLS Ph.D. Thesis
Yasuo Hirano 1988 151 p
Avail: Univ. Microfilms Order No. DA8824218

A nonlinear vibration analysis of composite circular cylinders, cylindrical panels and conical shells was performed. Influence of amplitude on frequency was studied for the large transverse deflection cases. Analysis begins with the derivation of governing equations of motion for composite shells of arbitrary shape. Galerkin's approximation method was applied to reduce those nonlinear partial differential equations to more feasible nonlinear ordinary differential equations which were subsequently analyzed by the Runge-Kutta method. The study includes the analysis of composite shells as well as isotropic shells. A soft spring type behavior was found for cylinders, panels and conical shells. It was found that the soft spring type behavior occurred within a limited amplitude and was followed by a hard spring type behavior as the amplitude increased further. Effects of anisotropy were revealed for any type of those shells. The influence of boundary conditions on the nonlinearity, about which very little is known, was also investigated. Comparison with the theoretical and experimental results by previous researchers was made. Qualitative agreement with experimental results was obtained.
Dissert. Abstr.

N89-19378# Utah Univ., Salt Lake City. Mechanics of Composites Lab.
CHARACTERIZATION OF IM7/8551-7 CARBON/EPOXY IN COMPRESSION AND SHEAR Final Report, Oct. 1987 - Sep. 1988
Stephen R. Swanson and Glenn E. Colvin, Jr. 27 Sep. 1988 16 p Prepared for Lawrence Livermore National Lab., CA
(Contract W-7405-eng-48)
(DE89-005544; UCRL-21135) Avail: NTIS HC A03/MF A01

This is a final report on a project entitled Characterization of IM7/8551-7 Carbon/Epoxy in Compression and Shear, for the period October 1987 to September 1988. The intent of this program is to determine the failure properties of carbon/epoxy laminates under multiaxial stress loadings, with particular emphasis on loadings involving compressive stresses. The work accomplished to date is summarized here, in the form of two published papers and a summary of other work. Appendix C contains a summary of the development of the multiaxial compression test fixture. DOE

N89-19379# McDonnell Aircraft Co., Saint Louis, MO.
DURABILITY AND DAMAGE TOLERANCE OF BISMALEIMIDE COMPOSITES. VOLUME 2: APPENDIX OF CRACK GROWTH AND LOW-VELOCITY IMPACT DATA Final Technical Report, 13 Sep. 1985 - 15 Jan. 1988
S. T. Tyahla and Paul S. McClellan, Jr. Jun. 1988 242 p
(Contract F33615-85-C-3212)
(AD-A201839; AFWAL-TR-88-3026-Vol-2) Avail: NTIS HC A11/MF A01 CSCL 11D

This program was the evaluation of durability and damage tolerance of bismaleimide (BMI) composites. BMI resins have been developed for structural applications in 350 F to 450 F environments. The represents an improvement over epoxy resin capability of approximately 100 F. In Task 1 of this program we experimentally evaluated two second generation BMI systems (IM6/3100 and IM6/F650) and compared their performance with that of baseline systems AS1/3501-6 and T300/V378A. The intermediate modulus fiber IM6 was chosen as the common fiber for both material systems because its high strength and stiffness are properties that are important for future fighter design. In Task II basic material properties were determined. The data included moisture absorption, glass transition temperature, thermal spike susceptibility, lamina properties, and interlaminar fracture toughness test results. Lamina properties and fracture toughness test data were used to correlate laminate behavior exhibited in Task III.
GRA

N89-19380# Naval Postgraduate School, Monterey, CA.
COMPOSITE RELIABILITY ENHANCEMENT VIA RELOADING M.S. Thesis
Mark C. Jones Sep. 1988 160 p
(AD-A201861) Avail: NTIS HC A08/MF A01 CSCL 11D

Composite strength is an inverse function of the size of the composite. As the use of composites expands into larger applications, such as airplane wings, missile components and ship superstructures the ability to accurately predict composite performance for large applications has become more important. The composite failure process is sequential and initiates with early breaking of the weak fibers. Concentration of breakage sites accumulate and lead to ultimately catastrophic failure. Prestressing fibers prior to solidification of the matrix has been demonstrated to increase the reliability of the composite by minimizing the spatial concentration of the breakage sights. This study concentrates on quantifying the level of preload and gauge length to optimize the prestress effect. Computer simulations of graphite bundle tests were used to validate actual AS-4 graphite bundle tests. The simulations were then extended to predict prestress performance.
GRA

N89-19381# Naval Postgraduate School, Monterey, CA.
FINITE ELEMENT ANALYSIS OF LAMINATED COMPOSITE PLATES M.S. Thesis
Myung-Ha Lee Sep. 1988 72 p
(AD-A202192) Avail: NTIS HC A04/MF A01 CSCL 13M

A biquadratic isoparametric plate/shell bending finite element is developed to study the behavior of isotropic and laminated composite plates. The element is based an Mindlin-Reissner's theory and the principle of virtual displacements. The element is implemented in a computer program. Results are presented and compared with analytical solutions to validate this element. Good agreement is observed for thin plates, while discrepancies are noted for thick plates. Effects of various integration schemes on the element performance are presented. Convergence studies for laminated composites for different fiber orientations are also discussed. GRA

N89-19382# Rolls-Royce Ltd., Derby (England). Composites Research and Development Group.
THERMAL CYCLING AND MECHANICAL PROPERTY ASSESSMENT OF CARBON FIBER (FABRIC) REINFORCED PMR-15 POLYIMIDE LAMINATES
G. A. Owens and S. E. Schofield 22 Jul. 1988 26 p Presented at the 6th International Conference on Composite Materials, London, England, 22-29 Jul. 1987
(PNR90522; ETN-89-93698) Copyright Avail: NTIS HC A03/MF A01

The effects on carbon fiber/PMR-15 polyimide mechanical properties of prolonged thermal cycling representative of a specific component application, and the resulting crack distribution within the laminate were studied. Potential life limitations were also addressed with respect to subsequent fatigue and aging behavior. The effects of absorbed moisture were also investigated. Thermal cycling produces microcracks initially in the outer laminate plies until a stress-relieved state is achieved. Continued cycling results in cracking of the inner plies. No evidence of a crack intensity plateau is observed at 5000 thermal cycles. Microcracking of the inner plies reduces matrix-dominated (compression and shear) residual strengths at RT and 232 C, although the effects are less pronounced at 232 C. Microcracking has no effect on fiber-dominated properties. A limited number of thermal cycles to

even lower temperatures (minus 55 C) can be tolerated by already cycled laminates without significant further detrimental effect. Isothermal aging after thermal cycling produces further microcracking in the inner plies, with associated further reduction in matrix-dominated residual strengths. This increased level of microcracking does not, however, produce additional weight loss after 1000 hr isothermal aging at 232 C. Thermal cycling of cracked samples having 1 percent moisture content gives no significant increase in microcracking compared to relatively dry samples.

ESA

N89-19383# Utah Univ., Salt Lake City. Dept. of Mechanical Engineering.

MEASUREMENTS OF THE COMPRESSIVE BEHAVIOR OF AS4/3501-6 AND IM7/8551-7 CARBON/EPOXY

Stephen R. Swanson, G. E. Colvin, Jr., and C. L. Haslam 1988 12 p Presented at the 33rd Symposium and Exhibit on Materials and Processes for All Industries: Materials-Pathway To the Future, Anaheim, CA, 7 Mar. 1988 Previously announced in IAA as A88-42428 Prepared in cooperation with Hercules Aerospace Corp., Magna, UT

(Contract W-7405-eng-48)

(DE89-005823; CONF-880312-2) Avail: NTIS HC A03/MF A01

The compressive strength of carbon/epoxy materials is of importance in design, and is typically somewhat lower than the strength in tension. The measurement of compressive strength has been subject to some uncertainty, as different experimental techniques can give somewhat different results. A new specimen for the determination of compressive strength has been developed, based on compression of a 38 mm (1.5 in) diameter tube. The tube has been designed to prevent overall structural buckling and also to minimize end effects. This and a larger tubular specimen have been utilized to determine the compressive strength of AS4/3501-6 and IM7/8551-7 carbon/epoxy prepregs. The results are compared with previous tests, indicating that the results are relatively independent of the test specimen. The comparison also supports a criterion for laminate failure prediction reported previously.

DOE

N89-19384# Oak Ridge National Lab., TN.

REINFORCEMENT/MATRIX INTERACTION IN SiC FIBER-REINFORCED Ni3Al MATRIX COMPOSITES

J.-M. Yang, W. H. Kao, and C. T. Liu 1988 6 p Presented at the Fall Meeting of the Materials Research Society, Boston, MA, 28 Nov. 1988

(Contract DE-AC05-84OR-21400)

(DE89-006041; CONF-881155-37) Avail: NTIS HC A02/MF A01

The interfacial reaction characteristics of two different types of SiC fibers with Ni3Al (Ni-Al-Cr-Zr-B) matrix have been investigated. The microstructure and chemical compositions across the reaction zones have been analyzed quantitatively using microscopy and electron probe microanalysis. In both types of SiC/Ni3Al composites, it was found that Ni was the dominant diffusing species responsible for the overall reaction. The C-rich layer outside the SCS-6 fiber provided an incubation period, but could not stop the inward diffusion of Ni. It could, however, effectively stop the diffusion of Al, Zr, and Cr. No significant increase in reaction zone thickness after exposure at temperatures below 900 C for up to 100 hours was observed. When the C-rich layer was depleted, a rapid increase in reaction zone thickness and the formation of multilayer reaction products occurred. In the case of Sigma/Ni3Al composite, extensive reaction between the fiber and the matrix occurred at all the temperatures studied. Diffusion barrier coating for both types of fibers is required to develop nickel aluminide matrix composites.

DOE

N89-19385*# National Aeronautics and Space Administration. Langley Research Center, Hampton, VA.

THE EFFECTS OF SIMULATED SPACE ENVIRONMENTAL PARAMETERS ON SIX COMMERCIALLY AVAILABLE COMPOSITE MATERIALS

Joan G. Funk and George F. Sykes, Jr. Apr. 1989 34 p (NASA-TP-2906; L-16549; NAS 1.60:2906) Avail: NTIS HC A03/MF A01 CSCL 11D

The effects of simulated space environmental parameters on microdamage induced by the environment in a series of commercially available graphite-fiber-reinforced composite materials were determined. Composites with both thermoset and thermoplastic resin systems were studied. Low-Earth-Orbit (LEO) exposures were simulated by thermal cycling; geosynchronous-orbit (GEO) exposures were simulated by electron irradiation plus thermal cycling. The thermal cycling temperature range was -250 F to either 200 F or 150 F. The upper limits of the thermal cycles were different to ensure that an individual composite material was not cycled above its glass transition temperature. Material response was characterized through assessment of the induced microcracking and its influence on mechanical property changes at both room temperature and -250 F. Microdamage was induced in both thermoset and thermoplastic advanced composite materials exposed to the simulated LEO environment. However, a 350 F cure single-phase toughened epoxy composite was not damaged during exposure to the LEO environment. The simuated GEO environment produced microdamage in all materials tested.

Author

25 INORGANIC AND PHYSICAL CHEMISTRY

Includes chemical analysis, e.g., chromatography; combustion theory; electrochemistry; and photochemistry.

For related information see also *77 Thermodynamics and Statistical Physics.*.

N89-19386 Georgia Inst. of Tech., Atlanta.

THE ANALYTICAL MODELING OF A TURBULENT DIFFUSION FLAME BEHIND A BACKWARD FACING STEP Ph.D. Thesis

Fang-Hei Tsau 1988 174 p

Avail: Univ. Microfilms Order No. DA8820831

Turbulent combustion flow fields behind a backward facing step are studied with various computational assumptions by using different boundary conditions. The degree of complexity of the problem increases as one relaxes the computational assumptions which consist of: (1) chemical equilibrium flow with species fluctuations neglected, (2) chemical equilibrium flow with species fluctuations taken into account, and (3) finite kinetic rate model with species fluctuations taken into account. A conventional high Reynolds number model using a law of the wall submodel as boundary conditions and a recently developed low Reynolds number model employing available experimental information in the near wall region are tested, respectively. When species fluctuations are taken into account in numerical simulations, two different statistical models are postulated and incorporated in the combustion models for this investigation to examine the effects on the species concentrations and the temperature field. The effects of combustion on the flow are also studied.

Dissert. Abstr.

N89-19387# Washington Univ., Seattle.

GAS HYDRATES THERMOMECHANICS Final Report

R. C. Corlett Apr. 1988 45 p

(Contract DE-AC21-84MC-21180)

(DE88-010280; DOE/MC-21180/2617) Avail: NTIS HC A03/MF A01

Solid CH4 hydrate samples can be built up by pulses of water spray onto a solid surface in a CH4 atmosphere at temperature and pressure within the hydrate stability domain. By pulse spraying into a cylindrical well, clean cylindrical samples approximately 4 cm diameter by 2.5 cm long can be obtained. There have been found experimentally simple means to achieve for such a cylindrical sample axial stress in excess above the radial and azimuthal stress imposed by gas pressure on the lateral face or excess radial and azimuthal stress above axial stress imposed by gas pressure on the end face. When uniaxially loaded

on the end faces, the samples have very little strength, crushing or fracturing at excess axial stress less than 0.2 MPa, at temperatures above 0 deg C, but can withstand at least 2 MPa at temperatures below 0 deg C. These results suggest that stress anisotropy is not a significant factor in the thermomechanics behavior of gas hydrates at temperatures above 0 deg C. Samples can be temporarily depressurized below the stability envelope at temperatures below 0 deg C and then be repressurized and have temperature raised above 0 deg C without any change of appearance, whereas, at temperatures above 0 deg C, samples decompose and dramatically alter in appearance upon depressurization below the stability envelope. DOE

N89-19388# California Univ., Berkeley.
THE COUPLED CLUSTER METHOD AND THE PROPERTIES OF ENERGETIC MATERIALS Final Report, 15 May 1986 - 14 May 1988
Henry F. Schaefer, III Sep. 1988 4 p
(Contract DAAL03-86-K-0077)
(AD-A201168; ARO-24083.8-CH) Avail: NTIS HC A02/MF A01 CSCL 07B

This research had two goals, the development of coupled cluster theory and the application of molecular electronic structure theory to the alkali dioxide molecules LiO2, NaO2, and KO2. The research on coupled cluster theory was successful. It was possible to take the single and double excitation coupled cluster method (CCSD) from an exotic, fringe technique to the very center of applied quantum chemistry. Critical to this remarkable transformation was the formulation of an analytic gradient method for the CCSD method. A sustained effort on the LiO2 and NaO2 molecules was begun, however, unusual difficulties (specifically symmetry-breaking) were discovered for LiO2. However, all these problems were eventually solved, resulting in a massive and truly definitive paper, to be submitted for publication very shortly. Work using the same methods is well underway for NaO2. GRA

N89-19389# Center for Naval Analyses, Alexandria, VA. Naval Warfare Analysis Group.
REACTION CHEMISTRY OF BORON HYDRIDES Final Report, 11 Sep. 1984 - 4 Feb. 1987
H. H. Nelson Sep. 1988 5 p Presented at the JANNAF Panel on Kinetic and Related Aspects of Propellant Combustion Chemistry, Laurel, MD, 2-4 May 1988 Submitted for publication
(AD-A201243; TR-7) Avail: NTIS HC A02/MF A01 CSCL 19A

We have recently begun a program of boron chemistry in the chemistry division at NRL. Our initial efforts have involved investigations with the room temperature reactions of BH3 and BH with various oxidants and hydrocarbons. In conjunction with the gas phase experimental work, we are pursuing a computational study of the heats of formation of boron compounds and reaction energetics. In addition, there is a compound of the program emphasizing the heterogenous chemistry of boron oxides. GRA

N89-19390# Wisconsin Univ., Madison. Center for Mathematical Sciences.
INTERDISCIPLINARY RESEARCH IN VISCOELASTICITY AND RHEOLOGY Annual Technical Report, 1 May 1987 - 31 May 1988
David S. Malkus, John A. Nohel, Robert C. Rogers, and Athannassios E. Tzavaras 22 Jun. 1988 9 p
(Grant AF-AFOSR-0191-87; AF Proj. 2304)
(AD-A201270; AFOSR-88-1189TR) Avail: NTIS HC A02/MF A01 CSCL 20D

Viscoelastic materials with fading memory exhibit behavior that is intermediate between the nonlinear hyperbolic response of purely elastic solids and the strongly diffusive, parabolic response of viscous fluids. The primary objective of current research is the modeling, analysis and computation of unsteady motions of viscoelastic materials with fading memory. During the first year of funding, progress has been made in: (1) Understanding spurt phenomena occurring in shearing flows of viscoelastic fluids; computational results for the unsteady equations produce qualitative and quantitative agreement with careful experimental results; (2) Understanding of weak solutions which are sufficiently broad to include shocks and acceleration waves. In (1), significant progress is being realized through insight gained from an interplay between careful numerical experiments and analysis. GRA

N89-19391# Colorado Univ., Boulder.
A FUNDAMENTAL MATHEMATICAL THEORY IN THE DYNAMICS OF COMBUSTION PROCESSES Final Report, 1 Aug. 1985 - 31 May 1988
J. Bebernes and D. R. Kassoy 8 Oct. 1988 20 p
(Contract DAAG29-85-K-0209)
(AD-A201284; CUCOMB-3; ARO-22520.10-MA) Avail: NTIS HC A03/MF A01 CSCL 21B

This research project has emphasized the formulation of rational mathematical models for transient and steady combustion processes. In particular thermal explosions, detonation wave initiation and high speed combustion waves have been examined. In each case the describing mathematical system is analyzed using both formal and constructive techniques. The former are employed to consider issues of existence and uniqueness, solution bonds and general trajectory properties. Constructive solution development is based on a combination of asymptotic and numerical methods. This hybrid approach to the study of combustion problems has permitted us to develop both a rigorous and quantitative understanding of complex, initial-boundary value problems. This report contains a summary description of each of the 15 papers contributed by the research group. GRA

N89-19392# Georgia Inst. of Tech., Atlanta. School of Aerospace Engineering.
FLAME DRIVING OF LONGITUDINAL INSTABILITIES IN LIQUID FUELED DUMP COMBUSTORS Final Report, 1 Jul. 1984 - 29 Feb. 1988
Ben T. Zinn, Uday G. Hegde, Dierk Reuter, and B. R. Daniel 1 Oct. 1988 126 p
(Contract N00014-84-K-0470)
(AD-A201293) Avail: NTIS HC A07/MF A01 CSCL 21E

This report describes the results of experimental and theoretical investigations of the mechanisms by which the core flow combustion process in coaxial, single inlet, dump type ramjet engines drives longitudinal combustion instabilities. To this end, the behavior of V-shaped flames, similar to those often occurring in ramjet combustors, stabilized in longitudinal acoustic fields has been studied. The presence of burning vortical structures is observed in the flame region. These structures appear at frequencies close to the first natural acoustic frequency of the combustor and are believed to be connected with a shear layer type of instability of the flame. Experiments conducted show that the unsteady combustion in these structures is capable of driving the acoustics at the fundamental acoustic mode frequency. With increase in fuel air ratio, a spontaneous instability involving the fundamental mode is observed and explained in terms of increased driving associated with the higher, unsteady heat release rates. GRA

N89-19393# University of Northern Illinois, De Kalb. Dept. of Chemistry.
INVESTIGATION OF THE INTERFACE BETWEEN TWO IMMISCIBLE ELECTROLYTES APPLIED TO MEMBRANE ELECTROCHEMISTRY Annual Report, 15 Oct. 1987 - 14 Oct. 1988
Petr Vanysek 13 Oct. 1988 10 p
(Contract N00014-88-K-0075; RR04108)
(AD-A201310; Rept-36-6008480) Avail: NTIS HC A02/MF A01 CSCL 07D

Four experimental studies were performed in the previous period: Effect of protein adsorption on capacitance of water/nitrobenzene interface, potentiometric study of fluorescent oxacyanine cation partitioning, frozen interfaces and microinterfaces. The most valuable experimental technique in use is impedance spectroscopy in the frequency range from 1 Hz to 65 kHz. Currently a new nonlinear least square software for data

evaluation is being utilized. In the study of oxacyanine dyes, both experimental and computational potentiometry were used. The results provided more insight in interfacial potential behavior. The contribution was particularly significant in providing large set of data previously unpublished. Liquid/liquid microinterface is in its initial stage of investigation. The phenomenon similar to microelectrodes is clearly present, current work is aimed at reproducibility. GRA

N89-19394# Birmingham Univ. (England).
ION AND ELECTRON INTERACTIONS AT THERMAL AND SUPRATHERMAL ENERGIES
David Smith, Nigel G. Adams, and Charles R. Herd 30 Sep. 1988 74 p
(Grant AF-AFOSR-0355-87; AF Proj. 2303)
(AD-A201418; AFGL-TR-88-0295; SR-1) Avail: NTIS HC A04/MF A01 CSCL 07D

The flowing afterglow/Langmuir probe (FALP) and the selected ion flow drift tube (SIFDT) apparatuses have been used to study dissociative electron attachment reactions of several organo-halogen molecules, including the unstable radical species CCl3 and CCl2Br. Dissociative recombination reactions of several polyatomic positive ions, and preliminary data on the neutral products of several such reactions are reported, as well as the proton affinities of several molecular species and the collisional breakup of C2H5OH2(+) ions. GRA

N89-19395# Utah Univ., Salt Lake City. Dept. of Chemistry.
ION PAIR SOLVATION Final Report, 1 Jul. 1984 - 30 Jun. 1988
Jack Simons 21 Sep. 1988 5 p
(Contract DAAG29-84-K-0086)
(AD-A201529; ARO-21401.14-CH) Avail: NTIS HC A02/MF A01 CSCL 07D

New tools for the computational simulation of ion and ion pair dynamics in the gas phase and in solution have been developed. Both classical and quantum mechanical methods were explored. Monte Carlo techniques for incorporating thermodynamic equilibrium effects of surrounding solvent molecules have been incorporated into the computer codes. New techniques for computing highly accurate weak interaction energies among anions and solvent molecules have been developed and tested. GRA

N89-19396# Pittsburgh Univ., PA. Surface Science Center.
THE DISSOCIATIVE ADSORPTION OF AMMONIA ON Si(100)
P. A. Taylor, R. M. Wallace, W. J. Choyke, M. J. Dresser (Washington State Univ., Pullman.), and J. T. Yates, Jr. 14 Dec. 1988 19 p
(Contract N00014-82-K-0280)
(AD-A201599; TR-19) Avail: NTIS HC A03/MF A01 CSCL 07B

The nature of the NH3 adsorption process on Si(100) at 120 K was studied by isotopic mixing with adsorbed atomic deuterium and thermal desorption spectroscopy. NH3 was found to dissociatively absorb onto Si(100) dimers sites at 120 K as NH2(a) and H(a). The NH2(a) species persist up to about 700 K where two reaction channels become available. The major reaction channel leads to the decomposition of NH2(a) to N(a) and H(a). The minor channel is a recombination reaction that leads to the desorption of ammonia. This recombination reaction exhibits a deuterium kinetic isotope effect. GRA

N89-19397# Pittsburgh Univ., PA. Surface Science Center.
THE ADSORPTION AND DECOMPOSITION OF NH3 ON Si(100): DETECTION OF THE NH2(a) SPECIES
M. J. Dresser (Washington State Univ., Pullman.), P. A. Taylor, R. M. Wallace, W. J. Choyke, and J. T. Yates, Jr. 14 Dec. 1988 70 p
(Contract N00014-82-K-0280)
(AD-A201601; TR-20) Avail: NTIS HC A04/MF A01 CSCL 07B

The dissociative adsorption of NH3 on Si(100)(2x1) has been studied using accurate coverage measurements, temperature programmed desorption, Auger spectroscopy and digital ESDIAD/LEED methods. It has been found that NH2 surface species (amino species) are produced to a saturation coverage of 1 NH2/Si dimer at 120 K. This is accompanied by the production of a Si-H surface species. Digital ESDIAD measurements of the H+ angular distribution from NH2(a) species indicate that torsional oscillations about the Si-NH2 bond are responsible for the characteristic elliptical H+ pattern whose long axis is perpendicular to the Si-Si dimer bond direction. It has been shown that NH3 dissociatively adsorbs with unity sticking probability at 120 K up to 86 percent of full coverage, indicative of a mobile precursor adsorption mechanism. The pre-adsorption of atomic H onto the Si dangling bond sites reduces the adsorptive capacity of the Si(100) surface, and 1 H/Si completely passivates the surface for NH3 chemisorption. GRA

N89-19398# California Inst. of Tech., Pasadena.
APPLICATIONS OF SCANNING TUNNELING MICROSCOPY TO ELECTROCHEMISTRY Technical Report, Sep. 1987 - Aug. 1988
Moris M. Dovek, Michael J. Heben, Nathan S. Lewis, Reginald M. Penner, and Calvin F. Quate 28 Oct. 1988 31 p
(Contract N00014-85-K-0805)
(AD-A201613; TR-1) Avail: NTIS HC A03/MF A01 CSCL 07D

The Scanning Tunneling Microscope (STM) has demonstrated unique capabilities for the examination of electrode topography, the vibrational spectroscopic imaging of surface adsorbed species, and the high resolution electrochemical modification of conductive surfaces. Here we discuss recent progress in electrochemical STM. Included are a comparison of STM with other ex situ and in situ surface analytic techniques, a discussion of relevant STM design considerations, and a semi-quantitative examination of faradaic current current contributions for STM at solution-covered surfaces. Applications of STM to the ex situ and in study of electrode surfaces are presented. GRA

N89-19399# Ballistic Research Labs., Aberdeen Proving Ground, MD.
SPECTRAL STUDIES OF PROPELLANT COMBUSTION: EXPERIMENTAL DETAILS AND EMISSION RESULTS FOR M-30 PROPELLANT Final Report, Jun. 1987 - Jun. 1988
John A. Vanderhoff Dec. 1988 29 p
(AD-A201634; BRL-TR-3714) Avail: NTIS HC A03/MF A01 CSCL 21B

A windowed strand burner has been constructed and used to characterize the steady state burning of propellants at moderate pressure using UV visible spectroscopic techniques. Emission spectroscopy has been performed on a triple base propellant (M-30) and three reactive transient combustion species (CN, NH and OH) have been profiled over a pressure range from 0.66 to 1.5 MPa. Reaction zone lengths on the order of 1 mm were determined from the CN and NH profiles. The strand burner is expected to be useful for future planned absorption and laser induced fluorescence studies on a variety of propellants. GRA

N89-19400# Pittsburgh Univ., PA. Dept. of Chemistry.
VIBRATIONAL SPECTROSCOPIC STUDIES OF SURFACE CHEMICAL INTERACTIONS IN CHEMISORPTION AND CATALYSIS Annual Progress Report
J. T. Yates, Jr. 31 Dec. 1988 3 p
(Contract DE-FG02-88ER-13864)
(DE89-005896; DOE/ER-13864/1) Avail: NTIS HC A02/MF A01

Vibrational spectroscopy, applied to the study of surface chemistry, is able to give detailed information about the structure and interactions of surface species at a level of sensitivity which is unrivaled by most other surface measurement methods. This work utilizes three different vibrational spectroscopic methods to study surface chemistry on both single crystal and supported metal catalyst surfaces. These methods are: (1) Reflection IR Spectroscopy, (2) Transmission IR Spectroscopy, and (3) High Resolution Electron Energy Loss Spectroscopy (HREELS). Current

activities include the construction of a novel FT Reflection IR Instrument with rapid background acquisition and subtraction procedures. Transmission IR studies on the behavior of absorbed hydrocarbon species are underway in a unique high temperature-low temperature cell. Here, an unusual ability of C-H bonds from butadiene-derived species on Rh has been observed spectroscopically. HREELS studies of model oxide-supported metal catalysts have been initiated and promise to give unique information about the nature of metal support interactions. DOE

N89-19401# Colorado School of Mines, Golden. Dept. of Physics.
FUNDAMENTAL OPTICAL STUDIES OF COMPETITIVE ADSORPTION AND THIN FILM PHENOMENA Progress Report, 1 Jul. 1986 - 31 Dec. 1988
T. E. Furtak Dec. 1988 19 p
(Contract DE-FG02-86ER-45253)
(DE89-005898; DOE/ER-45253/3) Avail: NTIS HC A03/MF A01

We have concentrated on understanding the mechanisms of unusual surface optical phenomena that show potential of development as tools for study of the electrolyte-solid interface. Our work has revealed the origin of the chemical component of surface enhanced Raman scattering (SERS). This was found to be concentrated at small Ag clusters, upon which special adsorption can take place and within which electronic resonance operates to increase the Raman cross section. Optical second harmonic generation (SHG) was studied with regard to its ability to determine the symmetry of adsorbed metal monolayers. Success was achieved in the cases of Cd, Tl, and Zn on Ag(111). Each example is unique, demonstrating a range of phenomena and showing how SHG can be used as an interfacial probe. Initiatives were generated in scanning tunneling microscopy and reflectance spectroscopy. Together these techniques have given us a powerful capability to examine the microscopic details of the electrolyte-solid interface. DOE

N89-19402*# National Aeronautics and Space Administration. Lewis Research Center, Cleveland, OH.
ACIDIC ATTACK OF PERFLUORINATED ALKYL ETHER LUBRICANT MOLECULES BY METAL OXIDE SURFACES
Michael J. Zehe and Owen D. Faut 1989 17 p Proposed for presentation at the Joint Tribology Conference, Fort Lauderdale, FL, 16-19 Oct. 1989; sponsored by STLE and ASME
(NASA-TM-101962; E-4660; NAS 1.15:101962) Avail: NTIS HC A03/MF A01 CSCL 07D

The reactions of linear perfluoropolyalkylether (PFAE) lubricants with alpha-Fe2O3 and Fe2O3-based solid superacids were studied. The reaction with alpha-Fe2O3 proceeds in two stages. The first stage is an initial slow catalytic decomposition of the fluid. This reaction releases reactive gaseous products which attach the metal oxide and convert it to FeF3. The second stage is a more rapid decomposition of the fluid, effected by the surface FeF3. A study of the inital breakdown step was performed using alpha-Fe2O3, alpha-Fe2O3 preconverted to FeF3, and sulfate-promoted alpha-Fe2O3 superacids. The results indicate that the breakdown reaction involves acidic attack at fluorine atoms on acetal carbons in the linear PFAE. Possible approaches to combat the problem are outlined. Author

N89-19403# Colorado Univ., Boulder. Dept. of Chemistry and Biochemistry.
STUDIES OF HYDROGEN-HYDROGEN AND CARBON-SULFUR BOND CLEAVAGE Progress Report, Aug. 1986 - Jul. 1989
M. R. DuBois 1989 16 p
(Contract DE-FG02-85ER-13451)
(DE89-006116; DOE/ER-13451/4) Avail: NTIS HC A03/MF A01

The primary goals of research were to synthesize new cationic dinuclear complexes and to further characterize the novel reactivity of the cations with hydrogen. These studies were proposed to have potential for providing relevant homogeneous models for hydrogen activation and hydrogenolysis reactions on molybdenum sulfide surfaces. Results in the following areas are discussed: synthesis of cations; reaction of the methylthiolate cation with H sub 2 to form a neutral derivative with an SH ligand; hydrogen activation as a function of thiolate substituent; effect of base on reactions; kinetics of hydrogen activation; reactions of Mo complexes with acyl halides and hydrogen; reactions of hydrogen with cations containing unsaturated thiolate; cation studies with a thiolate substituent; one electron reduction of cations; reactions of cations with nucleophiles; and oxidation chemistry. DOE

N89-19404# California Univ., Berkeley. Lawrence Berkeley Lab. Materials and Chemical Sciences Lab.
SCANNING TUNNELING MICROSCOPY OF METALS ON GRAPHITE Ph.D. Thesis
Eric David Ganz Aug. 1988 193 p Prepared in cooperation with California Univ., Berkeley
(Contract DE-AC03-76SF-00098)
(DE89-006608; LBL-25323) Avail: NTIS HC A10/MF A01

The use of scanning tunneling microscopy of gold and thin copper films on graphite is described. Discussions of the equipment, modifications of a gold surface, deformation of a graphite surface image interpretations, imaging of metal clusters on graphite in air and UHV, imaging of small two dimensional and three dimensional islands on graphite, and dynamics are included. DOE

N89-19687 Witten/Herdecke Univ. (Germany, F.R.). Inst. for Inorganic Chemistry.
KINETICS AND MECHANISM OF THE Fe CATALYZED AUTOXIDATION OF S(4)-OXIDES IN AQUEOUS SOLUTION
J. Kraft, M. Dellert, P. Braun, and R. vanEldik *In* Deutscher Wetterdienst, Annals from the German Meteorological Society, No. 25: 10th International Cloud Physics Conference Preprints, Volume 1 1988 p 246-247 (For primary document see N89-19605 12-42)
Copyright Avail: Deutscher Wetterdienst, Frankfurter Strasse 135, D-6050 Offenbach am Main, Fed. Republic of Germany

N89-20085*# Northeastern Univ., Boston, MA. Dept. of Chemical Engineering.
ARC JET DIAGNOSTICS TESTS Final Report
Ronald J. Willey *In* NASA, Lyndon B. Johnson Space Center, National Aeronautics and Space Administration (NASA)/American Society for Engineering Education (ASEE) Summer Faculty Fellowship Program 1988, Volume 2 Feb. 1989 15 p (For primary document see N89-20073 12-99)
Avail: NTIS HC A09/MF A01 CSCL 07D

26 METALLIC MATERIALS

Includes physical, chemical, and mechanical properties of metals, e.g., corrosion; and metallurgy.

N89-19405# Illinois Univ., Urbana. Dept. of Materials Science and Engineering.
ANOMALOUS SLIP IN AN FCC SYSTEM
T. C. Lee, I. M. Robertson, and H. K. Birnbaum 1988 13 p Presented at the Conference on Frontiers of Electron Microscopy, Chicago, IL, 1 Apr. 1988
(Contract DE-AC02-76ER-01198)
(DE89-002257; CONF-8804232-1) Avail: NTIS HC A03/MF A01

During in-situ TEM deformation of 310 stainless steel, it has been observed that a/2(110) axes dislocations are glissile on the (121) planes as well as on the more common (111) planes. The (121) slip plane was initiated by a grain-boundary dislocation source to relieve the stress concentrated on a grain boundary by a dislocation pile-up. This preference of slip on a (121) plane over a (111) plane can be understood by considering, in addition to the magnitude of the resolved shear stress on the plane, the angle between the lines of intersection of the slip systems in the boundary plane and the magnitude of the residual dislocation left in the grain boundary by the emission process. DOE

N89-19406*# National Aeronautics and Space Administration. Marshall Space Flight Center, Huntsville, AL.
AN ELECTROCHEMICAL STUDY OF CORROSION PROTECTION BY PRIMER-TOPCOAT SYSTEMS ON 4130 STEEL WITH ac IMPEDANCE AND dc METHODS
M. J. Mendrek, R. H. Higgins, and M. D. Danford May 1988 56 p
(NASA-TP-2820; NAS 1.60:2820) Avail: NTIS HC A04/MF A01 CSCL 11F

To investigate metal surface corrosion and the breakdown of metal protective coatings, the ac impedance method is applied to six systems of primer coated and primer topcoated 4130 steel. Two primers were used: a zinc-rich epoxy primer and a red lead oxide epoxy primer. The epoxy-polyamine topcoat was used in four of the systems. The EG and G-PARC Model 368 ac impedance measurement system, along with dc measurements with the same system using the polarization resistance method, were used to monitor changing properties of coated 4230 steel disks immersed in 3.5 percent NaCl solutions buffered at pH 5.4 over periods of 40 to 60 days. The corrosion system can be represented by an electronic analog called an equivalent circuit consisting of resistors and capacitors in specific arrangements. This equivalent circuit parallels the impedance behavior of the corrosion system during a frequency scan. Values for the resistors and capacitors, that can be assigned in the equivalent circuit following a least-squares analysis of the data, describe changes that occur on the corroding metal surface and in the protective coatings. Two equivalent circuits have been determined that predict the correct Bode phase and magnitude of the experimental sample at different immersion times. The dc corrosion current density data are related to equivalent circuit element parameters. Methods for determining corrosion rate with ac impedance parameters are verified by the dc method.
Author

N89-19407# Massachusetts Inst. of Tech., Cambridge.
TO MEASURE AND CHARACTERIZE METAL CORROSION IN ELECTROLYTE SOLUTIONS BY EXPLOITING THE PROPERTIES OF SUPERCONDUCTING Final Technical Report
Margaret L. MacVicar 30 Aug. 1988 173 p
(Contract N00014-85-K-0454)
(AD-A201484) Avail: NTIS HC A08/MF A01 CSCL 20A

A framework relating fluctuations in an electrochemical cell to fluctuations of the fundamental thermodynamic and kinetic parameters of the system is presented. A method for extracting critical interface parameters via noise measurements, such as the charge transfer resistance, is developed. The technique, called variable load analysis, does not require perturbation of the cell with applied voltage or current. The framework suggests measurements to distinguish between different noise sources superimposed in the same signal, and to determine the mechanisms underlying the observed noise. A cell geometry with two identical electrodes connected through an external resistive load is used. Fluctuations in the current flowing between the two electrodes under open circuit conditions (i.e., under no applied external potential) provide the detected signal. GRA

N89-19408# Brown Univ., Providence, RI. Div. of Engineering.
THE EFFECTS OF TEMPERING AND TEST TEMPERATURE ON THE DYNAMIC FRACTURE INITIATION BEHAVIOR OF AN AISI 4340 VAR STEEL
Y. C. Chi, S. H. Lee, K. Cho, and J. Duffy Aug. 1988 91 p
(Contract DAAL03-88-K-0015)
(AD-A201606; ARO-25544.3-EG) Avail: NTIS HC A05/MF A01 CSCL 11F

An investigation was conducted into the effect of tempering, test temperature and loading rate on the fracture initiation behavior of an AISI 4340 VAR steel. The fracture initiation tests were conducted by stress wave loading of a prefatigued circumferential crack in a notched round bar. The geometry provides for plane strain conditions at the fracture site, and the instrumentation gives records of average stress at the fracture site and of crack opening displacement, both as functions of time. GRA

N89-19409 Southampton Univ. (England).
SOLIDIFICATION, STRUCTURE AND MECHANICAL PROPERTIES OF A357 ALUMINUM ALLOY Ph.D. Thesis
Modjtaba Hashemi-Ahmady 1988 367 p
Avail: Univ. Microfilms Order No. BRD-82530

The microstructural variations in the A357 alloy were characterized as functions of: casting thickness (Z), casting process, modification and heat treatment. The growth rates (R), and temperature gradients (G), were obtained through a series of experiments and theoretical analysis of the casting process in sand and in graphite molds. Subsequently, the total solidification times (t sub F), and heat flow rates (Q) through each Z were also obtained. A complete survey of hardness, tensile and fracture toughness properties of the modified and unmodified A357 alloy was made by using very simple test techniques. These included tests on the A357 and a number of other Al-Si-Mg alloys in the as-cast and in various heat treated conditions. A series of tests on unidirectionally solidified (UDS) Al-Si entectic alloys (modified and unmodified) have established a strong Si orientation effect on the tensile and fracture properties. Increased Si volume fractions were found to increase proof stress and UTS, but at the expense of ductility and toughness. Increased Mg contents were also found to increase proof stress and UTS in the heat treated condition, but also at the significant expense of toughness. Dissert. Abstr.

N89-19410 Alabama Univ., University.
THE EFFECT OF HYDROGEN ON FATIGUE CRACK GROWTH RATE OF AISI 304 STAINLESS STEEL Ph.D. Thesis
Mohamed Riyad Husien Abdelkader 1988 173 p
Avail: Univ. Microfilms Order No. DA8821787

Fatigue crack growth behavior of AISI 304 stainless steel in dry hydrogen gas environment under low pressure and at room temperature was investigated under cyclic loading using fracture mechanics techniques. Fatigue crack propagation testing was accomplished by using precracked standard wedge opening load specimens. Three frequency levels and three environments were chosen to determine their effects on the fatigue behavior of 304 stainless steel. Comparison of the crack growth behavior in H2 environment with similar data generated in lab air and argon environments shows that H2 has a strong detrimental effect on the fatigue crack growth rate properties. Crack growth rates were measured as a function of the effective stress intensity, and the loading frequency. Generally, a decrease in frequency for a particular environment causes an increase in the fatigue crack propagation rate. Dissert. Abstr.

N89-19411# Naval Postgraduate School, Monterey, CA.
PROCESSING OF ALUMINUM ALLOY 2090 FOR SUPERPLASTICITY M.S. Thesis
Gary E. Groh Sep. 1988 82 p
(AD-A201865) Avail: NTIS HC A05/MF A01 CSCL 11F

Existing superplastic forming techniques for Al alloys rely on deformation at temperatures of 500 C to achieve the desired ductilities. The A1 alloy 2090 (Al-Li-Cu-Zr) has been successfully fabricated by such techniques, but at temperatures where cavitation during formation may significantly reduce the mechanical properties of the final product. It has been previously shown that cavitation can be effectively suppressed by forming at lower temperatures. The purpose of this research is to investigate the applicability of thermomechanical processing methods (developed at NPS for Al-Mg-X alloys) to produce a refined microstructure capable of supporting superplasticity at lower temperatures in Al 2090.
GRA

N89-19412# State Univ. of New York, Stony Brook. Dept. of Materials Science and Engineering.
EFFECT OF TEMPERATURE ON THE CORROSION RESISTANCE OF NITROGEN BEARING AL6X AND 904L STAINLESS STEELS Final Report
Kim G. Martin Oct. 1988 105 p
(Contract N00014-85-K-0437)
(AD-A201955) Avail: NTIS HC A06/MF A01 CSCL 11F

There has been a marked increase in the demand and use of

austenitic stainless steels as structural material, containing suitable levels of nitrogen in order to enhance strength characteristics. There is an obvious economic advantage in using nitrogen in stainless steels, for nitrogen can replace or supplement the element nickel. Nitrogen which is an austenite stabilizer like nickel, has the benefit of being much less expensive and having thirty times the austenite forming potential of nickel. Nitrogen has also been found to suppress the formation of secondary phases which are detrimental to corrosion resistance. GRA

N89-19413# Rolls-Royce Ltd., Derby (England).
MICROSTRUCTURAL OPTIMISATION OF TITANIUM ALLOYS FOR DEFECT TOLERANCE IN GAS TURBINE ENGINE COMPONENTS
M. T. Cope, P. J. Postans, and M. A. Hicks 15 Feb. 1987 9 p Presented at the TMS-AIME Meeting on Effect of Microstructures on Fracture Toughness and Fatigue Crack Growth Rate in Titanium Alloys, Denver, CO, Feb. 1987 Previously announced in IAA as A89-10069
(PNR90503; ETN-89-93347) Copyright Avail: NTIS HC A02/MF A01

Results for aligned and basketweave microstructures in near alpha alloys used on gas turbine engines are presented together with observations titanium alloy. To minimize crack propagation rates, it is important to minimize the prior beta grain size and the level of alpha platelet alignment. The propagation rate depends on the propagation mode which depends on the orientation of the structure presented to the crack tip. ESA

N89-19414# Rolls-Royce Ltd., Derby (England).
TENSILE PROPERTIES OF Ti-6Al-2Sn-4Zr-2Mo SHEET AFTER SUPERPLASTIC DEFORMATION
M. T. Cope, M. J. Hill, and D. R. Evetts 6 Jun. 1988 6 p Presented at the 6th World Conference on Titanium: Titanium '88, Cannes, France, 6-9 Jun. 1988
(PNR90499; ETN-89-93691) Copyright Avail: NTIS HC A02/MF A01

Ambient temperature tensile properties were studied after superplastic deformation at 940 C and up to 200 percent elongation at a strain rate of 0.00022 1/sec. The material was also tested after static annealing at 940 C to separate the effects of superplastic deformation from elevated temperature exposure. Preheating and furnace cooling results in a reduction of strength and an increase in elongation. Superplastic deformation produces a reduction both in tenacity and elongation. The variations in mechanical properties are related to variations in phase size and morphology, and crystallographic texture. ESA

N89-19415# Deutsche Forschungs- und Versuchsanstalt fuer Luft- und Raumfahrt, Cologne (Germany, F.R.). Inst. fuer Raumsimulation.
INVESTIGATIONS ON UNDERCOOLING, NUCLEATION AND RAPID SOLIDIFICATION OF METALLIC SYSTEMS Ph.D. Thesis - Bochum Univ.
Rainer Willnecker Aug. 1988 151 p In GERMAN; ENGLISH summary
(DFVLR-FB-88-39; ISSN-0171-1342; ETN-89-93973) Avail: NTIS HC A08/MF A01; DFVLR, VB-PL-DO, Postfach 90 60 58, 5000 Cologne, Federal Republic of Germany, 54 deutsche marks

Electromagnetic levitation was used for undercooling investigations and for studying rapid solidification processes of transition metals Cu, Ni, Fe, and their alloy systems. The application of levitation techniques results in an extension of the attainable undercooling range for bulk metallic samples. The undercooling behavior of the metals investigated was analyzed in the framework of classical nucleation theory. Measurements of the growth velocities of undercooled metals, performed on levitated droplets, are discussed within theoretical models of free dendritic growth. The growth behavior is controlled by the thermal and solutal gradients and additional kinetic effects at the solid-liquid interface. Investigations of microstructural changes with undercooling reveal aspects of the origin of grain refinement occurring at a critical undercooling. ESA

N89-19416# Duesseldorf Univ. (Germany, F.R.). Inst. fuer Physikalische Chemie und Elektrochemie.
PASSIVITY AND CORROSION OF PROBE METALS Final Report, 30 Sep. 1987
J. W. Schultze, L. Elfenthal, A. Hochfeld, and A. Meyer Apr. 1988 121 p In GERMAN; ENGLISH summary
(Contract BMFT-02-U-5594-0)
(ETN-89-93984) Avail: NTIS HC A06/MF A01

The corrosion stability of Zr and Ta, and Ti-alloys was investigated under the conditions of the Purex-process. Corrosion tests and simulations of technical conditions were developed. Laser microprobe analysis is described. While Ta is stable at all conditions Zr shows decreasing corrosion stability with increasing nitric acid concentration and temperature during potentiodynamic tests. Electrode modifications important for the Purex-process were checked. The stability of passive films against radiation was examined, using alpha radiation and hot atoms simulated by ion implantation. Amorphization occurs, making the layer more flexible and therefore more stable against mechanical stresses. The enhancement of electronic conductivity stabilizes the favorable potential region between 0 to 1 V. Electronic processes can be simulated by focused laser radiation which induces the growth of additional oxide. The dissolution of oxide films of Ta and Ti is investigated by analysis and electrochemical measurements, and is discussed with reference to decontamination processes. ESA

N89-19417# GKSS-Forschungszentrum Geesthacht (Germany, F.R.). Inst. fuer Werkstofforschung.
MICROSTRUCTURAL ANALYSES OF INTERMETALLIC TiAl (Nb)-COMPOUNDS PREPARED BY ARC MELTING AND BY POWDER METALLURGY Ph.D. Thesis - Technische Univ., Hamburg
S. Chen 1988 168 p
(GKSS-88/E/32; ISSN-0344-9629; ETN-89-93952) Copyright Avail: NTIS HC A08/MF A01

Intermetallic compounds based on TiAl with Nb or V as alloying additions prepared by powder metallurgy (P/M) and arc melting (A/M) techniques were investigated with respect to their potential as high temperature materials. All the alloys with nominal Al-concentrations 34 to 36 wt pct contain two phases, gamma-TiAl and alpha2-Ti3Al, but significant differences in the distribution of gamma and alpha2 are found between the P/M and A/M materials. The role of impurities during processing and the microstructural stability in the planned service temperature range 700 to 1000 C are discussed. In the P/M TiAl alloys two carbide precipitaties are found: the cubic perovskite-AlTi3C phase in the gamma-matrix and the hexagonal H-AlTi2 (C,N) phase at grain boundaries. At high temperatures the AlTi3C phase dissolves and is replaced by more stable H-phase, and therefore no longer contributes to the high temperature strength of the material. Mechanical properties of both the P/M and A/M alloys are compared in association with the processing methods and the resulting microstructures. ESA

N89-19418# Kernforschungszentrum G.m.b.H., Karlsruhe (Germany, F.R.). Inst. fuer Nukleare Festkoerperphysik.
IMPROVEMENTS IN THE PROPERTIES OF NbN LAYERS THROUGH THE PRESENCE OF SMALL AMOUNTS OF ALUMINUM DURING SPUTTERING
E. L. Haase and J. Ruzicka Sep. 1988 14 p
(KfK-4409; ISSN-0303-4003; ETN-89-93966) Copyright Avail: NTIS HC A03/MF A01

Pure phase B1 NbN layers could be sputtered only with a maximum Tc of 15.9 K and a residual resistance ratio (RRR) less than 0.9. Samples with a Tc of up to 16.7 K invariably had a large fraction of hexagonal foreign phase. It is shown that if under similar conditions one sputters layers in the presence of small amounts of Al, one obtains pure B1 phase NbN layers with a maximum Tc of 16.9 K. The RRR rises to values of up to 1.16. The specific resistance drops from typical values of around 400 micro Ohm cm to values as low as 73 micro Ohm cm. The width of the X-ray lines drops occasionally, indicating increased grain size. Aluminum acts like a catalyst, being substituted with less than 0.03 at pct for a high Tc layer. When Al is substituted for

Nb in detectable quantities both Tc and the lattice parameter drop. To verify the above results the experiment was repeated in a magnetron rather than an RF sputter system, with similar outcome. ESA

N89-19419# Kernforschungszentrum G.m.b.H., Karlsruhe (Germany, F.R.). Inst. fuer Radiochemie.
FORMATION OF TITANIUM NITRIDE LAYERS ON TITANIUN METAL: RESULTS OF XPS AND AES INVESTIGATIONS
H. Moers, G. Pfennig, H. Klewe-Nebenius, R.-D. Penzhorn, M. Sirch, and E. Willin Sep. 1988 65 p
(KfK-4449; ISSN-0303-4003; ETN-89-93968) Copyright Avail: NTIS HC A04/MF A01

The reaction of titanium metal with gaseous nitrogen and ammonia at 890 C was studied. Nitridic overlayers form on the metallic substrate. The thicknesses of the overlayers increase with increasing reaction time. Under comparable conditions ammonia reacts much slower than nitrogen. Depth profile analyses by XPS and AES show continuous changes of the in-depth compositions of the overlayers. This can be interpreted in terms of a very irregular thickness of the overlayers, an assumption which is substantiated by local AES analyses and by the observation of a pronounced crystalline structure of the substrate after annealing pretreatment, which can produce locally different reaction rates. The depth profile is also influenced by the broad ranges of stability of the titanium nitride phases formed during the reaction. The quantitative analysis of the titanium/nitrogen overlayers by AES is difficult because of the overlap of titanium and nitrogen Auger peaks. In quantitative XPS analysis problems arise due to difficulties in defining Ti 2p peak areas. Practical procedures for the quantitative evaluation by XPS and AES of nitridic overlayers with sufficient accuracy are presented. ESA

27 NONMETALLIC MATERIALS

Includes physical, chemical, and mechanical properties of plastics, elastomers, lubricants, polymers, textiles, adhesives, and ceramic materials.

For composite materials see *24 Composite Materials.*

N89-19420*# Engineering and Economics Research, Inc., Huntsville, AL.
PREPARATION OF NON-METALS PROPERTIES FOR DATA BASE Final Report
8 Jun. 1988 572 p
(Contract NAS8-36198)
(NASA-CR-183596; NAS 1.26:183596; EER58-36198-FR6/8)
Avail: NTIS HC A24/MF A01 CSCL 11B

The development of non-metallic material properties data bases is discussed. The data bases consist of the non-metallic material classes of adhesives, adhesive/sealants, plastics, and elastomers. A specifications data base was also developed to incorporate material specifications data as a supplement to the Elastomers Data Base. Examples of the forms used are provided to show the properties of the materials which appear in the data base. NASA

N89-19421*# AiResearch Casting Co., Torrance, CA.
IMPROVED SILICON NITRIDE FOR ADVANCED HEAT ENGINES Annual Contractor Report
Hun C. Yeh and Ho T. Fang (Garrett Turbine Engine Co., Phoenix, AZ.) Feb. 1987 113 p
(Contract NAS3-24385)
(NASA-CR-179525; NAS 1.26:179525; AiResearch-86-60365)
Avail: NTIS HC A06/MF A01 CSCL 11B

The technology base required to fabricate silicon nitride components with the strength, reliability, and reproducibility necessary for actual heat engine applications is presented. Task 2 was set up to develop test bars with high Weibull slope and greater high temperature strength, and to conduct an initial net shape component fabrication evaluation. Screening experiments were performed in Task 7 on advanced materials and processing for input to Task 2. The technical efforts performed in the second year of a 5-yr program are covered. The first iteration of Task 2 was completed as planned. Two half-replicated, fractional factorial (2 sup 5), statistically designed matrix experiments were conducted. These experiments have identified Denka 9FW Si3N4 as an alternate raw material to GTE SN502 Si3N4 for subsequent process evaluation. A detailed statistical analysis was conducted to correlate processing conditions with as-processed test bar properties. One processing condition produced a material with a 97 ksi average room temperature MOR (100 percent of goal) with 13.2 Weibull slope (83 percent of goal); another condition produced 86 ksi (6 percent over baseline) room temperature strength with a Weibull slope of 20 (125 percent of goal). Author

N89-19422# Pennsylvania State Univ., University Park.
THE MECHANICAL BEHAVIOR OF SURFACE MODIFIED CERAMICS Progress Report
D. J. Green 1988 6 p
(Contract DE-FG02-86ER-45252)
(DE89-004764; DOE/ER-45252/T3) Avail: NTIS HC A02/MF A01

This paper discusses the following topics: influence of surface residual stresses on strength variability; indentation of ion-exchanged glass; mechanical behavior of surface-modified alumina; and residual surface stress characterization. DOE

N89-19423# Idaho National Engineering Lab., Idaho Falls.
ELASTIC HYSTERESIS PHENOMENA IN ULE AND ZERODUR OPTICAL GLASSES AT ELEVATED TEMPERATURES
S. Curtis Wilkins, Dennis N. Coon, and Jonathan S. Epstein (Georgia Inst. of Tech., Atlanta.) 1988 7 p Presented at the 32nd International Technical Symposium on Optical and Opto-Electronic Applied Sciences and Engineering, San Diego, CA, 14 Aug. 1988
(Contract DE-AC07-76ID-01570)
(DE89-005183; EGG-M-88094; CONF-880887-28) Avail: NTIS HC A02/MF A01

Elastic hysteresis phenomena were observed in ULE and Zerodur glasses at elevated temperatures up to glass transition. These effects were found under load deformation testing using four-point bending. Permanent creep resulted in Zerodur at 900 C and in ULE at 1000 C. The deformation was monitored at mid-span of the samples with a capacitance-type transducer having 0.01 micrometer resolution. These hysteresis effects may be classified as elastic bimodulus between loading and unloading; that is, two different elastic moduli were observed between loading and unloading. Upon complete unloading, a minimal deformation state promptly returned, indicating little or no viscoelastic creep. The hysteresis effect may be attributed to a change in glass structure as a function of stress state. A description of the test apparatus and procedure, test results for both glasses at several elevated temperatures, and an elementary discussion of continuum theory of constitutive behavior are included. DOE

N89-19424# Pennsylvania State Univ., University Park.
POLYMER MORPHOLOGY AND TRANSPORT Final Report, 1 Sep. 1984 - 31 May 1988
H. J. Sha and I. R. Harrison 10 Aug. 1988 10 p
(Contract DAAG29-84-K-0175)
(AD-A201167; ARO-21364.1-MS) Avail: NTIS HC A02/MF A01 CSCL 07F

The goal of this research was to gain an understanding of the transport/morphology relationships in semi-crystalline polymers. It was hoped that this research would lead to the development of inexpensive high barrier materials with desirable mechanical properties. Briefly we have found that: (1) Uniaxial drawing is an extremely effective way to increase the barrier of semicrystalline films. For HDPE with a 20x draw, barrier improves by a factor of = 500 for carbon tetrachloride; = 50 to 100 for diatomic oxygen and carbon dioxide and = 25 for helium; and (2) The mechanism for this improvement is less clearly understood; however it is not due to major changes in percentages crystallinity or an increase in amorphous density. At this stage it appears to be due to a reduction in amorphous chain mobility. GRA

N89-19425# Maine Univ., Orono. Lab. for Surface Science and Technology.
PROPOSAL TO STUDY THE INTERACTION OF POLYIMIDE PRECURSORS AND THIN POLYIMIDE FILMS WITH SILICON AND SILICON OXIDE SURFACES Final Report, May 1985 - Sep. 1988
Michael Grunze Oct. 1988 5 p
(Contract N00014-85-K-0641)
(AD-A201183) Avail: NTIS HC A02/MF A01 CSCL 09A

The work performed within the research contract N00014-85-K-0641 produced results, which for the first time allowed us to derive a model for the detailed molecular mechanism of adhesion between a polymer and a metal surface. The spectroscopic characterization of polyimide/metal interface was made possible by a vapor deposition technique used to produce polyimide films sufficiently thin to access the interface by photoelectron spectroscopy and Infrared Reflection Absorption Spectroscopy. The polyimide films were prepared by codeposition of oxidianiline (ODA) and 1,2,4,5 Benzenetetracarboxylic Anhydride (PMDA) onto a surface held at 300 K to form polyamic acid. GRA

N89-19426# Pennsylvania Univ., Philadelphia. Dept. of Chemistry.
THE AQUEOUS ELECTROCHEMISTRY OF POLYACETYLENE (CH)x AND POLYPARAPHENYLENE Final Technical Report, 1 May 1983 - 30 Apr. 1986
Alan G. MacDiarmid 30 Apr. 1988 21 p
(Contract N00014-83-K-0209)
(AD-A201461) Avail: NTIS HC A03/MF A01 CSCL 07D

Polyacetylene, (CH)x, and polyaniline, two completely different types of conducting polymers, i.e., organic polymers which upon doping exhibit the electrical, electronic, and magnetic properties of metals while retaining the mechanical and related properties characteristic of conventional polymers, have been investigated. Studies include the synthesis, doping, electrochemistry and selected physical properties of these materials. It has been found that the polyacetylene chains in trans-(CH)x lie parallel to the fibril axis and that the electrical and optical properties are consistent with the principal pi electrical transport occurring along the (CH)x chains. Polyacetylene can be epitaxially polymerized from the gas phase on to single crystal faces of biphenyl which have been coated with a very thin layer of catalyst. GRA

N89-19427# Syracuse Univ., NY.
INTERACTIONS AND REACTIONS IN POLYMERIZED VESICLES Final Report, 1 Jun. 1985 - 31 May 1988
Janos H. Fendler 10 Aug. 1988 6 p
(Contract DAAG29-85-K-0127)
(AD-A201527; ARO-23034.11-CH) Avail: NTIS HC A02/MF A01 CSCL 07C

The term vesicle is used to describe spherical or ellipsoidal single (SUV = small unilamellar vesicle) or multicompartment (MLV = multilamellar vesicle) closed bilayer structures, regardless of their chemical compositions. Vesicles composed of naturally occurring or synthetic phospholipids are referred to as liposomes. In contrast, those formed from completely synthetic surfactants are designed as surfactant vesicles. Surfactant vesicles have been developed for the entrapment of a variety of molecules including drugs, herbicides, pesticides, and molecules capable of destroying nerve gases and their simulants. Lack of long term stabilities and controllable permeabilities has detracted somewhat from the use of surfactant vesicles as molecular containers. Polymerization of vesicles has been selected as a method of vesicle stabilization and of release control. Under the ARO support emphasis has been placed on vesicles prepared from n-hexadecyl 11-(4-vinylbenzamide) undecyl hydrogen phosphate, 1, and from mixtures of 1 and dioctadecyldimethylammonium bromide, 2. Irradiation by ultraviolet light resulted in the polymerization of vinyl groups in 1. Kinetics and mechanisms of photopolymerization have been established. The presence of ion-pair domains of 1 and 2 has been established in vesicles prepared from these surfactant mixtures. GRA

N89-19428 Massachusetts Univ., Amherst.
THE DETERMINATION OF THE MECHANICAL BEHAVIOR OF POLYAMIC ACID/POLYIMIDE COATINGS Ph.D. Thesis
Charles L. Bauer 1988 152 p
Avail: Univ. Microfilms Order No. DA8822638

The dimensional constraints imposed on polymeric coatings may significantly influence the final stress state in the coatings. For many polymeric coating materials the development of such stresses is dependent on the processing history of the coating. To accurately design devices that incorporate these types of coatings, the properties must be characterized as a function of the thermal and volvent history. The development of the stresses and mechanical properties in polyamic acid/polyimide coatings based on pyromellitic dianhydride and oxydianiline (PI5878 from DuPont) was studied as a function of processing history. Using techniques such as the propagating wave method and the Impulse Method, the stress, mass and modulus of the polyamic acid coating were determined as a function of temperature and time. For a coating under a two dimensional constraint, the stress due to solvent removal from the coating and subsequent imidization may be as large as 30 MPa. The solvent removal is dependent on temperature and stress in the polyamic acid coating. An energy balance approach qualitatively describes this coupled behavior. Mechanical properties such as modulus and thermal expansion coefficient were obtained throughout the processing of these coatings. The modulus of the polyamic acid coating was 2 GPa compared to 3 GPa for the fully cured polyimide. Dissert. Abstr.

N89-19429# Ceramic Process Systems Corp., Cambridge, MA.
COMPOSITE CERAMIC SUPERCONDUCTING WIRES FOR ELECTRIC MOTOR APPLICATIONS Quarterly Report No. 1, 30 Jun. - 30 Sep. 1988
John W. Halloran 30 Sep. 1988 155 p
(Contract N00014-88-C-0512)
(AD-A201810) Avail: NTIS HC A08/MF A01 CSCL 20C

This is the First Quarterly Report of a program to produce practical htsc wires, and build a htsc electric motor using this wire. The htsc ceramic wire will be a flexible composite of many fine ceramic filaments clad with copper or aluminum. The three basic elements of this method are: (1) spinning polymer-containing green fibers; (2) sintering the fibers to make bare superconducting ceramic filaments; and (3) cladding the filaments with copper. Albany International Research Corporation (AIResCo) is working with CPS to improve the green fiber spinning process and bring it to pilot scale production. During this quarter, most of the fibers were prepared from a Rhone-Poulenc powder. This material was suitable for spinning and highly sinterable, but contained excess copper oxide. Much effort went to scaling up in-house powder production of highly phase pure YBa2Cu3O7 powder to production rates adequate to supply the development program. The influence of powder characteristics on fiber spinning and sintering is now being studied to optimize the powder for the wire manufacturing. GRA

N89-19430# State Univ. of New York, Stony Brook. Dept. of Chemistry.
LASER SCATTERING STUDIES OF EPOXY POLYMERIZATION PROCESSES Final Report, 15 Mar. 1985 - 14 Sep. 1988
Ben Chu 4 Nov. 1988 13 p
(Contract DAAG29-85-K-0076)
(AD-A201925; ARO-22457.17-CH) Avail: NTIS HC A03/MF A01 CSCL 07F

The final technical report summarizes our development on the methodology to study the structure and dynamics of highly branched epoxy polymers. We have made advances in providing new approaches to this complex problem. Unfortunately, the project was not renewed for further studies. During the contract period, we have developed the methodology to study the structure and dynamics of epoxy polymer formation by using laser light scattering intensity and linewidth measurements, small angle X-ray scattering with a synchrotron X-ray source and chemical analysis. We have also tried to approach the kinetics and mechanisms of the epoxy

copolymerization reaction by using the Smoluchowski coagulation equation. GRA

N89-19431# Pennsylvania Univ., Philadelphia. Dept. of Chemistry.
CHEMISTRY AND PHYSICS OF POLYACETYLENE, (CH)x: THE PROTOTYPE CONDUCTING POLYMER Final Technical Report, 1 May 1981 - 30 Apr. 1983
Alan G. MacDiarmid 31 Oct. 1988 13 p
(Contract N00014-81-K-0648)
(AD-A201933) Avail: NTIS HC A03/MF A01 CSCL 07F

A method has been devised for synthesizing polyacetylene, (CH)x, of variable density ranging from 0.03 to 0.4 g/cc. The resulting polymer shows potential for microwave absorption. Polyacetylene can be chemically doped with resulting control of electrical conductivity over a range of 12 orders of magnitude. It has also been discovered that (CH)x can be reversibly p- and n-doped electrochemically, suggesting the possible use of conducting polymers in novel rechargeable batteries. Polyacetylene undergoes a semiconductor to metal transition upon p- and n-chemical or electrochemical doping. Magnetic, optical, I/R and phototransport changes associated with this transition show that soliton doping and soliton excitations play a dominant role in determining the electronic properties of the polymer. GRA

N89-19432# Southwest Research Inst., San Antonio, TX. Belvoir Fuels and Lubricants Research Facility.
PERFORMANCE EVALUATION OF MILITARY ENGINE AND GEAR OILS IN FRICTION AND WEAR DEVICES Final Report, Aug. 1987 - Aug. 1988
Howard W. Marbach, Jr. Sep. 1988 41 p
(Contract DAAK70-87-C-0029)
(AD-A202145; AD-E501048; BFLRF-256) Avail: NTIS HC A03/MF A01 CSCL 11H

For this program, eight lubricants were selected from three military lubricant specifications: three lubricants from MIL-L2105C multipurpose gear lubricants, grades 75W, 80W-90, and 85W-140; three reference grade MIL-L2104D tactical engine lubricants, grades 10W, 40, and 15W-40; one grade OW-20 MIL-L-46167A Arctic engine lubricant; and one grade CD/50 lubricant that met the MIL-L2104C specification. The lubricants were tested and evaluated under a wide range of lubrication environments using five friction-and-wear test devices. The results were analyzed by using a one-way analysis of variance (ANOVA) procedure. Also, a Tukey multiple comparison test was used to compare pairs of means among the gear and engine lubricants within a given test method. Lubricants were determined that had significantly different characteristics from the other lubricants. GRA

N89-19433# Clarkson Univ., Potsdam, NY. Div. of Research.
HOLE FORMATION (ETCHING) IN POLYMERS BY FAR (DEEP) UV HIGH INTENSITY LASER (EXCIMER) RADIATION PULSES AND ITS RELEVANCE TO PHOTORESISTS IN DEEP UV PHOTOLYSIS OF POLYMERS Final Report, 1 May 1985 - 31 Dec. 1987
H. G. Jellinek, R. Partch, and H. Kacki 20 Oct. 1988 38 p
(AD-A202274; ARO-22572.1-CH) Avail: NTIS HC A03/MF A01 CSCL 11I

Pulsed excimer laser light (193nm) has been used to study the photo and thermal induced degradation (ablation) of six common, industrially important polymers. A spoon gauge was employed to determine the rate loss of gaseous products from a film. Optical microscopy allowed visualization of the changes that take place in the polymer near the site of hole formation. Little correlation was observed between the depth of holes generated and average pulse power or total energy applied. Temperature increases in the polymer film were monitored during irradiation. An attempt was made to correlate calculated and experimental ejection velocities of oligomer fragments of polymer formal by irroliation. The amount of such sputtered material is small as opposed to gaseous products. Correlations were made between the percent transmission of infrared light through each type of polymer and the number of pulses. GRA

N89-19434# Virginia Polytechnic Inst. and State Univ., Blacksburg. Center for Adhesive and Sealant Science.
AN INTERDISCIPLINARY STUDY OF CATHODIC DEBONDING IN ELASTOMER/METAL ADHESIVE BONDS Final Report, Jan. 1985 - Oct. 1988
Ramzi F. Hamadeh and D. A. Dillard Oct. 1988 308 p
(Contract N00014-85-K-0145)
(AD-A202376; VPI-E-88-30; CASS/ESM-88-10) Avail: NTIS HC A14/MF A01 CSCL 11J

An interdisciplinary study concerning the durability of adhesively elastomer/metal bonded joints in marine environments is reported. The generation of OH-ions at the bondline due to an imposed cathodic current from an external source is suspected to be the predominant cause of failure. A surface analysis study was performed early in this research for the purpose of identifying the cause(s) of failure. Characterization of the rubber and the metal failure surfaces with XPS (X-ray Photoelectron Spectroscopy) showed similar composition on both sides and to that of the bulk degraded primer component of the adhesive. Saponification of the adhesive and the leaching of chlorine (forming HCl that attacks the oxide) are identified as two possible failure mechanisms. The locus of failure is believed to be very close to the adhesive/oxide interface. GRA

N89-19435*# National Aeronautics and Space Administration. Lewis Research Center, Cleveland, OH.
ADHESION IN CERAMICS AND MAGNETIC MEDIA
Kazuhisa Miyoshi Mar. 1989 19 p Prepared for presentation at the 5th International Congress on Tribology, Helsinki, Finland, 12-15 Jun. 1989
(NASA-TM-101476; E-4596; NAS 1.15:101476) Avail: NTIS HC A03/MF A01 CSCL 11B

When a ceramic is brought into contact with a metal or a polymeric material such as a magnetic medium, strong bonds form between the materials. For ceramic-to-metal contacts, adhesion and friction are strongly dependent on the ductility of the metals. Hardness of metals plays a much more important role in adhesion and friction than does the surface energy of metals. Adhesion, friction, surface energy, and hardness of a metal are all related to its Young's modulus and shear modulus, which have a marked dependence on the electron configuration of the metal. An increase in shear modulus results in a decrease in area of contact that is greater than the corresponding increase in surface energy (the fond energy) with shear modulus. Consequently, the adhesion and friction decrease with increasing shear modulus. For ceramics in contact with polymeric magnetic tapes, environment is extremely important. For example, a nitrogen environment reduces adhesion and friction when ferrite contacts polymeric tape, whereas a vacuum environment strengthens the ferrite-to-tape adhesion and increases friction. Adhesion and friction are strongly dependent on the particle loading of the tape. An increase in magnetic particle concentration increases the complex modulus of the tape, and a lower real area of contact and lower friction result. Author

N89-19436# Rolls-Royce Ltd., Watford (England). Material Engineering Dept.
SOME NOVEL TEST METHODS FOR, AND ASSOCIATED PROBLEMS OF MECHANICAL STRENGTH CHARACTERIZATION OF ENGINEERING CERAMICS
G. R. Essam and G. Syers 1 Aug. 1988 6 p Presented at the ICAS '88, Jerusalem, Israel, Aug. 1988 Previously announced in IAA as A89-13576
(PNR90492; ETN-89-93687) Copyright Avail: NTIS HC A02/MF A01

Multiple bend tests in one furnace load at elevatd temperature, a relatively inexpensive elevated temperature axial tensile test system, and an axial test system capable of complex thermomechanical cyclic loads are described. It is shown that bend tests are suitable for surface characterization and for material screening. Axial tests are the most reliable method of material assessment. ESA

N89-19437# Massachusetts Inst. of Tech., Cambridge. Dept. of Materials Science and Engineering.
GRAIN BOUNDARY NONSTOICHIOMETRY IN MULTICOMPONENT CERAMICS Progress Report
Yet-Ming Chiang Jan. 1989 3 p
(Contract DE-FG02-87ER-45307)
(DE89-006109; DOE/ER-45307/T1) Avail: NTIS HC A02/MF A01

The objectives of this research program are to investigate the relationships between lattice and grain boundary defect chemistry in multicomponent, nonstoichometric oxides, and their effects on grain boundary physical properties. Systems of current interest include titanates (TiO2, SrTiO3 and BaTiO3) and cuprate superconductors (primarily La sub 2-x Sr sub x CuO4 and YBa2Cu3O sub 7-y). DOE

N89-19438# Argonne National Lab., IL. Materials and Components Technology Div.
DEVELOPMENT OF NUCLEAR MAGNETIC RESONANCE (NMR) IMAGING TECHNOLOGY FOR ADVANCED CERAMICS
W. A. Ellingson, J. L. Ackerman, L. Garrido, P. S. Wong, and S. Gronemeyer Nov. 1988 51 p
(Contract W-31-109-eng-38)
(DE89-006400; ANL-87-53) Avail: NTIS HC A04/MF A01

In the work described in this report, we have explored both solid-state NMR imaging to map the distribution of binder/plasticizers (B/Ps) in cold-pressures ceramic parts and solution NMR to image the open, i.e., surface-connected porosity in dewaxed parts. The ability to detect B/Ps was initially evaluated on a state-of-the-art 1.5-T medical imager (Siemens Magnetom(trademark)) with T sub 1 weighted imaging techniques and a 10-cm standard eye coil. However, this system did not provide adequate image resolution. One problem is that at room temperature the waxy (soft-solid) B/Ps have spin-spin relaxation times (T sub 2 s) of approximately 1 msec using spin-echo, phase-encoding techniques. Short T sub 2 s imply long data acquisition times. We solved this problem by designing a special NMR probe for a 2-T, small-bore (approximately 15 cm) superconducting magnet system. The special NMR probe, designed and built with field gradients of approximately 10 gauss cm, has the ability to image material with T sub 2 less than msec by means of spin-echo phase-encoding techniques. The initial results show that a medical system may not be able to detect B/Ps unless elevated temperatures are used, whereas experimental small-bore systems with higher field gradients and shorter switching times detect B/P distribution quite well. DOE

N89-19439# Oak Ridge National Lab., TN. Metals and Ceramics Div.
FABRICATION OF XLWIR (EXTRA-LONG-WAVELENGTH-INFRARED) WINDOW MATERIALS
Hyoun-Ee Kim and A. J. Moorhead 1989 8 p Presented at the SPIE Conference on Optics, Electro-optics and Laser Applications in Science and Engineering: OE/LASE '89, Los Angeles, CA, 15 Jan. 1989
(Contract DE-AC05-84OR-21400)
(DE89-006418; CONF-890145-7) Avail: NTIS HC A02/MF A01

A technique was developed for fabrication of strong, fully dense, polycrystalline windows of CsI by hot-pressing in a steel die. We began with ultra-pure, ultra-dry CsI powder and conducted all processing operations within a glove box purged with dry N sub 2. We were able to hot-press 5.08 cm CsI discs having transmittance of about 80 percent in the extra long wavelength (greater than or equal to 10 microns) infrared range - equivalent to that of single crystal CsI. The flexural strength of CsI bars fabricated by hot pressing small-particle-size powder was 18 MPa, about 5 times higher than that of single crystal CsI. DOE

28 PROPELLANTS AND FUELS

Includes rocket propellants, igniters, and oxidizers; their storage and handling procedures; and aircraft fuels.

For related information see also *07 Aircraft Propulsion and Power, 20 Spacecraft Propulsion and Power,* and *44 Energy Production and Conversion.*

N89-19440# Naval Research Lab., Washington, DC. Chemistry Div.
NRL BORON PROPELLANTS COMBUSTION PROGRAM Technical Report No. 6, Sep. 1987 - Sep. 1988
H. H. Nelson Jun. 1988 4 p Presented at the AFOSR/ONR Contractor's Meeting on Combustion, Los Angeles, CA, 15-19 Jun. 1988 Submitted for publication
(AD-A201242) Avail: NTIS HC A02/MF A01 CSCL 19A

The NRL program on High-Energy Propellant Chemistry includes work in three project areas. The first of these is a mass spectrometry based study of the oxide layer formed at the surface of elemental boron. The second involves the study of chemical mechanisms of homogeneous boron combustion. This work has focussed on boron hydrides in the past year but is expanding to cover boron oxyhydrides. The third area is a theoretical investigation of important intermediates in boron combustion. Structures, thermodynamics and reaction pathways are being studied. All three projects are oriented to assist in the understanding and control of heterogeneous and homogeneous combustion of boron and boron-doped fuels. GRA

N89-19441# Southwest Research Inst., San Antonio, TX. Fuels and Lubricants Research Div.
APPLICATION OF NONDESTRUCTIVE EVALUATIONS TO THE PREDICTION OF TURBINE FUEL PEROXIDATION POTENTIAL Final Report, 5 Aug. 1987 - 5 Feb. 1988
G. E. Fodor, K. B. Kohl, and D. W. Naegeli Feb. 1988 17 p
(Contract DLA900-84-C-0910)
(AD-A202291; SWRI-17-7958-840) Avail: NTIS HC A03/MF A01 CSCL 21D

After the theoretical and experimental baselines were established to determine the potential peroxide content of jet fuels, nondestructive methods of analyses were evaluated to augment the procedures. The use of proton Nuclear Magnetic Resonance (NMR), ultraviolet (UV), and infrared (IR) spectroscopies were evaluated. UV and NMR did not respond to the trace-quantity compositional changes caused by autoxidation in the examined fuels. Direct detection and measurement of the primary autoxidation intermediates, that is, peroxides and hydroperoxides, were not feasible by the applied nondestructive analytical methods. Indications are that IR may be used for the detection and measurement of peroxide decomposition products such as alcohols and carbonyl compounds. GRA

29 MATERIALS PROCESSING

Includes space-based development of products and processes for commercial applications.

For biological materials see *55 Space Biology.*

N89-19442*# California Univ., Irvine.
EXPERIMENT PLANS TO STUDY PREIGNITION PROCESSES OF A POOL FIRE IN LOW GRAVITY M.S. Thesis - 1988 Final Report
David N. Schiller Mar. 1989 128 p
(Grant NAG3-627)
(NASA-CR-182256; NAS 1.26:182256) Avail: NTIS HC A07/MF A01 CSCL 22A

Science requirements are specified to guide experimental studies of transient heat transfer and fluid flow in an enclosure containing a two-layer gas-and-liquid system heated unevenly from above. Specifications are provided for experiments in three separate settings: (1) a normal gravity laboratory, (2) the NASA-LeRC Drop towers, and (3) a space-based laboratory (e.g., Shuttle, Space Station). A rationale is developed for both minimum

and desired requirement levels. The principal objective of the experimental effort is to validate a computational model of the enclosed liquid fuel pool during the preignition phase and to determine via measurement the role of gravity on the behavior of the system. Preliminary results of single-phase normal gravity experiments and simulations are also presented. Author

N89-19443# Consejo Superior de Investigaciones Cientificas, Madrid (Spain).
STUDY OF SPACE ALUMINUM COATING, EXECUTIVE SUMMARY
J. A. Aznarez, J. A. Mendez, J. L. Sacedon, and M. Sanchez-Avedillo Paris, France ESA May 1988 61 p Prepared in cooperation with CRISA, Madrid, Spain
(Contract ESTEC-7086/87-NL-PB(SC))
(IOM/CAEE-002/87(TR); ESA-CR(P)-2684; ETN-89-93917)
Avail: NTIS HC A04/MF A01

An experiment for demonstration of aluminum evaporation in orbit is proposed. The main objective is the preparation of aluminum layers, so verifying the feasibility of the technology and the high reflectance of the coated surfaces in the FUV. In order to take advantage of the possibilities offered by a space mission, at least two types of evaporation sources, filaments and effusion cells, are included in the experiment. Although both sources are fully operational in a terrestrial environment, space testing is thought necessary, in particular for effusion cells. Far ultraviolet reflectance is measured, and the recovery of that reflectance by a thin aluminum recoating after controlled oxidation of the initial layers is tested. ESA

N89-19444# Societe Nationale Industrielle Aerospatiale, Saint-Medard-en-Jalles (France).
MINI PROTEIN CRYSTALLIZATION FACILITY. PHASE A STUDY: EXECUTIVE SUMMARY
Paris, France ESA 28 Jul. 1988 52 p Prepared in cooperation with MBB GmbH, Ottobrunn, Germany, F.R.; Erno Raumfahrttechnik GmbH, Bremen, Germany, F.R.; CNRS, Paris, France
(Contract ESA-7382/87-F-FL(SC))
(Rept-AQ-ES-576/88; ESA-CR(P)-2692; ETN-89-93936)
Copyright Avail: NTIS HC A04/MF A01

The feasibility of a miniprotein crystallization facility to be flown on a KOSMOS system was established. Temperature regulation can be achieved within the 50 W allowed but for reentry and before recovery phases a battery is required to provide extra power. The payload can be accommodated within the volume allowed. Total mass is 50 kg. Reentry shocks can be absorbed if the 25 Hz frequency requirement is deviated for the orbital flight and the return phase. Up to 192 samples can be processed at 4 C before crystallization, 20 C during and after crystallization. However other crystallization temperatures are feasible. A mock-up and further tests are needed to improve the design of the compartments making up the experiment chambers (for instance syringe shape and volume decrease of the droplet after crystallization); investigate insulation improvement; assess the behavior of crystals submitted to residual shocks and vibrations; and optimize the Peltier elements consumption. Supersaturation, and storage life must also be examined. ESA

31 ENGINEERING (GENERAL)

Includes vacuum technology; control engineering; display engineering; cryogenics; and fire prevention.

N89-19445# Massachusetts Inst. of Tech., Cambridge. Artificial Intelligence Lab.
MODEL-BASED REASONING: TROUBLESHOOTING
Randall Davis and Walter C. Hamscher Jul. 1988 56 p
(Contract N00014-85-K-0124)
(AD-A201614; AI-M-1059) Avail: NTIS HC A04/MF A01 CSCL 12I

To determine why something has stopped working, its useful to know how it was supposed to work in the first place. That simple observation underlies some of the considerable interest generated in recent years on the topic of model-based reasoning, particularly its application to diagnosis and troubleshooting. This paper surveys the current state of the art, reviewing areas that are well understood and exploring areas that present challenging research topics. It views the fundamental paradigm as the interaction of prediction and observation, and explores it by examining three fundamental subproblems: generating hypotheses by reasoning from a symptom to a collection of components whose misbehavior may plausibly have caused that symptom; testing each hypothesis to see whether it can account for all available observations of device behavior; then discriminating among the ones that survive testing. We analyze each of these independently at the knowledge level i.e., attempting to understand what reasoning capabilities arise from the different varieties of knowledge available to the program. We find that while a wide range of apparently diverse model-based systems have been built for diagnosis and troubleshooting, they are for the most part variations on the central theme outlined here. Their diversity lies primarily in the varying amounts of kinds of knowledge they bring to bear at each stage of the process; the underlying paradigm is fundamentally the same. GRA

N89-19446*# National Aeronautics and Space Administration. Lewis Research Center, Cleveland, OH.
THE SOLID SURFACE COMBUSTION SPACE SHUTTLE EXPERIMENT HARDWARE DESCRIPTION AND GROUND-BASED TEST RESULTS
D. M. Vento, R. J. Zavesky, K. R. Sacksteder, and R. A. Altenkirch (Mississippi State Univ., Mississippi State.) Jan. 1989 9 p Presented at the 27th Aerospace Sciences Meeting, Reno, NV, 8-12 Jan. 1989; sponsored by AIAA Previously announced in IAA as A89-28419
(NASA-TM-101963; E-4661; NAS 1.15:101963) Avail: NTIS HC A02/MF A01 CSCL 22B

The Lewis Research Center is developing a series of microgravity combustion experiments for the Space Shuttle. The Solid Surface Combustion Experiment (SSCE) is the first to be completed. SSCE will study flame spreading over thermally thin fuels (ashless filter paper) under microgravity conditions. The flight hardware consists of a combustion chamber containing the sample and a computer which takes the data and controls the experiment. Experimental data will include gas-phase and solid-phase temperature measurements and motion pictures of the combustion process. Flame spread rates will be determined from the motion pictures. Author

N89-19447# MATRA Espace, Paris-Velizy (France).
SPECIFICATION VALIDATION TOOLS STUDY Final Report
J. P. Sotta Paris, France ESA 25 May 1987 99 p
(Contract ESTEC-6824/86-NL-PP(SC))
(MATRA-NT/139/1939; ESA-CR(P)-2542; ETN-89-93639) Avail: NTIS HC A05/MF

The use of the SMALLTALK language for specification of space mission information systems was assessed. It is shown that functional prototyping is possible. The SMALLTALK-80 language provides a complete development environment and powerful conceptual features that makes it a very good support for prototyping. Simple versions of both prototyping tool and demonstration examples were built rapidly. The prototyping approach should be introduced in the development cycle of space systems because it allows early verification of the functional analysis. However, it should not be limited to this phase and should be associated with the project data base to support various utilizations by keeping the unicity of the system definition. It is important that a model of the coordination tasks (e.g., mode management) in a space system is developed in order to make easier its verification and its implementation. This model should integrate the conventional way to define the management tasks and a more formal description. The approach could be applied to reliability analysis at functional level, and development of dynamic and hierarchic models of mode management. ESA

N89-19448# Istituto Elettrotecnico Nazionale (Galileo Ferraris), Turin (Italy).
[ACTIVITIES REPORT IN ELECTROTECHNOLOGY] Annual Report, 1987
May 1988 159 p Original contains color illustrations
(ETN-89-93715) Avail: NTIS HC A08/MF A01

Activities in time, frequency, and electromagnetic metrology; electrical metrology; photometry; acoustics; materials; electromechanics; and systems engineering are summarized. Engineering materials research includes magnetic materials and study of magnetic, electrical, radiometric, photometric, and acoustic properties of materials for specific applications. Electrical equipment research includes protection and reliability of low-voltage electrical installations and requirements to ensure electrical safety. Environment protection and human health research covers development of measurement and analysis techniques. Computer science includes development of techniques for image understanding, research on reliability of complex systems, and application of numerical techniques of computer aided design of electrical devices. ESA

32 COMMUNICATIONS AND RADAR

Includes radar; land and global communications; communications theory; and optical communications.

For related information see also *04 Aircraft Communications and Navigation* and *17 Space Communications, Spacecraft Communications, Command and Tracking.* For search and rescue see *03 Air Transportation and Safety,* and *16 Space Transportation.*

N89-19449*# Harris Corp., Melbourne, FL. Government Communication Systems Div.
A 20 GHz LOW NOISE, LOW COST RECEIVER FOR DIGITAL SATELLITE COMMUNICATION SYSTEM, GROUND TERMINAL APPLICATIONS Final Report
Glen Allen 15 Dec. 1988 244 p
(Contract NAS3-24244)
(NASA-CR-182243; NAS 1.26:182243) Avail: NTIS HC A11/MF A01 CSCL 17B

A 45 month effort for the development of a 20 GHz, low-noise, low-cost receiver for digital, satellite communication system, ground terminal applications is discussed. Six proof-of-concept receivers were built in two lots of three each. Performance was generally consistent between the two lots. Except for overall noise figure, parameters were within or very close to specification. While noise figure was specified as 3.5 dB, typical performance was measured at 3.0 to 5.5 dB, over the full temperature range of minus 30 C to plus 75 C. NASA

N89-19450 British Broadcasting Corp., Kingswood (England). Engineering Div.
ON THE DESIGN OF LOUDSPEAKERS FOR BROADCAST MONITORING
C. D. Mathers Dec. 1988 28 p
(BBC-RD-1988/14; PH-288) Avail: BBC, Kingswood Warren, Tadworth, Surrey, United Kingdom

By designing its own monitoring loudspeakers for about the past forty years, the BBC has achieved a degree of continuity and consensus in a subject where there are almost as many opinions as there are designers. The approach that has evolved within the BBC toward design and assessment is described. How calculation and objective measurement are supplemented by experience and subjective judgement to arrive at a design that is acceptable to users in the broadcasting service is indicated. Each component of the loudspeaker is considered, and the problems of achieving consistency and reliability are addressed. Author

N89-19451*# Jet Propulsion Lab., California Inst. of Tech., Pasadena.
THE TELECOMMUNICATIONS AND DATA ACQUISITION REPORT Progress Report, Oct. - Dec. 1988
E. C. Posner, ed. 15 Feb. 1989 210 p
(NASA-CR-184812; JPL-TDA-PR-42-96; NAS 1.26:184812) Avail: NTIS HC A10/MF A01 CSCL 17B

Deep Space Network advanced systems, very large scale integration architecture for decoders, radar interface and control units, microwave time delays, microwave antenna holography, and a radio frequency interference survey are among the topics discussed. For individual titles, see N89-19452 through N89-19466.

N89-19452*# Jet Propulsion Lab., California Inst. of Tech., Pasadena.
DESIGN AND TEST OF A 2.25-MW TRANSFORMER RECTIFIER ASSEMBLY **c33**
R. Cormier and J. Daeges *In its* The Telecommunications and Data Acquisition Report 15 Feb. 1989 p 1-13 (For primary document see N89-19451 12-32)
Avail: NTIS HC A10/MF A01 CSCL 17B

A new 2.25-MW transformer rectifier assembly was fabricated for DSS-13 at Goldstone, California. The transformer rectifier will provide constant output power of 2.25 MW at any voltage from 31 kV to 125 kV. This will give a new capability of 1 MW of RF power at X-band, provided appropriate microwave tubes are in the power amplifier. A description of the design and test results is presented. Author

N89-19453*# Jet Propulsion Lab., California Inst. of Tech., Pasadena.
ON SAMPLING BAND-PASS SIGNALS
R. Sadr and M. Shahshahani *In its* The Telecommunications and Data Acquisition Report 15 Feb. 1989 p 14-20 (For primary document see N89-19451 12-32)
Avail: NTIS HC A10/MF A01 CSCL 17B

Four techniques for uniform sampling of band-bass signals are examined. The in-phase and quadrature components of the band-pass signal are computed in terms of the samples of the original band-pass signal. The relative implementation merits of these techniques are discussed with reference to the Deep Space Network (DSN). Author

N89-19454*# Jet Propulsion Lab., California Inst. of Tech., Pasadena.
THE USE OF INTERLEAVING FOR REDUCING RADIO LOSS IN CONVOLUTIONALLY CODED SYSTEMS
D. Divsalar, M. K. Simon, and J. H. Yuen *In its* The Telecommunications and Data Acquisition Report 15 Feb. 1989 p 21-39 (For primary document see N89-19451 12-32)
Avail: NTIS HC A10/MF A01 CSCL 17B

The use of interleaving after convolutional coding and deinterleaving before Viterbi decoding is proposed. This effectively reduces radio loss at low-loop Signal to Noise Ratios (SNRs) by several decibels and at high-loop SNRs by a few tenths of a decibel. Performance of the coded system can further be enhanced if the modulation index is optimized for this system. This will correspond to a reduction of bit SNR at a certain bit error rate for the overall system. The introduction of interleaving/deinterleaving into communication systems designed for future deep space missions does not substantially complicate their hardware design or increase their system cost. Author

N89-19455*# Jet Propulsion Lab., California Inst. of Tech., Pasadena.
A NEW VLSI ARCHITECTURE FOR A SINGLE-CHIP-TYPE REED-SOLOMON DECODER
I. S. Hsu and T. K. Truong *In its* The Telecommunications and Data Acquisition Report 15 Feb. 1989 p 40-48 (For primary document see N89-19451 12-32)
Avail: NTIS HC A10/MF A01 CSCL 17B

A new very large scale integration (VLSI) architecture for implementing Reed-Solomon (RS) decoders that can correct both errors and erasures is described. This new architecture implements a Reed-Solomon decoder by using replication of a single VLSI chip. It is anticipated that this single chip type RS decoder approach

will save substantial development and production costs. It is estimated that reduction in cost by a factor of four is possible with this new architecture. Furthermore, this Reed-Solomon decoder is programmable between 8 bit and 10 bit symbol sizes. Therefore, both an 8 bit Consultative Committee for Space Data Systems (CCSDS) RS decoder and a 10 bit decoder are obtained at the same time, and when concatenated with a (15,1/6) Viterbi decoder, provide an additional 2.1-dB coding gain. Author

N89-19456*# Jet Propulsion Lab., California Inst. of Tech., Pasadena.

A SIMPLIFIED PROCEDURE FOR DECODING THE (23,12) AND (24,12) GOLAY CODES

T. K. Truong, J. K. Holmes, I. S. Reed, and X. Yin (University of Southern California, Los Angeles.) *In its* The Telecommunications and Data Acquisition Report 15 Feb. 1989 p 49-58 (For primary document see N89-19451 12-32)

Avail: NTIS HC A10/MF A01 CSCL 17B

A simplified procedure is developed to decode the three possible erors in a (23,12) Golay codeword. A computer simulation shows that this algorithm is modular, regular and naturally suitable for both Very Large Scale Integration (VLSI) and software implementation. An extension of this new decoding procedure is used also to decode the 1/2-rate (24,12) Golay code, thereby correcting three and detecting four errors. Author

N89-19457*# University of Southern California, Los Angeles. Dept. of Electrical Engineering.

TEST ASPECTS OF THE JPL VITERBI DECODER

M. A. Breuer *In* JPL, The Telecommunications and Data Acquisition Report 15 Feb. 1989 p 59-79 (For primary document see N89-19451 12-32)

Avail: NTIS HC A10/MF A01 CSCL 17B

The generation of test vectors and design-for-test aspects of the Jet Propulsion Laboratory (JPL) Very Large Scale Integration (VLSI) Viterbi decoder chip is discussed. Each processor integrated circuit (IC) contains over 20,000 gates. To achieve a high degree of testability, a scan architecture is employed. The logic has been partitioned so that very few test vectors are required to test the entire chip. In addition, since several blocks of logic are replicated numerous times on this chip, test vectors need only be generated for each block, rather than for the entire circuit. These unique blocks of logic have been identified and test sets generated for them. The approach employed for testing was to use pseudo-exhaustive test vectors whenever feasible. That is, each cone of logid is tested exhaustively. Using this approach, no detailed logic design or fault model is required. All faults which modify the function of a block of combinational logic are detected, such as all irredundant single and multiple stuck-at faults.

Author

N89-19458*# Jet Propulsion Lab., California Inst. of Tech., Pasadena.

ON TESTING VLSI CHIPS FOR THE BIG VITERBI DECODER **c33**

I. S. Hsu *In its* The Telecommunications and Data Acquisition Report 15 Feb. 1989 p 80-92 (For primary document see N89-19451 12-32)

Avail: NTIS HC A10/MF A01 CSCL 09C

A general technique that can be used in testing very large scale integrated (VLSI) chips for the Big Viterbi Decoder (BVD) system is described. The test technique is divided into functional testing and fault-coverage testing. The purpose of functional testing is to verify that the design works functionally. Functional test vectors are converted from outputs of software simulations which simulate the BVD functionally. Fault-coverage testing is used to detect and, in some cases, to locate faulty components caused by bad fabrication. This type of testing is useful in screening out bad chips. Finally, design for testability, which is included in the BVD VLSI chip design, is described in considerable detail. Both the observability and controllability of a VLSI chip are greatly enhanced by including the design for the testability feature. Author

N89-19459*# Jet Propulsion Lab., California Inst. of Tech., Pasadena.

WIRING VITERBI DECODERS (SPLITTING DEBRUIJN GRAPHS) **c33**

O. Collins, F. Pollara, S. Dolinar, and J. Statman *In its* The Telecommunications and Data Acquisition Report 15 Feb. 1989 p 93-104 (For primary document see N89-19451 12-32)

Avail: NTIS HC A10/MF A01 CSCL 09C

A new Viterbi decoder, capable of decoding convolutional codes with constraint lengths up to 15, is under development for the Deep Space Network (DSN). A key feature of this decoder is a two-level partitioning of the Viterbi state diagram into identical subgraphs. The larger subgraphs correspond to circuit boards, while the smaller subgraphs correspond to Very Large Scale Integration (VLSI) chips. The full decoder is built from identical boards, which in turn are built from identical chips. The resulting system is modular and hierarchical. The decoder is easy to implement, test, and repair because it uses a single VLSI chip design and a single board design. The partitioning is completely general in the sense that an appropriate number of boards or chips may be wired together to implement a Viterbi decoder of any size greater than or equal to the size of the module. Author

N89-19460*# Jet Propulsion Lab., California Inst. of Tech., Pasadena.

BLOCK DIAGRAMS OF THE RADAR INTERFACE AND CONTROL UNIT **c33**

J. W. Collier *In its* The Telecommunications and Data Acquisition Report 15 Feb. 1989 p 104-116 (For primary document see N89-19451 12-32)

Avail: NTIS HC A10/MF A01 CSCL 09C

The Interface and Control Unit is the heart of the radar module, which occupies one complex channel of the High-Speed Data Acquisition System of the Goldstone Solar System Radar. Block diagrams of the interface unit are presented as an aid to understanding its operation and interconnections to the rest of the radar module. Author

N89-19461*# Jet Propulsion Lab., California Inst. of Tech., Pasadena.

RF PERFORMANCE MEASUREMENT OF THE DSS-14 70-METER ANTENNA AT C-BAND/L-BAND

M. S. Gatti, A. J. Freiley, and D. Girdner *In its* The Telecommunications and Data Acquisition Report 15 Feb. 1989 p 117-125 (For primary document see N89-19451 12-32)

Avail: NTIS HC A10/MF A01 CSCL 17B

The calibration of the 70-meter antenna at C-band (5.01 GHz) and L-band (1.668 GHz) is described. This calibration comes after a modification to an existing L-band feed to include the C-band frequencies. The test technique employs noise-adding radiometers and associated equipment running simultaneously at both frequencies. The test procedure is described including block diagrams, and results are presented for efficiency, system temperature, and pointing. Author

N89-19462*# Jet Propulsion Lab., California Inst. of Tech., Pasadena.

MICROWAVE TIME DELAYS FOR THE DUAL L-C-BAND FEED SYSTEM **c33**

J. Chen *In its* The Telecommunications and Data Acquisition Report 15 Feb. 1989 p 126-131 (For primary document see N89-19451 12-32)

Avail: NTIS HC A10/MF A01 CSCL 09C

A new dual-frequency feed system at Goldstone is designed to receive the Phobos spacecraft signal at L-band (1668 + or - 40 MHz) and transmit to the spacecraft at C-band (5008.75 + or - 5.00 MHz) simultaneously. Hence, calculations of the time delay from the C-band range calibration coupler to the phase center of the L-C dual feed and back to the L-band range calibration coupler are required to correct the range measurements. Time delays of the elements in the dual-frequency feed system are obtained mostly from computer calculations and partly from experimental

measurements. The method used and results obtained are described. Author

N89-19463*# Jet Propulsion Lab., California Inst. of Tech., Pasadena.
SYSTEMS ANALYSIS FOR DSN MICROWAVE ANTENNA HOLOGRAPHY **c35**
D. J. Rochblatt *In its* The Telecommunications and Data Acquisition Report 15 Feb. 1989 p 132-157 (For primary document see N89-19451 12-32)
Avail: NTIS HC A10/MF A01 CSCL 14B

Proposed systems for Deep Space Network (DSN) microwave antenna holography are analyzed. Microwave holography, as applied to antennas, is a technique which utilizes the Fourier Transform relation between the complex far-field radiation pattern of an antenna and the complex aperture field distribution to provide a methodology for the analysis and evaluation of antenna performance. Resulting aperture phase and amplitude distribution data are used to precisely characterize various crucial performance parameters, including panel alignment, subreflector position, antenna aperture illumination, directivity at various frequencies, and gravity deformation. Microwave holographic analysis provides diagnostic capacity as well as being a powerful tool for evaluating antenna design specifications and their corresponding theoretical models. Author

N89-19464*# Jet Propulsion Lab., California Inst. of Tech., Pasadena.
Ka-BAND STUDY: 1988
J. W. Layland, R. L. Horttor, R. C. Clauss, J. H. Wilcher, R. J. Wallace, and D. J. Mudgway *In its* The Telecommunications and Data Acquisition Report 15 Feb. 1989 p 158-171 (For primary document see N89-19451 12-32)
Avail: NTIS HC A10/MF A01 CSCL 17B

The Ka-band study team was chartered in late 1987 to bring together all the planning elements for establishing 32 GHz (Ka-band) as the primary downlink frequency for deep-space operation, and to provide a stable baseline from which to pursue that development. This article summarizes the results of that study at its conclusion in mid-1988, and corresponds to material presented to NASA's Office of Space Operations on July 14, 1988. For a variety of reasons, Ka-band is the right next major step in deep-space communications. It offers improved radio metric accuracy through reduced plasma sensitivity and increased bandwidth. Because of these improvements, it offers the opportunity to reduce costs in the flight radio system or in the DSN by allocating part of the overall benefits of Ka-band to this cost reduction. A mission scenario is being planned that can drive at least two and possibly all three of the DSN subnets to provide a Ka-band downlink capability by the turn of the century. The implementation scenario devised by the study team is believed to be feasible within reasonable resource expectations, and capable of providing the needed upgrade as a natural follow-on to the technology development which is already underway. Author

N89-19465*# Jet Propulsion Lab., California Inst. of Tech., Pasadena.
A LOW-LOSS LINEAR ANALOG PHASE MODULATOR FOR 8415 MHz TRANSPONDER APPLICATION **c33**
N. Mysoor *In its* The Telecommunications and Data Acquisition Report 15 Feb. 1989 p 172-178 (For primary document see N89-19451 12-32)
Avail: NTIS HC A10/MF A01 CSCL 09C

A breadboard single-section low-loss analog phase modulator with good thermal stability for a spacecraft transponder application has been analyzed, fabricated, and evaluated. A linear phase shift of 70 degrees with a linearity tolerance of plus or minus 7 percent was measured for this modulator from 8257 to 8634 MHz over the temperature range -20 C to 75 C. The measured insertion loss and the static delay variation with temperature were within 2 plus or minus 0.3 dB and 0.16 ps/C, respectively. Four sections will be cascaded to provide the X-band (8415 MHz) phase modulator. The generic modulator design can also be utilized at 7950 to 8075 MHz followed by X4 multiplication to provide modulation of a Ka-band downlink signal. Author

N89-19466*# Jet Propulsion Lab., California Inst. of Tech., Pasadena.
RADIO FREQUENCY INTERFERENCE SURVEY OVER THE 1.0-10.4 GHz FREQUENCY RANGE AT THE GOLDSTONE-VENUS DEVELOPMENT STATION
S. Gulkis, E. T. Olsen, M. J. Klein, and E. B. Jackson *In its* The Telecommunications and Data Acquisition Report 15 Feb. 1989 p 179-190 (For primary document see N89-19451 12-32)
Avail: NTIS HC A10/MF A01 CSCL 17B

The results of a low sensitivity Radio Frequency Interference (RFI) survey carried out at the Venus Station of the Goldstone Communications Complex are reported. The data cover the spectral range from 1 GHz to 10.4 GHz with a 10-kHz instantaneous bandwidth. Frequency and power levels were observed using a sweep-frequency spectrum analyzer connected to a 1-m diameter antenna pointed at zenith. The survey was conducted from February 16, 1987 through February 24, 1987. Author

N89-19467# Illinois Univ., Chicago. Dept. of Electrical Engineering and Computer Science.
ADVANCEMENT OF HIGH RESOLUTION RADAR POLARIMETRY IN TARGET VERSES CLUTTER DETECTION, DISCRIMINATION, CLASSIFICATION. A: BASIC THEORY AND MODELING OF POLARIMETRIC CLUTTER PHENOMENOLOGY Final Report, 1 Mar. 1985 - 29 Feb. 1988
W. M. Boerner, H. J. Eom, A. B. Kostinski, A. P. Agrawal, and B. Y. Foo 15 Jul. 1988 396 p
(Contract DAAG29-85-K-0065)
(AD-A201240; UIC-EECS-88-07-15-Pt-A; ARO-22207.11-EL-Pt-A)
Avail: NTIS HC A17/MF A01 CSCL 17I

The overall objective of our polarimetric research is to conduct a unified and cohesive investigation to answer the question: How can polarization properties of targets/background speckle be utilized either by themselves or in concert with other electromagnetic probing methods such as Doppler, multispectral, pulse compression, etc., to best provide a basis for radar target classification, imaging, and identification. Scattering objects of interest include airborne/ground/marine targets of a large variety of sizes, shapes, and material decomposition and embedded in varied stationary/moving/fluctuating background scatter, which, we are confident, can most effectively be characterized via polarimetric radar/scatterometer methods including both coherent and partially coherent wave treatments. It is a specific objective of this task to approach and to investigate the polarimetric radar clutter problem using a unique approach of a strongly interdigitalizing analytical, modeling, computer-numerical/graphical, and measurement interpretive nature. A basic theory for a model-independent clutter description which can be applied to any specific type of clutter without a priori knowledge of the clutter model, i.e., a model-independent clutter description, in theory, is introduced. GRA

N89-19468# Army Missile Command, Redstone Arsenal, AL. Test and Evaluation Directorate.
ELECTROMAGNETIC COMPATIBILITY TEST REPORT FOR THE TETHERED SATELLITE DATA ACQUISITION AND CONTROL ASSEMBLY Final Report
Douglas Hoskins and Robert Snead 17 May 1988 75 p
(AD-A201549; AD-E951220; AMSMI/TR-RD-TE-88-2) Avail: NTIS HC A04/MF A01 CSCL 12F

This report details the results of an electromagnetic compatibility test on the SCI Systems Data Acquisition and Control Assembly (DACA). This assembly is an electronic processor which controls the central communication link from the Tethered Satellite System (TSS) to the Space Transportation System Orbiter Space Shuttle. GRA

N89-19469# Naval Postgraduate School, Monterey, CA.
COMPUTER ALGORITHMS FOR MEASUREMENT CONTROL AND SIGNAL PROCESSING OF TRANSIENT SCATTERING SIGNATURES M.S. Thesis
Chunk-Kiang Pang Sep. 1988 91 p
(AD-A201672) Avail: NTIS HC A05/MF A01 CSCL 17I

This thesis describes the development of computer algorithms for experimental measurement control and subsequent signal processing of transient signatures to synthesize scattering impulse responses of scale model targets. The theories behind transient scattering are considered in order to construct the algorithms. Up-to-date hardware and software technology are selectively implemented to optimize the resultant signal to noise ratio. The detailed explanation of the hardware and software operation is provided. A noise model for the system is also discussed. Measurement and programming validations are described, where comparisons are made with numerical computations for transient scattering by selected canonical targets. Results are documented for further research in the transient scattering problem. GRA

N89-19470 Brown Univ., Providence, RI.
STEADY WAVES IN A NONLINEAR THEORY OF VISCOELASTICITY Ph.D. Thesis
Gregory Thomas Warhola 1988 135 p
Avail: Univ. Microfilms Order No. DA8822611

The propagation of steady waves in viscoelastic materials for which the nonlinear strain measure is not necessarily convex is considered. The shape of such a wave is governed by an ordinary nonlinear integro-differential equation having a possibly singular difference kernel. The existence and structure of a solution depends upon the relation of the wavespeed, a parameter in the problem, to two speeds based upon the state of the material ahead of the wave. Solutions are constructed by a monotone iterative scheme which is proven to converge to a unique solution within restricted classes of functions depending upon the wavespeed. A simple numerical approximation to the iterative scheme is used to produce graphs of solutions. An algebraic quasielastic approximation produces upper bounds on discontinuous (shock and acceleration wave) solutions. For a material such as polymethyl methacrylate (PMMA) having a small power in a power-law model of its compliance, this approximation is found to be useful for accurately predicting the structure of shock solutions. Dissert. Abstr.

N89-19471# Kansas State Univ., Manhattan. Dept. of Electrical and Computer Engineering.
CALCULATION OF MUTUAL SELF INDUCTANCE AND COUPLING COEFFICIENT FOR CLOSELY SPACED LOOPS Final Report, 15 Apr. 1987 - 15 Apr. 1988
Kenneth H. Carpenter 20 Jun. 1988 99 p Prepared for Lawrence Livermore National Lab., CA
(Contract W-7405-eng-48)
(DE89-005546; UCRL-21140) Avail: NTIS HC A06/MF A01

The magnetic coupling of closely spaced, flat loops has been studied, assuming both coupling in air and coupling in the presence of ferrite cores. The equivalent circuits for such coupled loops have been derived, and the effect of resistance in the loops on measurements of coupling evaluated. For loops typically used, conductor resistance was found to have no significant effect on measurements. Series expansions for vector potential and mutual inductance have been derived for circular flat loops, and these expansions have been used to write a computer code, COUPM2IN, which simulates the magnetic coupling accurately enough to be used to aid air cored transformer design. With ferrite cores present the magnetizing current is a much smaller fraction of transformer current than with air cored design. Thus even though the models determined for the ferrite cored inductors only approximately simulate the saturation of the ferrite and the delay of the rotation of the magnetic domains, these models can be used to aid ferrite cored transformer design. The computer codes for both the air cored and ferrite cored cases are listed in appendices. It is recommended that follow up work be undertaken to refine the ferrite core modeling and to produce more robust computer programs for transformer designers. DOE

N89-19472# Virginia Polytechnic Inst. and State Univ., Blacksburg. Dept. of Electrical Engineering.
ANALYSIS AND SYNTHESIS OF MICROSTRIP ANTENNAS INCLUDING MUTUAL COUPLING Final Report, 1 Sep. 1984 - 31 Aug. 1988
Koichiro Takamizawa and Warren L. Stutzman Sep. 1988 257 p
(Contract DAAG29-84-K-0148)
(AD-A201783; ARO-22295.1-EL; VPI/EE-SATCOM-82-2) Avail: NTIS HC A12/MF A01 CSCL 09A

An array antenna is an assembly of radiating elements in one of many possible geometrical configurations with outputs of the individual elements in the array combined to produce radiation of desired pattern shape and gain. The advantages of array antennas over a single antenna include the following: (1) high gain and high resolution without increasing the physical size of each element, (2) electronic control of radiation patterns, such as scanning of main beam and shaping of radiation pattern, and (3) graceful degradation. Many techniques have been developed in the synthesis of array patterns. Most of the techniques, however, ignore mutual coupling between array elements. Mutual coupling is the electromagnetic interaction between array elements. In addition, unless the antenna elements are perfectly isolation power dividers are used, there will be coupling through the feed network. The two fold coupling problem (element-to-element and feed network coupling) then becomes difficult for analysis and very difficult for synthesis. This is because coupling from one element to another can travel through the feed network and reappear in other elements leading to further antenna coupling: this is an endless coupling effect. GRA

N89-19473# Massachusetts Inst. of Tech., Lexington. Lincoln Lab.
TDWR (TERMINAL DOPPLER WEATHER RADAR) SCAN STRATEGY REQUIREMENTS
S. D. Campbell and M. W. Merritt 3 Nov. 1988 21 p
(Contract F19628-85-C-0002)
(AD-A201785; DOT/FAA/PM-87-22) Avail: NTIS HC A03/MF A01 CSCL 17I

The requirements for the scan strategy to be employed in the Terminal Doppler Weather Radar (TDWR) are described. The report is divided into three main sections: rationale, example scan strategy and requirements. The rationale for the TDWR scan strategy is presented in terms of: (1) detection of meteorological phenomena, and (2) minimization of range and velocity folding effects. Next, an example is provided based on an experimental scan strategy used in Denver during the summer of 1987. Finally, the requirements for the TDWR scan strategy are presented based on the preceeding discussion. Also, an appendix is included describing the proposed criteria for switching between scan modes. GRA

N89-19474# Houston Univ., TX. Dept. of Electrical Engineering.
MILLIMETER WAVE ANTENNAS Final Report, 1 Sep. 1984 - 31 Aug. 1988
Stuart A. Long and David R. Jackson 28 Oct. 1988 63 p
(Contract DAAG29-84-K-0166)
(AD-A201919; ARO-21139.11-EL) Avail: NTIS HC A04/MF A01 CSCL 09A

The properties of two types of antennas suitable for operation at millimeter wave frequencies (100 to 300 GHz) have been investigated both theoretically and experimentally. The type of radiators considered were printed-circuit or microstrip antennas and dielectric resonator antennas. Special emphasis was placed on the problem of integrating the antenna with the waveguiding structure. The ultimate objective of the research was to provide aid in the selection and design of millimeter wave antennas for given systems applications within this frequency range. GRA

N89-19475# Massachusetts Univ., Amherst.
NORMALIZED RADAR CROSS SECTION OF NATURAL SURFACES AT MILLIMETER WAVELENGTHS Final Report, 22 - 23 Sep. 1985
Robert E. McIntosh Nov. 1988 11 p
(Contract DAAG29-85-K-0227)
(AD-A202252; ARO-22851.1-GS) Avail: NTIS HC A03/MF A01 CSCL 17I

The scattering of millimeter waves by foliated and snow-covered surfaces is of interest to designers of future radar and communication systems. It is also of interest to the remote sensing community, which is interested in the high-frequency behavior of radar signatures of natural surfaces. The University of Massachusetts Microwave Remote Sensing Laboratory developed a unique high-powered 215 GHz radar system. It used this system to measure the Normalized Radar Cross Section (NRCS) of trees and snow packs. Results of these studies are described in this report. GRA

N89-19476# Aerospace Corp., El Segundo, CA. Chemistry and Physics Lab.
AN INVARIANT IMBEDDING T MATRIX APPROACH TO ELECTROMAGNETIC SCATTERING
Bernard R. Johnson 31 Aug. 1988 50 p
(Contract F04701-85-C-0086)
(AD-A202298; TR-0088(3945-04)-1; SD-TR-88-108) Avail: NTIS HC A03/MF A01 CSCL 20N

A new method for calculating electromagnetic scattering from an arbitrary shaped, inhomogeneous, dielectric object is developed. The method is based on an invariant imbedding procedure for computing the T matrix that was originally developed to solve quantum mechanical scattering problems. The final outcome of this approach is a two-term recurrence relation which can be solved numerically for the T matrix. The limiting form of this recurrence relation is a first-order nonlinear differential equation that is identical in form to the quantum mechanical Calogero equation. The results of several test calculations are presented. GRA

N89-19477# Technical Univ. of Denmark, Lyngby. Inst. of Electromagnetics.
EXPERIMENTAL SPHERICAL NEAR-FIELD ANTENNA TEST FACILITY, PHASE 3. VOLUME 1: FACILITY UPDATES, EVALUATION AND SOFTWARE DOCUMENTATION Final Report
J. E. Hansen and F. Holm Larsen Paris, France ESA Aug. 1987 94 p
(Contract ESTEC-4682/81-NL-MS(SC))
(R-343; ESA-CR(P)-2591; ETN-89-93641) Avail: NTIS HC A05/MF A01

Improvements to the subsystems of the ESA spherical near-field test range are described. An antenna positioner steel tower allowing test antenna diameters of 6 m was installed. A series of 14 measuring probes (dual polarized) was designed, constructed, and tested. The probes cover the frequency range of 3 to 18 GHz. A spherical near-field transformation program SNIFN allowing test antenna diameters of 300 wavelengths was implemented on the system minicomputer. The alignment sequence was updated. A user guide to the measurement system and its software is presented. The information is sufficiently detailed to tell a test engineer how to operate the system manually and in the automatic mode. It also allows the operator to process data, including the near-field to far-field transformation, and to produce radiation patterns and contour plots. Measurements produced are reviewed. ESA

N89-19478# MATRA Espace, Paris-Velizy (France).
TELESCIENCE SYSTEM CONCEPT STUDY, VOLUME 2 Final Report
Paris, France ESA Nov. 1987 291 p Prepared in cooperation with Messerschmitt-Boelkow-Blohm/Entwicklungspring Nord, Bremen (Federal Republic of Germany)
(Contract ESTEC-6977/86-NL-PP(SC))
(MATRA-NT/2113/139-Vol-2; ESA-CR(P)-2592-Vol-2; ETN-89-93643) Copyright Avail: NTIS HC A13/MF A01

A demonstration test for Columbus interactive user operations is defined. The data management system (DMS) test bed and the crew work station (CWS) test bed represent the on-board facilities. A pilot experiment (PE), using the fluid physics module, is physically integrated into DMS/CWS test beds. The data management laboratory (DML), providing the necessary test environment, represents the ground segment and the space/ground links. A scientific user, interfaces the telescience test bed (TB) through a console of the DML. A payload on-board operator, interfaces the telescience test bed through CWS-TB facilities and has direct physical and visual contact with the PE. Hardware and basic software configurations necessary to run the telescience demonstration tests are defined. ESA

N89-19479 Politecnico di Milano (Italy). Dipartimento di Elettronica.
SYNTHETIC APERTURE RADAR (SAR) DATA FOCUSING USING SEISMIC MIGRATION TECHNIQUES
C. Caffario, C. Prati, and F. Rocca 1988 26 p
(Rept-88-015; ETN-89-93718) Avail: Politecnico di Milano, Piazza Leonardo da Vinci 32, 20133 Milan, Italy

Synthetic aperture radar (SAR) data were focused using migration techniques, similar to those used in geophysics. The frequency-wavenumber approach is extremely efficient: it attains almost the ultimate results in performance, with the efficiency of frequency domain implementation. The method is exact when the sensor flies among a rectilinear path, but even with a spherical Earth and a circular sensor trajectory the results are extremely good. Terrestrial swaths as wide as 100 km can be focused simultaneously with no serious degradation, at least with the spatial resolution used or envisaged in SAR missions. The algorithm was tested with synthetic data and with SEASAT-A data: results support the theoretical analysis. ESA

N89-19480 Politecnico di Milano (Italy). Dipartimento di Elettronica.
PROPAGATION PROBLEMS REGARDING 20/30 GHz BANDS IN EARTH-SPACE LINKS
A. Paraboni 1988 55 p
(Rept-88-022; ETN-89-93719) Avail: Politecnico di Milano, Piazza Leonardo da Vinci 32, 20133 Milan, Italy

Meteorological factors affecting slant path propagation in the 20/30 GHz bands are reviewed. Rain causes attenuation, depolarization and interference by scattering. Hail is probably unimportant in the sense that during severe storms links at 30 GHz are probably blinded by the accompanying rain. Snowflakes have a marginal importance as far as they are wet; in the opposite case, as in the brightband, they can constitute a problem. Clouds and fog give attenuation but no depolarization; ice needles can be a source of depolarization and occasional signal fading can occur as the result of polarization mismatch between the receiving antenna and the incoming wave. Gaseous water vapor absorption is a factor of fading according to its occasional concentration in the atmosphere; it is worth noting that the resonance line of the water vapor absorption is 22 GHz. The effect is then strongly dependent on the exact position of the 20 GHz band with respect to the absorption band. Air turbulence can be the source of rapid signal variations known as scintillations. ESA

N89-19481 Politecnico di Milano (Italy). Dipartimento di Elettronica.
PROPAGATION PROBLEMS REGARDING MILLIMETER WAVES (40/50 GHz)
A. Paraboni 1988 54 p
(Rept-88-023; ETN-89-93720) Avail: Politecnico di Milano, Piazza Leonardo da Vinci 32, 20133 Milan, Italy

Meteorological factors affecting slant path propagation in the 40/50 GHz bands are reviewed. Rain can cause attenuation, depolarization and interference by scattering; incoherent radiation can also be important when using medium gain antennas (40 dB). Hail is probably unimportant in the sense that during severe storms

links at 40/50 GHz are likely to be blinded by the accompanying rain. Snowflakes are of marginal importance as far as they are wet; in the opposite case, as in the brightband, they can constitute a problem. Clouds and fog give attenuation but no depolarization; ice needles can be a source of depolarization and signal fading can occur as the result of polarization mismatch between the receiving antenna and the incoming wave. Gaseous water vapor absorption is a factor of fading according to its occasional concentration in the atmosphere; for the remaining gaseous components the main effect is that of oxygen, whose resonance line is centered at 60 GHz but whose effects are already remarkable at 50 GHz. Air turbulence can be a source of rapid signal variations (possibly superimposed on those cause by rain incoherent radiation) known as scintillations. ESA

N89-19482# ANT Nachrichtentechnik, Backnang (Germany, F.R.). Space Communications Systems Div.
CODE PERFORMANCE SIMULATION STUDY FOR DRS S-BAND TRANSMISSION Final Report
S. Rasmussen, W. Schreitmueller, and J. Heichler Paris, France ESA Jun. 1988 181 p
(Contract ESA-7224/87-NL-PR)
(ESA-CR(P)-2688; ETN-89-93935) Copyright Avail: NTIS HC A09/MF A01

Performance of convolutional codes of rate R greater than 1/2 with respect to radio frequency interference (RFI) and thermal noise was evaluated for a data relay satellite. Improvement obtained by code concatenation with a Reed-Solomon-Code as outer code and a convolutional inner code was studied. Effectiveness of erasure strategies in an RFI environment was assessed. Interleaver performance in RFI conditions (channel interleaver and, in a concatenated scheme, character interleaving inserted between the two codecs) was investigated. The coding scheme recommended by the Consultative Committee for Space Data Systems for telemetry channel coding was examined. Codec implementation aspects are discussed; it is shown that implementation of a repeated codec, e.g., 1/2 repeated, is much simpler than that for a normal rate 1/n (e.g., 1/4) code. ESA

N89-19483# University Coll., London (England). Dept. of Electronic and Electrical Engineering.
A STUDY OF ADVANCED RADAR ALTIMETER TECHNIQUES Final Report
H. D. Griffiths and B. Purseyyed Paris, France ESA Jan. 1988 166 p
(Contract ESA-7088/87-NL-JG(SC))
(ESA-CR(P)-2699; ETN-89-93940) Avail: NTIS HC A08/MF A01

The use of synthetic aperture processing to provide a narrow antenna beamwidth and hence high spatial resolution, and the use of multiple off-nadir beams to provide swath coverage rather than just a single nadir-pointing altimeter beam were studied. It is demonstrated that synthetic aperture processing is compatible with the full-deramp pulse compression method conventionally employed on altimeters. Calculations indicate that a considerable amount of processing power is required for the aperture synthesis operation, and that this would be better carried out off-line on the ground. Transmit power requirements are modest, and likely to be compatible with the use of solid-state transmitters. An aircraft-borne proof-of-concept instrument which could be built and flown at a very low cost is proposed. A computer simulation to model the altimeter returns and extract the elevation and surface roughness information was developed. It is shown that surface elevation can be recovered to a similar precision to that achieved by the Seasat altimeter, but that proper recovery of significant waveheight from off-nadir beams needs an impractically-large antenna system. ESA

N89-19484# Los Alamos National Lab., NM.
DES CRYPTOGRAPHIC SERVICES DESIGNED FOR THE DOE WIDE BAND COMMUNICATIONS NETWORK
Sharon Hurdle and Blaine Burnham Nov. 1987 120 p
(LA-10966-MS) Avail: NTIS HC A06/MF A01

To exchange information between separate facilities of the Nuclear Weapons Complex quickly, accurately, and in computer-readable form, the Department of Energy (DOE) has built a secure data communicaitons facility called the Wide Band Communications Network. The network properly achieves security by using high-grade encryption for the communications links and strict physical security measures at the nodes. To provide need-to-know separation among various elements and users of the network, data are encrypted before transmission using the National Bureau of Standards' Data Encryption Standard (DES) algorithm. The software described here provides the key management, key distribution, and cipher processing for this network. Author

N89-19486# Joint Publications Research Service, Arlington, VA.
VARIATIONS OF THE TROPOSPHERIC PROPAGATION RANGE OF ULTRASHORT RADIO WAVES ABOVE THE SEA
A. R. Gliner, S. N. Krivonozhkin, and B. M. Shevtsov *In its* JPRS Report: Science and Technology. USSR: Electronics and Electrical Engineering 30 Aug. 1988 p 7-8 Transl. into ENGLISH from Izvestiya Vysshikh Uchebnykh Zavedeniy: Radiofizika (Gorkiy, USSR) v. 31, no. 2, Feb. 1988 p 238-240 Original language document was announced in IAA as A88-33920 (For primary document see N89-19485 12-33)
Avail: NTIS HC A04/MF A01

N89-19826*# Massachusetts Inst. of Tech., Lexington.
KNOWLEDGE-BASED OPERATION AND MANAGEMENT OF COMMUNICATIONS SYSTEMS
Harold M. Heggestad *In* NASA. Lyndon B. Johnson Space Center, 2nd Annual Workshop on Space Operations Automation and Robotics (SOAR 1988) Nov. 1988 p 53-57 Sponsored in part by the Defense Communications Agency and the Dept. of Air Force (For primary document see N89-19817 12-59)
Avail: NTIS HC A22/MF A01 CSCL 17B

N89-20064*# University of Southern Illinois, Carbondale. Dept. of Electrical Engineering.
AUTOMATIC VOICE RECOGNITION USING TRADITIONAL AND ARTIFICIAL NEURAL NETWORK APPROACHES Final Report
Nazeih M. Botros *In* NASA, Lyndon B. Johnson Space Center, National Aeronautics and Space Administration (NASA)/American Society for Engineering Education (ASEE) Summer Faculty Fellowship Program 1988, Volume 1 Feb. 1989 13 p (For primary document see N89-20058 12-99)
Avail: NTIS HC A09/MF A01 CSCL 17B

N89-20081*# Southern Univ., Baton Rouge, LA. Dept. of Electronics Engineering Technology.
FEASIBILITY OF USING HIGH TEMPERATURE SUPERCONDUCTING MAGNETS AND CONVENTIONAL MAGNETIC LOOP ANTENNAS TO ATTRACT OR REPEL OBJECTS AT THE SPACE STATION Final Report
Manjit S. Randhawa *In* NASA, Lyndon B. Johnson Space Center, National Aeronautics and Space Administration (NASA)/American Society for Engineering Education (ASEE) Summer Faculty Fellowship Program 1988, Volume 2 Feb. 1989 14 p (For primary document see N89-20073 12-99)
Avail: NTIS HC A09/MF A01 CSCL 20N

N89-20084*# Prairie View Agricultural and Mechanical Coll., TX. Dept. of Electrical Engineering.
TIME-DOMAIN IMAGING Final Report
C. L. Tolliver *In* NASA, Lyndon B. Johnson Space Center, National Aeronautics and Space Administration (NASA)/American Society for Engineering Education (ASEE) Summer Faculty Fellowship Program 1988, Volume 2 Feb. 1989 16 p (For primary document see N89-20073 12-99)
Avail: NTIS HC A09/MF A01 CSCL 17B

33 ELECTRONICS AND ELECTRICAL ENGINEERING

Includes test equipment and maintainability; components, e.g., tunnel diodes and transistors; microminiaturization; and integrated circuitry.

For related information see also *60 Computer Operations and Hardware* and *76 Solid-State Physics.*

N89-19485# Joint Publications Research Service, Arlington, VA.
JPRS REPORT: SCIENCE AND TECHNOLOGY. USSR: ELECTRONICS AND ELECTRICAL ENGINEERING
30 Aug. 1988 55 p Transl. into ENGLISH from various Russian articles
(JPRS-UEE-88-005) Avail: NTIS HC A04/MF A01

Various topics in electronics and electrical engineering and applications are addressed. Subject areas include broadcasting and consumer electronics, antennas and propagation, instrumentation and measurements, aerospace and electronic systems, industrial electronics and control instrumentation, electronic devices, communications, electromagnetic compatibility, power engineering, and quantum electronics and electro-optics. For individual titles, see N89-19486 through N89-19487.

N89-19486# Joint Publications Research Service, Arlington, VA.
VARIATIONS OF THE TROPOSPHERIC PROPAGATION RANGE OF ULTRASHORT RADIO WAVES ABOVE THE SEA **c32**
A. R. Gliner, S. N. Krivonozhkin, and B. M. Shevtsov *In its* JPRS Report: Science and Technology. USSR: Electronics and Electrical Engineering 30 Aug. 1988 p 7-8 Transl. into ENGLISH from Izvestiya Vysshikh Uchebnykh Zavedeniy: Radiofizika (Gorkiy, USSR) v. 31, no. 2, Feb. 1988 p 238-240 Original language document was announced in IAA as A88-33920 (For primary document see N89-19485 12-33)
Avail: NTIS HC A04/MF A01

In connection with the development of beyond-the-horizon radar, communications and remote sensing of the atmosphere, the problem of predicting the tropospheric propagation range of ultrashort (US) radio waves has assumed great practical importance. Therefore, the dependence of radio signal characteristics on the propagation conditions has been investigated over different radio paths. Of special interest are routes over oceans, where the conditions for long-range waveguide propagation can occur. In order to investigate the effects of radio-wave refraction and diffraction in the bottom, near-water layer of the troposphere and to record the variations in the radio-wave propagation range linked with these effects, the satellite observations must be made at small angles of elevation under conditions of very unstable radio communications, which poses considerable methodological difficulties. A measurement method and the results of observations of tropospheric variations in the propagation range of US radio waves above the ocean are discussed. The experiments were performed in the northern Indian Ocean in May and December with rising and setting satellites of the NOAA system. Author

N89-19487# Joint Publications Research Service, Arlington, VA.
PEACEFUL USES OF ELECTRICAL ENGINEERING IN SPACE
N. N. Sheremetyevskiy *In its* JPRS Report: Science and Technology. USSR: Electronics and Electrical Engineering 30 Aug. 1988 p 20-28 Transl. into ENGLISH from Elektrotekhnika (Moscow, USSR), no. 6, Jun. 1987 p 10-16 (For primary document see N89-19485 12-33)
Avail: NTIS HC A04/MF A01

In the 30 years since the world's first satellite was launched by the Soviet Union, space engineering has evolved into an independent field of science and engineering and one which is solving a broad range of scientific and technical problems concerning various branches of the national economy. Everyone knows of the Molniya and Raduga satellites, the Meteor weather satellites, the Salyut and Mir orbiting space stations and many others used to study near-earth and outer space, for radio and television broadcasting, weather forecasting and charting courses for ice-breakers. The collectives at the scientific research institutes and plants of the electrical equipment industry participate actively in solving the scientific-technical problems of space engineering. The branch has developed many tens of thousands of items for space engineering, including solar batteries, storage batteries, illumination engineering, cable products, and much more. Work done by electrical engineers to develop hardware components for orientation and power systems, automated systems, meteorology and resources-study is described and some important contributions to the peaceful use of space for the benefit of the Soviet people and all mankind are noted. Author

N89-19488# Societe Anonyme de Telecommunications, Paris (France).
DETERMINATION OF GENERAL AND SPECIFIC PROPERTIES OF WIDE ENERGY-BAND GAP HgCdTe IN THE 1 TO 2 MICROMETER WAVELENGTH RANGE Final Technical Report, 1987 - 1988
T. Nguyen-Duy, A. Durand, M. Royer, and F. Raymond 9 Sep. 1988 89 p
(Contract DAJA45-87-C-0020; DA Proj. 1L1-61103-BH-57)
(AD-A201341; Rept-7313/88; R/D-5574-EE-01) Avail: NTIS HC A05/MF A01 CSCL 11F

The metallurgical process of Wide Band Gap Mercury Cadmium Telluride (WBHCT) compound fabrication is briefly reviewed. Special emphasis is given to the Traveling Heater Method (THM) for HgCdTe growth. Physical and electronic properties are analyzed with particular attention to properties that apply to optoelectronic devices. Some special features, such as low intrinsic concentration, low band gap temperature coefficient and matching of band gap to spin orbit coupling appear to be of particular and unique interest in the fabrication of avalanche photodiodes (APD) in this spectral region. Electroluminescent properties have also been investigated. Light-emitting structures are discussed. GRA

N89-19489# Rochester Univ., NY.
INVESTIGATION OF THE PERFORMANCE OF PHOTOCONDUCTIVE SWITCHES Final Report, 1 Jul. 1984 - 30 Jun. 1988
William R. Donaldson Sep. 1988 59 p
(Grant AF-AFOSR-0175-84; AF Proj. 2301)
(AD-A201425; AFOSR-88-1292TR) Avail: NTIS HC A04/MF A01 CSCL 09E

The investigators have shown that photoconductive switches can be used to activate a switch in a radial transmission line geometry. The structure investigated has demonstrated gain in approximate agreement with theoretical predictions and the device may be useful as an accelerating element in a compact accelerator. They have shown that repetitive opening switches can be constructed from optically activated ceramic superconductors. GRA

N89-19490# Texas Technological Univ., Lubbock. Pulsed Power Lab.
HIGH CURRENT, HIGH COULOMB IGNITRONS Final Report, 20 May - 30 Sep. 1988
M. Giesselmann and M. Kristiansen 1988 29 p
(Contract W-7405-eng-48)
(DE89-005547; UCRL-21138) Avail: NTIS HC A03/MF A01

Texas Tech University is currently conducting research to develop high power ignitrons. The new ignitrons should be able to handle currents up to 1000 kA with a charge transfer of more than 500 C's per shot. Other requirements are a reasonable lifetime of 500 to 1000 shots and a low forward voltage drop. The project is carried out jointly between manufacturers, (Richardson Electronics/US and EEV/UK), Lawrence Livermore National Laboratory (LLNL) and Texas Tech University (TTU). Two Workshops have been held at TTU and LLNL to coordinate the work and address the research areas. Since the beginning of the ignitron work at TTU, a capacitor bank, a charging power supply, several test stands for critically damped and crowbarred operations, two high speed cameras, a Mach-Zehnder interferometer and

electrical diagnostics equipment were set up and tested. High power voltage and current measurements, as well as high speed photography of the discharge plasma, have been performed. The effects of axial magnetic fields on the discharge plasma and the holdoff voltage have also been studied. DOE

N89-19491# Fermi National Accelerator Lab., Batavia, IL. Advanced Computer Program

CROSSBAR SWITCH BACKPLANE AND ITS APPLICATION

R. Atac, A. Cook, J. Deepe, M. Fischler, I. Gaines, D. Husby, T. Nash, T. Pham, T. Zmuda, and E. Eichten et al Nov. 1988 5 p Presented at the IEEE Nuclear Science Symposium, Orlando, FL, 9 Nov. 1988

(Contract DE-AC02-76CH-03000)

(DE89-005621; FNAL/C-88/166; CONF-881103-28) Avail: NTIS HC A02/MF A01

A crossbar switch backplane design (Bus Switch Backplane) based on TI's crossbar switch chip is described. This backplane holds a maximum of 16 modules and allows simultaneous communications between up to 8 pairs of modules. The aggregate data transfer rate on the backplane is 160 Mbyte/sec. The Bus Switch Backplane is an essential part of the ACP Multi Array Processor, a supercomputer for site oriented problems. The first application of this machine is in Lattice Gauge Theory calculations. The Bus Switch Backplane also finds ready application in data acquisition schemes based on the ACP multi-microprocessor system. DOE

N89-19492# Rockwell International Science Center, Thousand Oaks, CA.

OHMIC CONTACTS TO GALLIUM ALUMINUM ARSENIDE FOR HIGH TEMPERATURE APPLICATIONS Final Technical Report, 1 Jul. 1985 - 29 Feb. 1988

R. W. Grant and J. R. Waldrop Nov. 1988 68 p

(Contract F49620-85-C-0120)

(AD-A202248; SC5485.FR; AFOSR-88-1249TR) Avail: NTIS HC A04/MF A01 CSCL 09A

A new approach for fabricating nonalloyed ohmic contacts to gallium arsenide was developed. The approach uses ultrathin layers of heavily doped germanium or silicon in contact with gallium arsenide to alter the Schottky barrier height(phi B) at the gallium arsenide interface. For n-type gallium arsenide phi B could be varied from about 0.3 to 1.0 eV. The low barriers are useful for tunneling ohmic contacts to n-gallium arsenide while the high barriers should be useful for p-gallium arsenide ohmic contacts and for Field Effect Transistor (FET) gate applications. In some instances it was necessary to interpose a thin nonmetallic electrically conducting barrier between the contact metal and the thin germanium or silicon layer to preserve optimum contact properties. Specific contact resistivity measurements indicated that contact resistivity < 10 to the -6 ohms/sq.cm should be obtainable in practical contacts to heavily doped material. It is generally observed that phi B at most gallium arsenide interfaces is confined to a relatively narrow range presumably due to a large concentration of acceptor and donor states closely spaced in energy near midgap. The new approach for normalized ohmic contact fabrication suggests that these states can be saturated with carriers from the heavily doped germanium silicon so as to substantially modify phi B. GRA

N89-19493*# National Aeronautics and Space Administration. Lewis Research Center, Cleveland, OH.

STARTING CHARACTERISTICS OF DIRECT CURRENT MOTORS POWERED BY SOLAR CELLS

S. Singer and J. Appelbaum Mar. 1989 20 p Prepared in cooperation with Tel-Aviv Univ. (Israel)

(NASA-TM-101981; E-4550-1; NAS 1.15:101981) Avail: NTIS HC A03/MF A01 CSCL 09A

Direct current motors are used in photovoltaic systems. Important characteristics of electric motors are the starting to rated current and torque ratios. These ratios are dictated by the size of the solar cell array and are different for the various dc motor types. Discussed here is the calculation of the starting to rated current ratio and starting to rated torque ratio of the permanent magnet, and series and shunt excited motors when powered by solar cells for two cases: with and without a maximum-power-point-tracker (MPPT) included in the system. Comparing these two cases, one gets a torque magnification of about 3 for the permanent magnet motor and about 7 for other motor types. The calculation of the torques may assist the PV system designer to determine whether or not to include an MPPT in the system. Author

N89-19494# Glasgow Univ. (Scotland). Dept. of Electronics and Electrical Engineering.

INTRINSIC HYBRID MODES IN A CORRUGATED CONICAL HORN

A. Dendane and J. M. Arnold Paris, France ESA 1988 46 p

(Contract ESA-5904/84-NL-GM/(3G63))

(ESA-CR(P)-2588; ETN-89-93640) Avail: NTIS HC A03/MF A01

Computational requirements for the generation of intrinsic modes in a nonseparable waveguide geometry requiring a full vector field description with anistropic impedance boundaries were derived. Good agreement is shown between computed and measured radiation patterns in copolar and crosspolar configurations. This agreement establishes that the intrinsic mode correctly accounts for the local normal mode conversion which takes place along the horn in a conventional mode coupling scheme, at least for cone semiangles up to 15 deg. The advantage of the intrinsic mode formulation over the conventional mode-coupling theory is that, to construct a single intrinsic mode throughout the horn, only one local normal mode field is required at each cross section, whereas mode conversion from the HE11 mode would require all the HE1n modes to be known at each cross section. The intrinsic mode accounts also for fields which would appear as backward modes in coupled-mode theory. A complete coupled-mode theory solution requires the inversion of a large matrix at each cross section, whereas the intrinsic mode can be constructed explicitly using a simple Fourier-like integral; the perturbation solution of Dragone (1977) is difficult to make rigorous. ESA

N89-19495# Interuniversity Micro-Electronics Center, Leuven (Belgium).

EVALUATION OF SCHOTTKY BARRIER AND PBTE IR-CCD DETECTORS FOR THE SWIR AND MIR WAVELENGTHS RANGE, EXECUTIVE SUMMARY Final Report

J. Vermeiren, R. VandeWalle, W. Stessens, W. Platz, M. Koeniger, G. Marangoni, M. DAntoni, and C. Musilli (Elettronica S.R.L., Rome, Italy) Paris, France ESA May 1988 46 p

(Contract ESTEC-6044/84-NL-PB)

(IMEC-SP/CCD-255/88-03; ESA-CR(P)-2681; ETN-89-93933) Avail: NTIS HC A03/MF A01

Platinum silicide Schottky barrier (SB) sensor arrays for the 1.5 to 3 micron wavelength range and lead telluride sensors combined with a silicon CCD multiplexer for the 3 to 45 micron range were studied. The choice of the application wavelength range for each sensor type is arbitrary, as they both are sensitive up to + or - 5 microns. However, the spectral response of SB diodes monotonically decreases from the cut on wavelength, whereas the response of the PbTe sensors can be tuned by applying the proper processing conditions. The refinement of the existing SB models in order to obtain a better understanding for the sensor improvement, and the introduction and optimization of the SB process steps into the existing tripple poly CCD process are described. The development of a combined CCD-PbTe process and the design of a parametric model as a tool for the optimization of the CCD multiplexer design are described. The designs for the SBCCD as well as for the PbTe CCD are realized. On the mask set several options concerning the PbTe readout and SB sensor design are implemented in order to verify design assumptions. ESA

N89-19496# Christian Rovsing Ltd., Copenhagen (Denmark). Technology Research Department.
ELECTRONIC POWER CONDITIONER (EPC) FOR CARCINOTRONS Final Report
F. H. Pedersen and S. Hartman Paris, France ESA 5 Aug. 1988 108 p
(Contract ESTEC-5607/83-NL-AN(SC))
(R/D/REPO/8801; ESA-CR(P)-2703; ETN-89-93941) Avail: NTIS HC A06/MF A01

A space qualified electronic power conditioner (EPC) for carcinotrons used in submillimeter atmospheric research heterodyne receivers was designed. The carcinotron is provided with the appropriate voltages by the EPC. The EPC is monitored and controlled via a serial data interface. In the test set up a personal computer controls the EPC. The carcinotron output frequency (fc) is tuned by the line to cathode voltage (VL,BWO.), fc = k.VL,BWO where k is a constant. Normal phase and frequency lock of the carcinotron is obtained by mixing the carcinotron signal with a harmonic of a crystal controlled oscillator and feeding the difference signal via phase and frequency detectors back to the EPC-PLL input such that: VL,BWO = VPLL + VL,EPC where VPLL is the feedback signal and VL, EPC is the line voltage produced by the EPC. The VL,EPC is independent of VPLL in as much as VL,EPC is returned to VPLL. The VPLL is called PLL-ground. In the EPC this is obtained by placing a PLL box between the floating box and chassis. The PLL box potential is equal to VPLL. A model EPC was designed, built, and tested with load simulators and with a real carcinotron. The noise and ripple specification inside the PLL bandwidth is met with a margin of 6 dB. ESA

N89-19497 Hahn-Meitner-Inst. G.m.b.H., Berlin (Germany, F.R.).
HIGH OUTPUT VOLTAGE MULTIOCTAVE BROADBAND AMPLIFIER WORKING BETWEEN 50 kHz AND 8 GHz Ph.D. Thesis - Technische Univ., Berlin
Michael Martin Jul. 1988 118 p In GERMAN; ENGLISH summary
(HMI-B-451; ISSN-0175-8349; ETN-89-93954) Copyright Avail: Hahn-Meitner-Institut Berlin GmbH, Gleinicker Strasse 100, D-1000 Berlin 39, Federal Republic of Germany

Using a circuit simulation computer program a medium power broadband amplifier was designed with a step by step optimization routine. In contrast to common circuit design practice, a miniaturization of the amplifier to minimize all parasitic elements is not necessary. To get a high output voltage swing from the final amplifier stage it has to be matched with a network, which is optimized for maximum power transfer to the load. The matching circuit configuration itself was optimized with a linear small signal CAD program by using only its analyzing capability. ESA

N89-19498# Idaho National Engineering Lab., Idaho Falls.
COMPARATIVE PERFORMANCE EVALUATION OF ADVANCED AC AND DC EV PROPULSION SYSTEMS
R. D. MacDowall and R. L. Crumley 1988 9 p Presented at the 9th Electric Vehicle Symposium, Toronto, Ontario, 13 Nov. 1988
(Contract DE-AC07-76ID-01570)
(DE89-005419; EGG-M-881162; CONF-881162-3) Avail: NTIS HC A02/MF A01

Idaho National Engineering Laboratory (INEL) evaluates EV propulsion systems and components for the U.S. Department of Energy (DOE) Electric and Hybrid Vehicle (EHV) Program. In this study, experimental data were used to evaluate the relative performances of the benchmark Chrysler/GE ETV-1 DC and the Ford/GE First Generation Single-Shaft AC (ETX-I) propulsion systems. Tests were conducted on the INEL's chassis dynamometer using identical aerodynamic and rolling resistance road-load coefficients and vehicle test weights. The results allowed a direct comparison of selected efficiency and performance characteristics for the two propulsion system technologies. The ETX-I AC system exhibited slightly lower system efficiency during constant speed testing than the ETV-1 DC propulsion system. DOE

N89-19452*# Jet Propulsion Lab., California Inst. of Tech., Pasadena.
DESIGN AND TEST OF A 2.25-MW TRANSFORMER RECTIFIER ASSEMBLY
R. Cormier and J. Daeges *In its* The Telecommunications and Data Acquisition Report 15 Feb. 1989 p 1-13 (For primary document see N89-19451 12-32)
Avail: NTIS HC A10/MF A01 CSCL 17B

N89-19458*# Jet Propulsion Lab., California Inst. of Tech., Pasadena.
ON TESTING VLSI CHIPS FOR THE BIG VITERBI DECODER
I. S. Hsu *In its* The Telecommunications and Data Acquisition Report 15 Feb. 1989 p 80-92 (For primary document see N89-19451 12-32)
Avail: NTIS HC A10/MF A01 CSCL 09C

N89-19459*# Jet Propulsion Lab., California Inst. of Tech., Pasadena.
WIRING VITERBI DECODERS (SPLITTING DEBRUIJN GRAPHS)
O. Collins, F. Pollara, S. Dolinar, and J. Statman *In its* The Telecommunications and Data Acquisition Report 15 Feb. 1989 p 93-104 (For primary document see N89-19451 12-32)
Avail: NTIS HC A10/MF A01 CSCL 09C

N89-19460*# Jet Propulsion Lab., California Inst. of Tech., Pasadena.
BLOCK DIAGRAMS OF THE RADAR INTERFACE AND CONTROL UNIT
J. W. Collier *In its* The Telecommunications and Data Acquisition Report 15 Feb. 1989 p 104-116 (For primary document see N89-19451 12-32)
Avail: NTIS HC A10/MF A01 CSCL 09C

N89-19462*# Jet Propulsion Lab., California Inst. of Tech., Pasadena.
MICROWAVE TIME DELAYS FOR THE DUAL L-C-BAND FEED SYSTEM
J. Chen *In its* The Telecommunications and Data Acquisition Report 15 Feb. 1989 p 126-131 (For primary document see N89-19451 12-32)
Avail: NTIS HC A10/MF A01 CSCL 09C

N89-19465*# Jet Propulsion Lab., California Inst. of Tech., Pasadena.
A LOW-LOSS LINEAR ANALOG PHASE MODULATOR FOR 8415 MHz TRANSPONDER APPLICATION
N. Mysoor *In its* The Telecommunications and Data Acquisition Report 15 Feb. 1989 p 172-178 (For primary document see N89-19451 12-32)
Avail: NTIS HC A10/MF A01 CSCL 09C

N89-19825*# National Aeronautics and Space Administration. Marshall Space Flight Center, Huntsville, AL.
AUTOMATIC DETECTION OF ELECTRIC POWER TROUBLES (ADEPT)
Caroline Wang, Hugh Zeanah, Audie Anderson, Clint Patrick, Mike Brady, and Donnie Ford (Alabama A & M Univ., Huntsville.) *In* NASA. Lyndon B. Johnson Space Center, 2nd Annual Workshop on Space Operations Automation and Robotics (SOAR 1988) Nov. 1988 p 47-50 (For primary document see N89-19817 12-59)
Avail: NTIS HC A22/MF A01 CSCL 09C

34 FLUID MECHANICS AND HEAT TRANSFER

Includes boundary layers; hydrodynamics; fluidics; mass transfer; and ablation cooling.

For related information see also *02 Aerodynamics* and *77 Thermodynamics and Statistical Physics.*

N89-19499*# National Aeronautics and Space Administration. Langley Research Center, Hampton, VA.
CONTAMINATION OF LIQUID OXYGEN BY PRESSURIZED GASEOUS NITROGEN
Allan J. Zuckerwar, Tracy K. King, and Kim Chi Ngo (Old Dominion Univ., Norfolk, VA.) Apr. 1989 26 p
(NASA-TP-2894; L-16526; NAS 1.60:2894) Avail: NTIS HC A03/MF A01 CSCL 20D

The penetration of pressurized gaseous nitrogen (GN2) into liquid oxygen (LOX) was investigated experimentally in the 7-inch High Temperature Tunnel, the pilot tunnel for the 8-foot High Temperature Tunnel (8'HTT) at Langley Research Center. A preliminary test using a nuclear monitor revealed the extent of the liquid nitrogen (LN2) build-up at the LOX interface as a function of GN2 pressure. Then an adaptation of the differential flash vaporization technique was used to determine the binary diffusivity of the LOX-LN2 system at a temperature of 90.2 K. The measured value D equals 0.000086 sq cm/s + or - 25 percent together with two prior measurements at lower temperatures revealed an excellent fit to the Arrhenius equation, yielding a pre-exponential factor D sub 0 equals 0.0452 sq cm/s and an activation enthalpy H equals 1.08 kcal/mol. At a pressure of 1700 psi and holding time of 15 min, the penetration of LN2 into LOX (to a 1 percent contamination level) was found to be 0.9 cm, indicating but minimal impact upon 8'HTT operations. Author

N89-19500 Virginia Polytechnic Inst. and State Univ., Blacksburg.
CURVATURE EFFECTS ON THE STABILITY OF THREE-DIMENSIONAL LAMINAR BOUNDARY LAYERS Ph.D. Thesis
Fayette Smith Collier, Jr. 1988 114 p
Avail: Univ. Microfilms Order No. DA8817402

The linear stability equations which govern the growth of small periodic disturbances for compressible, three-dimensional laminar boundary layer flow are derived in an orthogonal curvilinear coordinate system. The parallel flow assumption is utilized in the derivation. The system of equations is solved using a finite difference scheme similar to that in a current state-of-the-art stability analysis code, COSAL. The LR method and the inverse Rayleigh iteration procedure are used to calculate the eigenvalues. The stability of the three-dimensional compressible laminar boundary layer including the effects of streamline and surface curvature for flows past swept wings were crossflow type disturbances dominate is calculated. A parametric study is performed varying Reynolds number and sweep angle on an airfoil with a concave cutout in the leading edge region of the lower surface. The magnitude of these effects for swept wing flows is determined. Non-stationary as well as stationary disturbances are calculated, and the most amplified frequencies are identified. N-factor correlations at the measured location of transition are made utilizing flight test data. Dissert. Abstr.

N89-19501 Exeter Univ. (England).
SOME HYDRODYNAMIC INSTABILITIES OF BOUNDARY LAYER FLOWS Ph.D. Thesis
Sharon Olivia MacKerrell 1988 145 p
Avail: Univ. Microfilms Order No. BRDX82768

The breakdown of a laminar flow into a turbulent one is examined. This is investigated for boundary layer flows by employing linear and weakly nonlinear stability theory. Asymptotic methods are used to obtain approximate solutions along with triple deck theory in most cases. The flow induced by a rotation disc is considered. A triple deck structure is known to exist and weakly nonlinear stability theory is used to find asymptotic solutions for stationary 3-D modes of stability. The hydrodynamic stability of Blasius flow over a compliant plate is also studied. The results corresponding to the triple deck structure of a Blasius boundary layer are used, as well as linear stability theory, to obtain asymptotic solutions for the wavenumber of the disturbance. The 3-D breakdown to a time dependent flow of the Goertler vortex is also considered, as is the weakly nonlinear stability of the 3-D attachment line boundary layer is examined. A triple deck structure is appropriate here and the interaction between a 2-D and a 3-D unstable mode is investigated. Dissert. Abstr.

N89-19502*# Georgia Inst. of Tech., Atlanta. School of Mechanical Engineering.
MODELING OF TRANSIENT HEAT PIPE OPERATION Final Report, 19 Aug. 1983 - 31 Dec. 1988
Gene T. Colwell 15 Jan. 1989 216 p
(Grant NAG1-392)
(NASA-CR-184688; NAS 1.26:184688) Avail: NTIS HC A10/MF A01 CSCL 20D

Mathematical models and an associated computer program for heat pipe startup from the frozen state have been developed. Finite element formulations of the governing equations are written for each heat pipe region for each operating condition during startup from the frozen state. The various models were checked against analytical and experimental data available in the literature for three specific types of operation. Computations using the methods developed were made for a space shuttle reentry mission where a heat pipe cooled leading edge was used on the wing. NASA

N89-19503*# Purdue Univ., West Lafayette, IN. Thermal Sciences and Propulsion Center.
THE EFFECT OF PREWHIRL ON THE INTERNAL AERODYNAMICS AND PERFORMANCE OF A MIXED FLOW RESEARCH CENTRIFUGAL COMPRESSOR
William B. Bryan and Sanford Fleeter Dec. 1987 159 p
(Grant NsG-3285)
(NASA-CR-184756; NAS 1.26:184756; AVSCOM-TR-87-C-35; ME-TSPC-TR-87-13) Avail: NTIS HC A08/MF A01 CSCL 20D

The internal three-dimensional steady and time-varying flow through the diffusing elements of a centrifugal impeller were investigated using a moderate scale, subsonic, mixed flow research compressor facility. The characteristics of the test facility which permit the measurement of internal flow conditions throughout the entire research compressor and radial diffuser for various operating conditions are described. Results are presented in the form of graphs and charts to cover a range of mass flow rates with inlet guide vane settings varying from minus 15 degrees to plus 45 degrees. The static pressure distributions in the compressor inlet section and on the impeller and exit diffuser vanes, as well as the overall pressure and temperature rise and mass flow rate, were measured and analyzed at each operating point to determine the overall performance as well as the detailed aerodynamics throughout the compressor. NASA

N89-19504*# Pennsylvania State Univ., University Park. Dept. of Aerospace Engineering.
A COMPUTATIONALLY EFFICIENT MODELLING OF LAMINAR SEPARATION BUBBLES Semiannual Status Report, Jun. 1988 - Jan. 1989
Paolo Dini and Mark D. Maughmer Feb. 1989 48 p
(Grant NAG1-778)
(NASA-CR-184789; NAS 1.26:184789) Avail: NTIS HC A03/MF A01 CSCL 20D

The goal is to accurately predict the characteristics of the laminar separation bubble and its effects on airfoil performance. Toward this end, a computational model of the separation bubble was developed and incorporated into the Eppler and Somers airfoil design and analysis program. Thus far, the focus of the research was limited to the development of a model which can accurately predict situations in which the interaction between the bubble and the inviscid velocity distribution is weak, the so-called short bubble.

A summary of the research performed in the past nine months is presented. The bubble model in its present form is then described. Lastly, the performance of this model in predicting bubble characteristics is shown for a few cases. Author

N89-19505*# Boeing Commercial Airplane Co., Seattle, WA. New Product Development Organization.
FLIGHT SURVEY OF THE 757 WING NOISE FIELD AND ITS EFFECTS ON LAMINAR BOUNDARY LAYER TRANSITION. VOLUME 2: DATA COMPILATION Report, Nov. 1984 - Jul. 1985
Mar. 1987 382 p
(Contract NAS1-15325)
(NASA-CR-178217; NAS 1.26:178217; D6-53196-2-Vol-2) Avail: NTIS HC A17/MF A01 CSCL 20D

A flight test program was performed using the Boeing 757 flight research airplane to investigate the effect of noise from wing mounted engines on laminar boundary layer transition. An NLF glove was installed on the right wing panel just outboard of the engine. The extent of laminar flow on the glove was measured as a function of engine power setting for a range of flight conditions. A combination of surface and probe microphones was distributed over the upper and lower wing surfaces to measure sound spectra. The flight test program was completed in June 1985 and the results of preliminary analysis indicate that a maximum of about 29 percent of chord laminar flow was obtained on the upper surface and about 28 percent on the lower surface (at a high sideslip condition). The engine speed was varied from about 2600 (idle) to about 4500 (maximum continuous power) r/min. This produced changes in sound pressure level up to 20 dB on the lower surface. On the upper surface, the noise levels were independent of engine power but sensitive to airplane Mach number. No effect of engine power setting on upper surface transition location was observed, and only a small forward movement of the transition location on the lower surface was observed at the high power settings. Volume 1 of this report contains the program description and data analysis. Volume 2 is a compilation of all of the flight test data. Author

N89-19506# Japan Atomic Energy Research Inst., Tokyo.
VERIFICATION OF COMBINED THERMAL-HYDRAULIC AND HEAT CONDUCTION ANALYSIS CODE FLOWNET/TRUMP
Soh Maruyama, Nozomu Fujimoto, Yoshihiro Kiso, Tomoyuki Murakami (Fuji Electric Co. Ltd., Yokosuka, Japan), and Yukio Sudo Sep. 1988 80 p In JAPANESE; ENGLISH summary
(DE88-756063; JAERI-M-88-173) Avail: NTIS (US Sales Only) HC A05/MF A01

This report presents the verification results of the combined thermal-hydraulic and heat conduction analysis code, FLOWNET/TRUMP which has been utilized for the core thermal hydraulic design, especially for the analysis of flow distribution among fuel block coolant channels, the determination of thermal boundary conditions for fuel block stress analysis and the estimation of fuel temperature in the case of fuel block coolant channel blockage accident in the design of the High Temperature Engineering Test Reactor(HTTR), which the Japan Atomic Energy Research Institute has been planning to construct in order to establish basic technologies for future advanced very high temperature gas-cooled reactors and to be served as an irradiation test reactor for promotion of innovative high temperature new frontier technologies. The verification of the code was done through the comparison between the analytical results and experimental results of the Helium Engineering Demonstration Loop Multi-channel Test Section(HENDEL T(sub 1-M)) with simulated fuel rods and fuel blocks. DOE

N89-19507# Boeing Advanced Systems Co., Seattle, WA.
ERROR NORM GUIDED FLOW ANALYSIS OF SHOCK-WAVE/BOUNDARY-LAYER INTERACTIONS Final Report, 1 Aug. 1985 - 31 Jul. 1988
Gerald C. Paynter, Clifford K. Forester, David W. Mayer, and James Y. Baltar 30 Sep. 1988 108 p Original contains color illustrations
(Contract F49620-85-C-0126)
(AD-A201176; AFOSR-88-1180TR) Avail: NTIS HC A06/MF A01 CSCL 20D

Conventional means of assessing the accuracy of Navier-Stokes analyses are difficult to implement and may not be reliable. A new approach uses direct measures of solution error, both as accuracy monitors and as guides to grid adjustment. The artificial diffusion ratio (ADR) is a promising error monitor. As an example, ADR was used to guide the Navier-Stokes analysis of a supersonic external compression inlet with bleed flow. ADR was useful for guiding grid selection and seemed to provide a measure of solution accuracy as well. The algorithm dependence of ADR and the relationship between ADR and solution accuracy were explored in a follow-on study. This study investigated the algorithm and accuracy questions in two steps. First, modified equations were developed for the MacCormack explicit and Beam-Warming implicit algorithms for Burgers equation. Second, finite difference solutions were obtained (for a range of grid densities) and solution accuracy was established through comparisons with analytic solutions. This study established that ADR was useful as guide for grid adjustment, that only a qualitative relationship exists between ADR and solution accuracy, and that this relationship is algorithm dependent. The use of ADR error monitors for general purpose applications requires additional development. GRA

N89-19508# Naval Postgraduate School, Monterey, CA.
THE DEVELOPMENT AND STRUCTURAL CHARACTERISTICS OF DEAN VORTICES IN A CURVED RECTANGULAR CHANNEL M.S. Thesis
Lawrence R. Baun Sep. 1988 242 p
(AD-A201249) Avail: NTIS HC A11/MF A01 CSCL 20D

The development and structure of Dean vortices in a curved channel were measured and studied. A 40:1 aspect ratio channel with mild curvature was employed. Circulation of mean streamwise vorticity, and maxima of streamwise, spanwise and radial components of vorticity increase as the Dean number increases from 40 to 140. Mean vorticity components were determined from measurements of the three components of mean velocity using a miniature five hole pressure probe. Spectra obtained from a subminiature crossed wire probe show principal and harmonic frequencies for Dean numbers greater than 165, when vortices are twisting. Spectral peaks at other Dean numbers provide evidence of oscillations also observed during flow visualization. GRA

N89-19509# McDonnell-Douglas Corp., Long Beach, CA.
THE BIRTH OF OPEN SEPARATION ON A PROLATE SPHEROID Final Report, Mar. 1986 - Sep. 1988
Tuncer Cebeci and Wenhan Su Sep. 1988 30 p
(Contract F49620-84-C-0007)
(AD-A201350; MDC-K0171; AFOSR-88-1178TR) Avail: NTIS HC A03/MF A01 CSCL 20D

Results are presented to describe the laminar flow patterns around a prolate spheroid at angles of attack of 1, 2, 3, and 30 degrees and complement those obtained previously at 6 degrees. They were obtained by solving three-dimensional boundary layer equations with a combination of standard and characteristic box methods and with a stability criterion to ensure numerical accuracy. Emphasis is placed on the nature of separation which, in agreement with experiment but contrary to some theoretical claims, is shown to be open for all angles of attack and to be coincident with a particular skin friction line. GRA

N89-19510# Drexel Univ., Philadelphia, PA. Dept. of Mechanical Engineering and Mechanics.
CHARACTERISTIC TIME MODEL VALIDATION Final Technical Report, Oct. 1984 - Jun. 1988
K. V. Tallio, J. C. Prior, Jr., and A. M. Mellor Sep. 1988 182 p
(Contract DAAG29-84-K-0165)
(AD-A201374; ARO-21743.4-EG) Avail: NTIS HC A09/MF A01 CSCL 20D

An experimental program for validation of the semi-empirical Characteristic Time Model (CTM) is described. A two-dimensional

turbulent shear layer is generated in the experimental test section using a two-stream, vertically downflowing wind tunnel with a flat pre-filming airblast atomizer fitted along its centerline. This facility simulates the shear layer around the recirculation zone found in the primary zone of a gas turbine combustor. Experimental results are used to investigate CTM parameters for turbulent mixing and droplet lifetime and to examine current finite difference modeling techniques. Global mixing times evaluated at the origin of the shear layer and defined in terms of geometric macroscale and a reference velocity are compared with the locally measured values of turbulent mixing time. The results demonstrate that these global times, as defined for the CTM, do in fact accurately represent the events occurring on a local scale, as hypothesized. Modifications to the mixing time parameter to improve existing correlations are proposed. Due to restrictions imposed by the facility and instrumentation, validation of the droplet lifetime parameter was not possible. Measurements were restricted to mean spray diameters. These data and others demonstrate that current correlations for Sauter mean diameter do not adequately account for changes in atomizer geometry or liquid properties. GRA

N89-19511# Toronto Univ., Downsview (Ontario). Inst. for Aerospace Studies.
ANALYTICAL, NUMERICAL AND EXPERIMENTAL INVESTIGATIONS OF OBLIQUE-SHOCK-WAVE REFLECTIONS IN PURE AND DUSTY GASES Final Report, 1 Feb. 1987 - 30 Sep. 1988
I. I. Glass Oct. 1988 7 p
(Grant AF-AFOSR-0124-87; AF Proj. 2307)
(AD-A201438; AFOSR-88-1324TR) Avail: NTIS HC A02/MF A01 CSCL 20D

Over the last 18 months we have completed almost all of the tasks which we set for ourselves to accomplish, as enumerated below: (Problem 1) An Interferometric Investigation of Terminal Double Mach Reflections in low-Gamma Gases - isobutane (C4H10) and sulfurhexafluoride (SF6). This problem has been completed and resulted in the presentation of the paper. A Resolution of the von Neumann Paradox, by J. T. Urbanowicz and I. I. Glass at the 8th International Mach Reflection Symposium, held at UTIAS, during July 12 to 15, 1988; (Problem 2) An Interferometric Investigation of the Diffraction of a Planar Shock Wave over a Circular Cylinder in Air. This problem has been completed and resulted in the presentation of the paper with the same title by J. Kaca and I. I. Glass at the 8th International Mach Reflection Symposium, held at UTIAS, during July 12 to 15, 1988; (Problem 3) An Interferometric Investigation of the Diffraction of Planar Shock Waves; (Problem 4) Completion of Instrumentation, Calibration and Shakedown of the Shock-Tube; (Problem 5) Normal Shock-Wave Structure in a Dusty-Air Shock-Tube; (Problem 6) The Pitot Tube in a Dusty-Air Shock-Tube; (Problem 7) Laminar Sidewall Boundary Layer Induced by a Moving Shock Wave in a Dusty-Air Shock-Tube; and (Problem 8) Flat Plate Boundary Layer Induced by a Moving Shock Wave in a Dusty-Air Shock-Tube. GRA

N89-19512# Minnesota Univ., Minneapolis. Dept. of Aerospace Engineering and Mechanics.
THEORETICAL AND EXPERIMENTAL STUDIES OF SELECTED TOPICS IN THE RHEOLOGY OF FLUIDS Final Report, 1 May 1985 - 30 Apr. 1988
Daniel D. Joseph 28 Jul. 1988 6 p
(Contract DAAG29-85-K-0130)
(AD-A201460; ARO-22647.15-MA) Avail: NTIS HC A02/MF A01 CSCL 20D

Theoretical and experimental studies of the consequences of short-term elastic response in liquids are discussed. Theoretical studies include analysis of the origins of viscosity in relaxing elasticity, the analysis of equations of motions according to type; e.g., hyperbolic or elliptic, with particular attention to problems of identification of physical phenomena and numerical analysis of flow associated with: (1) change of type from subcritical to supercritical conditions in steady flow (transonic problems), (2) loss of well-posedness or short wave length instabilities in unsteady flow, and (3) regularization of short wave instabilities with viscosity. A wave speed meter enables us to measure the effective shear modulus in liquids. We discovered delayed die swell and demonstrated experimentally that it is a critical phenomenon which appears to be like a hydraulic jump with speed greater than the shear. The fluidization of particles at finite, but even small Reynold numbers was dominated by local mechanisms associated with wakes and turning couples on long bodies. GRA

N89-19513# Naval Postgraduate School, Monterey, CA.
NATURAL CONVECTION LIQUID IMMERSION COOLING OF A COLUMN OF DISCRETE HEAT SOURCES IN A VERTICAL CHANNEL M.S. Thesis
Daniel L. Knight Sep. 1988 63 p
(AD-A201676) Avail: NTIS HC A04/MF A01 CSCL 20M

Natural convection from a single column of eight in-line, rectangular, flush heat sources was examined. A vertical channel was formed by placing a movable shroud parallel to the test surface. The experimental program consisted of temperature measurements and flow visualizations. For a range of component power levels and channel spacings, surface temperatures of each heat source were measured at five locations using embedded thermocouples. The resulting steady state data was compared with corresponding measurements for an identical geometric arrangement of protruding heat sources. The flow visualization was carried out using a laser generated plane of light. GRA

N89-19514 Cincinnati Univ., OH.
THE USE OF DIRECT SPARSE MATRIX METHODS AND NEWTON ITERATION FOR THE NUMERICAL SOLUTION OF FLUID FLOWS Ph.D. Thesis
Erich Eduard Bender 1988 186 p
Avail: Univ. Microfilms Order No. DA8822812

Two modifications of Newton's method are investigated for the numerical solution of fluid flow problems. While Newton's method is guaranteed to have a quadratic convergence rate given a suitably close initial guess, the stability of the method can be very sensitive to the selection of this guess. This is the case for the fluid flows studied. The purpose of the modifications is to eliminate this limitation and produce a robust solution algorithm. The first modification uses the addition of a time term to provide underrelaxation. The second monitors the norm of the residuals to determine an underrelaxation parameter. The second method is shown to have a monotonic convergence property. All of these methods require the solution of large sparse linear systems. The use of sparse matrix methods is investigated for the efficient solution of these systems. These methods are tested on two flow problems: inviscid transonic flows and steady laminar separated flows. The stability problems of Newton's method appear to be associated with sharp shocks in the former problem, and by large gradients in the separated regions in the latter. Dissert. Abstr.

N89-19515 California Inst. of Tech., Pasadena.
MIXING IN GAS PHASE TURBULENT JETS Ph.D Thesis
David Russell Dowling 1988 269 p
Avail: Univ. Microfilms Order No. DA8820939

An experimental investigation is presented of the mixing of the nozzle fluid of a round, turbulent jet with the entrained reservoir fluid, using laser-Rayleigh scattering methods. The measurements, at Reynolds numbers of 5,000 and 16,000, cover the axial range from 20 to 90 jet exit diameters and resolve the full range of temporal and spatial concentration scales. The measured mean and rms values of the concentration, and the mean scalar dissipation rate, when estimated from the time derivative of concentration, are consistent with jet similarity laws. Concentration fluctuation power spectra are found to be self similar long rays eminating from the virtual origin of the jet, and are consistent with the universal form of scalar spectra proposed by Gibson. The probability density functions for the concentration, the time derivative of concentration, and the square of the time derivative of concentration, are compiled and are also found to be self similar along rays. Features of the measured distributions and spectra are consistent with the existence of large scale structures within

the flow that span the local diameter of the jet turbulent cone.
Dissert. Abstr.

N89-19516 Michigan Univ., Ann Arbor.
STUDY OF UNDEREXPANDED TURBULENT AIR JETS IN WATER Ph.D. Thesis
Eric Loth 1988 187 p
Avail: Univ. Microfilms Order No. DA8821614

An experimental and theoretical investigation of the structure of round and plane underexpanded air jets in water was conducted. To characterize the structure and mixing properties of these jets, the following measurements were made: (1) void fraction profiles; (2) static pressure distributions; and (3) entrainment rates. Measurements were made for various axial positions and flow rates including subsonic flow, sonic adapted flow and sonic underexpanded flow with underexpansion ratios as high as eight. Flow visualization was also used to investigate jet boundaries, dynamics of discharge, and compressible wave fields. A locally-homogeneous flow model (implying negligible velocity and temperature differences between the phases) was developed, with the external expansion region described by a simple equivalent adapted jet exit condition. In addition, a parabolized Navier-Stokes code was used to predict centerline static pressure distributions for baseline measurements in single-phase gas flows. Static pressure measurements confirmed the presence of a shock-wave-containing external-expansion region for under-expanded air jets in water, similar to results observed for under-expanded air jets in air. The fully-developed round and plane jets exhibited half-widths, based on void fractions, which were two to three times greater than half-widths, based on scalar properties, observed for single-phase jets. This is a result of the strong sensitivity of void fraction to mixing levels due to the large density ratio of the flow. Dissert. Abstr.

N89-19517# Illinois Univ., Urbana. Dept. of Chemical Engineering.
PRESSURE VARIATION OVER A SOLID WAVY SURFACE
David J. Countemanche and Thomas J. Hanratty Oct. 1988 107 p
(Contract N00014-82-K-0324)
(AD-A201724) Avail: NTIS HC A06/MF A01 CSCL 20D

Surface pressure variations for turbulent flow over solid wavy surfaces with a wavelength of 2 inches were studied. Measurements were made over waves of two amplitudes, 0.0123 inches and 0.03125 inches. The water flow rate and viscosity were varied so that a range of dimensionless wave numbers (scaled with the friction velocity and the kinematic viscosity) of alpha (+) = 0.0011 to 0.020 were covered. Pressure profiles are described using a three harmonic fit. A linear response, for which only a single harmonic is needed, was observed for all alpha (+) for the small amplitude wave and for small alpha (+) for the large amplitude wave. Of particular interest is the large phase shift of the pressure profile observed with increasing alpha (+). These results are used to test the quasi-laminar model for flow over wavy surfaces, widely used to predict wave generation and drag on small amplitude waves. GRA

N89-19518# National Oceanic and Atmospheric Administration, Oak Ridge, TN. Air Resources Lab.
AN INVESTIGATION OF THE INTERMITTENT TURBULENT BREAKDOWN OF THE NOCTURNAL PLANETARY BOUNDARY LAYER Final Report, 1 Apr. 1987 - 31 Mar. 1988
Carmen J. Nappo 15 Oct. 1988 17 p
(Contract MIPR-ARO-128-87)
(AD-A201743; ARO-23418.1-GS) Avail: NTIS HC A03/MF A01 CSCL 20D

A study of the statistics of the intermittent turbulent breakdown of the stable boundary layer over flat and complex terrain was made. The study is based on the temporal behavior of the covariance of wind speed and temperature (CST). During a breakdown event, the overturning of the Planetary Boundary Layer (PBL) results in high-speed warm air being transported downward toward the ground surface, and low-speed cool air being transported upward away from the ground surface. This results in a positive value of CST and a consequent flux of heat toward the ground surface. GRA

N89-19519# Naval Postgraduate School, Monterey, CA.
TRANSIENT THREE-DIMENSIONAL HEAT CONDUCTION COMPUTATIONS USING BRIAN'S TECHNIQUE M.S. Thesis
John A. Watson Sep. 1988 208 p
(AD-A201918) Avail: NTIS HC A10/MF A01 CSCL 20M

A transient three dimensional heat conduction code was developed using finite differences. A stability restriction on the time step was avoided using a technique proposed by Brian. Computations from the code were validated using both the explicit technique and an available closed from solution for small times. The maximum error was found to be within 0.019 percent for an 11 x 11 x 11 grid and time step of 17.117 seconds. The total CPU time to carry out the computations up to 3,600 seconds using Brian's techniques was six times that required for the explicit technique with the same time step of 17.117 seconds. However, as the time step was increased without altering the heometry, the CPU time using Brian's technique decreased and was less than that used in the explicit technique for time steps larger than 110 seconds. The validated code was also used in the analysis of the transient thermal response of a component on an orbiting spacecraft. GRA

N89-19520# Drexel Univ., Philadelphia, PA. Dept. of Mechanical Engineering and Mechanics.
COMPUTATIONAL STUDIES OF EVAPORATING SPRAYS IN A SHEAR LAYER Final Report, 14 Jan. 1987 - 14 May 1988
Bakhtier Farouk 21 Oct. 1988 79 p
(Contract DAAL03-87-K-0015)
(AD-A201932; ARO-24654.1-EG) Avail: NTIS HC A05/MF A01 CSCL 21B

The objective of the research project was to numerically predict the characteristics of evaporating sprays in a turbulent shear layer. The calculations were performed such that the essential physical processes in spray evaporation in gas turbine combustors are adequately realized. The calculations modeled parallel experiments (ARO Contract number DAAG29-84-K-0165) carried out in a vertically down-flowing wind tunnel where a splitter plate separates two air streams having different velocities. The two air streams meet at the end of the splitter plate and give rise to a confined shear layer. A flat prefilming airblast atomizer is located at the trip of the splitter plate. A liquid spray formed at the atomizer tip evaporates in the turbulent shear layer and is convected downstream. An Eulerian description of the turbulent gas phase flow and a Lagrangian formulation of the droplet size class motion and heat and mass transfer were considered. Single phase two dimensional turbulent flow calculations in a duct were considered. GRA

N89-19521# Purdue Univ., West Lafayette, IN. School of Mechanical Engineering.
TURBULENCE STRUCTURE AND MASS TRANSPORT IN A CHANNEL FLOW WITH POLYMER INJECTION Technical Report, 1 Dec. 1987 - 30 Nov. 1988
David T. Walker and William G. Tiederman Dec. 1988 158 p
(Contract N00014-83-K-0183)
(AD-A202237; PME-FM-88-2) Avail: NTIS HC A08/MF A01 CSCL 20D

This study which examined a fully developed turbulent channel flow with polymer injection at the wall had two complimentary objectives. The first objective was to gain more understanding of the way in which long-chain, high-molecular-weight, water soluble polymers effect viscous drag reduction in turbulent wall flows. The second was to acquire information useful in the modeling of the transport processes in flows with polymer injection at the wall, particularly the high Schmidt number mixing process. A fluorescence technique was developed for time-resolved measurements of species concentration profiles. This technique was combined with laser velocimetry to obtain measurements of turbulent mass transport in a flow with polymer injection and, for

comparison purposes, a flow with water injection. Two-component laser velocimeter measurements were made in both flows to examine the effect of both the injection process and the evolving polymer concentration field on the structure of turbulence. In the flows with injection, the major transport mechanism was identified as long (in the streamwise direction) filaments of high concentration fluid periodically lifting away from the near-wall region. GRA

N89-19522# Deutsche Forschungs- und Versuchsanstalt fuer Luft- und Raumfahrt, Oberpfaffenhofen (West Germany). Abteilung Atmosphaerische Dynamik.
LARGE-EDDY SIMULATION OF CONVECTIVE BOUNDARY LAYERS Ph.D. Thesis - Ludwig-Maximilians-Univ.
Helmut Schmidt Aug. 1988 146 p In GERMAN; ENGLISH summary Report will also be announced as translation (ESA-TT-1138)
(DFVLR-FB-88-30; ISSN-0171-1342; ETN-89-93969) Avail: NTIS HC A07/MF A01; DFVLR, VB-PL-DO, Postfach 90 60 58, 5000 Cologne, Federal Republic of Germany, 42.50 deutsche marks

A large-eddy simulation model is applied to free convection in the atmosphere. The three-dimensional data show coherent spoke patterns in the lower convective layer and isolated plumes and bubbles in the upper convective layer. Large-scale disturbances of the bottom heat flux increase horizontal velocity fluctuations compared to the homogeneous case. Diagnostic relationships for the subgrid-scale fluxes based on second order moment balance equations turn out to yield more exact results than eddy-diffusivity models for the same level of numerical expense. ESA

N89-19523# Oak Ridge National Lab., TN.
DETERMINATION OF LOCAL FLUID DRAG BY A LASER HEATING/THERMOGRAPHIC PHOSPHOR TECHNIQUE: APPLICABILITY OF THE H. LUDWIEG MODEL
J. J. Keyes, Jr. and W. K. Sartory Nov. 1988 9 p
(Contract DE-AC05-84OR-21400)
(DE89-006462; K/ETAC-80) Avail: NTIS HC A03/MF A01

A new application of laser thermography, that utilizes local heat- transfer measurements to deduce local fluid-induced drag is proposed and analyzed. The analytical model originally developed by H. Ludwieg is extended to account for heat conduction in the wall, and the limitations in Reynolds number that correspond to the Ludwieg assumption of a thin thermal boundary layer for air and water are discussed. DOE

N89-19524 Rensselaer Polytechnic Inst., Troy, NY.
THE STABILITY OF BOUNDARY LAYER FLOW OVER ELASTIC SUBSTRATES Ph.D. Thesis
David Lessen 1988 94 p
Avail: Univ. Microfilms Order No. DA8824698

A theoretical investigation of the stability of Boundary Layer flow over certain types of compliant surfaces was carried out. The models for compliant surfaces were: (1) an elastic half space; and (2) an elastic layer of finite thickness. In both cases the solid was modeled to be in a state of plane strain admitting small disturbances in the form of travelling transverse and longitudinal waves. Disturbances in the fluid were assumed to be self-excited and two dimensional and of the Tollmein-Schlichting class. The analysis consists of the calculation of stability boundaries in Reynolds number, wave number space by numerical solution of the Orr-Sommerfeld equation with associated interfacial boundary conditions. Those conditions demand continuous velocity and stress across the fluid-solid interface in both directions. Non-dimensional parameters measuring the relative wave speeds in shear and dilatation are developed. Neutral curves are calculated for various values of those parameters for both models. It is found that increased flexibility in the shear mode is highly destabilizing, causing the critical Reynolds number to decrease and the neutral stability curve to widen. Increased flexibility in the longitudinal mode has relatively little effect for thick layers but for decreased thickness was found to have a destabilizing effect in the range studied.
Dissert. Abstr.

N89-19525# Rolls-Royce Ltd., Derby (England).
COMPUTATIONAL FLUID DYNAMICS FOR COMBUSTION APPLICATIONS
C. H. Priddin 5 Sep. 1988 16 p Presented at Flucome '88, Sheffield, England, 5-8 Sep. 1988
(PNR90534; ETN-89-93703) Copyright Avail: NTIS HC A03/MF A01

Computational fluid dynamics as applied to combustion problems is summarized. Mesh generation, algorithm classification, combustion models, turbulence models, and pollutant emissions are surveyed. Aspects relevant to the calculation of gas turbine combustors, and the impact of such methods on the combustion development process are outlined. It is shown that although there are still large areas of research to be undertaken, models are already proving valuable in addressing real industrial combustion topics. Further developments to substantially advance the usefulness and reduce the cost of such calculations are predicted. ESA

N89-19526# Technische Hochschule, Darmstadt (Germany, F.R.). Fachbereich Mathematik.
ON BOUNDARY INTEGRAL EQUATION APPROACH TO A NONSTATIONARY PROBLEM OF ISOTHERMAL VISCOUS COMPRESSIBLE FLOWS
Friedrich K. Hebeker and George C. Hsiao (Delaware Univ., Newark.) May 1988 21 p
(Preprint-1134; ETN-89-93782) Avail: NTIS HC A03/MF A01

An approach to the initial boundary value problem of isothermal Navier Stokes equations is presented. It is based on a characteristics (Lagrangean) approximation locally in time and a boundary integral equation method using nonstationary potentials. As a basic problem, the latter leads to a Volterra integral equation of the first kind which is proved to be uniquely solvable and even coercive in certain anisotropic Sobolev spaces. The solution depends continuously upon the data and may be constructed by a quasioptimal Galerkin procedure. ESA

N89-19527# Max-Planck-Institut fuer Stroemungsforschung, Goettingen (Germany, F.R.).
VORTEX CONVECTION IN NONUNIFORM COMPRESSIBLE FLOW
A. P. Szumowski and G. E. A. Meier Mar. 1988 29 p
(MPIS-4/1988; ISSN-0436-1199; ETN-89-93812) Avail: NTIS HC A03/MF A01; Max-Planck Institut fuer Stroemungsforschung, Boettinger Strasse 6-8, 3400, Goettingen, Fed. Republic of Germany, 29 Deutsche marks

Vortex convection in longitudinally nonuniform transonic flow fields was studied. Vortices moving in moderately accelerated flow are distinct in the subsonic and supersonic range. Due to the acceleration, the vortices of the Karman street separate continuously one from another. They form a series of periodically shedding individual vortices. The density distribution of the accelerated vortices stays circular. Vortices in subsonic stream (behind the shock wave in the divergent part of the Laval nozzle) impinging on an obstacle (in this case on the regulating valve) cause shock fronts which move upstream. In a subsonic stream flowing out from the convergent nozzle, the primary vortices inside the stream significantly perturb its boundaries and induce secondary vortices (at the boundaries). Flow patterns in a duct with a sudden enlargement of cross section are influenced by the vortices convected in the flow too. However, the observed perturbations of these patterns are relatively weak. The unsteady behaviour of the free stream is not only the effect of the vortex convection but also of the unsteady interactions with the boundaries, i.e., the adjusting valve and the test-section walls. However, the effect of the vortex convection is the stronger. ESA

N89-19528# Technische Univ., Delft (Netherlands). Faculty of Technical Mathematics and Informatics.
MODELING OF INERTIAL EFFECTS IN TRANSIENT LIQUID-BUBBLE FLOWS
P. vanBeek 1988 12 p

(Rept-88-22; ISSN-0920-8577; ETN-89-94005) Copyright Avail: NTIS HC A03/MF A01

Models for liquid-bubble mixtures are reviewed, and the averaging procedure and microscopic equations are analyzed. It is shown that stability depends on the relation between the void-fraction and the ratio between macroscopic and microscopic length scales. This implies a transition to a different flow regime under certain flow conditions. ESA

N89-19237*# National Aeronautics and Space Administration. Ames Research Center, Moffett Field, CA.

ROLE OF COMPUTATIONAL FLUID DYNAMICS IN UNSTEADY AERODYNAMICS FOR AEROELASTICITY

Guru P. Guruswamy (Sterling Federal Systems, Moffett Field, CA.) and Peter M. Goorjian *In* NASA, Langley Research Center, Transonic Unsteady Aerodynamics and Aeroelasticity 1987, Part 1 Feb. 1989 p 47-61 (For primary document see N89-19234 12-02)

Avail: NTIS HC A12/MF A01 CSCL 20D

N89-19828*# National Aeronautics and Space Administration. Ames Research Center, Moffett Field, CA.

KNOWLEDGE-BASED ZONAL GRID GENERATION FOR COMPUTATIONAL FLUID DYNAMICS

Alison E. Andrews *In* NASA. Lyndon B. Johnson Space Center, 2nd Annual Workshop on Space Operations Automation and Robotics (SOAR 1988) Nov. 1988 p 73-80 (For primary document see N89-19817 12-59)

Avail: NTIS HC A22/MF A01 CSCL 20D

35 INSTRUMENTATION AND PHOTOGRAPHY

Includes remote sensors; measuring instruments and gages; detectors; cameras and photographic supplies; and holography.

For aerial photography see *43 Earth Resources and Remote Sensing.* For related information see also *06 Aircraft Instrumentation,* and *19 Spacecraft Instrumentation.*

N89-19529*# National Aeronautics and Space Administration. Langley Research Center, Hampton, VA.

HALOGEN OCCULTATION EXPERIMENT (HALOE) OPTICAL FILTER CHARACTERIZATION

Gale A. Harvey [1989] 28 p

(NASA-TM-4104; L-16538; NAS 1.15:4104) Avail: NTIS HC A03/MF A01 CSCL 14B

The Halogen Occultation Experiment (HALOE) is a solar occultation experiment that will fly on the Upper Atmosphere Research Satellite to measure mixing ratio profiles of O3, H2O, NO2, NO, CH4, HCl, and HF. The inversion of the HALOE data will be critically dependent on a detailed knowledge of eight optical filters. A filter characterization program was undertaken to measure in-band transmissions, out-of-band transmissions, in-band transmission shifts with temperature, reflectivities, and age stability. Fourier Transform Infrared Spectrometers were used to perform measurements over the spectral interval 400/cm to 6300/cm (25 micrometers to 1.6 micrometers). Very high precision (0.1 percent T) in-band measurements and very high resolution (0.0001 percent T) out-of-band measurements have been made. The measurements revealed several conventional leaks at 0.01 percent transmission and greatly enhanced (1,000) leaks to the 2-element filters when placed in a Fabry-Perot cavity. Filter throughput changes by 5 percent for a 25 C change in filter temperature. Author

N89-19530# Eikontech Ltd., Sheffield (England). Antenna Measurement and Consultant Services.

MICROWAVE HOLOGRAPHIC MEASUREMENTS OF LARGE REFLECTORS: PHASE 1 REPORT, VOLUME 1

P. Wright and M. P. Godwin Paris, France ESA May 1986 188 p

(Contract ESTEC-6487/85-NL-PB(SC))

(Rept-B090; ESA-CR(P)-2601-Vol-1; ETN-89-93645) Avail: NTIS HC A09/MF A01

The mathematical basis of holography is outlined. Recording and retrieval of complex radiated field distribution data are explained. Implementation of radiated field distribution measurement techniques is discussed. Implementation of holographic testing of satellite antennas in a space environment is considered. For spotbeam antennas, the aperture plane resolution attainable with likely in-orbit measurement parameter values, using either the aperture to far-field or the aperture to focal-plane transform, should be sufficient to provide useful diagnostic information. However, because of the limited scan angles available, the achievable resolution is probably limited to a few tenths of the antenna diameter. For this reason, the errors in the image of the reflector surface due to measurement system noise are not expected to pose a major problem. The passage of atmospheric irregularities through the signal propagation path does not introduce errors if the phase distribution is measured relative to a reference signal at the same frequency, which follows the same propagation path. Estimates of the change in the propagation path length due to atmospheric irregularities indicate that if the test and reference signals are at slightly different frequencies, or follow propagation paths spatially separated by less than 1 km, then only small errors in the reflector surface image result. ESA

N89-19531# Eikontech Ltd., Sheffield (England). Antenna Measurement and Consultant Services.

MICROWAVE HOLOGRAPHIC MEASUREMENTS OF LARGE REFLECTORS: PHASE 2 REPORT, VOLUME 2

P. Wright and M. P. Godwin Paris, France ESA Aug. 1987 101 p

(Contract ESTEC-6487/85-NL-PB(SC))

(Rept-B091; ESA-CR(P)-2601-Vol-2; ETN-89-93646) Avail: NTIS HC A06/MF A01

Holographic testing of the TVB1 antenna of the L-SAT spacecraft by measurement of the antenna radiation pattern and subsequent use of a phase retrieval algorithm to recover the phase information necessary for holographic surface mapping is discussed. The radiation pattern can be measured by monitoring the level of the transponded signal as the spacecraft is depointed by attitude control. The phase retrieval algorithm most suited to the recovery of the complex field distribution from far-field radiation pattern measurements is that suggested by Misell (1973) which requires the measurement of two patterns, one focussed and one defocussed. The extent of the antenna radiation patterns that can be measured using multiple receiving ground stations is sufficiently large to allow a useful measurement resolution to be achieved. The open loop pointing error of the TVB1 antenna is responsible for the major part of the estimated 0.11 radian phase error in the computed aperture field distribution. The corresponding error in the determination of the reflector surface profile is 0.2 mm at 12 GHz. The limiting constraint on the in-orbit implementation of holographic tests of the L-SAT TVB1 antenna is having to use a transponded signal to measure the radiation patterns. ESA

N89-19532# Rolls-Royce Ltd., Derby (England). Combustion Dept.

APPLICATION OF SCHLIEREN PHOTOGRAPHY IN GAS TURBINE COMBUSTION RESEARCH

B. Jones and A. Wynne 5 Sep. 1988 19 p Presented at Flucome '88, Sheffield, England, 5-8 Sep. 1988 Sponsored by the Ministry of Defence Procurement Executive, London, England

(PNR90495; ETN-89-93689) Copyright Avail: NTIS HC A03/MF A01

The Schlieren method of flow visualization is described. The primary sources of aberration are outlined together with methods to minimize them. The application of this technique in conjunction with high speed cinematography is discussed. The study of two nonsteady flow problems in gas turbine combustion is described. ESA

N89-19533# Rolls-Royce Ltd., Derby (England). Advanced Research Lab.
THE USE OF BURST-TRIGGERED CORRELATION FOR LASER ANEMOMETRY MEASUREMENTS IN TURBOMACHINERY
D. G. Jones and S. S. Wiseall 21 May 1988 6 p Presented at the Photon Correlation Techniques and Applications Conference, Washington, DC, 21 May - 1 Jun. 1988
(PNR90542; ETN-89-93706) Copyright Avail: NTIS HC A02/MF A01

The application of burst-triggered correlation to the processing of laser Doppler anemometry signals measured in rotating turbomachinery is described. The constraints imposed by measurements of high speed flows close to walls favor the use of laser transit anemometry. However, for applications in which a high data rate is required from flows with turbulence levels up to 25 percent, a two component Doppler-difference anemometer with a very good flare rejection capability was developed. It is possible to improve significantly the signal to noise by exploiting the transiently high rate of photon arrivals associated with light scattered from a particle rapidly transiting a small probe volume. Conditional correlation of only those signals which are significantly bunched within a time window comparable to a beam transit, provides a powerful method of enhancing the discrimination of particle signals from flare noise. A dual channel correlator was fitted with two fast preprocessor input boards which provide a burst detection capability for conditionally loading the parallel correlator channels with their respective time-expanded pulse trains. Tests show a strong motivation to exploit the individual event detection capability of burst processing, rather than simply time integrating in the correlator. ESA

N89-19534# Sandia National Labs., Albuquerque, NM.
COMPARISON OF AN ac AND A dc BRIDGE FOR STANDARD PLATINUM RESISTANCE THERMOMETER CALIBRATIONS
Mary K. Odom Jan. 1989 31 p
(Contract DE-AC04-76DP-00789)
(DE89-007060; SAND-88-2506) Avail: NTIS HC A03/MF A01

The Primary Standards Laboratory (PSL) presently uses a manually operated dc bridge to calibrate standard platinum resistance thermometers (SPRTs). The PSL will replace the dc bridge with a computer controlled ac bridge. The two bridges are compared for calibrating SPRTs. The results show that the two bridges are interchangeable within less than 3 C in the PSL environment. DOE

N89-19463*# Jet Propulsion Lab., California Inst. of Tech., Pasadena.
SYSTEMS ANALYSIS FOR DSN MICROWAVE ANTENNA HOLOGRAPHY
D. J. Rochblatt *In its* The Telecommunications and Data Acquisition Report 15 Feb. 1989 p 132-157 (For primary document see N89-19451 12-32)
Avail: NTIS HC A10/MF A01 CSCL 14B

N89-19653 Meteorological Research Inst., Tsukuba (Japan).
DEVELOPMENT OF HYDROMETEOR VIDEO SONDE
Masataka Murakami and Takayo Matsuo *In* Deutscher Wetterdienst, Annals from the German Meteorological Society, No. 25: 10th International Cloud Physics Conference Preprints, Volume 1 1988 p 144-147 (For primary document see N89-19605 12-42)
Copyright Avail: Deutscher Wetterdienst, Frankfurter Strasse 135, D-6050 Offenbach am Main, Fed. Republic of Germany

N89-19655 Stockholm Univ. (Sweden). Dept. of Meteorology.
ON THE DETERMINATION OF DROPLET SIZE DISTRIBUTIONS WITH THE COUNTERFLOW VIRTUAL IMPACTOR
B. Johansson and Jost Heintzenberg *In* Deutscher Wetterdienst, Annals from the German Meteorological Society, No. 25: 10th International Cloud Physics Conference Preprints, Volume 1 1988 p 151-153 (For primary document see N89-19605 12-42)
Copyright Avail: Deutscher Wetterdienst, Frankfurter Strasse 135, D-6050 Offenbach am Main, Fed. Republic of Germany

N89-19681 Drexel Univ., Philadelphia, PA. Dept. of Physics and Atmospheric Science.
AIRBORNE CLOUD SIEVING
Edward E. Hindman *In* Deutscher Wetterdienst, Annals from the German Meteorological Society, No. 25: 10th International Cloud Physics Conference Preprints, Volume 1 1988 p 229-231 (For primary document see N89-19605 12-42)
(Contract N00014-84-C-0591; NSF ATM-87-15060; NSF ATM-87-04776)
Copyright Avail: Deutscher Wetterdienst, Frankfurter Strasse 135, D-6050 Offenbach am Main, Fed. Republic of Germany

N89-19716 Netherlands Energy Research Foundation, Petten.
A POOR MAN'S OPTICAL FOG DETECTOR
Ronald K. A. M. Mallant *In* Deutscher Wetterdienst, Annals from the German Meteorological Society, No. 25: 10th International Cloud Physics Conference Preprints, Volume 1 1988 p 333-334 (For primary document see N89-19605 12-42)
Copyright Avail: Deutscher Wetterdienst, Frankfurter Strasse 135, D-6050 Offenbach am Main, Fed. Republic of Germany

N89-19719 Meteorological Research Inst., Tsukuba (Japan).
A NEW AIRBORNE DEVICE FOR MEASUREMENT OF CLOUD PARTICLES USING VIDEO MICROSCOPE
T. Tanaka, Takayo Matsuo, K. Okada, I. Ichimura, S. Ichikawa, and A. Tokuda (Sankei Co. Ltd., Tokyo, Japan) *In* Deutscher Wetterdienst, Annals from the German Meteorological Society, No. 25: 10th International Cloud Physics Conference Preprints, Volume 1 1988 p 341-343 (For primary document see N89-19605 12-42)
Copyright Avail: Deutscher Wetterdienst, Frankfurter Strasse 135, D-6050 Offenbach am Main, Fed. Republic of Germany

N89-19728 Institute of Hydrology and Meteorology, Sofia (Bulgaria).
A NEW DROPSONDE FOR CLOUD PROBINGS
Dimiter Gaytandjien *In* Deutscher Wetterdienst, Annals from the German Meteorological Society, No. 25: 10th International Cloud Physics Conference Preprints, Volume 1 1988 p 366-368 (For primary document see N89-19605 12-42)
Copyright Avail: Deutscher Wetterdienst, Frankfurter Strasse 135, D-6050 Offenbach am Main, Fed. Republic of Germany

36 LASERS AND MASERS

Includes parametric amplifiers.
For related information see also *76 Solid-State Physics.*

N89-19535# National Bureau of Standards, Gaithersburg, MD.
FREE-ELECTRON LASER DRIVEN BY THE NBS (NATIONAL BUREAU OF STANDARDS) CW MICROTRON Annual Report, 1 Apr. 1987 - 31 Mar. 1988
31 Mar. 1988 149 p
(Contract N00014-87-F-0066)
(AD-A201170) Avail: NTIS HC A07/MF A01 CSCL 09C

The overall goal of this project is to construct and bring into operation a free-electron laser (FEL) driven by the racetrack microtron (RTM) electron accelerator at NBS. NBS is providing the RTM, radiation shielded laboratory space for the RTM and FEL, and experimental areas. The scope of the project includes: modifying the RTM injector for increased peak current; developing electron beam transport from the RTM to the FEL: developing a wiggler and optical cavity; and developing optical beam transport and diagnostics. GRA

N89-19536# Cincinnati Univ., OH. Dept. of Electrical and Computer Engineering.
INTEGRATION OF DETECTORS AND OPTICAL WAVEGUIDE STRUCTURES Final Report, 15 Mar. 1985 - 15 Mar. 1988

J. T. Boyd 15 Sep. 1988 28 p
(Contract F49620-85-C-0044)
(AD-A201331; AFOSR-88-1175TR) Avail: NTIS HC A03/MF A01 CSCL 20F

Integrated detection of light propagating in an optical waveguide with a photodetector array fabricated directly on the waveguide surface has been demonstrated. Devices having very good performance were formed by depositing polycrystalline silicon and laser recrystallizing it prior to device fabrication. The use of two lasers has been shown to result in improved recrystallization. An analysis of a four-layer optical waveguide structure has been performed and applied to multiple layer gallium aluminum arsenide structures and SiO2/Si structures. Numerical calculations of waveguide attenuation due to substrate coupling for thermally-nitrided silicon dioxide and for gallium aluminum arsenide waveguides have been performed for a variety of layer thicknesses, layer material compositions, and wavelengths. Comparison with some experimental data has been carried out. Extensive Raman microprobe characterization has also been performed on laser recrystallized silicon and on GaAlAs dielectric strip waveguide structures. Use of rapid thermal annealing to initiate in-diffusion of Ti into LiNbO3 has yielded low loss optical waveguides. GRA

N89-19537# Howard Univ., Washington, DC.
KINETIC PROCESSES IN DISCHARGE PUMPED MERCURY HALIDE LASERS Final Report, May 1985 - Jul. 1988
Vikram S. Kushawaha 15 Aug. 1988 3 p
(Contract DAAG29-85-G-0081)
(AD-A201612; ARO-2279.14-PH-H) Avail: NTIS HC A02/MF A01 CSCL 07D

This report describes the formation of excited state species observed during collisions involving HgX2/CH3HgX(X=C,BR,I) molecules and electrons or ions at different laboratory kinetic energies. Electron impact dissociation of HgX2 and CH3HgX has been studied and formation of HgX (2sigma)-radicals and highly excited state of Hg atoms has been observed in the laboratory kinetic energy range of 1 to 100 eV. With electron and CH3HgX collisions, emissions from CH-radicals and atomic hydrogen have also been observed, in addition to the above mentioned species. GRA

N89-19538# Naval Research Lab., Washington, DC. Plasma Physics Div.
CHAOTIC ELECTRON MOTION CAUSED BY SIDEBANDS IN FREE ELECTRON LASERS Interim Report
S. Riyopoulos (Science Applications International Corp., McLean, VA.) and C. M. Tang 27 Oct. 1988 86 p Previously announced in IAA as A89-16893
(AD-A201635; NRL-MR-6365) Avail: NTIS HC A05/MF A01 CSCL 09C

The electron dynamics in a Free Electron Laser (FEL) is studied in the case when the radiation field contains many modes. This situation arises when unstable modes (sidebands) are excited during operation. It is observed that when the strength of these sidebands exceeds certain levels, the electron motion becomes chaotic. This may lead to extensive particle detrapping and loss of amplification for the FEL signal. The threshold for the onset of stochastic electron motion is computed. The evolution of the trapped electron distribution exhibits a diffusive behavior. The rate of particle detrapping is parameterized by the diffusion coefficient D in action space. It is found that the diffusion rates are connected to the type of the sideband spectrum. The diffusion coefficient is always proportional to the ratio of the sideband power in all frequencies to the power of the carrier signal. The coefficient of the proportionality however scales differentially to the FEL parameters for each of the three spectral categories: a narrow, a broad discrete and a broad continuous spectrum. The diffusion coefficient is computed analytically for the last two cases and is in good agreement with numerical results. The narrow spectrum yields the highest and the broad continuous the measured in wiggler periods, is independent of the electron energy. GRA

N89-19539*# City Coll. of the City Univ. of New York. Dept. of Physics.
NONRADIATIVE RELAXATION AND LASER ACTION IN TUNABLE SOLID STATE LASER CRYSTALS Final Technical Report, 1 Sep. 1987 - 31 Dec. 1988
V. Petricevic, S. K. Gayen, and R. R. Alfano 16 Mar. 1989 9 p
(Grant NAG1-810)
(NASA-CR-182820; NAS 1.26:182820) Avail: NTIS HC A02/MF A01 CSCL 20E

Room-temperature pulsed laser action was obtained in chromium-activated forsterite (Cr:Mg2SiO4) for both 532 and 1064 nm pumping. Free running laser emission in both cases is centered at 1235 nm and has a bandwidth of approximately 30 nm. Slope efficiency as high as 22 percent was measured. Using different sets of output mirrors and a single birefrigent plate as the intracavity wavelength selecting element tunability over the 1167 to 1268 nm spectral range was demonstrated. Continuous wave laser operation at room temperature was obtained for 1064 nm pumping from a CW Nd:YAG laser. The output power slope efficiency is 6.8 percent. The gain cross section is estimated to be 1.1 x 10 to the 19th sq cm. Spectroscopic studies suggest that the laser action is due to a center other than the trivalent chromium (Cr 3+), presumably the tetravalent chromium (Cr 4+) in a tetrahedrally coordinated site. Author

N89-19540# Brookhaven National Lab., Upton, NY.
DESCRIPTION OF FEL3D: A THREE DIMENSIONAL SIMULATION CODE FOR TOK AND FEL
S. Dutt, A. Friedman, and A. Gover 20 Oct. 1988 30 p
(Contract DE-AC02-76CH-00016)
(DE89-005529; BNL-41995) Avail: NTIS HC A03/MF A01

FEL3D is a three dimensional simulation code, written for the purpose of calculating the parameters of coherent radiation emitted by electrons in an undulator. The program was written predominantly for simulating the coherent super-radiant harmonic frequency emission of electrons which are being bunched by an external laser beam while propagating in an undulator magnet. This super-radiant emission is to be studied in the TOK (transverse optical klystron) experiment, which is under construction in the NSLS department at Brookhaven National Laboratory. The program can also calculate the stimulated emission radiometric properties of a free electron laser (FEL) taking into account three dimensional effects. While this application is presently limited to the small gain operation regime of FEL's, extension to the high gain regime is expected to be relatively easy. The code is based on a semi-analytical concept. Instead of a full numerical solution of the Maxwell-Lorentz equations, the trajectories of the electron in the wiggler field are calculated analytically, and the radiation fields are expanded in terms of free space eigen-modes. This approach permits efficient computation, with a computation time of about 0.1 sec/electron on the BNL IBM 3090. DOE

N89-19541# Medical Coll. of Virginia, Richmond.
BIOLOGICAL APPLICATIONS AND EFFECTS OF OPTICAL MASERS Midterm Report, 1 Sep. 1987 - 31 Aug. 1988
William T. Ham, Jr., Harold A. Mueller, R. K. Guerry, Dupont Guerry, III, and Stephan F. Cleary 29 Sep. 1988 20 p
(Contract DAMD17-87-C-7186; DA Proj. 3E1-62777-A-878)
(AD-A201834) Avail: NTIS HC A03/MF A01 CSCL 09C

Threshold radiant exposures for retinal damage in 3 macaque monkeys are given for exposures of 0.5, 0.125 and 0.016 seconds duration to laser wavelengths 514.5 and 488 nm. Intravitreal injections of 5 x .00005 gm of Cu-Zn SOD were toxic to cornea, lens and retina of the rhesus monkey after a radiant exposure of 33 j/sq cm of 440 nm light. No further experiments with SOD are contemplated. Similar experiments with catalase will be tried during the first quarter of the second contract year. The effect of oxygen on retinal toxicity during exposure to wave-lengths 540, 640 and 840 nm were delayed by the untimely death of Dr. Millen, our consultant on anesthesiology and oxygen administration. Arrangements have been made to activate this program during the second contract year. Threshold data on 40 microsecond pulse trains cannot be obtained until the acoustic modulator can be

incorporated into the Ar-Kr laser which was used during the contract year to produce exposures less than 1 second to 514.5 and 488 nm laser lines. Data on PRF's of 10 and 100 KHz and 1, 10 and 20 MHz will be obtained during the second contract year. The long-term experiment on cataractogenesis on 2 rhesus monkeys exposed to a near UV spectrum (330 to 420 nm) has been completed. GRA

N89-19542# Texas Univ., Dallas. Center for Quantum Electronics.
PROOF OF THE FEASIBILITY OF COHERENT AND INCOHERENT SCHEMES FOR PUMPING A GAMMA-RAY LASER Quarterly Technical Progress Report, 1 Jul. - 30 Sep. 1988
Carl B. Collins Oct. 1988 142 p
(Contract N00014-86-C-2488)
(AD-A201931; GRL/8802) Avail: NTIS HC A07/MF A01 CSCL 09C

This report focuses upon a breakthrough recently realized along the more complex direction toward the coherent pumping of a gamma-ray laser. The intent is to mix the quantum properties of long-lived nuclear states with those able to radiate freely. In this way the metastability of an isomeric state could be switched off. The critical experiment is to show that some laboratory level of coherent input power can affect the properties of a nuclear level. Reported here are the details of a series of experiments which clearly demonstrated that large levels of modulation of the phases of nuclear states can be obtained with relatively modest input powers. Now many more critical experiments become possible even along this more complex path toward a gamma-ray laser. Also reported here are the most recent advances we have made in the preparation of the thin film diamond materials. Efficacy of the unique laser plasma process we describe is so great that it already has become clear that applications will range far beyond the support of this gamma-ray laser project. GRA

N89-19543# Air Force Weapons Lab., Kirtland AFB, NM.
THE STANDARD CHEMICAL OXYGEN-IODINE LASER KINETICS PACKAGE Final Report, Aug. 1987 - Mar. 1988
Glen P. Perram and Gordon D. Hager Oct. 1988 33 p
(AD-A202223; AFWL-TR-88-50) Avail: NTIS HC A03/MF A01 CSCL 09C

This report presents the Air Force Weapons Laboratory Standard Chemical Oxygen-Iodine Laser Kinetics Package. A complete reaction scheme including recommended rate coefficients for modeling the gas phase kinetics of chemical oxygen-iodine lasers (COIL) was established to provide a common basis for the research and development of COIL devices. A review of the experimental kinetic data base from which this model was derived is also presented. However, the fully coupled, reactive mixing and optical physics problems inherent in supersonic chemical oxygen-iodine lasers are not addressed. GRA

N89-19544# Dayton Univ., OH.
HIGH-SPEED LASER PHOTOGRAPHY Final Report, 1 May 1983 - 30 Sep. 1987
Roger J. Becker Aug. 1988 84 p
(Contracts F04611-83-K-0023; F04611-83-K-0018)
(AD-A202293; UDRI-TR-88-45; AFAL-TR-88-050) Avail: NTIS HC A05/MF A01 CSCL 21H

High-speed movies of solid propellant deflagration have long provided useful qualitative information on propellant behavior. Consequently, an extension of performance to include quantitative behavior of the surface, particularly the spatial relationship of particles across the surface, the temporal behavior of particles through extended periods of time, and accurate measurements of particle sizes, is highly desirable. Such measurements require the ability to take detailed movies across an extensive surface through the propellant flame for longer periods than the residence time of a given particle. The modulation transfer function (MTF) of the camera optics and film will greatly affect performance. The MTF of the optics can be improved by a factor of two or more at practical spatial frequencies by the use of monochromatic light, such as the reflected light from a laser. The use of an intense, short-pulsed laser has the additional advantage of suppressing flame brightness and motion blur. High resolution at unity magnification is achieved by the use of 2 mJ of illumination energy per pulse in conjunction with a fine-grain film. The surfaces of the wide-distribution propellants were found to be molten. GRA

N89-19545*# Spectron Development Labs., Inc., Costa Mesa, CA.
LASER TRANSIT ANEMOMETER SOFTWARE DEVELOPMENT PROGRAM Final Report
John B. Abbiss Washington NASA Mar. 1989 56 p
(Contract NAS1-18311)
(NASA-CR-4225; NAS 1.26:4225; SDL-88-2513-27F/76) Avail: NTIS HC A04/MF A01 CSCL 20E

Algorithms were developed for the extraction of two components of mean velocity, standard deviation, and the associated correlation coefficient from laser transit anemometry (LTA) data ensembles. The solution method is based on an assumed two-dimensional Gaussian probability density function (PDF) model of the flow field under investigation. The procedure consists of transforming the data ensembles from the data acquisition domain (consisting of time and angle information) to the velocity space domain (consisting of velocity component information). The mean velocity results are obtained from the data ensemble centroid. Through a least squares fitting of the transformed data to an ellipse representing the intersection of a plane with the PDF, the standard deviations and correlation coefficient are obtained. A data set simulation method is presented to test the data reduction process. Results of using the simulation system with a limited test matrix of input values is also given. Author

N89-19546# Los Alamos National Lab., NM.
LIQUID EXCIMERS: LASING Xe2 AND Kr2 IN LIQUID ARGON
Thomas R. Loree, Robert R. Showalter, Brian S. Birmingham, Tamara M. Johnson, and William M. Hughes 1988 13 p Presented at the LASERS '88, Lake Tahoe, NV, 5 De c. 1988 Prepared in cooperation with Mission Research Corp., Los Alamos, NM
(Contract W-7405-eng-36)
(DE89-005449; LA-UR-88-4030; CONF-881244-2) Avail: NTIS HC A03/MF A01

By pumping a small cryogenic cell with a 40-ns, 1 MeV e-beam pulse, we have excited lasing in dilute mixtures of xenon or krypton in argon. The lasing occurred at 175 nm for the excimer Xe2 and 147 nm for Kr2. DOE

N89-19547# Los Alamos National Lab., NM.
XUV FREE-ELECTRON LASER DEVELOPMENT AT LOS ALAMOS
Brian E. Newnam 1988 13 p Presented at the International Conference on the Application of Accelerators in Research and Industry, Denton, TX, 7 Nov. 1988
(Contract W-7405-eng-36)
(DE89-005458; LA-UR-88-4114; CONF-881151-52) Avail: NTIS HC A03/MF A01

Free-electron lasers (FELs) for the vacuum-ultraviolet and soft X-ray spectral regions (together termed the XUV) are being developed at Los Alamos for integration into a proposed national UV/XUV FEL user facility for scientific experimentation. This facility would consist of a sequence of up to 15 FEL oscillators and amplifiers, driven by a single, RF-linear accelerator, that will generate broadly tunable, picosecond-pulse, coherent radiation over the range from 1 to 400 nm. Below 300 nm, the peak- and average-power output of these FEL devices should surpass the capabilities of any existing, continuously tunable photon sources by many orders of magnitude. We list the design parameters and predicted output of these FELs and make comparison with synchrotron radiation sources. Brief mention is given to our recent progress in developing the three primary components (electron beam, magnetic undulator, and resonator mirrors). DOE

N89-19548# Los Alamos National Lab., NM.
ULTRAHIGH-BRIGHTNESS XeCl LASER SYSTEM
R. B. Gibson, T. R. Gosnell, C. S. Lester, J. P. Robers, C. R. Tallman, and A. J. Taylor 1989 10 p Presented at the SPIE Conference on High Power and Solid State Lasers, Los Angeles, CA, 19 Jan. 1989
(Contract W-7405-eng-36)
(DE89-005467; LA-UR-88-4200; CONF-890157-1) Avail: NTIS HC A02/MF A01

A laser system that produces terawatt-level pulses of 308-nm light with near-diffraction-limited beam quality is under development. Pulses of 175-fs duration are generated at 616 nm in a synchronously-pumped mode-locked dye oscillator. These pulses are amplified in a three-stage dye amplifier longitudinally pumped by the frequency-doubled output of a regenerative Nd:YAG amplifier. Output of the dye amplifier is frequency-doubled in a BBO crystal and amplified in a chain of XeCl excimer stages. The optical design maintains high beam quality throughout. DOE

N89-19549# Los Alamos National Lab., NM.
ELECTRON-BEAM PUMPED LIQUID EXCIMER LASERS
Thomas R. Loree, Robert R. Showalter, Tamara M. Johnson, Brian S. Birmingham, and William M. Hughes 1988 31 p Presented at the LASERS '88, Lake Tahoe, NV, 5 De c. 1988
(Contract W-7405-eng-36)
(DE89-006549; LA-UR-89-19; CONF-881244-4) Avail: NTIS HC A03/MF A01

We have investigated the excimers formed in liquid argon when various cryogenic gas mixes were excited by 1-MeV electrons. Fluorescence was detected from many excimers at their new red-shifted wavelengths, and XeO, Xe2, and Kr2 were lased. DOE

N89-19550# Los Alamos National Lab., NM.
MODELING THE ENERGY DEPOSITION IN THE AURORA KrF LASER AMPLIFIER CHAIN
J. C. Comly, S. J. Czuchlewski, D. P. Greene, D. E. Hanson, B. J. Krohn, and A. W. McCown 1988 6 p Presented at the 35th National Vacuum Symposium and 4th International Laser Science Conference, Atlanta, GA, 2 Oct. 1988
(Contract W-7405-eng-36)
(DE89-006545; LA-UR-89-49; CONF-881002-4) Avail: NTIS HC A02/MF A01

Monte Carlo calculations model the energy depositions by highly energetic electron beams into the cavities of the four KrF laser amplifiers in the Aurora chain. Deposited energy density distributions are presented and studied as functions of e-beam energy and gas pressure. Results are useful for analyzing small signal gain (SSG) measurements and optimizing deposition in future experiments. DOE

N89-19551# Los Alamos National Lab., NM.
ON THE USE OF MULTIPLE PHOTON PROCESSES IN KRYPTON FOR LASER GUIDING OF ELECTRON BEAMS
Leon J. Radziemski, Noshir M. Khambatta, John A. Oertel, Robert Silk, Joseph M. Mack, and Dashan Mitrovich 1989 9 p Presented at the SPIE Conference on Optics, Electro-optics and Laser Applications in Science and Engineering: OE/LASE '89, Los Angeles, CA, 15-20 Jan. 1989
(Contract W-7405-eng-36)
(DE89-006546; LA-UR-89-48; CONF-890145-6) Avail: NTIS HC A02/MF A01

Neutral krypton atoms were excited from the ground state 4p(6) 1 sub S sub O to the 4p(5) 6p(3/2) sub 2 state by a resonant two-photon absorption from a line-narrowed ArF excimer laser operating at 193.41 nm. A third photon, absorbed while the atom is in the excited state, ionizes it. Excited state and ion densities were theoretically computed using a standard rate-equation analysis. The irradiance levels used (1 - 5 x 10 to the 8th power W/sq cm) were too low for significant ground and excited state ac Stark and Rabi effects. The photon detection system was calibrated with a standard tungsten lamp. Ion signals were measured with known electrical components. The resonance results were compared with predictions of non-resonant ionization based on a standard formulation. The ion and excited state densities have been used with a modified electron beam propagation code (IPROP) to model such propagation in a low pressure laser-excited krypton channel. The modifications included the effects to field ionization of the excited krypton atoms. Implications for guiding of e-beams using ArF excited krypton are discussed. DOE

N89-19552# Los Alamos National Lab., NM.
HIGH AVERAGE POWER EXCIMER LASER-PUMPED DYE OSCILLATORS
Roger A. Tennant, Michael C. Whitehead, Charles R. Tallman, and Richard W. Basinger 1988 16 p Presented at the LASERS '88, Lake Tahoe, NV, 4-9 Dec. 1988
(Contract W-7405-eng-36)
(DE89-006547; LA-UR-89-40; CONF-881244-3) Avail: NTIS HC A03/MF A01

The design, construction, and testing of a high-average-power excimer laser-pumped dye oscillator is described. The system is designed to produce up to 75 watts of average power in the near UV at a pulse repetition rate of 500 Hz. DOE

N89-19553# Los Alamos National Lab., NM.
IMPACT OF TARGET ALTITUDE RESTRICTIONS ON LASER PERFORMANCE
Gregory H. Canavan Jan. 1989 9 p
(Contract W-7405-eng-36)
(DE89-006567; LA-11382-MS) Avail: NTIS HC A02/MF A01

This report estimates the impact of Raman restrictions and shielding penalties separately and together. Its goal is an overall assessment of likely impact rather than a review of the details of missile trajectories, Raman physics, and shielding techniques, whose individual treatments matter less than their overall integration. Raman scattering could produce a factor of 2 to 3 reduction on the performance of repetitive pulse lasers with large fluences in each small pulse. Radio-frequency free-electron lasers (RF FELs), which have more frequent pulses with less energy in each, are impacted less. Shielding gives an independent penalty of about a factor of 2, but the combined effect of altitude and shielding penalizes lasers with large pulses by factors of 3 to 10. Those factors are significantly larger than any other factors differentiating between the two types of FELs. DOE

37 MECHANICAL ENGINEERING

Includes auxiliary systems (nonpower); machine elements and processes; and mechanical equipment.

N89-19554 North Carolina State Univ., Raleigh.
AN APPROACH TO SEMI-ACTIVE CONTROL OF MULTIPLE DEGREE-OF-FREEDOM SYSTEMS Ph.D. Thesis
Lane R. Miller 1988 213 p
Avail: Univ. Microfilms Order No. DA8815558

A system is semi-active when the control effort is generated passively. A natural application of this technology is to control vibratory systems. Because of power limitations, semi-active control is particularly attractive for vehicle suspensions. The benefits of semi-active control have been demonstrated on low-order systems. Mathematically, semi-active control is inherently highly nonlinear. This complication prevents the direct application of most of the standard techniques developed in modern control theory. While being highly nonlinear, semi-active systems can be described by piecewise linear differential equations. This description provides useful insight into the basic mathematical properties and performance of these systems. Using these properties, an approximate method for determining the frequency response is developed. Viewing semi-active systems as piecewise linear is useful in the development of a general control strategy. This control strategy makes use of an algorithm which includes parallel linear state observers, a cost function, and a logical decision. This strategy is called semi-active observer control and is a general technique

which can be applied to high-order dynamic systems, which possess competing performance criteria. By adjusting the weighting in the cost function, the dynamic response of a high-order system can be tailored. Dissert. Abstr.

N89-19555*# Texas A&M Univ., College Station. Turbomachinery Labs.
DESIGN IMPROVEMENT OF A PUMP WEAR RING LABYRINTH SEAL Final Report
David L. Rhode, G. L. Morrison, S. H. Ko, and S. P. Waughtal Feb. 1987 201 p
(Contract NAS8-36161)
(NASA-CR-179161; NAS 1.26:179161; TL-SEAL-2-87) Avail: NTIS HC A10/MF A01 CSCL 13I

The investigation was successful in obtaining two improved designs for the impeller wear ring seal of the liquid hydrogen turbopump of interest. A finite difference computer code was extensively used in a parametric computational study in determining a cavity configuration with high flow resistance due to turbulence dissipation. These two designs, along with that currently used, were fabricated and tested. The improved designs were denoted Type O and Type S. The measurements showed that Type O and Type S given 67 and 30 percent reduction in leakage over the current design, respectively. It was found that the number of cavities, the step height and the presence of a small stator groove are quite important design features. Also, the tooth thickness is of some significance. Finally, the tooth height and an additional large cavity cut out from the stator (upstream of the step) are of negligible importance. Author

N89-19556*# Boeing Commercial Airplane Co., Seattle, WA.
AN EXPERIMENTAL EVALUATION OF S-DUCT INLET-DIFFUSER CONFIGURATIONS FOR TURBOPROP OFFSET GEARBOX APPLICATIONS Final Report
Paul L. McDill Jul. 1986 126 p Sponsored by NASA, Lewis Research Center, Cleveland, Ohio
(NASA-CR-179454; NAS 1.26:179454; D6-53344) Avail: NTIS HC A07/MF A01 CSCL 13I

A test program, utilizing a large scale model, was run in the NASA Lewis Research Center 10- by 10-ft wind tunnel to examine the influence on performance of design parameters of turboprop S-duct inlet/diffuser systems. The parametric test program investigated inlet lip thickness, inlet/diffuser cross-sectional geometry, throat design Mach number, and shaft fairing shape. The test program was run at angles of attack to 15 deg and tunnel Mach numbers to 0.35. Results of the program indicate that current design techniques can be used to design inlet/diffuser systems with acceptable total pressure recovery, but several of the design parameters, notably lip thickness (contraction ratio) and shaft fairing cross section, must be optimized to prevent excessive distortion at the compressor face. Author

N89-19557# Idaho National Engineering Lab., Idaho Falls.
NONCONTACT ULTRASONIC SENSING OF WELD POOLS FOR AUTOMATED WELDING
John A. Johnson and Nancy M. Carlson 1988 8 p Presented at the Meeting on Nondestructive Characterization of Materials, Saarbrucken, Fed. Republic of Germany, 8 Oct. 1988
(Contract DE-AC07-76ID-01570)
(DE89-005185; EGG-M-88049; CONF-881081-1) Avail: NTIS HC A02/MF A01

Contacting ultrasonic techniques can determine the geometry of the molten/solid interface and detect conditions which could lead to defect formation. However, the couplant required is a potential source of contamination in the weld and may be difficult to use under industrial conditions. Stress waves can also be generated and detected using noncontacting techniques. Ultrasonic stress waves are generated by focusing a beam from a pulsed laser on a stationary weld pool formed on the surface of a steel plate or on a weld pool in a fillet weld. The transmitted ultrasound is detected by an electromagnetic-acoustic transducer (EMAT). The signal received by the EMAT provides information about the properties of the pool, including the geometry and defect generating conditions. This information can be input to an intelligent controller. The ultrasonic system described in this paper is being developed as a portion of the sensing and control system for a completely automated welder. DOE

N89-19558# Honeywell, Inc., Hopkins, MN.
A NEW PUMPJET DESIGN THEORY Final Report, 1 Jan. 1987 - 21 Dec. 1988
Okitsugu Furuya and Wen-Li Chiang 30 Jun. 1988 283 p
(Contract N00014-85-C-0050)
(AD-A201353) Avail: NTIS HC A13/MF A01 CSCL 19H

The pumpjet is considered to be one of the most promising candidate propulsors for high speed underwater vehicles and, as a matter of fact, it has recently been employed for MK 48 torpedoes, ALWT Advanced Light Weight Torpedo, now called MK 50 and other underwater vehicles. The pumpjet superiority over other propulsion devices is represented by two major factors, i.e., high efficiency and quietness. The pumpjet is one of few fluid devices which positively utilizes retarded wake flow and produces high propulsive efficiency. This peculiar situation may be understood readily by considering the momentum equation applied to a control volume surrounding an underwater vehicle, fixed to the inertial coordinate system. In the conventional propeller, for example, the velocity of flow coming into a propeller blade is approximately equal to the vehicle speed since the propeller diameter is large enough to enjoy the free stream flow. In order for the propeller to generate any effective thrust, it should accelerate the flow, the ejected flow speed being faster than the incoming flow. GRA

N89-19559# Army Missile Command, Redstone Arsenal, AL. Structures Directorate.
ANALYSIS OF PERSHING 2 REENTRY VEHICLE (RV) CONTROL RING CASTINGS Technical Report, Mar. - Aug. 1987
Albert S. Ingram May 1988 34 p
(AD-A201548; AD-E951221; AMSMI/TR-RD-ST-88-1) Avail: NTIS HC A03/MF A01 CSCL 11F

A comparative material analysis was performed on two PERSHING 2 RV control rings with reported differences in tensile properties and percent elongation. Both RV control rings were characterized by tensile tests, chemical analysis, fracture toughness tests, and metallography. The comparative analysis proved that the two examined RV rings were equivalent, though contractor tensile coupon tests showed otherwise. The average properties of the RV control ring were: 37.25 ksi (256.6 MPa) ultimate strength, 32.65 ksi (225 MPa) yield strength, 5.7 percent elongation, and 15.505 ksi sq.root (16.55 MPa sq.root) KIC fracture toughness. The RV rings are fabricated from A356-T6 aluminum. Analysis of cast tensile coupon specimens was also performed to determine the major reason for large differences in percent elongation resulting from quality control tensile tests. Electron microscopy and metallography revealed that large casting flaws (eutectic silicon segregation) had occurred in most tensile specimens with low percent elongation. Therefore, inaccurate (low) mechanical property and percent elongation data resulted from these tensile specimens with casting flaws. GRA

N89-19560# Rochester Univ., NY. Dept. of Computer Science.
COORDINATES, CONVERSIONS, AND KINEMATICS FOR THE ROCHESTER ROBOTICS LAB
Christopher M. Brown and Raymond D. Rimey Aug. 1988 22 p
(Contracts DACA76-85-C-0001; F30602-85-C-0008)
(AD-A201611; TR-259) Avail: NTIS HC A03/MF A01 CSCL 14D

This is a guide to coordinate systems, representations, and geometric relationships between them, for components of the Rochester Robotics Laboratory. The main entities at issue are the joint angles, location variables, and coordinate systems of the Puma, the camera angles and coordinate systems associated with the head, the spatial location of three-dimensional points, and the kinematic and inverse kinematic relationships between them. The robot-to-camera kinematic chain is described, conversions between

homogeneous transformations and VAL location descriptions are provided, and inverse problems (camera angles to aim cameras at a 3-D point given a robot configuration, binocular stereo calculations) are solved. Constants describing the robot head and sample robot description data structures are provided. GRA

N89-19561# Naval Postgraduate School, Monterey, CA.
IMPLEMENTATION OF DYNAMIC CONTROL OF A SINGLE-LINK FLEXIBLE ARM USING A GENERAL MICRO-COMPUTER M.S. Thesis
Michael Kirkland Sep. 1988 90 p
(AD-A201622) Avail: NTIS HC A05/MF A01 CSCL 12F

The purpose of this thesis is the implementation of a dynamic control of a single-link flexible arm and experimentation with various parameters to study the dynamic behavior of the control system. The tip position was determined by the outputs of a potentiometer and a strain gage. Data acquisition was performed using Data Translation high speed interface board (DT 2821-F-8DI). The board supports sixteen twelve bit A/D input channels with a maximum usable sampling rate of 130 kilohertz. The micro-computer used was the standard IBM AT. The support software (AT0-LAB) allowed direct manipulation of the data acquisition board through the use of provided subroutines which were compatible with FORTRAN, the language chosen to implement the controller. GRA

N89-19562 Brown Univ., Providence, RI.
MULTIPROCESSOR CONTROL OF ROBOTIC MANIPULATORS Ph.D. Thesis
Peter Kazanzides 1988 155 p
Avail: Univ. Microfilms Order No. DA8822537

SIERA (System for Implementing and Evaluating Robotic Algorithms) is a multiprocessor system that was developed to support research in robotic algorithms. It consists of the tightly-coupled, bus-based Real Time Servo System (RTSS) and the loosely-coupled, link-based Armstrong Multiprocessor. This hybrid architecture was selected to combine the benefits of both systems. The tightly-coupled RTSS provides the low communication overhead that is necessary for real time control. The loosely-coupled Armstrong Network provides expandability and reconfigurability, and can perform the high level planning required to coordinate robots and other devices in an intelligent manner. An important study is the demonstration that a hybrid architecture, such as the one employed in SIERA, is both desirable and feasible. SIERA is a flexible system that allows virtually all functions related to operation of the robot (control, kinematics, trajectory planning) to be interactively modified. The modular construction of the hardware and software allows SIERA to be applied to different robots. Various position and force controllers were implemented using SIERA. Some research results are presented.
Dissert. Abstr.

N89-19563 Ohio State Univ., Columbus.
A HEURISTICALLY BASED NAVIGATION SYSTEM FOR AN AUTONOMOUS WALKING MACHINE WITH A RANGE SCANNER Ph.D. Thesis
Ching-Long Shih 1988 141 p
Avail: Univ. Microfilms Order No. DA8820351

A simulation study is presented of full automation of a walking machine's navigation and guidance. A navigation system, which includes the adaptive gait control-, a terrain data analysis-, and the local and global path planning-modules, is developed for an autonomous walking machine. The optimal quadruped crab gait is developed and the properties of the optimal crab gait are used for basic decision strategy in the adaptive gait controller, so that the adaptive gait can perform a nearly optimal periodic gait when the vehicle travels on level ground. The adaptive quadruped gait has a three level hierarchical structure: the body motion adaptation, the leg sequence adaptation, and the leg position adaptation. This type of hierarchical structure works well for the walking machine on the H-type terrain, and is suitable for six-legged machines too.
Dissert. Abstr.

N89-19564 California Inst. of Tech., Pasadena.
EXPERIMENTAL INVESTIGATION OF ROTOR-STATOR INTERACTION IN DIFFUSER PUMPS Ph.D. Thesis
Norbert Karl Erhard Arndt 1988 237 p
Avail: Univ. Microfilms Order No. DA8820922

The interaction between impeller blades and diffuser vanes in diffuser pumps was investigated. Steady and unsteady pressure measurements were made on the diffuser vanes and on the front shroud wall of a vaned and a vaneless diffuser. Two different impellers were used, one half of the impeller of the double suction pump of the High Pressure Oxygen Turbopump (HPOTP) of the Space Shuttle Main Engine (SSME), and a two-dimensional impeller. The measurements were made for different flow coefficients, shaft speeds, and radial gaps between the impeller blades and the diffuser vanes. For the two-dimensional impeller, also unsteady impeller blade pressure measurements were made.
Dissert. Abstr.

N89-19565 Wisconsin Univ., Madison.
DESIGN OF AN OPTICAL SENSOR SYSTEM FOR ADAPTIVE CONTROL OF A SEAM TRACKING ROBOT Ph.D. Thesis
Behnam Bahrololoumi 1988 188 p
Avail: Univ. Microfilms Order No. DA8817110

High speed and high accuracy seam tracking for increased quality and productivity is limited by factors such as backlash, link flexibility, robot dynamics variations, and servo characteristics. An even more important limitation is imposed by the unavoidable mismatch between the actual trajectory to be followed and the programmed nominal trajectory caused by manufacturing and location errors of the workpiece. Commercial computer vision and ultrasonic sensors are not only slow for fast moving robots but also expensive. Therefore, the objective consists in developing a high speed and cost effective sensor system in conjunction with an adaptive controller for accurate seam tracking. The design of the sensor system was based on the use of the image of the seam on a linear detector to extract position and orientation information about the seam. A detailed mathematical model of the sensor operation along with a sensitivity analysis was introduced. The controller proposed for seam tracking was based on the developed sensor and an adaptive joint controller designed around the pole placement principle. The feature of the controller scheme was the use of the predicted seam errors as corrections superimposed onto the nominal sensor commands. The overall system was implemented in a multiprocessor environment capable of performing the image processing, joint dynamics identification, pole-assignment, and Cartesian to joint error transformations at sampling rates of 0.0055 Second. Dissert. Abstr.

N89-19566 Cornell Univ., Ithaca, NY.
CHAOTIC DYNAMICS AND CONTROL OF NONLINEAR AND FLEXIBLE ARM ROBOTIC DEVICES Ph.D. Thesis
Mohammad Farid Golnaraghi 1988 251 p
Avail: Univ. Microfilms Order No. DA8821209

Dynamical behavior and control of high speed robotic type mechanisms is the main focus with the major emphasis on the existence of chaotic oscillations associated with stiffness, Coriolis, inertia, and centripetal nonlinearities. The work is divided into two categories. In the first part the behavior of a one degree of freedom mechanical positioning device with nonlinear stiffness, subject to linear feedback, is described. In the second part, the effects of kinematic nonlinearities such as inertia, Coriolis, and centripetal forces, on the motion of a multi-degree of freedom high speed flexible arm robot, is considered. Dissert. Abstr.

N89-19567 Louisiana State Univ., Baton Rouge.
MINIMUM TIME MOTION OF A ROBOTIC MANIPULATOR Ph.D. Thesis
Heon Hwang 1988 230 p
Avail: Univ. Microfilms Order No. DA8819949

The modeling, analysis, and trajectory control of a robotic manipulator to execute specified point to point tasks is examined. The relative coordinate representation of kinematic and dynamic variable is defined using vectors and matrices based on coordinate

transformations. Two major formulations of robot dynamic modeling, the recursive Newton-Euler and the Lagrange-Euler are reviewed utilizing the results of the kinematic analysis. An efficient general solution algorithm for generating the minimum time trajectory for a point to point task subject to the actuator torque constraints is developed. A series of parametric cubic spline segments is used to represent the continuous joint trajectory. A formulation of an n segmented cubic spline satisfying second derivative continuity at knot points is derived. A Runge-Kutta 4th order, two starting point, forward and backward numerical integration and a nonderivative multivariable minimum search are performed with a penalty function imposing the constraints on search parameters and kinematic motion parameters. Information for manipulator structure and controller design and trajectory planning for a notable increase in dynamic performance are obtained using the algorithm.
Dissert. Abstr.

N89-19568# Naval Postgraduate School, Monterey, CA.
AN EXPERIMENTAL INVESTIGATION OF SOOTING CHARACTERISTICS OF A GAS TURBINE COMBUSTOR AND AUGMENTOR TUBE M.S. Thesis
Richard H. Lindsay Sep. 1988 72 p
(AD-A201804) Avail: NTIS HC A04/MF A01 CSCL 21D

An experimental investigation was conducted to examine the effects of fuel air ratio, fuel additives, fuel composition and inlet air temperature on particle sizes in a gas turbine combustor and augmentor tube. Equipment improvements led to validation of two optical sizing techniques, three-wavelength light transmittance and three-angle forward light scattering. Generally, data obtained agreed well with results of earlier investigations. Particle size variations within the combustor due to changing variables were documented. Effects of changing variables were dependent on inlet conditions and station. Fuel-air ratio had no effect on combustor or augmentor tube exhaust particle size. GRA

N89-19569# Naval Postgraduate School, Monterey, CA.
A THREE-DIMENSIONAL NONSINGULAR SIMULATION OF RIGID MANIPULATORS M.S. Thesis
Robert M. Verbos Sep. 1988 140 p
(AD-A201964) Avail: NTIS HC A07/MF A01 CSCL 12I

Robot manipulators have been studied, using various approaches to obtain the kinematic and dynamic equations which describe their motion. Conventional body-oriented robot arm kinematic equations have the disadvantage that a singular condition occurs when two successive links of the manipulator are aligned. When this occurs, the jacobian matrix which relates the end effector motion to the joint angle variations becomes singular and is not invertible, resulting in motion that can not be simulated. This thesis extends the previous work done in the investigation of a nonsingular Newton Euler approach to forward dynamic equations interpreted in a global (inertia) fixed reference frame. Specifically, the previous results are extended into validation of the approach for three-dimensional motion, including gravitational effects. In addition, the comparison and verification of the motion of an actual robotic manipulator to the simulation is investigated. GRA

N89-19570# Massachusetts Inst. of Tech., Cambridge. Artificial Intelligence Lab.
DEXTEROUS ROBOTIC HANDS: KINEMATICS AND CONTROL M.S. Thesis
Sundar Narasimhan Nov. 1988 30 p
(Contracts N00014-86-K-0685; N00014-85-K-0124)
(AD-A202183; AD-E801798; AI-TR-1056) Avail: NTIS HC A03/MF A01 CSCL 23C

This report presents issues relating to the kinematics and control of dextrous robot hands using the Utah-MIT hand as an illustrative example. The emphasis throughout is on the actual implementation and testing of the theoretical concepts presented. The kinematics of such hands is interesting and complicated owing to the large number of degrees of freedom involved. The implementation of position and force control algorithms on such tendon driven hands has previously suffered from inefficient formulations and a lack of sophisticated computer hardware. Both problems are addressed in this report. A multiprocessor architecture has been built with high performance microcomputers on which real-time algorithms can be efficiently implemented. A large software library has also been built to facilitate flexible software development of this architecture. The position and force control algorithms described herein have been implemented and tested on this hardware.
GRA

N89-19571# Rolls-Royce Ltd., Derby (England). Transmission Research and Development Dept.
GEAR TECHNOLOGY ACQUISITION FOR ADVANCED AERO ENGINES
G. A. Halls 10 Jun. 1987 19 p Presented at the International Mechanical Engineering Meeting, 10 Jun. 1987
(PNR90510; ETN-89-93694) Copyright Avail: NTIS HC A03/MF A01

Computer controlled facilities installed to test mechanical transmission systems are described, including program logic controllers which control the sequencing and operation of the main electrically driven machinery, the integrated instrumentation system, and the environment testing facilities. The main test programs are described, including large gearbox research, and gear dynamics and lubrication rig. ESA

N89-19572# Tennessee Univ., Knoxville. Dept. of Electrical and Computer Engineering.
EXTRACTING DEPTH BY BINOCULAR STEREO IN A ROBOT VISION SYSTEM
Suresh B Marapane and Mohan M. Trivedi 1988 7 p Presented at the 10th Conference on Applications of Digital Image Processing, San Diego, CA, 1 Aug. 1988
(Contract DE-FG02-86NE-37968)
(DE89-005016; DOE/NE-37968/5; CONF-8808176-1) Avail: NTIS HC A02/MF A01

New generation of robotic systems will operate in complex, unstructured environments utilizing sophisticated sensory mechanisms. Vision and range will be two of the most important sensory modalities such a system will utilize to sense their operating environment. Measurement of depth is critical for the success of many robotic tasks such as: object recognition and location; obstacle avoidance and navigation; and object inspection. In this paper we consider the development of a binocular stereo technique for extracting depth information in a robot vision system for inspection and manipulation tasks. Ability to produce precise depth measurements over a wide range of distances and the passivity of the approach make binocular stereo techniques attractive and appropriate for range finding in a robotic environment. This paper describes work in progress towards the development of a region-based binocular stereo technique for a robot vision system designed for inspection and manipulation and presents preliminary experiments designed to evaluate performance of the approach. Results of these studies show promise for the region-based stereo matching approach. DOE

N89-19573# Allied-Signal Aerospace Co., Kansas City, MO.
ELECTRON BEAM WELDING OF 6061-T6 COVERS TO A356-T6 MACHINED CAST HOUSINGS Final Report
G. P. Miller and H. B. Pressly Mar. 1988 54 p
(Contract DE-AC04-76DP-00613)
(BDX-613-3915) Avail: NTIS HC A04/MF A01

The objectives were: to determine an acceptable weld joint design for the large output cover of a filter pack assembly, and to determine design changes necessary to implement electron beam welding to replace the manual gas tungsten arc welding process currently being used in production to weld the output cover and the input cover to the cast housing. It was determined that a 0.060 by 0.100 inch or 0.040 by 0.100 inch step could be machined on the outer perimeter of the output cover, and the output cover could be welded to the cast housing. The input cover with the butt weld joint could be welded with minimal design changes in the cast housing. Although heat input was minimized and a more cost effective process was developed, distortion of the assembly was unavoidable. Author

N89-19574# Technische Univ., Eindhoven (Netherlands).
ON THE SEALING AND LUBRICATION MECHANISM OF RADIAL LIP SEALS Ph.D. Thesis
Marcel Jos Lou Stakenborg 1988 98 p
(ETN-89-93898) Avail: NTIS HC A05/MF A01

The sealing mechanism of radial lip seals was observed using a bundle of glass fibers fixed in the seal-shaft contact area. It is found that the sealing mechanism is based on an active pumping action of the seal, counterbalenced by capillary suction forces of the oil-air interface on the air-side of the seal. Above a certain angular velocity cavitation occurs in the contact area, starting at the edges of the contact area. The friction heat generated in the contact area raises seal lip temperature. Temperature effect on contact conditions is studied, using a coupled temperature-stress finite element method analysis. A numerical model to calculate the seal-shaft contact temperature for transient and steady-state situations is presented. Using the visco-seal principle a model which describes the active pumping action of radial lip seals is derived. A model is formulated which describes leakage at higher shaft angular velocities following a breakdown of the oil-air interface on the air-side of the seal, due to centrifugal forces acting on the oil. The interaction between the visco-elastic and inertial seal lip and the lubricating fluid film is investigated. It is shown how viscous and inertial effects can lead to a phenomenon designated as visco-elastohydrodynamic lubrication. ESA

N89-19575# Technische Univ., Delft (Netherlands).
A FINITE ELEMENT DYNAMIC ANALYSIS OF FLEXIBLE SPATIAL MECHANISMS AND MANIPULATORS Ph.D. Thesis
Ben Jonker 1988 162 p
(ETN-89-93901) Avail: NTIS HC A08/MF A01

A finite-element based method for the dynamic analysis of spatial mechanisms and manipulators with flexible links is presented. Finite element types, appropriate for modeling spatial mechanisms are presented. For each element, expressions for the deformation modes as analytical functions of the element nodal coordinates are defined. The angular orientations are described in terms of four Euler parameters; in contrast to Euler angles or any set of three angular generalized coordinates, these parameters display no singular behavior of the rotational transformations. The constraint condition for the Euler parameters can easily be incorporated in the theory as it is a condition similar to the constraint condition for undeformable finite elements. The kinematic description of multi degree of freedom mechanisms based on the geometric transfer function formalism is considered. The list of derivatives of the geometric transfer functions is extended up to the third order. The associated computation scheme for the kinematic analysis is described. The choice of the degrees of freedom is discussed. ESA

N89-19576# Technische Univ., Delft (Netherlands). Faculty of Technical Mathematics and Informatics.
ELASTIC CROSS-INFLUENCE BETWEEN TWO QUASI-HERTZIAN CONTACT ZONES
J. Piotrowski and J. J. Kalker 1988 28 p
(Rept-88-45; ISSN-0920-8577; ETN-89-94013) Copyright Avail: NTIS HC A03/MF A01

A contact of two bodies which leads to the formation of two separate contact zones is considered. The contact zones considered are Hertzian ellipses if the distance between them is large. When the distance between the zones is finite, it is necessary to take into account the elastic cross-influence of the two zones. An approximate method to determine the actual contact zones as Hertz's ellipses but without disregarding the cross-influence is proposed. Numerical results are presented for two two-humped bodies pressed against each other and for steady rolling of a flanged wheel along a steel rail. It is shown that neglecting the cross influence for a flanged wheel leads to a negligible error in the contact forces but the forces are transmitted between wheel and rail through contact patches which are generally more slender than with the cross-influence neglected. ESA

N89-19577# Technische Univ., Delft (Netherlands). Faculty of Technical Mathematics and Informatics.
SOME NEW RESULTS IN ROLLING CONTACT
J. J. Kalker and J. Piotrowski 1988 30 p
(Rept-88-46; ISSN-0920-8577; ETN-89-94014) Copyright Avail: NTIS HC A03/MF A01

Three problems of simplified theory of rolling are investigated. Two benchmark loadings for Hertzian rolling contact are added to the three already in existence. Each of these loadings gives a value of the flexibility parameter. The mean of these values is taken as the most probable value, an estimate of the error is found, and an empirical formula for the mean flexibility is given. The law of Colomb is generalized by introducing two values of the coefficient of friction. The Fastsim algorithm is adapted and it is found that the singularity in the traction and hence the displacement is removed by introducing damping in the simplified theory constitutive relations. The damping constant is determined experimentally but it appears that the simplified theory for two-constant friction does not compare well with the complete theory as implemented by the program Contact. It is shown that inertial effects may be neglected at speeds of around 30 m/s and also for much higher rolling velocities. ESA

N89-20072*# Michigan Technological Univ., Houghton. Dept. of Mechanical Engineering.
MODEL EVALUATION, RECOMMENDATION AND PRIORITIZING OF FUTURE WORK FOR THE MANIPULATOR EMULATOR TESTBED Final Report
Frederick A. Kelly *In* NASA, Lyndon B. Johnson Space Center, National Aeronautics and Space Administration (NASA)/American Society for Engineering Education (ASEE) Summer Faculty Fellowship Program 1988, Volume 1 Feb. 1989 10 p (For primary document see N89-20058 12-99)
Avail: NTIS HC A09/MF A01 CSCL 13I

N89-20082*# East Texas State Univ., Commerce. Dept. of Computer Science.
VISUAL PERCEPTION AND GRASPING FOR THE EXTRAVEHICULAR ACTIVITY ROBOT Final Report
Scott A. Starks *In* NASA, Lyndon B. Johnson Space Center, National Aeronautics and Space Administration (NASA)/American Society for Engineering Education (ASEE) Summer Faculty Fellowship Program 1988, Volume 2 Feb. 1989 14 p (For primary document see N89-20073 12-99)
Avail: NTIS HC A09/MF A01 CSCL 13I

38 QUALITY ASSURANCE AND RELIABILITY

Includes product sampling procedures and techniques; and quality control.

N89-19578*# National Aeronautics and Space Administration. Lewis Research Center, Cleveland, OH.
INTERFACING LABORATORY INSTRUMENTS TO MULTIUSER, VIRTUAL MEMORY COMPUTERS
Edward R. Generazio, David B. Stang (Sverdrup Technology, Inc., Cleveland, OH.), and Don J. Roth Washington Mar. 1989 29 p
(NASA-TM-4106; E-4510; NAS 1.15:4106) Avail: NTIS HC A03/MF A01 CSCL 14D

Incentives, problems and solutions associated with interfacing laboratory equipment with multiuser, virtual memory computers are presented. The major difficulty concerns how to utilize these computers effectively in a medium sized research group. This entails optimization of hardware interconnections and software to facilitate multiple instrument control, data acquisition and processing. The architecture of the system that was devised, and associated programming and subroutines are described. An example program involving computer controlled hardware for ultrasonic scan imaging is provided to illustrate the operational features. Author

39 STRUCTURAL MECHANICS

Includes structural element design and weight analysis; fatigue; and thermal stress.

For applications see *05 Aircraft Design, Testing and Performance* and *18 Spacecraft Design, Testing and Performance.*

N89-19579*# National Aeronautics and Space Administration, Washington, DC.
MIXED FINITE ELEMENT MODELS FOR FREE VIBRATIONS OF THIN-WALLED BEAMS
Ahmed K. Noor, Jeanne M. Peters, and Byung-Jin Min Feb. 1989 28 p Prepared in cooperation with Joint Inst. for Advancement of Flight Sciences, Hampton, VA
(NASA-TP-2868; L-16506; NAS 1.60:2868) Avail: NTIS HC A03/MF A01 CSCL 20K

Simple, mixed finite element models are developed for the free vibration analysis of curved thin-walled beams with arbitrary open cross section. The analytical formulation is based on a Vlasov's type thin-walled beam theory with the effects of flexural-torsional coupling, transverse shear deformation and rotary inertia included. The fundamental unknowns consist of seven internal forces and seven generalized displacements of the beam. The element characteristic arrays are obtained by using a perturbed Lagrangian-mixed variational principle. Only C(sup o) continuity is required for the generalized displacements. The internal forces and the Lagrange multiplier are allowed to be discontinuous at interelement boundaries. Numerical results are presented to demonstrate the high accuracy and effectiveness of the elements developed. The standard of comparison is taken to be the solutions obtained by using 2-D plate/shell models for the beams. Author

N89-19580*# National Aeronautics and Space Administration. Langley Research Center, Hampton, VA.
MIXED FORMULATION FOR FRICTIONLESS CONTACT PROBLEMS
Ahmed K. Noor and Kyun O. Kim [1989] 26 p Prepared in cooperation with George Washington Univ., Hampton, VA and Joint Inst. for Advancement of Flight Sciences, Hampton, VA
(NASA-TP-2897; L-16513; NAS 1.60:2897) Avail: NTIS HC A03/MF A01 CSCL 20K

Simple mixed finite element models and a computational precedure are presented for the solution of frictionless contact problems. The analytical formulation is based on a form of Reissner's large rotation theory of the structure with the effects of transverse shear deformation included. The contact conditions are incorporated into the formulation by using a perturbed Lagrangian approach with the fundamental unknowns consisting of the internal forces (stress resultants), the generalized displacements, and the Lagrange multipliers associated with the contact conditions. The element characteristic array are obtained by using a modified form of the two-field Hellinger-Reissner mixed variational principle. The internal forces and the Lagrange multipliers are allowed to be discontinuous at interelement boundaries. The Newton-Raphson iterative scheme is used for the solution of the nonlinear algebraic equations, and the determination of the contact area and the contact pressures.
Author

N89-19581*# Texas Univ., San Antonio. Div. of Engineering.
FATIGUE CRACK GROWTH MODEL RANDOM2 USER MANUAL. APPENDIX 1: DEVELOPMENT OF ADVANCED METHODOLOGIES FOR PROBABILISTIC CONSTITUTIVE RELATIONSHIPS OF MATERIAL STRENGTH MODELS Annual Report
Lola Boyce and Thomas B. Lovelace Jan. 1989 37 p
(Grant NAG3-867)
(NASA-CR-184775-App-1; NAS 1.26:184775-App-1) Avail: NTIS HC A03/MF A01 CSCL 20K

FORTRAN program RANDOM2 is presented in the form of a user's manual. RANDOM2 is based on fracture mechanics using a probabilistic fatigue crack growth model. It predicts the random lifetime of an engine component to reach a given crack size. Details of the theoretical background, input data instructions, and a sample problem illustrating the use of the program are included.
NASA

N89-19582*# Texas Univ., San Antonio. Div. of Engineering.
FATIGUE STRENGTH REDUCTION MODEL: RANDOM3 AND RANDOM4 USER MANUAL. APPENDIX 2: DEVELOPMENT OF ADVANCED METHODOLOGIES FOR PROBABILISTIC CONSTITUTIVE RELATIONSHIPS OF MATERIAL STRENGTH MODELS Annual Report
Lola Boyce and Thomas B. Lovelace Jan. 1989 80 p
(Grant NAG3-867)
(NASA-CR-184796-App-2; NAS 1.26:184796-App-2) Avail: NTIS HC A05/MF A01 CSCL 20K

FORTRAN programs RANDOM3 and RANDOM4 are documented in the form of a user's manual. Both programs are based on fatigue strength reduction, using a probabilistic constitutive model. The programs predict the random lifetime of an engine component to reach a given fatigue strength. The theoretical backgrounds, input data instructions, and sample problems illustrating the use of the programs are included.
NASA

N89-19583*# Aerostructures, Inc., Arlington, VA.
NASTRAN SUPPLEMENTAL DOCUMENTATION FOR MODAL FORCED VIBRATION ANALYSIS OF AERODYNAMICALLY EXCITED TURBOSYSTEMS Final Report
V. Elchuri and P. R. Pamidi (RPK Corp., Columbia, MD.) Jul. 1985 133 p
(Contract NAS3-24387)
(NASA-CR-174967; NAS 1.26:174967) Avail: NTIS HC A07/MF A01 CSCL 20K

This report is a supplemental NASTRAN document for a new capability to determine the vibratory response of turbosystems subjected to aerodynamic excitation. Supplements of NASTRAN Theoretical, User's, Programmer's, and Demonstration Manuals are included. Turbosystems such as advanced turbopropellers with highly swept blades, and axial-flow compressors and turbines can be analyzed using this capability, which has been developed and implemented in the April 1984 release of the general purpose finite element program NASTRAN. The dynamic response problem is addressed in terms of the normal modal coordinates of these tuned rotating cyclic structures. Both rigid and flexible hubs/disks are considered. Coriolis and centripetal accelerations, as well as differential stiffness effects are included. Generally nonuniform steady inflow fields and uniform flow fields arbitrarily inclined at small angles with respect to the axis of rotation of the turbosystem are considered as the sources of aerodynamic excitation. The spatial nonuniformities are considered to be small deviations from a principally uniform inflow. Subsonic relative inflows are addressed, with provision for linearly interpolating transonic airloads. Author

N89-19584# Virginia Polytechnic Inst. and State Univ., Blacksburg. Dept. of Engineering Science and Mechanics.
BOUNDARY LAYER AND SINGULARITY MEASUREMENT IN THREE DIMENSIONAL FRACTURE PROBLEMS Final Report, 31 Jul. 1987 - 31 Aug. 1988
D. Post, C. W. Smith, and R. Czarnek Oct. 1988 39 p
(Contract F04611-87-C-0057)
(AD-A201277; VPI-ESM-352-277-1; AFAL-TR-88-086) Avail: NTIS HC A03/MF A01 CSCL 21I

Experimental methods (coarse grid and high density moire interferometry) were used to measure near tip surface displacement during the opening and growth of cracks in biaxial specimens of inert propellant and pure binder in tests conducted at two different head rates (2.5 and 25.4 mm/min). Displacement data were collected from coarse grids at regular time intervals. An intense strain zone developed ahead of the crack tip in both materials. However, the size of the zone in the inert propellant was at least an order of magnitude larger than in the pure binder, shifting the high strain contours ahead of the crack tip. From such data, an idealized model for the intense strain zone in the inert propellant was postulated. Values of the dominant eigenvalue near the crack

tip were computed from appropriate algorithms where the crack intersected the free surface. Frozen stress photoelastic analysis of four point bend tests were used to infer the distribution of the dominant eigenvalue through the specimen thickness for both straight front and thumbnailed cracks. Results compared favorably with an analytical result obtained by Benthem. Results indicate an absence of transverse constraint in the intense strain zone of the inert propellant which suggests the absence of a strong thickness effect upon the threshold value of the stress intensity factor. GRA

N89-19585# Carnegie-Mellon Inst. of Research, Pittsburgh, PA. Dept. of Mechanical Engineering.
FUNDAMENTALS OF FATIGUE AND FRACTURE MECHANICS Final Report, 15 Feb. 1986 - 14 Aug. 1988
G. B. Sinclair Oct. 1988 37 p
(Grant AF-AFOSR-0113-86; AF Proj. 2302)
(AD-A201435; AFOSR-88-1294TR) Avail: NTIS HC A03/MF A01 CSCL 20K

The basic tenet of LEFM is that the stress intensity factor, K, is the key controlling parameter for fatigue crack growth and fast brittle fracture under monotonic loading. This research program examined whether or not this fundamental assumption formed an effective basis for an engineering technology. And, as needed, suggested directions for an improved technology. GRA

N89-19586# Army Armament Research, Development and Engineering Center, Watervliet, NY.
DETERMINATION OF RESIDUAL STRESS DISTRIBUTIONS IN AUTOFRETTAGED TUBING: A DISCUSSION Final Report
Boaz Avitzur Aug. 1988 24 p
(AD-A201454; ARCCB-MR-88034) Avail: NTIS HC A03/MF A01 CSCL 11F

There is a long-standing interest in developing a capability to predict the distribution of residual stresses in thick-wall tubes after internal pressurization--autofrettage. Since autofrettage involves partial or full plastic deformation of the tube, any computation of stress under pressure and, hence of the post-pressurization residual stresses, depends upon the assumed yield criterion. The latter may or may not include the material's strain hardening and/or strain softening capabilities. The most commonly used criteria are those named after Tresca and Mises. In the absence of exact solutions for plastic deformations, simplifying assumptions concerning the material's behavior are being made for the development of workable solutions, sometimes with the knowledge that certain physical principles are being violated. Many suggested solutions to the problem of autofrettage assume that Tresca's yield criterion prevails. Recent attempts to treat a modified Tresca's yield criterion as Mises' yield criterion and/or attempts to add strain-softening (Bauschinger effect) to Tresca's yield criterion are questioned. GRA

N89-19587# Northwestern Univ., Evanston, IL. Dept. of Civil Engineering.
SLIDING AND DEBONDING INCLUSIONS Final Report, 1 Jun. 1985 - 30 Jun. 1988
T. Mura 15 Aug. 1988 7 p
(Contract DAAG29-85-K-0134)
(AD-A201609; ARO-21817.23-EG) Avail: NTIS HC A02/MF A01 CSCL 11D

It was found by Mura and Furuhashi, J. App. Mech. 51 (1984) 308-310, when an ellipsoidal inclusion undergoes a uniform shear eigenstrain in the principal axis directions and the inclusion is free to slip along the interface, the stress field vanishes everywhere in the inclusion and the matrix. The main objective of the present grant DAAG29-85-K-0134 is to give more theoretical investigation on this amazing finding and to find applications to composite materials. This anomaly of sliding inclusions is based upon the fact that an ellipsoid is transformed into an identical ellipsoid by the uniform shear in the principle axis directions of the ellipsoid in the framework of linear theory as demonstrated by Mura. When the ellipsoidal inhomogeneity embedded in an infinite medium is subjected to an applied shear stress at infinity in the directions of the principle axes of the ellipsoid, the inhomogeneity behaves like a void if the interface can slide freely. GRA

N89-19588# Naval Postgraduate School, Monterey, CA.
THE MODELING OF VISCOELASTIC CIRCULAR PLATES FOR USE AS WAVEGUIDE ABSORBERS M.S. Thesis
Charles D. Hettema Sep. 1988 211 p
(AD-A201621) Avail: NTIS HC A10/MF A01 CSCL 20K

The need exists to reduce structural vibrations in plates, such as ship's hulls. It was proposed to use waveguide absorbers as a means to reduce structural vibrations. A waveguide absorber is a device which is made from damping material but mounted to the structure at a point rather than the full surface. A waveguide absorber removes and then dissipates vibrational energy from the structure through traveling waves. The performance of a waveguide absorber is determined from the driving point impedance, the ratio of force to velocity at the attachment point. This study has determined the theoretical driving point impedance for viscoelastic circular plates. The constitutive relations for viscoelastic material were evaluated and it was proven that a complex Young's modulus and shear modulus can be used to represent the viscoelastic material. Mindlin's theory for elastic isotropic plates, with complex moduli, was used to solve for the driving point impedance. The solutions are in terms of Bessel functions. Poisson's boundary conditions were used at the free edge of the circular plate, and clamped boundary conditions were used at the attachment point, which is at the center of the plate. A non-numeric language, REDUCE, was used to solve for the driving point impedance given the appropriate equations of motion and boundary conditions. GRA

N89-19589*# National Aeronautics and Space Administration. Langley Research Center, Hampton, VA.
EFFECT OF ADHESIVE INTERLEAVING AND DISCONTINUOUS PLIES ON FAILURE OF COMPOSITE LAMINATES SUBJECT TO TRANSVERSE NORMAL LOADS
Dawn C. Jegley Jan. 1989 28 p
(NASA-TM-101507; NAS 1.15:101507) Avail: NTIS HC A03/MF A01 CSCL 20K

Results of a series of tests to determine the effects of adhesive interleaving and discontinuous plies (plies with end-to-end gaps) on the displacements, failure loads and failure modes of graphite-epoxy laminates subjected to transverse normal loads are presented. Adhesive interleaving can be used to contain local damage within a group of plies, i.e., to arrest crack propagation on the interlaminate level, and it can increase the amount of normal displacement the laminate can withstand before failure. However, the addition of adhesive interleaving to a laminate does not significantly increase its load carrying capability. A few discontinuous plies in a laminate can reduce the normal displacement and load at failure by 10 to 40 percent compared to a laminate with no discontinuous plies, but the presence of the ply discontinuities does not generally change the failure location or the failure mode of the laminate. Author

N89-19590 Ohio State Univ., Columbus.
A DYNAMIC, TIME STEPPING BOUNDARY ELEMENT METHOD FOR FRICTIONAL CRACK AND INTERFACE PROBLEMS Ph.D. Thesis
Jia-maw Doong 1988 172 p
Avail: Univ. Microfilms Order No. DA8820286

Frictional interface problems have received a lot of attention due to their importance in, e.g., fracture mechanics, non-destructive evaluation (NDE) and soil-structure interaction. Due to the advantages of reduction of dimensionality and handling of full-plane and half-plane problems conveniently, the boundary element method (BEM) is used to solve some frictional interface and crack problems in this study. An incremental, iterative, time-domain 2-D BEM formulation is presented to treat the transient, non-linear anti-plane (SH) wave motions of two arbitrary rough frictional bodies, which may slide relative to each other, governed by Coulomb's law of sliding friction. Numerical examples of

time-harmonic and transient SH wave motions are presented for the interaction of: (1) cylindrical and plane waves with a rough interface between dissimilar elastic half-planes; (2) plane waves with a closed edge-crack with rough faces at the free-surface of a homogeneous half-plane; (3) cylindrical waves with an infinite long layer resting on a dissimilar half-plane; (4) cylindrical waves with a semi-infinite layer partially embedded in a dissimilar half-plane; and (5) cylindrical waves with a finite block partially embedded in a dissimilar half-plane. Comparisons are made whenever possible to available analytical solutions of several special cases of these problems. While no numerical examples were carried out, the formulation for the 2-D in-plane problem is also presented. This includes the possibility of multiple separation, stick and slip zones on the interface. The implementation of this formulation is recommended for further research. Dissert. Abstr.

N89-19591 California Inst. of Tech., Pasadena.
PLASTIC BUCKLING OF CYLINDERS UNDER BIAXIAL LOADING Ph.D. Thesis
Jurgen Johannes Giezen 1988 232 p
Avail: Univ. Microfilms Order No. DA8820947

An experimental investigation is carried out to study the effects of nonproportional loading in the plastic range on the buckling load. The discrepancy between experimental and theoretical results points to some principal shortcoming in the analysis. The problem was simplified by applying axial tensile load and external pressure to a simple cylindrical shell specimen and observing the buckling load for various nonproportional load-paths. Results are compared to numerical predictions (BOSOR5), using classical type plasticity models such as J(2) deformation and J(2) incremental theory. Significant discrepancy was found and attributed to inadequate modeling of the nonlinear material behavior. The effects of geometrical imperfections and large deflections were found to be insignificant, thereby leading to an idea how much of the discrepancy between test and theory is due to the use of an inadequate plastic model. The introduction of the Southwell plot into the plastic shell buckling problem reduced the already minor effects of geometric imperfections. The Christoffersen-Hutchinson corner theory model was introduced into BOSOR5 in its simplest form as presented by Poh-Sang Lam. Results obtained with this model, which allows corners to form on an initially smooth yield surface, displayed better agreement with experimental data. However, increased computational time and problems related to abrupt changes in load-path at the corner are a major concern at the present time. Dissert. Abstr.

N89-19592 Loughborough Univ. of Technology (England).
HIGH STRAIN-RATE BEHAVIOUR OF POLYMERS USING BLAST-WAVE AND IMPACT-LOADING METHODS Ph.D. Thesis
Sahrim Haji Ahmad 1988 377 p
Avail: Univ. Microfilms Order No. BRD-82828

There are a limited number of methods for quantitative investigation of the mechanical properties of materials at high rates of loading. A method of loading called the exploding wire technique was examined. The initial experimental work was concerned with the production of cylindrical blast waves in air at atmospheric pressure, these waves resulting from exploding copper wires. The wires are almost instantaneously vaporized by the rapid discharge of up to 8kJ of stores energy from 13.2 microF capacitor charged at up to 35kV. The blast waves were studied using an optical method called the Schlieren technique in conjunction with a high speed image converter camera. In order to determine the mechanical properties of the hollow cylindrical specimens it is necessary to measure the loading blast-wave pressure profile and the consequent hoop strain at the outer surface. The outer surface hoop strain was determined by a new technique using high-elongation foil strain gauges energized by a short-duration, high current pulse. The experimental recordings of hoop strain for thick cylinders as a function of time for several polymers were compared with corresponding computer predictions based on elastic wave theory. Two other experimental methods, the Split-Hopkinson pressure bar technique and Instron machine testing, were also employed in order to measure the mechanical properties of the polymers at high and low strain rates. These measurements were then compared with the blast wave results. Dissert. Abstr.

N89-19593# Cork Geotechnics Ltd., Castlemartyr (Ireland).
NONLINEAR DYNAMIC ANALYSIS OF EMBEDDED STRUCTURES Final Report, Jun. 1986 - Aug. 1987
W. D. Finn 7 Mar. 1988 87 p
(Contract DAJA45-86-C-0033; DA Proj. 1L1-61102-BH-57)
(AD-A201728; R/D-5491-EN-01-F) Avail: NTIS HC A05/MF A01 CSCL 13B

A computer program, TARA-3, developed for conducting nonlinear hysteretic dynamic response analysis is presented. The program can operate in either a total or effective stress mode. It may be used to analyse the seismic response of earth structures and soil-structures interaction systems such as nuclear containment structures. Validation studies of TARA-3 using data from seismic tests on centrifuged models are described. These studies confirm the capability of TARA-3 to predict accelerations, porewater pressures, and displacements in complex soil-structures systems during seismic loading with acceptable accuracy and reliability for engineering design. GRA

N89-19594# Naval Postgraduate School, Monterey, CA.
MACHINERY DIAGNOSTICS VIA MECHANICAL VIBRATION ANALYSIS USING SPECTRAL ANALYSIS TECHNIQUES M.S. Thesis
James A. Stamm Sep. 1988 100 p
(AD-A202089) Avail: NTIS HC A05/MF A01 CSCL 14B

Mechanical vibration analysis affords a reliable means to selectively identify specific machinery faults. As such, it plays a key role in diagnostic work on individual units and in progressive maintenance monitoring programs where substantial diagnostic and prognostic capabilities are considered essential. A physical machinery diagnostics model was developed that was designed to incorporate some of the more common machinery faults found in rotating machinery relating to shaft, bearing, gear, and alignment defects. The results of spectral analysis techniques used to detect these simulated faults are displayed and discussed, with special emphasis on gear train diagnostics. Also included are a description of one of the current U.S. Navy machinery vibration monitoring programs, and an initial study regarding a proposed technique for providing a graphic display of gear faults. GRA

N89-19595# Naval Postgraduate School, Monterey, CA.
PASSIVE VIBRATION CONTROL USING VISCOELASTIC AND CONSTRAINED LAYER BEAM WAVEGUIDE ABSORBERS M.S. Thesis
Charles T. Horne, III Sep. 1988 100 p
(AD-A202188) Avail: NTIS HC A05/MF A01 CSCL 13M

Reduction of noise and vibrations within structural systems has been a long standing problem. Recent studies have indicated that waveguide absorbers have been effective in the reduction of noise and vibrations over a broad frequency range. A waveguide absorber is a structure along which vibrational waves can travel. If the waveguide absorber is treated with an energy dissipation scheme, the amplitudes of the waves will decrease as they travel along the waveguide absorber. The test structure consisted of a rectangular aluminum plate with clamped boundary conditions. A finite element analysis approach theoretically predicted the test structure's mode shapes and modal strain energies. An experimental modal survey was conducted to compare with the theoretically predicted mode shapes and natural frequencies. The mode shapes and modal strain energies determined the optimum locations of the waveguide absorbers and their orientation on the test structure. The frequency range of interest and mode shapes determined the required number of waveguide absorbers. Experiments were conducted using viscoelastic and constrained layer beam waveguide absorbers over a 2000 Hertz frequency range. Significant reduction of the test structure's frequency response was demonstrated through the effective use of multiple beam waveguide absorbers. GRA

N89-19596# Texas A&M Univ., College Station. Dept. of Aerospace Engineering.
CONTROL OF FLEXIBLE STRUCTURES: MODEL ERRORS, ROBUSTNESS MEASURES, AND OPTIMIZATION OF FEEDBACK CONTROLLERS Final Report, 1 Jun. 1986 - 31 Aug. 1988
John L. Junkins and S. R. Vadali 31 Oct. 1988 300 p
(Contract F49620-86-K-0014)
(AD-A202234; AFOSR-88-1252TR) Avail: NTIS HC A13/MF A01 CSCL 22B

This report summarizes new methods for flexible structures' dynamic analysis, system identification, and maneuver controls. New control design methods are introduced for considering several competing performance measures simultaneously. A new attitude control method using single gimbal control moment gyros is introduced. New results and insights on singularity avoidance are presented. A method is given for simultaneous optimization of structural design parameters and feedback controller. GRA

N89-19597# General Dynamics Corp., Fort Worth, TX. Fort Worth Div.
ADVANCED DURABILITY ANALYSIS. VOLUME 4: EXECUTIVE SUMMARY Final Technical Report, Oct. 1984 - Sep. 1987
S. D. Manning and J. N. Yang 31 Jul. 1988 63 p Prepared in cooperation with United Analysis, Inc., Vienna, VA
(Contract F33615-84-C-3208)
(AD-A202304; AFWAL-TR-86-3017-Vol-4) Avail: NTIS HC A04/MF A01 CSCL 11F

This report is volume 4 of a 5-volume final report on the work conducted under AF contract F33615-84-C-3208. The objectives of this program were to: (1) recommend improvements to the current Air Force durability design requirements (i.e., MIL-A-8866B and MIL-A-87221), (2) develop a probabilistic durability analysis method capable of predicting the durability of advanced metallic aircraft structure for functional impairment such as excessive cracking, fuel leakage and ligament breakage, and (3) update the current Air Force Durability Design Handbook (AFWAL-TR-83-3027). Fatigue cracking is the form of degradation considered. This three-phase program consisted of eight tasks. Advanced durability analysis methods were developed and refined under Phase 1. Fatigue test results and fractographic data were acquired and evaluated under Phase 2. Phase 3 was concerned with durability, fatigue, equivalent initial flaw size (EIFS), initial fatigue quality (IFQ), time-to-crack initiation (TICI), deterministic and stochastic crack growth. GRA

N89-19598# California Univ., Los Angeles. Dept. of Civil Engineering.
RECIPROCAL THEOREM OF RESIDUAL STRESS AND INELASTIC STRAIN
T. H. Lin, S. R. Lin, X. Q. Wu, and Q. Y. Chen 1988 13 p Prepared in cooperation with Aerospace Corp., El Segundo, CA
(Contract N00014-86-K-0153)
(AD-A202353; UCLA-ENG-88-09) Avail: NTIS HC A03/MF A01 CSCL 20K

We consider a body to have an initial stress field. When the body is loaded beyond the elastic range, a plastic strain occurs in some part of the body. If the body is then unloaded, the plastic strain remains and causes a residual stress field. Now consider the load applied again. This applied load causes stress. There is no increase of plastic strain during this process of unloading and reloading. Plastic strain is one type on inelastic strain. Hence the reciprocal relation of inelastic strain and residual stress is very useful in numerical inelastic analyses. GRA

N89-19599*# Virginia Polytechnic Inst. and State Univ., Blacksburg. Dept. of Aerospace and Ocean Engineering.
COMPRESSION STRENGTH OF COMPOSITE PRIMARY STRUCTURAL COMPONENTS Semiannual Status Report, 1 May - 31 Oct. 1988
Eric R. Johnson 1988 16 p
(Grant NAG1-537)
(NASA-CR-184893; NAS 1.26:184893) Avail: NTIS HC A03/MF A01 CSCL 20K

The geometrically nonlinear response and failure of thin-walled structural components made from advanced composite materials is discussed. The materials involved are structural components in flight vehicle structures that are laminated from graphite-epoxy unidirectional tape. The investigation involves the buckling, postbuckling, and failure of structures subject to axial compression. The structural analysis was performed using the Structural Analysis of General Shells (STAGS) computer code. Experimental and theoretical methods are used to study the fundamental mechanisms limiting the load-carrying capacity of these components. NASA

N89-19600# Centro Informazioni Studi Esperienze, Milan (Italy).
ACOUSTIC EMISSION MEASUREMENTS DURING FATIGUE LOADING OF SCALED PRESSURIZED WATER REACTOR (PWR) VESSEL AT JOINT RESEARCH CENTER OF THE EUROPEAN COMMUNITIES (JRC), ISPRA (ITALY)
A. C. Lucia, A. Sala, and C. Scruby (United Kingdom Atomic Energy Authority, Harwell, England) 1987 21 p Presented at the SMIRT-9 Pre-Conference Seminar No. 15 on Acoustic Emission, Stuttgart, Germany, F.R., Aug. 12-13, 1987
(CISE-4476; ETN-89-93713) Avail: NTIS HC A03/MF A01

Fatigue tests on 1/5 scale models of PWR primary vessel are summarized. Acoustic emission (AE) measurements were made during hydrotests and fatigue cycling: continuously by JRC and CISE, periodically by UKAEA. Significant sources were detected and correctly located, also through the thickness. The fatigue propagation of a microdefect near the cladding (which gave clear signals during the first hydrotest) was clearly detected only during the last 30,000 cycles preceding the leak. The analysis of AE events clearly distinguishes friction/fretting noises from primary crack advance events, which, however, were too few or of too low energy to allow a completely satisfactory monitoring of crack propagation. ESA

N89-19601# Centro Informazioni Studi Esperienze, Milan (Italy).
GENERAL REVIEW OF RECENT ACTIVITIES IN ACOUSTIC EMISSION TECHNOLOGY IN ITALY
A. C. Lucia (Joint Research Centre of the European Communities, Ispra, Italy) and F. Tonolini 1987 18 p Presented at the SMIRT-9 Pre-Conference Seminar No. 15 on Acoustic Emission, Stuttgart, Germany, F.R., 12-13 Aug. 1987
(CISE-4477; ETN-89-93714) Avail: NTIS HC A03/MF A01

Instrumentation development for acoustic emission studies; pressure vessel examination during hydrotest; fatigue tests on experimental structures; leak monitoring; loose part monitoring; materials characterization; and standards and procedures are summarized. ESA

N89-19602# Technische Univ., Delft (Netherlands).
FATIGUE CRACK GROWTH IN ARALL: A HYBRID ALUMINUM ARAMID COMPOSITE MATERIAL. CRACK GROWTH MECHANISMS AND QUANTITATIVE PREDICTIONS OF THE CRACK GROWTH RATES Ph.D. Thesis
Roelof Marissen 1988 351 p
(ETN-89-93899) Avail: NTIS HC A15/MF A01

The fatigue crack growth behavior of small and large cracks in ARALL was investigated under constant amplitude and flight simulation loading. Static properties, delamination in the fiber-adhesive layer under cyclic loads, and shear deformations in the fiber-adhesive layer under static and cyclic loads were tested to provide material data for a model for the prediction of fatigue crack growth in ARALL. The thickness of the aluminum sheet layers and the fiber-adhesive layers; different types of adhesives and fibers; and residual stress systems introduced by prestraining or prestressing were examined. The excellent crack growth resistance of ARALL under constant-amplitude and variable-amplitude loading is confirmed. The resistance is considerably enhanced by a favorable residual stress system, i.e., compressive stress in the aluminum alloy layers and tensile stress in the aramid fibers. Thinner individual layers also lead to better properties. The favorable residual stress system is very effective

under constant-amplitude loading at low R-ratios. At high R-ratios the effect is less pronounced. Truncation of the TWIST load spectrum has a significant effect on fatigue crack growth in ARALL. A high truncation level considerably reduces crack growth rate. Initiation of small cracks in side notched specimens occurs relatively early in the fatigue life. The delamination growth rate observed in delamination tests, and crack opening displacements due to adhesive shear deformation, are directly dependent on the load transfer from the fibers to the aluminum alloy layers. ESA

N89-19603# Technische Univ., Delft (Netherlands). Faculty of Technical Mathematics and Informatics.
THE ELASTIC STRESS AND THE DISPLACEMENT ON THE SURFACES OF TWO RUBBER-CLAD STEEL CYLINDERS BETWEEN WHICH PAPER IS LED
J. J. Kalker 1988 27 p
(Rept-88-23; ISSN-0920-8577; ETN-89-94006) Copyright Avail: NTIS HC A03/MF A01

A method to determine the contact tractions and the surface displacements of two rubber-clad cylinders pressed together and rolling over each other is given. One of the layers may be absent, and paper may or may not be present between the cylinders. The conditions for contact formation between the bodies are discussed. An algorithm for determining the normally directed traction and the surface displacement at a given tangential traction is presented. The conditions for frictional behavior according to Coulomb-d'Amontons' law of dry friction are discussed. An algorithm for determining the tangentially directed traction and the surface displacement at a given normal traction is derived. The algorithms utilize influence numbers; these are the surface displacement components in a point x due to a traction element with centroid y. The method is implemented in the FORTRAN-77 program LAAGROL, which calculates a discretization of 30 points as well as a number of contact problems in 30 sec. ESA

N89-19604# Lawrence Livermore National Lab., CA.
ACOUSTOELASTICITY USING LONGITUDINAL WAVES FOR RESIDUAL STRESS EVALUATION
J. J. Dike, G. C. Johnson (California Univ., Berkeley.), and E. C. Flower 1988 8 p Presented at the Review of Progress in Quantitative Nondestructive Evaluation, La Jolla, CA, 31 Jul. - 5 Aug. 1988 Submitted for publication
(Contract W-7405-eng-48)
(DE89-006154; UCRL-100040; CONF-880760-10) Avail: NTIS HC A02/MF A01

Residual stresses play an important role in the behavior of structures during machining and under load. Knowledge of these residual stress states allows better and more efficient use of the structures, as well as more accurate predictions of their behavior. In this paper, a new method for nondestructively evaluating complete states of plane residual stress is presented. The basic analytical and experimental procedures are reviewed, and results of estimated residual stresses are compared with numerical predictions. Several methods are available for determining residual stresses. Nondestructive techniques include X-ray and neutron diffraction studies that measure residual strains through determination of crystal lattice spacing. Here we examine the application of a nondestructive technique called acoustoelasticity which employs ultrasonic waves in the evaluation of residual stress states. DOE

42 GEOSCIENCES (GENERAL)

N89-19605 Deutscher Wetterdienst, Offenbach am Main (Germany, F.R.).
ANNALS FROM THE GERMAN METEOROLOGICAL SOCIETY. NO. 25: 10TH INTERNATIONAL CLOUD PHYSICS CONFERENCE PREPRINTS, VOLUME 1
1988 395 p Conference held in Bad Homburg, Fed. Republic of Germany, 15-20 Aug. 1988
(ISBN-3-88-148240-7; ISSN-0072-4122; ETN-89-93655)
Copyright Avail: Deutscher Wetterdienst, Frankfurter Strasse 135, D-6050 Offenbach am Main, Fed. Republic of Germany

Cloud microphysics laboratory studies, field measurements, and theory; entrainment and mixing; clouds and radiation; cloud chemistry; acidic precipitation measurements and numerical modeling; instrumentation; orographic clouds; and cloud macrophysics were discussed. For individual titles, see N89-19606 through N89-19728.

N89-19606 Illinois State Water Survey, Champaign. Climate and Meteorology Section.
THE EFFECT OF CHARGE ON COALESCENCE OF SMALL PRECIPITATION DROPS AT TERMINAL VELOCITY **c47**
Harry T. Ochs, III, Robert R. Czys, and James Q. Feng *In* Deutscher Wetterdienst, Annals from the German Meteorological Society, No. 25: 10th International Cloud Physics Conference Preprints, Volume 1 1988 p 4-6 (For primary document see N89-19605 12-42)
(Grants NSF ATM-83-14072; NSF ATM-86-01549)
Copyright Avail: Deutscher Wetterdienst, Frankfurter Strasse 135, D-6050 Offenbach am Main, Fed. Republic of Germany

The effect of electric charge on water drops typical of drizzle drops or small precipitation drops was simulated. A computer controlled apparatus was used to produce drops which collided at terminal velocity. Results show that the charge required to induce complete coalescence differs from previous results for drop streams and suspended drops by an order of magnitude. A unique impact angle dividing the coalescence from the noncoalescence region that is independent of charge; a two order of magnitude range of relative charge between drop bounce and complete charge-induced coalescence; a wide range of charge where a satellite drop occurs with temporary coalescence; and, at higher charge levels, the beginning of charge induced permanent coalescence at the most grazing collisions are noted. ESA

N89-19607 Illinois State Water Survey, Champaign. Climate and Meteorology Section.
WAKE-EXCITED RAINDROP OSCILLATIONS **c47**
Kenneth V. Beard and Harry T. Ochs, III *In* Deutscher Wetterdienst, Annals from the German Meteorological Society, No. 25: 10th International Cloud Physics Conference Preprints, Volume 1 1988 p 7-8 (For primary document see N89-19605 12-42)
(Grants NSF ATM-84-19490; NSF ATM-86-01549)
Copyright Avail: Deutscher Wetterdienst, Frankfurter Strasse 135, D-6050 Offenbach am Main, Fed. Republic of Germany

The effect of wake forcing on raindrop shape under freefall conditions was studied. The apparatus minimized the lateral drift problem by generating drops at terminal veocity in still air. Wake excited oscillations were investigated over relatively short distances. Results confirm the hypothesis that small raindrops oscillate because of resonant interaction with eddy shedding, but for larger sizes, and possibly higher harmonics, than proposed by Gunn (1949). ESA

N89-19608 Hokkaido Univ., Sapporo (Japan). Inst. of Low Temperature Science.
TEMPORAL VARIATIONS OF SNOW CRYSTAL GROWTH PARAMETERS **c47**
Tsuneya Takahashi, Norihiko Fukuta (Utah Univ., Salt Lake City.), Tatsuo Endoh, and Gorow Wakahama *In* Deutscher Wetterdienst, Annals from the German Meteorological Society. No. 25: 10th International Cloud Physics Conference Preprints, Volume 1 1988 p 9-11 (For primary document see N89-19605 12-42)
(Grants NSF ATM-82-18966; JAPMINED-61020001)
Copyright Avail: Deutscher Wetterdienst, Frankfurter Strasse 135, D-6050 Offenbach am Main, Fed. Republic of Germany

Measurements on temporal variations of snow crystal growth parameters by vapor diffusion under water-saturation, and riming at -10 C are described. The observed crystal habits are needles at -5 C; columns at -8.5 C; and double plates at -10 C. At -14.5 C, crystal shape changes from sector to dendrite after 5 min of growth. At -8.5 and -10 C, crystal shapes are isometric. Temporal

variation of crystal masses for -10 C on liquid water content below 0.5 and 2 g/cu m is shown. Temporal variation is represented by 3 stages: vapor diffusional growth stage (d log m / d log t = 1.6); transitional growth stage (d log m / d log t = 2.3); and graupel growth stage (d log m / d log t = 6.2). ESA

N89-19609 Utah Univ., Salt Lake City. Dept. of Meteorology.
EMPIRICAL EQUATIONS OF ICE CRYSTAL GROWTH MICROPHYSICS FOR MODELING AND ANALYSIS **c47**
C. R. Redder and Norihiko Fukuta *In* Deutscher Wetterdienst, Annals from the German Meteorological Society, No. 25: 10th International Cloud Physics Conference Preprints, Volume 1 1988 p 12-14 (For primary document see N89-19605 12-42)
(Contract NOAA-87-1999; NSF ATM-86-16568)
Copyright Avail: Deutscher Wetterdienst, Frankfurter Strasse 135, D-6050 Offenbach am Main, Fed. Republic of Germany

Microphysical parameters of ice crystal growth were measured in a supercooled ice tunnel. By comparing tunnel data with theories of ice crystal growth, empirical expressions as a function of time up to 30 min at different temperatures in the range from -4 to -20 C, suitable for modeling and analysis, were derived. ESA

N89-19610 Academia Sinica, Beijing (China). Inst. of Atmospheric Physics.
THE CONTRAST STUDY OF NEW MODEL ON ICE CRYSTAL GROWTH **c47**
Ang-Sheng Wang *In* Deutscher Wetterdienst, Annals from the German Meteorological Society, No. 25: 10th International Cloud Physics Conference Preprints, Volume 1 1988 p 15-17 (For primary document see N89-19605 12-42)
Copyright Avail: Deutscher Wetterdienst, Frankfurter Strasse 135, D-6050 Offenbach am Main, Fed. Republic of Germany

The ice crystal growth models of Wang and Fukuta (1984) and Wang (1984) are reviewed. Results from the models are compared with qualitative studies, with Kobayashi's (1961) model, with dynamic experiments, and with field data on natural ice crystals. ESA

N89-19611 Johann-Wolfgang-Goethe-Univ., Frankfurt am Main (Germany, F.R.).
A WIND TUNNEL STUDY ON THE MELTING OF SNOW FLAKES **c47**
S. K. Mitra, O. Vohl, and H. R. Pruppacher *In* Deutscher Wetterdienst, Annals from the German Meteorological Society, No. 25: 10th International Cloud Physics Conference Preprints, Volume 1 1988 p 18-21 (For primary document see N89-19605 12-42)
Copyright Avail: Deutscher Wetterdienst, Frankfurter Strasse 135, D-6050 Offenbach am Main, Fed. Republic of Germany

Snow flake melting was studied in a vertical wind tunnel which allowed the ice particles to be kept at their terminal velocity freely floating in the tunnel air which can be warmed or cooled at the desired rate. Natural and artificial flakes were studied, suspended on a nylon thread, hovering on the surface of a nylon net, or freely suspended in the air stream. Melting occurs in four stages: (1) Small drops appear at the tips of crystal branches, melting being the most intense at the periphery and lower side of the flake. (2) Capillary action and surface tension cause melted water to flow from the periphery to the intersections of the snow crystal branches. The water keeps the aggregate together, but tries to collapse the crystal into a more compact shape. (3) The smallest branches of the flake interior melt and water flows to the intersection of the main branches. (4) The main ice frame collapses suddenly, and is transformed into a drop by being covered with water. ESA

N89-19612 Desert Research Inst., Reno, NV.
EVAPORATION AND MELTING OF ICE CRYSTALS: A LABORATORY STUDY **c47**
Riza G. Oraltay and John Hallett *In* Deutscher Wetterdienst, Annals from the German Meteorological Society, No. 25: 10th International Cloud Physics Conference Preprints, Volume 1 1988 p 22-24 (For primary document see N89-19605 12-42)
(Grant NSF ATM-87-15636)
Copyright Avail: Deutscher Wetterdienst, Frankfurter Strasse 135, D-6050 Offenbach am Main, Fed. Republic of Germany

A thermal diffusion chamber was used to grow ice crystals as a function of supersaturation, temperature, and air flow velocity; and melting and evaporation were studied under controlled relative humidity, temperature, and fall velocity. Results suggest that breakup and shedding are determined by the temperature and relative humidity of the ambient air, and produce quite different structures of the radar bright band. Secondary particle production only occurs for specific crystal habits (dendrites). The importance of recirculation of large drops and ice particles on the overall microphysical development depends on the probability of reincorporation of such particles into an appropriate updraft. ESA

N89-19613 Illinois State Water Survey, Champaign. Climate and Meteorology Section.
A NEW MECHANISM FOR ICE INITIATION IN WARM-BASED MIDWESTERN CUMULI **c47**
Robert R. Czys *In* Deutscher Wetterdienst, Annals from the German Meteorological Society, No. 25: 10th International Cloud Physics Conference Preprints, Volume 1 1988 p 25-27 (For primary document see N89-19605 12-42)
(Contracts COMM-NA-86-RAH-06051; COMM-NA-87-RAH-07077)
Copyright Avail: Deutscher Wetterdienst, Frankfurter Strasse 135, D-6050 Offenbach am Main, Fed. Republic of Germany

Collisions between supercooled precipitation drops are examined as a possible source for ice in warm-based summer convective clouds. Microphysical observations show that ice can originate at temperatures warmer and in concentrations higher than expected solely from ice-forming nuclei (IFN). Initial ice concentrations are up to 35 times larger than typical summer IFN concentrations. Clouds developed graupel concentrations between 10 to 20/liter, with mean diameters from 125 to 325 microns before cloud top temperature reached -11 C. All clouds develop ice in presence of supercooled rain. It is suggested that collisions between supercooled drops may result in freezing and thus be a strong source of ice having a powerful influence on the spectral evolution of liquid and solid particles. ESA

N89-19614 Desert Research Inst., Reno, NV.
SPREADING SUPERCOOLED WATER DROPLETS ON AN ICE SURFACE **c47**
Ya Yi Dong and John Hallett *In* Deutscher Wetterdienst, Annals from the German Meteorological Society, No. 25: 10th International Cloud Physics Conference Preprints, Volume 1 1988 p 28-30 (For primary document see N89-19605 12-42)
(Grant NSF ATM-87-15636)
Copyright Avail: Deutscher Wetterdienst, Frankfurter Strasse 135, D-6050 Offenbach am Main, Fed. Republic of Germany

The bahavior of supercooled water droplets spreading on different ice surfaces under various temperatures was investigated. It is found that the spreading ratio of water droplets slowly increases with temperature on a dry ice surface, but increases rapidly with temperature when a quasi-liquid layer exists on the ice surface above minus 4 C. The curvature of the ice surface has a strong influence on the water spreading. The traditional concept of contact angle is not applicable in this case. ESA

N89-19615 Illinois Univ., Urbana. Dept. of Atmospheric Sciences.
A MODEL OF THE ELECTROSTATIC-AERODYNAMIC SHAPE OF RAINDROPS **c47**
Catherine Chuang and Kenneth V. Beard *In* Deutscher Wetterdienst, Annals from the German Meteorological Society. No. 25: 10th International Cloud Physics Conference Preprints, Volume 1 1988 p 31-33 (For primary document see N89-19605 12-42)
(Grants NSF ATM-84-19490; NSF ATM-86-01549)
Copyright Avail: Deutscher Wetterdienst, Frankfurter Strasse 135, D-6050 Offenbach am Main, Fed. Republic of Germany

A model to predict the shape of raindrops, based on the

equilibrium equation across a curved surface, was developed by incorporating an aerodynamic pressure and electrostatic effects. The method of applying an empirical pressure distribution around a sphere, proposed by Savic (1983) was refined to include variations in the pressure distribution with Reynolds number and drop distortion. A finite volume technique was used to calculate the shape dependent electric effect with a numerically generated boundary-fitted coordinate system. Model results for aerodynamic shapes when compared with observations in wind tunnels follow the trend in measurements of the equilibrium axis ratios even for extremely large drops. The computed shapes for the pure electrostatic distortion are very close to the theoretical study by Taylor (1964). The results for aerodynamic-electrostatic drops are similar to the mean shapes and axis ratios obtained by Richards and Dawson (1973) from photographs of drops in a wind tunnel with a vertical electric field. ESA

N89-19616 Stockholm Univ. (Sweden). Dept. of Meteorology.
MEASUREMENTS OF THE PARTITIONING OF AEROSOL MASS AND NUMBER BETWEEN CLOUD DROPLETS AND INTERSTITIAL AIR **c47**
John A. Ogren, Jost Heintzenberg, and Kevin J. Noone *In* Deutscher Wetterdienst, Annals from the German Meteorological Society, No. 25: 10th International Cloud Physics Conference Preprints, Volume 1 1988 p 34-36 (For primary document see N89-19605 12-42)
Copyright Avail: Deutscher Wetterdienst, Frankfurter Strasse 135, D-6050 Offenbach am Main, Fed. Republic of Germany

Aerosol incorporation in clouds was studied using a counterflow virtual impactor (CVI) in a vertical tunnel, and submicrometer aerosol measurements obtained during field testing of a system for baseline measurements in Arctic air. In the relatively unpolluted, stratocumulus clouds frequently encountered at the site, well over half of the mass of submicrometer particles is typically found in the droplets. In contrast, fewer than half of the number of submicrometer particles is contained in the cloud droplets. In order to obtain more precise determinations of the scavenging efficiencies, the CVI is being redesigned to allow sampling of droplets down to 1 micron radius, and the time resolution of the submicrometer aerosol data is being improved. ESA

N89-19617 Manchester Univ. (England). Dept. of Pure and Applied Physics.
THE CALCULATION OF SUPERSATURATIONS AND GROWTH OF DROPLETS IN CONTINENTAL CUMULUS CLOUDS **c47**
Keith Bower and Tom W. Choularton *In* Deutscher Wetterdienst, Annals from the German Meteorological Society, No. 25: 10th International Cloud Physics Conference Preprints, Volume 1 1988 p 37-39 (For primary document see N89-19605 12-42)
Copyright Avail: Deutscher Wetterdienst, Frankfurter Strasse 135, D-6050 Offenbach am Main, Fed. Republic of Germany

Observations from aircraft passes through continental cumulus clouds were analyzed in an attempt to test results of dry air entrainment predicted by the model of Hill and Choularton (1986). A method to calculate supersaturation present in the passes was derived. For comparison purposes, a representative droplet spectrum developed from a measured cloud condensation nuclei distribution was allowed to develop adiabatically, from the observed cloud base conditions in a constant updraft profile to the observation level. The effect of the enhanced supersaturation on droplet growth was modelled by reducing the number concentration of activated droplets in the adiabatic model so as to reproduce the observed supersaturations at the observational level. Average droplet lifetimes were calculated by considering the time taken for embryo droplets to develop to an average size equal to the observed value in an adiabatic model. ESA

N89-19618 National Center for Atmospheric Research, Boulder, CO.
ON THE OBSERVATIONS OF CLOUD TEMPERATURE AND LIQUID WATER CONTENT USING A LYMAN-ALPHA AND AN FSSP SENSOR **c47**
Jorgen B. Jensen, Darrel G. Baumgardner, and Graciela Raga (Washington Univ., Seattle.) *In* Deutscher Wetterdienst, Annals from the German Meteorological Society, No. 25: 10th International Cloud Physics Conference Preprints, Volume 1 1988 p 40-42 (For primary document see N89-19605 12-42)
(Grant NSF ATM-84-20816)
Copyright Avail: Deutscher Wetterdienst, Frankfurter Strasse 135, D-6050 Offenbach am Main, Fed. Republic of Germany

An aircraft experiment was designed to explore the processes leading to warm rain in cumulus clouds off the coast of Hawaii. Data analyzed are 134 penetrations from 22 clouds sampled on 6 days during July. A total of 3126 1-sec samples are classified as in-cloud. The reverse flow temperature sensor, the dew-point thermometer, a Lyman-alpha humidity sensor mounted with a reverse flow shielding inside the fuselage, and a FSSP are discussed. ESA

N89-19619 National Center for Atmospheric Research, Boulder, CO.
EVALUATION OF DROPLET GROWTH RATES IN HAWAIIAN OROGRAPHIC CLOUDS **c47**
Darrel G. Baumgardner *In* Deutscher Wetterdienst, Annals from the German Meteorological Society. No. 25: 10th International Cloud Physics Conference Preprints, Volume 1 1988 p 43-45 Sponsored in part by NSF, Washington, DC (For primary document see N89-19605 12-42)
Copyright Avail: Deutscher Wetterdienst, Frankfurter Strasse 135, D-6050 Offenbach am Main, Fed. Republic of Germany

Evolving cloud droplet populations were measured. The orographic clouds formed by the island of Hawaii were selected for evaluation because of their temporal stability, relatively low levels of turbulence, and warmer than freezing cloud tops. Measurements are compared with predictions from a droplet growth model. The comparisons of predicted and measured droplet distributions in the relatively simple case of low turbulent, orographic, warm clouds indicate that larger droplets appear in quantities greater than predicted from conventional theories. There does not appear to be a fundamental physical processes that governs droplet growth. The model did not address the characterization of a fluctuating environment within which droplets grow and interact, although fluctuations in the velocity and moisture fields surrounding cloud droplets have major effects on their rates of growth. ESA

N89-19620* National Center for Atmospheric Research, Boulder, CO.
STUDIES OF WARM-RAIN DEVELOPMENT **c47**
William A. Cooper *In* Deutscher Wetterdienst, Annals from the German Meteorological Society. No. 25: 10th International Cloud Physics Conference Preprints, Volume 1 1988 p 46-48 Sponsored in part by NSF, Washington, DC (For primary document see N89-19605 12-42)
(Contract NAS5-27783)
Copyright Avail: Deutscher Wetterdienst, Frankfurter Strasse 135, D-6050 Offenbach am Main, Fed. Republic of Germany
CSCL 04B

The development of rain in warm (over 0 C) clouds due to the combined effects of condensation and coalescence following collisions is discussed. The detailed shape of the size distribution produced by condensation has a controlling influence on the rate of coalescence, and this shape is affected by entrainment of dry air, mixing of various cloud parcels, and radiative effects. Aspects of these processes in cloud types where rain formed through warm-rain processes are reviewed. Results suggest that diffusional growth may be enhanced in highly mixed regions of maritime cumulus in a manner similar to that in wave clouds, but that this effect is minor in updraft cores or in the stratocumulus layers examined. ESA

N89-19621 National Center for Atmospheric Research, Boulder, CO.
RADAR OBSERVATIONS AND MODELLING OF WARM RAIN INITIATION **c47**
Anthony J. Illingworth and I. Jeff Caylor (Manchester Univ., Eng-

land) *In* Deutscher Wetterdienst, Annals from the German Meteorological Society. No. 25: 10th International Cloud Physics Conference Preprints, Volume 1 1988 p 49-51 Sponsored in part by NSF, Washington, DC (For primary document see N89-19605 12-42)
(Grants NERC-GR3/5896; AF-AFOSR-0046-87)
Copyright Avail: Deutscher Wetterdienst, Frankfurter Strasse 135, D-6050 Offenbach am Main, Fed. Republic of Germany

Differential radar reflectivity observations of early echoes of rain in warm convective clouds in the UK and Alabama, USA, indicate that precipitation initially forms as raindrops greater than 4mm in size but present in concentrations of less than 1/cu m. The differential reflectivity, ZDR, = (10 log (ZH/ZV)), where ZH and ZV are the radar reflectivities measured with horizontal and vertical polarizations, respectively. The ZDR provides a measure of the shape of the hydrometeors, and because raindrops are oblate to a degree which depends upon their size, the magnitude of ZDR is a unique function of raindrop size. The ZDR is a ratio and so is independent of concentrations, but once the mean size is known then the conventional reflectivity, ZH, can be used to derive an estimate of raindrop concentration. ESA

N89-19622 Wyoming Univ., Laramie. Dept. of Atmospheric Science.
A TEST OF ICE CRYSTAL PRODUCTION BY AIRCRAFT **c47**
Gabor Vali, R. D. Kelly, and F. Serrano *In* Deutscher Wetterdienst, Annals from the German Meteorological Society, No. 25: 10th International Cloud Physics Conference Preprints, Volume 1 1988 p 52-54 (For primary document see N89-19605 12-42)
(Grant NSF ATM-86-11185)
Copyright Avail: Deutscher Wetterdienst, Frankfurter Strasse 135, D-6050 Offenbach am Main, Fed. Republic of Germany

Given the importance of aircraft observations in the studies of cloud and precipitation processes, the possibility that the aircraft themselves may modify the clouds was studied. Experiments were undertaken in order to provide a borader data base on the conditions of aircraft produced ice particle generation and on the controlling factors of the process. A tracer was used to ascertain proper sampling of the affected cloud volume so that both false positive and false negative conclusions could be avoided. Evidence suggests that aircraft may produce ice crystals when passing through supercooled water clouds, but only when certain combinations of conditions exist. ESA

N89-19623 Meteorological Office, Bracknell (England).
AIRBORNE STUDIES OF THE ICE PHASE IN MARITIME CLOUDS AROUND THE BRITISH ISLES **c47**
P. R. A. Brown and Tom W. Choularton (Manchester Univ., England) *In* Deutscher Wetterdienst, Annals from the German Meteorological Society, No. 25: 10th International Cloud Physics Conference Preprints, Volume 1 1988 p 55-57 (For primary document see N89-19605 12-42)
Copyright Avail: Deutscher Wetterdienst, Frankfurter Strasse 135, D-6050 Offenbach am Main, Fed. Republic of Germany

The Hallett-Mossop process is shown to be active within maritime convective clouds around the British Isles. The distribution of the secondary ice columns depends in detail on the cloud dynamics. Ice crystals are also generated separately at cloud top by a mechanism which may involve the freezing of large drops as suggested by Hobbs and Rangno (1985). The relationship between this process and the secondary ice production lower in the cloud was not determined. ESA

N89-19624 Indian Inst. of Tropical Meteorology, Poona.
PRECIPITATION INITIATION MECHANISMS IN CLOUDS OVER NORTH INDIA **c47**
R. N. Chatterjee, P. Prakash, G. Singh, and R. K. Kapoor *In* Deutscher Wetterdienst, Annals from the German Meteorological Society, No. 25: 10th International Cloud Physics Conference Preprints, Volume 1 1988 p 58-60 (For primary document see N89-19605 12-42)
Copyright Avail: Deutscher Wetterdienst, Frankfurter Strasse 135, D-6050 Offenbach am Main, Fed. Republic of Germany

The role of different precipitation initiation mechanisms in clouds over Delhi region in north India during different seasons was studied using radar observations of precipitation echoes collected during a 16 yr period. A year consisted of four seasons, namely, winter (December to February), premonsoon (March to June), monsoon (July to September) and postmonsoon (October to November). Heights of the freezing levels during winter, premonsoon, monsoon, and postmonsoon seasons are taken as 3.5, 5.0 and 4.5 kms respectively. Frequency distribution of precipitating clouds, and distribution of a, b, and c type rain cells are discussed. ESA

N89-19625 Clermont-Ferrand Univ. (France).
EVIDENCE OF PREFERENTIAL ZONES OF ICE MULTIPLICATION BY SPLINTERING IN CONVECTIVE CELLS **c47**
Jean-Francois Gayet, Christophe Duroure, and R. G. Soulage *In* Deutscher Wetterdienst, Annals from the German Meteorological Society, No. 25: 10th International Cloud Physics Conference Preprints, Volume 1 1988 p 61-63 (For primary document see N89-19605 12-42)
(Grants DRET/INSU-83-34308; DRET/INSU-85-34016)
Copyright Avail: Deutscher Wetterdienst, Frankfurter Strasse 135, D-6050 Offenbach am Main, Fed. Republic of Germany

It is shown from a small scale analysis of in-situ microphysical and dynamical measurements on clouds that the splintering process occurs on preferential zones in convective cells. Measurements were collected by an instrumented aircraft together with a ground meteorological radar system. The aircraft was equipped with a complete set of microphysical probes. ESA

N89-19626 Illinois State Water Survey, Champaign. Climate and Meteorology Section.
MICROPHYSICAL CHARACTERISTICS OF WARM-BASED CUMULI: OBSERVATIONS AT -10 C **c47**
Robert R. Czys *In* Deutscher Wetterdienst, Annals from the German Meteorological Society, No. 25: 10th International Cloud Physics Conference Preprints, Volume 1 1988 p 64-66 (For primary document see N89-19605 12-42)
(Contracts COMM-NA-86-RAH-06051; COMM-NA-87-RAH-07077)
Copyright Avail: Deutscher Wetterdienst, Frankfurter Strasse 135, D-6050 Offenbach am Main, Fed. Republic of Germany

As part of the Precipitation Augmentation for Crops Experiment (PACE), the microphysical properties of untreated and treated (with either AgI or placebo) cumulus clouds were investigated. The PACE objective is to determine precipitation alterations attainable by dynamic seeding during the growing season of the central United States and to determine the benefits and liabilities of such alterations. The microphysical features of the clouds observed suggest that supercooled liquid water is present in quantities sufficient for buoyancy enhancement by imposed glaciation. However, the clouds exhibit negative buoyancy by the time cloud top reaches the minus 10 C level. This suggests that the most attainable dynamic effect may be to only decrease the rate of updraft deceleration. ESA

N89-19627 Washington Univ., Seattle. Dept. of Aeronautics and Astronautics.
A COMPARATIVE STUDY OF LABORATORY THERMALS AND ATMOSPHERIC CLOUDS **c47**
H. Johari, Gregory R. Taylor, M. Baker, and R. Breidenthal *In* Deutscher Wetterdienst, Annals from the German Meteorological Society, No. 25: 10th International Cloud Physics Conference Preprints, Volume 1 1988 p 67-69 (For primary document see N89-19605 12-42)
(Grants NSF ATM-84-20816; NSF ATM-86-09376; NSF ATM-86-11225)
Copyright Avail: Deutscher Wetterdienst, Frankfurter Strasse 135, D-6050 Offenbach am Main, Fed. Republic of Germany

Conceptual models of cloud evolution are examined in the light of laboratory simulations of convective cloud development. According to the models, air rises adiabatically from cloud base in a thermal or plume. It mixes in a series of discrete gulps with the environment. After each gulp, the mixed fluid tends toward its

position of hydrostatic equilibrium. Most of the cloud mass is then this wake of mixed fluid. It is clear that atmospheric clouds are more complex than the laboratory flows, that they probably consist of collections of convective elements, and that intermixing of fluid from different parts of the cloud produces effects quite unlike those which can be reproduced in these experiments. The examination of laboratory flows, however, is an enlightening method with which to investigate individually certain interesting aspects of the atmospheric phenomenon. ESA

N89-19628 National Center for Atmospheric Research, Boulder, CO.
ENTRAINMENT AND FINE-SCALE (MOLECULAR) MIXING **c47**
Ilga R. Paluch and Darrel G. Baumgardner *In* Deutscher Wetterdienst, Annals from the German Meteorological Society, No. 25: 10th International Cloud Physics Conference Preprints, Volume 1 1988 p 70-72 Sponsored in part by NSF, Washington, DC (For primary document see N89-19605 12-42)
Copyright Avail: Deutscher Wetterdienst, Frankfurter Strasse 135, D-6050 Offenbach am Main, Fed. Republic of Germany

Fine-scale measurements of cloud-droplet concentrations indicate that entrainment in cumulus clouds can produce very nonuniform mixtures on the scale of meters. The data are interpreted to imply that the larger turbulent eddies cause most of the bulk entrainment and coarse mixing, while fine-scale (molecular) mixing takes place within intermittent small eddies or vortex cores. Observations indicate that most of the mixing takes place in narrow regions within tens of meters of clear-air boundaries. Substantially diluted, more or less uniformly mixed cloud volumes extending several hundreds of meters across are not observed, though such volumes are often postulated in microphysical parcel models. If the mixed airparcel concept is applicable to the type of continental cumulus investigated, then the mixed airparcels must be much smaller in size, perhaps only several meters or a few tens of meters across. ESA

N89-19629 Manchester Univ. (England). Dept. of Physics.
AIRBORNE STUDIES OF THE INFLUENCE OF ENTRAINMENT ON THE VERTICAL AND HORIZONTAL MICROPHYSICAL STRUCTURE OF SMALL CUMULUS CLOUDS **c47**
John Latham and Alan M. Blyth (New Mexico Inst. of Mining and Technology, Socorro.) *In* Deutscher Wetterdienst, Annals from the German Meteorological Society, No. 25: 10th International Cloud Physics Conference Preprints, Volume 1 1988 p 73-75 (For primary document see N89-19605 12-42)
Copyright Avail: Deutscher Wetterdienst, Frankfurter Strasse 135, D-6050 Offenbach am Main, Fed. Republic of Germany

The vertical structure of nonprecipitating, essentially ice-free cumulus clouds was studied by making a series of horizontal penetrations at different altitudes encompassing almost all of the depth of the cloud (typically 2 to 3 km) over as short a period as possible. The principal microphysical measurements were of liquid-water content, cloud droplet size distribution, and the droplet number concentration. Standard meteorological parameters and size distributions of larger hydrometeors were also measured, but it was necessary to sacrifice the quantity of the dynamical data in order to minimize the time over which the vertical structure was determined. The microphysical structure (especially in the vertical); the role of entrainment of environmental air in producing it; and the embryonic raindrops often present in particular regions of the clouds studied are discussed. ESA

N89-19630 Direction de la Meteorologie Nationale, Magny les Hameaux (France).
ENTRAINMENT SITES, MIXING PROCESSES IN WARM CONVECTIVE CLOUDS: EFFECT ON DROPLET GROWTH **c47**
Elizabeth Hicks, Arlette Rigaud, Jacqueline Gagneux, and Constantin Pontikis *In* Deutscher Wetterdienst, Annals from the German Meteorological Society, No. 25: 10th International Cloud Physics Conference Preprints, Volume 1 1988 p 76-78 (For primary document see N89-19605 12-42)
Copyright Avail: Deutscher Wetterdienst, Frankfurter Strasse 135, D-6050 Offenbach am Main, Fed. Republic of Germany

Entrainment and mixing of non-cloudy air into cumulus clouds as a mechanism which broadens the droplet spectrum and creates larger droplets which are the first to start growing by coalescence and may initiate precipitation are discussed. A field experiment was conducted to see if measurements made at different levels in a cloud indicate the same source of entrained air; if the mixing process during an entrainment event supports the droplet conserving or nonconserving hypothesis; and if entrainment and mixing enhance cloud droplet growth in the condensation spectrum. Results show that the source of entrained air observed at a given level is generally the cloud top, but lateral entrainment may affect the lower levels in a cloud. Mixing is a droplet nonconserving process. Dilution and buoyancy-driven recycling of cloudy parcels enhances droplet growth in shallow warm cumuli. ESA

N89-19631 Academy of Sciences (USSR), Tomsk. Inst. of Atmospheric Optics.
STRUCTURE OF UPPER CLOUDS BOUNDARY USING THE LIDAR DATA **c47**
V. E. Zuev, V. S. Shamanaev, I. E. Penner, and I. V. Samokhvalov *In* Deutscher Wetterdienst, Annals from the German Meteorological Society, No. 25: 10th International Cloud Physics Conference Preprints, Volume 1 1988 p 79-81 (For primary document see N89-19605 12-42)
Copyright Avail: Deutscher Wetterdienst, Frankfurter Strasse 135, D-6050 Offenbach am Main, Fed. Republic of Germany

An airborne lidar was used to study sizes and fluctuation characteristics of inhomogeneities forming the upper clouds boundary (UCB). The cloud field was studied for 2 hr. The average UCB of the stratocumulus field is 1660 to 1830 m. Only in one segment of the flight path a local cloudiness dome to the 1980 m CB is observed. Structural functions constructed with a minimal interval along the flight line (20 to 50 m) never have a saturation area smaller than 1 km. That is the small-scale UCB fluctuations (tens of meters) cannot be considered as a stationary random process on flight paths shorter than 1 km. The radiation temperature of clouds varies along the flight path by not more than 3 C and does not correlate with the UCB fluctuations. ESA

N89-19632 Deutsche Forschungs- und Versuchsanstalt fuer Luft- und Raumfahrt, Oberpfaffenhofen (West Germany). Inst. fuer Physik der Atmosphaere.
TURBULENT TRANSPORT PROCESSES WITHIN AND BELOW SMALL CUMULUS CLOUDS **c47**
Anne M. Jochum *In* Deutscher Wetterdienst, Annals from the German Meteorological Society, No. 25: 10th International Cloud Physics Conference Preprints, Volume 1 1988 p 82-84 (For primary document see N89-19605 12-42)
Copyright Avail: Deutscher Wetterdienst, Frankfurter Strasse 135, D-6050 Offenbach am Main, Fed. Republic of Germany

Multiple aircraft measurements were conducted in the cloud-topped convective boundary layer (cbl) over complex terrain to investigate the structure of turbulence and transport processes within and below clouds and to study the interaction between cloud and subcloud-layer. Physical properties of convective elements were derived from the conditional sampling data. The average temperature excess of updrafts compared to their environment is shown. For the cbl there is no region of negative buoyancy below the inversion, whereas in cloudfree cases the level of neutral buoyancy is in the upper third of the cbl. The average vertical wind velocity excess increases upwards in contrast to the cloudfree case. ESA

N89-19633 Meteorological Research Inst., Tsukuba (Japan).
INSTABILITY THEORY IN CLOUDS AND THE PARAMETERIZATION OF EDDY VISCOSITY COEFFICIENTS **c47**
Yoshimasa Takaya *In* Deutscher Wetterdienst, Annals from the German Meteorological Society, No. 25: 10th International Cloud Physics Conference Preprints, Volume 1 1988 p 85-87 (For

primary document see N89-19605 12-42)
Copyright Avail: Deutscher Wetterdienst, Frankfurter Strasse 135, D-6050 Offenbach am Main, Fed. Republic of Germany

A theory which describes the mechanism of the entrainment or mixing between cloudy air and the surrounding clear air which is a generalization of the conditional instability of the first kind, is proposed. There, the tilted stratification of the thermodynamical and cloud-physical variables in the cloud plays an important role. This theory explains the fractal-like structure of the convective cloud and predicts the horizontal angle of the node or the hollow of the cloud. The effect of this instability is included in the numerical simulation of the convective cloud as the eddy terms, obtaining the result that the history of the collective motion of the convective clouds sensitively depends on these eddy terms. ESA

N89-19634 National Center for Atmospheric Research, Boulder, CO.
THREE-DIMENSIONAL CUMULUS ENTRAINMENT STUDIES **c47**
Terry L. Clark, Piotr K. Smolarkiewicz, and William D. Hall *In* Deutscher Wetterdienst, Annals from the German Meteorological Society, No. 25: 10th International Cloud Physics Conference Preprints, Volume 1 1988 p 88-90 Sponsored in part by NSF, Washington, DC (For primary document see N89-19605 12-42)
Copyright Avail: Deutscher Wetterdienst, Frankfurter Strasse 135, D-6050 Offenbach am Main, Fed. Republic of Germany

The dynamics and thermodynamics of cumulocongestus are analyzed using kinetic energy and enstrophy budget analysis. The kinetic energy tends to emphasize the larger scales of motion whereas, since the vorticity tends to reside towards smaller scales, it emphasizes the smaller scales. Intercomparison of these two scalars indicates the degree of convergence attained for the various resolutions. Results indicate that large scale motions are well resolved using 100 m resolution. Smaller scale motions are very much affected by increased resolution as indicated by the enstrophy analysis. Entrainment is never active enough to limit the depth of growth of this cloud to below its equilibrium level. Two-dimensional Cartesian (x-z) calculations, however, do allow entrainment to limit cloud depth. The over emphasis of entrainment due to 2-D Cartesian geometry should be recognized. The source of entrained environmental air for this cumulocongestus cloud simulation is typically from below to 400 m above the level analyzed. The mechanism which leads to entrainment appears to be the inviscid production of cloud boundary vorticity similar to that found by Klaassen and Clark (1985). ESA

N89-19635 Centre National de Recherches Meteorologiques, Toulouse (France).
HETEROGENEOUS MIXING MEASUREMENTS IN SMALL NONPRECIPITATING CUMULI **c47**
J. L. Brenguier *In* Deutscher Wetterdienst, Annals from the German Meteorological Society, No. 25: 10th International Cloud Physics Conference Preprints, Volume 1 1988 p 91-93 (For primary document see N89-19605 12-42)
Copyright Avail: Deutscher Wetterdienst, Frankfurter Strasse 135, D-6050 Offenbach am Main, Fed. Republic of Germany

A method to correct the coincidence and dead-time losses in the forward scattering spectrometer probe is proposed. By adjusting the measured data to the predicted values of two independent parameters (nd and A, where A is activity, nd is counted particle rate, n is particle rate) it is possible to estimate high droplet rates for which the correction factor is important ($nd/n = 3$). The estimated values of the concentration are very high (2000/cc) compared to the values measured in the past. The method is also powerful to estimate the homogeneity of the samples. Thus it appears that 1 sec samples, with a low concentration (low values of nd and A) are in fact very heterogenous (high value of the mean transit duration). These regions are better described as a succession of cloudy patches inserted in clear air. This observation is confirmed by the fluctuations of the droplet counts measured at a high rate (5 Hz). The method is based on the evaluation of the probability of coincidence referred to as a Poisson distribution. The very high values of the concentration shows that droplets are probably distributed in space less uniformly than provided by this ideal distribution. ESA

N89-19636 National Oceanic and Atmospheric Administration, Princeton, NJ. Geophysical Fluid Dynamics Lab.
THE CASE FOR SUBGRID-SCALE CONDENSATION IN NUMERICAL CLOUD MODELS **c47**
Frank B. Lipps and Richard S. Hemler *In* Deutscher Wetterdienst, Annals from the German Meteorological Society, No. 25: 10th International Cloud Physics Conference Preprints, Volume 1 1988 p 94-96 (For primary document see N89-19605 12-42)
Copyright Avail: Deutscher Wetterdienst, Frankfurter Strasse 135, D-6050 Offenbach am Main, Fed. Republic of Germany

Calculations were carried out simulating midlatitude and tropical convection using a three-dimensional numerical cloud model with a Kessler-type warm rain bulk cloud physics. Inside clouds, where condensation is taking place, conservation of equivalent potential temperature is assumed for the subgrid-scale turbulence parameterization. In clear air, conservation of virtual potential temperature is assumed. Due to these different forms of turbulent mixing in clear and cloudy air, subgrid-scale condensation occurs just below cloud base with resultant latent heat release. For shallow and deep convection, this low level heating produces a more uniform vertical velocity maximum with time and maintains the cloud over a longer lifetime. For shallow convection, the rain reaching the ground is increased significantly. ESA

N89-19637 McGill Univ., Montreal (Quebec).
THE EFFECT OF TURBULENCE ON THE COLLECTION OF CLOUD DROPS: A STOCHASTIC MODEL **c47**
Gerhard Reuter *In* Deutscher Wetterdienst, Annals from the German Meteorological Society, No. 25: 10th International Cloud Physics Conference Preprints, Volume 1 1988 p 97-99 (For primary document see N89-19605 12-42)
Copyright Avail: Deutscher Wetterdienst, Frankfurter Strasse 135, D-6050 Offenbach am Main, Fed. Republic of Germany

Results of the growth of a cloud droplet population affected by gravitational collection and coalescence caused by overlapping eddies in turbulent air are presented. The collection equation is solved by a very economical numerical scheme (Eyre et al, 1988) and the collection kernel is approximated with the stochastic model of Reuter et al (1988). Numerical experiments are made with an exponential initial volume distribution. The liquid water content is 1g/cum, and the mean initial radius is 25 microns. Results show that the development of the coalescence is rather slow even for strong turbulence. If the turbulence is weaker, the growth is slower. However, the results clearly show that overlapping of turbulent eddies contributes to the collection process. ESA

N89-19638 National Center for Atmospheric Research, Boulder, CO.
THE EFFECT OF ICE PHYSICAL PROCESSES ON THE NUMERICAL SIMULATION OF WEST AFRICAN SQUALL LINES **c47**
William D. Hall and Jean Philippe Lafore (Centre National de Recherches Meteorologiques, Toulouse, France) *In* Deutscher Wetterdienst, Annals from the German Meteorological Society, No. 25: 10th International Cloud Physics Conference Preprints, Volume 1 1988 p 100-102 Sponsored in part by NSF, Washington, DC (For primary document see N89-19605 12-42)
Copyright Avail: Deutscher Wetterdienst, Frankfurter Strasse 135, D-6050 Offenbach am Main, Fed. Republic of Germany

Two-dimensional nested grid numerical experiments of Clark's 3-D cloud model were performed to study the thermodynamic and dynamic response of tropical squall lines by ice phase microphysical processes. The numerical framework consists of three nested models with increasing resolution moving at a constant speed to insure that the squall line remains in the center of the highest resolution domain. Results of two numerical experiments with and without ice are presented. In the ice case the Koenig and Murray (1976) ice parameterization with a high seeding nucleation rate is applied; in the no ice or warm rain case the parameterization is

of Kessler described by Clark (1979). In both experiments the model is initialized with a cooling rate of -0.01 C/sec maintained for 10 min over a 12 km region above the ground with a depth of 3 km. Results show that the inclusion of simple ice phase microphysics can significantly alter the simulated results of a fast moving tropical squall line. ESA

N89-19639 State Meteorological Inst., Beijing (China).
NUMERICAL SIMULATION OF MICROPHYSICAL PROCESSES IN CUMULONIMBUS **c47**
Zhijin Hu and Guanfang He *In* Deutscher Wetterdienst, Annals from the German Meteorological Society, No. 25: 10th International Cloud Physics Conference Preprints, Volume 1 1988 p 103-105 (For primary document see N89-19605 12-42)
Copyright Avail: Deutscher Wetterdienst, Frankfurter Strasse 135, D-6050 Offenbach am Main, Fed. Republic of Germany

A two-parameter model for simulating the microphysical processes in cumulonimbus clouds is presented. All the water substance is divided into six categories: vapor, cloud drops, rain drops, ice crystals, graupel, and hailstones. Case studies using the model combined with a one dimensional time dependent cumulus model are summarized. ESA

N89-19640 Clermont-Ferrand Univ. (France).
A COMPARATIVE STUDY OF TWO MICROPHYSICAL SCHEMES IN A BETA MESOSCALE MODEL **c47**
Evelyne Richard and Nadine Chaumerliac *In* Deutscher Wetterdienst, Annals from the German Meteorological Society, No. 25: 10th International Cloud Physics Conference Preprints, Volume 1 1988 p 106-108 (For primary document see N89-19605 12-42)
Copyright Avail: Deutscher Wetterdienst, Frankfurter Strasse 135, D-6050 Offenbach am Main, Fed. Republic of Germany

Two sets of microphysical parameterizations are compared under various orographic situations in a beta mesoscale model. One is the Kessler parameterization (Kessler, 1969) and the other is based upon Berry and Reinhardt (1973). In both cases, cloud water mixing ratio is diagnosed from the predicted value of q (equal to the sum of the vapor mixing ratio, qv and the cloud water mixing ratio). In the case of supersaturation, qv is set equal to the saturated vapor mixing ratio and excess vapor is converted into cloud water. Mountain wave simulations and feeder seeder simulations reveal different raindrop behavior between the two parameterizations. ESA

N89-19641 Wisconsin Univ., Madison.
GENERALIZED MICROPHYSICS SCHEME FOR USE IN MESOSCALE/CLOUD MODELS **c46**
Gregory J. Tripoli, Piotr J. Flatau, and William R. Cotton (Colorado State Univ., Fort Collins.) *In* Deutscher Wetterdienst, Annals from the German Meteorological Society, No. 25: 10th International Cloud Physics Conference Preprints, Volume 1 1988 p 109-111 (For primary document see N89-19605 12-42)
(Grant NSF ATM-85-12480)
Copyright Avail: Deutscher Wetterdienst, Frankfurter Strasse 135, D-6050 Offenbach am Main, Fed. Republic of Germany

A generalized bulk microphysics parameterization is outlined. Particle size spectra and their moments, including the gamma and normal distributions are discussed. An example of a bulk weighted parameterization formula for mass weighted terminal velocity is given. Treatment of hydrometeor classes and their interactions is shown. Implementation is summarized. ESA

N89-19642 Academia Sinica, Beijing (China). Inst. of Atmospheric Physics.
THE STUDY OF NUMERICAL SIMULATION ON THE FORMATION OF THE CLOUD DROPLET SPECTRA IN CUMULUS CLOUDS **c47**
Hui Xiao, Huaying Xu, and Meiyuan Huang *In* Deutscher Wetterdienst, Annals from the German Meteorological Society, No. 25: 10th International Cloud Physics Conference Preprints, Volume 1 1988 p 112-114 (For primary document see N89-19605 12-42)
Copyright Avail: Deutscher Wetterdienst, Frankfurter Strasse 135, D-6050 Offenbach am Main, Fed. Republic of Germany

A one dimensional time dependent cylindrical cumulus cloud model was used to study cloud droplets. Simulations show that the total concentration of cloud droplets in cumulus cloud has few changes with height, while the concentration of large cloud-droplets increases firstly with height in the middle-lower layer of cloud, reaches maximum in the middle-upper part, and then decreases rapidly again. The spectra of cloud droplets near the cloud top have a bimodal structure, linked to the entrainment characteristics between inside and outside of cloud at that height. In the spreading of the cloud droplet spectra in the earlier developing stage of cumulus clouds, gravitational collection process plays the most obvious role; the collection process caused by small-scale turbulence plays a greatly promoted role, which can accelerate the growth of big cloud-droplets, while the role of electric collection is not significant. ESA

N89-19643 Colorado State Univ., Fort Collins. Dept. of Atmospheric Science.
SOME OUTSTANDING PROBLEMS ON THE INFLUENCE OF CLOUDS ON RADIATION **c47**
Graeme L. Stephens *In* Deutscher Wetterdienst, Annals from the German Meteorological Society, No. 25: 10th International Cloud Physics Conference Preprints, Volume 1 1988 p 115-117 (For primary document see N89-19605 12-42)
(Grants NSF ATM-85-19160; NSF ATM-84-15127)
Copyright Avail: Deutscher Wetterdienst, Frankfurter Strasse 135, D-6050 Offenbach am Main, Fed. Republic of Germany

Issues that impact on ability to provide a meaningful description of the radiative processes in cloud both from the point of view of characterizing the radiative energy budgets of clouds and from the perspective of the remote sensing of cloud properties are reviewed. The relationship between radiative processes and microphysics is considered, including volume extinction and single scattering albedo. The impact of cloud structure, particularly scales of motion, on radiative transfer is noted. ESA

N89-19644* Utah Univ., Salt Lake City. Dept. of Meteorology.
THEORY ON THE UNCERTAINTY IN CLOUD MICROPHYSICAL PROCESSES AND CLIMATE **c47**
Kuo-Nan Liou and Szu-cheng S. Ou *In* Deutscher Wetterdienst, Annals from the German Meteorological Society, No. 25: 10th International Cloud Physics Conference Preprints, Volume 1 1988 p 118-120 Sponsored by NASA, Washington, DC (For primary document see N89-19605 12-42)
(Grants NAG7-32; AF-AFOSR-0294-87)
Copyright Avail: Deutscher Wetterdienst, Frankfurter Strasse 135, D-6050 Offenbach am Main, Fed. Republic of Germany
CSCL 04B

The interactive role of clouds and precipitation processes in a climate model is investigated. The basic model structure and parameterizations for condensation, evaporation, and precipitation are outlined. Results simulated from the cloud-climate model are discussed. The potential link between microphysical cloud processes and climate is theorized. The need to develop a climatology of the mean particle radius for clouds at the global scale, in order to understand the role of clouds in climate is stressed. ESA

N89-19645 Washington Univ., Seattle. Dept. of Atmospheric Sciences.
IN SITU MEASUREMENTS OF SHIP TRACKS **c47**
Lawrence F. Radke, Jamie H. Lyons, Peter V. Hobbs, and James E. Coakley (National Center for Atmospheric Research, Boulder, CO.) *In* Deutscher Wetterdienst, Annals from the German Meteorological Society, No. 25: 10th International Cloud Physics Conference Preprints, Volume 1 1988 p 121-123 (For primary document see N89-19605 12-42)
(Grant NSF ATM-86-15344)
Copyright Avail: Deutscher Wetterdienst, Frankfurter Strasse 135, D-6050 Offenbach am Main, Fed. Republic of Germany

Production of cloud condensation nuclei (CCN) by ships was investigated. Ship tracks detected in satellite imagery were intercepted by aircraft. Assuming a ship speed of 10 m/sec, and using the measurements of 16 km and 500 m for the width and depth, respectively, of the feature, and an increase in droplet concentration in the feature of 100/cc, it is calculated that in order for a ship to produce the observed changes in drop concentrations it has to produce 10 to the 16th power CCN/sec. This requires the ship to be a very large (perhaps unreasonably large) source of CCN. However, in addition to fuel combustion, a ship can cause CCN to be lofted into the atmosphere by generating sea-salt particles through cavitation, splashing, and bubble bursting. Particle production by these processes can produce substantial numbers of particles in the 0.1 to 1 micron size range. Since these particles serve as very efficient CCN, they could augment the combustion products from a ship and thereby play a role in the formation of ship tracks. Also, the dynamic effects suggested by the increase in liquid water content in the feature would increase the supersaturation in the cloud and thereby activate additional CCN. A ship might also loft additional water vapor through emissions and/or stirring of the boundary layer. ESA

N89-19646* National Aeronautics and Space Administration. Ames Research Center, Moffett Field, CA.

CLOUD AND AEROSOL OPTICAL DEPTHS **c47**

R. F. Pueschel, P. B. Russell, Thomas P. Ackerman, D. C. Colburn, R. C. Wrigley, M. A. Spanner, and J. M. Livingston (SRI International Corp., Menlo Park, CA.) *In* Deutscher Wetterdienst, Annals from the German Meteorological Society, No. 25: 10th International Cloud Physics Conference Preprints, Volume 1 1988 p 125-126 (For primary document see N89-19605 12-42)

Copyright Avail: Deutscher Wetterdienst, Frankfurter Strasse 135, D-6050 Offenbach am Main, Fed. Republic of Germany CSCL 04B

An airborne Sun photometer was used to measure optical depths in clear atmospheres between the appearances of broken stratus clouds, and the optical depths in the vicinity of smokes. Results show that (human) activities can alter the chemical and optical properties of background atmospheres to affect their spectral optical depths. Effects of water vapor adsorption on aerosol optical depths are apparent, based on data of the water vapor absorption band centered around 940 nm. Smoke optical depths show increases above the background atmosphere by up to two orders of magnitude. When the total optical depths measured through clouds were corrected for molecular scattering and gaseous absorption by subtracting the total optical depths measured through the background atmosphere, the resultant values are lower than those of the background aerosol at short wavelengths. The spectral dependence of these cloud optical depths is neutral, however, in contrast to that of the background aerosol or the molecular atmosphere. ESA

N89-19647 Meteorological Office, Bracknell (England).

AN OBSERVATIONAL STUDY OF RADIATIVELY DRIVEN CONVECTION **c47**

S. Nicholls *In* Deutscher Wetterdienst, Annals from the German Meteorological Society, No. 25: 10th International Cloud Physics Conference Preprints, Volume 1 1988 p 127-129 (For primary document see N89-19605 12-42)

Copyright Avail: Deutscher Wetterdienst, Frankfurter Strasse 135, D-6050 Offenbach am Main, Fed. Republic of Germany

Convective motion in the cloud top boundary layer, responsible for the cellular patterns observed in stratocumulus clouds, was studied using aircraft. It is suggested that horizontal circulations formed by updrafts spreading out under the inversion scour the cloud top interface, incorporating air which was radiatively cooled and/or partially mixed with inversion air before being forced down in narrow convergence zones. These downdrafts subsequently accelerate because of their net negative buoyancy, mixing internally and with the surrounding cloud. Updrafts compensating for this downward mass flux rise until they near the inversion where they are forced to spread out. This interpretation is also consistent with the measured turbulent kinetic energy balance. ESA

N89-19648 Colorado State Univ., Fort Collins. Dept. of Atmospheric Science.

RADIATIVE INFLUENCES ON PRECIPITATING MESOSCALE SYSTEMS **c47**

William R. Cotton, S. Chen, and Gregory J. Tripoli (Wisconsin Univ., Madison.) *In* Deutscher Wetterdienst, Annals from the German Meteorological Society, No. 25: 10th International Cloud Physics Conference Preprints, Volume 1 1988 p 130-132 (For primary document see N89-19605 12-42)

(Grant NSF ATM-85-12480)

Copyright Avail: Deutscher Wetterdienst, Frankfurter Strasse 135, D-6050 Offenbach am Main, Fed. Republic of Germany

The results of model sensitivity experiments to long and short-wave radiation using the Colorado State University Regional Atmospheric Modeling System (RAMS) is described. The model response to radiation is investigated for three different mesoscale convective systems (MCS): an isolated MCS over the High Plains of the United States; a pre-frontal squall line observed during the Australian Cold Fronts Research Program; and an orogenic MCS to the east of the Colorado mountains. The three cases illustrate that longwave radiation can have a significant influence on the behavior of mesoscale convective systems. The simulated interactions between radiation and the dynamics of MCS is strong enough to merit further refinement in the radiation and microphysical parameterizations. The impact of longwave radiation can involve very complex interactions that in some cases is directly related to the destabilization of the cloud layer while in other cases the link is more indirect through the trapping of gravity wave energy in the troposphere. ESA

N89-19649* National Aeronautics and Space Administration. Ames Research Center, Moffett Field, CA.

CIRRUS MICROPHYSICS AND INFRARED RADIATIVE TRANSFER: A CASE STUDY **c46**

Thomas P. Ackerman, Andrew J. Heymsfield (National Center for Atmospheric Research, Boulder, CO.), Francisco P. J. Valero, and Stefan Kinne *In* Deutscher Wetterdienst, Annals from the German Meteorological Society, No. 25: 10th International Cloud Physics Conference Preprints, Volume 1 1988 p 133-134 (For primary document see N89-19605 12-42)

Copyright Avail: Deutscher Wetterdienst, Frankfurter Strasse 135, D-6050 Offenbach am Main, Fed. Republic of Germany CSCL 04A

Coincident measurements of cirrus cloud microphysical properties such as particle size distribution and particle shape and morphology, and measurements of infrared intensity and flux were made. Data was acquired nearly simultaneously in space and time by a KingAir in cloud and by an ER-2 at an altitude of 19 km. Upwelling infrared intensities and fluxes measured from the ER-2 and observations of cloud particle size distributions and particle phase and morphology made from the KingAir are discussed. Broad-band flux measurements were available both in and below the cirrus layer from the KingAir. ESA

N89-19650 Atmospheric Environment Service, Downsview (Ontario).

THE COLLECTION EFFICIENCY OF A MASSIVE FOG COLLECTOR **c47**

Robert S. Schemenauer and Paul I. Joe *In* Deutscher Wetterdienst, Annals from the German Meteorological Society, No. 25: 10th International Cloud Physics Conference Preprints, Volume 1 1988 p 135-137 (For primary document see N89-19605 12-42)

Copyright Avail: Deutscher Wetterdienst, Frankfurter Strasse 135, D-6050 Offenbach am Main, Fed. Republic of Germany

Fog was collected in 10 m long, 4 m high meshes called atrapaniebla to see if fog water can be exploited in arid zones. The measured output is 58 percent of the expected output based on measured and calculated collection efficiencies at the center of the collector. Reduced collection efficiencies due to a lower average wind over the mesh cannot explain the discrepancy. It is postulated that blockage of the wind by the large collector results

in flow around the edges of the collector and thus a lower water droplet availability for collection. ESA

N89-19651 Meteorological Office, Bracknell (England).
THE USE OF AUTOMATIC PARTICLE RECOGNITION TO IMPROVE THE DETERMINATION OF BULK QUANTITIES FROM PMS 2-D PROBE DATA IN CIRRUS **c47**
A. G. Darlison and P. R. A. Brown *In* Deutscher Wetterdienst, Annals from the German Meteorological Society, No. 25: 10th International Cloud Physics Conference Preprints, Volume 1 1988 p 138-140 (For primary document see N89-19605 12-42)
Copyright Avail: Deutscher Wetterdienst, Frankfurter Strasse 135, D-6050 Offenbach am Main, Fed. Republic of Germany

An automatic particle recognition scheme based on Fourier transforms and geometry is found to successfully distinguish cirrus particles. Some poorly imaged crystals are misclassified as bullet rosettes. Such images are overcounted because of depth-of-field effects, but this does not seriously affect bulk quantities. Uncertainties in mass and fall speed relations introduce errors in the corresponding bulk quantities: a factor of 2 for IWC and 3 to 4 for precipitation rate. Number concentrations inferred for small particles depend on what is assumed about their shape in the depth of field calculation. However this source of error is unlikely to affect other bulk parameters. ESA

N89-19652 Meteorological Office, Bracknell (England).
THE COMPARISON OF HOLOGRAPHIC AND 2-D PROBE MEASUREMENTS OF ICE CRYSTALS **c46**
P. R. A. Brown and A. G. Darlison *In* Deutscher Wetterdienst, Annals from the German Meteorological Society. No. 25: 10th International Cloud Physics Conference Preprints, Volume 1 1988 p 141-143 (For primary document see N89-19605 12-42)
Copyright Avail: Deutscher Wetterdienst, Frankfurter Strasse 135, D-6050 Offenbach am Main, Fed. Republic of Germany

Ice crystal concentrations were measured in glaciating maritime cumulus clouds using PMS 2-D optical array probes and an airborne holographic system. For columnar crystals of length greater than 140 microns, the holographic values are a factor of 5 larger than those from the 2-D probes. Similar factors are also found for irregular ice particles larger than 140 microns and for all ice particles smaller than this limit. Sources of error in both instruments were investigated. The main causes of discrepancies lie with the 2-D system, but no single error source can account for the whole of the difference. ESA

N89-19653 Meteorological Research Inst., Tsukuba (Japan).
DEVELOPMENT OF HYDROMETEOR VIDEO SONDE **c35**
Masataka Murakami and Takayo Matsuo *In* Deutscher Wetterdienst, Annals from the German Meteorological Society, No. 25: 10th International Cloud Physics Conference Preprints, Volume 1 1988 p 144-147 (For primary document see N89-19605 12-42)
Copyright Avail: Deutscher Wetterdienst, Frankfurter Strasse 135, D-6050 Offenbach am Main, Fed. Republic of Germany

A sonde (HYVIS) for measuring cloud and precipitation particles is described. The HYVIS provides high quality images of hydrometeors from 7 microns to 2 cm in size and a fine vertical resolution (50 m) of microphysical structure in clouds. To obtain particle images together with meteorological data, the HYVIS and a standard rawinsonde are attached to the same balloon and are launched into clouds at ascent velocity of 5 m/sec. The HYVIS transmits images of hydrometeors taken by 2 TV cameras over a 1687 MHz microwave link to a ground station in real time so that it does not need to be retrieved later. At the same time, meteorological elements such as temperature, humidity, and pressure are also transmitted at a frequency of 1680 MHz. These two microwaves of different frequencies are received by 1 antenna assembly with a 1.2 m parabolic dish. ESA

N89-19654 Mainz Univ. (Germany, F.R.). Inst. for Meteorology.
THE STUDY OF THE INTERSTITIAL AEROSOL PARTICLES AND CLOUD DROPLETS WITH DIGITAL IMAGE ANALYSIS OF DIFFRACTION IMAGES **c47**
R. Jaenicke and R. Soerensen *In* Deutscher Wetterdienst, Annals from the German Meteorological Society, No. 25: 10th International Cloud Physics Conference Preprints, Volume 1 1988 p 148-150 Sponsored by the Deutsche Forschungsgemeinschaft, Bonn, Fed. Republic of Germany (For primary document see N89-19605 12-42)
Copyright Avail: Deutscher Wetterdienst, Frankfurter Strasse 135, D-6050 Offenbach am Main, Fed. Republic of Germany

A digital imaging technique for examining discrete airborne particles is presented. The particles are sent through a laser beam using clean air sheet technique so that single particles can be isolated. A spherical droplet shows a diffraction image of circular geometry, while a dry one does not. The diffraction image is directly recorded by a video camera connected to either a recorder or a personal computer. The time of processing can be regarded as nonsampling time. Processing of an image lasts 10 to 30 sec depending on the complexity of the scattered image. ESA

N89-19655 Stockholm Univ. (Sweden). Dept. of Meteorology.
ON THE DETERMINATION OF DROPLET SIZE DISTRIBUTIONS WITH THE COUNTERFLOW VIRTUAL IMPACTOR **c35**
B. Johansson and Jost Heintzenberg *In* Deutscher Wetterdienst, Annals from the German Meteorological Society, No. 25: 10th International Cloud Physics Conference Preprints, Volume 1 1988 p 151-153 (For primary document see N89-19605 12-42)
Copyright Avail: Deutscher Wetterdienst, Frankfurter Strasse 135, D-6050 Offenbach am Main, Fed. Republic of Germany

A way of obtaining particle size distribution through an inversion of parameters which are measured in the CVI is described. The method of retrieving the cloud drop size distribution has the advantage of yielding an internal consistency with the chemical properties measured in the same probe. It is a randomized minimization search technique, where the basic idea is to find a histogram-type size distribution whose properties have a minimum deviation from the measured properties. ESA

N89-19656 Deutsche Forschungs- und Versuchsanstalt fuer Luft- und Raumfahrt, Wesseling (Germany, F.R.). Inst. fuer HF-Technik.
MULTIPARAMETER CHARACTERIZATION OF RAINDROP SIZE DISTRIBUTION BY THE POLARIMETRIC DFVLR RADAR: FIRST RESULTS **c47**
M. Chandra, A. Schroth, and E. Lueneburg *In* Deutscher Wetterdienst, Annals from the German Meteorological Society, No. 25: 10th International Cloud Physics Conference Preprints, Volume 1 1988 p 154-157 (For primary document see N89-19605 12-42)
Copyright Avail: Deutscher Wetterdienst, Frankfurter Strasse 135, D-6050 Offenbach am Main, Fed. Republic of Germany

Radar determination of raindrop size distribution via a two parameter description was assessed. Using Z sub DR and Z sub HH measurements, radar estimates of D0 and N0 were obtained where Z = reflectivity; D = drop diameter; R = rain rate; and N(D) = raindrop size distribution. These were used to estimate rain rate, specific attenuation, and the accumulated attenuation along a ray. Comparison with empirical results reveals three observations linked to the magnitudes of Z sub DR values: (1) For Z sub DR greater than 2.5 dB, the radar predicted parameters (except N0) show satisfactory agreement with the empirical cases for -2 to 2 microns. (2) The Z sub DR values from 2.5 to 5.5 dB, interpreted as rain volumes, present large systematic departures from empirical results. (3) The Z sub DR greater than 6.5 dB results cannot be simply interpreted in terms of raindrop size distributions. ESA

N89-19657 Institute of Experimental Meteorology, Obninsk (USSR).
AN INVESTIGATION OF THE EFFECT OF ELECTRICAL CHARGES ON THE COLLISION EFFICIENCY OF CLOUD DROPS **c46**
V. M. Kim *In* Deutscher Wetterdienst, Annals from the German Meteorological Society, No. 25: 10th International Cloud Physics Conference Preprints, Volume 1 1988 p 158-160 (For primary document see N89-19605 12-42)
Copyright Avail: Deutscher Wetterdienst, Frankfurter Strasse 135, D-6050 Offenbach am Main, Fed. Republic of Germany

Theoretical investigations of the effects of drop electric charges on the gravitational coagulation process of drops of significantly varying sizes, while increasing their charge to the limiting values, are summarized. The intermediate Reynolds numbers ranging from 10 to 60, which correspond to fall velocities of the collector drops with radii ranging from 100 to 250 microns are studied because of the lack of data on the strongly charged drop growth velocity due to coagulation with neutral and charged droplets of radii from 1 to 20 microns. The drop size and charge range is the range in which particle growth occurs in clouds including thunderstorm clouds. Modification methods of warm clouds intended for precipitation growth enhancement are developed also in this range. ESA

N89-19658 High Mountain Geophysical Inst., Nalchik (USSR).
MICROPHYSICAL AND ELECTRICAL PHENOMENA DURING FREEZING OF WATER DROPS **c46**
A. Kh. Adzhiev and S. T. Tomazov *In* Deutscher Wetterdienst, Annals from the German Meteorological Society, No. 25: 10th International Cloud Physics Conference Preprints, Volume 1 1988 p 161-163 (For primary document see N89-19605 12-42)
Copyright Avail: Deutscher Wetterdienst, Frankfurter Strasse 135, D-6050 Offenbach am Main, Fed. Republic of Germany

The influence of various factors on electric charge separation during water droplet freezing was studied. Results indicate that a maximum charge, separated during explosive splitting of droplets, can attain 10 to the minus 11th power Coulombs. Electric charge separation time for the explosive splitting is from 0.001 to 0.1 sec. The rate of current build up is from 10 to the minus 10 to minus 11th power a/sec. Dynamic structural changes at interfaces are accompanied by electromagnetic emission in a wide range of frequencies. ESA

N89-19659 Academy of Sciences of the Georgian SSR, Tbilisi. Inst. of Geophysics.
EFFECT OF THE ELECTRIC FIELD ON THE RAINDROP SHAPE **c46**
Georgi Magradze *In* Deutscher Wetterdienst, Annals from the German Meteorological Society, No. 25: 10th International Cloud Physics Conference Preprints, Volume 1 1988 p 166-168 (For primary document see N89-19605 12-42)
Copyright Avail: Deutscher Wetterdienst, Frankfurter Strasse 135, D-6050 Offenbach am Main, Fed. Republic of Germany

Electric field effect on a raindrop falling with terminal velocity under the action of aerodynamic and gravitational forces is analyzed. The velocity vector is parallel to the electric field strength Eo and to the oz-axis directed downwards. An Eo less than 6 kV/cm has no effect on drops of radii less than 0.15 cm. An Eo less than 3 kV/cm has a weak effect on drops of radius 0.15 to 0.35 cm. For Eo greater than 3 kV/cm, large drops become elongated along the strength vector; the greater the radius, the stronger the elongation. ESA

N89-19660 Trinity Coll., Hartford, CT.
DAMPED-OSCILLATION REPRESENTATION OF DROP-SPECTRUM EVOLUTION DUE TO COALESCENCE AND BREAKUP **c46**
Philip S. Brown, Jr. *In* Deutscher Wetterdienst, Annals from the German Meteorological Society, No. 25: 10th International Cloud Physics Conference Preprints, Volume 1 1988 p 169-171 (For primary document see N89-19605 12-42)
(Grant NSF ATM-85-21417)
Copyright Avail: Deutscher Wetterdienst, Frankfurter Strasse 135, D-6050 Offenbach am Main, Fed. Republic of Germany

A mathematical form to describe the transient behavior which represents the departure of the raindrop spectrum from equilibrium is outlined. The exponential functions damp in time, while some oscillate as they decay. One particular damped oscillation represents extremely well the departure of the drop spectrum from equilibrium in the small-drop range. The damped oscillation explains the nonmonotonic behavior of a significant portion of the spectrum, and provides a convenient parameterization. Other representative functions can be found to describe the temporal behavior of the mid-size and large-drop portions of the drop-size distribution. ESA

N89-19661 Israel Meteorological Service, Bet Dagan. Dept. of Research and Development.
KINETIC EQUATION FOR POLLUTED CLOUD DROPLETS SPECTRUM **c46**
Isaac M. Enukashvily *In* Deutscher Wetterdienst, Annals from the German Meteorological Society, No. 25: 10th International Cloud Physics Conference Preprints, Volume 1 1988 p 172-174 (For primary document see N89-19605 12-42)
Copyright Avail: Deutscher Wetterdienst, Frankfurter Strasse 135, D-6050 Offenbach am Main, Fed. Republic of Germany

Pollutant distribution in polluted cloud droplets (PCD) was investigated. The kinetic equation for the time evolution of PCD number density function n(x,y,t) is derived; n(x,y,t) evolves with time as a result of microphysical processes of coalescence, of condensation/evaporation, and as a result of diffusion of pollutant gas molecules (or ions) from ambient air. Analytic solutions of the coalescence kinetic equation (CKE) with constant coalescence kernel are obtained for exponential and monodisperse initial spectra of PCD using the double Laplace transform. A numerical method of moments is developed for numerical integration of CKE with an arbitrary coalescence kernel. To test the numerical method of moments computations are performed using as a test problem the analytic solutions. ESA

N89-19662 Deutsche Forschungs- und Versuchsanstalt fuer Luft- und Raumfahrt, Oberpfaffenhofen (West Germany). Inst. fuer Physik der Atmosphaere.
LIQUID WATER CONTENT, MEDIAN VOLUME DIAMETER AND TEMPERATURE IN DEPENDENCE ON THE HEIGHT ABOVE THE CLOUD BASE FOR DIFFERENT TYPES OF CLOUDS **c47**
H.-E. Hoffmann and R. Roth *In* Deutscher Wetterdienst, Annals from the German Meteorological Society, No. 25: 10th International Cloud Physics Conference Preprints, Volume 1 1988 p 175-177 (For primary document see N89-19605 12-42)
Copyright Avail: Deutscher Wetterdienst, Frankfurter Strasse 135, D-6050 Offenbach am Main, Fed. Republic of Germany

Icing flights were conducted to investigate the dependence of the normalized icing on cloud physical parameters. To improve the forecast of normalized icing degrees, the flights were used to get information about the dependence of relevant icing cloud physical parameters on cloud parameters (cloud species and the height above the cloud base). The dependence of the cloud physical parameters liquid water content (LWC) temperature, and median volume diameter on the height above the cloudbase for different types of clouds is shown. To assess the reliability of measurements on LWC, values measured with the Johnson-Williams hot wire instrument and the Knollenberg instruments are plotted. ESA

N89-19663 Iowa State Univ. of Science and Technology, Ames. Dept. of Meteorology.
A DETAILED EXAMINATION OF DISCONTINUITIES IN NATURAL RAIN SPECTRA **c47**
Harry C. Vaughan *In* Deutscher Wetterdienst, Annals from the German Meteorological Society, No. 25: 10th International Cloud Physics Conference Preprints, Volume 1 1988 p 178-179 (For primary document see N89-19605 12-42)

Copyright Avail: Deutscher Wetterdienst, Frankfurter Strasse 135, D-6050 Offenbach am Main, Fed. Republic of Germany

The development of transient and seemingly stationary perturbations in raindrop spectra was studied, using a primitive cloud droplet growth model where only the accretion growth mechanism was considered. As the model output suggests, if in nature there is a tightly regimented mechanical growth process, the product would be perturbations resulting from discrete jumps where only selected drop size ratios make lasting coalescence. It is hard to reconcile the systematic distribution of these perturbations from the largest drop size down through the rain spectra by a breakup mechanism. The perturbations are real with differences as great as an order of magnitude, in mg, observed between adjacent null minim and peaks. When three point smoothing is applied to raw data the perturbations are lost, particularly in low rain rate samples. This suggests that a finely-balanced accretion process occurs in the development of the drop spectra. At least a portion of these data supports results reported by Niederdorfer (1932). ESA

N89-19664* Desert Research Inst., Reno, NV.
CRYSTALLIZATION OF SUPERCOOLED SOLUTIONS **c47**
K. Harrison and John Hallett *In* Deutscher Wetterdienst, Annals from the German Meteorological Society, No. 25: 10th International Cloud Physics Conference Preprints, Volume 1 1988 p 180-182 (For primary document see N89-19605 12-42)
(Contract NAS7-918)
Copyright Avail: Deutscher Wetterdienst, Frankfurter Strasse 135, D-6050 Offenbach am Main, Fed. Republic of Germany
CSCL 04B

Crystallization of uniformly supercooled solutions (Na2SO4, NaCl, H2SO4, HNO3, HCl) was studied. It is shown how crystal growth velocity and habit depend on solution and concentration. The segregation coefficient for the solute in ice is measured by analysis of ice and solution, separated immediately after initial freezing, at different supercoolings. Subsequent solidification gives ion rejection at a varying rate depending on the geometry of the freezing, and may result in separation of hydrates, particularly when the initial concentration is high, as in haze (inactivated) droplets and low temperatures found in the Antarctic stratosphere. Electrical effects associated with rapid freezing are also investigated. Results suggest that more extensive measurements need to be made in solutions at different supercoolings, and that substantial electrical effects may be present for higher concentrations under these conditions. Damage to vegetation could occur under specific conditions as concentrated solutions (possibly H2SO4) are rejected in the freezing of rime or dew. ESA

N89-19665 Institute of Chemical Kinetics and Combustion, Novosibirsk (USSR).
KINETICS OF ICE CRYSTAL FORMATION ON AEROSOL PARTICLES IN SUPERCOOLED FOG **c47**
Boris Gorbunov, Aleksandr Paschenko, and Hatalya Kakutkina *In* Deutscher Wetterdienst, Annals from the German Meteorological Society, No. 25: 10th International Cloud Physics Conference Preprints, Volume 1 1988 p 183-184 (For primary document see N89-19605 12-42)
Copyright Avail: Deutscher Wetterdienst, Frankfurter Strasse 135, D-6050 Offenbach am Main, Fed. Republic of Germany

Ice nucleation kinetics were studied in a cloud chamber under the action of silver iodide, cooper acetyl acetonate, floroglucine and metal oxides at 268, 263, and 253 K. To obtain the kinetic dependences, a two-section cloud chamber with automatic registration was constructed. The kinetic dependences were also determined in an isothermal cloud chamber. A mass-mean size of aerosol particles was determined by electron microscopy. Experimental kinetic curves exhibit three peculiarities: the presence of time lag in crystal formation, and the value of curve slopes at short and long times. ESA

N89-19666 Academy of Sciences of the Georgian SSR, Tbilisi. Inst. of Geophysics.
ABOUT SECONDARY ICE CRYSTAL PRODUCTION **c47**
T. Gzirishvili and V. Khorguani *In* Deutscher Wetterdienst, Annals from the German Meteorological Society, No. 25: 10th International Cloud Physics Conference Preprints, Volume 1 1988 p 185-187 (For primary document see N89-19605 12-42)
Copyright Avail: Deutscher Wetterdienst, Frankfurter Strasse 135, D-6050 Offenbach am Main, Fed. Republic of Germany

Collision of supercooled water drops with the ice surface, kinetics of the process of their solidification, and origin of secondary ice crystals in the presence or absence of the external electric field were investigated. Experiments were carried out in a small cloud chamber in the central part of which a vertically oriented electric field was established. Results delineate processes favoring the formation of ice crystals: in one case as a result of mechanical action, in another as a result of activation of heterogeneous nucleation of ice. A qualitative evaluation shows that the generation of ice crystals is much more in the latter case. The explanation of this phenomenon lies in the origin of comparatively significant over-saturation. ESA

N89-19667 Osaka Kyoiku Univ. (Japan).
EXPERIMENTAL STUDIES ON SECONDARY ICE PARTICLE PRODUCTION **c47**
Akira Yamashita, Hiroyuki Konishi, Wataru Shimada, Masayoshi Miyatake, and Keisuke Tani *In* Deutscher Wetterdienst, Annals from the German Meteorological Society, No. 25: 10th International Cloud Physics Conference Preprints, Volume 1 1988 p 188-189 (For primary document see N89-19605 12-42)
Copyright Avail: Deutscher Wetterdienst, Frankfurter Strasse 135, D-6050 Offenbach am Main, Fed. Republic of Germany

Mechanisms of secondary ice particle production were investigated by two series of experiments. Artificially grown ice needles were evaporated in a subsaturation chamber placed under a stereoscopic microscope, and the whole evaporating process of a needle was observed in situ by a video camera. The length of an ice needle decreases not only by evaporation but also by fragmentation, fracture or deformation of a tip. Ice crystals including many gas enclosures were broken in a supercooled cloud to clarify the effect of expanding enclosed gas. It is found that remarkable ice crystal enhancement occurs by the expansion of enclosed gas as large as 0.5 to 2.0 mm diameter. This type of secondary ice particle production may also be possible in natural clouds. ESA

N89-19668 Hokkaido Univ., Sapporo (Japan). Dept. of Geophysics.
PROPORTION OF RIMING GROWTH PROCESS IN SNOWFALL PHENOMENA **c47**
Toshio Harimaya and Misao Sato *In* Deutscher Wetterdienst, Annals from the German Meteorological Society, No. 25: 10th International Cloud Physics Conference Preprints, Volume 1 1988 p 190-192 (For primary document see N89-19605 12-42)
Copyright Avail: Deutscher Wetterdienst, Frankfurter Strasse 135, D-6050 Offenbach am Main, Fed. Republic of Germany

A method for measuring riming amount on a snowflake was developed to study the difference of riming proportion in the growth of snow particles due to the difference of meteorological conditions and stages in the life cycle of snow clouds. Snowflakes were caught on a piece of velvet cloth and a snowflake was disassembled into each snow crystal by a bamboo skewer on a glass plate as carefully as possible so that it would not fracture. All snow crystals constituting a snowflake were photographed, and classified. The lower limit of riming proportion tends to increase with the increase of snowfall intensity. Snowflakes with various values of riming proportion fall when the snowfall intensity is weak. This is explained by the sorting of snow particles and the difference of meteorological conditions. The riming proportion is large at the developing and mature stage of snow clouds and small at the dissipating stage. This may be explained by the formation of cloud droplets and the riming process by snow particles. ESA

N89-19669 Shinshu Univ., Nagano (Japan). Faculty of Education.
THREE-DIMENSIONAL STRUCTURES OF SNOW CRYSTALS SHOWN BY STEREO-PHOTOMICROGRAPHS **c47**
Kuniomoto Iwai *In* Deutscher Wetterdienst, Annals from the German Meteorological Society, No. 25: 10th International Cloud Physics Conference Preprints, Volume 1 1988 p 193-195 (For primary document see N89-19605 12-42)
Copyright Avail: Deutscher Wetterdienst, Frankfurter Strasse 135, D-6050 Offenbach am Main, Fed. Republic of Germany

The three-dimensional structure of snow crystals was studied by stereo-photomicrography. Most plate-like snow crystals (70 pct) consist of 2 or more plate-like crystals having different forms and sizes. A simple dendritic plate is rarely observed. Apparent pyramidal faces of bullet crystals are not crystallographic faces but mere skeleton structures. ESA

N89-19670 Akita Univ. (Japan). Dept. of Earth Science.
ON THE VARIATION OF FALLING VELOCITY OF EARLY SNOWFLAKES **c47**
Masahiro Kajikawa *In* Deutscher Wetterdienst, Annals from the German Meteorological Society, No. 25: 10th International Cloud Physics Conference Preprints, Volume 1 1988 p 196-198 (For primary document see N89-19605 12-42)
Copyright Avail: Deutscher Wetterdienst, Frankfurter Strasse 135, D-6050 Offenbach am Main, Fed. Republic of Germany

The falling motion in still air of early snowflakes, which are composed of two to six crystals, was analyzed by stereo-photogrammetry. The variations of vertical and horizontal velocity in the spiral or rotational falling motion were empirically obtained. The standard deviation of variation in vertical velocity is small; standard deviation of variation in horizontal velocity is considerbly larger and increases with mean horizontal velocity. It is concluded that the variation of horizontal velocity plays an important role in the aggregation process of snowflakes. The mean horizontal velocity can be estimated from the nondimensional amplitude of the spiral or rotational falling motion. The nondimensional amplitude is inversely related to the non-dimensional frequency of spiral or rotational motion. The nondimensional frequency can be estimated from the Reynolds number with respect to the mean vertical velocity of snowflakes. ESA

N89-19671 Johann-Wolfgang-Goethe-Univ., Frankfurt am Main (Germany, F.R.). Inst. fuer Meteorologie und Geophysik.
A PARAMETRIZATION SCHEME FOR THE COALESCENCE OF WATER DROPS USING THE STOCHASTIC COLLECTION EQUATION **c47**
C. Luepkes, K. D. Beheng, and S. Doms (Deutscher Wetterdienst, Offenbach am Main, Germany, F.R.) *In* Deutscher Wetterdienst, Annals from The German Meteorological Society, No. 25: 10th International Cloud Physics Conference Preprints, Volume 1 1988 p 199-201 (For primary document see N89-19605 12-42)
Copyright Avail: Deutscher Wetterdienst, Frankfurter Strasse 135, D-6050 Offenbach am Main, Fed. Republic of Germany

It is shown how the partitioning concept of Kessler (1969) can be applied to the stochastic collection equation governing the time evolution of a drop size spectrum, and how rate equations analogous to those presented by Kessler can be formulated. Results obtained by this method are compared with those obtained by Kessler's scheme. Starting from this basis a parametrization scheme is outlined. ESA

N89-19672 Missouri Univ., Rolla. Dept. of Mechanical and Aerospace Engineering.
ON THE DYNAMICS OF THE FALLING ICE CRYSTAL ZONE **c47**
Josef Podzimek *In* Deutscher Wetterdienst, Annals from the German Meteorological Society, No. 25: 10th International Cloud Physics Conference Preprints, Volume 1 1988 p 202-204 (For primary document see N89-19605 12-42)
(Contract DAAK11-83-K-0007)
Copyright Avail: Deutscher Wetterdienst, Frankfurter Strasse 135, D-6050 Offenbach am Main, Fed. Republic of Germany

The aerodynamics of ice crystals or snowflakes in reference to the evolution of the falling ice crystal zone was studied. It is shown that the most important parameter determining the evolution of a falling ice crystal zone is the effective mixing ratio of the crystals. The horizontal wind affects strongly the circulation inside and around the precipitation zone. Most of the crystals falling in nature do not perform an intense oscillatory motion except at side wind. Therefore the introduction of an effective mixing ratio in falling precipitation zone equations is feasible. ESA

N89-19673 Naval Research Lab., Washington, DC.
A NEW DATABASE OF ICE PARTICLE SIZE SPECTRA FOR ALTITUDES UP TO 10 km (30,000 ft) **c47**
Richard Jeck *In* Deutscher Wetterdienst, Annals from the German Meteorological Society, No. 25: 10th International Cloud Physics Conference Preprints, Volume 1 1988 p 205-207 Sponsored in part by the Dept. of Transportation, Washington, DC (For primary document see N89-19605 12-42)
Copyright Avail: Deutscher Wetterdienst, Frankfurter Strasse 135, D-6050 Offenbach am Main, Fed. Republic of Germany

About 7600 nautical miles (14,000 km) of ice particle measurements over the United States were compiled into a single, computerized database for use in characterizing ice/snow particle size distributions and mass concentrations at flight altitudes. Primary variables are average particle size spectra in the range 0.1 to 10 mm from each of 1625 microphysically uniform cloud intervals or other convenient distances in wintertime clouds, snowstorms, cirrus, and other high altitude clouds. The database provides a composite view of a large number of diverse ice particle measurements. Differences and similarities in ice particle characteristics among a wide variety of cloud and weather systems are evident. The database is illustrated by plots of particle size, number density, and total mass as a function of temperature. ESA

N89-19674 Nagoya Univ., Toyokawa (Japan).
A VERTICAL WIND TUNNEL FOR THE STUDY OF SNOWFLAKES AND EFFECTS OF ACCUMULATED SNOW ON MATERIALS **c47**
Kenki Isono, Jutaro Kobayashi, Takehiko Gonda, Yoshio Sasyo, and Taro Mori (Suga Test Instruments Co. Ltd., Japan) *In* Deutscher Wetterdienst, Annals from the German Meteorological Society, No. 25: 10th International Cloud Physics Conference Preprints, Volume 1 1988 p 208-210 (For primary document see N89-19605 12-42)
Copyright Avail: Deutscher Wetterdienst, Frankfurter Strasse 135, D-6050 Offenbach am Main, Fed. Republic of Germany

A vertical wind tunnel to study snow effects on industrial materials is presented. Photomicrographs of snowflakes, and test results for a typical plate are shown. ESA

N89-19675 Direction de la Meteorologie Nationale, Magny les Hameaux (France).
PROPERTIES OF THE PRECIPITATION EMBRYOS EVOLUTION IN CHARACTERISTIC HAWAIIAN BAND CLOUDS **c47**
Arlette Rigaud, Elizabeth Hicks, Jacqueline Gagneux, and Constantin Pontikis *In* Deutscher Wetterdienst, Annals from the German Meteorological Society, No. 25: 10th International Cloud Physics Conference Preprints, Volume 1 1988 p 211-213 (For primary document see N89-19605 12-42)
Copyright Avail: Deutscher Wetterdienst, Frankfurter Strasse 135, D-6050 Offenbach am Main, Fed. Republic of Germany

The formation and evolution of droplets in the radii range 20 to 75 micrometer (1DC probe range) are studied for clouds observed during the Joint Hawaiian Warm Rain Project. Cloud bands generated by the low level convergence between the trade wind flow and the nocturnal land breeze were sampled at different levels. This allows the analysis of the 1DC probe 10 Hz measurements according to the cloud depth. The 1DC data analysis

shows that the mean vertical concentration of the corresponding droplets can be represented using an empirical relation N bar = N (Delta Z), where Delta Z is the height above cloud base for Hawaiian warm convective clouds. The 1DC droplet concentrations even in nonprecipitating clouds are larger than the lower limit necessary to produce precipitation in models. Therefore the vertical extent may play the main role in warm rain production in these clouds. ESA

N89-19676 Clermont-Ferrand Univ. (France).
PATTERN OF AIR BUBBLE INCLUSIONS IN ATMOSPHERIC ICE FORMED DURING ACCRETION **c47**
Pascal Gribelin, Pascal Personne, and Harumi Isaka *In* Deutscher Wetterdienst, Annals from the German Meteorological Society, No. 25: 10th International Cloud Physics Conference Preprints, Volume 1 1988 p 214-216 (For primary document see N89-19605 12-42)
Copyright Avail: Deutscher Wetterdienst, Frankfurter Strasse 135, D-6050 Offenbach am Main, Fed. Republic of Germany

Riming experiments were carried out in an open wind tunnel. Fixed cylindrical rods of different diameters (from 0.3 to 5.0 cm) were used as rime collectors for different environmental conditions and for different airflow speeds (from 20 to 60 m/sec). The pattern formed by air bubble inclusions, in accreted ice deposits, obtained under dry growth conditions, shows a quasi-linear arrangement, like channels. The orientation of channels of air inclusions is strongly dependent upon the experimental conditions and can be classified according to the value of the inertial parameter. An analysis of simulation with a ballistic model shows that the columnar growth of aggregates occurs as a result of a statistical fluctuation and a shadowing of droplet impingement. The angle of channel orientation is found experimentally to vary linearly as a function of the angle of droplet impingement. This result agrees well with simulations. ESA

N89-19677 Servicio Meteorologico Nacional, Buenos Aires (Argentina).
ANALYSIS OF HAILSTONES FROM A SEVERE STORM AND THEIR SIMULATED EVOLUTION **c47**
Laura Levi and Luisa Lubart (Comision Nacional de Energia Atomica, Buenos Aires, Argentina) *In* Deutscher Wetterdienst, Annals from the German Meteorological Society, No. 25: 10th International Cloud Physics Conference Preprints, Volume 1 1988 p 217-219 Sponsored in part by the Consejo Nacional de Investigaciones Cientificas y Technicas, Buenos Aires, Argentina (For primary document see N89-19605 12-42)
Copyright Avail: Deutscher Wetterdienst, Frankfurter Strasse 135, D-6050 Offenbach am Main, Fed. Republic of Germany

Possible trajectories and environmental conditions for hailstones with a structure derived from the crystallographic analysis of a stone sample are discussed. A growth model is applied in a simulated updraft, the parameters of which are adjusted so to obtain the excepted trajectories. The simulated hailstone trajectories indicate that the growth process, initialized at the stage where the embryos are formed, should last 50 min (or less if liquid water content was larger). The stone analysis and the model application indicate that, during the growth period preceding the arrival at the main updraft, trajectories could be located at quite different altitudes. This is shown by the structure variety of the main layers following the embryo and is supported by the observation that drag values can vary with the embryo shape and fall mode, determining important changes in the free fall speed of the particle. ESA

N89-19678 Manchester Univ. (England). Dept. of Physics.
THE COLLECTION EFFICIENCIES OF SOFT-HAILSTONES FOR SUPER-COOLED WATER DROPLETS AND ICE CRYSTALS **c47**
W. D. Keith and C. P. R. Saunders *In* Deutscher Wetterdienst, Annals from the German Meteorological Society, No. 25: 10th International Cloud Physics Conference Preprints, Volume 1 1988 p 220-222 (For primary document see N89-19605 12-42)
Copyright Avail: Deutscher Wetterdienst, Frankfurter Strasse 135, D-6050 Offenbach am Main, Fed. Republic of Germany

Laboratory studies were performed to measure the increase, above the theoretical value, in the number of droplets collected by a hailstone rime surface under various conditions. The collision efficiency of a target for ice crystals was measured directly by comparing the number of ice crystals on the target with that number on a slide whose collision and adhesion efficiency was 100 pct. Results show that the theoretical collision efficiency equations cannot be accurately applied to a target with a rough surface as the equations tend to underestimate the efficiency of capture. Calculations show, however, that the growth rate of a hailstone by riming is only increased by 6 pct to 18 pct in the temperture range minus 5 to minus 20 C at an impact speed of 3 m/sec. At 5 m/sec, the increase is 2 pct. The collision efficiency ofa target for ice crystals was determined. The efficiency is less than 100 pct for small ice crystals and the efficiency is lower for column ice crystals than for plate ice crystals. ESA

N89-19679 Clermont-Ferrand Univ. (France).
SIMULATION OF CONICAL GRAUPEL BY USING A BALLISTIC MODEL **c47**
Pascal Personne, Christophe Duroure, and Harumi Isaka *In* Deutscher Wetterdienst, Annals from the German Meteorological Society, No. 25: 10th International Cloud Physics Conference Preprints, Volume 1 1988 p 223-225 (For primary document see N89-19605 12-42)
Copyright Avail: Deutscher Wetterdienst, Frankfurter Strasse 135, D-6050 Offenbach am Main, Fed. Republic of Germany

The extent to which the aggregation process determines by itself the form of rime deposits was studied. The aggregate growth was simulated by simple 2-D and 3-D ballistic models; characteristics of the form of simulated aggregates were compared with those of the rime deposits obtained in icing wind tunnel. Results show that, in spite of their much simplified physics, 2-D and 3-D ballistic models of aggregation can reproduce basic characteristics of fan-like and conical rime growth. Further comparison of simulated and observed rime growth, under various growth conditions, may provide a way to appreciate influences of other physical processes on the growth mechanism of rime. ESA

N89-19680 South Dakota School of Mines and Technology, Rapid City. Inst. of Atmospheric Sciences.
COMPARISON OF MODEL RESULTS FOR MODELS OF DIFFERING MICROPHYSICAL DETAIL **c46**
R. D. Farley and H. D. Orville *In* Deutscher Wetterdienst, Annals from the German Meteorological Society, No. 25: 10th International Cloud Physics Conference Preprints, Volume 1 1988 p 226-228 (For primary document see N89-19605 12-42) (Grants NSF ATM-85-16940; NSF ATM-86-03308)
Copyright Avail: Deutscher Wetterdienst, Frankfurter Strasse 135, D-6050 Offenbach am Main, Fed. Republic of Germany

The use of cloud models to test hail suppression concepts is discussed. Two versions of the same basic model are discussed: a relatively simple model employing bulk water parameterization techniques which is used mainly for diagnostic purposes; and a hybrid form of the parameterized model which treats the precipitating ice field as 20 discrete size categories allowing for more in depth studies of hail growth processes and possible responses to seeding strategies were compared for various hailstorm types. Model results for large scale structures, dynamic features, and evolution are similar. The hybrid model gives higher maximum and domain totals of cloud water and ice for continental cases. Precipitation production is more efficient in the bulk model. Maritime cases show a high degree of consistency in model results. ESA

N89-19681 Drexel Univ., Philadelphia, PA. Dept. of Physics and Atmospheric Science.
AIRBORNE CLOUD SIEVING **c35**
Edward E. Hindman *In* Deutscher Wetterdienst, Annals from

the German Meteorological Society, No. 25: 10th International Cloud Physics Conference Preprints, Volume 1 1988 p 229-231 (For primary document see N89-19605 12-42)
(Contract N00014-84-C-0591; NSF ATM-87-15060; NSF ATM-87-04776)
Copyright Avail: Deutscher Wetterdienst, Frankfurter Strasse 135, D-6050 Offenbach am Main, Fed. Republic of Germany

The Langmuir rotating-multicylinder was simulated to fly through the low liquid water content, wintertime clouds which occur over the northern Colorado Rockies. It was calculated that the multicylinder would collect insufficient cloud water for thorough chemical analyses. Consequently, an airborne cloud sieve was designed consisting of series of sets of nonrotating cylinders to collect drops greater than or equal to 4, 8, 13, and 18 micrometers in diameter. It is found that collecting droplets greater than 24 micrometers with the sieve may be impractical. The series of cylinders was designed so each set collects larger droplets than the previous set, but each set collects a similar amount of cloud water. The behavior of the airborne cloud sieve was simulated in winter mountain clouds and summer cumulus clouds. It is found the device should collect sufficient cloud water (2 to 9 g) over a droplet diameter range of 4 to 18 micrometers to perform thorough chemical characterizations. Such chemical information is valuable for improving understanding of the acidification of cloud droplets and the optical properties of cloud droplets. ESA

N89-19682 North Carolina State Univ., Raleigh. Dept. of Marine, Earth and Atmospheric Sciences.
CLOUD CAPTURE BY A MOUNTAIN TOP FOREST. PART 1: ACIDITY AND DOSAGE DURATION **c45**
V. K. Saxena and N.-H. Lin *In* Deutscher Wetterdienst, Annals from the German Meteorological Society, No. 25: 10th International Cloud Physics Conference Preprints, Volume 1 1988 p 232-234 (For primary document see N89-19605 12-42)
(Contracts EPA-81-39-3401-2; EPA-81-24-430)
Copyright Avail: Deutscher Wetterdienst, Frankfurter Strasse 135, D-6050 Offenbach am Main, Fed. Republic of Germany

The data base for Mt. Mitchell (North Carolina) for the summers of 1986 and 1987 regarding the acidity of cloud water and exposure of the mountain top forest to acidic substances in clouds is analyzed. Cloud events were categorized into 2 classes, long cloud events with a duration exceeding 8 hr and short cloud events lasting no more than 8 hr. The former are attributed to the frontal passages, and the latter to orographic lifting mechanisms. In addition to these two cloud event types, cloud events with precipitation are categorized as mixed events. A summary of the observed cloud events and the collected samples is given. The corresponding accumulative and average duration of events are listed. Both tables show that total samples collected in 1986 are 70 pct in excess of 1987, and the frequency of long cloud events is half that of short cloud events in 1986, but very few long cloud events were observed in 1987. However, the total number of cloud events for both years are not distinctly different. On average, cloud episodes in 1986 were significantly longer than in 1987. Sulfates account for 78 pct and 63 pct of acidity for 1986 and 1987 respectively. ESA

N89-19683 Technische Univ., Munich (Germany, F.R.). Meteorologisches Inst.
DETERMINATION OF CHEMICAL REACTION RATES IN FOG **c45**
Ralph Dlugi and Winfried Seidl *In* Deutscher Wetterdienst, Annals from the German Meteorological Society, No. 25: 10th International Cloud Physics Conference Preprints, Volume 1 1988 p 235-237 (For primary document see N89-19605 12-42)
Copyright Avail: Deutscher Wetterdienst, Frankfurter Strasse 135, D-6050 Offenbach am Main, Fed. Republic of Germany

Field experiments to study the oxidation and absorption of trace gases in radiation and advection fog are described. Most experiments were performed near the ground in polluted areas. Few data are available from vertically resolved measurements of microphysical and micrometeorological parameters and chemical compounds. Results from this kind of study are presented and are discussed with respect to the oxidation of traces gases like SO2 and NOx and the formation of H2O2. The effects of wind, and differences between night and daytime processes are noted. ESA

N89-19684 Mainz Univ. (Germany, F.R.). Inst. of Meteorology.
INSOLUBLE PARTICLES IN HYDROMETEORS **c45**
M. Kraemer and L. Schuetz *In* Deutscher Wetterdienst, Annals from the German Meteorological Society, No. 25: 10th International Cloud Physics Conference Preprints, Volume 1 1988 p 238-240 Sponsored in part by the Deutsche Forschungsgemeinschaft, Bonn, Fed. Republic of Germany (For primary document see N89-19605 12-42)
Copyright Avail: Deutscher Wetterdienst, Frankfurter Strasse 135, D-6050 Offenbach am Main, Fed. Republic of Germany

Studies of insoluble particles and dissolved material in cloud, fog, and rainwater are summarized. Results on number size and volume distributions, total mass, and elemental composition of the insoluble constituents are emphasized. For particles of radii greater than 0.5 micrometer, the shape of the number size distribution of insoluble particles in rain follows the shape of the average distribution of aerosol particles. In this size range no major size selective removal processes is seen. For smaller particles, number size and in particular volume distribution tends to flatten compared with the average distribution of aerosol particles. This is not caused by the increase of the fraction of soluble material in the atmospheric aerosol particles in this size range, but rather might be an indication of a size selective removal process. In the scavenging of aerosol particles a minimum between 0.1 and 1.0 micrometer particle radius is seen. The total insoluble mass in rainwater ranges between 1 and 4 mg per liter rainwater. The elemental composition of 60 single particles was determined for 1 sample. No correlation is found between the size of particles and their elemental composition or their appearance. The main elements contained in all investigated insoluble particles are Al, Si, Fe, followed by S and K; Na, Mg, Cl, Ca, Ti, Zn, Cu, and Au are present as trace substances. ESA

N89-19685 University Coll., Galway (Ireland).
BELOW CLOUD SCAVENGING BY RAIN AND DRIZZLE **c47**
Brendan Thomas McGann and S. Gerard Jennings *In* Deutscher Wetterdienst, Annals from the German Meteorological Society, No. 25: 10th International Cloud Physics Conference Preprints, Volume 1 1988 p 241-242 (For primary document see N89-19605 12-42)
Copyright Avail: Deutscher Wetterdienst, Frankfurter Strasse 135, D-6050 Offenbach am Main, Fed. Republic of Germany

Assuming a Marshall-Palmer distribution for the raindrop spectrum, precipitation scavenging rates for various sized aerosol particles were calculated. The scavenging rates correspond to atmospheric conditions of 900 mb, 10 C, 50 pct relative humidity. For each aerosol radius the scavenging rate was calculated with and without electric charges on the raindrop and aerosol particle. Results support the existence of the so-called Greenfield gap. ESA

N89-19686 Desert Research Inst., Reno, NV.
STUDIES OF CLOUD MICRO-CHEMICAL PHYSICS **c46**
Richard L. Pitter and William G. Finnegan *In* Deutscher Wetterdienst, Annals from the German Meteorological Society, No. 25: 10th International Cloud Physics Conference Preprints, Volume 1 1988 p 243-245 Sponsored in part by ONR, Washington, DC and NOAA, Washington, DC (For primary document see N89-19605 12-42)
Copyright Avail: Deutscher Wetterdienst, Frankfurter Strasse 135, D-6050 Offenbach am Main, Fed. Republic of Germany

A cloud chamber was used to conduct isothermal and isobaric studies of ice crystal formation and early growth. Water clouds were generated with ultrasonic nebulizers, using 0.0001 N solutions of salts commonly associated with cloud and precipitation water, in concentrations similar to those found in clouds and precipitation. Ice was nucleated by adiabatic expansion of moist air. Observations indicate that the solute present in the supercooled water is

incorporated into the growing ice crystals and subsequently plays important roles in microphysical processes which are highly pertinent to the formation of precipitation. Ice crystal habit, aggregation, and secondary ice formation results are highlighted. ESA

N89-19687 Witten/Herdecke Univ. (Germany, F.R.). Inst. for Inorganic Chemistry.

KINETICS AND MECHANISM OF THE Fe CATALYZED AUTOXIDATION OF S(4)-OXIDES IN AQUEOUS SOLUTION **c25**

J. Kraft, M. Dellert, P. Braun, and R. vanEldik *In* Deutscher Wetterdienst, Annals from the German Meteorological Society, No. 25: 10th International Cloud Physics Conference Preprints, Volume 1 1988 p 246-247 (For primary document see N89-19605 12-42)

Copyright Avail: Deutscher Wetterdienst, Frankfurter Strasse 135, D-6050 Offenbach am Main, Fed. Republic of Germany

The Fe(3)-catalyzed process was studied using fast kinetic and spectroscopic techniques. Model Fe(3) complexes were selected to investigate their interaction with S(4)-oxides and the catalytic nature of the produced sulfito complexes. Complex formation reactions and redox reactions are illustrated. ESA

N89-19688 Army Cold Regions Research and Engineering Lab., Hanover, NH.

THE EFFECT OF AEROSOLS ON pH OF SNOWFALLS **c45**

Motoi Kumai *In* Deutscher Wetterdienst, Annals from the German Meteorological Society, No. 25: 10th International Cloud Physics Conference Preprints, Volume 1 1988 p 249-250 (For primary document see N89-19605 12-42)

Copyright Avail: Deutscher Wetterdienst, Frankfurter Strasse 135, D-6050 Offenbach am Main, Fed. Republic of Germany

Chemical analysis of aerosols, aerosol concentration, pH, and electrolytic conductivity of fresh snowfalls were measured during 5 winters from 1972-1973 to 1983-1987 in New Hampshire. The relation between pH values and wind direction during snowfalls was examined. Fly-ash particles and other kinds of atmospheric aerosols in fresh snow were examined by scanning electron microscope and the elemental compositions were measured by energy dispersive analyzer to identify the minerals and their origins. The results on snow from New Hampshire are compared with those obtained from snow accumulated from 1981 to 1983 at Dye-3, Greenland. ESA

N89-19689 Nanjing Univ. (China). Dept. of Atmospheric Sciences.

IONIC CONCENTRATIONS OF RIME ICE AND SNOW AND BERGERON PROCESS **c47**

Shi-Hong Huang, R. A. Castillo, and V. K. Monhen (State Univ. of New York, Albany.) *In* Deutscher Wetterdienst, Annals from the German Meteorological Society, No. 25: 10th International Cloud Physics Conference Preprints, Volume 1 1988 p 251-253 (For primary document see N89-19605 12-42)

Copyright Avail: Deutscher Wetterdienst, Frankfurter Strasse 135, D-6050 Offenbach am Main, Fed. Republic of Germany

The effect of the Bergeron process in a supercooled cloud on snow ion concentrations is described. The data from two mountains show that ion concentrations in snow are generally lower than those measured in rime ice with a lower pH value. Results for one of the mountains demonstrate that the Bergeron process occurring in supercooled clouds may be the main reason for this ion concentration difference. The variation of ion concentrations in precipitation may in part be due to a higher percentage of solid precipitation. ESA

N89-19690 Technische Univ., Munich (Germany, F.R.). Meteorologisches Inst.

A ONE-DIMENSIONAL NUMERICAL MODEL TO SIMULATE LIQUID PHASE CHEMICAL REACTIONS WITHIN RADIATION FOG **c45**

Renate Forkel and Winfried Seidl *In* Deutscher Wetterdienst, Annals from the German Meteorological Society, No. 25: 10th International Cloud Physics Conference Preprints, Volume 1 1988 p 255-257 (For primary document see N89-19605 12-42)

Copyright Avail: Deutscher Wetterdienst, Frankfurter Strasse 135, D-6050 Offenbach am Main, Fed. Republic of Germany

A one-dimensional model for fog prediction is described. Fog chemistry is treated by a hybrid kinetic and equilibrium model for the bulk liquid phase. The model predicts vertical profiles of temperature, water vapor, liquid water, and gas and liquid phase reactant concentrations. A case study shows that for the case discussed the total deposition of S(6) due to sedimentations is 1.5 mg/sq m during the fog event. Since only the bulk properties of the liquid phase are calculated by the model, no size dependence of the aerosol composition can be taken into account. For aerosol types, which are acidic over the full range of size, the bulk model can yield reliable results. However, if for example, large basic aerosol particles are present, the oxidation rates calculated by the bulk model are not correct anymore. For this reason it is intended to introduce droplet microphysics into the model. This increases the range of application for the model, as it is then possible to account for size dependent aerosol composition and oxidation rates within the droplets. ESA

N89-19691 Toronto Univ. (Ontario). Physical Labs.

THE EFFECT OF FREEZING ON THE COMPOSITION OF CLOUD DROPLETS **c47**

J. V. Iribarne and T. Pyshnov *In* Deutscher Wetterdienst, Annals from the German Meteorological Society, No. 25: 10th International Cloud Physics Conference Preprints, Volume 1 1988 p 258-260 (For primary document see N89-19605 12-42)

Copyright Avail: Deutscher Wetterdienst, Frankfurter Strasse 135, D-6050 Offenbach am Main, Fed. Republic of Germany

The fraction of solutes retained by frozen droplets (retention coefficient) was studied in a cloud chamber. Experiments regarding possible losses of HC1, HNO3, NH3, and H2O2 during freezing indicate that these chemical species are totally retained by the ice. Experiments with SO2 relevant to cloud chemistry are those producing riming conditions. Values of retention coefficient for these conditions, to be used in chemistry models are given. Two-thirds of the S(4) contained in droplets remain in the ice after freezing, the remaining third being transferred to the interstitial air; there is only a slight dependence of the retention coefficient between minus 8 and minus 23 C. ESA

N89-19692 Washington Univ., Seattle. Dept. of Atmospheric Sciences.

SOME EFFECTS OF CLOUD MICROPHYSICS ON CLOUD CHEMISTRY **c46**

Dean A. Hegg and Peter V. Hobbs *In* Deutscher Wetterdienst, Annals from the German Meteorological Society, No. 25: 10th International Cloud Physics Conference Preprints, Volume 1 1988 p 261-263 (For primary document see N89-19605 12-42)

(Grant NSF ATM-84-19000)

Copyright Avail: Deutscher Wetterdienst, Frankfurter Strasse 135, D-6050 Offenbach am Main, Fed. Republic of Germany

The nucleation of cloud droplets on discreet nuclei is reviewed. The initiation of ice and interactions between ice and liquid water hydrometeors are discussed. It is shown that rapid condensational growth after nucleation on the largest condensation nuclei produces H(+) by progressive ionization of the bisulfate ion with decreasing solution strength. While NH3 is absorbed into these droplets as a consequence of the H(+) production, the rapidity of droplet growth precludes the attainment of gas-aqueous equilibrium. By the time that smaller CCN are activated and grow, the driving forces for NH3 redistribution between drops has decreased significantly and the NH(+) 4 distribution is essentially fixed for the remaining lifetime of the drops. A numerical rainband model shows that except for H2O2, chemical scavenging efficiencies are half the precipitation efficiency. The model calculations also show the ratio of accretional growth to total growth of the precipitation particles in the rainband to be 50 pct, the residual being due to depositional growth of the

ice. Clearly, such depositional growth, coupled with the initial cleanliness of the ice, act to reduce the chemical scavenging efficiencies. ESA

N89-19693 Brookhaven National Lab., Upton, NY. Environmental Chemistry Div.
PROCESSES DETERMINING CLOUDWATER COMPOSITION: FIELD EVIDENCE FOR IN-CLOUD REACTIVE SCAVENGING OF SO2 **c45**
Peter H. Daum *In* Deutscher Wetterdienst, Annals from the German Meteorological Society, No. 25: 10th International Cloud Physics Conference Preprints, Volume 1 1988 p 264-266 (For primary document see N89-19605 12-42)
(Contract DE-AC02-76CH-00016)
Copyright Avail: Deutscher Wetterdienst, Frankfurter Strasse 135, D-6050 Offenbach am Main, Fed. Republic of Germany

Sulfate incorporation into cloudwater and precipitation by aqueous-phase oxidation of SO2 was studied using aircraft and ground networks. It is shown that reactive scavenging of SO2 by H2O2 is an important atmospheric process. The amount of H2O2 available for this reaction appears seasonally dependent with concentrations lower in winter than summer. The SO2/H2O2 vertical profiles suggest that SO2 is largely confined to the lower part of the boundary layer whereas H2O2 is present at significant concentrations over a much wider range of altitudes. ESA

N89-19694 State Univ. of Western Connecticut, Danbury.
ACIDIFICATION OF STRATIFORM CLOUDS AND THEIR AEROSOL SCAVENGING PROPERTIES **c45**
R. A. Castillo and J. DeLuisi *In* Deutscher Wetterdienst, Annals from the German Meteorological Society, No. 25: 10th International Cloud Physics Conference Preprints, Volume 1 1988 p 267-269 (For primary document see N89-19605 12-42)
(Contracts NOAA-40-RANR-506003; NOAA-40-RANR-508854L)
Copyright Avail: Deutscher Wetterdienst, Frankfurter Strasse 135, D-6050 Offenbach am Main, Fed. Republic of Germany

Nephelometer data on unpolluted continental air masses were obtained to study the acidification of nonprecipitating stratiform clouds. The activation of cloud condensation nuclei to form a cloud is the predominant acidification process of the cloud water for nonprecipitating stratiform clouds. The ambient aerosol has a mean free acidity of pH 4.0. This is most likely associated with (N H4) HSO4. There is a consistent disagreement between the sum of the cloud water and interstitial sulfate concentrations when compared to the post event sulfate aerosol. ESA

N89-19695 Eidgenoessische Technische Hochschule, Zurich (Switzerland). Dept. of Atmospheric Physics.
MICROPHYSICAL, DYNAMICAL AND CHEMICAL ASPECTS OF SCAVENGING PROCESSES DURING WINTER PRECIPITATION **c46**
A. Waldvogel, T. Schumann, and B. Zinder *In* Deutscher Wetterdienst, Annals from the German Meteorological Society, No. 25: 10th International Cloud Physics Conference Preprints, Volume 1 1988 p 270-272 (For primary document see N89-19605 12-42)
Copyright Avail: Deutscher Wetterdienst, Frankfurter Strasse 135, D-6050 Offenbach am Main, Fed. Republic of Germany

The scavenging of aerosol particles by cloud droplets, ice crystals, snowflakes, and raindrops was investigated in a field experiment. Three ground stations and a mobile measuring platform (cable car) were instrumented, along a mountain slope between 430 and 1620 m. The mountain is an isolated precursor of the Alps giving a vertical profile of the incoming weather systems, which are mostly weak cold fronts. The quantitative contributions of in-cloud versus below-cloud scavenging; the efficiency of snow versus rain scavenging; and the distinction between dynamical and microphysical effects influencing the scavenging process as a whole were studied. Microphysical processes (scavenging due to nucleation, impaction, etc) dominate the changes of aerosol concentrations at the first mm of precipitation. Airmass changes govern the aerosol concentration later. In-cloud scavenging is the dominant removal process; the below-cloud scavenging is relatively small under normal conditions (no inversions). Very large below-cloud rates are found below inversions. This is due to large aerosol particles in the humid cold air mass. There is a large scatter in scavenging coefficients (up to 2 decades) obtained under different meteorological conditions. However, the variations can be reduced and the understanding of the processes can be increased under certain easily definable meteorological conditions. ESA

N89-19696 Atmospheric Environment Service, Downsview (Ontario).
VERTICAL PROFILES OF POLLUTANTS INSIDE AND OUTSIDE OF CLOUD **c45**
G. A. Isaac and W. R. Leaitch *In* Deutscher Wetterdienst, Annals from the German Meteorological Society, No. 25: 10th International Cloud Physics Conference Preprints, Volume 1 1988 p 273-275 (For primary document see N89-19605 12-42)
Copyright Avail: Deutscher Wetterdienst, Frankfurter Strasse 135, D-6050 Offenbach am Main, Fed. Republic of Germany

Vertical profiles of pollutants from clear air and cloud were obtained to characterize physical and chemical properties of clouds in different regions and during different seasons. The average out-of-cloud profiles of aerosol particles and NOy concentrations tend to decrease with increasing height. The highest and lowest concentrations tend to come with 48 hr back trajectories from the south and north respectively. In-cloud profiles show the interstitial aerosol is on average a significant fraction of the total number of particles bigger than 0.17 micrometer. The ratio of the cloud droplet concentration to the aerosol concentration is lower during the summer. Since supersaturations should not be lower in the summer versus winter, this suggests there are more holes due to entrainment of drier air in the summertime clouds. At all pressures, the ratio of the total particle number concentrations to that at the highest pressure or lowest elevations is always greater for the summer, suggesting that vertical transport is more efficient in summer. ESA

N89-19697 Kernforschungsanlage, Juelich (Germany, F.R.). Inst. fuer Atmosphaere Chemie.
RESULTS OF TIME AND HEIGHT RESOLVED SCAVENGING EXPERIMENTS **c45**
Lucia Kins, Franz X. Meixner, and Klaus-Peter Mueller *In* Deutscher Wetterdienst, Annals from the German Meteorological Society, No. 25: 10th International Cloud Physics Conference Preprints, Volume 1 1988 p 276-278 (For primary document see N89-19605 12-42)
Copyright Avail: Deutscher Wetterdienst, Frankfurter Strasse 135, D-6050 Offenbach am Main, Fed. Republic of Germany

The importance of the potential mechanisms responsible for the accumulation of trace substances in atmospheric hydrometeors was investigated. Nucleation scavenging of aerosol particles; uptake of particles and gases by cloud droplets; and scavenging of aerosols particles and highly soluble gases by falling rain were studied. Measurements reveal concentration difference between cloud water and rain uninfluenced by below-cloud scavenging. This is explained by assuming a concentration gradient inside the clouds, with decreasing concentrations with increasing height. Calculations suggest that the cloud water composition is mainly the result of particle scavenging, whereas rain water has a significantly different composition. Absorption of NH3 can hardly explain this neutralization. The question rises whether the rain composition reflects a selection of aerosol particles during condensation. ESA

N89-19698 Central Electricity Research Labs., Leatherhead (England).
OXIDATION REGIMES IN OROGRAPHIC CAPPING CLOUD **c45**
P. A. Clark, G. P. Gervat, T. A. Hill, A. R. W. Marsh, A. S. Chandler, Tom W. Choularton, and M. J. Gay (Manchester Univ., England) *In* Deutscher Wetterdienst, Annals from the German Meteorological Society, No. 25: 10th International Cloud Physics Conference

Preprints, Volume 1 1988 p 279-281 (For primary document see N89-19605 12-42)
Copyright Avail: Deutscher Wetterdienst, Frankfurter Strasse 135, D-6050 Offenbach am Main, Fed. Republic of Germany

During winter and spring, controlled releases of SO2 and SF6 (as a reference tracer) 5 km upwind of the summit into an airstream forming capping cloud over a fell were made. Measurements of cloud physics, meteorological, and chemical parameters were performed within the cloud and comparison made with upwind measurements of air composition. Results illustrate the importance of considering the full mix of species involved in determining cloud water composition when considering aqueous phase reactions. It is the imbalance of cations and anions which determines the cloud water pH, and hence the importance of oxidants such as O3. This imbalance may be very sensitive to small changes in the concentration of different species. Models which attempt to simulate chemical reactions in cloud systems must take account of sources of species that determine acidity or alkalinity, such as NH2 and HNO3, on appropriate spatial and temporal scales.
ESA

N89-19699 Stockholm Univ. (Sweden). Dept. of Meteorology.
AN EXAMINATION OF THE CHEMICAL AND PHYSICAL VARIABILITY OF CLOUDS AT A MOUNTAIN-TOP SITE IN CENTRAL SWEDEN **c46**
Kevin J. Noone, John A. Ogren, and Jost Heintzenberg *In* Deutscher Wetterdienst, Annals from the German Meteorological Society, No. 25: 10th International Cloud Physics Conference Preprints, Volume 1 1988 p 282-284 (For primary document see N89-19605 12-42)
Copyright Avail: Deutscher Wetterdienst, Frankfurter Strasse 135, D-6050 Offenbach am Main, Fed. Republic of Germany

Time series measurements of cloud parameters showing that despite large changes in parameters such as liquid water content (LWC) and droplet number, the distribution of the nonvolatile solute mass in two different droplet size classes remains relatively constant, are presented. Visual observations of the cloud during this period indicated that the variations in LWC are probably not due to entirely different clouds moving past the site, but rather to parts of the same cloud with different LWC values. This type of variation within a cloud indicates that mixing of environmental air is taking place. The constancy of the dissolved mass ratio for the two droplet size classes indicates that all the cloud droplets behave in a similar fashion. The variations in LWC are caused by all of the droplets evaporating or being diluted by environmental air, and not the smaller droplets evaporating with the large droplets remaining essentially unaffected.
ESA

N89-19700 National Oceanic and Atmospheric Administration, Boulder, CO. Environmental Sciences Group.
INFLUENCES OF CLOUD MICROPHYSICS ON CONTINENTAL AND MARINE PRECIPITATION CHEMISTRY **c45**
Farn Parungo and Clarence Nagamoto *In* Deutscher Wetterdienst, Annals from the German Meteorological Society, No. 25: 10th International Cloud Physics Conference Preprints, Volume 1 1988 p 285-287 (For primary document see N89-19605 12-42)
Copyright Avail: Deutscher Wetterdienst, Frankfurter Strasse 135, D-6050 Offenbach am Main, Fed. Republic of Germany

To investigate the mechanisms of acid rain formation and distribution, air chemistry and cloud microphysics in continental and marine environments were investigated. Results of chemical analyses of aerosol, cloud condensation nucleus, atmospheric cloudwater, snow, and rain samples are reported. The data are interpreted as stepwise incorporations of impurities into precipitation systems.
ESA

N89-19701 Paris VII Univ. (France). Lab. de Physico-Chimie de l'Atmosphere.
CONCENTRATIONS IN RAIN EVENTS COLLECTED SEQUENTIALLY: MEASUREMENTS VS RESULTS OF A SIMPLE SCAVENGING MODEL **c47**
J. L. Jaffrezo and J. L. Colin *In* Deutscher Wetterdienst, Annals from the German Meteorological Society, No. 25: 10th International Cloud Physics Conference Preprints, Volume 1 1988 p 288-290 (For primary document see N89-19605 12-42)
Copyright Avail: Deutscher Wetterdienst, Frankfurter Strasse 135, D-6050 Offenbach am Main, Fed. Republic of Germany

An air sampling campaign was conducted to study the scavenging of particulate nonreactive mineral aerosol by precipitations: sequential event-by-event sampling of wet deposition only; parallel aerosol collection with a short time period (6 hr). The physical and chemical data about the sequential events are compared with the results of a simple scavenging model. This is developed to determine more closely the effect on the chemical concentrations of parameters which vary during the precipitation, in particular the rain-rate. An example shows that it is possible to reveal the order of magnitude of the concentrations in the rain for a plausible scavenging height (here 3500 m for a ground level concentration of 0.145 microgram/cu m); the general evolution of the concentrations decreasing with the volume fallen; and second-order variations, which shows that they are clearly related in part to the rain-rate evolutions.
ESA

N89-19702 Johann-Wolfgang-Goethe-Univ., Frankfurt am Main (Germany, F.R.). Zentrum fuer Umweltforschung.
EXPERIMENTS ON MICROPHYSICS AND CHEMISTRY OF RADIATION FOGS
Karl-Heinz Enderle, Herbert Obenland, and Wolfgang Jaeschke *In* Deutscher Wetterdienst, Annals from the German Meteorological Society. No. 25: 10th International Cloud Physics Conference Preprints, Volume 1 1988 p 291-293 (For primary document see N89-19605 12-42)
(BMFT-Proj. 07vnd01-0)
Copyright Avail: Deutscher Wetterdienst, Frankfurter Strasse 135, D-6050 Offenbach am Main, Fed. Republic of Germany

An unidentified peak in the chromatograms of fog samples, which was below the detection limit in samples of a pH-value of less than 5.4, was found in a day old HMSA standard solution. It was assumed that this peak originates from a decomposition of the HMSA solution. A two point calibration for the unknown S(4)x concentration was done. Analytical results show that this compound of fog water significantly contributes to the S(4) budget at high pH-values. The concentrations of S(4)x and S(4)HMSA are in the same order of magnitude and both may contribute to S(4)tot' by up to 100 percent, a fact which is very important when Henry's law equilibrium is calculated.
ESA

N89-19703 Manchester Univ. (England).
CHEMICAL EVOLUTION WITHIN IN A CLOUD MODEL FEATURING A POLYDISPERSE DROPLET SIZE SPECTRUM
T. A. Hill *In* Deutscher Wetterdienst, Annals from the German Meteorological Society, No. 25: 10th International Cloud Physics Conference Preprints, Volume 1 1988 p 294-296 (For primary document see N89-19605 12-42)
Copyright Avail: Deutscher Wetterdienst, Frankfurter Strasse 135, D-6050 Offenbach am Main, Fed. Republic of Germany

The results of a model which features a realistic aerosol size spectrum on which droplets grow and within which solution chemistry takes place are discussed. Gases are absorbed or desorbed at a finite rate, and the rate of production of SO2/4 by SO2 oxidation is compared with the results of a model in which all the chemistry takes place in bulk water. Results show that concentrations of many species vary by orders of magnitude from droplet to droplet. Gas/aqueous equilibrium for NH3 is not necessarily established for all droplets within a cloud system simultaneously. Cloud condensation nuclei mass distribution changes as sulfate is produced. The reactivation of the nuclei already involved in the sulfate generation process takes precedence over those entrained with the external air, thus maintaining a lower average pH within the cloud and hence inhibiting the O3 reaction.
ESA

N89-19704 Kentucky Univ., Lexington. Dept. of Chemical Engineering.
MODELING STUDIES ON THE FORMATION, GROWTH, DISSIPATION AND ACIDIFICATION OF CUMULUS CLOUDS
Shyam K. Nair and Leonard K. Peters *In* Deutscher Wetterdienst, Annals from the German Meteorological Society, No. 25: 10th International Cloud Physics Conference Preprints, Volume 1 1988 p 297-299 Sponsored in part by DOE, Washington, DC and EPA, Washington, DC (For primary document see N89-19605 12-42)
Copyright Avail: Deutscher Wetterdienst, Frankfurter Strasse 135, D-6050 Offenbach am Main, Fed. Republic of Germany

A one-dimensional approach to cloud modeling is adopted so that both transport and chemistry of the gas and aqueous-phase species can be considered in detail. The one-dimensional model that is used as the basis for cumulus cloud acidification simulations is described. Detailed gas and aqueous-phase chemical kinetics are coupled to the cloud model. The chemical processes during the formation, growth, and dissipation periods of an entire cloud cycle are considered. Cumulus cloud runs with comprehensive gas-phase and aqueous-phase chemistries indicate that the final cloudwater pH depends primarily on the degree of oxidation of S(4) to S(6) by H2O2, and hence on the background H2O2 concentration. In these runs, H2O2 is the most important oxidant of S(4) in the aqueous phase; HO2, OH, O3, and other species make lesser contributions. Cumulus clouds can be considered to behave like giant variable volume reactors with entrainment of background air from below-cloud and above-cloud regions, and release of processed air from the sides. These simulations show S(4) to S(6) conversion rates ranging from 1 pct per min to greater than 30 pct per min in the presence of clouds. ESA

N89-19705 Washington Univ., Seattle. Geophysics Program.
A NUMERICAL INVESTIGATION OF SULFATE PRODUCTION AND DEPOSITION IN MIDLATITUDE CONTINENTAL CUMULUS CLOUDS **c45**
Gregory R. Taylor *In* Deutscher Wetterdienst, Annals from the German Meteorological Society, No. 25: 10th International Cloud Physics Conference Preprints, Volume 1 1988 p 300-302 (For primary document see N89-19605 12-42)
Copyright Avail: Deutscher Wetterdienst, Frankfurter Strasse 135, D-6050 Offenbach am Main, Fed. Republic of Germany

A time dependent cloud model developed for use in cloud chemistry and wet deposition studies, was used to examine the sensitivity of sulfate oxidation and deposition to the physical processes important in the development of midlatitude continental cumulus clouds. Model results for a small cumulonimbus indicate that for a continental background or moderately polluted atmosphere, aerosol scavenging accounts for between 50 pct and 80 pct of the in-cloud sulfate ultimately deposited; that ozone oxidation of sulfur dioxide may be important in the upper regions of the cloud; that although entrainment of environmental air is important in the cloud dynamics and microphysics, it is relatively unimportant in the chemistry for these clouds; and that neglect of the ice phase when considering chemistry in these clouds may lead to overestimates of up to 200 pct in sulfate deposition. ESA

N89-19706 Academia Sinica, Beijing (China). Inst. of Atmospheric Physics.
A NUMERICAL SIMULATION OF THE ACIDIFICATION PROCESS OF RAIN WATER BELOW THE CLOUD AND THE MECHANISM OF ACID RAIN FORMATION IN AREA OF CHONGQING, CHINA **c45**
Meiyuan Huang and Shuairen Liu *In* Deutscher Wetterdienst, Annals from the German Meteorological Society, No. 25: 10th International Cloud Physics Conference Preprints, Volume 1 1988 p 303-305 (For primary document see N89-19605 12-42)
Copyright Avail: Deutscher Wetterdienst, Frankfurter Strasse 135, D-6050 Offenbach am Main, Fed. Republic of Germany

Aircraft data and model simulations were used to study acid rain formation. Concentrations of (SO2)g up to 100 ppb, were studied, along with pollution gases and aerosols. Acidification of raindrops by absorption of pollution gases, and under the joint effects of aerosols and pollution gases is summarized. The acidification mechanism is outlined. ESA

N89-19707 Pennsylvania State Univ., University Park. Dept. of Meteorology.
EFFECTS OF CLOUD MICROPHYSICAL PROCESSES ON TRACE CHEMICAL REMOVAL EFFICIENCES **c45**
Dennis Lamb and Jen-Ping Chen *In* Deutscher Wetterdienst, Annals from the German Meteorological Society, No. 25: 10th International Cloud Physics Conference Preprints, Volume 1 1988 p 306-308 (For primary document see N89-19605 12-42)
(Contracts NOAA-50-EANR-6-00011; DE-FG02-85ER-60294; NSF ATM-85-20123; NSF ATM-87-16166)
Copyright Avail: Deutscher Wetterdienst, Frankfurter Strasse 135, D-6050 Offenbach am Main, Fed. Republic of Germany

The evolution of ideas related to wet deposition of trace chemicals is reviewed and it is shown how the concept of scavenging ratio was modified to improve understanding of storm-scale removal efficiency. A simple theoretical example shows that specific microphysical processes responsible for the growth of cloud and precipitation elements also lead to chemical fractionation and relative removal efficiencies which can vary by orders of magnitude. A real understanding of the wet deposition of trace chemicals cannot be achieved without a detailed study of traditional cloud and precipitation microphysics. ESA

N89-19708 State Univ. of New York, Albany. Atmospheric Sciences Research Center.
DYNAMIC, RADIATIVE AND CHEMICAL EFFECTS OF CLOUDS ON TROPOSPHERIC TRACE GASES **c46**
Chris J. Walcek *In* Deutscher Wetterdienst, Annals from the German Meteorological Society, No. 25: 10th International Cloud Physics Conference Preprints, Volume 1 1988 p 309-311 (For primary document see N89-19605 12-42)
Copyright Avail: Deutscher Wetterdienst, Frankfurter Strasse 135, D-6050 Offenbach am Main, Fed. Republic of Germany

It is demonstrated that calculations of regional or global tropospheric chemistry models are sensitive to the treatment of the microphysical and dynamical structure of clouds, suggesting the need for accurate models of these cloud effects in global and regional chemical models. Model results suggest that vertical motions associated with midlatitude cyclones over high NOx and organic compound emission areas can contribute significantly to the global formation of O3 since the necessary precursors are efficiently transported into the upper troposphere, where the lifetimes of these O3 precursors are much longer, and photolysis rates are significantly enhanced due to lower-level cloud fields. Regional-scale O3 production rates are extremely sensitive to the vertical and horizontal extent of cloudiness, as well as the microphysical structure of these clouds. Calculations of a radiative transfer model show that photolysis rates above clouds may be significantly enhanced, while below clouds, photolysis rates can be reduced to near zero. Since photolysis rates determine the rate at which tropospheric photochemistry is occurring, it is clear that models of tropospheric chemistry must accurately quantify the microphysics and dynamics of tropospheric cloud fields. ESA

N89-19709 Argonne National Lab., IL. Center for Environmental Research.
PARAMETERIZATIONS OF MICROPHYSICAL PROCESSES IN CLOUDS FOR APPLICATION IN MODELS OF REGIONAL ATMOSPHERIC DEPOSITION **c46**
In Young Lee *In* Deutscher Wetterdienst, Annals from the German Meteorological Society, No. 25: 10th International Cloud Physics Conference Preprints, Volume 1 1988 p 312-315 (For primary document see N89-19605 12-42)
(Contract W-31-109-eng-38)
Copyright Avail: Deutscher Wetterdienst, Frankfurter Strasse 135, D-6050 Offenbach am Main, Fed. Republic of Germany

Cloud physics parameterizations were reviewed in order to examine their theoretical basis and evaluate their applicability to regional models, and to obtain more efficient, improved parameterizations by optimization upon results of a detailed cloud model that incorporates treatments of microphysical processes and cloud dynamics too detailed for routine use in a regional model. Parameterizations for condensation of cloud droplets; evaporation of cloud droplets; condensation of raindrops; evaporation of raindrops; autoconversion of cloud droplets; accretion of cloud droplets; terminal velocity of cloud droplets; and terminal velocity of raindrops were derived. They are more efficient than parameterization used for comparison. The largest discrepancies occur in the autoconversion rates, whereas the accretion rates agree closely when the assumed collection efficiencies in other formulas are smaller than unity. ESA

N89-19710 Manchester Univ. (England). Dept. of Pure and Applied Physics.

A MODEL OF WET DEPOSITION TO COMPLEX TERRAIN BY THE SEEDER-FEEDER PROCESS **c47**

Andy Jones and Tom W. Choularton *In* Deutscher Wetterdienst, Annals from the German Meteorological Society, No. 25: 10th International Cloud Physics Conference Preprints, Volume 1 1988 p 316-318 (For primary document see N89-19605 12-42)

Copyright Avail: Deutscher Wetterdienst, Frankfurter Strasse 135, D-6050 Offenbach am Main, Fed. Republic of Germany

The seeder-feeder mechanism for the orographic enhancement of rainfall was studied. The terrain modelled consisted of two parallel hill ridges separated by a valley of comparable size. To investigate the effects on the rainfall and deposition patterns of different hill sizes, these parameters were modelled for hills of characteristic lengths 2 km and 20 km. The distributions were also modelled for conditions of potential and supercritical flow. ESA

N89-19711 Clermont-Ferrand Univ. (France).

METEOROLOGICAL AND CHEMICAL INFLUENCING FACTORS ON ACIDITY PRODUCTION IN A MESOSCALE MODEL WITH QUASI-SPECTRAL MICROPHYSICS **c45**

Nadine Chaumerliac and Robert Rosset *In* Deutscher Wetterdienst, Annals from the German Meteorological Society, No. 25: 10th International Cloud Physics Conference Preprints, Volume 1 1988 p 319-321 (For primary document see N89-19605 12-42)

Copyright Avail: Deutscher Wetterdienst, Frankfurter Strasse 135, D-6050 Offenbach am Main, Fed. Republic of Germany

To study gas and aerosol wet removal, an extended version of the mesoscale numerical model of Chaumerliac et al., (1987) was used. Concentrations of aqueous phase oxidants are explicitly predicted, neutralizing agents (NH3) are considered, and an ionic balance equation is added to predict cloud and rain acidity. Very tight and complex interactions are found between microphysical, dynamical, and chemical processes leading to acidity production in cloud and rain. Acidity load from nucleating particles and acidity production through SO2 oxidation compete to determine spatial cloud water pH distribution. Part of this cloud acidity is transferred to the rain through coalescence processes in the case of soluble species. This transfer is limited by the chemical reactivity of the species. The fate of insoluble species is less dependent on coalescence processes and depends on chemical and direct scavenging mechanisms. ESA

N89-19712 Meteorological Office, Bracknell (England).

A COMPARISON OF RADIOMETRIC AND IMMERSION TEMPERATURE MEASUREMENTS IN WATER CLOUDS **c46**

S. Nicholls, E. L. Simmons, N. C. Atkinson, and S. D. Rudman *In* Deutscher Wetterdienst, Annals from the German Meteorological Society, No. 25: 10th International Cloud Physics Conference Preprints, Volume 1 1988 p 322-324 (For primary document see N89-19605 12-42)

Copyright Avail: Deutscher Wetterdienst, Frankfurter Strasse 135, D-6050 Offenbach am Main, Fed. Republic of Germany

A fast response method for measuring temperature in clouds, the In-Cloud Temperature Probe (ICTP) was installed in an aircraft. This measures temperature radiometrically and avoids the problems associated with ill-defined heat balances entirely. Comparisons between the ICTP and a standard platinum resistance, cold wire thermometer, widely used in meteorological research, are discussed. Results show that commonly used airborne immersion thermometers may be significantly in error in water clouds because of undetermined partial evaporation. One fitted to the aircraft has errors of 0.5 C per g/kg of liquid water. The precise cause is still unknown, but the compressive heating correction is a prime suspect. Data from these instruments should be used with extreme care in studies of cloud thermodynamics. No large short period spikes or other disagreements are apparent in high resolution fluctuation data, even in fairly high liquid water clouds provided liquid water fluctuations remain fairly small. Heat flux measurements can probably be made with confidence in these conditions, although the spatial separation of the ICTP sampling volume from the other sensors should be remembered. ESA

N89-19713 Clermont-Ferrand Univ. (France).

CALIBRATION OF PMS FSSP AND 1D-C PROBES FOR CLOUD DROPLET MEASUREMENTS **c46**

Jean-Francois Gayet *In* Deutscher Wetterdienst, Annals from the German Meteorological Society, No. 25: 10th International Cloud Physics Conference Preprints, Volume 1 1988 p 325-327 (For primary document see N89-19605 12-42)

(Grant CEPr/ADER-86/00020)

Copyright Avail: Deutscher Wetterdienst, Frankfurter Strasse 135, D-6050 Offenbach am Main, Fed. Republic of Germany

An absolute diameter calibration of the Forward Scattering Spectrometer Probe (FSSP) is described. The probe output voltage is related to the diameter of a droplet passing through a laser beam. The accuracy of the calibration is confirmed by simultaneous holographic measurements carried out in a wet wind tunnel for airspeeds from 25 to 130 m/sec.These comparisons also shoW the air speed dependence of the undercounting of the 1D-C first five channels. ESA

N89-19714 National Center for Atmospheric Research, Boulder, CO.

RADAR OBSERVATIONS OF PRECIPITATION MICROSTRUCTURE: THE MORPHOLOGY OF LINEAR DEPOLARIZATION MEASUREMENTS IN CLOUD **c47**

Paul H. Herzegh and Arthur R. Jameson *In* Deutscher Wetterdienst, Annals from the German Meteorological Society, No. 25: 10th International Cloud Physics Conference Preprints, Volume 1 1988 p 328-329 Sponsored in part by ARO, Washington, DC (For primary document see N89-19605 12-42)

(Grant NSF ATM-86-01257)

Copyright Avail: Deutscher Wetterdienst, Frankfurter Strasse 135, D-6050 Offenbach am Main, Fed. Republic of Germany

Linear radar depolarization (LDR) measurements, which are sensitive to the degree of hydrometeor alignment and the occurrence of mixed-phase regions in cloud, were obtained to aid interpretation of hydrometeor characteristics. Differential reflectivity measurements were made at S-band, while LDR data were obtained at X-band, both during a severe convective storm. Measured LDR reveal interesting substructure in the precipitation and clear evidence of strong propagation effects. The high values of LDR behind the main precipitation shaft at the surface and aloft result from differential attenuation of the X-band signal. As expected, the strongest differential attenuation effects result from propagation through rain and are most visible near the surface. Regions of light precipitation show low depolarization values of -25 to -27 dB in the solid precipitation above the freezing level and in the rain below. High values of LDR are present in the high-reflectivity precipitation core, indicating a significant change in hydrometeor characteristics. The strong depolarization observed suggests that particles in the precipitation shaft are less-uniformly aligned in orientation and/or higher in dielectric constant than the lighter precipitation outside the shaft. ESA

N89-19715 Deutsche Forschungs- und Versuchsanstalt fuer Luft- und Raumfahrt, Oberpfaffenhofen (West Germany). Inst. fuer Physik der Atmosphaere.

MULTIPARAMETER DOPPLER RADAR OBSERVATIONS OF A SQUALL LINE WITH THE POLARIMETRIC DFVLR RADAR **c47**

P. Meischner, V. N. Bringi, and T. Jank *In* Deutscher Wetterdienst, Annals from the German Meteorological Society, No. 25: 10th International Cloud Physics Conference Preprints, Volume 1 1988 p 330-332 (For primary document see N89-19605 12-42)

Copyright Avail: Deutscher Wetterdienst, Frankfurter Strasse 135, D-6050 Offenbach am Main, Fed. Republic of Germany

Dynamic and microphysical structures of a squall line were measured using a C-band Doppler radar. The polarimetric versatility of the radar includes the transmitting of arbitrary elliptical polarizations, and the dual channel receiving of the backscattered co- and cross-signals. The transmitting polarization may be switched between orthogonal states from pulse to pulse. This way, depolarization ratios due to radar scattering at hydrometeors can be estimated for any transmitting radiation as well as the well established differential reflectivity, and the horizontal and vertical reflectivities. The three Doppler moments reflectivity, velocity, and spectral width as well as the polarimetric parameters are computed in near real time and displayed on a color screen. This combination of the polarimetric measurement capabilities together with the Doppler moments estimation gives insights into the precipitation formation process within deep convective cloud systems. ESA

N89-19716 Netherlands Energy Research Foundation, Petten.

A POOR MAN'S OPTICAL FOG DETECTOR **c35**

Ronald K. A. M. Mallant *In* Deutscher Wetterdienst, Annals from the German Meteorological Society, No. 25: 10th International Cloud Physics Conference Preprints, Volume 1 1988 p 333-334 (For primary document see N89-19605 12-42)

Copyright Avail: Deutscher Wetterdienst, Frankfurter Strasse 135, D-6050 Offenbach am Main, Fed. Republic of Germany

A detector that responds to the light that is near-forward scattered by fog droplets was developed. An unusual configuration of light source and detector was chosen to be able to detect this near-forward scattered light, without the use of highly collimated optics. The fog detector uses a low-cost commercially available source-receiver combination. The light source uses a pulsed LED (880 nm). The receiver electronics responds to pulsed signals only, so there is no influence of stray light. It is a switching device, with adjustable threshold. An algorithm to compute the Mie scattering coefficients, and a numerical integration method to calculate the contribution of various droplet sizes to the total signal reaching the receiver, were used to compute the response of the detector. Field and wind tunnel tests show that the detector can be used to control fog samplers. It can also be used to obtain statistics on fog occurrence or for traffic control. ESA

N89-19717 National Center for Atmospheric Research, Boulder, CO.

APPLICATIONS OF THE NCAR ELECTRA DOPPLER RADAR FOR THE STUDY OF PHYSICAL PARAMETERS OF CLOUDS **c46**

Craig Walther, Charles Frush, and Peter Hildebrand *In* Deutscher Wetterdienst, Annals from the German Meteorological Society, No. 25: 10th International Cloud Physics Conference Preprints, Volume 1 1988 p 335-337 (For primary document see N89-19605 12-42)

Copyright Avail: Deutscher Wetterdienst, Frankfurter Strasse 135, D-6050 Offenbach am Main, Fed. Republic of Germany

An airborne Doppler X-band radar to be mounted in the tail of a Lockheed Electra (ELDORA) is presented. The ELDORA is designed with a primary emphasis on the study of storm and mesoscale weather phenomena. However, the radar will also be very useful for the study of cloud physical parameters. Because the aircraft can be positioned close to the area of interest, reasonably fine scale data can be taken in a very short length of time. Since these types of measurements are not available, there is much to be learned even with the moderately course resolution of the ELDORA. The use of a larger, vertically pointing antenna will further enhance the ability of the ELDORA to measure these properties. Once this effort is completed, the information obtained will greatly enhance the cloud physics community's ability to determine what specific properties of airborne radar are necessary to measure their phenomena of interest. ESA

N89-19718 Atmospheric Environment Service, Downsview (Ontario).

INTERCOMPARISONS OF AIRCRAFT MEASUREMENTS WITH LIDAR RETURNS FOR AEROSOL, ICE CRYSTALS AND WATER DROPLETS **c47**

W. R. Leaitch, R. M. Hoff, A. I. Carswell, S. R. Pal, and A. G. Cunningham *In* Deutscher Wetterdienst, Annals from the German Meteorological Society, No. 25: 10th International Cloud Physics Conference Preprints, Volume 1 1988 p 338-340 (For primary document see N89-19605 12-42)

Copyright Avail: Deutscher Wetterdienst, Frankfurter Strasse 135, D-6050 Offenbach am Main, Fed. Republic of Germany

In situ observations of aerosol and cloud particles are compared with remote observations from ground-based lidars. The lidar backscatter profile (bsp) indicates about an order of magnitude increase in the backscatter from the ice crystals plus aerosol versus just the aerosol and is consistent with the value of aerosol volume scattering coefficient estimated for the ice crystals compared with the measured aerosol bsp. Temporal variations contribute to the discrepancies between the shapes of the lidar and aircraft data profiles. The results indicate promise for the simultaneous monitoring of aerosol and cloud extinction coefficients using lidar, however, much more research is needed. ESA

N89-19719 Meteorological Research Inst., Tsukuba (Japan).

A NEW AIRBORNE DEVICE FOR MEASUREMENT OF CLOUD PARTICLES USING VIDEO MICROSCOPE **c35**

T. Tanaka, Takayo Matsuo, K. Okada, I. Ichimura, S. Ichikawa, and A. Tokuda (Sankei Co. Ltd., Tokyo, Japan) *In* Deutscher Wetterdienst, Annals from the German Meteorological Society, No. 25: 10th International Cloud Physics Conference Preprints, Volume 1 1988 p 341-343 (For primary document see N89-19605 12-42)

Copyright Avail: Deutscher Wetterdienst, Frankfurter Strasse 135, D-6050 Offenbach am Main, Fed. Republic of Germany

An airborne cloud particle measuring system combining an impactor with a video-microscope is described. Comparative measurements with a hot-wire device in natural clouds are assessed. The airborne device provided high quality images of cloud particles in the size range of 5 to 150 micrometer with time resolution of 1.4 sec. The liquid water content (LWC) of clouds was calculated on the basis of the size distribution of particles. The results suggest that the LWC measured by the hot-wire device is closely related to particles up to 40 micrometer in diameter. It is stressed that with the device, the phase, shape, size, and number of cloud particles can be confirmed visually on board aircraft. ESA

N89-19720 National Center for Atmospheric Research, Boulder, CO.

ON THE SMALL SCALE TOPOGRAPHICAL INFLUENCES ON PRECIPITATION **c47**

Wojciech W. Grabowski *In* Deutscher Wetterdienst, Annals from the German Meteorological Society, No. 25: 10th International Cloud Physics Conference Preprints, Volume 1 1988 p 344-346 Sponsored in part by NSF, Washington, DC (For primary document see N89-19605 12-42)

Copyright Avail: Deutscher Wetterdienst, Frankfurter Strasse 135, D-6050 Offenbach am Main, Fed. Republic of Germany

A two-dimensional kinematic model was used to study topographic effects on precipitation (rain and snow cases). Results support Bergeron's idea that observed influence of small scale topography on precipitation may be explained in terms of the seeder-feeder mechanism. However, since raindrops are not very efficient in removing condensate that appears due to small vertical

displacements of air parcels, the influences on the snow stage of precipitation growth are very important. From the point of view of maximum to minimum ratio of precipitation intensity, the region just above melting level is the most sensitive to airflow perturbations. Although it is difficult to treat the results as qualitative for the region studied, they seem to represent a basic mechanism in which small scale topography influences the precipitation field. ESA

N89-19721 Colorado State Univ., Fort Collins. Dept. of Atmospheric Science.
A NUMERICAL INVESTIGATION OF AN OROGRAPHIC PRECIPITATION EVENT **c47**
Michael P. Meyers and William R. Cotton *In* Deutscher Wetterdienst, Annals from the German Meteorological Society, No. 25: 10th International Cloud Physics Conference Preprints, Volume 1 1988 p 347-349 (For primary document see N89-19605 12-42)
(Contract DAAL03-86-K-0175)
Copyright Avail: Deutscher Wetterdienst, Frankfurter Strasse 135, D-6050 Offenbach am Main, Fed. Republic of Germany

A prolonged orographic precipitation event, in a relatively steady-state synoptic environment over the Sierra Nevada range in central California was modeled. The numerical model employed is the two-dimensional nonhydrostatic option of Colorado State University's Regional Atmospheric Modeling System. The topography was rotated to a cross-barrier lifting. Full microphysics including vapor, cloud water, rainwater, pristine ice crystals, graupel, and aggregates was used. Horizontal and vertical turbulence are parameterized in the eddy viscosity closure as described by Tripoli and Cotton (1982). The equations are integrated numerically by a time-splitting procedure for a nonhydrostatic, compressible system with a large timestep of 10 sec and a small timestep of 5 sec. The control simulation is very consistent with the data observed. The dynamical and microphysical structure of the simulation exhibits the same basic features as the observed characteristics. ESA

N89-19722 Illinois Univ., Urbana. Dept. of Atmospheric Sciences.
COMPLEX MICROPHYSICAL INTERACTIONS WITHIN A CENTRAL SIERRA NEVADA OROGRAPHIC CLOUD SYSTEM **c47**
Robert M. Rauber *In* Deutscher Wetterdienst, Annals from the German Meteorological Society, No. 25: 10th International Cloud Physics Conference Preprints, Volume 1 1988 p 350-352 (For primary document see N89-19605 12-42)
Copyright Avail: Deutscher Wetterdienst, Frankfurter Strasse 135, D-6050 Offenbach am Main, Fed. Republic of Germany

Microphysical interactions that were observed within a shallow, stable wintertime orographic cloud system over the central Sierra Nevada Mountains were studied to evaluate the potential for precipitation enhancement from Sierra Nevada clouds through cloud seeding. Results show that shallow orographic cloud systems over the Sierra Nevada can produce considerable precipitation near the crest of the mountain despite the clouds characteristic warm temperatures. Of particular importance to the precipitation is the existence of an intersection region in the cloud where droplets advecting upward from cloud base encounter ice particles falling from cloud top. Within this region, secondary ice multiplication can occur and particle growth by diffusion, accretion, and aggregation all occur rapidly. These processes lead to rapid development of precipitation particles and lead to more effective precipitation processes in the cloud system. ESA

N89-19723 Bureau of Reclamation, Denver, CO.
COMPARISON OF OROGRAPHIC CLOUD AND PRECIPITATION DEVELOPMENT OF THREE DIFFERENT GEOGRAPHIC LOCATIONS USING A 3-D NESTED GRID CLOUD MODEL **c47**
Roy M. Rasmussen, Piotr K. Smolarkiewicz, William D. Hall, and T. Clark (National Center for Atmospheric Research, Boulder, CO.) *In* Deutscher Wetterdienst, Annals from the German Meteorological Society. No. 25: 10th International Cloud Physics Conference Preprints, Volume 1 1988 p 353-355 (For primary document see N89-19605 12-42)
Copyright Avail: Deutscher Wetterdienst, Frankfurter Strasse 135, D-6050 Offenbach am Main, Fed. Republic of Germany

Cloud and precipitation development was investigated at three different geographic locations using a three-dimensional nested cloud model. In many cases, the local Froude number could predict the likelihood of precipitation at a particular locality because it gives a good indication as to whether air will go over or around an obstacle. If the air goes over an obstacle, significant lifting can occur, resulting in the formation of clouds and precipitation. If air goes around an obstacle, it is not significantly lifted, but does experience horizontal acceleration. If the flow then encounters smaller obstacles, it has a larger local Froude number, and a better probability of going over the obstacle and producing clouds and precipitation. In some cases, low Froude number flow is found to produce low level convergence regions upstream of obstacles that produce significant amounts of clouds and precipitation. Additional factors important to cloud and precipitation formation at these three locations are the strength of the solar heating, the height and strength of inversions, and the cloud base temperature. Synoptic scale forcing also effects the formation of precipitation over these obstacles. ESA

N89-19724 Direction de la Meteorologie Nationale, Casablanca Royaume (Morocco). Div. de Developpement et de Recherche.
MICROPHYSICAL OBSERVATIONS OVER THE ATLAS MOUNTAINS IN MOROCCO **c47**
Omar Baddour and Roy M. Rasmussen (Bureau of Reclamation, Denver, CO.) *In* Deutscher Wetterdienst, Annals from the German Meteorological Society, No. 25: 10th International Cloud Physics Conference Preprints, Volume 1 1988 p 356-358 Sponsored by the Agency of International Development, Washington, DC (For primary document see N89-19605 12-42)
Copyright Avail: Deutscher Wetterdienst, Frankfurter Strasse 135, D-6050 Offenbach am Main, Fed. Republic of Germany

The natural precipitation processes active over the Atlas mountains (Morocco) were studied. Two case studies during winter are presented. The focus is on supercooled liquid water, and ice crystals analysis. Results show a typical winter storm sequence, and reveal basic cloud physics. During the frontal passage, a seeder-feeder type mechanism was active in the clouds over the mountains, with an upper level stratiform deck feeding aggregates of dendrites and stellars into a lower level supercooled cloud layer. Regions of the system had lower cloud top heights, and no upper level cloud to provide ice crystals, allowing for long-lived regions of supercooled liquid water. Post frontal stratocumulus clouds had an active coalescence process in convective regions, leading to drop freezing and subsequent riming. Aggregation of dendrites and stellars were observed in the stratiform regions. ESA

N89-19725 Colorado State Univ., Fort Collins. Dept. of Atmospheric Science.
MICROPHYSICAL AND DYNAMICAL INTERACTIONS IN COLORADO FRONT RANGE UPSLOPE STORMS **c47**
Douglas A. Wesley, Michael J. Weissbluth, Roger A. Pielke, and William R. Cotton *In* Deutscher Wetterdienst, Annals from the German Meteorological Society, No. 25: 10th International Cloud Physics Conference Preprints, Volume 1 1988 p 359-361 (For primary document see N89-19605 12-42)
(Contract DAAL03-36-K-0175)
Copyright Avail: Deutscher Wetterdienst, Frankfurter Strasse 135, D-6050 Offenbach am Main, Fed. Republic of Germany

An observational program with mesoscale model simulation was used to assess the physical processes which control microphysical and dynamical interactions in upslope snowstorms. Evidence of the roles of cold air damming, transient internal gravity wave disturbances, and seeder-feeder processes are emphasized. Simulations attempt to isolate these phenomena and assess their relative importance in the formation of snowfall ESA

N89-19726 Hokkaido Univ., Sapporo (Japan). Inst. of Low Temperature Science.
CHARACTERISTICS OF RADAR ECHO OF SNOW BAND FORMED IN THE LEE SIDE OF A MOUNTAIN **c47**
Yasushi Fujiyoshi, Tatsuo Endoh, and Gorow Wakahama *In* Deutscher Wetterdienst, Annals from the German Meteorological Society, No. 25: 10th International Cloud Physics Conference Preprints, Volume 1 1988 p 362-363 (For primary document see N89-19605 12-42)
Copyright Avail: Deutscher Wetterdienst, Frankfurter Strasse 135, D-6050 Offenbach am Main, Fed. Republic of Germany

Radar echo patterns of cloud bands associated with snow, in the lee of an island, are discussed. As excepted, the snow band becomes wavy with increase in Reynolds number. The weakly wavy snow band is composed of many small but intense convective echoes. The non-wavy snow band is composed of large and small numbers of echoes. The wavy snow band has the widest echo area and intermediate features of echo cells. The frequency of intense echoes is highest in the weakly wavy snow band, and that of weak echoes is highest in the non-wavy snow band. The wavy snow band is composed of echo cells with medium intensity. In other words, heavy snowfall tends to concentrate into a small area when the weakly wavy snow band is formed. Snow with medium intensity falls in a wider area when the wavy snow band is formed. Time change in snowfall intensity is large when the non-wavy snow band is formed. ESA

N89-19727 Beijing Univ. (China). Dept. of Geophysics.
STUDY ON CLOUD AND RAIN BY MICROWAVE RADIOMETER OBSERVATION **c47**
Bolin Zhao *In* Deutscher Wetterdienst, Annals from the German Meteorological Societyn No. 25: 10th International Cloud Physics Conference Preprints, Volume 1 1988 p 364-365 (For primary document see N89-19605 12-42)
Copyright Avail: Deutscher Wetterdienst, Frankfurter Strasse 135, D-6050 Offenbach am Main, Fed. Republic of Germany

A set of microwave radiometers from 5 mm to 3 cm waveband at 5 frequencies (9.37, 22.235, 35.5, 52.9, and 54.5 GHz) used in meteorology were developed. Experimental results from 8 mm and 1.35 cm radiometers in remote sensing of atmospheric water vapor content, liquid water content of cloud, and the process of rain are discussed. The results of microwave remote sensing of total water vapor content were compared with those obtained by radiosonde. The mean deviation between them is less than 7 pct. Results of rain intensity measured by the 3 cm radar-radiometer were compared with those obtained by raingage. The mean deviation between them is 25 pct. ESA

N89-19728 Institute of Hydrology and Meteorology, Sofia (Bulgaria).
A NEW DROPSONDE FOR CLOUD PROBINGS **c35**
Dimiter Gaytandjien *In* Deutscher Wetterdienst, Annals from the German Meteorological Society, No. 25: 10th International Cloud Physics Conference Preprints, Volume 1 1988 p 366-368 (For primary document see N89-19605 12-42)
Copyright Avail: Deutscher Wetterdienst, Frankfurter Strasse 135, D-6050 Offenbach am Main, Fed. Republic of Germany

A dropsonde was designed for measuring the air temperature, liquid water content, and air flow velocity in different types of clouds. The sonde is designed for measurements along only its descent trajectory, after being carried aloft in the cloud. After carrier separation (from a balloon, aircraft, or a modified antihail rocket) the 1 kg sonde is dropped inside the cloud and carried downwards by means of a specially designed parachute with a relative-to-ambient air fallspeed varying from 25 m/sec at altitude 9 km to 16 m/sec at sea level. A standard MARS-type transmitter is used in the dropsonde for tracking by an ordinary, 1782 MHz aerological radar. ESA

43 EARTH RESOURCES AND REMOTE SENSING

Includes remote sensing of earth resources by aircraft and spacecraft; photogrammetry; and aerial photography.

For instrumentation see *35 Instrumentation and Photography.*

N89-19729*# National Aeronautics and Space Administration. Goddard Space Flight Center, Greenbelt, MD.
MODIS INFORMATION, DATA AND CONTROL SYSTEM (MIDACS) OPERATIONS CONCEPTS
D. Han, V. Salomonson, J. Ormsby, P. Ardanuy, A. McKay, D. Hoyt, S. Jaffin, B. Vallette, B. Sharts, and D. Folta (General Sciences Corp., Laurel, MD.) et al Dec. 1988 84 p Prepared in cooperation with Interferometrics, Inc., Vienna, VA
(Contracts NAS5-29373; NAS5-28795)
(NASA-TM-100720; Rept-89B00065; NAS 1.15:100720) Avail: NTIS HC A05/MF A01 CSCL 05B

The MODIS Information, Data, and Control System (MIDACS) Operations Concepts Document provides a basis for the mutual understanding between the users and the designers of the MIDACS, including the requirements, operating environment, external interfaces, and development plan. In defining the concepts and scope of the system, how the MIDACS will operate as an element of the Earth Observing System (EOS) within the EosDIS environment is described. This version follows an earlier release of a preliminary draft version. The individual operations concepts for planning and scheduling, control and monitoring, data acquisition and processing, calibration and validation, data archive and distribution, and user access do not yet fully represent the requirements of the data system needed to achieve the scientific objectives of the MODIS instruments and science teams. The teams are not yet formed; however, it is possible to develop the operations concepts based on the present concept of EosDIS, the level 1 and level 2 Functional Requirements Documents, and through interviews and meetings with key members of the scientific community. The operations concepts were exercised through the application of representative scenarios. Author

N89-19730# Army Engineer Topographic Labs., Fort Belvoir, VA.
COMPUTER GENERATION OF FRACTAL TERRAINS
Eugene A. Margerum and Anne Werkheiser Sep. 1988 29 p
(AD-A201171; ETL-0504) Avail: NTIS HC A03/MF A01
CSCL 12E

The use of fractals for the generation of artificial terrains is presented. An introduction to the relevant basic properties of fractals is given and a method for the generation of artificial fractal landscapes is described. The algorithm has been used to develop a LISP computer program for synthesizing topographic surfaces. Examples of the resulting structures are given in the form of a series of profiled surfaces representing landscapes of varying fractal dimension and varying vertical dilation. The LISP computer programs are also given and described. GRA

N89-19731# Naval Postgraduate School, Monterey, CA.
LOCAL GEOID DETERMINATION USING THE GLOBAL POSITIONING SYSTEM M.S. Thesis
Wei-Ming Ma Sep. 1988 94 p
(AD-A202220) Avail: NTIS HC A05/MF A01 CSCL 08E

A local geoid model to predict the geoid heights in the vicinity of Monterey Bay, California, was developed to use Global Position System (GPS) differential positions and known Mean Sea Level (MSL) with the method of collocation. The local geoid models were based on Rapp's 360 degree x 360 order global geoid model determined from gravity measurements. Control data were adjusted by least squares to solve the parameters in the local geoid model. Also studied were factors that affected the GPS-measured ellipsoid height differences. These included: (1) comparing GPS differencing solutions; (2) standard error of GPS observations; (3) corrections for surface meteorological values; and (4) observation durations for GPS. The data used in this research were taken from GPS

measurements on the campus of the Naval Postgraduate School (NPS), an area about 100 m x 630 m, and in an area approximately 15 km x 33 km near Monterey, CA. The time period was from February 5, 1988, to May 12, 1988. The accuracy of the predicted geoid heights is + or - 2 cm if a six-parameter model is used for the larger area, and + or - 2 to 10 mm if a five-parameter model is used for the NPS campus. GRA

N89-19732# Begeleidingscommissie Remote Sensing, Delft (Netherlands).
THE USE OF LANDSAT IMAGERY FOR WATER QUALITY STUDIES IN THE IJSSELMEER AREA (NETHERLANDS) [HET GEBRUIK VAN LANDSAT OPNAMEN VOOR WATERKWALITEITSONDERZOEK IN HET IJSSELMEERGEBIED]
H. Buiteveld (Rijkswaterstaat, The Hague, Netherlands), C. Meulstee, and R. Jordans Dec. 1987 43 p In DUTCH Original contains color illustrations
(BCRS-87-18; ETN-89-93872) Avail: NTIS HC A03/MF A01

The procedure for the processing of satellite images to improve water quality aspects, such as sediments, is described. A procedure for airborne multispectral scanner pictures and field observations was extended for LANDSAT thematic mapper pictures. Via multiple linear regression a functional relation between ground observations and remote sensing data was established. This algorithm was applied to satellite pictures resulting in a concentration chart, e.g., of sediment. True color and false color composite pictures were also made. The results show the method to be suitable for the processing of satellite images for inland water applications. The processed images show significant optical differences between two stretches of water. ESA

N89-19733# Begeleidingscommissie Remote Sensing, Delft (Netherlands).
LAND USE ANALYSIS USING REMOTE SENSING TECHNIQUES. INVESTIGATION OF THE USEFULNESS OF LANDSAT THEMATIC MAPPER SATELLITE PICTURES FOR OBTAINING AND UP TO DATE PICTURE OF LAND USE IN THE PROVINCE SOUTH HOLLAND Final Report [LANDGEBRUIKSANALYSE MET BEHULP VAN REMOTE SENSING TECHNIEKEN. EEN ONDERZOEK NAAR DE BRUIKBAARHEID VAN LANDSAT THEMATIC MAPPER SATELLIETBEELDEN VOOR HET VERKRIJGEN VAN EEN AKTUEEL BEELD VAN HET LANDGEBRUIK IN DE PROVINCE ZUID-HOLLAND]
J. J. Cevat, F. B. vanderLaan (National Aerospace Lab., Amsterdam, Netherlands), and L. F. Verhelj Feb. 1988 31 p In DUTCH Original contains color illustrations
(BCRS-Proj. TO-3.4)
(BCRS-88-01; ETN-89-93873) Avail: NTIS HC A03/MF A01

The usefulness of LANDSAT thematic mapper to update land use maps was investigated in a test area of 300 sq km. Satellite pictures were processed for manual interpretation, for interpretation of the thermal IR image, as well as for automatic classification. Manual interpretation is found to be suitable for a survey on a scale 1:25,000; the result depends strongly on the spatial resolution of the satellite. The thermal IR image does not provide relevant information about the hydrological situation. The classification result varies strongly from class to class and from area to area; a minimum classification error of 10 pct has to be taken into account. ESA

N89-19734# Begeleidingscommissie Remote Sensing, Delft (Netherlands).
SALINITY MAPPING BASED ON SPOT IMAGES OF THE PUNJAB, PAKISTAN Final Report [ZOUTKARTERING MET BEHULP VAN SPOT-BEELDEN IN DE PUNJAB, PAKISTAN]
Feb. 1988 48 p In DUTCH Prepared in cooperation with EUROCONSULT B.V., Arnhem, Netherlands Original contains color illustrations
(BCRS-Proj. CO-1.6)
(BCRS-88-03; ETN-89-93874) Avail: NTIS HC A03/MF A01

Water logging and salinity in an irrigated agriculture area to the west of the Indus were inventoried using satellite images. Advanced image processing apparatus was used for the analysis of multispectral information and texture. Enlargements of false color images allowed a classification resulting in a salinity map. The combination of detailed panchromatic images and multispectral images proves to be very successful. ESA

N89-19735# Begeleidingscommissie Remote Sensing, Delft (Netherlands).
STUDY OF THE USE OF RADAR X-BAND DATA OF BARE SOIL IN A RADAR SCATTERING MODEL [ONDERZOEK NAAR DE TOEPASSING VAN RADAR X-BAND GEGEVENS VAN KALE GROND IN EEN RADARVERSTROOIINGSMODEL]
M. A. P. Vissers and J. Stolp Mar. 1988 28 p In DUTCH Original contains color illustrations
(BCRS-Proj. AO-2.1)
(BCRS-88-04; REPT-2021; ETN-89-93875) Avail: NTIS HC A03/MF A01

The combination of soil data and X-band side looking airborne radar data via a radar scattering was investigated. The radar reflection from the mainly bare soil of a test farm was measured, and samples of the moisture content of the top layer and of the soil roughness were determined. The calibrated radar data and soil data were coupled using a radar scattering model which describes the interaction mechanism radar-bare soil. It is shown that the standard deviation of the differences in height of the surface (i.e., as measure of the roughness) does not provide a correct adaptation in the correlation between radar backscatter and incidence angle of the scatter. A model parameter value of the soil roughness was deduced. The introduction of this value in the model provides a relation between radar backscatter and moisture content via regression, in agreement with previous experiments. ESA

N89-19736# Technische Univ., Delft (Netherlands).
THE GEOMETRY OF GEODETIC INVERSE LINEAR MAPPING AND NONLINEAR ADJUSTMENT Ph.D. Thesis
Peter J. G. Teunissen 1988 188 p Sponsored by The Netherlands Organization for the Advancement of Pure Research
(ETN-89-93900) Avail: NTIS HC A09/MF A01

It is shown that every inverse B of a linear map A can be uniquely characterized through the choice of three subspaces, S, C and D. Each of these three subspaces has an interesting interpretation of its own. The consequences of the inverse mapping problem for two- and three-dimensional geodetic networks are shown. The problem of nonlinear adjustment is considered, using a differential geometric approach throughout. Gauss method is analyzed, showing how the extrinsic curvatures of submanifold N affects its local behavior. It is also shown how in some cases the geometry of the problem suggests important simplifications. Typical examples are generalizations of the classical Helmert transformation. ESA

N89-19868*# Carnegie-Mellon Univ., Pittsburgh, PA. The Robotics Inst.
SENSOR FUSION OF RANGE AND REFLECTANCE DATA FOR OUTDOOR SCENE ANALYSIS
In So Kweon, Martial Hebvert, and Takeo Kanade *In* NASA. Lyndon B. Johnson Space Center, 2nd Annual Workshop on Space Operations Automation and Robotics (SOAR 1988) Nov. 1988 p 373-382 (For primary document see N89-19817 12-59)
(Contract NAGw-1175; DACA76-85-C-0003; NSF DCR-86-04199; ARPA Order 5351)
Avail: NTIS HC A22/MF A01 CSCL 20F

44 ENERGY PRODUCTION AND CONVERSION

Includes specific energy conversion systems, e.g., fuel cells; global sources of energy; geophysical conversion; and windpower.

For related information see also *07 Aircraft Propulsion and Power, 20 Spacecraft Propulsion and Power,* and *28 Propellants and Fuels.*

N89-19737*# National Aeronautics and Space Administration. Lewis Research Center, Cleveland, OH.
RE-1000 FREE-PISTON STIRLING ENGINE SENSITIVITY TEST RESULTS Final Report
Jeffrey G. Schreiber, Steven M. Geng, and Gary V. Lorenz Oct. 1986 130 p
(Contract DE-AI05-82OR-1005)
(NASA-TM-88846; DOE/NASA/1005-11; E-3277; NAS 1.15:88846) Avail: NTIS HC A07/MF A01 CSCL 10B

The NASA Lewis Research Center has been testing a 1 kW (1.33 hp) free-piston Stirling engine. The tests performed over the past several years have been on a single cylinder machine known as the RE-1000. The data recorded were to aid in the investigation of the dynamics and thermo-dynamics of the free-piston Stirling engine. The data are intended to be used primarily for computer code validation. NASA reports TM-82999, TM-83407, and TM-87126 give initial results of the engine tests. The tests were designed to investigate the sensitivity of the engine performance to variations on the mean pressure of the working space, the working fluid used, heater and cooler temperatures, regenerator porosity, power piston mass and displacer dynamics. These tests have now been completed. Some of the data collected in the sensitivity tests are presented. In all, 781 data points were recorded. A completed description of the engine and test facility is given. Many of the data can be found in tabular form, and a microfiche containing all of the data points can be requested from the NASA Lewis. Author

N89-19738# Sandia National Labs., Albuquerque, NM.
SOLAR THERMAL TECHNOLOGY Annual Report, fiscal year 1987
Sep. 1988 69 p Prepared in cooperation with Midwest Research Inst., Golden, CO
(Contract DE-AC02-83CH-10093)
(DE89-000818; DOE/CH-10093/36) Avail: NTIS HC A04/MF A01

This annual report describes the accomplishments and progress of government-funded activities initiated, renewed, or completed during Fiscal Year (FY) 1987 (October 1, 1986, through September 30, 1987). It highlights the program tasks conducted by participating federal laboratories and by industrial, academic, or other research under a subcontract. The emphasis of the Solar Thermal Technology Program during the year was: (1) to perform research and development leading to the economic viability of two primary solar thermal concepts, central receiver and parabolic dish, and (2) to explore applications of national significance where the special attributes of concentrated sunlight are appropriate. The report includes three appendices that cover principal contacts and sources of additional information (Appendix A), acronyms and abbreviations (Appendix B), and a glossary of terms (Appendix C). A bibliography of relevant publications from Sandia National Laboratories and the Solar Energy Research Institute completes this annual report. DOE

N89-19739# Energy Conversion Devices, Inc., Troy, MI.
RESEARCH ON HIGH-EFFICIENCY, MULTI-GAP, MULTIJUNCTION, AMORPHOUS-SILICON-BASED ALLOY THIN-FILM SOLAR CELLS, PHASE 1 Semiannual Subcontract Report, 1 Mar. - 31 Aug. 1987
S. Guha Aug. 1988 91 p Prepared for Midwest Research Inst., Golden, CO
(Contract DE-AC02-83CH-10093)
(DE89-000844; SERI/STR-211-3374) Avail: NTIS HC A05/MF A01

The research program described in this report is directed toward advancing our understanding of amorphous-silicon-based alloys and their use in small-area multijunction solar cells. Its principal objectives are: (1) to develop a broad scientific base for the chemical, structural, optical, and electronic properties of a-Si based alloys; (2) to determine the optimum properties of alloys materials as they relate to high-efficiency cells; (3) to determine the optimum device configuration for multijunction cells; and (4) to demonstrate a proof-of-concept multijunction a-Si alloy-based solar cell having an efficiency of 18 percent under standard AM1.5 global insolation conditions and having an area of at least 1 cm^2. This semiannual report describes some of the research results obtained in Phase 1. DOE

N89-19740# Sandia National Labs., Albuquerque, NM.
SILICON CONCENTRATOR SOLAR CELL RESEARCH
M. A. Green, Zhao Jianhua, Wang Aihua, A. W. Blakers, C. M. Chong, Zhang Fuzu, A. Sproul, S. R. Wenham, and P. Campbell (New South Wales Univ., Kensington, Australia) Dec. 1988 141 p
(Contract DE-AC04-76DP-00789)
(DE89-005490; SAND-88-7032) Avail: NTIS HC A07/MF A01

Research directed at improving the energy conversion efficiency of silicon concentrator solar cells over the year ending October 1987 is described. The most promising approach identified for fabricating high-efficiency, bifacially contacted cells is one whereby the effects of top metallization shading can be negated, such as by the use of prismatic covers. This approach is shown to be capable of producing 25 percent cell efficiency for relatively large-area cells for concentration in the 100 to 500 suns range. Increase beyond this efficiency figure is dependent upon improvements in rear surface passivation. Results reported include the first demonstration of 19 percent lens/cell efficiency with silicon, the demonstration of improved performance levels for bifacially contacted high-resistivity cells, and the demonstration of the feasibility of applying the laser-grooved approach to large-area, low-cost concentrator cells. The theory of sublinear effects in high-resistivity cells is developed and shown to accurately describe experimental results. Finally, a new light-trapping scheme based on tilted pyramids and slats is analyzed and shown to perform better than any other scheme analyzed to date. DOE

N89-19741# Little (Arthur D.), Inc., Cambridge, MA.
APPLICATIONS SURVEY FOR REMOTE PHOTOVOLTAIC POWER SYSTEMS
L. Frantzis and W. P. Teagan Oct. 1988 77 p
(AD-A201937; CERL-TR-E-89/01) Avail: NTIS HC A05/MF A01 CSCL 10B

As part of the Federal Photovoltaic Utilization Program, the U.S. Army determined that photovoltaic (PV) systems in the size range of 50 watts to 2 kilowatts are cost effective, reliable, and nearly maintenance free for remote, stand-alone applications. The objective of this study was to identify installations having potential PV applications and to determine the load and other system requirements. Recommendations for future activities to promote PV use at Army installations are included. GRA

N89-19742# Deutsche Forschungs- und Versuchsanstalt fuer Luft- und Raumfahrt, Stuttgart (Germany, F.R.). Forschungsbereich Energetik.
HORIZONS OF NEW ENERGY TECHNOLOGIES
Carl-Jochen Winter and Joachim Nitsch Jun. 1988 53 p In GERMAN; ENGLISH summary Presented at the 25th Arbeitstagung des Energiewirtschaftlichen Instituts, Cologne, Federal Republic of Germany 21-22 Apr. 1988
(DFVLR-Mitt-88-22; ISSN-0176-7739; ETN-89-93975) Avail: NTIS HC A04/MF A01; DFVLR, VB-PL-DO, Postfach 90 60 58, 5000 Cologne, Federal Republic of Germany, 19 deutsche marks

Three items, leading to new energy technologies are considered: consistent conservative energy usage in locally appropriate supply of the energy services heat, light, power, and communication;

indigenous solar energy in passive utilization: irradiation, ambient heat, wind, water power, and biomass; and solar energy import by means of solar hydrogen at the end of the adaption process. Lack of energy raw materials will be the main characteristic of these aspects. ESA

N89-19743# Midwest Research Inst., Golden, CO. Solar Energy Research Inst.
FIELD INVESTIGATION OF A WAKE STRUCTURE DOWNWIND OF A VANT (VERTICAL-AXIS WIND TURBINE) IN A WIND FARM ARRAY
H. T. Liu, J. W. Buck, A. C. Germain, M. E. Hinchee, T. S. Solt, G. M. LeRoy, and R. A. Srnsky Sep. 1988 80 p
(Contract DE-AC02-83CH-10093)
(DE89-000821; SERI/STR-217-3370) Avail: NTIS HC A05/MF A01

The effects of upwind turbine wakes on the performance of a FloWind 17-m vertical-axis wind turbine (VAWT) were investigated through a series of field experiments conducted at the FloWind wind farm on Cameron Ridge, Tehachapi, California. From the field measurements, we derived the velocity and power/energy deficits under various turbine on/off configurations. Much information was provided to characterize the structure of VAWT wakes and to assess their effects on the performance of downwind turbines. A method to estimate the energy deficit was developed based on the measured power deficit and the wind speed distributions. This method may be adopted for other turbine types and sites. Recommendations are made for optimizing wind farm design and operations, as well as for wind energy management. DOE

N89-19744# Midwest Research Inst., Golden, CO. Solar Energy Research Inst.
OPTICAL GOALS FOR POLYMERIC FILM REFLECTORS
Walter D. Short Oct. 1988 29 p
(Contract DE-AC02-83CH-10093)
(DE89-000836; SERI/SP-253-3383) Avail: NTIS HC A03/MF A01

This report provides guidelines and recommendations for research on polymeric film reflectors which have the potential to significantly reduce the weight and cost of concentrators for solar thermal systems. As with glass/metal reflectors, the primary performance criteria for film reflectors are reflectivity and specularity over the life of the film. The recommended reflectivity and specularity goals for polymer reflectors are made in the context of the cost of energy delivered and how that compares to the cost from alternative means of supplying the same energy. However, these optical goals should be considered only as guidelines, since many other parameters such as system capital cost can have a far larger impact on the cost of delivered energy. To ensure that these guidelines are correctly interpreted, the report includes definitions of the terms. The report also provides a summary listing of the recommendations and analysis details on which each recommendation is based. DOE

N89-19745# Texas A&M Univ., College Station. Dept. of Chemical Engineering.
OXYGEN ELECTRODE IN MOLTEN CARBONATE FUEL CELLS Quarterly Technical Progress Report No. 5, 1 Aug. - 31 Oct. 1988
B. Dave, P. K. Adanuvor, R. E. White, M. A. Enayetullah, S. Srinivasan, and A. J. Appleby 1988 19 p
(Contract DE-FG22-87PC-79931)
(DE89-005813; DOE/PC-79931/T3) Avail: NTIS HC A03/MF A01

Electrode kinetics of oxygen reduction on gold in molten lithium carbonate was investigated. Steady state cyclic voltammograms were obtained for the peroxide reduction at the gold electrode in Li2CO3 melt, results were found to be in good agreement with the data in the literature. Impedance measurements were made as a function of frequency to evaluate the kinetics and mass transfer related parameters. Impedance data were analyzed using a Complex Nonlinear Least Square (CNLS) parameter estimation program and a graphical procedure based upon the Randles-Ershler equivalent circuit. Parameters estimated by both the methods are in good agreement. One of the proposed micro electrodes is a micro ring, which involves a thin gold film positioned tightly between two alumina roots. As an initial study, the stability of gold films, sputter-deposited on alumina substrates, in the Li2CO3 melt was determined. DOE

N89-19746# Sandia National Labs., Albuquerque, NM.
A STUDY OF THE RELIABILITY OF STIRLING ENGINES FOR DISTRIBUTED RECEIVER SYSTEMS
R. E. Holtz and K. L. Uherka Nov. 1988 71 p Prepared in cooperation with Argonne National Lab., IL
(Contracts DE-AC04-76DP-00789; W-31-109-eng-38)
(DE89-006395; SAND-88-7028) Avail: NTIS HC A05/MF A01

The objective of this study was to examine the reliability of existing and improved Stirling engine concepts for dispersed solar dish/electric applications in the 25 to 50 kW sub e range. Five current kinematic Stirling engine designs have the capability to meet or exceed the 32 percent system efficiency goal of the DOE Solar Thermal Program. Experience with the Vanguard Solar-Dish/Stirling Engine module demonstrated that the 32 percent efficiency goal is realistic, but that improved Stirling engine reliability is necessary for successful implementation of dispersed solar power systems. A review of historical Stirling engine data illustrated that the three major reliability issues with kinematic Stirling engines are the piston-rod seals, engine hot parts and power control/drive systems. A specific kinematic engine concept that appears to have the potential for meeting the 50,000-hour operating lifetime requirement of solar power systems has a pressurized crankcase to reduce piston-rod seal problems, an indirectly heated hot-end section using heat pipes to smooth out temperature gradients in the heater tubes, and a variable-angle swashplate for power control. Further development efforts are required to establish reliability and validate performance goals of these engine concepts. DOE

45 ENVIRONMENT POLLUTION

Includes atmospheric, noise, thermal, and water pollution.

N89-19747# Fraunhofer-Inst. fuer Atmosphaerische Umweltforschung, Garmisch-Partenkirchen (Germany, F.R.).
MEASUREMENT OF THE GLOBAL DISTRIBUTION OF TROPOSPHERIC TRACE GASES AND THEIR TIME DEPENDENT VARIATIONS Final Report, 31 Jul. 1987
Hans-Eckhart Scheel, Franz Slemr, Pavel Matuska, Johannes Werhahn, and Wolfgang Seiler Jul. 1988 216 p In GERMAN; ENGLISH summary
(Contract BMFT-0704564-A)
(ETN-89-93987) Avail: NTIS HC A10/MF A01

An aircraft cargo container was fitted with instruments for measuring environmentally relevant trace gases. Flight missions were mainly performed between Frankfurt, FRG, and Sao Paulo, Brazil. Latitudinal distributions were determined for the trace gases CH4, H2O, O3, CO, NOy, CO2, N2O, CF2Cl2, CFCl3, C2F3Cl3, CHCl3, CH3CCl3, CCl4, C2H2, C2H6, C3H6, C3H8, C4H10, C5H12, C6H6, and C7H8. The data are presented. The results obtained between 1982 and 1987 show an increase of the upper tropospheric concentrations of several trace gases. The average annual increase is found to be 0.76 pct for CH4; 0.16 pct for N2O; 4.4 pct for CF2Cl2; 5.3 pct for CFCl3; 17.2 pct for C2F3Cl3; 4.5 pct for CH3CCl3; and 2.1 pct for CCl4. ESA

N89-19682 North Carolina State Univ., Raleigh. Dept. of Marine, Earth and Atmospheric Sciences.
CLOUD CAPTURE BY A MOUNTAIN TOP FOREST. PART 1: ACIDITY AND DOSAGE DURATION
V. K. Saxena and N.-H. Lin *In* Deutscher Wetterdienst, Annals from the German Meteorological Society, No. 25: 10th International Cloud Physics Conference Preprints, Volume 1 1988 p 232-234 (For primary document see N89-19605 12-42)

(Contracts EPA-81-39-3401-2; EPA-81-24-430)
Copyright Avail: Deutscher Wetterdienst, Frankfurter Strasse 135, D-6050 Offenbach am Main, Fed. Republic of Germany

N89-19683 Technische Univ., Munich (Germany, F.R.). Meteorologisches Inst.
DETERMINATION OF CHEMICAL REACTION RATES IN FOG
Ralph Dlugi and Winfried Seidl *In* Deutscher Wetterdienst, Annals from the German Meteorological Society, No. 25: 10th International Cloud Physics Conference Preprints, Volume 1 1988 p 235-237 (For primary document see N89-19605 12-42)
Copyright Avail: Deutscher Wetterdienst, Frankfurter Strasse 135, D-6050 Offenbach am Main, Fed. Republic of Germany

N89-19684 Mainz Univ. (Germany, F.R.). Inst. of Meteorology.
INSOLUBLE PARTICLES IN HYDROMETEORS
M. Kraemer and L. Schuetz *In* Deutscher Wetterdienst, Annals from the German Meteorological Society, No. 25: 10th International Cloud Physics Conference Preprints, Volume 1 1988 p 238-240 Sponsored in part by the Deutsche Forschungsgemeinschaft, Bonn, Fed. Republic of Germany (For primary document see N89-19605 12-42)
Copyright Avail: Deutscher Wetterdienst, Frankfurter Strasse 135, D-6050 Offenbach am Main, Fed. Republic of Germany

N89-19688 Army Cold Regions Research and Engineering Lab., Hanover, NH.
THE EFFECT OF AEROSOLS ON pH OF SNOWFALLS
Motoi Kumai *In* Deutscher Wetterdienst, Annals from the German Meteorological Society, No. 25: 10th International Cloud Physics Conference Preprints, Volume 1 1988 p 249-250 (For primary document see N89-19605 12-42)
Copyright Avail: Deutscher Wetterdienst, Frankfurter Strasse 135, D-6050 Offenbach am Main, Fed. Republic of Germany

N89-19690 Technische Univ., Munich (Germany, F.R.). Meteorologisches Inst.
A ONE-DIMENSIONAL NUMERICAL MODEL TO SIMULATE LIQUID PHASE CHEMICAL REACTIONS WITHIN RADIATION FOG
Renate Forkel and Winfried Seidl *In* Deutscher Wetterdienst, Annals from the German Meteorological Society, No. 25: 10th International Cloud Physics Conference Preprints, Volume 1 1988 p 255-257 (For primary document see N89-19605 12-42)
Copyright Avail: Deutscher Wetterdienst, Frankfurter Strasse 135, D-6050 Offenbach am Main, Fed. Republic of Germany

N89-19693 Brookhaven National Lab., Upton, NY. Environmental Chemistry Div.
PROCESSES DETERMINING CLOUDWATER COMPOSITION: FIELD EVIDENCE FOR IN-CLOUD REACTIVE SCAVENGING OF SO2
Peter H. Daum *In* Deutscher Wetterdienst, Annals from the German Meteorological Society, No. 25: 10th International Cloud Physics Conference Preprints, Volume 1 1988 p 264-266 (For primary document see N89-19605 12-42)
(Contract DE-AC02-76CH-00016)
Copyright Avail: Deutscher Wetterdienst, Frankfurter Strasse 135, D-6050 Offenbach am Main, Fed. Republic of Germany

N89-19694 State Univ. of Western Connecticut, Danbury.
ACIDIFICATION OF STRATIFORM CLOUDS AND THEIR AEROSOL SCAVENGING PROPERTIES
R. A. Castillo and J. DeLuisi *In* Deutscher Wetterdienst, Annals from the German Meteorological Society, No. 25: 10th International Cloud Physics Conference Preprints, Volume 1 1988 p 267-269 (For primary document see N89-19605 12-42)
(Contracts NOAA-40-RANR-506003; NOAA-40-RANR-508854L)
Copyright Avail: Deutscher Wetterdienst, Frankfurter Strasse 135, D-6050 Offenbach am Main, Fed. Republic of Germany

N89-19696 Atmospheric Environment Service, Downsview (Ontario).
VERTICAL PROFILES OF POLLUTANTS INSIDE AND OUTSIDE OF CLOUD
G. A. Isaac and W. R. Leaitch *In* Deutscher Wetterdienst, Annals from the German Meteorological Society, No. 25: 10th International Cloud Physics Conference Preprints, Volume 1 1988 p 273-275 (For primary document see N89-19605 12-42)
Copyright Avail: Deutscher Wetterdienst, Frankfurter Strasse 135, D-6050 Offenbach am Main, Fed. Republic of Germany

N89-19697 Kernforschungsanlage, Juelich (Germany, F.R.). Inst. fuer Atmosphaere Chemie.
RESULTS OF TIME AND HEIGHT RESOLVED SCAVENGING EXPERIMENTS
Lucia Kins, Franz X. Meixner, and Klaus-Peter Mueller *In* Deutscher Wetterdienst, Annals from the German Meteorological Society, No. 25: 10th International Cloud Physics Conference Preprints, Volume 1 1988 p 276-278 (For primary document see N89-19605 12-42)
Copyright Avail: Deutscher Wetterdienst, Frankfurter Strasse 135, D-6050 Offenbach am Main, Fed. Republic of Germany

N89-19698 Central Electricity Research Labs., Leatherhead (England).
OXIDATION REGIMES IN OROGRAPHIC CAPPING CLOUD
P. A. Clark, G. P. Gervat, T. A. Hill, A. R. W. Marsh, A. S. Chandler, Tom W. Choularton, and M. J. Gay (Manchester Univ., England) *In* Deutscher Wetterdienst, Annals from the German Meteorological Society, No. 25: 10th International Cloud Physics Conference Preprints, Volume 1 1988 p 279-281 (For primary document see N89-19605 12-42)
Copyright Avail: Deutscher Wetterdienst, Frankfurter Strasse 135, D-6050 Offenbach am Main, Fed. Republic of Germany

N89-19700 National Oceanic and Atmospheric Administration, Boulder, CO. Environmental Sciences Group.
INFLUENCES OF CLOUD MICROPHYSICS ON CONTINENTAL AND MARINE PRECIPITATION CHEMISTRY
Farn Parungo and Clarence Nagamoto *In* Deutscher Wetterdienst, Annals from the German Meteorological Society, No. 25: 10th International Cloud Physics Conference Preprints, Volume 1 1988 p 285-287 (For primary document see N89-19605 12-42)
Copyright Avail: Deutscher Wetterdienst, Frankfurter Strasse 135, D-6050 Offenbach am Main, Fed. Republic of Germany

N89-19705 Washington Univ., Seattle. Geophysics Program.
A NUMERICAL INVESTIGATION OF SULFATE PRODUCTION AND DEPOSITION IN MIDLATITUDE CONTINENTAL CUMULUS CLOUDS
Gregory R. Taylor *In* Deutscher Wetterdienst, Annals from the German Meteorological Society, No. 25: 10th International Cloud Physics Conference Preprints, Volume 1 1988 p 300-302 (For primary document see N89-19605 12-42)
Copyright Avail: Deutscher Wetterdienst, Frankfurter Strasse 135, D-6050 Offenbach am Main, Fed. Republic of Germany

N89-19706 Academia Sinica, Beijing (China). Inst. of Atmospheric Physics.
A NUMERICAL SIMULATION OF THE ACIDIFICATION PROCESS OF RAIN WATER BELOW THE CLOUD AND THE MECHANISM OF ACID RAIN FORMATION IN AREA OF CHONGQING, CHINA
Meiyuan Huang and Shuairen Liu *In* Deutscher Wetterdienst, Annals from the German Meteorological Society, No. 25: 10th International Cloud Physics Conference Preprints, Volume 1 1988 p 303-305 (For primary document see N89-19605 12-42)
Copyright Avail: Deutscher Wetterdienst, Frankfurter Strasse 135, D-6050 Offenbach am Main, Fed. Republic of Germany

N89-19707 Pennsylvania State Univ., University Park. Dept. of Meteorology.
EFFECTS OF CLOUD MICROPHYSICAL PROCESSES ON TRACE CHEMICAL REMOVAL EFFICIENCES
Dennis Lamb and Jen-Ping Chen *In* Deutscher Wetterdienst, Annals from the German Meteorological Society, No. 25: 10th International Cloud Physics Conference Preprints, Volume 1 1988 p 306-308 (For primary document see N89-19605 12-42)
(Contracts NOAA-50-EANR-6-00011; DE-FG02-85ER-60294; NSF ATM-85-20123; NSF ATM-87-16166)
Copyright Avail: Deutscher Wetterdienst, Frankfurter Strasse 135, D-6050 Offenbach am Main, Fed. Republic of Germany

N89-19711 Clermont-Ferrand Univ. (France).
METEOROLOGICAL AND CHEMICAL INFLUENCING FACTORS ON ACIDITY PRODUCTION IN A MESOSCALE MODEL WITH QUASI-SPECTRAL MICROPHYSICS
Nadine Chaumerliac and Robert Rosset *In* Deutscher Wetterdienst, Annals from the German Meteorological Society, No. 25: 10th International Cloud Physics Conference Preprints, Volume 1 1988 p 319-321 (For primary document see N89-19605 12-42)
Copyright Avail: Deutscher Wetterdienst, Frankfurter Strasse 135, D-6050 Offenbach am Main, Fed. Republic of Germany

46 GEOPHYSICS

Includes aeronomy; upper and lower atmosphere studies; ionospheric and magnetospheric physics; and geomagnetism.

For space radiation see *93 Space Radiation.*

N89-19748 Georgia Inst. of Tech., Atlanta.
AN INVESTIGATION OF THE RELATIONSHIP BETWEEN BEAM AND GLOBAL IRRADIATION WITH THE DEVELOPMENT OF NUMERICAL SOLAR RADIATION MODELS Ph.D. Thesis
Constantinos Agelou Balaras 1988 390 p
Avail: Univ. Microfilms Order No. DA8820810

A number of improved numerical models were developed to predict the beam radiation from global radiation data. The analysis was based on 5 years of hourly radiation data. Previously developed empirical correlations relate hourly values of the beam transmittance to clearness index. The relationship between these two values, though, is not deterministic. Some of the observed variation was explained by a seasonal dependence. Improved performance was achieved by introducing a third variable, either the atmospheric air mass, or the temporal variation coefficient, a new dimensionless parameter used to describe the sky condition without using any meteorological information. Two improved beam radiation models were developed, relating three of the variables at a time. These correlations have significantly improved the predictive powers of the beam radiation model, without compensating for additional input information. These models can predict different values of beam radiation for a given day and over the year, for the same value of global radiation which is what is observed. Dissert. Abstr.

N89-19749*# National Aeronautics and Space Administration. Marshall Space Flight Center, Huntsville, AL.
SUPERCONDUCTING GRAVITY GRADIOMETER MISSION. VOLUME 2: STUDY TEAM TECHNICAL REPORT
Samuel H. Morgan, ed. and Ho Jung Paik, ed. (Maryland Univ., College Park.) Nov. 1988 249 p
(NASA-TM-4091; NAS 1.15:4091) Avail: NTIS HC A11/MF A01 CSCL 08G

Scientific and engineering studies and developments performed or directed by a Study Team composed of various Federal and University activities involved with the development of a three-axis superconducting gravity gradiometer integrated with a six-axis superconducting accelerometer are examined. This instrument is being developed for a future orbital mission to make precise global gravity measurements. The scientific justification and requirements for such a mission are discussed. This includes geophysics, the primary mission objective, as well as secondary objective, such as navigation and feats of fundamental laws of physics, i.e., a null test of the inverse square law of gravitation and tests of general relativity. The instrument design and status along with mission analysis, engineering assessments, and preliminary spacecraft concepts are discussed. In addition, critical spacecraft systems and required technology advancements are examined. The mission requirements and an engineering assessment of a precursor flight test of the instrument are discussed. Author

N89-19750# Instituto de Pesquisas Espaciais, Sao Jose dos Campos (Brazil).
MEASUREMENT OF ATMOSPHERIC ELECTRICAL FIELDS IN PERIODS OF ELECTRICAL PERTURBATION AND CALM AT THE LATITUDE OF 23 C [MEDIDAS DO CAMPO ELETRICO ATMOSFERICO EM PERIODOS ELETRICAMENTE PERTURBADO E CALMOS NA LATITUDE DE 23 C]
S. L. G. Dutra, W. D. Gonzalez, O. Pinto, Jr., I. R. C. A. Pinto, and O. C. Pontieri Jul. 1988 16 p In PORTUGESE Presented at the 2nd Regional Meeting of the SBGF, Salvador, BA, 25-27 Nov. 1987
(Contract FINEP 537/CT)
(INPE-4626-PRE/1344) Avail: NTIS HC A03/MF A01

The atmospheric electric field was recently measured in the altitude band of 20 to 40 km, utilizing detectors on-board stratospheric balloons. The technique utilized was a duplicate sounding and the flight was performed during periods with atmospheric electrical storms (periods called perturbation) and without the storms (calm period). The balloons were launched from Cachoeira Paulista, SP, (22 deg 44 S, 44 deg 56 W) in the affected field during the period 1985 to 1986. The measurement of the 1986 flight is presented. The values observed in the periods of electrical perturbation were expected due to the influence of the storm clouds; in the calm periods, the observations should show the electrical structure related to fair weather and/or the penetration of magnetospheric/ionospheric fields. The preliminary values obtained, meanwhile, are of elevated magnitudes and may lead to a new source of the electrical field. Author

N89-19751# Utah State Univ., Logan. Center for Space Engineering.
INFRARED AND IONIZATION STRUCTURE OF THE POLAR MESOSPHERE Final Report, 19 Mar. 1985 - 15 May 1988
James C. Ulwick, Kay D. Baker, and Allan J. Steed Aug. 1988 27 p
(Grant AF-AFOSR-0163-85; AF Proj. 2310)
(AD-A201266; AFOSR-88-1182TR) Avail: NTIS HC A03/MF A01 CSCL 04A

The primary objective of this project was the investigation of the spatial and temporal structuring and photochemistry of the infrared airglow and the dynamic processes that modify the physical and radiative properties of the polar mesosphere. The approach was to conduct ground-based mesospheric stratospheric tropospheric (MST) radar measurements and rocket-borne probes. Rockets containing dec probes were launched to measure electron density irregularities with high spatial resolution. They were launched at times when the MST radar showed regions of intense backscatter in the mesosphere. Large changes and strong gradients in the electron density were observed in the region of most intense backscatter. Several results from the spectra which are in agreement with present theories are as follows: (1) The electron fluctuation spectrum displayed both a Kolmogorov inertial subrange and a viscous subrange characterized by an inner scale for turbulence; (2) The inner scale size for the electron gas varies with the energy dissipation rate in a manner predicted by classical turbulence theory; and (3) The 50 MHz scattering signal is in qualitative agreement with the in situ measurements. Some of the more controversial results we have found are: (1) The microscale for turbulence in the electron gas is much smaller than expected; (2) The electrons seem to behave as a passive scalar but one

with a large Schmidt number; and (3) The fact that strong high latitude mesospheric scatter occurs at all for a 50 MHz radar is due to the unusual character of the electron spectrum. GRA

N89-19752# Liverpool Univ. (England). Dept. of Geography.
HOMOGENIZING SURFACE AND SATELLITE OBSERVATIONS OF CLOUD Final Scientific Report, 1 Oct. 1987 - 30 Sep. 1988
Ann Henderson-Sellers and Alan H. Goodman Oct. 1988 60 p
(Grant AF-AFOSR-0299-85)
(AD-A201630; EOARD-TR-89-03) Avail: NTIS HC A04/MF A01 CSCL 04B

Using four months of global surface cloud observations an investigation has been made concerning both types of contingency probability as applied to different cloud levels. Analysis of the probability as applied to different cloud levels. Analysis of the probability of observing an upper cloud given the presence of a lower cloud, P(L approaches U) with varying lower level cloud amounts gives different results from those of Hahn et al. (1982) at a variety of spatial scales ranging from individual stations to the globe. The implications of this are discussed with respect to the probability of observing a lower cloud in the presence of an upper cloud, P(U approaches L). We find that their evaluation of P(U approaches L) is greater than our calculation which is modified to account for the variation in P(L approaches U). Their overestimate is most noticeable in low and middle latitudes and can be reversed (to an underestimate) in some high latitude areas. Plans for the investigations of temporal variations in cloud amount and type on the ocean surface radiation budget are also discussed in the contex of the first analysis of the large data set of all-sky camera imagery obtained from the Joint Air Sea Interaction Experiment (JASIN) conducted in 1978. Our results show a considerable temporal variability in total and high cloud amount cf. conventional (bridge) observations. GRA

N89-19753 Nevada Univ., Reno.
BOUNDARY LAYER DEVELOPMENT OVER THE EASTERN PACIFIC OCEAN Ph.D. Thesis
Guillermo Felix Almeyda 1988 206 p
Avail: Univ. Microfilms Order No. DA8820832

A model of the marine boundary layer was developed to study air sea interactions during El Nino Southern Oscillation (ENSO) and the ANTI-ENSO episodes. The model considers a marine boundary layer that grows by gaining water vapor from the ocean at its lower boundary and entrainment of overlying air at its upper boundary. This layer moves horizontally at a constant wind speed over an ocean initially colder than the overlying air. The sea surface temperature can either change or remain constant. It is assumed that the air temperature at sea level must be equal to the sea surface temperature during the whole process. The potential temperature, mixing ratio and liquid water content profiles of the marine boundary layer are calculated at the end of 1 hour time steps. The top boundary height, the cloud base height, the cloud depth, and the inversion intensity are evaluated as a function of time. This model has been applied to simulate properties of the marine boundary over the Southeastern Pacific off the coasts of Chile, Peru, and Ecuador. A well developed marine layer with a greater depth and a thicker cloud layer results from ENSO conditions, in contrast to a reduced well-mixed layer with thin stratus, capped by a stronger inversion for the ANTI-ENSO conditions. These results suggest that the evolution of the marine boundary layer is governed by both evaporation from the ocean and the entrainment of overlying air into the marine boundary layer. Dissert. Abstr.

N89-19754 Texas Univ. at Dallas, Richardson.
A STUDY OF THE IONOSPHERIC SIGNATURE OF ION SUPPLY FROM THE IONOSPHERE TO THE MAGNETOSPHERE Ph.D. Thesis
Mark Andre Peter Loranc 1988 174 p
Avail: Univ. Microfilms Order No. DA8822345

Recent studies have demonstrated the importance of the ionosphere as a source of magnetospheric plasma; in particular, the observations of upwelling ions (UWI) by the DE-1 Retarding Ion Mass Spectrometer have illustrated the significance of low-energy ion supply to the magnetosphere. The composition of the UWI implies an ionospheric source, and the Dynamics Explorer dual satellite mission provides an opportunity to search for the ionospheric signature of UWI. Magnetometer data from both satellites is used to determine magnetic conjunctions of the satellites; these conjunctions are searched for correlated observations of UWI and upward flowing thermal ion (UFI) events. Four cases of correlated observations are presented as proof that the UFI are indeed the ionospheric signature of UWI. Dissert. Abstr.

N89-19755 Texas Univ. at Dallas, Richardson.
CHARACTERISTICS OF OPTICAL EMISSIONS AND PARTICLE PRECIPITATION IN MID/LOW LATITUDE AURORAE Ph.D. Thesis
Hamid-Reza RassoulK 1987 207 p
Avail: Univ. Microfilms Order No. DA8809003

Ground-based optical observations were made at low/mid latitudes to study the auroral effects of particle precipitation. The measured optical emissions include (OI) 5577 A, (OI) 6300 A, and (OI) 7774 A of atomic oxygen; the Balmer Beta line of Hydrogen at 4861 A; and the emission bands from the first negative nitrogen system at 3914 A and 4278 A. Spectral characteristics of low latitude aurorae, the correlation of optical data with geomagnetic field variations, and the nature of the precipitating particles were established. The particle precipitation enhances at times when there is a populated and/or energized ring current and there exists a strong magnetic perturbation near the local meridian of the precipitation. The observed geomagnetic perturbations have the signature expected from a station on the low latitude side of the substorm auroral electrojets, and the effects are much more pronounced in the mid latitude than in the low latitude magnetometers. On the basis of the observed optical and geomagnetic field data a precipitation index was devised. The precipitation index reflects the variations of both the ring current intensity and magnetospheric substorm current at a given local time. Dissert. Abstr.

N89-19756 Nevada Univ., Reno.
LIDAR FOR THE DETERMINATION OF ANTARCTIC WATER VAPOR PROFILES Ph.D. Thesis
Bruce Magill Whitcomb 1988 156 p
Avail: Univ. Microfilms Order No. DA8820833

A differential lidar technique was demonstrated to be capable of determining water vapor profiles in the Antarctic atmosphere in the vicinity of clear air ice crystal precipitation events. A Candela flashlamp-pumped, tunable dye laser operating in the 930-nm spectral region proved to be an appropriate source for the system. Application of this system to the measurement of low concentrations of water vapor, such as those which would be observed during Antarctic precipitation events, was demonstrated in the laboratory. Dissert. Abstr.

N89-19757 Washington Univ., Seattle.
A CRITICAL EVALUATION OF THE VON KARMAN CONSTANT FROM A NEW ATMOSPHERIC SURFACE LAYER EXPERIMENT Ph.D. Thesis
Shi Feng Zhang 1988 148 p
Avail: Univ. Microfilms Order No. DA8820454

The von Karman constant (k) occupies an important position in modern turbulence theory. A systematic review of the previous studies of k for the atmospheric boundary layer (ABL) is presented. This review shows that over the last 40 years, the evaluated values of k for the ABL (mostly between 0.35 and 0.42) are controversial and have poor accuracy. Using up-to-date technology, a new field experiment to investigate turbulence structure for the atmospheric surface layer was carried out near Carpenter, Wyoming in September/October, 1986. This experiment and the collected data are described in detail. The propeller-vane anemometers were used for the wind profile measurements in the Wyoming experiment. In order to obtain accurate wind profiles, a model for calculating the propeller-vane anemometer overspeeding (error) was developed.

The model was tested by the comparison of wind speeds between sonic and propeller-vane anemometers. The sonic anemometer data were corrected for flow distortion. Field measurements appear to support the model. Hence, all the wind profile data were corrected according to the model. A feature of the experiment is that four PAM-II stations around the experimental site provided a data set which was used to calculate small-scale divergence (D) of horizontal winds. Dissert. Abstr.

N89-19758 Cornell Univ., Ithaca, NY.
ELECTROSTATIC PLASMA WAVES AND TURBULENCE NEAR AURORAL ARCS Ph.D. Thesis
Gregory Duane Earle 1988 233 p
Avail: Univ. Microfilms Order No. DA8821216

A cooperative experiment involving multiple probes was carried out in Greenland to measure the dynamic properties of the ionospheric plasma during active auroral conditions. The observations were made in a highly structured, low density plasma near a large scale convection shear at the edge of the auroral oval. Simultaneous observations by sounding rockets, incoherent scatter radar, and a high altitude satellite show good agreement between the various large scale plasma density and electric field measurements. The two sounding rockets involved in the experiment also made high resolution measurements as they simultaneously flew parallel to the oval along similar azimuths. A technique involving the simulation of a rocket flight through a medium of computer generated waves was used to directly compare the observations with theory. Dissert. Abstr.

N89-19759# Colorado State Univ., Fort Collins. Dept. of Physics.
A HIGH-SPECTRAL-RESOLUTION LIDAR SYSTEM: THE USE OF ATOMIC BLOCKING FILTER FOR MEASURING ATMOSPHERIC PARAMETERS Final Report, Jul. 1983 - Jun. 1988
Chiao-Yao She Oct. 1988 10 p
(Contract DAAG29-83-K-0095)
(AD-A201736; ARO-20157.6-GS) Avail: NTIS HC A02/MF A01 CSCL 04A

The objective of this project is to develop atomic-vapor absorption cells to be used as blocking filters for a high spectral resolution lidar (HSRL). Experimental assessment of the proposed new high-spectral-resolution lidar technique for backscatter ratio and atmospheric temperature measurements in the troposhere is presented. The feasibility of the proposed concept has been demonstrated by laboratory measurements using a CW tunable laser with an atomic vapor filter constructed for this purpose. The status of current laboratory experiment with pulsed system suggests that field measurement of backscatterer ratio can be made to 1 percent accuracy. A factor of 10 improvement in the accuracy in determining the molecular attenuation factor resulting from the atomic vapor filter is needed for field temperature measurement with a 1 K accuracy. GRA

N89-19760# McDonnell-Douglas Astronautics Co., Huntsville, AL.
ELECTRIC FIELDS IN EARTH ORBITAL SPACE Annual Report, Sep. 1987 - Sep. 1988
W. P. Olson and K. A. Pfitzer 19 Oct. 1988 26 p
(Contract N00014-80-C-0796; RR02101)
(AD-A201747) Avail: NTIS HC A03/MF A01 CSCL 04A

A model of the ground state magnetosphere was developed previously and it is suggested that the basic magnetosphere is formed and maintained simply by the interaction of the solar wind with the geomagnetic field. It is known, however, that the magnetosphere responds dynamically to changes in the interplanetary magnetic field (IMF). Instead of the qualitative reconnection theory (which we believe is basically incorrect), we have examined this response in terms of electromagnetic wave propagation in the interplanetary region. We suggest that the interplanetary plasma (solar wind) is magnetized by solar magnetic sector structure. Electromagnetic waves of higher frequency can propagate through the solar wind without appreciable attenuation. It is the interaction of these disturbance waves with the magnetosphere that causes the observed magnetospheric response to the IMF. The propagation of electromagnetic disturbances in the interplanetary region and their interaction with the magnetosphere are examined. Only certain modes propagate and there are further restrictions on the wave at the magnetopause. Southward and northward disturbances enter the magnetotail and then propagate within the magnetosphere. A magnetic field model is developed that includes propagating waves within the magnetosphere. These models will help us develop a quantitative model of magnetospheric tail dynamics. GRA

N89-19761# Lowell Univ., MA. Center for Atmospheric Research.
CALCULATION OF MOLECULAR ABSORPTION PARAMETERS AND UPDATING THE AFGL ATMOSPHERIC LINE PARAMETER COMPILATION Final Report, 31 May 1985 - 30 May 1988
Robert R. Gamache 15 Sep. 1988 177 p
(Contract F19628-85-K-0044)
(AD-A202113; ULRF-446/CAR; AFGL-TR-88-0228) Avail: NTIS HC A09/MF A01 CSCL 07B

The changes and updates made that produced the 1986 version of the HITRAN database are discussed. The new format adopted and the programs and files that are distributed with the database are reviewed. We present the new parameters added to the database and the sources of the data. We briefly discuss our work on the temperature dependence of the N2-broadened halfwidths and line shifts for ozone and water vapor. The work done on the calculation of line intensities for transitions in the visible region of the spectrum for water vapor is given. We discuss many of the miscellaneous tasks relating to the database that were done under this contract. Finally the work done on calculating the total internal partition sums and their temperature dependence for the species on the database is presented. GRA

N89-19762# Naval Postgraduate School, Monterey, CA.
REFRACTIVE TURBULENCE PROFILING VIA BINARY SOURCE INTENSITY SCINTILLATION CORRELATION M.S. Thesis
Ricky R. Holland Sep. 1988 73 p
(AD-A202189) Avail: NTIS HC A04/MF A01 CSCL 04A

This study examines the binary source correlation technique for determining vertical profiles of the refractive index structure parameter. Theoretical intensity scintillation covariance functions and power spectra for atmospheric layers of depth delta(h) at a mean altitude of h are derived. These functions are related to the photoelectron counting statistics and the spatial covariance of photoelectron counts for binary point sources. A linear detector array in the exit pupil of an optical system is examined, and the effects of the detection process uncertainty are explored. A lower bound for the expected error of an experimental determination of the spatioangular covariance of counts is derived. This error is then minimized via at least squares analysis using the redundant information available in pairwise multiple correlations of a signal from the detector elements of a ten element linear array. The refractive index structure parameter profile is then derived and found to be the undetermined coefficients of the spatial covariance weighting functions in the least squares analysis. GRA

N89-19763# Southwest Research Inst., San Antonio, TX.
STUDY OF THE CONTINUOUS/DIFFUSE AURORA USING PARTICLE OBSERVATIONS FROM THE DYNAMICS EXPLORER SATELLITES Final Technical Report, 1 Jan. 1985 - 17 Oct. 1988
J. R. Sharber and J. D. Winningham 17 Oct. 1988 72 p
(Contract F49620-85-C-0029)
(AD-A202241; AFOSR-88-1202TR) Avail: NTIS HC A04/MF A01 CSCL 04A

The continuous/diffuse (C/D) aurora and related auroral studies are used as the primary data observations from instruments on the Dynamics Explorer satellites. These satellites carried particle detection instrumentation referred to as the High Altitude Plasma

Instrument (HAPI) on the DE-1 and the Low Altitude Plasma Instrument (LAPI) on DE-2, and together provided high resolution spectral and angular measurements of electron and positive ions at altitudes between 500 km and 4 R sub E above the auroral region. The objectives of the research are: (1) to provide a thorough description of the particle populations which produce the quiet and activated continuous/diffuse aurora, (2) to attempt to determine what mechanisms act within the plasma sheet and on supra-auroral field lines to precipitate the continuous/diffuse auroral particles, (3) to attempt to find a simple and effective way to model the effects of this aurora and (4), added during the first year of the contract, applying the Dynamics Explorer database to selective investigations of of the high-latitude auroral regions. Research has included a description of quiet and disturbed diffuse auroral particles, a study of particles and waves in the diffuse aurora, an attempt to determine the mechanisms of the precipitation, and studies of polar arcs, ionization, and convection in the high-latitude regions. GRA

N89-19764*# Aerospace Corp., El Segundo, CA. Lab. Operations.
SUBSTORMS, PLASMOIDS, FLUX ROBES, AND MAGNETOTAIL FLUX LOSS ON MARCH 25, 1983: CDAW-8
D. H. Fairfield, D. N. Baker, J. A. Slavin, J. D. Craven, L. A. Frank, I. C. Elphic, J. F. Fennell, I. G. Richardson, H. J. Singer, and B. T. Tsurutani (Jet Propulsion Lab., California Inst. of Tech., Pasadena.) et al 3 Oct. 1988 70 p
(Contracts NAS5-28448; F04701-85-C-0086)
(NASA-CR-184823; NAS 1.26:184823; AD-A202278; TR-0088(3940-05)-1; SD-TR-88-85) Avail: NTIS HC A04/MF A01 CSCL 04A

During a 9-hour period following a storm-sudden commencement, six spacecraft near geosynchronous orbit, one over the pole, and three in the magnetotail, monitored a complex sequence of magnetospheric variations. Magnetic field compressions associated with the sudden commencement were seen first by the near earth spacecraft and subsequently by the three down-tail spacecraft with increasing time delays that were consistent with the tailward movement of an interplanetary-shock-associated pressure enhancement. Ground magnetograms and synchronous orbit data are used to identify 7 substorm intensifications during this geomagnetically active period. Six of these intensifications are clearly associated with tail lobe field decreases about 18 R sub E behind the earth. Four of these intensifications are followed by both Bz field increases in the tail lobes at about 18 and about 30 R sub E and by the subsequent observation of rapidly flowing plasma sheet plasma at ISEE 3 about 110 R sub E down the tail. During two substorms where DE 1 was optically observing the auroral oval, the area of the polar cap was observed to decrease as the tail lobe field decreased at 18 R sub E. All these observations are consistent with the substorm associated release of a plasmoid at a neutral line near 20 R sub E. GRA

N89-19765# Northwest Research Associates, Inc., Bellevue, WA.
AN ASSESSMENT OF THE APPLICATION OF IN SITU ION-DENSITY DATA FROM DMSP (DEFENSE METEOROLOGY SATELLITE PROGRAM) TO MODELING OF TRANSIONOSPHERIC SCINTILLATION Technical Report, 15 Sep. 1987 - 14 Sep. 1988
James A. Secan and Robert M. Bussey 15 Sep. 1988 86 p
(Contract F19628-86-C-0195)
(AD-A202415; NWRA-CR-88-R031; AFGL-TR-88-0280; SR-2)
Avail: NTIS HC A05/MF A01 CSCL 04A

Modern military communication, navigation, and surveillance systems depend on reliable, noise-free transionospheric radio frequency channels. They can be severely impacted by small scale electron density irregularities in the ionosphere which cause both phase and amplitude scintillation. Basic tools used in planning and mitigation schemes are climatological in nature and thus may greatly over- and under-estimate the effects of scintillation in a given scenario. This report describes the second year of an investigation into the feasibility of using in situ observations of the ionosphere from the U.S.A.F. DMSP satellite to calculate estimates of irregularity parameters which could be used to update scintillation models in near real-time. Methods for processing DMSP Scintillation Meter (SM) data and for calculating estimates of C sub K L from the SM data are described. Results of the analysis of DMSP SM data from a coordinated data-collection campaign run in January 1988 are presented. GRA

N89-19766# Compagnia Italiana Servizi Tecnici, Rome.
SOLID EARTH ARISTOTELES MISSION DATA PREPROCESSING SIMULATION OF GRAVITY GRADIOMETER Final Report
G. Avanzi, R. Stolfa, and B. Versini Paris, France ESA 1988 94 p
(Contract ESA-7388/87-NL-JS)
(ESA-CR(P)-2666; ETN-89-93912) Copyright Avail: NTIS HC A05/MF A01

Data preprocessing of the ARISTOTELES mission, which measures the Earth gravity gradient in a near polar orbit, was studied. The mission measures the gravity field at sea level through indirect measurements performed on the orbit, so that the evaluation steps consist in processing data from GRADIO accelerometer measurements. Due to the physical phenomena involved in the data collection experiment, it is possible to isolate at an initial stage a preprocessing of the gradiometer data based only on GRADIO measurements and not needing a detailed knowledge of the attitude and attitude rate sensors output. This preprocessing produces intermediate quantities used in future stages of the reduction. Software was designed and run to evaluate for this level of data reduction the achievable accuracy as a function of knowledge on instrument and satellite status parameters. The architecture of this element of preprocessing is described. ESA

N89-19767# Gesellschaft fuer Strahlen- und Umweltforschung m.b.H., Munich (Germany, F.R.).
DEVELOPMENT OF A DETECTION SYSTEM FOR ATMOSPHERIC TRACE GASES, IN PARTICULAR FOR OH MOLECULES AND REALIZATION OF FIELD MEASUREMENTS Final Report, 31 Oct. 1987
W. Armerding, A. Herbert, G. Mollekopf, T. Schindler, M. Spiekerman, and F. J. Comes Jun. 1988 91 p In GERMAN; ENGLISH summary Prepared in cooperation with Johann-Wolfgang-Goethe-Univ., Frankfurt am Main (Germany, F.R.).
(Contract BMFT-KFZ-0704587-2)
(BPT-11/88; ISSN-0176-0777; ETN-89-93955) Copyright Avail: NTIS HC A05/MF A01

A long-path absorption technique for the detection of tropospheric OH-concentration with excellent sensitivity, direct OH-identification, and self-calibration is described. A rapidly tunable, frequency-doubled laser-system was developed to eliminate atmospheric fluctuations. A range of 6 mm is scanned in less than 100 microsec. Output power of the laser is 10 mW with a bandwidth of 800 MHz. The main limitation of the sensitivity is the (unavoidable) modulation of the output power due to the angle tuning of the doubling crystal. With a real-time electronic demodulation of the outgoing signal, 8 ppb SO2 are detected with an absorption path length of 800 m. This is equivalent to 5 million OH/cc. Improvement in the detection limit to the order 100,000 OH/cc can be expected if the output power of the laser is stabilized and normalized by optical modulators. ESA

N89-19768 Utah State Univ., Logan.
A STUDY OF THE HIGH ALTITUDE THERMOSPHERIC DAYGLOW FROM SPACELAB 1 Ph.D. Thesis
Jong Won Eun 1988 237 p
Avail: Univ. Microfilms Order No. DA8823621

The optical emissions from the sunlit upper atmosphere contain detailed information concerning the composition of this region and on a variety of processes that occur as part of the overall photochemistry of the region. In order to survey the thermospheric dayglow, an array of spectrometers was developed to operate

from the vacuum ultraviolet to the near infrared. This instrument was tested on the Spacelab 1 mission. The results reported will deal with the observations made during the mission with that instrument, with the field of view looking tangentially from the orbit at 250 km, or looking above 250 km, namely, the high altitude dayglow. The purpose is to use these data to investigate the main features of the spectrum at these altitudes between 1150 A and 8000 A. The principal features are compared with the predictions of our present knowledge of the excitation process in the thermosphere. Particular consideration is given to the N2(+) first negative band system in the visible and near ultraviolet, and the N2 Lyman-Birge-Hopfield bands in the vacuum ultraviolet; vibrational population distributions are determined for the upper states of these two systems in the dayglow. Dissert. Abstr.

N89-19769 Institut d'Aeronomie Spatiale de Belgique, Brussels.
ULTRAVIOLET ABSORPTION CROSS-SECTIONS OF HALOCARBONS OF STRATOSPHERIC INTEREST
D. Gillotay and P. C. Simon 1988 128 p
(Aeronomica-Acta-A-336-1988; ISSN-0065-3715; ETN-89-93749)
Avail: Institut d'Aeronomie Spatiale de Belgique, 3 Avenue Circulaire, B-1180 Brussels, Belgium

Ultraviolet absorption cross-section values of 26 halocarbons of atmospheric interest are presented as a function of wavelength and temperature. Polynomial formulae to compute the absorption cross-sections for given temperature and wavelength ranges are also proposed. ESA

N89-19770# Institut d'Aeronomie Spatiale de Belgique, Brussels.
STRATOSPHERIC NITRIC ACID: FEASIBILITY OF ROUTINE MEASUREMENT BY OBSERVATION FROM COMMERCIAL AIRLINERS IN IR BANDS FROM 9 TO 14 MICRONS [ACIDE NITRIQUE STRATOSPHERIQUE: FAISABILITE DE LA MESURE DE RUTINE PAR OBSERVATION DES BANDES IR DE 9 A 14 MICRON A PARTIR DAVIONS DE LIGNES]
C. Lippens, C. Muller, and M. Ackerman 1989 34 p In FRENCH; ENGLISH summary
(C-48-1977) Avail: NTIS HC A03/MF A01

A radiometer developed for the observation of sky emissions in the 7 to 15 micrometer atmospheric window is described. A balloon flight performed in May 1976 permits the observation and the determination of an HNO3 vertical distribution in the stratosphere. The possibility of also making routine measurements of ozone and other constituents is discussed. The good performance of the instruments during flights on board the Caravelle of the Centre d'Essais en Vol is also shown. Author

N89-19641 Wisconsin Univ., Madison.
GENERALIZED MICROPHYSICS SCHEME FOR USE IN MESOSCALE/CLOUD MODELS
Gregory J. Tripoli, Piotr J. Flatau, and William R. Cotton (Colorado State Univ., Fort Collins.) *In* Deutscher Wetterdienst, Annals from the German Meteorological Society, No. 25: 10th International Cloud Physics Conference Preprints, Volume 1 1988 p 109-111 (For primary document see N89-19605 12-42)
(Grant NSF ATM-85-12480)
Copyright Avail: Deutscher Wetterdienst, Frankfurter Strasse 135, D-6050 Offenbach am Main, Fed. Republic of Germany

N89-19649* National Aeronautics and Space Administration. Ames Research Center, Moffett Field, CA.
CIRRUS MICROPHYSICS AND INFRARED RADIATIVE TRANSFER: A CASE STUDY
Thomas P. Ackerman, Andrew J. Heymsfield (National Center for Atmospheric Research, Boulder, CO.), Francisco P. J. Valero, and Stefan Kinne *In* Deutscher Wetterdienst, Annals from the German Meteorological Society, No. 25: 10th International Cloud Physics Conference Preprints, Volume 1 1988 p 133-134 (For primary document see N89-19605 12-42)
Copyright Avail: Deutscher Wetterdienst, Frankfurter Strasse 135, D-6050 Offenbach am Main, Fed. Republic of Germany CSCL 04A

N89-19652 Meteorological Office, Bracknell (England).
THE COMPARISON OF HOLOGRAPHIC AND 2-D PROBE MEASUREMENTS OF ICE CRYSTALS
P. R. A. Brown and A. G. Darlison *In* Deutscher Wetterdienst, Annals from the German Meteorological Society. No. 25: 10th International Cloud Physics Conference Preprints, Volume 1 1988 p 141-143 (For primary document see N89-19605 12-42)
Copyright Avail: Deutscher Wetterdienst, Frankfurter Strasse 135, D-6050 Offenbach am Main, Fed. Republic of Germany

N89-19657 Institute of Experimental Meteorology, Obninsk (USSR).
AN INVESTIGATION OF THE EFFECT OF ELECTRICAL CHARGES ON THE COLLISION EFFICIENCY OF CLOUD DROPS
V. M. Kim *In* Deutscher Wetterdienst, Annals from the German Meteorological Society, No. 25: 10th International Cloud Physics Conference Preprints, Volume 1 1988 p 158-160 (For primary document see N89-19605 12-42)
Copyright Avail: Deutscher Wetterdienst, Frankfurter Strasse 135, D-6050 Offenbach am Main, Fed. Republic of Germany

N89-19658 High Mountain Geophysical Inst., Nalchik (USSR).
MICROPHYSICAL AND ELECTRICAL PHENOMENA DURING FREEZING OF WATER DROPS
A. Kh. Adzhiev and S. T. Tomazov *In* Deutscher Wetterdienst, Annals from the German Meteorological Society, No. 25: 10th International Cloud Physics Conference Preprints, Volume 1 1988 p 161-163 (For primary document see N89-19605 12-42)
Copyright Avail: Deutscher Wetterdienst, Frankfurter Strasse 135, D-6050 Offenbach am Main, Fed. Republic of Germany

N89-19659 Academy of Sciences of the Georgian SSR, Tbilisi. Inst. of Geophysics.
EFFECT OF THE ELECTRIC FIELD ON THE RAINDROP SHAPE
Georgi Magradze *In* Deutscher Wetterdienst, Annals from the German Meteorological Society, No. 25: 10th International Cloud Physics Conference Preprints, Volume 1 1988 p 166-168 (For primary document see N89-19605 12-42)
Copyright Avail: Deutscher Wetterdienst, Frankfurter Strasse 135, D-6050 Offenbach am Main, Fed. Republic of Germany

N89-19660 Trinity Coll., Hartford, CT.
DAMPED-OSCILLATION REPRESENTATION OF DROP-SPECTRUM EVOLUTION DUE TO COALESCENCE AND BREAKUP
Philip S. Brown, Jr. *In* Deutscher Wetterdienst, Annals from the German Meteorological Society, No. 25: 10th International Cloud Physics Conference Preprints, Volume 1 1988 p 169-171 (For primary document see N89-19605 12-42)
(Grant NSF ATM-85-21417)
Copyright Avail: Deutscher Wetterdienst, Frankfurter Strasse 135, D-6050 Offenbach am Main, Fed. Republic of Germany

N89-19661 Israel Meteorological Service, Bet Dagan. Dept. of Research and Development.
KINETIC EQUATION FOR POLLUTED CLOUD DROPLETS SPECTRUM
Isaac M. Enukashvily *In* Deutscher Wetterdienst, Annals from the German Meteorological Society, No. 25: 10th International Cloud Physics Conference Preprints, Volume 1 1988 p 172-174 (For primary document see N89-19605 12-42)
Copyright Avail: Deutscher Wetterdienst, Frankfurter Strasse 135, D-6050 Offenbach am Main, Fed. Republic of Germany

N89-19680 South Dakota School of Mines and Technology, Rapid City. Inst. of Atmospheric Sciences.
COMPARISON OF MODEL RESULTS FOR MODELS OF DIFFERING MICROPHYSICAL DETAIL
R. D. Farley and H. D. Orville *In* Deutscher Wetterdienst, Annals from the German Meteorological Society, No. 25: 10th International

Cloud Physics Conference Preprints, Volume 1 1988 p 226-228 (For primary document see N89-19605 12-42)
(Grants NSF ATM-85-16940; NSF ATM-86-03308)
Copyright Avail: Deutscher Wetterdienst, Frankfurter Strasse 135, D-6050 Offenbach am Main, Fed. Republic of Germany

N89-19686 Desert Research Inst., Reno, NV.
STUDIES OF CLOUD MICRO-CHEMICAL PHYSICS
Richard L. Pitter and William G. Finnegan *In* Deutscher Wetterdienst, Annals from the German Meteorological Society, No. 25: 10th International Cloud Physics Conference Preprints, Volume 1 1988 p 243-245 Sponsored in part by ONR, Washington, DC and NOAA, Washington, DC (For primary document see N89-19605 12-42)
Copyright Avail: Deutscher Wetterdienst, Frankfurter Strasse 135, D-6050 Offenbach am Main, Fed. Republic of Germany

N89-19692 Washington Univ., Seattle. Dept. of Atmospheric Sciences.
SOME EFFECTS OF CLOUD MICROPHYSICS ON CLOUD CHEMISTRY
Dean A. Hegg and Peter V. Hobbs *In* Deutscher Wetterdienst, Annals from the German Meteorological Society, No. 25: 10th International Cloud Physics Conference Preprints, Volume 1 1988 p 261-263 (For primary document see N89-19605 12-42)
(Grant NSF ATM-84-19000)
Copyright Avail: Deutscher Wetterdienst, Frankfurter Strasse 135, D-6050 Offenbach am Main, Fed. Republic of Germany

N89-19695 Eidgenoessische Technische Hochschule, Zurich (Switzerland). Dept. of Atmospheric Physics.
MICROPHYSICAL, DYNAMICAL AND CHEMICAL ASPECTS OF SCAVENGING PROCESSES DURING WINTER PRECIPITATION
A. Waldvogel, T. Schumann, and B. Zinder *In* Deutscher Wetterdienst, Annals from the German Meteorological Society, No. 25: 10th International Cloud Physics Conference Preprints, Volume 1 1988 p 270-272 (For primary document see N89-19605 12-42)
Copyright Avail: Deutscher Wetterdienst, Frankfurter Strasse 135, D-6050 Offenbach am Main, Fed. Republic of Germany

N89-19699 Stockholm Univ. (Sweden). Dept. of Meteorology.
AN EXAMINATION OF THE CHEMICAL AND PHYSICAL VARIABILITY OF CLOUDS AT A MOUNTAIN-TOP SITE IN CENTRAL SWEDEN
Kevin J. Noone, John A. Ogren, and Jost Heintzenberg *In* Deutscher Wetterdienst, Annals from the German Meteorological Society, No. 25: 10th International Cloud Physics Conference Preprints, Volume 1 1988 p 282-284 (For primary document see N89-19605 12-42)
Copyright Avail: Deutscher Wetterdienst, Frankfurter Strasse 135, D-6050 Offenbach am Main, Fed. Republic of Germany

N89-19708 State Univ. of New York, Albany. Atmospheric Sciences Research Center.
DYNAMIC, RADIATIVE AND CHEMICAL EFFECTS OF CLOUDS ON TROPOSPHERIC TRACE GASES
Chris J. Walcek *In* Deutscher Wetterdienst, Annals from the German Meteorological Society, No. 25: 10th International Cloud Physics Conference Preprints, Volume 1 1988 p 309-311 (For primary document see N89-19605 12-42)
Copyright Avail: Deutscher Wetterdienst, Frankfurter Strasse 135, D-6050 Offenbach am Main, Fed. Republic of Germany

N89-19709 Argonne National Lab., IL. Center for Environmental Research.
PARAMETERIZATIONS OF MICROPHYSICAL PROCESSES IN CLOUDS FOR APPLICATION IN MODELS OF REGIONAL ATMOSPHERIC DEPOSITION
In Young Lee *In* Deutscher Wetterdienst, Annals from the German Meteorological Society, No. 25: 10th International Cloud Physics Conference Preprints, Volume 1 1988 p 312-315 (For primary document see N89-19605 12-42)
(Contract W-31-109-eng-38)
Copyright Avail: Deutscher Wetterdienst, Frankfurter Strasse 135, D-6050 Offenbach am Main, Fed. Republic of Germany

N89-19712 Meteorological Office, Bracknell (England).
A COMPARISON OF RADIOMETRIC AND IMMERSION TEMPERATURE MEASUREMENTS IN WATER CLOUDS
S. Nicholls, E. L. Simmons, N. C. Atkinson, and S. D. Rudman *In* Deutscher Wetterdienst, Annals from the German Meteorological Society, No. 25: 10th International Cloud Physics Conference Preprints, Volume 1 1988 p 322-324 (For primary document see N89-19605 12-42)
Copyright Avail: Deutscher Wetterdienst, Frankfurter Strasse 135, D-6050 Offenbach am Main, Fed. Republic of Germany

N89-19713 Clermont-Ferrand Univ. (France).
CALIBRATION OF PMS FSSP AND 1D-C PROBES FOR CLOUD DROPLET MEASUREMENTS
Jean-Francois Gayet *In* Deutscher Wetterdienst, Annals from the German Meteorological Society, No. 25: 10th International Cloud Physics Conference Preprints, Volume 1 1988 p 325-327 (For primary document see N89-19605 12-42)
(Grant CEPr/ADER-86/00020)
Copyright Avail: Deutscher Wetterdienst, Frankfurter Strasse 135, D-6050 Offenbach am Main, Fed. Republic of Germany

N89-19717 National Center for Atmospheric Research, Boulder, CO.
APPLICATIONS OF THE NCAR ELECTRA DOPPLER RADAR FOR THE STUDY OF PHYSICAL PARAMETERS OF CLOUDS
Craig Walther, Charles Frush, and Peter Hildebrand *In* Deutscher Wetterdienst, Annals from the German Meteorological Society, No. 25: 10th International Cloud Physics Conference Preprints, Volume 1 1988 p 335-337 (For primary document see N89-19605 12-42)
Copyright Avail: Deutscher Wetterdienst, Frankfurter Strasse 135, D-6050 Offenbach am Main, Fed. Republic of Germany

N89-20077*# Sul Ross State Univ., Alpine, TX. Dept. of Geology.
EVALUATION OF CRUSTAL RECYCLING DURING THE EVOLUTION OF ARCHEAN-AGE MATACHEWAN BASALTIC MAGMAS Final Report
Dennis O. Nelson *In* NASA, Lyndon B. Johnson Space Center, National Aeronautics and Space Administration (NASA)/American Society for Engineering Education (ASEE) Summer Faculty Fellowship Program 1988, Volume 2 Feb. 1989 15 p (For primary document see N89-20073 12-99)
Avail: NTIS HC A09/MF A01 CSCL 08G

N89-20078*# Sul Ross State Univ., Alpine, TX. Analytical Lab.
LITHOSPHERIC BUCKLING AND INTRA-ARC STRESSES: A MECHANISM FOR ARC SEGMENTATION Final Report
Kerri L. Nelson *In* NASA, Lyndon B. Johnson Space Center, National Aeronautics and Space Administration (NASA)/American Society for Engineering Education (ASEE) Summer Faculty Fellowship Program 1988, Volume 2 Feb. 1989 14 p (For primary document see N89-20073 12-99)
Avail: NTIS HC A09/MF A01 CSCL 08G

47 METEOROLOGY AND CLIMATOLOGY

Includes weather forecasting and modification.

N89-19771# National Weather Service, Kansas City, MO.
[CENTRAL REGION APPLIED RESEARCH ON SEVERE WEATHER FORECASTING] Research Papers 88-1 through 88-7
May 1988 84 p
(PB88-210836; NOAA-TM-NWS-CR-88) Avail: NTIS HC A05/MF A01 CSCL 04B

Weather forecasting as applied to the central region of the United States is discussed. Wind storms, real time analysis, lake

enhanced snow storms in Michigan, a collection of severe weather parameters used for a checklist, thunderstorm forecasting and the use of long waves in forecasting are among the topics discussed. For individual titles, see N89-19772 through N89-19778.

N89-19772# National Weather Service, Cheyanne, WY. Forecast Office.
THE CHEYENNE WINDSTORM THAT NEVER CAME: ANOTHER LESSON IN REAL TIME ANALYSIS
Edward K. Berry *In* National Weather Service, Central Region Applied Research on Severe Weather Forecasting May 1988 p 1-9 (For primary document see N89-19771 12-47)
(CRARP-88-1) Avail: NTIS HC A05/MF A01 CSCL 04B

A discussion is given of why a high event did not occur at Cheyenne, Wyoming. As a result of modeling errors, the magnitude of surface west to northwest geostrophic winds were forecasted to be high over eastern Wyoming valid 5:00 a.m. MST Monday, February 8. The main error in all the numerical guidance was the improper prediction of a middle and upper tropospheric short wave trough that originated in a relatively data void region of the eastern Pacific. It is speculated that this short wave trough initiated cyclogenesis on the leeside over northeastern Colorado causing a weak easterly gradient wind to occur over Cheyenne. Thus, the pressure gradient force was not favorable for a high wing event. A clue to this busted high wind forecast came Sunday afternoon, one day before this event was to occur when Satellite Weather Interpretation System (SWIS) animation indicated a fairly significant comma cloud feature moving through eastern Pacific, a feature not handled well by the models. If more consideration would have been given to what SWIS showed, the busted forecast may have been avoided. This case represents yet another example where real time monitoring of the atmosphere can be used as short time scale forecasting tool to possibly avoid a bust. This monitoring can be done using real time surface and constant pressure analyses, satellite imagery, radar data, etc. Author

N89-19773# National Weather Service, Ann Arbor, MI. Forecast Office.
A CASE STUDY OF SIGNIFICANT LAKE ENHANCED SNOW EVENT IN UPPER MICHIGAN
Richard Wagenmaker *In* National Weather Service, Central Region Applied Research on Severe Weather Forecasting May 1988 p 10-25 (For primary document see N89-19771 12-47)
(CRARP-88-2) Avail: NTIS HC A05/MF A01 CSCL 04B

Analyses of the heavy snowfalls of April 1 and 2, 1987, in Michigan illustrates the snowfall potential of slow moving synoptic scale storm systems through the Great Lakes in winter. For this particular storm, nearly 2 1/2 feet were verified while forecasts indicated no more than two inches in 24 hours for Michigan. Interestingly, the Nested Grid Model (NGM) performed rather well during this event. Using the NGM, Hank's method of forecasting snow amounts also gave a fairly accurate depiction of what was considered to be the synoptic scale contribution to the snowfall totals. But, subtracting this larger scale contribution still leaves a nearly two foot mesoscale contribution near the lake shore. In fact, from all appearances, some increadible snowfall rates. Even an estimate using the Dockus Decision Tree (Dockus, 1985) of nine to 12 inches in six hours was likely a bit conservative. The difficulty in forecasting an event of this magnitude is quite apparent. But, hopefully, results of this study will make it a bit easier to recognize the potential in such a system. And, once such an event is underway, researchers have shown that MESOS, in addition to radar, can be a valuable tool in making a timely snowcast. Author

N89-19774# National Weather Service, Sioux Falls, SD. Forecast Office.
A COLLECTION OF SEVERE WEATHER PARAMETERS USED FOR A CHECKLIST
Lee C. Anderson *In* National Weather Service, Central Region Applied Research on Severe Weather Forecasting May 1988 p 26-32 (For primary document see N89-19771 12-47)
(CRARP-88-3) Avail: NTIS HC A05/MF A01 CSCL 04B

Forecasters must examine a number of variables to acquire an adequate understanding of the current state of the atmosphere. In order to make specific forecasts of a particular type of phenomena, for example severe storms, many synoptic and subsynoptic parameters should be checked closely. The expected values of the variables for a forecast period can help the forecaster get a better understanding of the potential of significant weather developments. Several severe weather parameters have been compiled from three different sources including a work sheet from one of the references. The parameters have been organized into a checklist. A list of ratings of the parameters has been included. By using the list of ratings, the forecasters can assess a value to each parameter. Author

N89-19775# National Weather Service, Topeka, KS. Forecast Office.
A MEDITATION ON MILLER
Richard P. McNulty *In* National Weather Service, Central Region Applied Research on Severe Weather Forecasting May 1988 p 33-38 (For primary document see N89-19771 12-47)
(CRARP-88-4) Avail: NTIS HC A05/MF A01 CSCL 04B

A comparison of the four ingredients needed for the occurrence of thunderstorms and the 14 factors used to forecast severe weather leads to the conclusion that only three parameters (extreme instability, strong vertical wind shear and the mid-level dry intrusion) on Miller's Summary of Key Parameters actually indicate a potential for severe weather occurrence. The remaining factors on the list indicate a potential for significant convection. These results suggest that forecasters can first anticipate the occurrence of thunderstorms, and then decide if these storms will reach severe limits. This two step approach to severe weather forecasting differs from the more traditional one step approach described by Miller and employed by the National Severe Storms Forecast Center. Author

N89-19776# National Weather Service, Sioux Falls, SD. Forecast Office.
TECHNICAL REPORT ON TEMPERATURE, PRECIPITATION AND AVIATION VERIFICATION AT WSFO SIOUX FALLS FOR 1987
Jack Bier *In* National Weather Service, Central Region Applied Research on Severe Weather Forecasting May 1988 p 39-53 (For primary document see N89-19771 12-47)
(CRARP-88-5) Avail: NTIS HC A05/MF A01 CSCL 04B

The attached TEMPCHECK tables and graphs show that Sioux Falls forecasts were moderately better for Sioux Falls than were for Rapid City. However, improvements over guidance were made on all periods at both locations. The lowest improvement (+3 percent) occurred in the first period at Rapid City. This anomaly, although not very frequent, has appeared before. One possible explanation is that forecasters tend to expect that they will beat guidance in the first period and so vary from guidance on most forecasts, perhaps even when guidance is very good. In latter periods the technique may be to only change the guidance temperatures that stick out as bad. In 1987 no significant high or low bias was noted at Rapid City while a definite low bias was noted for local forecasters and especially for guidance. The opposite trend was noted in 1986. Since 1987 was Sioux Falls' fourth warmest year on record, so the low bias was not surprising. Finally, the bar graphs show that the greatest number of temperature forecasts by Sioux Falls forecasters were in the -3 to +3 error category. However, there were more temperature forecasts that were ten degrees or more too cold than in the previous year. Again, the extremely warm year certainly was most likely the reason for this low bias. However, local forecast error was less than guidance error, once again. Author

N89-19777# National Weather Service, Topeka, KS. Forecast Office.
PREPARING STORM DATA
Steven D. Schurr *In* National Weather Service, Central Region Applied Research on Severe Weather Forecasting May 1988

p 54-67 (For primary document see N89-19771 12-47)
(CRARP-88-6) Avail: NTIS HC A05/MF A01 CSCL 04B

The procedures for preparing the monthly Storm Data report for Kansas are discussed. These procedures proved an efficient as well as effective approach to compiling data and preparing required submissions. They are presented here with the hope they might assist other Warnings and Preparedness Meteorologists (WPM's) and others who prepare Storm Data. Storm Data serves two main functions. It is a record of all reported severe and damaging weather, and reported injuries and deaths related to adverse watches and warnings. This data base is used for variety of research purposes as well. It is important to keep these two purposes in mind through the entire preparation process, so the final report will satisfy both functions. The preparation process includes five general tasks. They are: gathering data, assembling data, writing the report, printing, and finally, submitting input to Outstanding Storms. Author

N89-19778# National Weather Service, Des Moines, IA. Forecast Office.

USE OF LONG-WAVES IN FORECASTING

Carl E. Weinbrecht and Charles Myers *In* National Weather Service, Central Region Applied Research on Severe Weather Forecasting May 1988 p 68-76 (For primary document see N89-19771 12-47)
(CRARP-88-7) Avail: NTIS HC A05/MF A01 CSCL 04B

This case study illustrates the usefulness of the long wave theory. This concept provides a framework for forecasting. It is one of the first steps of the forecast funnel as proposed by Snellman (1982) and Bullock (1986). This concept gives the forecaster a tool which enables him to choose the proper model in difficult situations. Author

N89-19779*# Kunz Associates, Inc., Albuquerque, NM.

GENERALIZED THREE-DIMENSIONAL EXPERIMENTAL LIGHTNING CODE (G3DXL) USER'S MANUAL Contractor Report, 1981 - 1986

Karl S. Kunz Feb. 1986 145 p
(Contract NAS1-16591)
(NASA-CR-166079; NAS 1.26:166079; KAI-R-1) Avail: NTIS HC A07/MF A01 CSCL 04B

Information concerning the programming, maintenance and operation of the G3DXL computer program is presented and the theoretical basis for the code is described. The program computes time domain scattering fields and surface currents and charges induced by a driving function on and within a complex scattering object which may be perfectly conducting or a lossy dielectric. This is accomplished by modeling the object with cells within a three-dimensional, rectangular problem space, enforcing the appropriate boundary conditions and differencing Maxwell's equations in time. In the present version of the program, the driving function can be either the field radiated by a lightning strike or a direct lightning strike. The F-106 B aircraft is used as an example scattering object. M.G.

N89-19780*# Kansas Univ. Center for Research, Inc., Lawrence.

THE ELECTROMAGNETIC MODELING OF THIN APERTURES USING THE FINITE-DIFFERENCE TIME-DOMAIN TECHNIQUE Final Contractor Report, 1985 - 1986

Kenneth R. Demarest Jun. 1987 104 p
(Grant NAG1-514)
(NASA-CR-178280; NAS 1.26:178280) Avail: NTIS HC A06/MF A01 CSCL 04B

A technique which computes transient electromagnetic responses of narrow apertures in complex conducting scatterers was implemented as an extension of previously developed Finite-Difference Time-Domain (FDTD) computer codes. Although these apertures are narrow with respect to the wavelengths contained within the power spectrum of excitation, this technique does not require significantly more computer resources to attain the increased resolution at the apertures. In the report, an analytical technique which utilizes Babinet's principle to model the apertures is developed, and an FDTD computer code which utilizes this technique is described. Author

N89-19781# Midwest Research Inst., Golden, CO. Solar Energy Research Inst.

LOCAL WIND MEASUREMENTS FOR MICROSITING Final Report

Stel N. Walker and John E. Wade (Pacific Wind Energy, Inc., Corvallis, OR.) Sep. 1988 107 p
(Contracts DE-FC02-86CH-10251; DE-AC02-83CH-10093)
(DE89-000829; SERI/STR-217-3320) Avail: NTIS HC A06/MF A01

An important consideration in determining the success or failure of wind energy conversion systems is site wind characteristics. Inadequate micrositing and subsequent poor placement of turbines may result in reductions of annual energy output up to two-thirds of predicted amounts. The objective of this study was to measure the effect of local terrain features on the wind flow at several locations over an array of wind turbines. The study was conducted as part of SERI's Cooperative Field Test Program. The investigation focused on the effect of a 100-ft bluff on wind characteristics. The characteristics investigated included speed, direction, wind speed distribution, turbulence intensity, shear, and power output. The wind energy generation facility at Whisky Run, in southern Oregon, is instrumented with a 350-ft tower in the center of the wind farm with speed and direction sensors at 50, 80, 100, and 200 ft. Four turbines are instrumented at 50 ft (turbines 4, 7, 18, and 21) with speed, direction, and power-output sensors. In addition, three 80-ft towers were instrumented at 50 and 80 ft with anemometers and direction sensors at one or two levels. Hourly and 10-min average data were collected for 1 yr. DOE

N89-19782# Massachusetts Inst. of Tech., Lexington. Lincoln Lab.

A PRELIMINARY STUDY OF PRECURSORS TO HUNTSVILLE MICROBURSTS

M. A. Isaminger 25 Oct. 1988 29 p
(Contract DTFA01-80-Y-10546)
(AD-A200914; ATC-153; DOT/FAA/PM-87/35) Avail: NTIS HC A03/MF A01 CSCL 01C

Automated algorithms are being developed for the detection of wind shears such as microbursts and gust fronts. Previous studies have shown that these outflows can be hazardous to an airplane during takeoffs and landings. The ultimate goal of a microburst detection algorithm is the timely warning of potentially hazardous wind shears through the detection of reliable precursors. Research in Colorado and Oklahoma documented the significance of precursors such as descending reflectivity cores, convergence, rotation, and reflectivity notching as indicators that a mircroburst will occur in the very near future. The overall importance of an individual feature varies between regions. This investigation will focus on those precursors which play a dominant role in the formation of wet microbursts in the southeastern United States. The data analyzed in this report was gathered by the FAA TDWR S-band Doppler radar during 1985 and 1986 in Memphis, Tennessee, and Huntsville, Alabama. GRA

N89-19783*# National Aeronautics and Space Administration. Langley Research Center, Hampton, VA.

A WIDE BANDWIDTH ELECTROSTATIC FIELD SENSOR FOR LIGHTNING RESEARCH

Klaus P. Zaepfel Jan. 1989 12 p Presented at the Conference on Lightning and Statis Electricity, Dayton, OH, 24-26 Jun. 1986 Previously announced in IAA as A86-50260
(NASA-TM-101539; NAS 1.15:101539) Avail: NTIS HC A03/MF A01 CSCL 04B

Data obtained from UHF radar observation of direct-lightning strikes to the NASA F-106B aircraft have indicated that most of the 690 strikes acquired during direct-strike lightning tests were triggered by the aircraft. As an aid in understanding the triggered lightning process, a wide bandwidth electric field measuring system was designed for the F-106B by implementing a clamped-detection

signal processing concept originated at the Air Force Cambridge Research Lab in 1953. The detection scheme combines the signals from complementary stator pairs clamped to zero bolts at the exact moment when each stator pair is maximally shielded by the rotor, a process that restores the dc level lost by the charge amplifier. The system was implemented with four shutter-type field mills located at strategic points on the aircraft. The bandwidth of the system was determined in the laboratory to be from dc to over 100 Hz, whereas past designs had upper limits of 10 to 100 Hz. To obtain the undisturbed electric field vector and total aircraft charge, the airborne field mill system is calibrated by using techniques involving results from ground and flight calibrations of the F-106B, laboratory tests of a metallized model, and a finite difference time-domain electromagnetic computer code. Author

N89-19784 North Carolina Univ., Chapel Hill.
THE CLIMATE INVERSION PROBLEM: A STATISTICAL/MODELING APPROACH Ph.D. Thesis
Robert S. Chen 1987 144 p
Avail: Univ. Microfilms Order No. DA8821453

A method is developed for inverting the climate, i.e., predicting the statistical behavior of the local climate from information about the regional climate. Specifically, the method links the monthly-average surface air temperature observed at selected stations in North Carolina and Virginia with the tropospheric free-air temperature and locally observed variables such as the surface solar radiation flux. Since these data are highly autocorrelated, weighted least squares regression is used to produce unbiased estimates of the strength of the relationships. A simple energy-balance climate model is developed to characterize possible non-linear interactions between climatic variables. With the seasonal cycle removed, the mean temperature of the 85 to 30 kPa (850 to 300 mb) layer can explain some 50 to 70 percent of the variance in the observed monthly surface air temperature at the four stations analyzed. Inclusion of selected local climate variables increases the explained variance by up to about 10 percent. Application of the local climate model also leads to small but statistically significant increases in predictability in some cases. Regional effects tend to dominate local effects. Using the regression estimates, it is possible either to develop an unbiased prediction of the monthly surface air temperature given normal or perturbed inputs or to generate hypothetical scenarios of monthly surface air temperature that retain the statistical characteristics of observed data. Dissert. Abstr.

N89-19785 Michigan Univ., Ann Arbor.
USE OF CLUSTER ANALYSIS TO DEFINE PERIODS OF SIMILAR METEOROLOGY AND PRECIPITATION CHEMISTRY IN EASTERN NORTH AMERICA Ph.D. Thesis
Mark Edward Fernau 1988 354 p
Avail: Univ. Microfilms Order No. DA8821570

An aggregation approach is needed to overcome the prohibitive expense involved in exercising the Regional Acid Deposition Model to determine annual deposition loads in eastern North America. A necessary first step in this process is to identify those events which are representative of annual meteorology and to determine their frequencies and pollutant loadings. The statistical technique of cluster analysis is applied to transport vectors and precipitation chemistry data to identify and define representative periods for use in aggregation schemes. Transport vectors representing the travel of air masses in the twelve hours preceding their daily arrival at chemistry sampling sites were calculated for 1979, 1981 and 1983 from mixed-layer back trajectories, arranged in a three-day moving format, and subjected to cluster analysis. The mean transport vectors at twenty-two sites were plotted for each resulting cluster to examine their flow patterns. The associated precipitation and analyte deposition fields were also studied. The sensitivity of the clustering process to differing methods, different sites or number of sites and other factors was assessed. Cluster analysis was shown to be useful in the computer-assisted classification of spatial patterns of weather and pollution data and should be considered for use along with more widely used synoptic climatological tools such as principal component analysis and correlation analysis. Dissert. Abstr.

N89-19786 Miami Univ., Coral Gables, FL.
SEMI-PROGNOSTIC TESTS OF CUMULUS PARAMETERIZATION SCHEMES IN THE MIDDLE LATITUDES Ph.D. Thesis
Georg Alfred Grell 1988 255 p
Avail: Univ. Microfilms Order No. DA8820785

The performance of three disparate cumulus parameterization schemes was tested semi-prognostically in the mid-latitude environment of severe convective storms. With the aid of the analysis package of a mesoscale model, three independent rawin data sets were analyzed on different grid sizes to provide the larger scale variables and the verifying heat and moisture budgets. The terminology of dynamic control, static control, and feedback was used to separate different assumptions used by various cumulus parameterization schemes. These assumptions were then tested rigorously to find systematic errors and show possible improvements. For the Arakawa-Schubert parameterization heating and drying in the lower troposphere were regularly overpredicted. This problem was fixed by adding a simple parameterization of moist convective-scale downdrafts to the dynamic control, static control and feedback of the scheme. For the Kuo-type parameterizations, assumptions used by the feedback led to serious errors in predicting the vertical heating distribution. For the Kreitzberg-Perkey scheme assumptions used by the dynamic control led to an erroneous reproduction of rainfall patterns. Furthermore, assumptions used by the feedback of this scheme led to too much moistening and cooling in the middle and upper troposphere. For all schemes, it was shown that moist convective scale downdrafts, which play a vital role in the mid-latitude environment of severe convective storms, should probably be a part of the feedback in any cumulus parameterization scheme.
Dissert. Abstr.

N89-19787 Delaware Univ., Newark.
A CLIMATOLOGY OF GLOBAL PRECIPITATION Ph.D. Thesis
David Russell Legates 1988 262 p
Avail: Univ. Microfilms Order No. DA8824245

A global climatology of mean monthly precipitation was developed using traditional land-based gage measurements as well as derived oceanic data. These data were screened for coding errors and redundant entries were removed. Oceanic precipitation estimates are most often extrapolated from coastal and island observations because few gage estimates of oceanic precipitation exist. One such procedure, developed by Dorman and Bourke and used here, employs a derived relationship between observed rainfall totals and the current weather at coastal stations. The combined data base contains 24,635 independent terrestial station records and 2223 oceanic grid-point records. Raingage catches are known to underestimate actual precipitation. Errors in the gage catch result from wind-field deformation, wetting losses, and evaporation from the gage and can amount to nearly 8, 2, and 1 percent of the global catch, respectively. A procedure was developed to correct many of these errors and was used to adjust the gage estimates of global precipitation. Space-time variations in gage type, air temperature, wind speed, and natural vegetation were incorporated into the correction procedure. Isohyetal maps displaying the mean annual, seasonal, and monthly precipitation are presented. Gage corrections and the standard error of the corrected estimates also are mapped. Dissert. Abstr.

N89-19788 Texas Technological Univ., Lubbock.
MESOSCALE CONVECTIVE SYSTEMS: STRUCTURE, DEVELOPMENT AND STORM-ENVIRONMENT INTERACTIONS Ph.D. Thesis
Edward N. Rappaport 1988 196 p
Avail: Univ. Microfilms Order No. DA8819422

Mesoscale Convective Systems (MCSs), clusterings of thunderstorms associated with significant weather events are described. Analyses focused on several objectives: a documentation of the condiitons in which MCSs form; an elucidation

of the life cycle and internal structure of a mid-latitude Mesoscale Convective Complex (MCC); and a systematic comparison of the precipitation structures and environments of many MCSs. In meeting the objectives the evolution of an episode of five MCSs over West Texas was investigated using as a principal source data collected by Texas Tech University as a participant in the Texas High Plains Cooperative Program (HIPLEX).

Dissert. Abstr.

N89-19789*# National Aeronautics and Space Administration. Goddard Space Flight Center, Greenbelt, MD.

TRMM (TROPICAL RAINFALL MEASURING MISSION): A SATELLITE MISSION TO MEASURE TROPICAL RAINFALL

Joanne Simpson, ed. Aug. 1988 104 p Original contains color illustrations

(NASA-TM-101288; NAS 1.15:101288) Avail: NTIS HC A06/MF A01 CSCL 04B

The Tropical Rainfall Measuring Mission (TRMM) is presented. TRMM is a satellite program being studied jointly by the United States and Japan which would carry out the systematic study of tropical rainfall required for major strides in weather and climate research. The scientific justification for TRMM is discussed. The implementation process for the scientific community, NASA management, and the other decision-makers and advisory personnel who are expected to evaluate the priority of the project is outlined. NASA

N89-19790# Universitaet der Bundeswehr, Neubiberg (Germany, F.R.). Forschungsschwerpunkt Simulation und Optimierung Deterministischer und Stochastischer Dynamischer Sy

INTERPRETATION OF ERS-1 WIND SCATTEROMETER DATA: WIND FIELD EXTRACTION

Ellmann, Humbert, and Schwenfeger Aug. 1988 33 p

(Contract ESA-EP/JVD/14.7/5234)

(ETN-89-93982) Avail: NTIS HC A03/MF A01

A wind extraction software for the ERS-1 wind scatterometer experiment is presented. It was tested using simulated measurements given as backscatter coefficients derived by evaluating the Long C-Band model function and adding Gaussian noise. A Bayesian estimator is used. The process depends on prior knowledge of the wind to be defined. This information might be taken from independent meteorological forcast wind fields or from the wind field itself within the estimation process. The tests give very good results in both operation modes, even given that working with simulated data gives accentuated agreement with the correct results. ESA

N89-19606 Illinois State Water Survey, Champaign. Climate and Meteorology Section.

THE EFFECT OF CHARGE ON COALESCENCE OF SMALL PRECIPITATION DROPS AT TERMINAL VELOCITY

Harry T. Ochs, III, Robert R. Czys, and James Q. Feng *In* Deutscher Wetterdienst, Annals from the German Meteorological Society, No. 25: 10th International Cloud Physics Conference Preprints, Volume 1 1988 p 4-6 (For primary document see N89-19605 12-42)

(Grants NSF ATM-83-14072; NSF ATM-86-01549)

Copyright Avail: Deutscher Wetterdienst, Frankfurter Strasse 135, D-6050 Offenbach am Main, Fed. Republic of Germany

N89-19607 Illinois State Water Survey, Champaign. Climate and Meteorology Section.

WAKE-EXCITED RAINDROP OSCILLATIONS

Kenneth V. Beard and Harry T. Ochs, III *In* Deutscher Wetterdienst, Annals from the German Meteorological Society, No. 25: 10th International Cloud Physics Conference Preprints, Volume 1 1988 p 7-8 (For primary document see N89-19605 12-42)

(Grants NSF ATM-84-19490; NSF ATM-86-01549)

Copyright Avail: Deutscher Wetterdienst, Frankfurter Strasse 135, D-6050 Offenbach am Main, Fed. Republic of Germany

N89-19608 Hokkaido Univ., Sapporo (Japan). Inst. of Low Temperature Science.

TEMPORAL VARIATIONS OF SNOW CRYSTAL GROWTH PARAMETERS

Tsuneya Takahashi, Norihiko Fukuta (Utah Univ., Salt Lake City.), Tatsuo Endoh, and Gorow Wakahama *In* Deutscher Wetterdienst, Annals from the German Meteorological Society. No. 25: 10th International Cloud Physics Conference Preprints, Volume 1 1988 p 9-11 (For primary document see N89-19605 12-42)

(Grants NSF ATM-82-18966; JAPMINED-61020001)

Copyright Avail: Deutscher Wetterdienst, Frankfurter Strasse 135, D-6050 Offenbach am Main, Fed. Republic of Germany

N89-19609 Utah Univ., Salt Lake City. Dept. of Meteorology.

EMPIRICAL EQUATIONS OF ICE CRYSTAL GROWTH MICROPHYSICS FOR MODELING AND ANALYSIS

C. R. Redder and Norihiko Fukuta *In* Deutscher Wetterdienst, Annals from the German Meteorological Society, No. 25: 10th International Cloud Physics Conference Preprints, Volume 1 1988 p 12-14 (For primary document see N89-19605 12-42)

(Contract NOAA-87-1999; NSF ATM-86-16568)

Copyright Avail: Deutscher Wetterdienst, Frankfurter Strasse 135, D-6050 Offenbach am Main, Fed. Republic of Germany

N89-19610 Academia Sinica, Beijing (China). Inst. of Atmospheric Physics.

THE CONTRAST STUDY OF NEW MODEL ON ICE CRYSTAL GROWTH

Ang-Sheng Wang *In* Deutscher Wetterdienst, Annals from the German Meteorological Society, No. 25: 10th International Cloud Physics Conference Preprints, Volume 1 1988 p 15-17 (For primary document see N89-19605 12-42)

Copyright Avail: Deutscher Wetterdienst, Frankfurter Strasse 135, D-6050 Offenbach am Main, Fed. Republic of Germany

N89-19611 Johann-Wolfgang-Goethe-Univ., Frankfurt am Main (Germany, F.R.).

A WIND TUNNEL STUDY ON THE MELTING OF SNOW FLAKES

S. K. Mitra, O. Vohl, and H. R. Pruppacher *In* Deutscher Wetterdienst, Annals from the German Meteorological Society, No. 25: 10th International Cloud Physics Conference Preprints, Volume 1 1988 p 18-21 (For primary document see N89-19605 12-42)

Copyright Avail: Deutscher Wetterdienst, Frankfurter Strasse 135, D-6050 Offenbach am Main, Fed. Republic of Germany

N89-19612 Desert Research Inst., Reno, NV.

EVAPORATION AND MELTING OF ICE CRYSTALS: A LABORATORY STUDY

Riza G. Oraltay and John Hallett *In* Deutscher Wetterdienst, Annals from the German Meteorological Society, No. 25: 10th International Cloud Physics Conference Preprints, Volume 1 1988 p 22-24 (For primary document see N89-19605 12-42)

(Grant NSF ATM-87-15636)

Copyright Avail: Deutscher Wetterdienst, Frankfurter Strasse 135, D-6050 Offenbach am Main, Fed. Republic of Germany

N89-19613 Illinois State Water Survey, Champaign. Climate and Meteorology Section.

A NEW MECHANISM FOR ICE INITIATION IN WARM-BASED MIDWESTERN CUMULI

Robert R. Czys *In* Deutscher Wetterdienst, Annals from the German Meteorological Society, No. 25: 10th International Cloud Physics Conference Preprints, Volume 1 1988 p 25-27 (For primary document see N89-19605 12-42)

(Contracts COMM-NA-86-RAH-06051; COMM-NA-87-RAH-07077)

Copyright Avail: Deutscher Wetterdienst, Frankfurter Strasse 135, D-6050 Offenbach am Main, Fed. Republic of Germany

N89-19614 Desert Research Inst., Reno, NV.

SPREADING SUPERCOOLED WATER DROPLETS ON AN ICE SURFACE

Ya Yi Dong and John Hallett *In* Deutscher Wetterdienst, Annals

from the German Meteorological Society, No. 25: 10th International Cloud Physics Conference Preprints, Volume 1 1988 p 28-30 (For primary document see N89-19605 12-42)
(Grant NSF ATM-87-15636)
Copyright Avail: Deutscher Wetterdienst, Frankfurter Strasse 135, D-6050 Offenbach am Main, Fed. Republic of Germany

N89-19615 Illinois Univ., Urbana. Dept. of Atmospheric Sciences.
A MODEL OF THE ELECTROSTATIC-AERODYNAMIC SHAPE OF RAINDROPS
Catherine Chuang and Kenneth V. Beard *In* Deutscher Wetterdienst, Annals from the German Meteorological Society. No. 25: 10th International Cloud Physics Conference Preprints, Volume 1 1988 p 31-33 (For primary document see N89-19605 12-42)
(Grants NSF ATM-84-19490; NSF ATM-86-01549)
Copyright Avail: Deutscher Wetterdienst, Frankfurter Strasse 135, D-6050 Offenbach am Main, Fed. Republic of Germany

N89-19616 Stockholm Univ. (Sweden). Dept. of Meteorology.
MEASUREMENTS OF THE PARTITIONING OF AEROSOL MASS AND NUMBER BETWEEN CLOUD DROPLETS AND INTERSTITIAL AIR
John A. Ogren, Jost Heintzenberg, and Kevin J. Noone *In* Deutscher Wetterdienst, Annals from the German Meteorological Society, No. 25: 10th International Cloud Physics Conference Preprints, Volume 1 1988 p 34-36 (For primary document see N89-19605 12-42)
Copyright Avail: Deutscher Wetterdienst, Frankfurter Strasse 135, D-6050 Offenbach am Main, Fed. Republic of Germany

N89-19617 Manchester Univ. (England). Dept. of Pure and Applied Physics.
THE CALCULATION OF SUPERSATURATIONS AND GROWTH OF DROPLETS IN CONTINENTAL CUMULUS CLOUDS
Keith Bower and Tom W. Choularton *In* Deutscher Wetterdienst, Annals from the German Meteorological Society, No. 25: 10th International Cloud Physics Conference Preprints, Volume 1 1988 p 37-39 (For primary document see N89-19605 12-42)
Copyright Avail: Deutscher Wetterdienst, Frankfurter Strasse 135, D-6050 Offenbach am Main, Fed. Republic of Germany

N89-19618 National Center for Atmospheric Research, Boulder, CO.
ON THE OBSERVATIONS OF CLOUD TEMPERATURE AND LIQUID WATER CONTENT USING A LYMAN-ALPHA AND AN FSSP SENSOR
Jorgen B. Jensen, Darrel G. Baumgardner, and Graciela Raga (Washington Univ., Seattle.) *In* Deutscher Wetterdienst, Annals from the German Meteorological Society, No. 25: 10th International Cloud Physics Conference Preprints, Volume 1 1988 p 40-42 (For primary document see N89-19605 12-42)
(Grant NSF ATM-84-20816)
Copyright Avail: Deutscher Wetterdienst, Frankfurter Strasse 135, D-6050 Offenbach am Main, Fed. Republic of Germany

N89-19619 National Center for Atmospheric Research, Boulder, CO.
EVALUATION OF DROPLET GROWTH RATES IN HAWAIIAN OROGRAPHIC CLOUDS
Darrel G. Baumgardner *In* Deutscher Wetterdienst, Annals from the German Meteorological Society. No. 25: 10th International Cloud Physics Conference Preprints, Volume 1 1988 p 43-45 Sponsored in part by NSF, Washington, DC (For primary document see N89-19605 12-42)
Copyright Avail: Deutscher Wetterdienst, Frankfurter Strasse 135, D-6050 Offenbach am Main, Fed. Republic of Germany

N89-19620* National Center for Atmospheric Research, Boulder, CO.
STUDIES OF WARM-RAIN DEVELOPMENT
William A. Cooper *In* Deutscher Wetterdienst, Annals from the German Meteorological Society. No. 25: 10th International Cloud Physics Conference Preprints, Volume 1 1988 p 46-48 Sponsored in part by NSF, Washington, DC (For primary document see N89-19605 12-42)
(Contract NAS5-27783)
Copyright Avail: Deutscher Wetterdienst, Frankfurter Strasse 135, D-6050 Offenbach am Main, Fed. Republic of Germany
CSCL 04B

N89-19621 National Center for Atmospheric Research, Boulder, CO.
RADAR OBSERVATIONS AND MODELLING OF WARM RAIN INITIATION
Anthony J. Illingworth and I. Jeff Caylor (Manchester Univ., England) *In* Deutscher Wetterdienst, Annals from the German Meteorological Society. No. 25: 10th International Cloud Physics Conference Preprints, Volume 1 1988 p 49-51 Sponsored in part by NSF, Washington, DC (For primary document see N89-19605 12-42)
(Grants NERC-GR3/5896; AF-AFOSR-0046-87)
Copyright Avail: Deutscher Wetterdienst, Frankfurter Strasse 135, D-6050 Offenbach am Main, Fed. Republic of Germany

N89-19622 Wyoming Univ., Laramie. Dept. of Atmospheric Science.
A TEST OF ICE CRYSTAL PRODUCTION BY AIRCRAFT
Gabor Vali, R. D. Kelly, and F. Serrano *In* Deutscher Wetterdienst, Annals from the German Meteorological Society, No. 25: 10th International Cloud Physics Conference Preprints, Volume 1 1988 p 52-54 (For primary document see N89-19605 12-42)
(Grant NSF ATM-86-11185)
Copyright Avail: Deutscher Wetterdienst, Frankfurter Strasse 135, D-6050 Offenbach am Main, Fed. Republic of Germany

N89-19623 Meteorological Office, Bracknell (England).
AIRBORNE STUDIES OF THE ICE PHASE IN MARITIME CLOUDS AROUND THE BRITISH ISLES
P. R. A. Brown and Tom W. Choularton (Manchester Univ., England) *In* Deutscher Wetterdienst, Annals from the German Meteorological Society, No. 25: 10th International Cloud Physics Conference Preprints, Volume 1 1988 p 55-57 (For primary document see N89-19605 12-42)
Copyright Avail: Deutscher Wetterdienst, Frankfurter Strasse 135, D-6050 Offenbach am Main, Fed. Republic of Germany

N89-19624 Indian Inst. of Tropical Meteorology, Poona.
PRECIPITATION INITIATION MECHANISMS IN CLOUDS OVER NORTH INDIA
R. N. Chatterjee, P. Prakash, G. Singh, and R. K. Kapoor *In* Deutscher Wetterdienst, Annals from the German Meteorological Society, No. 25: 10th International Cloud Physics Conference Preprints, Volume 1 1988 p 58-60 (For primary document see N89-19605 12-42)
Copyright Avail: Deutscher Wetterdienst, Frankfurter Strasse 135, D-6050 Offenbach am Main, Fed. Republic of Germany

N89-19625 Clermont-Ferrand Univ. (France).
EVIDENCE OF PREFERENTIAL ZONES OF ICE MULTIPLICATION BY SPLINTERING IN CONVECTIVE CELLS
Jean-Francois Gayet, Christophe Duroure, and R. G. Soulage *In* Deutscher Wetterdienst, Annals from the German Meteorological Society, No. 25: 10th International Cloud Physics Conference Preprints, Volume 1 1988 p 61-63 (For primary document see N89-19605 12-42)
(Grants DRET/INSU-83-34308; DRET/INSU-85-34016)
Copyright Avail: Deutscher Wetterdienst, Frankfurter Strasse 135, D-6050 Offenbach am Main, Fed. Republic of Germany

N89-19626 Illinois State Water Survey, Champaign. Climate and Meteorology Section.
MICROPHYSICAL CHARACTERISTICS OF WARM-BASED CUMULI: OBSERVATIONS AT -10 C
Robert R. Czys *In* Deutscher Wetterdienst, Annals from the German Meteorological Society, No. 25: 10th International Cloud Physics Conference Preprints, Volume 1 1988 p 64-66 (For

primary document see N89-19605 12-42)
(Contracts COMM-NA-86-RAH-06051; COMM-NA-87-RAH-07077)
Copyright Avail: Deutscher Wetterdienst, Frankfurter Strasse 135, D-6050 Offenbach am Main, Fed. Republic of Germany

N89-19627 Washington Univ., Seattle. Dept. of Aeronautics and Astronautics.
A COMPARATIVE STUDY OF LABORATORY THERMALS AND ATMOSPHERIC CLOUDS
H. Johari, Gregory R. Taylor, M. Baker, and R. Breidenthal *In* Deutscher Wetterdienst, Annals from the German Meteorological Society, No. 25: 10th International Cloud Physics Conference Preprints, Volume 1 1988 p 67-69 (For primary document see N89-19605 12-42)
(Grants NSF ATM-84-20816; NSF ATM-86-09376; NSF ATM-86-11225)
Copyright Avail: Deutscher Wetterdienst, Frankfurter Strasse 135, D-6050 Offenbach am Main, Fed. Republic of Germany

N89-19628 National Center for Atmospheric Research, Boulder, CO.
ENTRAINMENT AND FINE-SCALE (MOLECULAR) MIXING
Ilga R. Paluch and Darrel G. Baumgardner *In* Deutscher Wetterdienst, Annals from the German Meteorological Society, No. 25: 10th International Cloud Physics Conference Preprints, Volume 1 1988 p 70-72 Sponsored in part by NSF, Washington, DC (For primary document see N89-19605 12-42)
Copyright Avail: Deutscher Wetterdienst, Frankfurter Strasse 135, D-6050 Offenbach am Main, Fed. Republic of Germany

N89-19629 Manchester Univ. (England). Dept. of Physics.
AIRBORNE STUDIES OF THE INFLUENCE OF ENTRAINMENT ON THE VERTICAL AND HORIZONTAL MICROPHYSICAL STRUCTURE OF SMALL CUMULUS CLOUDS
John Latham and Alan M. Blyth (New Mexico Inst. of Mining and Technology, Socorro.) *In* Deutscher Wetterdienst, Annals from the German Meteorological Society, No. 25: 10th International Cloud Physics Conference Preprints, Volume 1 1988 p 73-75 (For primary document see N89-19605 12-42)
Copyright Avail: Deutscher Wetterdienst, Frankfurter Strasse 135, D-6050 Offenbach am Main, Fed. Republic of Germany

N89-19630 Direction de la Meteorologie Nationale, Magny les Hameaux (France).
ENTRAINMENT SITES, MIXING PROCESSES IN WARM CONVECTIVE CLOUDS: EFFECT ON DROPLET GROWTH
Elizabeth Hicks, Arlette Rigaud, Jacqueline Gagneux, and Constantin Pontikis *In* Deutscher Wetterdienst, Annals from the German Meteorological Society, No. 25: 10th International Cloud Physics Conference Preprints, Volume 1 1988 p 76-78 (For primary document see N89-19605 12-42)
Copyright Avail: Deutscher Wetterdienst, Frankfurter Strasse 135, D-6050 Offenbach am Main, Fed. Republic of Germany

N89-19631 Academy of Sciences (USSR), Tomsk. Inst. of Atmospheric Optics.
STRUCTURE OF UPPER CLOUDS BOUNDARY USING THE LIDAR DATA
V. E. Zuev, V. S. Shamanaev, I. E. Penner, and I. V. Samokhvalov *In* Deutscher Wetterdienst, Annals from the German Meteorological Society, No. 25: 10th International Cloud Physics Conference Preprints, Volume 1 1988 p 79-81 (For primary document see N89-19605 12-42)
Copyright Avail: Deutscher Wetterdienst, Frankfurter Strasse 135, D-6050 Offenbach am Main, Fed. Republic of Germany

N89-19632 Deutsche Forschungs- und Versuchsanstalt fuer Luft- und Raumfahrt, Oberpfaffenhofen (West Germany). Inst. fuer Physik der Atmosphaere.
TURBULENT TRANSPORT PROCESSES WITHIN AND BELOW SMALL CUMULUS CLOUDS
Anne M. Jochum *In* Deutscher Wetterdienst, Annals from the German Meteorological Society, No. 25: 10th International Cloud Physics Conference Preprints, Volume 1 1988 p 82-84 (For primary document see N89-19605 12-42)
Copyright Avail: Deutscher Wetterdienst, Frankfurter Strasse 135, D-6050 Offenbach am Main, Fed. Republic of Germany

N89-19633 Meteorological Research Inst., Tsukuba (Japan).
INSTABILITY THEORY IN CLOUDS AND THE PARAMETERIZATION OF EDDY VISCOSITY COEFFICIENTS
Yoshimasa Takaya *In* Deutscher Wetterdienst, Annals from the German Meteorological Society, No. 25: 10th International Cloud Physics Conference Preprints, Volume 1 1988 p 85-87 (For primary document see N89-19605 12-42)
Copyright Avail: Deutscher Wetterdienst, Frankfurter Strasse 135, D-6050 Offenbach am Main, Fed. Republic of Germany

N89-19634 National Center for Atmospheric Research, Boulder, CO.
THREE-DIMENSIONAL CUMULUS ENTRAINMENT STUDIES
Terry L. Clark, Piotr K. Smolarkiewicz, and William D. Hall *In* Deutscher Wetterdienst, Annals from the German Meteorological Society, No. 25: 10th International Cloud Physics Conference Preprints, Volume 1 1988 p 88-90 Sponsored in part by NSF, Washington, DC (For primary document see N89-19605 12-42)
Copyright Avail: Deutscher Wetterdienst, Frankfurter Strasse 135, D-6050 Offenbach am Main, Fed. Republic of Germany

N89-19635 Centre National de Recherches Meteorologiques, Toulouse (France).
HETEROGENEOUS MIXING MEASUREMENTS IN SMALL NONPRECIPITATING CUMULI
J. L. Brenguier *In* Deutscher Wetterdienst, Annals from the German Meteorological Society, No. 25: 10th International Cloud Physics Conference Preprints, Volume 1 1988 p 91-93 (For primary document see N89-19605 12-42)
Copyright Avail: Deutscher Wetterdienst, Frankfurter Strasse 135, D-6050 Offenbach am Main, Fed. Republic of Germany

N89-19636 National Oceanic and Atmospheric Administration, Princeton, NJ. Geophysical Fluid Dynamics Lab.
THE CASE FOR SUBGRID-SCALE CONDENSATION IN NUMERICAL CLOUD MODELS
Frank B. Lipps and Richard S. Hemler *In* Deutscher Wetterdienst, Annals from the German Meteorological Society, No. 25: 10th International Cloud Physics Conference Preprints, Volume 1 1988 p 94-96 (For primary document see N89-19605 12-42)
Copyright Avail: Deutscher Wetterdienst, Frankfurter Strasse 135, D-6050 Offenbach am Main, Fed. Republic of Germany

N89-19637 McGill Univ., Montreal (Quebec).
THE EFFECT OF TURBULENCE ON THE COLLECTION OF CLOUD DROPS: A STOCHASTIC MODEL
Gerhard Reuter *In* Deutscher Wetterdienst, Annals from the German Meteorological Society, No. 25: 10th International Cloud Physics Conference Preprints, Volume 1 1988 p 97-99 (For primary document see N89-19605 12-42)
Copyright Avail: Deutscher Wetterdienst, Frankfurter Strasse 135, D-6050 Offenbach am Main, Fed. Republic of Germany

N89-19638 National Center for Atmospheric Research, Boulder, CO.
THE EFFECT OF ICE PHYSICAL PROCESSES ON THE NUMERICAL SIMULATION OF WEST AFRICAN SQUALL LINES
William D. Hall and Jean Philippe Lafore (Centre National de Recherches Meteorologiques, Toulouse, France) *In* Deutscher Wetterdienst, Annals from the German Meteorological Society, No. 25: 10th International Cloud Physics Conference Preprints, Volume 1 1988 p 100-102 Sponsored in part by NSF, Washington, DC (For primary document see N89-19605 12-42)
Copyright Avail: Deutscher Wetterdienst, Frankfurter Strasse 135, D-6050 Offenbach am Main, Fed. Republic of Germany

N89-19639 State Meteorological Inst., Beijing (China).
NUMERICAL SIMULATION OF MICROPHYSICAL PROCESSES IN CUMULONIMBUS
Zhijin Hu and Guanfang He *In* Deutscher Wetterdienst, Annals from the German Meteorological Society, No. 25: 10th International Cloud Physics Conference Preprints, Volume 1 1988 p 103-105 (For primary document see N89-19605 12-42)
Copyright Avail: Deutscher Wetterdienst, Frankfurter Strasse 135, D-6050 Offenbach am Main, Fed. Republic of Germany

N89-19640 Clermont-Ferrand Univ. (France).
A COMPARATIVE STUDY OF TWO MICROPHYSICAL SCHEMES IN A BETA MESOSCALE MODEL
Evelyne Richard and Nadine Chaumerliac *In* Deutscher Wetterdienst, Annals from the German Meteorological Society, No. 25: 10th International Cloud Physics Conference Preprints, Volume 1 1988 p 106-108 (For primary document see N89-19605 12-42)
Copyright Avail: Deutscher Wetterdienst, Frankfurter Strasse 135, D-6050 Offenbach am Main, Fed. Republic of Germany

N89-19642 Academia Sinica, Beijing (China). Inst. of Atmospheric Physics.
THE STUDY OF NUMERICAL SIMULATION ON THE FORMATION OF THE CLOUD DROPLET SPECTRA IN CUMULUS CLOUDS
Hui Xiao, Huaying Xu, and Meiyuan Huang *In* Deutscher Wetterdienst, Annals from the German Meteorological Society, No. 25: 10th International Cloud Physics Conference Preprints, Volume 1 1988 p 112-114 (For primary document see N89-19605 12-42)
Copyright Avail: Deutscher Wetterdienst, Frankfurter Strasse 135, D-6050 Offenbach am Main, Fed. Republic of Germany

N89-19643 Colorado State Univ., Fort Collins. Dept. of Atmospheric Science.
SOME OUTSTANDING PROBLEMS ON THE INFLUENCE OF CLOUDS ON RADIATION
Graeme L. Stephens *In* Deutscher Wetterdienst, Annals from the German Meteorological Society, No. 25: 10th International Cloud Physics Conference Preprints, Volume 1 1988 p 115-117 (For primary document see N89-19605 12-42)
(Grants NSF ATM-85-19160; NSF ATM-84-15127)
Copyright Avail: Deutscher Wetterdienst, Frankfurter Strasse 135, D-6050 Offenbach am Main, Fed. Republic of Germany

N89-19644* Utah Univ., Salt Lake City. Dept. of Meteorology.
THEORY ON THE UNCERTAINTY IN CLOUD MICROPHYSICAL PROCESSES AND CLIMATE
Kuo-Nan Liou and Szu-cheng S. Ou *In* Deutscher Wetterdienst, Annals from the German Meteorological Society, No. 25: 10th International Cloud Physics Conference Preprints, Volume 1 1988 p 118-120 Sponsored by NASA, Washington, DC (For primary document see N89-19605 12-42)
(Grants NAG7-32; AF-AFOSR-0294-87)
Copyright Avail: Deutscher Wetterdienst, Frankfurter Strasse 135, D-6050 Offenbach am Main, Fed. Republic of Germany CSCL 04B

N89-19645 Washington Univ., Seattle. Dept. of Atmospheric Sciences.
IN SITU MEASUREMENTS OF SHIP TRACKS
Lawrence F. Radke, Jamie H. Lyons, Peter V. Hobbs, and James E. Coakley (National Center for Atmospheric Research, Boulder, CO.) *In* Deutscher Wetterdienst, Annals from the German Meteorological Society, No. 25: 10th International Cloud Physics Conference Preprints, Volume 1 1988 p 121-123 (For primary document see N89-19605 12-42)
(Grant NSF ATM-86-15344)
Copyright Avail: Deutscher Wetterdienst, Frankfurter Strasse 135, D-6050 Offenbach am Main, Fed. Republic of Germany

N89-19646* National Aeronautics and Space Administration. Ames Research Center, Moffett Field, CA.
CLOUD AND AEROSOL OPTICAL DEPTHS
R. F. Pueschel, P. B. Russell, Thomas P. Ackerman, D. C. Colburn, R. C. Wrigley, M. A. Spanner, and J. M. Livingston (SRI International Corp., Menlo Park, CA.) *In* Deutscher Wetterdienst, Annals from the German Meteorological Society, No. 25: 10th International Cloud Physics Conference Preprints, Volume 1 1988 p 125-126 (For primary document see N89-19605 12-42)
Copyright Avail: Deutscher Wetterdienst, Frankfurter Strasse 135, D-6050 Offenbach am Main, Fed. Republic of Germany CSCL 04B

N89-19647 Meteorological Office, Bracknell (England).
AN OBSERVATIONAL STUDY OF RADIATIVELY DRIVEN CONVECTION
S. Nicholls *In* Deutscher Wetterdienst, Annals from the German Meteorological Society, No. 25: 10th International Cloud Physics Conference Preprints, Volume 1 1988 p 127-129 (For primary document see N89-19605 12-42)
Copyright Avail: Deutscher Wetterdienst, Frankfurter Strasse 135, D-6050 Offenbach am Main, Fed. Republic of Germany

N89-19648 Colorado State Univ., Fort Collins. Dept. of Atmospheric Science.
RADIATIVE INFLUENCES ON PRECIPITATING MESOSCALE SYSTEMS
William R. Cotton, S. Chen, and Gregory J. Tripoli (Wisconsin Univ., Madison.) *In* Deutscher Wetterdienst, Annals from the German Meteorological Society, No. 25: 10th International Cloud Physics Conference Preprints, Volume 1 1988 p 130-132 (For primary document see N89-19605 12-42)
(Grant NSF ATM-85-12480)
Copyright Avail: Deutscher Wetterdienst, Frankfurter Strasse 135, D-6050 Offenbach am Main, Fed. Republic of Germany

N89-19650 Atmospheric Environment Service, Downsview (Ontario).
THE COLLECTION EFFICIENCY OF A MASSIVE FOG COLLECTOR
Robert S. Schemenauer and Paul I. Joe *In* Deutscher Wetterdienst, Annals from the German Meteorological Society, No. 25: 10th International Cloud Physics Conference Preprints, Volume 1 1988 p 135-137 (For primary document see N89-19605 12-42)
Copyright Avail: Deutscher Wetterdienst, Frankfurter Strasse 135, D-6050 Offenbach am Main, Fed. Republic of Germany

N89-19651 Meteorological Office, Bracknell (England).
THE USE OF AUTOMATIC PARTICLE RECOGNITION TO IMPROVE THE DETERMINATION OF BULK QUANTITIES FROM PMS 2-D PROBE DATA IN CIRRUS
A. G. Darlison and P. R. A. Brown *In* Deutscher Wetterdienst, Annals from the German Meteorological Society, No. 25: 10th International Cloud Physics Conference Preprints, Volume 1 1988 p 138-140 (For primary document see N89-19605 12-42)
Copyright Avail: Deutscher Wetterdienst, Frankfurter Strasse 135, D-6050 Offenbach am Main, Fed. Republic of Germany

N89-19654 Mainz Univ. (Germany, F.R.). Inst. for Meteorology.
THE STUDY OF THE INTERSTITIAL AEROSOL PARTICLES AND CLOUD DROPLETS WITH DIGITAL IMAGE ANALYSIS OF DIFFRACTION IMAGES
R. Jaenicke and R. Soerensen *In* Deutscher Wetterdienst, Annals from the German Meteorological Society, No. 25: 10th International Cloud Physics Conference Preprints, Volume 1 1988 p 148-150 Sponsored by the Deutsche Forschungsgemeinschaft, Bonn, Fed. Republic of Germany (For primary document see N89-19605 12-42)
Copyright Avail: Deutscher Wetterdienst, Frankfurter Strasse 135, D-6050 Offenbach am Main, Fed. Republic of Germany

N89-19656 Deutsche Forschungs- und Versuchsanstalt fuer Luft- und Raumfahrt, Wesseling (Germany, F.R.). Inst. fuer HF-Technik.

MULTIPARAMETER CHARACTERIZATION OF RAINDROP SIZE DISTRIBUTION BY THE POLARIMETRIC DFVLR RADAR: FIRST RESULTS

M. Chandra, A. Schroth, and E. Lueneburg *In* Deutscher Wetterdienst, Annals from the German Meteorological Society, No. 25: 10th International Cloud Physics Conference Preprints, Volume 1 1988 p 154-157 (For primary document see N89-19605 12-42)

Copyright Avail: Deutscher Wetterdienst, Frankfurter Strasse 135, D-6050 Offenbach am Main, Fed. Republic of Germany

N89-19662 Deutsche Forschungs- und Versuchsanstalt fuer Luft- und Raumfahrt, Oberpfaffenhofen (West Germany). Inst. fuer Physik der Atmosphaere.

LIQUID WATER CONTENT, MEDIAN VOLUME DIAMETER AND TEMPERATURE IN DEPENDENCE ON THE HEIGHT ABOVE THE CLOUD BASE FOR DIFFERENT TYPES OF CLOUDS

H.-E. Hoffmann and R. Roth *In* Deutscher Wetterdienst, Annals from the German Meteorological Society, No. 25: 10th International Cloud Physics Conference Preprints, Volume 1 1988 p 175-177 (For primary document see N89-19605 12-42)

Copyright Avail: Deutscher Wetterdienst, Frankfurter Strasse 135, D-6050 Offenbach am Main, Fed. Republic of Germany

N89-19663 Iowa State Univ. of Science and Technology, Ames. Dept. of Meteorology.

A DETAILED EXAMINATION OF DISCONTINUITIES IN NATURAL RAIN SPECTRA

Harry C. Vaughan *In* Deutscher Wetterdienst, Annals from the German Meteorological Society, No. 25: 10th International Cloud Physics Conference Preprints, Volume 1 1988 p 178-179 (For primary document see N89-19605 12-42)

Copyright Avail: Deutscher Wetterdienst, Frankfurter Strasse 135, D-6050 Offenbach am Main, Fed. Republic of Germany

N89-19664* Desert Research Inst., Reno, NV.

CRYSTALLIZATION OF SUPERCOOLED SOLUTIONS

K. Harrison and John Hallett *In* Deutscher Wetterdienst, Annals from the German Meteorological Society, No. 25: 10th International Cloud Physics Conference Preprints, Volume 1 1988 p 180-182 (For primary document see N89-19605 12-42)

(Contract NAS7-918)

Copyright Avail: Deutscher Wetterdienst, Frankfurter Strasse 135, D-6050 Offenbach am Main, Fed. Republic of Germany

CSCL 04B

N89-19665 Institute of Chemical Kinetics and Combustion, Novosibirsk (USSR).

KINETICS OF ICE CRYSTAL FORMATION ON AEROSOL PARTICLES IN SUPERCOOLED FOG

Boris Gorbunov, Aleksandr Paschenko, and Hatalya Kakutkina *In* Deutscher Wetterdienst, Annals from the German Meteorological Society, No. 25: 10th International Cloud Physics Conference Preprints, Volume 1 1988 p 183-184 (For primary document see N89-19605 12-42)

Copyright Avail: Deutscher Wetterdienst, Frankfurter Strasse 135, D-6050 Offenbach am Main, Fed. Republic of Germany

N89-19666 Academy of Sciences of the Georgian SSR, Tbilisi. Inst. of Geophysics.

ABOUT SECONDARY ICE CRYSTAL PRODUCTION

T. Gzirishvili and V. Khorguani *In* Deutscher Wetterdienst, Annals from the German Meteorological Society, No. 25: 10th International Cloud Physics Conference Preprints, Volume 1 1988 p 185-187 (For primary document see N89-19605 12-42)

Copyright Avail: Deutscher Wetterdienst, Frankfurter Strasse 135, D-6050 Offenbach am Main, Fed. Republic of Germany

N89-19667 Osaka Kyoiku Univ. (Japan).

EXPERIMENTAL STUDIES ON SECONDARY ICE PARTICLE PRODUCTION

Akira Yamashita, Hiroyuki Konishi, Wataru Shimada, Masayoshi Miyatake, and Keisuke Tani *In* Deutscher Wetterdienst, Annals from the German Meteorological Society, No. 25: 10th International Cloud Physics Conference Preprints, Volume 1 1988 p 188-189 (For primary document see N89-19605 12-42)

Copyright Avail: Deutscher Wetterdienst, Frankfurter Strasse 135, D-6050 Offenbach am Main, Fed. Republic of Germany

N89-19668 Hokkaido Univ., Sapporo (Japan). Dept. of Geophysics.

PROPORTION OF RIMING GROWTH PROCESS IN SNOWFALL PHENOMENA

Toshio Harimaya and Misao Sato *In* Deutscher Wetterdienst, Annals from the German Meteorological Society, No. 25: 10th International Cloud Physics Conference Preprints, Volume 1 1988 p 190-192 (For primary document see N89-19605 12-42)

Copyright Avail: Deutscher Wetterdienst, Frankfurter Strasse 135, D-6050 Offenbach am Main, Fed. Republic of Germany

N89-19669 Shinshu Univ., Nagano (Japan). Faculty of Education.

THREE-DIMENSIONAL STRUCTURES OF SNOW CRYSTALS SHOWN BY STEREO-PHOTOMICROGRAPHS

Kuniomoto Iwai *In* Deutscher Wetterdienst, Annals from the German Meteorological Society, No. 25: 10th International Cloud Physics Conference Preprints, Volume 1 1988 p 193-195 (For primary document see N89-19605 12-42)

Copyright Avail: Deutscher Wetterdienst, Frankfurter Strasse 135, D-6050 Offenbach am Main, Fed. Republic of Germany

N89-19670 Akita Univ. (Japan). Dept. of Earth Science.

ON THE VARIATION OF FALLING VELOCITY OF EARLY SNOWFLAKES

Masahiro Kajikawa *In* Deutscher Wetterdienst, Annals from the German Meteorological Society, No. 25: 10th International Cloud Physics Conference Preprints, Volume 1 1988 p 196-198 (For primary document see N89-19605 12-42)

Copyright Avail: Deutscher Wetterdienst, Frankfurter Strasse 135, D-6050 Offenbach am Main, Fed. Republic of Germany

N89-19671 Johann-Wolfgang-Goethe-Univ., Frankfurt am Main (Germany, F.R.). Inst. fuer Meteorologie und Geophysik.

A PARAMETRIZATION SCHEME FOR THE COALESCENCE OF WATER DROPS USING THE STOCHASTIC COLLECTION EQUATION

C. Luepkes, K. D. Beheng, and S. Doms (Deutscher Wetterdienst, Offenbach am Main, Germany, F.R.) *In* Deutscher Wetterdienst, Annals from The German Meteorological Society, No. 25: 10th International Cloud Physics Conference Preprints, Volume 1 1988 p 199-201 (For primary document see N89-19605 12-42)

Copyright Avail: Deutscher Wetterdienst, Frankfurter Strasse 135, D-6050 Offenbach am Main, Fed. Republic of Germany

N89-19672 Missouri Univ., Rolla. Dept. of Mechanical and Aerospace Engineering.

ON THE DYNAMICS OF THE FALLING ICE CRYSTAL ZONE

Josef Podzimek *In* Deutscher Wetterdienst, Annals from the German Meteorological Society, No. 25: 10th International Cloud Physics Conference Preprints, Volume 1 1988 p 202-204 (For primary document see N89-19605 12-42)

(Contract DAAK11-83-K-0007)

Copyright Avail: Deutscher Wetterdienst, Frankfurter Strasse 135, D-6050 Offenbach am Main, Fed. Republic of Germany

N89-19673 Naval Research Lab., Washington, DC.

A NEW DATABASE OF ICE PARTICLE SIZE SPECTRA FOR ALTITUDES UP TO 10 km (30,000 ft)

Richard Jeck *In* Deutscher Wetterdienst, Annals from the German Meteorological Society, No. 25: 10th International Cloud Physics Conference Preprints, Volume 1 1988 p 205-207 Sponsored in part by the Dept. of Transportation, Washington, DC (For

primary document see N89-19605 12-42)
Copyright Avail: Deutscher Wetterdienst, Frankfurter Strasse 135, D-6050 Offenbach am Main, Fed. Republic of Germany

N89-19674 Nagoya Univ., Toyokawa (Japan).
A VERTICAL WIND TUNNEL FOR THE STUDY OF SNOWFLAKES AND EFFECTS OF ACCUMULATED SNOW ON MATERIALS
Kenki Isono, Jutaro Kobayashi, Takehiko Gonda, Yoshio Sasyo, and Taro Mori (Suga Test Instruments Co. Ltd., Japan) *In* Deutscher Wetterdienst, Annals from the German Meteorological Society, No. 25: 10th International Cloud Physics Conference Preprints, Volume 1 1988 p 208-210 (For primary document see N89-19605 12-42)
Copyright Avail: Deutscher Wetterdienst, Frankfurter Strasse 135, D-6050 Offenbach am Main, Fed. Republic of Germany

N89-19675 Direction de la Meteorologie Nationale, Magny les Hameaux (France).
PROPERTIES OF THE PRECIPITATION EMBRYOS EVOLUTION IN CHARACTERISTIC HAWAIIAN BAND CLOUDS
Arlette Rigaud, Elizabeth Hicks, Jacqueline Gagneux, and Constantin Pontikis *In* Deutscher Wetterdienst, Annals from the German Meteorological Society, No. 25: 10th International Cloud Physics Conference Preprints, Volume 1 1988 p 211-213 (For primary document see N89-19605 12-42)
Copyright Avail: Deutscher Wetterdienst, Frankfurter Strasse 135, D-6050 Offenbach am Main, Fed. Republic of Germany

N89-19676 Clermont-Ferrand Univ. (France).
PATTERN OF AIR BUBBLE INCLUSIONS IN ATMOSPHERIC ICE FORMED DURING ACCRETION
Pascal Gribelin, Pascal Personne, and Harumi Isaka *In* Deutscher Wetterdienst, Annals from the German Meteorological Society, No. 25: 10th International Cloud Physics Conference Preprints, Volume 1 1988 p 214-216 (For primary document see N89-19605 12-42)
Copyright Avail: Deutscher Wetterdienst, Frankfurter Strasse 135, D-6050 Offenbach am Main, Fed. Republic of Germany

N89-19677 Servicio Meteorologico Nacional, Buenos Aires (Argentina).
ANALYSIS OF HAILSTONES FROM A SEVERE STORM AND THEIR SIMULATED EVOLUTION
Laura Levi and Luisa Lubart (Comision Nacional de Energia Atomica, Buenos Aires, Argentina) *In* Deutscher Wetterdienst, Annals from the German Meteorological Society, No. 25: 10th International Cloud Physics Conference Preprints, Volume 1 1988 p 217-219 Sponsored in part by the Consejo Nacional de Investigaciones Cientificas y Technicas, Buenos Aires, Argentina (For primary document see N89-19605 12-42)
Copyright Avail: Deutscher Wetterdienst, Frankfurter Strasse 135, D-6050 Offenbach am Main, Fed. Republic of Germany

N89-19678 Manchester Univ. (England). Dept. of Physics.
THE COLLECTION EFFICIENCIES OF SOFT-HAILSTONES FOR SUPER-COOLED WATER DROPLETS AND ICE CRYSTALS
W. D. Keith and C. P. R. Saunders *In* Deutscher Wetterdienst, Annals from the German Meteorological Society, No. 25: 10th International Cloud Physics Conference Preprints, Volume 1 1988 p 220-222 (For primary document see N89-19605 12-42)
Copyright Avail: Deutscher Wetterdienst, Frankfurter Strasse 135, D-6050 Offenbach am Main, Fed. Republic of Germany

N89-19679 Clermont-Ferrand Univ. (France).
SIMULATION OF CONICAL GRAUPEL BY USING A BALLISTIC MODEL
Pascal Personne, Christophe Duroure, and Harumi Isaka *In* Deutscher Wetterdienst, Annals from the German Meteorological Society, No. 25: 10th International Cloud Physics Conference Preprints, Volume 1 1988 p 223-225 (For primary document see N89-19605 12-42)
Copyright Avail: Deutscher Wetterdienst, Frankfurter Strasse 135, D-6050 Offenbach am Main, Fed. Republic of Germany

N89-19685 University Coll., Galway (Ireland).
BELOW CLOUD SCAVENGING BY RAIN AND DRIZZLE
Brendan Thomas McGann and S. Gerard Jennings *In* Deutscher Wetterdienst, Annals from the German Meteorological Society, No. 25: 10th International Cloud Physics Conference Preprints, Volume 1 1988 p 241-242 (For primary document see N89-19605 12-42)
Copyright Avail: Deutscher Wetterdienst, Frankfurter Strasse 135, D-6050 Offenbach am Main, Fed. Republic of Germany

N89-19689 Nanjing Univ. (China). Dept. of Atmospheric Sciences.
IONIC CONCENTRATIONS OF RIME ICE AND SNOW AND BERGERON PROCESS
Shi-Hong Huang, R. A. Castillo, and V. K. Monhen (State Univ. of New York, Albany.) *In* Deutscher Wetterdienst, Annals from the German Meteorological Society, No. 25: 10th International Cloud Physics Conference Preprints, Volume 1 1988 p 251-253 (For primary document see N89-19605 12-42)
Copyright Avail: Deutscher Wetterdienst, Frankfurter Strasse 135, D-6050 Offenbach am Main, Fed. Republic of Germany

N89-19691 Toronto Univ. (Ontario). Physical Labs.
THE EFFECT OF FREEZING ON THE COMPOSITION OF CLOUD DROPLETS
J. V. Iribarne and T. Pyshnov *In* Deutscher Wetterdienst, Annals from the German Meteorological Society, No. 25: 10th International Cloud Physics Conference Preprints, Volume 1 1988 p 258-260 (For primary document see N89-19605 12-42)
Copyright Avail: Deutscher Wetterdienst, Frankfurter Strasse 135, D-6050 Offenbach am Main, Fed. Republic of Germany

N89-19701 Paris VII Univ. (France). Lab. de Physico-Chimie de l'Atmosphere.
CONCENTRATIONS IN RAIN EVENTS COLLECTED SEQUENTIALLY: MEASUREMENTS VS RESULTS OF A SIMPLE SCAVENGING MODEL
J. L. Jaffrezo and J. L. Colin *In* Deutscher Wetterdienst, Annals from the German Meteorological Society, No. 25: 10th International Cloud Physics Conference Preprints, Volume 1 1988 p 288-290 (For primary document see N89-19605 12-42)
Copyright Avail: Deutscher Wetterdienst, Frankfurter Strasse 135, D-6050 Offenbach am Main, Fed. Republic of Germany

N89-19710 Manchester Univ. (England). Dept. of Pure and Applied Physics.
A MODEL OF WET DEPOSITION TO COMPLEX TERRAIN BY THE SEEDER-FEEDER PROCESS
Andy Jones and Tom W. Choularton *In* Deutscher Wetterdienst, Annals from the German Meteorological Society, No. 25: 10th International Cloud Physics Conference Preprints, Volume 1 1988 p 316-318 (For primary document see N89-19605 12-42)
Copyright Avail: Deutscher Wetterdienst, Frankfurter Strasse 135, D-6050 Offenbach am Main, Fed. Republic of Germany

N89-19714 National Center for Atmospheric Research, Boulder, CO.
RADAR OBSERVATIONS OF PRECIPITATION MICROSTRUCTURE: THE MORPHOLOGY OF LINEAR DEPOLARIZATION MEASUREMENTS IN CLOUD
Paul H. Herzegh and Arthur R. Jameson *In* Deutscher Wetterdienst, Annals from the German Meteorological Society, No. 25: 10th International Cloud Physics Conference Preprints, Volume 1 1988 p 328-329 Sponsored in part by ARO, Washington, DC (For primary document see N89-19605 12-42)
(Grant NSF ATM-86-01257)
Copyright Avail: Deutscher Wetterdienst, Frankfurter Strasse 135, D-6050 Offenbach am Main, Fed. Republic of Germany

N89-19715 Deutsche Forschungs- und Versuchsanstalt fuer Luft- und Raumfahrt, Oberpfaffenhofen (West Germany). Inst. fuer Physik der Atmosphaere.
MULTIPARAMETER DOPPLER RADAR OBSERVATIONS OF A SQUALL LINE WITH THE POLARIMETRIC DFVLR RADAR
P. Meischner, V. N. Bringi, and T. Jank *In* Deutscher Wetterdienst, Annals from the German Meteorological Society, No. 25: 10th International Cloud Physics Conference Preprints, Volume 1 1988 p 330-332 (For primary document see N89-19605 12-42)
Copyright Avail: Deutscher Wetterdienst, Frankfurter Strasse 135, D-6050 Offenbach am Main, Fed. Republic of Germany

N89-19718 Atmospheric Environment Service, Downsview (Ontario).
INTERCOMPARISONS OF AIRCRAFT MEASUREMENTS WITH LIDAR RETURNS FOR AEROSOL, ICE CRYSTALS AND WATER DROPLETS
W. R. Leaitch, R. M. Hoff, A. I. Carswell, S. R. Pal, and A. G. Cunningham *In* Deutscher Wetterdienst, Annals from the German Meteorological Society, No. 25: 10th International Cloud Physics Conference Preprints, Volume 1 1988 p 338-340 (For primary document see N89-19605 12-42)
Copyright Avail: Deutscher Wetterdienst, Frankfurter Strasse 135, D-6050 Offenbach am Main, Fed. Republic of Germany

N89-19720 National Center for Atmospheric Research, Boulder, CO.
ON THE SMALL SCALE TOPOGRAPHICAL INFLUENCES ON PRECIPITATION
Wojciech W. Grabowski *In* Deutscher Wetterdienst, Annals from the German Meteorological Society, No. 25: 10th International Cloud Physics Conference Preprints, Volume 1 1988 p 344-346 Sponsored in part by NSF, Washington, DC (For primary document see N89-19605 12-42)
Copyright Avail: Deutscher Wetterdienst, Frankfurter Strasse 135, D-6050 Offenbach am Main, Fed. Republic of Germany

N89-19721 Colorado State Univ., Fort Collins. Dept. of Atmospheric Science.
A NUMERICAL INVESTIGATION OF AN OROGRAPHIC PRECIPITATION EVENT
Michael P. Meyers and William R. Cotton *In* Deutscher Wetterdienst, Annals from the German Meteorological Society, No. 25: 10th International Cloud Physics Conference Preprints, Volume 1 1988 p 347-349 (For primary document see N89-19605 12-42)
(Contract DAAL03-86-K-0175)
Copyright Avail: Deutscher Wetterdienst, Frankfurter Strasse 135, D-6050 Offenbach am Main, Fed. Republic of Germany

N89-19722 Illinois Univ., Urbana. Dept. of Atmospheric Sciences.
COMPLEX MICROPHYSICAL INTERACTIONS WITHIN A CENTRAL SIERRA NEVADA OROGRAPHIC CLOUD SYSTEM
Robert M. Rauber *In* Deutscher Wetterdienst, Annals from the German Meteorological Society, No. 25: 10th International Cloud Physics Conference Preprints, Volume 1 1988 p 350-352 (For primary document see N89-19605 12-42)
Copyright Avail: Deutscher Wetterdienst, Frankfurter Strasse 135, D-6050 Offenbach am Main, Fed. Republic of Germany

N89-19723 Bureau of Reclamation, Denver, CO.
COMPARISON OF OROGRAPHIC CLOUD AND PRECIPITATION DEVELOPMENT OF THREE DIFFERENT GEOGRAPHIC LOCATIONS USING A 3-D NESTED GRID CLOUD MODEL
Roy M. Rasmussen, Piotr K. Smolarkiewicz, William D. Hall, and T. Clark (National Center for Atmospheric Research, Boulder, CO.) *In* Deutscher Wetterdienst, Annals from the German Meteorological Society. No. 25: 10th International Cloud Physics Conference Preprints, Volume 1 1988 p 353-355 (For primary document see N89-19605 12-42)
Copyright Avail: Deutscher Wetterdienst, Frankfurter Strasse 135, D-6050 Offenbach am Main, Fed. Republic of Germany

N89-19724 Direction de la Meteorologie Nationale, Casablanca Royaume (Morocco). Div. de Developpement et de Recherche.
MICROPHYSICAL OBSERVATIONS OVER THE ATLAS MOUNTAINS IN MOROCCO
Omar Baddour and Roy M. Rasmussen (Bureau of Reclamation, Denver, CO.) *In* Deutscher Wetterdienst, Annals from the German Meteorological Society, No. 25: 10th International Cloud Physics Conference Preprints, Volume 1 1988 p 356-358 Sponsored by the Agency of International Development, Washington, DC (For primary document see N89-19605 12-42)
Copyright Avail: Deutscher Wetterdienst, Frankfurter Strasse 135, D-6050 Offenbach am Main, Fed. Republic of Germany

N89-19725 Colorado State Univ., Fort Collins. Dept. of Atmospheric Science.
MICROPHYSICAL AND DYNAMICAL INTERACTIONS IN COLORADO FRONT RANGE UPSLOPE STORMS
Douglas A. Wesley, Michael J. Weissbluth, Roger A. Pielke, and William R. Cotton *In* Deutscher Wetterdienst, Annals from the German Meteorological Society, No. 25: 10th International Cloud Physics Conference Preprints, Volume 1 1988 p 359-361 (For primary document see N89-19605 12-42)
(Contract DAAL03-36-K-0175)
Copyright Avail: Deutscher Wetterdienst, Frankfurter Strasse 135, D-6050 Offenbach am Main, Fed. Republic of Germany

N89-19726 Hokkaido Univ., Sapporo (Japan). Inst. of Low Temperature Science.
CHARACTERISTICS OF RADAR ECHO OF SNOW BAND FORMED IN THE LEE SIDE OF A MOUNTAIN
Yasushi Fujiyoshi, Tatsuo Endoh, and Gorow Wakahama *In* Deutscher Wetterdienst, Annals from the German Meteorological Society, No. 25: 10th International Cloud Physics Conference Preprints, Volume 1 1988 p 362-363 (For primary document see N89-19605 12-42)
Copyright Avail: Deutscher Wetterdienst, Frankfurter Strasse 135, D-6050 Offenbach am Main, Fed. Republic of Germany

N89-19727 Beijing Univ. (China). Dept. of Geophysics.
STUDY ON CLOUD AND RAIN BY MICROWAVE RADIOMETER OBSERVATION
Bolin Zhao *In* Deutscher Wetterdienst, Annals from the German Meteorological Societyn No. 25: 10th International Cloud Physics Conference Preprints, Volume 1 1988 p 364-365 (For primary document see N89-19605 12-42)
Copyright Avail: Deutscher Wetterdienst, Frankfurter Strasse 135, D-6050 Offenbach am Main, Fed. Republic of Germany

48 OCEANOGRAPHY

Includes biological, dynamic, and physical oceanography; and marine resources.

For related information see also *43 Earth Resources and Remote Sensing.*

N89-19791# Naval Postgraduate School, Monterey, CA.
A MODAL/WKB INVERSION METHOD FOR DETERMINING SOUND SPEED PROFILES IN THE OCEAN AND OCEAN BOTTOM M.S. Thesis
Kevin D. Casey Jun. 1988 193 p
(AD-A201252) Avail: NTIS HC A09/MF A01 CSCL 20A

Two approaches to determining the ocean sound profile using measured acoustic modal eigenvalues are examined. Both methods use measured eigenvalues and mode dependent assumed values of the WKB phase integral as input data and use the WKB phase integral as a starting point for relating the index of refraction to depth. Inversion method one is restricted to monotonic or symmetric sound speed profiles and requires a measurement of the sound speed at one depth to convert the index of refraction profile to a

sound speed profile. Inversion method two assumes that the sound speed at the surface and the minimum sound speed in the profile are known and is applicable to monotonic profiles and to general single duct sound speed profiles. For asymmetric profiles, inversion method two gives the depth difference between two points of equal sound speed in the portion of the profile having two turning points, and in the remainder of the profile it gives sound speed versus depth directly. A numerical implementation of the methods is demonstrated using idealized ocean sound speed profiles numerical experiments used to test the performance of the inversions using noisy data. The two methods are used to determine the sediment sound speed profiles in two shallow water waveguide models, and inversion method one is used to find the sediment sound speed profile using data from an experiment performed in the Gulf of Mexico. GRA

N89-19792# Massachusetts Inst. of Tech., Cambridge. Research Lab. of Electronics.

ACTIVE AND PASSIVE REMOTE SENSING OF ICE Semiannual Report, 1 Feb. - 31 Jul. 1988

Jin Au Kong 1 Nov. 1988 54 p

(Contract N00014-83-K-0258)

(AD-A201915) Avail: NTIS HC A04/MF A01 CSCL 20N

Fully polarimetric scattering properties of earth terrain media are studied with three-layer random medium model. The top scattering layer is modeled as an isotropic random medium which is characterized by a scalar permittivity. The middle scattering layer is modeled as an anisotropic random medium with a symmetric permittivity tensor whose optic axis can be tilted depending on the preferred alignment of the embedded scatters. The bottom layer is considered as a homogeneous half-space. Volume scattering effects of both random media are described by three-dimensional correlation functions with variances and correlation lengths corresponding to the strengths of the permittivity fluctuations and the physical sizes of the inhomogeneities, respectively. The strong fluctuations theory is used to derive the mean fields in the random media under the bilocal approximation with singularities of the dyadic Green's functions properly taken into consideration. With the discrete scatterer concept, effective permittivities of the random media are calculated by two-phase mixing formulas. Then, the distorted Born approximation is used to calculate the covariance matrix which describes the fully polarimetric scattering properties of the remotely sensed media. The polarimetric information is useful in the identification, classification, and radar image simulation of earth terrain media. GRA

N89-19793# Institute of Oceanographic Sciences, Wormley (England). Deacon Lab.

DIRECTIONAL WAVE DATA RECORDED IN THE SOUTHERN NORTH SEA

C. H. Clayson and J. A. Ewing 1988 69 p

(Contract DEN-E/5B/CON/935/2043)

(IOS-258; ETN-89-93711) Avail: NTIS HC A04/MF A01; Institute of Oceanographic Sciences, Deacon Lab., Wormley, Godalming, Surrey GU8 5UB, United Kingdom, 19 pounds

A directional wave buoy was deployed 11 nm north-east of Cromer, in the southern North Sea during the period from December 1985 to June 1987, in an area which includes gas fields. The techniques used and results obtained are summarized. The basic nondirectional information consists of measurements of the frequency spectrum from which wave height and period statistics were computed. The buoy provides estimates of the directional spectrum from which the mean wave direction and directional spread are calculated. The results are presented in tables and figures which, in addition to wave height and period statistics, provide statistics of the joint occurrence of wave height, wave period, and wave direction. Information for each of four seasons and for the whole data set is given. ESA

N89-19794# Institute of Oceanographic Sciences, Wormley (England). Deacon Lab.

COMPRESSIONAL-WAVE VELOCITIES IN OCEAN SEDIMENTS EAST SOUTHESAST OF MADEIRA, ATLANTIC OCEAN

R. B. Whitmarsh, P. R. Miles, R. E. Kirk, and M. R. Saunders 1988 82 p Sponsored by the ARE, Portland, United Kingdom (IOS-257; ETN-89-93712) Avail: NTIS HC A05/MF A01; Institute of Oceanographic Sciences, Deacon Laboratory, Wormley, Godalming, Surrey GU8 5UB, United Kingdom, 22 pounds

Experiments were conducted to determine the seismic structure of oceanic sediments in an area ESE of Madeira, and to obtain data to assist the interpretation of acoustic propagation experiments. Simple velocity models were obtained from the travel-times of near-vertical-incidence reflections. Synthetic seismogram modeling applied to three wide-angle seismic refraction profiles identifies an unsuspected mid-sediment reflector which causes multiple reflection of energy refracted within the lower sediments. The reflector is associated with a small P-wave velocity contrast and a more substantial S-wave velocity difference. The seismic structure of the upper sediments could not be constrained by synthetic seismogram modeling because no arrivals from the upper sediments could be distinguished on the record-sections. This is essentially a geometrical problem only soluble in oceanic depths by using bottom sources. The calculated velocity/depth models were transformed to velocity/vertical travel-time and compared with a seismic reflection profile. The mid-sediment reflector was associated with a laterally extensive change in character in the upper part of the profile and the near-constant velocity layer with the transparent, probably pelagic, sediments draped over the volcanic basement. These correlations enabled an estimated depth section to the made from the whole reflection profile. ESA

51 LIFE SCIENCES (GENERAL)

N89-19795# National Lab. for High Energy Physics, Oho (Japan).

RADIATION BIOLOGY STUDIES IN SOFT X-RAY AND ULTRASOFT X-RAY REGION

Katsumi Kobayashi, ed. Feb. 1988 50 p In JAPANESE Presented at the Workshop on Radiation Biology Studies in Soft X-ray and Ultrasoft X-ray Region, Tsukuba, Japan, 17 Jun. 1987 (DE88-756071; KEK-87-29; CONF-8706364) Avail: NTIS (US Sales Only) HC A03/MF A01

The aim of the radiation biology group in the PF is to investigate into the radiation biological effect of monochromatic SR light from ultraviolet to X-ray region, and to clarify the mechanism of biological action of radiation including corpuscular beam and gamma ray, in particular, its initial process. As the requirement for the purpose, the equipment of irradiating the monochromatic SR light over the whole region on living things and the room for specimen preparation and effect test, in which the radioisotopes indispensable for elucidating the responding process of living things can be used, have been made to be ready for use. Two irradiation systems for the monochromatic X-ray from 0.8 A to 3 A and the monochromatic soft X-ray from 4 A to 7 A were provided. Besides, an oblique incidence spectroscope for the ultrasoft X-ray from 40 A to 400 A region is equipped. By the combined use with a vacuum irradiation equipment, the above mentioned aim approaches one step closer to the realization. Especially, the soft X-ray irradiation system is expected to contribute to the research on the mechanism of causing DNA injury and the response to it. The study meeting was held on June 17 and 18, 1987, and the reports are collected in this book. DOE

52 AEROSPACE MEDICINE

Includes physiological factors; biological effects of radiation; and effects of weightlessness on man and animals.

N89-19796# Krug International, San Antonio, TX. Technology Services Div.

AN ANNOTATED BIBLIOGRAPHY OF HYPOBARIC DECOMPRESSION SICKNESS RESEARCH CONDUCTED AT THE CREW TECHNOLOGY DIVISION, USAF SCHOOL OF AEROSPACE MEDICINE, BROOKS AFB, TEXAS FROM 1983 TO 1988 Interim Report, 1 Jun. 1983 - 15 Oct. 1988

James T. Webb, Robert W. Krutz, Jr., and Gene A. Dixon Oct. 1988 24 p

(Contract F33615-85-C-4503)

(AD-A201274; USAFSAM-TP-88-10) Avail: NTIS HC A03/MF A01 CSCL 06J

Four major protocols, one of which includes five studies, have been initiated or completed in the 5-year period from 1983 to 1988. The studies have resulted in numerous publications which are listed as the references for this review. The purpose of this review is to provide an accessible summary of these extensive efforts and document the history of their accomplishments. The cross-reference information contained in this review is intended to simplify data accession within both published and data base records. A listing of the abbreviated title, protocol approval information, sponsorship information, computer database (HYPOB) retrieval numbers/titles, dates of exposure, and information about subjects, prebreathe, and exposure parameters for each study is followed by the published abstracts from each publication. GRA

N89-19797# Navy Personnel Research and Development Center, San Diego, CA.

BRAIN ACTIVITY DURING TACTICAL DECISION-MAKING. PART 4: EVENT-RELATED POTENTIALS AS INDICES OF SELECTIVE ATTENTION AND COGNITIVE WORKLOAD

Leonard J. Trejo, Gregory W. Lewis, and Mark H. Blankenship Oct. 1988 24 p

(AD-A201370; NPRDC-TN-89-6) Avail: NTIS HC A03/MF A01 CSCL 05H

The demands of modern combat systems have the potential for exceeding the capacity of the human to accurately process information, especially during times of great stress. The capacity of the human to perceive, integrate, remember, and use information may be challenged when the individual is flying aircraft, monitoring radar and sonar displays, or operating electronic warfare systems. Exceeding the capacity of the human operator in such situations may impair decision-making and could result in costly tactical errors. Although much is being done to improve the reliability of combat systems, not enough is being done to improve the system operators. For these reasons, the most unpredictable element in combat systems is the human operator. Years of personnel testing have not eliminated this unpredictability. In part, this is because traditional testing methods tend to measure that a person knows rather than how a person thinks and processes information. This research is driven by the Navy's need for better methods of assessing combat system operators, particularly for predicting the ability of operators to continue to make accurate decisions under heavy workloads. This report, the fourth in a series of reports concerned with the use of neuroelectric signals to predict the decision-making performance of combat system operators, provides detailed analyses of the neuroelectric changes that occur as workload increases in a combat system simulation. GRA

N89-19798# Air Force Inst. of Tech., Wright-Patterson AFB, OH.

A STUDY TO ANALYZE THE DEGREE OF THE RELATIONSHIP BETWEEN HEALTH PRACTICES AND FATIGUE M.S. Thesis

Sherry L. Kennedy Sep. 1988 131 p

(AD-A201518; AFIT/GSM/LS/88S-12) Avail: NTIS HC A07/MF A01 CSCL 05I

The intention of this research was to examine the health practices of higher ranked individuals, both military and civilian, at Aeronautical Systems Division to determine if a relationship exists between the health practices they are following and the amount of fatigue they are experiencing. The health practices studied were: alcohol consumption, caffeine consumption, amount of exercise, eating habits, sleeping habits, smoking habits, and psychological stress management. These seven health practices were analyzed and compared to the amount of fatigue being experienced for both psychological and physiological fatigue. The level of fatigue was determined by individual responses to subjective self-analysis questions. Comparisons were also made between military and civilian personnel to determine if significant differences existed in health practices or in levels of fatigue. GRA

N89-19799# Army Research Inst. of Environmental Medicine, Natick, MA.

DEXAMETHASONE FOR PREVENTION AND TREATMENT OF ACUTE MOUNTAIN SICKNESS

Peter H. Hackett, Robert C. Roach, Robert A. Wood, Richard G. Foutch, Richard Meehan, Drummond Rennie, and William J. Mills, Jr. 3 Mar. 1988 17 p Submitted for publication

(AD-A201554; USARIEM-M39-88) Avail: NTIS HC A03/MF A01 CSCL 06J

Acute mountain sickness (AMS) is a common malady afflicting persons ascending quickly to high altitude. Although generally not life-threatening and usually self-limiting, AMS is often incapacitating. Potentially fatal pulmonary and cerebral edema may develop in as many as five to ten percent of those with AMS. Staged ascent with adequate time for acclimatization is optimal for prevention, but is not always effective and is often impractical. Therefore, pharmacological prophylaxis has been of great interest. The current agent of choice for prevention of AMS is acetazolamide. One field study found dexamethasone also effective in preventing symptoms of AMS. The investigators gave 4mg dexamethasone every six hours starting 48 hours prior to decompression or ascent. The subjects were sedentary. We also wished to study dexamethasone as a treatment for established cases of AMS. We rapidly transported fifteen soldiers from sea level to 4400m. The study included a double-blind, placebo-controlled trial of 2mg dexamethasone every six hours starting 1 hour before flight to high altitude; and subsequently a trial of 4mg dexamethasone every six hours for the treatment of AMS. We found that the lower dose dexamethasone did not prevent AMS in active soldiers, and that the higher dose of dexamethasone was an effective treatment for those ill with AMS. GRA

N89-19800# Army Research Inst. of Environmental Medicine, Natick, MA.

SATELLITE REMOTE SENSING OF HEAT STRESS DURING RESERVE TRAINING AT FORT HOOD

W. Matthew, G. Thomas, M. Rose, R. Hubbard, R. Whang, F. Schatzle, J. Baldwin, S. Hsu, O. Huh, and F. Quirk 17 Oct. 1988 9 p Presented at the 9th Annual EOSAEL/TWI Conference, Las Cruces, NM, 29 Nov. - 1 Dec. 1988

(AD-A201555; USARIEM-M2-89) Avail: NTIS HC A02/MF A01 CSCL 04B

Weather effects on soldiers have a profound impact on military operations in climatic extremes. In hot regions, soldier performance limits and drinking water requirements are crucial factors in mission planning and tactical options. The ability to quantify heat stress levels across an entire operational area would provide an information resource for optimizing soldier performance in high mobility Airland scenarios. Preliminary tests of satellite remote sensing methods currently under development (SBIR contract No. DAMD 17-86-C-6004), were conducted during reserve training operations at Fort Hood, Texas in June 1988. Data were obtained from the AVHRR (Advanced Very High Resolution Radiometer) and TOVS (TIROS Operational Vertical Sounder) instruments aboard NOAA polar orbiting satellites. WBGT (Wet Bulb Globe Temperature) index values derived from satellite data are compared with contemporary surface level measurements and heat casualty rates. Results and salient issues in further development of this capability are described. GRA

N89-19801# Delaware Univ., Newark.
BRAIN MECHANISMS UNDERLYING INDIVIDUAL DIFFERENCES IN REACTION TO STRESS: AN ANIMAL MODEL Final Report, 1 May 1985 - 31 Aug. 1988
Jerome Siegel, Patricia M. Saxton, and David F. Sisson 29 Oct. 1988 14 p
(Contract DAAG29-85-K-0085)
(AD-A201595; ARO-21733.4-LS) Avail: NTIS HC A03/MF A01 CSCL 06D

The research described in this final report is designed to expand the animal model for augmenting-reducing in rats and cats. Much effort has been put into developing an acute preparation in which VEPs variability is maintained at a manageable level. A two pronged effort is used to determine the neural mechanisms underlying augmenting-reducing. First, laminar origins of the components of VEPs. With this information, anatomical and physiological knowledge of visual cortex can be used to narrow down the putative mediators for this phenomenon. Second, determination of the effect of electrical and chemical lesions and electrical stimulation of subcortical nuclei on VEPs can be used to attempt to experimentally control the mechanisms that produce augmenting-reducing. GRA

N89-19802# Massachusetts Inst. of Tech., Cambridge. Center for Biological Information Processing.
COMPUTATION OF STEREO AND VISUAL MOTION: FROM BIOPHYSICS TO PSYCHOPHYSICS Progress Report, 1 Apr. - 30 Sep. 1988
Tomaso Poggio, Ellen Hildreth, Norberto Grzywacz, and Heinrich Buelthoff 30 Sep. 1988 8 p
(Contract N00014-85-C-0038)
(AD-A201873) Avail: NTIS HC A02/MF A01 CSCL 09A

During the second and third quarter of this stretchout year of funding, we have continued to explore a number of problems in motion analysis, including the parallel detection of motion using a correlation-based mechanism, motion correspondence, neural mechanisms for motion detection and measurement, and the recovery of 3-D structure and motion. We are also starting to focus more deeply on the integration of multiple visual cues. Described here is some work on the interaction between surface shape, albedo, and the illuminant direction. As we noted in our previous report, we are developing and testing some variations on a parallel network model recently proposed by Hutchinson, Koch, Luo and Mead for combining the computation of the smoothest velocity field with line processes (suggested by Geman and Geman) for handling motion discontinuities. Our modified network derives the initial motion measurements only at the locations of significant intensity changes, allows greater flexibility in the placement of the discontinuities and considers variations on the energy function being minimized to implement the smoothness constraint. The network is also designed in a way that more closely parallels physiological properties of motion-sensitive neurons in area MT of monkey visual cortex. GRA

N89-19803# Wright State Univ., Dayton, OH.
A STRESS TEST TO EVALUATE THE PHYSICAL CAPACITY OF PERFORMING L-1 ANTI-G STRAINING MANEUVERS Final Technical Report, Aug. 1987 - Aug. 1988
Wen-Yaw Chiou Sep. 1988 38 p
(AD-A202301; AAMRL-TR-88-047) Avail: NTIS HC A03/MF A01 CSCL 06J

To evaluate the physical capacity of performing L-1 anti-G straining maneuvers (AGSM), 9 subjects participated in stress test protocols which were designed to use repetitive AGSM exercise on the ground. Physiological responses of oxygen uptake (VO2), minute pulmonary ventilation (VE), respiratory exchange ratio (RER) and heart rate (HR) were determined for steady state exercises at AGSM duty cycles of 20, 25, 33, and 50 percent. The individual's physical capacity for performing AGSM can be objectively evaluated by the strength (peak output) and endurance (time to 40 percent fatigue) aspects of this continuous stress test. The higher peak VO achieved, the greater was considered the aerobic energy output for AGSM performance. This is dependent upon the muscle mass available, the condition of the muscles, as well as cardiopulmonary fitness of the individual. The longer endurance time for the ground test, the longer tolerance duration will most likely be obtained during actual centrifuge G-force testing. Therefore, the described AGSM stress test on the ground may be a convenient, inexpensive and useful tool to objectively evaluate the physical capacity of individuals for performing AGSM. Such a test may be used for pilot candidate screening prior to centrifuge and aircraft G-tolerance testing. GRA

N89-19804# Technische Univ., Eindhoven (Netherlands).
ULTRASOUND TRANSMISSION TOMOGRAPHY, A LOW-COST REALIZATION Ph.D. Thesis
Gerrit Sollie 1988 172 p
(ISBN-90-9002330-5; ETN-89-93894) Avail: NTIS HC A08/MF A01

A prototype transmission tomography system was developed and tested. Images can be obtained of the distributions of three independent physical quantities in a cross-section of the measured object: the local sound propagation velocity, the local attenuation coefficient, and the local derivative with respect to frequency of the attenuation coefficient. The images of these quantities are reconstructed from three sets of values that are measured simultaneously from one reverberating sound pulse. The measuring values, which are the time-of-flight, the amplitude, and the center frequency of the pulse, are obtained from this reverberating pulse without knowing the exact RF-signal. This eliminates the need of a very expensive, high-frequency sampling device. The tomography system offers the possibility of performing a limited degree of tissue characterization because of the specific combinations of the three physical quantities for different biological tissues. ESA

N89-20067*# Alma Coll., MI. Dept. of Exercise and Health Science.
A MODEL FOR PLASMA VOLUME CHANGES DURING SHORT DURATION SPACEFLIGHT Final Report
John E. Davis *In* NASA, Lyndon B. Johnson Space Center, National Aeronautics and Space Administration (NASA)/American Society for Engineering Education (ASEE) Summer Faculty Fellowship Program 1988, Volume 1 Feb. 1989 15 p (For primary document see N89-20058 12-99)
Avail: NTIS HC A09/MF A01 CSCL 06P

N89-20069*# University of Central Washington, Ellensburg. Dept. of Physical Education.
EFFECTS ON MOTOR UNIT POTENTIATION AND GROUND REACTION FORCE FROM TREADMILL EXERCISE Final Report
Reid P. Elam *In* NASA, Lyndon B. Johnson Space Center, National Aeronautics and Space Administration (NASA)/American Society for Engineering Education (ASEE) Summer Faculty Fellowship Program 1988, Volume 1 Feb. 1989 13 p (For primary document see N89-20058 12-99)
Avail: NTIS HC A09/MF A01 CSCL 06S

N89-20076*# Texas Univ., Galveston. Dept. of Pharmacology and Toxicology.
MALADJUSTMENT OF KIDNEYS TO MICROGRAVITY: DESIGN OF MEASURES TO REDUCE THE LOSS OF CALCIUM Final Report
Bohdan R. Nechay *In* NASA, Lyndon B. Johnson Space Center, National Aeronautics and Space Administration (NASA)/American Society for Engineering Education (ASEE) Summer Faculty Fellowship Program 1988, Volume 2 Feb. 1989 14 p (For primary document see N89-20073 12-99)
Avail: NTIS HC A09/MF A01 CSCL 06P

53 BEHAVIORAL SCIENCES

Includes psychological factors; individual and group behavior; crew training and evaluation; and psychiatric research.

N89-19805# Yale Univ., New Haven, CT. School of Medicine.
FEAR-POTENTIAL STARTLE AS A MODEL SYSTEM FOR ANALYZING LEARNING AND MEMORY Annual Report, 1 Jul. 1987 - 30 Jun. 1988
Michael Davis 21 Sep. 1988 4 p
(Grant AF-AFOSR-0336-87; AF Proj. 2312)
(AD-A201330; AFOSR-88-1171TR) Avail: NTIS HC A02/MF A01 CSCL 05H

Previous research has shown that the acoustic startle response, a simple reflex mediated by four synapsis in the brainstem and spinal cord, can be increased when elicited in the presence of a stimulus previously paired with a footshock. This fear-potentiated startle effect can be selectively blocked by drugs that decrease anxiety in humans as well as by lesions of the central nucleus of the amygdala, an area of the brain known to be critical for fear. This year it has been found that: (1) footshocks by themselves cause a marked increase in the startle reflex which appears to result from an activation of the central nucleus of the amygdala; (2) low level electrical stimulation of the central nucleus of the amygdala increases the acoustic startle reflex with a transit time of about 5 msec from the amygdala to the acoustic startle circuit; (3) a direct anatomical connection exists between the central nucleus of the nucleus of the amygdala and the acoustic startle pathway; and (4) lesions at several points along this pathway prevent a fear stimulus from potentiating the startle reflex. GRA

N89-19806# Massachusetts Inst. of Tech., Cambridge. Artificial Intelligence Lab.
STRUCTURAL SALIENCY: THE DETECTION OF GLOBALLY SALIENT STRUCTURES USING A LOCALLY CONNECTED NETWORK
Shimon Ullman and Amnon Shaashua Jul. 1988 15 p
(Contract N00014-85-K-0124)
(AD-A201619; AI-M-1061) Avail: NTIS HC A03/MF A01 CSCL 06D

When we look at images, certain salient structures often attract our immediate attention without requiring a systematic scan of the entire image. In subsequent stages, processing resources can be allocated preferentially to these salient structures. In many cases this saliency is a property of the structure as a whole, i.e., parts of the structure are not salient in isolation. In this paper we present a saliency measure based on curvature and curvature variation. The structures this measure emphasizes are also salient in human perception, and they often correspond to objects of interest in the image. We present a method for computing the saliency by a simple iterative scheme, using a uniform network of locally connected processing elements. The network uses an optimization approach to produce a saliency map, which is a representation of the image emphasizing salient locations. The main properties of the network are: (1) the computations are simple and local, (2) globally salient structures emerge with a small number of iterations, and (3) as a by-product of the computations, contours are smoothed and gaps are filled in. GRA

N89-19857*# Vector Research, Inc., Ann Arbor, MI.
PSYCHOLOGICAL TOOLS FOR KNOWLEDGE ACQUISITION
Henry H. Rueter and Judith Reitman Olson (Michigan Univ., Ann Arbor.) *In* NASA. Lyndon B. Johnson Space Center, 2nd Annual Workshop on Space Operations Automation and Robotics (SOAR 1988) Nov. 1988 p 293-297 (For primary document see N89-19817 12-59)
Avail: NTIS HC A22/MF A01 CSCL 05I

54 MAN/SYSTEM TECHNOLOGY AND LIFE SUPPORT

Includes human engineering; biotechnology; and space suits and protective clothing.

For related information see also *16 Space Transportation.*

N89-19807*# Texas Univ., Austin. Lunar Operations Co.
A BOOTSTRAP LUNAR BASE: PRELIMINARY DESIGN REVIEW 2 Final Report
25 Nov. 1987 180 p
(Grant NGT-21-002-080)
(NASA-CR-184753; NAS 1.26:184753) Avail: NTIS HC A09/MF A01 CSCL 06K

A bootstrap lunar base is the gateway to manned solar system exploration and requires new ideas and new designs on the cutting edge of technology. A preliminary design for a Bootstrap Lunar Base, the second provided by this contractor, is presented. An overview of the work completed is discussed as well as the technical, management, and cost strategies to complete the program requirements. The lunar base design stresses the transforming capabilities of its lander vehicles to aid in base construction. The design also emphasizes modularity and expandability in the base configuration to support the long-term goals of scientific research and profitable lunar resource exploitation. To successfully construct, develop, and inhabit a permanent lunar base, however, several technological advancements must first be realized. Some of these technological advancements are also discussed. Author

N89-19808*# Prairie View Agricultural and Mechanical Coll., TX. Coll. of Engineering.
DESIGN OF A SURFACE-BASED FACTORY FOR THE PRODUCTION OF LIFE SUPPORT AND TECHNOLOGY SUPPORT PRODUCTS. PHASE 2: INTEGRATED WATER SYSTEM FOR A SPACE COLONY Preliminary Final Report
[1989] 114 p
(Grant NGT-21-002-080)
(NASA-CR-184730; NAS 1.26:184730) Avail: NTIS HC A06/MF A01 CSCL 06K

Phase 2 of a conceptual design of an integrated water treatment system to support a space colony is presented. This includes a breathable air manufacturing system, a means of drilling for underground water, and storage of water for future use. The system is to supply quality water for biological consumption, farming, residential and industrial use and the water source is assumed to be artesian or subsurface and on Mars. Design criteria and major assumptions are itemized. A general block diagram of the expected treatment system is provided. The design capacity of the system is discussed, including a summary of potential users and the level of treatment required; and, finally, various treatment technologies are described. Author

N89-19809*# Essex Corp., Huntsville, AL.
ADVANCED EXTRAVEHICULAR ACTIVITY SYSTEMS REQUIREMENTS DEFINITION STUDY. PHASE 2: EXTRAVEHICULAR ACTIVITY AT A LUNAR BASE Final Report
Valerie Neal, Nicholas Shields, Jr., Gerald P. Carr, William Pogue, Harrison H. Schmitt, and Arthur E. Schulze (Lovelace Scientific Resources, Inc., Albuquerque, NM.) Sep. 1988 160 p
(Contract NAS9-17779)
(NASA-CR-172117; NAS 1.26:172117) Avail: NTIS HC A08/MF A01 CSCL 06K

The focus is on Extravehicular Activity (EVA) systems requirements definition for an advanced space mission: remote-from-main base EVA on the Moon. The lunar environment, biomedical considerations, appropriate hardware design criteria, hardware and interface requirements, and key technical issues for advanced lunar EVA were examined. Six remote EVA scenarios (three nominal operations and three contingency situations) were developed in considerable detail. B.G.

N89-19810# Aeronautical Research Labs., Melbourne (Australia).
THERMAL STRESS IN RAN SEA KING HELICOPTER OPERATIONS
J. G. Manton and K. C. Hendy Feb. 1988 50 p
(ARL-SYS-R-40; AR-004-592) Copyright Avail: NTIS HC A03/MF A01

Thermal stress in aircrew operating in the cabin and cockpit environment of the RAN's Sea King helicopter was examined. The high thermal loads experienced in the helicopter have previously been established and various options for ameliorating the conditions have also been proposed. A review of the literature on thermal stress research is presented. The development of an Index of Thermal Stress for the Sea King (SKITS) is reported along with the results of a study to determine the ameliorating effect of blown cooled air directed at the faces of subjects in a thermal chamber. Author

N89-19811# Army Natick Research and Development Command, MA.
COOLING EFFECTIVENESS OF A HYBRID MICROCLIMATE GARMENT Final Report, Jul. - Aug. 1987
Barry S. DeCristofano, Joseph S. Cohen, Bruce S. Cadarette, and Karen L. Speckman Apr. 1988 22 p
(AD-A201115; NATICK-TR-88/003) Avail: NTIS HC A03/MF A01 CSCL 05H

A prototype microclimate cooling garment that would allow the wearer to connect to either an air or a liquid cooling unit was tested and compared with existing air and liquid vests. Five male soldiers wore the three garments (hybrid, air, and liquid) on different days while walking on a treadmill in a climatically controlled environment. The chamber conditions were: dry bulb temperature, 38C (100F); relative humidity, 20 percent. The exercise generated a 332-W metabolic rate. The average metabolic rate (including rest periods) was 287 W. The hybrid garment, in either mode, performed as well as the individual air and liquid garments. Though the hybrid vest succeeded physiologically, comfort and fit problems were revealed that will require major changes in the next iteration. GRA

N89-19812# Anthropology Research Project, Yellow Springs, OH.
COMPUTER SOFTWARE USED IN US ARMY ANTHROPOMETRIC SURVEY 1987-1988 Final Report, Sep. 1986 - Mar. 1988
Thomas D. Churchill, Bruce Bradtmiller, and Claire C. Gordon 30 Jun. 1988 120 p
(Contract DAAK60-86-C-0128)
(AD-A201185; NATICK-TR-88/045) Avail: NTIS HC A06/MF A01 CSCL 05I

This report describes the hardware and software used in the 1987 to 1988 anthropometric survey of the U.S. Army. It includes a background section outlining how anthropometric data can be edited mathematically, and how such editing has been done in surveys of the past. It then describes the data entry and editing software which was created especially for the 1987 to 1988 survey, and how that software is based on historically proven techniques. Programs which randomly select subjects for measurement from among those who are screened and which calculate inter-observer measurement error are also described. The appendices include a self-contained hardware/software user's guide, and complete program listings for all software used in the survey. GRA

N89-19813# Anthropology Research Project, Yellow Springs, OH.
THE DEVELOPMENT AND VALIDATION OF AN AUTOMATED HEADBOARD DEVICE FOR MEASUREMENT OF THREE-DIMENSIONAL COORDINATES OF THE HEAD AND FACE Final Report, Sep. 1986 - Dec. 1987
James F. Annis and Claire C. Gordon 1 Jun. 1988 198 p
(Contract DAAK60-86-C-0128)
(AD-A201186; NATICK-TR-88/048) Avail: NTIS HC A09/MF A01 CSCL 05I

The measurement of three-dimensional (3-D) coordinates of the surface of the human body finds its justification in the applicability of such anthropometric information to the design of personal protective items for the head and face where good fit is critical. In the future, anthropologists and engineers will utilize remote imaging devices, such as lasers, video cameras, and holographic systems, to collect great quantities of 3-D shape information very rapidly. The measurement accuracy of such devices as well as the statistical means for analyzing large-sample data are still under investigation, however. For the present, we must be satisfied with 3-D information on a relatively low number of body landmark locations, particularly when measured on large samples under field survey conditions. The area of the body for which the collection of 3-D information in a major anthropometric survey seems most warranted is the head and face. GRA

N89-19814# Naval Postgraduate School, Monterey, CA.
THE EFFECTS OF A PITCHED FIELD ORIENTATION ON HAND/EYE COORDINATION M.S. Thesis
Cynthia J. Ballinger Sep. 1988 70 p
(AD-A201620) Avail: NTIS HC A04/MF A01 CSCL 06D

Ten subjects judged eye level by making verbal and pointing responses while looking into a box that was pitched at angles of approximately -15, -7.5, 0, 7.5 and 15 and 15 degrees. The mean verbal judgement changed as a function of the box's pitch angle according to the relationship: Judged Eye Level = 0.48 (Box Pitch Angle) - 0.31 Degrees which agrees with the results of previous studies. The mean pointing responses were also a function of the box's pitch angle: Pointing Response = -0.19 (Box Pitch Angle) - 5.39 Degrees Thus, the mean pointing responses change at approximately 40 percent of the rate of the perceptual responses, as indicated by the verbal judgements, and are in the opposite direction. These errors have implications for the design of displays and controls for vehicles that operate in environments where pitched visual fields are encountered. GRA

N89-19815# Naval Postgraduate School, Monterey, CA.
DEVELOPMENT OF A MODEL WHICH PROVIDES A TOTAL SYSTEM APPROACH TO INTEGRATING VOICE RECOGNITION AND SPEECH SYNTHESIS INTO THE COCKPIT OF US NAVY AIRCRAFT M.S. Thesis
Margaret A. Lee Sep. 1988 65 p
(AD-A202122; AD-E501048) Avail: NTIS HC A04/MF A01 CSCL 01D

Pilot workload saturation in the cockpit of U.S. Navy Aircraft has become a serious concern. Literature, studies, and flight tests indicate that utilizing a voice interactive system for certain cockpit tasks can reduce this workload by decreasing the time required to perform the task. This being the case, the problem which remains is one of deciding which tasks to convert. Therefore, a model has been developed which provides the designer with a total systems approach for use in deciding what combination of tasks, which if converted for performance by the voice interactive system, will result in the greatest workload reduction without overloading the pilot's voice channels. GRA

N89-19816# Messerschmitt-Boelkow-Blohm G.m.b.H., Ottobrunn (Germany, F.R.).
STUDY ON CHECKOUT OF FLIGHT UNITS AND SUBSYSTEMS Final Report
W. Berghofer and S. Y. Ovadya Paris, France ESA Jun. 1988 130 p
(Contract ESA-5974/84)
(ESA-CR(P)-2693; ETN-89-93937) Avail: NTIS HC A07/MF A01

Tradeoffs were performed to derive the ground support requirements of TV-SAT. The interfaces between checkout equipment, onboard data handling, and test facilities were defined. The European Test Operation Langage and AS-BASIC were compared in terms of utilization, support, and performance. Remote checkout for extravehicular activity (EVA) was studied. It is shown that it is not possible to perform EVA without local monitoring, control of the acquired data and their transmission. Thus, as a

windfall product remote checkout becomes available for the whole life of the EVA space suit system, and should be used to reduce cost and improve efficiency of the whole system. ESA

N89-19846*# National Aeronautics and Space Administration. Langley Research Center, Hampton, VA.
PHYSIOLOGICAL ASSESSMENT OF TASK UNDERLOAD
J. Raymond Comstock, Jr., Randall L. Harris, Sr., and Alan T. Pope *In* NASA. Lyndon B. Johnson Space Center, 2nd Annual Workshop on Space Operations Automation and Robotics (SOAR 1988) Nov. 1988 p 221-226 (For primary document see N89-19817 12-59)
Avail: NTIS HC A22/MF A01 CSCL 05H

N89-19847*# Aerospace Medical Research Labs., Wright-Patterson AFB, OH. Human Engineering Lab.
A SCHEMA-BASED MODEL OF SITUATION AWARENESS: IMPLICATIONS FOR MEASURING SITUATION AWARENESS
Martin L. Fracker *In* NASA. Lyndon B. Johnson Space Center, 2nd Annual Workshop on Space Operations Automation and Robotics (SOAR 1988) Nov. 1988 p 227-231 (For primary document see N89-19817 12-59)
Avail: NTIS HC A22/MF A01 CSCL 05H

N89-19860*# Essex Corp., Orlando, FL.
OPTIMAL SOLUTIONS FOR COMPLEX DESIGN PROBLEMS: USING ISOPERFORMANCE SOFTWARE FOR HUMAN FACTORS TRADE OFFS
Robert S. Kennedy, Marshall B. Jones (Pennsylvania State Univ., Hershey.), and Dennis R. Baltzley *In* NASA. Lyndon B. Johnson Space Center, 2nd Annual Workshop on Space Operations Automation and Robotics (SOAR 1988) Nov. 1988 p 313-319 (For primary document see N89-19817 12-59)
Avail: NTIS HC A22/MF A01 CSCL 05H

N89-19861*# Lockheed Engineering and Sciences Co., Houston, TX.
SIMULATION OF THE HUMAN-TELEROBOT INTERFACE
Mark A. Stuart and Randy L. Smith *In* NASA. Lyndon B. Johnson Space Center, 2nd Annual Workshop on Space Operations Automation and Robotics (SOAR 1988) Nov. 1988 p 321-326 (For primary document see N89-19817 12-59)
(Contract NAS9-17900)
Avail: NTIS HC A22/MF A01 CSCL 05H

N89-19862*# CAMUS, Inc., Huntsville, AL.
MAN-SYSTEMS REQUIREMENTS FOR THE CONTROL OF TELEOPERATORS IN SPACE
Nicholas L. Shields, Jr. *In* NASA. Lyndon B. Johnson Space Center, 2nd Annual Workshop on Space Operations Automation and Robotics (SOAR 1988) Nov. 1988 p 329-334 (For primary document see N89-19817 12-59)
Avail: NTIS HC A22/MF A01 CSCL 05H

N89-19863*# West Virginia Univ., Morgantown. Dept. of Mechanical and Aerospace Engineering.
INTEGRATION OF A COMPUTERIZED TWO-FINGER GRIPPER FOR ROBOT WORKSTATION SAFETY
John E. Sneckenberger and Kazuki Yoshikata *In* NASA. Lyndon B. Johnson Space Center, 2nd Annual Workshop on Space Operations Automation and Robotics (SOAR 1988) Nov. 1988 p 335-338 (For primary document see N89-19817 12-59)
Avail: NTIS HC A22/MF A01 CSCL 05H

N89-19864*# Michigan Technological Univ., Houghton. Dept. of Mechanical Engineering.
LOCAL POSITION CONTROL: A NEW CONCEPT FOR CONTROL OF MANIPULATORS
Frederick A. Kelly *In* NASA. Lyndon B. Johnson Space Center, 2nd Annual Workshop on Space Operations Automation and Robotics (SOAR 1988) Nov. 1988 p 339-341 (For primary document see N89-19817 12-59)
Avail: NTIS HC A22/MF A01 CSCL 05H

N89-19865*# Cincinnati Univ., OH. Dept. of Mechanical and Industrial Engineering.
DEXTERITY ANALYSIS AND ROBOT HAND DESIGN
Lu Li, A. H. Soni, Cai Chunsheng, and Max Brown *In* NASA. Lyndon B. Johnson Space Center, 2nd Annual Workshop on Space Operations Automation and Robotics (SOAR 1988) Nov. 1988 p 343-351 (For primary document see N89-19817 12-59)
Avail: NTIS HC A22/MF A01 CSCL 05H

N89-19866*# Central State Univ., Wilberforce, OH. Dept. of Manufacturing Engineering.
CONCEPT FOR A LARGE MASTER/SLAVE-CONTROLLED ROBOTIC HAND
William A. Grissom, Mahmoud A. AbdAllah, and Carl L. White (Computerized Technologies, Inc., Columbus, OH.) *In* NASA. Lyndon B. Johnson Space Center, 2nd Annual Workshop on Space Operations Automation and Robotics (SOAR 1988) Nov. 1988 p 353-359 Sponsored in part by an Ohio Board of Regeants Research Challenge grant (For primary document see N89-19817 12-59)
(Contract NAGw-1336; JPL-958292)
Avail: NTIS HC A22/MF A01 CSCL 05H

N89-19870*# National Aeronautics and Space Administration. Goddard Space Flight Center, Greenbelt, MD.
DESIGN CONCEPT FOR THE FLIGHT TELEROBOTIC SERVICER (FITS)
J. F. Andary, S. W. Hinkai, and J. G. Watzin *In* NASA. Lyndon B. Johnson Space Center, 2nd Annual Workshop on Space Operations Automation and Robotics (SOAR 1988) Nov. 1988 p 391-396 (For primary document see N89-19817 12-59)
Avail: NTIS HC A22/MF A01 CSCL 05H

N89-19871*# Wisconsin Univ., Madison. Coll. of Engineering.
THE WCSAR TELEROBOTICS TEST BED
N. Duffie, J. Zik, R. Teeter, and T. Crabb (Astronautics Corp. of America, Madison, WI.) *In* NASA. Lyndon B. Johnson Space Center, 2nd Annual Workshop on Space Operations Automation and Robotics (SOAR 1988) Nov. 1988 p 397-402 (For primary document see N89-19817 12-59)
(Grant NAGw-975)
Avail: NTIS HC A22/MF A01 CSCL 05H

N89-19872*# Aerospace Medical Research Labs., Wright-Patterson AFB, OH.
THE USE OF THE ARTICULATED TOTAL BODY MODEL AS A ROBOT DYNAMICS SIMULATION TOOL
Louise A. Obergfell, Xavier J. R. Avula, and Ints Kalegs *In* NASA. Lyndon B. Johnson Space Center, 2nd Annual Workshop on Space Operations Automation and Robotics (SOAR 1988) Nov. 1988 p 403-409 (For primary document see N89-19817 12-59)
Avail: NTIS HC A22/MF A01 CSCL 05H

N89-19873*# Martin Marietta Aero and Naval Systems, Baltimore, MD.
TELEPRESENCE AND TELEROBOTICS
John Garin, Joseph Matteo, and Von Ayre Jennings *In* NASA. Lyndon B. Johnson Space Center, 2nd Annual Workshop on Space Operations Automation and Robotics (SOAR 1988) Nov. 1988 p 411-420 (For primary document see N89-19817 12-59)
Avail: NTIS HC A22/MF A01 CSCL 05H

N89-19874*# Carnegie-Mellon Univ., Pittsburgh, PA. The Robotics Inst.
A NOVEL MANIPULATOR TECHNOLOGY FOR SPACE APPLICATIONS
Donald Schmitz, Pradeep Khosia, and Takeo Kanade *In* NASA. Lyndon B. Johnson Space Center, 2nd Annual Workshop on Space Operations Automation and Robotics (SOAR 1988) Nov. 1988 p 421-428 (For primary document see N89-19817 12-59)
Avail: NTIS HC A22/MF A01 CSCL 05H

N89-19875*# Carnegie-Mellon Univ., Pittsburgh, PA. Robotics Inst.
A ROBUST CONTROL SCHEME FOR FLEXIBLE ARMS WITH FRICTION IN THE JOINTS
Kuldip S. Rattan, Vicente Feliu (Universidad Nacional de Educacion a Distancia, Madrid, Spain), and H. Benjamin Brown, Jr. *In* NASA. Lyndon B. Johnson Space Center, 2nd Annual Workshop on Space Operations Automation and Robotics (SOAR 1988) Nov. 1988 p 429-435 (For primary document see N89-19817 12-59)
Avail: NTIS HC A22/MF A01 CSCL 05H

N89-19876*# Jet Propulsion Lab., California Inst. of Tech., Pasadena.
TELEROBOT OPERATOR CONTROL STATION REQUIREMENTS
Edwin P. Kan *In* NASA. Lyndon B. Johnson Space Center, 2nd Annual Workshop on Space Operations Automation and Robotics (SOAR 1988) Nov. 1988 p 437-443 (For primary document see N89-19817 12-59)
Avail: NTIS HC A22/MF A01 CSCL 05H

N89-19877*# Jet Propulsion Lab., California Inst. of Tech., Pasadena.
TIME-DELAYED OPERATION OF A TELEROBOT VIA GEOSYNCHRONOUS RELAY
Brian H. Wilcox *In* NASA. Lyndon B. Johnson Space Center, 2nd Annual Workshop on Space Operations Automation and Robotics (SOAR 1988) Nov. 1988 p 445-447 (For primary document see N89-19817 12-59)
Avail: NTIS HC A22/MF A01 CSCL 05H

N89-19878*# Texas Instruments, Inc., Dallas. Speech and Image Understanding Lab.
A REPRESENTATIONAL FRAMEWORK AND USER-INTERFACE FOR AN IMAGE UNDERSTANDING WORKSTATION
Joyce D. Schroeder *In* NASA. Lyndon B. Johnson Space Center, 2nd Annual Workshop on Space Operations Automation and Robotics (SOAR 1988) Nov. 1988 p 451-456 (For primary document see N89-19817 12-59)
Avail: NTIS HC A22/MF A01 CSCL 05H

N89-19879*# Jet Propulsion Lab., California Inst. of Tech., Pasadena.
MACHINE VISION FOR SPACE TELEROBOTICS AND PLANETARY ROVERS
Brian H. Wilcox *In* NASA. Lyndon B. Johnson Space Center, 2nd Annual Workshop on Space Operations Automation and Robotics (SOAR 1988) Nov. 1988 p 457-460 (For primary document see N89-19817 12-59)
Avail: NTIS HC A22/MF A01 CSCL 05H

N89-19880*# Texas Instruments, Inc., Dallas. Speech and Image Understanding Lab.
VOICE CONTROL OF COMPLEX WORKSTATIONS
Jeffrey L. Scruggs *In* NASA. Lyndon B. Johnson Space Center, 2nd Annual Workshop on Space Operations Automation and Robotics (SOAR 1988) Nov. 1988 p 461-466 (For primary document see N89-19817 12-59)
Avail: NTIS HC A22/MF A01 CSCL 05H

N89-19881*# National Aeronautics and Space Administration. Lyndon B. Johnson Space Center, Houston, TX.
A MULTI-SENSOR SYSTEM FOR ROBOTICS PROXIMITY OPERATIONS
J. B. Cheatham, C. K. Wu, P. L. Weiland (Rice Univ., Houston, TX.), and T. F. Cleghorn *In its* 2nd Annual Workshop on Space Operations Automation and Robotics (SOAR 1988) Nov. 1988 p 467-470 (For primary document see N89-19817 12-59)
(Contract NCC9-16; NAG9-208)
Avail: NTIS HC A22/MF A01 CSCL 05H

N89-19882*# Jet Propulsion Lab., California Inst. of Tech., Pasadena.
A METHODOLOGY FOR AUTOMATION AND ROBOTICS EVALUATION APPLIED TO THE SPACE STATION TELEROBOTIC SERVICER
Jeffrey H. Smith, Max Gyanfi, Kent Volkmer, and Wayne Zimmerman *In* NASA. Lyndon B. Johnson Space Center, 2nd Annual Workshop on Space Operations Automation and Robotics (SOAR 1988) Nov. 1988 p 471-479 (For primary document see N89-19817 12-59)
(Contract NAS7-918)
Avail: NTIS HC A22/MF A01 CSCL 05H

N89-19883*# Little (Arthur D.), Inc., Cambridge, MA. Center for Product Development.
SENSING HUMAN HAND MOTIONS FOR CONTROLLING DEXTEROUS ROBOTS
Beth A. Marcus, Philip J. Churchill, and Arthur D. Little *In* NASA. Lyndon B. Johnson Space Center, 2nd Annual Workshop on Space Operations Automation and Robotics (SOAR 1988) Nov. 1988 p 481-485 (For primary document see N89-19817 12-59)
Avail: NTIS HC A22/MF A01 CSCL 05H

N89-19884*# Westinghouse Electric Corp., Madison, PA. Robotics and Mechanical Design.
APPLICATION OF MODEL BASED CONTROL TO ROBOTIC MANIPULATORS
Lyman J. Petrosky and Irving J. Oppenheim (Carnegie-Mellon Univ., Pittsburgh, PA.) *In* NASA. Lyndon B. Johnson Space Center, 2nd Annual Workshop on Space Operations Automation and Robotics (SOAR 1988) Nov. 1988 p 487-493 (For primary document see N89-19817 12-59)
(Contract DE-AC02-85NE-37947)
Avail: NTIS HC A22/MF A01 CSCL 05H

N89-19885*# Rockwell International Corp., Downey, CA.
DESIGN GUIDELINES FOR REMOTELY MAINTAINABLE EQUIPMENT
Margaret M. Clarke and Davoud Manouchehri *In* NASA. Lyndon B. Johnson Space Center, 2nd Annual Workshop on Space Operations Automation and Robotics (SOAR 1988) Nov. 1988 p 495-497 (For primary document see N89-19817 12-59)
Avail: NTIS HC A22/MF A01 CSCL 05H

N89-19886*# Army Aviation Systems Command, Cleveland, OH.
AN EXPERT SYSTEM FOR RESTRUCTURABLE CONTROL
Jonathan Litt *In* NASA. Lyndon B. Johnson Space Center, 2nd Annual Workshop on Space Operations Automation and Robotics (SOAR 1988) Nov. 1988 p 503-507 (For primary document see N89-19817 12-59)
Avail: NTIS HC A22/MF A01 CSCL 05H

N89-19890*# Essex Corp., Alexandria, VA.
SARSCEST (HUMAN FACTORS)
H. McIlvaine Parsons *In* NASA. Lyndon B. Johnson Space Center, 2nd Annual Workshop on Space Operations Automation and Robotics (SOAR 1988) Nov. 1988 p 541-552 (For primary document see N89-19817 12-59)
Avail: NTIS HC A22/MF A01 CSCL 05H

N89-20059*# Texas Southern Univ., Houston. Dept. of Home Economics.
COMPARISON OF SOVIET AND US SPACE FOOD AND NUTRITION PROGRAMS Final Report
Selina Ahmed *In* NASA, Lyndon B. Johnson Space Center, National Aeronautics and Space Administration (NASA)/American Society for Engineering Education (ASEE) Summer Faculty Fellowship Program 1988, Volume 1 Feb. 1989 16 p (For primary document see N89-20058 12-99)
Avail: NTIS HC A09/MF A01 CSCL 06H

N89-20065*# Houston Univ., Clear Lake, TX. Div. of Life Sciences.
DEVELOPMENT OF AN ATMOSPHERIC MONITORING PLAN FOR SPACE STATION Final Report
Dennis M. Casserly *In* NASA, Lyndon B. Johnson Space Center, National Aeronautics and Space Administration (NASA)/American Society for Engineering Education (ASEE) Summer Faculty Fellowship Program 1988, Volume 1 Feb. 1989 16 p (For primary document see N89-20058 12-99)
Avail: NTIS HC A09/MF A01 CSCL 06K

N89-20071*# Montana State Univ., Bozeman. Dept. of Chemistry.
EVALUATION OF AVAILABLE ANALYTICAL TECHNIQUES FOR MONITORING THE QUALITY OF SPACE STATION POTABLE WATER Final Report
Richard D. Geer *In* NASA, Lyndon B. Johnson Space Center, National Aeronautics and Space Administration (NASA)/American Society for Engineering Education (ASEE) Summer Faculty Fellowship Program 1988, Volume 1 Feb. 1989 15 p (For primary document see N89-20058 12-99)
Avail: NTIS HC A09/MF A01 CSCL 06K

55 SPACE BIOLOGY

Includes exobiology; planetary biology; and extraterrestrial life.

No abstracts in this category.

59 MATHEMATICAL AND COMPUTER SCIENCES (GENERAL)

N89-19817*# National Aeronautics and Space Administration. Lyndon B. Johnson Space Center, Houston, TX.
SECOND ANNUAL WORKSHOP ON SPACE OPERATIONS AUTOMATION AND ROBOTICS (SOAR 1988)
Sandy Griffin, ed./comp. Washington, DC Nov. 1988 517 p Workshop held in Dayton, OH, 20-23 Jul. 1988; sponsored by NASA, Johnson Space Flight Center, USAF, Washington, DC, and Wright State Univ., Dayton, OH
(NASA-CP-3019; S-585; NAS 1.55:3019) Avail: NTIS HC A22/MF A01 CSCL 12A

Papers presented at the Second Annual Workshop on Space Operation Automation and Robotics (SOAR '88), hosted by Wright State University at Dayton, Ohio, on July 20, 21, 22, and 23, 1988, are documented herein. During the 4 days, approximately 100 technical papers were presented by experts from NASA, the USAF, universities, and technical companies. Panel discussions on Human Factors, Artificial Intelligence, Robotics, and Space Systems were held but are not documented herein. Technical topics addressed included knowledge-based systems, human factors, and robotics. For individual titles, see N89-19818 through N89-19891.

N89-19818*# National Aeronautics and Space Administration. Marshall Space Flight Center, Huntsville, AL.
THE SCHEDULING TECHNIQUES OF ESP2 **c81**
John P. Jaap and Elizabeth K. Davis *In* NASA. Lyndon B. Johnson Space Center, 2nd Annual Workshop on Space Operations Automation and Robotics (SOAR 1988) Nov. 1988 p 1-6 (For primary document see N89-19817 12-59)
Avail: NTIS HC A22/MF A01 CSCL 05A

The Mission Analysis Division of the Systems Analysis and Integration Laboratory at the Marshall Space Flight Center has developed a robust automatic scheduler which can produce detailed schedules for the multi-step activities required for payload operations on the Space Station. This scheduler, a part of the Expert Scheduling Program (ESP2), has five components: the bookkeeper, checker, loader, selector, and explainer. The bookkeeper maintains the usage profiles for nondepletable resources, consumables, equipment, crew, and the times of all the steps for the payload activities for several different schedules simultaneously. The checker searches the data maintained by the bookkeeper and finds times when the constraints of each step of an activity are satisfied. The loader is an expert system that uses the techniques of forward chaining, depth-first searching, and backtracking to manage the workings of the checker so that activities are placed in the schedule without violating constraints (such as crew, resources, and orbit opportunities). The checker searches the data maintained by the bookkeeper and finds times when the constraints of each step of an activity are satisfied. The loader is an expert system which uses the techniques of forward chaining, depth-first searching, and backtracking to manage the workings of the checker so that activities are placed in the schedule without violating the constraints. The selector has several methods of choosing the next activity for the loader to schedule. The explainer shows the user why an activity was or was not scheduled at a certain time; it offers a unique graphical explanation of how the expert system (the loader) works. Author

N89-19819*# National Aeronautics and Space Administration. Marshall Space Flight Center, Huntsville, AL.
SPACE STATION PAYLOAD OPERATIONS SCHEDULING WITH ESP2 **c18**
Kenneth L. Stacy and John P. Jaap *In* NASA. Lyndon B. Johnson Space Center, 2nd Annual Workshop on Space Operations Automation and Robotics (SOAR 1988) Nov. 1988 p 7-13 (For primary document see N89-19817 12-59)
Avail: NTIS HC A22/MF A01 CSCL 22B

The Mission Analysis Division of the Systems Analysis and Integration Laboratory at the Marshall Space Flight Center is developing a system of programs to handle all aspects of scheduling payload operations for Space Station. The Expert Scheduling Program (ESP2) is the heart of this system. The task of payload operations scheduling can be simply stated as positioning the payload activities in a mission so that they collect their desired data without interfering with other activities or violating mission constraints. ESP2 is an advanced version of the Experiment Scheduling Program (ESP) which was developed by the Mission Integration Branch beginning in 1979 to schedule Spacelab payload activities. The automatic scheduler in ESP2 is an expert system that embodies the rules that expert planners would use to schedule payload operations by hand. This scheduler uses depth-first searching, backtracking, and forward chaining techniques to place an activity so that constraints (such as crew, resources, and orbit opportunities) are not violated. It has an explanation facility to show why an activity was or was not scheduled at a certain time. The ESP2 user can also place the activities in the schedule manually. The program offers graphical assistance to the user and will advise when constraints are being violated. ESP2 also has an option to identify conflict introduced into an existing schedule by changes to payload requirements, mission constraints, and orbit opportunities. Author

N89-19820*# National Aeronautics and Space Administration. Ames Research Center, Moffett Field, CA.
A SURVEY OF PLANNING AND SCHEDULING RESEARCH AT THE NASA AMES RESEARCH CENTER **c81**
Monte Zweben *In* NASA. Lyndon B. Johnson Space Center, 2nd Annual Workshop on Space Operations Automation and Robotics (SOAR 1988) Nov. 1988 p 15-20 (For primary document see N89-19817 12-59)
Avail: NTIS HC A22/MF A01 CSCL 05A

NASA Ames Research Center has a diverse program in planning and scheduling. This paper highlights some of our research projects as well as some of our applications. Topics addressed include machine learning techniques, action representations and constraint-based scheduling systems. The applications discussed

are planetary rovers, Hubble Space Telescope scheduling, and Pioneer Venus orbit scheduling. Author

N89-19821*# National Aeronautics and Space Administration. Lyndon B. Johnson Space Center, Houston, TX.
AN EXPERT SYSTEM FOR SHUTTLE AND SATELLITE RADAR TRACKER SCHEDULING c81
Paul Mitchell *In its* 2nd Annual Workshop on Space Operations Automation and Robotics (SOAR 1988) Nov. 1988 p 21-23 (For primary document see N89-19817 12-59)
Avail: NTIS HC A22/MF A01 CSCL 05A

This expert system automates and optimizes radar tracker selection for shuttle missions. The expert system is written in the FORTRAN and C languages on an HP9000. It is portable to any UNIX machine having both ANSI-77 FORTRAN and C language compilers. It is a rule based expert system that selects tracking stations from the S-band and C-band radar stations and the TDRSS east and TDRSS west satellites under a variety of conditions. The expert system was prototyped on the Symbolics in the Automated Reasoning Tool (ART) and ZetaLisp. After the prototype demonstrated an acceptable automation of the process of selecting tracking stations to support the orbit determination requirements of Shuttle missions, the basic ART rules of the prototype were ported to the HP9000 computer using the CLIPS language. CLIPS is a forward-chaining rule-based expert system language written in C. Prior to the development of this expert system the selection process was a tedious manual process and expensive in terms of human resources. Manual tracking station selection required from 1 to 2 man weeks per mission; whereas the expert system can complete the selection process in about 2 hours. Author

N89-19822*# National Aeronautics and Space Administration. Marshall Space Flight Center, Huntsville, AL.
AUTOMATION OF THE SPACE STATION CORE MODULE POWER MANAGEMENT AND DISTRIBUTION SYSTEM c18
David J. Weeks *In* NASA. Lyndon B. Johnson Space Center, 2nd Annual Workshop on Space Operations Automation and Robotics (SOAR 1988) Nov. 1988 p 25-29 (For primary document see N89-19817 12-59)
Avail: NTIS HC A22/MF A01 CSCL 22B

Under the Advanced Development Program for Space Station, Marshall Space Flight Center has been developing advanced automation applications for the Power Management and Distribution (PMAD) system inside the Space Station modules for the past three years. The Space Station Module Power Management and Distribution System (SSM/PMAD) test bed features three artificial intelligence (AI) systems coupled with conventional automation software functioning in an autonomous or closed-loop fashion. The AI systems in the test bed include a baseline scheduler/dynamic rescheduler (LES), a load shedding management system (LPLMS), and a fault recovery and management expert system (FRAMES). This test bed will be part of the NASA Systems Autonomy Demonstration for 1990 featuring cooperating expert systems in various Space Station subsystem test beds. It is concluded that advanced automation technology involving AI approaches is sufficiently mature to begin applying the technology to current and planned spacecraft applications including the Space Station. Author

N89-19823*# Air Force Armament Lab., Eglin AFB, FL.
EMMA: THE EXPERT SYSTEM FOR MUNITION MAINTENANCE c81
Barry E. Mullins *In* NASA. Lyndon B. Johnson Space Center, 2nd Annual Workshop on Space Operations Automation and Robotics (SOAR 1988) Nov. 1988 p 31-39 (For primary document see N89-19817 12-59)
Avail: NTIS HC A22/MF A01 CSCL 05A

Expert Missile Maintenance Aid (EMMA) is a first attempt to enhance maintenance of the tactical munition at the field and depot level by using artificial intelligence (AI) techniques. The ultimate goal of EMMA is to help a novice maintenance technician isolate and diagnose electronic, electromechanical, and mechanical equipment faults to the board/chassis level more quickly and consistently than the best human expert using the best currently available automatic test equipment (ATE). To this end, EMMA augments existing ATE with an expert system that captures the knowledge of design and maintenance experts. The EMMA program is described, including the evaluation of field-level expert system prototypes, the description of several study tasks performed during EMMA, and future plans for a follow-on program. This paper will briefly address several study tasks performed during EMMA. The paper concludes with a discussion of future plans for a follow-on program and other areas of concern. Author

N89-19824*# Battelle Columbus Labs., OH.
DIAGNOSTICS IN THE EXTENDABLE INTEGRATED SUPPORT ENVIRONMENT (EISE) c62
James R. Brink and Paul Storey (Sacramento Air Logistics Center, McClellan AFB, CA.) *In* NASA. Lyndon B. Johnson Space Center, 2nd Annual Workshop on Space Operations Automation and Robotics (SOAR 1988) Nov. 1988 p 41-46 (For primary document see N89-19817 12-59)
Avail: NTIS HC A22/MF A01 CSCL 09B

Extendable Integrated Support Environment (EISE) is a real-time computer network consisting of commercially available hardware and software components to support systems level integration, modifications, and enhancement to weapons systems. The EISE approach offers substantial potential savings by eliminating unique support environments in favor of sharing common modules for the support of operational weapon systems. An expert system is being developed that will help support diagnosing faults in this network. This is a multi-level, multi-expert diagnostic system that uses experiential knowledge relating symptoms to faults and also reasons from structural and functional models of the underlying physical model when experiential reasoning is inadequate. The individual expert systems are orchestrated by a supervisory reasoning controller, a meta-level reasoner which plans the sequence of reasoning steps to solve the given specific problem. The overall system, termed the Diagnostic Executive, accesses systems level performance checks and error reports, and issues remote test procedures to formulate and confirm fault hypotheses. Author

N89-19825*# National Aeronautics and Space Administration. Marshall Space Flight Center, Huntsville, AL.
AUTOMATIC DETECTION OF ELECTRIC POWER TROUBLES (ADEPT) c33
Caroline Wang, Hugh Zeanah, Audie Anderson, Clint Patrick, Mike Brady, and Donnie Ford (Alabama A & M Univ., Huntsville.) *In* NASA. Lyndon B. Johnson Space Center, 2nd Annual Workshop on Space Operations Automation and Robotics (SOAR 1988) Nov. 1988 p 47-50 (For primary document see N89-19817 12-59)
Avail: NTIS HC A22/MF A01 CSCL 09C

Automatic Detection of Electric Power Troubles (A DEPT) is an expert system that integrates knowledge from three different suppliers to offer an advanced fault-detection system. It is designed for two modes of operation: real time fault isolation and simulated modeling. Real time fault isolation of components is accomplished on a power system breadboard through the Fault Isolation Expert System (FIES II) interface with a rule system developed in-house. Faults are quickly detected and displayed and the rules and chain of reasoning optionally provided on a laser printer. This system consists of a simulated space station power module using direct-current power supplies for solar arrays on three power buses. For tests of the system's ability to locate faults inserted via switches, loads are configured by an INTEL microcomputer and the Symbolics artificial intelligence development system. As these loads are resistive in nature, Ohm's Law is used as the basis for rules by which faults are located. The three-bus system can correct faults automatically where there is a surplus of power available on any of the three buses. Techniques developed and used can be applied readily to other control systems requiring rapid intelligent decisions. Simulated modeling, used for theoretical studies, is implemented using a modified version of Kennedy Space Center's KATE (Knowledge-Based Automatic Test Equipment), FIES II windowing, and an ADEPT knowledge base. Author

N89-19826*# Massachusetts Inst. of Tech., Lexington.
KNOWLEDGE-BASED OPERATION AND MANAGEMENT OF COMMUNICATIONS SYSTEMS **c32**
Harold M. Heggestad *In* NASA. Lyndon B. Johnson Space Center, 2nd Annual Workshop on Space Operations Automation and Robotics (SOAR 1988) Nov. 1988 p 53-57 Sponsored in part by the Defense Communications Agengy and the Dept. of Air Force (For primary document see N89-19817 12-59)
Avail: NTIS HC A22/MF A01 CSCL 17B

Expert systems techniques are being applied in operation and control of the Defense Communications System (DCS), which has the mission of providing reliable worldwide voice, data and message services for U.S. forces and commands. Thousands of personnel operate DCS facilities, and many of their functions match the classical expert system scenario: complex, skill-intensive environments with a full spectrum of problems in training and retention, cost containment, modernization, and so on. Two of these functions are: (1) fault isolation and restoral of dedicated circuits at Tech Control Centers, and (2) network management for the Defense Switched Network (the modernized dial-up voice system currently replacing AUTOVON). An expert system for the first of these is deployed for evaluation purposes at Andrews Air Force Base, and plans are being made for procurement of operational systems. In the second area, knowledge obtained with a sophisticated simulator is being embedded in an expert system. The background, design and status of both projects are described. Author

N89-19827*# Southwest Research Inst., San Antonio, TX.
NESSUS (NUMERICAL EVALUATION OF STOCHASTIC STRUCTURES UNDER STRESS)/EXPERT: BRIDGING THE GAP BETWEEN ARTIFICIAL INTELLIGENCE AND FORTRAN **c63**
Pamela K. Fink and Karol K. Palmer *In* NASA. Lyndon B. Johnson Space Center, 2nd Annual Workshop on Space Operations Automation and Robotics (SOAR 1988) Nov. 1988 p 59-67 (For primary document see N89-19817 12-59)
Avail: NTIS HC A22/MF A01 CSCL 09B

The development of a probabilistic structural analysis methodology (PSAM) is described. In the near-term, the methodology will be applied to designing critical components of the next generation space shuttle main engine. In the long-term, PSAM will be applied very broadly, providing designers with a new technology for more effective design of structures whose character and performance are significantly affected by random variables. The software under development to implement the ideas developed in PSAM resembles, in many ways, conventional deterministic structural analysis code. However, several additional capabilities regarding the probabilistic analysis makes the input data requirements and the resulting output even more complex. As a result, an intelligent front- and back-end to the code is being developed to assist the design engineer in providing the input data in a correct and appropriate manner. The type of knowledge that this entails is, in general, heuristically-based, allowing the fairly well-understood technology of production rules to apply with little difficulty. However, the PSAM code, called NESSUS, is written in FORTRAN-77 and runs on a DEC VAX. Thus, the associated expert system, called NESSUS/EXPERT, must run on a DEC VAX as well, and integrate effectively and efficiently with the existing FORTRAN code. This paper discusses the process undergone to select a suitable tool, identify an appropriate division between the functions that should be performed in FORTRAN and those that should be performed by production rules, and how integration of the conventional and AI technologies was achieved. Author

N89-19828*# National Aeronautics and Space Administration. Ames Research Center, Moffett Field, CA.
KNOWLEDGE-BASED ZONAL GRID GENERATION FOR COMPUTATIONAL FLUID DYNAMICS **c34**
Alison E. Andrews *In* NASA. Lyndon B. Johnson Space Center, 2nd Annual Workshop on Space Operations Automation and Robotics (SOAR 1988) Nov. 1988 p 73-80 (For primary document see N89-19817 12-59)
Avail: NTIS HC A22/MF A01 CSCL 20D

Automation of flow field zoning in two dimensions is an important step towards reducing the difficulty of three-dimensional grid generation in computational fluid dynamics. Using a knowledge-based approach makes sense, but problems arise which are caused by aspects of zoning involving perception, lack of expert consensus, and design processes. These obstacles are overcome by means of a simple shape and configuration language, a tunable zoning archetype, and a method of assembling plans from selected, predefined subplans. A demonstration system for knowledge-based two-dimensional flow field zoning has been successfully implemented and tested on representative aerodynamic configurations. The results show that this approach can produce flow field zonings that are acceptable to experts with differing evaluation criteria. Author

N89-19829*# National Aeronautics and Space Administration. John F. Kennedy Space Center, Cocoa Beach, FL.
CIRCA 2000 OPERATIONS CRITERIA **c16**
Arthur L. Scholz (Boeing Aerospace Co., Kennedy Space Center, FL.) and William J. Dickinson *In* NASA. Lyndon B. Johnson Space Center, 2nd Annual Workshop on Space Operations Automation and Robotics (SOAR 1988) Nov. 1988 p 81-85 (For primary document see N89-19817 12-59)
Avail: NTIS HC A22/MF A01 CSCL 22B

The current Shuttle Program was used as a working model and certified data source in the identification of Space Transportation System (STS) operational cost drivers. Changes to flight hardware, processing methodologies, and identification of automation applications that would reduce costs were derived by reference to that data. The CIRCA 2000 Criteria were developed using these critical analyses of the on-going Shuttle Program. Several innovative suggestions are reviewed. Author

N89-19830*# General Dynamics Corp., San Diego, CA.
ARTIFICIAL INTELLIGENT DECISION SUPPORT FOR LOW-COST LAUNCH VEHICLE INTEGRATED MISSION OPERATIONS **c15**
Gerard P. Szatkowski and Roger Schultz (Abacus Programming Corp., Van Nuys, CA.) *In* NASA. Lyndon B. Johnson Space Center, 2nd Annual Workshop on Space Operations Automation and Robotics (SOAR 1988) Nov. 1988 p 87-94 Sponsored in part by AF (For primary document see N89-19817 12-59)
Avail: NTIS HC A22/MF A01 CSCL 22B

The feasibility, benefits, and risks associated with Artificial Intelligence (AI) Expert Systems applied to low cost space expendable launch vehicle systems are reviewed. This study is in support of the joint USAF/NASA effort to define the next generation of a heavy-lift Advanced Launch System (ALS) which will provide economical and routine access to space. The significant technical goals of the ALS program include: a 10 fold reduction in cost per pound to orbit, launch processing in under 3 weeks, and higher reliability and safety standards than current expendables. Knowledge-based system techniques are being explored for the purpose of automating decision support processes in onboard and ground systems for pre-launch checkout and in-flight operations. Issues such as: satisfying real-time requirements, providing safety validation, hardware and Data Base Management System (DBMS) interfacing, system synergistic effects, human interfaces, and ease of maintainability, have an effect on the viability of expert systems as a useful tool. Author

N89-19831*# McDonnell-Douglas Corp., Houston, TX.
A DESIGN AND IMPLEMENTATION METHODOLOGY FOR DIAGNOSTIC SYSTEMS **c16**
Linda J. F. Williams *In* NASA. Lyndon B. Johnson Space Center, 2nd Annual Workshop on Space Operations Automation and Robotics (SOAR 1988) Nov. 1988 p 95-103 (For primary document see N89-19817 12-59)
Avail: NTIS HC A22/MF A01 CSCL 22B

A methodology for design and implementation of diagnostic systems is presented. Also discussed are the advantages of

embedding a diagnostic system in a host system environment. The methodology utilizes an architecture for diagnostic system development that is hierarchical and makes use of object-oriented representation techniques. Additionally, qualitative models are used to describe the host system components and their behavior. The methodology architecture includes a diagnostic engine that utilizes a combination of heuristic knowledge to control the sequence of diagnostic reasoning. The methodology provides an integrated approach to development of diagnostic system requirements that is more rigorous than standard systems engineering techniques. The advantages of using this methodology during various life cycle phases of the host systems (e.g., National Aerospace Plane (NASP)) include: the capability to analyze diagnostic instrumentation requirements during the host system design phase, a ready software architecture for implementation of diagnostics in the host system, and the opportunity to analyze instrumentation for failure coverage in safety critical host system operations. Author

N89-19832*# National Aeronautics and Space Administration. Hugh L. Dryden Flight Research Facility, Edwards, CA.

APPLICATION OF FLIGHT SYSTEMS METHODOLOGIES TO THE VALIDATION OF KNOWLEDGE-BASED SYSTEMS c03

Eugene L. Duke *In* NASA. Lyndon B. Johnson Space Center, 2nd Annual Workshop on Space Operations Automation and Robotics (SOAR 1988) Nov. 1988 p 107-121 Previously announced as N88-25207 (For primary document see N89-19817 12-59)

Avail: NTIS HC A22/MF A01 CSCL 01C

Flight and mission-critical systems are verified, qualified for flight, and validated using well-known and well-established techniques. These techniques define the validation methodology used for such systems. In order to verify, qualify, and validate knowledge-based systems (KBS's), the methodology used for conventional systems must be addressed, and the applicability and limitations of that methodology to KBS's must be identified. An outline of how this approach to the validation of KBS's is being developed and used is presented. Author

N89-19833*# National Aeronautics and Space Administration. Langley Research Center, Hampton, VA.

VALIDATION OF HIGHLY RELIABLE, REAL-TIME KNOWLEDGE-BASED SYSTEMS c61

Sally C. Johnson *In* NASA. Lyndon B. Johnson Space Center, 2nd Annual Workshop on Space Operations Automation and Robotics (SOAR 1988) Nov. 1988 p 123-129 (For primary document see N89-19817 12-59)

Avail: NTIS HC A22/MF A01 CSCL 09B

Knowledge-based systems have the potential to greatly increase the capabilities of future aircraft and spacecraft and to significantly reduce support manpower needed for the space station and other space missions. However, a credible validation methodology must be developed before knowledge-based systems can be used for life- or mission-critical applications. Experience with conventional software has shown that the use of good software engineering techniques and static analysis tools can greatly reduce the time needed for testing and simulation of a system. Since exhaustive testing is infeasible, reliability must be built into the software during the design and implementation phases. Unfortunately, many of the software engineering techniques and tools used for conventional software are of little use in the development of knowledge-based systems. Therefore, research at Langley is focused on developing a set of guidelines, methods, and prototype validation tools for building highly reliable, knowledge-based systems. The use of a comprehensive methodology for building highly reliable, knowledge-based systems should significantly decrease the time needed for testing and simulation. A proven record of delivering reliable systems at the beginning of the highly visible testing and simulation phases is crucial to the acceptance of knowledge-based systems in critical applications. Author

N89-19834*# Lockheed Missiles and Space Co., Austin, TX. Artificial Intelligence Center.

TESTING EXPERT SYSTEMS c61

C. L. Chang and R. A. Stachowitz *In* NASA. Lyndon B. Johnson Space Center, 2nd Annual Workshop on Space Operations Automation and Robotics (SOAR 1988) Nov. 1988 p 131-135 (For primary document see N89-19817 12-59)

Avail: NTIS HC A22/MF A01 CSCL 09B

Software quality is of primary concern in all large-scale expert system development efforts. Building appropriate validation and test tools for ensuring software reliability of expert systems is therefore required. The Expert Systems Validation Associate (EVA) is a validation system under development at the Lockheed Artificial Intelligence Center. EVA provides a wide range of validation and test tools to check correctness, consistency, and completeness of an expert system. Testing a major function of EVA. It means executing an expert system with test cases with the intent of finding errors. In this paper, we describe many different types of testing such as function-based testing, structure-based testing, and data-based testing. We describe how appropriate test cases may be selected in order to perform good and thorough testing of an expert system. Author

N89-19835*# Ohio State Univ., Columbus. Lab. for Artificial Intelligence Research.

DIAGNOSIS BY INTEGRATING MODEL-BASED REASONING WITH KNOWLEDGE-BASED REASONING c63

Tom Bylander *In* NASA. Lyndon B. Johnson Space Center, 2nd Annual Workshop on Space Operations Automation and Robotics (SOAR 1988) Nov. 1988 p 137-140 Sponsored in part by the National Inst. on Disability and Rehabilitation Research. (For primary document see N89-19817 12-59)

Avail: NTIS HC A22/MF A01 CSCL 09B

Our research investigates how observations can be categorized by integrating a qualitative physical model with experiential knowledge. Our domain is diagnosis of pathologic gait in humans, in which the observations are the gait motions, muscle activity during gait, and physical exam data, and the diagnostic hypotheses are the potential muscle weaknesses, muscle mistimings, and joint restrictions. Patients with underlying neurological disorders typically have several malfunctions. Among the problems that need to be faced are: the ambiguity of the observations, the ambiguity of the qualitative physical model, correspondence of the observations and hypotheses to the qualitative physical model, the inherent uncertainty of experiential knowledge, and the combinatorics involved in forming composite hypotheses. Our system divides the work so that the knowledge-based reasoning suggests which hypotheses appear more likely than others, the qualitative physical model is used to determine which hypotheses explain which observations, and another process combines these functionalities to construct a composite hypothesis based on explanatory power and plausibility. We speculate that the reasoning architecture of our system is generally applicable to complex domains in which a less-than-perfect physical model and less-than-perfect experiential knowledge need to be combined to perform diagnosis. Author

N89-19836*# Wright State Univ., Dayton, OH. Dept. of Computer Science.

TRANSFORMATION BASED ENDORSEMENT SYSTEMS c63

Thomas Sudkamp *In* NASA. Lyndon B. Johnson Space Center, 2nd Annual Workshop on Space Operations Automation and Robotics (SOAR 1988) Nov. 1988 p 143-147 (For primary document see N89-19817 12-59)

(MIPR-FY1175-87-04878/01)

Avail: NTIS HC A22/MF A01 CSCL 09B

Evidential reasoning techniques classically represent support for a hypothesis by a numeric value or an evidential interval. The combination of support is performed by an arithmetic rule which often requires restrictions to be placed on the set of possibilities. These assumptions usually require the hypotheses to be exhaustive and mutually exclusive. Endorsement based classification systems represent support for the alternatives symbolically rather than numerically. A framework for constructing endorsement systems

is presented in which transformations are defined to generate and update the knowledge base. The interaction of the knowledge base and transformations produces a non-monotonic reasoning system. Two endorsement based reasoning systems are presented to demonstrate the flexibility of the transformational approach for reasoning with ambiguous and inconsistent information. Author

N89-19837*# Ohio State Univ., Columbus.
REDUCING UNCERTAINTY BY USING EXPLANATORY RELATIONSHIPS **c61**
John R. Josephson *In* NASA. Lyndon B. Johnson Space Center, 2nd Annual Workshop on Space Operations Automation and Robotics (SOAR 1988) Nov. 1988 p 149-151 (For primary document see N89-19817 12-59)
Avail: NTIS HC A22/MF A01 CSCL 09B

Explanatory relationships can be used effectively to reduce the uncertainty that remains after diagnostic hypotheses have been scored using local matching. Author

N89-19838*# National Aeronautics and Space Administration. Ames Research Center, Moffett Field, CA.
SPACEBORNE VHSIC MULTIPROCESSOR SYSTEM FOR AI APPLICATIONS **c60**
Henry Lum, Jr., Howard E. Shrobe, and John G. Aspinall (Symbolics, Inc., Cambridge, MA.) *In* NASA. Lyndon B. Johnson Space Center, 2nd Annual Workshop on Space Operations Automation and Robotics (SOAR 1988) Nov. 1988 p 153-160 (For primary document see N89-19817 12-59)
Avail: NTIS HC A22/MF A01 CSCL 09B

A multiprocessor system, under design for space-station applications, makes use of the latest generation symbolic processor and packaging technology. The result will be a compact, space-qualified system two to three orders of magnitude more powerful than present-day symbolic processing systems. Author

N89-19839*# Rome Air Development Center, Griffiss AFB, NY.
AUTONOMOUS SATELLITE COMMAND AND CONTROL: A COMPARISON WITH OTHER MILITARY SYSTEMS **c18**
Robert J. Kruchten and Wayne Todd *In* NASA. Lyndon B. Johnson Space Center, 2nd Annual Workshop on Space Operations Automation and Robotics (SOAR 1988) Nov. 1988 p 161-166 (For primary document see N89-19817 12-59)
Avail: NTIS HC A22/MF A01 CSCL 22B

Existing satellite concepts of operation depend on readily available experts and are extremely manpower intensive. Areas of expertise required include mission planning, mission data interpretation, telemetry monitoring, and anomaly resolution. The concepts of operation have envolved to their current state in part because space systems have tended to be treated more as research and development assets rather than as operational assets. These methods of satellite command and control will be inadequate in the future because of the availability, survivability, and capability of human experts. Because space systems have extremely high reliability and limited access, they offer challenges not found in other military systems. Thus, automation techniques used elsewhere are not necessarily applicable to space systems. A program to make satellites much more autonomous has been developed, using a variety of advanced software techniques. The problem the program is addressing, some possible solutions, the goals of the Rome Air Development Center (RADC) program, the rationale as to why the goals are reasonable, and the current program status are discussed. Also presented are some of the concepts used in the program and how they differ from more traditional approaches. Author

N89-19840*# Integrated Inference Machines, Inc., Anaheim, CA.
GARBAGE COLLECTION CAN BE MADE REAL-TIME AND VERIFIABLE **c63**
James H. Hino and Charles L. Ross *In* NASA. Lyndon B. Johnson Space Center, 2nd Annual Workshop on Space Operations Automation and Robotics (SOAR 1988) Nov. 1988 p 167-170 (For primary document see N89-19817 12-59)
Avail: NTIS HC A22/MF A01 CSCL 09B

An efficient means of memory reclamation (also known as Garbage Collection) is essential for Machine Intelligence applications where dynamic storage allocation is desired or required. Solutions for real-time systems must introduce very small processing overhead and must also provide for the verification of the software in order to meet the application time budgets and to verify the correctness of the software. Garbage Collection (GC) techniques are proposed for symbolic processing systems which may simultaneously meet both real-time requirements and verification requirements. The proposed memory reclamation technique takes advantage of the strong points of both the earlier Mark and Sweep technique and the more recent Copy Collection approaches. At least one practical implementation of these new GC techniques has already been developed and tested on a very-high performance symbolic computing system. Complete GC processing of all generated garbage has been demonstrated to require as little as a few milliseconds to perform. This speed enables the effective operation of the GC function as either a background task or as an actual part of the application task itself. Author

N89-19841*# Mitre Corp., McLean, VA. Artificial Intelligence Technical Center.
AN ARCHITECTURE FOR INTEGRATING DISTRIBUTED AND COOPERATING KNOWLEDGE-BASED AIR FORCE DECISION AIDS **c60**
Richard O. Nugent and Richard W. Tucker *In* NASA. Lyndon B. Johnson Space Center, 2nd Annual Workshop on Space Operations Automation and Robotics (SOAR 1988) Nov. 1988 p 171-175 (For primary document see N89-19817 12-59)
(Contract F19628-86-C-0001)
Avail: NTIS HC A22/MF A01 CSCL 09B

MITRE has been developing a Knowledge-Based Battle Management Testbed for evaluating the viability of integrating independently-developed knowledge-based decision aids in the Air Force tactical domain. The primary goal for the testbed architecture is to permit a new system to be added to a testbed with little change to the system's software. Each system that connects to the testbed network declares that it can provide a number of services to other systems. When a system wants to use another system's service, it does not address the server system by name, but instead transmits a request to the testbed network asking for a particular service to be performed. A key component of the testbed architecture is a common database which uses a relational database management system (RDBMS). The RDBMS provides a database update notification service to requesting systems. Normally, each system is expected to monitor data relations of interest to it. Alternatively, a system may broadcast an announcement message to inform other systems that an event of potential interest has occurred. Current research is aimed at dealing with issues resulting from integration efforts, such as dealing with potential mismatches of each system's assumptions about the common database, decentralizing network control, and coordinating multiple agents. Author

N89-19842*# Air Force Wright Aeronautical Labs., Wright-Patterson AFB, OH. Avionics Lab.
A PARALLEL EXPERT SYSTEM FOR THE CONTROL OF A ROBOTIC AIR VEHICLE **c63**
Donald Shakley and Gary B. Lamont (Air Force Inst. of Tech., Wright-Patterson AFB, OH.) *In* NASA. Lyndon B. Johnson Space Center, 2nd Annual Workshop on Space Operations Automation and Robotics (SOAR 1988) Nov. 1988 p 179-186 (For primary document see N89-19817 12-59)
Avail: NTIS HC A22/MF A01 CSCL 09B

Expert systems can be used to govern the intelligent control of vehicles, for example the Robotic Air Vehicle (RAV). Due to the nature of the RAV system the associated expert system needs to perform in a demanding real-time environment. The use of a parallel processing capability to support the associated expert system's computational requirement is critical in this application.

Thus, algorithms for parallel real-time expert systems must be designed, analyzed, and synthesized. The design process incorporates a consideration of the rule-set/face-set size along with representation issues. These issues are looked at in reference to information movement and various inference mechanisms. Also examined is the process involved with transporting the RAV expert system functions from the TI Explorer, where they are implemented in the Automated Reasoning Tool (ART), to the iPSC Hypercube, where the system is synthesized using Concurrent Common LISP (CCLISP). The transformation process for the ART to CCLISP conversion is described. The performance characteristics of the parallel implementation of these expert systems on the iPSC Hypercube are compared to the TI Explorer implementation. Author

N89-19843*# Aerospace Corp., El Segundo, CA.
PORTABLE INFERENCE ENGINE: AN EXTENDED CLIPS FOR REAL-TIME PRODUCTION SYSTEMS c61
Thach Le and Peter Homeier *In* NASA. Lyndon B. Johnson Space Center, 2nd Annual Workshop on Space Operations Automation and Robotics (SOAR 1988) Nov. 1988 p 187-192 (For primary document see N89-19817 12-59)
Avail: NTIS HC A22/MF A01 CSCL 09B

The present C-Language Integrated Production System (CLIPS) architecture has not been optimized to deal with the constraints of real-time production systems. Matching in CLIPS is based on the Rete Net algorithm, whose assumption of working memory stability might fail to be satisfied in a system subject to real-time dataflow. Further, the CLIPS forward-chaining control mechanism with a predefined conflict resultion strategy may not effectively focus the system's attention on situation-dependent current priorties, or appropriately address different kinds of knowledge which might appear in a given application. Portable Inference Engine (PIE) is a production system architecture based on CLIPS which attempts to create a more general tool while addressing the problems of real-time expert systems. Features of the PIE design include a modular knowledge base, a modified Rete Net algorithm, a bi-directional control strategy, and multiple user-defined conflict resolution strategies. Problems associated with real-time applications are analyzed and an explanation is given for how the PIE architecture addresses these problems. Author

N89-19844*# Intellicorp, Mountain View, CA.
BROWSING SCHEMATICS: QUERY-FILTERED GRAPHS WITH CONTEXT NODES c61
Eugene C. Ciccarelli and Bonnie A. Nardi *In* NASA. Lyndon B. Johnson Space Center, 2nd Annual Workshop on Space Operations Automation and Robotics (SOAR 1988) Nov. 1988 p 193-204 (For primary document see N89-19817 12-59)
Avail: NTIS HC A22/MF A01 CSCL 09B

The early results of a research project to create tools for building interfaces to intelligent systems on the NASA Space Station are reported. One such tool is the Schematic Browser which helps users engaged in engineering problem solving find and select schematics from among a large set. Users query for schematics with certain components, and the Schematic Browser presents a graph whose nodes represent the schematics with those components. The query greatly reduces the number of choices presented to the user, filtering the graph to a manageable size. Users can reformulate and refine the query serially until they locate the schematics of interest. To help users maintain orientation as they navigate a large body of data, the graph also includes nodes that are not matches but provide global and local context for the matching nodes. Context nodes include landmarks, ancestors, siblings, children and previous matches. Author

N89-19845*# California Univ., Marina del Rey. Information Sciences Inst.
PRESENTATION PLANNING USING AN INTEGRATED KNOWLEDGE BASE c82
Yigal Arens, Lawrence Miller, and Norman Sondheimer *In* NASA. Lyndon B. Johnson Space Center, 2nd Annual Workshop on Space Operations Automation and Robotics (SOAR 1988) Nov. 1988 p 205-218 (For primary document see N89-19817 12-59)
(Contract N00014-87-K-0130)
Avail: NTIS HC A22/MF A01 CSCL 05B

A description is given of user interface research aimed at bringing together multiple unput and output modes in a way that handles mixed mode input (commands, menus, forms, natural language), interacts with a diverse collection of underlying software utilities in a uniform way, and presents the results through a combination of output modes including natural language text, maps, charts and graphs. The system, Integrated Interfaces, derives much of its ability to interact uniformly with the user and the underlying services and to build its presentations, from the information present in a central knowledge base. This knowledge base integrates models of the application domain (Navy ships in the Pacific region, in the current demonstration version); the structure of visual displays and their graphical features; the underlying services (data bases and expert systems); and interface functions. The emphasis is on a presentation planner that uses the knowledge base to produce multi-modal output. There has been a flurry of recent work in user interface management systems.(Several recent examples are listed in the references). Existing work is characterized by an attempt to relieve the software designer of the burden of handcrafting an interface for each application. The work has generally focused on intelligently handling input. This paper deals with the other end of the pipeline - presentations. Author

N89-19846*# National Aeronautics and Space Administration. Langley Research Center, Hampton, VA.
PHYSIOLOGICAL ASSESSMENT OF TASK UNDERLOAD c54
J. Raymond Comstock, Jr., Randall L. Harris, Sr., and Alan T. Pope *In* NASA. Lyndon B. Johnson Space Center, 2nd Annual Workshop on Space Operations Automation and Robotics (SOAR 1988) Nov. 1988 p 221-226 (For primary document see N89-19817 12-59)
Avail: NTIS HC A22/MF A01 CSCL 05H

The ultimate goal of research efforts directed at underload, boredom, or complacency in high-technology work environments is to detect conditions or states of the operator that can be demonstrated to lead to performance degradation, and then to intervene in the environment to restore acceptable system performance. Physiological measures may provide indices of changes in condition or state of the operator that may be of value in high-technology work environments. The focus of the present study was on the use of physiological measures in the assessment of operator condition or state in a task underload scenario. A fault acknowledgement task characterized by simple repetitive responses with minimal novelty, complexity, and uncertainty was employed to place subjects in a task underload situation. Physiological measures (electrocardiogram (ECG), electroencephalogram (EEG), and pupil diameter) were monitored during task performance over a one-hour test session for 12 subjects. Each of the physiological measures exhibited changes over the test session indicative of decrements in subject arousal level. While high correlations between physiological measures were found across subjects, individual differences between subjects support the use of profiling techniques to establish baselines unique to each subject. Author

N89-19847*# Aerospace Medical Research Labs., Wright-Patterson AFB, OH. Human Engineering Lab.
A SCHEMA-BASED MODEL OF SITUATION AWARENESS: IMPLICATIONS FOR MEASURING SITUATION AWARENESS c54
Martin L. Fracker *In* NASA. Lyndon B. Johnson Space Center, 2nd Annual Workshop on Space Operations Automation and Robotics (SOAR 1988) Nov. 1988 p 227-231 (For primary document see N89-19817 12-59)
Avail: NTIS HC A22/MF A01 CSCL 05H

Measures of pilot situation awareness (SA) are needed in order to know whether new concepts in display design help pilots keep track of rapidly changing tactical situations. In order to measure SA, a theory of situation assessment is needed. Such a theory is summarized, encompassing both a definition of SA and

a model of situation assessment. SA is defined as the pilot's knowledge about a zone of interest at a given level of abstraction. Pilots develop this knowledge by sampling data from the environment and matching the sampled data to knowledge structures stored in long-term memory. Matched knowledge structures then provide the pilot's assessment of the situation and serve to guide his attention. A number of cognitive biases that result from the knowledge matching process are discussed, as are implications for partial report measures of situation awareness. Author

N89-19848*# Computer Sciences Corp., Cincinnati, OH.
NEXT GENERATION KEYBOARDS: THE IMPORTANCE OF COGNITIVE COMPATIBILITY **c60**
John R. Amell, Michael E. Ewry, and Herbert A. Colle (Wright State Univ., Dayton, OH.) *In* NASA. Lyndon B. Johnson Space Center, 2nd Annual Workshop on Space Operations Automation and Robotics (SOAR 1988) Nov. 1988 p 233-236 (For primary document see N89-19817 12-59)
Avail: NTIS HC A22/MF A01 CSCL 09B

The computer keyboard of today is essentially the same as it has been for many years. Few advances have been made in keyboard design even though computer systems in general have made remarkable progress in improvements. This paper discusses the future of keyboards, their competition and compatibility with voice input systems, and possible special-application intelligent keyboards for controlling complex systems. Author

N89-19849*# Ohio State Univ., Columbus. Dept. of Psychology.
A METHOD FOR MODELING BIAS IN A PERSON'S ESTIMATES OF LIKELIHOODS OF EVENTS **c65**
Thomas E. Nygren and Osvaldo Morera *In* NASA. Lyndon B. Johnson Space Center, 2nd Annual Workshop on Space Operations Automation and Robotics (SOAR 1988) Nov. 1988 p 237-243 (For primary document see N89-19817 12-59)
(Contract F33615-85-D-0514)
Avail: NTIS HC A22/MF A01 CSCL 12A

It is of practical importance in decision situations involving risk to train individuals to transform uncertainties into subjective probability estimates that are both accurate and unbiased. We have found that in decision situations involving risk, people often introduce subjective bias in their estimation of the likelihoods of events depending on whether the possible outcomes are perceived as being good or bad. Until now, however, the successful measurement of individual differences in the magnitude of such biases has not been attempted. In this paper we illustrate a modification of a procedure originally outlined by Davidson, Suppes, and Siegel (3) to allow for a quantitatively-based methodology for simultaneously estimating an individual's subjective utility and subjective probability functions. The procedure is now an interactive computer-based algorithm, DSS, that allows for the measurement of biases in probability estimation by obtaining independent measures of two subjective probability functions (S+ and S-) for winning (i.e., good outcomes) and for losing (i.e., bad outcomes) respectively for each individual, and for different experimental conditions within individuals. The algorithm and some recent empirical data are described. Author

N89-19850*# Calspan-Buffalo Univ. Research Center, NY.
AN INTELLIGENT MULTI-MEDIA HUMAN-COMPUTER DIALOGUE SYSTEM **c60**
J. G. Neal, K. E. Bettinger, J. S. Byoun, Z. Dobes, and C. Y. Thielman *In* NASA. Lyndon B. Johnson Space Center, 2nd Annual Workshop on Space Operations Automation and Robotics (SOAR 1988) Nov. 1988 p 245-251 (For primary document see N89-19817 12-59)
(Contract F30603-87-C-0136)
Avail: NTIS HC A22/MF A01 CSCL 09B

Sophisticated computer systems are being developed to assist in the human decision-making process for very complex tasks performed under stressful conditions. The human-computer interface is a critical factor in these systems. The human-computer interface should be simple and natural to use, require a minimal learning period, assist the user in accomplishing his task(s) with a minimum of distraction, present output in a form that best conveys information to the user, and reduce cognitive load for the user. In pursuit of this ideal, the Intelligent Multi-Media Interfaces project is devoted to the development of interface technology that integrates speech, natural language text, graphics, and pointing gestures for human-computer dialogues. The objective of the project is to develop interface technology that uses the media/modalities intelligently in a flexible, context-sensitive, and highly integrated manner modelled after the manner in which humans converse in simultaneous coordinated multiple modalities. As part of the project, a knowledge-based interface system, called CUBRICON (CUBRC Intelligent CONversationalist) is being developed as a research prototype. The application domain being used to drive the research is that of military tactical air control. Author

N89-19851*# Columbia Univ., New York, NY. Dept. of Computer Science.
KNOWLEDGE-BASED GRAPHICAL INTERFACES FOR PRESENTING TECHNICAL INFORMATION **c61**
Steven Feiner *In* NASA. Lyndon B. Johnson Space Center, 2nd Annual Workshop on Space Operations Automation and Robotics (SOAR 1988) Nov. 1988 p 253-257 Sponsored in part by Hewlett-Packard Co. (For primary document see N89-19817 12-59)
(Contracts N00039-84-C-0165; NYSSTF-CAT(87)-5; N00014-78-C-0396; NSF INT-73-02268)
Avail: NTIS HC A22/MF A01 CSCL 09B

Designing effective presentations of technical information is extremely difficult and time-consuming. Moreover, the combination of increasing task complexity and declining job skills makes the need for high-quality technical presentations especially urgent. We believe that this need can ultimately be met through the development of knowledge-based graphical interfaces that can design and present technical information. Since much material is most naturally communicated through pictures, our work has stressed the importance of well-designed graphics, concentrating on generating pictures and laying out displays containing them. We describe APEX, a testbed picture generation system that creates sequences of pictures that depict the performance of simple actions in a world of 3D objects. Our system supports rules for determining automatically the objects to be shown in a picture, the style and level of detail with which they should be rendered, the method by which the action itself should be indicated, and the picture's camera specification. We then describe work on GRIDS, an experimental display layout system that addresses some of the problems in designing displays containing these pictures, determining the position and size of the material to be presented. Author

N89-19852*# RCA Advanced Technology Labs., Moorestown, NJ.
AN INTELLIGENT INTERFACE FOR SATELLITE OPERATIONS: YOUR ORBIT DETERMINATION ASSISTANT (YODA) **c18**
Anne Schur *In* NASA. Lyndon B. Johnson Space Center, 2nd Annual Workshop on Space Operations Automation and Robotics (SOAR 1988) Nov. 1988 p 259-265 (For primary document see N89-19817 12-59)
Avail: NTIS HC A22/MF A01 CSCL 22B

An intelligent interface is often characterized by the ability to adapt evaluation criteria as the environment and user goals change. Some factors that impact these adaptations are redefinition of task goals and, hence, user requirements; time criticality; and system status. To implement adaptations affected by these factors, a new set of capabilities must be incorporated into the human-computer interface design. These capabilities include: (1) dynamic update and removal of control states based on user inputs, (2) generation and removal of logical dependencies as change occurs, (3) uniform and smooth interfacing to numerous processes, databases, and expert systems, and (4) unobtrusive on-line assistance to users of concepts were applied and incorporated

into a human-computer interface using artificial intelligence techniques to create a prototype expert system, Your Orbit Determination Assistant (YODA). YODA is a smart interface that supports, in real teime, orbit analysts who must determine the location of a satellite during the station acquisition phase of a mission. Also described is the integration of four knowledge sources required to support the orbit determination assistant: orbital mechanics, spacecraft specifications, characteristics of the mission support software, and orbit analyst experience. This initial effort is continuing with expansion of YODA's capabilities, including evaluation of results of the orbit determination task. Author

N89-19853*# Search Technology, Inc., Norcross, GA.
AN INTELLIGENT TUTORING SYSTEM FOR SPACE SHUTTLE DIAGNOSIS c63
William B. Johnson, Jeffrey E. Norton, and Phillip C. Duncan *In* NASA. Lyndon B. Johnson Space Center, 2nd Annual Workshop on Space Operations Automation and Robotics (SOAR 1988) Nov. 1988 p 267-272 (For primary document see N89-19817 12-59)
Avail: NTIS HC A22/MF A01 CSCL 09B

An Intelligent Tutoring System (ITS) transcends conventional computer-based instruction. An ITS is capable of monitoring and understanding student performance thereby providing feedback, explanation, and remediation. This is accomplished by including models of the student, the instructor, and the expert technician or operator in the domain of interest. The space shuttle fuel cell is the technical domain for the project described below. One system, Microcomputer Intelligence for Technical Training (MITT), demonstrates that ITS's can be developed and delivered, with a reasonable amount of effort and in a short period of time, on a microcomputer. The MITT system capitalizes on the diagnostic training approach called Framework for Aiding the Understanding of Logical Troubleshooting (FAULT) (Johnson, 1987). The system's embedded procedural expert was developed with NASA's C-Language Integrated Production (CLIP) expert system shell (Cubert, 1987). Author

N89-19854*# Air Force Human Resources Lab., Wright-Patterson AFB, OH. Training Systems Div.
INTELLIGENT TUTORING SYSTEMS RESEARCH IN THE TRAINING SYSTEMS DIVISION: SPACE APPLICATIONS c63
J. Wesley Regian *In* NASA. Lyndon B. Johnson Space Center, 2nd Annual Workshop on Space Operations Automation and Robotics (SOAR 1988) Nov. 1988 p 273-277 (For primary document see N89-19817 12-59)
Avail: NTIS HC A22/MF A01 CSCL 09B

Computer-Aided Instruction (CAI) is a mature technology used to teach students in a wide variety of domains. The introduction of Artificial Intelligence (AI) technology of the field of CAI has prompted research and development efforts in an area known as Intelligent Computer-Aided Instruction (ICAI). In some cases, ICAI has been touted as a revolutionary alternative to traditional CAI. With the advent of powerful, inexpensive school computers, ICAI is emerging as a potential rival to CAI. In contrast to this, one may conceive of Computer-Based Training (CBT) systems as lying along a continuum which runs from CAI to ICAI. Although the key difference between the two is intelligence, there is not commonly accepted definition of what constitutes an intelligent instructional system. Author

N89-19855*# National Aeronautics and Space Administration. Goddard Space Flight Center, Greenbelt, MD.
INTELLIGENT TUTORING IN THE SPACECRAFT COMMAND/CONTROL ENVIRONMENT c63
Walter F. Truszkowski *In* NASA. Lyndon B. Johnson Space Center, 2nd Annual Workshop on Space Operations Automation and Robotics (SOAR 1988) Nov. 1988 p 279-286 (For primary document see N89-19817 12-59)
Avail: NTIS HC A22/MF A01 CSCL 09B

The spacecraft command/control environment is becoming increasingly complex. As we enter the era of Space Station and the era of more highly automated systems, it is evident that the critical roles played by operations personnel in supervising the many required control center system components is becoming more cognitively demanding. In addition, the changing and emerging roles in the operations picture have far-reaching effects on the achievement of mission objectives. Thus highly trained and competent operations personnel are mandatory for success. Keeping pace with these developments has been computer-aided instruction utilizing various artificial intelligence technologies. The impacts of this growing capability on the stringent requirements for efficient and effective control center operations personnel is an area of much concentrated study. Some of the research and development of automated tutoring systems for the spacecraft command/control environment is addressed. Author

N89-19856*# Yale Univ., New Haven, CT.
KNOWLEDGE ACQUISITION FOR CASE-BASED REASONING SYSTEMS c63
Christopher K. Riesbeck *In* NASA. Lyndon B. Johnson Space Center, 2nd Annual Workshop on Space Operations Automation and Robotics (SOAR 1988) Nov. 1988 p 289-292 Prepared in cooperation with Congitive Systems, Inc., New Haven, CT Sponsored in part by DARPA (For primary document see N89-19817 12-59)
(Contract F49620-82-K-0010)
Avail: NTIS HC A22/MF A01 CSCL 09B

Case-based reasoning (CBR) is a simple idea: solve new problems by adapting old solutions to similar problems. The CBR approach offers several potential advantages over rule-based reasoning: rules are not combined blindly in a search for solutions, solutions can be explained in terms of concrete examples, and performance can improve automatically as new problems are solved and added to the case library. Moving CBR for the university research environment to the real world requires smooth interfaces for getting knowledge from experts. Described are the basic elements of an interface for acquiring three basic bodies of knowledge that any case-based reasoner requires: the case library of problems and their solutions, the analysis rules that flesh out input problem specifications so that relevant cases can be retrieved, and the adaptation rules that adjust old solutions to fit new problems. Author

N89-19857*# Vector Research, Inc., Ann Arbor, MI.
PSYCHOLOGICAL TOOLS FOR KNOWLEDGE ACQUISITION c53
Henry H. Rueter and Judith Reitman Olson (Michigan Univ., Ann Arbor.) *In* NASA. Lyndon B. Johnson Space Center, 2nd Annual Workshop on Space Operations Automation and Robotics (SOAR 1988) Nov. 1988 p 293-297 (For primary document see N89-19817 12-59)
Avail: NTIS HC A22/MF A01 CSCL 05I

Knowledge acquisition is said to be the biggest bottleneck in the development of expert systems. The problem is getting the knowledge out of the expert's head and into a computer. In cognitive psychology, characterizing metal structures and why experts are good at what they do is an important research area. Is there some way that the tools that psychologists have developed to uncover mental structure can be used to benefit knowledge engineers? We think that the way to find out is to browse through the psychologist's toolbox to see what there is in it that might be of use to knowledge engineers. Expert system developers have relied on two standard methods for extracting knowledge from the expert: (1) the knowledge engineer engages in an intense bout of interviews with the expert or experts, or (2) the knowledge engineer becomes an expert himself, relying on introspection to uncover the basis of his own expertise. Unfortunately, these techniques have the difficulty that often the expert himself isn't consciously aware of the basis of his expertise. If the expert himself isn't conscious of how he solves problems, introspection is useless. Cognitive psychology has faced similar problems for many years and has developed exploratory methods that can be used to discover cognitive structure from simple data. Author

N89-19858*# Air Force Wright Aeronautical Labs., Wright-Patterson AFB, OH.

LIGHT WEIGHT ESCAPE CAPSULE FOR FIGHTER AIRCRAFT **c03**

James A. Robert *In* NASA. Lyndon B. Johnson Space Center, 2nd Annual Workshop on Space Operations Automation and Robotics (SOAR 1988) Nov. 1988 p 303-307 (For primary document see N89-19817 12-59)

Avail: NTIS HC A22/MF A01 CSCL 01C

Emergency crew escape capabilities have been less than adequate for fighter aircraft since before WW II. From the over-the-side bailout of those days through the current ejection seat with a rocket catapult, escaping from a disabled aircraft has been risky at best. Current efforts are underway toward developing a high-tech, smart ejection seat that will give fighter pilots more room to live in the sky, but an escape capsule is needed to meet current and future fighter envelopes. Escape capsules have a bad reputation due to past examples of high weight, poor performance and great complexity. However, the advantages available demand that a capsule be developed. This capsule concept will minimize the inherent disavantages and incorporate the benefits while integrating all aspects of crew station design. The resulting design is appropriate for a crew station of the year 2010 and includes improved combat acceleration protection, chemical or biological combat capability, improved aircraft to escape system interaction, and the highest level of escape performance achievable. The capsule is compact, which can ailow a reduced aircraft size and weighs only 1200 lb. The escape system weight penalty is only 120 lb higher than that for the next ejection seat and the capsule has a corresponding increase in performance. Author

N89-19859*# Air Force Wright Aeronautical Labs., Wright-Patterson AFB, OH.

CHEMICAL WARFARE PROTECTION FOR THE COCKPIT OF FUTURE AIRCRAFT **c05**

William C. Pickl *In* NASA. Lyndon B. Johnson Space Center, 2nd Annual Workshop on Space Operations Automation and Robotics (SOAR 1988) Nov. 1988 p 309-312 (For primary document see N89-19817 12-59)

Avail: NTIS HC A22/MF A01 CSCL 01C

Currently systems are being developed which will filter chemical and biological contaminants from crew station air. In order to maximize the benefits of these systems, a method of keeping the cockpit contaminant free during pilot ingress and egress is needed. One solution is to use a rectangular plastic curtain to seal the four edges of the canopy frame to the canopy sill. The curtain is stored in a tray which is recessed into the canopy sill and unfolds in accordion fashion as the canopy is raised. A two way zipper developed by Calspan could be used as an airlock between the pilot's oversuit and the cockpit. This system eliminates the pilot's need for heavy and restrictive CB gear because he would never be exposed to the chemical warfare environment. Author

N89-19860*# Essex Corp., Orlando, FL.

OPTIMAL SOLUTIONS FOR COMPLEX DESIGN PROBLEMS: USING ISOPERFORMANCE SOFTWARE FOR HUMAN FACTORS TRADE OFFS **c54**

Robert S. Kennedy, Marshall B. Jones (Pennsylvania State Univ., Hershey.), and Dennis R. Baltzley *In* NASA. Lyndon B. Johnson Space Center, 2nd Annual Workshop on Space Operations Automation and Robotics (SOAR 1988) Nov. 1988 p 313-319 (For primary document see N89-19817 12-59)

Avail: NTIS HC A22/MF A01 CSCL 05H

A major application of isoperformance is as a trade-off methodology of the three major drivers of system design; equipment, training variables, and user characteristics. The flexibility of isoperformance allows each of these three components to be nearly any rational variation. For example, aptitude may be military Armed Forces Qualification Testing (AFQT) categories, cutoff scores within a selection procedure, or simply dichotomizing high and low scorers (pass/fail). Equipment may be new versus old, 'smart' versus dumb, high versus low resolution, etc. Training may be short versus long or varieties of media types (lecture versus CAI/CBI versus self-paced workbooks). In its final computerized form isoperformance lets the user set an operational level of performance (e.g., a jet pilot in a simulated emergency must take prescribed corrective action and clear the plane in several seconds, pilot astronauts will check out all shuttle flight systems within 30 minutes, or Mission Specialists must handle sucdessfully a required number of job elements). At this point the computer program guides the user through any requested trade-offs of the three components while maintaining the specified operational level of performance through isoperformance curves. A demonstration of the computer program is currently available. Author

N89-19861*# Lockheed Engineering and Sciences Co., Houston, TX.

SIMULATION OF THE HUMAN-TELEROBOT INTERFACE **c54**

Mark A. Stuart and Randy L. Smith *In* NASA. Lyndon B. Johnson Space Center, 2nd Annual Workshop on Space Operations Automation and Robotics (SOAR 1988) Nov. 1988 p 321-326 (For primary document see N89-19817 12-59)

(Contract NAS9-17900)

Avail: NTIS HC A22/MF A01 CSCL 05H

A part of NASA's Space Station will be a Flight Telerobotic Servicer (FTS) used to help assemble, service, and maintain the Space Station. Since the human operator will be required to control the FTS, the design of the human-telerobot interface must be optimized from a human factors perspective. Simulation has been used as an aid in the development of complex systems. Simulation has been especially useful when it has been applied to the development of complex systems. Simulation should ensure that the hardware and software components of the human-telerobot interface have been designed and selected so that the operator's capabilities and limitations have been accommodated for since this is a complex system where few direct comparisons to existent systems can be made. Three broad areas of the human-telerobot interface where simulation can be of assistance are described. The use of simulation not only can result in a well-designed human-telerobot interface, but also can be used to ensure that components have been selected to best meet system's goals, and for operator training. Author

N89-19862*# CAMUS, Inc., Huntsville, AL.

MAN-SYSTEMS REQUIREMENTS FOR THE CONTROL OF TELEOPERATORS IN SPACE **c54**

Nicholas L. Shields, Jr. *In* NASA. Lyndon B. Johnson Space Center, 2nd Annual Workshop on Space Operations Automation and Robotics (SOAR 1988) Nov. 1988 p 329-334 (For primary document see N89-19817 12-59)

Avail: NTIS HC A22/MF A01 CSCL 05H

The microgravity of the space environment has profound effects on humans and, consequently, on the design requirements for subsystems and components with which humans interact. There are changes in the anthropometry, vision, the perception of orientation, posture, and the ways in which we exert energy. The design requirements for proper human engineering must reflect each of the changes that results, and this is especially true in the exercise of control over remote and teleoperated systems where the operator is removed from any direct sense of control. The National Aeronautics and Space Administration has recently completed the first NASA-wide human factors standard for microgravity. The Man-Systems Integration Standard, NASA-STD-3000, contains considerable information on the appropriate design criteria for microgravity, and there is information that is useful in the design for teleoperated systems. There is not, however, a dedicated collection of data which pertains directly to the special cases of remote and robotic operations. The design considerations for human-system interaction in the control of remote systems in space are discussed, with brief details on the information to be found in the NASA-STD-3000, and arguments for a dedicated section within the Standard which deals with robotic, teleoperated and remote systems and the design requirements for effective human control of these systems in the space environment, and from the space environment. Author

N89-19863*# West Virginia Univ., Morgantown. Dept. of Mechanical and Aerospace Engineering.

INTEGRATION OF A COMPUTERIZED TWO-FINGER GRIPPER FOR ROBOT WORKSTATION SAFETY **c54**

John E. Sneckenberger and Kazuki Yoshikata *In* NASA. Lyndon B. Johnson Space Center, 2nd Annual Workshop on Space Operations Automation and Robotics (SOAR 1988) Nov. 1988 p 335-338 (For primary document see N89-19817 12-59)

Avail: NTIS HC A22/MF A01 CSCL 05H

A microprocessor-based controller has been developed that continuously monitors and adjusts the gripping force applied by a special two-finger gripper. This computerized force sensing gripper system enables the endeffector gripping action to be independently detected and corrected. The gripping force applied to a manipulated object is real-time monitored for problem situations, situations which can occur during both planned and errant robot arm manipulation. When unspecified force conditions occur at the gripper, the gripping force controller initiates specific reactions to cause dynamic corrections to the continuously variable gripping action. The force controller for this intelligent gripper has been interfaced to the controller of an industrial robot. The gripper and robot controllers communicate to accomplish the successful completion of normal gripper operations as well as unexpected hazardous situations. An example of an unexpected gripping condition would be the sudden deformation of the object being manipulated by the robot. The capabilities of the interfaced gripper-robot system to apply workstation safety measures (e.g., stop the robot) when these unexpected gripping effects occur have been assessed. Author

N89-19864*# Michigan Technological Univ., Houghton. Dept. of Mechanical Engineering.

LOCAL POSITION CONTROL: A NEW CONCEPT FOR CONTROL OF MANIPULATORS **c54**

Frederick A. Kelly *In* NASA. Lyndon B. Johnson Space Center, 2nd Annual Workshop on Space Operations Automation and Robotics (SOAR 1988) Nov. 1988 p 339-341 (For primary document see N89-19817 12-59)

Avail: NTIS HC A22/MF A01 CSCL 05H

Resolved motion rate control is currently one of the most frequently used methods of manipulator control. It is currently used in the Space Shuttle remote manipulator system (RMS) and in prosthetic devices. Position control is predominately used in locating the end-effector of an industrial manipulator along a path with prescribed timing. In industrial applications, resolved motion rate control is inappropriate since position error accumulates. This is due to velocity being the control variable. In some applications this property is an advantage rather than a disadvantage. It may be more important for motion to end as soon as the input command is removed rather than reduce the position error to zero. Local position control is a new concept for manipulator control which retains the important properties of resolved motion rate control, but reduces the drift. Local position control can be considered to be a generalization of resolved position and resolved rate control. It places both control schemes on a common mathematical basis. Author

N89-19865*# Cincinnati Univ., OH. Dept. of Mechanical and Industrial Engineering.

DEXTERITY ANALYSIS AND ROBOT HAND DESIGN **c54**

Lu Li, A. H. Soni, Cai Chunsheng, and Max Brown *In* NASA. Lyndon B. Johnson Space Center, 2nd Annual Workshop on Space Operations Automation and Robotics (SOAR 1988) Nov. 1988 p 343-351 (For primary document see N89-19817 12-59)

Avail: NTIS HC A22/MF A01 CSCL 05H

Understanding about a dexterous robot hand's motion ranges is important to the precision grasping and precision manipulation. A planar robot hand is studied for object orientation, including ranges of motion, measures with respect to the palm, position reaching of a point in the grasped object, and rotation of the object about the reference point. The rotational dexterity index and dexterity chart are introduced and an analysis procedure is developed for calculating these quantities. A design procedure for determining the hand kinematic parameters based on a desired partial or complete dexterity chart is also developed. These procedures have been tested in detail for a planar robot hand with two 2- or 3-link fingers. The derived results are shown to be useful to performance evaluation, kinematic parameter design, and grasping motion planning for a planar robot hand. Author

N89-19866*# Central State Univ., Wilberforce, OH. Dept. of Manufacturing Engineering.

CONCEPT FOR A LARGE MASTER/SLAVE-CONTROLLED ROBOTIC HAND **c54**

William A. Grissom, Mahmoud A. AbdAllah, and Carl L. White (Computerized Technologies, Inc., Columbus, OH.) *In* NASA. Lyndon B. Johnson Space Center, 2nd Annual Workshop on Space Operations Automation and Robotics (SOAR 1988) Nov. 1988 p 353-359 Sponsored in part by an Ohio Board of Regeants Research Challenge grant (For primary document see N89-19817 12-59)

(Contract NAGw-1336; JPL-958292)

Avail: NTIS HC A22/MF A01 CSCL 05H

A strategy is presented for the design and construction of a large master/slave-controlled, five-finger robotic hand. Each of the five fingers will possess four independent axes each driven by a brushless DC servomotor and, thus, four degrees-of-freedom. It is proposed that commercially available components be utilized as much as possible to fabricate a working laboratory model of the device with an anticipated overall length of two-to-four feet (0.6 to 1.2 m). The fingers are to be designed so that proximity, tactile, or force/torque sensors can be imbedded in their structure. In order to provide for the simultaneous control of the twenty independent hand joints, a multilevel master/slave control strategy is proposed in which the operator wears a specially instrumented glove which produces control signals corresponding to the finger configurations and which is capable of conveying sensor feedback signals to the operator. Two dexterous hand master devices are currently commercially available for this application with both undergoing continuing development. A third approach to be investigated for the master control mode is the use of real-time image processing of a specially patterned master glove to provide the respective control signals for positioning the multiple finger joints. Author

N89-19867*# Washington Univ., Seattle. Dept. of Electrical Engineering.

CAD-MODEL-BASED VISION FOR SPACE APPLICATIONS **c61**

Linda G. Shapiro *In* NASA. Lyndon B. Johnson Space Center, 2nd Annual Workshop on Space Operations Automation and Robotics (SOAR 1988) Nov. 1988 p 361-367 (For primary document see N89-19817 12-59)

Avail: NTIS HC A22/MF A01 CSCL 09B

A pose acquisition system operating in space must be able to perform well in a variety of different applications including automated guidance and inspections tasks with many different, but known objects. Since the space station is being designed with automation in mind, there will be CAD models of all the objects, including the station itself. The construction of vision models and procedures directly from the CAD models is the goal of this project. The system that is being designed and implementing must convert CAD models to vision models, predict visible features from a given view point from the vision models, construct view classes representing views of the objects, and use the view class model thus derived to rapidly determine the pose of the object from single images and/or stereo pairs. Author

N89-19868*# Carnegie-Mellon Univ., Pittsburgh, PA. The Robotics Inst.

SENSOR FUSION OF RANGE AND REFLECTANCE DATA FOR OUTDOOR SCENE ANALYSIS **c43**

In So Kweon, Martial Hebvert, and Takeo Kanade *In* NASA. Lyndon B. Johnson Space Center, 2nd Annual Workshop on Space Operations Automation and Robotics (SOAR 1988) Nov. 1988 p 373-382 (For primary document see N89-19817 12-59)

(Contract NAGw-1175; DACA76-85-C-0003; NSF DCR-86-04199; ARPA Order 5351)
Avail: NTIS HC A22/MF A01 CSCL 20F

In recognizing objects in an outdoor scene, range and reflectance (or color) data provide complementary information. Results of experiments in recognizing outdoor scenes containing roads, trees, and cars are presented. The recognition program uses range and reflectance data obtained by a scanning laser range finder, as well as color data from a color TV camera. After segmentation of each image into primitive regions, models of objects are matched using various properties. Author

N89-19869*# National Aeronautics and Space Administration. Lyndon B. Johnson Space Center, Houston, TX.
ROBOT PATH PLANNING USING A GENETIC ALGORITHM **c61**
Timothy F. Cleghorn, Paul T. Baffes, and Liu Wang *In its* 2nd Annual Workshop on Space Operations Automation and Robotics (SOAR 1988) Nov. 1988 p 383-389 (For primary document see N89-19817 12-59)
Avail: NTIS HC A22/MF A01 CSCL 09B

Robot path planning can refer either to a mobile vehicle such as a Mars Rover, or to an end effector on an arm moving through a cluttered workspace. In both instances there may exist many solutions, some of which are better than others, either in terms of distance traversed, energy expended, or joint angle or reach capabilities. A path planning program has been developed based upon a genetic algorithm. This program assumes global knowledge of the terrain or workspace, and provides a family of good paths between the initial and final points. Initially, a set of valid random paths are constructed. Successive generations of valid paths are obtained using one of several possible reproduction strategies similar to those found in biological communities. A fitness function is defined to describe the goodness of the path, in this case including length, slope, and obstacle avoidance considerations. It was found that with some reproduction strategies, the average value of the fitness function improved for successive generations, and that by saving the best paths of each generation, one could quite rapidly obtain a collection of good candidate solutions. Author

N89-19870*# National Aeronautics and Space Administration. Goddard Space Flight Center, Greenbelt, MD.
DESIGN CONCEPT FOR THE FLIGHT TELEROBOTIC SERVICER (FITS) **c54**
J. F. Andary, S. W. Hinkai, and J. G. Watzin *In* NASA. Lyndon B. Johnson Space Center, 2nd Annual Workshop on Space Operations Automation and Robotics (SOAR 1988) Nov. 1988 p 391-396 (For primary document see N89-19817 12-59)
Avail: NTIS HC A22/MF A01 CSCL 05H

NASA has just completed an in-house Phase B Study (one of three studies) for the preliminary definition of a teleoperated robotic device that will be used on the National Space Transportation System (NSTS) and the Space Station to assist the astronauts in the performance of assembly, maintenance, servicing, and inspection tasks. This device, the Flight Telerobotic Servicer (FTS), will become a permanent element on the Space Station. Although it is primarily a teleoperated device, the FTS is being designed to grow and evolve to higher states of autonomy. Eventually, it will be capable of working from the Orbital Maneuvering Vehicle (OMV) to service free-flying spacecraft at great distances from the Space Station. A version of the FTS could also be resident on the large space platforms that are part of the Space Station Program. Author

N89-19871*# Wisconsin Univ., Madison. Coll. of Engineering.
THE WCSAR TELEROBOTICS TEST BED **c54**
N. Duffie, J. Zik, R. Teeter, and T. Crabb (Astronautics Corp. of America, Madison, WI.) *In* NASA. Lyndon B. Johnson Space Center, 2nd Annual Workshop on Space Operations Automation and Robotics (SOAR 1988) Nov. 1988 p 397-402 (For primary document see N89-19817 12-59)
(Grant NAGw-975)
Avail: NTIS HC A22/MF A01 CSCL 05H

Component technologies for use in telerobotic systems for space are being developed. As part of this effort, a test bed was established in which these technologies can be verified and integrated into telerobotic systems. The facility consists of two slave industrial robots, an articulated master arm controller, a cartesian coordinate master arm controller, and a variety of sensors, displays and stimulators for feedback to human operators. The controller of one of the slave robots remains in its commercial state, while the controller of the other robot has been replaced with a new controller that achieves high-performance in telerobotic operating modes. A dexterous slave hand which consists of two fingers and a thumb is being developed, along with a number of force-reflecting and non-force reflecting master hands, wrists and arms. A tactile sensing finger tip based on piezo-film technology has been developed, along with tactile stimulators and CAD-based displays for sensory feedback and sensory substitution. The telerobotics test bed and its component technologies are described, as well as the integration of these component technologies into telerobotic systems, and their performance in conjunction with human operators. Author

N89-19872*# Aerospace Medical Research Labs., Wright-Patterson AFB, OH.
THE USE OF THE ARTICULATED TOTAL BODY MODEL AS A ROBOT DYNAMICS SIMULATION TOOL **c54**
Louise A. Obergfell, Xavier J. R. Avula, and Ints Kalegs *In* NASA. Lyndon B. Johnson Space Center, 2nd Annual Workshop on Space Operations Automation and Robotics (SOAR 1988) Nov. 1988 p 403-409 (For primary document see N89-19817 12-59)
Avail: NTIS HC A22/MF A01 CSCL 05H

The Articulated Total Body (ATB) model is a computer sumulation program which was originally developed for the study of aircrew member dynamics during ejection from high-speed aircraft. This model is totally three-dimensional and is based on the rigid body dynamics of coupled systems which use Euler's equations of motion with constraint relations of the type employed in the Lagrange method. In this paper the use of the ATB model as a robot dynamics simulation tool is discussed and various simulations are demonstrated. For this purpose the ATB model has been modified to allow for the application of torques at the joints as functions of state variables of the system. Specifically, the motion of a robotic arm with six revolute articulations with joint torques prescribed as functions of angular displacement and angular velocity are demonstrated. The simulation procedures developed in this work may serve as valuable tools for analyzing robotic mechanisms, dynamic effects, joint load transmissions, feed-back control algorithms employed in the actuator control and end-effector trajectories. Author

N89-19873*# Martin Marietta Aero and Naval Systems, Baltimore, MD.
TELEPRESENCE AND TELEROBOTICS **c54**
John Garin, Joseph Matteo, and Von Ayre Jennings *In* NASA. Lyndon B. Johnson Space Center, 2nd Annual Workshop on Space Operations Automation and Robotics (SOAR 1988) Nov. 1988 p 411-420 (For primary document see N89-19817 12-59)
Avail: NTIS HC A22/MF A01 CSCL 05H

The capability for a single operator to simultaneously control complex remote multi degree of freedom robotic arms and associated dextrous end effectors is being developed. An optimal solution within the realm of current technology, can be achieved by recognizing that: (1) machines/computer systems are more effective than humans when the task is routine and specified, and (2) humans process complex data sets and deal with the unpredictable better than machines. These observations lead naturally to a philosophy in which the human's role becomes a higher level function associated with planning, teaching, initiating, monitoring, and intervening when the machine gets into trouble, while the machine performs the codifiable tasks with deliberate efficiency. This concept forms the basis for the integration of man

and telerobotics, i.e., robotics with the operator in the control loop. The concept of integration of the human in the loop and maximizing the feed-forward and feed-back data flow is referred to as telepresence. Author

N89-19874*# Carnegie-Mellon Univ., Pittsburgh, PA. The Robotics Inst.

A NOVEL MANIPULATOR TECHNOLOGY FOR SPACE APPLICATIONS **c54**

Donald Schmitz, Pradeep Khosia, and Takeo Kanade *In* NASA. Lyndon B. Johnson Space Center, 2nd Annual Workshop on Space Operations Automation and Robotics (SOAR 1988) Nov. 1988 p 421-428 (For primary document see N89-19817 12-59)

Avail: NTIS HC A22/MF A01 CSCL 05H

Modular manipulator designs have long been considered for use as research tools, and as the basis for easily modified industrial manipulators. In these manipulators the links and joints are discrete and modular components that can be assembled into a desired manipulator configuration. As hardware advances have made actual modular manipulators practical, various capabilities of such manipulators have gained interest. Particularly desirable is the ability to rapidly reconfigure such a manipulator, in order to custom tailor it to specific tasks. The reconfiguration greatly enhances the capability of a given amount of manipulator hardware. The development of a prototype modular manipulator is discussed as well as the implementation of a configuration independent manipulator kinematics algorithm used for path planning in the prototype. Author

N89-19875*# Carnegie-Mellon Univ., Pittsburgh, PA. Robotics Inst.

A ROBUST CONTROL SCHEME FOR FLEXIBLE ARMS WITH FRICTION IN THE JOINTS **c54**

Kuldip S. Rattan, Vicente Feliu (Universidad Nacional de Educacion a Distancia, Madrid, Spain), and H. Benjamin Brown, Jr. *In* NASA. Lyndon B. Johnson Space Center, 2nd Annual Workshop on Space Operations Automation and Robotics (SOAR 1988) Nov. 1988 p 429-435 (For primary document see N89-19817 12-59)

Avail: NTIS HC A22/MF A01 CSCL 05H

A general control scheme to control flexible arms with friction in the joints is proposed in this paper. This scheme presents the advantage of being robust in the sense that it minimizes the effects of the Coulomb friction existing in the motor and the effects of changes in the dynamic friction coefficient. A justification of the robustness properties of the scheme is given in terms of the sensitivity analysis. Author

N89-19876*# Jet Propulsion Lab., California Inst. of Tech., Pasadena.

TELEROBOT OPERATOR CONTROL STATION REQUIREMENTS **c54**

Edwin P. Kan *In* NASA. Lyndon B. Johnson Space Center, 2nd Annual Workshop on Space Operations Automation and Robotics (SOAR 1988) Nov. 1988 p 437-443 (For primary document see N89-19817 12-59)

Avail: NTIS HC A22/MF A01 CSCL 05H

The operator control station of a telerobot system has unique functional and human factors requirements. It has to satisfy the needs of a truly interactive and user-friendly complex system, a telerobot system being a hybrid between a teleoperated and an autonomous system. These functional, hardware and software requirements are discussed, with explicit reference to the design objectives and constraints of the JPL/NASA Telerobot Demonstrator System. Author

N89-19877*# Jet Propulsion Lab., California Inst. of Tech., Pasadena.

TIME-DELAYED OPERATION OF A TELEROBOT VIA GEOSYNCHRONOUS RELAY **c54**

Brian H. Wilcox *In* NASA. Lyndon B. Johnson Space Center, 2nd Annual Workshop on Space Operations Automation and Robotics (SOAR 1988) Nov. 1988 p 445-447 (For primary document see N89-19817 12-59)

Avail: NTIS HC A22/MF A01 CSCL 05H

Operation of a telerobot is compromised if a time delay of more than a few hundred milliseconds exists between the operator and remote manipulator. However, the most economically attractive way to perform telerobotic functions such as assembly, maintenance, and repair in Earth orbit is via geosynchronous relay satellites to a ground-based operator. This induces loop delays from one-half to two seconds, depending on how many relays are involved. Such large delays makes direct master-slave, force-reflecting teleoperated systems infeasible. Research at JPL on a useful telerobot that operates with such time delays is described. Author

N89-19878*# Texas Instruments, Inc., Dallas. Speech and Image Understanding Lab.

A REPRESENTATIONAL FRAMEWORK AND USER-INTERFACE FOR AN IMAGE UNDERSTANDING WORKSTATION **c54**

Joyce D. Schroeder *In* NASA. Lyndon B. Johnson Space Center, 2nd Annual Workshop on Space Operations Automation and Robotics (SOAR 1988) Nov. 1988 p 451-456 (For primary document see N89-19817 12-59)

Avail: NTIS HC A22/MF A01 CSCL 05H

Problems in image understanding involve a wide variety of data (e.g., image arrays, edge maps, 3-D shape models) and processes or algorithms (e.g., convolution, feature extraction, rendering). The underlying structure of an Image Understanding Workstation designed to support mulitple levels and types of representations for both data and processes is described, also the user-interface. The Image Understanding Workstation consists of two parts: the Image Understanding (IU) Framework, and the user-interface. The IU Framework is the set of data and process representations. It includes multiple levels of representation for data such as images (2-D), sketches (2-D), surfaces (2 1/2 D), and models (3-D). The representation scheme for processes characterizes their inputs, outputs, and parameters. Data and processes may reside on different classes of machines. The user-interface to the IU Workstation gives the user convenient access for creating, manipulating, transforming, and displaying image data. The user-interface follows the structure of the IU Framework and gives the user control over multiple types of data and processes. Both the IU Framework and user-interface are implemented on a LISP machine. Author

N89-19879*# Jet Propulsion Lab., California Inst. of Tech., Pasadena.

MACHINE VISION FOR SPACE TELEROBOTICS AND PLANETARY ROVERS **c54**

Brian H. Wilcox *In* NASA. Lyndon B. Johnson Space Center, 2nd Annual Workshop on Space Operations Automation and Robotics (SOAR 1988) Nov. 1988 p 457-460 (For primary document see N89-19817 12-59)

Avail: NTIS HC A22/MF A01 CSCL 05H

Machine vision allows a non-contact means of determining the three-dimensional shape of objects in the environment, enabling the control of contact forces when manipulation by a telerobot or traversal by a vehicle is desired. Telerobotic manipulation in Earth orbit requires a system that can recognize known objects in spite of harsh lighting conditions and highly specular or absorptive surfaces. Planetary surface traversal requires a system that can recognize the surface shape and properties of an unknown and arbitrary terrain. Research on these two rather disparate types of vision systems is described. Author

N89-19880*# Texas Instruments, Inc., Dallas. Speech and Image Understanding Lab.

VOICE CONTROL OF COMPLEX WORKSTATIONS **c54**

Jeffrey L. Scruggs *In* NASA. Lyndon B. Johnson Space Center, 2nd Annual Workshop on Space Operations Automation and Robotics (SOAR 1988) Nov. 1988 p 461-466 (For primary

document see N89-19817 12-59)
Avail: NTIS HC A22/MF A01 CSCL 05H

The use of a speaker-dependent connected word recognition system to control an Air Traffic Control (ATC) demonstration workstation is described, also the work that went into developing that speech system. The workstation with speech recognition was demonstrated live at an Air Traffic Controller's Association convention in 1987. The purpose of the demonstration workstation is discussed, with the development of the speech interface highlighted. Included are: a brief description of the speech hardware and software, and overview of the speech driven workstation functions, a description of the speech vocabulary/grammer, and details that the enrollment and training procedures used in preparing the controllers for the demonstrations. Although no quantitative results are available, the potential benefits of using voice as an interface to this type of workstation are discussed and limitations of current speech technology and areas where more work is required are highlighted. Author

N89-19881*# National Aeronautics and Space Administration. Lyndon B. Johnson Space Center, Houston, TX.
A MULTI-SENSOR SYSTEM FOR ROBOTICS PROXIMITY OPERATIONS **c54**
J. B. Cheatham, C. K. Wu, P. L. Weiland (Rice Univ., Houston, TX.), and T. F. Cleghorn *In its* 2nd Annual Workshop on Space Operations Automation and Robotics (SOAR 1988) Nov. 1988 p 467-470 (For primary document see N89-19817 12-59)
(Contract NCC9-16; NAG9-208)
Avail: NTIS HC A22/MF A01 CSCL 05H

Robots without sensors can perform only simple repetitive tasks and cannot cope with unplanned events. A multi-sensor system is needed for a robot to locate a target, move into its neighborhood and perform operations in contact with the object. Systems that can be used for such tasks are described. Author

N89-19882*# Jet Propulsion Lab., California Inst. of Tech., Pasadena.
A METHODOLOGY FOR AUTOMATION AND ROBOTICS EVALUATION APPLIED TO THE SPACE STATION TELEROBOTIC SERVICER **c54**
Jeffrey H. Smith, Max Gyanfi, Kent Volkmer, and Wayne Zimmerman *In* NASA. Lyndon B. Johnson Space Center, 2nd Annual Workshop on Space Operations Automation and Robotics (SOAR 1988) Nov. 1988 p 471-479 (For primary document see N89-19817 12-59)
(Contract NAS7-918)
Avail: NTIS HC A22/MF A01 CSCL 05H

The efforts of a recent study aimed at identifying key issues and trade-offs associated with using a Flight Telerobotic Servicer (FTS) to aid in Space Station assembly-phase tasks is described. The use of automation and robotic (A and R) technologies for large space systems would involve a substitution of automation capabilities for human extravehicular or intravehicular activities (EVA, IVA). A methodology is presented that incorporates assessment of candidate assembly-phase tasks, telerobotic performance capabilities, development costs, and effect of operational constraints (space transportation system (STS), attached payload, and proximity operations). Changes in the region of cost-effectiveness are examined under a variety of systems design assumptions. A discussion of issues is presented with focus on three roles the FTS might serve: (1) as a research-oriented testbed to learn more about space usage of telerobotics; (2) as a research based testbed having an experimental demonstration orientation with limited assembly and servicing applications; or (3) as an operational system to augment EVA and to aid the construction of the Space Station and to reduce the programmatic (schedule) risk by increasing the flexibility of mission operations.
Author

N89-19883*# Little (Arthur D.), Inc., Cambridge, MA. Center for Product Development.
SENSING HUMAN HAND MOTIONS FOR CONTROLLING DEXTEROUS ROBOTS **c54**
Beth A. Marcus, Philip J. Churchill, and Arthur D. Little *In* NASA. Lyndon B. Johnson Space Center, 2nd Annual Workshop on Space Operations Automation and Robotics (SOAR 1988) Nov. 1988 p 481-485 (For primary document see N89-19817 12-59)
Avail: NTIS HC A22/MF A01 CSCL 05H

The Dexterous Hand Master (DHM) system is designed to control dexterous robot hands such as the UTAH/MIT and Stanford/JPL hands. It is the first commercially available device which makes it possible to accurately and confortably track the complex motion of the human finger joints. The DHM is adaptable to a wide variety of human hand sizes and shapes, throughout their full range of motion. Author

N89-19884*# Westinghouse Electric Corp., Madison, PA. Robotics and Mechanical Design.
APPLICATION OF MODEL BASED CONTROL TO ROBOTIC MANIPULATORS **c54**
Lyman J. Petrosky and Irving J. Oppenheim (Carnegie-Mellon Univ., Pittsburgh, PA.) *In* NASA. Lyndon B. Johnson Space Center, 2nd Annual Workshop on Space Operations Automation and Robotics (SOAR 1988) Nov. 1988 p 487-493 (For primary document see N89-19817 12-59)
(Contract DE-AC02-85NE-37947)
Avail: NTIS HC A22/MF A01 CSCL 05H

A robot that can duplicate humam motion capabilities in such activities as balancing, reaching, lifting, and moving has been built and tested. These capabilities are achieved through the use of real time Model-Based Control (MBC) techniques which have recently been demonstrated. MBC accounts for all manipulator inertial forces and provides stable manipulator motion control even at high speeds. To effectively demonstrate the unique capabilities of MBC, an experimental robotic manipulator was constructed, which stands upright, balancing on a two wheel base. The mathematical modeling of dynamics inherent in MBC permit the control system to perform functions that are impossible with conventional non-model based methods. These capabilities include: (1) Stable control at all speeds of operation; (2) Operations requiring dynamic stability such as balancing; (3) Detection and monitoring of applied forces without the use of load sensors; (4) Manipulator safing via detection of abnormal loads. The full potential of MBC has yet to be realized. The experiments performed for this research are only an indication of the potential applications. MBC has no inherent stability limitations and its range of applicability is limited only by the attainable sampling rate, modeling accuracy, and sensor resolution. Manipulators could be designed to operate at the highest speed mechanically attainable without being limited by control inadequacies. Manipulators capable of operating many times faster than current machines would certainly increase productivity for many tasks. Author

N89-19885*# Rockwell International Corp., Downey, CA.
DESIGN GUIDELINES FOR REMOTELY MAINTAINABLE EQUIPMENT **c54**
Margaret M. Clarke and Davoud Manouchehri *In* NASA. Lyndon B. Johnson Space Center, 2nd Annual Workshop on Space Operations Automation and Robotics (SOAR 1988) Nov. 1988 p 495-497 (For primary document see N89-19817 12-59)
Avail: NTIS HC A22/MF A01 CSCL 05H

The quantity and complexity of on-orbit assets will increase significantly over the next decade. Maintaining and servicing these costly assets represent a difficult challenge. Three general methods are proposed to maintain equipment while it is still in orbit: an extravehicular activity (EVA) crew can perform the task in an unpressurized maintenance area outside any space vehicle; an intravehicular activity (IVA) crew can perform the maintenance in a shirt sleeve environment, perhaps at a special maintenance work station in a space vehicle; or a telerobotic manipulator can perform the maintenance in an unpressurized maintenance area at a distance from the crew (who may be EVA, IVA, or on the ground). However, crew EVA may not always be possible; the crew may have other demands on their time that take precedence. In addition, the orbit of the tasks themselves may be impossible for crew entry. Also crew IVA may not always be possible as option for

equipment maintenance. For example, the equipment may be too large to fit through the vehicle airlock. Therefore, in some circumstances, the third option, telerobotic manipulation, may be the only feasible option. Telerobotic manipulation has, therefore, an important role for on-orbit maintenance. It is not only used for the reasons outlined above, but also used in some cases as backup to the EVA crew in an orbit that they can reach. Author

N89-19886*# Army Aviation Systems Command, Cleveland, OH.

AN EXPERT SYSTEM FOR RESTRUCTURABLE CONTROL **c54**

Jonathan Litt *In* NASA. Lyndon B. Johnson Space Center, 2nd Annual Workshop on Space Operations Automation and Robotics (SOAR 1988) Nov. 1988 p 503-507 (For primary document see N89-19817 12-59)

Avail: NTIS HC A22/MF A01 CSCL 05H

Work in progrss on an expert system which restructures and tunes control systems online in real-time is presented. The expert system coordinates the different methods involved in redesigning and implementing the control strategies due to plant changes. Author

N89-19887*# Rockwell International Corp., Downey, CA. Space Transportation Systems Div.

EXPERT SYSTEMS APPLICATIONS FOR SPACE SHUTTLE PAYLOAD INTEGRATION AUTOMATION **c16**

Keith Morris *In* NASA. Lyndon B. Johnson Space Center, 2nd Annual Workshop on Space Operations Automation and Robotics (SOAR 1988) Nov. 1988 p 517-523 (For primary document see N89-19817 12-59)

Avail: NTIS HC A22/MF A01 CSCL 22B

Expert systems technologies have been and are continuing to be applied to NASA's Space Shuttle orbiter payload integration problems to provide a level of automation previously unrealizable. NASA's Space Shuttle orbiter was designed to be extremely flexible in its ability to accommodate many different types and combinations of satellites and experiments (payloads) within its payload bay. This flexibility results in differnet and unique engineering resource requirements for each of its payloads, creating recurring payload and cargo integration problems. Expert systems provide a successful solution for these recurring problems. The Orbiter Payload Bay Cabling Expert (EXCABL) was the first expert system, developed to solve the electrical services provisioning problem. A second expert system, EXMATCH, was developed to generate a list of the reusable installation drawings available for each EXCABL solution. These successes have proved the applicability of expert systems technologies to payload integration problems and consequently a third expert system is currently in work. These three expert systems, the manner in which they resolve payload problems and how they will be integrated are described. Author

N89-19888*# Softech, Inc., Fairborn, OH.

IDEAL: A METHOLOGY FOR DEVELOPING INFORMATION SYSTEMS **c82**

Ken H. Evers and Robert F. Bachert (Aerospace Medical Research Labs., Wright-Patterson AFB, OH.) *In* NASA. Lyndon B. Johnson Space Center, 2nd Annual Workshop on Space Operations Automation and Robotics (SOAR 1988) Nov. 1988 p 527-532 (For primary document see N89-19817 12-59)

Avail: NTIS HC A22/MF A01 CSCL 05B

As a result of improved capabilities obtained through current computer technologies, application programs and expert systems, Enterprises are being designed or upgraded to be highly integrated and automated information systems. To design or modify Enterprises, it is necessary to first define what functions are to be performed within the Enterprise, identify which functions are potential candidates for automation, and what automated or expert systems are available, or must be developed, to accomplish the selected function. Second, it is necessary to define and analyze the informational requirements for each function along with the informational relationships among the functions so that a database structure can be established to support the Enterprise. To perform this type of system design, an integrated set of analysis tools is required to support the information analysis process. The IDEAL (Integrated Design and Engineering Analysis Languages) methodology provides this integrated set of tools and is discussed. Author

N89-19889*# Computer Sciences Corp., Houston, TX.

DEVELOPMENT OF A PERSONAL-COMPUTER-BASED INTELLIGENT TUTORING SYSTEM **c63**

Stephen J. Mueller *In* NASA. Lyndon B. Johnson Space Center, 2nd Annual Workshop on Space Operations Automation and Robotics (SOAR 1988) Nov. 1988 p 535-540 (For primary document see N89-19817 12-59)

Avail: NTIS HC A22/MF A01 CSCL 09B

A large number of Intelligent Tutoring Systems (ITSs) have been built since they were first proposed in the early 1970's. Research conducted on the use of the best of these systems has demonstrated their effectiveness in tutoring in selected domains. A prototype ITS for tutoring students in the use of CLIPS language: CLIPSIT (CLIPS Intelligent Tutor) was developed. For an ITS to be widely accepted, not only must it be effective, flexible, and very responsive, it must also be capable of functioning on readily available computers. While most ITSs have been developed on powerful workstations, CLIPSIT is designed for use on the IBM PC/XT/AT personal computer family (and their clones). There are many issues to consider when developing an ITS on a personal computer such as the teaching strategy, user interface, knowledge representation, and program design methodology. Based on experiences in developing CLIPSIT, results on how to address some of these issues are reported and approaches are suggested for maintaining a powerful learning environment while delivering robust performance within the speed and memory constraints of the personal computer. Author

N89-19890*# Essex Corp., Alexandria, VA.

SARSCEST (HUMAN FACTORS) **c54**

H. McIlvaine Parsons *In* NASA. Lyndon B. Johnson Space Center, 2nd Annual Workshop on Space Operations Automation and Robotics (SOAR 1988) Nov. 1988 p 541-552 (For primary document see N89-19817 12-59)

Avail: NTIS HC A22/MF A01 CSCL 05H

People interact with the processes and products of contemporary technology. Individuals are affected by these in various ways and individuals shape them. Such interactions come under the label 'human factors'. To expand the understanding of those to whom the term is relatively unfamiliar, its domain includes both an applied science and applications of knowledge. It means both research and development, with implications of research both for basic science and for development. It encompasses not only design and testing but also training and personnel requirements, even though some unwisely try to split these apart both by name and institutionally. The territory includes more than performance at work, though concentration on that aspect, epitomized in the derivation of the term ergonomics, has overshadowed human factors interest in interactions between technology and the home, health, safety, consumers, children and later life, the handicapped, sports and recreation education, and travel. Two aspects of technology considered most significant for work performance, systems and automation, and several approaches to these, are discussed. Author

N89-19891*# Boeing Aerospace Co., Kennedy Space Center, FL.

ELECTRONIC DATA GENERATION AND DISPLAY SYSTEM **c82**

Jules Wetekamm *In* NASA. Lyndon B. Johnson Space Center, 2nd Annual Workshop on Space Operations Automation and Robotics (SOAR 1988) Nov. 1988 p 553-557 (For primary document see N89-19817 12-59)

Avail: NTIS HC A22/MF A01 CSCL 05B

The Electronic Data Generation and Display System (EDGADS) is a field tested paperless technical manual system. The authoring provides subject matter experts the option of developing

procedureware from digital or hardcopy inputs of technical information from text, graphics, pictures, and recorded media (video, audio, etc.). The display system provides multi-window presentations of graphics, pictures, animations, and action sequences with text and audio overlays on high resolution color CRT and monochrome portable displays. The database management system allows direct access via hierarchical menus, keyword name, ID number, voice command or touch of a screen pictoral of the item (ICON). It contains operations and maintenance technical information at three levels of intelligence for a total system. Author

N89-19892*# National Aeronautics and Space Administration. Langley Research Center, Hampton, VA.
OPERATION OF THE HP2250 WITH THE HP9000 SERIES 200 USING PASCAL 3.0
John Perry (PRC Kentron, Inc., Hampton, VA.) and C. W. Stroud Feb. 1986 35 p
(NASA-TM-87652; NAS 1.15:87652) Avail: NTIS HC A03/MF A01 CSCL 12A

A computer program has been written to provide an interface between the HP Series 200 desktop computers, operating under HP Standard Pascal 3.0, and the HP2250 Data Acquisition and Control System. Pascal 3.0 for the HP9000 desktop computer gives a number of procedures for handling bus communication at various levels. It is necessary, however, to reach the lowest possible level in Pascal to handle the bus protocols required by the HP2250. This makes programming extremely complex since these protocols are not documented. The program described solves those problems and allows the user to immediately program, simply and efficiently, any measurement and control language (MCL/50) application with a few procedure calls. The complete set of procedures is available on a 5 1/4 inch diskette from Cosmic. Included in this group of procedures is an Exerciser which allows the user to exercise his HP2250 interactively. The exerciser operates in a fashion similar to the Series 200 operating system programs, but is adapted to the requirements of the HP2250. The programs on the diskette and the user's manual assume the user is acquainted with both the MCL/50 programming language and HP Standard Pascal 3.0 for the HP series 200 desktop computers. Author

60 COMPUTER OPERATIONS AND HARDWARE

Includes hardware for computer graphics, firmware, and data processing.

For components see *33 Electronics and Electrical Engineering.*

N89-19893# Massachusetts Inst. of Tech., Cambridge. Artificial Intelligence Lab.
SCHEME86: AN ARCHITECTURE FOR MICROCODING A SCHEME INTERPRETER
Henry M. Wu Aug. 1988 38 p
(Contract N00014-86-K-0180)
(AD-A201258; AI-M-953) Avail: NTIS HC A03/MF A01 CSCL 12E

This document describes the design and implementation plans for a computer that is optimized as microcoded interpreter for Scheme. The native language of this computer is SCode, a tree-structured, typed-pointer representation of Scheme. The memory system is built with high speed RAM and offers low-latency as well as high throughput. Multiple execution units in the processor complete complex operations in less than one memory cycle to allow efficient use of memory bandwidth. The processor provides hardware support for tagged data objects and runtime type checking. The author will discuss the motivation for such a machine, its architecture, why it is expected to interpret Scheme efficiently, and the computer aided design tools I have developed for building this computer. GRA

N89-19894# Rolls-Royce Ltd., Derby (England). Performance Systems Dept.
COMPASS: A GENERALIZED GROUND-BASED MONITORING SYSTEM
M. J. Provost 30 May 1988 13 p Presented at the AGARD PEP 71st Symposium on Engine Condition Monitoring, Quebec, Canada, 30 May-3 Jun. 1988
(PNR90483; ETN-89-93681) Copyright Avail: NTIS HC A03/MF A01

The condition monitoring and performance analysis software system (COMPASS) is a ground based computer system being developed for application on the Rolls Royce RB211-542G and IAE V2500 turbofans. The diagnostic routines and the general host routines are described. The use of the general host routines could be extended to cover any operation which is to be monitored. Measures adopted to enable the COMPASS host to be made available for widespread application are outlined. ESA

N89-19895# ISEL, Madrid (Spain).
ADVANCED INFORMATION TECHNOLOGY MONITORING WITH MICROPROCESSORS Final Report
L. Guzman, A. Ferigle, and M. Admella Paris, France ESA 14 Jul. 1988 98 p
(Contract ESA-7254/87-D-IM(SC))
(MMP-1-IS-02-3302-FR; ESA-CR(P)-2677; ETN-89-93931) Avail: NTIS HC A05/MF A01

A decentralized spacecraft control and operation system (DSCOS) to provide the primary data processing support for spacecraft control centers is presented. The control systems of an electricity supply company and of a nuclear power plant were studied to derive DSCOS requirements. The hardware architecture places the workstations on the level below the back end and front end computers. Workstations are connected to local area networks according to their purpose, but an optical repeater allows data access between workstations, or between workstations and back end computers. A system oriented network assures functional connection between the front ends. It is possible to connect file servers and common resources (e.g., peripherals). The user interface is described. ESA

N89-19896# Deutsche Forschungs- und Versuchsanstalt fuer Luft- und Raumfahrt, Brunswick (Germany, F.R.). Abteilung Flugversuchstechnik.
APPLICATION OF THE OCCAM/TRANSPUTER CONCEPTION AS BUSLESS MULTIPROCESSOR SYSTEM IN A DIGITAL CONTROLLER
Hans-Peter Schwaneck Sep. 1988 54 p In GERMAN; ENGLISH summary
(DFVLR-FB-88-40; ISSN-0171-1342; ETN-89-93974) Avail: NTIS HC A04/MF A01; DFVLR, VB-PL-DO, Postfach 90 60 58, 5000 Cologne, Federal Republic of Germany, 21 deutsche marks

Increases in performance expected of busless multimicroprocessor systems, due to the architecture for multiprocessors are discussed. The transputer-OCCAM system overcomes the difficulties of handling such systems. With the application of a digital controller, which could not be realized with conventional systems, the experiences with OCCAM and transputers are described. ESA

N89-19897# Alabama Univ., Huntsville.
FONR OPTICAL COMPUTING ST Annual Report, 1 May 1987 - 30 Apr. 1988
H. J. Caulfield 13 Sep. 1988 15 p
(Contract N00014-86-K-0591)
(AD-A201002) Avail: NTIS HC A03/MF A01 CSCL 09B

As noted in the original proposal, most effort was in hybrid analog-digital algebra and in massively parallel processing based on hologram arrays. Both programs have exceeded the announced goals. In those primary studies, a number of other worthwhile applications were developed in optics as well. Future work will aim almost exclusively at the holographic interconnect as this is likely to be of most immediate value in meeting the announced DSI/ONR program needs. A satisfactory conclusion was reached

to the algebra study by lab demonstration and theoretical justification of the results previously obtained only by computer simulation and justifying arguments. An overview and detail parts for each application is presented. The detail is relegated to appendices to make reading of the overview more convenient.
E.R.

N89-19898# Nationaal Inst. voor Kernfysica en Hoge Energiefysica, Amsterdam (Netherlands).
BITBUS DATA TRANSMISSION WITH GALVANIC SEPARATIONS [BITBUS DATA TRANSPORT MET GALVANISCHE SCHEIDINGEN]
P. P. M. Jansweijer and J. J. Hogebirk 1988 24 p In DUTCH
(DIGEL-78; ETN-89-93879) Avail: NTIS HC A03/MF A01

The possibilities of implementing galvanic separations for a bitbus system in a raw environment are outlined. Bitbus is a multiprocessor system based on the Intel 8044 microprocessor. The physical and the datalink layer, which are important for the design of a galvanic separation for bitbus, are described. The use of transformers or optocouplers for the galvanic separation in magnetic-unit applications is discussed. The design of possible bitbus system with optical separation is presented. The different objects which have to be controlled are connected by a ring wiring, to which bitbus components are coupled by optocouplers. ESA

N89-19838*# National Aeronautics and Space Administration. Ames Research Center, Moffett Field, CA.
SPACEBORNE VHSIC MULTIPROCESSOR SYSTEM FOR AI APPLICATIONS
Henry Lum, Jr., Howard E. Shrobe, and John G. Aspinall (Symbolics, Inc., Cambridge, MA.) *In* NASA. Lyndon B. Johnson Space Center, 2nd Annual Workshop on Space Operations Automation and Robotics (SOAR 1988) Nov. 1988 p 153-160 (For primary document see N89-19817 12-59)
Avail: NTIS HC A22/MF A01 CSCL 09B

N89-19841*# Mitre Corp., McLean, VA. Artificial Intelligence Technical Center.
AN ARCHITECTURE FOR INTEGRATING DISTRIBUTED AND COOPERATING KNOWLEDGE-BASED AIR FORCE DECISION AIDS
Richard O. Nugent and Richard W. Tucker *In* NASA. Lyndon B. Johnson Space Center, 2nd Annual Workshop on Space Operations Automation and Robotics (SOAR 1988) Nov. 1988 p 171-175 (For primary document see N89-19817 12-59)
(Contract F19628-86-C-0001)
Avail: NTIS HC A22/MF A01 CSCL 09B

N89-19848*# Computer Sciences Corp., Cincinnati, OH.
NEXT GENERATION KEYBOARDS: THE IMPORTANCE OF COGNITIVE COMPATIBILITY
John R. Amell, Michael E. Ewry, and Herbert A. Colle (Wright State Univ., Dayton, OH.) *In* NASA. Lyndon B. Johnson Space Center, 2nd Annual Workshop on Space Operations Automation and Robotics (SOAR 1988) Nov. 1988 p 233-236 (For primary document see N89-19817 12-59)
Avail: NTIS HC A22/MF A01 CSCL 09B

N89-19850*# Calspan-Buffalo Univ. Research Center, NY.
AN INTELLIGENT MULTI-MEDIA HUMAN-COMPUTER DIALOGUE SYSTEM
J. G. Neal, K. E. Bettinger, J. S. Byoun, Z. Dobes, and C. Y. Thielman *In* NASA. Lyndon B. Johnson Space Center, 2nd Annual Workshop on Space Operations Automation and Robotics (SOAR 1988) Nov. 1988 p 245-251 (For primary document see N89-19817 12-59)
(Contract F30603-87-C-0136)
Avail: NTIS HC A22/MF A01 CSCL 09B

61 COMPUTER PROGRAMMING AND SOFTWARE

Includes computer programs, routines, alogorithms, and specific applications, e.g., CAD/CAM.

N89-19899*# National Aeronautics and Space Administration. Langley Research Center, Hampton, VA.
HIGH-SPEED REAL-TIME ANIMATED DISPLAYS ON THE ADAGE (TRADEMARK) RDS 3000 RASTER GRAPHICS SYSTEM
William M. Kahlbaum, Jr. and Katrina L. Ownbey Washington Apr. 1989 48 p
(NASA-TM-4095; L-16504; NAS 1.15:4095) Avail: NTIS HC A03/MF A01 CSCL 09B

Techniques which may be used to increase the animation update rate of real-time computer raster graphic displays are discussed. They were developed on the ADAGE RDS 3000 graphic system in support of the Advanced Concepts Simulator at the NASA Langley Research Center. These techniques involve the use of a special purpose parallel processor, for high-speed character generation. The description of the parallel processor includes the Barrel Shifter which is part of the hardware and is the key to the high-speed character rendition. The final result of this total effort was a fourfold increase in the update rate of an existing primary flight display from 4 to 16 frames per second.
Author

N89-19900# Tennessee Univ., Knoxville. Dept. of Electrical and Computer Engineering.
A 2-D AND 3-D ROBOT PATH PLANNING ALGORITHM BASED ON QUADTREE AND OCTREE REPRESENTATION OF WORKSPACE
A. K. HyderAli and M. A. Abidi 1988 6 p Presented at the Southeastcon '88 Conference and Exhibit, Knoxville, TN, 11 Apr. 1988
(Contract DE-FG02-86NE-37968)
(DE89-005014; DOE/NE-37968/1; CONF-880433-8) Avail: NTIS HC A02/MF A01

A 2-D and 3-D path planning algorithm for robot navigation and manipulation is developed in this paper. This method is of particular interest for robotic systems which require both 2-D navigation to reach the work site and 3-D path planning for on-site manipulation and inspection. This study extends the approach of 2-D path planning to 3-D with minimum effort. The quadtree and octree structures are used for 2-D and 3-D workspace representation, respectively. Quadtrees and octrees are generated from brightness image of the workspace obtained using a camera mounted on a robot. Path generation is based on the A* algorithm. The spatial length and the clearance space available for the robot are used as constraints in the path generation. The results of this approach are illustrated through an experimental system setup on a robotic workstation. DOE

N89-19901# Illinois Univ., Urbana. Applied Computation Theory Group.
DYNAMIC DATA STRUCTURES FOR TWO-DIMENSIONAL SEARCHING
Roberto Tamassia Aug. 1988 144 p
(Contract N00014-84-C-0149; NSF ECS-84-10902)
(AD-A201173; ACT-100; UILU-ENG-88-2250) Avail: NTIS HC A07/MF A01 CSCL 12D

This report investigates dynamic data structures and algorithms for searching in a subdivision of the plane. Three specific problems have been addressed in this area. The first problem, dynamic point location, considers a geometric subdivision of the plane into polygonal regions, and asks for the region that contains a given query point. The second problem, dynamic planar embedding, considers a topological subdivision of the plane induced by a planar embedding of a graph, and asks for a region that contains two given query vertices on its boundary (if one exists). The third problem, dynamic transitive closure, considers a planar acyclic

digraph embedded in the plane, and asks for testing the existence of and/or reporting a directed path between two query vertices. In all of the three problems the update operations consist of inserting/deleting vertices and edges. We present several dynamic techniques that improve previously published results in the area. The space requirement ranges from O(n) to O(nlogn), and the query and update times range from O(logn) to O(sq log), where n is the size of the subdivision. In addition to their good theoretical space/time performance, all the data structures and algorithms presented are also practical and easy to implement, and therefore suited for real-world applications. GRA

N89-19902# Nevada Univ., Las Vegas. Dept. of Computer Science and Electrical Engineering.
ON PURELY EXPONENTIAL LOGIC QUERIES
Kazem Taghva and Tian-Zheng Wu (New Mexico Inst. of Mining and Technology, Socorro.) May 1988 18 p
(Contract DAAL03-87-G-0004)
(AD-A201259; ARO-24960.19-MA) Avail: NTIS HC A03/MF A01 CSCL 12E

This paper, provides a syntactic condition under which these purely exponential queries can be rewritten as linear queries. As an application of this result, the authors give a new proof for Guessarian's theorem on converting binary chained exponential queries to linear queries. Moreover, an infinite chain of progressively weaker template dependencies is constructed via expansion of the logic program for transitive closure of a relation R. This natural chain yields another proof for the result of R, Fagin, et al. GRA

N89-19903# Carnegie-Mellon Univ., Pittsburgh, PA. Software Engineering Inst.
ISTAR EVALUATION Final Technical Report
Marc H. Graham and Daniel H. Miller Jul. 1988 212 p
(Contract F19628-85-C-0003)
(AD-A201345; CMU/SEI-88-TR-3; ESD-TR-88-004) Avail: NTIS HC A10/MF A01 CSCL 12F

ISTAR is a software development and project management environment that integrates management and technical development activities. It is based on the contract model, whose primary objective is that every individual in the organization know what is expected of him or her. To accomplish this, the relationships among the individuals of the organization are modeled as contracts. Each contract has a specification of the work to be performed under it, a person to whom it has been assigned, and a person for whom the work is being done. Chapter 2 describes the contract model both as a project management structure and as a data storage structure. It was found that the emphasis on project hygiene leads to a strict separation of user data spaces which causes excess data storage requirements and data movement operations. This, in turn, may make data sharing and cooperative work more difficult. ISTAR's user interface is also described in Chapter 2. That interface has a high degree of consistency because all user interaction is mediated through imperial Software's proprietary editor, E, which is window- and menu-oriented. Chapter 3, which forms the bulk of the report, deals with the functional areas (that is, those tool sets supplied with ISTAR) which were of most interest to us. The remaining tool sets are described in Chapter 4. GRA

N89-19904# Illinois Univ., Urbana. Coordinated Science Lab.
FAST AND PROCESSOR-EFFICIENT PARALLEL ALGORITHMS FOR REDUCIBLE FLOW GRAPHS
Vijaya Ramachandran Nov. 1988 28 p
(Contract N00014-84-C-0149)
(AD-A201651; UILU-ENG-88-2257; ACT-103) Avail: NTIS HC A03/MF A01 CSCL 12E

This document presents parallel NC algorithms for recognizing Reducible Flow Graphs (RFG), and for finding dominators, minimum feedback vertex sets, and a depth first search numbering in an RFG. All of these algorithms run in polylog parallel time using M (n) processors, where M (n) is the number of processors needed to multiply two nxn matrices in polylog time; this is the best processor bound currently known for polylog-time parallel algorithms for directed graphs. It is shown that finding a minimum feedback vertex is in vertex-weighted RFG's or finding a minimum feedback set in arc-weighted RFG's is complete. For arc or vertex weights in unary, RNC algorithms are presented for these problems and show that these problems are in NC if and only if the problem of finding a maximum matching is in NC. GRA

N89-19905# Naval Postgraduate School, Monterey, CA.
AN INTERROGATIVE MODEL OF COMPUTER-AIDED ADAPTIVE TESTING: SOME EXPERIMENTAL EVIDENCE M.S. Thesis
Patrick A. ODonnell Sep. 1988 101 p
(AD-A201675) Avail: NTIS HC A06/MF A01 CSCL 05H

This thesis proposes and validates an interrogative diagnostic model of computer-aided, adaptive testing. The model uses an algorithm based on Bayesian techniques to determine both the number and the difficulty level of questions to present. The power of the model lies in its ability to automatically adapt a testing session to the individual's level of knowledge by choosing the domain, type and number of questions. The model was implemented as a computer program and was tested in an experiment with 34 military officers who were masters degree students. Analysis of the results indicated that the IDM can evaluate student knowledge as effectively as traditional written examinations but with a significantly less number of questions and shorter test duration. GRA

N89-19906# Oak Ridge National Lab., TN. Engineering Physics and Mathematics Div.
BIFURCATING OPTIMIZATION ALGORITHMS AND THEIR POSSIBLE APPLICATION
J. C. Culioli and V. Protopopescu Nov. 1988 37 p
(Contract DE-AC05-84OR-21400)
(DE89-005692; ORNL/TM-10976) Avail: NTIS HC A03/MF A01

A new class of optimization algorithms for linear and nonlinear problems is proposed. The algorithms are based on sigmoidic updatings and can be looked upon as nonlinear multidimensional maps. The bifurcation and chaotic regimes of these maps are analyzed and their possible applications in optimization problems are indicated. DOE

N89-19907# Army Construction Engineering Research Lab., Champaign, IL.
INTELLIGENT EMBEDDED INSTRUCTION FOR COMPUTER-AIDED DESIGN (CAD) SYSTEMS
Doris S. Shaw, L. M. Golish, and Robert L. Johnson Oct. 1988 51 p
(AD-A201811; CERL-TR-P-89/03) Avail: NTIS HC A04/MF A01 CSCL 12E

User training on computer-aided design (CAD) systems traditionally has been expensive and ineffective. In addition, rapid changes in CAD software demand frequent update instruction to be able to take full advantage of the system's capabilities. As the U.S. Army Corps of Engineers begins using CAD technology to an increasing degree, there is a great need for low-cost, effective teaching programs. Embedded instruction programs represent a promising answer to this need. This technology involves the incorporation of tutorial programs directly into the software being taught, with the software used to drive the training session. Such a teaching method allows users to participate in self-paced study on the system they will be using in actual day-to-day operations. The U.S. Army Construction Engineering Research Laboratory (USE-CERL) has developed and tested an embedded instruction program for teaching CAD. The Program was demonstrated in a field test funded under the Technology Transfer Test Bed program. The field test results indicate that architects and engineers profit from online instruction embedded in the CAD system that they are learning. There is wide variability in the time spent studying the lessons as well as in learning strategies employed by different students. Follow-up questionnaires revealed a preference for this type of instruction over traditional methods. GRA

N89-19908# Stanford Univ., CA. Systems Optimization Lab.
SOFTWARE PERFORMANCE ON NONLINEAR LEAST-SQUARES PROBLEMS
Christina Fraley Sep. 1988 116 p
(Contract DE-FG03-87ER-25030; NSF ECS-87-15153)
(AD-A201879; SU-SOL-88-17) Avail: NTIS HC A06/MF A01 CSCL 12E

This paper presents numerical results for a large and varied set of problems using software that is widely available and has under gone extensive testing. The algorithms implemented in this software include Newton-based line search and trust-region methods for unconstrained optimization, as well as Gauss-Newton, Levenberg Marquardt, and special quasi-Newton methods for nonlinear least squares. Rather than give a critical assessment of the software itself, our original purpose was to use the best available software to compare the underlying algorithms, to identify classes of problems for each method on which the performance is either very good or very poor, and to provide benchmarks for future work in nonlinear least squares and unconstrained optimization. The variability in the results made it impossible to meet either of the first two goals; however the results are significant as a step toward explaining why these aims are so difficult to achieve. GRA

N89-19909# Howard Univ., Washington, DC.
ANALYSIS OF BLENDING ALGORITHMS IN COMPUTER GRAPHICS Final Report, 1 Aug. 1986 - 31 Jul. 1988
Ronald J. Leach 17 Oct. 1988 110 p
(Contract DAAL03-86-G-0085)
(AD-A201921; ARO-23714.7-MA-H) Avail: NTIS HC A06/MF A01 CSCL 12E

The research on this project centered around the analysis, development, and implementation of fast algorithms for representing a surface which blends together two or more intersecting surfaces. The blending surface should provide a smoother transition than is available when simply considering the intersection of the surfaces. The algorithms developed must be efficient because the major portion of computing time in a solid modeling system should be devoted to the important problems of data representation, object display, surface analysis (ray tracing, shadowing, etc.) and scene analysis (hidden line/surface removal, etc.) The important features of a blending surface are speed of computation, ability to be incorporated into the other features of a solid modeling system (such as hidden line/surface removal), and the visual quality of the blended image. This report is organized as follows. Section 1 is an introduction. Section 2 briefly describes some basic concepts from solid modeling. Section 3 is a description of the organization of the research, major findings, and publications. Section 4 describes additional directions for research. GRA

N89-19910# Naval Postgraduate School, Monterey, CA.
A SURVEY OF AUTOMATIC CODE GENERATING SOFTWARE M.S. Thesis
Sherman L. OBrien Sep. 1988 81 p
(AD-A201963) Avail: NTIS HC A05/MF A01 CSCL 12E

The advances made in computer hardware development have long outdistanced the computer software needed to make that hardware perform useful work for the user. This has precipitated a software crisis in the industry and spawned many potential solutions for alleviating the crisis. Among the various solutions are software systems that will automatically write program code. This thesis examines four such software systems currently available to a system developer giving a brief description of the product, principle behind its operation and possible applications. Additionally, it provides the reader background information on computer programming languages, reasons for the software crisis, the software development life cycle, and a method of classification and taxonomy of software development tools. The thesis concludes that these tools, properly applied, can be useful in relieving the software crisis in an organization but will not eliminate the crisis or the need for programmers. GRA

N89-19911# Massachusetts Inst. of Tech., Cambridge. Microsystems Research Center.
COMPUTER-AIDED FABRICATION SYSTEM IMPLEMENTATION Semiannual Technical Report, 1 Apr. - 30 Sep. 1988
Paul Penfield, Jr., Dimitri A. Antoniadis, Stanley B. Gershwin, Stephen D. Senturia, and Emanuel M. Sachs 30 Sep. 1988 32 p
(Contract N00014-85-K-0213)
(AD-A202128; AD-E501048) Avail: NTIS HC A03/MF A01 CSCL 09A

The objective of this contract is to do research supporting the development of a computer-aided fabrication system that will serve the needs of the American semiconductor industry and the VLSI design community. The semiconductor industry requires computer tools to enhance yields and reduce cost. VLSI designers can benefit from the ability to specify application-specific processes to fabricate their application-specific integrated circuits. In support of these goals, specific projects are in place to design, develop, and implement a hardware/software CAF system architecture; to develop aids to specifying process flows in a modular way; to develop models for semiconductor fabrication equipment; to develop technology computer aided design (TCAD) tools for the mechanical properties of integrated structures; and to develop and implement algorithms and programs to assist in scheduling of fabrication operations. GRA

N89-19912# Stanford Univ., CA. Systems Optimization Lab.
A HEURISTIC CEILING POINT ALGORITHM FOR GENERAL INTEGER LINEAR PROGRAMMING
Robert M. Saltzman Nov. 1988 84 p
(Contract N00014-85-K-0343)
(AD-A202285; SU-SOL-88-19) Avail: NTIS HC A05/MF A01 CSCL 12D

This report describes a heuristic algorithm for the pure, general Integer Linear Programming problem (ILP). In attempting to quickly obtain a near-optimal solution (with-out concern for establishing optimality), the algorithm searches for a feasible 1-ceiling point. A feasible 1-ceiling point may be thought of as an integer solution lying on or near the boundary of the feasible region for the LP-relaxation associated with the ILP. Precise definitions of 1-ceiling points and the role they play in an integer linear program are presented in a recent report by the authors. One key theorem therein demonstrates that all optimal solutions for an ILP whose feasible region is non-empty and bounded are feasible 1-ceiling points. Consequently, such a problem may be solved by enumerating just its feasible 1-ceiling points. Our heuristic approach is based upon the idea that a feasible 1-ceiling point found relatively near the optimal solution for the LP-relaxation is apt to have a high (possibly even optimal) objective function value. Having applied this Heuristic Ceiling Point Algorithm to 48 test problems taken from the literature, it appears that searching for such 1-ceiling points usually does provide a very good solution with a moderate amount of computational effort. GRA

N89-19913# Stanford Univ., CA. Systems Optimization Lab.
AN EXACT CEILING POINT ALGORITHM FOR GENERAL INTEGER LINEAR PROGRAMMING
Robert M. Saltzman and Frederick S. Hillier Nov. 1988 81 p
(Contract N00014-85-K-0343)
(AD-A202286; SU-SOL-88-20) Avail: NTIS HC A05/MF A01 CSCL 12D

This report describes an exact algorithm for the pure, general Integer Linear Programming problem (ILP). Common applications of this model occur in capital budgeting (project selection), resource allocation and fixed-charge (plant location) problems. The central theme of our algorithm is to enumerate a subset of all solutions called feasible 1-ceiling points. A feasible 1-ceiling point may be thought of as an integer solution lying on or near the boundary of the feasible region for the LP-relaxation associated with (ILP). Precise definitions of 1-ceiling points and the role they play in an integer linear program are presented in a recent report by the authors. One key theorem therein demonstrates that all optimal

solutions for an (ILP) whose feasible region is non-empty and bounded are feasible 1-ceiling points. Consequently, such a problem may be solved by enumerating just its feasible 1-ceiling points. Our approach is to implicitly enumerate 1-ceiling points with respect to one constraint at a time while simultaneously considering feasibility. Computational results from applying this incumbent-improving Exact Ceiling Point Algorithm to 48 test problems taken from the literature indicate that this enumeration scheme may hold potential as a practical approach for solving problems with certain types of structure. GRA

N89-19914 Politecnico di Milano (Italy). Dipt. di Elettronica.
A GENERAL WAY TO PUT TIME IN PETRI NETS
Carlo Ghezzi, Dino Mandrioli, Sandro Morasca, and Mauro Pezze 1988 26 p
(Rept-88-011; ETN-89-93716) Avail: Politecnico di Milano, Piazza Leonardo da Vinci 32, 20133 Milan, Italy

A way of putting time in Petri nets is proposed to unify and generalize previous proposals within a framework consistent with the rationale of the original Petri model, which requires that transition firing depends only on the marking of the places connected to the transition itself. The proposal consists of considering time as a stamp attached to each token. Transition firing can affect the value of the timestamp only consistently with suitable requirements. The user can specify time constraints of the system to be modelled using several external semantics that can be chosen according to the application needs. Semantics can then be rigorously defined in terms of a more basic model, that acts as a kernel for a variety of user interfaces. ESA

N89-19915 Politecnico di Milano (Italy). Dipartimento di Elettronica.
SPECIFICATION AND MANAGEMENT OF DATABASE INTEGRITY CONSTRAINTS THROUGH LOGIC PROGRAMMING
S. Ceri (Modena Univ., Italy) and F. Garzotto 1988 42 p
(Rept-88-025; ETN-89-93721) Avail: Politecnico di Milano, Piazza Leonardo da Vinci 32, 20133 Milan, Italy

The application of logic programming for expressing integrity constraints and for validating the correctness of transactions in data bases is described. Design and specification of a constraints management system which can verify the correctness of transactions, explain which constraints are violated, and suggest compensation actions to the user are illustrated. The proposed approach fits naturally within the conventional organization of data bases and can be easily integrated with transaction management systems. ESA

N89-19916# Sandia National Labs., Albuquerque, NM.
CAD DIRECTED ROBOTIC EDGE FINISHING
Cliff Loucks, Colin Selleck, and Sigfried Thunborg Dec. 1988 20 p Presented at the Deburring and Surface Conditioning, San Diego, CA, 14 Feb. 1989
(Contract DE-AC04-76DP-00789)
(DE89-005347; SAND-88-2251C; CONF-890253-1) Avail: NTIS HC A03/MF A01

The Robotic Edge Finishing Laboratory at Sandia National Laboratories is developing four areas of technology required for automated deburring and chamfering: (1) the automatic programming of robot trajectories and deburring processes using information derived from a CAD database, (2) the use of machine vision for locating the workpiece coupled with force control to ensure proper tool contact, (3) robotic deburring and machining of precision chamfered edges, and (4) in-process automated inspection of the formed edge. The Laboratory, its components, integration, and results from edge finishing experiments to date are described here. DOE

N89-19917# Nationaal Inst. voor Kernfysica en Hoge Energiefysica, Amsterdam (Netherlands).
REMOTE CONTROL SYSTEM [HET REMOTE CONTROL SYSTEEM]
P. P. M. Jansweijer 1988 43 p In DUTCH
(DIGEL-79; ETN-89-93880) Avail: NTIS HC A03/MF A01

A remote control system was designed for the different signals of a spectrometer. The system can control relay switches. The construction (hardware and software) as well as the operation of the remote control system are described. ESA

N89-19918# Technische Univ., Delft (Netherlands). Faculty of Technical Mathematics and Informatics.
LINEAR PROGRAMMING ALONG THE TRAJECTORY OF THE PROBLEM IN POLYNOMIAL TIME
C. Roos 1988 37 p
(Rept-88-17; ISSN-0920-8577; ETN-89-94001) Copyright Avail: NTIS HC A03/MF A01

An interior point method for the solution of the linear programming problem is presented. It is shown that the method admits a polynomial time bound. The method is based on the use of the trajectory of the problem, which makes it conceptually very simple. It has the advantage over related methods that it requires no problem transformation (either affine or projective) and that the feasible region may be unbounded. The method generates at each stage solutions of both the primal and the dual problem. This implies that, contrary to the Simplex method, the quality of the present solution is known at each stage. A practical (i.e., a deep step) version of the algorithm is included. ESA

N89-19919# Technische Univ., Delft (Netherlands). Faculty of Technical Mathematics and Informatics.
FROM ALGOL 60 TO Ada: PROBLEMS, SOLUTIONS, FEASIBILITY
R. D. Huijsman, J. vanKatwijk, C. Pronk, and W. J. Toetenel 1988 47 p
(Rept-88-41; ISSN-0920-8577; ETN-89-94010) Copyright Avail: NTIS HC A03/MF A01

Mechanical conversion of Algol 60 programs into Ada programs was studied. Major problem areas include handling goto's, handling procedures and parameters, and interaction with the environment. A large number of Algol 60 constructs turn out to be hard or even impossible to map. Tests, mainly in scientific computation, suggest that, depending on the amount of effort to be put into the project, between 80 pct and 90 pct of the source code can be translated mechanically. Translation based only on lexical and syntactical information is possible for about 50 pct of the source text. Taking semantics into account augments the percentage to 80 pct ot 90 pct. The remaining 10 pct to 20 pct of the code can be translated partly if certain forms of idiom are taken into account, the rest of the code being not mechanically translatable. The inability to translate 20 pct of the source is even worse than it seems. A manual translation of the remaining code often requires a complete restructuring of the program, including those parts that could be translated mechanically. Since translation is manual to a considerable extent, maintenance is also problematic and only possible when applied to the resulting Ada programs. Unfortunately, the readability and recognizability of the latter are seriously impaired by the consequences of partial manual translation. ESA

N89-19920# Technische Univ., Delft (Netherlands). Faculty of Technical Mathematics and Informatics.
THE INFLUENCE OF THE POTENTIAL FUNCTION ON THE PERFORMANCE OF A TRAJECTORY FOLLOWING ALGORITHM FOR THE LINEAR PROGRAMMING PROBLEM
C. Roos 1988 29 p
(Rept-88-44; ISSN-0920-8577; ETN-89-94012) Copyright Avail: NTIS HC A03/MF A01

The difference in (theoretical) performance of Karmarkar's (1984) projective method for linear programming, and more recent path following methods by a factor sq rt n, where n is the number of variables is studied. Results show that this difference in performance may well be due to the use of different potential functions. ESA

N89-19921# Royal Signals and Radar Establishment, Malvern (England).
USER-EXTENSIBLE GRAPHICS USING ABSTRACT STRUCTURE
P. W. Core Aug. 1987 79 p
(BR104469; RSRE-87011) Avail: NTIS HC A05/MF A01
A means of creating an editor which allows its users to extend the classes of objects manipulated by it is described. This was achieved by creating an abstract structure representing object classes. An example of such an editor was implemented on Perq Flex making use of the procedure values. Author

N89-19922# Los Alamos National Lab., NM.
A CURVE-FITTING PACKAGE FOR PERSONAL COMPUTERS
Celina M. Ortiz, P. M. Rinard, and A. Goldman Nov. 1987 55 p
(LA-11082-MS) Avail: NTIS HC A04/MF A01
A curve-fitting routine based on the Deming method was developed into a package for personal computers. In addition to the curve-fitting protion, the package includes a data editor, a plotting package, statistical analyses, and interpolation routines. The features of the package, the algorithms used, and suggestions on how to run it most effectively are described. Although several languages and computers were used with the package over the years, applications are generalized. Author

N89-19236*# Boeing Military Airplane Development, Seattle, WA.
EXTENSIONS AND IMPROVEMENTS ON XTRAN3S
C. J. Borland *In* NASA, Langley Research Center, Transonic Unsteady Aerodynamics and Aeroelasticity 1987, Part 1 Feb. 1989 p 15-45 (For primary document see N89-19234 12-02)
Avail: NTIS HC A12/MF A01 CSCL 09B

N89-19833*# National Aeronautics and Space Administration. Langley Research Center, Hampton, VA.
VALIDATION OF HIGHLY RELIABLE, REAL-TIME KNOWLEDGE-BASED SYSTEMS
Sally C. Johnson *In* NASA. Lyndon B. Johnson Space Center, 2nd Annual Workshop on Space Operations Automation and Robotics (SOAR 1988) Nov. 1988 p 123-129 (For primary document see N89-19817 12-59)
Avail: NTIS HC A22/MF A01 CSCL 09B

N89-19834*# Lockheed Missiles and Space Co., Austin, TX. Artificial Intelligence Center.
TESTING EXPERT SYSTEMS
C. L. Chang and R. A. Stachowitz *In* NASA. Lyndon B. Johnson Space Center, 2nd Annual Workshop on Space Operations Automation and Robotics (SOAR 1988) Nov. 1988 p 131-135 (For primary document see N89-19817 12-59)
Avail: NTIS HC A22/MF A01 CSCL 09B

N89-19837*# Ohio State Univ., Columbus.
REDUCING UNCERTAINTY BY USING EXPLANATORY RELATIONSHIPS
John R. Josephson *In* NASA. Lyndon B. Johnson Space Center, 2nd Annual Workshop on Space Operations Automation and Robotics (SOAR 1988) Nov. 1988 p 149-151 (For primary document see N89-19817 12-59)
Avail: NTIS HC A22/MF A01 CSCL 09B

N89-19843*# Aerospace Corp., El Segundo, CA.
PORTABLE INFERENCE ENGINE: AN EXTENDED CLIPS FOR REAL-TIME PRODUCTION SYSTEMS
Thach Le and Peter Homeier *In* NASA. Lyndon B. Johnson Space Center, 2nd Annual Workshop on Space Operations Automation and Robotics (SOAR 1988) Nov. 1988 p 187-192 (For primary document see N89-19817 12-59)
Avail: NTIS HC A22/MF A01 CSCL 09B

N89-19844*# Intellicorp, Mountain View, CA.
BROWSING SCHEMATICS: QUERY-FILTERED GRAPHS WITH CONTEXT NODES
Eugene C. Ciccarelli and Bonnie A. Nardi *In* NASA. Lyndon B. Johnson Space Center, 2nd Annual Workshop on Space Operations Automation and Robotics (SOAR 1988) Nov. 1988 p 193-204 (For primary document see N89-19817 12-59)
Avail: NTIS HC A22/MF A01 CSCL 09B

N89-19851*# Columbia Univ., New York, NY. Dept. of Computer Science.
KNOWLEDGE-BASED GRAPHICAL INTERFACES FOR PRESENTING TECHNICAL INFORMATION
Steven Feiner *In* NASA. Lyndon B. Johnson Space Center, 2nd Annual Workshop on Space Operations Automation and Robotics (SOAR 1988) Nov. 1988 p 253-257 Sponsored in part by Hewlett-Packard Co. (For primary document see N89-19817 12-59)
(Contracts N00039-84-C-0165; NYSSTF-CAT(87)-5; N00014-78-C-0396; NSF INT-73-02268)
Avail: NTIS HC A22/MF A01 CSCL 09B

N89-19867*# Washington Univ., Seattle. Dept. of Electrical Engineering.
CAD-MODEL-BASED VISION FOR SPACE APPLICATIONS
Linda G. Shapiro *In* NASA. Lyndon B. Johnson Space Center, 2nd Annual Workshop on Space Operations Automation and Robotics (SOAR 1988) Nov. 1988 p 361-367 (For primary document see N89-19817 12-59)
Avail: NTIS HC A22/MF A01 CSCL 09B

N89-19869*# National Aeronautics and Space Administration. Lyndon B. Johnson Space Center, Houston, TX.
ROBOT PATH PLANNING USING A GENETIC ALGORITHM
Timothy F. Cleghorn, Paul T. Baffes, and Liu Wang *In its* 2nd Annual Workshop on Space Operations Automation and Robotics (SOAR 1988) Nov. 1988 p 383-389 (For primary document see N89-19817 12-59)
Avail: NTIS HC A22/MF A01 CSCL 09B

N89-19928# Jet Propulsion Lab., California Inst. of Tech., Pasadena.
RECOGNITION OF OBJECT DOMAIN BY COLOR DISTRIBUTION
Takako Mugitani, Mitsuru Mifune, and Shigeki Nagata *In its* JPRS Report: Science and Technology. Japan: 7th Artificial Intelligence Symposium 14 Sep. 1988 p 49-54 Transl. into ENGLISH of paper presented at Dainanakai Chishiki Kogaku Symposium, Tokyo, Japan, 1988 p 125-128 (For primary document see N89-19924 12-63)
Avail: NTIS HC A04/MF A01

N89-20061*# Norwich Univ., Northfield, VT. Dept. of Computer Science Engineering.
DEVELOPMENT OF A SOFTWARE INTERFACE FOR OPTICAL DISK ARCHIVAL STORAGE FOR A NEW LIFE SCIENCES FLIGHT EXPERIMENTS COMPUTER Final Report
Peter N. Bartram *In* NASA, Lyndon B. Johnson Space Center, National Aeronautics and Space Administration (NASA)/American Society for Engineering Education (ASEE) Summer Faculty Fellowship Program 1988, Volume 1 Feb. 1989 10 p (For primary document see N89-20058 12-99)
Avail: NTIS HC A09/MF A01 CSCL 09B

N89-20062*# Illinois State Univ., Normal. Dept. of Applied Computer Science.
COMPUTER TECHNOLOGIES AND INSTITUTIONAL MEMORY Final Report
Christopher Bell and Roy Lachman (Houston Univ., TX.) *In* NASA, Lyndon B. Johnson Space Center, National Aeronautics and Space Administration (NASA)/American Society for Engineering Education (ASEE) Summer Faculty Fellowship Program 1988, Volume 1 Feb. 1989 22 p (For primary document see N89-20058 12-99)
Avail: NTIS HC A09/MF A01 CSCL 09B

N89-20079*# DePaul Univ., Chicago, IL. Dept. of Computer Science.
TOWARD AN IMAGE COMPRESSION ALGORITHM FOR THE HIGH-RESOLUTION ELECTRONIC STILL CAMERA Final Report
Rosalee Nerheim *In* NASA, Lyndon B. Johnson Space Center, National Aeronautics and Space Administration (NASA)/American Society for Engineering Education (ASEE) Summer Faculty Fellowship Program 1988, Volume 2 Feb. 1989 12 p (For primary document see N89-20073 12-99)
Avail: NTIS HC A09/MF A01 CSCL 09B

62 COMPUTER SYSTEMS

Includes computer networks and special application computer systems.

N89-19923# Massachusetts Inst. of Tech., Cambridge. Microsystems Research Center.
CRITICAL PROBLEMS IN VERY LARGE SCALE COMPUTER SYSTEMS Semiannual Technical Report, 1 Apr. - 30 Sep. 1988
Paul Penfield, Jr., Anant Agarwal, William J. Dally, Srinivas Devadas, and Thomas F. Knight, Jr. 30 Sep. 1988 86 p
(Contract N00014-85-K-0825)
(AD-A202129; AD-E501048) Avail: NTIS HC A05/MF A01 CSCL 12G

The research vehicle for this contract is the largest possible computer that could be conceived for the mid to late 1990s. The technical challenges of such a machine serve as the guiding stimulus for the research carried out and reported here. We imagine this machine to occupy a 14-story building, to cost upwards of $1,000,000,000, and to be so colossal that the nation can only afford one or two of them. The available chip technology and machine size are consistent with a million FLOPS (that's 10 to the 15th) and a million billion Bytes of memory. It will dissipate 50 megawatts of power using CMOS technology. Communication across the machine will be much slower than computation at a node. The architecture, software, interconnect technology, packaging, and operating system are unknown. This investigation deals with hardware technology, software techniques, programming algorithms, communications, processing elements, and applications. The study will determine the plausibility (not feasibility) of such a machine. Progress in these various areas are highlighted in the individual sections below. GRA

N89-19824*# Battelle Columbus Labs., OH.
DIAGNOSTICS IN THE EXTENDABLE INTEGRATED SUPPORT ENVIRONMENT (EISE)
James R. Brink and Paul Storey (Sacramento Air Logistics Center, McClellan AFB, CA.) *In* NASA. Lyndon B. Johnson Space Center, 2nd Annual Workshop on Space Operations Automation and Robotics (SOAR 1988) Nov. 1988 p 41-46 (For primary document see N89-19817 12-59)
Avail: NTIS HC A22/MF A01 CSCL 09B

63 CYBERNETICS

Includes feedback and control theory, artificial intelligence, robotics and expert systems.

For related information see also *54 Man/System Technology and Life Support.*

N89-19924# Joint Publications Research Service, Arlington, VA.
JPRS REPORT: SCIENCE AND TECHNOLOGY. JAPAN: 7TH ARTIFICIAL INTELLIGENCE SYMPOSIUM
14 Sep. 1988 57 p Transl. into ENGLISH of proceedings of Dainanakai Chishiki Kogaku Symposium, Tokyo, Japan, 22-23 Mar. 1988 Symposium held in Tokyo, Japan, 22-23 Mar. 1988
(JPRS-JST-88-020) Avail: NTIS HC A04/MF A01

Selections are presented from the 7th Artificial Intelligence Symposium held in Tokyo in March 1988. Topics discussed include problems in structuring a large-scale expert system, knowledge expression, production scheduling, evaluation support systems, robotics, and object recognition by color. For individual titles, see N89-19925 through N89-19928.

N89-19925# Joint Publications Research Service, Arlington, VA.
PROBLEMS IN STRUCTURING LARGE-SCALE EXPERT SYSTEM
Shigenbu Kobayashi, Katsuhiko Yui, and Masaharu Moritani *In its* JPRS Report: Science and Technology. Japan: 7th Artificial Intelligence Symposium 14 Sep. 1988 p 1-5 Transl. into ENGLISH of paper presented at Dainanakai Chishiki Kogaku Symposium, Tokyo, Japan, 1988 p 1-6 (For primary document see N89-19924 12-63)
Avail: NTIS HC A04/MF A01

The problems in regard to an expert system are largely divided into analysis and synthesis types. An analysis type problem is one in which, given the construction of a system and the features of its subsystem, the system's features are inferred. A synthesis type problem is one in which, given the features of a system, the system construction and its subsystem's features are inferred so that they can be realized. Generally speaking, given the construction of a system and its subsystem's features, there is only one choice for the system's features, whereas given the system's features, the choices for the subsystem features and system construction are infinete. Both analysis and synthesis types of problems are discussed. The influence of boundary conditions on the nonlinearity, about which very little is known, was also investigated. Comparison with the theoretical and experimental results by previous researchers was made. Qualitative agreement with experimental resuts was obtained. Author

N89-19926# Joint Publications Research Service, Arlington, VA.
EVALUATION SUPPORT SYSTEM FOR MULTIPLE R AND D PROJECTS
Yoshinori Katayama and Mitsuhiko Toda *In its* JPRS Report: Science and Technology. Japan: 7th Artificial Intelligence Symposium 14 Sep. 1988 p 27-40 Transl. into ENGLISH of paper presented at Dainanakai Chishiki Kogaku Symposium, Tokyo, Japan, 1988 p 31-36 (For primary document see N89-19924 12-63)
Avail: NTIS HC A04/MF A01

The evaluation of groups of research and development (R and D) projects largely depends on the experiential judgment of experts. A method is proposed for the total evaluation by experts of groups of projects and supporting decisionmaking based on it, focusing on engineering repercussion effects of project information. The basic framework of the support method involves knowledge of rules to deduce engineering impact relationships and relevant knowledge to expand the applicability of knowledge of these rules. An evaluation support system utilizes these rules as a knowledge base and supports experts' evaluation activities for multiple R and D projects. Examples are cited of groups of R and D projects that saved energy as application examples of this evaluation support system and results of their evaluations are shown.
Author

N89-19927# Joint Publications Research Service, Arlington, VA.
INTELLIGENT MOBILE ROBOT WORKING IN UNKNOWN ENVIRONMENT
Norio Baba and Yasuhiro Shiraishi *In its* JPRS Report: Science and Technology. Japan: 7th Artificial Intelligence Symposium 14 Sep. 1988 p 41-48 Transl. into ENGLISH of paper presented at Dainanakai Chishiki Kogaku Symposium, Tokyo, Japan, 1988 p 61-64 (For primary document see N89-19924 12-63)
Avail: NTIS HC A04/MF A01

In work that entails danger, robots should be used to replace human workers as much as possible. In fields such as those related to atomic energy, where direct harm to the human organism is likely to occur, in particular, the introduction of robots is indispensable. In such cases, however robots have to work under conditions of insufficient human monitoring. It is important to provide the robot with the ability to judge the situation and act on its

own--that is, with the intelligence to properly judge the circumstances. Research on the intellectualization of robots has begun, and great expectations are harbored for the research results to be accumulated. The problem of learning unknown environments for basic research on the intellectual action of mobile robots is the subject discussed. Author

N89-19928# Jet Propulsion Lab., California Inst. of Tech., Pasadena.
RECOGNITION OF OBJECT DOMAIN BY COLOR DISTRIBUTION **c61**
Takako Mugitani, Mitsuru Mifune, and Shigeki Nagata *In its* JPRS Report: Science and Technology. Japan: 7th Artificial Intelligence Symposium 14 Sep. 1988 p 49-54 Transl. into ENGLISH of paper presented at Dainanakai Chishiki Kogaku Symposium, Tokyo, Japan, 1988 p 125-128 (For primary document see N89-19924 12-63)
Avail: NTIS HC A04/MF A01

For the image processing of an object in its natural image, it is necessary to extract in advance the object to be processed from its image. To accomplish this the outer shape of an object is extracted through human instructions, which requires a great deal of time and patience. A method involving the setting of a model of color distribution on the surface of an object is described. This method automatically provides color recognition, a piece of knowledge that represents the properties of an object, from its natural image. A method for recognizing and extracting the object in the image according to the color recognized is also described. Author

N89-19929# Massachusetts Inst. of Tech., Lexington. Lincoln Lab.
THE BOLTZMANN MACHINE: A SURVEY AND GENERALIZATION
Mitchell D. Eggers 8 Jul. 1988 58 p
(Contract F19628-85-C-0002)
(AD-A197976; TR-805; ESD-TR-87-281) Avail: NTIS HC A04/MF A01 CSCL 23C

A tutorial is presented describing a general machine learning theory which spawns a class of energy minimizing machines useful in model identification, optimization, and associative memory. Special realizations of the theory include the Boltzmann machine and the Hopfield neural network. The theory is reinforced by appendices addressing particular facets of the machine, ranging from gradient descent to simulated annealing. The treatment is systematic, beginning with the description of the energy function. A defining relationship is established between the energy function and the optimal solution. Following, both classical and new learning algorithms are presented (directing the adaption of the free parameters) for numerically minimizing such function to yield the optimal solution. Finally, both computational burden and performance are assessed for several small-scale applications to date. GRA

N89-19930 Politecnico di Milano (Italy). Dipartimento di Elettronica.
STABILIZATION AND REGULATION OF MULTIRATE SAMPLED-DATE LINEAR SYSTEMS
P. Colaneri, R. Scattolini (Pavia Univ., Italy), and N. Schiavoni 1988 35 p Sponsored by the Ministry of Public Education, Italy and CNR, Italy
(Rept-88-013; ETN-89-93717) Avail: Politecnico di Milano, Piazza Leonardo di Vinci 32, 20133 Milan, Italy

The design of multiple-input multiple-output digital control systems characterized by a nonstandard sampling mechanism, fitting with peculiarities found in process instrumentation, is considered. It is assumed that the various outputs of the plant are measured at different rates, which can be definitely less than the unique rate adopted for input updating, or else at different times. With reference to such a situation and in a linear time-invariant environment, a pole-placement problem is solved by resorting to a periodic controller composed by an asymptotic state observer and a control law which turns out to be dynamic. It is shown how a regulator capable of robustly zeroing the steady-state error produced by constant exogenous signals can be synthesized. This regulator incorporates a stabilizer along with an appropriate number of suitably arranged discrete integral actions. ESA

N89-19931 Politecnico di Milano (Italy). Dipartimento di Elettronica.
FURTHER RESULTS ON THE DESIGN OF MULTIVARIABLE REGULATORS UNDER STRUCTURE AND ROBUSTNESS CONSTRAINTS. PART 1: THE INITIALIZATION PROBLEM
N. Schiavoni, M. Pedersoli, and F. Valle 1988 35 p Sponsored by the Ministry of Public Education, Italy and the CNR, Italy
(Rept-88-028; ETN-89-93722) Avail: Politecnico di Milano, Piazza Leonardo da Vinci 32, 20133 Milan, Italy

Parameter optimization methods for synthesizing multivariable regulators, especially when constraints are present on their structure and the robustness of the control system are considered. Most of the underlying numerical algorithms require preliminary selection of a regulator satisfying all the assigned constraints. Solutions to this subproblem, (which is generally nontrivial since, whenever robust zero-error regulation has to be guaranteed, the regulator cannot be asymptotically stable) are presented. Constructive sufficient conditions for the existence of low-gain regulators supplying the closed-loop system with asymptotic stability as well as robust zero-error regulation in the face of ramp type exogenous signals are given. The case where the regulator is constrained to be decentralized is emphasized. ESA

N89-19932 Politecnico di Milano (Italy). Dipartimento di Elettronica.
FURTHER RESULTS ON THE DESIGN OF MULTIVARIABLE REGULATORS UNDER STRUCTURE AND ROBUSTNESS CONSTRAINTS. PART 2: THE RELIABLE ROBUST DECENTRALIZED REGULATOR PROBLEM AND THE SIMULTANEOUS ROBUST DECENTRALIZED REGULATOR PROBLEM
N. Schiavoni 1988 34 p Sponsored by the Ministry of Public Education, Italy and the CNR, Italy
(Rept-88-029; ETN-89-93723) Avail: Politecnico di Milano, Piazza Leonardo da Vinci 32, 20133 Milan, Italy

The design of robust multivariable regulators which supply the control system with a satisfactory behavior even in the presence of large plant parameter variations is considered. With reference to decentralized regulators, constructive sufficient conditions are given for the existence of low-gain regulators capable of tackling the case where one of the feedback loops opens because of a failure of the corresponding sensor and/or actuator; and the case where the mode of the plant is an unknown element of a finite set of systems. ESA

N89-19933# Technische Univ., Delft (Netherlands). Faculty of Technical Mathematics and Informatics.
FORMAL ASPECTS OF A KNOWLEDGE SYSTEM: A LITERATURE REVIEW [FORMELE ASPEKTEN VAN EEN KENNISSYSTEEM; EEN LITERATUUROVERZICHT]
Nico Roos 1988 23 p In DUTCH
(Rept-88-12; B8809738; ISSN-0920-2358; ETN-89-93849)
Copyright Avail: NTIS HC A03/MF A01

The literature on knowledge systems was classified according to aspects that are important for a knowledge system: uncertainty, incompleteness, structure of the data, inconsistency, reflection of own knowledge, planning, and reasoning process. Many of these aspects cannot be described adequately, and are hence not present in existing implementations of knowledge systems. The structure of the knowledge and the form of the abstraction relations are found to be the most important aspects. ESA

N89-19934# Technische Univ., Eindhoven (Netherlands).
REGULATION OF LINEAR DISCRETE TIME-VARYING SYSTEMS Ph.D. Thesis
Jacob Christiaan Engwerda 1988 164 p
(ETN-89-93896) Avail: NTIS HC A08/MF A01

A necessary condition on the dynamic evolution of an admissible target path; and a method for checking the admissibility of a trajectory, and a controller which provides for the desired behavior of the system if it is admissible, are presented. It is shown that almost every admissible target path can be tracked by minimum-variance control. It is proved that stabilization of the closed-loop system matrix can be accomplished if the system satisfies a uniform periodic smooth exponential stabilizability and a periodic smooth exponential detectability condition. The state-space decomposition approach for studying stabilizability and detectability problems is studied. ESA

N89-19827*# Southwest Research Inst., San Antonio, TX.
NESSUS (NUMERICAL EVALUATION OF STOCHASTIC STRUCTURES UNDER STRESS)/EXPERT: BRIDGING THE GAP BETWEEN ARTIFICIAL INTELLIGENCE AND FORTRAN
Pamela K. Fink and Karol K. Palmer *In* NASA. Lyndon B. Johnson Space Center, 2nd Annual Workshop on Space Operations Automation and Robotics (SOAR 1988) Nov. 1988 p 59-67 (For primary document see N89-19817 12-59)
Avail: NTIS HC A22/MF A01 CSCL 09B

N89-19835*# Ohio State Univ., Columbus. Lab. for Artificial Intelligence Research.
DIAGNOSIS BY INTEGRATING MODEL-BASED REASONING WITH KNOWLEDGE-BASED REASONING
Tom Bylander *In* NASA. Lyndon B. Johnson Space Center, 2nd Annual Workshop on Space Operations Automation and Robotics (SOAR 1988) Nov. 1988 p 137-140 Sponsored in part by the National Inst. on Disability and Rehabilitation Research. (For primary document see N89-19817 12-59)
Avail: NTIS HC A22/MF A01 CSCL 09B

N89-19836*# Wright State Univ., Dayton, OH. Dept. of Computer Science.
TRANSFORMATION BASED ENDORSEMENT SYSTEMS
Thomas Sudkamp *In* NASA. Lyndon B. Johnson Space Center, 2nd Annual Workshop on Space Operations Automation and Robotics (SOAR 1988) Nov. 1988 p 143-147 (For primary document see N89-19817 12-59)
(MIPR-FY1175-87-04878/01)
Avail: NTIS HC A22/MF A01 CSCL 09B

N89-19840*# Integrated Inference Machines, Inc., Anaheim, CA.
GARBAGE COLLECTION CAN BE MADE REAL-TIME AND VERIFIABLE
James H. Hino and Charles L. Ross *In* NASA. Lyndon B. Johnson Space Center, 2nd Annual Workshop on Space Operations Automation and Robotics (SOAR 1988) Nov. 1988 p 167-170 (For primary document see N89-19817 12-59)
Avail: NTIS HC A22/MF A01 CSCL 09B

N89-19842*# Air Force Wright Aeronautical Labs., Wright-Patterson AFB, OH. Avionics Lab.
A PARALLEL EXPERT SYSTEM FOR THE CONTROL OF A ROBOTIC AIR VEHICLE
Donald Shakley and Gary B. Lamont (Air Force Inst. of Tech., Wright-Patterson AFB, OH.) *In* NASA. Lyndon B. Johnson Space Center, 2nd Annual Workshop on Space Operations Automation and Robotics (SOAR 1988) Nov. 1988 p 179-186 (For primary document see N89-19817 12-59)
Avail: NTIS HC A22/MF A01 CSCL 09B

N89-19853*# Search Technology, Inc., Norcross, GA.
AN INTELLIGENT TUTORING SYSTEM FOR SPACE SHUTTLE DIAGNOSIS
William B. Johnson, Jeffrey E. Norton, and Phillip C. Duncan *In* NASA. Lyndon B. Johnson Space Center, 2nd Annual Workshop on Space Operations Automation and Robotics (SOAR 1988) Nov. 1988 p 267-272 (For primary document see N89-19817 12-59)
Avail: NTIS HC A22/MF A01 CSCL 09B

N89-19854*# Air Force Human Resources Lab., Wright-Patterson AFB, OH. Training Systems Div.
INTELLIGENT TUTORING SYSTEMS RESEARCH IN THE TRAINING SYSTEMS DIVISION: SPACE APPLICATIONS
J. Wesley Regian *In* NASA. Lyndon B. Johnson Space Center, 2nd Annual Workshop on Space Operations Automation and Robotics (SOAR 1988) Nov. 1988 p 273-277 (For primary document see N89-19817 12-59)
Avail: NTIS HC A22/MF A01 CSCL 09B

N89-19855*# National Aeronautics and Space Administration. Goddard Space Flight Center, Greenbelt, MD.
INTELLIGENT TUTORING IN THE SPACECRAFT COMMAND/CONTROL ENVIRONMENT
Walter F. Truszkowski *In* NASA. Lyndon B. Johnson Space Center, 2nd Annual Workshop on Space Operations Automation and Robotics (SOAR 1988) Nov. 1988 p 279-286 (For primary document see N89-19817 12-59)
Avail: NTIS HC A22/MF A01 CSCL 09B

N89-19856*# Yale Univ., New Haven, CT.
KNOWLEDGE ACQUISITION FOR CASE-BASED REASONING SYSTEMS
Christopher K. Riesbeck *In* NASA. Lyndon B. Johnson Space Center, 2nd Annual Workshop on Space Operations Automation and Robotics (SOAR 1988) Nov. 1988 p 289-292 Prepared in cooperaion with Congitive Systems, Inc., New Haven, CT Sponsored in part by DARPA (For primary document see N89-19817 12-59)
(Contract F49620-82-K-0010)
Avail: NTIS HC A22/MF A01 CSCL 09B

N89-19889*# Computer Sciences Corp., Houston, TX.
DEVELOPMENT OF A PERSONAL-COMPUTER-BASED INTELLIGENT TUTORING SYSTEM
Stephen J. Mueller *In* NASA. Lyndon B. Johnson Space Center, 2nd Annual Workshop on Space Operations Automation and Robotics (SOAR 1988) Nov. 1988 p 535-540 (For primary document see N89-19817 12-59)
Avail: NTIS HC A22/MF A01 CSCL 09B

N89-20060*# Houston Univ., TX. Dept. of Mechanical Engineering.
PRODUCTION SYSTEM CHUNKING IN SOAR: CASE STUDIES IN AUTOMATED LEARNING Final Report
Robert Allen *In* NASA, Lyndon B. Johnson Space Center, National Aeronautics and Space Administration (NASA)/American Society for Engineering Education (ASEE) Summer Faculty Fellowship Program 1988, Volume 1 Feb. 1989 15 p (For primary document see N89-20058 12-99)
Avail: NTIS HC A09/MF A01 CSCL 09B

N89-20068*# Houston Univ., TX. Dept. of Applied Mathematical Sciences.
AN EVIDENTIAL APPROACH TO PROBLEM SOLVING WHEN A LARGE NUMBER OF KNOWLEDGE SYSTEMS IS AVAILABLE Final Report
Andre deKorvin *In* NASA, Lyndon B. Johnson Space Center, National Aeronautics and Space Administration (NASA)/American Society for Engineering Education (ASEE) Summer Faculty Fellowship Program 1988, Volume 1 Feb. 1989 15 p (For primary document see N89-20058 12-99)
Avail: NTIS HC A09/MF A01 CSCL 09B

N89-20075*# Texas A&I Univ., Kingsville. Dept. of Civil and Mechanical Engineering.
INTELLIGENT CONTROL OF ROBOTIC ARM/HAND SYSTEMS FOR THE NASA EVA RETRIEVER USING NEURAL NETWORKS Final Report
Robert A. McLauchlan *In* NASA, Lyndon B. Johnson Space Center, National Aeronautics and Space Administration (NASA)/American Society for Engineering Education (ASEE) Summer Faculty Fellowship Program 1988, Volume 2 Feb.

1989 15 p (For primary document see N89-20073 12-99)
Avail: NTIS HC A09/MF A01 CSCL 09B

N89-20080*# Baylor Univ., Waco, TX. Dept. of Mathematics.
EQUATING AN EXPERT SYSTEM TO A CLASSIFIER IN ORDER TO EVALUATE THE EXPERT SYSTEM Final Report
Patrick L. Odell *In* NASA, Lyndon B. Johnson Space Center, National Aeronautics and Space Administration (NASA)/American Society for Engineering Education (ASEE) Summer Faculty Fellowship Program 1988, Volume 2 Feb. 1989 14 p (For primary document see N89-20073 12-99)
Avail: NTIS HC A09/MF A01 CSCL 09B

64 NUMERICAL ANALYSIS

Includes iteration, difference equations, and numerical approximation.

N89-19935# Texas A&M Univ., College Station.
AN ASYMPTOTIC THEORY FOR WEIGHTED LEAST SQUARES WITH WEIGHTS ESTIMATED BY REPLICATION Technical Report No. 1, Aug. 1987 - Aug. 1988
Raymond J. Carroll and Daren B. Cline Aug. 1988 19 p
(Contract F49620-85-C-0144)
(AD-A198000; AFOSR-88-0844TR) Avail: NTIS HC A03/MF A01 CSCL 12C

This document considers a heteroscedastic linear regression model with replication. To estimate the variances, one can use the sample variances or the sample average squared errors from a regression fit. The authors study the large sample properties of these weighted least squares estimates with estimated weights when the number of replicates is small. The estimates are generally inconsistent for asymmetrically distributed data. If sample variances are used based on m replicates, the weighted least squares estimates are inconsistent for m=2 replicates even when the data are normally distributed. With between 3 and 5 replicates, the rates of convergence are slower than the usual square root of N. With m greater than or = 6 replicates, the effect of estimating the weights is to increase variances by (m-5)/(m-3), relative to weighted least squares estimates with known weights. GRA

N89-19936# Joint Inst. for Nuclear Research, Dubna (USSR). Lab. of Nuclear Problems.
BORN-INFELD EQUATIONS AND MINIMAL SURFACES
N. S. Shavokhina 1988 4 p In RUSSIAN; ENGLISH summary
(DE88-704966; JINR-R-2-88-132) Avail: NTIS (US Sales Only) HC A02/MF A01

In the N-dimensional flat space (N greater than or equal to 3) with symmetric nondegenerated metric of any index the systems are under consideration: (1) the system of Born - Infelds equations and (2) the system of equations defining K-dimensional surfaces in this space (1 less than or equal to K greater than or equal to N - 1). It is explicitly demonstrated that there exist solutions common for the considered systems and the possibility of these solutions follows from the variational principle. DOE

N89-19937# Texas Univ., Austin. Center for Cybernetic Studies.
A GEOMETRIC PROPERTY OF THE LEAST SQUARES SOLUTION OF LINEAR EQUATIONS
Aharon Ben-Tal and Marc Teboulle Jun. 1988 13 p
(Contract DAKF15-87-C-0110; NSF SES-85-20806)
(AD-A201342; CCS-RR-605) Avail: NTIS HC A03/MF A01 CSCL 12C

The authors derive an explicit determinantal formula for the least squares (LS) solution of an overdetermined system of linear equations. From this formula it follows that the LS solution lies in the convex hull S of points, each of which is a solution of a square subsystem of the whole system. The results are extended to weighted LS solution; it is shown that the convex hull S in which the solution must lie is independent of the weighting matrix. GRA

N89-19938# Air Force Inst. of Tech., Wright-Patterson AFB, OH. School of Systems and Logistics.
AN ANALYSIS OF THE IMPACT OF LOG-LINEAR REGRESSION ON THE ESTIMATED LEARNING CURVE PARAMETERS M.S. Thesis
Tom Tracht Sep. 1988 115 p
(AD-A201471; AFIT/GCA/LSQ/88S-9) Avail: NTIS HC A06/MF A01 CSCL 05H

This research had three main objectives. First, was to determine whether bias existed in the estimate of the learning curve parameters, as calculated by popular learning curve programs. Second, was to compare the fitting techniques of ordinary and weighted least-squares, with and without bias removed. Third, was to test the normality and constant variance assumptions of the average unit cost data. When using the least-squares fitting technique to fit production lot data to the unit formulation of learning curve theory, log-linear regression biases the estimate of the first unit cost parameter on the high side, resulting in overestimating program costs. The bias was shown to be almost exclusively a function of the variance in the production cost data. Factors which would reduce the bias were investigated. An approximation to the bias reduction factor proposed by Ilderton was used with excellent results. GRA

N89-19939# California Univ., Los Angeles. Dept. of Mathematics.
APPLIED PARTIAL DIFFERENTIAL EQUATIONS AND NUMERICAL ANALYSIS Final Technical Report, 1 Jul. 1985 - 30 Jun. 1988
Stanley Osher Sep. 1988 21 p
(Contract DAAG29-85-K-0190)
(AD-A201749; ARO-22759.8-MA) Avail: NTIS HC A03/MF A01 CSCL 12A

An hierarchy of uniformly high order accurate essentially non-oscillatory shock capturing algorithms was developed. Some theory and numerical experimentation was done. A correction to the unsteady full potential equation for flows with strong shocks was obtained. This modification inputs the correct entropy jumps at shocks. Numerical experiments on airfoils were sucessfully performed. A new family of paraxial wave approximations was derived and was applied to computational problems in seismology, underwater acoustics and artificial boundaries. Theoretical and experimental results were obtained. The family also included variants of parabolic approximations of scalar wave equations. A method for the computation of highly oscillatory solutions to hyperbolic equations was obtained. A convergence concept which makes analysis possible in the practical situation in which not all frequencies are well resolved is developed. Convergence of an average approximation is established for a general class of methods. Applications to particle methods were also obtained. GRA

N89-19940# Colorado School of Mines, Golden. Center for Wave Phenomena.
LARGE WAVE NUMBER APERTURE LIMITED FOURIER INVERSION AND INVERSE SCATTERING Technical Report, 1 Jan. - 30 Jun. 1988
Norman Bleistein 1 Jan. 1989 51 p
(Contract N00014-88-K-0092)
(AD-A202247; CWP-063R) Avail: NTIS HC A04/MF A01 CSCL 20N

Aperture limited Fourier operators are like pseudo-differential operators, except that the symbol of the latter is part of the unknown kernel function of the former. Such operators arise naturally in inverse scattering when one applies an integral inverse scattering operator to model data with an unknown (such as a reflection coefficient) which depends on the source/receiver location as well on interior medium coordinates. Large wave number aperture limited Fourier operators can be analyzed by multi-dimensional stationary phase. The nature of the asymptotic

expansion of such operators will then depend on the properties of the kernel function to which the operator is applied. Of interest in inverse scattering are distributions with support at a point or on a surface (the singular function of a surface) and piecewise smooth functions (whose discontinuity surfaces are reflectors). The purpose of this paper is to present some features of the asymptotics of large wave number aperture limited Fourier inversion operators and to relate these results to the application of a recently developed inverse scattering formalism as applied to Kirchhoff-approximate scattering data from a reflecting surface. GRA

N89-19941# Technische Univ., Delft (Netherlands). Lab. for Measurement and Control.
CRITERION BASED EQUIVALENCE FOR EQUATION ERROR MODELS
Paul M. J. vandenHof Apr. 1988 15 p
(WTHD-188; ISBN-9-03-700015-0; ETN-89-93838) Copyright Avail: NTIS HC A03/MF A01

The equivalence relation that is used when parametrizing a set of linear time invariant models for applying equation error system identification methods is investigated. In order to obtain identified models that are not dependent on the specific parametrization of the model set, a notion of model equivalence is introduced that is related to the identification criterion, leading to a nonconventional set of canonical forms. ESA

N89-19942# Technische Univ., Delft (Netherlands). Faculty of Technical Mathematics and Informatics.
CHARACTERIZATIONS OF CONDITIONAL EXPECTATION-TYPE OPERATORS
P. G. Dodds, C. B. Huijsmans, and B. dePagter 1988 34 p
(Rept-88-04; B8809730; ISSN-0920-8577; ETN-89-93841)
Copyright Avail: NTIS HC A03/MF A01

A complete description of positive projections in ideals of measurable functions is given in terms of conditional expectation-type operators. This theorem implies that each strictly positive order continuous projection for which the constant functions are invariant is of conditional expectation type. The extent to which the present approach yields characterizations of conditional expectation on Banach function spaces which extend those of Rota (1960) for averaging contractions and of Ando (1966) and Douglas (1965) for positive contractive projections and L sup p-spaces is shown. Satisfactory extensions are valid only under additional smoothness assumptions which are automatically satisfied in the L sup p setting. It is shown show that each contractive projection in a Banach function space with range a sublattice containing the constant functions is necessarily positive, provided a certain smoothness assumption is satisfied. While this smoothness assumption is necessarily satisfied in the case of L sup p spaces, an example shows that it cannot be omitted even in the finite dimensional setting. ESA

N89-19943# Technische Univ., Delft (Netherlands). Faculty of Technical Mathematics and Informatics.
THE BOX DIMENSION OF SELF-AFFINE GRAPHS AND REPELLORS
Tim Bedford 1988 22 p
(Rept-88-08; B8809736; ISSN-0920-8577; ETN-89-93845)
Copyright Avail: NTIS HC A03/MF A01

The box-dimension (or capacity) of a class of self-affine sets (fractal curves) in the plane is calculated. The formula for box dimension given has a similar form to Browen's (1979) formula for the Hausdorff dimension of self-similar sets, involving the topological pressure of certain functions. The sets studied appear in two contexts: as graphs of generalized Weierstrass functions, and as repellors in maps of the cylinder. The techniques of the singularity spectrum are used to carry out the calculations. ESA

N89-19944# Technische Univ., Delft (Netherlands). Faculty of Technical Mathematics and Informatics.
HAUSDORFF DIMENSION AND BOX DIMENSION IN SELF-SIMILAR SETS
Tim Bedford 1988 14 p
(Rept-88-09; B8809731; ISSN-0920-8577; ETN-89-93846)
Copyright Avail: NTIS HC A03/MF A01

A construction of self-similar sets is considered for which the Hausdorff and box dimensions are calculated and shown to be equal. The techniques of the singularity spectrum are used in the calculation. ESA

N89-19945# Technische Univ., Delft (Netherlands). Faculty of Technical Mathematics and Informatics.
HYPERBOLICITY PROPERTIES OF C SUP 2 MULTIMODAL COLLET-ECKMANN MAPS WITHOUT SCHWARZIAN DERIATIVE ASSUMPTIONS
Tomasz Nowicki and Sebastian vanStrien 1988 28 p
(Rept-88-10; B8809732; ISSN-0920-8577; ETN-89-93847)
Copyright Avail: NTIS HC A03/MF A01

The dynamical properties of general C sup 2 maps f: (0,1) to (0,1) with quadratic critical points (and not necessarily unimodal) are studied. It is shown that if such maps satisfy the Collet-Eckmann conditions, then one has: hyperbolicity on the set of periodic points; nonexistence of wandering intervals; sensitivity on initial conditions; and exponential decay of branches (intervals of monotonicity) of f sup n, as n tends to infinity. For these results, no assumptions are made on the Schwarzian derivative f. The return-time of points that start near critical points is estimated. ESA

N89-19946# Technische Univ., Delft (Netherlands). Faculty of Technical Mathematics and Informatics.
DISCRETE EVENT SYSTEMS WITH STOCHASTIC PROCESSING TIMES
G. J. Olsder, J. A. C. Resing, R. E. deVries, M. S. Keane, and G. Hooghiemstra 1988 23 p
(Rept-88-11; B8809737; ISSN-0920-8577; ETN-89-93848)
Copyright Avail: NTIS HC A03/MF A01

Discrete event dynamic systems in which the underlying algebra is the max-algebra and the coefficients in the system, referring to processing times in practice, are stochastic are studied. Restrictions are that the stochastic processing times of the nodes in the network are independent and identically distributed. These, however, are no fundamental restrictions since the same approach can essentially be used for dependent processing time and/or different distribution functions. The theory given may provide a bridge to another approach to discrete event dynamic systems, i.e., the perturbation analysis of trajectories. ESA

N89-19947# Kernforschungsanlage, Juelich (Germany, F.R.). Inst. fuer Reaktorentwicklung.
A MONTE CARLO TEST PROGRAM WITH VECTORIZED GEOMETRY ROUTINES
P. Cloth and D. Filges May 1988 48 p
(JUEL-2202; ISSN-0366-0885; ETN-89-93959) Avail: NTIS HC A03/MF A01

Utilization of parallel processing computers to perform radiation transport calculations is described. Vectorized geometry routines were coupled to a simple, scalar nuclear event generator and tracking routine for neutral particles, based on energy group principles, giving a test Monte Carlo program, which is partially vectorized. As the vectorized portion of this program is clearly separated from the scalar appendix, the performance of the vectorized part can be investigated and code acceleration can be easily measured. More than 1 billion distance-to-surface and region calculations were performed without any problems by the code with the tracking of particles between nuclear interaction points. The test was run on CRAY XMP48, XMP22 and, for comparison, on IBM 3081. The computing times are not significantly different on the CRAY machines. The CRAY performance speed is 16 times faster than IBM. Vectorization gives a speed-up factor of 4, compared to runs without vectorization. ESA

N89-19948# Technische Univ., Delft (Netherlands). Faculty of Technical Mathematics and Informatics.
NORMAL FORMS AND PERIODIC SOLUTIONS IN THE THEORY OF NONLINEAR OSCILLATIONS. EXISTENCE AND ASYMPTOTIC THEORY
C. G. A. vanderBeek 1988 45 p
(Rept-88-16; ISSN-0920-8577; ETN-89-94000) Copyright Avail: NTIS HC A03/MF A01

A concept of normal forms is presented to analyze a class of ordinary differential equations concerning nonlinear oscillations. An algorithm for the calculation of the normalized differential equations is presented as well as theorems on the existence, uniqueness, and stability of periodic solutions, and their calculation in an approximative way by using the normalized differential equations. As an application of the theory a simple model describing the flow-induced vibrations of an oscillator with one degree of freedom in a uniform wind field is discussed. The calculations to perform the analysis were done by an implementation of the algorithms for the calculation of higher order normal forms on the computer-algebra system Macsyma. ESA

N89-19949# Technische Univ., Delft (Netherlands). Faculty of Technical Mathematics and Informatics.
CELL-CENTERED AND VERTEX-CENTERED DISCRETIZATION OF INTERFACE PROBLEMS
M. Khalil and P. Wesseling 1988 44 p
(Rept-88-18; ISSN-0920-8577; ETN-89-94002) Copyright Avail: NTIS HC A03/MF A01

Cell-centered and vertex-centered finite volume discretization of the two-dimensional diffusion equation with discontinuous coefficients is described. Computer codes to generate these discretization are presented. ESA

N89-19950# Technische Univ., Delft (Netherlands). Faculty of Technical Mathematics and Informatics.
APPROXIMATION, SATURATION AND SEMIGROUPS OF OPERATORS IN BANACH SPACE
Cees A. Timmermans 1988 21 p
(Rept-88-19; ISSN-0920-8577; ETN-89-94003) Copyright Avail: NTIS HC A03/MF A01

The saturation problem for the Bernstein operators in a Banach space is addressed. Uniform saturation classes for Bernstein operators in C sup m (0,1) norms, where m is greater than or = 1 are derived. ESA

N89-19951# Technische Univ., Delft (Netherlands). Faculty of Technical Mathematics and Informatics.
VECTORIZATION OF LINEAR RECURRENCE RELATIONS
H. A. vanderVorst and K. Dekker 1988 18 p
(Rept-88-21; ISSN-0920-8577; ETN-89-94004) Copyright Avail: NTIS HC A03/MF A01

The usefulness of the partition method for solving linear bidiagonal systems on vector computers was tested. It is shown that the method is numerically stable for an interesting class of problems. For different vector computers, suitable variants of the method are formulated, and upper bounds for their performance are presented. Observed performances in a FORTRAN environment are discussed. ESA

N89-19952# Technische Univ., Delft (Netherlands). Faculty of Technical Mathematics and Informatics.
A GENERALIZATION OF LAGUERRE POLYNOMIALS
R. Koekoek and H. G. Meijer 1988 37 p
(Rept-88-28; ISSN-0920-8577; ETN-89-94008) Copyright Avail: NTIS HC A03/MF A01

The classical Laguerre polynomials are reviewed, and orthogonality and elementary properties are considered. A recurrence relation; a Christoffel-Darboux type formula; and representation as hypergeometric series are established. It is proved that under given conditions, some of the zeros of the polynomial considered are located within the interval of orthogonality. ESA

N89-19953# Technische Univ., Delft (Netherlands). Faculty of Technical Mathematics and Informatics.
VERTEX-CENTERED AND CELL-CENTERED MULTIGRID METHODS FOR INTERFACE PROBLEMS
M. Kahlil and P. Wesseling 1988 50 p
(Rept-88-42; ISSN-0920-8577; ETN-89-94011) Copyright Avail: NTIS HC A03/MF A01

Cell-centered and vertex-centered multigrid methods (MGCC, MGVC) for solving interface problems are compared. These methods differ in the location of the nodes in the grids and in the transfer operators. Numerical results of test problems with strong discontinuities in equation coefficients are presented. Storage and work required by each method are compared. The MGCC is more attractive than MGVC. The primary reason is the simplicity of the implementation of its components: restriction, interpolation, and Galerkin coarse grid approximation. The amount of preliminary work required is smaller in the cell-centered case than in the vertex-centered case. This difference is expected to be larger in the 3-D case. Numerical results show that MGCC is a robust as MGVC in the case of problems with discontinuous coefficients. ESA

65 STATISTICS AND PROBABILITY

Includes data sampling and smoothing; Monte Carlo method; and stochastic processes.

N89-19954# Old Dominion Univ., Norfolk, VA. Dept. of Mathematics and Statistics.
LARGE DEVIATION LOCAL LIMIT THEOREMS FOR RATIO STATISTICS
Narasinga R. Chaganty and Sanjeev Sabnis Jul. 1988 19 p
(Contract DAAL03-88-K-0076; NSF DMS-86-20007)
(AD-A201169; ARO-24834.1-MA) Avail: NTIS HC A03/MF A01 CSCL 12C

This document discusses an arbitrary sequence of non-lattice random variables and another sequence of positive random variables. Assume that the sequences are independent. This paper obtains asymptotic expression for the density function of the ratio statistic R sub n = T sub n/S sub n based on simple conditions on the moment generating functions of T sub n and S sub n. When S sub n = n, our main result reduces to that of Chaganty and Sethuraman. We also obtain analogous results when T sub n and S sub n are both lattice random variables. We call our theorems large deviation local limit theorems for R sub n, since the conditions of our theorems imply that R sub n approaches limit of c in probability for some constant c. We present some examples to illustrate our theorems. GRA

N89-19955# North Carolina Univ., Chapel Hill. Dept. of Operations Research.
SENSITIVITY ANALYSIS USING THE MONTE CARLO ACCEPTANCE-REJECTION METHOD Technical Report, Sep. 1987 - Sep. 1988
George S. Fishman Sep. 1988 36 p
(Grant AF-AFOSR-0140-84; AF Proj. 2304)
(AD-A201261; UNC/OR/TR-88/3; AFOSR-88-1179TR) Avail: NTIS HC A03/MF A01 CSCL 12C

This paper describes a Monte Carlo sampling plan for estimating how a function varies in response to changes in its arguments. Most notably, the plan effects this sensitivity analysis by applying the acceptance-rejection technique to data sampled at only one specified setting for the arguments, thus saving considerable computing time when compared to alternative methods. The plan which applies for a 0 to 1 response on each replication has immediate application when estimating variation in system performance measures in reliability analysis. The paper derives the variances of the proposed estimators and shows how to use worst case bounds on these or on corresponding coefficients of variation to choose the arguments, at which to sample, that minimize the worst case bounds. Individual and simultaneous confidence intervals are derived and an example based on s-t

reliability illustrates the method. The paper also compares the proposed method and an alternative Monte Carlo approach that uses an importance function. GRA

N89-19956# Michigan Univ., Ann Arbor. Dept. of Statistics.
ESTIMATION IN LARGE SAMPLES Final Report, 1 Jan. 1985 - 30 Jun. 1988
Michael Woodroofe Aug. 1988 23 p
(Contract DAAG29-85-K-0008)
(AD-A201459; ARO-22565.8-MA) Avail: NTIS HC A03/MF A01 CSCL 12C

Three problem areas were identified and studied: nonparametric estimation with truncated data; asymptotic expansions for randomly stopped sums (with a view towards finding corrected confidence intervals in sequential problems); and asymptotic local minimaxity in sequential estimation. In addition, some effort was devoted to understanding optimal sequential designs. The final report contains complete results of the research. GRA

N89-19957# Pennsylvania State Univ., University Park.
ROBUST BOUNDED INFLUENCE TESTS IN LINEAR MODELS
Marianthi Markatou and Thomas P. Hettmansperger Nov. 1988 28 p
(Contract N00014-80-C-0741)
(AD-A201896; Rept-77) Avail: NTIS HC A03/MF A01 CSCL 12C

A robust test, which we call an aligned generalized, M-test for testing subhypotheses in the general linear models is developed, and its asymptotic properties are studied. The test is a robustification of the well known F-test, and it is an elegant and practical alternative to Ronchetti's (1982) class of tau-tests. P-values associated with it can be approximated readily using existing chi square tables, unlike Ronchetti's test. The test is based on an appropriately constructed quadratic form, and uses the generalized M-estimators of the parameters in the reduced model. Under the null hypothesis the asymptotic distribution is a central chi square, and under contiguous alternatives is a non-central chi square with the same degrees of freedom. The test can also be viewed as a generalization of Sen's (1982) M-test for linear models. The influence function of the test is bounded. The bound not only applies to the influence of residuals but also to the influence of position in the factor space. Sen's test, on the other hand, has bounded influence only in residuals. GRA

N89-19958# Naval Postgraduate School, Monterey, CA.
MINIFICATION PROCESSES
Peter A. Lewis and Ed McKenzie Sep. 1988 26 p
(AD-A202219; NPS55-88-010) Avail: NTIS HC A03/MF A01 CSCL 12C

It is shown that the autoregressive, Markovian minification processes introduced by Tavares and Sim can be extended to marginal distributions other than the exponential and Weibull distributions. Necessary and sufficient conditions on the hazard rate of the marginal distributions are given for a minification process to exist. Results are given for the derivation of the autocorrelation function; these correct the expression for the Weibull given by Sim. Monotonic transformations of the minification processes are also discussed and generate a whole new class of autoregressive processes with fixed marginal distributions. Processes generated by a maximum operation are also introduced and a comparison of three different Markovian processes with uniform marginal distributions are given. GRA

N89-19959# Stanford Univ., CA. Dept. of Statistics.
ESTIMATION OF A RESTRICTED VARIANCE RATIO
Alan E. Gelfand 14 Dec. 1988 13 p
(Contract N00014-86-K-0156)
(AD-A202268; TR-410) Avail: NTIS HC A03/MF A01 CSCL 12C

The estimation of a variance ratio is studied under certain restrictions. A Bayesian viewpoint is taken. We then assume additional information on tau sub i is available in the form of an independent observation from a noncentral x squared distribution. A natural application arises when the u sub i are sums of squares in alpha variance components model. GRA

N89-19960# Stanford Univ., CA. Dept. of Statistics.
TIME SERIES ANALYSIS AND MULTIVARIATE STATISTICAL ANALYSIS Final Report, 23 Sep. 1985 - 22 Sep. 1988
Theodore W. Anderson Nov. 1988 6 p
(Contract DAAG29-85-K-0239)
(AD-A202273; ARO-22729.6-MA) Avail: NTIS HC A02/MF A01 CSCL 12C

Research was carried out mainly in the areas of time series analysis and multivariate statistical analysis. The most important results in the first area apply to autoregressive and moving average processes. In the second area emphasis was on parameter consistency and elliptically contoured distributions. To estimate the parameters of the moving average model 16 different iterative procedures have been devised. These involve alternative parametrizations, time and frequency domain representations, Newton-Raphson and scoring approaches, and use of likelihoods and concentrated likelihoods. Properties of the likelihood function, as well as the estimates, have been derived. GRA

N89-19961# Technische Univ., Delft (Netherlands). Faculty of Technical Mathematics and Informatics.
PROBABILITY THEORIES, FUZZY SET THEORY AND SYLLOGISMS; A LITERATURE REVIEW [KANSTHEORIEEN, VAGE-VERZAMELINGENTHEORIE EN SYLLOGISM; EEN LITERATUUROVERZICHT]
Hans Hellendoorn 1988 30 p In DUTCH
(Rept-88-13; B8809739; ISSN-0920-2358; ETN-89-93850)
Copyright Avail: NTIS HC A03/MF A01

A literature study of probability theories, fuzzy set theories and syllogisms was performed with a view to the modelling of incompleteness and uncertainty in reasonings. In probability theories, the Bayes probability calculation, the Dempster-Shafer and endorsement theories, the MYCIM medical expert system family, and the MUM system that manages uncertainty in medicine are treated. In fuzzy set theories interval-valued fuzzy sets, rough sets and twofold fuzzy sets, fuzzy logic and data bases, and approximation and entropy are discussed. Syllogisms as well as fuzzy set theory applications to robotics are presented. ESA

N89-19962# Technische Univ., Delft (Netherlands). Faculty of Technical Mathematics and Informatics.
HIGHLY EFFICIENT ESTIMATES OF MULTIVARIATE LOCATION WITH HIGH BREAKDOWN POINT
Hendrik P. Lopuhaa 1988 26 p
(Grant ZWO-10-62-10)
(Rept-88-14; ISSN-0920-8577; ETN-89-93999) Copyright Avail: NTIS HC A03/MF A01

A class of robust estimates for a multivariate location parameter is introduced. These estimates have the maximal breakdown point possible for affine equivariant estimates and are highly efficient as well in cases of normal data. They are defined by a two-stage procedure. In the first stage a simultaneous S-estimate of location and covariance is computed, and in the second stage a location M-equation based on the initial estimate is solved, using an appropriate redescending psi-function. Breakdown point and influence function of these estimates are obtained, and consistency and asymptotic normality is proved. ESA

N89-19963# Technische Univ., Delft (Netherlands). Faculty of Technical Mathematics and Informatics.
TAIL TRIVIALITY FOR SUMS OF STATIONARY RANDOM VARIABLES
H. C. P. Berbee and W. Th. F. denHollander 1988 16 p
(Rept-88-40; ISSN-0920-8577; ETN-89-94009) Copyright Avail: NTIS HC A03/MF A01

Tail sigma-fields and loss of memory associated with sums of stationary integer-valued random variables are studied. An application concerns convergence in distribution of interarrival times in 0 to 1 sequences. ESA

N89-19849*# Ohio State Univ., Columbus. Dept. of Psychology.
A METHOD FOR MODELING BIAS IN A PERSON'S ESTIMATES OF LIKELIHOODS OF EVENTS
Thomas E. Nygren and Osvaldo Morera *In* NASA. Lyndon B. Johnson Space Center, 2nd Annual Workshop on Space Operations Automation and Robotics (SOAR 1988) Nov. 1988 p 237-243
(For primary document see N89-19817 12-59)
(Contract F33615-85-D-0514)
Avail: NTIS HC A22/MF A01 CSCL 12A

66 SYSTEMS ANALYSIS

Includes mathematical modeling; network analysis; and operations research.

N89-19964# Los Alamos National Lab., NM.
SURVIVABILITY OF SPACE ASSETS IN THE LONG TERM
Gregory H. Canavan Jan. 1989 95 p
(Contract W-7405-eng-36)
(DE89-006563; LA-11395-MS) Avail: NTIS HC A05/MF A01

This report discusses the threats to strategic defense satellites over the next 20 to 30 years. It describes the purposes and sizes of the satellites, the types of attacks on them, the counters to those attacks, and the likely outcomes of the encounters. It concludes that their survivability and contribution to stability should increase over the next 20 to 30 years because of the advanced technologies that should become available then. DOE

67 THEORETICAL MATHEMATICS

Includes topology and number theory.

No abstracts in this category.

70 PHYSICS (GENERAL)

For precision time and time interval (PTTI) see *35 Instrumentation and Photography;* for geophysics, astrophysics or solar physics see *46 Geophysics, 90 Astrophysics,* or *92 Solar Physics.*

N89-19965*# National Aeronautics and Space Administration. Lewis Research Center, Cleveland, OH.
ACOUSTIC WAVE PROPAGATION IN HETEROGENEOUS STRUCTURES INCLUDING EXPERIMENTAL VALIDATION
Kenneth J. Baumeister and Milo D. Dahl Apr. 1989 19 p Prepared for presentation at the 12th Aeroacoustics Conference, San Antonio, TX, 10-12 Apr. 1989; sponsored by AIAA
(NASA-TM-101486; E-4622; NAS 1.15:101486) Avail: NTIS HC A03/MF A01 CSCL 20C

A finite element model was developed to solve for the acoustic pressure and energy fields in a heterogeneous suppressor. The derivations from the governing equations assumed that the material properties could vary with position resulting in a heterogeneous variable property two-dimensional wave equation. This eliminated the necessity of finding the boundary conditions between different materials. For a two media region consisting of part air and part bulk absorber, a model was used to describe the bulk absorber properties in two directions. Complex metallic structures inside the air duct are simulated by simply changing element properties from air to the structural material in a pattern to describe the desired shapes. To verify the numerical theory, experiments were conducted without flow in a rectangular duct with a single folded cavity mounted above the duct and absorbing material mounted inside a cavity. Changes in a nearly plane wave sound field were measured on the wall opposite the absorbing cavity. Fairly good agreement was found in the standing wave pattern upstream of the absorber and in the decay of pressure level opposite the absorber, as a function of distance along the duct. The finite element model provides a convenient method for evaluating the acoustic properties of bulk absorbers. Author

N89-19966# Deutsche Forschungs- und Versuchsanstalt fuer Luft- und Raumfahrt, Brunswick (Germany, F.R.). Abteilung Mathematische Verfahren und Datentechnik.
EQUILIBRIUM SOLUTIONS OF A SPHERICAL PENDULUM WITH ROTATING POINT OF SUSPENSION AND FRICTION
Ernst A. Bockemueller Oct. 1988 48 p In GERMAN; ENGLISH summary Report will also be announced as translation (ESA-TT-1139)
(DFVLR-Mitt-88-24; ISSN-0176-7739; ETN-89-93977) Avail: NTIS HC A03/MF A01; DFVLR, VB-PL-DO, Postfach 90 60 58, 5000 Cologne, Federal Republic of Germany, 21 deutsche marks

A spherical pendulum with rotating point of suspension and friction is investigated. For this nonlinear system with time dependent constraints, there exist multiple stationary solutions. Number and stability of these solutions depend on the system parameters. The investigations show that the gyroscopic coupling between the two degrees of freedom decides the stability of the solutions. ESA

71 ACOUSTICS

Includes sound generation, transmission and attenuation. For noise pollution see *45 Environmental Pollution.*

N89-19967# Idaho National Engineering Lab., Idaho Falls.
OPTICAL PARAMETER EFFECTS ON LASER GENERATED ULTRASOUND FOR MICROSTRUCTURE CHARACTERIZATION
K. L. Telschow and R. J. Conant (Montana State Univ., Bozeman.) 1988 8 p Presented at the Meeting on Nondestructive Characterization of Materials, Saarbrucken, Fed. Republic of Germany, 3 Oct. 1988
(Contract DE-AC07-76ID-01570)
(DE89-005193; EGG-M-88053; CONF-881081-2) Avail: NTIS HC A02/MF A01

Under appropriate conditions a significant feature of the laser generated elastic waveform in the thermoelastic regime is a precursor (sharp spike) signaling the arrival of the longitudinal wave. This paper shows that the observed precursor can be understood through the use of one-dimensional models that account for optical penetration and thermal diffusion into the material. Experimental results are compared with a two-dimensional analytic calculation including optical penetration. DOE

N89-19968# Washington State Univ., Pullman. Dept. of Physics.
RESEARCH IN ACOUSTICAL SCATTERING, DIFFRACTION CATASTROPHES, OPTICS OF BUBBLES AND ACOUSTICAL PHASE CONJUGATION Annual Summary Report, 16 Sep. 1987 - 15 Oct. 1988
Philip L. Marston 31 Oct. 1988 54 p
(Contract N00014-85-C-0141)
(AD-A201451) Avail: NTIS HC A04/MF A01 CSCL 20F

The research summarized concerns several aspects of propagation and scattering of acoustical and optical waves. The topics discussed fall under the following four categories: (1) A generalization of the geometrical theory of diffraction which describes surface-guided wave contributions to the scattering of sound from smooth elastic objects in water; the effect of curvature on Lamb wave velocities on thick shells; a product expansion of the S function for elastic spheres; (2) Acoustical and optical caustics and associated wavefields: unfolding axial caustics; observations of lips caustics in light backscattered from oblate drops; and observations of acoustical and optical transverse cusps produced by reflection; (3) Physical optics of bubbles in water: observations of Brewster angle light scattering; observations of backscattering from rising bubbles; asymptotic series for critical angle scattering

useful for determining bubble sizes; and (4) Acoustic phase conjugation and aspects of wavefront reversal via three-wave mixing in a layer of enhanced nonlinearity as caused, for example, by a layer of microbubbles in water; the present status of experiments on three-wave mixing; and the possibility of phase conjugation via reflection from curved vibrating surfaces. GRA

N89-19969# Rochester Univ., NY. Inst. of Optics.
OPTO-ELECTRONIC SYSTEMS RESEARCH. IMAGE RECOVERY FROM PARTIAL FRESNEL ZONE INFORMATION Ph.D. Thesis
Robert J. Rolleston Mar. 1988 201 p
(Contract DAAL03-87-K-0084)
(AD-A201556; ARO-24749.3-PH) Avail: NTIS HC A10/MF A01 CSCL 20F

The problem of reconstructing an unknown image from partial data in the Fresnel zone region is discussed. An iterative method of reconstructing an unknown image from either the phase-only or magnitude-only data in the transform domain, is investigated through the use of digital calculations. From the Fourier transform plane through the Fresnel region, it is demonstrated that the phase-only information in the transform allows for a very good reconstruction in just a few iterations. While reconstructing an image from the magnitude of the Fourier transform is very difficult, as one moves further into the Fresnel zone region, good reconstructions are obtained in only several iterations. GRA

N89-19970# Naval Postgraduate School, Monterey, CA.
DEVELOPMENT OF A SYSTEM FOR ACOUSTIC MEASUREMENTS OF BISTATIC TARGET STRENGTHS M.S. Thesis
Glenn R. Snyder Sep. 1988 90 p
(AD-A201673) Avail: NTIS HC A05/MF A01 CSCL 17A

A digital data acquisition system was implemented for the study and collection of scattered waveforms from various objects. Reflected waveforms were extracted from interference with other signals by a simple subtraction technique. Backscattered and bistatic reflections were observed and recorded. Various effects on scattered waveforms, including target composition, pulse length, and frequency, were experimentally observed. Bistatic scattering results from a styrofoam sphere at a ka value of 10 were in agreement with theoretical predictions for a rigid sphere. Bistatically measured data at 70 kHz from a styrofoam cylinder of length 20 cm and diameter 2.5 cm followed a trend for bistatic angles up to 150 degrees but became amorphous as the bistatic angle approached 180 degrees. GRA

N89-19971 Mississippi Univ., University.
AN EXAMINATION OF CAVITATION DUE TO SHORT PULSES OF MEGAHERTZ ULTRASOUND Ph.D. Thesis
Jeffrey Brian Fowlkes 1988 121 p
Avail: Univ. Microfilms Order No. DA8826316

The acoustic cavitation threshold of an aqueous solution was measured at megahertz frequencies as a function of pulse width and pulse repetition frequency for various combinations of these parameters. The fluid tested was a 0.1 M KOH - H3BO3 buffer solution at a pH of 10.9 which contained luminol, was saturated with argon, and filtered through a 25 micron filter. The presence of cavitation was detected by a photomultiplier tube which required the emission of visible light that was both larger in magnitude and longer in duration than a preset criterion. It was observed that the cavitation threshold of water under pulse conditions decreases both when the pulse width is fixed and the pulse repetition frequency is increased, and when the pulse repetition frequency is fixed and the pulse width is increased. Acoustic cavitation thresholds in aqueous solutions, as measured, are significantly less than those acoustic pressures associated with instruments that are currently in widespread use in medicine. In an attempt to explain the dependence of cavitation threshold on pulse parameters, a new solution to the problem of rectified diffusion is developed for short acoustic pulses. Results are examined. Dissert. Abstr.

N89-19972 Tennessee Univ., Knoxville.
GAUSSIAN BEAM REPRESENTATION OF BEAM-LIKE ULTRASONIC FIELDS Ph.D. Thesis
Jing Jiang Wen 1988 125 p
Avail: Univ. Microfilms Order No. DA8824336

A systematic method of analysis of beam-like wave fields (the Gaussian beam representation) is established. Through a computer determination of the coefficient and beam parameter sets based on optimization theory, any wave field satisfying the condition (ka) squared is much greater than 1 can be expressed as a superposition of a number of Gaussian beams with different beam waists, about the same (axisymmetric case) or different beam axes, and propagating in the same direction. Two typical beam fields -- the diffraction fields of axisymmetric piston radiators and the non-axisymmetric reflected field of a bounded beam incident at or near the Rayleigh angle -- are used as a demonstration of the new method. Experimental results obtained with a new Gaussian transducer are presented as a verification of the physical existence of a single ultrasonic Gaussian beam -- the basic unit of the Gaussian beam representation. Dissert. Abstr.

72 ATOMIC AND MOLECULAR PHYSICS

Includes atomic structure, electron properties, and molecular spectra.

N89-19973*# Colorado State Univ., Fort Collins. Dept. of Mechanical Engineering.
THE DIVERGENCE CHARACTERISTICS OF CONSTRAINED-SHEATH OPTICS SYSTEMS FOR USE WITH 5-eV ATOMIC OXYGEN SOURCES Final Report, Apr. 1987 - Sep. 1988
John R. Anderson and Paul J. Wilbur Jan. 1989 58 p
(Grant NAG3-791)
(NASA-CR-182238; NAS 1.26:182238) Avail: NTIS HC A04/MF A01 CSCL 20H

The potential usefulness of the constrained sheath optics concept as a means of controlling the divergence of low energy, high current density ion beams is examined numerically and experimentally. Numerical results demonstrate that some control of the divergence of typical ion beamlets can be achieved at perveance levels of interest by contouring the surface of the constrained sheath properly. Experimental results demonstrate that a sheath can be constrained by a wire mesh attached to the screen plate of the ion optics system. The numerically predicted beamlet divergence characteristics are shown to depart from those measured experimentally, and additional numerical analysis is used to demonstrate that this departure is probably due to distortions of the sheath caused by the fact that it attempts to conform to the individual wires that make up the sheath constraining mesh. The concept is considered potentially useful in controlling the divergence of ion beamlets in applications where low divergence, low energy, high current density beamlets are being sought, but more work is required to demonstrate this for net beam ion energies as low as 5 eV. Author

N89-19974# Rochester Univ., NY. Dept. of Chemistry.
INTERMOLECULAR AND INTRAMOLECULAR VIBRATIONAL RELAXATION AND ENERGY TRANSFER Final Report, 1 Apr. 1985 - 30 Sep. 1988
Shaul Mukamel 30 Sep. 1988 15 p
(Contract DAAG29-85-K-0059)
(AD-A201610; ARO-22396.21-CH) Avail: NTIS HC A03/MF A01 CSCL 07D

This research program resulted in 53 publications. Forty-three already appeared, 4 are accepted for publication, and 6 were submitted. These publications are listed at the end of the final report. The research focused in the following major areas: (1) molecular semi-classical dynamics in Liouville space; a unified description of vibrational relaxation nonlinear spectroscopy and rate processes; (2) intramolecular vibrational redistribution; (3) vibrational and radiative dynamics in molecular clusters; (4)

coherent and spontaneous Raman, fluorescence and four-wave mixing spectroscopy; (5) excitation transport, electron transfer, and localization in disordered molecular systems. The main accomplishments are summarized in the final report. GRA

N89-19975# Argonne National Lab., IL.
HIGH-PRECISION LASER AND RF SPECTROSCOPY OF ATOMIC, MOLECULAR, AND SLOW ION BEAMS
W. J. Childs, T. C. Steimle, A. Sen, and Y. Azuma 1988 3 p Presented at the DOE Atomic Physics Contractors' Meeting, Bethesda, MD, 31 Aug. 1988
(Contract W-31-109-eng-38)
(DE89-005870; CONF-880893-2) Avail: NTIS HC A02/MF A01

We have obtained extensive new structural information on the light diatomic radical ScO since the last report in this series. The new studies complete our systematic investigation of the fine and hyperfine structure (hfs) of the group IIIa monoxides LaO, YO, and ScO. The studies of the molecular X sup 2 sigma(+) electronic ground state were carried out using the molecular-beam laser-RF double-resonance method, and the excited electronic state information was obtained by complementing this data with Doppler-free laser fluorescence studies. DOE

N89-19976*# National Aeronautics and Space Administration. Goddard Space Flight Center, Greenbelt, MD.
THE V3, V4 AND V6 BANDS OF FORMALDEHYDE: A SPECTRAL CATALOG FROM 900 cm(-1) TO 1580 cm(-1)
Shachar Nadler, D. C. Reuter, S. J. Daunt, and J. W. C. Johns (Herzberg Inst. of Astrophysics, Ottawa, Ontario) Sep. 1988 199 p Prepared in cooperation with Tennessee Univ., Knoxville
(NASA-TM-100709; Rept-89B0005; NAS 1.15:100709) Avail: NTIS HC A09/MF A01 CSCL 20H

The results of a complete high resolution study of the three vibration-rotation bands v sub 3, v sub 4, and V sub 6 using both TDLs and FT-IR spectroscopy are presented. The reults are given in terms of a table of over 8000 predicted transition frequencies and strengths. A plot of the predicted and calculated spectra is shown. Over 3000 transitions were assigned and used in the simultaneous analysis of the three bands. The simultaneous fit permitted a rigorous study of Coriolis and other type iterations among bands yielding improved molecular constants. Line intensities of 28 transitions measured by a TDL and 20 transitions from FTS data were used, along with the eigenvectors from the frequency fitting, in a least squares analysis to evaluate the band strengths. NASA

N89-19977# Sandia National Labs., Albuquerque, NM.
MECHANISMS LEADING TO SINGLE EVENT UPSET
C. L. Axness, H. T. Weaver, J. S. Fu, R. Koga, and W. A. Kolasinski 15 Mar. 1988 9 p Prepared in cooperation with Aerospace Corp., El Segundo, CA
(ATR-86(8139)-5) Avail: NTIS HC A02/MF A01

The SRAM cell recovery time following a 140 MeV Krypton strike on a Sandia SRAM is modeled using a two-dimensional transient numerical simulator and circuit code. Strikes at both n- and p-channel off drains are investigated. Four principle results are obtained. The recovery time after a strike is strongly dependent on the drive of the restoring transistor. A struck off p-channel drain-to-gate capacitive coupling has a significant effect on recovery in SRAM with feedback resistors. Recovery time is approximately linear with LET over LET in the range to 0.4 pC/micrometer. Finally, an experimental n-channel Single Event Upset (SEU) was observed in a Sandia SRAM without feedback resistors. Author

73 NUCLEAR AND HIGH-ENERGY PHYSICS

Includes elementary and nuclear particles; and reactor theory.

For space radiation see *93 Space Radiation.*

N89-19978# Technische Univ., Eindhoven (Netherlands).
THEORY OF ACCELERATED ORBITS AND SPACE CHARGE EFFECTS IN AN AZIMUTHLY VARYING FIELD (AVF) CYCLOTRON Ph.D. Thesis
Willem Jan Gerard Ma Kleeven 1988 139 p
(ETN-89-93897) Avail: NTIS HC A07/MF A01

The motion of accelerated particles in a cyclotron was investigated. A general Hamiltonian theory for the simultaneous treatment of the transverse and the longitudinal motion and the coupling between both motions is derived. The theory describes phenomena which are due to the interfering influences of a given geometrical shape of the dee-structure and the flutter. An example is the electric gap crossing resonance. Also, another resonance which affects the central position phase may occur in a 3-fold symmetric magnetic field combined with a 3-dee system and also in a 4-fold symmetry combined with a 1-dee system or a 2-dee system. The effect of space charge in the cyclotron was studied. The properties of the bunch like the sizes, emittances, and momentum spread are represented in terms of the second order moments of phase space distribution function. Two sets of differential equations describe the time-evolution of these moments under space charge conditions. The model takes into account the coupling between the longitudinal and the radial motion. It also takes account of the fact that, in the ideal case, the revolution frequency of the particles is independent of their energy (isochronism), so there is no RF focusing in the longitudinal phase space to counteract the repulsive longitudinal space charge force. ESA

N89-19979# Kernforschungsanlage, Juelich (Germany, F.R.). Inst. fuer Reaktorentwicklung.
HERMES, A MONTE CARLO PROGRAM SYSTEM FOR BEAM-MATERIALS INTERACTION STUDIES
P. Cloth, D. Filges, R. D. Neef, G. Sterzenbach, Ch. Reul, T. W. Armstrong, B. L. Colborn, B. Anders, and H. Brueckmann May 1988 249 p
(JUEL-2203; ISSN-0366-0885; ETN-89-93960) Avail: NTIS HC A11/MF A01

The HERMES (High Energy Radiation Monte Carlo Elaborate System) system of Monte Carlo computer codes to treat the physics to be considered in computer simulation of radiation transport and interaction problems is described. The HERMES offers powerful capabilities of Monte Carlo analysis and of merging the outcomes of partial programs into final results. An interfacing system provides easy interchange of input/output data between programs by standardized data structures and allows unproblematic extension of the HERMES system by introducing new programs. The HERMES collection of physics programs permits the simulation of secondary particles histories induced by primary particles of any energy up to the regime of high-energy physics and down to thermal energies, e.g., for neutrons. The development of particle cascades can be simulated within very complex geometries and material configurations with only minor restrictions. To achieve portability of the HERMES system, the original coding of the programs was converted to the FORTRAN 77 standard. This, however, was verified only on two computer systems, the IBM 3081 and the CRAY-XMP22. ESA

N89-19980# Los Alamos National Lab., NM.
BEAM PROFILE EFFECTS ON NPB PERFORMANCE
Rene J. LeClaire, Jr. and Wilma J. Bunker, ed. Mar. 1988 19 p
(LA-11228-MS) Avail: NTIS HC A03/MF A01

A comparison of neutral particle beam (NPB) brightness for various neutral beam profiles indicates that the widely used assumption of a Gaussian profile may be misleading for collisional

neutralizers. An analysis of available experimental evidence shows that lower peaks and higher tails, compared to a Gaussian beam profile, are observed out of collisional neutralizers, which implies that peak brightness is over estimated, and for a given NPB platform-to-target range, the beam current (power), dwell time or some combination of such engagement parameters would have to be altered to maintain a fixed dose on the target. Based on the present analysis, this factor is nominally about 2.4 but may actually be as low as 1.8 or as high as 8. This is an important consideration in estimating NPB constellation performance in SDI engagement contexts. Author

74 OPTICS

Includes light phenomena; and optical devices.
For lasers see *36 Lasers and Masers.*

N89-19981# Dayton Univ., OH.
EVALUATION OF OPTICAL MATERIALS SAMPLES Final Report
Jul. 1988 81 p
(Contract DASG60-87-C-0029)
(AD-A199471; UDRI-TR-88-89) Avail: NTIS HC A05/MF A01 CSCL 02F

The primary objective of order subcontract was to prepare AGT and UGT test specimens, provide characterization data and provide damage assessments on tech base laser mirror materials being developed on other government contracts. The properties to be determined included flexural strength, Young's modulus, Poisson's ratio, fracture toughness (Klc), coefficient of thermal expansion, thermal diffusivity, hardness, and specific heat. In some cases Scanning Electron Microscopy (SEM), X-Ray Diffraction (XRD), energy dispersive X-ray analysis (EDAX), and Auger spectroscopy (AES) were to be performed to determine chemical composition and crystal structure and damage mechanisms. In addition if materials problems occurred, that could not be anticipated in advance, studies were to be initiated to aid the SDI optical materials efforts as required. GRA

N89-19982# University of Southern California, Los Angeles. Dept. of Electrical Engineering and Electrophysics.
NEW APPROACHES TO RECONFIGURABLE OPTICAL INTERCONNECTIONS FOR OPTICAL COMPUTING Annual Report, 1 Sep. 1987 - 30 Sep. 1988
William H. Steier 1 Oct. 1988 15 p
(Grant AF-AFOSR-0338-87; AF Proj. 2305)
(AD-A201307; AFOSR-88-1186TR) Avail: NTIS HC A03/MF A01 CSCL 20F

This report covers the period from October 1, 1987 through September 30, 1988, the first year under the contract. The objective of this effort is to define and evaluate new approaches to two-dimensional arrays of reconfigurable optical interconnections for optical computing. The emphasis is on optically controlled optical beam directors or switches which can be fabricated into high density 2-D arrays. The proposed applications in optical neural computers and other types of optical computers require reconfiguration speeds on the order of microseconds. The emphasis is therefore on devices and nonlinear optical materials with response times of microseconds but with the potential for high packing density. The approach to this research has two components: (1) nonlinear optical materials; and (2) optically controlled optical switching devices which can be integrated into 2-D arrays. The materials work stresses the transport assisted optical nonlinear materials since this is the only class of materials which exhibit a sufficiently large nonlinearity, in the response time required, and with a relatively low optical energy required. In these materials, optically excited electric charge is separated by an electric field to create a space charge field which reduces the total electric field. GRA

N89-19983# Massachusetts Inst. of Tech., Cambridge. Artificial Intelligence Lab.
ESTIMATING THE ILLUMINANT COLOR FROM THE SHADING OF A SMOOTH SURFACE
Hsien-Che Lee Aug. 1988 26 p
(Contract N00014-85-K-0124)
(AD-A201333; AI-M-1068) Avail: NTIS HC A03/MF A01 CSCL 06D

The image of a uniform wall illuminated by a spot light often gives a strong impression of the illuminant color. How can it be possible to know if it is a white wall illuminated by yellow light or a yellow wall illuminated by white light. If the wall is a Lambertian reflector, it would not be possible to tell the difference. However, in the real world, some amount of specular reflection is almost always present. In this memo, it is shown that the computation is possible in most practical cases. Light reflection from a surface is usually modeled as having two components: the interface (specular) reflection and the body (diffuse) reflection. For a surface of inhomogeneous material, the spectral composition of the interface reflection component is often similar to that of the illuminant. The problem of computing the illuminant chromaticity from the shading of a single smooth surface is to separate these two components. An image of an illuminated uniform wall, according to the above model, gives only one physical constraint about the illuminant chromaticity, not enough to determine a unique solution. However, since the spatial scale over which the interface reflection changes significantly is much smaller than that of the body reflection, it can be shown that one can effectively exploit the scale difference to find a unique solution, which is often very accurate. The method can also be generalized to compute the illuminant chromaticity for a nonuniform smooth surface. GRA

N89-19984# Los Alamos National Lab., NM.
HIGH-ORDER BEAM OPTICS: AN OVERVIEW
Edward A. Heighway 1988 7 p Presented at the Linear Accelerator Conference, Williamsburg, VA, 3 Oct. 1988
(Contract W-7405-eng-36)
(DE89-005441; LA-UR-88-3301; CONF-881049-60) Avail: NTIS HC A02/MF A01

Beam-transport codes have been around for as long as thirty years and high-order codes, second-order at least, for close to twenty years. Before this period of design-code development, there was considerable high-order treatment, but it was almost entirely analytical. History has a way of repeating itself, and the current excitement in the field of high-order optics is based on the application of Lie algebra and the so-called differential algebra to beam-transport codes, both of which are highly analytical in foundation. Some of the main design tools available today will be described, giving a little of their history, and will conclude by trying to convey some of the excitement in the field through a brief description of Lie and differential algebra. DOE

N89-19985# Brookhaven National Lab., Upton, NY.
LONG TRACE PROFILE MEASUREMENTS ON CYLINDRICAL ASPHERES
P. Z. Takacs, Su-chen Kate Feng, E. L. Church, Shi-nan Qian, and Wu-ming Liu 1988 11 p Presented at the 32nd International Technical Symposium on Optical and Opto-Electronic Applied Sciences and Engineering, San Diego, CA, 14 Aug. 1988
(Contract DE-AC02-76CH-00016)
(DE89-005661; BNL-40955; CONF-880887-29) Avail: NTIS HC A03/MF A01

A new long-trace optical profiling instrument is now in operation at Brookhaven National Laboratory measuring surface figure and macro-roughness on large optical components, principally long cylindrical mirrors for use in synchrotron radiation beam lines. The non-contact measurement technique is based upon a pencil-beam interferometer system. The optical head is mounted on a linear air bearing slide and has a free travel range of nearly one meter. We are able to sample surface spatial periods between 1 mm (the laser beam diameter) and 1 m. The input slope data is converted to surface height by a Fourier filtering technique which distributes the random noise error contributions evenly over the

entire trace length. A number of optical components have been measured with the instrument. Results are presented for fused silica cylinders 900 mm and 600 mm in length and for a fused silica toroid and several electroless nickel-plated paraboloids. DOE

N89-19986# Los Alamos National Lab., NM.
AN ACHROMATIC SUPER TELEPHOTO LENS
Yasuo Takahashi 1989 8 p
(Contract W-74U5-eng-36)
(DE89-006163; LA-tr-89-3) Avail: NTIS HC A02/MF A01

First, the structure is explained. The first lens is a positive lens, the second lens is a negative lens, the third lens is a positive lens, the fourth through the sixth lenses are the combination of a negative, a positive and a negative lens, the seventh lens is a negative lens, the eighth lens is a negative lens, the ninth lens is a positive lens, the eighth and the ninth lenses are placed immediately next to each other. The lens by this invention is characterized by the function of the 3-ply lens placed in the middle. If the 3-ply lens is not placed there, then the whole lens system will become a telephoto lens consisting of the frontal group (three lenses) and the rear group (three lenses). DOE

N89-19987# Consiglio Nazionale delle Ricerche, Frascati (Italy). Ist. di Fisica dello Spazio Interplanetario.
FOCUSING SYSTEM, ROTATION, AND MODULATION OF THE F 9 MIRROR OF THE IFSI 40 cm TELESCOPE [SISTEMA DI MESSA A FUOCO, ROTAZIONE E MODULAZIONE DELLO SPECCHIO SECONDARIO, F 9, DEL TELESCOPIO DA 40 CM, IFSI]
Paolo Baldetti Nov. 1987 36 p In ITALIAN
(IFSI-87-16; ETN-89-93463) Avail: NTIS HC A03/MF A01

The design of a control system for the secondary mirror of an infrared astronomic telescope is described. The mirror is 59.4 mm diameter and 76 g weight. The modulation is done using a highly asymmetric square wave to maximize the observation time. The design includes careful attention paid to vibrations induced by the modulation system. Drawings of the components and optical scheme are included. ESA

N89-20074*# Missouri Univ., Independence. Dept. of Electrical and Computer Engineering.
OPTICAL JOINT CORRELATION USING THE DEFORMABLE MIRROR DEVICE Final Report
Jerome Knopp *In* NASA, Lyndon B. Johnson Space Center, National Aeronautics and Space Administration (NASA)/American Society for Engineering Education (ASEE) Summer Faculty Fellowship Program 1988, Volume 2 Feb. 1989 14 p (For primary document see N89-20073 12-99)
Avail: NTIS HC A09/MF A01 CSCL 20F

75 PLASMA PHYSICS

Includes magnetohydrodynamics and plasma fusion.

For ionospheric plasmas see *46 Geophysics*. For space plasmas see *90 Astrophysics*.

N89-19988 California Univ., San Diego.
THERMONUCLEAR REACTIONS OF LIGHT NUCLEI IN ASTROPHYSICAL PLASMAS Ph.D. Thesis
Nidhal Guessoum 1988 216 p
Avail: Univ. Microfilms Order No. DA8817165

A very detailed and extensive calculation on the proton-proton fusion reaction, which takes place in the (high-temperature) central regions of young stars such as the sun is presented. A summary of the previous formulations of and results for the reaction rate is presented, and is then followed by calculations and results. Treatment consists of a recalculation of the lambda squared and S factors (defined therein) using different deuteron and p-p wave functions, but also includes evaluations of the various uncertainties attached to the determination of these quantities. The corrections applied to the (simplest) calculation of the reaction rate, and the relevance of these new results to the expected fluxes of the solar neutrinos are examined. The thermonuclear breakup processes which occur in astrophysical plasmas of ion temperatures kT(sub i) is approximately or greater than 1 MeV, is examined and some of their notable consequences investigated. Calculations of the rates of breakup of the (relevant) light species, as induced by protons, alphas, photons, and neutrons and electrons, respectively, are presented. The possibility of occurrence and the importance of these processes in accretion plasmas existing around compact stars (BHs, NSs, and WDs) are considered. Dissert. Abstr.

N89-19989# Gosudarstvennyi Komitet po Ispolzovaniyu Atomnoi Energii, Moscow (USSR). Inst. Atomnoj Ehnergii.
EFFECT OF LIMITER CURRENTS ON PLASMA EQUILIBRIUM AND STABILITY IN A TOKAMAK
V. I. Belashov, Yu. V. Gribov, S. V. Putvinskij, and N. N. Brevnov 1987 8 p In RUSSIAN
(DE88-704951; IAE-4477/7) Avail: NTIS (US Sales Only) HC A02/MF A01

The results of theoretical and experimental research of currents between diaphragms limiting plasma cord in tokamak on plasma equilibrium and stability with an arbitrary form of transverse cross section are presented. It is shown that plasma cord behaviour depends on applied voltage polarity. The phenomena considered can be important for tokamaks in which fast plasma compression in a big radius is invisaged. DOE

N89-19990# Tennessee Univ. Space Inst., Tullahoma.
AN INNOVATIVE DEMONSTRATION OF HIGH POWER DENSITY IN A COMPACT MHD GENERATOR Semiannual Report
J. T. Lineberry, H. J. Schmidt, and J. N. Chapman May 1988 104 p
(Contract DE-AC22-87PC-79678)
(DE89-002159; DOE/PC-79678/T1) Avail: NTIS HC A06/MF A01

This document is the first semi-annual report for this project. It has been prepared in accordance with contractual reporting obligations and contains a written summary of the research work which has been performed since the beginning of the project through March 31, 1988. During this period, research work has included a variety of studies on several aspects of the overall project as was needed to scope out the requirements for proceeding with a detailed design of experimental hardware. One of the major objectives of these efforts was to provide a definition of operating conditions that are required to allow this MHD system to meet the program objectives. These background studies encompassed detailed analyses of the combustion of the aluminum/carbon (Al:C) solid fuel and evaluations of the gas dynamic characteristics of the combustion plasma produced by combustion. Another major effort was that of analyses and predictions of the performance of conceptual designs for the MHD generator. Both of these tasks were directed at obtaining necessary information which would allow geometric scaling of the experimental MHD system. A summary of the design studies that were performed is given within the body of this report. DOE

N89-19991# Ruhr Univ., Bochum (Germany, F.R.). Abteilung fuer Physik und Astronomie.
EXCITATION OF STRONG HIGH-FREQUENCY ELECTRIC FIELDS AND THEIR DETECTION USING THE DYNAMIC STARK EFFECT Ph.D. Thesis [ERZEUGUNG STARKER ELEKTRISCHER HF-FELDER UND NACHWEIS DURCH DEN DYNAMISCHEN STARKEFFEKT]
Armin Kamp 1987 100 p In GERMAN
(ETN-89-93794) Avail: NTIS HC A05/MF A01

The effects of monochromatic high frequency electric fields on deuterium spectral lines in plasma were investigated. Field and plasma excitation were separated in order to obtain clearly defined test conditions. The electric field of the microwaves (mm range) was enhanced by a lens. Plasma satellites of first and second order were observed in the line profile, the distance to the main component of which corresponds to an integer multiple of the

microwave frequency. The electric field strength (of order kV/Cm) was deduced from the satellite intensities, leading to consistent results. The satellite intensities are very sensitive to the polarization direction. The results show that the determination of high frequency field strengths in hydrogen and deuterium plasmas is possible using the dynamic Stark effect. ESA

N89-19992# Kernforschungszentrum G.m.b.H., Karlsruhe (Germany, F.R.). Projekt Kernfusion.
POSSIBILITIES FOR BREAKEVEN AND IGNITION OF D-He3 FUSION FUEL IN A NEAR TERM TOKAMAK Final Report
G. A. Emmert, L. El-Guebaly, R. Klingelhofer, G. L. Kulcinski, J. F. Santarius, J. E. Scharer, I. N. Sviatoslavsky, P. L. Walstrom, and J. L. Wittenburg Sep. 1988 151 p Partly in ENGLISH and GERMAN
(KfK-4433; FPA-88-2; ISSN-0303-4003; ETN-89-93967)
Copyright Avail: NTIS HC A08/MF A01

The feasibility of investigating D-He3 reactor plasma conditions in a tokamak of the NET/INTOR class was investigated. Depending on the energy confinement scaling law, energy breakeven may be achieved without significant modification to the NET design. The best results are for the more optimistic ASDEX H-mode scaling law. Kaye-Goldston scaling with a modest improvement due to the H-mode is more pessimistic and makes achieving breakeven more difficult. Significant improvement in Q (ratio of the fusion power to the injected power), or the ignition margin, can be achieved by taking advantage of the much reduced neutron production of the D-He3 fuel cycle. Removal of the tritium producing blanket and replacing the inboard neutron shield by a thinner shield optimized for the neutron spectrum in D-He3 allows the plasma to be increased without changing the magnetic field at the toroidal field magnet. This allows the plasma to achieve higher beta and Q values up to 3. The implications of D-He3 operation for fast ion loss, neutron sheilding, heat loads on the first wall and divertor, plasma refuelling, changes to the poloidal field coil system, and pumping of the helium from the vacuum chamber are considered. ESA

N89-19993# Ruhr Univ., Bochum (Germany, F.R.). Inst. fuer Experimentalphysik.
RESONANCE CONES IN NON MAXWELLIAN PLASMAS
G. Oelerich-Hill and A. Piel May 1988 53 p Submitted for publication Sponsored by Deutsch Forschungsgeimschaft, Bonn, Federal Republic of Germany
(Rept-88-N4-173; ETN-89-93983) Avail: NTIS HC A04/MF A01

Resonance cones in hot drifting plasmas and in various beam-plasma situations are studied. In a drifting plasma the upstream-downstream asymmetry of the main cone is suitable for diagnostics of plasma drifts. The evaluation of electron temperature from the interference pattern is discussed in terms of the low temperature low drift-approximation (LTLDA) and by comparison with numerical kinetic theory calculations. In this way the range of applicability of this method is extended compared to LTLDA. In a beam-plasma situation, the downstream resonance cone exhibits an interference pattern which can be attributed to resonant particle effects. The upstream resonance cone is only slightly affected and is still applicable for Te and ne diagnostics. As a result of the comparison with numerical calculations, in which the actual distribution function is used, the downstream interference pattern is proposed as a diagnostic method for obtaining the mean beam energy. The waves generated by the beam plasma interaction are analyzed by digital cross correlation techniques. They are found to be Whistler waves propagating obliquely to the magnetic field direction at the resonance cone angle. ESA

N89-19994# Max-Planck-Inst. fuer Plasmaphysik, Garching (Germany, F.R.).
NUMERICAL STUDIES OF MHD TURBULENCE IN THE REVERSED FIELD PINCH
David Merlin and Dieter Biskamp Aug. 1988 53 p
(IPP-6/276; ETN-89-93990) Copyright Avail: NTIS HC A04/MF A01

Nonlinear numerical studies of the MHD turbulence generated in a reversed field pinch (RFP) configuration are presented. The resistive MHD equations are solved by using a three-dimensional semi-implicit spectral code. While a qualitative picture of the global RFP behavior is readily obtained, the possibility of obtaining reliable results for Reynolds numbers of practical interest is a major problem. For this reason particular attention is payed to the convergence properties of the spectral methods. Results on the dependence of the fluctuations on the Reynolds numbers are given. ESA

N89-19995 Max-Planck-Inst. fuer Physik und Astrophysik, Garching (Germany, F.R.). Inst. fuer Extraterrestrische Physik.
ION BEAM DRIVEN ELECTROSTATIC SHOCKS
R. Pottellette, R. A. Treumann, O. H. Bauer, and J. P. Lebreton Jul. 1988 33 p Sponsored in part by CNES, France Original contains color illustrations
(MPE-Preprint-127; ETN-89-93993) Copyright Avail: Fachinformationszentrum Karlsruhe, 7514
Eggentein-Leopoldshafen 2, Fed. Republic of Germany

Electrostatic shock waves were detected during the injection of an artificial xenon ion beam into the collisionless ionospheric plasma. The beam was directed quasiperpendicular to the ambient magnetic field. The shock structure develops at distances where the apparent azimuthal speed of the beam fan is comparable to the phase velocity of ion acoustic waves sustained by background O(+) ions. The shock is characterized by a decrease in the local density up to 10 percent of the background density, strong shear motion visible in the convection electric field, field-aligned potential drops of the order of several tens of mV, increased electron temperatures, and fluxes of reflected ions. Probably also suprathermal electron fluxes along the magnetic field were present, but were not measured. The Mach number is 1.09 and thus the shock is weak and turbulent generated by ion-acoustic turbulence observed throughout the shock region. It is suggested that this turbulence is driven by an ion-ion instability excited by reflected background ions. Estimates of the number density of reflected ions show that 50 percent of the background ion population may be reflected from the shock potential. On a larger spatial scale these reflected ions may be responsible for the excitation of the observed lower-hybrid and ion-cyclotron harmonic waves in front of the leading edge of the beam. No shock is found on the trailing edge of the beam suggesting that different physical conditions apply there. ESA

N89-19996 Max-Planck-Inst. fuer Physik und Astrophysik, Garching (Germany, F.R.). Inst. fuer Extraterrestrische Physik.
PLASMA WAVES AT THE DAYSIDE MAGNETOPAUSE
J. LaBelle and R. A. Treumann Jul. 1988 43 p Submitted for publication
(MPE-Preprint-128; ETN-89-93994) Copyright Avail: Fachinformationszentrum Karlsruhe, 7514
Egenstein-Leopoldshafen 2, Fed. Republic of Germany

Investigations of plasma waves at the magnetopause, including results from the AMPTE/IRM satellite, show that delta E and delta B fluctuations typically have a featureless spectrum which monotonically decreases with frequency; integrated rms amplitudes are typically a few mV/m for delta E and 10 nT for delta B, though delta E can be an order of magnitude larger. Surveys show a lack of correlation between wave parameters and the magnetopause parameters. Assuming that crossing the diffusion region would give a pronounced signature in the waves, the survey data allow an upper limit of 1000 km to be placed on the latitude extent of the diffusion region, implying that it is not surprising that wave data surveys fail to detect it. The observed wave turbulence levels were used to estimate diffusion coefficients under different assumptions for the wave mode, but the resulting diffusion coefficient is always too small to explain either reconnection or boundary layer formation. Galeev et al (1986) suggest that the dominant diffusion process may be magnetic field migration, a macroscopic process involving the interaction of tearing mode islands. Assuming this mode to be present at the observed level of beta B, the particle diffusion coefficient is 1 billion/sq m/sec.

Another macroscopic diffusive process which could occur at the magnetopause is stochastic E x B scattering, which also implies a diffusion coefficient the same order if the observed delta E spectrum is assumed to be a turbulent cascade consisting of convective cells. ESA

76 SOLID-STATE PHYSICS

Includes superconductivity.

For related information, see also *33 Electronics and Electrical Engineering* and *36 Lasers and Masers.*

N89-19997# National Lab. for High Energy Physics, Oho (Japan).
XPS AND AES STUDIES OF THIN OXIDE LAYERS ON NIOBIUM FOR SUPERCONDUCTING RF CAVITIES
Kiyomitsu Asano, Takaaki Furuya, Yuzo Kojima, Shinji Mitsunobu, Hirotaka Nakai, Syuichi Noguchi, Kenji Saito, Tsuyoshi Tajima, Masahiro Tosa, and Kazuhiro Yoshihara (National Research Inst. for Metals, Ibaraki, Japan) May 1988 25 p
(DE88-756073; KEK-88-2) Avail: NTIS (US Sales Only) HC A03/MF A01

Results from X-ray photoelectron spectroscopy (XPS) and Auger electron spectroscopy (AES) studies of thin oxide layers formed on niobium by surface treatments, which can be applied to superconducting RF cavities, are presented. DOE

N89-19998# North Carolina Univ., Chapel Hill. Dept. of Chemistry.
SOME 2H NMR STUDIES OF ORIENTED FLUID PHASES Interim Technical Report
Edward T. Samulski 19 Oct. 1988 9 p Presented at the Micromolecules International Symposium, Kyoto, Japan, Aug. 1988 Submitted for publication
(Contract N00014-86-K-0772)
(AD-A201241; TR-29) Avail: NTIS HC A02/MF A01 CSCL 07F

Deuterium nuclear magnetic resonance (NMR) observations are presented for two kinds of liquid crystals, thermotropic dimer mesogens and lyotropic polypeptide liquid crystals. In the former intramolecular averaging within the dimer spacer chain is suggestive of translational ordering within the nematic phase which is sensitive to the dimer's terminal chain length. The averaging within the polypeptide sidechain appears to be dominated by intramolecular constraints -- dihedral angle rotations. GRA

N89-19999# Draper (Charles Stark) Lab., Inc., Cambridge, MA.
RCS/PIEZOELECTRIC DISTRIBUTED ACTUATOR STUDY Final Report, Aug. 1985 - Mar. 1988
Thomas Bailey, Alexander Gruzen, and Paul Madden Aug. 1988 113 p
(Contract F04611-85-K-0050)
(AD-A201276; CSDL-R-2076; AFAL-TR-88-038) Avail: NTIS HC A06/MF A01 CSCL 22B

The objective of the program was to develop the technology of piezoelectric distributed actuators, and to test the effectiveness and performance of the actuators when used to augment the damping of a simulated large flexible space structure. The CSDL/AFAL experimental test facility located at CSDL, Inc. was used to test and demonstrate the technology. GRA

N89-20000# California Univ., Davis. Dept. of Physics.
QUANTUM LIMITS OF SUPERCONDUCTING HETERODYNE RECEIVERS Final Report, 15 May 1986 - 14 May 1988
Paul L. Richards 23 Sep. 1988 12 p
(Grant AF-AFOSR-0230-85; AF Proj. 2305)
(AD-A201303; AFOSR-88-1169TR) Avail: NTIS HC A03/MF A01 CSCL 20M

An investigation of the behavior of superconducting heterodyne receivers in the quantum limit can be carried out using very low leakage tunnel junctions and relatively low frequencies, such as W-band. Alternatively, very low capacitance small-area junctions with moderate leakage can be used at much higher frequencies. It is necessary in either case to make precise measurements of mixer noise and gain. It is also essential to make precise determinations of the embedding admittances in order to permit comparison between experiment and theory. In addition, extensive computer software must be written in order to carry out the comparisons with quantum mixer theory. In this project, the technology has been developed for both approaches to the study of the quantum limits of semiconductor insulator semiconductors (SIS) heterodyne mixers. All of the factors necessary to make these coparisons in a W-band waveguide mixer have been in place since early 1977. GRA

N89-20001# Hughes Research Labs., Malibu, CA.
DEVELOPMENT OF Si/SiGe HETEROSTRUCTURES Annual Report, Sep. 1987 - Sep. 1988
R. J. Hauenstein Oct. 1988 30 p
(Contract F49620-87-C-0104)
(AD-A201440) Avail: NTIS HC A03/MF A01 CSCL 09A

With the recent advances in Si molecular beam epitaxy (MBE) and limited-reaction processing (LRP), a viable, heterojunction-based device technology for Si may soon be at hand. Strained-Layer Si(sub 1-x)Ge(sub x) epitaxial alloy films and coherently strained Si(sub1-x)Ge(sub x)Si multilayer structures have been grown very successfully by MBE. More recently, high quality Si/Si(sub 1-x)Ge(sub x)Si heterojunction bipolar transistors (HBT) having been fabricated by LRP techniques. Si(sub 1-x)Ge(sub x)Si systems are of considerable interest because they provide Si-based semiconductor device technology with a practical heterojunction capability which is also compatible with exiting device processing techniques. GRA

N89-20002# Wayne State Univ., Detroit, MI.
JOSEPHSON EFFECT RESEARCH IN HIGH-TEMPERATURE SUPERCONDUCTORS Interim Report, 30 Sep. 1987 - 29 Sep. 1988
Juei-Teng Cheng and Lowell E. Wenger Aug. 1988 35 p
(Contract N00014-88-K-0191)
(AD-A201483) Avail: NTIS HC A03/MF A01 CSCL 20L

The original research proposal to ONR/SDIO had outlined two major goals to be accomplished during the three and half year period from July 1987 to December 1990. The first task was: (1) the fabrication and characterization of thin film superconductors with the high-temperature oxide materials, and secondly (2) the fabrication and characterization of Josephson tunnel junctions. These tasks included the following: (1) fabrication and characterization of thin film superconductors, and (2) fabrication and characterization of Josephson tunnel junctions. Although the administration/contracting of funds were not formally authorized until January 1988, the progress has been quite successful with regard to the first goal of fabrication and characterization of thin/film superconducting oxide films. Similar to all other research groups in being unable to fabricate simple Josephson tunnel junctions with superconducting oxides, we have however been unable to initiate some characterization of the electromagnetic response observed in these films due to the inherent granular Josephson-coupled networks. The progress attained in the research proposal to date, a summary of the major accomplishments, an index of publications attributable to the present funding period, and the proposed program for continued research are presented. GRA

N89-20003# Oak Ridge National Lab., TN.
QUENCH PRESSURE, THERMAL EXPULSION, AND NORMAL ZONE PROPAGATION IN INTERNALLY COOLED SUPERCONDUCTORS
Lawrence Dresner 1988 3 p Presented at the Applied Superconductivity Conference, San Francisco, CA, 21 Aug. 1988
(Contract DE-AC05-84OR-21400)
(DE89-005668; CONF-880812-34) Avail: NTIS HC A02/MF A01

When a nonrecovering normal zone appears in an internally cooled superconductor, the pressure in the conductor rises, helium

is expelled from its ends, and the normal zone grows in size. This paper presents a model of these processes that allows calculation of the pressure, the expulsion velocity, and the propagation velocity with simple formulas. The model is intended to apply to conductors such as the cable-in-conduit conductor of the Westinghouse LCT (WH-LCT) coil, the helium volumes of which have very large length-to-diameter ratios (3 x 10 to the 5th). The predictions of the model agree with the rather limited data available from propagation experiments carried out on the WH-LCT coil. DOE

N89-20004# Space Power, Inc., San Jose, CA.
THE 30 kWe CLASS HIGH EFFICIENCY ARCJET POWER CONDITIONER, VOLUME 1 Final Report, 6 Sep. 1986 - 11Jul 1988
See-Pok Wong, Edward J. Britt, and Kevin McCracken Aug. 1988 43 p
(Contract F04611-86-C-0052)
(AD-A202244; SPI-13-14-Vol-1; AFAL-TR-88-049-Vol-1) Avail: NTIS HC A03/MF A01 CSCL 10B

A 30 kWe arcjet power conditioning unit (PCU) has been designed, built and tested, both with a solid state load and with a 30 kWe arcjet thruster. The arcjet PCU has accumulated over 40 hours full power or nearly full power operating time, and showed no sign of degradation. The measured efficiency was 94 percent, which can easily be increased to 95 percent by substitution of some recently available semiconductors. The stability of output current has been demonstrated while using current-mode, pulse-width modulation control. GRA

N89-20005# Purdue Univ., West Lafayette, IN. School of Electrical Engineering.
THE 2-4 SEMICONDUCTOR SUPERLATTICES Annual Technical Report, 30 Jun. 1987 - 1 Jul. 1988
Robert L. Gunshor, Leslie A. Kolodziejski, Supriyo Datta, and Nobuo Otsuka 18 Oct. 1988 44 p
(Grant AF-AFOSR-0185-85; AF Proj. 2306)
(AD-A202369; AFOSR-88-1219TR) Avail: NTIS HC A03/MF A01 CSCL 20L

The research program is directed toward achieving controlled substitutional doping of the wide bandgap semiconductor ZnSe, ZnSe alloys, and ZnSe-based heterostructures. To achieve this goal the incorporation processes involved in the molecular beam epitaxial and atomic beam epitaxial growth techniques are under study by comparing the experiments with the results of Monte Carlo simulations. As a first approach the n-type doping of zinc selenide with gallium has been investigated and analyzed by both optical (photoluminescence) and electrical (Hall effect) characterization. GRA

N89-20006# Technische Univ., Berlin (Germany, F.R.). Fachbereich Physik.
INVESTIGATIONS OF THE STATICS AND DYNAMICS OF THE JAHN-TELLER SYSTEM RbCrCl3 USING NEUTRON SCATTERING Ph.D. Thesis [UNTERSUCHUNGEN ZUR STATIK UND DYNAMIK DES JAHN-TELLER SYSTEMS RBCRCL3 MITTELS NEUTRONENSTREUUNG]
Niels Michael Pyka 1988 113 p In GERMAN
(ETN-89-93790) Avail: NTIS HC A06/MF A01

As an example of the Rb-group, the Jahn-Teller system RbCrCl3 was investigated to understand the occurrence of a beta-phase between the disordered alpha high and the ordered gamma low phase. Huang scattering in the high and middle phase, dynamic effects, phase transitions, possible cell enlargement ordering effects, critical phenomena, and the magnetic structure below 16 K were analyzed. ESA

N89-20007# Technische Univ., Berlin (Germany, F.R.). Fachbereich Physik.
LASER-SPECTROSCOPIC INVESTIGATIONS OF MANGANESE CENTERS IN THE ZINC SULFIDE HOST LATTICE Ph.D. Thesis [LASERSPEKTORSKOPISCHE UNTERSUNCHUNGEN AN MANGAN-ZENTREN IM ZINKSULFID-WIRTSGITTER]
Udo W. Pohl 1988 172 p In GERMAN
(ETN-89-93791) Avail: NTIS HC A08/MF A01

Laser-spectroscopic measurements were performed on ZnS samples doped with Mn (ZnS:Mn) for the investigation of the electronic structure of the Mn centers. The electronic and crystallographic characteristics of the ZnS host lattice as well as the properties of Mn in the ZnS crystal are depicted. The measuring equipment and the samples are described, with emphasis on the Zeeman apparatus. The composition of the samples was determined analytically using electron beam microprobe and mass spectroscopic measurements. The spectroscopic measurements provide a classification of the electronic transitions, and the effect of codoping of the ZnSiMn samples with foreign substances. The theoretical fundamentals of crystal field theory, spin-orbit coupling, Jahn-Teller effect, and the distribution laws for clusters in zinc lattices are presented. ESA

N89-20008# Los Alamos National Lab., NM. Center for Materials Sciences.
RADIATION INDUCED AMORPHIZATION IN YBa2Cu3O7 AND GdBa2Cu3O7 SUPERCONDUCTORS
Don M. Parkin and Michael Nastasi 1988 7 p Presented at the Fall Meeting of the Materials Research Society, Boston, MA, 28 Nov. 1988
(Contract W-7405-eng-36)
(DE89-005451; LA-UR-88-4038; CONF-881155-34) Avail: NTIS HC A02/MF A01

The response of YBa2Cu3O7 and GdBa2Cu3O7 high temperature superconductors to particle irradiation is examined. Both ion and electron irradiations have been shown to first produce an orthorhombic-to-tetragonal transformation at doses roughly a factor of 10 higher. Analysis of the displacement stoichiometry that results from 120, 300, and 1000 keV electron irradiations, 400 and 500 keV O irradiations, and 300 keV helium irradiations indicate that the orthorhombic-to-tetragonal transformation is driven by O atoms displacements either alone or in the presence of metal atom displacements and that the transformation to the amorphous phase is driven by displacements on the Y, Gd, or other rare earth atom site. DOE

N89-20009# Cornell Univ., Ithaca, NY.
STUDIES OF 3-5 COMPOUNDS IN THE MEGABAR REGIME: Progress Report
A. L. Ruoff 1988 7 p
(Contract DE-FG02-87ER-45320)
(DE89-005722; DOE/ER-45320/2) Avail: NTIS HC A02/MF A01

In this project we make systematic studies of the crystal structure changes of the 3-5 compounds as a function of pressure. The broad objective of the proposed research is to provide experimental data over a broad range of coordination number and interatomic spacing which can play a leading role in the testing and development of theoretical models of bonding. Phase transformations of GaAs, CeO2, InSb are discussed. DOE

N89-20010# University of Western Ontario, London. Dept. of Physics.
POSITRON SPECTROSCOPY FOR MATERIALS CHARACTERIZATION
Peter J. Schultz and C. L. Snead, Jr. 1988 45 p Presented at the Metallurgical Society Fall Meeting and American Society for Metals Materials Week, Chicago, IL, 24 Sep. 1988 Prepared in cooperation with Brookhaven National Lab., Upton, NY
(Contract DE-AC02-76CH-00016)
(DE89-005766; BNL-41959; CONF-880901-15) Avail: NTIS HC A03/MF A01

One of the more active areas of research on materials involves the observation and characterization of defects. The discovery of positron localization in vacancy-type defects in solids in the 1960's initiated a vast number of experimental and theoretical investigations which continue to this day. Traditional positron annihilation spectroscopic techniques, including lifetime studies, angular correlation, and Doppler broadening of annihilation

radiation, are still being applied to new problems in the bulk properties of simple metals and their alloys. In addition new techniques based on tunable sources of monoenergetic positron beams have, in the last 5 years, expanded the horizons to studies of surfaces, thin films, and interfaces. In the present paper we briefly review these experimental techniques, illustrating with some of the important accomplishments of the field. DOE

N89-20011# Argonne National Lab., IL.
OXYGEN DIFFUSION IN YBa2Cu3O7-DELTA
J. L. Routbort, S. J. Rothman, L. J. Nowicki, and K. C. Goretta Jun. 1988 9 p Presented at the AUSTCERAM '88: International Conference on Ceramics, Sidney, Australia, 20 Aug. 1988
(Contract W-31-109-eng-38)
(DE89-005831; CONF-8808187-1) Avail: NTIS HC A02/MF A01

The tracer diffusion coefficient of O-18 in the 90 K superconducting oxide, YBa2Cu3O sub 7-delta, in the temperature range of 300 to 600 C was measured using the SIMS technique. An activation energy of 0.95 eV was obtained which we believe represents the temperature dependence of volume diffusion. Techniques to measure more accurately diffusion at higher temperature are being devised and diffusion experiments on single crystals are in progress. DOE

N89-20012# Argonne National Lab., IL.
MOSSBAUER EFFECT STUDIES OF MAGNETISM IN SUPERCONDUCTING SYSTEMS
B. D. Dunlap and C. W. Kimball 1988 29 p Presented at the Meeting on Nuclear Methods in Magnetism, Munich, (Federal Republic of Germany), 1 Aug. 1988 Prepared in cooperation with Northern Illinois Univ., Dekalb
(Contract W-31-109-eng-38)
(DE89-005844; CONF-880845-2) Avail: NTIS HC A03/MF A01

The use of magnetism in the study of superconducting materials has gone from a time when the sole purpose was the introduction of magnetic ions for the specific purpose of degrading superconducting properties to a time when magnetic and superconductivity take comparable roles, with comparably sized interactions, in determining the overall properties of a material. Magnetic hyperfine measurements have been very useful, e.g., in sorting out values of exchange parameters, values of crystal field interactions, details of magnetic ordering, and spatial distribution of magnetism. As with most such measurements, Mossbauer data do not specifically provide a great deal of information on superconducting properties themselves, but they have provided an important complement to bulk property measurements such as heat capacity, susceptibility and magnetization, and have also been very important when taken together with neutron diffraction data on structural and magnetic properties. With the oxide superconductors, it seems clear that we may deal with rather complex magnetic phenomena, and it is clear that this type of research will continue to play an important part in developing our understanding of these phenomena. DOE

N89-20013# Argonne National Lab., IL.
ATOMIC STRUCTURE OF TILT GRAIN BOUNDARIES IN NiO
Karl L. Merkle and David J. Smith May 1988 6 p Presented at the Spring Meeting of the Materials Research Society, Reno, NV, 4 Apr. 1988 Prepared in cooperation with Arizona State Univ., Tempe
(Contract W-31-109-eng-38)
(DE89-005847; CONF-880408-44) Avail: NTIS HC A02/MF A01

High-resolution electron microscopy at 400 kV has been used to study the core structure of large-angle (001) tilt grain boundaries in NiO. The deduced atomic structures show considerable variety and complexity, even for boundaries with the same tilt axis and misorientation. The coexistence of asymmetric and symmetric boundaries which is observed at each misorientation suggests that asymmetric grain boundaries containing densely packed planes are associated with relatively low free energies. A multiplicity of core structures is found for the sigma=5 and the sigma=13 grain boundaries. The normal component of the rigid-body translation in these boundaries is quite small in view of the relatively open structure that is expected for grain boundaries in ionic solids. Substantial concentrations of Schottky pairs near the boundary cores, as well as relaxations parallel to the misorientation axis, are indicated. DOE

N89-20014# Argonne National Lab., IL.
SIMS MEASUREMENT OF OXYGEN TRACER DIFFUSION IN YBa2Cu3O7-DELTA
S. J. Rothman, J. L. Routbort, J. E. Baker (Illinois Univ., Urbana.), L. J. Nowicki, K. C. Goretta, L. J. Thompson, and J. N. Mundy Sep. 1988 18 p Presented at the American Institute of Mechanical Engineers Meeting, Chicago, IL, 25 Sep. 1988
(Contracts W-31-109-eng-38; DE-AC02-76ER-01198)
(DE89-005884; CONF-8809201-3) Avail: NTIS HC A03/MF A01

The present paper describes experiments to measure the tracer diffusion of 18O in the high T sub c superconductor YBa2Cu3O sub 7-delta, with special emphasis on depth profiling by secondary ion mass spectrometry (SIMS) and the analysis of the SIMS data. The tracer diffusion coefficients are given by an Arrhenius type expression: $D^* = (9 + \text{or} - 8) \times 0.000001 \exp(- (0.89 + \text{or} - 0.05\ eV)/kT)$ sq cm/s. These results are discussed in the framework of the theory of Bakker et al. DOE

N89-20015# Los Alamos National Lab., NM.
USE OF SUPERCONDUCTING IMAGING SURFACES TO ENHANCE DETECTION OF WEAK MAGNETIC SOURCES BY SQUID SYSTEMS
W. C. Overton, Jr., D. B. vanHulsteyn, and E. R. Flynn Jan. 1989 94 p
(Contract W-7405-eng-36)
(DE89-006568; LA-11473-MS) Avail: NTIS HC A05/MF A01

The use of superconducting magnetometers and gradiometers to detect weak magnetic signals is well known. The weak sources produce small field changes in the vicinity of superconducting pickup coil combinations which respond to changes in the local magnetic flux. When coupled to SQUID detectors, these systems can respond to changes as small as 10 ft. However, magnetic noise severely restricts the operation of such systems. We show that combinations of flat and curved superconducting sheets in combination with superconducting pickup coils can enhance the detection capability and improve noise rejection. Surface currents induced in the sheets are represented by the source dipole and its image. They give rise to signals similar to those of the first-order gradiometer. The theory of images is used to analyze the signals. Several configurations of sense coils and superconducting imaging surfaces are analyzed. DOE

N89-20016 Portland State Univ., OR.
THE TENSILE STRENGTH OF LIQUID HELIUM FOUR Ph.D. Thesis
Joel Alan Nissen 1988 120 p
Avail: Univ. Microfilms Order No. DA8827193

It is well known that most liquids exhibit a tensile strength which is much smaller in magnitude than the tensile strength predicted by homogeneous nucleation theory. Liquid helium occupies a unique place among liquids for tensile strength measurements because all foreign gases are frozen out at liquid temperatures. Moreover, superfluid He-4 should fill all crevises on solid surfaces, eliminating the chance of heterogeneous nucleation on helium vapor pockets. A piezoelectric transducer in the form of a hemispherical shell was used to focus high intensity ultrasound into a small volume of He-4. The transducer was gated at its resonant frequency of 566 kHz with gate widths of less than 1 msec in order to minimize the effects of transducer heating and acoustic streaming. The onset of nucleation was detected from the absorption of acoustic energy and the scattering of laser light from microscopic bubbles. A theory for light diffraction from the focal zone of a spherical converging sound wave was developed to confirm calculations of the acoustic pressure amplitude at the

focus of the transducer, calculations based on the acoustic power radiated into the liquid and nonlinear sound absorption.
Dissert. Abstr.

N89-20017 Ohio State Univ., Columbus.
STATIC AND DYNAMIC PROPERTIES OF ARRAYS OF SUPERCONDUCTORS Ph.D. Thesis
Jean Soo Chung 1988 103 p
Avail: Univ. Microfilms Order No. DA8824478

Static and dynamic properties of two dimensional arrays of superconductors were studied. It is shown that in the fully frustrated case, weak positional disorder does not change the critical behavior of the ordered system although the critical temperature is lowered. For sufficiently strong disorder, evidence of the transition disappears. Phase transitions of the arrays in novel types of lattices were analyzed. The ground state configurations and the nature of the transitions of the arrays are found for certain values of frustrations. The variation of the transition temperature with magnetic field is estimated. A method for solving the dynamics of two dimensional arrays of Josephson junctions with shunt resistance was developed. Using this method, I-V characteristics, consistent with experiments, are obtained and the nature of the superconducting transition is analyzed. Dissert. Abstr.

N89-20018 Ohio State Univ., Columbus.
SUPERFLUID TURBULENCE IN TWO-FLUID FLOW OF HELIUM II Ph.D. Thesis
Samuel Scott Courts 1988 169 p
Avail: Univ. Microfilms Order No. DA8824481

The completion of measurements of the dissipation for independently varied normal-fluid and superfluid velocities is presented. These measurements show the propagation of the first and second critical velocities into the (V sub n, V sub s) plane above the thermal counterflow line and provide a data base with which to compare theoretical predictions. The steady state dissipation delta T was measured across the ends of a flow tube (d = 134 micrometers) during laminar and turbulent flow. These flow states were produced using a combination of thermal counterflow procedures and using a very fine fiberglass bundle to produce a pure superflow via film flow of the superfluid component. These data show that the first critical velocity is actually a closed boundary separating laminar flow at small normal-fluid and superfluid velocities from turbulent flow at higher combinations. It was also found that the second critical velocity propagates into the (V sub n, V sub s) plane above thermal counterflow. The transition becomes increasingly abrupt as V sub n is increased. These two boundaries define three regions of turbulence in the (V sub n, V sub s) plane. The turbulence in regions for high V sub n appears to be homogeneous fitting a simple mutual friction model. The TI/TII Boundary separates this region from one of low-level dissipation. These flow states are very complicated and the dissipation here can oscillate between two values. The first critical velocity separates laminar flow states from a turbulent state obeying a modified mutual friction model suggested by Baehr and Tough. This type of turbulence exists both above and below the thermal counterflow line. Dissert. Abstr.

N89-20019# Oak Ridge National Lab., TN.
PYROLYTIC AND LASER PHOTOLYTIC GROWTH OF CRYSTALLINE AND AMORPHOUS GERMANIUM FILMS FROM DIGERMANE (GE2H6)
Djula Eres, D. H. Lowndes, J. Z. Tischler, J. W. Sharp, D. B. Geohegan, and S. J. Pennycook Nov. 1988 6 p Presented at the Fall Meeting of the Materials Research Society, Boston, MA, 28 Nov. - 3 Dec. 1988 Submitted for publication
(Contract DE-AC05-84OR-21400)
(DE89-006125; CONF-881155-36) Avail: NTIS HC A02/MF A01

High-purity digermane (Ge sub 2 H sub 6, 5 percent in He) has been used to grow epitaxially oriented crystalline Ge films by pyrolysis. Amorphous Ge:H films also have been deposited by pyrolysis and ArF (193 nm) laser-induced photolysis. The amorphous-to-crystalline transition and the film's morphology were studied as a function of deposition conditions. The film's microstructure, strain and epitaxial quality were assessed using X-ray diffraction curves and scanning and transmission electron microscopy. It was found that commensurate, coherently strained epitaxial Ge films could be grown pyrolytically on (100) GaAs at low (0.05 to 40 m Torr) Ge sub 2 H sub 6 partial pressures for substrate temperatures above 380 C. DOE

N89-20020# California Univ., Berkeley. Dept. of Materials Science and Mineral Engineering.
THERMAL OXIDATION OF 3-5 COMPOUND SEMICONDUCTORS Ph.D. Thesis
Othon deRego MonteiroNeto Nov. 1988 105 p
(Contract DE-AC03-76SF-00098)
(DE89-007127; LBL-26337) Avail: NTIS HC A06/MF A01

Thermal oxidation of 3-5 compound semiconductors has been studied in the temperature range of 300 to 600 C. Two members of this class of materials, namely InP and GaAs, were the object of the experimental work carried out here. The main analytical tools used were transmission electron microscopy (TEM) and secondary ion mass spectroscopy (SIMS). TEM was employed to access microstructural changes and SIMS to access the composition redistribution that takes place as a consequence of the oxidation reaction. Below 400 C oxidation of both materials led to the formation of amorphous scales, which consisted of a mixture of gallium and arsenic oxides in the case of GaAs, and indium phosphate and oxide in the case of InP. The oxidation kinetics of InP was found to be slower than that of GaAs. In the high temperature regime, i.e., above 400 C, the oxidation of both materials resulted in crystalline products. Precipitation of the group 5 element at the scale/semiconductor interface took place during oxidation. At the GaAs/Ga2O3 interface, As precipitates were formed with a truncated square pyramid shape bound by (111) sub GaAs planes. The precipitates found at the InPO4/InP interface were either a phosphorus rich phase or red phosphorus. Strong vaporization under the electron beam prohibited a more accurate determination. The morphology of those precipitates were very similar to the As ones in GaAs. DOE

N89-20021# Aerospace Corp., El Segundo, CA. Chemistry and Physics Lab.
RAMAN AND RBS STUDIES OF ION IMPLANTED SEMICONDUCTORS
R. C. Bowman, Jr. and D. N. Jamieson 17 May 1988 14 p Prepared in cooperation with California Inst. of Tech., Pasadena
(ATR-88(8359)-5) Avail: NTIS HC A03/MF A01

Raman spectroscopy and Rutherford backscattering spectrometry (RBS) were used to assess boron and silicon implants on the properties of single crystal silicon, GaAs, and CdTe. The behavior of these different semiconductors under identical implant conditions was compared. Changes in the Raman optic phonon spectra reflect the extent of lattice damage caused by the ion implants as well as the ability of various annealing procedures to remove this damage. The Raman results are generally confirmed by RBS ion-channeling measurements. Furthermore, these techniques are shown to provide complementary information on the distribution and nature of implant damages. Author

77 THERMODYNAMICS AND STATISTICAL PHYSICS

Includes quantum mechanics; theoretical physics; and Bose and Fermi statistics.

For related information see also *25 Inorganic and Physical Chemistry* and *34 Fluid Mechanics and Heat Transfer.*

N89-20022# Hiroshima Univ., Takehara (Japan). Research Inst. for Theoretical Physics.
QUANTUM FIELD THEORY OF UNIVERSE
Akio Hosoya and Masahiro Morikawa (Kyoto Univ., Japan) Aug. 1988 21 p

(DE88-756084; RRK-88-20) Avail: NTIS (US Sales Only) HC A03/MF A01

As is well-known, the wave function of universe dictated by the Wheeler-DeWitt equation has a difficulty in its probabilistic interpretation. In order to overcome this difficulty, we explore a theoretical possibility of the second quantization of universe, following the same passage historically taken for the Klein-Gordon particles and the Nambu-Goto strings. It turns out that multiple production of universes is an inevitable consequence even if the initial state is nothing. The problematical interpretation of wave function of universe is circumvented by introducing an internal comoving model detector, which is an analogue of the DeWitt-Unruh detector in the quantum field theory in curved space-time. DOE

N89-20023# Washington Univ., Seattle.
STUDIES IN QUANTUM FIELD THEORY Progress Report
S. K. Polmar 1988 6 p
(Contract DE-AC02-78ER-04915)
(DE89-006286; DOE/ER-04915/3) Avail: NTIS HC A02/MF A01

The theoretical physics group at Washington University has been devoted to the solution of problems in theoretical and mathematical physics. All of the personnel on this task have a similar approach to their research in that they apply sophisticated analytical and numerical techniques to problems primarily in quantum field theory. Specifically, this group has worked on quantum chromodynamics, classical Yang-Mills fields, chiral symmetry breaking condensates, lattice field theory, strong-coupling approximations, perturbation theory in large order, nonlinear waves, 1/N expansions, quantum solitons, phase transitions, nuclear potentials, and early universe calculations. DOE

80 SOCIAL SCIENCES (GENERAL)

Includes educational matters.

No abstracts in this category.

81 ADMINISTRATION AND MANAGEMENT

Includes management planning and research.

N89-20024# Advisory Group for Aerospace Research and Development, Neuilly-Sur-Seine (France).
CALENDAR OF SELECTED AERONAUTICAL AND SPACE MEETINGS: JANUARY 1989 ONWARDS
Dec. 1988 154 p
(AGARD-CAL-89/1; ISBN-92-835-0488-7) Copyright Avail: NTIS HC A08/MF A01

Three kinds of events are covered by this calendar: technical meetings, conferences, and symposia; exhibitions and technical displays; and educational courses. For each meeting, exhibition, or course, the following information is given: reference number, data, location, title and sponsor, keywords indicating main topics covered, and contact code for inquiries. A subject index in the form of keywords is given, each keyword being followed by reference numbers of all the meetings relevant to that particular keyword. Author

N89-20025# Air Force Inst. of Tech., Wright-Patterson AFB, OH.
FACTORS AFFECTING THE ADOPTION OF R AND D PROJECT SELECTION TECHNIQUES AT THE AIR FORCE WRITE AERONAUTICAL LABORATORIES M.S. Thesis
Jonathan D. Congdon Sep. 1988 122 p
(AD-A201543; AD-E951221; AFIT/GSM/LSY/88S-4) Avail: NTIS HC A06/MF A01 CSCL 05A

Although several techniques have been developed to enhance R and D project selection decision-making in research laboratories, they have not been widely accepted by management. This research examined three aspects relating to the implementation of R and D project selection techniques at the Air Force Wright Aeronautical Laboratories (AFWAL). It examined: (1) the methods used by managers to make R and D project selection decisions; (2) the attitudes and perceptions of managers toward the utility of R and D project selection techniques; and (3) the specific factors affecting the adoption of these techniques by R and D managers. Findings showed that R and D project selection techniques play a minor role in the project selection process, and that managers are generally unfamiliar with these techniques. Instead, project selection decisions are often made by top-level laboratory managers through a review process. Findings also showed that the project selection process at AFWAL is primarily driven by requirements pull as opposed to technology push. Factor analysis was used to identify an initial set of variables which affect management's willingness to adopt R and D project selection techniques. GRA

N89-20026# Technische Univ., Delft (Netherlands). Faculty of Technical Mathematics and Informatics.
MULTICRITERIA ANALYSIS AND BUDGET ALLOCATION, WITH APPLICATIONS IN ENERGY R AND D PLANNING: A FEASIBILITY STUDY
F. A. Lootsma, T. C. A. Mensch, and F. A. Vos 1988 70 p
(Contracts EN3M-0048-NL(GDF); DUT-5-35362)
(Rept-88-07; B8809735; ISSN-0920-8577; ETN-89-93844)
Copyright Avail: NTIS HC A04/MF A01

A method of pairwise comparisons was used to rank and rate a number of nonnuclear energy research programs under the relevant criteria. The final scores of the programs were used to calculate an optimal reallocation of the research budget, assuming that there is only a small number of distinct support levels for each program. ESA

N89-20027# Technische Univ., Delft (Netherlands). Faculty of Technical Mathematics and Informatics.
STOCHASTIC AND FUZZY PERT
F. A. Lootsma 1988 25 p Presented at the Workshop on Representation of Uncertainty, Delft, The Netherlands, 22 Sep. 1987
(Rept-88-26; ISSN-0920-8577; ETN-89-94007) Copyright Avail: NTIS HC A03/MF A01

Network-planning techniques based on stochastic and fuzzy models of the activity durations is considered. The stochastic versions of PERT are generally intractable, and cannot be used to draw up tight plans for action. Fuzzy models are closer to reality, simpler to use, but theoretically not well established. The impact of a stochastic and a fuzzy version of PERT is illustrated via a numerical example. The representation of uncertainty in network planning, when the activity durations are estimated by human experts is discussed. Stochastic models are unsuitable in PERT planning when the activity durations are estimated by human experts. However, fuzzy arithmetic, in its present form, is not sufficiently well established to model the vagueness of human judgement. ESA

N89-19818*# National Aeronautics and Space Administration. Marshall Space Flight Center, Huntsville, AL.
THE SCHEDULING TECHNIQUES OF ESP2
John P. Jaap and Elizabeth K. Davis *In* NASA. Lyndon B. Johnson Space Center, 2nd Annual Workshop on Space Operations Automation and Robotics (SOAR 1988) Nov. 1988 p 1-6 (For primary document see N89-19817 12-59)
Avail: NTIS HC A22/MF A01 CSCL 05A

N89-19820*# National Aeronautics and Space Administration. Ames Research Center, Moffett Field, CA.
A SURVEY OF PLANNING AND SCHEDULING RESEARCH AT THE NASA AMES RESEARCH CENTER
Monte Zweben *In* NASA. Lyndon B. Johnson Space Center,

2nd Annual Workshop on Space Operations Automation and Robotics (SOAR 1988) Nov. 1988 p 15-20 (For primary document see N89-19817 12-59)
Avail: NTIS HC A22/MF A01 CSCL 05A

N89-19821*# National Aeronautics and Space Administration. Lyndon B. Johnson Space Center, Houston, TX.
AN EXPERT SYSTEM FOR SHUTTLE AND SATELLITE RADAR TRACKER SCHEDULING
Paul Mitchell *In its* 2nd Annual Workshop on Space Operations Automation and Robotics (SOAR 1988) Nov. 1988 p 21-23 (For primary document see N89-19817 12-59)
Avail: NTIS HC A22/MF A01 CSCL 05A

N89-19823*# Air Force Armament Lab., Eglin AFB, FL.
EMMA: THE EXPERT SYSTEM FOR MUNITION MAINTENANCE
Barry E. Mullins *In* NASA. Lyndon B. Johnson Space Center, 2nd Annual Workshop on Space Operations Automation and Robotics (SOAR 1988) Nov. 1988 p 31-39 (For primary document see N89-19817 12-59)
Avail: NTIS HC A22/MF A01 CSCL 05A

82 DOCUMENTATION AND INFORMATION SCIENCE

Includes information management; information storage and retrieval technology; technical writing; graphic arts; and micrography.

For computer documentation see *61 Computer Programming and Software*.

N89-20028# Idaho National Engineering Lab., Idaho Falls.
STATUS OF DOE INFORMATION NETWORK MODIFICATIONS
Ron Fuchs 1988 6 p Presented at the 10th Annual DOE Low-Level Waste Management Conference, Denver, CO, 30 Aug. 1988
(Contract DE-AC07-76ID-01570)
(DE89-005191; EGG-M-88377; CONF-880839-13) Avail: NTIS HC A02/MF A01

This paper provides an update for conference participants on changes, that have been made, or are taking place, to the Department of Energy's National Information Network. A question and answer period is anticipated. Areas of focus are data acquisition from commercial disposal site operators, improved access methods to DOE Information network, progress on personnel computer interfaces, and availability of end user support. DOE

N89-20029# Massachusetts Univ., Amherst.
USING THE SENTENCE VERIFICATION TECHNIQUE TO ASSESS STORAGE AND RETRIEVAL PROCESSES Final Report, 1 Aug. 1987 - 30 Jul. 1988
James M. Royer and Gale M. Sinatra Jul. 1988 96 p
(Grant AF-AFOSR-0309-87; AF Proj. 2313)
(AD-A201632; AFOSR-88-1170TR) Avail: NTIS HC A05/MF A01 CSCL 05H

The research described in this report had two purposes: first, to determine if meaning change and paraphrase test sentences (which are two of the test item types in the Sentence Verification Technique of Measuring reading comprehension) could be used to assess and examinee's capacity to store information that had been read and to retrieve information that had been previously stored; and second, to evaluate two procedures that could enhance the reliability of SVT tests. The two procedures were a new form of the Sentence Verification Technique called the Meaning Identification Technique which asked examinees to rate their confidence in responses to the items. GRA

N89-20030# Defense Applied Information Technology Center, Alexandria, VA.
GLOBAL SCIENTIFIC AND TECHNICAL INFORMATION NETWORK
Gladys A. Cotter Dec. 1988 10 p
(AD-A201902; DAITC/TR-88/007; DTIC-TR-89/2) Avail: NTIS HC A02/MF A01 CSCL 12G

This paper describes the foundations for a global scientific and technical information network which is currently under development at the Defense Applied Information Technology Center (DAITC). The paper highlights advances in information technology which are creating an environment where networking and interoperability strategies are possible on a global basis. Applied information technology modules which have been created to support the Global Scientific and Technical Information Network are described. The network is purposefully designed to incorporate both end-users and their information management intermediaries in a complementary manner making them resolute partners in the work and its rewards. GRA

N89-19845*# California Univ., Marina del Rey. Information Sciences Inst.
PRESENTATION PLANNING USING AN INTEGRATED KNOWLEDGE BASE
Yigal Arens, Lawrence Miller, and Norman Sondheimer *In* NASA. Lyndon B. Johnson Space Center, 2nd Annual Workshop on Space Operations Automation and Robotics (SOAR 1988) Nov. 1988 p 205-218 (For primary document see N89-19817 12-59)
(Contract N00014-87-K-0130)
Avail: NTIS HC A22/MF A01 CSCL 05B

N89-19888*# Softech, Inc., Fairborn, OH.
IDEAL: A METHOLOGY FOR DEVELOPING INFORMATION SYSTEMS
Ken H. Evers and Robert F. Bachert (Aerospace Medical Research Labs., Wright-Patterson AFB, OH.) *In* NASA. Lyndon B. Johnson Space Center, 2nd Annual Workshop on Space Operations Automation and Robotics (SOAR 1988) Nov. 1988 p 527-532 (For primary document see N89-19817 12-59)
Avail: NTIS HC A22/MF A01 CSCL 05B

N89-19891*# Boeing Aerospace Co., Kennedy Space Center, FL.
ELECTRONIC DATA GENERATION AND DISPLAY SYSTEM
Jules Wetekamm *In* NASA. Lyndon B. Johnson Space Center, 2nd Annual Workshop on Space Operations Automation and Robotics (SOAR 1988) Nov. 1988 p 553-557 (For primary document see N89-19817 12-59)
Avail: NTIS HC A22/MF A01 CSCL 05B

83 ECONOMICS AND COST ANALYSIS

Includes cost effectiveness studies.

No abstracts in this category.

84 LAW, POLITICAL SCIENCE AND SPACE POLICY

Includes NASA appropriation hearings; aviation law; space law and policy; international law; international cooperation; and patent policy.

N89-20031# Committee on Commerce, Science, and Transportation (U.S. Senate).
NATIONAL AERONAUTICS AND SPACE ADMINISTRATION AUTHORIZATION
Washington GPO 1988 101 p Hearing before the Subcommittee on Science, Technology and Space of the Committee on Commerce, Science and Transportation, 100th Congress, 2d Session, 10 Mar. 1988, part 2
(S-Hrg-100-579-Pt-2; GPO-84-990) Avail: Subcommittee on Science, Technology and Space

Hearings before a subcommittee of the Senate on How the U.S. equips itself to be competitive in space in the 21st century: Maintaining momentum in high technology research and develop are presented. The statements of various NASA officials as well as those of university and aerospace industry are also presented.
E.R.

85 URBAN TECHNOLOGY AND TRANSPORTATION

Includes applications of space technology to urban problems; technology transfer; technology assessment; and surface and mass transportation.

For related information see also *03 Air Transportation and Safety, 16 Space Transportation,* and *44 Energy Production and Conversion.*

N89-20032# Air Force Inst. of Tech., Wright-Patterson AFB, OH. School of Systems and Logistics.
AN INVESTIGATION OF FACTORS AFFECTING DOMESTIC TECHNOLOGY TRANSFER AT THE WRIGHT AERONAUTICAL LABORATORIES M.S. Thesis
Mark A. Leuthold Sep. 1988 107 p
(AD-A201581; AFIT/GSM/LSM/88S-16) Avail: NTIS HC A06/MF A01 CSCL 09C

The purpose of this project is to construct and study a laser trap for neutral atoms, initially potassium (K). At low densities, such a trap could be used to address a number of fundamental questions, e.g., the interaction of an individual atom with an electromagnetic field, collision dynamics and recombination. We have studied the feasibility and limitations of a purely laser trap concept, a corner cube trap, for trapping neutral K atoms. The confinement of the atoms in the two dimensions perpendicular to the laser is provided in the cavity of a newly constructed high power alexandrite laser operating in the CW TEM*01 mode (doughnut mode) tuned slightly to the blueside of the resonance line of the K atom. By reflecting the TEM*01 laser back on itself with two mirrors, one cap the ends of the cylindrical trap, resulting in a slightly weaker ends plug. GRA

88 SPACE SCIENCES (GENERAL)

No abstracts in this category.

89 ASTRONOMY

Includes radio, gamma-ray, and infrared astronomy, and astrometry.

N89-20033 Texas Univ., Austin.
NEAR-INFRARED SPECTROSCOPY OF YOUNG STELLAR OBJECTS Ph.D. Thesis
John Sherman Carr 1988 219 p
Avail: Univ. Microfilms Order No. DA8816413

Near-infrared spectroscopic observations of young stellar objects are presented. Spectra were obtained of the first overtone bands of CO, the hydrogen Br gamma line, and the S(1)v=1-0 line of H2. The majority of objects observed have luminosities less than 1000 solar luminosity. The CO overtone bands were found in emission in 6 out of 31 objects. Two models are discussed for producing the CO emission. In the first, models are calculated for steady state accretion disks. The radial distribution of temperature in the disk was calculated by balancing the heating and cooling in the disk. The resulting model disks have optically thin regions with sufficient temperatures and densities for vibrational excitation of CO. The models also reproduce the observed increase in CO luminosity with increasing stellar luminosity. The second model considered is a spherical, stellar wind with velocities of 100 to 300 km/s. The CO emission from the wind is computed as a function of mass loss rate. Thirty objects were measured for Br gamma emission. Four new detections of H2 emission in young stars are also reported. It was also verified that the proportionality between hydrogen recombination line strength and stellar luminosity extends down to 1 solar luminosity objects. The relation of recombination line emission to radio continuum emission, the momentum in the ionized wind, and the relationship of the ionized gas to large scale molecular outflows are discussed.
Dissert. Abstr.

N89-20034 Washington Univ., Seattle.
THE SCINTILLATING OPTICAL FIBER ISOTOPE EXPERIMENT (SOFIE): BEVALAC CALIBRATIONS OF TEST MODELS Ph.D. Thesis
James Joseph Connell 1988 203 p
Avail: Univ. Microfilms Order No. DA8818502

The Scintillating Optical Fiber Isotope Experiment (SOFIE) is a Cherenkov-dE/dx-Range experiment being developed to study the isotopic composition of cosmic rays in the iron region. Such measurements are crucial to a better understanding of cosmic ray origins and propagation. The goal of measuring the isotopic abundances of cosmic rays in the silicon to iron region has required the development of a new generation of instruments, such as SOFIE's electronic charged-particle track-imaging detector. This consists of a bundle of scintillating optical fibers coupled to an image intensified CID video camera; from the digitized video data the trajectory and range of stopping particles can be determined. This information, together with a Cherenkov measurement, is used to determine the mass of stopping charged particles. Test models of SOPHIE were calibrated at the Lawrence Berkeley Laboratory's Bevalac heavy ion accelerator in 1985 and 1986 using beams of iron nuclei with energies of 465 MeV/nucleon to 515 MeV/nucleon. This was done to demonstrate the feasibility of the detector system before attempting a balloon flight to measure cosmic rays. The design and construction of the SOFIE Bevalac test models are discussed in the context of the scientific objectives and goals of the eventual balloon experiment. A new Cherenkov response equation is derived for heavy ions at energies near threshold in a thick Cherenkov radiator. The results of the analysis of the Bevalac calibration data are presented. Dissert. Abstr.

N89-20035 Brandeis Univ., Waltham, MA.
VLBI POLARIZATION MEASUREMENTS OF BL LACERTAE OBJECTS Ph.D. Thesis
Denise Carmen Gabuzda 1988 158 p
Avail: Univ. Microfilms Order No. DA8819751

The milliarcsecond resolution total intensity and polarization structures of six BL Lacertae objects were determined at 6 centimeters wavelength using very long baseline interferometry. The sources 0454+844, 0735+178, and 1749+096 were observed at only one epoch; 0235+164, OJ287, and BL Lac were observed at three epochs, though polarization information was not available for the latest epoch. BL Lac, O454+844, 0735+178, and OJ287 display polarization structure, sometimes to a considerably greater extent that is indicated by the corresponding total intensity maps. In all cases, the core components are polarized less than approximately 5 percent. Jet components may be polarized as much as approximately 60 percent, although several instances of very weakly polarized knots also were observed. In addition, different knots in the same source may have very different polarization properties. Integrated polarization measurements of BL Lacertae objects have shown a tendency for the polarization postion angle to be parallel to the VLBI structure. Each of the four sources that show polarization structure has knots whose intrinsic polarization position angles are close to parallel to the jet axes. This result suggests that in BL Lacertae objects as a class, the radio polarization is dominated by knots in which the magnetic field is perpendicular to the jet. Dissert. Abstr.

N89-20036 New Mexico Univ., Albuquerque.
POWER SPECTRA DECOMPOSITION OF 36 RS CVn UBV PHOTOMETRIC LIGHT CURVES FROM THE FIRST TWO YEARS OF THE AUTOMATIC PHOTOELECTRIC TELESCOPE Ph.D. Thesis
Eric Raymond Nelson 1988 753 p
Avail: Univ. Microfilms Order No. DA8820689

The first search for multiple periodic structure of a major subset of the RS CVn class of interacting binary stars systems, using a rigorous numerical approach appropriate to unevenly-spaced gapped data, is presented. The main intent is to characterize properly the power spectral content of RS CVn binary light curves and describe how this information can constrain the current models for the systems. If the light curve can be considered as a tracer of stellar surface activity, then the photometric distortions can be used to characterize magnetic activity cycles and add to the understanding of stellar dynamics. The data set is provided by the Fairborn Observatory from the first two years of observing with the first generation Automatic Photoelectric Telescope (APT). An interactive analysis environment, for the 8086/80286/80386 based workstations, is described that was specifically developed in order to analyze the volumes of time-serial data generated by the APT. Most of the systems exhibit multiple periodic structure, 40 percent of which show changes in the photometric period on a time scale of a few hundred days. Changes in the photometric period are associated with variations in the amplitude of the distortion wave, which would indicate the growth and decay of spot groups. The growth and decay of pairs of spot groups, arbitrarily separated in phase, on a differentially rotating star is the model most consistent with the results of my analysis. High resolution, long term observations are needed to properly address the details of differential rotations. Dissert. Abstr.

N89-20037 Arizona Univ., Tucson.
AN INFRARED REFLECTANCE STUDY OF WATER IN OUTER BELT ASTEROIDS Ph.D. Thesis
Thomas David Jones 1988 286 p
Avail: Univ. Microfilms Order No. DA8824279

A lab and telescopic investigation is presented of H2O distribution among the low-albedo, outer belt asteroids. The water distribution was determined by surveying asteroids for the 3 micron molecular H2O and structural OH ion absorption, the spectral signature of meteorite and asteroid hydrated silicates. Survey results were interpreted using the midinfrared reflectance spectra of 16 carbonaceous chondrites and other asteroidal materials. The 19 asteroids observed, augmented by earlier reflectance data, yielded 3 micron band depth measurements that reflect the present outer belt H2O distribution. Of the 32 C class sampled asteroids, 66 percent have hydrated silicate surfaces, indicating a mild aqueous alteration episode early in solar system history. Strictly speaking, the C class is thus not a primitive asteroid group, but the anhydrous objects appear little altered, as do the P and D asteroid classes beyond 3.5 AU. In addition to this pronounced difference in hydration state among the outer belt classes, the C region shows a gradual decline in hydrated silicate abundance from 2.5 to 3.5 AU. This trend is consistent with an original outer belt asteroid composition of anhydrous silicates, water ice, and complex organic material. Dissert. Abstr.

N89-20038# Technische Univ., Delft (Netherlands).
ON THE GREAT CIRCLE REDUCTION IN THE DATA ANALYSIS FOR THE ASTROMETRIC SATELLITE HIPPARCOS Ph.D. Thesis
Hans vanderMarel 1988 240 p Sponsored by The Netherlands Organization for the Advancement of Pure Research, CNRS, Paris, France and the Centre d'Etudes et Recherches Geodynamiques et Astronomiques, Grasse, France
(ETN-89-93902) Avail: NTIS HC A11/MF A01

Scientific data reduction for HIPPARCOS is considered, including model assumptions, estimability, and accuracy of the great circle reduction; attitude smoothing, which improves the results of the great circle reduction; and numerical methods for the reduction. The great circle reduction comprises a half-daily least squares solution of 80,000 observations with 2,000 unknown star abscissae and 50 instrumental parameters. Depending on the solution method chosen, also 18,000, or in case of attitude smoothing 600, attitude parameters have to be solved. The reduction processes only observations of stars within a small band on the celestial sphere. Therefore, only one coordinate can be improved, i.e., the abscissae on a reference great circle in the middle of the band. The ordinates are not improved, i.e., they are fixed on their approximate values, which results in errors in the estimated star abscissae. By iterating the complete data reduction several times, in order to obtain better approximate values for the ordinates, the modeling error becomes very small and can be neglected. Analytical formulae for the magnitude of this error are derived. Instrument parameters appear to be estimable. The covariance function of the star abscissae is computed for a regular star network using Fourier analysis. Attitude smoothing is described. ESA

90 ASTROPHYSICS

Includes cosmology; celestial mechanics; space plasmas; and interstellar and interplanetary gases and dust.
For related information see also *75 Plasma Physics*.

N89-20039 Rochester Univ., NY.
ROTATION AND MAGNETIC FIELDS AS AN ACCELERATION MECHANISM IN ASTROPHYSICAL JETS Ph.D. Thesis
Theodoros Koupelis 1988 211 p
Avail: Univ. Microfilms Order No. DA8817083

The importance of the combined effects of rotation and magnetic fields on the acceleration of the longitudinal motion of jets is examined in three related models. In the Helix model, a plasma blob is emitted by a massive, rotation body along the common magnetic/rotation axis. The blob's expansion produces helical twisting of the lines, generating a magnetic pressure that accelerates the blob. In the Narrow jet model, the system of ideal MHD equations is projected onto the axis and approximate the unknown parameters with their average values. In the r sup 2 model, the initial and boundary conditions at the origin are used to find the general forms of the integrals of motion, and thus obtain a 2-D model for narrow jets, which was reduced to 1-D by following the motion of the flow along stream surfaces. It is concluded that the combination of rotation and magnetic fields is a very important acceleration mechanism for black holes and neutron stars, resulting in relativistic velocities at large distances. For protostars, it sustains an increase in the velocity along the length of the jet. Dissert. Abstr.

N89-20040*# Auburn Univ., AL. Dept. of Aerospace Engineering.
THE NINEVAH MISSION: A DESIGN SUMMARY FOR AN UNMANNED MISSION TO VENUS, VOLUME 1
Jun. 1988 66 p
(Grant NGT-21-002-080)
(NASA-CR-184705; NAS 1.26:184705) Avail: NTIS HC A04/MF A01 CSCL 03B

The design summary for an unmanned mission to the planet Venus, with code name Ninevah, is presented. The design includes a Hohmann transfer trajectory analysis, propulsion trade study, an overview of the communication and instrumentation systems, power requirements, probe and lander analysis, and a weight and cost analysis. NASA

N89-20041*# Auburn Univ., AL. Dept. of Aerospace Engineering.
THE NINEVAH MISSION: ANALYTICAL ANALYSES AND CALCULATIONS FOR TRAJECTORY AND PROPULSION, VOLUME 2
Jun. 1988 55 p
(Grant NGT-21-002-080)
(NASA-CR-184706; NAS 1.26:184706) Avail: NTIS HC A04/MF A01 CSCL 03B

Mathematical models, diagrams, and computer programs involving an unmanned mission to the planet Venus are presented. This work was done in support of the proposed project called Ninevah. The specific subjects covered are trajectory analysis, propulsion analysis, and structural analysis. NASA

N89-20042 California Univ., Los Angeles.
INTERSTELLAR MATTER IN EARLY TYPE GALAXIES Ph.D. Thesis
Dong-Woo Kim 1988 146 p
Avail: Univ. Microfilms Order No. DA8822330

Multi-wavelength observations were performed in order to investigate various phases of interstellar matter in early type galaxies. From the IRAS coadding procedure for a large sample of galaxies, it was found that about half of early type galaxies contain detectable amounts of cold interstellar dust. Selecting galaxies with strong far infrared fluxes, optical imaging and spectroscopy, H I lambda 21 cm line observations and CO J = 1-0 line observations were undertaken. Cold dust, H I gas, ionized gas and molecular material were successfully detected; proving that the far infrared flux is indeed a good indicator for the presence of interstellar matter. The infrared emission mechanism and origin and fate of interstellar matter are discussed using the date obtained from various phases of interstellar matter. The interstellar matter is also used as a probe of dynamical structure, nuclear activity and star formation in early type galaxies. Dissert. Abstr.

N89-20043 Massachusetts Univ., Amherst.
THE DISTRIBUTION OF THE INTERSTELLAR MEDIUM IN THE Scd GALAXY NGC 6946 AND IN A SAMPLE OF DWARF IRREGULAR GALAXIES Ph.D. Thesis
Linda Jean Tacconi-Garman 1988 238 p
Avail: Univ. Microfilms Order No. DA8822863

The atomic and molecular hydrogen distributions in the spiral galaxy NGC 6946 and in 15 dwarf irregular galaxies were compared. Observations were made of the COJ = 1 yields 0 transition to obtain a fully sampled map to a radium of 10 kpc in NGC 6946, using the 14-meter telescope of the Five College Radio Astronomy Observatory, and have also completely mapped the 21-cm line of neutral hydrogen with the Very Large Array. The CO observations were made at FCRAO in 15 dwarf irregular galaxies spanning a wide range of infrared luminosity and color. In NGC 6946 the CO and HI maps were used to investigate the radial and azimuthal variations in the atomic and molecular gas. Dissert. Abstr.

N89-20044 Wisconsin Univ., Madison.
ULTRACOMPACT HII REGIONS ASSOCIATED WITH MASSIVE STAR FORMATION Ph.D. Thesis
Douglas Owen Starkey Wood 1988 243 p
Avail: Univ. Microfilms Order No. DA8817156

The physical properties of ultracompact (UC) HII regions are established and their interaction with the interstellar medium investigated. The UC HII regions are small photoionized nebulae produced by massive stars embedded in clouds of molecular gas and dust. New observations were made using the Very Large Array (VLA) at cm wavelengths and single dish telescopes at mm wavelengths. Data were also collected from the Infrared Astronomical Satellite (IRAS) and from the literature. The VLA was used at 2 and 6 cm to identify 75 UC HII regions. Radio continuum brightness distributions with 0.4 minute resolution are presented in the form of contour plots. H76 alpha recombination line profiles were obtained for six sources. The flux density distributions of the sources from radio to near infrared wavelengths are assembled using the IRAS Point Source Catalog and data from the literature. It is shown that UC HII regions have a characteristic FIR flux density distribution that is very different from typical entries in the IRAS Point Source Catalog. A two-color selection criterion based on the known UC HII regions is developed and when applied to the entire PSC a total of 1708 embedded OB star candidates are found. This represents a direct measure of the population and distribution of galactic OB stars embedded in molecular clouds. Dissert. Abstr.

N89-20045 Sussex Univ., Brighton (England).
PHENOMENOLOGICAL MODELS FROM HIGHER DIMENSIONS WITH AND WITHOUT SUPERGRAVITY Ph.D. Thesis
A. F. Zerrouk 1987 449 p
Avail: Univ. Microfilms Order No. BRDX83016

A brief survey on Kaluza-Klein theories is given. It is emphasized that for a maximally supersymmetric universe, the only way to do Kaluza-Klein theory is through supergravity. Bearing this in mind, a seven-dimensional internal compact manifold is considered. It is described as being the most general type of coset spaces containing the standard model group. Dissert. Abstr.

N89-20046# Ruhr Univ., Bochum (Germany, F.R.). Abteilung fuer Physik und Astronomie.
MORPHOLOGY AND NATURE OF THE DUST OF THE DARK CLOUD COAL SACK Ph.D. Thesis [MORPHOLOGIE UND NATUR DES STAUBES DER DUNKELWOLKE KOHLENSACK]
Klaus J. Seidensticker 1988 236 p In GERMAN
(ETN-89-93795) Avail: NTIS HC A11/MF A01

Measurements were performed on 284 stars of the spectral classes B to F, in the region of the dark cloud Coal Sack in order to study the morphological structure and the chemical composition of the interstellar dust. Photometric as well as spectrophotometric measurements in the visible and UV range were conducted using a 61 cm telescope. The method for the determination of interstellar extinction from photometric data was extended and its validity domain was checked. A method for the analysis of extinction curves was developed, which is very useful for deciphering the physical and chemical nature of the interstellar dust. The dust and gas masses were calculated using the calibrated and corrected extinction data. No stellar development of Coal Sack is found. ESA

N89-20047 Princeton Univ., NJ.
IMPLICATIONS OF THE OBSERVED CONTRACTION OF ACCRETION DISKS IN QUIESCENT DWARF NOVAE Ph.D. Thesis
Nels Eric Anderson 1988 114 p
Avail: Univ. Microfilms Order No. DA8816043

The observed contraction of the accretion disks in the dwarf novae U Gem and Z Cha during quiescence is interpreted with simple dynamical models. The standard alpha-parameter viscosity prescription is replaced by macroscopic constraints that are both computationally convenient and appropriate for the study of an extensive characteristic such as the disk radius. In the first model, quiescent phase mass accumulation occurs in a torus located at the outer edge of the disk proper. Interaction between the torus and the disk itself is minimal, there being no torque between the two. Contraction occurs as the torus accretes matter of low specific angular momentum from the companion star. The second model corresponds to a torus-disk interaction so large that the torus is no longer a separate entity: mass accumulates throughout the disk in such a way that the surface density has a specified power law form at all times. These two extreme models thus bracket the range of possible accretion modes. Both models fit U Gem's radius vs time curve, but surface density measurements favor a torus. Neither model fits Z Cha's ill defined radius behavior well, although its surface brightness profile suggests accretion throughout the disk rather than in a torus. Dissert. Abstr.

N89-20048 Wisconsin Univ., Madison.
GROUND-BASED FABRY-PEROT OBSERVATIONS OF NEUTRAL AND IONIC ATOMS AND MOLECULES OF COMET HALLEY Ph.D. Thesis
Karen Patricia Magee-Sauer 1988 278 p
Avail: Univ. Microfilms Order No. DA8810026

A series of observations were conducted from Nov. 1985 to May 1986 of comet Halley using a 150 mm dual etalon Fabry-Perot spectrometer coupled to a 32 inch west auxiliary of the McMath Solar Telescope on Kitt Peak. High spectral resolution scans and images were obtained. Spatial images of comet Halley in (OI)6300 A emission were used to deduce the distribution of cometary O(1D). The 10/kms bandpass of the system allowed the distribution to

be measured with little comtamination from airglow (OI)6300 and cometary NH2 lines in the nearby spectrum. The results were modeled to provide photodestruction lifetimes for cometary H2O and OH, the predominant parents of O(1D). Measurements of (OI)6300 and Balmer alpha (H alpha) emissions were used to determine the H production rate Q(H), and O(1D) production rate Q(O(1D)) and their dependence on heliocentric distance R sub h. Dissert. Abstr.

N89-20049# Consiglio Nazionale delle Ricerche, Frascati (Italy). Ist. di Fisica dello Spazio Interplanetario.
JETS PHYSICS IN COMET P/HALLEY
V. Formisano, G. Bellucci, F. Tripodi, and E. Amata Apr. 1988 22 p Original contains color illustrations
(IFSI-88-3; ETN-89-93470) Avail: NTIS HC A03/MF A01

CCD images of comet P/Halley taken from Catania Observatory in April 1986 with IHW filters are analyzed. On scale distances larger than 200,000 Km these images show the presence of jets in the Cont....A, H2O(+) and C2 filters. The jet maximum intensity is at less than 1000 Km from the nucleus for dust, at 20,000 to 30,000 Km for H2O(+) and at 60,000 to 90,000 Km for C2, implying 20,000 s or 100,000 s formation time for the last two molecules. Comparison of various images shown that H2O(+) and C2 jets are in very different directions, the first one coinciding with the main dust jet, the second one appearing as a continuation in space of a very short dust jet. It is speculated that dust grains have different sizes and chemical composition from the moment they leave the cometary nucleus, and that grains in the small dust jet undergo fragmentation and chemical reactions to produce C2 jets. ESA

N89-20050# Technische Univ., Hanover (Germany, F.R.). Astronomische Station.
MASS-RADIUS STAR EVOLUTION SUN ACTIVITY PLANETS SURFACES ON PURELY EMPIRICAL BASIS. EMPIRY THEORY REALITY: THE USE OF STATISTICS
Karl Pilowski 1988 36 p
(Rept-18; ETN-89-93780) Avail: NTIS HC A03/MF A01

Investigations on the integral state quantities of the stars, the Hertzsprung-Russel diagram, and mass-radius diagram are reviewed. Continental motions, and solar activity effects on the Earth surface and Earth atmosphere are discussed. ESA

91 LUNAR AND PLANETARY EXPLORATION

Includes planetology; and manned and unmanned flights.

For spacecraft design or space stations see *18 Spacecraft Design, Testing and Performance.*

N89-20051*# Cornell Univ., Ithaca, NY. Dept. of Astronomy.
TEMPERATURE AND CIRCULATION IN THE STRATOSPHERES OF THE OUTER PLANETS
Barney J. Conrath, Peter J. Gierasch, and Stephen S. Leroy (California Inst. of Tech., Pasadena.) Jan. 1989 51 p
(Grant NAG5-813)
(NASA-CR-184826; NAS 1.26:184826) Avail: NTIS HC A04/MF A01 CSCL 03B

A zonally symmetric, linear radiative-dynamical model is compared with observations of the upper tropospheres and stratospheres of the outer planets. Seasonal variation is included in the model. Friction is parameterized by linear drag (Rayleigh friction). Gas opacities are accounted for but aerosols are omitted. Horizontal temperature gradients are small on all the planets. Seasonal effects are strongest on Saturn and Neptune but are weak even in these cases, because the latitudinal gradient of radiative heating is weak. Seasonal effects on Uranus are extremely weak because the radiative time constant is longer that the orbital period. One free parameter in the model is the frictional time constant. Comparison with observed temperature perturbations over zonal currents in the troposphere shows that the frictional time constant is on the same order as the radiative time constant for all these objects. Vertical motions predicted by the model are extremely weak. They are much smaller than one scale height per orbital period, except in the immediate neighborhood of tropospheric and zonal currents. Author

N89-20052 California Inst. of Tech., Pasadena.
EPISODIC VOLCANISM OF TIDALLY HEATED SATELLITES WITH APPLICATION TO Io. THERMAL STATE OF AN ICE SHELL ON EUROPA. POLAR WANDER OF A SYNCHRONOUSLY ROTATING SATELLITE WITH APPLICATION TO EUROPA Ph.D. Thesis
Gregory Wayne Ojakangas 1988 186 p
Avail: Univ. Microfilms Order No. DA8820978

Two examples of planetary bodies that may have coupled thermal and dynamical evolutions are investigated. The work is presented in three individual papers. The first example is that of a tidally heated satellite in an orbital resonance, for which the tidal dissipation rate is a strongly increasing function of the internal temperature. For such a satellite, a feedback mechanism exists between the orbital and thermal energies, which may lead to periodic variations in tidal heating within the satellite and its orbital eccentricity. A simple model of this mechanism is presented in the first paper and is applied specifically to Io. The second example is that of an ice shell on Europa, which is decoupled from the silicate core by a layer of liquid water. In the second paper, the spatially varying thickness that such a shell would have in thermal equilibrium with tidal dissipation within it, surface solar insolation and heat flow from the core is calculated for reasonable rheological laws for ice. The contribution of these variations in ice thickness to Europa's inertia tensor is estimated, and the implications for non-synchronous rotation of Europa are discussed. In the third paper, a detailed dynamical model is developed, which demonstrates that such a shell may exhibit large-scale polar wander as it approaches thermal equilibrium, because of the destabilizing effect of the variations in ice thickness on the enertia tensor of the shell. Dissert. Abstr.

N89-20070*# State Univ. of New York, Plattsburgh. Dept. of Physics.
AN ASSESSMENT OF THE MICROMETEORITIC COMPONENT IN THE MARTIAN SOIL Final Report
George J. Flynn *In* NASA, Lyndon B. Johnson Space Center, National Aeronautics and Space Administration (NASA)/American Society for Engineering Education (ASEE) Summer Faculty Fellowship Program 1988, Volume 1 Feb. 1989 15 p (For primary document see N89-20058 12-99)
Avail: NTIS HC A09/MF A01 CSCL 03B

92 SOLAR PHYSICS

Includes solar activity, solar flares, solar radiation and sunspots.

For related information see *93 Space Radiation.*

N89-20053# California Inst. of Tech., Pasadena. Solar Astronomy Group.
STUDIES OF FLARES AND DISAPPEARING MAGNETIC FLUX Final Report, 1 Oct. 1986 - 31 Mar. 1988
Sara F. Martin 31 Mar. 1988 13 p
(Contract N00014-86-K-0138)
(AD-A201456) Avail: NTIS HC A02/MF A01 CSCL 03B

Research accomplishments include: (1) research on flaring arches; (2) a collaborative paper on Anomalously Dense Flare Loops was published; (3) the footprints of the giant arches previously discovered by Z. Svestka were found in hydrogen alpha observations from the Big Bear Solar Observatory and the Udaipur Solar Observatory; (4) several sets of new observations showing a relationship between cancelling magnetic fields and flares were acquired and analyzed; and (5) a new hypothesis is advanced that cancelling magnetic fields are necessary conditions for the energy build-up to solar flares. GRA

N89-20054# Technische Univ., Delft (Netherlands). Faculty of Technical Mathematics and Informatics.
EXISTENCE OF STATIONARY SOLUTIONS IN THE CORONAL LOOP PROBLEM
J. Hulshof, D. Terman (Ohio State Univ., Columbus.), and F. Verhulst 1988 27 p Sponsored in part by NATO Science Fellowship
(Grant NSF DMS-87-02693)
(Rept-88-06; B8809733; ISSN-0920-8577; ETN-89-93843)
Copyright Avail: NTIS HC A03/MF A01

The study of a hot plasma confined to a magnetic loop in the Sun's corona leads to a singularly perturbed nonlinear reaction-diffusion equation with unusual side conditions. Monotone solutions of the stationary problem appear as fixed points of an iteration map which is contractive if the perturbation parameter is sufficiently small. ESA

93 SPACE RADIATION

Includes cosmic radiation; and inner and outer earth's radiation belts.

For biological effects of radiation see *52 Aerospace Medicine*. For theory see *73 Nuclear and High-Energy Physics*.

N89-20055 Minnesota Univ., Minneapolis.
AN OBSERVATIONAL AND NUMERICAL STUDY OF EXTRAGALACTIC RADIO SOURCES Ph.D. Thesis
Jeffrey Alan Pedelty 1988 321 p
Avail: Univ. Microfilms Order No. DA8820491

The Very Large Array is used to make radio continuum observations of a sample of 12 distant ($z = 1$) high luminosity 3CR galaxies. Images with arcsecond resolution are produced at wavelength 20 and 6 cm. The total and polarized intensity images are used to create maps of the fractional polarization, depolarization, rotation measure, and spectral index distributions. Additional arcsecond resolution observations at wavelength 2 cm, higher resolution wavelength 6 and 2 cm maps, and optical R band continuum and emission-line images of (OII) wavelength 3727 are presented for 3C337. Suggestive evidence for dynamically significant interactions between the emission-line gas and the radio sources is presented. Numerical simulations of the interaction of a Mach 4 relative velocity slip surface with several trains of incident nonlinear sound waves are performed using the Piecewise-Parabolic Method. PPM simulations of the supersonic slip surface between 10:1 density ratio fluids are made at $M = 1$, 1.9, and 4. Further simulations test the effects of grid resolution, the SLIC interface tracking method, and the initial transverse perturbation. Dissert. Abstr.

N89-20056 Max-Planck-Inst. fuer Physik und Astrophysik, Garching (Germany, F.R.). Inst. fuer Extraterrestrische Physik.
SOLAR AND INERPLANETARY COSMIC RAY COMPOSITION
Dietrich Huvestadt Feb. 1988 11 p Presented at the 20th International Cosmic Ray Conference
(MPE-Preprint-108; ETN-89-93802) Copyright Avail: Fachinformationszentrum Karlsruhe, 7514
Eggenstein-Leopoldshafen 2, Federal Republic of Germany

Research on solar cosmic rays and the anomalous cosmic ray (ACR) component, and experimental methods and installations is summarized. Solar cosmic ray elemental and isotopic abundances, and ionic charges are discussed. The ACR at 1AU and in the outer heliosphere, and ACR charge states are reviewed. ESA

N89-20057 Indiana Univ., Bloomington.
THE COSMIC RAY ANTIPROTON SPECTRUM BETWEEN 0.1 AND 1.5 GeV KINETIC ENERGY Ph.D. Thesis
Charles Raymond Bower 1988 218 p
Avail: Univ. Microfilms Order No. DA8824153

In the summer of 1980, a balloon-borne cosmic ray experiment reported the detection of 14 low energy antiprotons during an 18 hour flight. This measurement represented an antiproton intensity two orders of magnitude greater than that predicted by conventional theories. This surprising result triggered a flurry of papers theorizing the origin of these particles, including the prediction of domains of primary antimatter, and evidence for supersymmetric particle annihilation. Not until the summer of 1987 was a followup experiment (PBAR) performed. The PBAR detector has both better resolution and a larger dynamic range in energy than the previous detector. It measured the energy spectrum of antiprotons in the 0.1 to 1.5 GeV kinetic energy range. The present work describes the instrument, the experiment, and the results. Analysis of the PBAR data reveals no antiprotons in the energy range of 0.13 to 0.64 GeV and only one antiproton candidate for energies between 0.64 and 1.5 GeV. The numbers of protons detected to date in these energy bins are 75,000 and 6,400 respectively. This result is in disagreement with the 1980 findings and rules out some of the exotic theories of antiproton production. Dissert. Abstr.

99 GENERAL

N89-20058*# National Aeronautics and Space Administration. Lyndon B. Johnson Space Center, Houston, TX.
NATIONAL AERONAUTICS AND SPACE ADMINISTRATION (NASA)/AMERICAN SOCIETY FOR ENGINEERING EDUCATION (ASEE) SUMMER FACULTY FELLOWSHIP PROGRAM 1988, VOLUME 1
Richard B. Bannerot, ed. (Houston Univ., TX.) and Stanley H. Goldstein, ed. Feb. 1989 199 p Program held in Houston, TX, 1988 Sponsored by NASA, Washington
(Grant NGT-44-005-803)
(NASA-CR-172118-Vol-1; NAS 1.26:172118-Vol-1) Avail: NTIS HC A09/MF A01 CSCL 05I

The 1988 Johnson Space Center (JSC) National Aeronautics and Space Administration (NASA)/American Society for Engineering Education (ASEE) Summer Faculty Fellowship Program was conducted by the University of Houston and JSC. The 10-week program was operated under the auspices of the ASEE. The program at JSC, as well as the programs at other NASA Centers, was funded by the Office of University Affairs, NASA Headquarters, Washington, D.C. The objectives of the program, which began in 1965 at JSC and in 1964 nationally, are (1) to further the professional knowledge of qualified engineering and science faculty members; (2) to stimulate an exchange of ideas between participants and NASA; (3) to enrich and refresh the research and teaching activities of participants' institutions; and (4) to contribute to the research objectives of the NASA Centers. For individual titles, see N89-20059 through N89-20072.

N89-20059*# Texas Southern Univ., Houston. Dept. of Home Economics.
COMPARISON OF SOVIET AND US SPACE FOOD AND NUTRITION PROGRAMS Final Report **c54**
Selina Ahmed *In* NASA, Lyndon B. Johnson Space Center, National Aeronautics and Space Administration (NASA)/American Society for Engineering Education (ASEE) Summer Faculty Fellowship Program 1988, Volume 1 Feb. 1989 16 p (For primary document see N89-20058 12-99)
Avail: NTIS HC A09/MF A01 CSCL 06H

The Soviet Space Food and Nutrition programs are compared with those of the U.S. The Soviets established the first Space Food programs in 1961, when one of the Soviet Cosmonauts experienced eating in zero gravity. This study indicates that some major differences exist between the two space food and nutrition programs regarding dietary habits. The major differences are in recommended nutrient intake and dietary patterns between the cosmonauts and astronauts. The intake of protein, carbohydrates and fats are significantly higher in cosmonaut diets compared to astronauts. Certain mineral elements such as phosphorus, sodium and iron are also significantly higher in the cosmonauts' diets. Cosmonauts also experience intake of certain unconventional food and plant extracts to resist stress and increase stamina. Author

N89-20060*# Houston Univ., TX. Dept. of Mechanical Engineering.

PRODUCTION SYSTEM CHUNKING IN SOAR: CASE STUDIES IN AUTOMATED LEARNING Final Report **c63**

Robert Allen *In* NASA, Lyndon B. Johnson Space Center, National Aeronautics and Space Administration (NASA)/American Society for Engineering Education (ASEE) Summer Faculty Fellowship Program 1988, Volume 1 Feb. 1989 15 p (For primary document see N89-20058 12-99)

Avail: NTIS HC A09/MF A01 CSCL 09B

A preliminary study of SOAR, a general intelligent architecture for automated problem solving and learning, is presented. The underlying principles of universal subgoaling and chunking were applied to a simple, yet representative, problem in artificial intelligence. A number of problem space representations were examined and compared. It is concluded that learning is an inherent and beneficial aspect of problem solving. Additional studies are suggested in domains relevant to mission planning and to SOAR itself. Author

N89-20061*# Norwich Univ., Northfield, VT. Dept. of Computer Science Engineering.

DEVELOPMENT OF A SOFTWARE INTERFACE FOR OPTICAL DISK ARCHIVAL STORAGE FOR A NEW LIFE SCIENCES FLIGHT EXPERIMENTS COMPUTER Final Report **c61**

Peter N. Bartram *In* NASA, Lyndon B. Johnson Space Center, National Aeronautics and Space Administration (NASA)/American Society for Engineering Education (ASEE) Summer Faculty Fellowship Program 1988, Volume 1 Feb. 1989 10 p (For primary document see N89-20058 12-99)

Avail: NTIS HC A09/MF A01 CSCL 09B

The current Life Sciences Laboratory Equipment (LSLE) microcomputer for life sciences experiment data acquisition is now obsolete. Among the weaknesses of the current microcomputer are small memory size, relatively slow analog data sampling rates, and the lack of a bulk data storage device. While life science investigators normally prefer data to be transmitted to Earth as it is taken, this is not always possible. No down-link exists for experiments performed in the Shuttle middeck region. One important aspect of a replacement microcomputer is provision for in-flight storage of experimental data. The Write Once, Read Many (WORM) optical disk was studied because of its high storage density, data integrity, and the availability of a space-qualified unit. In keeping with the goals for a replacement microcomputer based upon commercially available components and standard interfaces, the system studied includes a Small Computer System Interface (SCSI) for interfacing the WORM drive. The system itself is designed around the STD bus, using readily available boards. Configurations examined were: (1) master processor board and slave processor board with the SCSI interface; (2) master processor with SCSI interface; (3) master processor with SCSI and Direct Memory Access (DMA); (4) master processor controlling a separate STD bus SCSI board; and (5) master processor controlling a separate STD bus SCSI board with DMA. Author

N89-20062*# Illinois State Univ., Normal. Dept. of Applied Computer Science.

COMPUTER TECHNOLOGIES AND INSTITUTIONAL MEMORY Final Report **c61**

Christopher Bell and Roy Lachman (Houston Univ., TX.) *In* NASA, Lyndon B. Johnson Space Center, National Aeronautics and Space Administration (NASA)/American Society for Engineering Education (ASEE) Summer Faculty Fellowship Program 1988, Volume 1 Feb. 1989 22 p (For primary document see N89-20058 12-99)

Avail: NTIS HC A09/MF A01 CSCL 09B

NASA programs for manned space flight are in their 27th year. Scientists and engineers who worked continuously on the development of aerospace technology during that period are approaching retirement. The resulting loss to the organization will be considerable. Although this problem is general to the NASA community, the problem was explored in terms of the institutional memory and technical expertise of a single individual in the Man-Systems division. The main domain of the expert was spacecraft lighting, which became the subject area for analysis in these studies. The report starts with an analysis of the cumulative expertise and institutional memory of technical employees of organizations such as NASA. A set of solutions to this problem are examined and found inadequate. Two solutions were investigated at length: hypertext and expert systems. Illustrative examples were provided of hypertext and expert system representation of spacecraft lighting. These computer technologies can be used to ameliorate the problem of the loss of invaluable personnel. Author

N89-20063*# Louisiana Tech Univ., Ruston. Dept. of Electrical Engineering.

DEVELOPMENT OF PARALLEL ALGORITHMS FOR ELECTRICAL POWER MANAGEMENT IN SPACE APPLICATIONS Final Report **c20**

Frederick C. Berry *In* NASA, Lyndon B. Johnson Space Center, National Aeronautics and Space Administration (NASA)/American Society for Engineering Education (ASEE) Summer Faculty Fellowship Program 1988, Volume 1 Feb. 1989 9 p (For primary document see N89-20058 12-99)

Avail: NTIS HC A09/MF A01 CSCL 10B

The application of parallel techniques for electrical power system analysis is discussed. The Newton-Raphson method of load flow analysis was used along with the decomposition-coordination technique to perform load flow analysis. The decomposition-coordination technique enables tasks to be performed in parallel by partitioning the electrical power system into independent local problems. Each independent local problem represents a portion of the total electrical power system on which a loan flow analysis can be performed. The load flow analysis is performed on these partitioned elements by using the Newton-Raphson load flow method. These independent local problems will produce results for voltage and power which can then be passed to the coordinator portion of the solution procedure. The coordinator problem uses the results of the local problems to determine if any correction is needed on the local problems. The coordinator problem is also solved by an iterative method much like the local problem. The iterative method for the coordination problem will also be the Newton-Raphson method. Therefore, each iteration at the coordination level will result in new values for the local problems. The local problems will have to be solved again along with the coordinator problem until some convergence conditions are met. Author

N89-20064*# University of Southern Illinois, Carbondale. Dept. of Electrical Engineering.

AUTOMATIC VOICE RECOGNITION USING TRADITIONAL AND ARTIFICIAL NEURAL NETWORK APPROACHES Final Report **c32**

Nazeih M. Botros *In* NASA, Lyndon B. Johnson Space Center, National Aeronautics and Space Administration (NASA)/American Society for Engineering Education (ASEE) Summer Faculty Fellowship Program 1988, Volume 1 Feb. 1989 13 p (For primary document see N89-20058 12-99)

Avail: NTIS HC A09/MF A01 CSCL 17B

The main objective of this research is to develop an algorithm for isolated-word recognition. This research is focused on digital signal analysis rather than linguistic analysis of speech. Features extraction is carried out by applying a Linear Predictive Coding (LPC) algorithm with order of 10. Continuous-word and speaker independent recognition will be considered in future study after accomplishing this isolated word research. To examine the similarity between the reference and the training sets, two approaches are explored. The first is implementing traditional pattern recognition techniques where a dynamic time warping algorithm is applied to align the two sets and calculate the probability of matching by measuring the Euclidean distance between the two sets. The second is implementing a backpropagation artificial neural net model with three layers as the pattern classifier. The adaptation rule implemented in this network is the generalized least mean square (LMS) rule. The first approach has been accomplished. A

vocabulary of 50 words was selected and tested. The accuracy of the algorithm was found to be around 85 percent. The second approach is in progress at the present time. Author

N89-20065*# Houston Univ., Clear Lake, TX. Div. of Life Sciences.
DEVELOPMENT OF AN ATMOSPHERIC MONITORING PLAN FOR SPACE STATION Final Report **c54**
Dennis M. Casserly *In* NASA, Lyndon B. Johnson Space Center, National Aeronautics and Space Administration (NASA)/American Society for Engineering Education (ASEE) Summer Faculty Fellowship Program 1988, Volume 1 Feb. 1989 16 p (For primary document see N89-20058 12-99)
Avail: NTIS HC A09/MF A01 CSCL 06K

An environmental health monitoring plan for Space Station will ensure crew health during prolonged habitation. The Space Station, Freedom, will operate for extended periods, 90+ days, without resupply. A regenerative, closed loop life support system will be utilized in order to minimize resupply logistics and costs. Overboard disposal of wastes and venting of gases to space will be minimal. All waste material will be treated and recycled. The concentrated wastes will be stabilized and stored for ground disposal. The expected useful life of the station (decades) and the diversity of materials brought aboard for experimental or manufacturing purposes, increases the likelihood of cabin contamination. Processes by which cabin contamination can occur include: biological waste production, material off-gassing, process leakage, accidental containment breach, and accumulation due to poor removal efficiencies of the purification units. An industrial hygiene approach was taken to rationalize monitoring needs and to identify the substances likely to be present, the amount, and their hazard. Author

N89-20066*# Prairie View Agricultural and Mechanical Coll., TX. Dept. of Mechanical Engineering.
MODEL FORMULATION OF NON-EQUILIBRIUM GAS RADIATION FOR HYPERSONIC FLIGHT VEHICLES Final Report **c18**
Ing Chang *In* NASA, Lyndon B. Johnson Space Center, National Aeronautics and Space Administration (NASA)/American Society for Engineering Education (ASEE) Summer Faculty Fellowship Program 1988, Volume 1 Feb. 1989 10 p (For primary document see N89-20058 12-99)
Avail: NTIS HC A09/MF A01 CSCL 22B

Several radiation models for low density nonequilibrium hypersonic flow are studied. It is proposed that these models should be tested by the 3-D VRFL code developed at NASA/JSC. A modified and optimized radiation model may be obtained from the testing. Then, the current VRFL code could be expanded to solve hypersonic flow problems with nonequilibrium thermal radiation. Author

N89-20067*# Alma Coll., MI. Dept. of Exercise and Health Science.
A MODEL FOR PLASMA VOLUME CHANGES DURING SHORT DURATION SPACEFLIGHT Final Report **c52**
John E. Davis *In* NASA, Lyndon B. Johnson Space Center, National Aeronautics and Space Administration (NASA)/American Society for Engineering Education (ASEE) Summer Faculty Fellowship Program 1988, Volume 1 Feb. 1989 15 p (For primary document see N89-20058 12-99)
Avail: NTIS HC A09/MF A01 CSCL 06P

It is well established that plasma volume decreases during spaceflight and simulated weightlessness (bedrest). The decrement in plasma volume is thought to contribute to the orthostatic intolerance that has been observed in some crew members following spaceflight. To date, no studies have evaluated the effectiveness of fluid countermeasures of varying osmolality in the restoration of plasma volume and orthostatic tolerance in a controlled study. The overall objectives of this project were to: (1) provide a model that would rapidly and safely produce a fluid loss comparable to that which occurs during short duration spaceflight; and (2) design a study that would determine the optimal drink solution to restore orthostatic tolerance and describe the mechanism(s) whereby orthostatic tolerance is restored. In summary, Lasix can be used as a way of simulating the plasma volume changes that occur during short duration spaceflight. The total loss of plasma is comparable to spaceflight. Lasix is fast acting, and has relatively few side effects. The present design for evaluating the optimal fluid countermeasures will have important implications in restoring orthostatic tolerance and function in the latter stages of spaceflight when it is essential for safe operation of the spacecraft. Author

N89-20068*# Houston Univ., TX. Dept. of Applied Mathematical Sciences.
AN EVIDENTIAL APPROACH TO PROBLEM SOLVING WHEN A LARGE NUMBER OF KNOWLEDGE SYSTEMS IS AVAILABLE Final Report **c63**
Andre deKorvin *In* NASA, Lyndon B. Johnson Space Center, National Aeronautics and Space Administration (NASA)/American Society for Engineering Education (ASEE) Summer Faculty Fellowship Program 1988, Volume 1 Feb. 1989 15 p (For primary document see N89-20058 12-99)
Avail: NTIS HC A09/MF A01 CSCL 09B

Some recent problems are no longer formulated in terms of imprecise facts, missing data or inadequate measuring devices. Instead, questions pertaining to knowledge and information itself arise and can be phrased independently of any particular area of knowledge. The problem considered in the present work is how to model a problem solver that is trying to find the answer to some query. The problem solver has access to a large number of knowledge systems that specialize in diverse features. In this context, feature means an indicator of what the possibilities for the answer are. The knowledge systems should not be accessed more than once, in order to have truly independent sources of information. Moreover, these systems are allowed to run in parallel. Since access might be expensive, it is necessary to construct a management policy for accessing these knowledge systems. To help in the access policy, some control knowledge systems are available. Control knowledge systems have knowledge about the performance parameters status of the knowledge systems. In order to carry out the double goal of estimating what units to access and to answer the given query, diverse pieces of evidence must be fused. The Dempster-Shafer Theory of Evidence is used to pool the knowledge bases. Author

N89-20069*# University of Central Washington, Ellensburg. Dept. of Physical Education.
EFFECTS ON MOTOR UNIT POTENTIATION AND GROUND REACTION FORCE FROM TREADMILL EXERCISE Final Report **c52**
Reid P. Elam *In* NASA, Lyndon B. Johnson Space Center, National Aeronautics and Space Administration (NASA)/American Society for Engineering Education (ASEE) Summer Faculty Fellowship Program 1988, Volume 1 Feb. 1989 13 p (For primary document see N89-20058 12-99)
Avail: NTIS HC A09/MF A01 CSCL 06S

This study was conducted to analyze the characteristics of motor unit potentiation (MUP) and ground reaction force (GRF) in treadmill exercise at the inclines of 0, 5.5 and 11 percent with conjuctive speeds of 7.5, 6, and 5 mph respectively. These speeds and corresponding inclines were set to provide equivalent physiological workloads at 12.5 METS. EMG recordings were taken from the rectus femoris and gastrocnemius of the right leg from 5 subjects. Simultaneous GRF recordings were obtained from a Delmar Avionic treadmill rigged with load cells. Measures for MUP and GRF were taken over a period containing 10 strides at steady pace. It was concluded that the gastrocnemius was more evident in EMG activity in all speed/incline settings over the rectus femoris, and that inclines from 5.5 to 11 percent produced greater GRF's over 0 percent. Recommendations for future studies was made. Author

N89-20070*# State Univ. of New York, Plattsburgh. Dept. of Physics.
AN ASSESSMENT OF THE MICROMETEORITIC COMPONENT IN THE MARTIAN SOIL Final Report **c91**
George J. Flynn *In* NASA, Lyndon B. Johnson Space Center, National Aeronautics and Space Administration (NASA)/American Society for Engineering Education (ASEE) Summer Faculty Fellowship Program 1988, Volume 1 Feb. 1989 15 p (For primary document see N89-20058 12-99)
Avail: NTIS HC A09/MF A01 CSCL 03B

Particles in the mass range from 10 to the minus 7th power to 10 to the minus 3rd power grams contribute 80 percent of the total mass influx of meteoritic material in the 10 to the minus 13th power to 10 to the 6th power gram mass range at Earth (Hughes, 1978). On Earth atmospheric entry, all but the smallest particles in the 10 to the minus 7th power to 10 to the minus 3rd power gram mass range, about 60 to 1200 micrometers in diameter, are heated sufficiently to melt and vaporize. Mars, because of its lower escape velocity and larger atmospheric scale height, is a much more favorable site for unmelted survival of micrometeorites on atmospheric deceleration. Researchers calculate that a significant fraction of particles throughout the 60 to 1200 micrometer diameter range will survive atmospheric entry unmelted. Thus returned Mars soils may offer a resource for sampling micrometeorites in a size range uncollectable in unaltered form at Earth. The addition of meteoritic material to the Mars soils should perturb their chemical composition, as has been detected using the soils on the Moon (Anders, et al., 1973). Using measured mass influx at Earth and estimates of the Mars/Earth flux ratio, researchers estimate a mass influx at Mars of between 2,700 and 202,000 metric tons per year. Author

N89-20071*# Montana State Univ., Bozeman. Dept. of Chemistry.
EVALUATION OF AVAILABLE ANALYTICAL TECHNIQUES FOR MONITORING THE QUALITY OF SPACE STATION POTABLE WATER Final Report **c54**
Richard D. Geer *In* NASA, Lyndon B. Johnson Space Center, National Aeronautics and Space Administration (NASA)/American Society for Engineering Education (ASEE) Summer Faculty Fellowship Program 1988, Volume 1 Feb. 1989 15 p (For primary document see N89-20058 12-99)
Avail: NTIS HC A09/MF A01 CSCL 06K

To assure the quality of potable water (PW) on the Space Station (SS) a number of chemical and physical tests must be conducted routinely. After reviewing the requirements for potable water, both direct and indirect analytical methods are evaluated that could make the required tests and improvements compatible with the Space Station operation. A variety of suggestions are made to improve the analytical techniques for SS operation. The most important recommendations are: (1) the silver/silver chloride electrode (SB) method of removing I sub 2/I (-) biocide from the water, since it may interfere with analytical procedures for PW and also its end uses; (2) the orbital reactor (OR) method of carrying out chemistry and electrochemistry in microgravity by using a disk shaped reactor on an orbital table to impart artificial G force to the contents, allowing solution mixing and separation of gases and liquids; and (3) a simple ultra low volume highly sensitive electrochemical/conductivity detector for use with a capillary zone electrophoresis apparatus. It is also recommended, since several different conductivity and resistance measurements are made during the analysis of PW, that the bipolar pulse measuring circuit be used in all these applications for maximum compatibility and redundancy of equipment. Author

N89-20072*# Michigan Technological Univ., Houghton. Dept. of Mechanical Engineering.
MODEL EVALUATION, RECOMMENDATION AND PRIORITIZING OF FUTURE WORK FOR THE MANIPULATOR EMULATOR TESTBED Final Report **c37**
Frederick A. Kelly *In* NASA, Lyndon B. Johnson Space Center, National Aeronautics and Space Administration (NASA)/American Society for Engineering Education (ASEE) Summer Faculty Fellowship Program 1988, Volume 1 Feb. 1989 10 p (For primary document see N89-20058 12-99)
Avail: NTIS HC A09/MF A01 CSCL 13I

The Manipulator Emulator Testbed (MET) is to provide a facility capable of hosting the simulation of various manipulator configurations to support concept studies, evaluation, and other engineering development activities. Specifically, the testbed is intended to support development of the Space Station Remote Manipulator System (SSRMS) and related systems. The objective of this study is to evaluate the math models developed for the MET simulation of a manipulator's rigid body dynamics and the servo systems for each of the driven manipulator joints. Specifically, the math models are examined with regard to their amenability to pipeline and parallel processing. Based on this evaluation and the project objectives, a set of prioritized recommendations are offered for future work. Author

N89-20073*# National Aeronautics and Space Administration. Lyndon B. Johnson Space Center, Houston, TX.
NATIONAL AERONAUTICS AND SPACE ADMINISTRATION (NASA)/AMERICAN SOCIETY FOR ENGINEERING EDUCATION (ASEE) SUMMER FACULTY FELLOWSHIP PROGRAM 1988, VOLUME 2
Richard B. Bannerot and Stanley H. Goldstein Feb. 1989 177 p Program held in Houston, TX, 1988 Sponsored by NASA, Washington
(Grant NGT-44-005-803)
(NASA-CR-172118-Vol-2; NAS 1.26:172118-Vol-2) Avail: NTIS HC A09/MF A01 CSCL 05I

The 1988 Johnson Space Center (JSC) National Aeronautics and Space Administration (NASA)/American Society for Engineering Education (ASEE) Summer Faculty Fellowship Program was conducted by the University of Houston and JCS. The 10-week program was operated under the auspices of the ASEE. The program at JSC, as well as the programs at other NASA Centers, was funded by the Office of University Affairs, NASA Headquarters, Washington, D.C. The objectives of the program, which began in 1965 at JSC and in 1964 nationally, are: (1) to further the professional knowledge of qualified engineering and science faculty members; (2) to stimulate an exchange of ideas between participants and NASA; (3) to enrich and refresh the research and teaching activities of participants' institutions; and (4) to contribute to the research objectives of the NASA Centers. For individual titles, see N89-20074 through N89-20085.

N89-20074*# Missouri Univ., Independence. Dept. of Electrical and Computer Engineering.
OPTICAL JOINT CORRELATION USING THE DEFORMABLE MIRROR DEVICE Final Report **c74**
Jerome Knopp *In* NASA, Lyndon B. Johnson Space Center, National Aeronautics and Space Administration (NASA)/American Society for Engineering Education (ASEE) Summer Faculty Fellowship Program 1988, Volume 2 Feb. 1989 14 p (For primary document see N89-20073 12-99)
Avail: NTIS HC A09/MF A01 CSCL 20F

An experimental investigation of the Deformable Mirror Device (DMD) developed by Texas Instruments at Dallas for use in object identification was completed. The DMD was tested as a joint correlator. The DMD was used as a spatial light modulator on which the squared modulus of the Fourier transform of test object pairs was written. The squared modulus was phase encoded on the DMD after it had been thresholded and rewritten as a binary phase function. The thresholding was found to produce a sharp peak in the autocorrelation when the test objects were matched and no significant peak in the case of distinct objects. It was concluded that the use of the DMD as a joint correlator looks promising and further studies should be carried out. Author

N89-20075*# Texas A&I Univ., Kingsville. Dept. of Civil and Mechanical Engineering.
INTELLIGENT CONTROL OF ROBOTIC ARM/HAND SYSTEMS FOR THE NASA EVA RETRIEVER USING NEURAL NETWORKS Final Report **c63**

Robert A. McLauchlan *In* NASA, Lyndon B. Johnson Space Center, National Aeronautics and Space Administration (NASA)/American Society for Engineering Education (ASEE) Summer Faculty Fellowship Program 1988, Volume 2 Feb. 1989 15 p (For primary document see N89-20073 12-99)
Avail: NTIS HC A09/MF A01 CSCL 09B

Adaptive/general learning algorithms using varying neural network models are considered for the intelligent control of robotic arm plus dextrous hand/manipulator systems. Results are summarized and discussed for the use of the Barto/Sutton/Anderson neuronlike, unsupervised learning controller as applied to the stabilization of an inverted pendulum on a cart system. Recommendations of an inverted pendulum of the controller and a kinematic analysis for trajectory planning to simple object retrieval (chase/approach and capture/grasp) scenarios in two dimensions. Author

N89-20076*# Texas Univ., Galveston. Dept. of Pharmacology and Toxicology.
MALADJUSTMENT OF KIDNEYS TO MICROGRAVITY: DESIGN OF MEASURES TO REDUCE THE LOSS OF CALCIUM Final Report **c52**
Bohdan R. Nechay *In* NASA, Lyndon B. Johnson Space Center, National Aeronautics and Space Administration (NASA)/American Society for Engineering Education (ASEE) Summer Faculty Fellowship Program 1988, Volume 2 Feb. 1989 14 p (For primary document see N89-20073 12-99)
Avail: NTIS HC A09/MF A01 CSCL 06P

Losses of skeletal calcium and body fluids occur during prolonged exposure to microgravity. The kidney plays a major role in regulating the physiological functions involved. Relative to this regulatory function, the kidney performs three operations: filtration of blood plasma through the glomeruli, reabsorption, and secretion of fluid and electrolytes so that needed components are retained and only waste is eliminated in the urine. Using data published in Biomedical Results from Skylab, researchers performed new calculations that reflect more directly the operations of the kidney in the handling of calcium, sodium, chloride, potassium and phosphate during space flight. These calculations revealed that the fraction of filtered calcium that was rejected by renal tubules and excreted in the urine increased by 71 percent, from 1.77 percent (preflight) to 3.02 percent (inflight) of the filtered load. This represents a large absolute increase because the total filtered amount is huge. Because the tubular rejection fraction of other ions increased relatively less than that of calcium, researchers postulate the inflight development of a specific renal defect that causes an excessive loss of calcium in urine and thereby contributes to the weakening of bones. Author

N89-20077*# Sul Ross State Univ., Alpine, TX. Dept. of Geology.
EVALUATION OF CRUSTAL RECYCLING DURING THE EVOLUTION OF ARCHEAN-AGE MATACHEWAN BASALTIC MAGMAS Final Report **c46**
Dennis O. Nelson *In* NASA, Lyndon B. Johnson Space Center, National Aeronautics and Space Administration (NASA)/American Society for Engineering Education (ASEE) Summer Faculty Fellowship Program 1988, Volume 2 Feb. 1989 15 p (For primary document see N89-20073 12-99)
Avail: NTIS HC A09/MF A01 CSCL 08G

The simplest model for the Matachewan-Hearst Dike (MHD) magmas is assimilation-fractional crystallization (AFC), presumably occurring at the base of the crust during underplating. Subduction zone enriched mantle sources are not required. Trace elements suggest that the mantle sources for the MHD were depleted, but possessed a degree of heterogeneity. Rates of assimilation were approximately 0.5 (= Ma/Mc); the contaminant mass was less than 20 percent. The contaminant was dominated by tonalites-randodiorites, similar to xenoliths and rocks in the Kapuskasing Structural Zone (KSZ). Assimilation of partial melts of light-rare earth and garnet-bearing basaltic precursors may have produced some the MHD magmas. Apparently, previous underplating-AFC processes had already produced a thick crust. The silicic granitoid assimilant for the MHD magmas was probably produced by earlier processing of underplated mafic crust (4, 5, 10, 21 and 30). Calculations suggest that the derived silicic rocks possess negative Ta and Ti anomalies even though they were not the product of subduction. Author

N89-20078*# Sul Ross State Univ., Alpine, TX. Analytical Lab.
LITHOSPHERIC BUCKLING AND INTRA-ARC STRESSES: A MECHANISM FOR ARC SEGMENTATION Final Report **c46**
Kerri L. Nelson *In* NASA, Lyndon B. Johnson Space Center, National Aeronautics and Space Administration (NASA)/American Society for Engineering Education (ASEE) Summer Faculty Fellowship Program 1988, Volume 2 Feb. 1989 14 p (For primary document see N89-20073 12-99)
Avail: NTIS HC A09/MF A01 CSCL 08G

Comparison of segment development of a number of arcs has shown that consistent relationships between segmentation, volcanism and variable stresses exists. Researchers successfully modeled these relationships using the conceptual model of lithospheric buckling of Yamaoka et al. (1986; 1987). Lithosphere buckling (deformation) provides the needed mechanism to explain segmentation phenomenon; offsets in volcanic fronts, distribution of calderas within segments, variable segment stresses and the chemical diversity seen between segment boundary and segment interior magmas. Author

N89-20079*# DePaul Univ., Chicago, IL. Dept. of Computer Science.
TOWARD AN IMAGE COMPRESSION ALGORITHM FOR THE HIGH-RESOLUTION ELECTRONIC STILL CAMERA Final Report **c61**
Rosalee Nerheim *In* NASA, Lyndon B. Johnson Space Center, National Aeronautics and Space Administration (NASA)/American Society for Engineering Education (ASEE) Summer Faculty Fellowship Program 1988, Volume 2 Feb. 1989 12 p (For primary document see N89-20073 12-99)
Avail: NTIS HC A09/MF A01 CSCL 09B

Taking pictures with a camera that uses a digital recording medium instead of film has the advantage of recording and transmitting images without the use of a darkroom or a courier. However, high-resolution images contain an enormous amount of information and strain data-storage systems. Image compression will allow multiple images to be stored in the High-Resolution Electronic Still Camera. The camera is under development at Johnson Space Center. Fidelity of the reproduced image and compression speed are of tantamount importance. Lossless compression algorithms are fast and faithfully reproduce the image, but their compression ratios will be unacceptably low due to noise in the front end of the camera. Future efforts will include exploring methods that will reduce the noise in the image and increase the compression ratio. Author

N89-20080*# Baylor Univ., Waco, TX. Dept. of Mathematics.
EQUATING AN EXPERT SYSTEM TO A CLASSIFIER IN ORDER TO EVALUATE THE EXPERT SYSTEM Final Report **c63**
Patrick L. Odell *In* NASA, Lyndon B. Johnson Space Center, National Aeronautics and Space Administration (NASA)/American Society for Engineering Education (ASEE) Summer Faculty Fellowship Program 1988, Volume 2 Feb. 1989 14 p (For primary document see N89-20073 12-99)
Avail: NTIS HC A09/MF A01 CSCL 09B

A strategy to evaluate an expert system is formulated. The strategy proposed is based on finding an equivalent classifier to an expert system and evaluate that classifier with respect to an optimal classifier, a Bayes classifier. Here it is shown that for the rules considered an equivalent classifier exists. Also, a brief consideration of meta and meta-meta rules is included. Also, a taxonomy of expert systems is presented and an assertion made that an equivalent classifier exists for each type of expert system in the taxonomy with associated sets of underlying assumptions. Author

N89-20081*# Southern Univ., Baton Rouge, LA. Dept. of Electronics Engineering Technology.
FEASIBILITY OF USING HIGH TEMPERATURE SUPERCONDUCTING MAGNETS AND CONVENTIONAL MAGNETIC LOOP ANTENNAS TO ATTRACT OR REPEL OBJECTS AT THE SPACE STATION Final Report **c32**
Manjit S. Randhawa *In* NASA, Lyndon B. Johnson Space Center, National Aeronautics and Space Administration (NASA)/American Society for Engineering Education (ASEE) Summer Faculty Fellowship Program 1988, Volume 2 Feb. 1989 14 p (For primary document see N89-20073 12-99)
Avail: NTIS HC A09/MF A01 CSCL 20N

A study was undertaken to see if magnetic forces can be used at the Space Station to attract or repel spacecrafts such as the Orbital Manuevering Vehicle (OMV) or the Orbiter. A large magnet, in the form of a current loop, is assumed to be placed at the Space Station and another one on the spacecraft. The expression for the force between the two dipoles (loops) is obtained. Using a force of 15 Newtons (3.4 pounds) in order to move the spacecraft, the number of ampere-turn needed in the current loops was calculated at various distances between them. The expression for the force of attraction between a current loop and a soft magnetic material was also examined and the number of amp-turn needed to provide a force of one-tenth of a pound at various distances is also calculated. This one tenth of a pound force would be used in a life line system for the retrieval of an adrift crewman or tool at the Space Station. The feasibility of using conventional antenna on the Station and the incoming vehicle for attraction or repulsion was also examined. Author

N89-20082*# East Texas State Univ., Commerce. Dept. of Computer Science.
VISUAL PERCEPTION AND GRASPING FOR THE EXTRAVEHICULAR ACTIVITY ROBOT Final Report **c37**
Scott A. Starks *In* NASA, Lyndon B. Johnson Space Center, National Aeronautics and Space Administration (NASA)/American Society for Engineering Education (ASEE) Summer Faculty Fellowship Program 1988, Volume 2 Feb. 1989 14 p (For primary document see N89-20073 12-99)
Avail: NTIS HC A09/MF A01 CSCL 13I

The development of an approach to the visual perception of object surface information using laser range data in support of robotic grasping is discussed. This is a very important problem area in that a robot such as the EVAR must be able to formulate a grasping strategy on the basis of its knowledge of the surface structure of the object. A description of the problem domain is given as well as a formulation of an algorithm which derives an object surface description adequate to support robotic grasping. The algorithm is based upon concepts of differential geometry namely, Gaussian and mean curvature. Author

N89-20083*# Alabama A & M Univ., Normal. Dept. of Physics.
ESTIMATION OF VELOCITY PERTURBATIONS IN SATELLITE FRAGMENTATION EVENTS Final Report **c18**
Arjun Tan *In* NASA, Lyndon B. Johnson Space Center, National Aeronautics and Space Administration (NASA)/American Society for Engineering Education (ASEE) Summer Faculty Fellowship Program 1988, Volume 2 Feb. 1989 15 p (For primary document see N89-20073 12-99)
Avail: NTIS HC A09/MF A01 CSCL 22B

The magnitude, variance and directionality of the velocity perturbations of the fragments of a satellite can shed valuable information regarding the nature and intensity of the fragmentation. Up until now, the only method used to calculate the three orthogonal components of the velocity change consisted of inverting the process of evaluating the changes in the orbital elements of the fragments due to velocity perturbing forces. But the traditional method failed in five different cases: (1) when the parent satellite's orbit was circular; (2) and (3) when the true anomaly of the parent was either 0 deg or 180 deg; and (4) and (5) when the argument of latitude of the parent was 90 deg or 270 deg. Described here is a new method of calculating the velocity perturbations which is free from the shortcomings of the traditional method and could be used in all occasions, provided the fragmentation data and the orbital elements data are consistent with one another. Author

N89-20084*# Prairie View Agricultural and Mechanical Coll., TX. Dept. of Electrical Engineering.
TIME-DOMAIN IMAGING Final Report **c32**
C. L. Tolliver *In* NASA, Lyndon B. Johnson Space Center, National Aeronautics and Space Administration (NASA)/American Society for Engineering Education (ASEE) Summer Faculty Fellowship Program 1988, Volume 2 Feb. 1989 16 p (For primary document see N89-20073 12-99)
Avail: NTIS HC A09/MF A01 CSCL 17B

The quest for the highest resolution microwave imaging and principle of time-domain imaging has been the primary motivation for recent developments in time-domain techniques. With the present technology, fast time varying signals can now be measured and recorded both in magnitude and in-phase. It has also enhanced our ability to extract relevant details concerning the scattering object. In the past, the interface of object geometry or shape for scattered signals has received substantial attention in radar technology. Various scattering theories were proposed to develop analytical solutions to this problem. Furthermore, the random inversion, frequency swept holography, and the synthetic radar imaging, have two things in common: (1) the physical optic far-field approximation, and (2) the utilization of channels as an extra physical dimension, were also advanced. Despite the inherent vectorial nature of electromagnetic waves, these scalar treatments have brought forth some promising results in practice with notable examples in subsurface and structure sounding. The development of time-domain techniques are studied through the theoretical aspects as well as experimental verification. The use of time-domain imaging for space robotic vision applications has been suggested. Author

N89-20085*# Northeastern Univ., Boston, MA. Dept. of Chemical Engineering.
ARC JET DIAGNOSTICS TESTS Final Report **c25**
Ronald J. Willey *In* NASA, Lyndon B. Johnson Space Center, National Aeronautics and Space Administration (NASA)/American Society for Engineering Education (ASEE) Summer Faculty Fellowship Program 1988, Volume 2 Feb. 1989 15 p (For primary document see N89-20073 12-99)
Avail: NTIS HC A09/MF A01 CSCL 07D

Two objectives were addressed during a 10 week 1988 NASA/ASEE summer faculty fellowship at the Johnson Space Center Atmospheric Reentry Materials Structures Evaluation Facility (ARMSEF). These objectives were the evaluation of mass spectrometry for the measurement of atomic and molecular species in an arc jet environment, and the determination of atomic recombination coefficients for reaction cured glass (RCG) coated high temperature surface insulation (HRSI) materials subjected to simulated reentry conditions. Evaluation of mass spectrometry for the measurement of atomic and molecular species provided some of the first measurements of point compositions in arc jet tunnel environments. A major objective of this project centered around the sampling residence time. A three staged vacuum sampling system pulled the molecules and atoms from the arc jet to a quadrupole ionization mass spectrometer in 400 milliseconds. Conditions investigated included a composition survey across the nozzle exit at 3 cm z-distance from the nozzle exit for 3 different currents. Also, a point composition survey was taken around a shock created by the presence of a blunt body. Author

Typical Subject Index Listing

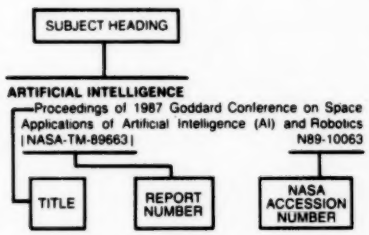

The subject heading is the key to the subject content of the document. Titles, report numbers, and accession numbers of pertinent documents are provided under each subject heading. When the title is insufficiently descriptive of the document content, a title extension has been added, separated from the title by three hyphens. The report number helps to indicate the type of document cited (e.g., NASA report, NASA translation, NASA contractor report). The NASA accession number is the number by which the document abstracts are arranged in this journal and by which the document is sold or requested. The titles, with title extensions if present, are arranged under each subject heading in ascending accession number order. The subject headings have been selected from the latest revision of the *NASA Thesaurus* (NASA SP-7064).

A

ABSORPTION CROSS SECTIONS
Fundamental optical studies of competitive adsorption and thin film phenomena
[DE89-005898] N89-19401
Ultraviolet absorption cross-sections of halocarbons of stratospheric interest
[AERONOMICA-ACTA-A-336-1988] N89-19769

ACCELERATION TOLERANCE
A stress test to evaluate the physical capacity of performing L-1 anti-G straining maneuvers
[AD-A202301] N89-19803

ACCELEROMETERS
Superconducting gravity gradiometer mission. Volume 2: Study team technical report
[NASA-TM-4091] N89-19749

ACCESS CONTROL
An evidential approach to problem solving when a large number of knowledge systems is available N89-20068

ACCIDENT INVESTIGATION
The Atlas/Centaur 67 launch mishap
[GPO-80-201] N89-19332

ACCLIMATIZATION
Dexamethasone for prevention and treatment of acute mountain sickness
[AD-A201554] N89-19799

ACCRETION DISKS
Near-infrared spectroscopy of young stellar objects N89-20033
Implications of the observed contraction of accretion disks in quiescent dwarf novae N89-20047

ACCURACY
Estimating aircraft airframe tooling cost: An alternative to DAPCA 3
[AD-A201506] N89-19226
Testing expert systems N89-19834
Next generation keyboards: The importance of cognitive compatibility N89-19848

ACETAZOLAMIDE
Dexamethasone for prevention and treatment of acute mountain sickness
[AD-A201554] N89-19799

ACID RAIN
Cloud capture by a mountain top forest. Part 1: Acidity and dosage duration N89-19682
Influences of cloud microphysics on continental and marine precipitation chemistry N89-19700
Modeling studies on the formation, growth, dissipation and acidification of cumulus clouds N89-19704
A numerical simulation of the acidification process of rain water below the cloud and the mechanism of acid rain formation in area of Chongqing, China N89-19706
Meteorological and chemical influencing factors on acidity production in a mesoscale model with quasi-spectral microphysics N89-19711
Use of cluster analysis to define periods of similar meteorology and precipitation chemistry in eastern North America N89-19785

ACIDITY
Acidification of stratiform clouds and their aerosol scavenging properties N89-19694

ACOUSTIC DUCTS
Acoustic wave propagation in heterogeneous structures including experimental validation
[NASA-TM-101486] N89-19965

ACOUSTIC EMISSION
Acoustic emission measurements during fatigue loading of scaled Pressurized Water Reactor (PWR) vessel at Joint Research Center of the European Communities (JRC), Ispra (Italy)
[CISE-4476] N89-19600
General review of recent activities in acoustic emission technology in Italy
[CISE-4477] N89-19601

ACOUSTIC MEASUREMENT
Noise assessment of the rocket sled test track operation at Holloman AFB, New Mexico
[AD-A201279] N89-19317
Development of a system for acoustic measurements of bistatic target strengths
[AD-A201673] N89-19970

ACOUSTIC SCATTERING
Research in acoustical scattering, diffraction catastrophes, optics of bubbles and acoustical phase conjugation
[AD-A201451] N89-19968
Development of a system for acoustic measurements of bistatic target strengths
[AD-A201673] N89-19970

ACOUSTIC VELOCITY
A modal/WKB inversion method for determining sound speed profiles in the ocean and ocean bottom
[AD-A201252] N89-19791

ACOUSTICS
Activities report in electrotechnology
[ETN-89-93715] N89-19448
On the design of loudspeakers for broadcast monitoring
[BBC-RD-1988/14] N89-19450
Acoustoelasticity using longitudinal waves for residual stress evaluation
[DE89-006154] N89-19604
Acoustic wave propagation in heterogeneous structures including experimental validation
[NASA-TM-101486] N89-19965

ACTIVATION ENERGY
Oxygen diffusion in YBa2Cu3O7-delta
[DE89-005831] N89-20011

ACTIVE CONTROL
Active control of elastic wave motion in structural networks N89-19342
An approach to semi-active control of multiple degree-of-freedom systems N89-19554

ACTUATORS
Integrated tools for control-system analysis
[NASA-TP-2885] N89-19309
Proceedings of the Fifth AFOSR Forum on Space Structures
[AD-A194761] N89-19333
Comments on electromechanical actuators for controlling flexible structures N89-19339
Decentralized/relegated control for large space structures N89-19346
Robust eigenstructure assignment by a projection method: Application using multiple optimization criteria N89-19349
Investigation of flight sensors and actuators for the vibration damping augmentation of large flexible space structures
[ESA-CR(P)-2670] N89-19362
RCS/piezoelectric distributed actuator study
[AD-A201276] N89-19999

ADA (PROGRAMMING LANGUAGE)
From Algol 60 to Ada: Problems, solutions, feasibility
[REPT-88-41] N89-19919

ADAPTATION
Concept of adaptive structures N89-19338

ADAPTERS
Maximum entropy/optimal projection design synthesis for decentralized control of large space structures
[AD-A202375] N89-19358

ADAPTIVE CONTROL
Adaptive control of large space structures N89-19343
Design of an optical sensor system for adaptive control of a seam tracking robot N89-19565

ADDITIVES
An experimental investigation of sooting characteristics of a gas turbine combustor and augmentor tube
[AD-A201804] N89-19568

ADHESION
Adhesion in ceramics and magnetic media
[NASA-TM-101476] N89-19435
Effect of adhesive interleaving and discontinuous plies on failure of composite laminates subject to transverse normal loads
[NASA-TM-101507] N89-19589

ADHESIVE BONDING
An interdisciplinary study of cathodic debonding in elastomer/metal adhesive bonds
[AD-A202376] N89-19434
Adhesion in ceramics and magnetic media
[NASA-TM-101476] N89-19435

ADHESIVES
Preparation of non-metals properties for data base
[NASA-CR-183596] N89-19420
An interdisciplinary study of cathodic debonding in elastomer/metal adhesive bonds
[AD-A202376] N89-19434
Effect of adhesive interleaving and discontinuous plies on failure of composite laminates subject to transverse normal loads
[NASA-TM-101507] N89-19589

ADJUSTING
The geometry of geodetic inverse linear mapping and nonlinear adjustment
[ETN-89-93900] N89-19736

ADSORPTION
The dissociative adsorption of ammonia on Si(100)
[AD-A201599] N89-19396
The adsorption and decomposition of NH3 on Si(100): Detection of the NH2(a) species
[AD-A201601] N89-19397
Fundamental optical studies of competitive adsorption and thin film phenomena
[DE89-005898] N89-19401

AEROACOUSTICS
Unsteady aerodynamics of blade rows N89-19263

AERODYNAMIC BALANCE
Drag measurements on a laminar-flow body of revolution in the 13-inch magnetic suspension and balance system
[NASA-TP-2895] N89-19232

AERODYNAMIC CHARACTERISTICS
Numerical simulation of the aerodynamics of turbulent transonic flow past a projectile N89-19270
Experimental simulation of transonic vortex-airfoil interactions
[AD-A201934] N89-19274
Numerical computations of transonic critical aerodynamic behavior
[AD-A202412] N89-19277

Multiple Application Propfan Study (MAPS): Advanced tactical transport
[NASA-CR-175003] N89-19300

AERODYNAMIC COEFFICIENTS
Drag coefficients for irregular fragments
[AD-A201943] N89-19276

AERODYNAMIC CONFIGURATIONS
Knowledge-based zonal grid generation for computational fluid dynamics N89-19828

AERODYNAMIC DRAG
Use of riblets to obtain drag reduction on airfoils at high Reynolds number flows
[AD-A201485] N89-19267
Drag coefficients for irregular fragments
[AD-A201943] N89-19276

AERODYNAMIC FORCES
Numerical simulation of the aerodynamics of turbulent transonic flow past a projectile N89-19270

AERODYNAMIC LOADS
Application of a full potential method to AGARD standard airfoils N89-19242
NASTRAN supplemental documentation for modal forced vibration analysis of aerodynamically excited turbosystems
[NASA-CR-174967] N89-19583

AERODYNAMIC STABILITY
Turbomachinery aeroelasticity at NASA Lewis Research Center N89-19262
Time periodic control of a multiblade helicopter N89-19312
A systems approach to rotorcraft stability and control research
[AD-A201784] N89-19314

AERODYNAMIC STALLING
Airfoil stall penetration at constant pitch rate and high Reynolds number N89-19260

AERODYNAMICS
Hypervelocity technology escape system concepts. Volume 1: Development and evaluation
[AD-A201719] N89-19280
The design and initial construction of a composite RPV (Remotely Piloted Vehicle) for flight research applications
[AD-A201884] N89-19291
A model of the electrostatic-aerodynamic shape of raindrops N89-19615
On the dynamics of the falling ice crystal zone N89-19672

AEROELASTICITY
Transonic Unsteady Aerodynamics and Aeroelasticity 1987, part 1
[NASA-CP-3022-PT-1] N89-19234
Unsteady aerodynamics and aeroelastic research at AFWAL N89-19235
Extensions and improvements on XTRAN3S N89-19236
Role of computational fluid dynamics in unsteady aerodynamics for aeroelasticity N89-19237
Full potential unsteady computations including aeroelastic effects N89-19243
AGARD standard aeroelastic configurations for dynamic response N89-19246
Transonic Unsteady Aerodynamics and Aeroelasticity 1987, part 2
[NASA-CP-3022-PT-2] N89-19247
The oblique-wing research aircraft: A test bed for unsteady aerodynamic and aeroelastic research N89-19253
Static aeroelasticity of a composite oblique wing in transonic flows N89-19254
Investigation and suppression of high dynamic response encountered on an elastic supercritical wing N89-19255
Initial application of CAP-TSD to wing flutter N89-19257
Turbomachinery aeroelasticity at NASA Lewis Research Center N89-19262
Unsteady aerodynamics of blade rows N89-19263
Computational aeroelasticity challenges and resources N89-19264

AERONAUTICAL ENGINEERING
R and M (Reliability and Maintainability) quality team concept and C-17 design at Douglas Aircraft Company: An R and M 2000 initiative case study
[AD-A201574] N89-19228

AEROSOLS
Measurements of the partitioning of aerosol mass and number between cloud droplets and interstitial air N89-19616
Cloud and aerosol optical depths N89-19646
The study of the interstitial aerosol particles and cloud droplets with digital image analysis of diffraction images N89-19654
Kinetics of ice crystal formation on aerosol particles in supercooled fog N89-19665
Insoluble particles in hydrometeors N89-19684
Below cloud scavenging by rain and drizzle N89-19685
The effect of aerosols on pH of snowfalls N89-19688
Acidification of stratiform clouds and their aerosol scavenging properties N89-19694
Microphysical, dynamical and chemical aspects of scavenging processes during winter precipitation N89-19695
Intercomparisons of aircraft measurements with lidar returns for aerosol, ice crystals and water droplets N89-19718
A high-spectral-resolution lidar system: The use of atomic blocking filter for measuring atmospheric parameters
[AD-A201736] N89-19759

AEROSPACE ENGINEERING
Minimax and maximax optimal control problems with applications in aerospace engineering N89-19311
Advanced extravehicular activity systems requirements definition study. Phase 2: Extravehicular activity at a lunar base
[NASA-CR-172117] N89-19809
Validation of highly reliable, real-time knowledge-based systems N89-19833

AEROSPACE INDUSTRY
Analysis of cost growth and cost composition in the defense aerospace industry
[AD-A201544] N89-19227

AEROSPACE MEDICINE
An annotated bibliography of hypobaric decompression sickness research conducted at the Crew Technology Division, USAF School of Aerospace Medicine, Brooks AFB, Texas from 1983 to 1988
[AD-A201274] N89-19796
Advanced extravehicular activity systems requirements definition study. Phase 2: Extravehicular activity at a lunar base
[NASA-CR-172117] N89-19809

AEROSPACE SYSTEMS
Experimental verification of an innovative performance-validation methodology for large space systems
[AD-A202243] N89-19357
Maximum entropy/optimal projection design synthesis for decentralized control of large space structures
[AD-A202375] N89-19358

AEROTHERMODYNAMICS
Aerothermodynamics of a jet cell facility
[AD-A202142] N89-19318

AGROMETEOROLOGY
Microphysical characteristics of warm-based cumuli: Observations at -10 C --- weather modification N89-19626

AIR
Pattern of air bubble inclusions in atmospheric ice formed during accretion N89-19676

AIR COOLING
Cooling effectiveness of a hybrid microclimate garment
[AD-A201115] N89-19811

AIR DUCTS
Acoustic wave propagation in heterogeneous structures including experimental validation
[NASA-TM-101486] N89-19965

AIR FLOW
A model of wet deposition to complex terrain by the seeder-feeder process N89-19710

AIR JETS
Study of underexpanded turbulent air jets in water N89-19516

AIR LAND INTERACTIONS
On the small scale topographical influences on precipitation N89-19720

AIR LOCKS
Chemical warfare protection for the cockpit of future aircraft N89-19859

AIR POLLUTION
Kinetic equation for polluted cloud droplets spectrum N89-19661
Determination of chemical reaction rates in fog N89-19683
Vertical profiles of pollutants inside and outside of cloud N89-19696
Effects of cloud microphysical processes on trace chemical removal efficiences N89-19707
Measurement of the global distribution of tropospheric trace gases and their time dependent variations
[ETN-89-93987] N89-19747

AIR SAMPLING
Concentrations in rain events collected sequentially: Measurements vs results of a simple scavenging model N89-19701

AIR TO SURFACE MISSILES
Short-range anti-armour flight vehicles of the Apache/CWS family
[DRIC-T-8130] N89-19296
EMMA: The expert system for munition maintenance N89-19823

AIR TRAFFIC
Simultaneous three-dimensional modeling of commercial flights within the airspace of the Federal Republic of Germany
[DFVLR-FB-88-31] N89-19282

AIR TRAFFIC CONTROL
The efficacy of color-coded symbols to enhance air-traffic control displays
[AD-A201594] N89-19284

AIR TRAFFIC CONTROLLERS (PERSONNEL)
Voice control of complex workstations N89-19880

AIR WATER INTERACTIONS
In situ measurements of ship tracks N89-19645
Boundary layer development over the eastern Pacific Ocean N89-19753

AIRBORNE EQUIPMENT
Calibration of PMS FSSP and 1D-C probes for cloud droplet measurements N89-19713
Applications of the NCAR Electra Doppler radar for the study of physical parameters of clouds N89-19717
A new airborne device for measurement of cloud particles using video microscope N89-19719

AIRBORNE/SPACEBORNE COMPUTERS
Spaceborne VHSIC multiprocessor system for AI applications N89-19838
Development of a software interface for optical disk archival storage for a new life sciences flight experiments computer N89-20061

AIRCRAFT APPROACH SPACING
Simultaneous three-dimensional modeling of commercial flights within the airspace of the Federal Republic of Germany
[DFVLR-FB-88-31] N89-19282

AIRCRAFT CONFIGURATIONS
Transonic Unsteady Aerodynamics and Aeroelasticity 1987, part 1
[NASA-CP-3022-PT-1] N89-19234
Unsteady aerodynamics and aeroelastic research at AFWAL N89-19235
Extensions and improvements on XTRAN3S N89-19236
CAP-TSD: A program for unsteady transonic analysis of realistic aircraft configurations N89-19238
CAP-TSD analysis of the F-15 aircraft N89-19239
Calculation of steady and unsteady pressures at supersonic speeds with CAP-TSD N89-19240
Application of a full potential method to AGARD standard airfoils N89-19242
Full potential unsteady computations including aeroelastic effects N89-19243
AGARD standard aeroelastic configurations for dynamic response N89-19246
Numerical solution of unsteady rotational flow past fixed and rotary wing configurations N89-19251
The oblique-wing research aircraft: A test bed for unsteady aerodynamic and aeroelastic research N89-19253
Static aeroelasticity of a composite oblique wing in transonic flows N89-19254

AIRCRAFT CONTROL
A parallel expert system for the control of a robotic air vehicle N89-19842

AIRCRAFT DESIGN
Control of nonlinear systems using partial dynamic inversion N89-19310
Light weight escape capsule for fighter aircraft N89-19858

AIRCRAFT ENGINES
Propulsion
[PNR90472] N89-19302
The gas turbine engine and its certification
[PNR90496] N89-19303
The relationship between manufacturing technology and design --- aircraft engines
[PNR90537] N89-19307
The diffusion bonding of aeroengine components
[PNR90540] N89-19308
Gear technology acquisition for advanced aero engines
[PNR90510] N89-19571
COMPASS: A generalized ground-based monitoring system
[PNR90483] N89-19894

AIRCRAFT GUIDANCE
Simultaneous three-dimensional modeling of commercial flights within the airspace of the Federal Republic of Germany
[DFVLR-FB-88-31] N89-19282

AIRCRAFT HAZARDS
Generalized three-dimensional experimental lightning code (G3DXL) user's manual
[NASA-CR-166079] N89-19779
AIRCRAFT INDUSTRY
R and M (Reliability and Maintainability) quality team concept and C-17 design at Douglas Aircraft Company: An R and M 2000 initiative case study
[AD-A201574] N89-19228
AIRCRAFT INSTRUMENTS
A schema-based model of situation awareness: Implications for measuring situation awareness N89-19847
Light weight escape capsule for fighter aircraft N89-19858
AIRCRAFT MAINTENANCE
R and M (Reliability and Maintainability) quality team concept and C-17 design at Douglas Aircraft Company: An R and M 2000 initiative case study
[AD-A201574] N89-19228
AIRCRAFT MODELS
Icing research tunnel test of a model helicopter rotor
[NASA-TM-101978] N89-19305
AIRCRAFT PERFORMANCE
Multiple Application Propfan Study (MAPS): Advanced tactical transport
[NASA-CR-175003] N89-19300
AIRCRAFT RELIABILITY
Combined preliminary airworthiness evaluation and airworthiness and flight characteristics evaluation of the UH-1H with preproduction hub spring and composite main rotor blades installed
[AD-A202316] N89-19295
AIRCRAFT STABILITY
Unsteady aerodynamics and aeroelastic research at AFWAL N89-19235
Extensions and improvements on XTRAN3S N89-19236
Transonic Unsteady Aerodynamics and Aeroelasticity 1987, part 2
[NASA-CP-3022-PT-2] N89-19247
AIRCRAFT STRUCTURES
Advanced durability analysis. Volume 4: Executive summary
[AD-A202304] N89-19597
AIRFOIL OSCILLATIONS
The role of shock induced trailing-edge separation in limit cycle oscillations N89-19256
Initial application of CAP-TSD to wing flutter N89-19257
Experimental transonic steady state and unsteady pressure measurements on a supercritical wing during flutter and forced discrete frequency oscillations N89-19261
AIRFOIL PROFILES
Solution of steady and unsteady transonic-vortex flows using Euler and full-potential equations N89-19248
Viscous flow calculations for the AGARD standard configuration airfoils with experimental comparisons N89-19249
Unsteady Navier-Stokes computations over airfoils using both fixed and dynamic meshes N89-19252
AIRFOILS
A data analysis system for unsteady turbulence measurements
[AD-A201662] N89-19268
Experimental simulation of transonic vortex-airfoil interactions
[AD-A201934] N89-19274
A computationally efficient modelling of laminar separation bubbles
[NASA-CR-184789] N89-19504
AIRFRAMES
Estimating aircraft airframe tooling cost: An alternative to DAPCA 3
[AD-A201506] N89-19226
AIRGLOW
Ion and electron interactions at thermal and suprathermal energies
[AD-A201418] N89-19394
Infrared and ionization structure of the polar mesosphere
[AD-A201266] N89-19751
A study of the high altitude thermospheric dayglow from Spacelab 1 N89-19768
AIRLINE OPERATIONS
Simultaneous three-dimensional modeling of commercial flights within the airspace of the Federal Republic of Germany
[DFVLR-FB-88-31] N89-19282
AIRPORT LIGHTS
Airfield lighting: Future trends
[RAE-TM-FM-6] N89-19319
AIRSPACE
Minimum required heliport airspace under visual flight rules
[AD-A201433] N89-19283
ALGEBRA
FONR optical computing ST
[AD-A201002] N89-19897
ALGOL
From Algol 60 to Ada: Problems, solutions, feasibility
[REPT-88-41] N89-19919
ALGORITHMS
CAP-TSD: A program for unsteady transonic analysis of realistic aircraft configurations N89-19238
Flux-vector splitting for unsteady calculations on dynamic meshes N89-19244
Unsteady transonic flow using Euler equations N89-19245
A data analysis system for unsteady turbulence measurements
[AD-A201662] N89-19268
Robust control for linear systems with structured uncertainty
[AD-A201947] N89-19315
A variable-gain output feedback control design methodology
[NASA-CR-4226] N89-19316
A simplified procedure for decoding the (23,12) and (24,12) Golay codes N89-19456
DES cryptographic services designed for the DOE wide band communications network
[LA-10966-MS] N89-19484
The use of direct sparse matrix methods and Newton iteration for the numerical solution of fluid flows N89-19514
Laser transit anemometer software development program
[NASA-CR-4225] N89-19545
Multiprocessor control of robotic manipulators N89-19562
Minimum time motion of a robotic manipulator N89-19567
A preliminary study of precursors to Huntsville microbursts
[AD-A200914] N89-19782
Testing expert systems N89-19834
A method for modeling bias in a person's estimates of likelihoods of events N89-19849
Robot path planning using a genetic algorithm N89-19869
A novel manipulator technology for space applications N89-19874
A representational framework and user-interface for an image understanding workstation N89-19878
A 2-D and 3-D robot path planning algorithm based on quadtree and octree representation of workspace
[DE89-005014] N89-19900
Dynamic data structures for two-dimensional searching
[AD-A201173] N89-19901
Fast and processor-efficient parallel algorithms for reducible flow graphs
[AD-A201651] N89-19904
Bifurcating optimization algorithms and their possible application
[DE89-005692] N89-19906
Software performance on nonlinear least-squares problems
[AD-A201879] N89-19908
Analysis of blending algorithms in computer graphics
[AD-A201921] N89-19909
Computer-aided fabrication system implementation
[AD-A202128] N89-19911
A heuristic ceiling point algorithm for general integer linear programming
[AD-A202285] N89-19912
An exact ceiling point algorithm for general integer linear programming
[AD-A202286] N89-19913
The influence of the potential function on the performance of a trajectory following algorithm for the linear programming problem
[REPT-88-44] N89-19920
The Boltzmann machine: A survey and generalization
[AD-A197976] N89-19929
Applied partial differential equations and numerical analysis
[AD-A201749] N89-19939
Development of parallel algorithms for electrical power management in space applications N89-20063
Automatic voice recognition using traditional and artificial neural network approaches N89-20064
Toward an image compression algorithm for the high-resolution electronic still camera N89-20079
ALPINE METEOROLOGY
Microphysical, dynamical and chemical aspects of scavenging processes during winter precipitation N89-19695
ALTERNATING CURRENT
An electrochemical study of corrosion protection by primer-topcoat systems on 4130 steel with ac impedance and dc methods
[NASA-TP-2820] N89-19406
Comparison of an ac and a dc bridge for standard platinum resistance thermometer calibrations
[DE89-007060] N89-19534
ALTITUDE
Impact of target altitude restrictions on laser performance
[DE89-006567] N89-19553
Homogenizing surface and satellite observations of cloud
[AD-A201630] N89-19752
ALTITUDE SICKNESS
Dexamethasone for prevention and treatment of acute mountain sickness
[AD-A201554] N89-19799
ALUMINIDES
Reinforcement/matrix interaction in SiC fiber-reinforced Ni3Al matrix composites
[DE89-006041] N89-19384
ALUMINUM
Improvements in the properties of NbN layers through the presence of small amounts of aluminum during sputtering
[KFK-4409] N89-19418
ALUMINUM ALLOYS
Solidification, structure and mechanical properties of A357 aluminum alloy N89-19409
Processing of aluminum alloy 2090 for superplasticity
[AD-A201865] N89-19411
Analysis of PERSHING 2 Reentry Vehicle (RV) control ring castings
[AD-A201548] N89-19559
Fatigue crack growth in ARALL: A hybrid aluminum Aramid composite material. Crack growth mechanisms and quantitative predictions of the crack growth rates
[ETN-89-93899] N89-19602
ALUMINUM ARSENIDES
Ohmic contacts to gallium aluminum arsenide for high temperature applications
[AD-A202248] N89-19492
ALUMINUM COATINGS
Study of space aluminum coating, executive summary --- telescope mirrors
[IOM/CAEE-002/87(TR)] N89-19443
ALUMINUM GALLIUM ARSENIDES
Integration of detectors and optical waveguide structures
[AD-A201331] N89-19536
AMIDES
The determination of the mechanical behavior of polyamic acid/polyimide coatings N89-19428
AMINES
The dissociative adsorption of ammonia on Si(100)
[AD-A201599] N89-19396
The adsorption and decomposition of NH3 on Si(100): Detection of the NH2(a) species
[AD-A201601] N89-19397
AMMONIA
The dissociative adsorption of ammonia on Si(100)
[AD-A201599] N89-19396
The adsorption and decomposition of NH3 on Si(100): Detection of the NH2(a) species
[AD-A201601] N89-19397
AMORPHOUS MATERIALS
Pyrolytic and laser photolytic growth of crystalline and amorphous germanium films from digermane (GE2H6)
[DE89-006125] N89-20019
AMORPHOUS SILICON
Research on high-efficiency, multi-gap, multijunction, amorphous-silicon-based alloy thin-film solar cells, phase 1
[DE89-000844] N89-19739
AMPLIFICATION
A variable-gain output feedback control design methodology
[NASA-CR-4226] N89-19316
AMPLIFIER DESIGN
High output voltage multioctave broadband amplifier working between 50 kHz and 8 GHz
[HMI-B-451] N89-19497
ANALOG TO DIGITAL CONVERTERS
FONR optical computing ST
[AD-A201002] N89-19897
ANALYSIS OF VARIANCE
Performance evaluation of military engine and gear oils in friction and wear devices
[AD-A202145] N89-19432

Estimation of a restricted variance ratio
[AD-A202268] N89-19959

ANECHOIC CHAMBERS
Experimental spherical near-field antenna test facility, phase 3. Volume 1: Facility updates, evaluation and software documentation
[R-343] N89-19477

ANGLE OF ATTACK
Analytical interpretation on lateral/directional stability and controllability of high angle-of-attack reentry flight
[ISAS-630] N89-19353

ANGULAR ACCELERATION
Rotation and magnetic fields as an acceleration mechanism in astrophysical jets N89-20039

ANGULAR VELOCITY
On the variation of falling velocity of early snowflakes N89-19670
A vertical wind tunnel for the study of snowflakes and effects of accumulated snow on materials N89-19674

ANILINE
The aqueous electrochemistry of polyacetylene (CH)x and polyparaphenylene
[AD-A201461] N89-19426

ANIMALS
Brain mechanisms underlying individual differences in reaction to stress: An animal model
[AD-A201595] N89-19801

ANISOTROPY
Gas hydrates thermomechanics
[DE88-010260] N89-19387

ANOMALIES
Sliding and debonding inclusions
[AD-A201609] N89-19587
Autonomous satellite command and control: A comparison with other military systems N89-19839

ANTARCTIC REGIONS
Lidar for the determination of Antarctic water vapor profiles N89-19756

ANTENNA ARRAYS
Analysis and synthesis of microstrip antennas including mutual coupling
[AD-A201783] N89-19472

ANTENNA COMPONENTS
Analysis and synthesis of microstrip antennas including mutual coupling
[AD-A201783] N89-19472

ANTENNA COUPLERS
Microwave time delays for the dual L-C-band feed system N89-19462
Analysis and synthesis of microstrip antennas including mutual coupling
[AD-A201783] N89-19472

ANTENNA DESIGN
Meteosat Millimetre Wave Sounder (MWS) study
[BAE-TP-9119] N89-19363

ANTENNA FEEDS
Microwave time delays for the dual L-C-band feed system N89-19462
Analysis and synthesis of microstrip antennas including mutual coupling
[AD-A201783] N89-19472
Intrinsic hybrid modes in a corrugated conical horn
[ESA-CR(P)-2588] N89-19494

ANTENNA RADIATION PATTERNS
Systems analysis for DSN microwave antenna holography N89-19463
Experimental spherical near-field antenna test facility, phase 3. Volume 1: Facility updates, evaluation and software documentation
[R-343] N89-19477
A study of advanced radar altimeter techniques --- satellite altimetry
[ESA-CR(P)-2699] N89-19483
Intrinsic hybrid modes in a corrugated conical horn
[ESA-CR(P)-2588] N89-19494
Microwave holographic measurements of large reflectors: Phase 1 report, volume 1 --- spacecraft antennas
[REPT-B090] N89-19530

ANTENNAS
Concept of adaptive structures N89-19338

ANTHROPOMETRY
Computer software used in US Army Anthropometric Survey 1987-1988
[AD-A201185] N89-19812
The development and validation of an automated headboard device for measurement of three-dimensional coordinates of the head and face
[AD-A201186] N89-19813

ANTIGRAVITY
A stress test to evaluate the physical capacity of performing L-1 anti-G straining maneuvers
[AD-A202301] N89-19803

ANTIMATTER
The cosmic ray antiproton spectrum between 0.1 and 1.5 GeV kinetic energy N89-20057

ANTIMISSILE MISSILES
Survivability of space assets in the long term
[DE89-006563] N89-19964

ANTIPROTONS
The cosmic ray antiproton spectrum between 0.1 and 1.5 GeV kinetic energy N89-20057

ANTITANK MISSILES
Short-range anti-armour flight vehicles of the Apache/CWS family
[DRIC-T-8130] N89-19296

APERTURES
The electromagnetic modeling of thin apertures using the finite-difference time-domain technique
[NASA-CR-178280] N89-19780
Large wave number aperture limited Fourier inversion and inverse scattering
[AD-A202247] N89-19940

APPALACHIAN MOUNTAINS (NORTH AMERICA)
Cloud capture by a mountain top forest. Part 1: Acidity and dosage duration N89-19682

APPLICATIONS PROGRAMS (COMPUTERS)
Design improvement of a pump wear ring labyrinth seal
[NASA-CR-179161] N89-19555
Generalized three-dimensional experimental lightning code (G3DXL) user's manual
[NASA-CR-166079] N89-19779
The scheduling techniques of ESP2 N89-19818
Space station payload operations scheduling with ESP2 N89-19819
An expert system for shuttle and satellite radar tracker scheduling N89-19821
EMMA: The expert system for munition maintenance N89-19823
Diagnostics in the Extendable Integrated Support Environment (EISE) N89-19824
Automatic Detection of Electric Power Troubles (ADEPT) N89-19825
Knowledge-based operation and management of communications systems N89-19826
NESSUS (Numerical Evaluation of Stochastic Structures Under Stress)/EXPERT: Bridging the gap between artificial intelligence and FORTRAN N89-19827
Artificial intelligent decision support for low-cost launch vehicle integrated mission operations N89-19830
Diagnosis by integrating model-based reasoning with knowledge-based reasoning N89-19835
Transformation based endorsement systems N89-19836
Autonomous satellite command and control: A comparison with other military systems N89-19839
Garbage collection can be made real-time and verifiable N89-19840
Portable inference engine: An extended CLIPS for real-time production systems N89-19843
Browsing schematics: Query-filtered graphs with context nodes N89-19844
An intelligent interface for satellite operations: Your Orbit Determination Assistant (YODA) N89-19852
Intelligent tutoring systems research in the training systems division: Space applications N89-19854
Intelligent tutoring in the spacecraft command/control environment N89-19855
Optimal solutions for complex design problems: Using isoperformance software for human factors trade offs N89-19860
A novel manipulator technology for space applications N89-19874
A robust control scheme for flexible arms with friction in the joints N89-19875
Telerobot operator control station requirements N89-19876
A representational framework and user-interface for an image understanding workstation N89-19878
Machine vision for space telerobotics and planetary rovers N89-19879

APPROACH CONTROL
A systems approach to rotorcraft stability and control research
[AD-A201784] N89-19314
Airfield lighting: Future trends
[RAE-TM-FM-6] N89-19319

AQUEOUS SOLUTIONS
Crystallization of supercooled solutions --- atmosphere N89-19664
Kinetics and mechanism of the Fe catalyzed autoxidation of S(4)-oxides in aqueous solution N89-19687

ARC JET ENGINES
MPD (Magnetoplasmadynamic) thrust chamber flow dynamics
[AD-A201263] N89-19368
The 30 kWe class high efficiency arcjet power conditioner, volume 1
[AD-A202244] N89-20004
National Aeronautics and Space Administration (NASA)/American Society for Engineering Education (ASEE) Summer Faculty Fellowship Program 1988, volume 2 --- Author
[NASA-CR-172118-VOL-2] N89-20073
Arc jet diagnostics tests N89-20085

ARC MELTING
Microstructural analyses of intermetallic TiAl (Nb)-compounds prepared by arc melting and by powder metallurgy
[GKSS-88/E/32] N89-19417

ARCHITECTURE (COMPUTERS)
A new VLSI architecture for a single-chip-type Reed-Solomon decoder N89-19455
Test aspects of the JPL Viterbi decoder N89-19457
Crossbar switch backplane and its application
[DE89-005621] N89-19491
A design and implementation methodology for diagnostic systems N89-19831
Spaceborne VHSIC multiprocessor system for AI applications N89-19838
An architecture for integrating distributed and cooperating knowledge-based Air Force decision aids N89-19841
A parallel expert system for the control of a robotic air vehicle N89-19842
Portable inference engine: An extended CLIPS for real-time production systems N89-19843
Scheme86: An architecture for microcoding a scheme interpreter
[AD-A201258] N89-19893
Critical problems in very large scale computer systems
[AD-A202129] N89-19923
Production system chunking in SOAR: Case studies in automated learning N89-20060

ARGON
Liquid excimers: Lasing Xe2 and Kr2 in liquid argon
[DE89-005449] N89-19546

ARID LANDS
The collection efficiency of a massive fog collector N89-19650

ARRAYS
Static and dynamic properties of arrays of superconductors N89-20017

ARTIFICIAL INTELLIGENCE
A survey of planning and scheduling research at the NASA Ames Research Center N89-19820
NESSUS (Numerical Evaluation of Stochastic Structures Under Stress)/EXPERT: Bridging the gap between artificial intelligence and FORTRAN N89-19827
Application of flight systems methodologies to the validation of knowledge-based systems N89-19832
Spaceborne VHSIC multiprocessor system for AI applications N89-19838
A parallel expert system for the control of a robotic air vehicle N89-19842
CAD-model-based vision for space applications N89-19867
Time-delayed operation of a telerobot via geosynchronous relay N89-19877
Development of a personal-computer-based intelligent tutoring system N89-19889
JPRS report: Science and technology. Japan: 7th Artificial Intelligence Symposium
[JPRS-JST-88-020] N89-19924
Recognition of object domain by color distribution N89-19926
The Boltzmann machine: A survey and generalization
[AD-A197976] N89-19929
Estimating the illuminant color from the shading of a smooth surface
[AD-A201333] N89-19983
Production system chunking in SOAR: Case studies in automated learning N89-20060

ARTIFICIAL SATELLITES
Halogen Occultation Experiment (HALOE) optical filter characterization
[NASA-TM-4104] N89-19529
Survivability of space assets in the long term
[DE89-006563] N89-19964
Estimation of velocity perturbations in satellite fragmentation events N89-20083

ASSOCIATIVE PROCESSING (COMPUTERS)
The Boltzmann machine: A survey and generalization
[AD-A197976] N89-19929

ASTEROIDS
An infrared reflectance study of water in outer belt asteroids N89-20037

ASTRIONICS
JPRS report: Science and technology. USSR: Electronics and electrical engineering
[JPRS-UEE-88-005] N89-19485

ASTROMETRY
On the great circle reduction in the data analysis for the astrometric satellite HIPPARCOS
[ETN-89-93902] N89-20038

ASTRONAUT PERFORMANCE
Simulation of the human-telerobot interface N89-19861
Man-systems requirements for the control of teleoperators in space N89-19862
ASTRONAUTS
Comparison of Soviet and US space food and nutrition programs N89-20059
ASTROPHYSICS
Thermonuclear reactions of light nuclei in astrophysical plasmas N89-19988
ASYMPTOTIC METHODS
Robust bounded influence tests in linear models [AD-A201896] N89-19957
ASYMPTOTIC PROPERTIES
Normal forms and periodic solutions in the theory of nonlinear oscillations. Existence and asymptotic theory [REPT-88-16] N89-19948
ASYMPTOTIC SERIES
An asymptotic theory for weighted least squares with weights estimated by replication [AD-A198000] N89-19935
Large wave number aperture limited Fourier inversion and inverse scattering [AD-A202247] N89-19940
Large deviation local limit theorems for ratio statistics [AD-A201169] N89-19954
Estimation in large samples [AD-A201459] N89-19956
ATLANTIC OCEAN
Compressional-wave velocities in ocean sediments east southesast of Madeira, Atlantic Ocean [IOS-257] N89-19794
ATLAS CENTAUR LAUNCH VEHICLE
The Atlas/Centaur 67 launch mishap [GPO-80-201] N89-19332
ATMOSPHERIC BOUNDARY LAYER
Large-eddy simulation of convective boundary layers [DFVLR-FB-88-30] N89-19522
Boundary layer development over the eastern Pacific Ocean N89-19753
A critical evaluation of the von Karman constant from a new atmospheric surface layer experiment N89-19757
ATMOSPHERIC CHEMISTRY
Annals from the German Meteorological Society. No. 25: 10th International Cloud Physics Conference Preprints, volume 1 [ISBN-3-88-148240-7] N89-19605
On the determination of droplet size distributions with the counterflow virtual impactor --- cloud physics N89-19655
Kinetic equation for polluted cloud droplets spectrum N89-19661
Crystallization of supercooled solutions --- atmosphere N89-19664
Cloud capture by a mountain top forest. Part 1: Acidity and dosage duration N89-19682
Determination of chemical reaction rates in fog N89-19683
Insoluble particles in hydrometeors N89-19684
Below cloud scavenging by rain and drizzle N89-19685
Studies of cloud micro-chemical physics N89-19686
Kinetics and mechanism of the Fe catalyzed autoxidation of S(4)-oxides in aqueous solution N89-19687
The effect of aerosols on pH of snowfalls N89-19688
A one-dimensional numerical model to simulate liquid phase chemical reactions within radiation fog N89-19690
The effect of freezing on the composition of cloud droplets N89-19691
Some effects of cloud microphysics on cloud chemistry N89-19692
Processes determining cloudwater composition: Field evidence for in-cloud reactive scavenging of SO2 N89-19693
Acidification of stratiform clouds and their aerosol scavenging properties N89-19694
Microphysical, dynamical and chemical aspects of scavenging processes during winter precipitation N89-19695
Results of time and height resolved scavenging experiments --- atmospheric chemistry N89-19697
Oxidation regimes in orographic capping cloud N89-19698
An examination of the chemical and physical variability of clouds at a mountain-top site in central Sweden N89-19699
Influences of cloud microphysics on continental and marine precipitation chemistry N89-19700
Experiments on microphysics and chemistry of radiation fogs N89-19702
Chemical evolution within in a cloud model featuring a polydisperse droplet size spectrum N89-19703
A numerical investigation of sulfate production and deposition in midlatitude continental cumulus clouds N89-19705
A numerical simulation of the acidification process of rain water below the cloud and the mechanism of acid rain formation in area of Chongqing, China N89-19706
Dynamic, radiative and chemical effects of clouds on tropospheric trace gases N89-19708
Parameterizations of microphysical processes in clouds for application in models of regional atmospheric deposition N89-19709
Meteorological and chemical influencing factors on acidity production in a mesoscale model with quasi-spectral microphysics N89-19711
ATMOSPHERIC CIRCULATION
An investigation of the intermittent turbulent breakdown of the nocturnal planetary boundary layer [AD-A201743] N89-19518
Large-eddy simulation of convective boundary layers [DFVLR-FB-88-30] N89-19522
A collection of severe weather parameters used for a checklist [CRARP-88-3] N89-19774
Temperature and circulation in the stratospheres of the outer planets [NASA-CR-184826] N89-20051
ATMOSPHERIC COMPOSITION
Cloud capture by a mountain top forest. Part 1: Acidity and dosage duration N89-19682
A numerical investigation of sulfate production and deposition in midlatitude continental cumulus clouds N89-19705
A numerical simulation of the acidification process of rain water below the cloud and the mechanism of acid rain formation in area of Chongqing, China N89-19706
Effects of cloud microphysical processes on trace chemical removal efficiences N89-19707
Dynamic, radiative and chemical effects of clouds on tropospheric trace gases N89-19708
Parameterizations of microphysical processes in clouds for application in models of regional atmospheric deposition N89-19709
A model of wet deposition to complex terrain by the seeder-feeder process N89-19710
Meteorological and chemical influencing factors on acidity production in a mesoscale model with quasi-spectral microphysics N89-19711
A comparison of radiometric and immersion temperature measurements in water clouds N89-19712
A poor man's optical fog detector N89-19716
Applications of the NCAR Electra Doppler radar for the study of physical parameters of clouds N89-19717
A numerical investigation of an orographic precipitation event N89-19721
Lidar for the determination of Antarctic water vapor profiles N89-19756
A study of the high altitude thermospheric dayglow from Spacelab 1 N89-19768
Stratospheric nitric acid: Feasibility of routine measurement by observation from commercial airliners in IR bands from 9 to 14 microns [C-48-1977] N89-19770
ATMOSPHERIC ELECTRICITY
Measurement of atmospheric electrical fields in periods of electrical perturbation and calm at the latitude of 23 C [INPE-4626-PRE/1344] N89-19750
A wide bandwidth electrostatic field sensor for lightning research [NASA-TM-101539] N89-19783
ATMOSPHERIC LASERS
Development of a detection system for atmospheric trace gases, in particular for OH molecules and realization of field measurements [BPT-11/88] N89-19767
ATMOSPHERIC MODELS
Large-eddy simulation of convective boundary layers [DFVLR-FB-88-30] N89-19522
Empirical equations of ice crystal growth microphysics for modeling and analysis N89-19609
The contrast study of new model on ice crystal growth N89-19610
A comparative study of laboratory thermals and atmospheric clouds N89-19627
The case for subgrid-scale condensation in numerical cloud models N89-19636
The effect of turbulence on the collection of cloud drops: A stochastic model N89-19637
A comparative study of two microphysical schemes in a beta mesoscale model N89-19640
Generalized microphysics scheme for use in mesoscale/cloud models N89-19641
The study of numerical simulation on the formation of the cloud droplet spectra in cumulus clouds N89-19642
Theory on the uncertainty in cloud microphysical processes and climate N89-19644
Radiative influences on precipitating mesoscale systems N89-19648
Comparison of model results for models of differing microphysical detail --- hailstorms N89-19680
Concentrations in rain events collected sequentially: Measurements vs results of a simple scavenging model N89-19701
Chemical evolution within in a cloud model featuring a polydisperse droplet size spectrum N89-19703
Modeling studies on the formation, growth, dissipation and acidification of cumulus clouds N89-19704
Parameterizations of microphysical processes in clouds for application in models of regional atmospheric deposition N89-19709
A model of wet deposition to complex terrain by the seeder-feeder process N89-19710
A numerical investigation of an orographic precipitation event N89-19721
Comparison of orographic cloud and precipitation development of three different geographic locations using a 3-D nested grid cloud model N89-19723
Use of cluster analysis to define periods of similar meteorology and precipitation chemistry in eastern North America N89-19785
Temperature and circulation in the stratospheres of the outer planets [NASA-CR-184826] N89-20051
ATMOSPHERIC MOISTURE
On the observations of cloud temperature and liquid water content using a Lyman-alpha and an FSSP sensor --- forward scattering spectrometer probe (FSSP) N89-19618
An examination of the chemical and physical variability of clouds at a mountain-top site in central Sweden N89-19699
Intercomparisons of aircraft measurements with lidar returns for aerosol, ice crystals and water droplets N89-19718
Semi-prognostic tests of cumulus parameterization schemes in the middle latitudes N89-19786
ATMOSPHERIC OPTICS
Cloud and aerosol optical depths N89-19646
ATMOSPHERIC PHYSICS
Influences of cloud microphysics on continental and marine precipitation chemistry N89-19700
On the small scale topographical influences on precipitation N89-19720
Comparison of orographic cloud and precipitation development of three different geographic locations using a 3-D nested grid cloud model N89-19723
Microphysical and dynamical interactions in Colorado front range upslope storms N89-19725
A new dropsonde for cloud probings N89-19728
ATMOSPHERIC RADIATION
Radiative influences on precipitating mesoscale systems N89-19648
Cirrus microphysics and infrared radiative transfer: A case study N89-19649
ATMOSPHERIC REFRACTION
Refractive turbulence profiling via binary source intensity scintillation correlation [AD-A202189] N89-19762
ATMOSPHERIC SCATTERING
Propagation problems regarding 20/30 GHz bands in Earth-space links [REPT-88-022] N89-19480
Propagation problems regarding millimeter waves (40/50 GHz) [REPT-88-023] N89-19481
Some outstanding problems on the influence of clouds on radiation N89-19643
ATMOSPHERIC SOUNDING
Electronic Power Conditioner (EPC) for carcinotrons [R/D/REPO/8801] N89-19496
Measurement of atmospheric electrical fields in periods of electrical perturbation and calm at the latitude of 23 C [INPE-4626-PRE/1344] N89-19750
Development of a detection system for atmospheric trace gases, in particular for OH molecules and realization of field measurements [BPT-11/88] N89-19767
ATMOSPHERIC STRATIFICATION
Airborne studies of the influence of entrainment on the vertical and horizontal microphysical structure of small cumulus clouds N89-19629
ATMOSPHERIC TEMPERATURE
A comparison of radiometric and immersion temperature measurements in water clouds N89-19712
A high-spectral-resolution lidar system: The use of atomic blocking filter for measuring atmospheric parameters [AD-A201736] N89-19759
Technical report on temperature, precipitation and aviation verification at WSFO Sioux Falls for 1987 [CRARP-88-5] N89-19776

Semi-prognostic tests of cumulus parameterization schemes in the middle latitudes N89-19786
Temperature and circulation in the stratospheres of the outer planets
[NASA-CR-184826] N89-20051

ATMOSPHERIC TURBULENCE
An investigation of the intermittent turbulent breakdown of the nocturnal planetary boundary layer
[AD-A201743] N89-19518
Turbulent transport processes within and below small cumulus clouds N89-19632

ATOMIC BEAMS
Gaussian beam representation of beam-like ultrasonic fields N89-19972
High-precision laser and RF spectroscopy of atomic, molecular, and slow ion beams
[DE89-005870] N89-19975

ATOMIC ENERGY LEVELS
Proof of the feasibility of coherent and incoherent schemes for pumping a gamma-ray laser
[AD-A201931] N89-19542

ATOMIC MOBILITIES
An investigation of factors affecting domestic technology transfer at the Wright Aeronautical Laboratories
[AD-A201581] N89-20032

ATOMIC RECOMBINATION
Arc jet diagnostics tests N89-20085

ATOMIC STRUCTURE
Kinetic processes in discharge pumped mercury halide lasers
[AD-A201612] N89-19537
Atomic structure of tilt grain boundaries in NiO
[DE89-005847] N89-20013

ATTENTION
A schema-based model of situation awareness: Implications for measuring situation awareness N89-19847

ATTITUDE CONTROL
SCD2 satellite spin axis reorientation and feasibility study
[INPE-4688-NTE/285] N89-19351
Control of flexible structures: Model errors, robustness measures, and optimization of feedback controllers
[AD-A202234] N89-19596

AUGER SPECTROSCOPY
The adsorption and decomposition of NH3 on Si(100): Detection of the NH2(a) species
[AD-A201601] N89-19397
Formation of titanium nitride layers on titanium metal: Results of XPS and AES investigations
[KFK-4449] N89-19419
XPS and AES studies of thin oxide layers on niobium for superconducting RF cavities
[DE88-756073] N89-19997

AUGMENTATION
An experimental investigation of sooting characteristics of a gas turbine combustor and augmentor tube
[AD-A201804] N89-19568
Brain mechanisms underlying individual differences in reaction to stress: An animal model
[AD-A201595] N89-19801

AURORAL ARCS
Electrostatic plasma waves and turbulence near auroral arcs N89-19758

AURORAL IONIZATION
Study of the continuous/diffuse aurora using particle observations from the Dynamics Explorer satellites
[AD-A202241] N89-19763

AURORAS
Modeling the energy deposition in the Aurora KrF laser amplifier chain
[DE89-006545] N89-19550
Characteristics of optical emissions and particle precipitation in mid/low latitude aurorae N89-19755
Study of the continuous/diffuse aurora using particle observations from the Dynamics Explorer satellites
[AD-A202241] N89-19763

AUSTENITIC STAINLESS STEELS
Effect of temperature on the corrosion resistance of nitrogen bearing AL6X and 904L stainless steels
[AD-A201955] N89-19412

AUTOCORRELATION
A data analysis system for unsteady turbulence measurements
[AD-A201662] N89-19268

AUTOMATA THEORY
Intelligent mobile robot working in unknown environment N89-19927

AUTOMATIC CONTROL
Automation of the space station core module power management and distribution system N89-19822
Knowledge-based operation and management of communications systems N89-19826
CIRCA 2000 operations criteria N89-19829
Autonomous satellite command and control: A comparison with other military systems N89-19839
An architecture for integrating distributed and cooperating knowledge-based Air Force decision aids N89-19841
Physiological assessment of task underload N89-19846
A robust control scheme for flexible arms with friction in the joints N89-19875

AUTOMATIC TEST EQUIPMENT
EMMA: The expert system for munition maintenance N89-19823
CIRCA 2000 operations criteria N89-19829

AUTONOMOUS NAVIGATION
CIRCA 2000 operations criteria N89-19829

AUTOREGRESSIVE PROCESSES
Minification processes
[AD-A202219] N89-19958

AVALANCHE DIODES
Determination of general and specific properties of wide energy-band gap HgCdTe in the 1 to 2 micrometer wavelength range
[AD-A201341] N89-19488

AVIONICS
Joint University Program for Air Transportation Research, 1987
[NASA-CP-3028] N89-19230
CIRCA 2000 operations criteria N89-19829
A schema-based model of situation awareness: Implications for measuring situation awareness N89-19847

AXIAL COMPRESSION LOADS
Compression strength of composite primary structural components
[NASA-CR-184893] N89-19599

AXIAL LOADS
Plastic buckling of cylinders under biaxial loading N89-19591

B

BACKSCATTERING
Research in acoustical scattering, diffraction catastrophes, optics of bubbles and acoustical phase conjugation
[AD-A201451] N89-19968
Raman and RBS studies of ion implanted semiconductors
[ATR-88(8359)-5] N89-20021

BACKWARD FACING STEPS
Computational study of incompressible turbulent flow over a swept rearward-facing step N89-19272
The analytical modeling of a turbulent diffusion flame behind a backward facing step N89-19386

BALLISTICS
Simulation of conical graupel by using a ballistic model N89-19679

BALLOON-BORNE INSTRUMENTS
Measurement of atmospheric electrical fields in periods of electrical perturbation and calm at the latitude of 23 C
[INPE-4626-PRE/1344] N89-19750
The cosmic ray antiproton spectrum between 0.1 and 1.5 GeV kinetic energy N89-20057

BANACH SPACE
Approximation, saturation and semigroups of operators in Banach space
[REPT-88-19] N89-19950

BANDPASS FILTERS
On sampling band-pass signals N89-19453

BARIUM OXIDES
Radiation induced amorphization in YBa2Cu3O7 and GdBa2Cu3O7 superconductors
[DE89-005451] N89-20008

BASALT
Evaluation of crustal recycling during the evolution of Archean-age Matachewan basaltic magmas N89-20077

BAYES THEOREM
An interrogative model of computer-aided adaptive testing: Some experimental evidence
[AD-A201675] N89-19905
Estimation of a restricted variance ratio
[AD-A202268] N89-19959

BEAM INTERACTIONS
Gaussian beam representation of beam-like ultrasonic fields N89-19972

BEAMS (RADIATION)
An investigation of the relationship between beam and global irradiation with the development of numerical solar radiation models N89-19748
High-order beam optics: An overview
[DE89-005441] N89-19984

BEAMS (SUPPORTS)
Comments on electromechanical actuators for controlling flexible structures N89-19339
Mixed finite element models for free vibrations of thin-walled beams
[NASA-TP-2868] N89-19579

BEARING (DIRECTION)
Directional wave data recorded in the southern North Sea
[IOS-258] N89-19793

BEHAVIOR
Model-based reasoning: Troubleshooting
[AD-A201614] N89-19445

BIAS
An analysis of the impact of log-linear regression on the estimated learning curve parameters
[AD-A201471] N89-19938

BIBLIOGRAPHIES
An annotated bibliography of hypobaric decompression sickness research conducted at the Crew Technology Division, USAF School of Aerospace Medicine, Brooks AFB, Texas from 1983 to 1988
[AD-A201274] N89-19796

BINARY DATA
CAD-model-based vision for space applications N89-19867

BINOCULAR VISION
Extracting depth by binocular stereo in a robot vision system
[DE89-005016] N89-19572

BIOLOGICAL EFFECTS
Biological applications and effects of optical masers
[AD-A201834] N89-19541

BIOPHYSICS
Computation of stereo and visual motion: From biophysics to psychophysics
[AD-A201873] N89-19802

BIPOLAR TRANSISTORS
Development of Si/SiGe heterostructures
[AD-A201440] N89-20001

BISMALEIMIDE
Durability and damage tolerance of bismaleimide composites, volume 1
[AD-A201273] N89-19374
Durability and damage tolerance of bismaleimide composites. Volume 2: Appendix of crack growth and low-velocity impact data
[AD-A201839] N89-19379

BISTATIC REFLECTIVITY
Development of a system for acoustic measurements of bistatic target strengths
[AD-A201673] N89-19970

BL LACERTAE OBJECTS
VLBI polarization measurements of BL Lacertae objects N89-20035

BLADE-VORTEX INTERACTION
Experimental simulation of transonic vortex-airfoil interactions
[AD-A201934] N89-19274

BLOCK DIAGRAMS
Block diagrams of the radar interface and control unit N89-19460

BLOCKING
A high-spectral-resolution lidar system: The use of atomic blocking filter for measuring atmospheric parameters
[AD-A201736] N89-19759

BLOOD
Maladjustment of kidneys to microgravity: Design of measures to reduce the loss of calcium N89-20076

BLOOD PLASMA
A model for plasma volume changes during short duration spaceflight N89-20067

BODIES OF REVOLUTION
Drag measurements on a laminar-flow body of revolution in the 13-inch magnetic suspension and balance system
[NASA-TP-2895] N89-19232

BODY-WING AND TAIL CONFIGURATIONS
Multiple Application Propfan Study (MAPS): Advanced tactical transport
[NASA-CR-175003] N89-19300

BONDING
Sliding and debonding inclusions
[AD-A201609] N89-19587

BONE DEMINERALIZATION
Maladjustment of kidneys to microgravity: Design of measures to reduce the loss of calcium N89-20076

BONES
Maladjustment of kidneys to microgravity: Design of measures to reduce the loss of calcium N89-20076

BOOSTER ROCKET ENGINES
Booster propulsion/vehicle impact study
[NASA-CR-183584] N89-19366

BOREDOM
Physiological assessment of task underload N89-19846

BORN-INFELD THEORY
Born-Infeld equations and minimal surfaces
[DE88-704966] N89-19936

BORON
NRL boron propellants combustion program
[AD-A201242] N89-19440

BORON HYDRIDES
Reaction chemistry of boron hydrides
[AD-A201243] N89-19389
BORON OXIDES
Reaction chemistry of boron hydrides
[AD-A201243] N89-19389
BOUNDARY ELEMENT METHOD
The boundary element method for the diffusion equation N89-19233
BOUNDARY INTEGRAL METHOD
On boundary integral equation approach to a nonstationary problem of isothermal viscous compressible flows
[PREPRINT-1134] N89-19526
BOUNDARY LAYER CONTROL
The NASA Langley laminar-flow-control experiment on a swept, supercritical airfoil - Drag equations
[NASA-TM-4096] N89-19231
BOUNDARY LAYER EQUATIONS
Unsteady transonic viscous-inviscid interaction using Euler and boundary-layer equations N89-19250
The birth of open separation on a prolate spheroid
[AD-A201350] N89-19509
BOUNDARY LAYER FLOW
Some hydrodynamic instabilities of boundary layer flows N89-19501
Error norm guided flow analysis of shock-wave/boundary-layer interactions
[AD-A201176] N89-19507
The birth of open separation on a prolate spheroid
[AD-A201350] N89-19509
BOUNDARY LAYER SEPARATION
The role of shock induced trailing-edge separation in limit cycle oscillations N89-19256
BOUNDARY LAYER STABILITY
Some hydrodynamic instabilities of boundary layer flows N89-19501
The stability of boundary layer flow over elastic substrates N89-19524
BOUNDARY LAYER TRANSITION
Flight survey of the 757 wing noise field and its effects on laminar boundary layer transition. Volume 2: Data compilation
[NASA-CR-178217] N89-19505
BOUNDARY LAYERS
A data analysis system for unsteady turbulence measurements
[AD-A201662] N89-19268
BOUNDARY VALUE PROBLEMS
A fundamental mathematical theory in the dynamics of combustion processes
[AD-A201284] N89-19391
On boundary integral equation approach to a nonstationary problem of isothermal viscous compressible flows
[PREPRINT-1134] N89-19526
Further results on the design of multivariable regulators under structure and robustness constraints. Part 1: The initialization problem
[REPT-88-028] N89-19931
Cell-centered and vertex-centered discretization of interface problems
[REPT-88-18] N89-19949
BRAIN
Brain activity during tactical decision-making. Part 4: Event-related potentials as indices of selective attention and cognitive workload
[AD-A201370] N89-19797
Brain mechanisms underlying individual differences in reaction to stress: An animal model
[AD-A201595] N89-19801
BRANCHING (MATHEMATICS)
Bifurcating optimization algorithms and their possible application
[DE89-005692] N89-19906
BRIGHTNESS
Ultrahigh-brightness XeCl laser system
[DE89-005467] N89-19548
Beam profile effects on NPB performance
[LA-11228-MS] N89-19980
BRIGHTNESS DISTRIBUTION
Ultracompact HII regions associated with massive star formation N89-20044
BROADBAND AMPLIFIERS
High output voltage multioctave broadband amplifier working between 50 kHz and 8 GHz
[HMI-B-451] N89-19497
BROADCASTING
On the design of loudspeakers for broadcast monitoring
[BBC-RD-1988/14] N89-19450
BROKEN SYMMETRY
Studies in quantum field theory
[DE89-006286] N89-20023
BUBBLES
A computationally efficient modelling of laminar separation bubbles
[NASA-CR-184789] N89-19504
Modeling of inertial effects in transient liquid-bubble flows
[REPT-88-22] N89-19528
Pattern of air bubble inclusions in atmospheric ice formed during accretion N89-19676
BUCKLING
Plastic buckling of cylinders under biaxial loading N89-19591
Compression strength of composite primary structural components
[NASA-CR-184893] N89-19599
Lithospheric buckling and intra-arc stresses: A mechanism for arc segmentation N89-20078
BUDGETING
Multicriteria analysis and budget allocation, with applications in energy R and D planning: A feasibility study
[REPT-88-07] N89-20026
BURNERS
Spectral studies of propellant combustion: Experimental details and emission results for M-30 propellant
[AD-A201634] N89-19399
BURSTS
The use of burst-triggered correlation for laser anemometry measurements in turbomachinery
[PNR90542] N89-19533
BYPASS RATIO
Propulsion
[PNR90472] N89-19302

C

C (PROGRAMMING LANGUAGE)
Development of a personal-computer-based intelligent tutoring system N89-19889
C BAND
Microwave time delays for the dual L-C-band feed system N89-19462
Multiparameter Doppler radar observations of a squall line with the polarimetric DFVLR radar N89-19715
C-160 AIRCRAFT
Lightning campaign 85/86 Transall C160 A04: Flying tests
[REPT-85/535800] N89-19297
CABIN ATMOSPHERES
Chemical warfare protection for the cockpit of future aircraft N89-19859
CALCIUM
Maladjustment of kidneys to microgravity: Design of measures to reduce the loss of calcium N89-20076
CALDERAS
Lithospheric buckling and intra-arc stresses: A mechanism for arc segmentation N89-20078
CALENDARS
Calendar of selected aeronautical and space meetings: January 1989 onwards
[AGARD-CAL-89/1] N89-20024
CALIBRATING
RF performance measurement of the DSS-14 70-meter antenna at C-band/L-band N89-19461
Comparison of an ac and a dc bridge for standard platinum resistance thermometer calibrations
[DE89-007060] N89-19534
MODIS information, data and control system (MIDACS) operations concepts
[NASA-TM-100720] N89-19729
CALIFORNIA
Local geoid determination using the global positioning system
[AD-A202220] N89-19731
CAMERAS
High-speed laser photography
[AD-A202293] N89-19544
Toward an image compression algorithm for the high-resolution electronic still camera N89-20079
CAPACITANCE
Investigation of the interface between two immiscible electrolytes applied to membrane electrochemistry
[AD-A201310] N89-19393
CARBON
Characterization of IM7/8551-7 carbon/epoxy in compression and shear
[DE89-005544] N89-19378
CARBON FIBER REINFORCED PLASTICS
Thermal cycling and mechanical property assessment of carbon fiber (fabric) reinforced PMR-15 polyimide laminates
[PNR90522] N89-19382
CARBONATES
Oxygen electrode in molten carbonate fuel cells
[DE89-005813] N89-19745
CARCINOTRONS
Electronic Power Conditioner (EPC) for carcinotrons
[R/D/REPO/8801] N89-19496
CARDIOVASCULAR SYSTEM
A model for plasma volume changes during short duration spaceflight N89-20067
CARRIER FREQUENCIES
Chaotic electron motion caused by sidebands in free electron lasers
[AD-A201635] N89-19538
CASE HISTORIES
A case study of significant lake enhanced snow event in upper Michigan
[CRARP-88-2] N89-19773
Use of long-waves in forecasting
[CRARP-88-7] N89-19778
Knowledge acquisition for case-based reasoning systems N89-19856
CASTINGS
Electron beam welding of 6061-T6 covers to A356-T6 machined cast housings
[BDX-613-3915] N89-19573
CATALYSIS
Vibrational spectroscopic studies of surface chemical interactions in chemisorption and catalysis
[DE89-005896] N89-19400
Improvements in the properties of NbN layers through the presence of small amounts of aluminum during sputtering
[KFK-4409] N89-19418
Kinetics and mechanism of the Fe catalyzed autoxidation of S(4)-oxides in aqueous solution N89-19687
CATARACTS
Biological applications and effects of optical masers
[AD-A201834] N89-19541
CATS
Brain mechanisms underlying individual differences in reaction to stress: An animal model
[AD-A201595] N89-19801
CAVITATION FLOW
Tip vortices: Single phase and cavitating flow phenomena N89-19271
An examination of cavitation due to short pulses of megahertz ultrasound N89-19971
CAVITIES
XPS and AES studies of thin oxide layers on niobium for superconducting RF cavities
[DE88-756073] N89-19997
CAVITY RESONATORS
Acoustic wave propagation in heterogeneous structures including experimental validation
[NASA-TM-101486] N89-19965
CEILINGS (METEOROLOGY)
Structure of upper clouds boundary using the lidar data N89-19631
The study of numerical simulation on the formation of the cloud droplet spectra in cumulus clouds N89-19642
CENTRIFUGAL COMPRESSORS
The effect of prewhirl on the internal aerodynamics and performance of a mixed flow research centrifugal compressor
[NASA-CR-184756] N89-19503
CERAMICS
Improved silicon nitride for advanced heat engines
[NASA-CR-179525] N89-19421
The mechanical behavior of surface modified ceramics
[DE89-004764] N89-19422
Composite ceramic superconducting wires for electric motor applications
[AD-A201810] N89-19429
Adhesion in ceramics and magnetic media
[NASA-TM-101476] N89-19435
Some novel test methods for, and associated problems of mechanical strength characterization of engineering ceramics
[PNR90492] N89-19436
Grain boundary nonstoichiometry in multicomponent ceramics
[DE89-006109] N89-19437
Development of Nuclear Magnetic Resonance (NMR) imaging technology for advanced ceramics
[DE89-006400] N89-19438
CHAINS
On purely exponential logic queries
[AD-A201259] N89-19902
CHANNEL FLOW
The development and structural characteristics of Dean vortices in a curved rectangular channel
[AD-A201249] N89-19508
Turbulence structure and mass transport in a channel flow with polymer injection
[AD-A202237] N89-19521
CHANNELS (DATA TRANSMISSION)
Bitbus data transmission with galvanic separations
[DIGEL-78] N89-19898

CHARACTERISTICS
The divergence characteristics of constrained-sheath optics systems for use with 5-eV atomic oxygen sources
[NASA-CR-182238] N89-19973
CHARACTERIZATION
Characterizations of conditional expectation-type operators
[REPT-88-04] N89-19942
CHARGE COUPLED DEVICES
Evaluation of Schottky barrier and PBTE IR-CCD detectors for the SWIR and MIR wavelengths range, executive summary
[IMEC-SP/CCD-255/88-03] N89-19495
CHARGE TRANSFER
High current, high Coulomb ignitrons
[DE89-005547] N89-19490
CHARGED PARTICLES
Chaotic electron motion caused by sidebands in free electron lasers
[AD-A201635] N89-19538
The scintillating optical fiber isotope experiment (SOFIE): Bevalac calibrations of test models N89-20034
CHECKOUT
Study on checkout of flight units and subsystems --- ground support
[ESA-CR(P)-2693] N89-19816
CHEMICAL ANALYSIS
Laser scattering studies of epoxy polymerization processes
[AD-A201925] N89-19430
Analysis of PERSHING 2 Reentry Vehicle (RV) control ring castings
[AD-A201548] N89-19559
Positron spectroscopy for materials characterization
[DE89-005766] N89-20010
Arc jet diagnostics tests N89-20085
CHEMICAL BONDS
The adsorption and decomposition of NH3 on Si(100): Detection of the NH2(a) species
[AD-A201601] N89-19397
Studies of hydrogen-hydrogen and carbon-sulfur bond cleavage
[DE89-006116] N89-19403
Studies of 3-5 compounds in the megabar regime:
[DE89-005722] N89-20009
CHEMICAL COMPOSITION
Interactions and reactions in polymerized vesicles
[AD-A201527] N89-19427
Insoluble particles in hydrometeors N89-19684
Ionic concentrations of rime ice and snow and Bergeron process N89-19689
The effect of freezing on the composition of cloud droplets N89-19691
Evaluation of optical materials samples
[AD-A199471] N89-19981
Thermal oxidation of 3-5 compound semiconductors
[DE89-007127] N89-20020
An infrared reflectance study of water in outer belt asteroids N89-20037
Solar and interplanetary cosmic ray composition
[MPE-PREPRINT-108] N89-20056
CHEMICAL ENERGY
Ion and electron interactions at thermal and suprathermal energies
[AD-A201418] N89-19394
CHEMICAL LASERS
The standard chemical oxygen-iodine laser kinetics package
[AD-A202223] N89-19543
CHEMICAL REACTION CONTROL
Acidic attack of perfluorinated alkyl ether lubricant molecules by metal oxide surfaces
[NASA-TM-101962] N89-19402
CHEMICAL REACTIONS
Reaction chemistry of boron hydrides
[AD-A201243] N89-19389
Ion pair solvation
[AD-A201529] N89-19395
Studies of hydrogen-hydrogen and carbon-sulfur bond cleavage
[DE89-006116] N89-19403
NRL boron propellants combustion program
[AD-A201242] N89-19440
CHEMICAL WARFARE
Chemical warfare protection for the cockpit of future aircraft N89-19859
CHEMISORPTION
Vibrational spectroscopic studies of surface chemical interactions in chemisorption and catalysis
[DE89-005896] N89-19400
CHIPS (ELECTRONICS)
The Telecommunications and Data Acquisition Report
[NASA-CR-184812] N89-19451
A new VLSI architecture for a single-chip-type Reed-Solomon decoder N89-19455
Test aspects of the JPL Viterbi decoder N89-19457
On testing VLSI chips for the big Viterbi decoder N89-19458
Wiring Viterbi decoders (splitting deBruijn graphs) N89-19459
Critical problems in very large scale computer systems
[AD-A202129] N89-19923
CHROMATOGRAPHY
Evaluation of available analytical techniques for monitoring the quality of space station potable water N89-20071
CHROMIUM COMPOUNDS
Investigations of the statics and dynamics of the Jahn-Teller system RbCrCl3 using neutron scattering
[ETN-89-93790] N89-20008
CIRCUIT BOARDS
Wiring Viterbi decoders (splitting deBruijn graphs) N89-19459
CIRCUIT DIAGRAMS
Browsing schematics: Query-filtered graphs with context nodes N89-19844
CIRCULAR PLATES
The modeling of viscoelastic circular plates for use as waveguide absorbers
[AD-A201621] N89-19588
CIRRUS CLOUDS
Cirrus microphysics and infrared radiative transfer: A case study N89-19649
The use of automatic particle recognition to improve the determination of bulk quantities from PMS 2-D probe data in cirrus N89-19651
CIVIL AVIATION
General aviation activity and avionics survey
[AD-A201760] N89-19229
Simultaneous three-dimensional modeling of commercial flights within the airspace of the Federal Republic of Germany
[DFVLR-FB-88-31] N89-19282
CLASSIFICATIONS
Advancement of high resolution radar polarimetry in target verses clutter detection, discrimination, classification. A: Basic theory and modeling of polarimetric clutter phenomenology
[AD-A201240] N89-19467
Use of cluster analysis to define periods of similar meteorology and precipitation chemistry in eastern North America N89-19785
Transformation based endorsement systems N89-19836
User-extensible graphics using abstract structure
[BR104469] N89-19921
Equating an expert system to a classifier in order to evaluate the expert system N89-20080
CLASSIFIERS
Equating an expert system to a classifier in order to evaluate the expert system N89-20080
CLEAR AIR TURBULENCE
Instability theory in clouds and the parameterization of eddy viscosity coefficients N89-19633
CLEAVAGE
Studies of hydrogen-hydrogen and carbon-sulfur bond cleavage
[DE89-006116] N89-19403
CLIMATE
Theory on the uncertainty in cloud microphysical processes and climate N89-19644
CLIMATOLOGY
The climate inversion problem: A statistical/modeling approach N89-19784
A climatology of global precipitation N89-19787
TRMM (Tropical Rainfall Measuring Mission): A satellite mission to measure tropical rainfall
[NASA-TM-101288] N89-19789
CLOUD GLACIATION
Airborne studies of the ice phase in maritime clouds around the British Isles N89-19623
Evidence of preferential zones of ice multiplication by splintering in convective cells N89-19625
The effect of ice physical processes on the numerical simulation of West African squall lines N89-19638
The comparison of holographic and 2-D probe measurements of ice crystals N89-19652
Microphysical and electrical phenomena during freezing of water drops N89-19658
Studies of cloud micro-chemical physics N89-19686
Some effects of cloud microphysics on cloud chemistry N89-19692
CLOUD PHYSICS
Annals from the German Meteorological Society. No. 25: 10th International Cloud Physics Conference Preprints, volume 1
[ISBN-3-88-148240-7] N89-19605
Empirical equations of ice crystal growth microphysics for modeling and analysis N89-19609
A new mechanism for ice initiation in warm-based midwestern cumuli N89-19613
The calculation of supersaturations and growth of droplets in continental cumulus clouds N89-19617
Evaluation of droplet growth rates in Hawaiian orographic clouds N89-19619
Studies of warm-rain development N89-19620
Radar observations and modelling of warm rain initiation N89-19621
Airborne studies of the ice phase in maritime clouds around the British Isles N89-19623
Precipitation initiation mechanisms in clouds over north India N89-19624
Evidence of preferential zones of ice multiplication by splintering in convective cells N89-19625
A comparative study of laboratory thermals and atmospheric clouds N89-19627
Airborne studies of the influence of entrainment on the vertical and horizontal microphysical structure of small cumulus clouds N89-19629
Entrainment sites, mixing processes in warm convective clouds: Effect on droplet growth N89-19630
Structure of upper clouds boundary using the lidar data N89-19631
Turbulent transport processes within and below small cumulus clouds N89-19632
Instability theory in clouds and the parameterization of eddy viscosity coefficients N89-19633
Three-dimensional cumulus entrainment studies N89-19634
The case for subgrid-scale condensation in numerical cloud models N89-19636
The effect of turbulence on the collection of cloud drops: A stochastic model N89-19637
The effect of ice physical processes on the numerical simulation of West African squall lines N89-19638
Numerical simulation of microphysical processes in cumulonimbus N89-19639
A comparative study of two microphysical schemes in a beta mesoscale model N89-19640
Generalized microphysics scheme for use in mesoscale/cloud models N89-19641
Some outstanding problems on the influence of clouds on radiation N89-19643
Theory on the uncertainty in cloud microphysical processes and climate N89-19644
In situ measurements of ship tracks N89-19645
Cloud and aerosol optical depths N89-19646
An observational study of radiatively driven convection --- clouds N89-19647
Cirrus microphysics and infrared radiative transfer: A case study N89-19649
Development of hydrometeor video sonde N89-19653
The study of the interstitial aerosol particles and cloud droplets with digital image analysis of diffraction images N89-19654
On the determination of droplet size distributions with the counterflow virtual impactor --- cloud physics N89-19655
An investigation of the effect of electrical charges on the collision efficiency of cloud drops N89-19657
Kinetic equation for polluted cloud droplets spectrum N89-19661
Liquid water content, median volume diameter and temperature in dependence on the height above the cloud base for different types of clouds --- aircraft icing N89-19662
About secondary ice crystal production N89-19666
Experimental studies on secondary ice particle production N89-19667
Properties of the precipitation embryos evolution in characteristic Hawaiian band clouds N89-19675
Comparison of model results for models of differing microphysical detail --- hailstorms N89-19680
Airborne cloud sieving N89-19681
Studies of cloud micro-chemical physics N89-19686
Some effects of cloud microphysics on cloud chemistry N89-19692
Processes determining cloudwater composition: Field evidence for in-cloud reactive scavenging of SO2 N89-19693
Microphysical, dynamical and chemical aspects of scavenging processes during winter precipitation N89-19695
Vertical profiles of pollutants inside and outside of cloud N89-19696
Oxidation regimes in orographic capping cloud N89-19698
An examination of the chemical and physical variability of clouds at a mountain-top site in central Sweden N89-19699
Experiments on microphysics and chemistry of radiation fogs N89-19702
Chemical evolution within in a cloud model featuring a polydisperse droplet size spectrum N89-19703
Modeling studies on the formation, growth, dissipation and acidification of cumulus clouds N89-19704

A numerical simulation of the acidification process of rain water below the cloud and the mechanism of acid rain formation in area of Chongqing, China N89-19706
Effects of cloud microphysical processes on trace chemical removal efficiences N89-19707
Dynamic, radiative and chemical effects of clouds on tropospheric trace gases N89-19708
Parameterizations of microphysical processes in clouds for application in models of regional atmospheric deposition N89-19709
Meteorological and chemical influencing factors on acidity production in a mesoscale model with quasi-spectral microphysics N89-19711
Applications of the NCAR Electra Doppler radar for the study of physical parameters of clouds N89-19717
A new airborne device for measurement of cloud particles using video microscope N89-19719
Complex microphysical interactions within a central Sierra Nevada orographic cloud system N89-19722
Comparison of orographic cloud and precipitation development of three different geographic locations using a 3-D nested grid cloud model N89-19723
Microphysical observations over the Atlas Mountains in Morocco N89-19724
A new dropsonde for cloud probings N89-19728

CLOUD SEEDING
Microphysical characteristics of warm-based cumuli: Observations at -10 C --- weather modification N89-19626
A model of wet deposition to complex terrain by the seeder-feeder process N89-19710
Complex microphysical interactions within a central Sierra Nevada orographic cloud system N89-19722

CLOUDS
Measurements of the partitioning of aerosol mass and number between cloud droplets and interstitial air N89-19616

CLOUDS (METEOROLOGY)
A comparative study of laboratory thermals and atmospheric clouds N89-19627
Cloud capture by a mountain top forest. Part 1: Acidity and dosage duration N89-19682
The effect of freezing on the composition of cloud droplets N89-19691
Vertical profiles of pollutants inside and outside of cloud N89-19696
Study on cloud and rain by microwave radiometer observation N89-19727
Homogenizing surface and satellite observations of cloud
[AD-A201630] N89-19752

CLUSTER ANALYSIS
Use of cluster analysis to define periods of similar meteorology and precipitation chemistry in eastern North America N89-19785
Psychological tools for knowledge acquisition N89-19857

CLUTTER
Advancement of high resolution radar polarimetry in target verses clutter detection, discrimination, classification. A: Basic theory and modeling of polarimetric clutter phenomenology
[AD-A201240] N89-19467

CN EMISSION
Spectral studies of propellant combustion: Experimental details and emission results for M-30 propellant
[AD-A201634] N89-19399

COALESCING
The effect of charge on coalescence of small precipitation drops at terminal velocity N89-19606
Studies of warm-rain development N89-19620
The effect of turbulence on the collection of cloud drops: A stochastic model N89-19637
Damped-oscillation representation of drop-spectrum evolution due to coalescence and breakup N89-19660
A parametrization scheme for the coalescence of water drops using the stochastic collection equation N89-19671

COATINGS
The determination of the mechanical behavior of polyamic acid/polyimide coatings N89-19428

COCKPIT SIMULATORS
A comparative analysis of tilt rotor aircraft versus helicopters using simulator results
[AD-A202190] N89-19294

COCKPITS
Development of a model which provides a total system approach to integrating voice recognition and speech synthesis into the cockpit of US Navy aircraft
[AD-A202122] N89-19815
Light weight escape capsule for fighter aircraft N89-19858
Chemical warfare protection for the cockpit of future aircraft N89-19859

CODING
The Telecommunications and Data Acquisition Report
[NASA-CR-184812] N89-19451
The use of interleaving for reducing radio loss in convolutionally coded systems N89-19454
A new VLSI architecture for a single-chip-type Reed-Solomon decoder N89-19455

COEFFICIENT OF FRICTION
A robust control scheme for flexible arms with friction in the joints N89-19875

COGNITIVE PSYCHOLOGY
Psychological tools for knowledge acquisition N89-19857

COHERENT LIGHT
Proof of the feasibility of coherent and incoherent schemes for pumping a gamma-ray laser
[AD-A201931] N89-19542

COLLECTION
The collection efficiencies of soft-hailstones for super-cooled water droplets and ice crystals N89-19678

COLLISIONS
An investigation of the effect of electrical charges on the collision efficiency of cloud drops N89-19657

COLOR
Recognition of object domain by color distribution N89-19928
Estimating the illuminant color from the shading of a smooth surface
[AD-A201333] N89-19983
An achromatic super telephoto lens
[DE89-006163] N89-19986

COLOR CODING
The efficacy of color-coded symbols to enhance air-traffic control displays
[AD-A201594] N89-19284

COLOR VISION
Estimating the illuminant color from the shading of a smooth surface
[AD-A201333] N89-19983

COLUMBUS SPACE STATION
Telescience system concept study, volume 2 --- Columbus space station
[MATRA-NT/2113/139-VOL-2] N89-19478

COMBAT
The importance of aircraft performance and signature reduction upon combat survivability
[AD-A202106] N89-19292

COMBUSTIBLE FLOW
The analytical modeling of a turbulent diffusion flame behind a backward facing step N89-19386
Flame driving of longitudinal instabilities in liquid fueled dump combustors
[AD-A201293] N89-19392

COMBUSTION
A fundamental mathematical theory in the dynamics of combustion processes
[AD-A201284] N89-19391
The solid surface combustion space shuttle experiment hardware description and ground-based test results
[NASA-TM-101963] N89-19446
Application of Schlieren photography in gas turbine combustion research
[PNR90495] N89-19532

COMBUSTION CHAMBERS
Current diagnostic practice in gas turbine combustors
[PNR90530] N89-19306
Flame driving of longitudinal instabilities in liquid fueled dump combustors
[AD-A201293] N89-19392
Computational studies of evaporating sprays in a shear layer
[AD-A201932] N89-19520
High-speed laser photography
[AD-A202293] N89-19544
An experimental investigation of sooting characteristics of a gas turbine combustor and augmentor tube
[AD-A201804] N89-19568

COMBUSTION PHYSICS
A fundamental mathematical theory in the dynamics of combustion processes
[AD-A201284] N89-19391
Computational fluid dynamics for combustion applications
[PNR90534] N89-19525
High-speed laser photography
[AD-A202293] N89-19544

COMET NUCLEI
Jets physics in Comet P/Halley
[IFSI-88-3] N89-20049

COMET TAILS
Jets physics in Comet P/Halley
[IFSI-88-3] N89-20049

COMMAND AND CONTROL
Autonomous satellite command and control: A comparison with other military systems N89-19839

COMMUNICATION NETWORKS
Knowledge-based operation and management of communications systems N89-19826
Global scientific and technical information network
[AD-A201902] N89-20030

COMMUNICATION SATELLITES
PSDE/SAT-2 preliminary spacecraft configuration study, executive summary
[ESA-CR(P)-2689] N89-19360
PSDE/SAT-2: Preliminary spacecraft configuration study, executive summary
[ESA-CR(P)-2704] N89-19364
Design and test of a 2.25-MW transformer rectifier assembly N89-19452

COMMUNITIES
Noise assessment of the rocket sled test track operation at Holloman AFB, New Mexico
[AD-A201279] N89-19317

COMPATIBILITY
Next generation keyboards: The importance of cognitive compatibility N89-19848
Design guidelines for remotely maintainable equipment N89-19865

COMPLEX VARIABLES
Two-dimensional test section with preadjusted adaptive walls for low speed wind tunnel
[KTH-AERO-REPT-57] N89-19278

COMPONENT RELIABILITY
Composite reliability enhancement via reloading
[AD-A201861] N89-19380

COMPOSITE MATERIALS
Heat transfer properties of satellite component materials N89-19375
Nonlinear vibrations of composite material shells N89-19377
Composite reliability enhancement via reloading
[AD-A201861] N89-19380
Finite element analysis of laminated composite plates
[AD-A202192] N89-19381
The effects of simulated space environmental parameters on six commercially available composite materials
[NASA-TP-2906] N89-19385
Composite ceramic superconducting wires for electric motor applications
[AD-A201810] N89-19429
Sliding and debonding inclusions
[AD-A201609] N89-19587
Compression strength of composite primary structural components
[NASA-CR-184893] N89-19599

COMPOSITE STRUCTURES
A Monte Carlo simulation of the single-filament-composite test N89-19376
Nonlinear vibrations of composite material shells N89-19377
Finite element analysis of laminated composite plates
[AD-A202192] N89-19381
Compression strength of composite primary structural components
[NASA-CR-184893] N89-19599

COMPRESSIBLE FLOW
On boundary integral equation approach to a nonstationary problem of isothermal viscous compressible flows
[PREPRINT-1134] N89-19526
Vortex convection in nonuniform compressible flow
[MPIS-4/1988] N89-19527

COMPRESSIVE STRENGTH
Measurements of the compressive behavior of AS4/3501-6 and IM7/8551-7 carbon/epoxy
[DE89-005823] N89-19383

COMPRESSOR ROTORS
The effect of prewhirl on the internal aerodynamics and performance of a mixed flow research centrifugal compressor
[NASA-CR-184756] N89-19503

COMPUTATION
Calculation of molecular absorption parameters and updating the AFGL atmospheric line parameter compilation
[AD-A202113] N89-19761
Structural saliency: The detection of globally salient structures using a locally connected network
[AD-A201619] N89-19806

COMPUTATIONAL FLUID DYNAMICS
Transonic Unsteady Aerodynamics and Aeroelasticity 1987, part 1
[NASA-CP-3022-PT-1] N89-19234
Role of computational fluid dynamics in unsteady aerodynamics for aeroelasticity N89-19237
An efficient method for computing unsteady transonic aerodynamics of swept wings with control surfaces
[AIAA-85-4058] N89-19241
Numerical simulation of the aerodynamics of turbulent transonic flow past a projectile N89-19270

Computational study of incompressible turbulent flow over a swept rearward-facing step N89-19272
A study of flow separation in transonic flow using inviscid and viscous CFD schemes N89-19273
Theoretical and experimental investigations on shocks losses in transonic axial flow compressors [DFVLR-FB-88-38] N89-19304
Computational fluid dynamics for combustion applications [PNR90534] N89-19525
Modeling of inertial effects in transient liquid-bubble flows [REPT-88-22] N89-19528
Design improvement of a pump wear ring labyrinth seal [NASA-CR-179161] N89-19555
Knowledge-based zonal grid generation for computational fluid dynamics N89-19828

COMPUTATIONAL GRIDS
Full potential unsteady computations including aeroelastic effects N89-19243
Flux-vector splitting for unsteady calculations on dynamic meshes N89-19244
Computational aeroelasticity challenges and resources N89-19264
Numerical computations of transonic critical aerodynamic behavior [AD-A202412] N89-19277
Psychological tools for knowledge acquisition N89-19657
Vertex-centered and cell-centered multigrid methods for interface problems [REPT-88-42] N89-19953

COMPUTER AIDED DESIGN
Design of digital filters for navigation receivers --- GPS [DFVLR-MITT-88-23] N89-19288
Integrated Structural Analysis And Control (ISAAC): Issues and progress N89-19341
Calculation of mutual self inductance and coupling coefficient for closely spaced loops [DE89-005546] N89-19471
High output voltage multioctave broadband amplifier working between 50 kHz and 8 GHz [HMI-B-451] N89-19497
NESSUS (Numerical Evaluation of Stochastic Structures Under Stress)/EXPERT: Bridging the gap between artificial intelligence and FORTRAN N89-19827
Knowledge-based zonal grid generation for computational fluid dynamics N89-19828
CIRCA 2000 operations criteria N89-19829
Optimal solutions for complex design problems: Using isoperformance software for human factors trade offs N89-19860
Expert systems applications for space shuttle payload integration automation N89-19887
Intelligent embedded instruction for Computer-Aided Design (CAD) systems [AD-A201811] N89-19907
Computer-aided fabrication system implementation [AD-A202128] N89-19911
CAD directed robotic edge finishing [DE89-005347] N89-19916

COMPUTER AIDED TOMOGRAPHY
Ultrasound transmission tomography, a low-cost realization --- medical equipment [ISBN-90-9002330-5] N89-19804

COMPUTER ANIMATION
High-speed real-time animated displays on the ADAGE (trademark) RDS 3000 raster graphics system [NASA-TM-4095] N89-19899

COMPUTER ASSISTED INSTRUCTION
Second Annual Workshop on Space Operations Automation and Robotics (SOAR 1988) [NASA-CP-3019] N89-19817
An intelligent tutoring system for space shuttle diagnosis N89-19853
Intelligent tutoring systems research in the training systems division: Space applications N89-19854
Intelligent tutoring in the spacecraft command/control environment N89-19855
Development of a personal-computer-based intelligent tutoring system N89-19889
Intelligent embedded instruction for Computer-Aided Design (CAD) systems [AD-A201811] N89-19907

COMPUTER GRAPHICS
Study of a software system concept for mission analysis presentation [ESA-CR(P)-2661] N89-19320
Computer generation of fractal terrains [AD-A201171] N89-19730
Analysis of blending algorithms in computer graphics [AD-A201921] N89-19909
User-extensible graphics using abstract structure [BR104469] N89-19921
Recognition of object domain by color distribution N89-19928
Estimating the illuminant color from the shading of a smooth surface [AD-A201333] N89-19983

COMPUTER INFORMATION SECURITY
DES cryptographic services designed for the DOE wide band communications network [LA-10966-MS] N89-19484

COMPUTER NETWORKS
DES cryptographic services designed for the DOE wide band communications network [LA-10966-MS] N89-19484
Crossbar switch backplane and its application [DE89-005621] N89-19491
Interfacing laboratory instruments to multiuser, virtual memory computers [NASA-TM-4106] N89-19578

COMPUTER PROGRAMMING
On purely exponential logic queries [AD-A201259] N89-19902
A survey of automatic code generating software [AD-A201963] N89-19910
Critical problems in very large scale computer systems [AD-A202129] N89-19923

COMPUTER PROGRAMS
Unsteady aerodynamics and aeroelastic research at AFWAL N89-19235
Extensions and improvements on XTRAN3S N89-19236
CAP-TSD: A program for unsteady transonic analysis of realistic aircraft configurations N89-19238
CAP-TSD analysis of the F-15 aircraft N89-19239
Viscous flow calculations for the AGARD standard configuration airfoils with experimental comparisons N89-19249
A data analysis system for unsteady turbulence measurements [AD-A201662] N89-19268
Integrated tools for control-system analysis [NASA-TP-2885] N89-19309
Aerothermodynamics of a jet cell facility [AD-A202142] N89-19318
Computer algorithms for measurement control and signal processing of transient scattering signatures [AD-A201672] N89-19469
Verification of combined thermal-hydraulic and heat conduction analysis code FLOWNET/TRUMP [DE88-756063] N89-19506
Description of FEL3D: A three dimensional simulation code for TOK and FEL [DE89-005529] N89-19540
Dexterous robotic hands: Kinematics and control [AD-A202183] N89-19570
Gear technology acquisition for advanced aero engines [PNR90510] N89-19571
Interfacing laboratory instruments to multiuser, virtual memory computers [NASA-TM-4106] N89-19578
Fatigue crack growth model RANDOM2 user manual. Appendix 1: Development of advanced methodologies for probabilistic constitutive relationships of material strength models [NASA-CR-184775-APP-1] N89-19581
Fatigue strength reduction model: RANDOM3 and RANDOM4 user manual. Appendix 2: Development of advanced methodologies for probabilistic constitutive relationships of material strength models [NASA-CR-184796-APP-2] N89-19582
Nonlinear dynamic analysis of embedded structures [AD-A201728] N89-19593
Computer generation of fractal terrains [AD-A201171] N89-19730
A climatology of global precipitation N89-19787
On purely exponential logic queries [AD-A201259] N89-19902
ISTAR evaluation [AD-A201345] N89-19903
An interrogative model of computer-aided adaptive testing: Some experimental evidence [AD-A201675] N89-19905
A survey of automatic code generating software [AD-A201963] N89-19910
Computer-aided fabrication system implementation [AD-A202128] N89-19911
Quantum limits of superconducting heterodyne receivers [AD-A201303] N89-20000
Development of a software interface for optical disk archival storage for a new life sciences flight experiments computer N89-20061
Automatic voice recognition using traditional and artificial neural network approaches N89-20064
Model formulation of non-equilibrium gas radiation for hypersonic flight vehicles N89-20066

COMPUTER SYSTEMS DESIGN
Specification validation tools study [MATRA-NT/139/1939] N89-19447
Scheme86: An architecture for microcoding a scheme interpreter [AD-A201258] N89-19893
Advanced information technology monitoring with microprocessors --- spacecraft control [MMP-1-IS-02-3302-FR] N89-19895
Application of the OCCAM/transputer conception as busless multiprocessor system in a digital controller [DFVLR-FB-88-40] N89-19896

COMPUTER SYSTEMS PERFORMANCE
Validation of highly reliable, real-time knowledge-based systems N89-19833
Testing expert systems N89-19834
Scheme86: An architecture for microcoding a scheme interpreter [AD-A201258] N89-19893
A Monte Carlo test program with vectorized geometry routines --- radiation transport [JUEL-2202] N89-19947

COMPUTER SYSTEMS PROGRAMS
Spaceborne VHSIC multiprocessor system for AI applications N89-19838
Operation of the HP2250 with the HP9000 series 200 using PASCAL 3.0 [NASA-TM-87652] N89-19892
HERMES, a Monte Carlo program system for beam-materials interaction studies --- radiation transport [JUEL-2203] N89-19979

COMPUTER TECHNIQUES
Joint University Program for Air Transportation Research, 1987 [NASA-CP-3028] N89-19230
Computer software used in US Army Anthropometric Survey 1987-1988 [AD-A201185] N89-19812
Second Annual Workshop on Space Operations Automation and Robotics (SOAR 1988) [NASA-CP-3019] N89-19817
The scheduling techniques of ESP2 N89-19818
Space station payload operations scheduling with ESP2 N89-19819
EMMA: The expert system for munition maintenance N89-19823
Diagnostics in the Extendable Integrated Support Environment (EISE) N89-19824
Knowledge-based operation and management of communications systems N89-19826
Knowledge-based zonal grid generation for computational fluid dynamics N89-19828
Artificial intelligent decision support for low-cost launch vehicle integrated mission operations N89-19830
Autonomous satellite command and control: A comparison with other military systems N89-19839
Portable inference engine: An extended CLIPS for real-time production systems N89-19843
Presentation planning using an integrated knowledge base N89-19845
Integration of a computerized two-finger gripper for robot workstation safety N89-19863
Local position control: A new concept for control of manipulators N89-19864
IDEAL: A methology for developing information systems N89-19888
SARSCEST (human factors) N89-19890
Electronic data generation and display system N89-19891
An interrogative model of computer-aided adaptive testing: Some experimental evidence [AD-A201675] N89-19905
Software performance on nonlinear least-squares problems [AD-A201879] N89-19908
Computer-aided fabrication system implementation [AD-A202128] N89-19911

COMPUTER VISION
Design of an optical sensor system for adaptive control of a seam tracking robot N89-19565
Extracting depth by binocular stereo in a robot vision system [DE89-005016] N89-19572
CAD-model-based vision for space applications N89-19867
Sensor fusion of range and reflectance data for outdoor scene analysis N89-19868
Machine vision for space telerobotics and planetary rovers N89-19879
A multi-sensor system for robotics proximity operations N89-19881
Optical joint correlation using the deformable mirror device N89-20074
Visual perception and grasping for the extravehicular activity robot N89-20082

COMPUTERIZED SIMULATION
Hypervelocity technology escape system concepts. Volume 2: Software manual
[AD-A201720] N89-19281
Study of a software system concept for mission analysis presentation
[ESA-CR(P)-2661] N89-19320
Variable gravity research facility
[NASA-CR-184714] N89-19324
A Monte Carlo simulation of the single-filament-composite test N89-19376
Composite reliability enhancement via reloading
[AD-A201861] N89-19380
A simplified procedure for decoding the (23,12) and (24,12) Golay codes N89-19456
Calculation of mutual self inductance and coupling coefficient for closely spaced loops
[DE89-005546] N89-19471
Description of FEL3D: A three dimensional simulation code for TOK and FEL
[DE89-005529] N89-19540
A heuristically based navigation system for an autonomous walking machine with a range scanner N89-19563
A three-dimensional nonsingular simulation of rigid manipulators
[AD-A201964] N89-19569
Instability theory in clouds and the parameterization of eddy viscosity coefficients N89-19633
The case for subgrid-scale condensation in numerical cloud models N89-19636
The effect of ice physical processes on the numerical simulation of West African squall lines N89-19638
Numerical simulation of microphysical processes in cumulonimbus N89-19639
The study of numerical simulation on the formation of the cloud droplet spectra in cumulus clouds N89-19642
Automatic Detection of Electric Power Troubles (ADEPT) N89-19825
Knowledge-based zonal grid generation for computational fluid dynamics N89-19828
Presentation planning using an integrated knowledge base N89-19845
A schema-based model of situation awareness: Implications for measuring situation awareness N89-19847
Simulation of the human-telerobot interface N89-19861
The use of the articulated total body model as a robot dynamics simulation tool N89-19872
Numerical studies of MHD turbulence in the reversed field pinch
[IPP-6/276] N89-19994
An observational and numerical study of extragalactic radio sources N89-20055

COMPUTERS
Critical problems in very large scale computer systems
[AD-A202129] N89-19923

CONDENSATION NUCLEI
In situ measurements of ship tracks N89-19645
Acidification of stratiform clouds and their aerosol scavenging properties N89-19694

CONDUCTIVE HEAT TRANSFER
Verification of combined thermal-hydraulic and heat conduction analysis code FLOWNET/TRUMP
[DE88-756063] N89-19506
Transient three-dimensional heat conduction computations using Brian's technique
[AD-A201918] N89-19519
Determination of local fluid drag by a laser heating/thermographic phosphor technique: Applicability of the H. Ludwieg model
[DE89-006462] N89-19523

CONFERENCES
Proceedings of the Fifth AFOSR Forum on Space Structures
[AD-A194761] N89-19333
Annals from the German Meteorological Society. No. 25: 10th International Cloud Physics Conference Preprints, volume 1
[ISBN-3-88-148240-7] N89-19605
Calendar of selected aeronautical and space meetings: January 1989 onwards
[AGARD-CAL-89/1] N89-20024
National Aeronautics and Space Administration (NASA)/American Society for Engineering Education (ASEE) Summer Faculty Fellowship Program 1988, volume 2 --- Author
[NASA-CR-172118-VOL-2] N89-20073

CONFIDENCE
Reducing uncertainty by using explanatory relationships N89-19837

CONFIDENCE LIMITS
Estimation in large samples
[AD-A201459] N89-19956

CONFORMAL MAPPING
The geometry of geodetic inverse linear mapping and nonlinear adjustment
[ETN-89-93900] N89-19736
Hyperbolicity properties of C sup 2 multimodal Collet-Eckmann maps without Schwarzian deriative assumptions
[REPT-88-10] N89-19945

CONGRESSIONAL REPORTS
Commercial expendable launch vehicle liability
[S-HRG-100-750] N89-19325
The Atlas/Centaur 67 launch mishap
[GPO-80-201] N89-19332
National Aeronautics and Space Administration authorization
[S-HRG-100-579-PT-2] N89-20031

CONSERVATION
Interdisciplinary research in viscoelasticity and rheology
[AD-A201270] N89-19390

CONSISTENCY
Validation of highly reliable, real-time knowledge-based systems N89-19833
Testing expert systems N89-19834

CONSTRUCTION
The design and initial construction of a composite RPV (Remotely Piloted Vehicle) for flight research applications
[AD-A201884] N89-19291

CONTACT LOADS
Mixed formulation for frictionless contact problems
[NASA-TP-2897] N89-19580

CONTAMINANTS
Kinetic equation for polluted cloud droplets spectrum N89-19661
Chemical warfare protection for the cockpit of future aircraft N89-19859

CONTINUOUS SPECTRA
Chaotic electron motion caused by sidebands in free electron lasers
[AD-A201635] N89-19538

CONTINUOUS WAVE LASERS
The standard chemical oxygen-iodine laser kinetics package
[AD-A202223] N89-19543
A high-spectral-resolution lidar system: The use of atomic blocking filter for measuring atmospheric parameters
[AD-A201736] N89-19759

CONTINUUM MECHANICS
Integrated Structural Analysis And Control (ISAAC): Issues and progress N89-19341

CONTOUR SENSORS
CAD-model-based vision for space applications N89-19867

CONTRACT MANAGEMENT
ISTAR evaluation
[AD-A201345] N89-19903

CONTROL STABILITY
Stabilization and regulation of multirate sampled-date linear systems
[REPT-88-013] N89-19930

CONTROL SYSTEMS DESIGN
Integrated tools for control-system analysis
[NASA-TP-2885] N89-19309
Robust control for linear systems with structured uncertainty
[AD-A201947] N89-19315
A variable-gain output feedback control design methodology
[NASA-CR-4226] N89-19316
Proceedings of the Fifth AFOSR Forum on Space Structures
[AD-A194761] N89-19333
Adaptive control of large space structures N89-19343
Majorant analysis of performance degradation due to uncertainty N89-19344
Decentralized/relegated control for large space structures N89-19346
Frobenius-Hankel norm framework for disturbance rejection and low order decentralized controller design N89-19347
Robust eigenstructure assignment by a projection method: Application using multiple optimization criteria N89-19349
Damage detection and location in large space trusses N89-19350
Effects of reduced order modeling on the control of a large space structure
[AD-A201674] N89-19355
Maximum entropy/optimal projection design synthesis for decentralized control of large space structures
[AD-A202375] N89-19358
Integration of a computerized two-finger gripper for robot workstation safety N89-19863
Local position control: A new concept for control of manipulators N89-19864
Dexterity analysis and robot hand design N89-19865
Concept for a large master/slave-controlled robotic hand N89-19866
A novel manipulator technology for space applications N89-19874
An expert system for restructurable control N89-19886
Advanced information technology monitoring with microprocessors --- spacecraft control
[MMP-1-IS-02-3302-FR] N89-19895
Remote control system --- spectrometer
[DIGEL-79] N89-19917
Stabilization and regulation of multirate sampled-date linear systems
[REPT-88-013] N89-19930
Further results on the design of multivariable regulators under structure and robustness constraints. Part 1: The initialization problem
[REPT-88-028] N89-19931
Further results on the design of multivariable regulators under structure and robustness constraints. Part 2: The reliable robust decentralized regulator problem and the simultaneous robust decentralized regulator problem
[REPT-88-029] N89-19932
Focusing system, rotation, and modulation of the F 9 mirror of the IFSI 40 cm telescope
[IFSI-87-16] N89-19987

CONTROL THEORY
Joint University Program for Air Transportation Research, 1987
[NASA-CP-3028] N89-19230
Control of nonlinear systems using partial dynamic inversion N89-19310
A variable-gain output feedback control design methodology
[NASA-CR-4226] N89-19316
Proceedings of the Fifth AFOSR Forum on Space Structures
[AD-A194761] N89-19333
Majorant analysis of performance degradation due to uncertainty N89-19344
Decentralized/relegated control for large space structures N89-19346
Robust eigenstructure assignment by a projection method: Application using multiple optimization criteria N89-19349
An approach to semi-active control of multiple degree-of-freedom systems N89-19554
Regulation of linear discrete time-varying systems
[ETN-89-93896] N89-19934

CONTROLLABILITY
Analytical interpretation on lateral/directional stability and controllability of high angle-of-attack reentry flight
[ISAS-630] N89-19353

CONTROLLED FUSION
Possibilities for breakeven and ignition of D-He3 fusion fuel in a near term tokamak
[KFK-4433] N89-19992

CONTROLLERS
Integrated tools for control-system analysis
[NASA-TP-2885] N89-19309
Proceedings of the Fifth AFOSR Forum on Space Structures
[AD-A194761] N89-19333
System identification of suboptimal feedback control parameters based on limiting-performance/minimum-time characteristics N89-19340
Integrated Structural Analysis And Control (ISAAC): Issues and progress N89-19341
Majorant analysis of performance degradation due to uncertainty N89-19344
The optimal projection equations for fixed-order dynamic compensation: Existence, convergence and global optimality N89-19345
Decentralized/relegated control for large space structures N89-19346
Frobenius-Hankel norm framework for disturbance rejection and low order decentralized controller design N89-19347
A controlled component synthesis method for truss structure vibration control N89-19348
Maximum entropy/optimal projection design synthesis for decentralized control of large space structures
[AD-A202375] N89-19358
Block diagrams of the radar interface and control unit N89-19460
RF performance measurement of the DSS-14 70-meter antenna at C-band/L-band N89-19461
Design of an optical sensor system for adaptive control of a seam tracking robot N89-19585
An expert system for restructurable control N89-19886
Intelligent control of robotic arm/hand systems for the NASA EVA retriever using neural networks N89-20075

CONVECTION
Mesoscale Convective Systems: Structure, development and storm-environment interactions N89-19788
CONVECTION CLOUDS
Evidence of preferential zones of ice multiplication by splintering in convective cells N89-19625
Entrainment sites, mixing processes in warm convective clouds: Effect on droplet growth N89-19630
Properties of the precipitation embryos evolution in characteristic Hawaiian band clouds N89-19675
CONVECTIVE FLOW
Large-eddy simulation of convective boundary layers [DFVLR-FB-88-30] N89-19522
Vortex convection in nonuniform compressible flow [MPIS-4/1988] N89-19527
Semi-prognostic tests of cumulus parameterization schemes in the middle latitudes N89-19786
CONVECTIVE HEAT TRANSFER
Natural convection liquid immersion cooling of a column of discrete heat sources in a vertical channel [AD-A201676] N89-19513
COORDINATES
Maneuvering equations in terms of quasi-coordinate N89-19337
Coordinates, conversions, and kinematics for the Rochester Robotics Lab [AD-A201611] N89-19560
The development and validation of an automated headboard device for measurement of three-dimensional coordinates of the head and face [AD-A201186] N89-19813
COORDINATION
The effects of a pitched field orientation on hand/eye coordination [AD-A201620] N89-19814
COPPER
Scanning tunneling microscopy of metals on graphite [DE89-006608] N89-19404
COPPER ALLOYS
Investigations on undercooling, nucleation and rapid solidification of metallic systems [DFVLR-FB-88-39] N89-19415
COPPER OXIDES
Radiation induced amorphization in YBa2Cu3O7 and GdBa2Cu3O7 superconductors [DE89-005451] N89-20008
CORIOLIS EFFECT
Chaotic dynamics and control of nonlinear and flexible arm robotic devices N89-19566
CORNEA
Biological applications and effects of optical masers [AD-A201834] N89-19541
CORONAL LOOPS
Existence of stationary solutions in the coronal loop problem [REPT-88-06] N89-20054
CORRELATION COEFFICIENTS
Variations of the tropospheric propagation range of ultrashort radio waves above the sea N89-19486
CORRELATORS
Optical joint correlation using the deformable mirror device N89-20074
CORROSION RESISTANCE
Effect of temperature on the corrosion resistance of nitrogen bearing AL6X and 904L stainless steels [AD-A201955] N89-19412
Passivity and corrosion of probe metals [ETN-89-93984] N89-19416
CORROSION TESTS
Passivity and corrosion of probe metals [ETN-89-93984] N89-19416
COSMIC DUST
Morphology and nature of the dust of the dark cloud Coal Sack [ETN-89-93795] N89-20046
Jets physics in Comet P/Halley [IFSI-88-3] N89-20049
COSMIC RAYS
The scintillating optical fiber isotope experiment (SOFIE): Bevalac calibrations of test models N89-20034
The cosmic ray antiproton spectrum between 0.1 and 1.5 GeV kinetic energy N89-20057
COSMOCHEMISTRY
Solar and interplanetary cosmic ray composition [MPE-PREPRINT-108] N89-20056
COSMOLOGY
Studies in quantum field theory [DE89-006286] N89-20023
Mass-radius star evolution Sun activity planets surfaces on purely empirical basis. Empiry theory reality: The use of statistics [REPT-18] N89-20050
COSMONAUTS
Comparison of Soviet and US space food and nutrition programs N89-20059
COSMOS SATELLITES
Mini protein crystallization facility. Phase A study: Executive summary [REPT-AQ-ES-576/88] N89-19444
COST ANALYSIS
Estimating aircraft airframe tooling cost: An alternative to DAPCA 3 [AD-A201506] N89-19226
Analysis of cost growth and cost composition in the defense aerospace industry [AD-A201544] N89-19227
COST EFFECTIVENESS
The development of a cislunar space infrastructure [NASA-CR-184728] N89-19352
A methodology for automation and robotics evaluation applied to the space station telerobotic servicer N89-19882
COST ESTIMATES
Estimating aircraft airframe tooling cost: An alternative to DAPCA 3 [AD-A201506] N89-19226
Preliminary cost model for a commercial geostationary transportation company (GRET) [ILR-MITT-208] N89-19330
COST REDUCTION
CIRCA 2000 operations criteria N89-19829
Autonomous satellite command and control: A comparison with other military systems N89-19839
COSTS
Estimating aircraft airframe tooling cost: An alternative to DAPCA 3 [AD-A201506] N89-19226
COUNTERFLOW
Superfluid turbulence in two-fluid flow of helium II N89-20018
COUNTERMEASURES
A model for plasma volume changes during short duration spaceflight N89-20067
COUPLING
The coupled cluster method and the properties of energetic materials [AD-A201168] N89-19388
COUPLING COEFFICIENTS
Calculation of mutual self inductance and coupling coefficient for closely spaced loops [DE89-005546] N89-19471
COVARIANCE
Refractive turbulence profiling via binary source intensity scintillation correlation [AD-A202189] N89-19762
CRACK INITIATION
The effects of tempering and test temperature on the dynamic fracture initiation behavior of an AISI 4340 VAR steel [AD-A201606] N89-19408
A dynamic, time stepping boundary element method for frictional crack and interface problems N89-19590
CRACK PROPAGATION
A new approach to the evaluation of the effects of stress state and interfacial properties on the behavior of advanced metal matrix composites [AD-A201246] N89-19373
Durability and damage tolerance of bismaleimide composites. Volume 2: Appendix of crack growth and low-velocity impact data [AD-A201839] N89-19379
The effect of hydrogen on fatigue crack growth rate of AISI 304 stainless steel N89-19410
Fatigue crack growth model RANDOM2 user manual. Appendix 1: Development of advanced methodologies for probabilistic constitutive relationships of material strength models [NASA-CR-184775-APP-1] N89-19581
Boundary layer and singularity measurement in three dimensional fracture problems [AD-A201277] N89-19584
Advanced durability analysis. Volume 4: Executive summary [AD-A202304] N89-19597
Fatigue crack growth in ARALL: A hybrid aluminum Aramid composite material. Crack growth mechanisms and quantitative predictions of the crack growth rates [ETN-89-93899] N89-19602
CRACKING (FRACTURING)
The effects of tempering and test temperature on the dynamic fracture initiation behavior of an AISI 4340 VAR steel [AD-A201606] N89-19408
CRACKS
A new approach to the evaluation of the effects of stress state and interfacial properties on the behavior of advanced metal matrix composites [AD-A201246] N89-19373
Boundary layer and singularity measurement in three dimensional fracture problems [AD-A201277] N89-19584
CREEP PROPERTIES
Elastic hysteresis phenomena in ULE and Zerodur optical glasses at elevated temperatures [DE89-005183] N89-19423
CREEP RUPTURE STRENGTH
Tensile and creep rupture behavior of P/M processed Nb-base alloy, WC-3009 [NASA-TM-101954] N89-19371
CREW WORKSTATIONS
Light weight escape capsule for fighter aircraft N89-19858
CROSS CORRELATION
A data analysis system for unsteady turbulence measurements [AD-A201662] N89-19268
CRYSTAL DEFECTS
Grain boundary nonstoichiometry in multicomponent ceramics [DE89-006109] N89-19437
Positron spectroscopy for materials characterization [DE89-005766] N89-20010
CRYSTAL DISLOCATIONS
Anomalous slip in an FCC system [DE89-002257] N89-19405
CRYSTAL GROWTH
Temporal variations of snow crystal growth parameters N89-19608
Empirical equations of ice crystal growth microphysics for modeling and analysis N89-19609
The contrast study of new model on ice crystal growth N89-19610
Proportion of riming growth process in snowfall phenomena N89-19668
Pattern of air bubble inclusions in atmospheric ice formed during accretion N89-19676
Pyrolytic and laser photolytic growth of crystalline and amorphous germanium films from digermane (GE2H6) [DE89-006125] N89-20019
CRYSTAL LATTICES
Grain boundary nonstoichiometry in multicomponent ceramics [DE89-006109] N89-19437
Laser-spectroscopic investigations of manganese centers in the zinc sulfide host lattice [ETN-89-93791] N89-20007
CRYSTAL STRUCTURE
Anomalous slip in an FCC system [DE89-002257] N89-19405
Evaluation of optical materials samples [AD-A199471] N89-19981
Radiation induced amorphization in YBa2Cu3O7 and GdBa2Cu3O7 superconductors [DE89-005451] N89-20008
Studies of 3-5 compounds in the megabar regime: [DE89-005722] N89-20009
Positron spectroscopy for materials characterization [DE89-005766] N89-20010
Atomic structure of tilt grain boundaries in NiO [DE89-005847] N89-20013
CRYSTALLINITY
Pyrolytic and laser photolytic growth of crystalline and amorphous germanium films from digermane (GE2H6) [DE89-006125] N89-20019
CRYSTALLIZATION
Polymer morphology and transport [AD-A201167] N89-19424
Mini protein crystallization facility. Phase A study: Executive summary [REPT-AQ-ES-576/88] N89-19444
Crystallization of supercooled solutions --- atmosphere N89-19664
Kinetics of ice crystal formation on aerosol particles in supercooled fog N89-19665
About secondary ice crystal production N89-19666
CRYSTALLOGRAPHY
Three-dimensional structures of snow crystals shown by stereo-photomicrographs N89-19669
Analysis of hailstones from a severe storm and their simulated evolution N89-19677
CRYSTALS
The comparison of holographic and 2-D probe measurements of ice crystals N89-19652
The collection efficiencies of soft-hailstones for super-cooled water droplets and ice crystals N89-19678
CUES
Computation of stereo and visual motion: From biophysics to psychophysics [AD-A201873] N89-19802
CUMULONIMBUS CLOUDS
Numerical simulation of microphysical processes in cumulonimbus N89-19639
CUMULUS CLOUDS
A new mechanism for ice initiation in warm-based midwestern cumuli N89-19613

The calculation of supersaturations and growth of droplets in continental cumulus clouds N89-19617
On the observations of cloud temperature and liquid water content using a Lyman-alpha and an FSSP sensor --- forward scattering spectrometer probe (FSSP) N89-19618
Microphysical characteristics of warm-based cumuli: Observations at -10 C --- weather modification N89-19626
Entrainment and fine-scale (molecular) mixing --- clouds N89-19628
Turbulent transport processes within and below small cumulus clouds N89-19632
Three-dimensional cumulus entrainment studies N89-19634
Heterogeneous mixing measurements in small nonprecipitating cumuli N89-19635
The study of numerical simulation on the formation of the cloud droplet spectra in cumulus clouds N89-19642
Modeling studies on the formation, growth, dissipation and acidification of cumulus clouds N89-19704
A numerical investigation of sulfate production and deposition in midlatitude continental cumulus clouds N89-19705
Semi-prognostic tests of cumulus parameterization schemes in the middle latitudes N89-19786

CURTAINS
Chemical warfare protection for the cockpit of future aircraft N89-19859

CURVATURE
Curvature effects on the stability of three-dimensional laminar boundary layers N89-19500
The development and structural characteristics of Dean vortices in a curved rectangular channel [AD-A201249] N89-19508
Structural saliency: The detection of globally salient structures using a locally connected network [AD-A201619] N89-19806

CURVE FITTING
A curve-fitting package for personal computers [LA-11082-MS] N89-19922

CURVED BEAMS
Mixed formulation for frictionless contact problems [NASA-TP-2897] N89-19580

CYCLIC LOADS
Fatigue crack growth in ARALL: A hybrid aluminum Aramid composite material. Crack growth mechanisms and quantitative predictions of the crack growth rates [ETN-89-93899] N89-19602

CYCLOTRONS
Theory of accelerated orbits and space charge effects in an Azimuthly Varying Field (AVF) cyclotron [ETN-89-93897] N89-19978

CYLINDRICAL BODIES
Plastic buckling of cylinders under biaxial loading N89-19591
Development of a system for acoustic measurements of bistatic target strengths [AD-A201673] N89-19970

CYLINDRICAL WAVES
A dynamic, time stepping boundary element method for frictional crack and interface problems N89-19590

D

DAMAGE
Raman and RBS studies of ion implanted semiconductors [ATR-88(8359)-5] N89-20021

DAMAGE ASSESSMENT
Ice/frost/debris assessment for space shuttle mission STS-27R, December 2, 1988 [NASA-TM-102144] N89-19326
Damage detection and location in large space trusses N89-19350
Evaluation of optical materials samples [AD-A199471] N89-19981

DARK MATTER
Morphology and nature of the dust of the dark cloud Coal Sack [ETN-89-93795] N89-20046

DATA ACQUISITION
General aviation activity and avionics survey [AD-A201760] N89-19229
In-line wear monitor [AD-A201292] N89-19301
Block diagrams of the radar interface and control unit N89-19460
MODIS information, data and control system (MIDACS) operations concepts [NASA-TM-100720] N89-19729
TRMM (Tropical Rainfall Measuring Mission): A satellite mission to measure tropical rainfall [NASA-TM-101288] N89-19789
Knowledge acquisition for case-based reasoning systems N89-19856
Psychological tools for knowledge acquisition N89-19857
Status of DOE information network modifications [DE89-005191] N89-20028
Development of a software interface for optical disk archival storage for a new life sciences flight experiments computer N89-20061

DATA BASE MANAGEMENT SYSTEMS
An architecture for integrating distributed and cooperating knowledge-based Air Force decision aids N89-19841
ISTAR evaluation [AD-A201345] N89-19903
Specification and management of database integrity constraints through logic programming [REPT-88-025] N89-19915
Status of DOE information network modifications [DE89-005191] N89-20028

DATA BASES
Analysis of cost growth and cost composition in the defense aerospace industry [AD-A201544] N89-19227
An examination of the fatigue meter records from the RAAF (Royal Australian Air Force) caribou fleet [AD-A201074] N89-19290
Preparation of non-metals properties for data base [NASA-CR-183596] N89-19420
The standard chemical oxygen-iodine laser kinetics package [AD-A202223] N89-19543
Coordinates, conversions, and kinematics for the Rochester Robotics Lab [AD-A201611] N89-19560
A new database of ice particle size spectra for altitudes up to 10 km (30,000 ft) N89-19673
Calculation of molecular absorption parameters and updating the AFGL atmospheric line parameter compilation [AD-A202113] N89-19761
Preparing storm data [CRARP-88-6] N89-19777
An annotated bibliography of hypobaric decompression sickness research conducted at the Crew Technology Division, USAF School of Aerospace Medicine, Brooks AFB, Texas from 1983 to 1988 [AD-A201274] N89-19796
Testing expert systems N89-19834

DATA INTEGRATION
An architecture for integrating distributed and cooperating knowledge-based Air Force decision aids N89-19841
Presentation planning using an integrated knowledge base N89-19845

DATA LINKS
Electromagnetic compatibility test report for the tethered satellite data acquisition and control assembly [AD-A201549] N89-19468
Bitbus data transmission with galvanic separations [DIGEL-78] N89-19898

DATA MANAGEMENT
General aviation activity and avionics survey [AD-A201760] N89-19229
Electronic data generation and display system N89-19891
Computer technologies and institutional memory N89-20062

DATA PROCESSING
A data analysis system for unsteady turbulence measurements [AD-A201662] N89-19268
MODIS information, data and control system (MIDACS) operations concepts [NASA-TM-100720] N89-19729
Analysis of blending algorithms in computer graphics [AD-A201921] N89-19909

DATA PROCESSING TERMINALS
Next generation keyboards: The importance of cognitive compatibility N89-19848

DATA REDUCTION
Solid Earth ARISTOTELES mission data preprocessing simulation of gravity gradiometer [ESA-CR(P)-2666] N89-19766
Problems in structuring large-scale expert system N89-19925
On the great circle reduction in the data analysis for the astrometric satellite HIPPARCOS [ETN-89-93902] N89-20038

DATA SAMPLING
Stabilization and regulation of multirate sampled-date linear systems [REPT-88-013] N89-19930

DATA SIMULATION
Code performance simulation study for DRS S-band transmission [ESA-CR(P)-2688] N89-19482
Solid Earth ARISTOTELES mission data preprocessing simulation of gravity gradiometer [ESA-CR(P)-2666] N89-19766

DATA STORAGE
Computer technologies and institutional memory N89-20062

DATA STRUCTURES
Dynamic data structures for two-dimensional searching [AD-A201173] N89-19901

DATA TRANSFER (COMPUTERS)
Crossbar switch backplane and its application [DE89-005621] N89-19491

DATA TRANSMISSION
A new dropsonde for cloud probings N89-19728
Bitbus data transmission with galvanic separations [DIGEL-78] N89-19898

DAYTIME
Plasma waves at the dayside magnetopause [MPE-PREPRINT-128] N89-19996

DEBRIS
In-line wear monitor [AD-A201292] N89-19301
Ice/frost/debris assessment for space shuttle mission STS-27R, December 2, 1988 [NASA-TM-102144] N89-19326

DECEPTION
The importance of aircraft performance and signature reduction upon combat survivability [AD-A202106] N89-19292

DECISION MAKING
A case study of small group decision-making as influenced by the Abilene Paradox: The Challenger mishap [AD-A202102] N89-19328
Brain activity during tactical decision-making. Part 4: Event-related potentials as indices of selective attention and cognitive workload [AD-A201370] N89-19797
Artificial intelligent decision support for low-cost launch vehicle integrated mission operations N89-19830
An architecture for integrating distributed and cooperating knowledge-based Air Force decision aids N89-19841
A schema-based model of situation awareness: Implications for measuring situation awareness N89-19847
A method for modeling bias in a person's estimates of likelihoods of events N89-19849
An intelligent multi-media human-computer dialogue system N89-19850
Optimal solutions for complex design problems: Using isoperformance software for human factors trade offs N89-19860
JPRS report: Science and technology. Japan: 7th Artificial Intelligence Symposium [JPRS-JST-88-020] N89-19924
Evaluation support system for multiple R and D projects N89-19926
Factors affecting the adoption of R and D project selection techniques at the Air Force Write Aeronautical Laboratories [AD-A201543] N89-20025
Multicriteria analysis and budget allocation, with applications in energy R and D planning: A feasibility study [REPT-88-07] N89-20026
Stochastic and fuzzy PERT [REPT-88-26] N89-20027

DECODERS
The Telecommunications and Data Acquisition Report [NASA-CR-184812] N89-19451
A new VLSI architecture for a single-chip-type Reed-Solomon decoder N89-19455
Test aspects of the JPL Viterbi decoder N89-19457
On testing VLSI chips for the big Viterbi decoder N89-19458
Wiring Viterbi decoders (splitting deBruijn graphs) N89-19459

DECODING
A simplified procedure for decoding the (23,12) and (24,12) Golay codes N89-19456
Scheme86: An architecture for microcoding a scheme interpreter [AD-A201258] N89-19893

DECOMPOSITION
The dissociative adsorption of ammonia on Si(100) [AD-A201599] N89-19396
Power spectra decomposition of 36 RS CVn UBV photometric light curves from the first two years of the automatic photoelectric telescope N89-20036

DECOMPRESSION SICKNESS
An annotated bibliography of hypobaric decompression sickness research conducted at the Crew Technology Division, USAF School of Aerospace Medicine, Brooks AFB, Texas from 1983 to 1988
[AD-A201274] N89-19796
DEEP SPACE NETWORK
The Telecommunications and Data Acquisition Report
[NASA-CR-184812] N89-19451
Design and test of a 2.25-MW transformer rectifier assembly N89-19452
RF performance measurement of the DSS-14 70-meter antenna at C-band/L-band N89-19461
Systems analysis for DSN microwave antenna holography N89-19463
Ka-band study: 1988 N89-19464
DEFECTS
On testing VLSI chips for the big Viterbi decoder N89-19458
Machinery diagnostics via mechanical vibration analysis using spectral analysis techniques
[AD-A202089] N89-19594
DEFENSE COMMUNICATIONS SYSTEM (DCS)
Knowledge-based operation and management of communications systems N89-19826
DEFENSE INDUSTRY
Analysis of cost growth and cost composition in the defense aerospace industry
[AD-A201544] N89-19227
DEFENSE PROGRAM
Analysis of cost growth and cost composition in the defense aerospace industry
[AD-A201544] N89-19227
DEFORMATION
Processing of aluminum alloy 2090 for superplasticity
[AD-A201865] N89-19411
Elastic hysteresis phenomena in ULE and Zerodur optical glasses at elevated temperatures
[DE89-005183] N89-19423
Mixed formulation for frictionless contact problems
[NASA-TP-2897] N89-19580
DEGREES OF FREEDOM
An approach to semi-active control of multiple degree-of-freedom systems N89-19554
Dexterous robotic hands: Kinematics and control
[AD-A202183] N89-19570
Dexterity analysis and robot hand design N89-19865
Concept for a large master/slave-controlled robotic hand N89-19866
The WCSAR telerobotics test bed N89-19871
Telepresence and telerobotics N89-19873
A multi-sensor system for robotics proximity operations N89-19881
Normal forms and periodic solutions in the theory of nonlinear oscillations. Existence and asymptotic theory
[REPT-88-16] N89-19948
DELTA WINGS
Unsteady low-speed wind tunnel test of a straked delta wing, oscillating in pitch. Part 2: Plots of steady and zeroth and first harmonic unsteady pressure distributions
[AD-A201936] N89-19275
DEMODULATION
The Telecommunications and Data Acquisition Report
[NASA-CR-184812] N89-19451
The use of interleaving for reducing radio loss in convolutionally coded systems N89-19454
DEPOLARIZATION
Radar observations of precipitation microstructure: The morphology of linear depolarization measurements in cloud N89-19714
DEPOSITION
Pattern of air bubble inclusions in atmospheric ice formed during accretion N89-19676
Parameterizations of microphysical processes in clouds for application in models of regional atmospheric deposition N89-19709
DEPTH
Extracting depth by binocular stereo in a robot vision system
[DE89-005016] N89-19572
DESIGN ANALYSIS
Propulsion
[PNR90472] N89-19302
Maximum entropy/optimal projection design synthesis for decentralized control of large space structures
[AD-A202375] N89-19358
Booster propulsion/vehicle impact study
[NASA-CR-183584] N89-19366
Design improvement of a pump wear ring labyrinth seal
[NASA-CR-179161] N89-19555
Advanced extravehicular activity systems requirements definition study. Phase 2: Extravehicular activity at a lunar base
[NASA-CR-172117] N89-19809
Next generation keyboards: The importance of cognitive compatibility N89-19848
Dexterity analysis and robot hand design N89-19865
DESORPTION
The adsorption and decomposition of NH3 on Si(100): Detection of the NH2(a) species
[AD-A201601] N89-19397
DETECTION
Advancement of high resolution radar polarimetry in target verses clutter detection, discrimination, classification. A: Basic theory and modeling of polarimetric clutter phenomenology
[AD-A201240] N89-19467
Noncontact ultrasonic sensing of weld pools for automated welding
[DE89-005185] N89-19557
Structural saliency: The detection of globally salient structures using a locally connected network
[AD-A201619] N89-19806
DETECTORS
Evaluation of available analytical techniques for monitoring the quality of space station potable water N89-20071
DETONATION WAVES
A fundamental mathematical theory in the dynamics of combustion processes
[AD-A201284] N89-19391
High strain-rate behaviour of polymers using blast-wave and impact-loading methods N89-19592
DEUTERIUM
The dissociative adsorption of ammonia on Si(100)
[AD-A201599] N89-19396
DEUTERIUM PLASMA
Possibilities for breakeven and ignition of D-He3 fusion fuel in a near term tokamak
[KFK-4433] N89-19992
DHC 4 AIRCRAFT
An examination of the fatigue meter records from the RAAF (Royal Australian Air Force) caribou fleet
[AD-A201074] N89-19290
DIAGNOSIS
A design and implementation methodology for diagnostic systems N89-19831
Diagnosis by integrating model-based reasoning with knowledge-based reasoning N89-19835
DIAMETERS
Liquid water content, median volume diameter and temperature in dependence on the height above the cloud base for different types of clouds --- aircraft icing N89-19662
DIELECTRIC PROPERTIES
Active and passive remote sensing of ice
[AD-A201915] N89-19792
DIELECTRICS
Millimeter wave antennas
[AD-A201919] N89-19474
DIETS
Comparison of Soviet and US space food and nutrition programs N89-20059
DIFFERENTIAL EQUATIONS
Born-Infeld equations and minimal surfaces
[DE88-704966] N89-19936
Normal forms and periodic solutions in the theory of nonlinear oscillations. Existence and asymptotic theory
[REPT-88-16] N89-19948
DIFFUSERS
An experimental evaluation of S-duct inlet-diffuser configurations for turboprop offset gearbox applications
[NASA-CR-179454] N89-19556
DIFFUSION
The boundary element method for the diffusion equation N89-19233
DIFFUSION COEFFICIENT
Oxygen diffusion in YBa2Cu3O7-delta
[DE89-005831] N89-20011
SIMS measurement of oxygen tracer diffusion in YBa2Cu3O7-delta
[DE89-005884] N89-20014
DIFFUSION FLAMES
The analytical modeling of a turbulent diffusion flame behind a backward facing step N89-19386
DIFFUSION THEORY
Cell-centered and vertex-centered discretization of interface problems
[REPT-88-18] N89-19949
DIFFUSION WELDING
The diffusion bonding of aeroengine components
[PNR90540] N89-19308
DIGITAL FILTERS
Design of digital filters for navigation receivers --- GPS
[DFVLR-MITT-88-23] N89-19288
DIGITAL SYSTEMS
A variable-gain output feedback control design methodology
[NASA-CR-4226] N89-19316
Opto-electronic systems research. Image recovery from partial Fresnel zone information
[AD-A201556] N89-19969
DIGITAL TECHNIQUES
Application of the OCCAM/transputer conception as busless multiprocessor system in a digital controller
[DFVLR-FB-88-40] N89-19896
DIMERS
Some 2H NMR studies of oriented fluid phases
[AD-A201241] N89-19998
DIOXIDES
The coupled cluster method and the properties of energetic materials
[AD-A201168] N89-19388
DIRECT BROADCAST SATELLITES
Study on checkout of flight units and subsystems --- ground support
[ESA-CR(P)-2693] N89-19816
DIRECT CURRENT
An electrochemical study of corrosion protection by primer-topcoat systems on 4130 steel with ac impedance and dc methods
[NASA-TP-2820] N89-19406
Comparison of an ac and a dc bridge for standard platinum resistance thermometer calibrations
[DE89-007060] N89-19534
DIRECTIONAL STABILITY
Analytical interpretation on lateral/directional stability and controllability of high angle-of-attack reentry flight
[ISAS-630] N89-19353
DISCONTINUITY
Computation of stereo and visual motion: From biophysics to psychophysics
[AD-A201873] N89-19802
Large wave number aperture limited Fourier inversion and inverse scattering
[AD-A202247] N89-19940
DISORDERS
Diagnosis by integrating model-based reasoning with knowledge-based reasoning N89-19835
DISPENSERS
Short-range anti-armour flight vehicles of the Apache/CWS family
[DRIC-T-8130] N89-19296
DISPLACEMENT
The elastic stress and the displacement on the surfaces of two rubber-clad steel cylinders between which paper is led
[REPT-88-23] N89-19603
DISPLACEMENT MEASUREMENT
Boundary layer and singularity measurement in three dimensional fracture problems
[AD-A201277] N89-19584
DISPLAY DEVICES
The efficacy of color-coded symbols to enhance air-traffic control displays
[AD-A201594] N89-19284
A schema-based model of situation awareness: Implications for measuring situation awareness N89-19847
An intelligent multi-media human-computer dialogue system N89-19850
Knowledge-based graphical interfaces for presenting technical information N89-19851
A representational framework and user-interface for an image understanding workstation N89-19878
Electronic data generation and display system N89-19891
High-speed real-time animated displays on the ADAGE (trademark) RDS 3000 raster graphics system
[NASA-TM-4095] N89-19899
DISSOCIATION
The dissociative adsorption of ammonia on Si(100)
[AD-A201599] N89-19396
DISTORTION
Electron beam welding of 6061-T6 covers to A356-T6 machined cast housings
[BDX-613-3915] N89-19573
DISTRIBUTED PROCESSING
CIRCA 2000 operations criteria N89-19829
DISTRIBUTION (PROPERTY)
A study of the ionospheric signature of ion supply from the ionosphere to the magnetosphere N89-19754
DISTRIBUTION FUNCTIONS
Discrete event systems with stochastic processing times
[REPT-88-11] N89-19946
Minification processes
[AD-A202219] N89-19958
Estimation of a restricted variance ratio
[AD-A202268] N89-19959
DISTRIBUTION MOMENTS
Large deviation local limit theorems for ratio statistics
[AD-A201169] N89-19954

DIVERGENCE
The divergence characteristics of constrained-sheath optics systems for use with 5-eV atomic oxygen sources [NASA-CR-182238] N89-19973
DOCUMENTATION
Electronic data generation and display system N89-19891
DOMAINS
The electromagnetic modeling of thin apertures using the finite-difference time-domain technique [NASA-CR-178280] N89-19780
DOPED CRYSTALS
Laser-spectroscopic investigations of manganese centers in the zinc sulfide host lattice [ETN-89-93791] N89-20007
Thermal oxidation of 3-5 compound semiconductors [DE89-007127] N89-20020
DOPPLER RADAR
TDWR (Terminal Doppler Weather Radar) scan strategy requirements [AD-A201785] N89-19473
Multiparameter Doppler radar observations of a squall line with the polarimetric DFVLR radar N89-19715
Applications of the NCAR Electra Doppler radar for the study of physical parameters of clouds N89-19717
A preliminary study of precursors to Huntsville microbursts [AD-A200914] N89-19782
DOWNLINKING
The Telecommunications and Data Acquisition Report [NASA-CR-184812] N89-19451
A new VLSI architecture for a single-chip-type Reed-Solomon decoder N89-19455
Microwave time delays for the dual L-C-band feed system N89-19462
Ka-band study: 1988 N89-19464
A low-loss linear analog phase modulator for 8415 MHz transponder application N89-19465
DRAG MEASUREMENT
Drag measurements on a laminar-flow body of revolution in the 13-inch magnetic suspension and balance system [NASA-TP-2895] N89-19232
Drag coefficients for irregular fragments [AD-A201943] N89-19276
DRAG REDUCTION
Use of riblets to obtain drag reduction on airfoils at high Reynolds number flows [AD-A201485] N89-19267
Turbulence structure and mass transport in a channel flow with polymer injection [AD-A202237] N89-19521
DRONE AIRCRAFT
RPV (Remote Piloted Vehicle) applications in the US Navy [AD-A202151] N89-19293
DROP SIZE
The use of automatic particle recognition to improve the determination of bulk quantities from PMS 2-D probe data in cirrus N89-19651
On the determination of droplet size distributions with the counterflow virtual impactor --- cloud physics N89-19655
Multiparameter characterization of raindrop size distribution by the polarimetric DFVLR radar: First results N89-19656
Chemical evolution within in a cloud model featuring a polydisperse droplet size spectrum N89-19703
DROPS (LIQUIDS)
Characteristic time model validation [AD-A201374] N89-19510
Computational studies of evaporating sprays in a shear layer [AD-A201932] N89-19520
Spreading supercooled water droplets on an ice surface N89-19614
Measurements of the partitioning of aerosol mass and number between cloud droplets and interstitial air N89-19616
The calculation of supersaturations and growth of droplets in continental cumulus clouds N89-19617
Evaluation of droplet growth rates in Hawaiian orographic clouds N89-19619
Entrainment sites, mixing processes in warm convective clouds: Effect on droplet growth N89-19630
Heterogeneous mixing measurements in small nonprecipitating cumuli N89-19635
The effect of turbulence on the collection of cloud drops: A stochastic model N89-19637
The study of numerical simulation on the formation of the cloud droplet spectra in cumulus clouds N89-19642
An investigation of the effect of electrical charges on the collision efficiency of cloud drops N89-19657
Microphysical and electrical phenomena during freezing of water drops N89-19658
Kinetic equation for polluted cloud droplets spectrum N89-19661
A parametrization scheme for the coalescence of water drops using the stochastic collection equation N89-19671
The collection efficiencies of soft-hailstones for super-cooled water droplets and ice crystals N89-19678
DROPSONDES
A new dropsonde for cloud probings N89-19728
DUCTED FLOW
Duct flow nonuniformities for Space Shuttle Main Engine (SSME) [NASA-CR-183595] N89-19367
DUCTILITY
Processing of aluminum alloy 2090 for superplasticity [AD-A201865] N89-19411
DUCTS
An experimental evaluation of S-duct inlet-diffuser configurations for turboprop offset gearbox applications [NASA-CR-179454] N89-19556
DURABILITY
The gas turbine engine and its certification [PNR90496] N89-19303
DUST
Analytical, numerical and experimental investigations of oblique-shock-wave reflections in pure and dusty gases [AD-A201438] N89-19511
DWARF GALAXIES
The distribution of the interstellar medium in the Scd galaxy NGC 6946 and in a sample of dwarf irregular galaxies N89-20043
DWARF NOVAE
Implications of the observed contraction of accretion disks in quiescent dwarf novae N89-20047
DYE LASERS
High average power excimer laser-pumped dye oscillators [DE89-006547] N89-19552
DYNAMIC CHARACTERISTICS
Laser scattering studies of epoxy polymerization processes [AD-A201925] N89-19430
A three-dimensional nonsingular simulation of rigid manipulators [AD-A201964] N89-19569
Dynamic data structures for two-dimensional searching [AD-A201173] N89-19901
Intermolecular and intramolecular vibrational relaxation and energy transfer [AD-A201610] N89-19974
DYNAMIC CONTROL
Estimating projected controllable sets for dynamical control systems N89-19313
Implementation of dynamic control of a single-link flexible arm using a general micro-computer [AD-A201622] N89-19561
Control of flexible structures: Model errors, robustness measures, and optimization of feedback controllers [AD-A202234] N89-19596
DYNAMIC MODELS
Hypervelocity technology escape system concepts. Volume 2: Software manual [AD-A201720] N89-19281
Intelligent tutoring in the spacecraft command/control environment N89-19855
The use of the articulated total body model as a robot dynamics simulation tool N89-19872
Temperature and circulation in the stratospheres of the outer planets [NASA-CR-184826] N89-20051
Episodic volcanism of tidally heated satellites with application to Io. Thermal state of an ice shell on Europa. Polar wander of a synchronously rotating satellite with application to Europa N89-20052
DYNAMIC RESPONSE
AGARD standard aeroelastic configurations for dynamic response N89-19246
Investigation and suppression of high dynamic response encountered on an elastic supercritical wing N89-19255
Turbomachinery aeroelasticity at NASA Lewis Research Center N89-19262
Nonlinear dynamic analysis of embedded structures [AD-A201728] N89-19593
DYNAMIC STABILITY
Application of model based control to robotic manipulators N89-19884
DYNAMIC STRUCTURAL ANALYSIS
Proceedings of the Fifth AFOSR Forum on Space Structures [AD-A194761] N89-19333
Wave propagation in large space structures N89-19335
A recursive method for parallel processor multiflexible body dynamic simulation N89-19336
Concept of adaptive structures N89-19338
Comments on electromechanical actuators for controlling flexible structures N89-19339
Active control of elastic wave motion in structural networks N89-19342
Adaptive control of large space structures N89-19343
A finite element dynamic analysis of flexible spatial mechanisms and manipulators [ETN-89-93901] N89-19575
Nonlinear dynamic analysis of embedded structures [AD-A201728] N89-19593
Machinery diagnostics via mechanical vibration analysis using spectral analysis techniques [AD-A202089] N89-19594
DYNAMICAL SYSTEMS
Estimating projected controllable sets for dynamical control systems N89-19313
Hyperbolicity properties of C sup 2 multimodal Collet-Eckmann maps without Schwarzian deriative assumptions [REPT-88-10] N89-19945
DYNAMICS EXPLORER SATELLITES
Study of the continuous/diffuse aurora using particle observations from the Dynamics Explorer satellites [AD-A202241] N89-19763

E

EARTH ATMOSPHERE
Results of time and height resolved scavenging experiments --- atmospheric chemistry N89-19697
Oxidation regimes in orographic capping cloud N89-19698
An examination of the chemical and physical variability of clouds at a mountain-top site in central Sweden N89-19699
Influences of cloud microphysics on continental and marine precipitation chemistry N89-19700
Concentrations in rain events collected sequentially: Measurements vs results of a simple scavenging model N89-19701
Experiments on microphysics and chemistry of radiation fogs N89-19702
Chemical evolution within in a cloud model featuring a polydisperse droplet size spectrum N89-19703
Modeling studies on the formation, growth, dissipation and acidification of cumulus clouds N89-19704
A numerical investigation of sulfate production and deposition in midlatitude continental cumulus clouds N89-19705
A numerical simulation of the acidification process of rain water below the cloud and the mechanism of acid rain formation in area of Chongqing, China N89-19706
Effects of cloud microphysical processes on trace chemical removal efficiences N89-19707
Dynamic, radiative and chemical effects of clouds on tropospheric trace gases N89-19708
Parameterizations of microphysical processes in clouds for application in models of regional atmospheric deposition N89-19709
A model of wet deposition to complex terrain by the seeder-feeder process N89-19710
Meteorological and chemical influencing factors on acidity production in a mesoscale model with quasi-spectral microphysics N89-19711
A comparison of radiometric and immersion temperature measurements in water clouds N89-19712
A poor man's optical fog detector N89-19716
Applications of the NCAR Electra Doppler radar for the study of physical parameters of clouds N89-19717
On the small scale topographical influences on precipitation N89-19720
A numerical investigation of an orographic precipitation event N89-19721
Complex microphysical interactions within a central Sierra Nevada orographic cloud system N89-19722
Comparison of orographic cloud and precipitation development of three different geographic locations using a 3-D nested grid cloud model N89-19723
Microphysical and dynamical interactions in Colorado front range upslope storms N89-19725
Characteristics of radar echo of snow band formed in the lee side of a mountain N89-19726
Study on cloud and rain by microwave radiometer observation N89-19727
A new dropsonde for cloud probings N89-19728
EARTH CRUST
Evaluation of crustal recycling during the evolution of Archean-age Matachewan basaltic magmas N89-20077
Lithospheric buckling and intra-arc stresses: A mechanism for arc segmentation N89-20078
EARTH GRAVITATION
Variable gravity research facility [NASA-CR-184714] N89-19324

EARTH IONOSPHERE
A study of the ionospheric signature of ion supply from the ionosphere to the magnetosphere N89-19754
EARTH MAGNETOSPHERE
Electric fields in earth orbital space
[AD-A201747] N89-19760
Substorms, plasmoids, flux robes, and magnetotail flux loss on March 25, 1983: CDAW-8
[NASA-CR-184823] N89-19764
EARTH ORBITAL ENVIRONMENTS
Flight model discharge system
[AD-A201605] N89-19354
The effects of simulated space environmental parameters on six commercially available composite materials
[NASA-TP-2906] N89-19385
EARTH ORBITS
Electric fields in earth orbital space
[AD-A201747] N89-19760
EARTH SURFACE
Mass-radius star evolution Sun activity planets surfaces on purely empirical basis. Empiry theory reality: The use of statistics
[REPT-18] N89-20050
EARTH-VENUS TRAJECTORIES
The Ninevah Mission: A design summary for an unmanned mission to Venus, volume 1
[NASA-CR-184705] N89-20040
The Ninevah Mission: Analytical analyses and calculations for trajectory and propulsion, volume 2
[NASA-CR-184706] N89-20041
ECONOMIC ANALYSIS
Economic analysis of NAVSAT system
[REPT-1013-CA/TS] N89-19285
ECONOMIC FACTORS
The development of a cislunar space infrastructure
[NASA-CR-184728] N89-19352
EDDY VISCOSITY
Instability theory in clouds and the parameterization of eddy viscosity coefficients N89-19633
EDITING ROUTINES (COMPUTERS)
Computer software used in US Army Anthropometric Survey 1987-1988
[AD-A201165] N89-19812
User-extensible graphics using abstract structure
[BR104469] N89-19921
A curve-fitting package for personal computers
[LA-11082-MS] N89-19922
EDUCATION
An intelligent tutoring system for space shuttle diagnosis N89-19853
Optimal solutions for complex design problems: Using isoperformance software for human factors trade offs N89-19860
Simulation of the human-telerobot interface N89-19861
Development of a personal-computer-based intelligent tutoring system N89-19889
Intelligent embedded instruction for Computer-Aided Design (CAD) systems
[AD-A201811] N89-19907
Calendar of selected aeronautical and space meetings: January 1989 onwards
[AGARD-CAL-89/1] N89-20024
EFFICIENCY
Wind-tunnel results of advanced high-speed propellers at takeoff, climb, and landing Mach numbers
[NASA-TM-87030] N89-19265
EIGENVECTORS
Robust eigenstructure assignment by a projection method: Application using multiple optimization criteria N89-19349
ELASTIC BODIES
Elastic cross-influence between two quasi-Hertzian contact zones
[REPT-88-45] N89-19576
Some new results in rolling contact
[REPT-88-46] N89-19577
ELASTIC DEFORMATION
Modeling of flexible spacecraft accounting for orbital effects N89-19334
ELASTIC MEDIA
The stability of boundary layer flow over elastic substrates N89-19524
ELASTIC PROPERTIES
Concept of adaptive structures N89-19338
Interdisciplinary research in viscoelasticity and rheology
[AD-A201270] N89-19390
Elastic cross-influence between two quasi-Hertzian contact zones
[REPT-88-45] N89-19576
ELASTIC WAVES
Active control of elastic wave motion in structural networks N89-19342
Theoretical and experimental studies of selected topics in the rheology of fluids
[AD-A201460] N89-19512
Pressure variation over a solid wavy surface
[AD-A201724] N89-19517
ELASTOMERS
Preparation of non-metals properties for data base
[NASA-CR-183596] N89-19420
ELECTRIC BRIDGES
Comparison of an ac and a dc bridge for standard platinum resistance thermometer calibrations
[DE89-007060] N89-19534
ELECTRIC CHARGE
The effect of charge on coalescence of small precipitation drops at terminal velocity N89-19606
An investigation of the effect of electrical charges on the collision efficiency of cloud drops N89-19657
Microphysical and electrical phenomena during freezing of water drops N89-19658
ELECTRIC CONNECTORS
New approaches to reconfigurable optical interconnections for optical computing
[AD-A201307] N89-19982
ELECTRIC CONTACTS
Ohmic contacts to gallium aluminum arsenide for high temperature applications
[AD-A202248] N89-19492
ELECTRIC CONTROL
Remote control system --- spectrometer
[DIGEL-79] N89-19917
ELECTRIC FIELDS
Effect of the electric field on the raindrop shape N89-19659
Measurement of atmospheric electrical fields in periods of electrical perturbation and calm at the latitude of 23 C
[INPE-4626-PRE/1344] N89-19750
Electric fields in earth orbital space
[AD-A201747] N89-19760
Excitation of strong high-frequency electric fields and their detection using the dynamic Stark effect
[ETN-89-93794] N89-19991
ELECTRIC MOTORS
Starting characteristics of direct current motors powered by solar cells
[NASA-TM-101981] N89-19493
ELECTRIC PROPULSION
MPD (Magnetoplasmadynamic) thrust chamber flow dynamics
[AD-A201263] N89-19368
ELECTRIC STIMULI
Fear-potential startle as a model system for analyzing learning and memory
[AD-A201330] N89-19805
ELECTRIC SWITCHES
Investigation of the performance of photoconductive switches
[AD-A201425] N89-19489
ELECTRICAL ENGINEERING
Activities report in electrotechnology
[ETN-89-93715] N89-19448
Peaceful uses of electrical engineering in space N89-19487
ELECTRICAL FAULTS
Automatic Detection of Electric Power Troubles (ADEPT) N89-19825
Knowledge-based operation and management of communications systems N89-19826
ELECTRICAL MEASUREMENT
Lightning campaign 85/86 Transall C160 A04: Flying tests
[REPT-85/535800] N89-19297
Measurement of atmospheric electrical fields in periods of electrical perturbation and calm at the latitude of 23 C
[INPE-4626-PRE/1344] N89-19750
ELECTRICAL PROPERTIES
The aqueous electrochemistry of polyacetylene (CH)x and polyparaphenylene
[AD-A201461] N89-19426
ELECTRO-OPTICAL PHOTOGRAPHY
National Aeronautics and Space Administration (NASA)/American Society for Engineering Education (ASEE) Summer Faculty Fellowship Program 1988, volume 2 --- Author
[NASA-CR-172118-VOL-2] N89-20073
Toward an image compression algorithm for the high-resolution electronic still camera N89-20079
ELECTRO-OPTICS
Determination of general and specific properties of wide energy-band gap HgCdTe in the 1 to 2 micrometer wavelength range
[AD-A201341] N89-19488
Opto-electronic systems research. Image recovery from partial Fresnel zone information
[AD-A201556] N89-19969
ELECTROCHEMICAL CELLS
To measure and characterize metal corrosion in electrolyte solutions by exploiting the properties of superconducting
[AD-A201484] N89-19407
ELECTROCHEMICAL CORROSION
An electrochemical study of corrosion protection by primer-topcoat systems on 4130 steel with ac impedance and dc methods
[NASA-TP-2820] N89-19406
To measure and characterize metal corrosion in electrolyte solutions by exploiting the properties of superconducting
[AD-A201484] N89-19407
Passivity and corrosion of probe metals
[ETN-89-93984] N89-19416
ELECTROCHEMISTRY
Investigation of the interface between two immiscible electrolytes applied to membrane electrochemistry
[AD-A201310] N89-19393
Applications of scanning tunneling microscopy to electrochemistry
[AD-A201613] N89-19398
The aqueous electrochemistry of polyacetylene (CH)x and polyparaphenylene
[AD-A201461] N89-19426
Chemistry and physics of polyacetylene, (CH)x: The prototype conducting polymer
[AD-A201933] N89-19431
ELECTRODES
To measure and characterize metal corrosion in electrolyte solutions by exploiting the properties of superconducting
[AD-A201484] N89-19407
Oxygen electrode in molten carbonate fuel cells
[DE89-005813] N89-19745
ELECTROLUMINESCENCE
Determination of general and specific properties of wide energy-band gap HgCdTe in the 1 to 2 micrometer wavelength range
[AD-A201341] N89-19488
ELECTROLYTES
To measure and characterize metal corrosion in electrolyte solutions by exploiting the properties of superconducting
[AD-A201484] N89-19407
ELECTROMAGNETIC COMPATIBILITY
Electromagnetic compatibility test report for the tethered satellite data acquisition and control assembly
[AD-A201549] N89-19468
ELECTROMAGNETIC FIELDS
Generalized three-dimensional experimental lightning code (G3DXL) user's manual
[NASA-CR-166079] N89-19779
ELECTROMAGNETIC INTERACTIONS
MPD (Magnetoplasmadynamic) thrust chamber flow dynamics
[AD-A201263] N89-19368
Analysis and synthesis of microstrip antennas including mutual coupling
[AD-A201783] N89-19472
ELECTROMAGNETIC NOISE
The importance of aircraft performance and signature reduction upon combat survivability
[AD-A202106] N89-19292
Computer algorithms for measurement control and signal processing of transient scattering signatures
[AD-A201672] N89-19469
ELECTROMAGNETIC PROPERTIES
The electromagnetic modeling of thin apertures using the finite-difference time-domain technique
[NASA-CR-178280] N89-19780
Josephson effect research in high-temperature superconductors
[AD-A201483] N89-20002
ELECTROMAGNETIC RADIATION
Normalized radar cross section of natural surfaces at millimeter wavelengths
[AD-A202252] N89-19475
An invariant imbedding T matrix approach to electromagnetic scattering
[AD-A202298] N89-19476
ELECTROMAGNETIC SCATTERING
An invariant imbedding T matrix approach to electromagnetic scattering
[AD-A202298] N89-19476
ELECTROMAGNETIC WAVE TRANSMISSION
Electric fields in earth orbital space
[AD-A201747] N89-19760
ELECTROMAGNETISM
MPD (Magnetoplasmadynamic) thrust chamber flow dynamics
[AD-A201263] N89-19368
ELECTROMECHANICS
Comments on electromechanical actuators for controlling flexible structures N89-19339

JPRS report: Science and technology. USSR: Electronics and electrical engineering
[JPRS-UEE-88-005] N89-19485
Peaceful uses of electrical engineering in space N89-19487

ELECTRON ACCELERATORS
Free-electron laser driven by the NBS (National Bureau of Standards) CW microtron
[AD-A201170] N89-19535

ELECTRON BEAM WELDING
Electron beam welding of 6061-T6 covers to A356-T6 machined cast housings
[BDX-613-3915] N89-19573

ELECTRON BEAMS
Free-electron laser driven by the NBS (National Bureau of Standards) CW microtron
[AD-A201170] N89-19535
Description of FEL3D: A three dimensional simulation code for TOK and FEL
[DE89-005529] N89-19540
Electron-beam pumped liquid excimer lasers
[DE89-006549] N89-19549
Modeling the energy deposition in the Aurora KrF laser amplifier chain
[DE89-006545] N89-19550
On the use of multiple photon processes in krypton for laser guiding of electron beams
[DE89-006546] N89-19551

ELECTRON DENSITY (CONCENTRATION)
Infrared and ionization structure of the polar mesosphere
[AD-A201266] N89-19751
Study of the continuous/diffuse aurora using particle observations from the Dynamics Explorer satellites
[AD-A202241] N89-19763
An assessment of the application of in situ ion-density data from DMSP (Defense Meteorology Satellite Program) to modeling of transionospheric scintillation
[AD-A202415] N89-19765

ELECTRON DISTRIBUTION
Chaotic electron motion caused by sidebands in free electron lasers
[AD-A201635] N89-19538

ELECTRON ENERGY
Chaotic electron motion caused by sidebands in free electron lasers
[AD-A201635] N89-19538

ELECTRON IMPACT
Kinetic processes in discharge pumped mercury halide lasers
[AD-A201612] N89-19537

ELECTRON MICROSCOPY
Analysis of PERSHING 2 Reentry Vehicle (RV) control ring castings
[AD-A201548] N89-19559

ELECTRON SCATTERING
Ion and electron interactions at thermal and suprathermal energies
[AD-A201418] N89-19394

ELECTRON SPECTROSCOPY
The adsorption and decomposition of NH3 on Si(100): Detection of the NH2(a) species
[AD-A201601] N89-19397
XPS and AES studies of thin oxide layers on niobium for superconducting RF cavities
[DE88-756073] N89-19997

ELECTRON TRANSFER
Studies of hydrogen-hydrogen and carbon-sulfur bond cleavage
[DE89-006116] N89-19403

ELECTRON TUNNELING
Josephson effect research in high-temperature superconductors
[AD-A201483] N89-20002

ELECTRON-ION RECOMBINATION
Ion and electron interactions at thermal and suprathermal energies
[AD-A201418] N89-19394

ELECTRONIC CONTROL
Analysis and synthesis of microstrip antennas including mutual coupling
[AD-A201783] N89-19472

ELECTRONIC SPECTRA
Determination of general and specific properties of wide energy-band gap HgCdTe in the 1 to 2 micrometer wavelength range
[AD-A201341] N89-19488

ELECTROPHYSICS
Chemistry and physics of polyacetylene, (CH)x: The prototype conducting polymer
[AD-A201933] N89-19431

ELECTROPHYSIOLOGY
Brain mechanisms underlying individual differences in reaction to stress: An animal model
[AD-A201595] N89-19801

ELECTROSTATIC PROBES
Ion and electron interactions at thermal and suprathermal energies
[AD-A201418] N89-19394

ELECTROSTATIC WAVES
Ion beam driven electrostatic shocks --- ionosphere
[MPE-PREPRINT-127] N89-19995

ELECTROSTATICS
A model of the electrostatic-aerodynamic shape of raindrops N89-19615
Electrostatic plasma waves and turbulence near auroral arcs N89-19758
A wide bandwidth electrostatic field sensor for lightning research
[NASA-TM-101539] N89-19783

ELEMENTARY PARTICLE INTERACTIONS
HERMES, a Monte Carlo program system for beam-materials interaction studies --- radiation transport
[JUEL-2203] N89-19979

ELLIPTIC DIFFERENTIAL EQUATIONS
Vertex-centered and cell-centered multigrid methods for interface problems
[REPT-88-42] N89-19953

ELONGATION
Tensile properties of Ti-6Al-2Sn-4Zr-2Mo sheet after superplastic deformation
[PNR90499] N89-19414

EMBEDDED COMPUTER SYSTEMS
A design and implementation methodology for diagnostic systems N89-19831
Portable inference engine: An extended CLIPS for real-time production systems N89-19843

EMBEDDING
Nonlinear dynamic analysis of embedded structures
[AD-A201728] N89-19593
Intelligent embedded instruction for Computer-Aided Design (CAD) systems
[AD-A201811] N89-19907

EMISSION SPECTRA
Spectral studies of propellant combustion: Experimental details and emission results for M-30 propellant
[AD-A201634] N89-19399
Ground-based Fabry-Perot observations of neutral and ionic atoms and molecules of comet Halley N89-20048

END EFFECTORS
Integration of a computerized two-finger gripper for robot workstation safety N89-19863
Local position control: A new concept for control of manipulators N89-19864
Dexterity analysis and robot hand design N89-19865
Concept for a large master/slave-controlled robotic hand N89-19866
The WCSAR telerobotics test bed N89-19871
Sensing human hand motions for controlling dexterous robots N89-19883

ENERGY BUDGETS
Some outstanding problems on the influence of clouds on radiation N89-19643
The climate inversion problem: A statistical/modeling approach N89-19784
Possibilities for breakeven and ignition of D-He3 fusion fuel in a near term tokamak
[KFK-4433] N89-19992

ENERGY CONSERVATION
Wind-tunnel results of advanced high-speed propellers at takeoff, climb, and landing Mach numbers
[NASA-TM-87030] N89-19265

ENERGY CONSUMPTION
Comparative performance evaluation of advanced AC and DC EV propulsion systems
[DE89-005419] N89-19498
Applications survey for remote photovoltaic power systems
[AD-A201937] N89-19741

ENERGY CONVERSION EFFICIENCY
Solar thermal technology
[DE89-000818] N89-19738
Research on high-efficiency, multi-gap, multijunction, amorphous-silicon-based alloy thin-film solar cells, phase 1
[DE89-000844] N89-19739
Silicon concentrator solar cell research
[DE89-005490] N89-19740
A study of the reliability of Stirling engines for distributed receiver systems
[DE89-006395] N89-19746

ENERGY GAPS (SOLID STATE)
Determination of general and specific properties of wide energy-band gap HgCdTe in the 1 to 2 micrometer wavelength range
[AD-A201341] N89-19488

ENERGY POLICY
Multicriteria analysis and budget allocation, with applications in energy R and D planning: A feasibility study
[REPT-88-07] N89-20026

ENERGY SPECTRA
The cosmic ray antiproton spectrum between 0.1 and 1.5 GeV kinetic energy N89-20057

ENERGY TECHNOLOGY
Solar thermal technology
[DE89-000818] N89-19738
Horizons of new energy technologies
[DFVLR-MITT-88-22] N89-19742
Multicriteria analysis and budget allocation, with applications in energy R and D planning: A feasibility study
[REPT-88-07] N89-20026

ENERGY TRANSFER
Proof of the feasibility of coherent and incoherent schemes for pumping a gamma-ray laser
[AD-A201931] N89-19542
Modeling the energy deposition in the Aurora KrF laser amplifier chain
[DE89-006545] N89-19550
Applications survey for remote photovoltaic power systems
[AD-A201937] N89-19741
Intermolecular and intramolecular vibrational relaxation and energy transfer
[AD-A201610] N89-19974

ENGINE CONTROL
The Atlas/Centaur 67 launch mishap
[GPO-80-201] N89-19332

ENGINE DESIGN
Large-scale Advanced Prop-fan (LAP) hub/blade retention design report
[NASA-CR-174786] N89-19299
Propulsion
[PNR90472] N89-19302
The relationship between manufacturing technology and design --- aircraft engines
[PNR90537] N89-19307

ENGINE MONITORING INSTRUMENTS
COMPASS: A generalized ground-based monitoring system
[PNR90483] N89-19894

ENGINE NOISE
Flight survey of the 757 wing noise field and its effects on laminar boundary layer transition. Volume 2: Data compilation
[NASA-CR-178217] N89-19505

ENGINE PARTS
The relationship between manufacturing technology and design --- aircraft engines
[PNR90537] N89-19307
The diffusion bonding of aeroengine components
[PNR90540] N89-19308
Improved silicon nitride for advanced heat engines
[NASA-CR-179525] N89-19421
Fatigue strength reduction model: RANDOM3 and RANDOM4 user manual. Appendix 2: Development of advanced methodologies for probabilistic constitutive relationships of material strength models
[NASA-CR-184796-APP-2] N89-19582

ENGINE TESTING LABORATORIES
Current diagnostic practice in gas turbine combustors
[PNR90530] N89-19306

ENGINE TESTS
The gas turbine engine and its certification
[PNR90496] N89-19303
Current diagnostic practice in gas turbine combustors
[PNR90530] N89-19306
Performance evaluation of military engine and gear oils in friction and wear devices
[AD-A202145] N89-19432
RE-1000 free-piston Stirling engine sensitivity test results
[NASA-TM-88846] N89-19737

ENGINEERING DRAWINGS
Browsing schematics: Query-filtered graphs with context nodes N89-19844

ENTRAINMENT
Entrainment and fine-scale (molecular) mixing --- clouds N89-19628
Airborne studies of the influence of entrainment on the vertical and horizontal microphysical structure of small cumulus clouds N89-19629
Entrainment sites, mixing processes in warm convective clouds: Effect on droplet growth N89-19630
Three-dimensional cumulus entrainment studies N89-19634

ENTROPY
Application of a full potential method to AGARD standard airfoils N89-19242
Applied partial differential equations and numerical analysis
[AD-A201749] N89-19939

ENVIRONMENT EFFECTS
A test of ice crystal production by aircraft N89-19622

ENVIRONMENTAL CONTROL
A bootstrap lunar base: Preliminary design review 2 [NASA-CR-184753] N89-19807
ENVIRONMENTAL ENGINEERING
Development of an atmospheric monitoring plan for space station N89-20065
ENVIRONMENTAL SURVEYS
Noise assessment of the rocket sled test track operation at Holloman AFB, New Mexico [AD-A201279] N89-19317
ENVIRONMENTS
Intelligent mobile robot working in unknown environment N89-19927
EPOXY COMPOUNDS
Laser scattering studies of epoxy polymerization processes [AD-A201925] N89-19430
EPOXY MATRIX COMPOSITES
Durability and damage tolerance of bismaleimide composites, volume 1 [AD-A201273] N89-19374
Characterization of IM7/8551-7 carbon/epoxy in compression and shear [DE89-005544] N89-19378
Durability and damage tolerance of bismaleimide composites. Volume 2: Appendix of crack growth and low-velocity impact data [AD-A201839] N89-19379
Measurements of the compressive behavior of AS4/3501-6 and IM7/8551-7 carbon/epoxy [DE89-005823] N89-19383
EQUATIONS OF MOTION
Time periodic control of a multiblade helicopter N89-19312
A recursive method for parallel processor multiflexible body dynamic simulation N89-19336
Maneuvering equations in terms of quasi-coordinate N89-19337
Nonlinear vibrations of composite material shells N89-19377
Interdisciplinary research in viscoelasticity and rheology [AD-A201270] N89-19390
Local position control: A new concept for control of manipulators N89-19864
A novel manipulator technology for space applications N89-19874
EQUILIBRIUM FLOW
Unsteady low-speed wind tunnel test of a straked delta wing, oscillating in pitch. Part 2: Plots of steady and zeroth and first harmonic unsteady pressure distributions [AD-A201936] N89-19275
EQUIPMENT SPECIFICATIONS
Superconducting gravity gradiometer mission. Volume 2: Study team technical report [NASA-TM-4091] N89-19749
Stratospheric nitric acid: Feasibility of routine measurement by observation from commercial airliners in IR bands from 9 to 14 microns [C-48-1977] N89-19770
The scintillating optical fiber isotope experiment (SOFIE): Bevalac calibrations of test models N89-20034
EQUIVALENCE
Criterion based equivalence for equation error models [WTHD-188] N89-19941
ERROR ANALYSIS
Examinations on TERCOM navigation by evaluation of test flights done over the testing areas Deister and Harz (Germany, F.R.) [DFVLR-FB-88-37] N89-19287
SCD2 satellite spin axis reorientation and feasibility study [INPE-4688-NTE/285] N89-19351
Error localization and updating of spacecraft structures mathematical models [YMD/EF/0175] N89-19361
Error norm guided flow analysis of shock-wave/boundary-layer interactions [AD-A201176] N89-19507
Criterion based equivalence for equation error models [WTHD-188] N89-19941
ERROR CORRECTING CODES
A simplified procedure for decoding the (23,12) and (24,12) Golay codes N89-19456
ERRORS
Error norm guided flow analysis of shock-wave/boundary-layer interactions [AD-A201176] N89-19507
Transient three-dimensional heat conduction computations using Brian's technique [AD-A201918] N89-19519
Control of flexible structures: Model errors, robustness measures, and optimization of feedback controllers [AD-A202234] N89-19596
The Cheyenne windstorm that never came: Another lesson in real time analysis [CRARP-88-1] N89-19772
A climatology of global precipitation N89-19787
ERS-1 (ESA SATELLITE)
Interpretation of ERS-1 wind scatterometer data: Wind field extraction [ETN-89-93982] N89-19790
ESA SATELLITES
Study of NAVSAT for precise positioning [IKU-88.068] N89-19286
Definition of the transmission system for a European data relay satellite [ESA-CR(P)-2632] N89-19359
PSDE/SAT-2 preliminary spacecraft configuration study, executive summary [ESA-CR(P)-2689] N89-19360
PSDE/SAT-2: Preliminary spacecraft configuration study, executive summary [ESA-CR(P)-2704] N89-19364
ESCAPE CAPSULES
Light weight escape capsule for fighter aircraft N89-19858
ESCAPE SYSTEMS
Hypervelocity technology escape system concepts. Volume 2: Software manual [AD-A201720] N89-19281
ESTIMATING
Estimating aircraft airframe tooling cost: An alternative to DAPCA 3 [AD-A201506] N89-19226
Optimal solutions for complex design problems: Using isoperformance software for human factors trade offs N89-19860
ETCHING
Hole formation (etching) in polymers by far (deep) UV high intensity laser (excimer) radiation pulses and its relevance to photoresists in deep UV photolysis of polymers [AD-A202274] N89-19433
EULER EQUATIONS OF MOTION
Unsteady transonic flow using Euler equations N89-19245
Solution of steady and unsteady transonic-vortex flows using Euler and full-potential equations N89-19248
Unsteady transonic viscous-inviscid interaction using Euler and boundary-layer equations N89-19250
Numerical solution of unsteady rotational flow past fixed and rotary wing configurations N89-19251
Transonic flutter calculations using the Euler equations N89-19258
Minimum time motion of a robotic manipulator N89-19567
EULER-LAGRANGE EQUATION
The use of the articulated total body model as a robot dynamics simulation tool N89-19872
Application of model based control to robotic manipulators N89-19884
EUROPA
Episodic volcanism of tidally heated satellites with application to Io. Thermal state of an ice shell on Europa. Polar wander of a synchronously rotating satellite with application to Europa N89-20052
EUROPEAN SPACE AGENCY
Experimental spherical near-field antenna test facility, phase 3. Volume 1: Facility updates, evaluation and software documentation [R-343] N89-19477
EUROPEAN SPACE PROGRAMS
Economic analysis of NAVSAT system [REPT-1013-CA/TS] N89-19285
EVALUATION
A methodology for automation and robotics evaluation applied to the space station telerobotic servicer N89-19882
JPRS report: Science and technology. Japan: 7th Artificial Intelligence Symposium [JPRS-JST-88-020] N89-19924
Evaluation support system for multiple R and D projects N89-19926
Equating an expert system to a classifier in order to evaluate the expert system N89-20080
EVAPORATION
Study of space aluminum coating, executive summary --- telescope mirrors [IOM/CAEE-002/87(TR)] N89-19443
Computational studies of evaporating sprays in a shear layer [AD-A201932] N89-19520
Evaporation and melting of ice crystals: A laboratory study N89-19612
EVOLUTION (DEVELOPMENT)
Analysis of hailstones from a severe storm and their simulated evolution N89-19677
EXCIMER LASERS
Hole formation (etching) in polymers by far (deep) UV high intensity laser (excimer) radiation pulses and its relevance to photoresists in deep UV photolysis of polymers [AD-A202274] N89-19433
Electron-beam pumped liquid excimer lasers [DE89-006549] N89-19549
On the use of multiple photon processes in krypton for laser guiding of electron beams [DE89-006546] N89-19551
EXCIMERS
Liquid excimers: Lasing Xe2 and Kr2 in liquid argon [DE89-005449] N89-19546
High average power excimer laser-pumped dye oscillators [DE89-006547] N89-19552
EXCITATION
NASTRAN supplemental documentation for modal forced vibration analysis of aerodynamically excited turbosystems [NASA-CR-174967] N89-19583
EXERCISE PHYSIOLOGY
National Aeronautics and Space Administration (NASA)/American Society for Engineering Education (ASEE) Summer Faculty Fellowship Program 1988, volume 1 [NASA-CR-172118-VOL-1] N89-20058
Effects on motor unit potentiation and ground reaction force from treadmill exercise N89-20069
EXHAUST NOZZLES
Arc jet diagnostics tests N89-20085
EXISTENCE THEOREMS
Normal forms and periodic solutions in the theory of nonlinear oscillations. Existence and asymptotic theory [REPT-88-16] N89-19948
EXPECTATION
Characterizations of conditional expectation-type oeprators [REPT-88-04] N89-19942
EXPERIMENT DESIGN
Variable gravity research facility [NASA-CR-184714] N89-19324
Telescience system concept study, volume 2 --- Columbus space station [MATRA-NT/2113/139-VOL-2] N89-19478
EXPERIMENTATION
Experiment plans to study preignition processes of a pool fire in low gravity [NASA-CR-182256] N89-19442
EXPERT SYSTEMS
Second Annual Workshop on Space Operations Automation and Robotics (SOAR 1988) [NASA-CP-3019] N89-19817
The scheduling techniques of ESP2 N89-19818
Space station payload operations scheduling with ESP2 N89-19819
A survey of planning and scheduling research at the NASA Ames Research Center N89-19820
An expert system for shuttle and satellite radar tracker scheduling N89-19821
Automation of the space station core module power management and distribution system N89-19822
EMMA: The expert system for munition maintenance N89-19823
Diagnostics in the Extendable Integrated Support Environment (EISE) N89-19824
Automatic Detection of Electric Power Troubles (ADEPT) N89-19825
Knowledge-based operation and management of communications systems N89-19826
NESSUS (Numerical Evaluation of Stochastic Structures Under Stress)/EXPERT: Bridging the gap between artificial intelligence and FORTRAN N89-19827
Knowledge-based zonal grid generation for computational fluid dynamics N89-19828
Artificial intelligent decision support for low-cost launch vehicle integrated mission operations N89-19830
A design and implementation methodology for diagnostic systems N89-19831
Application of flight systems methodologies to the validation of knowledge-based systems N89-19832
Validation of highly reliable, real-time knowledge-based systems N89-19833
Testing expert systems N89-19834
Diagnosis by integrating model-based reasoning with knowledge-based reasoning N89-19835
Transformation based endorsement systems N89-19836
Reducing uncertainty by using explanatory relationships N89-19837
Spaceborne VHSIC multiprocessor system for AI applications N89-19838
Autonomous satellite command and control: A comparison with other military systems N89-19839

Garbage collection can be made real-time and verifiable N89-19840
An architecture for integrating distributed and cooperating knowledge-based Air Force decision aids N89-19841
A parallel expert system for the control of a robotic air vehicle N89-19842
Portable inference engine: An extended CLIPS for real-time production systems N89-19843
Browsing schematics: Query-filtered graphs with context nodes N89-19844
Presentation planning using an integrated knowledge base N89-19845
An intelligent multi-media human-computer dialogue system N89-19850
An intelligent interface for satellite operations: Your Orbit Determination Assistant (YODA) N89-19852
An intelligent tutoring system for space shuttle diagnosis N89-19853
Intelligent tutoring systems research in the training systems division: Space applications N89-19854
Intelligent tutoring in the spacecraft command/control environment N89-19855
Knowledge acquisition for case-based reasoning systems N89-19856
Psychological tools for knowledge acquisition N89-19857
Design concept for the Flight Telerobotic Servicer (FITS) N89-19870
Telepresence and telerobotics N89-19873
A multi-sensor system for robotics proximity operations N89-19881
An expert system for restructurable control N89-19886
Expert systems applications for space shuttle payload integration automation N89-19887
Development of a personal-computer-based intelligent tutoring system N89-19889
SARSCEST (human factors) N89-19890
Electronic data generation and display system N89-19891
JPRS report: Science and technology. Japan: 7th Artificial Intelligence Symposium
[JPRS-JST-88-020] N89-19924
Problems in structuring large-scale expert system N89-19925
Evaluation support system for multiple R and D projects N89-19926
Intelligent mobile robot working in unknown environment N89-19927
Formal aspects of a knowledge system: A literature review
[REPT-88-12] N89-19933
National Aeronautics and Space Administration (NASA)/American Society for Engineering Education (ASEE) Summer Faculty Fellowship Program 1988, volume 1
[NASA-CR-172118-VOL-1] N89-20058
Computer technologies and institutional memory N89-20062
An evidential approach to problem solving when a large number of knowledge systems is available N89-20068
National Aeronautics and Space Administration (NASA)/American Society for Engineering Education (ASEE) Summer Faculty Fellowship Program 1988, volume 2 — Author
[NASA-CR-172118-VOL-2] N89-20073
Equating an expert system to a classifier in order to evaluate the expert system N89-20080

EXPLODING WIRES
High strain-rate behaviour of polymers using blast-wave and impact-loading methods N89-19592

EXPLOSIONS
A fundamental mathematical theory in the dynamics of combustion processes
[AD-A201284] N89-19391

EXPLOSIVES
Reaction chemistry of boron hydrides
[AD-A201243] N89-19389

EXPONENTIAL FUNCTIONS
On purely exponential logic queries
[AD-A201259] N89-19902

EXPULSION
Quench pressure, thermal expulsion, and normal zone propagation in internally cooled superconductors
[DE89-005668] N89-20003

EXTRACTION
Extracting depth by binocular stereo in a robot vision system
[DE89-005016] N89-19572

EXTRAGALACTIC RADIO SOURCES
An observational and numerical study of extragalactic radio sources N89-20055

EXTRAVEHICULAR ACTIVITY
Advanced extravehicular activity systems requirements definition study. Phase 2: Extravehicular activity at a lunar base
[NASA-CR-172117] N89-19809
Study on checkout of flight units and subsystems — ground support
[ESA-CR(P)-2693] N89-19816
National Aeronautics and Space Administration (NASA)/American Society for Engineering Education (ASEE) Summer Faculty Fellowship Program 1988, volume 2 — Author
[NASA-CR-172118-VOL-2] N89-20073
Visual perception and grasping for the extravehicular activity robot N89-20082

EXTREME ULTRAVIOLET RADIATION
XUV free-electron laser development at Los Alamos
[DE89-005458] N89-19547

EXTREMELY HIGH FREQUENCIES
Ka-band study: 1988 N89-19464

EYE (ANATOMY)
Development of a low-cost helmet mounted eye gaze sensor
[AD-A202303] N89-19298
The effects of a pitched field orientation on hand/eye coordination
[AD-A201620] N89-19814

F

F REGION
Electrostatic plasma waves and turbulence near auroral arcs N89-19758

F-15 AIRCRAFT
CAP-TSD analysis of the F-15 aircraft N89-19239

FABRICATION
Tensile and creep rupture behavior of P/M processed Nb-base alloy, WC-3009
[NASA-TM-101954] N89-19371
Improved silicon nitride for advanced heat engines
[NASA-CR-179525] N89-19421
Fabrication of XLWIR (Extra-Long-Wavelength-Infrared) window materials
[DE89-006418] N89-19439
Research on high-efficiency, multi-gap, multijunction, amorphous-silicon-based alloy thin-film solar cells, phase 1
[DE89-000844] N89-19739
Silicon concentrator solar cell research
[DE89-005490] N89-19740
Computer-aided fabrication system implementation
[AD-A202128] N89-19911

FABRICS
Preparation of non-metals properties for data base
[NASA-CR-183596] N89-19420

FABRY-PEROT SPECTROMETERS
Ground-based Fabry-Perot observations of neutral and ionic atoms and molecules of comet Halley N89-20048

FACE CENTERED CUBIC LATTICES
Anomalous slip in an FCC system
[DE89-002257] N89-19405

FAILURE
Safe, compact nuclear propulsion: Solid core nuclear propulsion concept
[AD-A202339] N89-19369
An interdisciplinary study of cathodic debonding in elastomer/metal adhesive bonds
[AD-A202376] N89-19434

FAILURE ANALYSIS
Composite reliability enhancement via reloading
[AD-A201861] N89-19380
Measurements of the compressive behavior of AS4/3501-6 and IM7/8551-7 carbon/epoxy
[DE89-005823] N89-19383
Diagnostics in the Extendable Integrated Support Environment (EISE) N89-19824
Problems in structuring large-scale expert system N89-19925

FAILURE MODES
Effect of adhesive interleaving and discontinuous plies on failure of composite laminates subject to transverse normal loads
[NASA-TM-101507] N89-19589

FAR FIELDS
Systems analysis for DSN microwave antenna holography N89-19463

FAR ULTRAVIOLET RADIATION
Hole formation (etching) in polymers by far (deep) UV high intensity laser (excimer) radiation pulses and its relevance to photoresists in deep UV photolysis of polymers
[AD-A202274] N89-19433

FARADAY EFFECT
Applications of scanning tunneling microscopy to electrochemistry
[AD-A201613] N89-19398

FATIGUE (BIOLOGY)
A study to analyze the degree of the relationship between health practices and fatigue
[AD-A201518] N89-19798
A stress test to evaluate the physical capacity of performing L-1 anti-G straining maneuvers
[AD-A202301] N89-19803

FATIGUE (MATERIALS)
An examination of the fatigue meter records from the RAAF (Royal Australian Air Force) caribou fleet
[AD-A201074] N89-19290
Fundamentals of fatigue and fracture mechanics
[AD-A201435] N89-19585

FATIGUE LIFE
Fatigue crack growth in ARALL: A hybrid aluminum Aramid composite material. Crack growth mechanisms and quantitative predictions of the crack growth rates
[ETN-89-93899] N89-19602

FATIGUE TESTS
Fatigue crack growth model RANDOM2 user manual. Appendix 1: Development of advanced methodologies for probabilistic constitutive relationships of material strength models
[NASA-CR-184775-APP-1] N89-19581
Fatigue strength reduction model: RANDOM3 and RANDOM4 user manual. Appendix 2: Development of advanced methodologies for probabilistic constitutive relationships of material strength models
[NASA-CR-184796-APP-2] N89-19582
Advanced durability analysis. Volume 4: Executive summary
[AD-A202304] N89-19597
Acoustic emission measurements during fatigue loading of scaled Pressurized Water Reactor (PWR) vessel at Joint Research Center of the European Communities (JRC), Ispra (Italy)
[CISE-4476] N89-19600
General review of recent activities in acoustic emission technology in Italy
[CISE-4477] N89-19601

FAULT TOLERANCE
CIRCA 2000 operations criteria N89-19829

FEAR
Fear-potential startle as a model system for analyzing learning and memory
[AD-A201330] N89-19805

FEASIBILITY ANALYSIS
Mini protein crystallization facility. Phase A study: Executive summary
[REPT-AQ-ES-576/88] N89-19444

FEEDBACK
Telepresence and telerobotics N89-19873

FEEDBACK CONTROL
A variable-gain output feedback control design methodology
[NASA-CR-4226] N89-19316
Comments on electromechanical actuators for controlling flexible structures N89-19339
System identification of suboptimal feedback control parameters based on limiting-performance/minimum-time characteristics N89-19340
Integrated Structural Analysis And Control (ISAAC): Issues and progress N89-19341
Majorant analysis of performance degradation due to uncertainty N89-19344
Decentralized/relegated control for large space structures N89-19346
Frobenius-Hankel norm framework for disturbance rejection and low order decentralized controller design N89-19347
Control of flexible structures: Model errors, robustness measures, and optimization of feedback controllers
[AD-A202234] N89-19596
The use of the articulated total body model as a robot dynamics simulation tool N89-19872

FERROUS METALS
In-line wear monitor
[AD-A201292] N89-19301

FIBER COMPOSITES
Heat transfer properties of satellite component materials N89-19375
Measurements of the compressive behavior of AS4/3501-6 and IM7/8551-7 carbon/epoxy
[DE89-005823] N89-19383
Reinforcement/matrix interaction in SiC fiber-reinforced Ni3Al matrix composites
[DE89-006041] N89-19384
The effects of simulated space environmental parameters on six commercially available composite materials
[NASA-TP-2906] N89-19385

Fatigue crack growth in ARALL: A hybrid aluminum Aramid composite material. Crack growth mechanisms and quantitative predictions of the crack growth rates
[ETN-89-93899] N89-19602

FIBERS
Durability and damage tolerance of bismaleimide composites, volume 1
[AD-A201273] N89-19374
A Monte Carlo simulation of the single-filament-composite test N89-19376

FIELD EFFECT TRANSISTORS
Ohmic contacts to gallium aluminum arsenide for high temperature applications
[AD-A202248] N89-19492

FIELD OF VIEW
Light weight escape capsule for fighter aircraft N89-19858

FIELD STRENGTH
Effect of the electric field on the raindrop shape N89-19659

FIGHTER AIRCRAFT
The importance of aircraft performance and signature reduction upon combat survivability
[AD-A202106] N89-19292
Durability and damage tolerance of bismaleimide composites. Volume 2: Appendix of crack growth and low-velocity impact data
[AD-A201839] N89-19379
Light weight escape capsule for fighter aircraft N89-19858

FINANCE
Commercial expendable launch vehicle liability
[S-HRG-100-750] N89-19325
Preliminary cost model for a commercial geostationary transportation company (GRET)
[ILR-MITT-208] N89-19330
Preliminary project plan for a GEO regional transportation and servicing company
[ILR-MITT-210] N89-19331

FINITE DIFFERENCE THEORY
Characteristic time model validation
[AD-A201374] N89-19510
The electromagnetic modeling of thin apertures using the finite-difference time-domain technique
[NASA-CR-178280] N89-19780

FINITE ELEMENT METHOD
Error localization and updating of spacecraft structures mathematical models
[YMD/EF/0175] N89-19361
Finite element analysis of laminated composite plates
[AD-A202192] N89-19381
Interdisciplinary research in viscoelasticity and rheology
[AD-A201270] N89-19390
A finite element dynamic analysis of flexible spatial mechanisms and manipulators
[ETN-89-93901] N89-19575
Mixed finite element models for free vibrations of thin-walled beams
[NASA-TP-2868] N89-19579
Mixed formulation for frictionless contact problems
[NASA-TP-2897] N89-19580
Passive vibration control using viscoelastic and constrained layer beam waveguide absorbers
[AD-A202188] N89-19595
Acoustic wave propagation in heterogeneous structures including experimental validation
[NASA-TM-101486] N89-19965

FINITE VOLUME METHOD
Transonic flutter calculations using the Euler equations N89-19258
Cell-centered and vertex-centered discretization of interface problems
[REPT-88-18] N89-19949

FIRES
Experiment plans to study preignition processes of a pool fire in low gravity
[NASA-CR-182256] N89-19442

FISSION PRODUCTS
Safe, compact nuclear propulsion: Solid core nuclear propulsion concept
[AD-A202339] N89-19369

FIXED WINGS
Numerical solution of unsteady rotational flow past fixed and rotary wing configurations N89-19251

FLAME PROPAGATION
Experiment plans to study preignition processes of a pool fire in low gravity
[NASA-CR-182256] N89-19442
The solid surface combustion space shuttle experiment hardware description and ground-based test results
[NASA-TM-101963] N89-19446

FLAME STABILITY
Flame driving of longitudinal instabilities in liquid fueled dump combustors
[AD-A201293] N89-19392

FLAPPING
Time periodic control of a multiblade helicopter N89-19312

FLEXIBLE BODIES
Proceedings of the Fifth AFOSR Forum on Space Structures
[AD-A194761] N89-19333
Comments on electromechanical actuators for controlling flexible structures N89-19339
Active control of elastic wave motion in structural networks N89-19342
The optimal projection equations for fixed-order dynamic compensation: Existence, convergence and global optimality N89-19345
Robust eigenstructure assignment by a projection method: Application using multiple optimization criteria N89-19349
Damage detection and location in large space trusses N89-19350
Control of flexible structures: Model errors, robustness measures, and optimization of feedback controllers
[AD-A202234] N89-19596
A robust control scheme for flexible arms with friction in the joints N89-19875
RCS/piezoelectric distributed actuator study
[AD-A201276] N89-19999

FLEXIBLE SPACECRAFT
Modeling of flexible spacecraft accounting for orbital effects N89-19334
A recursive method for parallel processor multiflexible body dynamic simulation N89-19336
Maneuvering equations in terms of quasi-coordinate N89-19337
Investigation of flight sensors and actuators for the vibration damping augmentation of large flexible space structures
[ESA-CR(P)-2670] N89-19362
A finite element dynamic analysis of flexible spatial mechanisms and manipulators
[ETN-89-93901] N89-19575

FLEXING
Chaotic dynamics and control of nonlinear and flexible arm robotic devices N89-19566

FLIGHT
Generalized three-dimensional experimental lightning code (G3DXL) user's manual
[NASA-CR-166079] N89-19779

FLIGHT ALTITUDE
Dexamethasone for prevention and treatment of acute mountain sickness
[AD-A201554] N89-19799

FLIGHT CHARACTERISTICS
Combined preliminary airworthiness evaluation and airworthiness and flight characteristics evaluation of the UH-1H with preproduction hub spring and composite main rotor blades installed
[AD-A202316] N89-19295

FLIGHT CONTROL
Hypervelocity technology escape system concepts. Volume 1: Development and evaluation
[AD-A201719] N89-19280
A systems approach to rotorcraft stability and control research
[AD-A201784] N89-19314

FLIGHT CREWS
A comparative analysis of tilt rotor aircraft versus helicopters using simulator results
[AD-A202190] N89-19294
Thermal stress in Ran Sea King Helicopter operations
[ARL-SYS-R-40] N89-19810

FLIGHT HAZARDS
TDWR (Terminal Doppler Weather Radar) scan strategy requirements
[AD-A201785] N89-19473
Liquid water content, median volume diameter and temperature in dependence on the height above the cloud base for different types of clouds --- aircraft icing N89-19662
A wide bandwidth electrostatic field sensor for lightning research
[NASA-TM-101539] N89-19783

FLIGHT MANAGEMENT SYSTEMS
Application of flight systems methodologies to the validation of knowledge-based systems N89-19832

FLIGHT OPERATIONS
Artificial intelligent decision support for low-cost launch vehicle integrated mission operations N89-19830

FLIGHT PATHS
Minimum required heliport airspace under visual flight rules
[AD-A201433] N89-19283

FLIGHT SIMULATION
Simultaneous three-dimensional modeling of commercial flights within the airspace of the Federal Republic of Germany
[DFVLR-FB-88-31] N89-19282

Fatigue crack growth in ARALL: A hybrid aluminum Aramid composite material. Crack growth mechanisms and quantitative predictions of the crack growth rates
[ETN-89-93899] N89-19602

FLIGHT TESTS
Examinations on TERCOM navigation by evaluation of test flights done over the testing areas Deister and Harz (Germany, F.R.)
[DFVLR-FB-88-37] N89-19287
Combined preliminary airworthiness evaluation and airworthiness and flight characteristics evaluation of the UH-1H with preproduction hub spring and composite main rotor blades installed
[AD-A202316] N89-19295
Lightning campaign 85/86 Transall C160 A04: Flying tests
[REPT-85/535800] N89-19297
Development of a low-cost helmet mounted eye gaze sensor
[AD-A202303] N89-19298
Flight survey of the 757 wing noise field and its effects on laminar boundary layer transition. Volume 2: Data compilation
[NASA-CR-178217] N89-19505

FLIGHT TIME
General aviation activity and avionics survey
[AD-A201760] N89-19229

FLOTATION
Positive Flotation Harness (PFH) for use by Canadian Forces search and rescue technicians
[AD-A200727] N89-19279

FLOW CHARACTERISTICS
The effect of prewhirl on the internal aerodynamics and performance of a mixed flow research centrifugal compressor
[NASA-CR-184756] N89-19503
A computationally efficient modelling of laminar separation bubbles
[NASA-CR-184789] N89-19504
Error norm guided flow analysis of shock-wave/boundary-layer interactions
[AD-A201176] N89-19507

FLOW CHARTS
Fast and processor-efficient parallel algorithms for reducible flow graphs
[AD-A201651] N89-19904

FLOW DISTRIBUTION
CAP-TSD analysis of the F-15 aircraft N89-19239
Flux-vector splitting for unsteady calculations on dynamic meshes N89-19244
Unsteady transonic flow using Euler equations N89-19245
Transonic Unsteady Aerodynamics and Aeroelasticity 1987, part 2
[NASA-CP-3022-PT-2] N89-19247
Solution of steady and unsteady transonic-vortex flows using Euler and full-potential equations N89-19248
Viscous flow calculations for the AGARD standard configuration airfoils with experimental comparisons N89-19249
Unsteady Navier-Stokes computations over airfoils using both fixed and dynamic meshes N89-19252
The oblique-wing research aircraft: A test bed for unsteady aerodynamic and aeroelastic research N89-19253
Static aeroelasticity of a composite oblique wing in transonic flows N89-19254
Investigation and suppression of high dynamic response encountered on an elastic supercritical wing N89-19255
Numerical computations of transonic critical aerodynamic behavior
[AD-A202412] N89-19277
Duct flow nonuniformities for Space Shuttle Main Engine (SSME)
[NASA-CR-183595] N89-19367
The analytical modeling of a turbulent diffusion flame behind a backward facing step N89-19386
The birth of open separation on a prolate spheroid
[AD-A201350] N89-19509
Application of Schlieren photography in gas turbine combustion research
[PNR90495] N89-19532
Laser transit anemometer software development program
[NASA-CR-4225] N89-19545
Experimental investigation of rotor-stator interaction in diffuser pumps N89-19564
The collection efficiency of a massive fog collector N89-19650
Knowledge-based zonal grid generation for computational fluid dynamics N89-19828
Model formulation of non-equilibrium gas radiation for hypersonic flight vehicles N89-20066

FLOW EQUATIONS
Calculation of steady and unsteady pressures at supersonic speeds with CAP-TSD N89-19240
A new pumpjet design theory
[AD-A201353] N89-19558
FLOW GEOMETRY
Duct flow nonuniformities for Space Shuttle Main Engine (SSME)
[NASA-CR-183595] N89-19367
FLOW MEASUREMENT
The effect of prewhirl on the internal aerodynamics and performance of a mixed flow research centrifugal compressor
[NASA-CR-184756] N89-19503
FLOW THEORY
Orientation of orbits in flows
[REPT-88-05] N89-19322
A new pumpjet design theory
[AD-A201353] N89-19558
FLOW VELOCITY
Use of riblets to obtain drag reduction on airfoils at high Reynolds number flows
[AD-A201485] N89-19267
Pressure variation over a solid wavy surface
[AD-A201724] N89-19517
The use of burst-triggered correlation for laser anemometry measurements in turbomachinery
[PNR90542] N89-19533
FLOW VISUALIZATION
Natural convection liquid immersion cooling of a column of discrete heat sources in a vertical channel
[AD-A201676] N89-19513
Application of Schlieren photography in gas turbine combustion research
[PNR90495] N89-19532
The use of burst-triggered correlation for laser anemometry measurements in turbomachinery
[PNR90542] N89-19533
FLUID DYNAMICS
National Aeronautics and Space Administration (NASA)/American Society for Engineering Education (ASEE) Summer Faculty Fellowship Program 1988, volume 1
[NASA-CR-172118-VOL-1] N89-20058
Model formulation of non-equilibrium gas radiation for hypersonic flight vehicles N89-20066
FLUID FLOW
Experiment plans to study preignition processes of a pool fire in low gravity
[NASA-CR-182256] N89-19442
Theoretical and experimental studies of selected topics in the rheology of fluids
[AD-A201460] N89-19512
FLUID MECHANICS
Superfluid turbulence in two-fluid flow of helium II N89-20018
FLUORESCENCE
In-line wear monitor
[AD-A201292] N89-19301
FLUTTER ANALYSIS
Transonic Unsteady Aerodynamics and Aeroelasticity 1987, part 1
[NASA-CP-3022-PT-1] N89-19234
Role of computational fluid dynamics in unsteady aerodynamics for aeroelasticity N89-19237
Initial application of CAP-TSD to wing flutter N89-19257
Transonic flutter calculations using the Euler equations N89-19258
Experimental transonic steady state and unsteady pressure measurements on a supercritical wing during flutter and forced discrete frequency oscillations N89-19261
Turbomachinery aeroelasticity at NASA Lewis Research Center N89-19262
Computational aeroelasticity challenges and resources N89-19264
FLUX VECTOR SPLITTING
Flux-vector splitting for unsteady calculations on dynamic meshes N89-19244
Unsteady transonic flow using Euler equations N89-19245
FLYWHEELS
Peaceful uses of electrical engineering in space N89-19487
FOAMS
Preparation of non-metals properties for data base
[NASA-CR-183596] N89-19420
FOCUSING
Synthetic aperture radar (SAR) data focusing using seismic migration techniques
[REPT-88-015] N89-19479
Focusing system, rotation, and modulation of the F 9 mirror of the IFSI 40 cm telescope
[IFSI-87-16] N89-19987
FOG
The collection efficiency of a massive fog collector N89-19650
Kinetics of ice crystal formation on aerosol particles in supercooled fog N89-19665
Determination of chemical reaction rates in fog N89-19683
A one-dimensional numerical model to simulate liquid phase chemical reactions within radiation fog N89-19690
Experiments on microphysics and chemistry of radiation fogs N89-19702
A poor man's optical fog detector N89-19716
FORCED VIBRATION
NASTRAN supplemental documentation for modal forced vibration analysis of aerodynamically excited turbosystems
[NASA-CR-174967] N89-19583
FORESTS
Cloud capture by a mountain top forest. Part 1: Acidity and dosage duration N89-19682
FORMALDEHYDE
The V3, V4 and V6 bands of formaldehyde: A spectral catalog from 900 cm(-1) to 1580 cm(-1)
[NASA-TM-100709] N89-19976
FORMALISM
Formal aspects of a knowledge system: A literature review
[REPT-88-12] N89-19933
FORTRAN
A data analysis system for unsteady turbulence measurements
[AD-A201662] N89-19268
FORWARD SCATTERING
Heterogeneous mixing measurements in small nonprecipitating cumuli N89-19635
FOURIER ANALYSIS
Large wave number aperture limited Fourier inversion and inverse scattering
[AD-A202247] N89-19940
FOURIER TRANSFORMATION
Systems analysis for DSN microwave antenna holography N89-19463
Opto-electronic systems research. Image recovery from partial Fresnel zone information
[AD-A201556] N89-19969
The V3, V4 and V6 bands of formaldehyde: A spectral catalog from 900 cm(-1) to 1580 cm(-1)
[NASA-TM-100709] N89-19976
FRACTALS
Computer generation of fractal terrains
[AD-A201171] N89-19730
The box dimension of self-affine graphs and repellors
[REPT-88-08] N89-19943
Hausdorff dimension and box dimension in self-similar sets
[REPT-88-09] N89-19944
FRACTOGRAPHY
Advanced durability analysis. Volume 4: Executive summary
[AD-A202304] N89-19597
FRACTURE MECHANICS
The effects of tempering and test temperature on the dynamic fracture initiation behavior of an AISI 4340 VAR steel
[AD-A201606] N89-19408
Solidification, structure and mechanical properties of A357 aluminum alloy N89-19409
The effect of hydrogen on fatigue crack growth rate of AISI 304 stainless steel N89-19410
Analysis of PERSHING 2 Reentry Vehicle (RV) control ring castings
[AD-A201548] N89-19559
Fatigue crack growth model RANDOM2 user manual. Appendix 1: Development of advanced methodologies for probabilistic constitutive relationships of material strength models
[NASA-CR-184775-APP-1] N89-19581
Boundary layer and singularity measurement in three dimensional fracture problems
[AD-A201277] N89-19584
Fundamentals of fatigue and fracture mechanics
[AD-A201435] N89-19585
A dynamic, time stepping boundary element method for frictional crack and interface problems N89-19590
FRACTURE STRENGTH
A new approach to the evaluation of the effects of stress state and interfacial properties on the behavior of advanced metal matrix composites
[AD-A201246] N89-19373
Durability and damage tolerance of bismaleimide composites, volume 1
[AD-A201273] N89-19374
Durability and damage tolerance of bismaleimide composites. Volume 2: Appendix of crack growth and low-velocity impact data
[AD-A201839] N89-19379
Evaluation of optical materials samples
[AD-A199471] N89-19981
FRACTURING
Boundary layer and singularity measurement in three dimensional fracture problems
[AD-A201277] N89-19584
FRAGMENTATION
Estimation of velocity perturbations in satellite fragmentation events N89-20083
FRAGMENTS
Drag coefficients for irregular fragments
[AD-A201943] N89-19276
FREE CONVECTION
Turbulent transport processes within and below small cumulus clouds N89-19632
The case for subgrid-scale condensation in numerical cloud models N89-19636
An observational study of radiatively driven convection --- clouds N89-19647
FREE ELECTRON LASERS
Free-electron laser driven by the NBS (National Bureau of Standards) CW microtron
[AD-A201170] N89-19535
Chaotic electron motion caused by sidebands in free electron lasers
[AD-A201635] N89-19538
Description of FEL3D: A three dimensional simulation code for TOK and FEL
[DE89-005529] N89-19540
XUV free-electron laser development at Los Alamos
[DE89-005458] N89-19547
Impact of target altitude restrictions on laser performance
[DE89-006567] N89-19553
FREE FALL
On the variation of falling velocity of early snowflakes N89-19670
On the dynamics of the falling ice crystal zone N89-19672
A vertical wind tunnel for the study of snowflakes and effects of accumulated snow on materials N89-19674
FREE VIBRATION
Mixed finite element models for free vibrations of thin-walled beams
[NASA-TP-2868] N89-19579
FREEZING
A new mechanism for ice initiation in warm-based midwestern cumuli N89-19613
Microphysical and electrical phenomena during freezing of water drops N89-19658
Kinetics of ice crystal formation on aerosol particles in supercooled fog N89-19665
The effect of freezing on the composition of cloud droplets N89-19691
FREQUENCY ANALYZERS
Radio frequency interference survey over the 1.0-10.4 GHz frequency range at the Goldstone-Venus Development Station N89-19466
FREQUENCY CONTROL
Passive vibration control using viscoelastic and constrained layer beam waveguide absorbers
[AD-A202188] N89-19595
FREQUENCY DISTRIBUTION
Time series analysis and multivariate statistical analysis
[AD-A202273] N89-19960
FRESNEL REGION
Opto-electronic systems research. Image recovery from partial Fresnel zone information
[AD-A201556] N89-19969
FRICTION
Performance evaluation of military engine and gear oils in friction and wear devices
[AD-A202145] N89-19432
Adhesion in ceramics and magnetic media
[NASA-TM-101476] N89-19435
A robust control scheme for flexible arms with friction in the joints N89-19875
FRICTION DRAG
Pressure variation over a solid wavy surface
[AD-A201724] N89-19517
FRICTION FACTOR
Mixed formulation for frictionless contact problems
[NASA-TP-2897] N89-19580
FRICTION MEASUREMENT
A dynamic, time stepping boundary element method for frictional crack and interface problems N89-19590
FROST
Ice/frost/debris assessment for space shuttle mission STS-27R, December 2, 1988
[NASA-TM-102144] N89-19326

FROUDE NUMBER
Comparison of orographic cloud and precipitation development of three different geographic locations using a 3-D nested grid cloud model N89-19723
FUEL CELLS
Oxygen electrode in molten carbonate fuel cells [DE89-005813] N89-19745
FUEL COMBUSTION
An innovative demonstration of high power density in a compact MHD generator [DE89-002159] N89-19990
FUEL CONSUMPTION
General aviation activity and avionics survey [AD-A201760] N89-19229
FUEL CONTAMINATION
Contamination of liquid oxygen by pressurized gaseous nitrogen [NASA-TP-2894] N89-19499
FUEL SYSTEMS
Studies and analyses of the space shuttle main engine. Appendix B: SSME FIPM drawings [NASA-CR-183594] N89-19365
FUEL-AIR RATIO
Flame driving of longitudinal instabilities in liquid fueled dump combustors [AD-A201293] N89-19392
An experimental investigation of sooting characteristics of a gas turbine combustor and augmentor tube [AD-A201804] N89-19568
FUELS
An experimental investigation of sooting characteristics of a gas turbine combustor and augmentor tube [AD-A201804] N89-19568
An innovative demonstration of high power density in a compact MHD generator [DE89-002159] N89-19990
FUNCTIONAL DESIGN SPECIFICATIONS
Specification validation tools study [MATRA-NT/139/1939] N89-19447
Telerobot operator control station requirements N89-19876
IDEAL: A methology for developing information systems N89-19888
FUNCTIONS (MATHEMATICS)
A data analysis system for unsteady turbulence measurements [AD-A201662] N89-19268
FUZZY SYSTEMS
Probability theories, fuzzy set theory and syllogisms; a literature review [REPT-88-13] N89-19961
Stochastic and fuzzy PERT [REPT-88-26] N89-20027

G

GADOLINIUM
Radiation induced amorphization in YBa2Cu3O7 and GdBa2Cu3O7 superconductors [DE89-005451] N89-20008
GALAXIES
Interstellar matter in early type galaxies N89-20042
GALLIUM ARSENIDES
Ohmic contacts to gallium aluminum arsenide for high temperature applications [AD-A202248] N89-19492
Thermal oxidation of 3-5 compound semiconductors [DE89-007127] N89-20020
GAMMA RAY LASERS
Proof of the feasibility of coherent and incoherent schemes for pumping a gamma-ray laser [AD-A201931] N89-19542
GAS DYNAMICS
A fundamental mathematical theory in the dynamics of combustion processes [AD-A201284] N89-19391
GAS FLOW
Computational studies of evaporating sprays in a shear layer [AD-A201932] N89-19520
GAS JETS
Mixing in gas phase turbulent jets N89-19515
GAS MIXTURES
Electron-beam pumped liquid excimer lasers [DE89-006549] N89-19549
GAS TEMPERATURE
Hole formation (etching) in polymers by far (deep) UV high intensity laser (excimer) radiation pulses and its relevance to photoresists in deep UV photolysis of polymers [AD-A202274] N89-19433
GAS TURBINE ENGINES
Propulsion [PNR90472] N89-19302
The gas turbine engine and its certification [PNR90496] N89-19303
Current diagnostic practice in gas turbine combustors [PNR90530] N89-19306
Aerothermodynamics of a jet cell facility [AD-A202142] N89-19318
Computational fluid dynamics for combustion applications [PNR90534] N89-19525
GAS TURBINES
Microstructural optimisation of titanium alloys for defect tolerance in gas turbine engine components [PNR90503] N89-19413
Computational studies of evaporating sprays in a shear layer [AD-A201932] N89-19520
Application of Schlieren photography in gas turbine combustion research [PNR90495] N89-19532
An experimental investigation of sooting characteristics of a gas turbine combustor and augmentor tube [AD-A201804] N89-19568
GAS-GAS INTERACTIONS
Contamination of liquid oxygen by pressurized gaseous nitrogen [NASA-TP-2894] N89-19499
GAS-METAL INTERACTIONS
Effect of temperature on the corrosion resistance of nitrogen bearing AL6X and 904L stainless steels [AD-A201955] N89-19412
Formation of titanium nitride layers on titaniun metal: Results of XPS and AES investigations [KFK-4449] N89-19419
GASEOUS DIFFUSION
Contamination of liquid oxygen by pressurized gaseous nitrogen [NASA-TP-2894] N89-19499
Oxygen diffusion in YBa2Cu3O7-delta [DE89-005831] N89-20011
SIMS measurement of oxygen tracer diffusion in YBa2Cu3O7-delta [DE89-005884] N89-20014
GASES
Analytical, numerical and experimental investigations of oblique-shock-wave reflections in pure and dusty gases [AD-A201438] N89-19511
GEARS
Performance evaluation of military engine and gear oils in friction and wear devices [AD-A202145] N89-19432
An experimental evaluation of S-duct inlet-diffuser configurations for turboprop offset gearbox applications [NASA-CR-179454] N89-19556
Gear technology acquisition for advanced aero engines [PNR90510] N89-19571
Machinery diagnostics via mechanical vibration analysis using spectral analysis techniques [AD-A202089] N89-19594
GENERAL AVIATION AIRCRAFT
General aviation activity and avionics survey [AD-A201760] N89-19229
GENERALIZATION (PSYCHOLOGY)
Psychological tools for knowledge acquisition N89-19857
GEOCHEMISTRY
Evaluation of crustal recycling during the evolution of Archean-age Matachewan basaltic magmas N89-20077
GEODESY
The geometry of geodetic inverse linear mapping and nonlinear adjustment [ETN-89-93900] N89-19736
GEODETIC COORDINATES
The geometry of geodetic inverse linear mapping and nonlinear adjustment [ETN-89-93900] N89-19736
GEODETIC SATELLITES
Solid Earth ARISTOTELES mission data preprocessing simulation of gravity gradiometer [ESA-CR(P)-2666] N89-19766
GEOIDS
Local geoid determination using the global positioning system [AD-A202220] N89-19731
GEOMAGNETISM
Characteristics of optical emissions and particle precipitation in mid/low latitude aurorae N89-19755
GEOMETRICAL OPTICS
Research in acoustical scattering, diffraction catastrophes, optics of bubbles and acoustical phase conjugation [AD-A201451] N89-19968
GEOMETRICAL THEORY OF DIFFRACTION
Research in acoustical scattering, diffraction catastrophes, optics of bubbles and acoustical phase conjugation [AD-A201451] N89-19968
GEOMETRY
A geometric property of the least squares solution of linear equations [AD-A201342] N89-19937
GEOPHYSICS
Superconducting gravity gradiometer mission. Volume 2: Study team technical report [NASA-TM-4091] N89-19749
GEOSYNCHRONOUS ORBITS
A model for the geostationary orbital infrastructure, system analysis [ILR-MITT-205] N89-19323
Model of a geostationary regional transportation company (GRET): Fleet composition and facility layout [ILR-MITT-207] N89-19329
Preliminary project plan for a GEO regional transportation and servicing company [ILR-MITT-210] N89-19331
GERMANIUM
Ohmic contacts to gallium aluminum arsenide for high temperature applications [AD-A202248] N89-19492
Pyrolytic and laser photolytic growth of crystalline and amorphous germanium films from digermane (GE2H6) [DE89-006125] N89-20019
GET AWAY SPECIALS (STS)
Get Away Special (GAS): Educational applications of space flight [NASA-TM-101287] N89-19321
GLASS
The mechanical behavior of surface modified ceramics [DE89-004764] N89-19422
Elastic hysteresis phenomena in ULE and Zerodur optical glasses at elevated temperatures [DE89-005183] N89-19423
GLASS COATINGS
Arc jet diagnostics tests N89-20085
GLASS FIBERS
Heat transfer properties of satellite component materials N89-19375
GLOBAL POSITIONING SYSTEM
Design of digital filters for navigation receivers --- GPS [DFVLR-MITT-88-23] N89-19288
Local geoid determination using the global positioning system [AD-A202220] N89-19731
GLOVES
Concept for a large master/slave-controlled robotic hand N89-19866
GOALS
Optical goals for polymeric film reflectors [DE89-000836] N89-19744
GOLD
Scanning tunneling microscopy of metals on graphite [DE89-006608] N89-19404
GRAIN BOUNDARIES
Anomalous slip in an FCC system [DE89-002257] N89-19405
Microstructural analyses of intermetallic TiAl (Nb)-compounds prepared by arc melting and by powder metallurgy [GKSS-88/E/32] N89-19417
Grain boundary nonstoichiometry in multicomponent ceramics [DE89-006109] N89-19437
High-speed laser photography [AD-A202293] N89-19544
Atomic structure of tilt grain boundaries in NiO [DE89-005847] N89-20013
GRAPH THEORY
The box dimension of self-affine graphs and repellors [REPT-88-08] N89-19943
Hausdorff dimension and box dimension in self-similar sets [REPT-88-09] N89-19944
GRAPHIC ARTS
Hypervelocity technology escape system concepts. Volume 2: Software manual [AD-A201720] N89-19281
GRAPHITE
Scanning tunneling microscopy of metals on graphite [DE89-006608] N89-19404
GRAPHITE-EPOXY COMPOSITES
Composite materials at high temperatures [AD-A201163] N89-19372
Measurements of the compressive behavior of AS4/3501-6 and IM7/8551-7 carbon/epoxy [DE89-005823] N89-19383

Effect of adhesive interleaving and discontinuous plies on failure of composite laminates subject to transverse normal loads
[NASA-TM-101507] N89-19589
Compression strength of composite primary structural components
[NASA-CR-184893] N89-19599

GRAPHS (CHARTS)
Wiring Viterbi decoders (splitting deBruijn graphs) N89-19459
Fast and processor-efficient parallel algorithms for reducible flow graphs
[AD-A201651] N89-19904

GRAVIMETRY
Local geoid determination using the global positioning system
[AD-A202220] N89-19731
Solid Earth ARISTOTELES mission data preprocessing simulation of gravity gradiometer
[ESA-CR(P)-2666] N89-19766

GRAVITATION THEORY
Theoretical and experimental studies of selected topics in the rheology of fluids
[AD-A201460] N89-19512

GRAVITATIONAL EFFECTS
Maladjustment of kidneys to microgravity: Design of measures to reduce the loss of calcium N89-20076

GRAVITATIONAL PHYSIOLOGY
Maladjustment of kidneys to microgravity: Design of measures to reduce the loss of calcium N89-20076

GRAVITY GRADIOMETERS
Superconducting gravity gradiometer mission. Volume 2: Study team technical report
[NASA-TM-4091] N89-19749
Solid Earth ARISTOTELES mission data preprocessing simulation of gravity gradiometer
[ESA-CR(P)-2666] N89-19766

GREAT CIRCLES
On the great circle reduction in the data analysis for the astrometric satellite HIPPARCOS
[ETN-89-93902] N89-20038

GRID GENERATION (MATHEMATICS)
Knowledge-based zonal grid generation for computational fluid dynamics N89-19828

GROUND BASED CONTROL
Advanced information technology monitoring with microprocessors --- spacecraft control
[MMP-1-IS-02-3302-FR] N89-19895

GROUND STATE
Electric fields in earth orbital space
[AD-A201747] N89-19760
High-precision laser and RF spectroscopy of atomic, molecular, and slow ion beams
[DE89-005870] N89-19975

GROUND SUPPORT SYSTEMS
Study on checkout of flight units and subsystems --- ground support
[ESA-CR(P)-2693] N89-19816
EMMA: The expert system for munition maintenance N89-19823
Diagnostics in the Extendable Integrated Support Environment (EISE) N89-19824
Intelligent tutoring in the spacecraft command/control environment N89-19855
COMPASS: A generalized ground-based monitoring system
[PNR90483] N89-19894

GROUP DYNAMICS
A case study of small group decision-making as influenced by the Abilene Paradox: The Challenger mishap
[AD-A202102] N89-19328

GUIDANCE (MOTION)
Joint University Program for Air Transportation Research, 1987
[NASA-CP-3028] N89-19230

GUST LOADS
An examination of the fatigue meter records from the RAAF (Royal Australian Air Force) caribou fleet
[AD-A201074] N89-19290

GUSTS
A preliminary study of precursors to Huntsville microbursts
[AD-A200914] N89-19782

GYROSCOPIC COUPLING
Equilibrium solutions of a spherical pendulum with rotating point of suspension and friction
[DFVLR-MITT-88-24] N89-19966

GYROSCOPIC PENDULUMS
Equilibrium solutions of a spherical pendulum with rotating point of suspension and friction
[DFVLR-MITT-88-24] N89-19966

GYROSCOPIC STABILITY
Peaceful uses of electrical engineering in space N89-19487
Equilibrium solutions of a spherical pendulum with rotating point of suspension and friction
[DFVLR-MITT-88-24] N89-19966

H

H II REGIONS
Ultracompact HII regions associated with massive star formation N89-20044

HABITS
A study to analyze the degree of the relationship between health practices and fatigue
[AD-A201518] N89-19798

HAIL
About secondary ice crystal production N89-19666
Analysis of hailstones from a severe storm and their simulated evolution N89-19677
The collection efficiencies of soft-hailstones for super-cooled water droplets and ice crystals N89-19678
Simulation of conical graupel by using a ballistic model N89-19679

HAILSTORMS
Comparison of model results for models of differing microphysical detail --- hailstorms N89-19680
A numerical investigation of an orographic precipitation event N89-19721

HALF SPACES
The stability of boundary layer flow over elastic substrates N89-19524

HALL EFFECT
Sensing human hand motions for controlling dexterous robots N89-19883
The 2-4 semiconductor superlattices
[AD-A202369] N89-20005

HALLEY'S COMET
Ground-based Fabry-Perot observations of neutral and ionic atoms and molecules of comet Halley N89-20048
Jets physics in Comet P/Halley
[IFSI-88-3] N89-20049

HALOCARBONS
Ultraviolet absorption cross-sections of halocarbons of stratospheric interest
[AERONOMICA-ACTA-A-336-1988] N89-19769

HALOGEN OCCULTATION EXPERIMENT
Halogen Occultation Experiment (HALOE) optical filter characterization
[NASA-TM-4104] N89-19529

HAND (ANATOMY)
Dexterous robotic hands: Kinematics and control
[AD-A202183] N89-19570
Concept for a large master/slave-controlled robotic hand N89-19866
Sensing human hand motions for controlling dexterous robots N89-19883

HARDWARE
Telerobot operator control station requirements N89-19876

HARMONIC ANALYSIS
Pressure variation over a solid wavy surface
[AD-A201724] N89-19517

HARMONIC OSCILLATION
The development and structural characteristics of Dean vortices in a curved rectangular channel
[AD-A201249] N89-19508
Wake-excited raindrop oscillations N89-19607

HARNESSES
Positive Flotation Harness (PFH) for use by Canadian Forces search and rescue technicians
[AD-A200727] N89-19279

HEAD (ANATOMY)
The development and validation of an automated headboard device for measurement of three-dimensional coordinates of the head and face
[AD-A201186] N89-19813

HEAD-UP DISPLAYS
Light weight escape capsule for fighter aircraft N89-19858

HEALTH
A study to analyze the degree of the relationship between health practices and fatigue
[AD-A201518] N89-19798
Development of an atmospheric monitoring plan for space station N89-20065

HEAT FLUX
An investigation of the intermittent turbulent breakdown of the nocturnal planetary boundary layer
[AD-A201743] N89-19518

HEAT MEASUREMENT
Natural convection liquid immersion cooling of a column of discrete heat sources in a vertical channel
[AD-A201676] N89-19513
Satellite remote sensing of heat stress during reserve training at Fort Hood
[AD-A201555] N89-19800

HEAT PIPES
Modeling of transient heat pipe operation
[NASA-CR-184688] N89-19502

HEAT RESISTANT ALLOYS
Microstructural optimisation of titanium alloys for defect tolerance in gas turbine engine components
[PNR90503] N89-19413

HEAT TRANSFER
Experiment plans to study preignition processes of a pool fire in low gravity
[NASA-CR-182256] N89-19442
Modeling of transient heat pipe operation
[NASA-CR-184688] N89-19502
Quench pressure, thermal expulsion, and normal zone propagation in internally cooled superconductors
[DE89-005668] N89-20003
Model formulation of non-equilibrium gas radiation for hypersonic flight vehicles N89-20066

HEAT TRANSMISSION
Episodic volcanism of tidally heated satellites with application to Io. Thermal state of an ice shell on Europa. Polar wander of a synchronously rotating satellite with application to Europa N89-20052

HEIGHT
Results of time and height resolved scavenging experiments --- atmospheric chemistry N89-19697

HELICOPTER CONTROL
Time periodic control of a multiblade helicopter N89-19312

HELICOPTER PERFORMANCE
Combined preliminary airworthiness evaluation and airworthiness and flight characteristics evaluation of the UH-1H with preproduction hub spring and composite main rotor blades installed
[AD-A202316] N89-19295

HELICOPTER TAIL ROTORS
Icing research tunnel test of a model helicopter rotor
[NASA-TM-101978] N89-19305

HELICOPTERS
Minimum required heliport airspace under visual flight rules
[AD-A201433] N89-19283
A comparative analysis of tilt rotor aircraft versus helicopters using simulator results
[AD-A202190] N89-19294
A systems approach to rotorcraft stability and control research
[AD-A201784] N89-19314

HELIPORTS
Minimum required heliport airspace under visual flight rules
[AD-A201433] N89-19283

HELIUM ISOTOPES
The tensile strength of liquid helium four N89-20016

HELMET MOUNTED DISPLAYS
Development of a low-cost helmet mounted eye gaze sensor
[AD-A202303] N89-19298

HELMETS
Development of a low-cost helmet mounted eye gaze sensor
[AD-A202303] N89-19298

HELMHOLTZ RESONATORS
Acoustic wave propagation in heterogeneous structures including experimental validation
[NASA-TM-101486] N89-19965

HETEROJUNCTIONS
Development of Si/SiGe heterostructures
[AD-A201440] N89-20001

HEURISTIC METHODS
A heuristically based navigation system for an autonomous walking machine with a range scanner N89-19563
Transformation based endorsement systems N89-19836
Portable inference engine: An extended CLIPS for real-time production systems N89-19843
A heuristic ceiling point algorithm for general integer linear programming
[AD-A202285] N89-19912

HEWLETT-PACKARD COMPUTERS
Operation of the HP2250 with the HP9000 series 200 using PASCAL 3.0
[NASA-TM-87652] N89-19892

HIGH CURRENT
High current, high Coulomb ignitrons
[DE89-005547] N89-19490

HIGH ENERGY FUELS
Booster propulsion/vehicle impact study
[NASA-CR-183584] N89-19366

HIGH ENERGY PROPELLANTS
NRL boron propellants combustion program
[AD-A201242] N89-19440

HIGH FREQUENCIES
Normalized radar cross section of natural surfaces at millimeter wavelengths
[AD-A202252] N89-19475
Excitation of strong high-frequency electric fields and their detection using the dynamic Stark effect
[ETN-89-93794] N89-19991
HIGH GAIN
Analysis and synthesis of microstrip antennas including mutual coupling
[AD-A201783] N89-19472
HIGH POWER LASERS
An investigation of factors affecting domestic technology transfer at the Wright Aeronautical Laboratories
[AD-A201581] N89-20032
HIGH RESOLUTION
Analysis and synthesis of microstrip antennas including mutual coupling
[AD-A201783] N89-19472
Toward an image compression algorithm for the high-resolution electronic still camera N89-20079
HIGH REYNOLDS NUMBER
Unsteady pressure measurements on a supercritical airfoil at high Reynolds numbers N89-19259
Airfoil stall penetration at constant pitch rate and high Reynolds number N89-19260
Use of riblets to obtain drag reduction on airfoils at high Reynolds number flows
[AD-A201485] N89-19267
HIGH SPEED
High-speed real-time animated displays on the ADAGE (trademark) RDS 3000 raster graphics system
[NASA-TM-4095] N89-19899
HIGH SPEED PHOTOGRAPHY
High-speed laser photography
[AD-A202293] N89-19544
HIGH STRENGTH
Durability and damage tolerance of bismaleimide composites, volume 1
[AD-A201273] N89-19374
Durability and damage tolerance of bismaleimide composites. Volume 2: Appendix of crack growth and low-velocity impact data
[AD-A201839] N89-19379
HIGH TEMPERATURE
Composite materials at high temperatures
[AD-A201163] N89-19372
Elastic hysteresis phenomena in ULE and Zerodur optical glasses at elevated temperatures
[DE89-005183] N89-19423
HIGH TEMPERATURE PLASMAS
Existence of stationary solutions in the coronal loop problem
[REPT-88-06] N89-20054
HIGH TEMPERATURE SUPERCONDUCTORS
Josephson effect research in high-temperature superconductors
[AD-A201483] N89-20002
HIGH TEMPERATURE TESTS
Some novel test methods for, and associated problems of mechanical strength characterization of engineering ceramics
[PNR90492] N89-19436
HIPPARCOS SATELLITE
On the great circle reduction in the data analysis for the astrometric satellite HIPPARCOS
[ETN-89-93902] N89-20038
HISTOLOGY
Biological applications and effects of optical masers
[AD-A201834] N89-19541
HOLE BURNING
Hole formation (etching) in polymers by far (deep) UV high intensity laser (excimer) radiation pulses and its relevance to photoresists in deep UV photolysis of polymers
[AD-A202274] N89-19433
HOLOGRAPHY
Systems analysis for DSN microwave antenna holography N89-19463
The comparison of holographic and 2-D probe measurements of ice crystals N89-19652
HOMOGENIZING
Homogenizing surface and satellite observations of cloud
[AD-A201630] N89-19752
HORN ANTENNAS
Microwave time delays for the dual L-C-band feed system N89-19462
Intrinsic hybrid modes in a corrugated conical horn
[ESA-CR(P)-2586] N89-19494
HOT PRESSING
Fabrication of XLWIR (Extra-Long-Wavelength-Infrared) window materials
[DE89-006418] N89-19439
HOUSINGS
Electron beam welding of 6061-T6 covers to A356-T6 machined cast housings
[BDX-613-3915] N89-19573
HOVERING
Combined preliminary airworthiness evaluation and airworthiness and flight characteristics evaluation of the UH-1H with preproduction hub spring and composite main rotor blades installed
[AD-A202316] N89-19295
HOVERING STABILITY
A systems approach to rotorcraft stability and control research
[AD-A201784] N89-19314
HUBS
Large-scale Advanced Prop-fan (LAP) hub/blade retention design report
[NASA-CR-174786] N89-19299
HUMAN BEHAVIOR
A case study of small group decision-making as influenced by the Abilene Paradox: The Challenger mishap
[AD-A202102] N89-19328
HUMAN FACTORS ENGINEERING
The efficacy of color-coded symbols to enhance air-traffic control displays
[AD-A201594] N89-19284
Development of a low-cost helmet mounted eye gaze sensor
[AD-A202303] N89-19298
Advanced extravehicular activity systems requirements definition study. Phase 2: Extravehicular activity at a lunar base
[NASA-CR-172117] N89-19809
The development and validation of an automated headboard device for measurement of three-dimensional coordinates of the head and face
[AD-A201186] N89-19813
Second Annual Workshop on Space Operations Automation and Robotics (SOAR 1988)
[NASA-CP-3019] N89-19817
A schema-based model of situation awareness: Implications for measuring situation awareness N89-19847
An intelligent multi-media human-computer dialogue system N89-19850
Knowledge-based graphical interfaces for presenting technical information N89-19851
An intelligent tutoring system for space shuttle diagnosis N89-19853
Light weight escape capsule for fighter aircraft N89-19858
Optimal solutions for complex design problems: Using isoperformance software for human factors trade offs N89-19860
Simulation of the human-telerobot interface N89-19861
Man-systems requirements for the control of teleoperators in space N89-19862
The WCSAR telerobotics test bed N89-19871
Telerobot operator control station requirements N89-19876
A representational framework and user-interface for an image understanding workstation N89-19878
Voice control of complex workstations N89-19880
SARSCEST (human factors) N89-19890
HUMAN PATHOLOGY
Diagnosis by integrating model-based reasoning with knowledge-based reasoning N89-19835
HUMAN PERFORMANCE
The effects of a pitched field orientation on hand/eye coordination
[AD-A201620] N89-19814
HYDRATES
Gas hydrates thermomechanics
[DE88-010280] N89-19387
Crystallization of supercooled solutions --- atmosphere N89-19664
HYDRAULIC JETS
Study of underexpanded turbulent air jets in water N89-19516
HYDRIDES
Studies of hydrogen-hydrogen and carbon-sulfur bond cleavage
[DE89-006116] N89-19403
HYDROCARBON COMBUSTION
Reaction chemistry of boron hydrides
[AD-A201243] N89-19389
HYDRODYNAMICS
Study of underexpanded turbulent air jets in water N89-19516
HYDROGEN
Studies of hydrogen-hydrogen and carbon-sulfur bond cleavage
[DE89-006116] N89-19403
The effect of hydrogen on fatigue crack growth rate of AISI 304 stainless steel N89-19410
HYDROGEN COMPOUNDS
Interactions and reactions in polymerized vesicles
[AD-A201527] N89-19427
HYDROGEN FUELS
Booster propulsion/vehicle impact study
[NASA-CR-183584] N89-19366
HYDROMETEOROLOGY
Development of hydrometeor video sonde N89-19653
Insoluble particles in hydrometeors N89-19684
Results of time and height resolved scavenging experiments --- atmospheric chemistry N89-19697
HYDROXIDES
Development of a detection system for atmospheric trace gases, in particular for OH molecules and realization of field measurements
[BPT-11/88] N89-19767
HYPERBOLIC COORDINATES
Hyperbolicity properties of C sup 2 multimodal Collet-Eckmann maps without Schwarzian deriative assumptions
[REPT-88-10] N89-19945
HYPERCUBE MULTIPROCESSORS
A parallel expert system for the control of a robotic air vehicle N89-19842
HYPERFINE STRUCTURE
Mossbauer effect studies of magnetism in superconducting systems
[DE89-005844] N89-20012
HYPERSONIC FLOW
Model formulation of non-equilibrium gas radiation for hypersonic flight vehicles N89-20066
HYPERSONIC REENTRY
Analytical interpretation on lateral/directional stability and controllability of high angle-of-attack reentry flight
[ISAS-630] N89-19353
HYPERSONIC VEHICLES
Hypervelocity technology escape system concepts. Volume 2: Software manual
[AD-A201720] N89-19281
National Aeronautics and Space Administration (NASA)/American Society for Engineering Education (ASEE) Summer Faculty Fellowship Program 1988, volume 1
[NASA-CR-172118-VOL-1] N89-20058
Model formulation of non-equilibrium gas radiation for hypersonic flight vehicles N89-20066
HYPERSONIC WIND TUNNELS
Contamination of liquid oxygen by pressurized gaseous nitrogen
[NASA-TP-2894] N89-19499
HYPOBARIC ATMOSPHERES
An annotated bibliography of hypobaric decompression sickness research conducted at the Crew Technology Division, USAF School of Aerospace Medicine, Brooks AFB, Texas from 1983 to 1988
[AD-A201274] N89-19796
HYPOTHESES
Reducing uncertainty by using explanatory relationships N89-19837
Robust bounded influence tests in linear models
[AD-A201896] N89-19957
HYSTERESIS
The role of shock induced trailing-edge separation in limit cycle oscillations N89-19256
Elastic hysteresis phenomena in ULE and Zerodur optical glasses at elevated temperatures
[DE89-005183] N89-19423
Nonlinear dynamic analysis of embedded structures
[AD-A201726] N89-19593

I

ICE
Ice/frost/debris assessment for space shuttle mission STS-27R, December 2, 1988
[NASA-TM-102144] N89-19326
Evaporation and melting of ice crystals: A laboratory study N89-19612
Spreading supercooled water droplets on an ice surface N89-19614
The comparison of holographic and 2-D probe measurements of ice crystals N89-19652
On the dynamics of the falling ice crystal zone N89-19672
A new database of ice particle size spectra for altitudes up to 10 km (30,000 ft) N89-19673
Pattern of air bubble inclusions in atmospheric ice formed during accretion N89-19676
The collection efficiencies of soft-hailstones for super-cooled water droplets and ice crystals N89-19678

Ionic concentrations of rime ice and snow and Bergeron process N89-19689

ICE FORMATION

Icing research tunnel test of a model helicopter rotor [NASA-TM-101978] N89-19305

Empirical equations of ice crystal growth microphysics for modeling and analysis N89-19609

The contrast study of new model on ice crystal growth N89-19610

A new mechanism for ice initiation in warm-based midwestern cumuli N89-19613

A test of ice crystal production by aircraft N89-19622

The effect of ice physical processes on the numerical simulation of West African squall lines N89-19638

Numerical simulation of microphysical processes in cumulonimbus N89-19639

Liquid water content, median volume diameter and temperature in dependence on the height above the cloud base for different types of clouds --- aircraft icing N89-19662

About secondary ice crystal production N89-19666

Experimental studies on secondary ice particle production N89-19667

ICE REPORTING

Intercomparisons of aircraft measurements with lidar returns for aerosol, ice crystals and water droplets N89-19718

Active and passive remote sensing of ice [AD-A201915] N89-19792

IGNITION

Experiment plans to study preignition processes of a pool fire in low gravity [NASA-CR-182256] N89-19442

Possibilities for breakeven and ignition of D-He3 fusion fuel in a near term tokamak [KFK-4433] N89-19992

IGNITRONS

High current, high Coulomb ignitrons [DE89-005547] N89-19490

IMAGE ANALYSIS

The use of LANDSAT imagery for water quality studies in the Ijsselmeer area (Netherlands) [BCRS-87-18] N89-19732

A representational framework and user-interface for an image understanding workstation N89-19878

IMAGE PROCESSING

Development of a low-cost helmet mounted eye gaze sensor [AD-A202303] N89-19298

Extracting depth by binocular stereo in a robot vision system [DE89-005016] N89-19572

The use of automatic particle recognition to improve the determination of bulk quantities from PMS 2-D probe data in cirrus N89-19651

The use of LANDSAT imagery for water quality studies in the Ijsselmeer area (Netherlands) [BCRS-87-18] N89-19732

Toward an image compression algorithm for the high-resolution electronic still camera N89-20079

IMAGE RECONSTRUCTION

Opto-electronic systems research. Image recovery from partial Fresnel zone information [AD-A201556] N89-19969

Time-domain imaging N89-20084

IMAGERY

Measurements of shuttle glow on mission STS 41-G [AD-A201769] N89-19327

IMAGES

Scanning tunneling microscopy of metals on graphite [DE89-006608] N89-19404

Computation of stereo and visual motion: From biophysics to psychophysics [AD-A201873] N89-19802

Structural saliency: The detection of globally salient structures using a locally connected network [AD-A201619] N89-19806

Knowledge-based graphical interfaces for presenting technical information N89-19851

CAD-model-based vision for space applications N89-19867

IMAGING TECHNIQUES

Development of Nuclear Magnetic Resonance (NMR) imaging technology for advanced ceramics [DE89-006400] N89-19438

The study of the interstitial aerosol particles and cloud droplets with digital image analysis of diffraction images N89-19654

Analysis of blending algorithms in computer graphics [AD-A201921] N89-19909

Use of superconducting imaging surfaces to enhance detection of weak magnetic sources by SQUID systems [DE89-006568] N89-20015

National Aeronautics and Space Administration (NASA)/American Society for Engineering Education (ASEE) Summer Faculty Fellowship Program 1988, volume 2 --- Author [NASA-CR-172118-VOL-2] N89-20073

Time-domain imaging N89-20084

IMPACT DAMAGE

Durability and damage tolerance of bismaleimide composites, volume 1 [AD-A201273] N89-19374

Durability and damage tolerance of bismaleimide composites. Volume 2: Appendix of crack growth and low-velocity impact data [AD-A201839] N89-19379

IMPACT LOADS

High strain-rate behaviour of polymers using blast-wave and impact-loading methods N89-19592

IMPACT TOLERANCES

Durability and damage tolerance of bismaleimide composites, volume 1 [AD-A201273] N89-19374

Durability and damage tolerance of bismaleimide composites. Volume 2: Appendix of crack growth and low-velocity impact data [AD-A201839] N89-19379

IMPEDANCE

An electrochemical study of corrosion protection by primer-topcoat systems on 4130 steel with ac impedance and dc methods [NASA-TP-2820] N89-19406

IMPEDANCE MEASUREMENT

Investigation of the interface between two immiscible electrolytes applied to membrane electrochemistry [AD-A201310] N89-19393

IMPELLERS

Experimental investigation of rotor-stator interaction in diffuser pumps N89-19564

INCLUSIONS

Sliding and debonding inclusions [AD-A201609] N89-19587

Pattern of air bubble inclusions in atmospheric ice formed during accretion N89-19676

INCOMPRESSIBLE FLOW

Computational study of incompressible turbulent flow over a swept rearward-facing step N89-19272

INDEPENDENT VARIABLES

A data analysis system for unsteady turbulence measurements [AD-A201662] N89-19268

INDEXES (DOCUMENTATION)

Calendar of selected aeronautical and space meetings: January 1989 onwards [AGARD-CAL-89/1] N89-20024

INDIA

Precipitation initiation mechanisms in clouds over north India N89-19624

INDIUM PHOSPHIDES

Thermal oxidation of 3-5 compound semiconductors [DE89-007127] N89-20020

INDUCTANCE

Calculation of mutual self inductance and coupling coefficient for closely spaced loops [DE89-005546] N89-19471

INERTIA

Modeling of inertial effects in transient liquid-bubble flows [REPT-88-22] N89-19528

Chaotic dynamics and control of nonlinear and flexible arm robotic devices N89-19566

INFERENCE

Reducing uncertainty by using explanatory relationships N89-19837

A parallel expert system for the control of a robotic air vehicle N89-19842

Portable inference engine: An extended CLIPS for real-time production systems N89-19843

INFORMATION

Global scientific and technical information network [AD-A201902] N89-20030

INFORMATION PROCESSING (BIOLOGY)

Brain activity during tactical decision-making. Part 4: Event-related potentials as indices of selective attention and cognitive workload [AD-A201370] N89-19797

INFORMATION RETRIEVAL

An annotated bibliography of hypobaric decompression sickness research conducted at the Crew Technology Division, USAF School of Aerospace Medicine, Brooks AFB, Texas from 1983 to 1988 [AD-A201274] N89-19796

Browsing schematics: Query-filtered graphs with context nodes N89-19844

Presentation planning using an integrated knowledge base N89-19845

Using the sentence verification technique to assess storage and retrieval processes [AD-A201632] N89-20029

Computer technologies and institutional memory N89-20062

INFORMATION SYSTEMS

Specification validation tools study [MATRA-NT/139/1939] N89-19447

Second Annual Workshop on Space Operations Automation and Robotics (SOAR 1988) [NASA-CP-3019] N89-19817

IDEAL: A methology for developing information systems N89-19888

Electronic data generation and display system N89-19891

Status of DOE information network modifications [DE89-005191] N89-20028

INFRARED ASTRONOMY

Focusing system, rotation, and modulation of the F 9 mirror of the IFSI 40 cm telescope [IFSI-87-16] N89-19987

Near-infrared spectroscopy of young stellar objects N89-20033

Interstellar matter in early type galaxies N89-20042

INFRARED DETECTORS

Evaluation of Schottky barrier and PBTE IR-CCD detectors for the SWIR and MIR wavelengths range, executive summary [IMEC-SP/CCD-255/88-03] N89-19495

INFRARED LASERS

Free-electron laser driven by the NBS (National Bureau of Standards) CW microtron [AD-A201170] N89-19535

INFRARED RADIATION

Hole formation (etching) in polymers by far (deep) UV high intensity laser (excimer) radiation pulses and its relevance to photoresists in deep UV photolysis of polymers [AD-A202274] N89-19433

Fabrication of XLWIR (Extra-Long-Wavelength-Infrared) window materials [DE89-006418] N89-19439

Cirrus microphysics and infrared radiative transfer: A case study N89-19649

Infrared and ionization structure of the polar mesosphere [AD-A201266] N89-19751

INFRARED SPECTROSCOPY

Application of nondestructive evaluations to the prediction of turbine fuel peroxidation potential [AD-A202291] N89-19441

The V3, V4 and V6 bands of formaldehyde: A spectral catalog from 900 cm(-1) to 1580 cm(-1) [NASA-TM-100709] N89-19976

Near-infrared spectroscopy of young stellar objects N89-20033

INFRARED TELESCOPES

Focusing system, rotation, and modulation of the F 9 mirror of the IFSI 40 cm telescope [IFSI-87-16] N89-19987

INHOMOGENEITY

Structure of upper clouds boundary using the lidar data N89-19631

INITIATORS (EXPLOSIVES)

A fundamental mathematical theory in the dynamics of combustion processes [AD-A201284] N89-19391

INJECTION

Turbulence structure and mass transport in a channel flow with polymer injection [AD-A202237] N89-19521

INJECTORS

Studies and analyses of the space shuttle main engine. Appendix B: SSME FIPM drawings [NASA-CR-183594] N89-19365

INLET FLOW

Theoretical and experimental investigations on shocks losses in transonic axial flow compressors [DFVLR-FB-88-38] N89-19304

INLET NOZZLES

An experimental evaluation of S-duct inlet-diffuser configurations for turboprop offset gearbox applications [NASA-CR-179454] N89-19556

INPUT

Presentation planning using an integrated knowledge base N89-19845

INSTRUMENT ERRORS

Calibration of PMS FSSP and 1D-C probes for cloud droplet measurements N89-19713

INSURANCE (CONTRACTS)

Commercial expendable launch vehicle liability [S-HRG-100-750] N89-19325

INTAKE SYSTEMS

Flame driving of longitudinal instabilities in liquid fueled dump combustors [AD-A201293] N89-19392

INTEGRAL EQUATIONS
The boundary element method for the diffusion equation N89-19233
INTEGRATED OPTICS
Optical joint correlation using the deformable mirror device N89-20074
INTERACTIONAL AERODYNAMICS
Unsteady transonic viscous-inviscid interaction using Euler and boundary-layer equations N89-19250
Time periodic control of a multiblade helicopter N89-19312
INTERFACES
A new approach to the evaluation of the effects of stress state and interfacial properties on the behavior of advanced metal matrix composites
[AD-A201246] N89-19373
Fundamental optical studies of competitive adsorption and thin film phenomena
[DE89-005898] N89-19401
Proposal to study the interaction of polyimide precursors and thin polyimide films with silicon and silicon oxide surfaces
[AD-A201183] N89-19425
Block diagrams of the radar interface and control unit N89-19460
Interfacing laboratory instruments to multiuser, virtual memory computers
[NASA-TM-4106] N89-19578
Advanced extravehicular activity systems requirements definition study. Phase 2: Extravehicular activity at a lunar base
[NASA-CR-172117] N89-19809
An architecture for integrating distributed and cooperating knowledge-based Air Force decision aids N89-19841
Presentation planning using an integrated knowledge base N89-19845
Development of a personal-computer-based intelligent tutoring system N89-19889
SARSCEST (human factors) N89-19890
Operation of the HP2250 with the HP9000 series 200 using PASCAL 3.0
[NASA-TM-87652] N89-19892
INTERFEROMETERS
Long trace profile measurements on cylindrical aspheres
[DE89-005661] N89-19985
INTERFEROMETRY
Analytical, numerical and experimental investigations of oblique-shock-wave reflections in pure and dusty gases
[AD-A201438] N89-19511
INTERMETALLICS
Microstructural analyses of intermetallic TiAl (Nb)-compounds prepared by arc melting and by powder metallurgy
[GKSS-88/E/32] N89-19417
INTERPLANETARY MAGNETIC FIELDS
Electric fields in earth orbital space
[AD-A201747] N89-19760
INTERPOLATION
A curve-fitting package for personal computers
[LA-11082-MS] N89-19922
INTERPROCESSOR COMMUNICATION
Critical problems in very large scale computer systems
[AD-A202129] N89-19923
INTERSTELLAR MATTER
Interstellar matter in early type galaxies N89-20042
The distribution of the interstellar medium in the Scd galaxy NGC 6946 and in a sample of dwarf irregular galaxies N89-20043
Morphology and nature of the dust of the dark cloud Coal Sack
[ETN-89-93795] N89-20046
INVERSE SCATTERING
Large wave number aperture limited Fourier inversion and inverse scattering
[AD-A202247] N89-19940
INVERSIONS
Control of nonlinear systems using partial dynamic inversion N89-19310
Coordinates, conversions, and kinematics for the Rochester Robotics Lab
[AD-A201611] N89-19560
The geometry of geodetic inverse linear mapping and nonlinear adjustment
[ETN-89-93900] N89-19736
INVISCID FLOW
Unsteady transonic viscous-inviscid interaction using Euler and boundary-layer equations N89-19250
A study of flow separation in transonic flow using inviscid and viscous CFD schemes N89-19273
IO
Episodic volcanism of tidally heated satellites with application to Io. Thermal state of an ice shell on Europa. Polar wander of a synchronously rotating satellite with application to Europa N89-20052
IODINE LASERS
The standard chemical oxygen-iodine laser kinetics package
[AD-A202223] N89-19543
ION BEAMS
The divergence characteristics of constrained-sheath optics systems for use with 5-eV atomic oxygen sources
[NASA-CR-182238] N89-19973
High-precision laser and RF spectroscopy of atomic, molecular, and slow ion beams
[DE89-005870] N89-19975
Ion beam driven electrostatic shocks --- ionosphere
[MPE-PREPRINT-127] N89-19995
ION CONCENTRATION
Ionic concentrations of rime ice and snow and Bergeron process N89-19689
ION DENSITY (CONCENTRATION)
An assessment of the application of in situ ion-density data from DMSP (Defense Meteorology Satellite Program) to modeling of transionospheric scintillation
[AD-A202415] N89-19765
ION EMISSION
Kinetic processes in discharge pumped mercury halide lasers
[AD-A201612] N89-19537
ION IMPLANTATION
Raman and RBS studies of ion implanted semiconductors
[ATR-88(8359)-5] N89-20021
IONIC DIFFUSION
Reinforcement/matrix interaction in SiC fiber-reinforced Ni3Al matrix composites
[DE89-006041] N89-19384
IONIZATION
Infrared and ionization structure of the polar mesosphere
[AD-A201266] N89-19751
Mechanisms leading to single event upset
[ATR-86(8139)-5] N89-19977
IONOSPHERIC PROPAGATION
An assessment of the application of in situ ion-density data from DMSP (Defense Meteorology Satellite Program) to modeling of transionospheric scintillation
[AD-A202415] N89-19765
IONOSPHERIC SOUNDING
Ion beam driven electrostatic shocks --- ionosphere
[MPE-PREPRINT-127] N89-19995
IONS
A study of the ionospheric signature of ion supply from the ionosphere to the magnetosphere N89-19754
IOWA
Technical report on temperature, precipitation and aviation verification at WSFO Sioux Falls for 1987
[CRARP-88-5] N89-19776
IRON
The scintillating optical fiber isotope experiment (SOFIE): Bevalac calibrations of test models N89-20034
IRON ALLOYS
Investigations on undercooling, nucleation and rapid solidification of metallic systems
[DFVLR-FB-88-39] N89-19415
IRON COMPOUNDS
Kinetics and mechanism of the Fe catalyzed autoxidation of S(4)-oxides in aqueous solution N89-19687
IRRADIATION
Radiation biology studies in soft X-ray and ultrasoft X-ray region
[DE88-756071] N89-19795
IRREGULAR GALAXIES
The distribution of the interstellar medium in the Scd galaxy NGC 6946 and in a sample of dwarf irregular galaxies N89-20043
ISENTROPIC PROCESSES
Application of a full potential method to AGARD standard airfoils N89-19242
ISOLATION
Structural saliency: The detection of globally salient structures using a locally connected network
[AD-A201619] N89-19806
ISOTHERMAL FLOW
On boundary integral equation approach to a nonstationary problem of isothermal viscous compressible flows
[PREPRINT-1134] N89-19526
ISOTOPE EFFECT
The dissociative adsorption of ammonia on Si(100)
[AD-A201599] N89-19396
ISOTOPES
The scintillating optical fiber isotope experiment (SOFIE): Bevalac calibrations of test models N89-20034
Solar and interplanetary cosmic ray composition
[MPE-PREPRINT-108] N89-20056
ITERATIVE SOLUTION
Vectorization of linear recurrence relations
[REPT-88-21] N89-19951
Vertex-centered and cell-centered multigrid methods for interface problems
[REPT-88-42] N89-19953

J

JAHN-TELLER EFFECT
Investigations of the statics and dynamics of the Jahn-Teller system RbCrCl3 using neutron scattering
[ETN-89-93790] N89-20006
JAMMING
The importance of aircraft performance and signature reduction upon combat survivability
[AD-A202106] N89-19292
JET AIRCRAFT
Aerothermodynamics of a jet cell facility
[AD-A202142] N89-19318
JET ENGINE FUELS
Application of nondestructive evaluations to the prediction of turbine fuel peroxidation potential
[AD-A202291] N89-19441
JET FLOW
Study of underexpanded turbulent air jets in water N89-19516
Rotation and magnetic fields as an acceleration mechanism in astrophysical jets N89-20039
JET IMPINGEMENT
Experimental investigation on plume contamination and surface effects, phase 2 --- spacecraft
[TUHH-TRI-ESA-1987] N89-19370
JET MIXING FLOW
Mixing in gas phase turbulent jets N89-19515
JOINTS (ANATOMY)
Sensing human hand motions for controlling dexterous robots N89-19883
JOINTS (JUNCTIONS)
An interdisciplinary study of cathodic debonding in elastomer/metal adhesive bonds
[AD-A202376] N89-19434
Electron beam welding of 6061-T6 covers to A356-T6 machined cast housings
[BDX-613-3915] N89-19573
JOSEPHSON JUNCTIONS
Josephson effect research in high-temperature superconductors
[AD-A201483] N89-20002
Static and dynamic properties of arrays of superconductors N89-20017
JOUKOWSKI TRANSFORMATION
Two-dimensional test section with preadjusted adaptive walls for low speed wind tunnel
[KTH-AERO-REPT-57] N89-19278
JUDGMENTS
The effects of a pitched field orientation on hand/eye coordination
[AD-A201620] N89-19814
A method for modeling bias in a person's estimates of likelihoods of events N89-19849
JUPITER ATMOSPHERE
Temperature and circulation in the stratospheres of the outer planets
[NASA-CR-184826] N89-20051

K

KALMAN FILTERS
Time series analysis and multivariate statistical analysis
[AD-A202273] N89-19960
KERNEL FUNCTIONS
Large wave number aperture limited Fourier inversion and inverse scattering
[AD-A202247] N89-19940
KEYING
Next generation keyboards: The importance of cognitive compatibility N89-19848
KIDNEYS
National Aeronautics and Space Administration (NASA)/American Society for Engineering Education (ASEE) Summer Faculty Fellowship Program 1988, volume 2 --- Author
[NASA-CR-172118-VOL-2] N89-20073
Maladjustment of kidneys to microgravity: Design of measures to reduce the loss of calcium N89-20076
KINEMATIC EQUATIONS
A three-dimensional nonsingular simulation of rigid manipulators
[AD-A201964] N89-19569
KINEMATICS
Coordinates, conversions, and kinematics for the Rochester Robotics Lab
[AD-A201611] N89-19560
Dexterous robotic hands: Kinematics and control
[AD-A202183] N89-19570

Telepresence and telerobotics N89-19873
A novel manipulator technology for space applications N89-19874
Machine vision for space telerobotics and planetary rovers N89-19879
Sensing human hand motions for controlling dexterous robots N89-19883
Intelligent control of robotic arm/hand systems for the NASA EVA retriever using neural networks N89-20075

KINETIC EQUATIONS
Kinetic equation for polluted cloud droplets spectrum N89-19661

KINETICS
To measure and characterize metal corrosion in electrolyte solutions by exploiting the properties of superconducting
[AD-A201484] N89-19407
Kinetic processes in discharge pumped mercury halide lasers
[AD-A201612] N89-19537
The standard chemical oxygen-iodine laser kinetics package
[AD-A202223] N89-19543

KLYSTRONS
Description of FEL3D: A three dimensional simulation code for TOK and FEL
[DE89-005529] N89-19540

KNOWLEDGE BASES (ARTIFICIAL INTELLIGENCE)
Second Annual Workshop on Space Operations Automation and Robotics (SOAR 1988)
[NASA-CP-3019] N89-19817
Artificial intelligent decision support for low-cost launch vehicle integrated mission operations N89-19830
Validation of highly reliable, real-time knowledge-based systems N89-19833
Diagnosis by integrating model-based reasoning with knowledge-based reasoning N89-19835
Reducing uncertainty by using explanatory relationships N89-19837
An architecture for integrating distributed and cooperating knowledge-based Air Force decision aids N89-19841
Presentation planning using an integrated knowledge base N89-19845
An intelligent multi-media human-computer dialogue system N89-19850
Knowledge-based graphical interfaces for presenting technical information N89-19851
An intelligent interface for satellite operations: Your Orbit Determination Assistant (YODA) N89-19852
Intelligent tutoring systems research in the training systems division: Space applications N89-19854
Intelligent tutoring in the spacecraft command/control environment N89-19855
Knowledge acquisition for case-based reasoning systems N89-19856
Telerobot operator control station requirements N89-19876
Machine vision for space telerobotics and planetary rovers N89-19879
SARSCEST (human factors) N89-19890
Evaluation support system for multiple R and D projects N89-19926
intelligent mobile robot working in unknown environment N89-19927

KNOWLEDGE REPRESENTATION
Knowledge-based zonal grid generation for computational fluid dynamics N89-19828
A design and implementation methodology for diagnostic systems N89-19831
Application of flight systems methodologies to the validation of knowledge-based systems N89-19832
Transformation based endorsement systems N89-19836
Portable inference engine: An extended CLIPS for real-time production systems N89-19843
A method for modeling bias in a person's estimates of likelihoods of events N89-19849
Knowledge-based graphical interfaces for presenting technical information N89-19851
An intelligent tutoring system for space shuttle diagnosis N89-19853
Intelligent tutoring systems research in the training systems division: Space applications N89-19854
Knowledge acquisition for case-based reasoning systems N89-19856
Psychological tools for knowledge acquisition N89-19857
A representational framework and user-interface for an image understanding workstation N89-19878
JPRS report: Science and technology. Japan: 7th Artificial Intelligence Symposium
[JPRS-JST-88-020] N89-19924
Formal aspects of a knowledge system: A literature review
[REPT-88-12] N89-19933
Stochastic and fuzzy PERT
[REPT-88-26] N89-20027

KRYPTON
On the use of multiple photon processes in krypton for laser guiding of electron beams
[DE89-006546] N89-19551

L

L-SAT
Microwave holographic measurements of large reflectors: Phase 2 report, volume 2
[REPT-B091] N89-19531

LABORATORY EQUIPMENT
Current diagnostic practice in gas turbine combustors
[PNR90530] N89-19306
Mini protein crystallization facility. Phase A study: Executive summary
[REPT-AQ-ES-576/88] N89-19444

LABYRINTH SEALS
Design improvement of a pump wear ring labyrinth seal
[NASA-CR-179161] N89-19555

LAGUERRE FUNCTIONS
A generalization of Laguerre polynomials
[REPT-88-28] N89-19952

LAMINAR BOUNDARY LAYER
Curvature effects on the stability of three-dimensional laminar boundary layers N89-19500
Flight survey of the 757 wing noise field and its effects on laminar boundary layer transition. Volume 2: Data compilation
[NASA-CR-178217] N89-19505

LAMINAR FLOW
The NASA Langley laminar-flow-control experiment on a swept, supercritical airfoil - Drag equations
[NASA-TM-4096] N89-19231
Drag measurements on a laminar-flow body of revolution in the 13-inch magnetic suspension and balance system
[NASA-TP-2895] N89-19232
Some hydrodynamic instabilities of boundary layer flows N89-19501
A computationally efficient modelling of laminar separation bubbles
[NASA-CR-184789] N89-19504
The birth of open separation on a prolate spheroid
[AD-A201350] N89-19509
Superfluid turbulence in two-fluid flow of helium II N89-20018

LAMINAR FLOW AIRFOILS
Two experimental supercritical laminar-flow-control swept-wing airfoils
[NASA-TM-89073] N89-19266

LAMINATES
Durability and damage tolerance of bismaleimide composites, volume 1
[AD-A201273] N89-19374
Characterization of IM7/8551-7 carbon/epoxy in compression and shear
[DE89-005544] N89-19378
Durability and damage tolerance of bismaleimide composites. Volume 2: Appendix of crack growth and low-velocity impact data
[AD-A201839] N89-19379
Finite element analysis of laminated composite plates
[AD-A202192] N89-19381
Thermal cycling and mechanical property assessment of carbon fiber (fabric) reinforced PMR-15 polyimide laminates
[PNR90522] N89-19382
Effect of adhesive interleaving and discontinuous plies on failure of composite laminates subject to transverse normal loads
[NASA-TM-101507] N89-19589

LAND USE
Land use analysis using remote sensing techniques. Investigation of the usefulness of LANDSAT Thematic Mapper satellite pictures for obtaining and up to date picture of land use in the province South Holland
[BCRS-88-01] N89-19733

LANDSAT SATELLITES
Land use analysis using remote sensing techniques. Investigation of the usefulness of LANDSAT Thematic Mapper satellite pictures for obtaining and up to date picture of land use in the province South Holland
[BCRS-88-01] N89-19733

LARGE SPACE STRUCTURES
Proceedings of the Fifth AFOSR Forum on Space Structures
[AD-A194761] N89-19333
Modeling of flexible spacecraft accounting for orbital effects N89-19334
Wave propagation in large space structures N89-19335
System identification of suboptimal feedback control parameters based on limiting-performance/minimum-time characteristics N89-19340
Integrated Structural Analysis And Control (ISAAC): Issues and progress N89-19341
Adaptive control of large space structures N89-19343
The optimal projection equations for fixed-order dynamic compensation: Existence, convergence and global optimality N89-19345
Decentralized/relegated control for large space structures N89-19346
Frobenius-Hankel norm framework for disturbance rejection and low order decentralized controller design N89-19347
A controlled component synthesis method for truss structure vibration control N89-19348
Damage detection and location in large space trusses N89-19350
Effects of reduced order modeling on the control of a large space structure
[AD-A201674] N89-19355
Experimental verification of an innovative performance-validation methodology for large space systems
[AD-A202243] N89-19357
Maximum entropy/optimal projection design synthesis for decentralized control of large space structures
[AD-A202375] N89-19358
Investigation of flight sensors and actuators for the vibration damping augmentation of large flexible space structures
[ESA-CR(P)-2670] N89-19362
RCS/piezoelectric distributed actuator study
[AD-A201276] N89-19999

LASER ANEMOMETERS
The use of burst-triggered correlation for laser anemometry measurements in turbomachinery
[PNR90542] N89-19533
Laser transit anemometer software development program
[NASA-CR-4225] N89-19545

LASER APPLICATIONS
Natural convection liquid immersion cooling of a column of discrete heat sources in a vertical channel
[AD-A201676] N89-19513
High-speed laser photography
[AD-A202293] N89-19544
Lidar for the determination of Antarctic water vapor profiles N89-19756
An investigation of factors affecting domestic technology transfer at the Wright Aeronautical Laboratories
[AD-A201581] N89-20032

LASER BEAMS
On the use of multiple photon processes in krypton for laser guiding of electron beams
[DE89-006546] N89-19551

LASER CAVITIES
Free-electron laser driven by the NBS (National Bureau of Standards) CW microtron
[AD-A201170] N89-19535

LASER DAMAGE
Biological applications and effects of optical masers
[AD-A201834] N89-19541

LASER DOPPLER VELOCIMETERS
The use of burst-triggered correlation for laser anemometry measurements in turbomachinery
[PNR90542] N89-19533

LASER GUIDANCE
On the use of multiple photon processes in krypton for laser guiding of electron beams
[DE89-006546] N89-19551

LASER HEATING
Determination of local fluid drag by a laser heating/thermographic phosphor technique: Applicability of the H. Ludwieg model
[DE89-006462] N89-19523

LASER INDUCED FLUORESCENCE
Spectral studies of propellant combustion: Experimental details and emission results for M-30 propellant
[AD-A201634] N89-19399
Electron-beam pumped liquid excimer lasers
[DE89-006549] N89-19549

LASER MATERIALS
Nonradiative relaxation and laser action in tunable solid state laser crystals
[NASA-CR-182820] N89-19539
Evaluation of optical materials samples
[AD-A199471] N89-19981

LASER OUTPUTS
Hole formation (etching) in polymers by far (deep) UV high intensity laser (excimer) radiation pulses and its relevance to photoresists in deep UV photolysis of polymers
[AD-A202274] N89-19433

Biological applications and effects of optical masers
[AD-A201834] N89-19541
Ultrahigh-brightness XeCl laser system
[DE89-005467] N89-19548
LASER PUMPING
Nonradiative relaxation and laser action in tunable solid state laser crystals
[NASA-CR-182820] N89-19539
Proof of the feasibility of coherent and incoherent schemes for pumping a gamma-ray laser
[AD-A201931] N89-19542
Electron-beam pumped liquid excimer lasers
[DE89-006549] N89-19549
LASER RANGE FINDERS
Sensor fusion of range and reflectance data for outdoor scene analysis N89-19868
Visual perception and grasping for the extravehicular activity robot N89-20082
LASER SPECTROSCOPY
High-precision laser and RF spectroscopy of atomic, molecular, and slow ion beams
[DE89-005870] N89-19975
Laser-spectroscopic investigations of manganese centers in the zinc sulfide host lattice
[ETN-89-93791] N89-20007
LASER WEAPONS
Impact of target altitude restrictions on laser performance
[DE89-006567] N89-19553
Survivability of space assets in the long term
[DE89-006563] N89-19964
LASERS
Laser scattering studies of epoxy polymerization processes
[AD-A201925] N89-19430
Noncontact ultrasonic sensing of weld pools for automated welding
[DE89-005185] N89-19557
Optical parameter effects on laser generated ultrasound for microstructure characterization
[DE89-005193] N89-19967
LASING
Liquid excimers: Lasing Xe2 and Kr2 in liquid argon
[DE89-005449] N89-19546
LATERAL STABILITY
Analytical interpretation on lateral/directional stability and controllability of high angle-of-attack reentry flight
[ISAS-630] N89-19353
LAUNCH ESCAPE SYSTEMS
Hypervelocity technology escape system concepts. Volume 1: Development and evaluation
[AD-A201719] N89-19280
LAUNCH VEHICLES
Commercial expendable launch vehicle liability
[S-HRG-100-750] N89-19325
Booster propulsion/vehicle impact study
[NASA-CR-183584] N89-19366
LAYOUTS
Knowledge-based graphical interfaces for presenting technical information N89-19851
Telerobot operator control station requirements N89-19876
Expert systems applications for space shuttle payload integration automation N89-19887
LEACHING
An interdisciplinary study of cathodic debonding in elastomer/metal adhesive bonds
[AD-A202376] N89-19434
LEAD TELLURIDES
Evaluation of Schottky barrier and PBTE IR-CCD detectors for the SWIR and MIR wavelengths range, executive summary
[IMEC-SP/CCD-255/88-03] N89-19495
LEAKAGE
Design improvement of a pump wear ring labyrinth seal
[NASA-CR-179161] N89-19555
General review of recent activities in acoustic emission technology in Italy
[CISE-4477] N89-19601
LEARNING
Fear-potential startle as a model system for analyzing learning and memory
[AD-A201330] N89-19805
Intelligent embedded instruction for Computer-Aided Design (CAD) systems
[AD-A201811] N89-19907
Production system chunking in SOAR: Case studies in automated learning N89-20060
LEARNING CURVES
An analysis of the impact of log-linear regression on the estimated learning curve parameters
[AD-A201471] N89-19938
LEARNING MACHINES
Voice control of complex workstations N89-19880
The Boltzmann machine: A survey and generalization
[AD-A197976] N89-19929
LEAST SQUARES METHOD
A comparative analysis of tilt rotor aircraft versus helicopters using simulator results
[AD-A202190] N89-19294
Local geoid determination using the global positioning system
[AD-A202220] N89-19731
Refractive turbulence profiling via binary source intensity scintillation correlation
[AD-A202189] N89-19762
Software performance on nonlinear least-squares problems
[AD-A201879] N89-19908
An asymptotic theory for weighted least squares with weights estimated by replication
[AD-A198000] N89-19935
A geometric property of the least squares solution of linear equations
[AD-A201342] N89-19937
An analysis of the impact of log-linear regression on the estimated learning curve parameters
[AD-A201471] N89-19938
LEE WAVES
Characteristics of radar echo of snow band formed in the lee side of a mountain N89-19726
LEGAL LIABILITY
Commercial expendable launch vehicle liability
[S-HRG-100-750] N89-19325
LENS DESIGN
An achromatic super telephoto lens
[DE89-006163] N89-19986
LENSES
An achromatic super telephoto lens
[DE89-006163] N89-19986
LEVITATION
Investigations on undercooling, nucleation and rapid solidification of metallic systems
[DFVLR-FB-88-39] N89-19415
LIE GROUPS
High-order beam optics: An overview
[DE89-005441] N89-19984
LIFE (DURABILITY)
A survey of automatic code generating software
[AD-A201963] N89-19910
LIFE CYCLE COSTS
Preliminary project plan for a GEO regional transportation and servicing company
[ILR-MITT-210] N89-19331
LIFE SUPPORT SYSTEMS
Hypervelocity technology escape system concepts. Volume 1: Development and evaluation
[AD-A201719] N89-19280
A bootstrap lunar base: Preliminary design review 2
[NASA-CR-184753] N89-19807
Development of an atmospheric monitoring plan for space station N89-20065
Evaluation of available analytical techniques for monitoring the quality of space station potable water N89-20071
LIGHT (VISIBLE RADIATION)
Integration of detectors and optical waveguide structures
[AD-A201331] N89-19536
LIGHT AMPLIFIERS
Modeling the energy deposition in the Aurora KrF laser amplifier chain
[DE89-006545] N89-19550
LIGHT CURVE
Power spectra decomposition of 36 RS CVn UBV photometric light curves from the first two years of the automatic photoelectric telescope N89-20036
LIGHT MODULATION
High-speed laser photography
[AD-A202293] N89-19544
LIGHT TRANSMISSION
Hole formation (etching) in polymers by far (deep) UV high intensity laser (excimer) radiation pulses and its relevance to photoresists in deep UV photolysis of polymers
[AD-A202274] N89-19433
LIGHTNING
Lightning campaign 85/86 Transall C160 A04: Flying tests
[REPT-85/535800] N89-19297
Generalized three-dimensional experimental lightning code (G3DXL) user's manual
[NASA-CR-166079] N89-19779
A wide bandwidth electrostatic field sensor for lightning research
[NASA-TM-101539] N89-19783
LIKELIHOOD RATIO
A method for modeling bias in a person's estimates of likelihoods of events N89-19849
LIMITERS (FUSION REACTORS)
Effect of limiter currents on plasma equilibrium and stability in a tokamak
[DE88-704951] N89-19989
LINE OF SIGHT
The effects of a pitched field orientation on hand/eye coordination
[AD-A201620] N89-19814
LINE SPECTRA
Calculation of molecular absorption parameters and updating the AFGL atmospheric line parameter compilation
[AD-A202113] N89-19761
Ground-based Fabry-Perot observations of neutral and ionic atoms and molecules of comet Halley N89-20048
LINEAR ACCELERATORS
XUV free-electron laser development at Los Alamos
[DE89-005458] N89-19547
LINEAR ARRAYS
Refractive turbulence profiling via binary source intensity scintillation correlation
[AD-A202189] N89-19762
LINEAR ENERGY TRANSFER (LET)
Mechanisms leading to single event upset
[ATR-86(8139)-5] N89-19977
LINEAR EQUATIONS
A geometric property of the least squares solution of linear equations
[AD-A201342] N89-19937
LINEAR PROGRAMMING
Bifurcating optimization algorithms and their possible application
[DE89-005692] N89-19906
A heuristic ceiling point algorithm for general integer linear programming
[AD-A202285] N89-19912
An exact ceiling point algorithm for general integer linear programming
[AD-A202286] N89-19913
Linear programming along the trajectory of the problem in polynomial time
[REPT-88-17] N89-19918
The influence of the potential function on the performance of a trajectory following algorithm for the linear programming problem
[REPT-88-44] N89-19920
LINEAR RECEIVERS
Design of digital filters for navigation receivers --- GPS
[DFVLR-MITT-88-23] N89-19288
LINEAR SYSTEMS
Integrated tools for control-system analysis
[NASA-TP-2885] N89-19309
Robust control for linear systems with structured uncertainty
[AD-A201947] N89-19315
The use of direct sparse matrix methods and Newton iteration for the numerical solution of fluid flows N89-19514
Stabilization and regulation of multirate sampled-date linear systems
[REPT-88-013] N89-19930
Regulation of linear discrete time-varying systems
[ETN-89-93896] N89-19934
Vectorization of linear recurrence relations
[REPT-88-21] N89-19951
LINEARIZATION
Unsteady aerodynamics of blade rows N89-19263
LIQUEFACTION
Studies of warm-rain development N89-19620
The case for subgrid-scale condensation in numerical cloud models N89-19636
LIQUID ATOMIZATION
Characteristic time model validation
[AD-A201374] N89-19510
Computational studies of evaporating sprays in a shear layer
[AD-A201932] N89-19520
LIQUID COOLING
Natural convection liquid immersion cooling of a column of discrete heat sources in a vertical channel
[AD-A201676] N89-19513
Cooling effectiveness of a hybrid microclimate garment
[AD-A201115] N89-19811
LIQUID CRYSTALS
Some 2H NMR studies of oriented fluid phases
[AD-A201241] N89-19998
LIQUID FUELS
Experiment plans to study preignition processes of a pool fire in low gravity
[NASA-CR-182256] N89-19442
LIQUID HELIUM
The tensile strength of liquid helium four N89-20016
LIQUID HELIUM 2
Superfluid turbulence in two-fluid flow of helium II N89-20018

LIQUID LASERS
Electron-beam pumped liquid excimer lasers
[DE89-006549] N89-19549
LIQUID NITROGEN
Contamination of liquid oxygen by pressurized gaseous nitrogen
[NASA-TP-2894] N89-19499
LIQUID OXYGEN
Contamination of liquid oxygen by pressurized gaseous nitrogen
[NASA-TP-2894] N89-19499
LIQUID PROPELLANT ROCKET ENGINES
The Atlas/Centaur 67 launch mishap
[GPO-80-201] N89-19332
Studies and analyses of the space shuttle main engine. Appendix B: SSME FIPM drawings
[NASA-CR-183594] N89-19365
Safe, compact nuclear propulsion: Solid core nuclear propulsion concept
[AD-A202239] N89-19369
LIQUIDS
Liquid excimers: Lasing Xe2 and Kr2 in liquid argon
[DE89-005449] N89-19546
LITHIUM COMPOUNDS
The coupled cluster method and the properties of energetic materials
[AD-A201168] N89-19388
Oxygen electrode in molten carbonate fuel cells
[DE89-005813] N89-19745
LOAD TESTS
Some new results in rolling contact
[REPT-88-46] N89-19577
LOGIC CIRCUITS
Test aspects of the JPL Viterbi decoder N89-19457
LOGIC PROGRAMMING
Specification and management of database integrity constraints through logic programming
[REPT-88-025] N89-19915
LONG DURATION SPACE FLIGHT
Effects on motor unit potentiation and ground reaction force from treadmill exercise N89-20069
LONG TERM EFFECTS
Advanced durability analysis. Volume 4: Executive summary
[AD-A202304] N89-19597
LONGITUDINAL WAVES
The stability of boundary layer flow over elastic substrates N89-19524
Acoustoelasticity using longitudinal waves for residual stress evaluation
[DE89-006154] N89-19604
LOOPS
Calculation of mutual self inductance and coupling coefficient for closely spaced loops
[DE89-005546] N89-19471
LOSSES
A model for plasma volume changes during short duration spaceflight N89-20067
LOUDSPEAKERS
On the design of loudspeakers for broadcast monitoring
[BBC-RD-1988/14] N89-19450
LOW COST
Artificial intelligent decision support for low-cost launch vehicle integrated mission operations N89-19830
LOW LEVEL TURBULENCE
Turbulence structure and mass transport in a channel flow with polymer injection
[AD-A202237] N89-19521
LOW TEMPERATURE TESTS
Icing research tunnel test of a model helicopter rotor
[NASA-TM-101978] N89-19305
LUBRICANT TESTS
Performance evaluation of military engine and gear oils in friction and wear devices
[AD-A202145] N89-19432
LUBRICATION
In-line wear monitor
[AD-A201292] N89-19301
On the sealing and lubrication mechanism of radial lip seals
[ETN-89-93898] N89-19574
LUBRICATION SYSTEMS
Acidic attack of perfluorinated alkyl ether lubricant molecules by metal oxide surfaces
[NASA-TM-101962] N89-19402
LUNAR BASES
The development of a cislunar space infrastructure
[NASA-CR-184728] N89-19352
A bootstrap lunar base: Preliminary design review 2
[NASA-CR-184753] N89-19807

M

MACH NUMBER
Drag coefficients for irregular fragments
[AD-A201943] N89-19276
MACHINE TRANSLATION
From Algol 60 to Ada: Problems, solutions, feasibility
[REPT-88-41] N89-19919
MACHINING
Electron beam welding of 6061-T6 covers to A356-T6 machined cast housings
[BDX-613-3915] N89-19573
CAD directed robotic edge finishing
[DE89-005347] N89-19916
MAGMA
Evaluation of crustal recycling during the evolution of Archean-age Matachewan basaltic magmas N89-20077
Lithospheric buckling and intra-arc stresses: A mechanism for arc segmentation N89-20078
MAGNETIC CONTROL
Existence of stationary solutions in the coronal loop problem
[REPT-88-06] N89-20054
MAGNETIC EFFECTS
Mossbauer effect studies of magnetism in superconducting systems
[DE89-005844] N89-20012
MAGNETIC FIELDS
Substorms, plasmoids, flux robes, and magnetotail flux loss on March 25, 1983: CDAW-8
[NASA-CR-184823] N89-19764
Rotation and magnetic fields as an acceleration mechanism in astrophysical jets N89-20039
Studies of flares and disappearing magnetic flux
[AD-A201456] N89-20053
Feasibility of using high temperature superconducting magnets and conventional magnetic loop antennas to attract or repel objects at the space station N89-20081
MAGNETIC FLUX
Studies of flares and disappearing magnetic flux
[AD-A201456] N89-20053
MAGNETIC MATERIALS
Activities report in electrotechnology
[ETN-89-93715] N89-19448
MAGNETIC PROBES
MPD (Magnetoplasmadynamic) thrust chamber flow dynamics
[AD-A201263] N89-19368
MAGNETIC PROPERTIES
The aqueous electrochemistry of polyacetylene (CH)x and polyparaphenylene
[AD-A201461] N89-19426
MAGNETIC RECORDING
Substorms, plasmoids, flux robes, and magnetotail flux loss on March 25, 1983: CDAW-8
[NASA-CR-184823] N89-19764
MAGNETIC SIGNALS
Use of superconducting imaging surfaces to enhance detection of weak magnetic sources by SQUID systems
[DE89-006568] N89-20015
MAGNETIC SUSPENSION
Drag measurements on a laminar-flow body of revolution in the 13-inch magnetic suspension and balance system
[NASA-TP-2895] N89-19232
MAGNETIC TAPES
Adhesion in ceramics and magnetic media
[NASA-TM-101476] N89-19435
MAGNETOHYDRODYNAMIC GENERATORS
An innovative demonstration of high power density in a compact MHD generator
[DE89-002159] N89-19990
MAGNETOHYDRODYNAMIC STABILITY
Effect of limiter currents on plasma equilibrium and stability in a tokamak
[DE88-704951] N89-19989
Numerical studies of MHD turbulence in the reversed field pinch
[IPP-6/276] N89-19994
MAGNETOMETERS
Use of superconducting imaging surfaces to enhance detection of weak magnetic sources by SQUID systems
[DE89-006568] N89-20015
MAGNETOPAUSE
Plasma waves at the dayside magnetopause
[MPE-PREPRINT-128] N89-19996
MAGNETOPLASMADYNAMICS
MPD (Magnetoplasmadynamic) thrust chamber flow dynamics
[AD-A201263] N89-19368
MAGNETOSPHERES
A study of the ionospheric signature of ion supply from the ionosphere to the magnetosphere N89-19754
MAINTENANCE
Machinery diagnostics via mechanical vibration analysis using spectral analysis techniques
[AD-A202089] N89-19594
EMMA: The expert system for munition maintenance N89-19823
Diagnostics in the Extendable Integrated Support Environment (EISE) N89-19824
Knowledge-based operation and management of communications systems N89-19826
Design concept for the Flight Telerobotic Servicer (FITS) N89-19870
Design guidelines for remotely maintainable equipment N89-19885
MAN MACHINE SYSTEMS
Physiological assessment of task underload N89-19846
A schema-based model of situation awareness: Implications for measuring situation awareness N89-19847
Next generation keyboards: The importance of cognitive compatibility N89-19848
Simulation of the human-telerobot interface N89-19861
Man-systems requirements for the control of teleoperators in space N89-19862
Concept for a large master/slave-controlled robotic hand N89-19866
The WCSAR telerobotics test bed N89-19871
Telepresence and telerobotics N89-19873
A novel manipulator technology for space applications N89-19874
Time-delayed operation of a telerobot via geosynchronous relay N89-19877
Voice control of complex workstations N89-19880
An expert system for restructurable control N89-19886
Development of a personal-computer-based intelligent tutoring system N89-19889
SARSCEST (human factors) N89-19890
MAN-COMPUTER INTERFACE
An intelligent multi-media human-computer dialogue system N89-19850
Knowledge-based graphical interfaces for presenting technical information N89-19851
An intelligent interface for satellite operations: Your Orbit Determination Assistant (YODA) N89-19852
An intelligent tutoring system for space shuttle diagnosis N89-19853
Intelligent tutoring systems research in the training systems division: Space applications N89-19854
ISTAR evaluation
[AD-A201345] N89-19903
MANAGEMENT PLANNING
R and M (Reliability and Maintainability) quality team concept and C-17 design at Douglas Aircraft Company: An R and M 2000 initiative case study
[AD-A201574] N89-19228
MANAGEMENT SYSTEMS
Automation of the space station core module power management and distribution system N89-19822
MANEUVERABILITY
Combined preliminary airworthiness evaluation and airworthiness and flight characteristics evaluation of the UH-1H with preproduction hub spring and composite main rotor blades installed
[AD-A202316] N89-19295
MANEUVERS
Combined preliminary airworthiness evaluation and airworthiness and flight characteristics evaluation of the UH-1H with preproduction hub spring and composite main rotor blades installed
[AD-A202316] N89-19295
Maneuvering equations in terms of quasi-coordinate N89-19337
MANGANESE IONS
Laser-spectroscopic investigations of manganese centers in the zinc sulfide host lattice
[ETN-89-93791] N89-20007
MANIPULATORS
Implementation of dynamic control of a single-link flexible arm using a general micro-computer
[AD-A201622] N89-19561
Multiprocessor control of robotic manipulators N89-19562
Minimum time motion of a robotic manipulator N89-19567
A three-dimensional nonsingular simulation of rigid manipulators
[AD-A201964] N89-19569
Dexterous robotic hands: Kinematics and control
[AD-A202183] N89-19570
A finite element dynamic analysis of flexible spatial mechanisms and manipulators
[ETN-89-93901] N89-19575

Local position control: A new concept for control of manipulators N89-19864
Dexterity analysis and robot hand design N89-19865
Design concept for the Flight Telerobotic Servicer (FITS) N89-19870
A novel manipulator technology for space applications N89-19874
A robust control scheme for flexible arms with friction in the joints N89-19875
Machine vision for space telerobotics and planetary rovers N89-19879
Application of model based control to robotic manipulators N89-19884
Design guidelines for remotely maintainable equipment N89-19885
Model evaluation, recommendation and prioritizing of future work for the manipulator emulator testbed N89-20072
National Aeronautics and Space Administration (NASA)/American Society for Engineering Education (ASEE) Summer Faculty Fellowship Program 1988, volume 2 --- Author
[NASA-CR-172118-VOL-2] N89-20073
Intelligent control of robotic arm/hand systems for the NASA EVA retriever using neural networks N89-20075
Visual perception and grasping for the extravehicular activity robot N89-20082

MANNED SPACE FLIGHT
A model for plasma volume changes during short duration spaceflight N89-20067

MANUFACTURING
Estimating aircraft airframe tooling cost: An alternative to DAPCA 3
[AD-A201506] N89-19226
The relationship between manufacturing technology and design --- aircraft engines
[PNR90537] N89-19307

MAPPING
CAD-model-based vision for space applications N89-19867

MARINE ENVIRONMENTS
Variations of the tropospheric propagation range of ultrashort radio waves above the sea N89-19486
Boundary layer development over the eastern Pacific Ocean N89-19753

MARINE METEOROLOGY
Airborne studies of the ice phase in maritime clouds around the British Isles N89-19623
Influences of cloud microphysics on continental and marine precipitation chemistry N89-19700

MARKET RESEARCH
Economic analysis of NAVSAT system
[REPT-1013-CA/TS] N89-19265

MARKOV PROCESSES
Minification processes
[AD-A202219] N89-19958

MARS SURFACE SAMPLES
An assessment of the micrometeoritic component in the Martian soil N89-20070

MASERS
Biological applications and effects of optical masers
[AD-A201834] N89-19541

MASS FLOW
MPD (Magnetoplasmadynamic) thrust chamber flow dynamics
[AD-A201263] N89-19368

MASS SPECTROSCOPY
Arc jet diagnostics tests N89-20085

MASS TRANSFER
Turbulence structure and mass transport in a channel flow with polymer injection
[AD-A202237] N89-19521

MASSIVELY PARALLEL PROCESSORS
FONR optical computing ST
[AD-A201002] N89-19897

MATHEMATICAL LOGIC
On purely exponential logic queries
[AD-A201259] N89-19902

MATHEMATICAL MODELS
Modeling of flexible spacecraft accounting for orbital effects N89-19334
Majorant analysis of performance degradation due to uncertainty N89-19344
Decentralized/relegated control for large space structures N89-19346
Error localization and updating of spacecraft structures mathematical models
[YMD/EF/0175] N89-19361
A Monte Carlo simulation of the single-filament-composite test N89-19376
A fundamental mathematical theory in the dynamics of combustion processes
[AD-A201284] N89-19391
A computationally efficient modelling of laminar separation bubbles
[NASA-CR-184789] N89-19504
Computational fluid dynamics for combustion applications
[PNR90534] N89-19525
Modeling of inertial effects in transient liquid-bubble flows
[REPT-88-22] N89-19528
Design of an optical sensor system for adaptive control of a seam tracking robot N89-19565
Plastic buckling of cylinders under biaxial loading N89-19591
A model of the electrostatic-aerodynamic shape of raindrops N89-19615
Damped-oscillation representation of drop-spectrum evolution due to coalescence and breakup N89-19660
Simulation of conical graupel by using a ballistic model N89-19679
Study of the use of radar X-band data of bare soil in a radar scattering model
[BCRS-88-04] N89-19735
An investigation of the relationship between beam and global irradiation with the development of numerical solar radiation models N89-19748
The climate inversion problem: A statistical/modeling approach N89-19784
A method for modeling bias in a person's estimates of likelihoods of events N89-19849
Application of model based control to robotic manipulators N89-19884
An asymptotic theory for weighted least squares with weights estimated by replication
[AD-A196000] N89-19935
Criterion based equivalence for equation error models
[WTHD-188] N89-19941
The divergence characteristics of constrained-sheath optics systems for use with 5-eV atomic oxygen sources
[NASA-CR-182238] N89-19973
Quench pressure, thermal expulsion, and normal zone propagation in internally cooled superconductors
[DE89-005668] N89-20003
Near-infrared spectroscopy of young stellar objects N89-20033
Rotation and magnetic fields as an acceleration mechanism in astrophysical jets N89-20039
Phenomenological models from higher dimensions with and without supergravity N89-20045

MATHEMATICAL PROGRAMMING
A heuristic ceiling point algorithm for general integer linear programming
[AD-A202265] N89-19912
An exact ceiling point algorithm for general integer linear programming
[AD-A202286] N89-19913

MATRICES (MATHEMATICS)
Estimating projected controllable sets for dynamical control systems N89-19313

MATRIX MATERIALS
A Monte Carlo simulation of the single-filament-composite test N89-19376
Reinforcement/matrix interaction in SiC fiber-reinforced Ni3Al matrix composites
[DE89-006041] N89-19384

MATRIX THEORY
Robust control for linear systems with structured uncertainty
[AD-A201947] N89-19315

MAXIMUM PRINCIPLE
Minimax and maximax optimal control problems with applications in aerospace engineering N89-19311

MEAN
The development and structural characteristics of Dean vortices in a curved rectangular channel
[AD-A201249] N89-19508

MECHANICAL PROPERTIES
Experimental simulation of transonic vortex-airfoil interactions
[AD-A201934] N89-19274
A new approach to the evaluation of the effects of stress state and interfacial properties on the behavior of advanced metal matrix composites
[AD-A201246] N89-19373
Composite reliability enhancement via reloading
[AD-A201861] N89-19380
Gas hydrates thermomechanics
[DE88-010280] N89-19387
Solidification, structure and mechanical properties of A357 aluminum alloy N89-19409
Processing of aluminum alloy 2090 for superplasticity
[AD-A201865] N89-19411
The mechanical behavior of surface modified ceramics
[DE89-004764] N89-19422
The determination of the mechanical behavior of polyamic acid/polyimide coatings N89-19428
Some novel test methods for, and associated problems of mechanical strength characterization of engineering ceramics
[PNR90492] N89-19436
High strain-rate behaviour of polymers using blast-wave and impact-loading methods N89-19592

MEDICAL EQUIPMENT
Ultrasound transmission tomography, a low-cost realization --- medical equipment
[ISBN-90-9002330-5] N89-19804

MEDICAL PHENOMENA
Probability theories, fuzzy set theory and syllogisms; a literature review
[REPT-88-13] N89-19961

MELTING
A wind tunnel study on the melting of snow flakes N89-19611
Evaporation and melting of ice crystals: A laboratory study N89-19612

MEMBRANES
Investigation of the interface between two immiscible electrolytes applied to membrane electrochemistry
[AD-A201310] N89-19393

MEMORY
Fear-potential startle as a model system for analyzing learning and memory
[AD-A201330] N89-19805
Computer technologies and institutional memory N89-20062

MEMORY (COMPUTERS)
Garbage collection can be made real-time and verifiable N89-19840

MENTAL PERFORMANCE
Model-based reasoning: Troubleshooting
[AD-A201614] N89-19445
Brain activity during tactical decision-making. Part 4: Event-related potentials as indices of selective attention and cognitive workload
[AD-A201370] N89-19797
A method for modeling bias in a person's estimates of likelihoods of events N89-19849
Psychological tools for knowledge acquisition N89-19857

MERCURY (METAL)
Kinetic processes in discharge pumped mercury halide lasers
[AD-A201612] N89-19537

MERCURY CADMIUM TELLURIDES
Determination of general and specific properties of wide energy-band gap HgCdTe in the 1 to 2 micrometer wavelength range
[AD-A201341] N89-19488

MESOSCALE PHENOMENA
A comparative study of two microphysical schemes in a beta mesoscale model N89-19640
Generalized microphysics scheme for use in mesoscale/cloud models N89-19641
Radiative influences on precipitating mesoscale systems N89-19648
Meteorological and chemical influencing factors on acidity production in a mesoscale model with quasi-spectral microphysics N89-19711
Microphysical and dynamical interactions in Colorado front range upslope storms N89-19725
Mesoscale Convective Systems: Structure, development and storm-environment interactions N89-19788

MESOSPHERE
Infrared and ionization structure of the polar mesosphere
[AD-A201266] N89-19751

METAL COMBUSTION
NRL boron propellants combustion program
[AD-A201242] N89-19440

METAL FATIGUE
A new approach to the evaluation of the effects of stress state and interfacial properties on the behavior of advanced metal matrix composites
[AD-A201246] N89-19373
The effect of hydrogen on fatigue crack growth rate of AISI 304 stainless steel N89-19410
Advanced durability analysis. Volume 4: Executive summary
[AD-A202304] N89-19597

METAL HALIDES
Kinetic processes in discharge pumped mercury halide lasers
[AD-A201612] N89-19537

METAL MATRIX COMPOSITES
A new approach to the evaluation of the effects of stress state and interfacial properties on the behavior of advanced metal matrix composites
[AD-A201246] N89-19373

METAL OXIDES
Acidic attack of perfluorinated alkyl ether lubricant molecules by metal oxide surfaces
[NASA-TM-101962] N89-19402
An interdisciplinary study of cathodic debonding in elastomer/metal adhesive bonds
[AD-A202376] N89-19434

METAL PLATES
Passive vibration control using viscoelastic and constrained layer beam waveguide absorbers
[AD-A202188] N89-19595
METAL SURFACES
An electrochemical study of corrosion protection by primer-topcoat systems on 4130 steel with ac impedance and dc methods
[NASA-TP-2820] N89-19406
METAL VAPOR LASERS
Kinetic processes in discharge pumped mercury halide lasers
[AD-A201612] N89-19537
METALLOGRAPHY
Analysis of PERSHING 2 Reentry Vehicle (RV) control ring castings
[AD-A201548] N89-19559
METALS
Adhesion in ceramics and magnetic media
[NASA-TM-101476] N89-19435
Positron spectroscopy for materials characterization
[DE89-005766] N89-20010
METASTABLE STATE
Proof of the feasibility of coherent and incoherent schemes for pumping a gamma-ray laser
[AD-A201931] N89-19542
METEOROID CONCENTRATION
An assessment of the micrometeoritic component in the Martian soil N89-20070
METEOROLOGICAL FLIGHT
On the observations of cloud temperature and liquid water content using a Lyman-alpha and an FSSP sensor --- forward scattering spectrometer probe (FSSP) N89-19618
A test of ice crystal production by aircraft N89-19622
Intercomparisons of aircraft measurements with lidar returns for aerosol, ice crystals and water droplets N89-19718
METEOROLOGICAL INSTRUMENTS
On the observations of cloud temperature and liquid water content using a Lyman-alpha and an FSSP sensor --- forward scattering spectrometer probe (FSSP) N89-19618
Airborne cloud sieving N89-19681
Calibration of PMS FSSP and 1D-C probes for cloud droplet measurements N89-19713
A poor man's optical fog detector N89-19716
METEOROLOGICAL PARAMETERS
TDWR (Terminal Doppler Weather Radar) scan strategy requirements
[AD-A201785] N89-19473
Propagation problems regarding 20/30 GHz bands in Earth-space links
[REPT-88-022] N89-19480
Propagation problems regarding millimeter waves (40/50 GHz)
[REPT-88-023] N89-19481
An investigation of the intermittent turbulent breakdown of the nocturnal planetary boundary layer
[AD-A201743] N89-19518
Proportion of riming growth process in snowfall phenomena N89-19668
A new database of ice particle size spectra for altitudes up to 10 km (30,000 ft) N89-19673
Meteorological and chemical influencing factors on acidity production in a mesoscale model with quasi-spectral microphysics N89-19711
METEOROLOGICAL RADAR
TDWR (Terminal Doppler Weather Radar) scan strategy requirements
[AD-A201785] N89-19473
Radar observations and modelling of warm rain initiation N89-19621
Radar observations of precipitation microstructure: The morphology of linear depolarization measurements in cloud N89-19714
Multiparameter Doppler radar observations of a squall line with the polarimetric DFVLR radar N89-19715
Applications of the NCAR Electra Doppler radar for the study of physical parameters of clouds N89-19717
Intercomparisons of aircraft measurements with lidar returns for aerosol, ice crystals and water droplets N89-19718
Characteristics of radar echo of snow band formed in the lee side of a mountain N89-19726
Study on cloud and rain by microwave radiometer observation N89-19727
A preliminary study of precursors to Huntsville microbursts
[AD-A200914] N89-19782
METEOROLOGICAL SATELLITES
JPRS report: Science and technology. USSR: Electronics and electrical engineering
[JPRS-UEE-88-005] N89-19485
Peaceful uses of electrical engineering in space N89-19487
TRMM (Tropical Rainfall Measuring Mission): A satellite mission to measure tropical rainfall
[NASA-TM-101288] N89-19789
METEOROLOGY
Use of cluster analysis to define periods of similar meteorology and precipitation chemistry in eastern North America N89-19785
Mesoscale Convective Systems: Structure, development and storm-environment interactions N89-19788
METEOSAT SATELLITE
Meteosat Millimetre Wave Sounder (MWS) study
[BAE-TP-9119] N89-19363
METHANE
Booster propulsion/vehicle impact study
[NASA-CR-183584] N89-19366
METROLOGY
Activities report in electrotechnology
[ETN-89-93715] N89-19448
Microwave holographic measurements of large reflectors: Phase 1 report, volume 1 --- spacecraft antennas
[REPT-B090] N89-19530
Microwave holographic measurements of large reflectors: Phase 2 report, volume 2
[REPT-B091] N89-19531
MICROBURSTS (METEOROLOGY)
TDWR (Terminal Doppler Weather Radar) scan strategy requirements
[AD-A201785] N89-19473
A preliminary study of precursors to Huntsville microbursts
[AD-A200914] N89-19782
MICROCLIMATOLOGY
Cooling effectiveness of a hybrid microclimate garment
[AD-A201115] N89-19811
MICROCOMPUTERS
Implementation of dynamic control of a single-link flexible arm using a general micro-computer
[AD-A201622] N89-19561
Dexterous robotic hands: Kinematics and control
[AD-A202183] N89-19570
An intelligent tutoring system for space shuttle diagnosis N89-19853
MICROMECHANICS
Thermal cycling and mechanical property assessment of carbon fiber (fabric) reinforced PMR-15 polyimide laminates
[PNR90522] N89-19382
MICROMETEORITES
National Aeronautics and Space Administration (NASA)/American Society for Engineering Education (ASEE) Summer Faculty Fellowship Program 1988, volume 1
[NASA-CR-172118-VOL-1] N89-20058
An assessment of the micrometeoritic component in the Martian soil N89-20070
MICROPROCESSORS
Advanced information technology monitoring with microprocessors --- spacecraft control
[MMP-1-IS-02-3302-FR] N89-19895
MICROPROGRAMMING
Scheme86: An architecture for microcoding a scheme interpreter
[AD-A201258] N89-19893
MICROSCOPES
Applications of scanning tunneling microscopy to electrochemistry
[AD-A201613] N89-19398
MICROSTRUCTURE
A new approach to the evaluation of the effects of stress state and interfacial properties on the behavior of advanced metal matrix composites
[AD-A201246] N89-19373
Solidification, structure and mechanical properties of A357 aluminum alloy N89-19409
Processing of aluminum alloy 2090 for superplasticity
[AD-A201865] N89-19411
Microstructural optimisation of titanium alloys for defect tolerance in gas turbine engine components
[PNR90503] N89-19413
Microstructural analyses of intermetallic TiAl (Nb)-compounds prepared by arc melting and by powder metallurgy
[GKSS-88/E/32] N89-19417
Radar observations of precipitation microstructure: The morphology of linear depolarization measurements in cloud N89-19714
Optical parameter effects on laser generated ultrasound for microstructure characterization
[DE89-005193] N89-19967
SIMS measurement of oxygen tracer diffusion in YBa2Cu3O7-delta
[DE89-005884] N89-20014
MICROTRONS
Free-electron laser driven by the NBS (National Bureau of Standards) CW microtron
[AD-A201170] N89-19535
MICROWAVE ANTENNAS
Systems analysis for DSN microwave antenna holography N89-19463
Millimeter wave antennas
[AD-A201919] N89-19474
MICROWAVE ATTENUATION
Propagation problems regarding 20/30 GHz bands in Earth-space links
[REPT-88-022] N89-19480
Propagation problems regarding millimeter waves (40/50 GHz)
[REPT-88-023] N89-19481
MICROWAVE HOLOGRAPHY
Microwave holographic measurements of large reflectors: Phase 1 report, volume 1 --- spacecraft antennas
[REPT-B090] N89-19530
Microwave holographic measurements of large reflectors: Phase 2 report, volume 2
[REPT-B091] N89-19531
MICROWAVE RADIOMETERS
Study on cloud and rain by microwave radiometer observation N89-19727
MICROWAVE SOUNDING
Meteosat Millimetre Wave Sounder (MWS) study
[BAE-TP-9119] N89-19363
MICROWAVE TRANSMISSION
The Telecommunications and Data Acquisition Report
[NASA-CR-184812] N89-19451
Microwave time delays for the dual L-C-band feed system N89-19462
Propagation problems regarding 20/30 GHz bands in Earth-space links
[REPT-88-022] N89-19480
Propagation problems regarding millimeter waves (40/50 GHz)
[REPT-88-023] N89-19481
MICROWAVE TUBES
Design and test of a 2.25-MW transformer rectifier assembly N89-19452
MICROWAVES
Time-domain imaging N89-20084
MILITARY AIRCRAFT
Multiple-Purpose Subsonic Naval Aircraft (MPSNA) Multiple Application Propfan Study (MAPS)
[NASA-CR-175096] N89-19289
Multiple Application Propfan Study (MAPS): Advanced tactical transport
[NASA-CR-175003] N89-19300
MILITARY OPERATIONS
RPV (Remote Piloted Vehicle) applications in the US Navy
[AD-A202151] N89-19293
Performance evaluation of military engine and gear oils in friction and wear devices
[AD-A202145] N89-19432
MILLIMETER WAVES
Meteosat Millimetre Wave Sounder (MWS) study
[BAE-TP-9119] N89-19363
Millimeter wave antennas
[AD-A201919] N89-19474
Normalized radar cross section of natural surfaces at millimeter wavelengths
[AD-A202252] N89-19475
MINIMAL SURFACES
Born-Infeld equations and minimal surfaces
[DE88-704966] N89-19936
MINIMAX TECHNIQUE
Minimax and maximax optimal control problems with applications in aerospace engineering N89-19311
MIRRORS
Study of space aluminum coating, executive summary --- telescope mirrors
[IOM/CAEE-002/87(TR)] N89-19443
Evaluation of optical materials samples
[AD-A199471] N89-19981
National Aeronautics and Space Administration (NASA)/American Society for Engineering Education (ASEE) Summer Faculty Fellowship Program 1988, volume 2 --- Author
[NASA-CR-172118-VOL-2] N89-20073
Optical joint correlation using the deformable mirror device N89-20074
MISSION PLANNING
MODIS information, data and control system (MIDACS) operations concepts
[NASA-TM-100720] N89-19729
Superconducting gravity gradiometer mission. Volume 2: Study team technical report
[NASA-TM-4091] N89-19749

Satellite remote sensing of heat stress during reserve training at Fort Hood
[AD-A201555] N89-19800
A bootstrap lunar base: Preliminary design review 2
[NASA-CR-184753] N89-19807
The scheduling techniques of ESP2 N89-19818
Space station payload operations scheduling with ESP2 N89-19819
The Ninevah Mission: A design summary for an unmanned mission to Venus, volume 1
[NASA-CR-184705] N89-20040
The Ninevah Mission: Analytical analyses and calculations for trajectory and propulsion, volume 2
[NASA-CR-184706] N89-20041

MIXING
Heterogeneous mixing measurements in small nonprecipitating cumuli N89-19635

MIXING HEIGHT
Boundary layer development over the eastern Pacific Ocean N89-19753

MIXING LENGTH FLOW THEORY
Mixing in gas phase turbulent jets N89-19515

MOBILITY
Intelligent mobile robot working in unknown environment N89-19927

MODEL REFERENCE ADAPTIVE CONTROL
Application of model based control to robotic manipulators N89-19884

MODELS
Computation of stereo and visual motion: From biophysics to psychophysics
[AD-A201873] N89-19802
Development of a model which provides a total system approach to integrating voice recognition and speech synthesis into the cockpit of US Navy aircraft
[AD-A202122] N89-19815
A schema-based model of situation awareness: Implications for measuring situation awareness N89-19847
Analysis of blending algorithms in computer graphics
[AD-A201921] N89-19909

MODULARITY
A novel manipulator technology for space applications N89-19674

MODULATORS
A low-loss linear analog phase modulator for 8415 MHz transponder application N89-19465

MODULES
An intelligent tutoring system for space shuttle diagnosis N89-19853
Computer-aided fabrication system implementation
[AD-A202128] N89-19911

MODULUS OF ELASTICITY
Composite materials at high temperatures
[AD-A201163] N89-19372

MOIRE INTERFEROMETRY
Boundary layer and singularity measurement in three dimensional fracture problems
[AD-A201277] N89-19584

MOISTURE CONTENT
Liquid water content, median volume diameter and temperature in dependence on the height above the cloud base for different types of clouds --- aircraft icing N89-19662
Lidar for the determination of Antarctic water vapor profiles N89-19756

MOLECULAR ABSORPTION
Calculation of molecular absorption parameters and updating the AFGL atmospheric line parameter compilation
[AD-A202113] N89-19761

MOLECULAR BEAM EPITAXY
Development of Si/SiGe heterostructures
[AD-A201440] N89-20001
The 2-4 semiconductor superlattices
[AD-A202369] N89-20005

MOLECULAR BEAMS
High-precision laser and RF spectroscopy of atomic, molecular, and slow ion beams
[DE89-005870] N89-19975

MOLECULAR COLLISIONS
Ion and electron interactions at thermal and suprathermal energies
[AD-A201418] N89-19394

MOLECULAR EXCITATION
Intermolecular and intramolecular vibrational relaxation and energy transfer
[AD-A201610] N89-19974

MOLECULAR FLOW
Ion and electron interactions at thermal and suprathermal energies
[AD-A201418] N89-19394

MOLECULAR INTERACTIONS
Intermolecular and intramolecular vibrational relaxation and energy transfer
[AD-A201610] N89-19974

MOLECULAR IONS
High-precision laser and RF spectroscopy of atomic, molecular, and slow ion beams
[DE89-005870] N89-19975

MOLECULAR OSCILLATIONS
Intermolecular and intramolecular vibrational relaxation and energy transfer
[AD-A201610] N89-19974

MOLECULAR RELAXATION
Nonradiative relaxation and laser action in tunable solid state laser crystals
[NASA-CR-182820] N89-19539
Intermolecular and intramolecular vibrational relaxation and energy transfer
[AD-A201610] N89-19974

MOLECULAR ROTATION
Some 2H NMR studies of oriented fluid phases
[AD-A201241] N89-19998

MOLECULAR SPECTROSCOPY
Calculation of molecular absorption parameters and updating the AFGL atmospheric line parameter compilation
[AD-A202113] N89-19761
The V3, V4 and V6 bands of formaldehyde: A spectral catalog from 900 cm(-1) to 1580 cm(-1)
[NASA-TM-100709] N89-19976

MOLECULAR STRUCTURE
The coupled cluster method and the properties of energetic materials
[AD-A201168] N89-19388
Intermolecular and intramolecular vibrational relaxation and energy transfer
[AD-A201610] N89-19974
Atomic structure of tilt grain boundaries in NiO
[DE89-005847] N89-20013

MOMENTUM THEORY
A new pumpjet design theory
[AD-A201353] N89-19558

MONITORS
In-line wear monitor
[AD-A201292] N89-19301
Development of an atmospheric monitoring plan for space station N89-20065
Evaluation of available analytical techniques for monitoring the quality of space station potable water N89-20071

MONKEYS
Computation of stereo and visual motion: From biophysics to psychophysics
[AD-A201873] N89-19802

MONOTONY
Physiological assessment of task underload N89-19846

MONTE CARLO METHOD
A Monte Carlo simulation of the single-filament-composite test N89-19376
Ion pair solvation
[AD-A201529] N89-19395
A Monte Carlo test program with vectorized geometry routines --- radiation transport
[JUEL-2202] N89-19947
Sensitivity analysis using the Monte Carlo acceptance-rejection method
[AD-A201261] N89-19955
HERMES, a Monte Carlo program system for beam-materials interaction studies --- radiation transport
[JUEL-2203] N89-19979
The 2-4 semiconductor superlattices
[AD-A202369] N89-20005

MOROCCO
Microphysical observations over the Atlas Mountains in Morocco N89-19724

MORPHOLOGY
Solidification, structure and mechanical properties of A357 aluminum alloy N89-19409
Polymer morphology and transport
[AD-A201167] N89-19424
Thermal oxidation of 3-5 compound semiconductors
[DE89-007127] N89-20020
Morphology and nature of the dust of the dark cloud Coal Sack
[ETN-89-93795] N89-20046

MOSSBAUER EFFECT
Mossbauer effect studies of magnetism in superconducting systems
[DE89-005844] N89-20012

MOTION SIMULATION
The use of the articulated total body model as a robot dynamics simulation tool N89-19872

MOUNTAINS
Microphysical observations over the Atlas Mountains in Morocco N89-19724
Characteristics of radar echo of snow band formed in the lee side of a mountain N89-19726

MRCA AIRCRAFT
Short-range anti-armour flight vehicles of the Apache/CWS family
[DRIC-T-8130] N89-19296

MULTIPLE ACCESS
PSDE/SAT-2 preliminary spacecraft configuration study, executive summary
[ESA-CR(P)-2689] N89-19360
PSDE/SAT-2: Preliminary spacecraft configuration study, executive summary
[ESA-CR(P)-2704] N89-19364

MULTIPROCESSING (COMPUTERS)
Multiprocessor control of robotic manipulators N89-19562
Dexterous robotic hands: Kinematics and control
[AD-A202183] N89-19570
Interfacing laboratory instruments to multiuser, virtual memory computers
[NASA-TM-4106] N89-19578
Spaceborne VHSIC multiprocessor system for AI applications N89-19838
Application of the OCCAM/transputer conception as busless multiprocessor system in a digital controller
[DFVLR-FB-88-40] N89-19896
Bitbus data transmission with galvanic separations
[DIGEL-78] N89-19898
Development of a software interface for optical disk archival storage for a new life sciences flight experiments computer N89-20061

MULTISENSOR APPLICATIONS
A multi-sensor system for robotics proximity operations N89-19881

MULTIVARIATE STATISTICAL ANALYSIS
Time series analysis and multivariate statistical analysis
[AD-A202273] N89-19960
Highly efficient estimates of multivariate location with high breakdown point
[REPT-88-14] N89-19962

N

N-TYPE SEMICONDUCTORS
Ohmic contacts to gallium aluminum arsenide for high temperature applications
[AD-A202248] N89-19492
The 2-4 semiconductor superlattices
[AD-A202369] N89-20005

NASA PROGRAMS
National Aeronautics and Space Administration authorization
[S-HRG-100-579-PT-2] N89-20031
Computer technologies and institutional memory N89-20062

NASTRAN
NASTRAN supplemental documentation for modal forced vibration analysis of aerodynamically excited turbosystems
[NASA-CR-174967] N89-19583

NAVIER-STOKES EQUATION
Numerical solution of unsteady rotational flow past fixed and rotary wing configurations N89-19251
Unsteady Navier-Stokes computations over airfoils using both fixed and dynamic meshes N89-19252
Numerical simulation of the aerodynamics of turbulent transonic flow past a projectile N89-19270
Numerical computations of transonic critical aerodynamic behavior
[AD-A202412] N89-19277
Error norm guided flow analysis of shock-wave/boundary-layer interactions
[AD-A201176] N89-19507
On boundary integral equation approach to a nonstationary problem of isothermal viscous compressible flows
[PREPRINT-1134] N89-19526

NAVIGATION
A 2-D and 3-D robot path planning algorithm based on quadtree and octree representation of workspace
[DE89-005014] N89-19900

NAVIGATION AIDS
A heuristically based navigation system for an autonomous walking machine with a range scanner N89-19563

NAVIGATION SATELLITES
Economic analysis of NAVSAT system
[REPT-1013-CA/TS] N89-19285
Study of NAVSAT for precise positioning
[IKU-88.068] N89-19286

NEODYMIUM LASERS
JPRS report: Science and technology. USSR: Electronics and electrical engineering
[JPRS-UEE-88-005] N89-19485
Ultrahigh-brightness XeCl laser system
[DE89-005467] N89-19548

NERVOUS SYSTEM
Computation of stereo and visual motion: From biophysics to psychophysics
[AD-A201873] N89-19802
NETWORK ANALYSIS
Status of DOE information network modifications
[DE89-005191] N89-20028
Global scientific and technical information network
[AD-A201902] N89-20030
NETWORK CONTROL
Knowledge-based operation and management of communications systems N89-19826
Discrete event systems with stochastic processing times
[REPT-88-11] N89-19946
NEURAL NETS
The Boltzmann machine: A survey and generalization
[AD-A197976] N89-19929
NEUTRAL ATOMS
Ground-based Fabry-Perot observations of neutral and ionic atoms and molecules of comet Halley N89-20048
NEUTRAL BEAMS
Beam profile effects on NPB performance
[LA-11228-MS] N89-19980
NEUTRALIZERS
Beam profile effects on NPB performance
[LA-11228-MS] N89-19980
NEUTRON SCATTERING
Investigations of the statics and dynamics of the Jahn-Teller system RbCrCl3 using neutron scattering
[ETN-89-93790] N89-20006
NEWTON METHODS
The use of direct sparse matrix methods and Newton iteration for the numerical solution of fluid flows N89-19514
NICKEL ALLOYS
Investigations on undercooling, nucleation and rapid solidification of metallic systems
[DFVLR-FB-88-39] N89-19415
NICKEL COMPOUNDS
Reinforcement/matrix interaction in SiC fiber-reinforced Ni3Al matrix composites
[DE89-006041] N89-19384
NICKEL OXIDES
Atomic structure of tilt grain boundaries in NiO
[DE89-005847] N89-20013
NIOBIUM
XPS and AES studies of thin oxide layers on niobium for superconducting RF cavities
[DE88-756073] N89-19997
NIOBIUM ALLOYS
Tensile and creep rupture behavior of P/M processed Nb-base alloy, WC-3009
[NASA-TM-101954] N89-19371
NIOBIUM COMPOUNDS
Improvements in the properties of NbN layers through the presence of small amounts of aluminum during sputtering
[KFK-4409] N89-19418
NITRIC ACID
Stratospheric nitric acid: Feasibility of routine measurement by observation from commercial airliners in IR bands from 9 to 14 microns
[C-48-1977] N89-19770
NITROBENZENES
Investigation of the interface between two immiscible electrolytes applied to membrane electrochemistry
[AD-A201310] N89-19393
NITROGEN
Effect of temperature on the corrosion resistance of nitrogen bearing AL6X and 904L stainless steels
[AD-A201955] N89-19412
Adhesion in ceramics and magnetic media
[NASA-TM-101476] N89-19435
NOAA SATELLITES
Variations of the tropospheric propagation range of ultrashort radio waves above the sea N89-19486
NOCTURNAL VARIATIONS
An investigation of the intermittent turbulent breakdown of the nocturnal planetary boundary layer
[AD-A201743] N89-19518
NOISE (SOUND)
Noise assessment of the rocket sled test track operation at Holloman AFB, New Mexico
[AD-A201279] N89-19317
NOISE POLLUTION
Noise assessment of the rocket sled test track operation at Holloman AFB, New Mexico
[AD-A201279] N89-19317
NOISE REDUCTION
Acoustic wave propagation in heterogeneous structures including experimental validation
[NASA-TM-101486] N89-19965
NOISE TEMPERATURE
RF performance measurement of the DSS-14 70-meter antenna at C-band/L-band N89-19461
NONDESTRUCTIVE TESTS
Application of nondestructive evaluations to the prediction of turbine fuel peroxidation potential
[AD-A202291] N89-19441
A dynamic, time stepping boundary element method for frictional crack and interface problems N89-19590
Acoustoelasticity using longitudinal waves for residual stress evaluation
[DE89-006154] N89-19604
Optical parameter effects on laser generated ultrasound for microstructure characterization
[DE89-005193] N89-19967
NONEQUILIBRIUM FLOW
Model formulation of non-equilibrium gas radiation for hypersonic flight vehicles N89-20066
NONLINEAR EQUATIONS
An invariant imbedding T matrix approach to electromagnetic scattering
[AD-A202298] N89-19476
Development of parallel algorithms for electrical power management in space applications N89-20063
NONLINEAR FEEDBACK
Nonlinear optimal control and near-optimal guidance strategies in spacecraft general attitude maneuvers N89-19356
NONLINEAR SYSTEMS
Control of nonlinear systems using partial dynamic inversion N89-19310
Majorant analysis of performance degradation due to uncertainty N89-19344
Nonlinear vibrations of composite material shells N89-19377
Chaotic dynamics and control of nonlinear and flexible arm robotic devices N89-19566
New approaches to reconfigurable optical interconnections for optical computing
[AD-A201307] N89-19982
NONLINEARITY
Steady waves in a nonlinear theory of viscoelasticity N89-19470
Software performance on nonlinear least-squares problems
[AD-A201879] N89-19908
NONNEWTONIAN FLUIDS
Interdisciplinary research in viscoelasticity and rheology
[AD-A201270] N89-19390
NONPARAMETRIC STATISTICS
Estimation in large samples
[AD-A201459] N89-19956
NONSTABILIZED OSCILLATION
Damped-oscillation representation of drop-spectrum evolution due to coalescence and breakup N89-19660
NORMAL DENSITY FUNCTIONS
Large deviation local limit theorems for ratio statistics
[AD-A201169] N89-19954
NORTH SEA
Directional wave data recorded in the southern North Sea
[IOS-258] N89-19793
NOWCASTING
A case study of significant lake enhanced snow event in upper Michigan
[CRARP-88-2] N89-19773
NOZZLE FLOW
Mixing in gas phase turbulent jets N89-19515
Vortex convection in nonuniform compressible flow
[MPIS-4/1988] N89-19527
NUCLEAR MAGNETIC RESONANCE
Development of Nuclear Magnetic Resonance (NMR) imaging technology for advanced ceramics
[DE89-006400] N89-19438
Application of nondestructive evaluations to the prediction of turbine fuel peroxidation potential
[AD-A202291] N89-19441
Some 2H NMR studies of oriented fluid phases
[AD-A201241] N89-19998
NUCLEAR PROPULSION
Safe, compact nuclear propulsion: Solid core nuclear propulsion concept
[AD-A202339] N89-19369
NUCLEATION
Investigations on undercooling, nucleation and rapid solidification of metallic systems
[DFVLR-FB-88-39] N89-19415
The tensile strength of liquid helium four N89-20016
NUCLEI (NUCLEAR PHYSICS)
Thermonuclear reactions of light nuclei in astrophysical plasmas N89-19988
NUCLEOGENESIS
In situ measurements of ship tracks N89-19645
NUMERICAL ANALYSIS
Numerical computations of transonic critical aerodynamic behavior
[AD-A202412] N89-19277
Two-dimensional test section with preadjusted adaptive walls for low speed wind tunnel
[KTH-AERO-REPT-57] N89-19278
A fundamental mathematical theory in the dynamics of combustion processes
[AD-A201284] N89-19391
Computational studies of evaporating sprays in a shear layer
[AD-A201932] N89-19520
Chaotic dynamics and control of nonlinear and flexible arm robotic devices N89-19566
Reciprocal theorem of residual stress and inelastic strain
[AD-A202353] N89-19598
A numerical investigation of sulfate production and deposition in midlatitude continental cumulus clouds N89-19705
Linear programming along the trajectory of the problem in polynomial time
[REPT-88-17] N89-19918
Applied partial differential equations and numerical analysis
[AD-A201749] N89-19939
The box dimension of self-affine graphs and repellors
[REPT-88-08] N89-19943
Hausdorff dimension and box dimension in self-similar sets
[REPT-88-09] N89-19944
Probability theories, fuzzy set theory and syllogisms; a literature review
[REPT-88-13] N89-19961
An observational and numerical study of extragalactic radio sources N89-20055
NUMERICAL CONTROL
Implementation of dynamic control of a single-link flexible arm using a general micro-computer
[AD-A201622] N89-19561
NUMERICAL WEATHER FORECASTING
A one-dimensional numerical model to simulate liquid phase chemical reactions within radiation fog N89-19690
NUTRITION
Comparison of Soviet and US space food and nutrition programs N89-20059

O

OBLATE SPHEROIDS
Effect of the electric field on the raindrop shape N89-19659
OBLIQUE SHOCK WAVES
Analytical, numerical and experimental investigations of oblique-shock-wave reflections in pure and dusty gases
[AD-A201438] N89-19511
OBLIQUE WINGS
The oblique-wing research aircraft: A test bed for unsteady aerodynamic and aeroelastic research N89-19253
Static aeroelasticity of a composite oblique wing in transonic flows N89-19254
OBSTACLE AVOIDANCE
Robot path planning using a genetic algorithm N89-19869
OCEAN BOTTOM
A modal/WKB inversion method for determining sound speed profiles in the ocean and ocean bottom
[AD-A201252] N89-19791
Compressional-wave velocities in ocean sediments east southeast of Madeira, Atlantic Ocean
[IOS-257] N89-19794
OCEAN DATA ACQUISITIONS SYSTEMS
Directional wave data recorded in the southern North Sea
[IOS-258] N89-19793
OCEAN MODELS
Boundary layer development over the eastern Pacific Ocean N89-19753
OCULOMETERS
Development of a low-cost helmet mounted eye gaze sensor
[AD-A202303] N89-19298
ON-LINE SYSTEMS
An expert system for restructurable control N89-19886
Electronic data generation and display system N89-19891
Intelligent embedded instruction for Computer-Aided Design (CAD) systems
[AD-A201811] N89-19907
OPERATOR PERFORMANCE
Brain activity during tactical decision-making. Part 4: Event-related potentials as indices of selective attention and cognitive workload
[AD-A201370] N89-19797

Thermal stress in Ran Sea King Helicopter operations
[ARL-SYS-R-40] N89-19810
Physiological assessment of task underload N89-19846
Intelligent tutoring in the spacecraft command/control environment N89-19855
Optimal solutions for complex design problems: Using isoperformance software for human factors trade offs N89-19860
SARSCEST (human factors) N89-19890

OPERATORS (MATHEMATICS)
Characterizations of conditional expectation-type oeprators
[REPT-88-04] N89-19942
Approximation, saturation and semigroups of operators in Banach space
[REPT-88-19] N89-19950

OPTICAL COMMUNICATION
PSDE/SAT-2 preliminary spacecraft configuration study, executive summary
[ESA-CR(P)-2689] N89-19360
PSDE/SAT-2: Preliminary spacecraft configuration study, executive summary
[ESA-CR(P)-2704] N89-19364

OPTICAL COMPUTERS
FONR optical computing ST
[AD-A201002] N89-19897
New approaches to reconfigurable optical interconnections for optical computing
[AD-A201307] N89-19982

OPTICAL DATA PROCESSING
FONR optical computing ST
[AD-A201002] N89-19897
New approaches to reconfigurable optical interconnections for optical computing
[AD-A201307] N89-19982
Optical joint correlation using the deformable mirror device N89-20074

OPTICAL DATA STORAGE MATERIALS
Development of a software interface for optical disk archival storage for a new life sciences flight experiments computer N89-20061

OPTICAL EQUIPMENT
Elastic hysteresis phenomena in ULE and Zerodur optical glasses at elevated temperatures
[DE89-005183] N89-19423
New approaches to reconfigurable optical interconnections for optical computing
[AD-A201307] N89-19982

OPTICAL FILTERS
Halogen Occultation Experiment (HALOE) optical filter characterization
[NASA-TM-4104] N89-19529

OPTICAL MATERIALS
Elastic hysteresis phenomena in ULE and Zerodur optical glasses at elevated temperatures
[DE89-005183] N89-19423
Fabrication of XLWIR (Extra-Long-Wavelength-Infrared) window materials
[DE89-006418] N89-19439
Evaluation of optical materials samples
[AD-A199471] N89-19981

OPTICAL MEASURING INSTRUMENTS
A poor man's optical fog detector N89-19716

OPTICAL MICROSCOPES
A new airborne device for measurement of cloud particles using video microscope N89-19719

OPTICAL PROPERTIES
The aqueous electrochemistry of polyacetylene (CH)x and polyparaphenylene
[AD-A201461] N89-19426
Ultrahigh-brightness XeCl laser system
[DE89-005467] N89-19548
Optical goals for polymeric film reflectors
[DE89-000836] N89-19744
Remote control system --- spectrometer
[DIGEL-79] N89-19917
Optical parameter effects on laser generated ultrasound for microstructure characterization
[DE89-005193] N89-19967
High-order beam optics: An overview
[DE89-005441] N89-19984
Long trace profile measurements on cylindrical aspheres
[DE89-005661] N89-19985

OPTICAL PUMPING
Liquid excimers: Lasing Xe2 and Kr2 in liquid argon
[DE89-005449] N89-19546
High average power excimer laser-pumped dye oscillators
[DE89-006547] N89-19552

OPTICAL RADAR
Intercomparisons of aircraft measurements with lidar returns for aerosol, ice crystals and water droplets N89-19718
Lidar for the determination of Antarctic water vapor profiles N89-19756
A high-spectral-resolution lidar system: The use of atomic blocking filter for measuring atmospheric parameters
[AD-A201736] N89-19759

OPTICAL THICKNESS
Cloud and aerosol optical depths N89-19646
Research in acoustical scattering, diffraction catastrophes, optics of bubbles and acoustical phase conjugation
[AD-A201451] N89-19968

OPTICAL WAVEGUIDES
Integration of detectors and optical waveguide structures
[AD-A201331] N89-19536

OPTIMAL CONTROL
Minimax and maximax optimal control problems with applications in aerospace engineering N89-19311
Nonlinear optimal control and near-optimal guidance strategies in spacecraft general attitude maneuvers N89-19356
Further results on the design of multivariable regulators under structure and robustness constraints. Part 1: The initialization problem
[REPT-88-028] N89-19931

OPTIMIZATION
The optimal projection equations for fixed-order dynamic compensation: Existence, convergence and global optimality N89-19345
Robust eigenstructure assignment by a projection method: Application using multiple optimization criteria N89-19349
Maximum entropy/optimal projection design synthesis for decentralized control of large space structures
[AD-A202375] N89-19358
Microstructural optimisation of titanium alloys for defect tolerance in gas turbine engine components
[PNR90503] N89-19413
Improved silicon nitride for advanced heat engines
[NASA-CR-179525] N89-19421
Simulation of the human-telerobot interface N89-19861
Man-systems requirements for the control of teleoperators in space N89-19862
Bifurcating optimization algorithms and their possible application
[DE89-005692] N89-19906

OPTOELECTRONIC DEVICES
Bitbus data transmission with galvanic separations
[DIGEL-78] N89-19898

ORBIT CALCULATION
An intelligent interface for satellite operations: Your Orbit Determination Assistant (YODA) N89-19852

ORBITAL ASSEMBLY
A multi-sensor system for robotics proximity operations N89-19881
A methodology for automation and robotics evaluation applied to the space station telerobotic servicer N89-19882

ORBITAL MANEUVERING VEHICLES
Design concept for the Flight Telerobotic Servicer (FITS) N89-19870
Feasibility of using high temperature superconducting magnets and conventional magnetic loop antennas to attract or repel objects at the space station N89-20081

ORBITAL MECHANICS
Modeling of flexible spacecraft accounting for orbital effects N89-19334
On the great circle reduction in the data analysis for the astrometric satellite HIPPARCOS
[ETN-89-93902] N89-20038

ORBITAL SERVICING
Design concept for the Flight Telerobotic Servicer (FITS) N89-19870
A multi-sensor system for robotics proximity operations N89-19881
A methodology for automation and robotics evaluation applied to the space station telerobotic servicer N89-19882
Design guidelines for remotely maintainable equipment N89-19885

ORBITS
Orientation of orbits in flows
[REPT-88-05] N89-19322

ORDER-DISORDER TRANSFORMATIONS
Intermolecular and intramolecular vibrational relaxation and energy transfer
[AD-A201610] N89-19974

ORGANIZATIONS
A case study of small group decision-making as influenced by the Abilene Paradox: The Challenger mishap
[AD-A202102] N89-19328
Calendar of selected aeronautical and space meetings: January 1989 onwards
[AGARD-CAL-89/1] N89-20024
Computer technologies and institutional memory N89-20062

OROGRAPHY
Evaluation of droplet growth rates in Hawaiian orographic clouds N89-19619
A comparative study of two microphysical schemes in a beta mesoscale model N89-19640
Oxidation regimes in orographic capping cloud N89-19698
A model of wet deposition to complex terrain by the seeder-feeder process N89-19710
On the small scale topographical influences on precipitation N89-19720
A numerical investigation of an orographic precipitation event N89-19721
Complex microphysical interactions within a central Sierra Nevada orographic cloud system N89-19722
Comparison of orographic cloud and precipitation development of three different geographic locations using a 3-D nested grid cloud model N89-19723
Microphysical observations over the Atlas Mountains in Morocco N89-19724

ORTHOGONAL FUNCTIONS
A generalization of Laguerre polynomials
[REPT-88-28] N89-19952

OSCILLATIONS
Unsteady low-speed wind tunnel test of a straked delta wing, oscillating in pitch. Part 2: Plots of steady and zeroth and first harmonic unsteady pressure distributions
[AD-A201936] N89-19275
Chaotic dynamics and control of nonlinear and flexible arm robotic devices N89-19566
Normal forms and periodic solutions in the theory of nonlinear oscillations. Existence and asymptotic theory
[REPT-88-16] N89-19948

OSCILLATORS
High average power excimer laser-pumped dye oscillators
[DE89-006547] N89-19552

OUTPUT
Presentation planning using an integrated knowledge base N89-19845

OVER-THE-HORIZON RADAR
Variations of the tropospheric propagation range of ultrashort radio waves above the sea N89-19486

OXIDATION
Studies of hydrogen-hydrogen and carbon-sulfur bond cleavage
[DE89-006116] N89-19403
Thermal oxidation of 3-5 compound semiconductors
[DE89-007127] N89-20020

OXIDE FILMS
Proposal to study the interaction of polyimide precursors and thin polyimide films with silicon and silicon oxide surfaces
[AD-A201183] N89-19425

OXIDES
XPS and AES studies of thin oxide layers on niobium for superconducting RF cavities
[DE88-756073] N89-19997

OXYGEN
Oxygen electrode in molten carbonate fuel cells
[DE89-005813] N89-19745
The divergence characteristics of constrained-sheath optics systems for use with 5-eV atomic oxygen sources
[NASA-CR-182238] N89-19973

OXYGEN 18
Oxygen diffusion in YBa2Cu3O7-delta
[DE89-005831] N89-20011
SIMS measurement of oxygen tracer diffusion in YBa2Cu3O7-delta
[DE89-005884] N89-20014

OZONE
Dynamic, radiative and chemical effects of clouds on tropospheric trace gases N89-19708
Calculation of molecular absorption parameters and updating the AFGL atmospheric line parameter compilation
[AD-A202113] N89-19761

P

PAINTS
Preparation of non-metals properties for data base
[NASA-CR-183596] N89-19420

PANEL METHOD (FLUID DYNAMICS)
A vortex panel method for potential flows with applications to dynamics and controls N89-19269

PARABOLIC ANTENNAS
Microwave holographic measurements of large reflectors: Phase 1 report, volume 1 --- spacecraft antennas
[REPT-B090] N89-19530
Microwave holographic measurements of large reflectors: Phase 2 report, volume 2
[REPT-B091] N89-19531
PARABOLIC DIFFERENTIAL EQUATIONS
The boundary element method for the diffusion equation N89-19233
PARABOLIC REFLECTORS
Microwave holographic measurements of large reflectors: Phase 1 report, volume 1 --- spacecraft antennas
[REPT-B090] N89-19530
Microwave holographic measurements of large reflectors: Phase 2 report, volume 2
[REPT-B091] N89-19531
PARALLEL FLOW
Fast and processor-efficient parallel algorithms for reducible flow graphs
[AD-A201651] N89-19904
PARALLEL PROCESSING (COMPUTERS)
A recursive method for parallel processor multiflexible body dynamic simulation N89-19336
A parallel expert system for the control of a robotic air vehicle N89-19842
Application of the OCCAM/transputer conception as busless multiprocessor system in a digital controller
[DFVLR-FB-88-40] N89-19896
FONR optical computing ST
[AD-A201002] N89-19897
Fast and processor-efficient parallel algorithms for reducible flow graphs
[AD-A201651] N89-19904
A Monte Carlo test program with vectorized geometry routines --- radiation transport
[JUEL-2202] N89-19947
Development of parallel algorithms for electrical power management in space applications N89-20063
Model evaluation, recommendation and prioritizing of future work for the manipulator emulator testbed N89-20072
PARAMETER IDENTIFICATION
Control of flexible structures: Model errors, robustness measures, and optimization of feedback controllers
[AD-A202234] N89-19596
Highly efficient estimates of multivariate location with high breakdown point
[REPT-88-14] N89-19962
PARAMETERIZATION
The optimal projection equations for fixed-order dynamic compensation: Existence, convergence and global optimality N89-19345
XUV free-electron laser development at Los Alamos
[DE89-005458] N89-19547
Instability theory in clouds and the parameterization of eddy viscosity coefficients N89-19633
A comparative study of two microphysical schemes in a beta mesoscale model N89-19640
Generalized microphysics scheme for use in mesoscale/cloud models N89-19641
Multiparameter characterization of raindrop size distribution by the polarimetric DFVLR radar: First results N89-19656
Damped-oscillation representation of drop-spectrum evolution due to coalescence and breakup N89-19660
A parametrization scheme for the coalescence of water drops using the stochastic collection equation N89-19671
Parameterizations of microphysical processes in clouds for application in models of regional atmospheric deposition N89-19709
PARTIAL DIFFERENTIAL EQUATIONS
Applied partial differential equations and numerical analysis
[AD-A201749] N89-19939
PARTICLE ACCELERATION
Theory of accelerated orbits and space charge effects in an Azimuthly Varying Field (AVF) cyclotron
[ETN-89-93897] N89-19978
PARTICLE ACCELERATORS
Ion and electron interactions at thermal and suprathermal energies
[AD-A201418] N89-19394
Investigation of the performance of photoconductive switches
[AD-A201425] N89-19489
PARTICLE BEAMS
Positron spectroscopy for materials characterization
[DE89-005766] N89-20010
PARTICLE DIFFUSION
Chaotic electron motion caused by sidebands in free electron lasers
[AD-A201635] N89-19538
PARTICLE ENERGY
High-speed laser photography
[AD-A202293] N89-19544
PARTICLE MASS
Measurements of the partitioning of aerosol mass and number between cloud droplets and interstitial air N89-19616
PARTICLE MOTION
Theoretical and experimental studies of selected topics in the rheology of fluids
[AD-A201460] N89-19512
Chaotic electron motion caused by sidebands in free electron lasers
[AD-A201635] N89-19538
Theory of accelerated orbits and space charge effects in an Azimuthly Varying Field (AVF) cyclotron
[ETN-89-93897] N89-19978
PARTICLE PRECIPITATION
Characteristics of optical emissions and particle precipitation in mid/low latitude aurorae N89-19755
PARTICLE PRODUCTION
Experimental studies on secondary ice particle production N89-19667
The cosmic ray antiproton spectrum between 0.1 and 1.5 GeV kinetic energy N89-20057
PARTICLE SIZE DISTRIBUTION
An experimental investigation of sooting characteristics of a gas turbine combustor and augmentor tube
[AD-A201804] N89-19568
On the determination of droplet size distributions with the counterflow virtual impactor --- cloud physics N89-19655
A new database of ice particle size spectra for altitudes up to 10 km (30,000 ft) N89-19673
PARTICLE THEORY
Theoretical and experimental studies of selected topics in the rheology of fluids
[AD-A201460] N89-19512
PARTICLE TRACKS
The scintillating optical fiber isotope experiment (SOFIE): Bevalac calibrations of test models N89-20034
PATHOLOGY
Biological applications and effects of optical masers
[AD-A201834] N89-19541
PATTERN RECOGNITION
CAD-model-based vision for space applications N89-19867
Sensor fusion of range and reflectance data for outdoor scene analysis N89-19868
A 2-D and 3-D robot path planning algorithm based on quadtree and octree representation of workspace
[DE89-005014] N89-19900
Recognition of object domain by color distribution N89-19928
PATTERN REGISTRATION
Sensor fusion of range and reflectance data for outdoor scene analysis N89-19868
PAYLOAD CONTROL
Intelligent tutoring in the spacecraft command/control environment N89-19855
PAYLOAD INTEGRATION
PSDE/SAT-2 preliminary spacecraft configuration study, executive summary
[ESA-CR(P)-2689] N89-19360
PSDE/SAT-2: Preliminary spacecraft configuration study, executive summary
[ESA-CR(P)-2704] N89-19364
Expert systems applications for space shuttle payload integration automation N89-19887
PAYLOADS
Get Away Special (GAS): Educational applications of space flight
[NASA-TM-101287] N89-19321
Application of model based control to robotic manipulators N89-19884
PEPTIDES
Some 2H NMR studies of oriented fluid phases
[AD-A201241] N89-19998
PERCEPTION
Structural saliency: The detection of globally salient structures using a locally connected network
[AD-A201619] N89-19806
The effects of a pitched field orientation on hand/eye coordination
[AD-A201620] N89-19814
PERFORMANCE PREDICTION
An examination of the fatigue meter records from the RAAF (Royal Australian Air Force) caribou fleet
[AD-A201074] N89-19290
A comparative analysis of tilt rotor aircraft versus helicopters using simulator results
[AD-A202190] N89-19294
PERFORMANCE TESTS
Positive Flotation Harness (PFH) for use by Canadian Forces search and rescue technicians
[AD-A200727] N89-19279
Icing research tunnel test of a model helicopter rotor
[NASA-TM-101978] N89-19305
Flight model discharge system
[AD-A201605] N89-19354
Composite reliability enhancement via reloading
[AD-A201861] N89-19380
Test aspects of the JPL Viterbi decoder N89-19457
On testing VLSI chips for the big Viterbi decoder N89-19458
RF performance measurement of the DSS-14 70-meter antenna at C-band/L-band N89-19461
Comparative performance evaluation of advanced AC and DC EV propulsion systems
[DE89-005419] N89-19498
RE-1000 free-piston Stirling engine sensitivity test results
[NASA-TM-88846] N89-19737
Research on high-efficiency, multi-gap, multijunction, amorphous-silicon-based alloy thin-film solar cells, phase 1
[DE89-000844] N89-19739
Testing expert systems N89-19834
PERIODIC VARIATIONS
Temperature and circulation in the stratospheres of the outer planets
[NASA-CR-184826] N89-20051
PERMANENT MAGNETS
Starting characteristics of direct current motors powered by solar cells
[NASA-TM-101981] N89-19493
PEROXIDES
Application of nondestructive evaluations to the prediction of turbine fuel peroxidation potential
[AD-A202291] N89-19441
PERSONAL COMPUTERS
Development of a personal-computer-based intelligent tutoring system N89-19889
A curve-fitting package for personal computers
[LA-11082-MS] N89-19922
PERSONNEL
Computer technologies and institutional memory N89-20062
PERSONNEL DEVELOPMENT
Optimal solutions for complex design problems: Using isoperformance software for human factors trade offs N89-19860
PERT
Stochastic and fuzzy PERT
[REPT-88-26] N89-20027
PERTURBATION
Maneuvering equations in terms of quasi-coordinate N89-19337
PERTURBATION THEORY
A detailed examination of discontinuities in natural rain spectra N89-19663
Studies in quantum field theory
[DE89-006286] N89-20023
PETRI NETS
A general way to put time in Petri nets
[REPT-88-011] N89-19914
PH
The effect of aerosols on pH of snowfalls N89-19688
PHASE MODULATION
The use of interleaving for reducing radio loss in convolutionally coded systems N89-19454
A low-loss linear analog phase modulator for 8415 MHz transponder application N89-19465
Proof of the feasibility of coherent and incoherent schemes for pumping a gamma-ray laser
[AD-A201931] N89-19542
PHASE TRANSFORMATIONS
Studies of 3-5 compounds in the megabar regime:
[DE89-005722] N89-20009
Static and dynamic properties of arrays of superconductors N89-20017
PHENOMENOLOGY
Phenomenological models from higher dimensions with and without supergravity N89-20045
PHOSPHORS
Determination of local fluid drag by a laser heating/thermographic phosphor technique: Applicability of the H. Ludwieg model
[DE89-006462] N89-19523
PHOTOCHEMICAL REACTIONS
Interactions and reactions in polymerized vesicles
[AD-A201527] N89-19427
Infrared and ionization structure of the polar mesosphere
[AD-A201266] N89-19751
PHOTOCONDUCTIVITY
Investigation of the performance of photoconductive switches
[AD-A201425] N89-19489

PHOTOCONDUCTORS
Investigation of the performance of photoconductive switches
[AD-A201425] N89-19489
PHOTODIODES
Determination of general and specific properties of wide energy-band gap HgCdTe in the 1 to 2 micrometer wavelength range
[AD-A201341] N89-19488
PHOTOLUMINESCENCE
The 2-4 semiconductor superlattices
[AD-A202369] N89-20005
PHOTOLYSIS
Pyrolytic and laser photolytic growth of crystalline and amorphous germanium films from digermane (GE2H6)
[DE89-006125] N89-20019
PHOTOMETERS
Integration of detectors and optical waveguide istructures
[AD-A201331] N89-19536
PHOTOMETRY
Activities report in electrotechnology
[ETN-89-93715] N89-19448
Evaluation of available analytical techniques for monitoring the quality of space station potable water N89-20071
PHOTOMICROGRAPHY
Three-dimensional structures of snow crystals shown by stereo-photomicrographs N89-19669
PHOTON BEAMS
On the use of multiple photon processes in krypton for laser guiding of electron beams
[DE89-006546] N89-19551
PHOTOOXIDATION
Oxidation regimes in orographic capping cloud N89-19698
PHOTOVOLTAIC CELLS
Applications survey for remote photovoltaic power systems
[AD-A201937] N89-19741
PHOTOVOLTAIC CONVERSION
Applications survey for remote photovoltaic power systems
[AD-A201937] N89-19741
PHOTOVOLTAIC EFFECT
Starting characteristics of direct current motors powered by solar cells
[NASA-TM-101981] N89-19493
PHYSIOLOGICAL EFFECTS
Computation of stereo and visual motion: From biophysics to psychophysics
[AD-A201873] N89-19802
A model for plasma volume changes during short duration spaceflight N89-20067
Effects on motor unit potentiation and ground reaction force from treadmill exercise N89-20069
PHYSIOLOGICAL FACTORS
Man-systems requirements for the control of teleoperators in space N89-19862
PHYSIOLOGICAL RESPONSES
Brain mechanisms underlying individual differences in reaction to stress: An animal model
[AD-A201595] N89-19801
A stress test to evaluate the physical capacity of performing L-1 anti-G straining maneuvers
[AD-A202301] N89-19803
Diagnosis by integrating model-based reasoning with knowledge-based reasoning N89-19835
Physiological assessment of task underload N89-19846
PHYSIOLOGICAL TESTS
Physiological assessment of task underload N89-19846
PIEZOELECTRICITY
RCS/piezoelectric distributed actuator study
[AD-A201276] N89-19999
PILOT ERROR
Brain activity during tactical decision-making. Part 4: Event-related potentials as indices of selective attention and cognitive workload
[AD-A201370] N89-19797
PILOT PERFORMANCE
A stress test to evaluate the physical capacity of performing L-1 anti-G straining maneuvers
[AD-A202301] N89-19803
A schema-based model of situation awareness: Implications for measuring situation awareness N89-19847
Chemical warfare protection for the cockpit of future aircraft N89-19859
PILOTLESS AIRCRAFT
RPV (Remote Piloted Vehicle) applications in the US Navy
[AD-A202151] N89-19293
PIPELINING (COMPUTERS)
Model evaluation, recommendation and prioritizing of future work for the manipulator emulator testbed N89-20072
PIPES (TUBES)
Determination of residual stress distributions in autofrettaged tubing: A discussion
[AD-A201454] N89-19586
PITCH (INCLINATION)
Airfoil stall penetration at constant pitch rate and high Reynolds number N89-19260
The effects of a pitched field orientation on hand/eye coordination
[AD-A201620] N89-19814
PITCHING MOMENTS
Numerical computations of transonic critical aerodynamic behavior
[AD-A202412] N89-19277
PLAN POSITION INDICATORS
A preliminary study of precursors to Huntsville microbursts
[AD-A200914] N89-19782
PLANAR STRUCTURES
Dynamic data structures for two-dimensional searching
[AD-A201173] N89-19901
PLANE WAVES
A dynamic, time stepping boundary element method for frictional crack and interface problems N89-19590
PLANETARY BOUNDARY LAYER
An investigation of the intermittent turbulent breakdown of the nocturnal planetary boundary layer
[AD-A201743] N89-19518
PLANETARY EVOLUTION
Evaluation of crustal recycling during the evolution of Archean-age Matachewan basaltic magmas N89-20077
PLANETARY TEMPERATURE
Temperature and circulation in the stratospheres of the outer planets
[NASA-CR-184826] N89-20051
PLANETARY WAVES
Use of long-waves in forecasting
[CRARP-88-7] N89-19778
PLANNING
Robot path planning using a genetic algorithm N89-19869
PLASMA COMPRESSION
Effect of limiter currents on plasma equilibrium and stability in a tokamak
[DE88-704951] N89-19989
PLASMA CONTROL
Effect of limiter currents on plasma equilibrium and stability in a tokamak
[DE88-704951] N89-19989
Existence of stationary solutions in the coronal loop problem
[REPT-88-06] N89-20054
PLASMA DIAGNOSTICS
Theory of accelerated orbits and space charge effects in an Azimuthly Varying Field (AVF) cyclotron
[ETN-89-93897] N89-19978
Resonance cones in non Maxwellian plasmas
[REPT-88-N4-173] N89-19993
Ion beam driven electrostatic shocks --- ionosphere
[MPE-PREPRINT-127] N89-19995
PLASMA DIFFUSION
Study of the continuous/diffuse aurora using particle observations from the Dynamics Explorer satellites
[AD-A202241] N89-19763
PLASMA DRIFT
Resonance cones in non Maxwellian plasmas
[REPT-88-N4-173] N89-19993
PLASMA EQUILIBRIUM
Effect of limiter currents on plasma equilibrium and stability in a tokamak
[DE88-704951] N89-19989
PLASMA GENERATORS
Flight model discharge system
[AD-A201605] N89-19354
PLASMA JETS
Jets physics in Comet P/Halley
[IFSI-88-3] N89-20049
PLASMA PHYSICS
Existence of stationary solutions in the coronal loop problem
[REPT-88-06] N89-20054
PLASMA PINCH
Numerical studies of MHD turbulence in the reversed field pinch
[IPP-6/276] N89-19994
PLASMA RESONANCE
Resonance cones in non Maxwellian plasmas
[REPT-88-N4-173] N89-19993
PLASMA TURBULENCE
Numerical studies of MHD turbulence in the reversed field pinch
[IPP-6/276] N89-19994
PLASMA WAVES
Electrostatic plasma waves and turbulence near auroral arcs N89-19758
Plasma waves at the dayside magnetopause
[MPE-PREPRINT-128] N89-19996
PLASMAS (PHYSICS)
Substorms, plasmoids, flux robes, and magnetotail flux loss on March 25, 1983: CDAW-8
[NASA-CR-184823] N89-19764
PLASTIC PROPERTIES
Processing of aluminum alloy 2090 for superplasticity
[AD-A201865] N89-19411
Plastic buckling of cylinders under biaxial loading N89-19591
Reciprocal theorem of residual stress and inelastic strain
[AD-A202353] N89-19598
PLATES (STRUCTURAL MEMBERS)
Finite element analysis of laminated composite plates
[AD-A202192] N89-19381
The modeling of viscoelastic circular plates for use as waveguide absorbers
[AD-A201621] N89-19588
PLATES (TECTONICS)
Lithospheric buckling and intra-arc stresses: A mechanism for arc segmentation N89-20078
POLAR ORBITS
Substorms, plasmoids, flux robes, and magnetotail flux loss on March 25, 1983: CDAW-8
[NASA-CR-184823] N89-19764
Solid Earth ARISTOTELES mission data preprocessing simulation of gravity gradiometer
[ESA-CR(P)-2666] N89-19766
Satellite remote sensing of heat stress during reserve training at Fort Hood
[AD-A201555] N89-19800
POLAR REGIONS
Infrared and ionization structure of the polar mesosphere
[AD-A201266] N89-19751
Study of the continuous/diffuse aurora using particle observations from the Dynamics Explorer satellites
[AD-A202241] N89-19763
POLARIMETRY
Advancement of high resolution radar polarimetry in target verses clutter detection, discrimination, classification. A: Basic theory and modeling of polarimetric clutter phenomenology
[AD-A201240] N89-19467
Multiparameter Doppler radar observations of a squall line with the polarimetric DFVLR radar N89-19715
POLARIZATION (WAVES)
VLBI polarization measurements of BL Lacertae objects N89-20035
POLLUTION MONITORING
Measurement of the global distribution of tropospheric trace gases and their time dependent variations
[ETN-89-93987] N89-19747
POLLUTION TRANSPORT
Use of cluster analysis to define periods of similar meteorology and precipitation chemistry in eastern North America N89-19785
POLYACETYLENE
The aqueous electrochemistry of polyacetylene (CH)x and polyparaphemylene
[AD-A201461] N89-19426
Chemistry and physics of polyacetylene, (CH)x: The prototype conducting polymer
[AD-A201933] N89-19431
POLYATOMIC MOLECULES
Ion and electron interactions at thermal and suprathermal energies
[AD-A201418] N89-19394
POLYCARBONATES
Hole formation (etching) in polymers by far (deep) UV high intensity laser (excimer) radiation pulses and its relevance to photoresists in deep UV photolysis of polymers
[AD-A202274] N89-19433
POLYCRYSTALS
Polymer morphology and transport
[AD-A201167] N89-19424
POLYETHYLENES
Polymer morphology and transport
[AD-A201167] N89-19424
POLYGONS
Dynamic data structures for two-dimensional searching
[AD-A201173] N89-19901

POLYIMIDE RESINS
Thermal cycling and mechanical property assessment of carbon fiber (fabric) reinforced PMR-15 polyimide laminates
[PNR90522] N89-19382
POLYIMIDES
Proposal to study the interaction of polyimide precursors and thin polyimide films with silicon and silicon oxide surfaces
[AD-A201183] N89-19425
The determination of the mechanical behavior of polyamic acid/polyimide coatings N89-19428
POLYMER CHEMISTRY
Chemistry and physics of polyacetylene, (CH)x: The prototype conducting polymer
[AD-A201933] N89-19431
POLYMER PHYSICS
Chemistry and physics of polyacetylene, (CH)x: The prototype conducting polymer
[AD-A201933] N89-19431
POLYMERIC FILMS
Adhesion in ceramics and magnetic media
[NASA-TM-101476] N89-19435
Optical goals for polymeric film reflectors
[DE89-000836] N89-19744
POLYMERIZATION
The aqueous electrochemistry of polyacetylene (CH)x and polyparaphenylene
[AD-A201461] N89-19426
Interactions and reactions in polymerized vesicles
[AD-A201527] N89-19427
Laser scattering studies of epoxy polymerization processes
[AD-A201925] N89-19430
POLYNOMIALS
Linear programming along the trajectory of the problem in polynomial time
[REPT-88-17] N89-19918
A generalization of Laguerre polynomials
[REPT-88-28] N89-19952
POLYPHENYLS
The aqueous electrochemistry of polyacetylene (CH)x and polyparaphenylene
[AD-A201461] N89-19426
POROSITY
Development of Nuclear Magnetic Resonance (NMR) imaging technology for advanced ceramics
[DE89-006400] N89-19438
PORTABLE EQUIPMENT
Portable inference engine: An extended CLIPS for real-time production systems N89-19843
SARSCEST (human factors) N89-19890
PORTABLE LIFE SUPPORT SYSTEMS
Cooling effectiveness of a hybrid microclimate garment
[AD-A201115] N89-19811
POSITION (LOCATION)
Orientation of orbits in flows
[REPT-88-05] N89-19322
An intelligent interface for satellite operations: Your Orbit Determination Assistant (YODA) N89-19852
POSITION SENSING
CAD-model-based vision for space applications N89-19867
POSITIONING
Local position control: A new concept for control of manipulators N89-19864
Dexterity analysis and robot hand design N89-19865
Concept for a large master/slave-controlled robotic hand N89-19866
POSITRONS
Positron spectroscopy for materials characterization
[DE89-005766] N89-20010
POTABLE WATER
Design of a surface-based factory for the production of life support and technology support products. Phase 2: Integrated water system for a space colony
[NASA-CR-184730] N89-19808
Evaluation of available analytical techniques for monitoring the quality of space station potable water N89-20071
POTASSIUM COMPOUNDS
The coupled cluster method and the properties of energetic materials
[AD-A201168] N89-19388
POTENTIAL FLOW
Solution of steady and unsteady transonic-vortex flows using Euler and full-potential equations N89-19248
A vortex panel method for potential flows with applications to dynamics and controls N89-19269
POTENTIAL THEORY
Application of a full potential method to AGARD standard airfoils N89-19242
Full potential unsteady computations including aeroelastic effects N89-19243
The influence of the potential function on the performance of a trajectory following algorithm for the linear programming problem
[REPT-88-44] N89-19920
POTENTIOMETRIC ANALYSIS
Investigation of the interface between two immiscible electrolytes applied to membrane electrochemistry
[AD-A201310] N89-19393
POWDER METALLURGY
Tensile and creep rupture behavior of P/M processed Nb-base alloy, WC-3009
[NASA-TM-101954] N89-19371
Microstructural analyses of intermetallic TiAl (Nb)-compounds prepared by arc melting and by powder metallurgy
[GKSS-88/E/32] N89-19417
POWER CONDITIONING
Electronic Power Conditioner (EPC) for carcinotrons
[R/D/REPO/8801] N89-19496
Free-electron laser driven by the NBS (National Bureau of Standards) CW microtron
[AD-A201170] N89-19535
The 30 kWe class high efficiency arcjet power conditioner, volume 1
[AD-A202244] N89-20004
POWER EFFICIENCY
Field investigation of a wake structure downwind of a VANT (Vertical-Axis Wind Turbine) in a wind farm array
[DE89-000821] N89-19743
The 30 kWe class high efficiency arcjet power conditioner, volume 1
[AD-A202244] N89-20004
POWER LINES
Expert systems applications for space shuttle payload integration automation N89-19887
POWER SPECTRA
Power spectra decomposition of 36 RS CVn UBV photometric light curves from the first two years of the automatic photoelectric telescope N89-20036
PRECIPITATION (METEOROLOGY)
Propagation problems regarding 20/30 GHz bands in Earth-space links
[REPT-88-022] N89-19480
Propagation problems regarding millimeter waves (40/50 GHz)
[REPT-88-023] N89-19481
Annals from the German Meteorological Society. No. 25: 10th International Cloud Physics Conference Preprints, volume 1
[ISBN-3-88-148240-7] N89-19605
Precipitation initiation mechanisms in clouds over north India N89-19624
Theory on the uncertainty in cloud microphysical processes and climate N89-19644
An investigation of the effect of electrical charges on the collision efficiency of cloud drops N89-19657
Radar observations of precipitation microstructure: The morphology of linear depolarization measurements in cloud N89-19714
On the small scale topographical influences on precipitation N89-19720
Comparison of orographic cloud and precipitation development of three different geographic locations using a 3-D nested grid cloud model N89-19723
Microphysical observations over the Atlas Mountains in Morocco N89-19724
Technical report on temperature, precipitation and aviation verification at WSFO Sioux Falls for 1987
[CRARP-88-5] N89-19776
A climatology of global precipitation N89-19787
PRECIPITATION PARTICLE MEASUREMENT
The use of automatic particle recognition to improve the determination of bulk quantities from PMS 2-D probe data in cirrus N89-19651
Development of hydrometeor video sonde N89-19653
The study of the interstitial aerosol particles and cloud droplets with digital image analysis of diffraction images N89-19654
On the determination of droplet size distributions with the counterflow virtual impactor --- cloud physics N89-19655
A new airborne device for measurement of cloud particles using video microscope N89-19719
PRECISION
Dexterity analysis and robot hand design N89-19865
PREDICTION ANALYSIS TECHNIQUES
A computationally efficient modelling of laminar separation bubbles
[NASA-CR-184789] N89-19504
An investigation of the relationship between beam and global irradiation with the development of numerical solar radiation models N89-19748
PREDICTIONS
Steady waves in a nonlinear theory of viscoelasticity N89-19470
High strain-rate behaviour of polymers using blast-wave and impact-loading methods N89-19592
Quench pressure, thermal expulsion, and normal zone propagation in internally cooled superconductors
[DE89-005668] N89-20003
PRESSES
The elastic stress and the displacement on the surfaces of two rubber-clad steel cylinders between which paper is led
[REPT-88-23] N89-19603
PRESSURE DISTRIBUTION
Unsteady pressure measurements on a supercritical airfoil at high Reynolds numbers N89-19259
Airfoil stall penetration at constant pitch rate and high Reynolds number N89-19260
A vortex panel method for potential flows with applications to dynamics and controls N89-19269
Unsteady low-speed wind tunnel test of a straked delta wing, oscillating in pitch. Part 2: Plots of steady and zeroth and first harmonic unsteady pressure distributions
[AD-A201936] N89-19275
Pressure variation over a solid wavy surface
[AD-A201724] N89-19517
PRESSURE EFFECTS
CAP-TSD analysis of the F-15 aircraft N89-19239
Calculation of steady and unsteady pressures at supersonic speeds with CAP-TSD N89-19240
Full potential unsteady computations including aeroelastic effects N89-19243
The role of shock induced trailing-edge separation in limit cycle oscillations N89-19256
Initial application of CAP-TSD to wing flutter N89-19257
Computational aeroelasticity challenges and resources N89-19264
Contamination of liquid oxygen by pressurized gaseous nitrogen
[NASA-TP-2894] N89-19499
Studies of 3-5 compounds in the megabar regime:
[DE89-005722] N89-20009
PRESSURE MEASUREMENT
Experimental transonic steady state and unsteady pressure measurements on a supercritical wing during flutter and forced discrete frequency oscillations N89-19261
The effect of prewhirl on the internal aerodynamics and performance of a mixed flow research centrifugal compressor
[NASA-CR-184756] N89-19503
PRESSURE REDUCTION
Dexamethasone for prevention and treatment of acute mountain sickness
[AD-A201554] N89-19799
PRESSURE SENSORS
Integration of a computerized two-finger gripper for robot workstation safety N89-19863
PRESSURE VESSELS
Characterization of IM7/8551-7 carbon/epoxy in compression and shear
[DE89-005544] N89-19378
Acoustic emission measurements during fatigue loading of scaled Pressurized Water Reactor (PWR) vessel at Joint Research Center of the European Communities (JRC), Ispra (Italy)
[CISE-4476] N89-19600
General review of recent activities in acoustic emission technology in Italy
[CISE-4477] N89-19601
PRESSURIZED WATER REACTORS
Acoustic emission measurements during fatigue loading of scaled Pressurized Water Reactor (PWR) vessel at Joint Research Center of the European Communities (JRC), Ispra (Italy)
[CISE-4476] N89-19600
PRESTRESSING
Determination of residual stress distributions in autofrettaged tubing: A discussion
[AD-A201454] N89-19586
PRIMERS (COATINGS)
An electrochemical study of corrosion protection by primer-topcoat systems on 4130 steel with ac impedance and dc methods
[NASA-TP-2820] N89-19406
PRINCIPAL COMPONENTS ANALYSIS
Transformation based endorsement systems N89-19836
PROBABILITY DENSITY FUNCTIONS
Laser transit anemometer software development program
[NASA-CR-4225] N89-19545
PROBABILITY DISTRIBUTION FUNCTIONS
Highly efficient estimates of multivariate location with high breakdown point
[REPT-88-14] N89-19962
Tail triviality for sums of stationary random variables
[REPT-88-40] N89-19963

PROBABILITY THEORY
A method for modeling bias in a person's estimates of likelihoods of events N89-19849
Probability theories, fuzzy set theory and syllogisms; a literature review
[REPT-88-13] N89-19961
An evidential approach to problem solving when a large number of knowledge systems is available N89-20068
PROBLEM SOLVING
R and M (Reliability and Maintainability) quality team concept and C-17 design at Douglas Aircraft Company: An R and M 2000 initiative case study
[AD-A201574] N89-19228
The boundary element method for the diffusion equation N89-19233
Minimax and maximax optimal control problems with applications in aerospace engineering N89-19311
Model-based reasoning: Troubleshooting
[AD-A201614] N89-19445
Reducing uncertainty by using explanatory relationships N89-19837
Autonomous satellite command and control: A comparison with other military systems N89-19839
Browsing schematics: Query-filtered graphs with context nodes N89-19844
Knowledge acquisition for case-based reasoning systems N89-19856
Robot path planning using a genetic algorithm N89-19869
An exact ceiling point algorithm for general integer linear programming
[AD-A202286] N89-19913
Production system chunking in SOAR: Case studies in automated learning N89-20060
An evidential approach to problem solving when a large number of knowledge systems is available N89-20068
PROCEDURES
A meditation on Miller
[CRARP-88-4] N89-19775
Preparing storm data
[CRARP-88-6] N89-19777
PROCESS CONTROL (INDUSTRY)
The relationship between manufacturing technology and design — aircraft engines
[PNR90537] N89-19307
PRODUCTION COSTS
An analysis of the impact of log-linear regression on the estimated learning curve parameters
[AD-A201471] N89-19938
PRODUCTION ENGINEERING
Portable inference engine: An extended CLIPS for real-time production systems N89-19843
PRODUCTION MANAGEMENT
IDEAL: A methology for developing information systems N89-19888
PRODUCTION PLANNING
IDEAL: A methology for developing information systems N89-19888
PRODUCTIVITY
Design of an optical sensor system for adaptive control of a seam tracking robot N89-19565
PROGNOSIS
Semi-prognostic tests of cumulus parameterization schemes in the middle latitudes N89-19786
PROGRAM VERIFICATION (COMPUTERS)
Verification of combined thermal-hydraulic and heat conduction analysis code FLOWNET/TRUMP
[DE88-756063] N89-19506
A three-dimensional nonsingular simulation of rigid manipulators
[AD-A201964] N89-19569
MODIS information, data and control system (MIDACS) operations concepts
[NASA-TM-100720] N89-19729
Validation of highly reliable, real-time knowledge-based systems N89-19833
Testing expert systems N89-19834
Garbage collection can be made real-time and verifiable N89-19840
PROGRAMMERS
A survey of automatic code generating software
[AD-A201963] N89-19910
PROGRAMMING LANGUAGES
A survey of automatic code generating software
[AD-A201963] N89-19910
PROJECT PLANNING
A survey of planning and scheduling research at the NASA Ames Research Center N89-19820
PROJECTILES
Numerical simulation of the aerodynamics of turbulent transonic flow past a projectile N89-19270
Numerical computations of transonic critical aerodynamic behavior
[AD-A202412] N89-19277
PROLATE SPHEROIDS
The birth of open separation on a prolate spheroid
[AD-A201350] N89-19509
PROP-FAN TECHNOLOGY
Wind-tunnel results of advanced high-speed propellers at takeoff, climb, and landing Mach numbers
[NASA-TM-87030] N89-19265
Multiple-Purpose Subsonic Naval Aircraft (MPSNA) Multiple Application Propfan Study (MAPS)
[NASA-CR-175096] N89-19289
Large-scale Advanced Prop-fan (LAP) hub/blade retention design report
[NASA-CR-174786] N89-19299
PROPAGATION VELOCITY
Compressional-wave velocities in ocean sediments east southesast of Madeira, Atlantic Ocean
[IOS-257] N89-19794
PROPANE
Booster propulsion/vehicle impact study
[NASA-CR-183584] N89-19366
PROPELLANT CHEMISTRY
NRL boron propellants combustion program
[AD-A201242] N89-19440
PROPELLANT COMBUSTION
Safe, compact nuclear propulsion: Solid core nuclear propulsion concept
[AD-A202339] N89-19369
Spectral studies of propellant combustion: Experimental details and emission results for M-30 propellant
[AD-A201634] N89-19399
NRL boron propellants combustion program
[AD-A201242] N89-19440
PROPELLER BLADES
Large-scale Advanced Prop-fan (LAP) hub/blade retention design report
[NASA-CR-174786] N89-19299
A new pumpjet design theory
[AD-A201353] N89-19558
PROPELLER EFFICIENCY
A new pumpjet design theory
[AD-A201353] N89-19558
PROPULSION SYSTEM CONFIGURATIONS
Comparative performance evaluation of advanced AC and DC EV propulsion systems
[DE89-005419] N89-19498
PROPULSION SYSTEM PERFORMANCE
Turbomachinery aeroelasticity at NASA Lewis Research Center N89-19262
Comparative performance evaluation of advanced AC and DC EV propulsion systems
[DE89-005419] N89-19498
PROTECTIVE CLOTHING
Cooling effectiveness of a hybrid microclimate garment
[AD-A201115] N89-19811
Chemical warfare protection for the cockpit of future aircraft N89-19859
PROTECTIVE COATINGS
An electrochemical study of corrosion protection by primer-topcoat systems on 4130 steel with ac impedance and dc methods
[NASA-TP-2820] N89-19406
PROTEINS
Mini protein crystallization facility. Phase A study: Executive summary
[REPT-AQ-ES-576/88] N89-19444
PROTOCOL (COMPUTERS)
DES cryptographic services designed for the DOE wide band communications network
[LA-10966-MS] N89-19484
PROTOTYPES
Positive Flotation Harness (PFH) for use by Canadian Forces search and rescue technicians
[AD-A200727] N89-19279
PROVING
Technical report on temperature, precipitation and aviation verification at WSFO Sioux Falls for 1987
[CRARP-88-5] N89-19776
Application of flight systems methodologies to the validation of knowledge-based systems N89-19832
Validation of highly reliable, real-time knowledge-based systems N89-19833
Using the sentence verification technique to assess storage and retrieval processes
[AD-A201632] N89-20029
PROXIMITY
A multi-sensor system for robotics proximity operations N89-19881
PSYCHOLOGICAL TESTS
Using the sentence verification technique to assess storage and retrieval processes
[AD-A201632] N89-20029
PSYCHOLOGY
A case study of small group decision-making as influenced by the Abilene Paradox: The Challenger mishap
[AD-A202102] N89-19328
Structural saliency: The detection of globally salient structures using a locally connected network
[AD-A201619] N89-19806
PSYCHOMETRICS
Using the sentence verification technique to assess storage and retrieval processes
[AD-A201632] N89-20029
PSYCHOPHYSICS
Computation of stereo and visual motion: From biophysics to psychophysics
[AD-A201873] N89-19802
PULSE COMMUNICATION
A 20 GHz low noise, low cost receiver for digital satellite communication system, ground terminal applications
[NASA-CR-182243] N89-19449
PULSE DURATION
Nonradiative relaxation and laser action in tunable solid state laser crystals
[NASA-CR-182820] N89-19539
Ultrahigh-brightness XeCl laser system
[DE89-005467] N89-19548
PULSE DURATION MODULATION
The 30 kWe class high efficiency arcjet power conditioner, volume 1
[AD-A202244] N89-20004
PUMP SEALS
On the sealing and lubrication mechanism of radial lip seals
[ETN-89-93898] N89-19574
PUMPS
A new pumpjet design theory
[AD-A201353] N89-19558
PYROLYSIS
Pyrolytic and laser photolytic growth of crystalline and amorphous germanium films from digermane (GE2H6)
[DE89-006125] N89-20019

Q

QUALITY
Testing expert systems N89-19834
QUALITY CONTROL
R and M (Reliability and Maintainability) quality team concept and C-17 design at Douglas Aircraft Company: An R and M 2000 initiative case study
[AD-A201574] N89-19228
The gas turbine engine and its certification
[PNR90496] N89-19303
QUANTITATIVE ANALYSIS
Diagnosis by integrating model-based reasoning with knowledge-based reasoning N89-19835
QUANTUM CHEMISTRY
The coupled cluster method and the properties of energetic materials
[AD-A201168] N89-19388
QUANTUM MECHANICS
An invariant imbedding T matrix approach to electromagnetic scattering
[AD-A202298] N89-19476
QUANTUM THEORY
Ion pair solvation
[AD-A201529] N89-19395
Quantum limits of superconducting heterodyne receivers
[AD-A201303] N89-20000
Quantum field theory of universe
[DE88-756084] N89-20022
Studies in quantum field theory
[DE89-006286] N89-20023

R

RADAR
Block diagrams of the radar interface and control unit N89-19460
RADAR CROSS SECTIONS
Computer algorithms for measurement control and signal processing of transient scattering signatures
[AD-A201672] N89-19469
Normalized radar cross section of natural surfaces at millimeter wavelengths
[AD-A202252] N89-19475
RADAR DATA
Synthetic aperture radar (SAR) data focusing using seismic migration techniques
[REPT-88-015] N89-19479
RADAR ECHOES
Characteristics of radar echo of snow band formed in the lee side of a mountain N89-19726

RADAR IMAGERY
Active and passive remote sensing of ice
[AD-A201915] N89-19792
RADAR MEASUREMENT
Advancement of high resolution radar polarimetry in target verses clutter detection, discrimination, classification. A: Basic theory and modeling of polarimetric clutter phenomenology
[AD-A201240] N89-19467
Radar observations and modelling of warm rain initiation N89-19621
Structure of upper clouds boundary using the lidar data N89-19631
Multiparameter characterization of raindrop size distribution by the polarimetric DFVLR radar: First results N89-19656
Radar observations of precipitation microstructure: The morphology of linear depolarization measurements in cloud N89-19714
RADAR SCATTERING
Normalized radar cross section of natural surfaces at millimeter wavelengths
[AD-A202252] N89-19475
Study of the use of radar X-band data of bare soil in a radar scattering model
[BCRS-88-04] N89-19735
Active and passive remote sensing of ice
[AD-A201915] N89-19792
RADAR SIGNATURES
The importance of aircraft performance and signature reduction upon combat survivability
[AD-A202106] N89-19292
Normalized radar cross section of natural surfaces at millimeter wavelengths
[AD-A202252] N89-19475
RADAR TARGETS
Advancement of high resolution radar polarimetry in target verses clutter detection, discrimination, classification. A: Basic theory and modeling of polarimetric clutter phenomenology
[AD-A201240] N89-19467
RADAR TRACKING
An expert system for shuttle and satellite radar tracker scheduling N89-19821
RADIAL FLOW
The effect of prewhirl on the internal aerodynamics and performance of a mixed flow research centrifugal compressor
[NASA-CR-184756] N89-19503
RADIANT FLUX DENSITY
Hole formation (etching) in polymers by far (deep) UV high intensity laser (excimer) radiation pulses and its relevance to photoresists in deep UV photolysis of polymers
[AD-A202274] N89-19433
RADIATION DISTRIBUTION
Analysis and synthesis of microstrip antennas including mutual coupling
[AD-A201783] N89-19472
RADIATION DOSAGE
Biological applications and effects of optical masers
[AD-A201834] N89-19541
RADIATION EFFECTS
The effects of simulated space environmental parameters on six commercially available composite materials
[NASA-TP-2906] N89-19385
Radiative influences on precipitating mesoscale systems N89-19648
Radiation biology studies in soft X-ray and ultrasoft X-ray region
[DE88-756071] N89-19795
Optical parameter effects on laser generated ultrasound for microstructure characterization
[DE89-005193] N89-19967
Radiation induced amorphization in YBa2Cu3O7 and GdBa2Cu3O7 superconductors
[DE89-005451] N89-20008
RADIATION SHIELDING
Free-electron laser driven by the NBS (National Bureau of Standards) CW microtron
[AD-A201170] N89-19535
RADIATION TRANSPORT
A Monte Carlo test program with vectorized geometry routines --- radiation transport
[JUEL-2202] N89-19947
HERMES, a Monte Carlo program system for beam-materials interaction studies --- radiation transport
[JUEL-2203] N89-19979
RADIATIVE TRANSFER
Some outstanding problems on the influence of clouds on radiation N89-19643
An observational study of radiatively driven convection --- clouds N89-19647
Cirrus microphysics and infrared radiative transfer: A case study N89-19649
Dynamic, radiative and chemical effects of clouds on tropospheric trace gases N89-19708
RADII
Implications of the observed contraction of accretion disks in quiescent dwarf novae N89-20047
RADIO ALTIMETERS
A study of advanced radar altimeter techniques --- satellite altimetry
[ESA-CR(P)-2699] N89-19483
RADIO ANTENNAS
Design and test of a 2.25-MW transformer rectifier assembly N89-19452
RF performance measurement of the DSS-14 70-meter antenna at C-band/L-band N89-19461
RADIO ASTRONOMY
The distribution of the interstellar medium in the Scd galaxy NGC 6946 and in a sample of dwarf irregular galaxies N89-20043
RADIO COMMUNICATION
A 20 GHz low noise, low cost receiver for digital satellite communication system, ground terminal applications
[NASA-CR-182243] N89-19449
RADIO FREQUENCIES
RF performance measurement of the DSS-14 70-meter antenna at C-band/L-band N89-19461
An assessment of the application of in situ ion-density data from DMSP (Defense Meteorology Satellite Program) to modeling of transionospheric scintillation
[AD-A202415] N89-19765
XPS and AES studies of thin oxide layers on niobium for superconducting RF cavities
[DE88-756073] N89-19997
RADIO FREQUENCY INTERFERENCE
Radio frequency interference survey over the 1.0-10.4 GHz frequency range at the Goldstone-Venus Development Station N89-19466
RADIO RECEIVERS
A 20 GHz low noise, low cost receiver for digital satellite communication system, ground terminal applications
[NASA-CR-182243] N89-19449
On sampling band-pass signals N89-19453
The use of interleaving for reducing radio loss in convolutionally coded systems N89-19454
RADIO SIGNALS
A new dropsonde for cloud probings N89-19728
RADIO TRANSMISSION
JPRS report: Science and technology. USSR: Electronics and electrical engineering
[JPRS-UEE-88-005] N89-19485
RADIOBIOLOGY
Radiation biology studies in soft X-ray and ultrasoft X-ray region
[DE88-756071] N89-19795
RADIOMETERS
Stratospheric nitric acid: Feasibility of routine measurement by observation from commercial airliners in IR bands from 9 to 14 microns
[C-48-1977] N89-19770
RAIN
Studies of warm-rain development N89-19620
Radar observations and modelling of warm rain initiation N89-19621
Properties of the precipitation embryos evolution in characteristic Hawaiian band clouds N89-19675
Below cloud scavenging by rain and drizzle N89-19685
Concentrations in rain events collected sequentially: Measurements vs results of a simple scavenging model N89-19701
A model of wet deposition to complex terrain by the seeder-feeder process N89-19710
Study on cloud and rain by microwave radiometer observation N89-19727
TRMM (Tropical Rainfall Measuring Mission): A satellite mission to measure tropical rainfall
[NASA-TM-101288] N89-19789
RAIN GAGES
A climatology of global precipitation N89-19787
RAINDROPS
The effect of charge on coalescence of small precipitation drops at terminal velocity N89-19606
Wake-excited raindrop oscillations N89-19607
A model of the electrostatic-aerodynamic shape of raindrops N89-19615
Multiparameter characterization of raindrop size distribution by the polarimetric DFVLR radar: First results N89-19656
Effect of the electric field on the raindrop shape N89-19659
Damped-oscillation representation of drop-spectrum evolution due to coalescence and breakup N89-19660
A detailed examination of discontinuities in natural rain spectra N89-19663
A numerical simulation of the acidification process of rain water below the cloud and the mechanism of acid rain formation in area of Chongqing, China N89-19706
RAINMAKING
Microphysical characteristics of warm-based cumuli: Observations at -10 C --- weather modification N89-19626
RAINSTORMS
Radar observations of precipitation microstructure: The morphology of linear depolarization measurements in cloud N89-19714
RAMAN LASERS
Integration of detectors and optical waveguide structures
[AD-A201331] N89-19536
RAMAN SPECTRA
Fundamental optical studies of competitive adsorption and thin film phenomena
[DE89-005898] N89-19401
RAMAN SPECTROSCOPY
Raman and RBS studies of ion implanted semiconductors
[ATR-88(8359)-5] N89-20021
RAMJET ENGINES
Flame driving of longitudinal instabilities in liquid fueled dump combustors
[AD-A201293] N89-19392
RANDOM VARIABLES
Large deviation local limit theorems for ratio statistics
[AD-A201169] N89-19954
Tail triviality for sums of stationary random variables
[REPT-88-40] N89-19963
RANGE FINDERS
A heuristically based navigation system for an autonomous walking machine with a range scanner N89-19563
RANKING
Multicriteria analysis and budget allocation, with applications in energy R and D planning: A feasibility study
[REPT-88-07] N89-20026
RATS
Brain mechanisms underlying individual differences in reaction to stress: An animal model
[AD-A201595] N89-19801
RAWINSONDES
Development of hydrometeor video sonde N89-19653
RAYLEIGH WAVES
Gaussian beam representation of beam-like ultrasonic fields N89-19972
REACTION KINETICS
Ion pair solvation
[AD-A201529] N89-19395
Vibrational spectroscopic studies of surface chemical interactions in chemisorption and catalysis
[DE89-005896] N89-19400
The standard chemical oxygen-iodine laser kinetics package
[AD-A202223] N89-19543
Kinetics of ice crystal formation on aerosol particles in supercooled fog N89-19665
Determination of chemical reaction rates in fog N89-19683
Kinetics and mechanism of the Fe catalyzed autoxidation of S(4)-oxides in aqueous solution N89-19687
A one-dimensional numerical model to simulate liquid phase chemical reactions within radiation fog N89-19690
Oxidation regimes in orographic capping cloud N89-19698
Oxygen electrode in molten carbonate fuel cells
[DE89-005813] N89-19745
REACTION PRODUCTS
Formation of titanium nitride layers on titanium metal: Results of XPS and AES investigations
[KFK-4449] N89-19419
REACTOR TECHNOLOGY
Safe, compact nuclear propulsion: Solid core nuclear propulsion concept
[AD-A202339] N89-19369
READING
Using the sentence verification technique to assess storage and retrieval processes
[AD-A201632] N89-20029
REAL TIME OPERATION
Dexterous robotic hands: Kinematics and control
[AD-A202183] N89-19570
MODIS information, data and control system (MIDACS) operations concepts
[NASA-TM-100720] N89-19729
Central Region applied research on severe weather forecasting
[PB88-210836] N89-19771
The Cheyenne windstorm that never came: Another lesson in real time analysis
[CRARP-88-1] N89-19772
Automatic Detection of Electric Power Troubles (ADEPT) N89-19825

Validation of highly reliable, real-time knowledge-based systems N89-19833
Garbage collection can be made real-time and verifiable N89-19840
A parallel expert system for the control of a robotic air vehicle N89-19842
Portable inference engine: An extended CLIPS for real-time production systems N89-19843
An intelligent interface for satellite operations: Your Orbit Determination Assistant (YODA) N89-19852
A novel manipulator technology for space applications N89-19874
Application of model based control to robotic manipulators N89-19884
An expert system for restructurable control N89-19886
High-speed real-time animated displays on the ADAGE (trademark) RDS 3000 raster graphics system [NASA-TM-4095] N89-19899

RECOMBINATION REACTIONS
The dissociative adsorption of ammonia on Si(100) [AD-A201599] N89-19396

RECRYSTALLIZATION
Integration of detectors and optical waveguide structures [AD-A201331] N89-19536

RECTIFIERS
The Telecommunications and Data Acquisition Report [NASA-CR-184812] N89-19451
Design and test of a 2.25-MW transformer rectifier assembly N89-19452

RECURSIVE FUNCTIONS
A recursive method for parallel processor multiflexible body dynamic simulation N89-19336

REDUCED GRAVITY
Experiment plans to study preignition processes of a pool fire in low gravity [NASA-CR-182256] N89-19442
The solid surface combustion space shuttle experiment hardware description and ground-based test results [NASA-TM-101963] N89-19446
Man-systems requirements for the control of teleoperators in space N89-19862
Effects on motor unit potentiation and ground reaction force from treadmill exercise N89-20069
Maladjustment of kidneys to microgravity: Design of measures to reduce the loss of calcium N89-20076

REDUCTION (CHEMISTRY)
Oxygen electrode in molten carbonate fuel cells [DE89-005813] N89-19745

REDUNDANCY
Refractive turbulence profiling via binary source intensity scintillation correlation [AD-A202189] N89-19762
Autonomous satellite command and control: A comparison with other military systems N89-19839

REENTRY VEHICLES
Analysis of PERSHING 2 Reentry Vehicle (RV) control ring castings [AD-A201548] N89-19559

REFRACTIVITY
Refractive turbulence profiling via binary source intensity scintillation correlation [AD-A202189] N89-19762

REFRACTORY MATERIALS
Microstructural analyses of intermetallic TiAl (Nb)-compounds prepared by arc melting and by powder metallurgy [GKSS-88/E/32] N89-19417
Josephson effect research in high-temperature superconductors [AD-A201483] N89-20002

REFRACTORY METAL ALLOYS
Microstructural analyses of intermetallic TiAl (Nb)-compounds prepared by arc melting and by powder metallurgy [GKSS-88/E/32] N89-19417

REGRESSION ANALYSIS
A comparative analysis of tilt rotor aircraft versus helicopters using simulator results [AD-A202190] N89-19294
An asymptotic theory for weighted least squares with weights estimated by replication [AD-A198000] N89-19935
An analysis of the impact of log-linear regression on the estimated learning curve parameters [AD-A201471] N89-19938

REGULATORS
Further results on the design of multivariable regulators under structure and robustness constraints. Part 1: The initialization problem [REPT-88-028] N89-19931
Further results on the design of multivariable regulators under structure and robustness constraints. Part 2: The reliable robust decentralized regulator problem and the simultaneous robust decentralized regulator problem [REPT-88-029] N89-19932

RELATIONSHIPS
Reducing uncertainty by using explanatory relationships N89-19837

RELAY SATELLITES
Time-delayed operation of a telerobot via geosynchronous relay N89-19877

RELIABILITY
Technical report on temperature, precipitation and aviation verification at WSFO Sioux Falls for 1987 [CRARP-88-5] N89-19776
Artificial intelligent decision support for low-cost launch vehicle integrated mission operations N89-19830
A design and implementation methodology for diagnostic systems N89-19831
Validation of highly reliable, real-time knowledge-based systems N89-19833
Testing expert systems N89-19834
Autonomous satellite command and control: A comparison with other military systems N89-19839
Garbage collection can be made real-time and verifiable N89-19840
A methodology for automation and robotics evaluation applied to the space station telerobotic servicer N89-19882
An expert system for restructurable control N89-19886
Sensitivity analysis using the Monte Carlo acceptance-rejection method [AD-A201261] N89-19955

RELIABILITY ENGINEERING
R and M (Reliability and Maintainability) quality team concept and C-17 design at Douglas Aircraft Company: An R and M 2000 initiative case study [AD-A201574] N89-19228
Composite reliability enhancement via reloading [AD-A201861] N89-19380
On the design of loudspeakers for broadcast monitoring [BBC-RD-1988/14] N89-19450
Fatigue strength reduction model: RANDOM3 and RANDOM4 user manual. Appendix 2: Development of advanced methodologies for probabilistic constitutive relationships of material strength models [NASA-CR-184796-APP-2] N89-19582
A study of the reliability of Stirling engines for distributed receiver systems [DE89-006395] N89-19746
CIRCA 2000 operations criteria N89-19829

REMOTE CONTROL
Telescience system concept study, volume 2 --- Columbus space station [MATRA-NT/2113/139-VOL-2] N89-19478
Man-systems requirements for the control of teleoperators in space N89-19862
Integration of a computerized two-finger gripper for robot workstation safety N89-19863
Remote control system --- spectrometer [DIGEL-79] N89-19917
Model evaluation, recommendation and prioritizing of future work for the manipulator emulator testbed N89-20072

REMOTE HANDLING
Telescience system concept study, volume 2 --- Columbus space station [MATRA-NT/2113/139-VOL-2] N89-19478

REMOTE MANIPULATOR SYSTEM
Simulation of the human-telerobot interface N89-19861

REMOTE SENSING
Some outstanding problems on the influence of clouds on radiation N89-19643
Land use analysis using remote sensing techniques. Investigation of the usefulness of LANDSAT Thematic Mapper satellite pictures for obtaining and up to date picture of land use in the province South Holland [BCRS-88-01] N89-19733
Salinity mapping based on SPOT images of the Punjab, Pakistan [BCRS-88-03] N89-19734
Active and passive remote sensing of ice [AD-A201915] N89-19792
Satellite remote sensing of heat stress during reserve training at Fort Hood [AD-A201555] N89-19800

REMOTE SENSORS
Normalized radar cross section of natural surfaces at millimeter wavelengths [AD-A202252] N89-19475
On the observations of cloud temperature and liquid water content using a Lyman-alpha and an FSSP sensor --- forward scattering spectrometer probe (FSSP) N89-19618
Heterogeneous mixing measurements in small nonprecipitating cumuli N89-19635
The comparison of holographic and 2-D probe measurements of ice crystals N89-19652
Development of hydrometeor video sonde N89-19653
Calibration of PMS FSSP and 1D-C probes for cloud droplet measurements N89-19713
A poor man's optical fog detector N89-19716
Satellite remote sensing of heat stress during reserve training at Fort Hood [AD-A201555] N89-19800

REMOTELY PILOTED VEHICLES
The design and initial construction of a composite RPV (Remotely Piloted Vehicle) for flight research applications [AD-A201884] N89-19291
RPV (Remote Piloted Vehicle) applications in the US Navy [AD-A202151] N89-19293
A parallel expert system for the control of a robotic air vehicle N89-19842

RENAL FUNCTION
National Aeronautics and Space Administration (NASA)/American Society for Engineering Education (ASEE) Summer Faculty Fellowship Program 1988, volume 2 --- Author [NASA-CR-172118-VOL-2] N89-20073
Maladjustment of kidneys to microgravity: Design of measures to reduce the loss of calcium N89-20076

REPORT GENERATORS
Electronic data generation and display system N89-19891

REPORTS
Preparing storm data [CRARP-88-6] N89-19777

REQUIREMENTS
Hypervelocity technology escape system concepts. Volume 1: Development and evaluation [AD-A201719] N89-19280
Advanced extravehicular activity systems requirements definition study. Phase 2: Extravehicular activity at a lunar base [NASA-CR-172117] N89-19809
Telerobot operator control station requirements N89-19876

RESCUE OPERATIONS
Positive Flotation Harness (PFH) for use by Canadian Forces search and rescue technicians [AD-A200727] N89-19279

RESEARCH AND DEVELOPMENT
Evaluation support system for multiple R and D projects N89-19926
Factors affecting the adoption of R and D project selection techniques at the Air Force Write Aeronautical Laboratories [AD-A201543] N89-20025
Multicriteria analysis and budget allocation, with applications in energy R and D planning: A feasibility study [REPT-88-07] N89-20026
National Aeronautics and Space Administration authorization [S-HRG-100-579-PT-2] N89-20031

RESEARCH FACILITIES
Variable gravity research facility [NASA-CR-184714] N89-19324
Gear technology acquisition for advanced aero engines [PNR90510] N89-19571
Factors affecting the adoption of R and D project selection techniques at the Air Force Write Aeronautical Laboratories [AD-A201543] N89-20025

RESEARCH MANAGEMENT
Factors affecting the adoption of R and D project selection techniques at the Air Force Write Aeronautical Laboratories [AD-A201543] N89-20025

RESIDUAL STRESS
The mechanical behavior of surface modified ceramics [DE89-004764] N89-19422
Determination of residual stress distributions in autofrettaged tubing: A discussion [AD-A201454] N89-19586
Reciprocal theorem of residual stress and inelastic strain [AD-A202353] N89-19598
Acoustoelasticity using longitudinal waves for residual stress evaluation [DE89-006154] N89-19604

RESIN MATRIX COMPOSITES
Heat transfer properties of satellite component materials N89-19375
RESISTANCE THERMOMETERS
Comparison of an ac and a dc bridge for standard platinum resistance thermometer calibrations [DE89-007060] N89-19534
A comparison of radiometric and immersion temperature measurements in water clouds N89-19712
RESONANT FREQUENCIES
Passive vibration control using viscoelastic and constrained layer beam waveguide absorbers [AD-A202188] N89-19595
RESOURCE ALLOCATION
Knowledge-based operation and management of communications systems N89-19826
Garbage collection can be made real-time and verifiable N89-19840
An exact ceiling point algorithm for general integer linear programming [AD-A202286] N89-19913
RESPIRATORY PHYSIOLOGY
A stress test to evaluate the physical capacity of performing L-1 anti-G straining maneuvers [AD-A202301] N89-19803
RESPONSE BIAS
A method for modeling bias in a person's estimates of likelihoods of events N89-19849
RETIREMENT
Computer technologies and institutional memory N89-20062
REVERSE FIELD PINCH
Numerical studies of MHD turbulence in the reversed field pinch [IPP-6/276] N89-19994
REYNOLDS NUMBER
Use of riblets to obtain drag reduction on airfoils at high Reynolds number flows [AD-A201485] N89-19267
RHEOLOGY
Interdisciplinary research in viscoelasticity and rheology [AD-A201270] N89-19390
Theoretical and experimental studies of selected topics in the rheology of fluids [AD-A201460] N89-19512
RIBLETS
Use of riblets to obtain drag reduction on airfoils at high Reynolds number flows [AD-A201485] N89-19267
RICCATI EQUATION
Effects of reduced order modeling on the control of a large space structure [AD-A201674] N89-19355
RIGID STRUCTURES
A recursive method for parallel processor multiflexible body dynamic simulation N89-19336
RISK
A method for modeling bias in a person's estimates of likelihoods of events N89-19849
ROBOTICS
Coordinates, conversions, and kinematics for the Rochester Robotics Lab [AD-A201611] N89-19560
Implementation of dynamic control of a single-link flexible arm using a general micro-computer [AD-A201622] N89-19561
Multiprocessor control of robotic manipulators N89-19562
Chaotic dynamics and control of nonlinear and flexible arm robotic devices N89-19566
Minimum time motion of a robotic manipulator N89-19567
A three-dimensional nonsingular simulation of rigid manipulators [AD-A201964] N89-19569
Dexterous robotic hands: Kinematics and control [AD-A202183] N89-19570
Second Annual Workshop on Space Operations Automation and Robotics (SOAR 1988) [NASA-CP-3019] N89-19817
A parallel expert system for the control of a robotic air vehicle N89-19842
Simulation of the human-telerobot interface N89-19861
Concept for a large master/slave-controlled robotic hand N89-19866
Sensor fusion of range and reflectance data for outdoor scene analysis N89-19868
Design concept for the Flight Telerobotic Servicer (FITS) N89-19870
The WCSAR telerobotics test bed N89-19871
Telepresence and telerobotics N89-19873
A novel manipulator technology for space applications N89-19874
A robust control scheme for flexible arms with friction in the joints N89-19875
Telerobot operator control station requirements N89-19876
Time-delayed operation of a telerobot via geosynchronous relay N89-19877
Machine vision for space telerobotics and planetary rovers N89-19879
A multi-sensor system for robotics proximity operations N89-19881
A methodology for automation and robotics evaluation applied to the space station telerobotic servicer N89-19882
Application of model based control to robotic manipulators N89-19884
Design guidelines for remotely maintainable equipment N89-19885
SARSCEST (human factors) N89-19890
CAD directed robotic edge finishing [DE89-005347] N89-19916
JPRS report: Science and technology. Japan: 7th Artificial Intelligence Symposium [JPRS-JST-88-020] N89-19924
National Aeronautics and Space Administration (NASA)/American Society for Engineering Education (ASEE) Summer Faculty Fellowship Program 1988, volume 2 --- Author [NASA-CR-172118-VOL-2] N89-20073
Intelligent control of robotic arm/hand systems for the NASA EVA retriever using neural networks N89-20075
Visual perception and grasping for the extravehicular activity robot N89-20082
Time-domain imaging N89-20084
ROBOTS
Concept of adaptive structures N89-19338
Coordinates, conversions, and kinematics for the Rochester Robotics Lab [AD-A201611] N89-19560
Design of an optical sensor system for adaptive control of a seam tracking robot N89-19565
Chaotic dynamics and control of nonlinear and flexible arm robotic devices N89-19566
Extracting depth by binocular stereo in a robot vision system [DE89-005016] N89-19572
Integration of a computerized two-finger gripper for robot workstation safety N89-19863
Dexterity analysis and robot hand design N89-19865
Robot path planning using a genetic algorithm N89-19869
The use of the articulated total body model as a robot dynamics simulation tool N89-19872
Sensing human hand motions for controlling dexterous robots N89-19883
A 2-D and 3-D robot path planning algorithm based on quadtree and octree representation of workspace [DE89-005014] N89-19900
CAD directed robotic edge finishing [DE89-005347] N89-19916
Intelligent mobile robot working in unknown environment N89-19927
National Aeronautics and Space Administration (NASA)/American Society for Engineering Education (ASEE) Summer Faculty Fellowship Program 1988, volume 2 --- Author [NASA-CR-172118-VOL-2] N89-20073
Intelligent control of robotic arm/hand systems for the NASA EVA retriever using neural networks N89-20075
Visual perception and grasping for the extravehicular activity robot N89-20082
ROBUSTNESS (MATHEMATICS)
Robust eigenstructure assignment by a projection method: Application using multiple optimization criteria N89-19349
Stabilization and regulation of multirate sampled-date linear systems [REPT-88-013] N89-19930
Further results on the design of multivariable regulators under structure and robustness constraints. Part 1: The initialization problem [REPT-88-028] N89-19931
Further results on the design of multivariable regulators under structure and robustness constraints. Part 2: The reliable robust decentralized regulator problem and the simultaneous robust decentralized regulator problem [REPT-88-029] N89-19932
Robust bounded influence tests in linear models [AD-A201896] N89-19957
ROCK INTRUSIONS
Evaluation of crustal recycling during the evolution of Archean-age Matachewan basaltic magmas N89-20077
ROCKET EXHAUST
Experimental investigation on plume contamination and surface effects, phase 2 --- spacecraft [TUHH-TRI-ESA-1987] N89-19370
ROCKET LAUNCHING
The Atlas/Centaur 67 launch mishap [GPO-80-201] N89-19332
ROCKET NOZZLES
Studies and analyses of the space shuttle main engine. Appendix B: SSME FIPM drawings [NASA-CR-183594] N89-19365
ROCKET PROPELLED SLEDS
Noise assessment of the rocket sled test track operation at Holloman AFB, New Mexico [AD-A201279] N89-19317
ROCKS
An assessment of the micrometeoritic component in the Martian soil N89-20070
ROCKY MOUNTAINS (NORTH AMERICA)
Microphysical and dynamical interactions in Colorado front range upslope storms N89-19725
ROLLING CONTACT LOADS
Elastic cross-influence between two quasi-Hertzian contact zones [REPT-88-45] N89-19576
Some new results in rolling contact [REPT-88-46] N89-19577
The elastic stress and the displacement on the surfaces of two rubber-clad steel cylinders between which paper is led [REPT-88-23] N89-19603
ROTARY WINGS
Numerical solution of unsteady rotational flow past fixed and rotary wing configurations N89-19251
Experimental simulation of transonic vortex-airfoil interactions [AD-A201934] N89-19274
Combined preliminary airworthiness evaluation and airworthiness and flight characteristics evaluation of the UH-1H with preproduction hub spring and composite main rotor blades installed [AD-A202316] N89-19295
Icing research tunnel test of a model helicopter rotor [NASA-TM-101978] N89-19305
Time periodic control of a multiblade helicopter N89-19312
ROTATING CYLINDERS
Airborne cloud sieving N89-19681
ROTATING MIRRORS
Focusing system, rotation, and modulation of the F 9 mirror of the IFSI 40 cm telescope [IFSI-87-16] N89-19987
ROTATION
On the variation of falling velocity of early snowflakes N89-19670
Rotation and magnetic fields as an acceleration mechanism in astrophysical jets N89-20039
ROTORS
Experimental investigation of rotor-stator interaction in diffuser pumps N89-19564
ROUTES
Robot path planning using a genetic algorithm N89-19869
ROVING VEHICLES
Machine vision for space telerobotics and planetary rovers N89-19879
RUBBER
An interdisciplinary study of cathodic debonding in elastomer/metal adhesive bonds [AD-A202376] N89-19434
RUBIDIUM COMPOUNDS
Investigations of the statics and dynamics of the Jahn-Teller system RbCrCl3 using neutron scattering [ETN-89-93790] N89-20006
RULES
Equating an expert system to a classifier in order to evaluate the expert system N89-20080

S

SAFETY
Validation of highly reliable, real-time knowledge-based systems N89-19833
SAFETY DEVICES
Chemical warfare protection for the cockpit of future aircraft N89-19859
SAFETY FACTORS
Light weight escape capsule for fighter aircraft N89-19858
Integration of a computerized two-finger gripper for robot workstation safety N89-19863
SALINITY
Salinity mapping based on SPOT images of the Punjab, Pakistan [BCRS-88-03] N89-19734
SAMPLING
On sampling band-pass signals N89-19453
Arc jet diagnostics tests N89-20085

SATELLITE COMMUNICATION
A 20 GHz low noise, low cost receiver for digital satellite communication system, ground terminal applications
[NASA-CR-182243] N89-19449
Electromagnetic compatibility test report for the tethered satellite data acquisition and control assembly
[AD-A201549] N89-19458
SATELLITE CONFIGURATIONS
PSDE/SAT-2 preliminary spacecraft configuration study, executive summary
[ESA-CR(P)-2689] N89-19360
PSDE/SAT-2: Preliminary spacecraft configuration study, executive summary
[ESA-CR(P)-2704] N89-19364
SATELLITE CONTROL
Electromagnetic compatibility test report for the tethered satellite data acquisition and control assembly
[AD-A201549] N89-19458
SATELLITE DESIGN
Definition of the transmission system for a European data relay satellite
[ESA-CR(P)-2632] N89-19359
Heat transfer properties of satellite component materials N89-19375
SATELLITE DOPPLER POSITIONING
Study of NAVSAT for precise positioning
[IKU-88.068] N89-19286
SATELLITE GROUND SUPPORT
A 20 GHz low noise, low cost receiver for digital satellite communication system, ground terminal applications
[NASA-CR-182243] N89-19449
SATELLITE IMAGERY
The use of LANDSAT imagery for water quality studies in the Ijsselmeer area (Netherlands)
[BCRS-87-18] N89-19732
Land use analysis using remote sensing techniques. Investigation of the usefulness of LANDSAT Thematic Mapper satellite pictures for obtaining and up to date picture of land use in the province South Holland
[BCRS-88-01] N89-19733
Salinity mapping based on SPOT images of the Punjab, Pakistan
[BCRS-88-03] N89-19734
SATELLITE NAVIGATION SYSTEMS
Study of NAVSAT for precise positioning
[IKU-88.068] N89-19286
SATELLITE NETWORKS
Economic analysis of NAVSAT system
[REPT-1013-CA/TS] N89-19285
SATELLITE OBSERVATION
Homogenizing surface and satellite observations of cloud
[AD-A201630] N89-19752
An assessment of the application of in situ ion-density data from DMSP (Defense Meteorology Satellite Program) to modeling of transionospheric scintillation
[AD-A202415] N89-19765
Satellite remote sensing of heat stress during reserve training at Fort Hood
[AD-A201555] N89-19800
SATELLITE ORIENTATION
SCD2 satellite spin axis reorientation and feasibility study
[INPE-4688-NTE/285] N89-19351
JPRS report: Science and technology. USSR: Electronics and electrical engineering
[JPRS-UEE-88-005] N89-19485
Peaceful uses of electrical engineering in space N89-19487
SATELLITE PERTURBATION
National Aeronautics and Space Administration (NASA)/American Society for Engineering Education (ASEE) Summer Faculty Fellowship Program 1988, volume 2 --- Author
[NASA-CR-172118-VOL-2] N89-20073
Estimation of velocity perturbations in satellite fragmentation events N89-20083
SATELLITE ROTATION
Episodic volcanism of tidally heated satellites with application to Io. Thermal state of an ice shell on Europa. Polar wander of a synchronously rotating satellite with application to Europa N89-20052
SATELLITE SOUNDING
Satellite remote sensing of heat stress during reserve training at Fort Hood
[AD-A201555] N89-19800
SATELLITE TRACKING
An expert system for shuttle and satellite radar tracker scheduling N89-19821
SATELLITE TRANSMISSION
Definition of the transmission system for a European data relay satellite
[ESA-CR(P)-2632] N89-19359
Code performance simulation study for DRS S-band transmission
[ESA-CR(P)-2688] N89-19482
SATELLITE-BORNE PHOTOGRAPHY
Homogenizing surface and satellite observations of cloud
[AD-A201630] N89-19752
SATURN ATMOSPHERE
Temperature and circulation in the stratospheres of the outer planets
[NASA-CR-184826] N89-20051
SCALE MODELS
Control of nonlinear systems using partial dynamic inversion N89-19310
SCANNING
Structural saliency: The detection of globally salient structures using a locally connected network
[AD-A201619] N89-19806
SCANNING TUNNELING MICROSCOPY
Applications of scanning tunneling microscopy to electrochemistry
[AD-A201613] N89-19398
Scanning tunneling microscopy of metals on graphite
[DE89-006608] N89-19404
SCATTERING
Time-domain imaging N89-20084
SCATTERING COEFFICIENTS
Interpretation of ERS-1 wind scatterometer data: Wind field extraction
[ETN-89-93982] N89-19790
SCATTEROMETERS
Interpretation of ERS-1 wind scatterometer data: Wind field extraction
[ETN-89-93982] N89-19790
SCAVENGING
Measurements of the partitioning of aerosol mass and number between cloud droplets and interstitial air N89-19616
Below cloud scavenging by rain and drizzle N89-19685
Processes determining cloudwater composition: Field evidence for in-cloud reactive scavenging of SO2 N89-19693
Acidification of stratiform clouds and their aerosol scavenging properties N89-19694
Microphysical, dynamical and chemical aspects of scavenging processes during winter precipitation N89-19695
Results of time and height resolved scavenging experiments --- atmospheric chemistry N89-19697
Concentrations in rain events collected sequentially: Measurements vs results of a simple scavenging model N89-19701
Effects of cloud microphysical processes on trace chemical removal efficiences N89-19707
SCENE ANALYSIS
Sensor fusion of range and reflectance data for outdoor scene analysis N89-19868
Analysis of blending algorithms in computer graphics
[AD-A201921] N89-19909
SCHEDULING
The scheduling techniques of ESP2 N89-19818
Space station payload operations scheduling with ESP2 N89-19819
A survey of planning and scheduling research at the NASA Ames Research Center N89-19820
An expert system for shuttle and satellite radar tracker scheduling N89-19821
JPRS report: Science and technology. Japan: 7th Artificial Intelligence Symposium
[JPRS-JST-88-020] N89-19924
Problems in structuring large-scale expert system N89-19925
Calendar of selected aeronautical and space meetings: January 1989 onwards
[AGARD-CAL-89/1] N89-20024
SCHLIEREN PHOTOGRAPHY
Application of Schlieren photography in gas turbine combustion research
[PNR90495] N89-19532
SCHOTTKY DIODES
Ohmic contacts to gallium aluminum arsenide for high temperature applications
[AD-A202248] N89-19492
Evaluation of Schottky barrier and PBTE IR-CCD detectors for the SWIR and MIR wavelengths range, executive summary
[IMEC-SP/CCD-255/88-03] N89-19495
SCINTILLATION
An assessment of the application of in situ ion-density data from DMSP (Defense Meteorology Satellite Program) to modeling of transionospheric scintillation
[AD-A202415] N89-19765
SEAMS (JOINTS)
Design of an optical sensor system for adaptive control of a seam tracking robot N89-19565
SEASONS
Precipitation initiation mechanisms in clouds over north India N89-19624
SEDIMENTS
Compressional-wave velocities in ocean sediments east southeast of Madeira, Atlantic Ocean
[IOS-257] N89-19794
SEISMOLOGY
Compressional-wave velocities in ocean sediments east southeast of Madeira, Atlantic Ocean
[IOS-257] N89-19794
SELF SEALING
On the sealing and lubrication mechanism of radial lip seals
[ETN-89-93898] N89-19574
SEMANTICS
A general way to put time in Petri nets
[REPT-88-011] N89-19914
SEMICONDUCTORS (MATERIALS)
Chemistry and physics of polyacetylene, (CH)x: The prototype conducting polymer
[AD-A201933] N89-19431
Computer-aided fabrication system implementation
[AD-A202128] N89-19911
Development of Si/SiGe heterostructures
[AD-A201440] N89-20001
The 2-4 semiconductor superlattices
[AD-A202369] N89-20005
Thermal oxidation of 3-5 compound semiconductors
[DE89-007127] N89-20020
Raman and RBS studies of ion implanted semiconductors
[ATR-88(8359)-5] N89-20021
SENSITIVITY
RE-1000 free-piston Stirling engine sensitivity test results
[NASA-TM-88846] N89-19737
SENTENCES
Using the sentence verification technique to assess storage and retrieval processes
[AD-A201632] N89-20029
SEPARATED FLOW
A study of flow separation in transonic flow using inviscid and viscous CFD schemes N89-19273
A computationally efficient modelling of laminar separation bubbles
[NASA-CR-184789] N89-19504
The use of direct sparse matrix methods and Newton iteration for the numerical solution of fluid flows N89-19514
SERIES (MATHEMATICS)
Estimation in large samples
[AD-A201459] N89-19956
SERVICE LIFE
Fatigue strength reduction model: RANDOM3 and RANDOM4 user manual. Appendix 2: Development of advanced methodologies for probabilistic constitutive relationships of material strength models
[NASA-CR-184796-APP-2] N89-19582
SERVOCONTROL
Multiprocessor control of robotic manipulators N89-19562
Telepresence and telerobotics N89-19873
SERVOMECHANISMS
Model evaluation, recommendation and prioritizing of future work for the manipulator emulator testbed N89-20072
SH-3 HELICOPTER
Thermal stress in Ran Sea King Helicopter operations
[ARL-SYS-R-40] N89-19810
SHAPE CONTROL
The efficacy of color-coded symbols to enhance air-traffic control displays
[AD-A201594] N89-19284
Modeling of flexible spacecraft accounting for orbital effects N89-19334
SHAPES
A model of the electrostatic-aerodynamic shape of raindrops N89-19615
The development and validation of an automated headboard device for measurement of three-dimensional coordinates of the head and face
[AD-A201186] N89-19813
Time-domain imaging N89-20084
SHEAR LAYERS
Flame driving of longitudinal instabilities in liquid fueled dump combustors
[AD-A201293] N89-19392
Characteristic time model validation
[AD-A201374] N89-19510
Computational studies of evaporating sprays in a shear layer
[AD-A201932] N89-19520
SHEAR PROPERTIES
Finite element analysis of laminated composite plates
[AD-A202192] N89-19381
Sliding and debonding inclusions
[AD-A201609] N89-19587

SHELLS (STRUCTURAL FORMS)
Modeling of flexible spacecraft accounting for orbital effects N89-19334
Nonlinear vibrations of composite material shells N89-19377
SHIELDING
Impact of target altitude restrictions on laser performance
[DE89-006567] N89-19553
SHIP HULLS
The modeling of viscoelastic circular plates for use as waveguide absorbers
[AD-A201621] N89-19588
SHIPS
In situ measurements of ship tracks N89-19645
SHOCK (PHYSIOLOGY)
Fear-potential startle as a model system for analyzing learning and memory
[AD-A201330] N89-19805
SHOCK LOADS
The role of shock induced trailing-edge separation in limit cycle oscillations N89-19256
SHOCK TUBES
Analytical, numerical and experimental investigations of oblique-shock-wave reflections in pure and dusty gases
[AD-A201438] N89-19511
SHOCK WAVE INTERACTION
Error norm guided flow analysis of shock-wave/boundary-layer interactions
[AD-A201176] N89-19507
SHOCK WAVES
Investigation and suppression of high dynamic response encountered on an elastic supercritical wing N89-19255
Numerical computations of transonic critical aerodynamic behavior
[AD-A202412] N89-19277
Ion beam driven electrostatic shocks --- ionosphere
[MPE-PREPRINT-127] N89-19995
SHORT CRACKS
Fatigue crack growth model RANDOM2 user manual. Appendix 1: Development of advanced methodologies for probabilistic constitutive relationships of material strength models
[NASA-CR-184775-APP-1] N89-19581
SHORT WAVE RADIO TRANSMISSION
Variations of the tropospheric propagation range of ultrashort radio waves above the sea N89-19486
SIDE-LOOKING RADAR
Study of the use of radar X-band data of bare soil in a radar scattering model
[BCRS-88-04] N89-19735
SIDEBANDS
Chaotic electron motion caused by sidebands in free electron lasers
[AD-A201635] N89-19538
SIERRA NEVADA MOUNTAINS (CA)
Complex microphysical interactions within a central Sierra Nevada orographic cloud system N89-19722
SIEVES
Airborne cloud sieving N89-19681
SIGNAL ANALYSIS
The use of interleaving for reducing radio loss in convolutionally coded systems N89-19454
The use of burst-triggered correlation for laser anemometry measurements in turbomachinery
[PNR90542] N89-19533
Automatic voice recognition using traditional and artificial neural network approaches N89-20064
SIGNAL DETECTION
Development of a system for acoustic measurements of bistatic target strengths
[AD-A201673] N89-19970
SIGNAL ENCODING
Code performance simulation study for DRS S-band transmission
[ESA-CR(P)-2688] N89-19482
SIGNAL PROCESSING
On sampling band-pass signals N89-19453
Computer algorithms for measurement control and signal processing of transient scattering signatures
[AD-A201672] N89-19469
A study of advanced radar altimeter techniques --- satellite altimetry
[ESA-CR(P)-2699] N89-19483
The WCSAR telerobotics test bed N89-19871
SIGNAL REFLECTION
Time-domain imaging N89-20084
SIGNAL TO NOISE RATIOS
The use of interleaving for reducing radio loss in convolutionally coded systems N89-19454
Computer algorithms for measurement control and signal processing of transient scattering signatures
[AD-A201672] N89-19469
SILICON CARBIDES
Reinforcement/matrix interaction in SiC fiber-reinforced Ni3Al matrix composites
[DE89-006041] N89-19384
Evaluation of optical materials samples
[AD-A199471] N89-19981
SILICON ISOTOPES
The dissociative adsorption of ammonia on Si(100)
[AD-A201599] N89-19396
SILICON NITRIDES
The dissociative adsorption of ammonia on Si(100)
[AD-A201599] N89-19396
Improved silicon nitride for advanced heat engines
[NASA-CR-179525] N89-19421
SILICON OXIDES
Proposal to study the interaction of polyimide precursors and thin polyimide films with silicon and silicon oxide surfaces
[AD-A201183] N89-19425
SIMULATION
Experimental simulation of transonic vortex-airfoil interactions
[AD-A201934] N89-19274
A recursive method for parallel processor multiflexible body dynamic simulation N89-19336
A comparative study of laboratory thermals and atmospheric clouds N89-19627
Analysis of hailstones from a severe storm and their simulated evolution N89-19677
Simulation of conical graupel by using a ballistic model N89-19679
A one-dimensional numerical model to simulate liquid phase chemical reactions within radiation fog N89-19690
Some effects of cloud microphysics on cloud chemistry N89-19692
Model evaluation, recommendation and prioritizing of future work for the manipulator emulator testbed N89-20072
SINGLE EVENT UPSETS
Mechanisms leading to single event upset
[ATR-86(8139)-5] N89-19977
SINTERED ALUMINUM POWDER
Composite ceramic superconducting wires for electric motor applications
[AD-A201810] N89-19429
SITE SELECTION
Local wind measurements for micrositing
[DE89-000829] N89-19781
SIZE DETERMINATION
The development and validation of an automated headboard device for measurement of three-dimensional coordinates of the head and face
[AD-A201186] N89-19813
SIZE DISTRIBUTION
Evaluation of droplet growth rates in Hawaiian orographic clouds N89-19619
An examination of the chemical and physical variability of clouds at a mountain-top site in central Sweden N89-19699
SLIDING
Sliding and debonding inclusions
[AD-A201609] N89-19587
SLIPSTREAMS
A data analysis system for unsteady turbulence measurements
[AD-A201662] N89-19268
SMALL PERTURBATION FLOW
Role of computational fluid dynamics in unsteady aerodynamics for aeroelasticity N89-19237
CAP-TSD: A program for unsteady transonic analysis of realistic aircraft configurations N89-19238
CAP-TSD analysis of the F-15 aircraft N89-19239
Calculation of steady and unsteady pressures at supersonic speeds with CAP-TSD N89-19240
Initial application of CAP-TSD to wing flutter N89-19257
Transonic flutter calculations using the Euler equations N89-19258
SNOW
Temporal variations of snow crystal growth parameters N89-19608
A wind tunnel study on the melting of snow flakes N89-19611
Proportion of riming growth process in snowfall phenomena N89-19668
Three-dimensional structures of snow crystals shown by stereo-photomicrographs N89-19669
On the variation of falling velocity of early snowflakes N89-19670
On the dynamics of the falling ice crystal zone N89-19672
A vertical wind tunnel for the study of snowflakes and effects of accumulated snow on materials N89-19674
Simulation of conical graupel by using a ballistic model N89-19679
The effect of aerosols on pH of snowfalls N89-19688
Ionic concentrations of rime ice and snow and Bergeron process N89-19689
Characteristics of radar echo of snow band formed in the lee side of a mountain N89-19726
A case study of significant lake enhanced snow event in upper Michigan
[CRARP-88-2] N89-19773
Use of long-waves in forecasting
[CRARP-88-7] N89-19778
SNOW COVER
Normalized radar cross section of natural surfaces at millimeter wavelengths
[AD-A202252] N89-19475
SNOWSTORMS
A numerical investigation of an orographic precipitation event N89-19721
Microphysical and dynamical interactions in Colorado front range upslope storms N89-19725
SODIUM COMPOUNDS
The coupled cluster method and the properties of energetic materials
[AD-A201168] N89-19388
SOFTWARE ENGINEERING
Laser transit anemometer software development program
[NASA-CR-4225] N89-19545
ISTAR evaluation
[AD-A201345] N89-19903
Software performance on nonlinear least-squares problems
[AD-A201879] N89-19908
Critical problems in very large scale computer systems
[AD-A202129] N89-19923
Development of a software interface for optical disk archival storage for a new life sciences flight experiments computer N89-20061
SOFTWARE TOOLS
Integrated tools for control-system analysis
[NASA-TP-2885] N89-19309
NESSUS (Numerical Evaluation of Stochastic Structures Under Stress)/EXPERT: Bridging the gap between artificial intelligence and FORTRAN N89-19827
A design and implementation methodology for diagnostic systems N89-19831
An intelligent tutoring system for space shuttle diagnosis N89-19853
ISTAR evaluation
[AD-A201345] N89-19903
SOIL MAPPING
Salinity mapping based on SPOT images of the Punjab, Pakistan
[BCRS-88-03] N89-19734
Study of the use of radar X-band data of bare soil in a radar scattering model
[BCRS-88-04] N89-19735
SOILS
An assessment of the micrometeoritic component in the Martian soil N89-20070
SOLAR ACTIVITY EFFECTS
Mass-radius star evolution Sun activity planets surfaces on purely empirical basis. Empiry theory reality: The use of statistics
[REPT-18] N89-20050
SOLAR CELLS
Peaceful uses of electrical engineering in space N89-19487
Starting characteristics of direct current motors powered by solar cells
[NASA-TM-101981] N89-19493
Research on high-efficiency, multi-gap, multijunction, amorphous-silicon-based alloy thin-film solar cells, phase 1
[DE89-000844] N89-19739
Silicon concentrator solar cell research
[DE89-005490] N89-19740
SOLAR COLLECTORS
Silicon concentrator solar cell research
[DE89-005490] N89-19740
A study of the reliability of Stirling engines for distributed receiver systems
[DE89-006395] N89-19746
SOLAR COSMIC RAYS
Solar and interplanetary cosmic ray composition
[MPE-PREPRINT-108] N89-20056
SOLAR ENERGY
Solar thermal technology
[DE89-000818] N89-19738
Studies of flares and disappearing magnetic flux
[AD-A201456] N89-20053
SOLAR ENERGY CONVERSION
Horizons of new energy technologies
[DFVLR-MITT-88-22] N89-19742

A study of the reliability of Stirling engines for distributed receiver systems
[DE89-006395] N89-19746
SOLAR FLARES
Studies of flares and disappearing magnetic flux
[AD-A201456] N89-20053
SOLAR RADIATION
An investigation of the relationship between beam and global irradiation with the development of numerical solar radiation models N89-19748
SOLAR REFLECTORS
Optical goals for polymeric film reflectors
[DE89-000836] N89-19744
SOLAR THERMAL ELECTRIC POWER PLANTS
Solar thermal technology
[DE89-000818] N89-19738
SOLAR WIND
Electric fields in earth orbital space
[AD-A201747] N89-19760
Substorms, plasmoids, flux robes, and magnetotail flux loss on March 25, 1983: CDAW-8
[NASA-CR-184823] N89-19764
SOLID ELECTROLYTES
Fundamental optical studies of competitive adsorption and thin film phenomena
[DE89-005898] N89-19401
SOLID PROPELLANTS
Spectral studies of propellant combustion: Experimental details and emission results for M-30 propellant
[AD-A201634] N89-19399
SOLID ROCKET BINDERS
Boundary layer and singularity measurement in three dimensional fracture problems
[AD-A201277] N89-19584
SOLID ROCKET PROPELLANTS
High-speed laser photography
[AD-A202293] N89-19544
Boundary layer and singularity measurement in three dimensional fracture problems
[AD-A201277] N89-19584
SOLID STATE LASERS
Nonradiative relaxation and laser action in tunable solid state laser crystals
[NASA-CR-182820] N89-19539
SOLID SURFACES
The solid surface combustion space shuttle experiment hardware description and ground-based test results
[NASA-TM-101963] N89-19446
Pressure variation over a solid wavy surface
[AD-A201724] N89-19517
SOLID-SOLID INTERFACES
A dynamic, time stepping boundary element method for frictional crack and interface problems N89-19590
SOLIDIFICATION
Solidification, structure and mechanical properties of A357 aluminum alloy N89-19409
SOLUBILITY
Insoluble particles in hydrometeors N89-19684
SOLUTES
The effect of freezing on the composition of cloud droplets N89-19691
An examination of the chemical and physical variability of clouds at a mountain-top site in central Sweden N89-19699
SOLUTIONS
To measure and characterize metal corrosion in electrolyte solutions by exploiting the properties of superconducting
[AD-A201484] N89-19407
A survey of automatic code generating software
[AD-A201963] N89-19910
SOLVATION
Ion pair solvation
[AD-A201529] N89-19395
SONIC BOOMS
Noise assessment of the rocket sled test track operation at Holloman AFB, New Mexico
[AD-A201279] N89-19317
SOOT
An experimental investigation of sooting characteristics of a gas turbine combustor and augmentor tube
[AD-A201804] N89-19568
SORPTION
Polymer morphology and transport
[AD-A201167] N89-19424
SOUND INTENSITY
An examination of cavitation due to short pulses of megahertz ultrasound N89-19971
SOUND PRESSURE
An examination of cavitation due to short pulses of megahertz ultrasound N89-19971
SOUND WAVES
Acoustic wave propagation in heterogeneous structures including experimental validation
[NASA-TM-101486] N89-19965
Development of a system for acoustic measurements of bistatic target strengths
[AD-A201673] N89-19970
SPACE CHARGE
Theory of accelerated orbits and space charge effects in an Azimuthly Varying Field (AVF) cyclotron
[ETN-89-93897] N89-19978
SPACE COLONIES
A bootstrap lunar base: Preliminary design review 2
[NASA-CR-184753] N89-19807
Design of a surface-based factory for the production of life support and technology support products. Phase 2: Integrated water system for a space colony
[NASA-CR-184730] N89-19808
SPACE COMMERCIALIZATION
Model of a geostationary regional transportation company (GRET): Fleet composition and facility layout
[ILR-MITT-207] N89-19329
Preliminary cost model for a commercial geostationary transportation company (GRET)
[ILR-MITT-208] N89-19330
Preliminary project plan for a GEO regional transportation and servicing company
[ILR-MITT-210] N89-19331
The development of a cislunar space infrastructure
[NASA-CR-184728] N89-19352
SPACE DEBRIS
Estimation of velocity perturbations in satellite fragmentation events N89-20083
SPACE ENVIRONMENT SIMULATION
The effects of simulated space environmental parameters on six commercially available composite materials
[NASA-TP-2906] N89-19385
SPACE EXPLORATION
A case study of small group decision-making as influenced by the Abilene Paradox: The Challenger mishap
[AD-A202102] N89-19328
National Aeronautics and Space Administration authorization
[S-HRG-100-579-PT-2] N89-20031
SPACE FLIGHT
Flight model discharge system
[AD-A201605] N89-19354
SPACE FLIGHT FEEDING
National Aeronautics and Space Administration (NASA)/American Society for Engineering Education (ASEE) Summer Faculty Fellowship Program 1988, volume 1
[NASA-CR-172118-VOL-1] N89-20058
Comparison of Soviet and US space food and nutrition programs N89-20059
SPACE FLIGHT STRESS
A model for plasma volume changes during short duration spaceflight N89-20067
SPACE HABITATS
The development of a cislunar space infrastructure
[NASA-CR-184728] N89-19352
A bootstrap lunar base: Preliminary design review 2
[NASA-CR-184753] N89-19807
SPACE MANUFACTURING
Study of space aluminum coating, executive summary --- telescope mirrors
[IOM/CAEE-002/87(TR)] N89-19443
SPACE MISSIONS
Study of a software system concept for mission analysis presentation
[ESA-CR(P)-2661] N89-19320
Specification validation tools study
[MATRA-NT/139/1939] N89-19447
The Ninevah Mission: A design summary for an unmanned mission to Venus, volume 1
[NASA-CR-184705] N89-20040
The Ninevah Mission: Analytical analyses and calculations for trajectory and propulsion, volume 2
[NASA-CR-184706] N89-20041
SPACE PLASMAS
Substorms, plasmoids, flux robes, and magnetotail flux loss on March 25, 1983: CDAW-8
[NASA-CR-184823] N89-19764
Thermonuclear reactions of light nuclei in astrophysical plasmas N89-19988
Ion beam driven electrostatic shocks --- ionosphere
[MPE-PREPRINT-127] N89-19995
Existence of stationary solutions in the coronal loop problem
[REPT-88-06] N89-20054
SPACE PROCESSING
Mini protein crystallization facility. Phase A study: Executive summary
[REPT-AQ-ES-576/88] N89-19444
SPACE SHUTTLE MAIN ENGINE
Studies and analyses of the space shuttle main engine. Appendix B: SSME FIPM drawings
[NASA-CR-183594] N89-19365
Duct flow nonuniformities for Space Shuttle Main Engine (SSME)
[NASA-CR-183595] N89-19367
SPACE SHUTTLE MISSION 41-G
Measurements of shuttle glow on mission STS 41-G
[AD-A201769] N89-19327
SPACE SHUTTLE MISSIONS
Get Away Special (GAS): Educational applications of space flight
[NASA-TM-101287] N89-19321
Ice/frost/debris assessment for space shuttle mission STS-27R, December 2, 1988
[NASA-TM-102144] N89-19326
SPACE SHUTTLE ORBITERS
Expert systems applications for space shuttle payload integration automation N89-19887
SPACE SHUTTLE PAYLOADS
The solid surface combustion space shuttle experiment hardware description and ground-based test results
[NASA-TM-101963] N89-19446
Expert systems applications for space shuttle payload integration automation N89-19887
SPACE SHUTTLES
Measurements of shuttle glow on mission STS 41-G
[AD-A201769] N89-19327
Electromagnetic compatibility test report for the tethered satellite data acquisition and control assembly
[AD-A201549] N89-19468
Modeling of transient heat pipe operation
[NASA-CR-184688] N89-19502
Artificial intelligent decision support for low-cost launch vehicle integrated mission operations N89-19830
SPACE STATION PAYLOADS
The scheduling techniques of ESP2 N89-19818
Space station payload operations scheduling with ESP2 N89-19819
SPACE STATION POWER SUPPLIES
Automation of the space station core module power management and distribution system N89-19822
Automatic Detection of Electric Power Troubles (ADEPT) N89-19825
SPACE STATIONS
A model for the geostationary orbital infrastructure, system analysis
[ILR-MITT-205] N89-19323
Model of a geostationary regional transportation company (GRET): Fleet composition and facility layout
[ILR-MITT-207] N89-19329
Preliminary cost model for a commercial geostationary transportation company (GRET)
[ILR-MITT-208] N89-19330
Preliminary project plan for a GEO regional transportation and servicing company
[ILR-MITT-210] N89-19331
The development of a cislunar space infrastructure
[NASA-CR-184728] N89-19352
Effects of reduced order modeling on the control of a large space structure
[AD-A201674] N89-19355
The scheduling techniques of ESP2 N89-19818
Space station payload operations scheduling with ESP2 N89-19819
A methodology for automation and robotics evaluation applied to the space station telerobotic servicer N89-19882
National Aeronautics and Space Administration (NASA)/American Society for Engineering Education (ASEE) Summer Faculty Fellowship Program 1988, volume 1
[NASA-CR-172118-VOL-1] N89-20058
Development of an atmospheric monitoring plan for space station N89-20065
Evaluation of available analytical techniques for monitoring the quality of space station potable water N89-20071
Model evaluation, recommendation and prioritizing of future work for the manipulator emulator testbed N89-20072
National Aeronautics and Space Administration (NASA)/American Society for Engineering Education (ASEE) Summer Faculty Fellowship Program 1988, volume 2 --- Author
[NASA-CR-172118-VOL-2] N89-20073
Feasibility of using high temperature superconducting magnets and conventional magnetic loop antennas to attract or repel objects at the space station N89-20081
SPACE TRANSPORTATION SYSTEM
A model for the geostationary orbital infrastructure, system analysis
[ILR-MITT-205] N89-19323
Preliminary cost model for a commercial geostationary transportation company (GRET)
[ILR-MITT-208] N89-19330
Preliminary project plan for a GEO regional transportation and servicing company
[ILR-MITT-210] N89-19331

The development of a cislunar space infrastructure [NASA-CR-184728] N89-19352
CIRCA 2000 operations criteria N89-19829
Artificial intelligent decision support for low-cost launch vehicle integrated mission operations N89-19830
A design and implementation methodology for diagnostic systems N89-19831

SPACE VEHICLE CHECKOUT PROGRAM
CIRCA 2000 operations criteria N89-19829

SPACE WEAPONS
Survivability of space assets in the long term [DE89-006563] N89-19964

SPACEBORNE EXPERIMENTS
Get Away Special (GAS): Educational applications of space flight [NASA-TM-101287] N89-19321
The solid surface combustion space shuttle experiment hardware description and ground-based test results [NASA-TM-101963] N89-19446
The scheduling techniques of ESP2 N89-19818
Space station payload operations scheduling with ESP2 N89-19819
Development of a software interface for optical disk archival storage for a new life sciences flight experiments computer N89-20061

SPACEBORNE TELESCOPES
Study of space aluminum coating, executive summary --- telescope mirrors [IOM/CAEE-002/87(TR)] N89-19443

SPACECRAFT ANTENNAS
Meteosat Millimetre Wave Sounder (MWS) study [BAE-TP-9119] N89-19363
Experimental spherical near-field antenna test facility, phase 3. Volume 1: Facility updates, evaluation and software documentation [R-343] N89-19477
Intrinsic hybrid modes in a corrugated conical horn [ESA-CR(P)-2588] N89-19494
Microwave holographic measurements of large reflectors: Phase 1 report, volume 1 --- spacecraft antennas [REPT-B090] N89-19530
Microwave holographic measurements of large reflectors: Phase 2 report, volume 2 [REPT-B091] N89-19531

SPACECRAFT CABIN ATMOSPHERES
National Aeronautics and Space Administration (NASA)/American Society for Engineering Education (ASEE) Summer Faculty Fellowship Program 1988, volume 1 [NASA-CR-172118-VOL-1] N89-20058
Development of an atmospheric monitoring plan for space station N89-20065

SPACECRAFT CHARGING
Flight model discharge system [AD-A201605] N89-19354

SPACECRAFT COMMUNICATION
Radio frequency interference survey over the 1.0-10.4 GHz frequency range at the Goldstone-Venus Development Station N89-19466

SPACECRAFT COMPONENTS
Experimental verification of an innovative performance-validation methodology for large space systems [AD-A202243] N89-19357
Modeling of transient heat pipe operation [NASA-CR-184688] N89-19502

SPACECRAFT CONFIGURATIONS
Experimental investigation on plume contamination and surface effects, phase 2 --- spacecraft [TUHH-TRI-ESA-1987] N89-19370

SPACECRAFT CONTROL
Nonlinear optimal control and near-optimal guidance strategies in spacecraft general attitude maneuvers N89-19356
Maximum entropy/optimal projection design synthesis for decentralized control of large space structures [AD-A202375] N89-19358
Advanced information technology monitoring with microprocessors --- spacecraft control [MMP-1-IS-02-3302-FR] N89-19895

SPACECRAFT DESIGN
A model for the geostationary orbital infrastructure, system analysis [ILR-MITT-205] N89-19323
Model of a geostationary regional transportation company (GRET): Fleet composition and facility layout [ILR-MITT-207] N89-19329
Integrated Structural Analysis And Control (ISAAC): Issues and progress N89-19341
Booster propulsion/vehicle impact study [NASA-CR-183584] N89-19366

SPACECRAFT DOCKING
Feasibility of using high temperature superconducting magnets and conventional magnetic loop antennas to attract or repel objects at the space station N89-20081

SPACECRAFT ELECTRONIC EQUIPMENT
A low-loss linear analog phase modulator for 8415 MHz transponder application N89-19465

SPACECRAFT GLOW
Measurements of shuttle glow on mission STS 41-G [AD-A201769] N89-19327

SPACECRAFT GUIDANCE
Nonlinear optimal control and near-optimal guidance strategies in spacecraft general attitude maneuvers N89-19356

SPACECRAFT MANEUVERS
Nonlinear optimal control and near-optimal guidance strategies in spacecraft general attitude maneuvers N89-19356
Control of flexible structures: Model errors, robustness measures, and optimization of feedback controllers [AD-A202234] N89-19596

SPACECRAFT MODELS
Flight model discharge system [AD-A201605] N89-19354
Control of flexible structures: Model errors, robustness measures, and optimization of feedback controllers [AD-A202234] N89-19596

SPACECRAFT ORBITS
Substorms, plasmoids, flux robes, and magnetotail flux loss on March 25, 1983: CDAW-8 [NASA-CR-184823] N89-19764

SPACECRAFT POWER SUPPLIES
Electronic Power Conditioner (EPC) for carcinotrons [R/D/REPO/8801] N89-19496
Automation of the space station core module power management and distribution system N89-19822
National Aeronautics and Space Administration (NASA)/American Society for Engineering Education (ASEE) Summer Faculty Fellowship Program 1988, volume 1 [NASA-CR-172118-VOL-1] N89-20058
Development of parallel algorithms for electrical power management in space applications N89-20063

SPACECRAFT REENTRY
Analytical interpretation on lateral/directional stability and controllability of high angle-of-attack reentry flight [ISAS-630] N89-19353

SPACECRAFT STABILITY
Analytical interpretation on lateral/directional stability and controllability of high angle-of-attack reentry flight [ISAS-630] N89-19353
Transient three-dimensional heat conduction computations using Brian's technique [AD-A201918] N89-19519

SPACECRAFT STRUCTURES
A recursive method for parallel processor multiflexible body dynamic simulation N89-19336
Error localization and updating of spacecraft structures mathematical models [YMD/EF/0175] N89-19361
Heat transfer properties of satellite component materials N89-19375
A finite element dynamic analysis of flexible spatial mechanisms and manipulators [ETN-89-93901] N89-19575

SPACECRAFT SURVIVABILITY
Survivability of space assets in the long term [DE89-006563] N89-19964

SPACECRAFT TRACKING
Nonlinear optimal control and near-optimal guidance strategies in spacecraft general attitude maneuvers N89-19356
An expert system for shuttle and satellite radar tracker scheduling N89-19821

SPACECREWS
An annotated bibliography of hypobaric decompression sickness research conducted at the Crew Technology Division, USAF School of Aerospace Medicine, Brooks AFB, Texas from 1983 to 1988 [AD-A201274] N89-19796
Development of an atmospheric monitoring plan for space station N89-20065
A model for plasma volume changes during short duration spaceflight N89-20067

SPATIAL DISTRIBUTION
Verification of combined thermal-hydraulic and heat conduction analysis code FLOWNET/TRUMP [DE88-756063] N89-19506

SPATIAL RESOLUTION
A study of advanced radar altimeter techniques --- satellite altimetry [ESA-CR(P)-2699] N89-19483

SPECIFICATIONS
Performance evaluation of military engine and gear oils in friction and wear devices [AD-A202145] N89-19432
Comparative performance evaluation of advanced AC and DC EV propulsion systems [DE89-005419] N89-19498

SPECTRAL REFLECTANCE
Sensor fusion of range and reflectance data for outdoor scene analysis N89-19868
An infrared reflectance study of water in outer belt asteroids N89-20037

SPECTRAL SIGNATURES
A study of the ionospheric signature of ion supply from the ionosphere to the magnetosphere N89-19754
Recognition of object domain by color distribution N89-19928

SPECTROMETERS
Remote control system --- spectrometer [DIGEL-79] N89-19917

SPECTROPHOTOMETERS
Calibration of PMS FSSP and 1D-C probes for cloud droplet measurements N89-19713

SPECTROSCOPY
MPD (Magnetoplasmadynamic) thrust chamber flow dynamics [AD-A201263] N89-19368
Applications of scanning tunneling microscopy to electrochemistry [AD-A201613] N89-19398
Spectral studies of propellant combustion: Experimental details and emission results for M-30 propellant [AD-A201634] N89-19399

SPECTRUM ANALYSIS
Machinery diagnostics via mechanical vibration analysis using spectral analysis techniques [AD-A202089] N89-19594
Damped-oscillation representation of drop-spectrum evolution due to coalescence and breakup N89-19660
A detailed examination of discontinuities in natural rain spectra N89-19663
Excitation of strong high-frequency electric fields and their detection using the dynamic Stark effect [ETN-89-93794] N89-19991

SPECULAR REFLECTION
Estimating the illuminant color from the shading of a smooth surface [AD-A201333] N89-19983

SPEECH
Development of a model which provides a total system approach to integrating voice recognition and speech synthesis into the cockpit of US Navy aircraft [AD-A202122] N89-19815

SPEECH RECOGNITION
Next generation keyboards: The importance of cognitive compatibility N89-19848
Voice control of complex workstations N89-19880

SPIN STABILIZATION
SCD2 satellite spin axis reorientation and feasibility study [INPE-4688-NTE/285] N89-19351

SPOT (FRENCH SATELLITE)
Salinity mapping based on SPOT images of the Punjab, Pakistan [BCRS-88-03] N89-19734

SPRAY CHARACTERISTICS
Characteristic time model validation [AD-A201374] N89-19510

SPRAYERS
Computational studies of evaporating sprays in a shear layer [AD-A201932] N89-19520

SPREADING
Spreading supercooled water droplets on an ice surface N89-19614

SPUTTERING
Improvements in the properties of NbN layers through the presence of small amounts of aluminum during sputtering [KFK-4409] N89-19418

SQUALLS
The effect of ice physical processes on the numerical simulation of West African squall lines N89-19638
Multiparameter Doppler radar observations of a squall line with the polarimetric DFVLR radar N89-19715

SQUID (DETECTORS)
Use of superconducting imaging surfaces to enhance detection of weak magnetic sources by SQUID systems [DE89-006568] N89-20015

STAINLESS STEELS
Anomalous slip in an FCC system [DE89-002257] N89-19405
An electrochemical study of corrosion protection by primer-topcoat systems on 4130 steel with ac impedance and dc methods [NASA-TP-2820] N89-19406
The effect of hydrogen on fatigue crack growth rate of AISI 304 stainless steel N89-19410

STANDARDS
Man-systems requirements for the control of teleoperators in space N89-19862

STAR FORMATION
Near-infrared spectroscopy of young stellar objects N89-20033
Interstellar matter in early type galaxies N89-20042
The distribution of the interstellar medium in the Scd galaxy NGC 6946 and in a sample of dwarf irregular galaxies N89-20043
Ultracompact HII regions associated with massive star formation N89-20044
STARK EFFECT
Excitation of strong high-frequency electric fields and their detection using the dynamic Stark effect
[ETN-89-93794] N89-19991
STARTING
Starting characteristics of direct current motors powered by solar cells
[NASA-TM-101981] N89-19493
STATE ESTIMATION
Regulation of linear discrete time-varying systems
[ETN-89-93896] N89-19934
STATIC FIRING
Experimental investigation on plume contamination and surface effects, phase 2 --- spacecraft
[TUHH-TRI-ESA-1967] N89-19370
STATIC MODELS
CAD-model-based vision for space applications N89-19867
STATIC PRESSURE
Study of underexpanded turbulent air jets in water N89-19516
STATISTICAL ANALYSIS
Performance evaluation of military engine and gear oils in friction and wear devices
[AD-A202145] N89-19432
A curve-fitting package for personal computers
[LA-11082-MS] N89-19922
Discrete event systems with stochastic processing times
[REPT-88-11] N89-19946
Large deviation local limit theorems for ratio statistics
[AD-A201169] N89-19954
Sensitivity analysis using the Monte Carlo acceptance-rejection method
[AD-A201261] N89-19955
Estimation of a restricted variance ratio
[AD-A202268] N89-19959
STATISTICAL CORRELATION
Refractive turbulence profiling via binary source intensity scintillation correlation
[AD-A202189] N89-19762
STATISTICAL DISTRIBUTIONS
Minimum required heliport airspace under visual flight rules
[AD-A201433] N89-19283
STATISTICAL TESTS
Robust bounded influence tests in linear models
[AD-A201896] N89-19957
STATISTICAL WEATHER FORECASTING
The climate inversion problem: A statistical/modeling approach N89-19784
STATORS
Experimental investigation of rotor-stator interaction in diffuser pumps N89-19564
STEADY FLOW
Unsteady aerodynamics of blade rows N89-19263
Steady waves in a nonlinear theory of viscoelasticity N89-19470
STEADY STATE
Experimental transonic steady state and unsteady pressure measurements on a supercritical wing during flutter and forced discrete frequency oscillations N89-19261
STEELS
The effects of tempering and test temperature on the dynamic fracture initiation behavior of an AISI 4340 VAR steel
[AD-A201606] N89-19408
STELLAR EVOLUTION
An infrared reflectance study of water in outer belt asteroids N89-20037
Mass-radius star evolution Sun activity planets surfaces on purely empirical basis. Empiry theory reality: The use of statistics
[REPT-18] N89-20050
STELLAR INTERIORS
Thermonuclear reactions of light nuclei in astrophysical plasmas N89-19988
STELLAR LUMINOSITY
Near-infrared spectroscopy of young stellar objects N89-20033
STELLAR MASS ACCRETION
Implications of the observed contraction of accretion disks in quiescent dwarf novae N89-20047
STELLAR WINDS
Near-infrared spectroscopy of young stellar objects N89-20033
STEREOPHOTOGRAPHY
Three-dimensional structures of snow crystals shown by stereo-photomicrographs N89-19669
STEREOSCOPIC VISION
Extracting depth by binocular stereo in a robot vision system
[DE89-005016] N89-19572
STIFFENING
Concept of adaptive structures N89-19338
STIRLING CYCLE
RE-1000 free-piston Stirling engine sensitivity test results
[NASA-TM-88846] N89-19737
STIRLING ENGINES
RE-1000 free-piston Stirling engine sensitivity test results
[NASA-TM-88846] N89-19737
A study of the reliability of Stirling engines for distributed receiver systems
[DE89-006395] N89-19746
STOCHASTIC PROCESSES
The effect of turbulence on the collection of cloud drops: A stochastic model N89-19637
A parametrization scheme for the coalescence of water drops using the stochastic collection equation N89-19671
Discrete event systems with stochastic processing times
[REPT-88-11] N89-19946
Sensitivity analysis using the Monte Carlo acceptance-rejection method
[AD-A201261] N89-19955
Stochastic and fuzzy PERT
[REPT-88-26] N89-20027
STOICHIOMETRY
Grain boundary nonstoichiometry in multicomponent ceramics
[DE89-006109] N89-19437
STORMS (METEOROLOGY)
Analysis of hailstones from a severe storm and their simulated evolution N89-19677
Central Region applied research on severe weather forecasting
[PB88-210836] N89-19771
The Cheyenne windstorm that never came: Another lesson in real time analysis
[CRARP-88-1] N89-19772
A case study of significant lake enhanced snow event in upper Michigan
[CRARP-88-2] N89-19773
A collection of severe weather parameters used for a checklist
[CRARP-88-3] N89-19774
Preparing storm data
[CRARP-88-6] N89-19777
Use of long-waves in forecasting
[CRARP-88-7] N89-19778
STRAIN MEASUREMENT
Steady waves in a nonlinear theory of viscoelasticity N89-19470
STRAIN RATE
Tensile properties of Ti-6Al-2Sn-4Zr-2Mo sheet after superplastic deformation
[PNR90499] N89-19414
High strain-rate behaviour of polymers using blast-wave and impact-loading methods N89-19592
STRATOCUMULUS CLOUDS
Structure of upper clouds boundary using the lidar data N89-19631
An observational study of radiatively driven convection --- clouds N89-19647
STRATOSPHERE
Ultraviolet absorption cross-sections of halocarbons of stratospheric interest
[AERONOMICA-ACTA-A-336-1988] N89-19769
Temperature and circulation in the stratospheres of the outer planets
[NASA-CR-184826] N89-20051
STRATUS CLOUDS
Acidification of stratiform clouds and their aerosol scavenging properties N89-19694
STRESS (PHYSIOLOGY)
A study to analyze the degree of the relationship between health practices and fatigue
[AD-A201518] N89-19798
Satellite remote sensing of heat stress during reserve training at Fort Hood
[AD-A201555] N89-19800
A stress test to evaluate the physical capacity of performing L-1 anti-G straining maneuvers
[AD-A202301] N89-19803
Thermal stress in Ran Sea King Helicopter operations
[ARL-SYS-R-40] N89-19810
STRESS (PSYCHOLOGY)
A study to analyze the degree of the relationship between health practices and fatigue
[AD-A201518] N89-19798
Fear-potential startle as a model system for analyzing learning and memory
[AD-A201330] N89-19805
STRESS ANALYSIS
A new approach to the evaluation of the effects of stress state and interfacial properties on the behavior of advanced metal matrix composites
[AD-A201246] N89-19373
Durability and damage tolerance of bismaleimide composites, volume 1
[AD-A201273] N89-19374
Characterization of IM7/8551-7 carbon/epoxy in compression and shear
[DE89-005544] N89-19378
Elastic hysteresis phenomena in ULE and Zerodur optical glasses at elevated temperatures
[DE89-005183] N89-19423
The determination of the mechanical behavior of polyamic acid/polyimide coatings N89-19428
Mixed formulation for frictionless contact problems
[NASA-TP-2897] N89-19580
Boundary layer and singularity measurement in three dimensional fracture problems
[AD-A201277] N89-19584
Determination of residual stress distributions in autofrettaged tubing: A discussion
[AD-A201454] N89-19586
The elastic stress and the displacement on the surfaces of two rubber-clad steel cylinders between which paper is led
[REPT-88-23] N89-19603
A stress test to evaluate the physical capacity of performing L-1 anti-G straining maneuvers
[AD-A202301] N89-19803
STRESS CONCENTRATION
Analysis of PERSHING 2 Reentry Vehicle (RV) control ring castings
[AD-A201548] N89-19559
STRESS DISTRIBUTION
Determination of residual stress distributions in autofrettaged tubing: A discussion
[AD-A201454] N89-19586
STRESS INTENSITY FACTORS
The effect of hydrogen on fatigue crack growth rate of AISI 304 stainless steel N89-19410
Fundamentals of fatigue and fracture mechanics
[AD-A201435] N89-19585
STRESS WAVES
The effects of tempering and test temperature on the dynamic fracture initiation behavior of an AISI 4340 VAR steel
[AD-A201606] N89-19408
STRESS-STRAIN RELATIONSHIPS
Nonlinear dynamic analysis of embedded structures
[AD-A201728] N89-19593
Reciprocal theorem of residual stress and inelastic strain
[AD-A202353] N89-19598
STRESSES
Reciprocal theorem of residual stress and inelastic strain
[AD-A202353] N89-19598
Acoustoelasticity using longitudinal waves for residual stress evaluation
[DE89-006154] N89-19604
STRIP TRANSMISSION LINES
Millimeter wave antennas
[AD-A201919] N89-19474
STRUCTURAL ANALYSIS
Majorant analysis of performance degradation due to uncertainty N89-19344
Error localization and updating of spacecraft structures mathematical models
[YMD/EF/0175] N89-19361
Finite element analysis of laminated composite plates
[AD-A202192] N89-19381
The modeling of viscoelastic circular plates for use as waveguide absorbers
[AD-A201621] N89-19588
Control of flexible structures: Model errors, robustness measures, and optimization of feedback controllers
[AD-A202234] N89-19596
Compression strength of composite primary structural components
[NASA-CR-184893] N89-19599
NESSUS (Numerical Evaluation of Stochastic Structures Under Stress)/EXPERT: Bridging the gap between artificial intelligence and FORTRAN N89-19827

STRUCTURAL DESIGN
The design and initial construction of a composite RPV (Remotely Piloted Vehicle) for flight research applications
[AD-A201884] N89-19291
Variable gravity research facility
[NASA-CR-184714] N89-19324
XUV free-electron laser development at Los Alamos
[DE89-005458] N89-19547
Ultrahigh-brightness XeCl laser system
[DE89-005467] N89-19548
A bootstrap lunar base: Preliminary design review 2
[NASA-CR-184753] N89-19807
Concept for a large master/slave-controlled robotic hand N89-19866
Design concept for the Flight Telerobotic Servicer (FITS) N89-19870
An innovative demonstration of high power density in a compact MHD generator
[DE89-002159] N89-19990

STRUCTURAL DESIGN CRITERIA
Design improvement of a pump wear ring labyrinth seal
[NASA-CR-179161] N89-19555

STRUCTURAL ENGINEERING
Nonlinear dynamic analysis of embedded structures
[AD-A201728] N89-19593

STRUCTURAL FAILURE
Advanced durability analysis. Volume 4: Executive summary
[AD-A202304] N89-19597

STRUCTURAL VIBRATION
Proceedings of the Fifth AFOSR Forum on Space Structures
[AD-A194761] N89-19333
Wave propagation in large space structures N89-19335
Maneuvering equations in terms of quasi-coordinate N89-19337
System identification of suboptimal feedback control parameters based on limiting-performance/minimum-time characteristics N89-19340
Active control of elastic wave motion in structural networks N89-19342
A controlled component synthesis method for truss structure vibration control N89-19348
Maximum entropy/optimal projection design synthesis for decentralized control of large space structures
[AD-A202375] N89-19358
An approach to semi-active control of multiple degree-of-freedom systems N89-19554
Passive vibration control using viscoelastic and constrained layer beam waveguide absorbers
[AD-A202188] N89-19595

STRUCTURAL WEIGHT
Light weight escape capsule for fighter aircraft N89-19858

SUBSONIC FLOW
Computational study of incompressible turbulent flow over a swept rearward-facing step N89-19272

SULFATES
Experiments on microphysics and chemistry of radiation fogs N89-19702
A numerical investigation of sulfate production and deposition in midlatitude continental cumulus clouds N89-19705

SULFUR COMPOUNDS
Studies of hydrogen-hydrogen and carbon-sulfur bond cleavage
[DE89-006116] N89-19403

SULFUR DIOXIDES
Processes determining cloudwater composition: Field evidence for in-cloud reactive scavenging of SO2 N89-19693
Oxidation regimes in orographic capping cloud N89-19698

SULFUR OXIDES
Kinetics and mechanism of the Fe catalyzed autoxidation of S(4)-oxides in aqueous solution N89-19687

SUMS
Tail triviality for sums of stationary random variables
[REPT-88-40] N89-19963

SUPERCONDUCTING MAGNETS
National Aeronautics and Space Administration (NASA)/American Society for Engineering Education (ASEE) Summer Faculty Fellowship Program 1988, volume 2 --- Author
[NASA-CR-172118-VOL-2] N89-20073
Feasibility of using high temperature superconducting magnets and conventional magnetic loop antennas to attract or repel objects at the space station N89-20081

SUPERCONDUCTIVITY
To measure and characterize metal corrosion in electrolyte solutions by exploiting the properties of superconducting
[AD-A201484] N89-19407
Composite ceramic superconducting wires for electric motor applications
[AD-A201810] N89-19429
XPS and AES studies of thin oxide layers on niobium for superconducting RF cavities
[DE88-756073] N89-19997
Oxygen diffusion in YBa2Cu3O7-delta
[DE89-005831] N89-20011
Mossbauer effect studies of magnetism in superconducting systems
[DE89-005844] N89-20012

SUPERCONDUCTORS
improvements in the properties of NbN layers through the presence of small amounts of aluminum during sputtering
[KFK-4409] N89-19418
Composite ceramic superconducting wires for electric motor applications
[AD-A201810] N89-19429
Superconducting gravity gradiometer mission. Volume 2: Study team technical report
[NASA-TM-4091] N89-19749
Quantum limits of superconducting heterodyne receivers
[AD-A201303] N89-20000
Quench pressure, thermal expulsion, and normal zone propagation in internally cooled superconductors
[DE89-005668] N89-20003
Radiation induced amorphization in YBa2Cu3O7 and GdBa2Cu3O7 superconductors
[DE89-005451] N89-20008
SIMS measurement of oxygen tracer diffusion in YBa2Cu3O7-delta
[DE89-005884] N89-20014
Use of superconducting imaging surfaces to enhance detection of weak magnetic sources by SQUID systems
[DE89-006568] N89-20015
Static and dynamic properties of arrays of superconductors N89-20017

SUPERCOOLING
Spreading supercooled water droplets on an ice surface N89-19614
Crystallization of supercooled solutions --- atmosphere N89-19664
Kinetics of ice crystal formation on aerosol particles in supercooled fog N89-19665
The collection efficiencies of soft-hailstones for super-cooled water droplets and ice crystals N89-19678

SUPERCRITICAL AIRFOILS
The NASA Langley laminar-flow-control experiment on a swept, supercritical airfoil - Drag equations
[NASA-TM-4096] N89-19231
Unsteady pressure measurements on a supercritical airfoil at high Reynolds numbers N89-19259
Two experimental supercritical laminar-flow-control swept-wing airfoils
[NASA-TM-89073] N89-19266
Use of riblets to obtain drag reduction on airfoils at high Reynolds number flows
[AD-A201485] N89-19267

SUPERCRITICAL WINGS
Investigation and suppression of high dynamic response encountered on an elastic supercritical wing N89-19255
Experimental transonic steady state and unsteady pressure measurements on a supercritical wing during flutter and forced discrete frequency oscillations N89-19261

SUPERGRAVITY
Phenomenological models from higher dimensions with and without supergravity N89-20045

SUPERHETERODYNE RECEIVERS
Electronic Power Conditioner (EPC) for carcinotrons
[R/D/REPO/8801] N89-19496
Quantum limits of superconducting heterodyne receivers
[AD-A201303] N89-20000

SUPERHIGH FREQUENCIES
Code performance simulation study for DRS S-band transmission
[ESA-CR(P)-2688] N89-19482
Applications of the NCAR Electra Doppler radar for the study of physical parameters of clouds N89-19717
Study of the use of radar X-band data of bare soil in a radar scattering model
[BCRS-88-04] N89-19735

SUPERLATTICES
The 2-4 semiconductor superlattices
[AD-A202369] N89-20005

SUPERPLASTICITY
Processing of aluminum alloy 2090 for superplasticity
[AD-A201865] N89-19411
Tensile properties of Ti-6Al-2Sn-4Zr-2Mo sheet after superplastic deformation
[PNR90499] N89-19414

SUPERSATURATION
The calculation of supersaturations and growth of droplets in continental cumulus clouds N89-19617

SUPERSONIC FLOW
The standard chemical oxygen-iodine laser kinetics package
[AD-A202223] N89-19543

SUPERSONIC SPEED
Calculation of steady and unsteady pressures at supersonic speeds with CAP-TSD N89-19240

SUPERSONIC WIND TUNNELS
Wind-tunnel results of advanced high-speed propellers at takeoff, climb, and landing Mach numbers
[NASA-TM-87030] N89-19265

SUPPORT SYSTEMS
Transformation based endorsement systems N89-19836

SUPPRESSORS
The importance of aircraft performance and signature reduction upon combat survivability
[AD-A202106] N89-19292

SURFACE COOLING
Investigations on undercooling, nucleation and rapid solidification of metallic systems
[DFVLR-FB-88-39] N89-19415

SURFACE LAYERS
A critical evaluation of the von Karman constant from a new atmospheric surface layer experiment N89-19757

SURFACE NAVIGATION
Joint University Program for Air Transportation Research, 1987
[NASA-CP-3028] N89-19230

SURFACE PROPERTIES
An interdisciplinary study of cathodic debonding in elastomer/metal adhesive bonds
[AD-A202376] N89-19434
Pressure variation over a solid wavy surface
[AD-A201724] N89-19517
Estimating the illuminant color from the shading of a smooth surface
[AD-A201333] N89-19983

SURFACE REACTIONS
Experimental investigation on plume contamination and surface effects, phase 2 --- spacecraft
[TUHH-TRI-ESA-1987] N89-19370
Vibrational spectroscopic studies of surface chemical interactions in chemisorption and catalysis
[DE89-005896] N89-19400

SURFACE ROUGHNESS
Long trace profile measurements on cylindrical aspheres
[DE89-005661] N89-19985
Visual perception and grasping for the extravehicular activity robot N89-20082

SURFACE TEMPERATURE
Natural convection liquid immersion cooling of a column of discrete heat sources in a vertical channel
[AD-A201676] N89-19513

SURFACE TO SURFACE MISSILES
Analysis of PERSHING 2 Reentry Vehicle (RV) control ring castings
[AD-A201548] N89-19559

SURGES
Transient three-dimensional heat conduction computations using Brian's technique
[AD-A201918] N89-19519

SURVEYS
R and M (Reliability and Maintainability) quality team concept and C-17 design at Douglas Aircraft Company: An R and M 2000 initiative case study
[AD-A201574] N89-19228
Radio frequency interference survey over the 1.0-10.4 GHz frequency range at the Goldstone-Venus Development Station N89-19466

SURVIVAL EQUIPMENT
Positive Flotation Harness (PFH) for use by Canadian Forces search and rescue technicians
[AD-A200727] N89-19279

SUSPENSION SYSTEMS (VEHICLES)
An approach to semi-active control of multiple degree-of-freedom systems N89-19554

SWATH WIDTH
A study of advanced radar altimeter techniques --- satellite altimetry
[ESA-CR(P)-2699] N89-19483

SWEEP ANGLE
Computational study of incompressible turbulent flow over a swept rearward-facing step N89-19272

SWEEP FREQUENCY
Radio frequency interference survey over the 1.0-10.4 GHz frequency range at the Goldstone-Venus Development Station N89-19466

SWEPT WINGS
The NASA Langley laminar-flow-control experiment on a swept, supercritical airfoil - Drag equations
[NASA-TM-4096] N89-19231
An efficient method for computing unsteady transonic aerodynamics of swept wings with control surfaces
[AIAA-85-4058] N89-19241
Curvature effects on the stability of three-dimensional laminar boundary layers N89-19500
SWEPTBACK WINGS
Two experimental supercritical laminar-flow-control swept-wing airfoils
[NASA-TM-89073] N89-19266
SWITCHES
Investigation of the performance of photoconductive switches
[AD-A201425] N89-19489
SWITCHING CIRCUITS
Crossbar switch backplane and its application
[DE89-005621] N89-19491
SYNCHRONOUS SATELLITES
Substorms, plasmoids, flux robes, and magnetotail flux loss on March 25, 1983: CDAW-8
[NASA-CR-184823] N89-19764
SYNOPTIC METEOROLOGY
A collection of severe weather parameters used for a checklist
[CRARP-88-3] N89-19774
SYNTHETIC APERTURE RADAR
Synthetic aperture radar (SAR) data focusing using seismic migration techniques
[REPT-88-015] N89-19479
SYNTHETIC APERTURES
A study of advanced radar altimeter techniques --- satellite altimetry
[ESA-CR(P)-2699] N89-19483
SYSTEM IDENTIFICATION
Proceedings of the Fifth AFOSR Forum on Space Structures
[AD-A194761] N89-19333
System identification of suboptimal feedback control parameters based on limiting-performance/minimum-time characteristics N89-19340
Criterion based equivalence for equation error models
[WTHD-188] N89-19941
SYSTEMS ANALYSIS
Integrated tools for control-system analysis
[NASA-TP-2885] N89-19309
Experimental verification of an innovative performance-validation methodology for large space systems
[AD-A202243] N89-19357
Systems analysis for DSN microwave antenna holography N89-19463
Ka-band study: 1988 N89-19464
Development of a model which provides a total system approach to integrating voice recognition and speech synthesis into the cockpit of US Navy aircraft
[AD-A202122] N89-19815
IDEAL: A methology for developing information systems N89-19888
Critical problems in very large scale computer systems
[AD-A202129] N89-19923
JPRS report: Science and technology. Japan: 7th Artificial Intelligence Symposium
[JPRS-JST-88-020] N89-19924
SYSTEMS ENGINEERING
R and M (Reliability and Maintainability) quality team concept and C-17 design at Douglas Aircraft Company: An R and M 2000 initiative case study
[AD-A201574] N89-19228
A model for the geostationary orbital infrastructure, system analysis
[ILR-MITT-205] N89-19323
Model of a geostationary regional transportation company (GRET): Fleet composition and facility layout
[ILR-MITT-207] N89-19329
Mini protein crystallization facility. Phase A study: Executive summary
[REPT-AQ-ES-576/88] N89-19444
Activities report in electrotechnology
[ETN-89-93715] N89-19448
Block diagrams of the radar interface and control unit N89-19460
A bootstrap lunar base: Preliminary design review 2
[NASA-CR-184753] N89-19807
Problems in structuring large-scale expert system N89-19925
Evaluation support system for multiple R and D projects N89-19926
SYSTEMS INTEGRATION
Integrated Structural Analysis And Control (ISAAC): Issues and progress N89-19341
Second Annual Workshop on Space Operations Automation and Robotics (SOAR 1988)
[NASA-CP-3019] N89-19817
NESSUS (Numerical Evaluation of Stochastic Structures Under Stress)/EXPERT: Bridging the gap between artificial intelligence and FORTRAN N89-19827
A design and implementation methodology for diagnostic systems N89-19831
An architecture for integrating distributed and cooperating knowledge-based Air Force decision aids N89-19841
An intelligent multi-media human-computer dialogue system N89-19850
Integration of a computerized two-finger gripper for robot workstation safety N89-19863
Sensor fusion of range and reflectance data for outdoor scene analysis N89-19868
SYSTEMS MANAGEMENT
Automation of the space station core module power management and distribution system N89-19822
Knowledge-based operation and management of communications systems N89-19826
Garbage collection can be made real-time and verifiable N89-19840
Browsing schematics: Query-filtered graphs with context nodes N89-19844
Presentation planning using an integrated knowledge base N89-19845
SYSTEMS SIMULATION
Problems in structuring large-scale expert system N89-19925

T

TABLES (DATA)
Preparing storm data
[CRARP-88-6] N89-19777
TACTICS
The importance of aircraft performance and signature reduction upon combat survivability
[AD-A202106] N89-19292
TANKS (COMBAT VEHICLES)
Short-range anti-armour flight vehicles of the Apache/CWS family
[DRIC-T-8130] N89-19296
TANTALUM
Passivity and corrosion of probe metals
[ETN-89-93984] N89-19416
TARGET ACQUISITION
Advancement of high resolution radar polarimetry in target verses clutter detection, discrimination, classification. A: Basic theory and modeling of polarimetric clutter phenomenology
[AD-A201240] N89-19467
Local position control: A new concept for control of manipulators N89-19864
TARGET RECOGNITION
Machine vision for space telerobotics and planetary rovers N89-19879
TARGET SIMULATORS
A comparative analysis of tilt rotor aircraft versus helicopters using simulator results
[AD-A202190] N89-19294
TARGETS
Advancement of high resolution radar polarimetry in target verses clutter detection, discrimination, classification. A: Basic theory and modeling of polarimetric clutter phenomenology
[AD-A201240] N89-19467
Impact of target altitude restrictions on laser performance
[DE89-006567] N89-19553
TASKS
Development of a model which provides a total system approach to integrating voice recognition and speech synthesis into the cockpit of US Navy aircraft
[AD-A202122] N89-19815
TDR SATELLITES
Definition of the transmission system for a European data relay satellite
[ESA-CR(P)-2632] N89-19359
Code performance simulation study for DRS S-band transmission
[ESA-CR(P)-2688] N89-19482
TEACHING MACHINES
An intelligent tutoring system for space shuttle diagnosis N89-19853
TECHNICAL WRITING
Electronic data generation and display system N89-19891
TECHNOLOGICAL FORECASTING
Horizons of new energy technologies
[DFVLR-MITT-88-22] N89-19742
TECHNOLOGY ASSESSMENT
Model-based reasoning: Troubleshooting
[AD-A201614] N89-19445
Solar thermal technology
[DE89-000818] N89-19738
Superconducting gravity gradiometer mission. Volume 2: Study team technical report
[NASA-TM-4091] N89-19749
IDEAL: A methology for developing information systems N89-19888
National Aeronautics and Space Administration authorization
[S-HRG-100-579-PT-2] N89-20031
TECHNOLOGY TRANSFER
An investigation of factors affecting domestic technology transfer at the Wright Aeronautical Laboratories
[AD-A201581] N89-20032
TELEMETRY
A new VLSI architecture for a single-chip-type Reed-Solomon decoder N89-19455
Ka-band study: 1988 N89-19464
TELEOPERATORS
Second Annual Workshop on Space Operations Automation and Robotics (SOAR 1988)
[NASA-CP-3019] N89-19817
Simulation of the human-telerobot interface N89-19861
Man-systems requirements for the control of teleoperators in space N89-19862
Local position control: A new concept for control of manipulators N89-19864
Concept for a large master/slave-controlled robotic hand N89-19866
Design concept for the Flight Telerobotic Servicer (FITS) N89-19870
The WCSAR telerobotics test bed N89-19871
Telepresence and telerobotics N89-19873
Telerobot operator control station requirements N89-19876
Time-delayed operation of a telerobot via geosynchronous relay N89-19877
Machine vision for space telerobotics and planetary rovers N89-19879
A methodology for automation and robotics evaluation applied to the space station telerobotic servicer N89-19882
TELESCOPES
Power spectra decomposition of 36 RS CVn UBV photometric light curves from the first two years of the automatic photoelectric telescope N89-20036
TELEVISION SYSTEMS
Development of hydrometeor video sonde N89-19653
TEMPERATURE CONTROL
Modeling of transient heat pipe operation
[NASA-CR-184688] N89-19502
TEMPERATURE DEPENDENCE
Oxygen diffusion in YBa2Cu3O7-delta
[DE89-005831] N89-20011
Mossbauer effect studies of magnetism in superconducting systems
[DE89-005844] N89-20012
TEMPERATURE EFFECTS
The effects of tempering and test temperature on the dynamic fracture initiation behavior of an AISI 4340 VAR steel
[AD-A201606] N89-19408
Effect of temperature on the corrosion resistance of nitrogen bearing AL6X and 904L stainless steels
[AD-A201955] N89-19412
Tensile properties of Ti-6Al-2Sn-4Zr-2Mo sheet after superplastic deformation
[PNR90499] N89-19414
Liquid water content, median volume diameter and temperature in dependence on the height above the cloud base for different types of clouds --- aircraft icing N89-19662
TEMPERATURE INVERSIONS
The climate inversion problem: A statistical/modeling approach N89-19784
TEMPERATURE MEASUREMENT
The adsorption and decomposition of NH3 on Si(100): Detection of the NH2(a) species
[AD-A201601] N89-19397
Natural convection liquid immersion cooling of a column of discrete heat sources in a vertical channel
[AD-A201676] N89-19513
On the observations of cloud temperature and liquid water content using a Lyman-alpha and an FSSP sensor --- forward scattering spectrometer probe (FSSP) N89-19618
A comparison of radiometric and immersion temperature measurements in water clouds N89-19712
A high-spectral-resolution lidar system: The use of atomic blocking filter for measuring atmospheric parameters
[AD-A201736] N89-19759
TENSILE PROPERTIES
Tensile and creep rupture behavior of P/M processed Nb-base alloy, WC-3009
[NASA-TM-101954] N89-19371

TENSILE STRENGTH
Composite materials at high temperatures
[AD-A201163] N89-19372
Tensile properties of Ti-6Al-2Sn-4Zr-2Mo sheet after superplastic deformation
[PNR90499] N89-19414
The tensile strength of liquid helium four N89-20016
TENSILE TESTS
Some novel test methods for, and associated problems of mechanical strength characterization of engineering ceramics
[PNR90492] N89-19436
TERCOM
Examinations on TERCOM navigation by evaluation of test flights done over the testing areas Deister and Harz (Germany, F.R.)
[DFVLR-FB-88-37] N89-19287
TERMINAL VELOCITY
The effect of charge on coalescence of small precipitation drops at terminal velocity N89-19606
TERRAIN
Computer generation of fractal terrains
[AD-A201171] N89-19730
TERRAIN ANALYSIS
Machine vision for space telerobotics and planetary rovers N89-19879
TEST EQUIPMENT
The WCSAR telerobotics test bed N89-19871
TEST FACILITIES
Icing research tunnel test of a model helicopter rotor
[NASA-TM-101978] N89-19305
Aerothermodynamics of a jet cell facility
[AD-A202142] N89-19318
The effect of prewhirl on the internal aerodynamics and performance of a mixed flow research centrifugal compressor
[NASA-CR-184756] N89-19503
TESTING TIME
An interrogative model of computer-aided adaptive testing: Some experimental evidence
[AD-A201675] N89-19905
TETHERED SATELLITES
Electromagnetic compatibility test report for the tethered satellite data acquisition and control assembly
[AD-A201549] N89-19468
TEXTS
Computer technologies and institutional memory N89-20062
THEMATIC MAPPERS (LANDSAT)
Land use analysis using remote sensing techniques. Investigation of the usefulness of LANDSAT Thematic Mapper satellite pictures for obtaining and up to date picture of land use in the province South Holland
[BCRS-88-01] N89-19733
THEMATIC MAPPING
Land use analysis using remote sensing techniques. Investigation of the usefulness of LANDSAT Thematic Mapper satellite pictures for obtaining and up to date picture of land use in the province South Holland
[BCRS-88-01] N89-19733
THERMAL ABSORPTION
Durability and damage tolerance of bismaleimide composites, volume 1
[AD-A201273] N89-19374
Durability and damage tolerance of bismaleimide composites. Volume 2: Appendix of crack growth and low-velocity impact data
[AD-A201839] N89-19379
THERMAL ANALYSIS
An innovative demonstration of high power density in a compact MHD generator
[DE89-002159] N89-19990
THERMAL CONDUCTIVITY
Heat transfer properties of satellite component materials N89-19375
Transient three-dimensional heat conduction computations using Brian's technique
[AD-A201918] N89-19519
THERMAL CYCLING TESTS
Thermal cycling and mechanical property assessment of carbon fiber (fabric) reinforced PMR-15 polyimide laminates
[PNR90522] N89-19382
THERMAL DIFFUSION
Optical parameter effects on laser generated ultrasound for microstructure characterization
[DE89-005193] N89-19967
THERMAL INSULATION
Arc jet diagnostics tests N89-20085
THERMAL PLASMAS
Resonance cones in non Maxwellian plasmas
[REPT-88-N4-173] N89-19993
THERMAL PROTECTION
Hypervelocity technology escape system concepts. Volume 1: Development and evaluation
[AD-A201719] N89-19280
THERMAL RADIATION
Model formulation of non-equilibrium gas radiation for hypersonic flight vehicles N89-20066
THERMAL STABILITY
Acidic attack of perfluorinated alkyl ether lubricant molecules by metal oxide surfaces
[NASA-TM-101962] N89-19402
THERMAL STRESSES
Thermal stress in Ran Sea King Helicopter operations
[ARL-SYS-R-40] N89-19810
THERMODYNAMIC PROPERTIES
Transient three-dimensional heat conduction computations using Brian's technique
[AD-A201918] N89-19519
Quench pressure, thermal expulsion, and normal zone propagation in internally cooled superconductors
[DE89-005668] N89-20003
Episodic volcanism of tidally heated satellites with application to Io. Thermal state of an ice shell on Europa. Polar wander of a synchronously rotating satellite with application to Europa N89-20052
THERMODYNAMICS
Gas hydrates thermomechanics
[DE88-010280] N89-19387
Experiment plans to study preignition processes of a pool fire in low gravity
[NASA-CR-182256] N89-19442
Verification of combined thermal-hydraulic and heat conduction analysis code FLOWNET/TRUMP
[DE88-756063] N89-19506
THERMOELASTICITY
Optical parameter effects on laser generated ultrasound for microstructure characterization
[DE89-005193] N89-19967
THERMOGRAPHY
Determination of local fluid drag by a laser heating/thermographic phosphor technique: Applicability of the H. Ludwieg model
[DE89-006462] N89-19523
THERMONUCLEAR REACTIONS
Thermonuclear reactions of light nuclei in astrophysical plasmas N89-19988
THERMOSPHERE
A study of the high altitude thermospheric dayglow from Spacelab 1 N89-19768
THICK PLATES
Finite element analysis of laminated composite plates
[AD-A202192] N89-19381
THIN FILMS
Fundamental optical studies of competitive adsorption and thin film phenomena
[DE89-005898] N89-19401
Proposal to study the interaction of polyimide precursors and thin polyimide films with silicon and silicon oxide surfaces
[AD-A201183] N89-19425
Research on high-efficiency, multi-gap, multijunction, amorphous-silicon-based alloy thin-film solar cells, phase 1
[DE89-000844] N89-19739
Josephson effect research in high-temperature superconductors
[AD-A201483] N89-20002
Positron spectroscopy for materials characterization
[DE89-005766] N89-20010
THIN PLATES
Finite element analysis of laminated composite plates
[AD-A202192] N89-19381
THIN WALLED SHELLS
Compression strength of composite primary structural components
[NASA-CR-184893] N89-19599
THIN WALLS
Mixed finite element models for free vibrations of thin-walled beams
[NASA-TP-2868] N89-19579
THREE DIMENSIONAL BODIES
Three-dimensional structures of snow crystals shown by stereo-photomicrographs N89-19669
CAD-model-based vision for space applications N89-19867
THREE DIMENSIONAL BOUNDARY LAYER
Curvature effects on the stability of three-dimensional laminar boundary layers N89-19500
THREE DIMENSIONAL FLOW
Computational study of incompressible turbulent flow over a swept rearward-facing step N89-19272
Numerical computations of transonic critical aerodynamic behavior
[AD-A202412] N89-19277
The birth of open separation on a prolate spheroid
[AD-A201350] N89-19509
Three-dimensional cumulus entrainment studies N89-19634
THREE DIMENSIONAL MOTION
A three-dimensional nonsingular simulation of rigid manipulators
[AD-A201964] N89-19569
Robot path planning using a genetic algorithm N89-19869
THRUST CHAMBERS
MPD (Magnetoplasmadynamic) thrust chamber flow dynamics
[AD-A201263] N89-19368
THUNDERSTORMS
A meditation on Miller
[CRARP-88-4] N89-19775
Mesoscale Convective Systems: Structure, development and storm-environment interactions N89-19788
TILT ROTOR AIRCRAFT
A comparative analysis of tilt rotor aircraft versus helicopters using simulator results
[AD-A202190] N89-19294
TIME
The use of direct sparse matrix methods and Newton iteration for the numerical solution of fluid flows N89-19514
TIME DEPENDENCE
Temporal variations of snow crystal growth parameters N89-19608
Measurement of the global distribution of tropospheric trace gases and their time dependent variations
[ETN-89-93987] N89-19747
TIME FUNCTIONS
A general way to put time in Petri nets
[REPT-88-011] N89-19914
Linear programming along the trajectory of the problem in polynomial time
[REPT-88-17] N89-19918
Regulation of linear discrete time-varying systems
[ETN-89-93896] N89-19934
TIME LAG
Microwave time delays for the dual L-C-band feed system N89-19462
Time-delayed operation of a telerobot via geosynchronous relay N89-19877
TIME SERIES ANALYSIS
Minification processes
[AD-A202219] N89-19958
Time series analysis and multivariate statistical analysis
[AD-A202273] N89-19960
TIROS SATELLITES
Satellite remote sensing of heat stress during reserve training at Fort Hood
[AD-A201555] N89-19800
TITANIUM
Formation of titanium nitride layers on titaniun metal: Results of XPS and AES investigations
[KFK-4449] N89-19419
TITANIUM ALLOYS
Microstructural optimisation of titanium alloys for defect tolerance in gas turbine engine components
[PNR90503] N89-19413
Passivity and corrosion of probe metals
[ETN-89-93984] N89-19416
TITANIUM NITRIDES
Formation of titanium nitride layers on titaniun metal: Results of XPS and AES investigations
[KFK-4449] N89-19419
TOKAMAK DEVICES
Effect of limiter currents on plasma equilibrium and stability in a tokamak
[DE88-704951] N89-19989
Possibilities for breakeven and ignition of D-He3 fusion fuel in a near term tokamak
[KFK-4433] N89-19992
TOLERANCES (PHYSIOLOGY)
An annotated bibliography of hypobaric decompression sickness research conducted at the Crew Technology Division, USAF School of Aerospace Medicine, Brooks AFB, Texas from 1983 to 1988
[AD-A201274] N89-19796
A stress test to evaluate the physical capacity of performing L-1 anti-G straining maneuvers
[AD-A202301] N89-19803
A model for plasma volume changes during short duration spaceflight N89-20067
TOOLING
Estimating aircraft airframe tooling cost: An alternative to DAPCA 3
[AD-A201506] N89-19226
TOOLS
Estimating aircraft airframe tooling cost: An alternative to DAPCA 3
[AD-A201506] N89-19226
TOPOGRAPHY
On the small scale topographical influences on precipitation N89-19720

TRACE CONTAMINANTS
Determination of chemical reaction rates in fog N89-19683
Vertical profiles of pollutants inside and outside of cloud N89-19696
Results of time and height resolved scavenging experiments --- atmospheric chemistry N89-19697
Effects of cloud microphysical processes on trace chemical removal efficiences N89-19707
Measurement of the global distribution of tropospheric trace gases and their time dependent variations [ETN-89-93987] N89-19747
Development of a detection system for atmospheric trace gases, in particular for OH molecules and realization of field measurements [BPT-11/88] N89-19767

TRADEOFFS
Optimal solutions for complex design problems: Using isoperformance software for human factors trade offs N89-19860

TRAILING EDGES
The role of shock induced trailing-edge separation in limit cycle oscillations N89-19256

TRAINING EVALUATION
An interrogative model of computer-aided adaptive testing: Some experimental evidence [AD-A201675] N89-19905

TRAJECTORY ANALYSIS
Analysis of hailstones from a severe storm and their simulated evolution N89-19677
Linear programming along the trajectory of the problem in polynomial time [REPT-88-17] N89-19918
The influence of the potential function on the performance of a trajectory following algorithm for the linear programming problem [REPT-88-44] N89-19920

TRAJECTORY CONTROL
Minimum time motion of a robotic manipulator N89-19567

TRANSCONTINENTAL SYSTEMS
Influences of cloud microphysics on continental and marine precipitation chemistry N89-19700

TRANSDUCERS
Noncontact ultrasonic sensing of weld pools for automated welding [DE89-005185] N89-19557
Sensing human hand motions for controlling dexterous robots N89-19883

TRANSFER OF TRAINING
A comparative analysis of tilt rotor aircraft versus helicopters using simulator results [AD-A202190] N89-19294

TRANSFORMATIONS
Transformation based endorsement systems N89-19836

TRANSFORMATIONS (MATHEMATICS)
Control of nonlinear systems using partial dynamic inversion N89-19310
Estimating projected controllable sets for dynamical control systems N89-19313

TRANSFORMERS
Design and test of a 2.25-MW transformer rectifier assembly N89-19452

TRANSMISSION LINES
Investigation of the performance of photoconductive switches [AD-A201425] N89-19489

TRANSMISSION LOSS
The Telecommunications and Data Acquisition Report [NASA-CR-184812] N89-19451

TRANSMISSIONS (MACHINE ELEMENTS)
Gear technology acquisition for advanced aero engines [PNR90510] N89-19571

TRANSONIC COMPRESSORS
Theoretical and experimental investigations on shocks losses in transonic axial flow compressors [DFVLR-FB-88-38] N89-19304

TRANSONIC FLOW
Transonic Unsteady Aerodynamics and Aeroelasticity 1987, part 1 [NASA-CP-3022-PT-1] N89-19234
Unsteady aerodynamics and aeroelastic research at AFWAL N89-19235
Extensions and improvements on XTRAN3S N89-19236
Role of computational fluid dynamics in unsteady aerodynamics for aeroelasticity N89-19237
CAP-TSD: A program for unsteady transonic analysis of realistic aircraft configurations N89-19238
CAP-TSD analysis of the F-15 aircraft N89-19239
Calculation of steady and unsteady pressures at supersonic speeds with CAP-TSD N89-19240
An efficient method for computing unsteady transonic aerodynamics of swept wings with control surfaces [AIAA-85-4058] N89-19241
Unsteady transonic flow using Euler equations N89-19245
AGARD standard aeroelastic configurations for dynamic response N89-19246
Transonic Unsteady Aerodynamics and Aeroelasticity 1987, part 2 [NASA-CP-3022-PT-2] N89-19247
Solution of steady and unsteady transonic-vortex flows using Euler and full-potential equations N89-19248
Viscous flow calculations for the AGARD standard configuration airfoils with experimental comparisons N89-19249
Unsteady transonic viscous-inviscid interaction using Euler and boundary-layer equations N89-19250
Numerical solution of unsteady rotational flow past fixed and rotary wing configurations N89-19251
Static aeroelasticity of a composite oblique wing in transonic flows N89-19254
Initial application of CAP-TSD to wing flutter N89-19257
Transonic flutter calculations using the Euler equations N89-19258
Unsteady pressure measurements on a supercritical airfoil at high Reynolds numbers N89-19259
Experimental transonic steady state and unsteady pressure measurements on a supercritical wing during flutter and forced discrete frequency oscillations N89-19261
Computational aeroelasticity challenges and resources N89-19264
Numerical simulation of the aerodynamics of turbulent transonic flow past a projectile N89-19270
A study of flow separation in transonic flow using inviscid and viscous CFD schemes N89-19273
Experimental simulation of transonic vortex-airfoil interactions [AD-A201934] N89-19274
Numerical computations of transonic critical aerodynamic behavior [AD-A202412] N89-19277
The use of direct sparse matrix methods and Newton iteration for the numerical solution of fluid flows N89-19514
Vortex convection in nonuniform compressible flow [MPIS-4/1988] N89-19527

TRANSONIC FLUTTER
An efficient method for computing unsteady transonic aerodynamics of swept wings with control surfaces [AIAA-85-4058] N89-19241

TRANSONIC WIND TUNNELS
Two experimental supercritical laminar-flow-control swept-wing airfoils [NASA-TM-89073] N89-19266

TRANSPONDERS
A low-loss linear analog phase modulator for 8415 MHz transponder application N89-19465

TRANSPORT AIRCRAFT
Multiple Application Propfan Study (MAPS): Advanced tactical transport [NASA-CR-175003] N89-19300

TRANSPORT PROPERTIES
Polymer morphology and transport [AD-A201167] N89-19424
Turbulent transport processes within and below small cumulus clouds N89-19632

TRANSPORT THEORY
High-order beam optics: An overview [DE89-005441] N89-19984

TRANSVERSE WAVES
The stability of boundary layer flow over elastic substrates N89-19524

TRAPPED PARTICLES
Chaotic electron motion caused by sidebands in free electron lasers [AD-A201635] N89-19538

TRAVELING WAVES
The modeling of viscoelastic circular plates for use as waveguide absorbers [AD-A201621] N89-19588

TREADMILLS
Effects on motor unit potentiation and ground reaction force from treadmill exercise N89-20069

TRIBOLOGY
Acidic attack of perfluorinated alkyl ether lubricant molecules by metal oxide surfaces [NASA-TM-101962] N89-19402

TROPICAL METEOROLOGY
The effect of ice physical processes on the numerical simulation of West African squall lines N89-19638
TRMM (Tropical Rainfall Measuring Mission): A satellite mission to measure tropical rainfall [NASA-TM-101288] N89-19769

TROPOSPHERE
Dynamic, radiative and chemical effects of clouds on tropospheric trace gases N89-19708
Measurement of the global distribution of tropospheric trace gases and their time dependent variations [ETN-89-93987] N89-19747
Temperature and circulation in the stratospheres of the outer planets [NASA-CR-184826] N89-20051

TROPOSPHERIC SCATTERING
Variations of the tropospheric propagation range of ultrashort radio waves above the sea N89-19486

TRUSSES
A controlled component synthesis method for truss structure vibration control N89-19348
Damage detection and location in large space trusses N89-19350

TUNABLE LASERS
Nonradiative relaxation and laser action in tunable solid state laser crystals [NASA-CR-182820] N89-19539
A high-spectral-resolution lidar system: The use of atomic blocking filter for measuring atmospheric parameters [AD-A201736] N89-19759
The V3, V4 and V6 bands of formaldehyde: A spectral catalog from 900 cm(-1) to 1580 cm(-1) [NASA-TM-100709] N89-19976

TURBINE ENGINES
In-line wear monitor [AD-A201292] N89-19301

TURBINE PUMPS
Studies and analyses of the space shuttle main engine. Appendix B: SSME FIPM drawings [NASA-CR-183594] N89-19365

TURBOCOMPRESSORS
Theoretical and experimental investigations on shocks losses in transonic axial flow compressors [DFVLR-FB-88-38] N89-19304

TURBOFAN AIRCRAFT
Multiple-Purpose Subsonic Naval Aircraft (MPSNA) Multiple Application Propfan Study (MAPS) [NASA-CR-175096] N89-19289
Multiple Application Propfan Study (MAPS): Advanced tactical transport [NASA-CR-175003] N89-19300

TURBOFANS
COMPASS: A generalized ground-based monitoring system [PNR90483] N89-19894

TURBOMACHINERY
Turbomachinery aeroelasticity at NASA Lewis Research Center N89-19262
Unsteady aerodynamics of blade rows N89-19263
The use of burst-triggered correlation for laser anemometry measurements in turbomachinery [PNR90542] N89-19533
NASTRAN supplemental documentation for modal forced vibration analysis of aerodynamically excited turbosystems [NASA-CR-174967] N89-19583

TURBOPROP ENGINES
Wind-tunnel results of advanced high-speed propellers at takeoff, climb, and landing Mach numbers [NASA-TM-87030] N89-19265
An experimental evaluation of S-duct inlet-diffuser configurations for turboprop offset gearbox applications [NASA-CR-179454] N89-19556

TURBULENCE
Turbulence structure and mass transport in a channel flow with polymer injection [AD-A202237] N89-19521
A critical evaluation of the von Karman constant from a new atmospheric surface layer experiment N89-19757
Electrostatic plasma waves and turbulence near auroral arcs N89-19758

TURBULENCE EFFECTS
The effect of turbulence on the collection of cloud drops: A stochastic model N89-19637

TURBULENCE MODELS
Numerical simulation of the aerodynamics of turbulent transonic flow past a projectile N89-19270
Computational study of incompressible turbulent flow over a swept rearward-facing step N89-19272

TURBULENT BOUNDARY LAYER
An investigation of the intermittent turbulent breakdown of the nocturnal planetary boundary layer [AD-A201743] N89-19518
Turbulent transport processes within and below small cumulus clouds N89-19632

TURBULENT DIFFUSION
The analytical modeling of a turbulent diffusion flame behind a backward facing step N89-19386

TURBULENT FLOW
Unsteady Navier-Stokes computations over airfoils using both fixed and dynamic meshes N89-19252
Numerical simulation of the aerodynamics of turbulent transonic flow past a projectile N89-19270
Computational study of incompressible turbulent flow over a swept rearward-facing step N89-19272
Some hydrodynamic instabilities of boundary layer flows N89-19501
Computational studies of evaporating sprays in a shear layer
[AD-A201932] N89-19520
Turbulence structure and mass transport in a channel flow with polymer injection
[AD-A202237] N89-19521
Field investigation of a wake structure downwind of a VANT (Vertical-Axis Wind Turbine) in a wind farm array
[DE89-000821] N89-19743
Superfluid turbulence in two-fluid flow of helium II N89-20018

TURBULENT JETS
Mixing in gas phase turbulent jets N89-19515
Study of underexpanded turbulent air jets in water N89-19516

TURBULENT MIXING
Characteristic time model validation
[AD-A201374] N89-19510
Entrainment and fine-scale (molecular) mixing --- clouds N89-19628
Entrainment sites, mixing processes in warm convective clouds: Effect on droplet growth N89-19630
Instability theory in clouds and the parameterization of eddy viscosity coefficients N89-19633

TWO PHASE FLOW
Modeling of inertial effects in transient liquid-bubble flows
[REPT-88-22] N89-19528

U

ULTRAHIGH FREQUENCIES
Microwave time delays for the dual L-C-band feed system N89-19462
Code performance simulation study for DRS S-band transmission
[ESA-CR(P)-2688] N89-19482

ULTRASONIC RADIATION
Gaussian beam representation of beam-like ultrasonic fields N89-19972

ULTRASONIC SCANNERS
Ultrasound transmission tomography, a low-cost realization --- medical equipment
[ISBN-90-9002330-5] N89-19804

ULTRASONIC WELDING
Noncontact ultrasonic sensing of weld pools for automated welding
[DE89-005185] N89-19557

ULTRASONICS
Optical parameter effects on laser generated ultrasound for microstructure characterization
[DE89-005193] N89-19967
An examination of cavitation due to short pulses of megahertz ultrasound N89-19971
The tensile strength of liquid helium four N89-20016

ULTRAVIOLET ABSORPTION
Ultraviolet absorption cross-sections of halocarbons of stratospheric interest
[AERONOMICA-ACTA-A-336-1988] N89-19769

ULTRAVIOLET SPECTROSCOPY
Application of nondestructive evaluations to the prediction of turbine fuel peroxidation potential
[AD-A202291] N89-19441

UNDERWATER ACOUSTICS
A modal/WKB inversion method for determining sound speed profiles in the ocean and ocean bottom
[AD-A201252] N89-19791
An examination of cavitation due to short pulses of megahertz ultrasound N89-19971

UNDERWATER VEHICLES
A new pumpjet design theory
[AD-A201353] N89-19558

UNITED KINGDOM
Airborne studies of the ice phase in maritime clouds around the British Isles N89-19623

UNIVERSAL TIME
Characteristic time model validation
[AD-A201374] N89-19510

UNIVERSE
Quantum field theory of universe
[DE88-756084] N89-20022
Studies in quantum field theory
[DE89-006286] N89-20023
Phenomenological models from higher dimensions with and without supergravity N89-20045

UNMANNED SPACECRAFT
The Ninevah Mission: A design summary for an unmanned mission to Venus, volume 1
[NASA-CR-184705] N89-20040
The Ninevah Mission: Analytical analyses and calculations for trajectory and propulsion, volume 2
[NASA-CR-184706] N89-20041

UNSTEADY AERODYNAMICS
Transonic Unsteady Aerodynamics and Aeroelasticity 1987, part 1
[NASA-CP-3022-PT-1] N89-19234
Unsteady aerodynamics and aeroelastic research at AFWAL N89-19235
Extensions and improvements on XTRAN3S N89-19236
Role of computational fluid dynamics in unsteady aerodynamics for aeroelasticity N89-19237
CAP-TSD: A program for unsteady transonic analysis of realistic aircraft configurations N89-19238
Calculation of steady and unsteady pressures at supersonic speeds with CAP-TSD N89-19240
An efficient method for computing unsteady transonic aerodynamics of swept wings with control surfaces
[AIAA-85-4058] N89-19241
Application of a full potential method to AGARD standard airfoils N89-19242
Full potential unsteady computations including aeroelastic effects N89-19243
Flux-vector splitting for unsteady calculations on dynamic meshes N89-19244
AGARD standard aeroelastic configurations for dynamic response N89-19246
Transonic Unsteady Aerodynamics and Aeroelasticity 1987, part 2
[NASA-CP-3022-PT-2] N89-19247
Unsteady transonic viscous-inviscid interaction using Euler and boundary-layer equations N89-19250
The oblique-wing research aircraft: A test bed for unsteady aerodynamic and aeroelastic research N89-19253
Investigation and suppression of high dynamic response encountered on an elastic supercritical wing N89-19255
Unsteady aerodynamics of blade rows N89-19263

UNSTEADY FLOW
An efficient method for computing unsteady transonic aerodynamics of swept wings with control surfaces
[AIAA-85-4058] N89-19241
Unsteady transonic flow using Euler equations N89-19245
Numerical solution of unsteady rotational flow past fixed and rotary wing configurations N89-19251
Unsteady Navier-Stokes computations over airfoils using both fixed and dynamic meshes N89-19252
Unsteady pressure measurements on a supercritical airfoil at high Reynolds numbers N89-19259
Experimental transonic steady state and unsteady pressure measurements on a supercritical wing during flutter and forced discrete frequency oscillations N89-19261
Unsteady low-speed wind tunnel test of a straked delta wing, oscillating in pitch. Part 2: Plots of steady and zeroth and first harmonic unsteady pressure distributions
[AD-A201936] N89-19275

UPLINKING
The Telecommunications and Data Acquisition Report
[NASA-CR-184812] N89-19451
Design and test of a 2.25-MW transformer rectifier assembly N89-19452
Microwave time delays for the dual L-C-band feed system N89-19462
Propagation problems regarding 20/30 GHz bands in Earth-space links
[REPT-88-022] N89-19480
Propagation problems regarding millimeter waves (40/50 GHz)
[REPT-88-023] N89-19481

UPPER ATMOSPHERE
Halogen Occultation Experiment (HALOE) optical filter characterization
[NASA-TM-4104] N89-19529
A study of the high altitude thermospheric dayglow from Spacelab 1 N89-19768

URANUS ATMOSPHERE
Temperature and circulation in the stratospheres of the outer planets
[NASA-CR-184826] N89-20051

USER MANUALS (COMPUTER PROGRAMS)
NASTRAN supplemental documentation for modal forced vibration analysis of aerodynamically excited turbosystems
[NASA-CR-174967] N89-19583
Generalized three-dimensional experimental lightning code (G3DXL) user's manual
[NASA-CR-166079] N89-19779
Computer software used in US Army Anthropometric Survey 1987-1988
[AD-A201185] N89-19812

USER REQUIREMENTS
An intelligent interface for satellite operations: Your Orbit Determination Assistant (YODA) N89-19852
IDEAL: A methology for developing information systems N89-19888

V

V/STOL AIRCRAFT
Multiple-Purpose Subsonic Naval Aircraft (MPSNA) Multiple Application Propfan Study (MAPS)
[NASA-CR-175096] N89-19289

VACUUM SYSTEMS
Arc jet diagnostics tests N89-20085

VANELESS DIFFUSERS
Experimental investigation of rotor-stator interaction in diffuser pumps N89-19564

VAPOR PHASES
Ion pair solvation
[AD-A201529] N89-19395

VARIABLE PITCH PROPELLERS
Wind-tunnel results of advanced high-speed propellers at takeoff, climb, and landing Mach numbers
[NASA-TM-87030] N89-19265

VECTOR ANALYSIS
Vectorization of linear recurrence relations
[REPT-88-21] N89-19951

VECTOR SPACES
A Monte Carlo test program with vectorized geometry routines --- radiation transport
[JUEL-2202] N89-19947

VELOCITY
Estimation of velocity perturbations in satellite fragmentation events N89-20083

VELOCITY COUPLING
Theoretical and experimental studies of selected topics in the rheology of fluids
[AD-A201460] N89-19512

VELOCITY DISTRIBUTION
On the variation of falling velocity of early snowflakes N89-19670
A modal/WKB inversion method for determining sound speed profiles in the ocean and ocean bottom
[AD-A201252] N89-19791
Compressional-wave velocities in ocean sediments east southesast of Madeira, Atlantic Ocean
[IOS-257] N89-19794

VELOCITY MEASUREMENT
Turbulence structure and mass transport in a channel flow with polymer injection
[AD-A202237] N89-19521

VENUS (PLANET)
The Ninevah Mission: A design summary for an unmanned mission to Venus, volume 1
[NASA-CR-184705] N89-20040
The Ninevah Mission: Analytical analyses and calculations for trajectory and propulsion, volume 2
[NASA-CR-184706] N89-20041

VENUS PROBES
The Ninevah Mission: A design summary for an unmanned mission to Venus, volume 1
[NASA-CR-184705] N89-20040
The Ninevah Mission: Analytical analyses and calculations for trajectory and propulsion, volume 2
[NASA-CR-184706] N89-20041

VERTICAL AIR CURRENTS
A comparative study of laboratory thermals and atmospheric clouds N89-19627
Analysis of hailstones from a severe storm and their simulated evolution N89-19677

VERTICAL DISTRIBUTION
Vertical profiles of pollutants inside and outside of cloud N89-19696

VERTICAL ORIENTATION
Satellite remote sensing of heat stress during reserve training at Fort Hood
[AD-A201555] N89-19800

VERY LARGE SCALE INTEGRATION
The Telecommunications and Data Acquisition Report
[NASA-CR-184812] N89-19451
A new VLSI architecture for a single-chip-type Reed-Solomon decoder N89-19455
Test aspects of the JPL Viterbi decoder N89-19457
On testing VLSI chips for the big Viterbi decoder N89-19458
Wiring Viterbi decoders (splitting deBruijn graphs) N89-19459

VERY LONG BASE INTERFEROMETRY
VLBI polarization measurements of BL Lacertae objects N89-20035

VESTS
Positive Flotation Harness (PFH) for use by Canadian Forces search and rescue technicians
[AD-A200727] N89-19279
Cooling effectiveness of a hybrid microclimate garment
[AD-A201115] N89-19811
VHSIC (CIRCUITS)
Spaceborne VHSIC multiprocessor system for AI applications N89-19838
VIBRATION
Nonlinear vibrations of composite material shells N89-19377
Machinery diagnostics via mechanical vibration analysis using spectral analysis techniques
[AD-A202089] N89-19594
VIBRATION DAMPING
Proceedings of the Fifth AFOSR Forum on Space Structures
[AD-A194761] N89-19333
Active control of elastic wave motion in structural networks N89-19342
The optimal projection equations for fixed-order dynamic compensation: Existence, convergence and global optimality N89-19345
Frobenius-Hankel norm framework for disturbance rejection and low order decentralized controller design N89-19347
A controlled component synthesis method for truss structure vibration control N89-19348
Maximum entropy/optimal projection design synthesis for decentralized control of large space structures
[AD-A202375] N89-19358
Investigation of flight sensors and actuators for the vibration damping augmentation of large flexible space structures
[ESA-CR(P)-2670] N89-19362
An approach to semi-active control of multiple degree-of-freedom systems N89-19554
The modeling of viscoelastic circular plates for use as waveguide absorbers
[AD-A201621] N89-19588
Passive vibration control using viscoelastic and constrained layer beam waveguide absorbers
[AD-A202188] N89-19595
RCS/piezoelectric distributed actuator study
[AD-A201276] N89-19999
VIBRATION ISOLATORS
Investigation of flight sensors and actuators for the vibration damping augmentation of large flexible space structures
[ESA-CR(P)-2670] N89-19362
The modeling of viscoelastic circular plates for use as waveguide absorbers
[AD-A201621] N89-19588
VIBRATION MODE
Normal forms and periodic solutions in the theory of nonlinear oscillations. Existence and asymptotic theory
[REPT-88-16] N89-19948
VIBRATIONAL SPECTRA
Vibrational spectroscopic studies of surface chemical interactions in chemisorption and catalysis
[DE89-005896] N89-19400
Passive vibration control using viscoelastic and constrained layer beam waveguide absorbers
[AD-A202188] N89-19595
VIDEO EQUIPMENT
A new airborne device for measurement of cloud particles using video microscope N89-19719
VINYL POLYMERS
Interactions and reactions in polymerized vesicles
[AD-A201527] N89-19427
VIRTUAL MEMORY SYSTEMS
Interfacing laboratory instruments to multiuser, virtual memory computers
[NASA-TM-4106] N89-19578
Spaceborne VHSIC multiprocessor system for AI applications N89-19838
VISCOELASTICITY
Steady waves in a nonlinear theory of viscoelasticity N89-19470
VISCOUS DRAG
Determination of local fluid drag by a laser heating/thermographic phosphor technique: Applicability of the H. Ludwieg model
[DE89-006462] N89-19523
VISCOUS FLOW
Transonic Unsteady Aerodynamics and Aeroelasticity 1987, part 2
[NASA-CP-3022-PT-2] N89-19247
Viscous flow calculations for the AGARD standard configuration airfoils with experimental comparisons N89-19249
Unsteady transonic viscous-inviscid interaction using Euler and boundary-layer equations N89-19250
A study of flow separation in transonic flow using inviscid and viscous CFD schemes N89-19273
On boundary integral equation approach to a nonstationary problem of isothermal viscous compressible flows
[PREPRINT-1134] N89-19526
VISCOUS FLUIDS
Interdisciplinary research in viscoelasticity and rheology
[AD-A201270] N89-19390
Theoretical and experimental studies of selected topics in the rheology of fluids
[AD-A201460] N89-19512
VISUAL FLIGHT RULES
Minimum required heliport airspace under visual flight rules
[AD-A201433] N89-19283
VISUAL PERCEPTION
The effects of a pitched field orientation on hand/eye coordination
[AD-A201620] N89-19814
VOICE COMMUNICATION
Development of a model which provides a total system approach to integrating voice recognition and speech synthesis into the cockpit of US Navy aircraft
[AD-A202122] N89-19815
VOICE CONTROL
Voice control of complex workstations N89-19880
VOICE DATA PROCESSING
Next generation keyboards: The importance of cognitive compatibility N89-19848
National Aeronautics and Space Administration (NASA)/American Society for Engineering Education (ASEE) Summer Faculty Fellowship Program 1988, volume 1
[NASA-CR-172118-VOL-1] N89-20058
Automatic voice recognition using traditional and artificial neural network approaches N89-20064
VOLCANOES
Lithospheric buckling and intra-arc stresses: A mechanism for arc segmentation N89-20078
VOLCANOLOGY
Episodic volcanism of tidally heated satellites with application to Io. Thermal state of an ice shell on Europa. Polar wander of a synchronously rotating satellite with application to Europa N89-20052
VOLUME
A model for plasma volume changes during short duration spaceflight N89-20067
VON KARMAN EQUATION
A critical evaluation of the von Karman constant from a new atmospheric surface layer experiment N89-19757
VORTEX ALLEVIATION
Experimental simulation of transonic vortex-airfoil interactions
[AD-A201934] N89-19274
Unsteady low-speed wind tunnel test of a straked delta wing, oscillating in pitch. Part 2: Plots of steady and zeroth and first harmonic unsteady pressure distributions
[AD-A201936] N89-19275
VORTEX FILAMENTS
A vortex panel method for potential flows with applications to dynamics and controls N89-19269
VORTEX SHEDDING
Tip vortices: Single phase and cavitating flow phenomena N89-19271
VORTEX SHEETS
Unsteady low-speed wind tunnel test of a straked delta wing, oscillating in pitch. Part 2: Plots of steady and zeroth and first harmonic unsteady pressure distributions
[AD-A201936] N89-19275
VORTICES
A vortex panel method for potential flows with applications to dynamics and controls N89-19269
Tip vortices: Single phase and cavitating flow phenomena N89-19271
The development and structural characteristics of Dean vortices in a curved rectangular channel
[AD-A201249] N89-19508
Large-eddy simulation of convective boundary layers
[DFVLR-FB-88-30] N89-19522
Vortex convection in nonuniform compressible flow
[MPIS-4/1988] N89-19527
VORTICITY
Three-dimensional cumulus entrainment studies N89-19634
Field investigation of a wake structure downwind of a VAWT (Vertical-Axis Wind Turbine) in a wind farm array
[DE89-000821] N89-19743
VULNERABILITY
Hypervelocity technology escape system concepts. Volume 1: Development and evaluation
[AD-A201719] N89-19280
The importance of aircraft performance and signature reduction upon combat survivability
[AD-A202106] N89-19292

W

WAKES
Wake-excited raindrop oscillations N89-19607
WALKING
Diagnosis by integrating model-based reasoning with knowledge-based reasoning N89-19835
WALKING MACHINES
A heuristically based navigation system for an autonomous walking machine with a range scanner N89-19563
WALL FLOW
Two-dimensional test section with preadjusted adaptive walls for low speed wind tunnel
[KTH-AERO-REPT-57] N89-19278
WALLS
Turbulence structure and mass transport in a channel flow with polymer injection
[AD-A202237] N89-19521
Acoustic wave propagation in heterogeneous structures including experimental validation
[NASA-TM-101486] N89-19965
WASTE WATER
Design of a surface-based factory for the production of life support and technology support products. Phase 2: Integrated water system for a space colony
[NASA-CR-184730] N89-19808
WATER
Spreading supercooled water droplets on an ice surface N89-19614
A parametrization scheme for the coalescence of water drops using the stochastic collection equation N89-19671
An infrared reflectance study of water in outer belt asteroids N89-20037
WATER MANAGEMENT
Salinity mapping based on SPOT images of the Punjab, Pakistan
[BCRS-88-03] N89-19734
Design of a surface-based factory for the production of life support and technology support products. Phase 2: Integrated water system for a space colony
[NASA-CR-184730] N89-19808
WATER QUALITY
The use of LANDSAT imagery for water quality studies in the Ijsselmeer area (Netherlands)
[BCRS-87-18] N89-19732
Evaluation of available analytical techniques for monitoring the quality of space station potable water N89-20071
WATER RECLAMATION
Design of a surface-based factory for the production of life support and technology support products. Phase 2: Integrated water system for a space colony
[NASA-CR-184730] N89-19808
WATER RESOURCES
The collection efficiency of a massive fog collector N89-19650
Design of a surface-based factory for the production of life support and technology support products. Phase 2: Integrated water system for a space colony
[NASA-CR-184730] N89-19808
WATER TREATMENT
Design of a surface-based factory for the production of life support and technology support products. Phase 2: Integrated water system for a space colony
[NASA-CR-184730] N89-19808
WATER VAPOR
Lidar for the determination of Antarctic water vapor profiles N89-19756
Calculation of molecular absorption parameters and updating the AFGL atmospheric line parameter compilation
[AD-A202113] N89-19761
WATER WAVES
Directional wave data recorded in the southern North Sea
[IOS-258] N89-19793
WAVE EQUATIONS
Applied partial differential equations and numerical analysis
[AD-A201749] N89-19939
WAVE FUNCTIONS
Quantum field theory of universe
[DE88-756084] N89-20022
WAVE INTERACTION
Characteristics of radar echo of snow band formed in the lee side of a mountain N89-19726
WAVE PROPAGATION
Wave propagation in large space structures N89-19335

Microwave time delays for the dual L-C-band feed system N89-19462
Steady waves in a nonlinear theory of viscoelasticity N89-19470
Propagation problems regarding 20/30 GHz bands in Earth-space links
[REPT-88-022] N89-19480
Propagation problems regarding millimeter waves (40/50 GHz)
[REPT-88-023] N89-19481
Directional wave data recorded in the southern North Sea
[IOS-258] N89-19793
Acoustic wave propagation in heterogeneous structures including experimental validation
[NASA-TM-101486] N89-19965
Research in acoustical scattering, diffraction catastrophes, optics of bubbles and acoustical phase conjugation
[AD-A201451] N89-19968
Gaussian beam representation of beam-like ultrasonic fields N89-19972
An observational and numerical study of extragalactic radio sources N89-20055

WAVE REFLECTION
Active control of elastic wave motion in structural networks N89-19342

WAVE SCATTERING
Large wave number aperture limited Fourier inversion and inverse scattering
[AD-A202247] N89-19940

WAVEGUIDES
The modeling of viscoelastic circular plates for use as waveguide absorbers
[AD-A201621] N89-19588
Passive vibration control using viscoelastic and constrained layer beam waveguide absorbers
[AD-A202188] N89-19595

WEAK ENERGY INTERACTIONS
Ion pair solvation
[AD-A201529] N89-19395

WEAPON SYSTEMS
Short-range anti-armour flight vehicles of the Apache/CWS family
[DRIC-T-8130] N89-19296
EMMA: The expert system for munition maintenance N89-19823
Diagnostics in the Extendable Integrated Support Environment (EISE) N89-19824

WEAPONS DELIVERY
Short-range anti-armour flight vehicles of the Apache/CWS family
[DRIC-T-8130] N89-19296

WEAR
In-line wear monitor
[AD-A201292] N89-19301

WEAR TESTS
Performance evaluation of military engine and gear oils in friction and wear devices
[AD-A202145] N89-19432

WEATHER FORECASTING
Central Region applied research on severe weather forecasting
[PB88-210836] N89-19771
The Cheyenne windstorm that never came: Another lesson in real time analysis
[CRARP-88-1] N89-19772
A collection of severe weather parameters used for a checklist
[CRARP-88-3] N89-19774
A meditation on Milier
[CRARP-88-4] N89-19775
Technical report on temperature, precipitation and aviation verification at WSFO Sioux Falls for 1987
[CRARP-88-5] N89-19776
Preparing storm data
[CRARP-88-6] N89-19777
Use of long-waves in forecasting
[CRARP-88-7] N89-19778

WEATHER MODIFICATION
A model of wet deposition to complex terrain by the seeder-feeder process N89-19710
Complex microphysical interactions within a central Sierra Nevada orographic cloud system N89-19722
Microphysical and dynamical interactions in Colorado front range upslope storms N89-19725

WEIBULL DENSITY FUNCTIONS
Minification processes
[AD-A202219] N89-19958

WEIERSTRASS FUNCTIONS
The box dimension of self-affine graphs and repellors
[REPT-88-08] N89-19943

WEIGHT REDUCTION
Peaceful uses of electrical engineering in space N89-19487

WEIGHTING FUNCTIONS
An asymptotic theory for weighted least squares with weights estimated by replication
[AD-A198000] N89-19935

WEIGHTLESSNESS
A model for plasma volume changes during short duration spaceflight N89-20067
Maladjustment of kidneys to microgravity: Design of measures to reduce the loss of calcium N89-20076

WELD STRENGTH
The diffusion bonding of aeroengine components
[PNR90540] N89-19308

WENTZEL-KRAMER-BRILLOUIN METHOD
A modal/WKB inversion method for determining sound speed profiles in the ocean and ocean bottom
[AD-A201252] N89-19791

WHEELS
Some new results in rolling contact
[REPT-88-46] N89-19577

WIND (METEOROLOGY)
Central Region applied research on severe weather forecasting
[PB88-210836] N89-19771
The Cheyenne windstorm that never came: Another lesson in real time analysis
[CRARP-88-1] N89-19772
A collection of severe weather parameters used for a checklist
[CRARP-88-3] N89-19774

WIND MEASUREMENT
Local wind measurements for micrositing
[DE89-000829] N89-19781
Interpretation of ERS-1 wind scatterometer data: Wind field extraction
[ETN-89-93982] N89-19790

WIND PROFILES
Interpretation of ERS-1 wind scatterometer data: Wind field extraction
[ETN-89-93982] N89-19790

WIND SHEAR
A preliminary study of precursors to Huntsville microbursts
[AD-A200914] N89-19782

WIND TUNNEL TESTS
Wind-tunnel results of advanced high-speed propellers at takeoff, climb, and landing Mach numbers
[NASA-TM-87030] N89-19265
Two experimental supercritical laminar-flow-control swept-wing airfoils
[NASA-TM-89073] N89-19266
Unsteady low-speed wind tunnel test of a straked delta wing, oscillating in pitch. Part 2: Plots of steady and zeroth and first harmonic unsteady pressure distributions
[AD-A201936] N89-19275
Drag coefficients for irregular fragments
[AD-A201943] N89-19276
A wind tunnel study on the melting of snow flakes N89-19611

WIND TUNNEL WALLS
Two-dimensional test section with preadjusted adaptive walls for low speed wind tunnel
[KTH-AERO-REPT-57] N89-19278

WIND TUNNELS
A vertical wind tunnel for the study of snowflakes and effects of accumulated snow on materials N89-19674

WIND TURBINES
Field investigation of a wake structure downwind of a VANT (Vertical-Axis Wind Turbine) in a wind farm array
[DE89-000821] N89-19743
Local wind measurements for micrositing
[DE89-000829] N89-19781

WINDOWS (APERTURES)
Fabrication of XLWIR (Extra-Long-Wavelength-Infrared) window materials
[DE89-006418] N89-19439

WINDPOWER UTILIZATION
Field investigation of a wake structure downwind of a VANT (Vertical-Axis Wind Turbine) in a wind farm array
[DE89-000821] N89-19743
Local wind measurements for micrositing
[DE89-000829] N89-19781

WING PLANFORMS
An efficient method for computing unsteady transonic aerodynamics of swept wings with control surfaces
[AIAA-85-4058] N89-19241

WING PROFILES
Airfoil stall penetration at constant pitch rate and high Reynolds number N89-19260
Flight survey of the 757 wing noise field and its effects on laminar boundary layer transition. Volume 2: Data compilation
[NASA-CR-178217] N89-19505

WING TIPS
Tip vortices: Single phase and cavitating flow phenomena N89-19271

WINTER
Microphysical, dynamical and chemical aspects of scavenging processes during winter precipitation N89-19695

WIRE
Composite ceramic superconducting wires for electric motor applications
[AD-A201810] N89-19429

WIRELESS COMMUNICATION
The use of interleaving for reducing radio loss in convolutionally coded systems N89-19454

WIRING
Wiring Viterbi decoders (splitting deBruijn graphs) N89-19459

WORDS (LANGUAGE)
Using the sentence verification technique to assess storage and retrieval processes
[AD-A201632] N89-20029
Automatic voice recognition using traditional and artificial neural network approaches N89-20064

WORK CAPACITY
Physiological assessment of task underload N89-19846

WORKLOADS (PSYCHOPHYSIOLOGY)
Brain activity during tactical decision-making. Part 4: Event-related potentials as indices of selective attention and cognitive workload
[AD-A201370] N89-19797
Physiological assessment of task underload N89-19846

WORKSTATIONS
Telerobot operator control station requirements N89-19876
A representational framework and user-interface for an image understanding workstation N89-19878
Voice control of complex workstations N89-19880
A 2-D and 3-D robot path planning algorithm based on quadtree and octree representation of workspace
[DE89-005014] N89-19900

X

X RAY ANALYSIS
In-line wear monitor
[AD-A201292] N89-19301

X RAY SCATTERING
Laser scattering studies of epoxy polymerization processes
[AD-A201925] N89-19430

X RAY SPECTROSCOPY
Formation of titanium nitride layers on titaniun metal: Results of XPS and AES investigations
[KFK-4449] N89-19419

X RAYS
Radiation biology studies in soft X-ray and ultrasoft X-ray region
[DE88-756071] N89-19795

Y

YAG LASERS
Ultrahigh-brightness XeCl laser system
[DE89-005467] N89-19548

YIELD POINT
Determination of residual stress distributions in autofrettaged tubing: A discussion
[AD-A201454] N89-19586

YTTRIUM OXIDES
Radiation induced amorphization in YBa2Cu3O7 and GdBa2Cu3O7 superconductors
[DE89-005451] N89-20008
Mossbauer effect studies of magnetism in superconducting systems
[DE89-005844] N89-20012

Z

ZINC SELENIDES
The 2-4 semiconductor superlattices
[AD-A202369] N89-20005

ZINC SULFIDES
Laser-spectroscopic investigations of manganese centers in the zinc sulfide host lattice
[ETN-89-93791] N89-20007

ZIRCONIUM
Passivity and corrosion of probe metals
[ETN-89-93984] N89-19416

ZONAL FLOW (METEOROLOGY)
Temperature and circulation in the stratospheres of the outer planets
[NASA-CR-184826] N89-20051

Typical Personal Author Index Listing

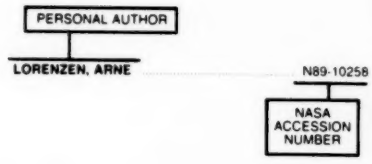

Listings in this index are arranged alphabetically by personal author. The NASA accession number denotes the number by which the citation is identified.

A

AARTS, J. M. N89-19322
ABBISS, JOHN B. N89-19545
ABDALLAH, MAHMOUD A. N89-19866
ABDELKADER, MOHAMED RIYAD HUSIEN N89-19410
ABIDI, M. A. N89-19900
ABITZSCH, SVEN N89-19331
ACKERMAN, J. L. N89-19438
ACKERMAN, M. N89-19770
ACKERMAN, THOMAS P. N89-19646
N89-19649
ADAMS, NIGEL G. N89-19394
ADAMS, WILLIAM M., JR. N89-19255
ADANUVOR, P. K. N89-19745
ADMELLA, M. N89-19895
ADZHIEV, A. KH. N89-19658
AGARWAL, ANANT N89-19923
AGRAWAL, A. P. N89-19467
AHMAD, SAHRIM HAJI N89-19592
AHMED, SELINA N89-20059
AIHUA, WANG N89-19740
AL-KENANY, S. N89-19329
ALEXANDER, J. D. N89-19307
ALFANO, R. R. N89-19539
ALLAN, SEAN N89-19324
ALLEN, GLEN N89-19449
ALLEN, ROBERT N89-20060
ALLISON, DENNIS O. N89-19266
ALMEYDA, GUILLERMO FELIX N89-19753
ALTENKIRCH, R. A. N89-19446
AMATA, E. N89-20049
AMELL, JOHN R. N89-19848
ANCHETA, STAN N89-19324
ANDARY, J. F. N89-19870
ANDERS, B. N89-19979
ANDERSON, AUDIE N89-19825
ANDERSON, JOHN R. N89-19973
ANDERSON, LEE C. N89-19774
ANDERSON, NELS ERIC N89-20047
ANDERSON, THEODORE W. N89-19960
ANDERSON, W. KYLE N89-19244
N89-19252
ANDREWS, ALISON E. N89-19828
ANNIS, JAMES F. N89-19813
ANTONIADIS, DIMITRI A. N89-19911
APPELBAUM, J. N89-19493
APPLEBY, A. J. N89-19745
ARDANUY, P. N89-19729
ARENS, YIGAL N89-19845
ARMERDING, W. N89-19767
ARMSTRONG, T. W. N89-19979
ARNDT, NORBERT KARL ERHARD N89-19564
ARNOLD, J. M. N89-19494
ASANO, KIYOMITSU N89-19997
ASPINALL, JOHN G. N89-19838
ASSELINEAU, ITEF M. N89-19297
ASWANI, M. N89-19341
ATAC, R. N89-19491
ATKINSON, N. C. N89-19712
ATTAWAY, DOROTHY CLAIRE N89-19233
AVANZI, G. N89-19766
AVITZUR, BOAZ N89-19586
AVULA, XAVIER J. R. N89-19872
AXNESS, C. L. N89-19977
AZNAREZ, J. A. N89-19443
AZUMA, Y. N89-19975

B

BABA, NORIO N89-19927
BACHERT, ROBERT F. N89-19888
BADDOUR, OMAR N89-19724
BAFFES, PAUL T. N89-19869
BAHROLOLOUMI, BEHNAM N89-19565
BAILEY, THOMAS N89-19999
BAINUM, PETER M. N89-19334
BAKER, D. N. N89-19764
BAKER, J. E. N89-20014
BAKER, KAY D. N89-19751
BAKER, M. N89-19627
BALARAS, CONSTANTINOS AGELOU N89-19748
BALDETTI, PAOLO N89-19987
BALDWIN, J. N89-19800
BALLINGER, CYNTHIA J. N89-19814
BALTAR, JAMES Y. N89-19507
BALTZERSEN, OYSTEIN N89-19286
BALTZLEY, DENNIS R. N89-19860
BANNEROT, RICHARD B. N89-20058
N89-20073
BARELA, MAXIMO A. N89-19293
BARTRAM, PETER N. N89-20061
BASINGER, RICHARD W. N89-19552
BATINA, JOHN T. N89-19238
N89-19240
N89-19257
BAUER, CHARLES L. N89-19428
BAUER, O. H. N89-19995
BAUMEISTER, KENNETH J. N89-19965
BAUMGARDNER, DARREL G. N89-19618
N89-19619
N89-19628
BAUN, LAWRENCE R. N89-19508
BEARD, KENNETH V. N89-19607
N89-19615
BEBERNES, J. N89-19391
BECKER, ROGER J. N89-19544
BEDFORD, TIM N89-19943
N89-19944
BEHENG, K. D. N89-19671
BEINE, DONNA N89-19324
BELASHOV, V. I. N89-19989
BELK, DAVE M. N89-19245
BELL, CHRISTOPHER N89-20062
BELLUCCI, G. N89-20049
BEMIS, S. V. N89-19284
BEN-TAL, AHARON N89-19937
BENDER, ERICH EDUARD N89-19514
BENDIKSEN, ODDVAR O. N89-19258
BENNETT, ROBERT M. N89-19238
N89-19240
N89-19257
BERBEE, H. C. P. N89-19963
BERG, KJELL N89-19286
BERGHOFER, W. N89-19816
BERNSTEIN, DENNIS S. N89-19358
BERRY, EDWARD K. N89-19772
BERRY, FREDERICK C. N89-20063
BESS, CHARLES R. N89-19372
BETTINGER, K. E. N89-19850
BIER, JACK N89-19776
BINDEMANN, I. N89-19370
BIRMINGHAM, BRIAN S. N89-19546
N89-19549
BIRNBAUM, H. K. N89-19405
BISKAMP, DIETER N89-19994
BLAKERS, A. W. N89-19740
BLAND, SAMUEL R. N89-19234
N89-19238
N89-19240
N89-19247
BLANKENSHIP, MARK H. N89-19797
BLEISTEIN, NORMAN N89-19940
BLYTH, ALAN M. N89-19629
BOCKEMUELLER, ERNST A. N89-19966
BOERNER, W. M. N89-19467
BOHLMANN, JONATHAN D. N89-19254
BOND, THOMAS H. N89-19305
BORLAND, C. J. N89-19236
BOTROS, NAZEIH M. N89-20064
BOWER, CHARLES RAYMOND N89-20057
BOWER, KEITH N89-19617
BOWMAN, R. C., JR. N89-20021
BOYCE, LOLA N89-19581
N89-19582
BOYD, J. T. N89-19536
BRADTMILLER, BRUCE N89-19812
BRADY, MIKE N89-19825
BRAUN, P. N89-19687
BREIDENTHAL, R. N89-19627
BRENGUIER, J. L. N89-19635
BREUER, M. A. N89-19457
BREVNOV, N. N. N89-19989
BRINGI, V. N. N89-19715
BRINK, JAMES R. N89-19824
BRITT, EDWARD J. N89-20004
BRITTEN, M. N89-19285
BROOKS, CUYLER W., JR. N89-19231
BROUGHTON, T. N89-19308
BROUSSARD, JOHN R. N89-19316
BROWN, CHRISTOPHER M. N89-19560
BROWN, H. BENJAMIN, JR. N89-19875
BROWN, JAMES D. N89-19295
BROWN, MAX N89-19865
BROWN, P. R. A. N89-19623
N89-19651
N89-19652
BROWN, PHILIP S., JR. N89-19660
BRUECKMANN, H. N89-19979
BRYAN, WILLIAM B. N89-19503
BUCK, C. A. N89-19352
BUCK, J. W. N89-19743
BUELTHOFF, HEINRICH N89-19802
BUITEVELD, H. N89-19732
BUNKER, WILMA J. N89-19980
BURNHAM, BLAINE N89-19484
BUSSEY, ROBERT M. N89-19765
BYLANDER, TOM N89-19835
BYOUN, J. S. N89-19850

C

CADARETTE, BRUCE S. N89-19811
CAFFARIO, C. N89-19479
CAMPBELL, P. N89-19740
CAMPBELL, S. D. N89-19473
CANAVAN, GREGORY H. N89-19553
N89-19964
CANPOLAT, B. N89-19329
CARLSON, NANCY M. N89-19557
CARNEBIANCA, C. N89-19285
CARPENTER, KENNETH H. N89-19471
CARR, GERALD P. N89-19809
CARR, JOHN SHERMAN N89-20033
CARRARA, VALDEMIR N89-19351
CARROLL, RAYMOND J. N89-19935
CARSWELL, A. I. N89-19718
CARTA, FRANKLIN O. N89-19260
CASEY, KEVIN D. N89-19791
CASSERLY, DENNIS M. N89-20065
CASTILLO, R. A. N89-19689
N89-19694
CAULFIELD, H. J. N89-19897
CAYLOR, I. JEFF N89-19621
CAZIER, FRANK W., JR. N89-19261
CEBECI, TUNCER N89-19509
CERI, S. N89-19915
CEVAT, J. J. N89-19733
CHAGANTY, NARASINGA R. N89-19954
CHAN, K. S. N89-19373
CHANDLER, A. S. N89-19698
CHANDRA, M. N89-19656
CHANG, C. L. N89-19834
CHANG, ING N89-20066
CHAPMAN, J. N. N89-19990
CHATTERJEE, R. N. N89-19624

CHAUMERLIAC, NADINE N89-19640
N89-19711
CHEATHAM, J. B. N89-19881
CHEN, J. N89-19462
CHEN, JEN-PING N89-19707
CHEN, P. C. N89-19280
N89-19281
CHEN, Q. Y. N89-19598
CHEN, ROBERT S. N89-19784
CHEN, S. N89-19417
N89-19648
CHENG, JUEI-TENG N89-20002
CHI, Y. C. N89-19408
CHIANG, WEN-LI N89-19558
CHIANG, YET-MING N89-19437
CHILDS, W. J. N89-19975
CHIOU, WEN-YAW N89-19803
CHO, K. N89-19408
CHOGNOT, M. N89-19360
CHONG, C. M. N89-19740
CHOULARTON, TOM W. N89-19617
N89-19623
N89-19698
N89-19710
CHOYKE, W. J. N89-19396
N89-19397
CHU, BEN N89-19430
CHUANG, ANDREW H. N89-19248
CHUANG, CATHERINE N89-19615
CHUNG, JEAN SOO N89-20017
CHUNSHENG, CAI N89-19665
CHURCH, E. L. N89-19985
CHURCHILL, PHILIP J. N89-19883
CHURCHILL, THOMAS D. N89-19812
CICCARELLI, EUGENE C. N89-19844
CINK, BRIAN N89-19324
CLARK, DAVID R. N89-19309
CLARK, P. A. N89-19698
CLARK, T. N89-19723
CLARK, TERRY L. N89-19634
CLARKE, MARGARET M. N89-19885
CLAUSS, R. C. N89-19464
CLAYSON, C. H. N89-19793
CLEARY, STEPHAN F. N89-19541
CLEGHORN, T. F. N89-19881
CLEGHORN, TIMOTHY F. N89-19869
CLINE, DAREN B. N89-19935
CLOTH, P. N89-19947
N89-19979
COAKLEY, JAMES E. N89-19645
COHEN, JOSEPH S. N89-19811
COLANERI, P. N89-19930
COLBORN, B. L. N89-19979
COLBURN, D. C. N89-19646
COLIN, J. L. N89-19701
COLLE, HERBERT A. N89-19848
COLLIER, FAYETTE SMITH, JR. N89-19500
COLLIER, J. W. N89-19460
COLLINS, CARL B. N89-19542
COLLINS, EMMANUEL G., JR. N89-19358
COLLINS, O. N89-19459
COLVIN, G. E., JR. N89-19383
COLVIN, GLENN E., JR. N89-19378
COLWELL, GENE T. N89-19502
COMES, F. J. N89-19767
COMLY, J. C. N89-19550
COMSTOCK, J. RAYMOND, JR. N89-19846
CONANT, R. J. N89-19967
CONGDON, JONATHAN D. N89-20025
CONNELL, JAMES JOSEPH N89-20034
CONRATH, BARNEY J. N89-20051
COOK, A. N89-19491
COON, DENNIS N. N89-19423
COOPER, WILLIAM A. N89-19620
COPE, M. T. N89-19413
N89-19414
CORE, P. W. N89-19921
CORLETT, R. C. N89-19387
CORMIER, R. N89-19452
COTTER, GLADYS A. N89-20030
COTTON, WILLIAM R. N89-19641
N89-19648
N89-19721
N89-19725
COUNTEMANCHE, DAVID J. N89-19517
COURTS, SAMUEL SCOTT N89-20018
CRABB, T. N89-19871
CRAVEN, J. D. N89-19764
CRUMLEY, R. L. N89-19498
CULIOLI, J. C. N89-19906
CUNNINGHAM, A. G. N89-19718
CUNNINGHAM, A. M., JR. N89-19275
CUNNINGHAM, ATLEE M., JR. N89-19256
CUNNINGHAM, HERBERT J. N89-19257
CZARNEK, R. N89-19584
CZARNITZKI, J. N89-19330
CZUCHLEWSKI, S. J. N89-19550
CZYS, ROBERT R. N89-19606
N89-19613
N89-19626

D

DACRUZ, JOSE JAIME N89-19351
DAEGES, J. N89-19452
DAGENHART, J. RAY N89-19266
DAHL, MILO D. N89-19965
DALLMANN, D. N89-19329
DALLY, WILLIAM J. N89-19923
DAMASCENOFERREIRA, LUIZ DANILO N89-19351
DANFORD, M. D. N89-19406
DANIEL, B. R. N89-19392
DANTONI, M. N89-19495
DARLISON, A. G. N89-19651
N89-19652
DATTA, SUPRIYO N89-20005
DAUM, PETER H. N89-19693
DAUNT, S. J. N89-19976
DAVE, B. N89-19745
DAVIS, ELIZABETH K. N89-19818
DAVIS, JOHN E. N89-20067
DAVIS, MICHAEL N89-19805
DAVIS, RANDALL N89-19445
DECRISTOFANO, BARRY S. N89-19811
DEEPE, J. N89-19491
DEKKER, K. N89-19951
DEKORVIN, ANDRE N89-20068
DELANDELONG, M. A. N89-19320
DELLERT, M. N89-19687
DELUISI, J. N89-19694
DEMAREST, KENNETH R. N89-19780
DENBOER, R. G. N89-19275
DENDANE, A. N89-19494
DENHOLLANDER, W. TH. F. N89-19963
DENIG, W. F. N89-19327
DEPAGTER, B. N89-19942
DEVADAS, SRINIVAS N89-19923
DEVRIES, R. E. N89-19946
DICKINSON, WILLIAM J. N89-19829
DIENER, F. N89-19359
DIKE, J. J. N89-19604
DILLARD, D. A. N89-19434
DINI, PAOLO N89-19504
DIVSALAR, D. N89-19454
DIXON, GENE A. N89-19796
DLUGI, RALPH N89-19683
DOBES, Z. N89-19850
DODDS, P. G. N89-19942
DOGGER, C. S. G. N89-19275
DOLINAR, S. N89-19459
DOMS, S. N89-19671
DONALDSON, WILLIAM R. N89-19489
DONG, YA YI N89-19614
DOONG, JIA-MAW N89-19590
DOVEK, MORIS M. N89-19398
DOWLING, DAVID RUSSELL N89-19515
DRESNER, LAWRENCE N89-20003
DRESS, DAVID A. N89-19232
DRESSER, M. J. N89-19396
N89-19397
DUBOIS, M. R. N89-19403
DUFFIE, N. N89-19871
DUFFY, J. N89-19408
DUKE, EUGENE L. N89-19832
DUNCAN, PHILLIP C. N89-19853
DUNKER, REINER N89-19304
DUNLAP, B. D. N89-20012
DUNN, MICHAEL N89-19366
DUNN, RICHARD S. N89-19298
DURAND, A. N89-19488
DUROURE, CHRISTOPHE N89-19625
N89-19679
DUTRA, S. L. G. N89-19750
DUTT, S. N89-19540

E

EAGON, MARK N89-19324
EARLE, GREGORY DUANE N89-19758
ECKERT, A. N89-19329
ECKSTEIN, BRETT N89-19324
ECKSTROM, CLINTON V. N89-19255
EDWARDS, JOHN W. N89-19264
EGGERS, MITCHELL D. N89-19929
EICHTEN, E. N89-19491
EILINGSFELD, FABIAN N89-19331
EL-GUEBALY, L. N89-19992
ELAM, REID P. N89-20069
ELCHURI, V. N89-19583
ELFENTHAL, L. N89-19416
ELGERSMA, MICHAEL RAY N89-19310
ELLINGSON, W. A. N89-19438
ELLMANN N89-19790
ELPHIC, I. C. N89-19764
EMMERT, G. A. N89-19992
ENAYETULLAH, M. A. N89-19745
ENDERLE, KARL-HEINZ N89-19702
ENDOH, TATSUO N89-19608
N89-19726
ENGWERDA, JACOB CHRISTIAAN N89-19934
ENUKASHVILY, ISAAC M. N89-19661
EOM, H. J. N89-19467
EPSTEIN, JONATHAN S. N89-19423
ERES, DJULA N89-20019
ESSAM, G. R. N89-19436
EUN, JONG WON N89-19768
EVERS, KEN H. N89-19888
EVETTS, D. R. N89-19414
EWERING, W. N89-19370
EWING, J. A. N89-19793
EWRY, MICHAEL E. N89-19848

F

FAIRFIELD, D. H. N89-19764
FANG, HO T. N89-19421
FARBMAN, GERRY N89-19369
FARLEY, R. D. N89-19680
FAROUK, BAKHTIER N89-19520
FAUT, OWEN D. N89-19402
FEINER, STEVEN N89-19851
FELIU, VICENTE N89-19875
FENDLER, JANOS H. N89-19427
FENG, JAMES Q. N89-19606
FENG, SU-CHEN KATE N89-19985
FENNELL, J. F. N89-19764
FERIGLE, A. N89-19895
FERNAU, MARK EDWARD N89-19785
FETZER, H. N89-19360
FILGES, D. N89-19947
N89-19979
FINK, LAWRENCE N89-19366
FINK, PAMELA K. N89-19827
FINN, W. D. N89-19593
FINNEGAN, WILLIAM G. N89-19686
FIORITO, P. N89-19285
FIRTH, JAMES A. N89-19279
FISCHLER, M. N89-19491
FISHMAN, GEORGE S. N89-19955
FISSETTE, E. N89-19361
FITZPATRICK, G. A. N89-19308
FITZSIMMONS, P. N89-19314
FLAMM, D. S. N89-19341
FLATAU, PIOTR J. N89-19641
FLEETER, SANFORD N89-19503
FLOWER, E. C. N89-19604
FLYNN, E. R. N89-20015
FLYNN, GEORGE J. N89-20070
FODOR, G. E. N89-19441
FOLTA, D. N89-19729
FOO, B. Y. N89-19467
FORD, DONNIE N89-19825
FORESTER, CLIFFORD K. N89-19507
FORKEL, RENATE N89-19690
FORMISANO, V. N89-20049
FORSSELL, BORJE N89-19286
FOSTER, P. N89-19363
FOUTCH, RICHARD G. N89-19799
FOWLKES, JEFFREY BRIAN N89-19971
FRACKER, MARTIN L. N89-19847
FRALEY, CHRISTINA N89-19908
FRANK, L. A. N89-19764
FRANTZIS, L. N89-19741
FREILEY, A. J. N89-19461
FRIEDMAN, A. N89-19540
FRUSH, CHARLES N89-19717
FU, J. S. N89-19977
FUCHS, RON N89-20028
FUJIMOTO, NOZOMU N89-19506
FUJIYOSHI, YASUSHI N89-19726
FUKUTA, NORIHIKO N89-19608
N89-19609
FUNG, K. Y. N89-19241
FUNK, JOAN G. N89-19385
FURTAK, T. E. N89-19401
FURUYA, OKITSUGU N89-19558
FURUYA, TAKAAKI N89-19997
FUZU, ZHANG N89-19740

G

GABUZDA, DENISE CARMEN N89-20035
GAGNEUX, JACQUELINE N89-19630
N89-19675

GAINES, I. N89-19491
GAMACHE, ROBERT R. N89-19761
GANZ, ERIC DAVID N89-19404
GARIN, JOHN N89-19873
GARRIDO, L. N89-19438
GARZOTTO, F. N89-19915
GASKINS, JAMES Y. N89-19328
GATTI, M. S. N89-19461
GATTINGER, R. L. N89-19327
GAY, M. J. N89-19698
GAYEN, S. K. N89-19539
GAYET, JEAN-FRANCOIS N89-19625
N89-19713
GAYTANDJIEN, DIMITER N89-19728
GEER, RICHARD D. N89-20071
GELFAND, ALAN E. N89-19959
GENERAZIO, EDWARD R. N89-19578
GENG, STEVEN M. N89-19737
GEOHEGAN, D. B. N89-20019
GERMAIN, A. C. N89-19743
GERONDAKIS, GEORGE G. N89-19321
GERSHWIN, STANLEY B. N89-19911
GERVAT, G. P. N89-19698
GHEZZI, CARLO N89-19914
GIBBONS, MICHAEL D. N89-19240
GIBSON, R. B. N89-19548
GIERASCH, PETER J. N89-20051
GIESSELMANN, M. N89-19490
GIEZEN, JURGEN JOHANNES N89-19591
GILLOTAY, D. N89-19769
GILYARD, GLENN B. N89-19253
GIOVAGNOLI, F. N89-19285
GIRDNER, D. N89-19461
GIRLICH, A. N89-19370
GLASS, I. I. N89-19511
GLINER, A. R. N89-19486
GODWIN, M. P. N89-19530
N89-19531
GOLDMAN, A. N89-19922
GOLDSTEIN, STANLEY H. N89-20058
N89-20073
GOLISH, L. M. N89-19907
GOLNARAGHI, MOHAMMAD FARID N89-19566
GONDA, TAKEHIKO N89-19674
GONZALEZ, W. D. N89-19750
GOODMAN, ALAN H. N89-19752
GOORJIAN, PETER M. N89-19237
GORBUNOV, BORIS N89-19665
GORDON, CLAIRE C. N89-19812
N89-19813
GORETTA, K. C. N89-20011
N89-20014
GOSNELL, T. R. N89-19548
GOVER, A. N89-19540
GRABOWSKI, WOJCIECH W. N89-19720
GRAHAM, MARC H. N89-19903
GRANT, R. W. N89-19492
GREEN, D. J. N89-19422
GREEN, M. A. N89-19740
GREEN, SHELDON ISAIAH N89-19271
GREENE, D. P. N89-19550
GRELL, GEORG ALFRED N89-19786
GRIBELIN, PASCAL N89-19676
GRIBOV, YU. V. N89-19989
GRIFFIN, SANDY N89-19817
GRIFFITHS, H. D. N89-19483
GRISSOM, WILLIAM A. N89-19866
GROH, GARY E. N89-19411
GRONEMEYER, S. N89-19438
GRUNZE, MICHAEL N89-19425
GRUZEN, ALEXANDER N89-19999
GRZYWACZ, NORBERTO N89-19802
GUERRY, DUPONT, III N89-19541
GUERRY, R. K. N89-19541
GUERTS, E. G. M. N89-19275
GUESSOUM, NIDHAL N89-19988
GUHA, S. N89-19739
GULKIS, S. N89-19466
GUNSHOR, ROBERT L. N89-20005
GURUSWAMY, GURU P. N89-19237
GUSTAFSON, C. L. N89-19341
GUZMAN, L. N89-19895
GYANFI, MAX N89-19882
GZIRISHVILI, T. N89-19666

H

HAASE, E. L. N89-19418
HACKETT, PETER H. N89-19799
HAGER, GORDON D. N89-19543
HALL, WILLIAM D. N89-19634
N89-19638
N89-19723
HALLETT, JOHN N89-19612
N89-19614
N89-19664
HALLORAN, JOHN W. N89-19429
HALLS, G. A. N89-19571
HALS, TORBJORN N89-19286
HALYO, NESIM N89-19316
HAM, WILLIAM T., JR. N89-19541
HAMADEH, RAMZI F. N89-19434
HAMSCHER, WALTER C. N89-19445
HAN, D. N89-19729
HANRATTY, THOMAS J. N89-19517
HANSEN, J. E. N89-19477
HANSON, D. E. N89-19550
HARIMAYA, TOSHIO N89-19668
HARRIS, CHARLES D. N89-19231
HARRIS, PAUL N89-19369
HARRIS, RANDALL L., SR. N89-19846
HARRISON, I. R. N89-19424
HARRISON, K. N89-19664
HARTMAN, ROBERT MARSHALL N89-19272
HARTMAN, S. N89-19496
HARVEY, GALE A. N89-19529
HARVEY, WILLIAM D. N89-19231
HASHEMI-AHMADY, MODJTABA N89-19409
HASLAM, C. L. N89-19383
HASPEL, DONNA L. N89-19298
HAUENSTEIN, R. J. N89-20001
HAUG, EDWARD J. N89-19336
HE, GUANFANG N89-19639
HEBEKER, FRIEDRICH K. N89-19526
HEBEN, MICHAEL J. N89-19398
HEBSUR, MOHAN G. N89-19371
HEBVERT, MARTIAL N89-19868
HEGDE, UDAY G. N89-19392
HEGG, DEAN A. N89-19692
HEGGESTAD, HAROLD M. N89-19826
HEICHLER, J. N89-19482
HEIGHWAY, EDWARD A. N89-19984
HEINE, W. N89-19359
HEINEMANN, KLAUS N89-19329
N89-19330
HEINTZENBERG, JOST N89-19616
N89-19655
N89-19699
HELLENDOORN, HANS N89-19961
HEMLER, RICHARD S. N89-19636
HENDERSON-SELLERS, ANN N89-19752
HENDY, K. C. N89-19810
HENSTENBURG, ROBERT BROWN N89-19376
HERBERT, A. N89-19767
HERD, CHARLES R. N89-19394
HERZEGH, PAUL H. N89-19714
HESS, R. W. N89-19259
HETTEMA, CHARLES D. N89-19588
HETTMANSPERGER, THOMAS P. N89-19957
HEYLEN, W. N89-19361
HEYMSFIELD, ANDREW J. N89-19649
HICKS, ELIZABETH N89-19630
N89-19675
HICKS, M. A. N89-19413
HIGGINBOTHAM, SCOTT A. N89-19326
HIGGINS, R. H. N89-19406
HILDEBRAND, PETER N89-19717
HILDRETH, ELLEN N89-19802
HILL, M. J. N89-19414
HILL, T. A. N89-19698
N89-19703
HILLIER, FREDERICK S. N89-19913
HINCHEE, M. E. N89-19743
HINDMAN, EDWARD E. N89-19681
HINKAI, S. W. N89-19870
HINO, JAMES H. N89-19840
HIRANO, YASUO N89-19377
HOBBS, PETER V. N89-19645
N89-19692
HOCHFELD, A. N89-19416
HOFF, R. M. N89-19718
HOFFMANN, H.-E. N89-19662
HOGEBIRK, J. J. N89-19898
HOLLAND, RICKY R. N89-19762
HOLMES, J. K. N89-19456
HOLTZ, R. E. N89-19746
HOMEIER, PETER N89-19843
HOOGHIEMSTRA, G. N89-19946
HORNE, CHARLES T., III N89-19595
HORTTOR, R. L. N89-19464
HOSKINS, DOUGLAS N89-19468
HOSOYA, AKIO N89-20022
HOWLETT, JAMES T. N89-19249
HOYT, D. N89-19729
HSIAO, GEORGE C. N89-19526
HSU, I. S. N89-19455
N89-19458
HSU, S. N89-19800
HU, HONG N89-19248
HU, ZHIJIN N89-19639
HUANG, MEIYUAN N89-19642
N89-19706
HUANG, SHI-HONG N89-19689
HUBBARD, R. N89-19800
HUGHES, WILLIAM M. N89-19546
N89-19549
HUH, O. N89-19800
HUIJSMAN, R. D. N89-19919
HUIJSMANS, C. B. N89-19942
HULSHOF, J. N89-20054
HUMBERT N89-19790
HURDLE, SHARON N89-19484
HUSBY, D. N89-19491
HUTTSELL, L. J. N89-19235
HUVESTADT, DIETRICH N89-20056
HWANG, HEON N89-19567
HYDERALI, A. K. N89-19900
HYLAND, DAVID C. N89-19344
N89-19345
N89-19357
N89-19358

I

ICHIKAWA, S. N89-19719
ICHIMURA, I. N89-19719
IDE, HIROSHI N89-19243
ILLINGWORTH, ANTHONY J. N89-19621
INATANI, YOSHIFUMI N89-19353
INGRAM, ALBERT S. N89-19559
INMAN, D. J. N89-19339
IRIBARNE, J. V. N89-19691
ISAAC, G. A. N89-19696
ISAKA, HARUMI N89-19676
N89-19679
ISAMINGER, M. A. N89-19782
ISONO, KENKI N89-19674
IWAI, KUNIOMOTO N89-19669

J

JAAP, JOHN P. N89-19818
N89-19819
JACKSON, DAVID R. N89-19474
JACKSON, E. B. N89-19466
JACKSON, JAMES N89-19293
JAENICKE, R. N89-19654
JAESCHKE, WOLFGANG N89-19702
JAFFIN, S. N89-19729
JAFFREZO, J. L. N89-19701
JAMESON, ARTHUR R. N89-19714
JAMIESON, D. N. N89-20021
JANK, T. N89-19715
JANSWEIJER, P. P. M. N89-19898
N89-19917
JANTER, T. N89-19361
JECK, RICHARD N89-19673
JEGLEY, DAWN C. N89-19589
JELLINEK, H. G. N89-19433
JENKIN, A. B. N89-19341
JENNINGS, S. GERARD N89-19685
JENNINGS, VON AYRE N89-19873
JENSEN, JORGEN B. N89-19618
JERACKI, ROBERT J. N89-19265
JEZIORO, M. N89-19307
JIANHUA, ZHAO N89-19740
JOCHUM, ANNE M. N89-19632
JOE, PAUL I. N89-19650
JOHANSSON, B. N89-19655
JOHARI, H. N89-19627
JOHNS, J. W. C. N89-19976
JOHNSON, A. S. N89-19352
JOHNSON, BERNARD R. N89-19476
JOHNSON, DONALD K. N89-19268
JOHNSON, ERIC R. N89-19599
JOHNSON, G. C. N89-19604
JOHNSON, JOHN A. N89-19557
JOHNSON, ROBERT L. N89-19907
JOHNSON, SALLY C. N89-19833
JOHNSON, TAMARA M. N89-19546
N89-19549
JOHNSON, WILLIAM B. N89-19853
JONES, ANDY N89-19710
JONES, B. N89-19306
N89-19532
JONES, D. G. N89-19533
JONES, MARK C. N89-19380
JONES, MARSHALL B. N89-19860
JONES, THOMAS DAVID N89-20037
JONKER, BEN N89-19575
JORDANS, R. N89-19732
JOSEPH, DANIEL D. N89-19512
JOSEPHSON, JOHN R. N89-19837
JUANG, J. N. N89-19349
JUNKINS, J. L. N89-19349
JUNKINS, JOHN L. N89-19596

K

KACKI, H. N89-19433
KAHLBAUM, WILLIAM M., JR. N89-19899
KAHLIL, M. N89-19953
KAJIKAWA, MASAHIRO N89-19670
KAKUTKINA, HATALYA N89-19665
KALEGS, INTS N89-19872
KALKER, J. J. N89-19576
N89-19577
N89-19603
KAMP, ARMIN N89-19991
KAN, EDWIN P. N89-19876
KANADE, TAKEO N89-19868
N89-19874
KANDIL, OSAMA A. N89-19248
KAO, W. H. N89-19384
KAO, Y. F. N89-19241
KAPOOR, R. K. N89-19624
KASSOY, D. R. N89-19391
KATAYAMA, YOSHINORI N89-19926
KATNIK, GREGORY N. N89-19326
KAWAMOTO, J. D. N89-19341
KAYAL, HAKAN N89-19330
KAZA, KRISHNA RAO V. N89-19262
KAZANZIDES, PETER N89-19562
KEANE, M. S. N89-19946
KEITH, W. D. N89-19678
KELLERMEIER, H. N89-19360
KELLY, FREDERICK A. N89-19864
N89-20072
KELLY, R. D. N89-19622
KENDALL, D. J. N89-19327
KENNEDY, ROBERT S. N89-19860
KENNEDY, SHERRY L. N89-19798
KEYES, J. J., JR. N89-19523
KHADJAVI, F. N89-19278
KHALID, M. N89-19267
KHALIL, M. N89-19949
KHAMBATTA, NOSHIR M. N89-19551
KHORGUANI, V. N89-19666
KHOSIA, PRADEEP N89-19874
KIM, DONG-WOO N89-20042
KIM, HYOUN-EE N89-19439
KIM, KYUN O. N89-19580
KIM, V. M. N89-19657
KIMBALL, C. W. N89-20012
KING, TRACY K. N89-19499
KINNE, STEFAN N89-19649
KINS, LUCIA N89-19697
KIRK, R. E. N89-19794
KIRKLAND, MICHAEL N89-19561
KISO, YOSHIHIRO N89-19506
KLEESSEN, R. N89-19329
KLEEVEN, WILLEM JAN GERARD MARIE N89-19978
KLEIN, M. J. N89-19466
KLEWE-NEBENIUS, H. N89-19419
KLINGELHOFER, R. N89-19992
KNABE, FRANZ N89-19287
KNIGHT, DANIEL L. N89-19513
KNIGHT, THOMAS F., JR. N89-19923
KNOPP, JEROME N89-20074
KO, S. H. N89-19555
KOBAYASHI, JUTARO N89-19674
KOBAYASHI, KATSUMI N89-19795
KOBAYASHI, SHIGENBU N89-19925
KOEKOEK, R. N89-19352
KOELLE, H. H. N89-19323
N89-19330
KOENIGER, M. N89-19495
KOGA, R. N89-19977
KOHL, K. B. N89-19441
KOJIMA, YUZO N89-19997
KOLASINSKI, W. A. N89-19977
KOLODZIEJSKI, LESLIE A. N89-20005
KONG, JIN AU N89-19792
KONISHI, HIROYUKI N89-19667
KOSTINSKI, A. B. N89-19467
KOSUT, ROBERT L. N89-19333
N89-19343
KOUPELIS, THEODOROS N89-20039
KOUSEN, KENNETH A. N89-19258
KRAEMER, M. N89-19684
KRAFT, J. N89-19687
KRISTIANSEN, M. N89-19490
KRIVONOZHKIN, S. N. N89-19488
KROHN, B. J. N89-19550
KRUCHTEN, ROBERT J. N89-19839
KRUTZ, ROBERT W., JR. N89-19796
KUHLEN, H. N89-19360
KULCINSKI, G. L. N89-19992
KUMAI, MOTOI N89-19688
KUNZ, KARL S. N89-19779
KUSHAWAHA, VIKRAM S. N89-19537
KWEON, IN SO N89-19868

L

LABELLE, J. N89-19996
LACHMAN, ROY N89-20062
LAFORE, JEAN PHILIPPE N89-19638
LAMB, DENNIS N89-19707
LAMONT, GARY B. N89-19842
LANGE, TH. N89-19362
LANGFORD, JOHN D., JR. N89-19292
LARSEN, F. HOLM N89-19477
LATHAM, JOHN N89-19629
LAYLAND, J. W. N89-19464
LE, THACH N89-19843
LEACH, RONALD J. N89-19905
LEAITCH, W. R. N89-19696
N89-19718
LEBRETON, J. P. N89-19995
LECLAIRE, RENE J., JR. N89-19980
LEE, HSIEN-CHE N89-19983
LEE, IN YOUNG N89-19709
LEE, MARGARET A. N89-19815
LEE, MYUNG-HA N89-19381
LEE, S. H. N89-19408
LEE, T. C. N89-19405
LEEDS, J. L. N89-19284
LEGATES, DAVID RUSSELL N89-19787
LEROY, G. M. N89-19743
LEROY, STEPHEN S. N89-20051
LESSEN, DAVID N89-19524
LESTER, C. S. N89-19548
LEUTHOLD, MARK A. N89-20032
LEVERANT, G. R. N89-19373
LEVI, LAURA N89-19677
LEVRINI N89-19364
LEWIS, GREGORY W. N89-19797
LEWIS, NATHAN S. N89-19398
LEWIS, PETER A. N89-19958
LI, LU N89-19865
LIEBECK, R. H. N89-19300
LIEFOOGHE, C. N89-19361
LIMBOURG, N. N89-19360
LIN, N.-H. N89-19682
LIN, S. R. N89-19598
LIN, T. H. N89-19598
LIN, YIING-YUH N89-19356
LINDSAY, RICHARD H. N89-19568
LINEBERRY, J. T. N89-19990
LIOU, KUO-NAN N89-19644
LIPPENS, C. N89-19770
LIPPS, FRANK B. N89-19636
LITT, JONATHAN N89-19886
LITTLE, ARTHUR D. N89-19883
LIU, C. T. N89-19384
LIU, D. D. N89-19241
LIU, H. T. N89-19743
LIU, SHUAIREN N89-19706
LIU, WU-MING N89-19985
LIVINGSTON, J. M. N89-19646
LLEWELLYN, E. J. N89-19327
LONG, STUART A. N89-19474
LOOTSMA, F. A. N89-20026
N89-20027
LOPUHAA, HENDRIK P. N89-19962
LORANC, MARK ANDRE PETER N89-19754
LORBER, PETER F. N89-19260
LOREE, THOMAS R. N89-19546
N89-19549
LORENZ, GARY V. N89-19737
LOTH, ERIC N89-19516
LOTZE, CLAUDIA N89-19330
LOUCKS, CLIFF N89-19916
LOVELACE, THOMAS B. N89-19581
N89-19582
LOWNDES, D. H. N89-20019
LU, PING N89-19311
LUBART, LUISA N89-19677
LUCIA, A. C. N89-19600
N89-19601
LUENEBURG, E. N89-19656
LUEPKES, C. N89-19671
LUHMAN, DAN N89-19324
LUM, HENRY, JR. N89-19838
LYONS, JAMIE H. N89-19645

M

MA, WEI-MING N89-19731
MABEY, DENNIS G. N89-19240
MACDIARMID, ALAN G. N89-19426
N89-19431
MACDOWALL, R. D. N89-19498
MACK, JOSEPH M. N89-19551
MACKERRELL, SHARON OLIVIA N89-19501
MACVICAR, MARGARET L. N89-19407
MADDEN, PAUL N89-19999
MAGEE-SAUER, KAREN PATRICIA N89-20048
MAGRADZE, GEORGI N89-19659
MALKUS, DAVID S. N89-19390
MALLANT, RONALD K. A. M. N89-19716
MALONE, J. B. N89-19251
MANDRIOLI, DINO N89-19914
MANNING, S. D. N89-19597
MANONI N89-19364
MANOUCHEHRI, DAVOUD N89-19885
MANTON, J. G. N89-19810
MARANGONI, G. N89-19495
MARAPANE, SURESH B N89-19572
MARBACH, HOWARD W., JR. N89-19432
MARCUS, BETH A. N89-19883
MARGERUM, EUGENE A. N89-19730
MARISSEN, ROELOF N89-19602
MARKATOU, MARIANTHI N89-19957
MARSH, A. R. W. N89-19698
MARSTON, PHILIP L. N89-19968
MARTIN, KIM G. N89-19412
MARTIN, MICHAEL N89-19497
MARTIN, SARA F. N89-20053
MARUYAMA, SOH N89-19506
MATHERS, C. D. N89-19450
MATIJEVIC, Z. N89-19330
MATSUO, TAKAYO N89-19653
N89-19719
MATTEO, JOSEPH N89-19873
MATTHEW, W. N89-19800
MATUSKA, PAVEL N89-19747
MAUGHMER, MARK D. N89-19504
MAYER, DAVID W. N89-19507
MAYER, JUERGEN N89-19330
MAYNE, R. W. N89-19339
MAYRAND, C. H. N89-19289
MAZZINI N89-19364
MCCLELLAN, PAUL S., JR. N89-19374
N89-19379
MCCLESKEY, FRANK N89-19276
MCCOWAN, DANIEL N89-19324
MCCOWN, A. W. N89-19550
MCCRACKEN, KEVIN N89-20004
MCDILL, PAUL L. N89-19556
MCGANN, BRENDAN THOMAS N89-19685
MCGLINCHEY, J. M. N89-19352
MCINTOSH, ROBERT E. N89-19475
MCIVOR, STUART DONALD N89-19375
MCKAY, A. N89-19729
MCKEITHAN, C. M. N89-19314
MCKENZIE, ED N89-19958
MCLAUCHLAN, ROBERT A. N89-20075
MCNULTY, RICHARD P. N89-19775
MEDANIC, J. N89-19347
MEEHAN, RICHARD N89-19799
MEIER, G. E. A. N89-19527
MEIJER, H. G. N89-19952
MEIROVITCH, LEONARD N89-19337
MEISCHNER, P. N89-19715
MEIXNER, FRANZ X. N89-19697
MELLOR, A. M. N89-19510
MENDE, S. B. N89-19327
MENDEZ, J. A. N89-19443
MENDREK, M. J. N89-19406
MENSCH, T. C. A. N89-20026
MERKLE, KARL L. N89-20013
MERLIN, DAVID N89-19994
MERRITT, M. W. N89-19473
MEULSTEE, C. N89-19732
MEYER, A. N89-19416
MEYER, PATRICIA L. N89-19226
MEYERS, MICHAEL P. N89-19721
MIELKE, MICHAEL N89-19331
MIFUNE, MITSURU N89-19928
MILES, P. R. N89-19794
MILLER, DANIEL H. N89-19903
MILLER, DAVID W. N89-19342
MILLER, G. P. N89-19573
MILLER, LANE R. N89-19554
MILLER, LAWRENCE N89-19845
MILLER, THOMAS L. N89-19305
MILLIN, N. N89-19323
MILLS, WILLIAM J., JR. N89-19799
MIN, BYUNG-JIN N89-19579
MISLICK, GREGORY K. N89-19294
MITCHELL, G. H. N89-19300
MITCHELL, PAUL N89-19821
MITRA, S. K. N89-19611
MITROVICH, DASHAN N89-19551
MITSUNOBU, SHINJI N89-19997
MIYATAKE, MASAYOSHI N89-19667
MIYOSHI, KAZUHISA N89-19435
MOERDER, DANIEL D. N89-19316
MOERS, H. N89-19419
MOLLEKOPF, G. N89-19767
MONHEN, V. K. N89-19689

MONTEDORI N89-19364
MONTEIRONETO, OTHON DEREGO N89-20020
MOOIWEER, A. N89-19300
MOORHEAD, A. J. N89-19439
MORASCA, SANDRO N89-19914
MORERA, OSVALDO N89-19849
MORGAN, SAMUEL H. N89-19749
MORI, TARO N89-19674
MORIKAWA, MASAHIRO N89-20022
MORITANI, MASAHARU N89-19925
MORRELL, FREDERICK R. N89-19230
MORRIS, KEITH N89-19887
MORRISON, G. L. N89-19555
MRACEK, CURTIS PAUL N89-19269
MUDGWAY, D. J. N89-19464
MUELLER, HAROLD A. N89-19541
MUELLER, KLAUS-PETER N89-19697
MUELLER, STEPHEN J. N89-19889
MUGITANI, TAKAKO N89-19928
MUKAMEL, SHAUL N89-19974
MULLER, C. N89-19770
MULLINS, BARRY E. N89-19823
MUNDY, J. N. N89-20014
MURA, T. N89-19587
MURAKAMI, MASATAKA N89-19653
MURAKAMI, TOMOYUKI N89-19506
MUSILLI, C. N89-19495
MYERS, CHARLES N89-19778
MYSOOR, N. N89-19465

N

NADLER, SHACHAR N89-19976
NAEGELI, D. W. N89-19441
NAGAMOTO, CLARENCE N89-19700
NAGATA, SHIGEKI N89-19928
NAGEM, RAYMOND J. N89-19335
NAIR, SHYAM K. N89-19704
NAKAI, HIROTAKA N89-19997
NAPPO, CARMEN J. N89-19518
NARASIMHAN, SUNDAR N89-19570
NARDI, BONNIE A. N89-19844
NASH, T. N89-19491
NASTASI, MICHAEL N89-20008
NATIONS, JAMES N89-19324
NEAL, J. G. N89-19850
NEAL, VALERIE N89-19809
NECHAY, BOHDAN R. N89-20076
NEEF, R. D. N89-19979
NELSON, DENNIS O. N89-20077
NELSON, ERIC RAYMOND N89-20036
NELSON, H. H. N89-19389
N89-19440
NELSON, KERRI L. N89-20078
NERHEIM, ROSALEE N89-20079
NEWNAM, BRIAN E. N89-19547
NEWTON, F. C. N89-19300
NGO, KIM CHI N89-19499
NGUYEN-DUY, T. N89-19488
NICHOLLS, S. N89-19647
N89-19712
NICOLAUS, ERIC A. N89-19318
NISSEN, JOEL ALAN N89-20016
NITSCH, JOACHIM N89-19742
NOGUCHI, SYUICHI N89-19997
NOHEL, JOHN A. N89-19390
NOONE, KEVIN J. N89-19616
N89-19699
NOOR, AHMED K. N89-19579
N89-19580
NORDTVEDT, TODD N89-19324
NORTON, JEFFREY E. N89-19853
NOWICKI, L. J. N89-20011
N89-20014
NOWICKI, TOMASZ N89-19945
NUGENT, RICHARD O. N89-19841
NYGREN, THOMAS E. N89-19849

O

OBENLAND, HERBERT N89-19702
OBERGFELL, LOUISE A. N89-19872
OBRIEN, SHERMAN L. N89-19910
OBRINGER, THOMAS M. N89-19227
OCHS, HARRY T., III N89-19606
N89-19607
ODELL, PATRICK L. N89-20080
ODOM, MARY K. N89-19534
ODONNELL, PATRICK A. N89-19905
OELERICH-HILL, G. N89-19993
OERTEL, JOHN A. N89-19551
OGREN, JOHN A. N89-19616
N89-19699
OJAKANGAS, GREGORY WAYNE N89-20052
OKADA, K. N89-19719
OLSDER, G. J. N89-19946
OLSEN, E. T. N89-19466
OLSON, JUDITH REITMAN N89-19857
OLSON, W. P. N89-19760
OMLIE, AUSTIN R. N89-19295
OPPENHEIM, IRVING J. N89-19884
ORALTAY, RIZA G. N89-19612
ORMSBY, J. N89-19729
ORTIZ, CELINA M. N89-19922
ORVILLE, H. D. N89-19680
OSHER, STANLEY N89-19939
OSTROFF, AARON J. N89-19309
OTSUKA, NOBUO N89-20005
OU, SZU-CHENG S. N89-19644
OVADYA, S. Y. N89-19816
OVERTON, W. C., JR. N89-20015
OWENS, G. A. N89-19382
OWNBEY, KATRINA L. N89-19899
OZGUNER, UMIT N89-19346

P

PAIK, HO JUNG N89-19749
PAL, S. R. N89-19718
PALMER, KAROL K. N89-19827
PALUCH, ILGA R. N89-19628
PAMIDI, P. R. N89-19583
PANG, CHUNK-KIANG N89-19469
PARABONI, A. N89-19480
N89-19481
PARKER, H. KEITH N89-19291
PARKIN, DON M. N89-20008
PARSONS, H. MCILVAINE N89-19890
PARTCH, R. N89-19433
PARUNGO, FARN N89-19700
PASCHENKO, ALEKSANDR N89-19665
PATRICK, CLINT N89-19825
PAVESI, B. N89-19285
PAYNTER, GERALD C. N89-19507
PEDELTY, JEFFREY ALAN N89-20055
PEDERSEN, F. H. N89-19496
PEDERSOLI, M. N89-19931
PENFIELD, PAUL, JR. N89-19911
N89-19923
PENNER, I. E. N89-19631
PENNER, REGINALD M. N89-19398
PENNYCOOK, S. J. N89-20019
PENZHORN, R.-D. N89-19419
PERKINS, W. R. N89-19347
PERRAM, GLEN P. N89-19543
PERROTTA N89-19364
PERRY, JOHN N89-19892
PERSONNE, PASCAL N89-19676
N89-19679
PERSOON, A. J. N89-19275
PETERS, HANNS-JUERGEN N89-19282
PETERS, JEANNE M. N89-19579
PETERS, LEONARD K. N89-19704
PETRICEVIC, V. N89-19539
PETROSKY, LYMAN J. N89-19884
PEZZE, MAURO N89-19914
PFENNIG, G. N89-19419
PFITZER, K. A. N89-19760
PHAM, T. N89-19491
PHILLIPS, DWIGHT N89-19366
PHILLIPS, R. ANTHONY N89-19228
PICKERELL, D. J. N89-19302
PICKL, WILLIAM C. N89-19859
PIEL, A. N89-19993
PIELKE, ROGER A. N89-19725
PIEPER, KEITH A. N89-19301
PIETTE, DOUGLAS S. N89-19261
PILKEY, WALTER D. N89-19333
N89-19340
PILOWSKI, KARL N89-20050
PINTO, I. R. C. A. N89-19750
PINTO, O., JR. N89-19750
PIOTROWSKI, J. N89-19576
N89-19577
PIOTROWSKI, JOSEPH N89-19295
PIRZADEH, SHAHYAR N89-19250
PITT, DALE M. N89-19239
PITTER, RICHARD L. N89-19686
PLATTE, M. M. N89-19300
PLATZ, W. N89-19495
PODZIMEK, JOSEF N89-19672
POGGIO, TOMASO N89-19802
POGUE, WILLIAM N89-19809
POHL, UDO W. N89-20007
POLLARA, F. N89-19459
POLMAR, S. K. N89-20023
PONTIERI, O. C. N89-19750
PONTIKIS, CONSTANTIN N89-19630
N89-19675
POPE, ALAN T. N89-19846
POSNER, E. C. N89-19451
POST, D. N89-19584
POSTANS, P. J. N89-19413
POTTELLETTE, R. N89-19995
PRAKASH, P. N89-19624
PRASAD, J. V. N89-19314
PRATI, C. N89-19479
PRESSLY, H. B. N89-19573
PRESTON, WILLIAM J. N89-19355
PRIDDIN, C. H. N89-19525
PRIOR, J. C., JR. N89-19510
PROFFITT, MELISSA S. N89-19309
PRONK, C. N89-19919
PROTOPOPESCU, V. N89-19906
PROTTO N89-19364
PROVOST, M. J. N89-19894
PRUPPACHER, H. R. N89-19611
PUESCHEL, R. F. N89-19646
PURSEYYED, B. N89-19483
PUTVINSKIJ, S. V. N89-19989
PYKA, NIELS MICHAEL N89-20006
PYSHNOV, T. N89-19691

Q

QIAN, SHI-NAN N89-19985
QUATE, CALVIN F. N89-19398
QUIRK, F. N89-19800

R

RADKE, LAWRENCE F. N89-19645
RADZIEMSKI, LEON J. N89-19551
RAGA, GRACIELA N89-19618
RAMACHANDRAN, VIJAYA N89-19904
RAMSTHALER, JACK H. N89-19369
RANDHAWA, MANJIT S. N89-20081
RAPPAPORT, EDWARD N. N89-19788
RASMUSSEN, ROY M. N89-19723
N89-19724
RASMUSSEN, S. N89-19359
N89-19482
RASSOULK, HAMID-REZA N89-19755
RATTAN, KULDIP S. N89-19875
RAUBER, ROBERT M. N89-19722
RAYMOND, F. N89-19488
REDDER, C. R. N89-19609
REED, I. S. N89-19456
REGIAN, J. WESLEY N89-19854
RENN, H. W. N89-19329
RENN, HATTO W. N89-19330
RENNIE, DRUMMOND N89-19799
RESING, J. A. C. N89-19946
RETEL, A. P. N89-19275
REUL, CH. N89-19979
REUTER, D. C. N89-19976
REUTER, DIERK N89-19392
REUTER, GERHARD N89-19637
REW, D. W. N89-19349
RHODE, DAVID L. N89-19555
RHODES, JAMES ANDREW N89-19273
RICHARD, EVELYNE N89-19640
RICHARDS, PAUL L. N89-20000
RICHARDSON, I. G. N89-19764
RIESBECK, CHRISTOPHER K. N89-19856
RIGAUD, ARLETTE N89-19630
N89-19675
RIMEY, RAYMOND D. N89-19560
RINARD, P. M. N89-19922
RIYOPOULOS, S. N89-19538
ROACH, ROBERT C. N89-19799
ROBERS, J. P. N89-19548
ROBERT, JAMES A. N89-19858
ROBERTSON, I. M. N89-19405
ROBSON, R. R. N89-19354
ROCCA, F. N89-19479
ROCHBLATT, D. J. N89-19463
ROGERS, ROBERT C. N89-19390
ROLLESTON, ROBERT J. N89-19969
ROOS, C. N89-19918
N89-19920
ROOS, NICO N89-19933
ROSE, M. N89-19800
ROSS, CHARLES L. N89-19840
ROSSET, ROBERT N89-19711
ROSSETTI, MICHAEL A. N89-19229
ROTH, DON J. N89-19578
ROTH, R. N89-19662
ROTHMAN, S. J. N89-20011
N89-20014
ROUTBORT, J. L. N89-20011
N89-20014
ROYER, JAMES M. N89-20029

ROYER, M. N89-19488
RUDMAN, S. D. N89-19712
RUETER, HENRY H. N89-19857
RUMSEY, CHRISTOPHER L. N89-19244
N89-19252
RUO, S. Y. N89-19251
RUOFF, A. L. N89-20009
RUPP, W. N89-19360
RUSSELL, P. B. N89-19646
RUZICKA, J. N89-19418
RYAN, K. D. N89-19352

S

SABNIS, SANJEEV N89-19954
SACEDON, J. L. N89-19443
SACHS, EMANUEL M. N89-19911
SACKSTEDER, K. R. N89-19446
SADR, R. N89-19453
SAHU, JUBARAJ N89-19277
SAITO, KENJI N89-19997
SALA, A. N89-19600
SALOMONSON, V. N89-19729
SALTZMAN, ROBERT M. N89-19912
N89-19913
SAMOKHVALOV, I. V. N89-19631
SAMULSKI, EDWARD T. N89-19998
SANCHEZ-AVEDILLO, M. N89-19443
SANDFORD, MAYNARD C. N89-19255
SANKAR, N. L. N89-19251
SANTARIUS, J. F. N89-19992
SARTORY, W. K. N89-19523
SAS, P. N89-19361
SASYO, YOSHIO N89-19674
SATO, MISAO N89-19668
SAUNDERS, C. P. R. N89-19678
SAUNDERS, M. R. N89-19794
SAXENA, V. K. N89-19682
SAXTON, PATRICIA M. N89-19801
SCATTOLINI, R. N89-19930
SCHAEFER, HENRY F., III N89-19388
SCHARER, J. E. N89-19992
SCHATZLE, F. N89-19800
SCHEEL, HANS-ECKHART N89-19747
SCHEMENAUER, ROBERT S. N89-19650
SCHIAVONI, N. N89-19930
N89-19931
N89-19932
SCHILLER, DAVID N. N89-19442
SCHINDLER, T. N89-19767
SCHMIDT, H. J. N89-19990
SCHMIDT, HELMUT N89-19522
SCHMITT, HARRISON H. N89-19809
SCHMITZ, DONALD N89-19874
SCHMUDLACH, R. N89-19329
SCHNEIDER, FRANK N89-19330
SCHOFIELD, S. E. N89-19382
SCHOLZ, ARTHUR L. N89-19829
SCHRAGE, D. P. N89-19314
SCHREIBER, JEFFREY G. N89-19737
SCHREITMUELLER, W. N89-19359
N89-19482
SCHROEDER, JOYCE D. N89-19878
SCHROTH, A. N89-19656
SCHUETZ, L. N89-19684
SCHULTZ, PETER J. N89-20010
SCHULTZ, ROGER N89-19830
SCHULTZE, J. W. N89-19416
SCHULZE, ARTHUR E. N89-19809
SCHUMANN, T. N89-19695
SCHUR, ANNE N89-19852
SCHURR, STEVEN D. N89-19777
SCHWANECK, HANS-PETER N89-19896
SCHWENFEGER N89-19790
SCRUBY, C. N89-19600
SCRUGGS, JEFFREY L. N89-19880
SEATH, DONALD D. N89-19274
SECAN, JAMES A. N89-19765
SEIDEL, DAVID A. N89-19238
N89-19255
SEIDENSTICKER, KLAUS J. N89-20046
SEIDL, WINFRIED N89-19683
N89-19690
SEILER, WOLFGANG N89-19747
SELLECK, COLIN N89-19916
SEN, A. N89-19975
SENTURIA, STEPHEN D. N89-19911
SERRANO, F. N89-19622
SHA, H. J. N89-19424
SHAASHUA, AMNON N89-19806
SHAFFER, WINSTON J., II N89-19317
SHAHSHAHANI, M. N89-19453
SHAKLEY, DONALD N89-19842
SHAMANAEV, V. S. N89-19631
SHANKAR, VIJAYA N89-19243
SHAPIRO, LINDA G. N89-19867
SHARBER, J. R. N89-19763
SHARP, J. W. N89-20019
SHARTS, B. N89-19729
SHAVOKHINA, N. S. N89-19936
SHAW, DORIS S. N89-19907
SHE, CHIAO-YAO N89-19759
SHEREMETYEVSKIY, N. N. N89-19487
SHERMAN, DOUGLAS J. N89-19290
SHEVTSOV, B. M. N89-19486
SHIAU, NAE-HAUR ERIC N89-19270
SHIELDS, NICHOLAS L., JR. N89-19862
SHIELDS, NICHOLAS, JR. N89-19809
SHIH, CHING-LONG N89-19563
SHIMADA, WATARU N89-19667
SHIRAISHI, YASUHIRO N89-19927
SHORT, WALTER D. N89-19744
SHOWALTER, ROBERT R. N89-19546
N89-19549
SHROBE, HOWARD E. N89-19838
SIEGEL, JEROME N89-19801
SIELAFF, S. F. N89-19280
SILK, ROBERT N89-19551
SIMMONS, E. L. N89-19712
SIMON, M. K. N89-19454
SIMON, P. C. N89-19769
SIMONS, JACK N89-19395
SIMPSON, JOANNE N89-19789
SIMPSON, L. BRUCE N89-19245
SINATRA, GALE M. N89-20029
SINCLAIR, G. B. N89-19585
SINGER, H. J. N89-19764
SINGER, S. N89-19493
SINGH, G. N89-19624
SIRCH, M. N89-19419
SISSON, DAVID F. N89-19801
SKINNER, GARY L. N89-19295
SLAVIN, J. A. N89-19764
SLEMR, FRANZ N89-19747
SMITH, A. J. N89-19319
SMITH, C. W. N89-19584
SMITH, DAVID N89-19394
SMITH, DAVID J. N89-20013
SMITH, JEFFREY H. N89-19682
SMITH, RANDY L. N89-19861
SMITH, ROBERT D. N89-19283
SMITH, SUZANNE WEAVER N89-19350
SMOLARKIEWICZ, PIOTR K. N89-19634
N89-19723
SNEAD, C. L., JR. N89-20010
SNEAD, ROBERT N89-19468
SNECKENBERGER, JOHN E. N89-19863
SNYDER, GLENN R. N89-19970
SOERENSEN, R. N89-19654
SOLLIE, GERRIT N89-19804
SOLT, T. S. N89-19743
SONDHEIMER, NORMAN N89-19845
SONI, A. H. N89-19865
SOTOMAYER, W. A. N89-19235
SOTTA, J. P. N89-19447
SOULAGE, R. G. N89-19625
SOULE, MATTHEW N89-19299
SPANNER, M. A. N89-19646
SPECKMAN, KAREN L. N89-19811
SPIEKERMAN, M. N89-19767
SPROUL, A. N89-19740
SRINIVASAN, S. N89-19745
SRNSKY, R. A. N89-19743
STACHOWITZ, R. A. N89-19834
STACY, KENNETH L. N89-19819
STAKENBORG, MARCEL JOS LOU N89-19574
STAMM, JAMES A. N89-19594
STANG, DAVID B. N89-19578
STARKS, SCOTT A. N89-20082
STATMAN, J. N89-19459
STAVRINIDIS, C. N89-19361
STEED, ALLAN J. N89-19751
STEFFLER, JEAN C. N89-19279
STEFKO, GEORGE L. N89-19265
STEIER, WILLIAM H. N89-19982
STEIMLE, T. C. N89-19975
STEINERT, W. N89-19359
STEPHENS, GRAEME L. N89-19643
STERZENBACH, G. N89-19979
STESSENS, W. N89-19495
STIMPSON, R. N89-19303
STOLFA, R. N89-19766
STOLP, J. N89-19735
STOREY, PAUL N89-19824
STROUD, C. W. N89-19892
STUART, MARK A. N89-19861
STUTZMAN, WARREN L. N89-19472
STUURMAN, CAREL N89-19329
N89-19330
SU, WENHAN N89-19509
SUDKAMP, THOMAS N89-19836
SUDO, YUKIO N89-19506
SULMEISTERS, TAL N89-19369
SVIATOSLAVSKY, I. N. N89-19992
SWANSON, STEPHEN R. N89-19378
N89-19383
SWENSON, G. R. N89-19327
SYERS, G. N89-19436
SYKES, GEORGE F., JR. N89-19385
SZATKOWSKI, GERARD P. N89-19830
SZUMOWSKI, A. P. N89-19527

T

TACCONI-GARMAN, LINDA JEAN N89-20043
TAGHVA, KAZEM N89-19902
TAJIMA, TSUYOSHI N89-19997
TAKACS, P. Z. N89-19985
TAKAHASHI, TSUNEYA N89-19608
TAKAHASHI, YASUO N89-19986
TAKAMIZAWA, KOICHIRO N89-19472
TAKAYA, YOSHIMASA N89-19633
TALLIO, K. V. N89-19510
TALLMAN, C. R. N89-19548
TALLMAN, CHARLES R. N89-19552
TAMASSIA, ROBERTO N89-19901
TAN, ARJUN N89-20083
TANAKA, T. N89-19719
TANG, C. M. N89-19538
TANI, KEISUKE N89-19667
TATNALL, A. R. L. N89-19363
TAYLOR, A. J. N89-19548
TAYLOR, DEBORAH B. N89-19316
TAYLOR, GREGORY R. N89-19627
N89-19705
TAYLOR, IVOR J. N89-19301
TAYLOR, P. A. N89-19396
N89-19397
TEAGAN, W. P. N89-19741
TEARE, D. N89-19314
TEBOULLE, MARC N89-19937
TEETER, R. N89-19871
TELSCHOW, K. L. N89-19967
TENNANT, ROGER A. N89-19552
TERMAN, D. N89-20054
TEUNISSEN, PETER J. G. N89-19736
THIELMAN, C. Y. N89-19850
THOMAS, G. N89-19800
THOMAS, JAMES L. N89-19244
THOMPSON, L. J. N89-20014
THUNBORG, SIGFRIED N89-19916
TIEDERMAN, WILLIAM G. N89-19521
TIMMERMANS, CEES A. N89-19950
TISCHLER, J. Z. N89-20019
TITRAN, ROBERT H. N89-19371
TODA, MITSUHIKO N89-19926
TODD, WAYNE N89-19839
TOETENEL, W. J. N89-19919
TOKUDA, A. N89-19719
TOLLIVER, C. L. N89-20084
TOMAZOV, S. T. N89-19658
TONGUE, B. H. N89-19314
TONOLINI, F. N89-19601
TOOGOOD, T. L. N89-19300
TORKILDSEN, T. N89-19285
TOSA, MASAHIRO N89-19997
TRACHT, TOM N89-19938
TREJO, LEONARD J. N89-19797
TREUMANN, R. A. N89-19995
N89-19996
TRIKHA, A. K. N89-19280
N89-19281
TRINKS, H. N89-19370
TRIPODI, F. N89-20049
TRIPOLI, GREGORY J. N89-19641
N89-19648
TRIVEDI, MOHAN M. N89-19572
TRUONG, T. K. N89-19455
N89-19456
TRUSZKOWSKI, WALTER F. N89-19855
TSAU, FANG-HEI N89-19386
TSENG, G. T. N89-19341
TSURUTANI, B. T. N89-19764
TUCKER, RICHARD W. N89-19841
TYAHLA, S. T. N89-19374
N89-19379
TZAVARAS, ATHANNASSIOS E. N89-19390

U

UHERKA, K. L. N89-19746
ULLMAN, SHIMON N89-19806
ULWICK, JAMES C. N89-19751

V

VADALI, S. R. N89-19596
VALERO, FRANCISCO P. J. N89-19649
VALI, GABOR N89-19622
VALLE, F. N89-19931
VALLETTE, B. N89-19729
VANBEEK, P. N89-19528
VANDENHOF, PAUL M. J. N89-19941
VANDERBEEK, C. G. A. N89-19948
VANDERHOFF, JOHN A. N89-19399
VANDERLAAN, F. B. N89-19733
VANDERMAREL, HANS N89-20038
VANDERVORST, H. A. N89-19951
VANDEWALLE, R. N89-19495
VANELDIK, R. N89-19687
VANHULSTEYN, D. B. N89-20015
VANKATWIJK, J. N89-19919
VANSTRIEN, SEBASTIAN N89-19945
VANYSEK, PETR N89-19393
VAUGHAN, HARRY C. N89-19663
VENTO, D. M. N89-19446
VERBOS, ROBERT M. N89-19569
VERDON, JOSEPH M. N89-19263
VERHEIJ, L. F. N89-19733
VERHULST, F. N89-20054
VERMEIREN, J. N89-19495
VERSINI, B. N89-19766
VISSERS, M. A. P. N89-19735
VOHL, O. N89-19611
VOLKMER, KENT N89-19882
VONFLOTOW, ANDREAS H. N89-19342
VORBRUGG, H. N89-19360
VOS, F. A. N89-20026

W

WADE, JOHN E. N89-19781
WAGENMAKER, RICHARD N89-19773
WAKAHAMA, GOROW N89-19608
N89-19726
WAKE, B. E. N89-19251
WALCEK, CHRIS J. N89-19708
WALDROP, J. R. N89-19492
WALDVOGEL, A. N89-19695
WALKER, DAVID T. N89-19521
WALKER, STEL N. N89-19781
WALLACE, R. J. N89-19464
WALLACE, R. M. N89-19396
N89-19397
WALSTROM, P. L. N89-19992
WALTHER, CRAIG N89-19717
WANG, ANG-SHENG N89-19610
WANG, CAROLINE N89-19825
WANG, LIU N89-19869
WARHOLA, GREGORY THOMAS N89-19470
WATSON, JOHN A. N89-19519
WATZIN, J. G. N89-19870
WAUGHTAL, S. P. N89-19555
WEAVER, H. T. N89-19977
WEBB, JAMES T. N89-19796
WEBB, STEVEN GARNETT N89-19312
WEEKS, DAVID J. N89-19822
WEIDENHAGEN, DIETER N89-19296
WEILAND, P. L. N89-19881
WEINBRECHT, CARL E. N89-19778
WEISSBLUTH, MICHAEL J. N89-19725
WELDON, VINCENT N89-19366
WEN, JING JIANG N89-19972
WENGER, LOWELL E. N89-20002
WENHAM, S. R. N89-19740
WERHAHN, JOHANNES N89-19747
WERKHEISER, ANNE N89-19730
WESLEY, DOUGLAS A. N89-19725
WESSELING, P. N89-19949
N89-19953
WETEKAMM, JULES N89-19891
WETZEL, ERIC N89-19366
WHANG, R. N89-19800
WHITCOMB, BRUCE MAGILL N89-19756
WHITE, CARL L. N89-19866
WHITE, MICHAEL E. N89-19295
WHITE, R. E. N89-19745
WHITEHEAD, MICHAEL C. N89-19552
WHITFIELD, DAVE N89-19250
WHITLOW, WOODROW, JR. N89-19242
WHITMARSH, R. B. N89-19794
WILBUR, PAUL J. N89-19973
WILCHER, J. H. N89-19464
WILCOX, BRIAN H. N89-19877
N89-19879
WILKINS, S. CURTIS N89-19423
WILLEY, RONALD J. N89-20085
WILLIAMS, JAMES H., JR. N89-19335
WILLIAMS, LINDA J. F. N89-19831
WILLIAMSON, W. W. N89-19354
WILLIN, E. N89-19419
WILLNECKER, RAINER N89-19415
WILLNER, JOACHIM N89-19288
WILSON, DONALD R. N89-19274
WINER, E. A. N89-19284
WINKELJOHN, D. M. N89-19289
WINNINGHAM, J. D. N89-19763
WINTER, CARL-JOCHEN N89-19742
WIRT, U. N89-19329
WISEALL, S. S. N89-19533
WITTENBURG, J. L. N89-19992
WONG, P. S. N89-19438
WONG, SEE-POK N89-20004
WOOD, DOUGLAS OWEN STARKEY N89-20044
WOOD, ROBERT A. N89-19799
WOODROOFE, MICHAEL N89-19956
WRIGHT, P. N89-19530
N89-19531
WRIGHT, R. A. N89-19300
WRIGLEY, R. C. N89-19646
WU, C. K. N89-19881
WU, HENRY M. N89-19893
WU, TIAN-ZHENG N89-19902
WU, X. Q. N89-19598
WU, ZONG YENG N89-19313
WYNNE, A. N89-19532

X

XIAO, HUI N89-19642
XU, HUAYING N89-19642

Y

YAMASHITA, AKIRA N89-19667
YANG, J. N. N89-19597
YANG, J.-M. N89-19384
YATES, E. CARSON, JR. N89-19246
YATES, J. T., JR. N89-19396
N89-19397
N89-19400
YEDAVALLI, RAMA K. N89-19315
YEH, HUN C. N89-19421
YIN, X. N89-19456
YONEMOTO, KOICHI N89-19353
YOSHIHARA, KAZUHIRO N89-19997
YOSHIKATA, KAZUKI N89-19863
YOUNG, K. DAVID N89-19348
YUEN, J. H. N89-19454
YUI, KATSUHIKO N89-19925
YURKOVICH, STEVE N89-19346

Z

ZAEPFEL, KLAUS P. N89-19783
ZAK, MICHAIL N89-19338
ZAVESKY, R. J. N89-19446
ZEANAH, HUGH N89-19825
ZEHE, MICHAEL J. N89-19402
ZERROUK, A. F. N89-20045
ZHANG, SHI FENG N89-19757
ZHAO, BOLIN N89-19727
ZIK, J. N89-19871
ZIMMERMAN, D. C. N89-19339
ZIMMERMAN, WAYNE N89-19882
ZINDER, B. N89-19695
ZINN, BEN T. N89-19392
ZMUDA, T. N89-19491
ZUCKERWAR, ALLAN J. N89-19499
ZUEV, V. E. N89-19631
ZWAAN, R. J. N89-19275
ZWEBEN, MONTE N89-19820

Typical Corporate Source Index Listing

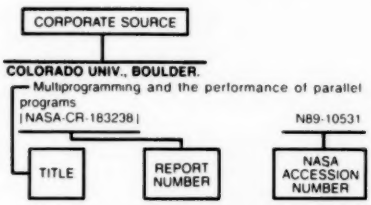

Listings in this index are arranged alphabetically by corporate source. The title of the document provides the user with a brief description of the subject matter. The report number helps to indicate the type of document cited (e.g., NASA report, translation, NASA contractor report). The NASA accession number denotes the number by which the citation is identified. The titles are arranged under each corporate source in ascending accession number order.

A

ACADEMIA SINICA, BEIJING (CHINA).
The contrast study of new model on ice crystal growth N89-19610
The study of numerical simulation on the formation of the cloud droplet spectra in cumulus clouds N89-19642
A numerical simulation of the acidification process of rain water below the cloud and the mechanism of acid rain formation in area of Chongqing, China N89-19706

ACADEMY OF SCIENCES OF THE GEORGIAN SSR, TBILISI.
Effect of the electric field on the raindrop shape N89-19659
About secondary ice crystal production N89-19666

ACADEMY OF SCIENCES (USSR), TOMSK.
Structure of upper clouds boundary using the lidar data N89-19631

ADVISORY GROUP FOR AEROSPACE RESEARCH AND DEVELOPMENT, NEUILLY-SUR-SEINE (FRANCE).
Calendar of selected aeronautical and space meetings: January 1989 onwards
[AGARD-CAL-89/1] N89-20024

AERONAUTICAL RESEARCH LABS., MELBOURNE (AUSTRALIA).
An examination of the fatigue meter records from the RAAF (Royal Australian Air Force) caribou fleet
[AD-A201074] N89-19290
Thermal stress in Ran Sea King Helicopter operations
[ARL-SYS-R-40] N89-19810

AEROSPACE CORP., EL SEGUNDO, CA.
An invariant imbedding T matrix approach to electromagnetic scattering
[AD-A202298] N89-19476
Reciprocal theorem of residual stress and inelastic strain
[AD-A202353] N89-19598
Substorms, plasmoids, flux robes, and magnetotail flux loss on March 25, 1983: CDAW-8
[NASA-CR-184823] N89-19764
Portable inference engine: An extended CLIPS for real-time production systems N89-19843
Mechanisms leading to single event upset
[ATR-86(8139)-5] N89-19977
Raman and RBS studies of ion implanted semiconductors
[ATR-88(8359)-5] N89-20021

AEROSPACE CORP., LOS ANGELES, CA.
Integrated Structural Analysis And Control (ISAAC): Issues and progress N89-19341

AEROSPACE MEDICAL RESEARCH LABS., WRIGHT-PATTERSON AFB, OH.
A schema-based model of situation awareness: Implications for measuring situation awareness N89-19847
The use of the articulated total body model as a robot dynamics simulation tool N89-19872

AEROSTRUCTURES, INC., ARLINGTON, VA.
NASTRAN supplemental documentation for modal forced vibration analysis of aerodynamically excited turbosystems
[NASA-CR-174967] N89-19583

AIR FORCE ARMAMENT LAB., EGLIN AFB, FL.
Unsteady transonic flow using Euler equations N89-19245
EMMA: The expert system for munition maintenance N89-19823

AIR FORCE GEOPHYSICS LAB., HANSCOM AFB, MA.
Measurements of shuttle glow on mission STS 41-G
[AD-A201769] N89-19327

AIR FORCE HUMAN RESOURCES LAB., WRIGHT-PATTERSON AFB, OH.
Intelligent tutoring systems research in the training systems division: Space applications N89-19854

AIR FORCE INST. OF TECH., WRIGHT-PATTERSON AFB, OH.
Estimating aircraft airframe tooling cost: An alternative to DAPCA 3
[AD-A201506] N89-19226
Analysis of cost growth and cost composition in the defense aerospace industry
[AD-A201544] N89-19227
R and M (Reliability and Maintainability) quality team concept and C-17 design at Douglas Aircraft Company: An R and M 2000 initiative case study
[AD-A201574] N89-19228
Time periodic control of a multiblade helicopter N89-19312
A study to analyze the degree of the relationship between health practices and fatigue
[AD-A201518] N89-19798
An analysis of the impact of log-linear regression on the estimated learning curve parameters
[AD-A201471] N89-19938
Factors affecting the adoption of R and D project selection techniques at the Air Force Write Aeronautical Laboratories
[AD-A201543] N89-20025
An investigation of factors affecting domestic technology transfer at the Wright Aeronautical Laboratories
[AD-A201581] N89-20032

AIR FORCE OCCUPATIONAL AND ENVIRONMENTAL HEALTH LAB., BROOKS AFB, TX.
Noise assessment of the rocket sled test track operation at Holloman AFB, New Mexico
[AD-A201279] N89-19317

AIR FORCE WEAPONS LAB., KIRTLAND AFB, NM.
The standard chemical oxygen-iodine laser kinetics package
[AD-A202223] N89-19543

AIR FORCE WRIGHT AERONAUTICAL LABS., WRIGHT-PATTERSON AFB, OH.
Unsteady aerodynamics and aeroelastic research at AFWAL N89-19235
A parallel expert system for the control of a robotic air vehicle N89-19842
Light weight escape capsule for fighter aircraft N89-19858
Chemical warfare protection for the cockpit of future aircraft N89-19859

AIR WAR COLL., MAXWELL AFB, AL.
RPV (Remote Piloted Vehicle) applications in the US Navy
[AD-A202151] N89-19293
A case study of small group decision-making as influenced by the Abilene Paradox: The Challenger mishap
[AD-A202102] N89-19328

AIRESEARCH CASTING CO., TORRANCE, CA.
Improved silicon nitride for advanced heat engines
[NASA-CR-179525] N89-19421

AKITA UNIV. (JAPAN).
On the variation of falling velocity of early snowflakes N89-19670

ALABAMA A & M UNIV., NORMAL.
Estimation of velocity perturbations in satellite fragmentation events N89-20083

ALABAMA UNIV., HUNTSVILLE.
FONR optical computing ST
[AD-A201002] N89-19897

ALABAMA UNIV., UNIVERSITY.
The effect of hydrogen on fatigue crack growth rate of AISI 304 stainless steel N89-19410

ALCATEL ESPACE, TOULOUSE (FRANCE).
Meteosat Millimetre Wave Sounder (MWS) study
[BAE-TP-9119] N89-19363

ALLIED-SIGNAL AEROSPACE CO., KANSAS CITY, MO.
Electron beam welding of 6061-T6 covers to A356-T6 machined cast housings
[BDX-613-3915] N89-19573

ANT NACHRICHTENTECHNIK, BACKNANG (GERMANY, F.R.).
Definition of the transmission system for a European data relay satellite
[ESA-CR(P)-2632] N89-19359
Code performance simulation study for DRS S-band transmission
[ESA-CR(P)-2688] N89-19482

ANTHROPOLOGY RESEARCH PROJECT, YELLOW SPRINGS, OH.
Computer software used in US Army Anthropometric Survey 1987-1988
[AD-A201185] N89-19812
The development and validation of an automated headboard device for measurement of three-dimensional coordinates of the head and face
[AD-A201186] N89-19813

ARGONNE NATIONAL LAB., IL.
Development of Nuclear Magnetic Resonance (NMR) imaging technology for advanced ceramics
[DE89-006400] N89-19438
Parameterizations of microphysical processes in clouds for application in models of regional atmospheric deposition N89-19709
A study of the reliability of Stirling engines for distributed receiver systems
[DE89-006395] N89-19746
High-precision laser and RF spectroscopy of atomic, molecular, and slow ion beams
[DE89-005870] N89-19975
Oxygen diffusion in YBa2Cu3O7-delta
[DE89-005831] N89-20011
Mossbauer effect studies of magnetism in superconducting systems
[DE89-005844] N89-20012
Atomic structure of tilt grain boundaries in NiO
[DE89-005847] N89-20013
SIMS measurement of oxygen tracer diffusion in YBa2Cu3O7-delta
[DE89-005884] N89-20014

ARIZONA STATE UNIV., TEMPE.
An efficient method for computing unsteady transonic aerodynamics of swept wings with control surfaces
[AIAA-85-4058] N89-19241
Atomic structure of tilt grain boundaries in NiO
[DE89-005847] N89-20013

ARIZONA UNIV., TUCSON.
Estimating projected controllable sets for dynamical control systems N89-19313
An infrared reflectance study of water in outer belt asteroids N89-20037

ARMY ARMAMENT RESEARCH, DEVELOPMENT AND ENGINEERING CENTER, WATERVLIET, NY.
Determination of residual stress distributions in autofrettaged tubing: A discussion
[AD-A201454] N89-19586

ARMY AVIATION ENGINEERING FLIGHT ACTIVITY, EDWARDS AFB, CA.
Combined preliminary airworthiness evaluation and airworthiness and flight characteristics evaluation of the UH-1H with preproduction hub spring and composite main rotor blades installed
[AD-A202316] N89-19295

ARMY AVIATION SYSTEMS COMMAND, CLEVELAND, OH.
An expert system for restructurable control N89-19886

ARMY COLD REGIONS RESEARCH AND ENGINEERING LAB., HANOVER, NH.
The effect of aerosols on pH of snowfalls N89-19688
ARMY CONSTRUCTION ENGINEERING RESEARCH LAB., CHAMPAIGN, IL.
Intelligent embedded instruction for Computer-Aided Design (CAD) systems
[AD-A201811] N89-19907
ARMY ENGINEER TOPOGRAPHIC LABS., FORT BELVOIR, VA.
Computer generation of fractal terrains
[AD-A201171] N89-19730
ALMA COLL., MI.
A model for plasma volume changes during short duration spaceflight N89-20067
ARMY MISSILE COMMAND, REDSTONE ARSENAL, AL.
Electromagnetic compatibility test report for the tethered satellite data acquisition and control assembly
[AD-A201549] N89-19468
Analysis of PERSHING 2 Reentry Vehicle (RV) control ring castings
[AD-A201548] N89-19559
ARMY NATICK RESEARCH AND DEVELOPMENT COMMAND, MA.
Cooling effectiveness of a hybrid microclimate garment
[AD-A201115] N89-19811
ARMY RESEARCH INST. OF ENVIRONMENTAL MEDICINE, NATICK, MA.
Dexamethasone for prevention and treatment of acute mountain sickness
[AD-A201554] N89-19799
Satellite remote sensing of heat stress during reserve training at Fort Hood
[AD-A201555] N89-19800
ATMOSPHERIC ENVIRONMENT SERVICE, DOWNSVIEW (ONTARIO).
The collection efficiency of a massive fog collector N89-19650
Vertical profiles of pollutants inside and outside of cloud N89-19696
Intercomparisons of aircraft measurements with lidar returns for aerosol, ice crystals and water droplets N89-19718
AUBURN UNIV., AL.
The Ninevah Mission: A design summary for an unmanned mission to Venus, volume 1
[NASA-CR-184705] N89-20040
The Ninevah Mission: Analytical analyses and calculations for trajectory and propulsion, volume 2
[NASA-CR-184706] N89-20041

B

BALLISTIC RESEARCH LABS., ABERDEEN PROVING GROUND, MD.
Numerical computations of transonic critical aerodynamic behavior
[AD-A202412] N89-19277
Spectral studies of propellant combustion: Experimental details and emission results for M-30 propellant
[AD-A201634] N89-19399
BATTELLE COLUMBUS LABS., OH.
Studies and analyses of the space shuttle main engine. Appendix B: SSME FIPM drawings
[NASA-CR-183594] N89-19365
Diagnostics in the Extendable Integrated Support Environment (EISE) N89-19824
BAYLOR UNIV., WACO, TX.
Equating an expert system to a classifier in order to evaluate the expert system N89-20080
BEGELEIDINGSCOMMISSIE REMOTE SENSING, DELFT (NETHERLANDS).
The use of LANDSAT imagery for water quality studies in the Ijsselmeer area (Netherlands)
[BCRS-87-18] N89-19732
Land use analysis using remote sensing techniques. Investigation of the usefulness of LANDSAT Thematic Mapper satellite pictures for obtaining and up to date picture of land use in the province South Holland
[BCRS-88-01] N89-19733
Salinity mapping based on SPOT images of the Punjab, Pakistan
[BCRS-88-03] N89-19734
Study of the use of radar X-band data of bare soil in a radar scattering model
[BCRS-88-04] N89-19735
BEIJING UNIV. (CHINA).
Study on cloud and rain by microwave radiometer observation N89-19727
BIRMINGHAM UNIV. (ENGLAND).
Ion and electron interactions at thermal and suprathermal energies
[AD-A201418] N89-19394
BOEING ADVANCED SYSTEMS CO., SEATTLE, WA.
Hypervelocity technology escape system concepts. Volume 1: Development and evaluation
[AD-A201719] N89-19280
Hypervelocity technology escape system concepts. Volume 2: Software manual
[AD-A201720] N89-19281
Error norm guided flow analysis of shock-wave/boundary-layer interactions
[AD-A201176] N89-19507
BOEING AEROSPACE CO., KENNEDY SPACE CENTER, FL.
Electronic data generation and display system N89-19891
BOEING AEROSPACE CO., SEATTLE, WA.
Booster propulsion/vehicle impact study
[NASA-CR-183584] N89-19366
BOEING COMMERCIAL AIRPLANE CO., SEATTLE, WA.
Flight survey of the 757 wing noise field and its effects on laminar boundary layer transition. Volume 2: Data compilation
[NASA-CR-178217] N89-19505
An experimental evaluation of S-duct inlet-diffuser configurations for turboprop offset gearbox applications
[NASA-CR-179454] N89-19556
BOEING MILITARY AIRPLANE DEVELOPMENT, SEATTLE, WA.
Extensions and improvements on XTRAN3S N89-19236
BOSTON UNIV., MA.
The boundary element method for the diffusion equation N89-19233
BRANDEIS UNIV., WALTHAM, MA.
VLBI polarization measurements of BL Lacertae objects N89-20035
BRITISH AEROSPACE PUBLIC LTD. CO., STEVENAGE (ENGLAND).
Meteosat Millimetre Wave Sounder (MWS) study
[BAE-TP-9119] N89-19363
BRITISH BROADCASTING CORP., KINGSWOOD (ENGLAND).
On the design of loudspeakers for broadcast monitoring
[BBC-RD-1988/14] N89-19450
BROOKHAVEN NATIONAL LAB., UPTON, NY.
Description of FEL3D: A three dimensional simulation code for TOK and FEL
[DE89-005529] N89-19540
Processes determining cloudwater composition: Field evidence for in-cloud reactive scavenging of SO2 N89-19693
Long trace profile measurements on cylindrical aspheres
[DE89-005661] N89-19985
Positron spectroscopy for materials characterization
[DE89-005766] N89-20010
BROWN UNIV., PROVIDENCE, RI.
The effects of tempering and test temperature on the dynamic fracture initiation behavior of an AISI 4340 VAR steel
[AD-A201606] N89-19408
Steady waves in a nonlinear theory of viscoelasticity N89-19470
Multiprocessor control of robotic manipulators N89-19562
BUREAU OF RECLAMATION, DENVER, CO.
Comparison of orographic cloud and precipitation development of three different geographic locations using a 3-D nested grid cloud model N89-19723

C

CALIFORNIA INST. OF TECH., PASADENA.
Tip vortices: Single phase and cavitating flow phenomena N89-19271
Applications of scanning tunneling microscopy to electrochemistry
[AD-A201613] N89-19398
Mixing in gas phase turbulent jets N89-19515
Experimental investigation of rotor-stator interaction in diffuser pumps N89-19564
Plastic buckling of cylinders under biaxial loading N89-19591
Raman and RBS studies of ion implanted semiconductors
[ATR-88(8359)-5] N89-20021
Episodic volcanism of tidally heated satellites with application to Io. Thermal state of an ice shell on Europa. Polar wander of a synchronously rotating satellite with application to Europa N89-20052
Studies of flares and disappearing magnetic flux
[AD-A201456] N89-20053
CALIFORNIA UNIV., BERKELEY.
The coupled cluster method and the properties of energetic materials
[AD-A201168] N89-19388
Scanning tunneling microscopy of metals on graphite
[DE89-006608] N89-19404
Thermal oxidation of 3-5 compound semiconductors
[DE89-007127] N89-20020
CALIFORNIA UNIV., BERKELEY. LAWRENCE BERKELEY LAB.
Scanning tunneling microscopy of metals on graphite
[DE89-006608] N89-19404
Thermal oxidation of 3-5 compound semiconductors
[DE89-007127] N89-20020
CALIFORNIA UNIV., DAVIS.
Quantum limits of superconducting heterodyne receivers
[AD-A201303] N89-20000
CALIFORNIA UNIV., IRVINE.
Experiment plans to study preignition processes of a pool fire in low gravity
[NASA-CR-182256] N89-19442
CALIFORNIA UNIV., LOS ANGELES.
Reciprocal theorem of residual stress and inelastic strain
[AD-A202353] N89-19598
Applied partial differential equations and numerical analysis
[AD-A201749] N89-19939
Interstellar matter in early type galaxies N89-20042
CALIFORNIA UNIV., MARINA DEL REY.
Presentation planning using an integrated knowledge base N89-19845
CALIFORNIA UNIV., SAN DIEGO.
Thermonuclear reactions of light nuclei in astrophysical plasmas N89-19988
CALSPAN-BUFFALO UNIV. RESEARCH CENTER, NY.
An intelligent multi-media human-computer dialogue system N89-19850
CAMUS, INC., HUNTSVILLE, AL.
Man-systems requirements for the control of teleoperators in space N89-19862
CARNEGIE-MELLON INST. OF RESEARCH, PITTSBURGH, PA.
Fundamentals of fatigue and fracture mechanics
[AD-A201435] N89-19585
CARNEGIE-MELLON UNIV., PITTSBURGH, PA.
Sensor fusion of range and reflectance data for outdoor scene analysis N89-19868
A novel manipulator technology for space applications N89-19874
A robust control scheme for flexible arms with friction in the joints N89-19875
ISTAR evaluation
[AD-A201345] N89-19903
CENTER FOR NAVAL ANALYSES, ALEXANDRIA, VA.
Reaction chemistry of boron hydrides
[AD-A201243] N89-19389
CENTRAL ELECTRICITY RESEARCH LABS., LEATHERHEAD (ENGLAND).
Oxidation regimes in orographic capping cloud N89-19698
CENTRAL STATE UNIV., WILBERFORCE, OH.
Concept for a large master/slave-controlled robotic hand N89-19866
CENTRE D'ESSAIS AERONAUTIQUE TOULOUSE (FRANCE).
Lightning campaign 85/86 Transall C160 A04: Flying tests
[REPT-85/535800] N89-19297
CENTRE NATIONAL DE LA RECHERCHE SCIENTIFIQUE, PARIS (FRANCE).
Mini protein crystallization facility. Phase A study: Executive summary
[REPT-AQ-ES-576/88] N89-19444
CENTRE NATIONAL DE RECHERCHES METEOROLOGIQUES, TOULOUSE (FRANCE).
Heterogeneous mixing measurements in small nonprecipitating cumuli N89-19635
CENTRO INFORMAZIONI STUDI ESPERIENZE, MILAN (ITALY).
Acoustic emission measurements during fatigue loading of scaled Pressurized Water Reactor (PWR) vessel at Joint Research Center of the European Communities (JRC), Ispra (Italy)
[CISE-4476] N89-19600
General review of recent activities in acoustic emission technology in Italy
[CISE-4477] N89-19601
CERAMIC PROCESS SYSTEMS CORP., CAMBRIDGE, MA.
Composite ceramic superconducting wires for electric motor applications
[AD-A201810] N89-19429

CHRISTIAN ROVSING LTD., COPENHAGEN (DENMARK).
Electronic Power Conditioner (EPC) for carcinotrons [R/D/REPO/8801] N89-19496
CINCINNATI UNIV., OH.
The use of direct sparse matrix methods and Newton iteration for the numerical solution of fluid flows N89-19514
Integration of detectors and optical waveguide structures [AD-A201331] N89-19536
Dexterity analysis and robot hand design N89-19865
CITY COLL. OF THE CITY UNIV. OF NEW YORK.
Nonradiative relaxation and laser action in tunable solid state laser crystals [NASA-CR-182820] N89-19539
CLARKSON UNIV., POTSDAM, NY.
Hole formation (etching) in polymers by far (deep) UV high intensity laser (excimer) radiation pulses and its relevance to photoresists in deep UV photolysis of polymers [AD-A202274] N89-19433
CLERMONT-FERRAND UNIV. (FRANCE).
Evidence of preferential zones of ice multiplication by splintering in convective cells N89-19625
A comparative study of two microphysical schemes in a beta mesoscale model N89-19640
Pattern of air bubble inclusions in atmospheric ice formed during accretion N89-19676
Simulation of conical graupel by using a ballistic model N89-19679
Meteorological and chemical influencing factors on acidity production in a mesoscale model with quasi-spectral microphysics N89-19711
Calibration of PMS FSSP and 1D-C probes for cloud droplet measurements N89-19713
COGNITIVE SYSTEMS, INC., NEW HAVEN, CT.
Knowledge acquisition for case-based reasoning systems N89-19856
COLORADO SCHOOL OF MINES, GOLDEN.
Fundamental optical studies of competitive adsorption and thin film phenomena [DE89-005898] N89-19401
Large wave number aperture limited Fourier inversion and inverse scattering [AD-A202247] N89-19940
COLORADO STATE UNIV., FORT COLLINS.
Some outstanding problems on the influence of clouds on radiation N89-19643
Radiative influences on precipitating mesoscale systems N89-19648
A numerical investigation of an orographic precipitation event N89-19721
Microphysical and dynamical interactions in Colorado front range upslope storms N89-19725
A high-spectral-resolution lidar system: The use of atomic blocking filter for measuring atmospheric parameters [AD-A201736] N89-19759
The divergence characteristics of constrained-sheath optics systems for use with 5-eV atomic oxygen sources [NASA-CR-182238] N89-19973
COLORADO UNIV., BOULDER.
The development of a cislunar space infrastructure [NASA-CR-184728] N89-19352
A fundamental mathematical theory in the dynamics of combustion processes [AD-A201284] N89-19391
Studies of hydrogen-hydrogen and carbon-sulfur bond cleavage [DE89-006116] N89-19403
COLUMBIA UNIV., NEW YORK, NY.
Knowledge-based graphical interfaces for presenting technical information N89-19851
COMMITTEE ON COMMERCE, SCIENCE, AND TRANSPORTATION (U.S. SENATE).
Commercial expendable launch vehicle liability [S-HRG-100-750] N89-19325
National Aeronautics and Space Administration authorization [S-HRG-100-579-PT-2] N89-20031
COMMITTEE ON SCIENCE, SPACE AND TECHNOLOGY (U.S. HOUSE).
The Atlas/Centaur 67 launch mishap [GPO-80-201] N89-19332
COMPAGNIA ITALIANA SERVIZI TECNICI, ROME.
Solid Earth ARISTOTELES mission data preprocessing simulation of gravity gradiometer [ESA-CR(P)-2666] N89-19766
COMPUTER SCIENCES CORP., CINCINNATI, OH.
Next generation keyboards: The importance of cognitive compatibility N89-19848
COMPUTER SCIENCES CORP., HOUSTON, TX.
Development of a personal-computer-based intelligent tutoring system N89-19889
CONSEJO SUPERIOR DE INVESTIGACIONES CIENTIFICAS, MADRID (SPAIN).
Study of space aluminum coating, executive summary [IOM/CAEE-002/87(TR)] N89-19443
CONSIGLIO NAZIONALE DELLE RICERCHE, FRASCATI (ITALY).
Focusing system, rotation, and modulation of the F 9 mirror of the IFSI 40 cm telescope [IFSI-87-16] N89-19987
Jets physics in Comet P/Halley [IFSI-88-3] N89-20049
CONSTRUCCIONES AERONAUTICAS S.A., MADRID (SPAIN).
Meteosat Millimetre Wave Sounder (MWS) study [BAE-TP-9119] N89-19363
CONTINENTAL SHELF INST., TRONDHEIM (NORWAY).
Economic analysis of NAVSAT system [REPT-1013-CA/TS] N89-19285
Study of NAVSAT for precise positioning [IKU-88.068] N89-19286
CORK GEOTECHNICS LTD., CASTLEMARTYR (IRELAND).
Nonlinear dynamic analysis of embedded structures [AD-A201728] N89-19593
CORNELL UNIV., ITHACA, NY.
A Monte Carlo simulation of the single-filament-composite test N89-19376
Chaotic dynamics and control of nonlinear and flexible arm robotic devices N89-19566
Electrostatic plasma waves and turbulence near auroral arcs N89-19758
Studies of 3-5 compounds in the megabar regime: [DE89-005722] N89-20009
Temperature and circulation in the stratospheres of the outer planets [NASA-CR-184826] N89-20051
CRISA, MADRID (SPAIN).
Study of space aluminum coating, executive summary [IOM/CAEE-002/87(TR)] N89-19443

D

DAYTON UNIV., OH.
High-speed laser photography [AD-A202293] N89-19544
Evaluation of optical materials samples [AD-A199471] N89-19981
DEFENCE AND CIVIL INST. OF ENVIRONMENTAL MEDICINE, DOWNSVIEW (ONTARIO).
Positive Flotation Harness (PFH) for use by Canadian Forces search and rescue technicians [AD-A200727] N89-19279
DEFENCE RESEARCH INFORMATION CENTRE, ORPINGTON (ENGLAND).
Short-range anti-armour flight vehicles of the Apache/CWS family [DRIC-T-8130] N89-19296
DEFENSE APPLIED INFORMATION TECHNOLOGY CENTER, ALEXANDRIA, VA.
Global scientific and technical information network [AD-A201902] N89-20030
DELANDE LONG (I. B. AND M. A.) SOFTWARE AND CONSULTANCY, SEEHEIM (GERMANY, F.R.).
Study of a software system concept for mission analysis presentation [ESA-CR(P)-2661] N89-19320
DELAWARE UNIV., NEWARK.
Computational study of incompressible turbulent flow over a swept rearward-facing step N89-19272
Nonlinear vibrations of composite material shells N89-19377
A climatology of global precipitation N89-19787
Brain mechanisms underlying individual differences in reaction to stress: An animal model [AD-A201595] N89-19801
DEPAUL UNIV., CHICAGO, IL.
Toward an image compression algorithm for the high-resolution electronic still camera N89-20079
DESERT RESEARCH INST., RENO, NV.
Evaporation and melting of ice crystals: A laboratory study N89-19612
Spreading supercooled water droplets on an ice surface N89-19614
Crystallization of supercooled solutions N89-19664
Studies of cloud micro-chemical physics N89-19686
DETROIT DIESEL ALLISON, INDIANAPOLIS, IN.
In-line wear monitor [AD-A201292] N89-19301
DEUTSCHE FORSCHUNGS- UND VERSUCHSANSTALT FUER LUFT- UND RAUMFAHRT, BRUNSWICK (GERMANY, F.R.).
Examinations on TERCOM navigation by evaluation of test flights done over the testing areas Deister and Harz (Germany, F.R.) [DFVLR-FB-88-37] N89-19287
Application of the OCCAM/transputer conception as busless multiprocessor system in a digital controller [DFVLR-FB-88-40] N89-19896
Equilibrium solutions of a spherical pendulum with rotating point of suspension and friction [DFVLR-MITT-88-24] N89-19966
DEUTSCHE FORSCHUNGS- UND VERSUCHSANSTALT FUER LUFT- UND RAUMFAHRT, COLOGNE (GERMANY, F.R.).
Simultaneous three-dimensional modeling of commercial flights within the airspace of the Federal Republic of Germany [DFVLR-FB-88-31] N89-19282
Theoretical and experimental investigations on shocks losses in transonic axial flow compressors [DFVLR-FB-88-38] N89-19304
Investigations on undercooling, nucleation and rapid solidification of metallic systems [DFVLR-FB-88-39] N89-19415
DEUTSCHE FORSCHUNGS- UND VERSUCHSANSTALT FUER LUFT- UND RAUMFAHRT, OBERPFAFFENHOFEN (WEST GERMANY).
Design of digital filters for navigation receivers [DFVLR-MITT-88-23] N89-19288
Investigation of flight sensors and actuators for the vibration damping augmentation of large flexible space structures [ESA-CR(P)-2670] N89-19362
Large-eddy simulation of convective boundary layers [DFVLR-FB-88-30] N89-19522
Turbulent transport processes within and below small cumulus clouds N89-19632
Liquid water content, median volume diameter and temperature in dependence on the height above the cloud base for different types of clouds N89-19662
Multiparameter Doppler radar observations of a squall line with the polarimetric DFVLR radar N89-19715
DEUTSCHE FORSCHUNGS- UND VERSUCHSANSTALT FUER LUFT- UND RAUMFAHRT, STUTTGART (GERMANY, F.R.).
Horizons of new energy technologies [DFVLR-MITT-88-22] N89-19742
DEUTSCHE FORSCHUNGS- UND VERSUCHSANSTALT FUER LUFT- UND RAUMFAHRT, WESSELING (GERMANY, F.R.).
Multiparameter characterization of raindrop size distribution by the polarimetric DFVLR radar: First results N89-19658
DEUTSCHER WETTERDIENST, OFFENBACH AM MAIN (GERMANY, F.R.).
Annals from the German Meteorological Society. No. 25: 10th International Cloud Physics Conference Preprints, volume 1 [ISBN-3-88-148240-7] N89-19605
DIRECTION DE LA METEOROLOGIE NATIONALE, CASABLANCA ROYAUME (MOROCCO).
Microphysical observations over the Atlas Mountains in Morocco N89-19724
DIRECTION DE LA METEOROLOGIE NATIONALE, MAGNY LES HAMEAUX (FRANCE).
Entrainment sites, mixing processes in warm convective clouds: Effect on droplet growth N89-19630
Properties of the precipitation embryos evolution in characteristic Hawaiian band clouds N89-19675
DOUGLAS AIRCRAFT CO., INC., LONG BEACH, CA.
Multiple Application Propfan Study (MAPS): Advanced tactical transport [NASA-CR-175003] N89-19300
DRAPER (CHARLES STARK) LAB., INC., CAMBRIDGE, MA.
RCS/piezoelectric distributed actuator study [AD-A201276] N89-19999
DREXEL UNIV., PHILADELPHIA, PA.
Characteristic time model validation [AD-A201374] N89-19510
Computational studies of evaporating sprays in a shear layer [AD-A201932] N89-19520
Airborne cloud sieving N89-19681
DUESSELDORF UNIV. (GERMANY, F.R.).
Passivity and corrosion of probe metals [ETN-89-93984] N89-19416

E

EAST TEXAS STATE UNIV., COMMERCE.
Visual perception and grasping for the extravehicular activity robot N89-20082
EDGERTON, GERMESHAUSEN AND GRIER, INC., IDAHO FALLS, ID.
Safe, compact nuclear propulsion: Solid core nuclear propulsion concept [AD-A202339] N89-19369

EIDGENOESSISCHE TECHNISCHE HOCHSCHULE, ZURICH (SWITZERLAND).
Microphysical, dynamical and chemical aspects of scavenging processes during winter precipitation N89-19695
EIKONTECH LTD., SHEFFIELD (ENGLAND).
Microwave holographic measurements of large reflectors: Phase 1 report, volume 1 [REPT-B090] N89-19530
Microwave holographic measurements of large reflectors: Phase 2 report, volume 2 [REPT-B091] N89-19531
ENERGY CONVERSION DEVICES, INC., TROY, MI.
Research on high-efficiency, multi-gap, multijunction, amorphous-silicon-based alloy thin-film solar cells, phase 1 [DE89-000844] N89-19739
ENGINEERING AND ECONOMICS RESEARCH, INC., HUNTSVILLE, AL.
Preparation of non-metals properties for data base [NASA-CR-183596] N89-19420
ENTWICKLUNGSRING NORD, BREMEN (GERMANY, F.R.).
Mini protein crystallization facility. Phase A study: Executive summary [REPT-AQ-ES-576/88] N89-19444
ESSEX CORP., ALEXANDRIA, VA.
SARSCEST (human factors) N89-19890
ESSEX CORP., HUNTSVILLE, AL.
Advanced extravehicular activity systems requirements definition study. Phase 2: Extravehicular activity at a lunar base [NASA-CR-172117] N89-19609
ESSEX CORP., ORLANDO, FL.
Optimal solutions for complex design problems: Using isoperformance software for human factors trade offs N89-19860
ETUDES TECHNIQUES ET CONSTRUCTIONS AEROSPATIALES, CHARLEROI (BELGIUM).
PSDE/SAT-2 preliminary spacecraft configuration study, executive summary [ESA-CR(P)-2689] N89-19360
EUROCONSULT B.V., ARNHEM (NETHERLANDS).
Salinity mapping based on SPOT images of the Punjab, Pakistan [BCRS-88-03] N89-19734
EXETER UNIV. (ENGLAND).
Some hydrodynamic instabilities of boundary layer flows N89-19501

F

FARRAN TECHNOLOGY LTD., BALLINCOLLIG (IRELAND).
Meteosat Millimetre Wave Sounder (MWS) study [BAE-TP-9119] N89-19363
FEDERAL AVIATION ADMINISTRATION, WASHINGTON, DC.
Minimum required heliport airspace under visual flight rules [AD-A201433] N89-19283
FERMI NATIONAL ACCELERATOR LAB., BATAVIA, IL.
Crossbar switch backplane and its application [DE89-005621] N89-19491
FLORIDA UNIV., GAINESVILLE.
Numerical simulation of the aerodynamics of turbulent transonic flow past a projectile N89-19270
FRAUNHOFER-INST. FUER ATMOSPHAERISCHE UMWELTFORSCHUNG, GARMISCH-PARTENKIRCHEN (GERMANY, F.R.).
Measurement of the global distribution of tropospheric trace gases and their time dependent variations [ETN-89-93987] N89-19747

G

GENERAL DYNAMICS CORP., FORT WORTH, TX.
The role of shock induced trailing-edge separation in limit cycle oscillations N89-19256
Unsteady low-speed wind tunnel test of a straked delta wing, oscillating in pitch. Part 2: Plots of steady and zeroth and first harmonic unsteady pressure distributions [AD-A201936] N89-19275
Advanced durability analysis. Volume 4: Executive summary [AD-A202304] N89-19597
GENERAL DYNAMICS CORP., SAN DIEGO, CA.
Artificial intelligent decision support for low-cost launch vehicle integrated mission operations N89-19830
GEORGE WASHINGTON UNIV., HAMPTON, VA.
Mixed formulation for frictionless contact problems [NASA-TP-2897] N89-19580
GEORGIA INST. OF TECH., ATLANTA.
Numerical solution of unsteady rotational flow past fixed and rotary wing configurations N89-19251
A systems approach to rotorcraft stability and control research [AD-A201784] N89-19314
The analytical modeling of a turbulent diffusion flame behind a backward facing step N89-19386
Flame driving of longitudinal instabilities in liquid fueled dump combustors [AD-A201293] N89-19392
Modeling of transient heat pipe operation [NASA-CR-184688] N89-19502
An investigation of the relationship between beam and global irradiation with the development of numerical solar radiation models N89-19748
GESELLSCHAFT FUER STRAHLEN- UND UMWELTFORSCHUNG M.B.H., MUNICH (GERMANY, F.R.).
Development of a detection system for atmospheric trace gases, in particular for OH molecules and realization of field measurements [BPT-11/88] N89-19767
GKSS-FORSCHUNGSZENTRUM GEESTHACHT (GERMANY, F.R.).
Microstructural analyses of intermetallic TiAl (Nb)-compounds prepared by arc melting and by powder metallurgy [GKSS-88/E/32] N89-19417
GLASGOW UNIV. (SCOTLAND).
Intrinsic hybrid modes in a corrugated conical horn [ESA-CR(P)-2586] N89-19494
GOSUDARSTVENNYI KOMITET PO ISPOLZOVANIYU ATOMNOI ENERGII, MOSCOW (USSR).
Effect of limiter currents on plasma equilibrium and stability in a tokamak [DE88-704951] N89-19989

H

HAHN-MEITNER-INST. G.M.B.H., BERLIN (GERMANY, F.R.).
High output voltage multioctave broadband amplifier working between 50 kHz and 8 GHz [HMI-B-451] N89-19497
HAMILTON STANDARD DIV., UNITED AIRCRAFT CORP., WINDSOR LOCKS, CT.
Large-scale Advanced Prop-fan (LAP) hub/blade retention design report [NASA-CR-174786] N89-19299
HARRIS CORP., MELBOURNE, FL.
Majorant analysis of performance degradation due to uncertainty N89-19344
The optimal projection equations for fixed-order dynamic compensation: Existence, convergence and global optimality N89-19345
Experimental verification of an innovative performance-validation methodology for large space systems [AD-A202243] N89-19357
Maximum entropy/optimal projection design synthesis for decentralized control of large space structures [AD-A202375] N89-19358
A 20 GHz low noise, low cost receiver for digital satellite communication system, ground terminal applications [NASA-CR-182243] N89-19449
HERCULES AEROSPACE CO., MAGNA, UT.
Measurements of the compressive behavior of AS4/3501-6 and IM7/8551-7 carbon/epoxy [DE89-005823] N89-19383
HIGH MOUNTAIN GEOPHYSICAL INST., NALCHIK (USSR).
Microphysical and electrical phenomena during freezing of water drops N89-19658
HIROSHIMA UNIV., TAKEHARA (JAPAN).
Quantum field theory of universe [DE88-756084] N89-20022
HOKKAIDO UNIV., SAPPORO (JAPAN).
Temporal variations of snow crystal growth parameters N89-19608
Proportion of riming growth process in snowfall phenomena N89-19668
Characteristics of radar echo of snow band formed in the lee side of a mountain N89-19726
HONEYWELL, INC., HOPKINS, MN.
A new pumpjet design theory [AD-A201353] N89-19558
HOUSTON UNIV., CLEAR LAKE, TX.
Development of an atmospheric monitoring plan for space station N89-20065
HOUSTON UNIV., TX.
Millimeter wave antennas [AD-A201919] N89-19474
Production system chunking in SOAR: Case studies in automated learning N89-20060
An evidential approach to problem solving when a large number of knowledge systems is available N89-20068
HOWARD UNIV., WASHINGTON, DC.
Modeling of flexible spacecraft accounting for orbital effects N89-19334
Kinetic processes in discharge pumped mercury halide lasers [AD-A201612] N89-19537
Analysis of blending algorithms in computer graphics [AD-A201921] N89-19909
HUGHES RESEARCH LABS., MALIBU, CA.
Flight model discharge system [AD-A201605] N89-19354
Development of Si/SiGe heterostructures [AD-A201440] N89-20001

I

IDAHO NATIONAL ENGINEERING LAB., IDAHO FALLS.
Safe, compact nuclear propulsion: Solid core nuclear propulsion concept [AD-A202339] N89-19369
Elastic hysteresis phenomena in ULE and Zerodur optical glasses at elevated temperatures [DE89-005183] N89-19423
Comparative performance evaluation of advanced AC and DC EV propulsion systems [DE89-005419] N89-19498
Noncontact ultrasonic sensing of weld pools for automated welding [DE89-005185] N89-19557
Optical parameter effects on laser generated ultrasound for microstructure characterization [DE89-005193] N89-19967
Status of DOE information network modifications [DE89-005191] N89-20028
ILLINOIS STATE UNIV., NORMAL.
Computer technologies and institutional memory N89-20062
ILLINOIS STATE WATER SURVEY, CHAMPAIGN.
The effect of charge on coalescence of small precipitation drops at terminal velocity N89-19606
Wake-excited raindrop oscillations N89-19607
A new mechanism for ice initiation in warm-based midwestern cumuli N89-19613
Microphysical characteristics of warm-based cumuli: Observations at -10 C N89-19626
ILLINOIS UNIV., CHICAGO.
Advancement of high resolution radar polarimetry in target verses clutter detection, discrimination, classification. A: Basic theory and modeling of polarimetric clutter phenomenology [AD-A201240] N89-19467
ILLINOIS UNIV., URBANA.
Frobenius-Hankel norm framework for disturbance rejection and low order decentralized controller design N89-19347
Anomalous slip in an FCC system [DE89-002257] N89-19405
Pressure variation over a solid wavy surface [AD-A201724] N89-19517
A model of the electrostatic-aerodynamic shape of raindrops N89-19615
Complex microphysical interactions within a central Sierra Nevada orographic cloud system N89-19722
Dynamic data structures for two-dimensional searching [AD-A201173] N89-19901
Fast and processor-efficient parallel algorithms for reducible flow graphs [AD-A201651] N89-19904
INDIAN INST. OF TROPICAL METEOROLOGY, POONA.
Precipitation initiation mechanisms in clouds over north India N89-19624
INDIANA UNIV., BLOOMINGTON.
The cosmic ray antiproton spectrum between 0.1 and 1.5 GeV kinetic energy N89-20057
INFORMATION AND CONTROL SYSTEMS, INC., HAMPTON, VA.
A variable-gain output feedback control design methodology [NASA-CR-4226] N89-19316
INSTITUT D'AERONOMIE SPATIALE DE BELGIQUE, BRUSSELS.
Ultraviolet absorption cross-sections of halocarbons of stratospheric interest [AERONOMICA-ACTA-A-336-1988] N89-19769
Stratospheric nitric acid: Feasibility of routine measurement by observation from commercial airliners in IR bands from 9 to 14 microns [C-48-1977] N89-19770
INSTITUTE OF CHEMICAL KINETICS AND COMBUSTION, NOVOSIBIRSK (USSR).
Kinetics of ice crystal formation on aerosol particles in supercooled fog N89-19665

INSTITUTE OF EXPERIMENTAL METEOROLOGY, OBNINSK (USSR).
An investigation of the effect of electrical charges on the collision efficiency of cloud drops N89-19657
INSTITUTE OF HYDROLOGY AND METEOROLOGY, SOFIA (BULGARIA).
A new dropsonde for cloud probings N89-19728
INSTITUTE OF OCEANOGRAPHIC SCIENCES, WORMLEY (ENGLAND).
Directional wave data recorded in the southern North Sea
[IOS-258] N89-19793
Compressional-wave velocities in ocean sediments east southeast of Madeira, Atlantic Ocean
[IOS-257] N89-19794
INSTITUTO DE ELECTRONICA DE COMMUNICACIONES, MADRID (SPAIN).
Meteosat Millimetre Wave Sounder (MWS) study
[BAE-TP-9119] N89-19363
INSTITUTO DE PESQUISAS ESPACIAIS, SAO JOSE DOS CAMPOS (BRAZIL).
SCD2 satellite spin axis reorientation and feasibility study
[INPE-4688-NTE/285] N89-19351
Measurement of atmospheric electrical fields in periods of electrical perturbation and calm at the latitude of 23 C
[INPE-4626-PRE/1344] N89-19750
INTEGRATED INFERENCE MACHINES, INC., ANAHEIM, CA.
Garbage collection can be made real-time and verifiable N89-19840
INTEGRATED SYSTEMS, INC., SANTA CLARA, CA.
Adaptive control of large space structures N89-19343
INTELLICORP, MOUNTAIN VIEW, CA.
Browsing schematics: Query-filtered graphs with context nodes N89-19844
INTERFEROMETRICS, INC., VIENNA, VA.
MODIS information, data and control system (MIDACS) operations concepts
[NASA-TM-100720] N89-19729
INTERUNIVERSITY MICRO-ELECTRONICS CENTER, LEUVEN (BELGIUM).
Evaluation of Schottky barrier and PBTE IR-CCD detectors for the SWIR and MIR wavelengths range, executive summary
[IMEC-SP/CCD-255/88-03] N89-19495
IOWA STATE UNIV. OF SCIENCE AND TECHNOLOGY, AMES.
A detailed examination of discontinuities in natural rain spectra N89-19663
IOWA UNIV., IOWA CITY.
A recursive method for parallel processor multiflexible body dynamic simulation N89-19336
ISEL, MADRID (SPAIN).
Advanced information technology monitoring with microprocessors
[MMP-1-IS-02-3302-FR] N89-19895
ISRAEL METEOROLOGICAL SERVICE, BET DAGAN.
Kinetic equation for polluted cloud droplets spectrum N89-19661
ISTITUTO ELETTROTECNICO NAZIONALE (GALILEO FERRARIS), TURIN (ITALY).
Activities report in electrotechnology
[ETN-89-93715] N89-19448
ITALSPAZIO, ROME (ITALY).
Economic analysis of NAVSAT system
[REPT-1013-CA/TS] N89-19285

J

JAPAN ATOMIC ENERGY RESEARCH INST., TOKYO.
Verification of combined thermal-hydraulic and heat conduction analysis code FLOWNET/TRUMP
[DE88-756063] N89-19506
JET PROPULSION LAB., CALIFORNIA INST. OF TECH., PASADENA.
Concept of adaptive structures N89-19338
The Telecommunications and Data Acquisition Report
[NASA-CR-184812] N89-19451
Design and test of a 2.25-MW transformer rectifier assembly N89-19452
On sampling band-pass signals N89-19453
The use of interleaving for reducing radio loss in convolutionally coded systems N89-19454
A new VLSI architecture for a single-chip-type Reed-Solomon decoder N89-19455
A simplified procedure for decoding the (23,12) and (24,12) Golay codes N89-19456
On testing VLSI chips for the big Viterbi decoder N89-19458
Wiring Viterbi decoders (splitting deBruijn graphs) N89-19459
Block diagrams of the radar interface and control unit N89-19460
RF performance measurement of the DSS-14 70-meter antenna at C-band/L-band N89-19461
Microwave time delays for the dual L-C-band feed system N89-19462
Systems analysis for DSN microwave antenna holography N89-19463
Ka-band study: 1988 N89-19464
A low-loss linear analog phase modulator for 8415 MHz transponder application N89-19465
Radio frequency interference survey over the 1.0-10.4 GHz frequency range at the Goldstone-Venus Development Station N89-19466
Telerobot operator control station requirements N89-19876
Time-delayed operation of a telerobot via geosynchronous relay N89-19877
Machine vision for space telerobotics and planetary rovers N89-19879
A methodology for automation and robotics evaluation applied to the space station telerobotic servicer N89-19882
Recognition of object domain by color distribution N89-19928
JOHANN-WOLFGANG-GOETHE-UNIV., FRANKFURT AM MAIN (GERMANY, F.R.).
A wind tunnel study on the melting of snow flakes N89-19611
A parametrization scheme for the coalescence of water drops using the stochastic collection equation N89-19671
Experiments on microphysics and chemistry of radiation fogs N89-19702
Development of a detection system for atmospheric trace gases, in particular for OH molecules and realization of field measurements
[BPT-11/88] N89-19767
JOINT INST. FOR ADVANCEMENT OF FLIGHT SCIENCES, HAMPTON, VA.
Mixed finite element models for free vibrations of thin-walled beams
[NASA-TP-2868] N89-19579
Mixed formulation for frictionless contact problems
[NASA-TP-2897] N89-19580
JOINT INST. FOR NUCLEAR RESEARCH, DUBNA (USSR).
Born-Infeld equations and minimal surfaces
[DE88-704966] N89-19936
JOINT PUBLICATIONS RESEARCH SERVICE, ARLINGTON, VA.
JPRS report: Science and technology. USSR: Electronics and electrical engineering
[JPRS-UEE-88-005] N89-19485
Variations of the tropospheric propagation range of ultrashort radio waves above the sea N89-19486
Peaceful uses of electrical engineering in space N89-19487
JPRS report: Science and technology. Japan: 7th Artificial Intelligence Symposium
[JPRS-JST-88-020] N89-19924
Problems in structuring large-scale expert system N89-19925
Evaluation support system for multiple R and D projects N89-19926
Intelligent mobile robot working in unknown environment N89-19927

K

KANSAS STATE UNIV., MANHATTAN.
Calculation of mutual self inductance and coupling coefficient for closely spaced loops
[DE89-005546] N89-19471
KANSAS UNIV. CENTER FOR RESEARCH, INC., LAWRENCE.
The electromagnetic modeling of thin apertures using the finite-difference time-domain technique
[NASA-CR-178280] N89-19780
KATHOLIEKE UNIVERSITEIT TE LEUVEN (BELGIUM).
Error localization and updating of spacecraft structures mathematical models
[YMD/EF/0175] N89-19361
KENTUCKY UNIV., LEXINGTON.
Modeling studies on the formation, growth, dissipation and acidification of cumulus clouds N89-19704
KERNFORSCHUNGSANLAGE, JUELICH (GERMANY, F.R.).
Results of time and height resolved scavenging experiments N89-19697
A Monte Carlo test program with vectorized geometry routines
[JUEL-2202] N89-19947
HERMES, a Monte Carlo program system for beam-materials interaction studies
[JUEL-2203] N89-19979
KERNFORSCHUNGSZENTRUM G.M.B.H., KARLSRUHE (GERMANY, F.R.).
Improvements in the properties of NbN layers through the presence of small amounts of aluminum during sputtering
[KFK-4409] N89-19418
Formation of titanium nitride layers on titaniun metal: Results of XPS and AES investigations
[KFK-4449] N89-19419
Possibilities for breakeven and ignition of D-He3 fusion fuel in a near term tokamak
[KFK-4433] N89-19992
KRUG INTERNATIONAL, SAN ANTONIO, TX.
An annotated bibliography of hypobaric decompression sickness research conducted at the Crew Technology Division, USAF School of Aerospace Medicine, Brooks AFB, Texas from 1983 to 1988
[AD-A201274] N89-19796
KUNZ ASSOCIATES, INC., ALBUQUERQUE, NM.
Generalized three-dimensional experimental lightning code (G3DXL) user's manual
[NASA-CR-166079] N89-19779

L

LABORATORI ELETTRONICI E NUCLEARI, MILAN (ITALY).
Meteosat Millimetre Wave Sounder (MWS) study
[BAE-TP-9119] N89-19363
LAWRENCE LIVERMORE NATIONAL LAB., CA.
A controlled component synthesis method for truss structure vibration control N89-19348
Characterization of IM7/8551-7 carbon/epoxy in compression and shear
[DE89-005544] N89-19378
Calculation of mutual self inductance and coupling coefficient for closely spaced loops
[DE89-005546] N89-19471
Acoustoelasticity using longitudinal waves for residual stress evaluation
[DE89-006154] N89-19604
LITTLE (ARTHUR D.), INC., CAMBRIDGE, MA.
Applications survey for remote photovoltaic power systems
[AD-A201937] N89-19741
Sensing human hand motions for controlling dexterous robots N89-19883
LIVERPOOL UNIV. (ENGLAND).
Homogenizing surface and satellite observations of cloud
[AD-A201630] N89-19752
LOCKHEED ENGINEERING AND SCIENCES CO., HOUSTON, TX.
Simulation of the human-telerobot interface N89-19861
LOCKHEED-GEORGIA CO., MARIETTA.
Multiple-Purpose Subsonic Naval Aircraft (MPSNA) Multiple Application Propfan Study (MAPS)
[NASA-CR-175096] N89-19289
LOCKHEED MISSILES AND SPACE CO., AUSTIN, TX.
Testing expert systems N89-19834
LOCKHEED MISSILES AND SPACE CO., HUNTSVILLE, AL.
Duct flow nonuniformities for Space Shuttle Main Engine (SSME)
[NASA-CR-183595] N89-19367
LOS ALAMOS NATIONAL LAB., NM.
DES cryptographic services designed for the DOE wide band communications network
[LA-10966-MS] N89-19484
Liquid excimers: Lasing Xe2 and Kr2 in liquid argon
[DE89-005449] N89-19546
XUV free-electron laser development at Los Alamos
[DE89-005458] N89-19547
Ultrahigh-brightness XeCl laser system
[DE89-005467] N89-19548
Electron-beam pumped liquid excimer lasers
[DE89-006549] N89-19549
Modeling the energy deposition in the Aurora KrF laser amplifier chain
[DE89-006545] N89-19550
On the use of multiple photon processes in krypton for laser guiding of electron beams
[DE89-006546] N89-19551
High average power excimer laser-pumped dye oscillators
[DE89-006547] N89-19552
Impact of target altitude restrictions on laser performance
[DE89-006567] N89-19553
A curve-fitting package for personal computers
[LA-11082-MS] N89-19922
Survivability of space assets in the long term
[DE89-006563] N89-19964

Beam profile effects on NPB performance
[LA-11228-MS] N89-19980
High-order beam optics: An overview
[DE89-005441] N89-19984
An achromatic super telephoto lens
[DE89-006163] N89-19986
Radiation induced amorphization in YBa2Cu3O7 and GdBa2Cu3O7 superconductors
[DE89-005451] N89-20008
Use of superconducting imaging surfaces to enhance detection of weak magnetic sources by SQUID systems
[DE89-006568] N89-20015

LOUGHBOROUGH UNIV. OF TECHNOLOGY (ENGLAND).
High strain-rate behaviour of polymers using blast-wave and impact-loading methods N89-19592

LOUISIANA STATE UNIV., BATON ROUGE.
Minimum time motion of a robotic manipulator N89-19567

LOUISIANA TECH UNIV., RUSTON.
Development of parallel algorithms for electrical power management in space applications N89-20063

LOWELL UNIV., MA.
Calculation of molecular absorption parameters and updating the AFGL atmospheric line parameter compilation
[AD-A202113] N89-19761

M

MAINE UNIV., ORONO.
Proposal to study the interaction of polyimide precursors and thin polyimide films with silicon and silicon oxide surfaces
[AD-A201183] N89-19425

MAINZ UNIV. (GERMANY, F.R.).
The study of the interstitial aerosol particles and cloud droplets with digital image analysis of diffraction images N89-19654
Insoluble particles in hydrometeors N89-19684

MANCHESTER UNIV. (ENGLAND).
The calculation of supersaturations and growth of droplets in continental cumulus clouds N89-19617
Airborne studies of the influence of entrainment on the vertical and horizontal microphysical structure of small cumulus clouds N89-19629
The collection efficiencies of soft-hailstones for super-cooled water droplets and ice crystals N89-19678
Chemical evolution within in a cloud model featuring a polydisperse droplet size spectrum N89-19703
A model of wet deposition to complex terrain by the seeder-feeder process N89-19710

MARTIN MARIETTA AERO AND NAVAL SYSTEMS, BALTIMORE, MD.
Telepresence and telerobotics N89-19873

MARTIN MARIETTA CORP., ENGLEWOOD, CO.
Safe, compact nuclear propulsion: Solid core nuclear propulsion concept
[AD-A202339] N89-19369

MASSACHUSETTS INST. OF TECH., CAMBRIDGE.
Wave propagation in large space structures N89-19335
Active control of elastic wave motion in structural networks N89-19342
To measure and characterize metal corrosion in electrolyte solutions by exploiting the properties of superconducting
[AD-A201484] N89-19407
Grain boundary nonstoichiometry in multicomponent ceramics
[DE89-006109] N89-19437
Model-based reasoning: Troubleshooting
[AD-A201614] N89-19445
Dexterous robotic hands: Kinematics and control
[AD-A202183] N89-19570
Active and passive remote sensing of ice
[AD-A201915] N89-19792
Computation of stereo and visual motion: From biophysics to psychophysics
[AD-A201873] N89-19802
Structural saliency: The detection of globally salient structures using a locally connected network
[AD-A201619] N89-19806
Scheme86: An architecture for microcoding a scheme interpreter
[AD-A201258] N89-19893
Computer-aided fabrication system implementation
[AD-A202128] N89-19911
Critical problems in very large scale computer systems
[AD-A202129] N89-19923
Estimating the illuminant color from the shading of a smooth surface
[AD-A201333] N89-19983

MASSACHUSETTS INST. OF TECH., LEXINGTON.
TDWR (Terminal Doppler Weather Radar) scan strategy requirements
[AD-A201785] N89-19473
A preliminary study of precursors to Huntsville microbursts
[AD-A200914] N89-19782
Knowledge-based operation and management of communications systems N89-19826
The Boltzmann machine: A survey and generalization
[AD-A197976] N89-19929

MASSACHUSETTS UNIV., AMHERST.
The determination of the mechanical behavior of polyamic acid/polyimide coatings N89-19428
Normalized radar cross section of natural surfaces at millimeter wavelengths
[AD-A202252] N89-19475
Using the sentence verification technique to assess storage and retrieval processes
[AD-A201632] N89-20029
The distribution of the interstellar medium in the Scd galaxy NGC 6946 and in a sample of dwarf irregular galaxies N89-20043

MATRA ESPACE, PARIS-VELIZY (FRANCE).
Specification validation tools study
[MATRA-NT/139/1939] N89-19447
Telescience system concept study, volume 2
[MATRA-NT/2113/139-VOL-2] N89-19478

MAX-PLANCK-INST. FUER PHYSIK UND ASTROPHYSIK, GARCHING (GERMANY, F.R.).
Ion beam driven electrostatic shocks
[MPE-PREPRINT-127] N89-19995
Plasma waves at the dayside magnetopause
[MPE-PREPRINT-128] N89-19996
Solar and inerplanetary cosmic ray composition
[MPE-PREPRINT-108] N89-20056

MAX-PLANCK-INST. FUER PLASMAPHYSIK, GARCHING (GERMANY, F.R.).
Numerical studies of MHD turbulence in the reversed field pinch
[IPP-6/276] N89-19994

MAX-PLANCK-INSTITUT FUER STROEMUNGSFORSCHUNG, GOETTINGEN (GERMANY, F.R.).
Vortex convection in nonuniform compressible flow
[MPIS-4/1988] N89-19527

MCDONNELL AIRCRAFT CO., SAINT LOUIS, MO.
CAP-TSD analysis of the F-15 aircraft N89-19239
Durability and damage tolerance of bismaleimide composites, volume 1
[AD-A201273] N89-19374
Durability and damage tolerance of bismaleimide composites. Volume 2: Appendix of crack growth and low-velocity impact data
[AD-A201839] N89-19379

MCDONNELL-DOUGLAS ASTRONAUTICS CO., HUNTSVILLE, AL.
Electric fields in earth orbital space
[AD-A201747] N89-19760

MCDONNELL-DOUGLAS CORP., HOUSTON, TX.
A design and implementation methodology for diagnostic systems N89-19831

MCDONNELL-DOUGLAS CORP., LONG BEACH, CA.
The birth of open separation on a prolate spheroid
[AD-A201350] N89-19509

MCGILL UNIV., MONTREAL (QUEBEC).
The effect of turbulence on the collection of cloud drops: A stochastic model N89-19637

MEDICAL COLL. OF VIRGINIA, RICHMOND.
Biological applications and effects of optical masers
[AD-A201834] N89-19541

MESSERSCHMITT-BOELKOW-BLOHM/ENTWICKLUNG SPRING NORD, BREMEN (GERMANY, F.R.).
Telescience system concept study, volume 2
[MATRA-NT/2113/139-VOL-2] N89-19478

MESSERSCHMITT-BOELKOW-BLOHM G.M.B.H., OTTOBRUNN (GERMANY, F.R.).
PSDE/SAT-2 preliminary spacecraft configuration study, executive summary
[ESA-CR(P)-2689] N89-19360
Mini protein crystallization facility. Phase A study: Executive summary
[REPT-AQ-ES-576/88] N89-19444
Study on checkout of flight units and subsystems
[ESA-CR(P)-2693] N89-19816

METEOROLOGICAL OFFICE, BRACKNELL (ENGLAND).
Airborne studies of the ice phase in maritime clouds around the British Isles N89-19623
An observational study of radiatively driven convection N89-19647
The use of automatic particle recognition to improve the determination of bulk quantities from PMS 2-D probe data in cirrus N89-19651
The comparison of holographic and 2-D probe measurements of ice crystals N89-19652
A comparison of radiometric and immersion temperature measurements in water clouds N89-19712

METEOROLOGICAL OFFICE, LONDON (ENGLAND).
Meteosat Millimetre Wave Sounder (MWS) study
[BAE-TP-9119] N89-19363

METEOROLOGICAL RESEARCH INST., TSUKUBA (JAPAN).
Instability theory in clouds and the parameterization of eddy viscosity coefficients N89-19633
Development of hydrometeor video sonde N89-19653
A new airborne device for measurement of cloud particles using video microscope N89-19719

MIAMI UNIV., CORAL GABLES, FL.
Semi-prognostic tests of cumulus parameterization schemes in the middle latitudes N89-19786

MICHIGAN TECHNOLOGICAL UNIV., HOUGHTON.
Local position control: A new concept for control of manipulators N89-19864
Model evaluation, recommendation and prioritizing of future work for the manipulator emulator testbed N89-20072

MICHIGAN UNIV., ANN ARBOR.
Minimax and maximax optimal control problems with applications in aerospace engineering N89-19311
Study of underexpanded turbulent air jets in water N89-19516
Use of cluster analysis to define periods of similar meteorology and precipitation chemistry in eastern North America N89-19785
Estimation in large samples
[AD-A201459] N89-19956

MIDWEST RESEARCH INST., GOLDEN, CO.
Solar thermal technology
[DE89-000818] N89-19738
Research on high-efficiency, multi-gap, multijunction, amorphous-silicon-based alloy thin-film solar cells, phase 1
[DE89-000844] N89-19739
Field investigation of a wake structure downwind of a VANT (Vertical-Axis Wind Turbine) in a wind farm array
[DE89-000821] N89-19743
Optical goals for polymeric film reflectors
[DE89-000836] N89-19744
Local wind measurements for micrositing
[DE89-000829] N89-19781

MINNESOTA UNIV., MINNEAPOLIS.
Control of nonlinear systems using partial dynamic inversion N89-19310
Theoretical and experimental studies of selected topics in the rheology of fluids
[AD-A201460] N89-19512
An observational and numerical study of extragalactic radio sources N89-20055

MISSION RESEARCH CORP., LOS ALAMOS, NM.
Liquid excimers: Lasing Xe2 and Kr2 in liquid argon
[DE89-005449] N89-19546

MISSISSIPPI STATE UNIV., MISSISSIPPI STATE.
Unsteady transonic viscous-inviscid interaction using Euler and boundary-layer equations N89-19250

MISSISSIPPI UNIV., UNIVERSITY.
An examination of cavitation due to short pulses of megahertz ultrasound N89-19971

MISSOURI UNIV., INDEPENDENCE.
Optical joint correlation using the deformable mirror device N89-20074

MISSOURI UNIV., ROLLA.
On the dynamics of the falling ice crystal zone N89-19672

MITRE CORP., MCLEAN, VA.
An architecture for integrating distributed and cooperating knowledge-based Air Force decision aids N89-19941

MONTANA STATE UNIV., BOZEMAN.
Evaluation of available analytical techniques for monitoring the quality of space station potable water N89-20071

N

NAGOYA UNIV., TOYOKAWA (JAPAN).
A vertical wind tunnel for the study of snowflakes and effects of accumulated snow on materials N89-19674

NANJING UNIV. (CHINA).
Ionic concentrations of rime ice and snow and Bergeron process N89-19689

NATIONAAL INST. VOOR KERNFYSICA EN HOGE ENERGIEFYSICA, AMSTERDAM (NETHERLANDS).
Bitbus data transmission with galvanic separations
[DIGEL-78] N89-19898
Remote control system
[DIGEL-79] N89-19917

NATIONAL AERONAUTICS AND SPACE ADMINISTRATION, WASHINGTON, DC.
Mixed finite element models for free vibrations of thin-walled beams
[NASA-TP-2868] N89-19579

NATIONAL AERONAUTICS AND SPACE ADMINISTRATION. AMES RESEARCH CENTER, MOFFETT FIELD, CA.
Role of computational fluid dynamics in unsteady aerodynamics for aeroelasticity N89-19237
The oblique-wing research aircraft: A test bed for unsteady aerodynamic and aeroelastic research N89-19253
Cloud and aerosol optical depths N89-19646
Cirrus microphysics and infrared radiative transfer: A case study N89-19649
A survey of planning and scheduling research at the NASA Ames Research Center N89-19820
Knowledge-based zonal grid generation for computational fluid dynamics N89-19828
Spaceborne VHSIC multiprocessor system for AI applications N89-19838

NATIONAL AERONAUTICS AND SPACE ADMINISTRATION. GODDARD SPACE FLIGHT CENTER, GREENBELT, MD.
Get Away Special (GAS): Educational applications of space flight
[NASA-TM-101287] N89-19321
MODIS information, data and control system (MIDACS) operations concepts
[NASA-TM-100720] N89-19729
TRMM (Tropical Rainfall Measuring Mission): A satellite mission to measure tropical rainfall
[NASA-TM-101288] N89-19789
Intelligent tutoring in the spacecraft command/control environment N89-19855
Design concept for the Flight Telerobotic Servicer (FITS) N89-19870
The V3, V4 and V6 bands of formaldehyde: A spectral catalog from 900 cm(-1) to 1580 cm(-1)
[NASA-TM-100709] N89-19976

NATIONAL AERONAUTICS AND SPACE ADMINISTRATION. HUGH L. DRYDEN FLIGHT RESEARCH FACILITY, EDWARDS, CA.
Application of flight systems methodologies to the validation of knowledge-based systems N89-19832

NATIONAL AERONAUTICS AND SPACE ADMINISTRATION. JOHN F. KENNEDY SPACE CENTER, COCOA BEACH, FL.
Ice/frost/debris assessment for space shuttle mission STS-27R, December 2, 1988
[NASA-TM-102144] N89-19326
CIRCA 2000 operations criteria N89-19829

NATIONAL AERONAUTICS AND SPACE ADMINISTRATION. LYNDON B. JOHNSON SPACE CENTER, HOUSTON, TX.
Second Annual Workshop on Space Operations Automation and Robotics (SOAR 1988)
[NASA-CP-3019] N89-19817
An expert system for shuttle and satellite radar tracker scheduling N89-19821
Robot path planning using a genetic algorithm N89-19869
A multi-sensor system for robotics proximity operations N89-19881
National Aeronautics and Space Administration (NASA)/American Society for Engineering Education (ASEE) Summer Faculty Fellowship Program 1988, volume 1
[NASA-CR-172118-VOL-1] N89-20058
National Aeronautics and Space Administration (NASA)/American Society for Engineering Education (ASEE) Summer Faculty Fellowship Program 1988, volume 2
[NASA-CR-172118-VOL-2] N89-20073

NATIONAL AERONAUTICS AND SPACE ADMINISTRATION. LANGLEY RESEARCH CENTER, HAMPTON, VA.
Joint University Program for Air Transportation Research, 1987
[NASA-CP-3028] N89-19230
The NASA Langley laminar-flow-control experiment on a swept, supercritical airfoil - Drag equations
[NASA-TM-4096] N89-19231
Drag measurements on a laminar-flow body of revolution in the 13-inch magnetic suspension and balance system
[NASA-TP-2895] N89-19232
Transonic Unsteady Aerodynamics and Aeroelasticity 1987, part 1
[NASA-CP-3022-PT-1] N89-19234
CAP-TSD: A program for unsteady transonic analysis of realistic aircraft configurations N89-19238
Calculation of steady and unsteady pressures at supersonic speeds with CAP-TSD N89-19240
Application of a full potential method to AGARD standard airfoils N89-19242
Flux-vector splitting for unsteady calculations on dynamic meshes N89-19244
AGARD standard aeroelastic configurations for dynamic response N89-19246
Transonic Unsteady Aerodynamics and Aeroelasticity 1987, part 2
[NASA-CP-3022-PT-2] N89-19247
Viscous flow calculations for the AGARD standard configuration airfoils with experimental comparisons N89-19249
Unsteady Navier-Stokes computations over airfoils using both fixed and dynamic meshes N89-19252
Investigation and suppression of high dynamic response encountered on an elastic supercritical wing N89-19255
Initial application of CAP-TSD to wing flutter N89-19257
Unsteady pressure measurements on a supercritical airfoil at high Reynolds numbers N89-19259
Experimental transonic steady state and unsteady pressure measurements on a supercritical wing during flutter and forced discrete frequency oscillations N89-19261
Computational aeroelasticity challenges and resources N89-19264
Two experimental supercritical laminar-flow-control swept-wing airfoils
[NASA-TM-89073] N89-19266
Integrated tools for control-system analysis
[NASA-TP-2885] N89-19309
Robust eigenstructure assignment by a projection method: Application using multiple optimization criteria N89-19349
The effects of simulated space environmental parameters on six commercially available composite materials
[NASA-TP-2906] N89-19385
Contamination of liquid oxygen by pressurized gaseous nitrogen
[NASA-TP-2894] N89-19499
Halogen Occultation Experiment (HALOE) optical filter characterization
[NASA-TM-4104] N89-19529
Mixed formulation for frictionless contact problems
[NASA-TP-2897] N89-19580
Effect of adhesive interleaving and discontinuous plies on failure of composite laminates subject to transverse normal loads
[NASA-TM-101507] N89-19589
A wide bandwidth electrostatic field sensor for lightning research
[NASA-TM-101539] N89-19783
Validation of highly reliable, real-time knowledge-based systems N89-19833
Physiological assessment of task underload N89-19846
Operation of the HP2250 with the HP9000 series 200 using PASCAL 3.0
[NASA-TM-87652] N89-19892
High-speed real-time animated displays on the ADAGE (trademark) RDS 3000 raster graphics system
[NASA-TM-4095] N89-19899

NATIONAL AERONAUTICS AND SPACE ADMINISTRATION. LEWIS RESEARCH CENTER, CLEVELAND, OH.
Turbomachinery aeroelasticity at NASA Lewis Research Center N89-19262
Wind-tunnel results of advanced high-speed propellers at takeoff, climb, and landing Mach numbers
[NASA-TM-87030] N89-19265
Icing research tunnel test of a model helicopter rotor
[NASA-TM-101978] N89-19305
Tensile and creep rupture behavior of P/M processed Nb-base alloy, WC-3009
[NASA-TM-101954] N89-19371
Acidic attack of perfluorinated alkyl ether lubricant molecules by metal oxide surfaces
[NASA-TM-101962] N89-19402
Adhesion in ceramics and magnetic media
[NASA-TM-101476] N89-19435
The solid surface combustion space shuttle experiment hardware description and ground-based test results
[NASA-TM-101963] N89-19446
Starting characteristics of direct current motors powered by solar cells
[NASA-TM-101981] N89-19493
Interfacing laboratory instruments to multiuser, virtual memory computers
[NASA-TM-4106] N89-19578
RE-1000 free-piston Stirling engine sensitivity test results
[NASA-TM-88846] N89-19737
Acoustic wave propagation in heterogeneous structures including experimental validation
[NASA-TM-101486] N89-19965

NATIONAL AERONAUTICS AND SPACE ADMINISTRATION. MARSHALL SPACE FLIGHT CENTER, HUNTSVILLE, AL.
An electrochemical study of corrosion protection by primer-topcoat systems on 4130 steel with ac impedance and dc methods
[NASA-TP-2820] N89-19406
Superconducting gravity gradiometer mission. Volume 2: Study team technical report
[NASA-TM-4091] N89-19749
The scheduling techniques of ESP2 N89-19818
Space station payload operations scheduling with ESP2 N89-19819
Automation of the space station core module power management and distribution system N89-19822
Automatic Detection of Electric Power Troubles (ADEPT) N89-19825

NATIONAL BUREAU OF STANDARDS, GAITHERSBURG, MD.
Free-electron laser driven by the NBS (National Bureau of Standards) CW microtron
[AD-A201170] N89-19535

NATIONAL CENTER FOR ATMOSPHERIC RESEARCH, BOULDER, CO.
On the observations of cloud temperature and liquid water content using a Lyman-alpha and an FSSP sensor N89-19618
Evaluation of droplet growth rates in Hawaiian orographic clouds N89-19619
Studies of warm-rain development N89-19620
Radar observations and modelling of warm rain initiation N89-19621
Entrainment and fine-scale (molecular) mixing N89-19628
Three-dimensional cumulus entrainment studies N89-19634
The effect of ice physical processes on the numerical simulation of West African squall lines N89-19638
Radar observations of precipitation microstructure: The morphology of linear depolarization measurements in cloud N89-19714
Applications of the NCAR Electra Doppler radar for the study of physical parameters of clouds N89-19717
On the small scale topographical influences on precipitation N89-19720

NATIONAL LAB. FOR HIGH ENERGY PHYSICS, OHO (JAPAN).
Radiation biology studies in soft X-ray and ultrasoft X-ray region
[DE88-756071] N89-19795
XPS and AES studies of thin oxide layers on niobium for superconducting RF cavities
[DE88-756073] N89-19997

NATIONAL OCEANIC AND ATMOSPHERIC ADMINISTRATION, BOULDER, CO.
Influences of cloud microphysics on continental and marine precipitation chemistry N89-19700

NATIONAL OCEANIC AND ATMOSPHERIC ADMINISTRATION, OAK RIDGE, TN.
An investigation of the intermittent turbulent breakdown of the nocturnal planetary boundary layer
[AD-A201743] N89-19518

NATIONAL OCEANIC AND ATMOSPHERIC ADMINISTRATION, PRINCETON, NJ.
The case for subgrid-scale condensation in numerical cloud models N89-19636

NATIONAL RESEARCH COUNCIL OF CANADA, OTTAWA (ONTARIO).
Use of riblets to obtain drag reduction on airfoils at high Reynolds number flows
[AD-A201485] N89-19267

NATIONAL WEATHER SERVICE, ANN ARBOR, MI.
A case study of significant lake enhanced snow event in upper Michigan
[CRARP-88-2] N89-19773

NATIONAL WEATHER SERVICE, CHEYANNE, WY.
The Cheyenne windstorm that never came: Another lesson in real time analysis
[CRARP-88-1] N89-19772

NATIONAL WEATHER SERVICE, DES MOINES, IA.
Use of long-waves in forecasting
[CRARP-88-7] N89-19778

NATIONAL WEATHER SERVICE, KANSAS CITY, MO.
Central Region applied research on severe weather forecasting
[PB88-210836] N89-19771

NATIONAL WEATHER SERVICE, SIOUX FALLS, SD.
A collection of severe weather parameters used for a checklist
[CRARP-88-3] N89-19774
Technical report on temperature, precipitation and aviation verification at WSFO Sioux Falls for 1987
[CRARP-88-5] N89-19776

NATIONAL WEATHER SERVICE, TOPEKA, KS.
A meditation on Miller
[CRARP-88-4] N89-19775

Preparing storm data
[CRARP-88-6] N89-19777

NAVAL AIR TEST CENTER, PATUXENT RIVER, MD.
Development of a low-cost helmet mounted eye gaze sensor
[AD-A202303] N89-19298

NAVAL OCEAN SYSTEMS CENTER, SAN DIEGO, CA.
The efficacy of color-coded symbols to enhance air-traffic control displays
[AD-A201594] N89-19284

NAVAL POSTGRADUATE SCHOOL, MONTEREY, CA.
A data analysis system for unsteady turbulence measurements
[AD-A201662] N89-19268
The design and initial construction of a composite RPV (Remotely Piloted Vehicle) for flight research applications
[AD-A201884] N89-19291
The importance of aircraft performance and signature reduction upon combat survivability
[AD-A202106] N89-19292
A comparative analysis of tilt rotor aircraft versus helicopters using simulator results
[AD-A202190] N89-19294
Aerothermodynamics of a jet cell facility
[AD-A202142] N89-19318
Effects of reduced order modeling on the control of a large space structure
[AD-A201674] N89-19355
Composite reliability enhancement via reloading
[AD-A201861] N89-19380
Finite element analysis of laminated composite plates
[AD-A202192] N89-19381
Processing of aluminum alloy 2090 for superplasticity
[AD-A201865] N89-19411
Computer algorithms for measurement control and signal processing of transient scattering signatures
[AD-A201672] N89-19469
The development and structural characteristics of Dean vortices in a curved rectangular channel
[AD-A201249] N89-19508
Natural convection liquid immersion cooling of a column of discrete heat sources in a vertical channel
[AD-A201676] N89-19513
Transient three-dimensional heat conduction computations using Brian's technique
[AD-A201918] N89-19519
Implementation of dynamic control of a single-link flexible arm using a general micro-computer
[AD-A201622] N89-19561
An experimental investigation of sooting characteristics of a gas turbine combustor and augmentor tube
[AD-A201804] N89-19568
A three-dimensional nonsingular simulation of rigid manipulators
[AD-A201964] N89-19569
The modeling of viscoelastic circular plates for use as waveguide absorbers
[AD-A201621] N89-19588
Machinery diagnostics via mechanical vibration analysis using spectral analysis techniques
[AD-A202089] N89-19594
Passive vibration control using viscoelastic and constrained layer beam waveguide absorbers
[AD-A202188] N89-19595
Local geoid determination using the global positioning system
[AD-A202220] N89-19731
Refractive turbulence profiling via binary source intensity scintillation correlation
[AD-A202189] N89-19762
A modal/WKB inversion method for determining sound speed profiles in the ocean and ocean bottom
[AD-A201252] N89-19791
The effects of a pitched field orientation on hand/eye coordination
[AD-A201620] N89-19814
Development of a model which provides a total system approach to integrating voice recognition and speech synthesis into the cockpit of US Navy aircraft
[AD-A202122] N89-19815
An interrogative model of computer-aided adaptive testing: Some experimental evidence
[AD-A201675] N89-19905
A survey of automatic code generating software
[AD-A201963] N89-19910
Minification processes
[AD-A202219] N89-19958
Development of a system for acoustic measurements of bistatic target strengths
[AD-A201673] N89-19970

NAVAL RESEARCH LAB., WASHINGTON, DC.
Composite materials at high temperatures
[AD-A201163] N89-19372
NRL boron propellants combustion program
[AD-A201242] N89-19440
Chaotic electron motion caused by sidebands in free electron lasers
[AD-A201635] N89-19538
A new database of ice particle size spectra for altitudes up to 10 km (30,000 ft) N89-19673

NAVAL SURFACE WARFARE CENTER, DAHLGREN, VA.
Drag coefficients for irregular fragments
[AD-A201943] N89-19276

NAVY PERSONNEL RESEARCH AND DEVELOPMENT CENTER, SAN DIEGO, CA.
Brain activity during tactical decision-making. Part 4: Event-related potentials as indices of selective attention and cognitive workload
[AD-A201370] N89-19797

NETHERLANDS ENERGY RESEARCH FOUNDATION, PETTEN.
A poor man's optical fog detector N89-19716

NEVADA UNIV., LAS VEGAS.
On purely exponential logic queries
[AD-A201259] N89-19902

NEVADA UNIV., RENO.
Boundary layer development over the eastern Pacific Ocean N89-19753
Lidar for the determination of Antarctic water vapor profiles N89-19756

NEW MEXICO UNIV., ALBUQUERQUE.
Power spectra decomposition of 36 RS CVn UBV photometric light curves from the first two years of the automatic photoelectric telescope N89-20036

NORGES TEKNISKE HOEGSKOLE, TRONDHEIM.
Economic analysis of NAVSAT system
[REPT-1013-CA/TS] N89-19285

NORTH CAROLINA STATE UNIV., RALEIGH.
An approach to semi-active control of multiple degree-of-freedom systems N89-19554
Cloud capture by a mountain top forest. Part 1: Acidity and dosage duration N89-19682

NORTH CAROLINA UNIV., CHAPEL HILL.
The climate inversion problem: A statistical/modeling approach N89-19784
Sensitivity analysis using the Monte Carlo acceptance-rejection method
[AD-A201261] N89-19955
Some 2H NMR studies of oriented fluid phases
[AD-A201241] N89-19998

NORTH DAKOTA UNIV., GRAND FORKS.
Variable gravity research facility
[NASA-CR-184714] N89-19324

NORTHEASTERN UNIV., BOSTON, MA.
Arc jet diagnostics tests N89-20085

NORTHWEST RESEARCH ASSOCIATES, INC., BELLEVUE, WA.
An assessment of the application of in situ ion-density data from DMSP (Defense Meteorology Satellite Program) to modeling of transionospheric scintillation
[AD-A202415] N89-19765

NORTHWESTERN UNIV., EVANSTON, IL.
Sliding and debonding inclusions
[AD-A201609] N89-19587

NORWICH UNIV., NORTHFIELD, VT.
Development of a software interface for optical disk archival storage for a new life sciences flight experiments computer N89-20061

O

OAK RIDGE NATIONAL LAB., TN.
Reinforcement/matrix interaction in SiC fiber-reinforced Ni3Al matrix composites
[DE89-006041] N89-19384
Fabrication of XLWIR (Extra-Long-Wavelength-Infrared) window materials
[DE89-006418] N89-19439
Determination of local fluid drag by a laser heating/thermographic phosphor technique: Applicability of the H. Ludwieg model
[DE89-006462] N89-19523
Bifurcating optimization algorithms and their possible application
[DE89-005692] N89-19906
Quench pressure, thermal expulsion, and normal zone propagation in internally cooled superconductors
[DE89-005668] N89-20003
Pyrolytic and laser photolytic growth of crystalline and amorphous germanium films from digermane (GE2H6)
[DE89-006125] N89-20019

OHIO STATE UNIV., COLUMBUS.
Decentralized/relegated control for large space structures N89-19346
A heuristically based navigation system for an autonomous walking machine with a range scanner N89-19563
A dynamic, time stepping boundary element method for frictional crack and interface problems N89-19590
Diagnosis by integrating model-based reasoning with knowledge-based reasoning N89-19835
Reducing uncertainty by using explanatory relationships N89-19837
A method for modeling bias in a person's estimates of likelihoods of events N89-19849
Static and dynamic properties of arrays of superconductors N89-20017
Superfluid turbulence in two-fluid flow of helium II N89-20018

OLD DOMINION UNIV., NORFOLK, VA.
Solution of steady and unsteady transonic-vortex flows using Euler and full-potential equations N89-19248
A study of flow separation in transonic flow using inviscid and viscous CFD schemes N89-19273
Large deviation local limit theorems for ratio statistics
[AD-A201169] N89-19954

OSAKA KYOIKU UNIV. (JAPAN).
Experimental studies on secondary ice particle production N89-19667

P

PARIS VII UNIV. (FRANCE).
Concentrations in rain events collected sequentially: Measurements vs results of a simple scavenging model N89-19701

PENNSYLVANIA STATE UNIV., UNIVERSITY PARK.
The mechanical behavior of surface modified ceramics
[DE89-004764] N89-19422
Polymer morphology and transport
[AD-A201167] N89-19424
A computationally efficient modelling of laminar separation bubbles
[NASA-CR-184789] N89-19504
Effects of cloud microphysical processes on trace chemical removal efficiences N89-19707
Robust bounded influence tests in linear models
[AD-A201896] N89-19957

PENNSYLVANIA UNIV., PHILADELPHIA.
The aqueous electrochemistry of polyacetylene (CH)x and polyparaphenylene
[AD-A201461] N89-19426
Chemistry and physics of polyacetylene, (CH)x: The prototype conducting polymer
[AD-A201933] N89-19431

PITTSBURGH UNIV., PA.
The dissociative adsorption of ammonia on Si(100)
[AD-A201599] N89-19396
The adsorption and decomposition of NH3 on Si(100): Detection of the NH2(a) species
[AD-A201601] N89-19397
Vibrational spectroscopic studies of surface chemical interactions in chemisorption and catalysis
[DE89-005896] N89-19400

POLITECNICO DI MILANO (ITALY).
Synthetic aperture radar (SAR) data focusing using seismic migration techniques
[REPT-88-015] N89-19479
Propagation problems regarding 20/30 GHz bands in Earth-space links
[REPT-88-022] N89-19480
Propagation problems regarding millimeter waves (40/50 GHz)
[REPT-88-023] N89-19481
A general way to put time in Petri nets
[REPT-88-011] N89-19914
Specification and management of database integrity constraints through logic programming
[REPT-88-025] N89-19915
Stabilization and regulation of multirate sampled-date linear systems
[REPT-88-013] N89-19930
Further results on the design of multivariable regulators under structure and robustness constraints. Part 1: The initialization problem
[REPT-88-028] N89-19931
Further results on the design of multivariable regulators under structure and robustness constraints. Part 2: The reliable robust decentralized regulator problem and the simultaneous robust decentralized regulator problem
[REPT-88-029] N89-19932

PORTLAND STATE UNIV., OR.
The tensile strength of liquid helium four N89-20016

PRAIRIE VIEW AGRICULTURAL AND MECHANICAL COLL., TX.
Design of a surface-based factory for the production of life support and technology support products. Phase 2: Integrated water system for a space colony
[NASA-CR-184730] N89-19808
Model formulation of non-equilibrium gas radiation for hypersonic flight vehicles N89-20066
Time-domain imaging N89-20084

PRINCETON UNIV., NJ.
Transonic flutter calculations using the Euler equations N89-19258
Implications of the observed contraction of accretion disks in quiescent dwarf novae N89-20047
PURDUE UNIV., WEST LAFAYETTE, IN.
Static aeroelasticity of a composite oblique wing in transonic flows N89-19254
The effect of prewhirl on the internal aerodynamics and performance of a mixed flow research centrifugal compressor
[NASA-CR-184756] N89-19503
Turbulence structure and mass transport in a channel flow with polymer injection
[AD-A202237] N89-19521
The 2-4 semiconductor superlattices
[AD-A202369] N89-20005

R

R AND D ASSOCIATES, ALEXANDRIA, VA.
MPD (Magnetoplasmadynamic) thrust chamber flow dynamics
[AD-A201263] N89-19368
RACAL-DECCA ADVANCED DEVELOPMENT LTD., WALTON-ON-THAMES (ENGLAND).
Economic analysis of NAVSAT system
[REPT-1013-CA/TS] N89-19285
RCA ADVANCED TECHNOLOGY LABS., MOORESTOWN, NJ.
An intelligent interface for satellite operations: Your Orbit Determination Assistant (YODA) N89-19852
RENSSELAER POLYTECHNIC INST., TROY, NY.
The stability of boundary layer flow over elastic substrates N89-19524
ROCHESTER UNIV., NY.
Investigation of the performance of photoconductive switches
[AD-A201425] N89-19489
Coordinates, conversions, and kinematics for the Rochester Robotics Lab
[AD-A201611] N89-19560
Opto-electronic systems research. Image recovery from partial Fresnel zone information
[AD-A201556] N89-19969
Intermolecular and intramolecular vibrational relaxation and energy transfer
[AD-A201610] N89-19974
Rotation and magnetic fields as an acceleration mechanism in astrophysical jets N89-20039
ROCKWELL INTERNATIONAL CORP., CANOGA PARK, CA.
Safe, compact nuclear propulsion: Solid core nuclear propulsion concept
[AD-A202339] N89-19369
ROCKWELL INTERNATIONAL CORP., DOWNEY, CA.
Design guidelines for remotely maintainable equipment N89-19885
Expert systems applications for space shuttle payload integration automation N89-19887
ROCKWELL INTERNATIONAL SCIENCE CENTER, THOUSAND OAKS, CA.
Full potential unsteady computations including aeroelastic effects N89-19243
Ohmic contacts to gallium aluminum arsenide for high temperature applications
[AD-A202248] N89-19492
ROLLS-ROYCE LTD., DERBY (ENGLAND).
Propulsion
[PNR90472] N89-19302
The gas turbine engine and its certification
[PNR90496] N89-19303
Current diagnostic practice in gas turbine combustors
[PNR90530] N89-19306
The relationship between manufacturing technology and design
[PNR90537] N89-19307
The diffusion bonding of aeroengine components
[PNR90540] N89-19308
Thermal cycling and mechanical property assessment of carbon fiber (fabric) reinforced PMR-15 polyimide laminates
[PNR90522] N89-19382
Microstructural optimisation of titanium alloys for defect tolerance in gas turbine engine components
[PNR90503] N89-19413
Tensile properties of Ti-6Al-2Sn-4Zr-2Mo sheet after superplastic deformation
[PNR90499] N89-19414
Computational fluid dynamics for combustion applications
[PNR90534] N89-19525
Application of Schlieren photography in gas turbine combustion research
[PNR90495] N89-19532
The use of burst-triggered correlation for laser anemometry measurements in turbomachinery
[PNR90542] N89-19533
Gear technology acquisition for advanced aero engines
[PNR90510] N89-19571
COMPASS: A generalized ground-based monitoring system
[PNR90483] N89-19894
ROLLS-ROYCE LTD., WATFORD (ENGLAND).
Some novel test methods for, and associated problems of mechanical strength characterization of engineering ceramics
[PNR90492] N89-19436
ROME AIR DEVELOPMENT CENTER, GRIFFISS AFB, NY.
Autonomous satellite command and control: A comparison with other military systems N89-19839
ROYAL AEROSPACE ESTABLISHMENT, FARNBOROUGH (ENGLAND).
Airfield lighting: Future trends
[RAE-TM-FM-6] N89-19319
ROYAL INST. OF TECH., STOCKHOLM (SWEDEN).
Two-dimensional test section with preadjusted adaptive walls for low speed wind tunnel
[KTH-AERO-REPT-57] N89-19278
ROYAL SIGNALS AND RADAR ESTABLISHMENT, MALVERN (ENGLAND).
User-extensible graphics using abstract structure
[BR104469] N89-19921
RUHR UNIV., BOCHUM (GERMANY, F.R.).
Excitation of strong high-frequency electric fields and their detection using the dynamic Stark effect
[ETN-89-93794] N89-19991
Resonance cones in non Maxwellian plasmas
[REPT-88-N4-173] N89-19993
Morphology and nature of the dust of the dark cloud Coal Sack
[ETN-89-93795] N89-20046

S

SALFORD UNIV. (ENGLAND).
Heat transfer properties of satellite component materials N89-19375
SANDIA NATIONAL LABS., ALBUQUERQUE, NM.
Comparison of an ac and a dc bridge for standard platinum resistance thermometer calibrations
[DE89-007060] N89-19534
Solar thermal technology
[DE89-000818] N89-19738
Silicon concentrator solar cell research
[DE89-005490] N89-19740
A study of the reliability of Stirling engines for distributed receiver systems
[DE89-006395] N89-19746
CAD directed robotic edge finishing
[DE89-005347] N89-19916
Mechanisms leading to single event upset
[ATR-86(8139)-5] N89-19977
SEARCH TECHNOLOGY, INC., NORCROSS, GA.
An intelligent tutoring system for space shuttle diagnosis N89-19853
SELENIA SPAZIO S.P.A., ROME (ITALY).
PSDE/SAT-2: Preliminary spacecraft configuration study, executive summary
[ESA-CR(P)-2704] N89-19364
SERVICIO METEOROLOGICO NACIONAL, BUENOS AIRES (ARGENTINA).
Analysis of hailstones from a severe storm and their simulated evolution N89-19677
SHINSHU UNIV., NAGANO (JAPAN).
Three-dimensional structures of snow crystals shown by stereo-photomicrographs N89-19669
SOCIETE ANONYME DE TELECOMMUNICATIONS, PARIS (FRANCE).
Determination of general and specific properties of wide energy-band gap HgCdTe in the 1 to 2 micrometer wavelength range
[AD-A201341] N89-19488
SOCIETE NATIONALE INDUSTRIELLE AEROSPATIALE, CANNES (FRANCE).
Economic analysis of NAVSAT system
[REPT-1013-CA/TS] N89-19285
PSDE/SAT-2 preliminary spacecraft configuration study, executive summary
[ESA-CR(P)-2689] N89-19360
SOCIETE NATIONALE INDUSTRIELLE AEROSPATIALE, SAINT-MEDARD-EN-JALLES (FRANCE).
Mini protein crystallization facility. Phase A study: Executive summary
[REPT-AQ-ES-576/88] N89-19444
SOFTECH, INC., FAIRBORN, OH.
IDEAL: A methology for developing information systems N89-19888
SOUTH DAKOTA SCHOOL OF MINES AND TECHNOLOGY, RAPID CITY.
Comparison of model results for models of differing microphysical detail N89-19680
SOUTHAMPTON UNIV. (ENGLAND).
Solidification, structure and mechanical properties of A357 aluminum alloy N89-19409
SOUTHERN UNIV., BATON ROUGE, LA.
Feasibility of using high temperature superconducting magnets and conventional magnetic loop antennas to attract or repel objects at the space station N89-20081
SOUTHWEST RESEARCH INST., SAN ANTONIO, TX.
A new approach to the evaluation of the effects of stress state and interfacial properties on the behavior of advanced metal matrix composites
[AD-A201246] N89-19373
Performance evaluation of military engine and gear oils in friction and wear devices
[AD-A202145] N89-19432
Application of nondestructive evaluations to the prediction of turbine fuel peroxidation potential
[AD-A202291] N89-19441
Study of the continuous/diffuse aurora using particle observations from the Dynamics Explorer satellites
[AD-A202241] N89-19763
NESSUS (Numerical Evaluation of Stochastic Structures Under Stress)/EXPERT: Bridging the gap between artificial intelligence and FORTRAN N89-19827
SPACE POWER, INC., SAN JOSE, CA.
The 30 kWe class high efficiency arcjet power conditioner, volume 1
[AD-A202244] N89-20004
SPECTRON DEVELOPMENT LABS., INC., COSTA MESA, CA.
Laser transit anemometer software development program
[NASA-CR-4225] N89-19545
STANFORD UNIV., CA.
Software performance on nonlinear least-squares problems
[AD-A201879] N89-19908
A heuristic ceiling point algorithm for general integer linear programming
[AD-A202285] N89-19912
An exact ceiling point algorithm for general integer linear programming
[AD-A202286] N89-19913
Estimation of a restricted variance ratio
[AD-A202268] N89-19959
Time series analysis and multivariate statistical analysis
[AD-A202273] N89-19960
STATE METEOROLOGICAL INST., BEIJING (CHINA).
Numerical simulation of microphysical processes in cumulonimbus N89-19639
STATE UNIV. OF NEW YORK, ALBANY.
Dynamic, radiative and chemical effects of clouds on tropospheric trace gases N89-19708
STATE UNIV. OF NEW YORK, BUFFALO.
Comments on electromechanical actuators for controlling flexible structures N89-19339
STATE UNIV. OF NEW YORK, PLATTSBURGH.
An assessment of the micrometeoritic component in the Martian soil N89-20070
STATE UNIV. OF NEW YORK, STONY BROOK.
Effect of temperature on the corrosion resistance of nitrogen bearing AL6X and 904L stainless steels
[AD-A201955] N89-19412
Laser scattering studies of epoxy polymerization processes
[AD-A201925] N89-19430
STATE UNIV. OF WESTERN CONNECTICUT, DANBURY.
Acidification of stratiform clouds and their aerosol scavenging properties N89-19694
STOCKHOLM UNIV. (SWEDEN).
Measurements of the partitioning of aerosol mass and number between cloud droplets and interstitial air N89-19616
On the determination of droplet size distributions with the counterflow virtual impactor N89-19655
An examination of the chemical and physical variability of clouds at a mountain-top site in central Sweden N89-19699
SUL ROSS STATE UNIV., ALPINE, TX.
Evaluation of crustal recycling during the evolution of Archean-age Matachewan basaltic magmas N89-20077
Lithospheric buckling and intra-arc stresses: A mechanism for arc segmentation N89-20078
SUSSEX UNIV., BRIGHTON (ENGLAND).
Phenomenological models from higher dimensions with and without supergravity N89-20045
SYRACUSE UNIV., NY.
Interactions and reactions in polymerized vesicles
[AD-A201527] N89-19427

T

TECHNICAL UNIV. OF DENMARK, LYNGBY.
Experimental spherical near-field antenna test facility, phase 3. Volume 1: Facility updates, evaluation and software documentation
[R-343] N89-19477

TECHNISCHE HOCHSCHULE, DARMSTADT (GERMANY, F.R.).
On boundary integral equation approach to a nonstationary problem of isothermal viscous compressible flows
[PREPRINT-1134] N89-19526

TECHNISCHE UNIV., BERLIN (GERMANY, F.R.).
A model for the geostationary orbital infrastructure, system analysis
[ILR-MITT-205] N89-19323
Model of a geostationary regional transportation company (GRET): Fleet composition and facility layout
[ILR-MITT-207] N89-19329
Preliminary cost model for a commercial geostationary transportation company (GRET)
[ILR-MITT-208] N89-19330
Preliminary project plan for a GEO regional transportation and servicing company
[ILR-MITT-210] N89-19331
Investigations of the statics and dynamics of the Jahn-Teller system RbCrCl3 using neutron scattering
[ETN-89-93790] N89-20006
Laser-spectroscopic investigations of manganese centers in the zinc sulfide host lattice
[ETN-89-93791] N89-20007

TECHNISCHE UNIV., DELFT (NETHERLANDS).
Orientation of orbits in flows
[REPT-88-05] N89-19322
Modeling of inertial effects in transient liquid-bubble flows
[REPT-88-22] N89-19528
A finite element dynamic analysis of flexible spatial mechanisms and manipulators
[ETN-89-93901] N89-19575
Elastic cross-influence between two quasi-Hertzian contact zones
[REPT-88-45] N89-19576
Some new results in rolling contact
[REPT-88-46] N89-19577
Fatigue crack growth in ARALL: A hybrid aluminum Aramid composite material. Crack growth mechanisms and quantitative predictions of the crack growth rates
[ETN-89-93899] N89-19602
The elastic stress and the displacement on the surfaces of two rubber-clad steel cylinders between which paper is led
[REPT-88-23] N89-19603
The geometry of geodetic inverse linear mapping and nonlinear adjustment
[ETN-89-93900] N89-19736
Linear programming along the trajectory of the problem in polynomial time
[REPT-88-17] N89-19918
From Algol 60 to Ada: Problems, solutions, feasibility
[REPT-88-41] N89-19919
The influence of the potential function on the performance of a trajectory following algorithm for the linear programming problem
[REPT-88-44] N89-19920
Formal aspects of a knowledge system: A literature review
[REPT-88-12] N89-19933
Criterion based equivalence for equation error models
[WTHD-188] N89-19941
Characterizations of conditional expectation-type oeprators
[REPT-88-04] N89-19942
The box dimension of self-affine graphs and repellors
[REPT-88-08] N89-19943
Hausdorff dimension and box dimension in self-similar sets
[REPT-88-09] N89-19944
Hyperbolicity properties of C sup 2 multimodal Collet-Eckmann maps without Schwarzian deriative assumptions
[REPT-88-10] N89-19945
Discrete event systems with stochastic processing times
[REPT-88-11] N89-19946
Normal forms and periodic solutions in the theory of nonlinear oscillations. Existence and asymptotic theory
[REPT-88-16] N89-19948
Cell-centered and vertex-centered discretization of interface problems
[REPT-88-18] N89-19949
Approximation, saturation and semigroups of operators in Banach space
[REPT-88-19] N89-19950
Vectorization of linear recurrence relations
[REPT-88-21] N89-19951
A generalization of Laguerre polynomials
[REPT-88-28] N89-19952
Vertex-centered and cell-centered multigrid methods for interface problems
[REPT-88-42] N89-19953
Probability theories, fuzzy set theory and syllogisms; a literature review
[REPT-88-13] N89-19961
Highly efficient estimates of multivariate location with high breakdown point
[REPT-88-14] N89-19962
Tail triviality for sums of stationary random variables
[REPT-88-40] N89-19963
Multicriteria analysis and budget allocation, with applications in energy R and D planning: A feasibility study
[REPT-88-07] N89-20026
Stochastic and fuzzy PERT
[REPT-88-26] N89-20027
On the great circle reduction in the data analysis for the astrometric satellite HIPPARCOS
[ETN-89-93902] N89-20038
Existence of stationary solutions in the coronal loop problem
[REPT-88-06] N89-20054

TECHNISCHE UNIV., EINDHOVEN (NETHERLANDS).
On the sealing and lubrication mechanism of radial lip seals
[ETN-89-93898] N89-19574
Ultrasound transmission tomography, a low-cost realization
[ISBN-90-9002330-5] N89-19804
Regulation of linear discrete time-varying systems
[ETN-89-93896] N89-19934
Theory of accelerated orbits and space charge effects in an Azimuthly Varying Field (AVF) cyclotron
[ETN-89-93897] N89-19978

TECHNISCHE UNIV., HAMBURG (GERMANY, F.R.).
Experimental investigation on plume contamination and surface effects, phase 2
[TUHH-TRI-ESA-1987] N89-19370

TECHNISCHE UNIV., HANOVER (GERMANY, F.R.).
Mass-radius star evolution Sun activity planets surfaces on purely empirical basis. Empiry theory reality: The use of statistics
[REPT-18] N89-20050

TECHNISCHE UNIV., MUNICH (GERMANY, F.R.).
Determination of chemical reaction rates in fog N89-19683
A one-dimensional numerical model to simulate liquid phase chemical reactions within radiation fog N89-19690

TEL-AVIV UNIV. (ISRAEL).
Starting characteristics of direct current motors powered by solar cells
[NASA-TM-101981] N89-19493

TENNESSEE UNIV., KNOXVILLE.
Extracting depth by binocular stereo in a robot vision system
[DE89-005016] N89-19572
A 2-D and 3-D robot path planning algorithm based on quadtree and octree representation of workspace
[DE89-005014] N89-19900
Gaussian beam representation of beam-like ultrasonic fields N89-19972
The V3, V4 and V6 bands of formaldehyde: A spectral catalog from 900 cm(-1) to 1580 cm(-1)
[NASA-TM-100709] N89-19976

TENNESSEE UNIV. SPACE INST., TULLAHOMA.
An innovative demonstration of high power density in a compact MHD generator
[DE89-002159] N89-19990

TEXAS A&I UNIV., KINGSVILLE.
Intelligent control of robotic arm/hand systems for the NASA EVA retriever using neural networks N89-20075

TEXAS A&M UNIV., COLLEGE STATION.
Design improvement of a pump wear ring labyrinth seal
[NASA-CR-179161] N89-19555
Control of flexible structures: Model errors, robustness measures, and optimization of feedback controllers
[AD-A202234] N89-19596
Oxygen electrode in molten carbonate fuel cells
[DE89-005813] N89-19745
An asymptotic theory for weighted least squares with weights estimated by replication
[AD-A198000] N89-19935

TEXAS INSTRUMENTS, INC., DALLAS.
A representational framework and user-interface for an image understanding workstation N89-19878
Voice control of complex workstations N89-19880

TEXAS SOUTHERN UNIV., HOUSTON.
Comparison of Soviet and US space food and nutrition programs N89-20059

TEXAS TECHNOLOGICAL UNIV., LUBBOCK.
High current, high Coulomb ignitrons
[DE89-005547] N89-19490
Mesoscale Convective Systems: Structure, development and storm-environment interactions N89-19788

TEXAS UNIV., ARLINGTON.
Experimental simulation of transonic vortex-airfoil interactions
[AD-A201934] N89-19274

TEXAS UNIV., AUSTIN.
A bootstrap lunar base: Preliminary design review 2
[NASA-CR-184753] N89-19807
A geometric property of the least squares solution of linear equations
[AD-A201342] N89-19937
Near-infrared spectroscopy of young stellar objects N89-20033

TEXAS UNIV., DALLAS.
Proof of the feasibility of coherent and incoherent schemes for pumping a gamma-ray laser
[AD-A201931] N89-19542

TEXAS UNIV., GALVESTON.
Maladjustment of kidneys to microgravity: Design of measures to reduce the loss of calcium N89-20076

TEXAS UNIV., SAN ANTONIO.
Fatigue crack growth model RANDOM2 user manual. Appendix 1: Development of advanced methodologies for probabilistic constitutive relationships of material strength models
[NASA-CR-184775-APP-1] N89-19581
Fatigue strength reduction model: RANDOM3 and RANDOM4 user manual. Appendix 2: Development of advanced methodologies for probabilistic constitutive relationships of material strength models
[NASA-CR-184796-APP-2] N89-19582

TEXAS UNIV. AT DALLAS, RICHARDSON.
A study of the ionospheric signature of ion supply from the ionosphere to the magnetosphere N89-19754
Characteristics of optical emissions and particle precipitation in mid/low latitude aurorae N89-19755

TICRA A/S, LYNGBY (DENMARK).
Meteosat Millimetre Wave Sounder (MWS) study
[BAE-TP-9119] N89-19363

TOKYO UNIV. (JAPAN).
Analytical interpretation on lateral/directional stability and controllability of high angle-of-attack reentry flight
[ISAS-630] N89-19353

TOLEDO UNIV., OH.
Robust control for linear systems with structured uncertainty
[AD-A201947] N89-19315

TORONTO UNIV., DOWNSVIEW (ONTARIO).
Analytical, numerical and experimental investigations of oblique-shock-wave reflections in pure and dusty gases
[AD-A201438] N89-19511

TORONTO UNIV. (ONTARIO).
The effect of freezing on the composition of cloud droplets N89-19691

TRANSPORTATION SYSTEMS CENTER, CAMBRIDGE, MA.
General aviation activity and avionics survey
[AD-A201760] N89-19229

TRINITY COLL., HARTFORD, CT.
Damped-oscillation representation of drop-spectrum evolution due to coalescence and breakup N89-19660

U

UNITED ANALYSIS, INC., VIENNA, VA.
Advanced durability analysis. Volume 4: Executive summary
[AD-A202304] N89-19597

UNITED TECHNOLOGIES RESEARCH CENTER, EAST HARTFORD, CT.
Airfoil stall penetration at constant pitch rate and high Reynolds number N89-19260
Unsteady aerodynamics of blade rows N89-19263

UNIVERSITAET DER BUNDESWEHR, NEUBIBERG (GERMANY, F.R.).
Interpretation of ERS-1 wind scatterometer data: Wind field extraction
[ETN-89-93982] N89-19790

UNIVERSITY COLL., GALWAY (IRELAND).
Below cloud scavenging by rain and drizzle N89-19685

UNIVERSITY COLL., LONDON (ENGLAND).
A study of advanced radar altimeter techniques
[ESA-CR(P)-2699] N89-19483

UNIVERSITY OF CENTRAL WASHINGTON, ELLENSBURG.
Effects on motor unit potentiation and ground reaction force from treadmill exercise N89-20069

UNIVERSITY OF NORTHERN ILLINOIS, DE KALB.
Investigation of the interface between two immiscible electrolytes applied to membrane electrochemistry
[AD-A201310] N89-19393
Mossbauer effect studies of magnetism in superconducting systems
[DE89-005844] N89-20012
UNIVERSITY OF SOUTHERN CALIFORNIA, LOS ANGELES.
Test aspects of the JPL Viterbi decoder N89-19457
New approaches to reconfigurable optical interconnections for optical computing
[AD-A201307] N89-19982
UNIVERSITY OF SOUTHERN ILLINOIS, CARBONDALE.
Automatic voice recognition using traditional and artificial neural network approaches N89-20064
UNIVERSITY OF WESTERN ONTARIO, LONDON.
Positron spectroscopy for materials characterization
[DE89-005766] N89-20010
UTAH STATE UNIV., LOGAN.
Infrared and ionization structure of the polar mesosphere
[AD-A201266] N89-19751
A study of the high altitude thermospheric dayglow from Spacelab 1 N89-19768
UTAH UNIV., SALT LAKE CITY.
Characterization of IM7/8551-7 carbon/epoxy in compression and shear
[DE89-005544] N89-19378
Measurements of the compressive behavior of AS4/3501-6 and IM7/8551-7 carbon/epoxy
[DE89-005823] N89-19383
Ion pair solvation
[AD-A201529] N89-19395
Empirical equations of ice crystal growth microphysics for modeling and analysis N89-19609
Theory on the uncertainty in cloud microphysical processes and climate N89-19644

V

VECTOR RESEARCH, INC., ANN ARBOR, MI.
Psychological tools for knowledge acquisition N89-19857
VIRGINIA POLYTECHNIC INST. AND STATE UNIV., BLACKSBURG.
A vortex panel method for potential flows with applications to dynamics and controls N89-19269
Maneuvering equations in terms of quasi-coordinate N89-19337
Damage detection and location in large space trusses N89-19350
Nonlinear optimal control and near-optimal guidance strategies in spacecraft general attitude maneuvers N89-19356
An interdisciplinary study of cathodic debonding in elastomer/metal adhesive bonds
[AD-A202376] N89-19434
Analysis and synthesis of microstrip antennas including mutual coupling
[AD-A201783] N89-19472
Curvature effects on the stability of three-dimensional laminar boundary layers N89-19500
Boundary layer and singularity measurement in three dimensional fracture problems
[AD-A201277] N89-19584
Compression strength of composite primary structural components
[NASA-CR-184893] N89-19599
VIRGINIA UNIV., CHARLOTTESVILLE.
Proceedings of the Fifth AFOSR Forum on Space Structures
[AD-A194761] N89-19333
System identification of suboptimal feedback control parameters based on limiting-performance/minimum-time characteristics N89-19340

W

WASHINGTON STATE UNIV., PULLMAN.
Research in acoustical scattering, diffraction catastrophes, optics of bubbles and acoustical phase conjugation
[AD-A201451] N89-19968
WASHINGTON UNIV., SEATTLE.
Gas hydrates thermomechanics
[DE88-010280] N89-19387
A comparative study of laboratory thermals and atmospheric clouds N89-19627
In situ measurements of ship tracks N89-19645
Some effects of cloud microphysics on cloud chemistry N89-19692
A numerical investigation of sulfate production and deposition in midlatitude continental cumulus clouds N89-19705
A critical evaluation of the von Karman constant from a new atmospheric surface layer experiment N89-19757
CAD-model-based vision for space applications N89-19867
Studies in quantum field theory
[DE89-006286] N89-20023
The scintillating optical fiber isotope experiment (SOFIE): Bevalac calibrations of test models N89-20034
WAYNE STATE UNIV., DETROIT, MI.
Josephson effect research in high-temperature superconductors
[AD-A201483] N89-20002
WEST VIRGINIA UNIV., MORGANTOWN.
Integration of a computerized two-finger gripper for robot workstation safety N89-19863
WESTINGHOUSE ELECTRIC CORP., MADISON, PA.
Application of model based control to robotic manipulators N89-19884
WESTINGHOUSE ELECTRIC CORP., PITTSBURGH, PA.
Safe, compact nuclear propulsion: Solid core nuclear propulsion concept
[AD-A202339] N89-19369
WISCONSIN UNIV., MADISON.
Interdisciplinary research in viscoelasticity and rheology
[AD-A201270] N89-19390
Design of an optical sensor system for adaptive control of a seam tracking robot N89-19565
Generalized microphysics scheme for use in mesoscale/cloud models N89-19641
The WCSAR telerobotics test bed N89-19871
Ultracompact HII regions associated with massive star formation N89-20044
Ground-based Fabry-Perot observations of neutral and ionic atoms and molecules of comet Halley N89-20048
WITTEN/HERDECKE UNIV. (GERMANY, F.R.).
Kinetics and mechanism of the Fe catalyzed autoxidation of S(4)-oxides in aqueous solution N89-19687
WRIGHT STATE UNIV., DAYTON, OH.
A stress test to evaluate the physical capacity of performing L-1 anti-G straining maneuvers
[AD-A202301] N89-19803
Transformation based endorsement systems N89-19836
WYOMING UNIV., LARAMIE.
A test of ice crystal production by aircraft N89-19622

Y

YALE UNIV., NEW HAVEN, CT.
Fear-potential startle as a model system for analyzing learning and memory
[AD-A201330] N89-19805
Knowledge acquisition for case-based reasoning systems N89-19856

Typical Contract Number Index Listing

Listings in this index are arranged alphanumerically by contract number. Under each contract number the NASA accession numbers denoting documents that have been produced as a result of research done under that contract are arranged in ascending order. The NASA accession number denotes the number by which the citation is identified.

AF PROJ. 2301 ..... N89-19489
AF PROJ. 2302 ..... N89-19333
N89-19585
AF PROJ. 2303 ..... N89-19394
AF PROJ. 2304 ..... N89-19390
N89-19955
AF PROJ. 2305 ..... N89-19982
N89-20000
AF PROJ. 2306 ..... N89-20005
AF PROJ. 2307 ..... N89-19511
AF PROJ. 2310 ..... N89-19751
AF PROJ. 2312 ..... N89-19805
AF PROJ. 2313 ..... N89-20029
AF PROJ. 3058 ..... N89-19369
AF-AFOSR-0046-87 ..... N89-19621
AF-AFOSR-0113-86 ..... N89-19585
AF-AFOSR-0124-87 ..... N89-19511
AF-AFOSR-0140-84 ..... N89-19955
AF-AFOSR-0163-85 ..... N89-19751
AF-AFOSR-0175-84 ..... N89-19489
AF-AFOSR-0185-85 ..... N89-20005
AF-AFOSR-0191-87 ..... N89-19390
AF-AFOSR-0230-85 ..... N89-20000
AF-AFOSR-0294-87 ..... N89-19644
AF-AFOSR-0299-85 ..... N89-19752
AF-AFOSR-0309-87 ..... N89-20029
AF-AFOSR-0336-87 ..... N89-19805
AF-AFOSR-0338-87 ..... N89-19982
AF-AFOSR-0355-87 ..... N89-19394
AFAL-89-014 ..... N89-19369
ARPA ORDER 5351 ..... N89-19868
BCRS-PROJ. AO-2.1 ..... N89-19735
BCRS-PROJ. CO-1.6 ..... N89-19734
BCRS-PROJ. TO-3.4 ..... N89-19733
BMFT-KFZ-0704587-2 ..... N89-19767
BMFT-PROJ. 07VND01-0 ..... N89-19702
BMFT-02-U-5594-0 ..... N89-19416
BMFT-0704564-A N89-19747
CEPR/ADER-86/00020 ..... N89-19713
COMM-NA-86-RAH-06051 ..... N89-19613
N89-19626
COMM-NA-87-RAH-07077 ..... N89-19613
N89-19626
DA PROJ. 1L1-61102-BH-57 ..... N89-19593
DA PROJ. 1L1-61103-BH-57 ..... N89-19488
DA PROJ. 3E1-62777-A-878 ..... N89-19541
DAAG29-83-K-0095 ..... N89-19759
DAAG29-84-K-0086 ..... N89-19395
DAAG29-84-K-0131 ..... N89-19274
DAAG29-84-K-0148 ..... N89-19472
DAAG29-84-K-0165 ..... N89-19510
DAAG29-84-K-0166 ..... N89-19474
DAAG29-84-K-0175 ..... N89-19424
DAAG29-85-G-0081 ..... N89-19537
DAAG29-85-K-0008 ..... N89-19956
DAAG29-85-K-0050 ..... N89-19373
DAAG29-85-K-0059 ..... N89-19974
DAAG29-85-K-0065 ..... N89-19467
DAAG29-85-K-0076 ..... N89-19430
DAAG29-85-K-0085 ..... N89-19801
DAAG29-85-K-0127 ..... N89-19427
DAAG29-85-K-0130 ..... N89-19512
DAAG29-85-K-0134 ..... N89-19587
DAAG29-85-K-0190 ..... N89-19939
DAAG29-85-K-0209 ..... N89-19391
DAAG29-85-K-0227 ..... N89-19475
DAAG29-85-K-0239 ..... N89-19960
DAAK11-83-K-0007 ..... N89-19672
DAAK60-86-C-0128 ..... N89-19812
N89-19813
DAAK70-87-C-0029 ..... N89-19432
DAAL03-36-K-0175 ..... N89-19725
DAAL03-86-G-0085 ..... N89-19909
DAAL03-86-K-0077 ..... N89-19388
DAAL03-86-K-0160 ..... N89-19314
DAAL03-86-K-0175 ..... N89-19721
DAAL03-87-G-0004 ..... N89-19902
DAAL03-87-K-0015 ..... N89-19520
DAAL03-87-K-0084 ..... N89-19969
DAAL03-88-K-0015 ..... N89-19408
DAAL03-88-K-0076 ..... N89-19954
DACA76-85-C-0001 ..... N89-19560
DACA76-85-C-0003 ..... N89-19868
DAJA45-86-C-0033 ..... N89-19593
DAJA45-87-C-0020 ..... N89-19488
DAKF15-87-C-0110 ..... N89-19937
DAMD17-87-C-7186 ..... N89-19541
DASG60-87-C-0029 ..... N89-19981
DE-AC02-76CH-00016 ..... N89-19540
N89-19693
N89-19985
N89-20010
DE-AC02-76CH-03000 ..... N89-19491
DE-AC02-76ER-01198 ..... N89-19405
N89-20014
DE-AC02-78ER-04915 ..... N89-20023
DE-AC02-83CH-10093 ..... N89-19738
N89-19739
N89-19743
N89-19744
N89-19781
DE-AC02-85NE-37947 ..... N89-19684
DE-AC03-76SF-00098 ..... N89-19404
N89-20020
DE-AC04-76DP-00613 ..... N89-19573
DE-AC04-76DP-00789 ..... N89-19534
N89-19740
N89-19746
N89-19916
DE-AC05-84OR-21400 ..... N89-19384
N89-19439
N89-19523
N89-19906
N89-20003
N89-20019
DE-AC07-76ID-01570 ..... N89-19389
N89-19423
N89-19498
N89-19557
N89-19967
N89-20028
DE-AC21-84MC-21180 ..... N89-19387
DE-AC22-87PC-79678 ..... N89-19990
DE-AI05-82OR-1005 ..... N89-19737
DE-FC02-86CH-10251 ..... N89-19781
DE-FG02-85ER-13451 ..... N89-19403
DE-FG02-85ER-60294 ..... N89-19707
DE-FG02-86ER-45252 ..... N89-19422
DE-FG02-86ER-45253 ..... N89-19401
DE-FG02-86NE-37968 ..... N89-19572
N89-19900
DE-FG02-87ER-45307 ..... N89-19437
DE-FG02-87ER-45320 ..... N89-20009
DE-FG02-88ER-13864 ..... N89-19400
DE-FG03-87ER-25030 ..... N89-19908
DE-FG22-87PC-79931 ..... N89-19745
DEN-E/5B/CON/935/2043 ..... N89-19793
DLA900-84-C-0910 ..... N89-19441
DRET/INSU-83-34308 ..... N89-19625
DRET/INSU-85-34016 ..... N89-19625
DTFA01-80-Y-10546 ..... N89-19782
DUT-5-35362 ..... N89-20026
EN3M-0048-NL(GDF) N89-20026
EPA-81-24-430 ..... N89-19682
EPA-81-39-3401-2 ..... N89-19682
ESA-CR(P)-6499/85-NL-DG N89-19359
ESA-EP/JVD/14.7/5234 ..... N89-19790
ESA-5904/84-NL-GM/(3G63) N89-19494
ESA-5974/84 ..... N89-19816
ESA-6864/86-D-MD N89-19320
ESA-7088/87-NL-JG(SC) N89-19483
ESA-7112/87-S-RD(SC) N89-19285
ESA-7189/87-NL-DG N89-19360
ESA-7224/87-NL-PR N89-19482
ESA-7231/87-NL-JS N89-19363
ESA-7254/87-D-IM(SC) N89-19895
ESA-7312/87-F-RD(SC) N89-19286
ESA-7382/87-F-FL(SC) N89-19444
ESA-7388/87-NL-JS N89-19766
ESA-7574/88 ..... N89-19364
ESTEC-1511/87-NL-PH N89-19361
ESTEC-4682/81-NL-MS(SC) N89-19477
ESTEC-5607/83-NL-AN(SC) N89-19496
ESTEC-6044/84-NL-PB N89-19495
ESTEC-6487/85-NL-PB(SC) N89-19530
N89-19531
ESTEC-6559/85-NL-PH(SC) N89-19370
ESTEC-6824/86-NL-PP(SC) N89-19447
ESTEC-6902/86-NL-MAC(SC) N89-19362
ESTEC-6977/86-NL-PP(SC) N89-19478
ESTEC-7086/87-NL-PB(SC) N89-19443
FINEP 537/CT N89-19750
F04611-83-K-0018 ..... N89-19544
F04611-83-K-0023 ..... N89-19544
F04611-85-K-0050 ..... N89-19999
F04611-86-C-0052 ..... N89-20004
F04611-87-C-0057 ..... N89-19584
F04701-85-C-0086 ..... N89-19476
N89-19764
F19628-83-C-0143 ..... N89-19354
F19628-85-C-0002 ..... N89-19473
N89-19929
F19628-85-C-0003 ..... N89-19903
F19628-85-K-0044 ..... N89-19761
F19628-86-C-0001 ..... N89-19841
F19628-86-C-0195 ..... N89-19765
F30602-85-C-0008 ..... N89-19560
F30603-87-C-0136 ..... N89-19850
F33615-84-C-3208 ..... N89-19597
F33615-85-C-2537 ..... N89-19301
F33615-85-C-3013 ..... N89-19275
F33615-85-C-3212 ..... N89-19374
N89-19379
F33615-85-C-4503 ..... N89-19796
F33615-85-D-0514 ..... N89-19849
F33615-86-C-3410 ..... N89-19280
N89-19281
F33615-86-K-3611 ..... N89-19315
F49620-82-K-0010 ..... N89-19856
F49620-84-C-0007 ..... N89-19509
F49620-85-C-0029 ..... N89-19763
F49620-85-C-0044 ..... N89-19536
F49620-85-C-0120 ..... N89-19492
F49620-85-C-0126 ..... N89-19507
F49620-85-C-0144 ..... N89-19935
F49620-86-C-0038 ..... N89-19358
F49620-86-C-0117 ..... N89-19368
F49620-86-K-0009 ..... N89-19333
F49620-86-K-0014 ..... N89-19596
F49620-87-C-0104 ..... N89-20001
F49620-87-C-0108 ..... N89-19357
JAPMINED-61020001 ..... N89-19608
JPL-958292 ..... N89-19866
MIPR-ARO-128-87 ..... N89-19518
MIPR-FY1175-87-04878/01 ..... N89-19836
NAGW-975 ..... N89-19871
NAGW-1175 ..... N89-19868
NAGW-1336 ..... N89-19866
NAG1-392 ..... N89-19502
NAG1-514 ..... N89-19780
NAG1-537 ..... N89-19599
NAG1-648 ..... N89-19248
NAG1-778 ..... N89-19504
NAG1-810 ..... N89-19539
NAG3-627 ..... N89-19442
NAG3-791 ..... N89-19973
NAG3-867 ..... N89-19581

N89-19582
NAG5-813 ..... N89-20051
NAG7-32 ..... N89-19644
NAG9-208 ..... N89-19881
NASW-3737 ..... N89-19365
NAS1-15325 ..... N89-19505
NAS1-16591 ..... N89-19779
NAS1-17493 ..... N89-19316
NAS1-18311 ..... N89-19545
NAS3-23051 ..... N89-19299
NAS3-24244 ..... N89-19449
NAS3-24348 ..... N89-19300
NAS3-24385 ..... N89-19421
NAS3-24387 ..... N89-19583
NAS3-24528 ..... N89-19289
NAS4-2577 ..... N89-19256
NAS5-27783 ..... N89-19620
NAS5-28448 ..... N89-19764
NAS5-28795 ..... N89-19729
NAS5-29373 ..... N89-19729
NAS7-918 ..... N89-19664
N89-19882
NAS8-34507 ..... N89-19367
NAS8-36161 ..... N89-19555
NAS8-36198 ..... N89-19420
NAS8-36944 ..... N89-19366
NAS9-17779 ..... N89-19809
NAS9-17900 ..... N89-19861
NCC9-16 ..... N89-19881
NERC-GR3/5896 ..... N89-19621
NGT-21-002-080 ..... N89-19324
N89-19352
N89-19807
N89-19808
N89-20040
N89-20041
NGT-44-005-803 ..... N89-20058
N89-20073
NOAA-40-RANR-506003 ..... N89-19694
NOAA-40-RANR-508854L N89-19694
NOAA-50-EANR-6-00011 ..... N89-19707
NOAA-87-1999 ..... N89-19609
NSF ATM-82-18066 ..... N89-19608
NSF ATM-83-14072 ..... N89-19606
NSF ATM-84-15127 ..... N89-19643
NSF ATM-84-19000 ..... N89-19692
NSF ATM-84-19490 ..... N89-19607
N89-19615
NSF ATM-84-20816 ..... N89-19618
N89-19627
NSF ATM-85-12480 ..... N89-19641
N89-19648
NSF ATM-85-16940 ..... N89-19680
NSF ATM-85-19160 ..... N89-19643
NSF ATM-85-20123 ..... N89-19707
NSF ATM-85-21417 ..... N89-19660
NSF ATM-86-01257 ..... N89-19714
NSF ATM-86-01549 ..... N89-19606
N89-19607
N89-19615
NSF ATM-86-03308 ..... N89-19680
NSF ATM-86-09376 ..... N89-19627
NSF ATM-86-11185 ..... N89-19622
NSF ATM-86-11225 ..... N89-19627
NSF ATM-86-15344 ..... N89-19645
NSF ATM-86-16568 ..... N89-19609
NSF ATM-87-04776 ..... N89-19681
NSF ATM-87-15060 ..... N89-19681
NSF ATM-87-15636 ..... N89-19812
N89-19614
NSF ATM-87-16166 ..... N89-19707
NSF DCR-86-04199 ..... N89-19868
NSF DMS-86-20007 ..... N89-19954
NSF DMS-87-02693 ..... N89-20054
NSF ECS-84-10902 ..... N89-19901
NSF ECS-87-15153 ..... N89-19908
NSF INT-73-02268 ..... N89-19851
NSF SES-85-20806 ..... N89-19937
NSG-3285 ..... N89-19503
NYSSTF-CAT(87)-5 ..... N89-19851
N00014-78-C-0396 ..... N89-19851
N00014-80-C-0741 ..... N89-19957
N00014-80-C-0796 ..... N89-19760
N00014-81-K-0648 ..... N89-19431
N00014-82-K-0280 ..... N89-19396
N89-19397
N00014-82-K-0324 ..... N89-19517
N00014-83-K-0183 ..... N89-19521
N00014-83-K-0209 ..... N89-19426
N00014-83-K-0258 ..... N89-19792
N00014-84-C-0149 ..... N89-19901
N89-19904
N00014-84-C-0591 ..... N89-19681
N00014-84-K-0470 ..... N89-19392
N00014-85-C-0038 ..... N89-19802
N00014-85-C-0050 ..... N89-19558
N00014-85-C-0141 ..... N89-19968
N00014-85-K-0124 ..... N89-19445
N89-19570
N89-19806
N89-19983
N00014-85-K-0145 ..... N89-19434
N00014-85-K-0213 ..... N89-19911
N00014-85-K-0343 ..... N89-19912
N89-19913
N00014-85-K-0437 ..... N89-19412
N00014-85-K-0454 ..... N89-19407
N00014-85-K-0641 ..... N89-19425
N00014-85-K-0805 ..... N89-19398
N00014-85-K-0825 ..... N89-19923
N00014-86-C-2488 ..... N89-19542
N00014-86-K-0138 ..... N89-20053
N00014-86-K-0153 ..... N89-19598
N00014-86-K-0156 ..... N89-19959
N00014-86-K-0180 ..... N89-19893
N00014-86-K-0591 ..... N89-19897
N00014-86-K-0685 ..... N89-19570
N00014-86-K-0772 ..... N89-19998
N00014-87-F-0066 ..... N89-19535
N00014-87-K-0130 ..... N89-19845
N00014-88-C-0512 ..... N89-19429
N00014-88-K-0075 ..... N89-19393
N00014-88-K-0092 ..... N89-19940
N00014-88-K-0191 ..... N89-20002
N00039-84-C-0165 ..... N89-19851
RR02101 ..... N89-19760
RR04108 ..... N89-19393
W-31-109-ENG-38 ..... N89-19438
N89-19709
N89-19746
N89-19975
N89-20011
N89-20012
N89-20013
N89-20014
W-7405-ENG-36 ..... N89-19546
N89-19547
N89-19548
N89-19549
N89-19550
N89-19551
N89-19552
N89-19553
N89-19964
N89-19984
N89-19986
N89-20008
N89-20015
W-7405-ENG-48 ..... N89-19348
N89-19378
N89-19383
N89-19471
N89-19490
N89-19604
ZWO-10-62-10 ..... N89-19962
505-43-31-05 ..... N89-19499
505-45-48 ..... N89-19265
505-60-21-02 ..... N89-19266
505-60-31-03 ..... N89-19231
505-60-41-01 ..... N89-19505
505-61-01 ..... N89-19545
505-61-01-02 ..... N89-19232
505-62-21 ..... N89-19965
505-63-21-01 ..... N89-19234
N89-19247
505-63-41-02 ..... N89-19579
N89-19580
505-66-01-02 ..... N89-19230
N89-19309
N89-19316
505-66-21-04 ..... N89-19779
N89-19780
N89-19783
505-66-41-05 ..... N89-19899
505-66-11 ..... N89-19305
506-41-11 ..... N89-19493
506-43-11 ..... N89-19402
N89-19435
506-43-21-04 ..... N89-19385
506-43-81 ..... N89-19892
506-55-6E N89-19737
510-01-01 ..... N89-19371
510-02-21-01 ..... N89-19589
533-05-01 ..... N89-19421
535-03-01 ..... N89-19289
N89-19556
535-07-01 ..... N89-19578
674-22-05 ..... N89-19442
676-59-33 ..... N89-19749
678-12-04-07 ..... N89-19529
694-03-03 ..... N89-19446

Typical Report Number Index Listing

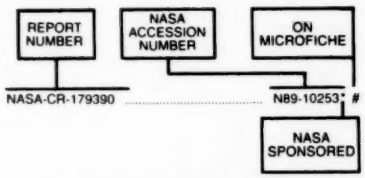

Listings in this index are arranged alphanumerically by report number. The NASA accession number denotes the number by which the citation is identified. An asterisk (*) indicates that the item is a NASA report. A pound sign (#) indicates that the item is available on microfiche.

AAMRL-TR-88-047 ..... N89-19803 #

ACT-100 ..... N89-19901 #
ACT-103 ..... N89-19904 #

AD-A194761 ..... N89-19333 #
AD-A197976 ..... N89-19929 #
AD-A198000 ..... N89-19935 #
AD-A199471 ..... N89-19981 #
AD-A200727 ..... N89-19279 #
AD-A200914 ..... N89-19782 #
AD-A201002 ..... N89-19897 #
AD-A201074 ..... N89-19290 #
AD-A201115 ..... N89-19811 #
AD-A201163 ..... N89-19372 #
AD-A201167 ..... N89-19424 #
AD-A201168 ..... N89-19388 #
AD-A201169 ..... N89-19954 #
AD-A201170 ..... N89-19535 #
AD-A201171 ..... N89-19730 #
AD-A201173 ..... N89-19901 #
AD-A201176 ..... N89-19507 #
AD-A201183 ..... N89-19425 #
AD-A201185 ..... N89-19812 #
AD-A201186 ..... N89-19813 #
AD-A201240 ..... N89-19467 #
AD-A201241 ..... N89-19998 #
AD-A201242 ..... N89-19440 #
AD-A201243 ..... N89-19389 #
AD-A201246 ..... N89-19373 #
AD-A201249 ..... N89-19508 #
AD-A201252 ..... N89-19791 #
AD-A201258 ..... N89-19893 #
AD-A201259 ..... N89-19902 #
AD-A201261 ..... N89-19955 #
AD-A201263 ..... N89-19368 #
AD-A201266 ..... N89-19751 #
AD-A201270 ..... N89-19390 #
AD-A201273 ..... N89-19374 #
AD-A201274 ..... N89-19796 #
AD-A201276 ..... N89-19999 #
AD-A201277 ..... N89-19584 #
AD-A201279 ..... N89-19317 #
AD-A201284 ..... N89-19391 #
AD-A201292 ..... N89-19301 #
AD-A201293 ..... N89-19392 #
AD-A201303 ..... N89-20000 #
AD-A201307 ..... N89-19982 #
AD-A201310 ..... N89-19393 #
AD-A201330 ..... N89-19805 #
AD-A201331 ..... N89-19536 #
AD-A201333 ..... N89-19983 #
AD-A201341 ..... N89-19488 #
AD-A201342 ..... N89-19937 #
AD-A201345 ..... N89-19903 #
AD-A201350 ..... N89-19509 #
AD-A201353 ..... N89-19558 #
AD-A201370 ..... N89-19797 #
AD-A201374 ..... N89-19510 #
AD-A201418 ..... N89-19394 #
AD-A201425 ..... N89-19489 #
AD-A201433 ..... N89-19283 #
AD-A201435 ..... N89-19585 #
AD-A201438 ..... N89-19511 #
AD-A201440 ..... N89-20001 #
AD-A201451 ..... N89-19968 #
AD-A201454 ..... N89-19586 #
AD-A201456 ..... N89-20053 #
AD-A201459 ..... N89-19956 #
AD-A201460 ..... N89-19512 #
AD-A201461 ..... N89-19426 #
AD-A201471 ..... N89-19938 #
AD-A201483 ..... N89-20002 #
AD-A201484 ..... N89-19407 #
AD-A201485 ..... N89-19267 #
AD-A201506 ..... N89-19226 #
AD-A201518 ..... N89-19798 #
AD-A201527 ..... N89-19427 #
AD-A201529 ..... N89-19395 #
AD-A201543 ..... N89-20025 #
AD-A201544 ..... N89-19227 #
AD-A201548 ..... N89-19559 #
AD-A201549 ..... N89-19468 #
AD-A201554 ..... N89-19799 #
AD-A201555 ..... N89-19800 #
AD-A201556 ..... N89-19969 #
AD-A201574 ..... N89-19228 #
AD-A201581 ..... N89-20032 #
AD-A201594 ..... N89-19284 #
AD-A201595 ..... N89-19801 #
AD-A201599 ..... N89-19396 #
AD-A201601 ..... N89-19397 #
AD-A201605 ..... N89-19354 #
AD-A201606 ..... N89-19408 #
AD-A201609 ..... N89-19587 #
AD-A201610 ..... N89-19974 #
AD-A201611 ..... N89-19560 #
AD-A201612 ..... N89-19537 #
AD-A201613 ..... N89-19398 #
AD-A201614 ..... N89-19445 #
AD-A201619 ..... N89-19806 #
AD-A201620 ..... N89-19814 #
AD-A201621 ..... N89-19588 #
AD-A201622 ..... N89-19561 #
AD-A201630 ..... N89-19752 #
AD-A201632 ..... N89-20029 #
AD-A201634 ..... N89-19399 #
AD-A201635 ..... N89-19538 #
AD-A201651 ..... N89-19904 #
AD-A201662 ..... N89-19268 #
AD-A201672 ..... N89-19469 #
AD-A201673 ..... N89-19970 #
AD-A201674 ..... N89-19355 #
AD-A201675 ..... N89-19905 #
AD-A201676 ..... N89-19513 #
AD-A201719 ..... N89-19280 #
AD-A201720 ..... N89-19281 #
AD-A201724 ..... N89-19517 #
AD-A201728 ..... N89-19593 #
AD-A201736 ..... N89-19759 #
AD-A201743 ..... N89-19518 #
AD-A201747 ..... N89-19760 #
AD-A201749 ..... N89-19939 #
AD-A201760 ..... N89-19229 #
AD-A201769 ..... N89-19327 #
AD-A201783 ..... N89-19472 #
AD-A201784 ..... N89-19314 #
AD-A201785 ..... N89-19473 #
AD-A201804 ..... N89-19568 #
AD-A201810 ..... N89-19429 #
AD-A201811 ..... N89-19907 #
AD-A201834 ..... N89-19541 #
AD-A201839 ..... N89-19379 #
AD-A201861 ..... N89-19380 #
AD-A201865 ..... N89-19411 #
AD-A201873 ..... N89-19802 #
AD-A201879 ..... N89-19908 #
AD-A201884 ..... N89-19291 #
AD-A201896 ..... N89-19957 #
AD-A201902 ..... N89-20030 #
AD-A201915 ..... N89-19792 #
AD-A201918 ..... N89-19519 #
AD-A201919 ..... N89-19474 #
AD-A201921 ..... N89-19909 #
AD-A201925 ..... N89-19430 #
AD-A201931 ..... N89-19542 #
AD-A201932 ..... N89-19520 #
AD-A201933 ..... N89-19431 #
AD-A201934 ..... N89-19274 #
AD-A201936 ..... N89-19275 #
AD-A201937 ..... N89-19741 #
AD-A201943 ..... N89-19276 #
AD-A201947 ..... N89-19315 #
AD-A201955 ..... N89-19412 #
AD-A201963 ..... N89-19910 #
AD-A201964 ..... N89-19569 #
AD-A202089 ..... N89-19594 #
AD-A202102 ..... N89-19328 #
AD-A202106 ..... N89-19292 #
AD-A202113 ..... N89-19761 #
AD-A202122 ..... N89-19815 #
AD-A202128 ..... N89-19911 #
AD-A202129 ..... N89-19923 #
AD-A202142 ..... N89-19318 #
AD-A202145 ..... N89-19432 #
AD-A202151 ..... N89-19293 #
AD-A202183 ..... N89-19570 #
AD-A202188 ..... N89-19595 #
AD-A202189 ..... N89-19762 #
AD-A202190 ..... N89-19294 #
AD-A202192 ..... N89-19381 #
AD-A202219 ..... N89-19958 #
AD-A202220 ..... N89-19731 #
AD-A202223 ..... N89-19543 #
AD-A202234 ..... N89-19596 #
AD-A202237 ..... N89-19521 #
AD-A202241 ..... N89-19763 #
AD-A202243 ..... N89-19357 #
AD-A202244 ..... N89-20004 #
AD-A202247 ..... N89-19940 #
AD-A202248 ..... N89-19492 #
AD-A202252 ..... N89-19475 #
AD-A202268 ..... N89-19959 #
AD-A202273 ..... N89-19960 #
AD-A202274 ..... N89-19433 #
AD-A202278 ..... N89-19764* #
AD-A202285 ..... N89-19912 #
AD-A202286 ..... N89-19913 #
AD-A202291 ..... N89-19441 #
AD-A202293 ..... N89-19544 #
AD-A202298 ..... N89-19476 #
AD-A202301 ..... N89-19803 #
AD-A202303 ..... N89-19298 #
AD-A202304 ..... N89-19597 #
AD-A202316 ..... N89-19295 #
AD-A202339 ..... N89-19369 #
AD-A202353 ..... N89-19598 #
AD-A202369 ..... N89-20005 #
AD-A202375 ..... N89-19358 #
AD-A202376 ..... N89-19434 #
AD-A202412 ..... N89-19277 #
AD-A202415 ..... N89-19765 #

AD-E501048 ..... N89-19318 #
AD-E501048 ..... N89-19432 #
AD-E501048 ..... N89-19815 #
AD-E501048 ..... N89-19911 #
AD-E501048 ..... N89-19923 #
AD-E801798 ..... N89-19570 #
AD-E951220 ..... N89-19468 #
AD-E951221 ..... N89-19227 #
AD-E951221 ..... N89-19559 #
AD-E951221 ..... N89-20025 #

AERONOMICA-ACTA-A-336-1988 ..... N89-19769

AFAL-TR-88-033 ..... N89-19369 #
AFAL-TR-88-038 ..... N89-19999 #
AFAL-TR-88-049-VOL-1 ..... N89-20004 #
AFAL-TR-88-050 ..... N89-19544 #
AFAL-TR-88-086 ..... N89-19584 #

AFGL-TR-88-0150 ..... N89-19354 #
AFGL-TR-88-0228 ..... N89-19761 #
AFGL-TR-88-0262 ..... N89-19327 #
AFGL-TR-88-0280 ..... N89-19765 #
AFGL-TR-88-0295 ..... N89-19394 #

AFIT/GCA/LSQ/88S-6 ..... N89-19226 #
AFIT/GCA/LSQ/88S-9 ..... N89-19938 #

AFIT/GCA/LSY/88S-7 ..... N89-19227 #

AFIT/GLM/LSM/88S-56 ..... N89-19228 #

AFIT/GSM/LS/88S-12 ..... N89-19798 #

AFIT/GSM/LSM/88S-16 ..... N89-20032 #

AFIT/GSM/LSY/88S-4 ..... N89-20025 #

AFOSR-88-0477TR ..... N89-19333 #
AFOSR-88-0844TR ..... N89-19935 #
AFOSR-88-1169TR ..... N89-20000 #
AFOSR-88-1170TR ..... N89-20029 #
AFOSR-88-1171TR ..... N89-19805 #
AFOSR-88-1175TR ..... N89-19536 #
AFOSR-88-1178TR ..... N89-19509 #
AFOSR-88-1179TR ..... N89-19955 #
AFOSR-88-1180TR ..... N89-19507 #
AFOSR-88-1182TR ..... N89-19751 #
AFOSR-88-1183TR ..... N89-19368 #
AFOSR-88-1186TR ..... N89-19982 #
AFOSR-88-1189TR ..... N89-19390 #
AFOSR-88-1192TR ..... N89-19357 #
AFOSR-88-1202TR ..... N89-19763 #
AFOSR-88-1203TR ..... N89-19358 #
AFOSR-88-1219TR ..... N89-20005 #
AFOSR-88-1249TR ..... N89-19492 #
AFOSR-88-1252TR ..... N89-19596 #
AFOSR-88-1292TR ..... N89-19489 #
AFOSR-88-1294TR ..... N89-19585 #
AFOSR-88-1324TR ..... N89-19511 #

AFWAL-TR-86-3017-VOL-4 ..... N89-19597 #
AFWAL-TR-87-3098-PT-2 ..... N89-19275 #
AFWAL-TR-88-2095 ..... N89-19301 #
AFWAL-TR-88-3026-VOL-1 ..... N89-19374 #
AFWAL-TR-88-3026-VOL-2 ..... N89-19379 #
AFWAL-TR-88-3044-VOL-1 ..... N89-19280 #
AFWAL-TR-88-3044-VOL-2 ..... N89-19281 #
AFWAL-TR-88-3077 ..... N89-19315 #

AFWL-TR-88-50 ..... N89-19543 #

AGARD-CAL-89/1 ..... N89-20024 #

AI-M-953 ..... N89-19893 #
AI-M-1059 ..... N89-19445 #
AI-M-1061 ..... N89-19806 #
AI-M-1068 ..... N89-19983 #

AI-TR-1056 ..... N89-19570 #

AIAA-85-4058 ..... N89-19241* #

AIRESEARCH-86-60365 ..... N89-19421* #

AMSMI/TR-RD-ST-88-1 ..... N89-19559 #

AMSMI/TR-RD-TE-88-2 ..... N89-19468 #

ANL-87-53 ..... N89-19438 #

AR-004-592 ..... N89-19810 #

ARCCB-MR-88034 ..... N89-19586 #

ARL-SYS-R-40 ..... N89-19810 #

ARL/STRUC-TM-489 ..... N89-19290 #

ARO-2279.14-PH-H ..... N89-19537 #
ARO-20157.6-GS ..... N89-19759 #
ARO-21139.11-EL ..... N89-19474 #
ARO-21346.4-EG ..... N89-19274 #
ARO-21364.1-MS ..... N89-19424 #
ARO-21401.14-CH ..... N89-19395 #
ARO-21569.3-MS ..... N89-19373 #
ARO-21733.4-LS ..... N89-19801 #
ARO-21743.4-EG ..... N89-19510 #
ARO-21817.23-EG ..... N89-19587 #
ARO-22207.11-EL-PT-A ..... N89-19467 #
ARO-22295.1-EL ..... N89-19472 #
ARO-22396.21-CH ..... N89-19974 #
ARO-22457.17-CH ..... N89-19430 #
ARO-22520.10-MA ..... N89-19391 #
ARO-22565.8-MA ..... N89-19956 #
ARO-22572.1-CH ..... N89-19433 #
ARO-22647.15-MA ..... N89-19512 #
ARO-22729.6-MA ..... N89-19960 #
ARO-22759.8-MA ..... N89-19939 #
ARO-22851.1-GS ..... N89-19475 #
ARO-23034.11-CH ..... N89-19427 #
ARO-23246.1-EG ..... N89-19314 #
ARO-23418.1-GS ..... N89-19518 #
ARO-23714.7-MA-H ..... N89-19909 #
ARO-24083.8-CH ..... N89-19388 #
ARO-24654.1-EG ..... N89-19520 #
ARO-24749.3-PH ..... N89-19969 #
ARO-24834.1-MA ..... N89-19954 #
ARO-24960.19-MA ..... N89-19902 #
ARO-25544.3-EG ..... N89-19408 #

ATC-153 ..... N89-19782 #

ATR-86(8139)-5 ..... N89-19977 #
ATR-88(8359)-5 ..... N89-20021 #

AU-AWC-88-052 ..... N89-19293 #

AVSCOM-TR-87-C-35 ..... N89-19503* #

BAE-TP-9119 ..... N89-19363 #

BBC-RD-1988/14 ..... N89-19450

BCD-SSME-TR-87-3-APP-B N89-19365*

BCRS-87-18 ..... N89-19732 #
BCRS-88-01 ..... N89-19733 #
BCRS-88-03 ..... N89-19734 #
BCRS-88-04 ..... N89-19735 #

BDX-613-3915 ..... N89-19573 #

BFLRF-256 ..... N89-19432 #

BNL-40955 ..... N89-19985 #
BNL-41959 ..... N89-20010 #
BNL-41995 ..... N89-19540 #

BPT-11/88 ..... N89-19767 #

BRL-TR-2962 ..... N89-19277 #
BRL-TR-3714 ..... N89-19399 #

BR104469 ..... N89-19921 #
BR107591 ..... N89-19319 #
BR107730 ..... N89-19296 #

B8809730 ..... N89-19942 #
B8809731 ..... N89-19944 #
B8809732 ..... N89-19945 #
B8809733 ..... N89-20054 #
B8809734 ..... N89-19322 #
B8809735 ..... N89-20026 #
B8809736 ..... N89-19943 #
B8809737 ..... N89-19946 #
B8809738 ..... N89-19933 #
B8809739 ..... N89-19961 #

C-48-1977 ..... N89-19770 #

CASS/ESM-88-10 ..... N89-19434 #

CCS-RR-605 ..... N89-19937 #

CERL-TR-E-89/01 ..... N89-19741 #

CERL-TR-P-89/03 ..... N89-19907 #

CISE-4476 ..... N89-19600 #
CISE-4477 ..... N89-19601 #

CMU/SEI-88-TR-3 ..... N89-19903 #

CONF-880312-2 ..... N89-19383 #
CONF-880408-44 ..... N89-20013 #
CONF-880433-8 ..... N89-19900 #
CONF-880760-10 ..... N89-19604 #
CONF-880812-34 ..... N89-20003 #
CONF-880839-13 ..... N89-20028 #
CONF-880845-2 ..... N89-20012 #
CONF-880887-28 ..... N89-19423 #
CONF-880887-29 ..... N89-19985 #
CONF-880893-2 ..... N89-19975 #
CONF-880901-15 ..... N89-20010 #
CONF-881002-4 ..... N89-19550 #
CONF-881049-60 ..... N89-19984 #
CONF-881081-1 ..... N89-19557 #
CONF-881081-2 ..... N89-19967 #
CONF-881103-28 ..... N89-19491 #
CONF-881151-52 ..... N89-19547 #
CONF-881155-34 ..... N89-20008 #
CONF-881155-36 ..... N89-20019 #
CONF-881155-37 ..... N89-19384 #
CONF-881162-3 ..... N89-19496 #
CONF-881244-2 ..... N89-19546 #
CONF-881244-3 ..... N89-19552 #
CONF-881244-4 ..... N89-19549 #
CONF-890145-6 ..... N89-19551 #
CONF-890145-7 ..... N89-19439 #
CONF-890157-1 ..... N89-19548 #
CONF-890253-1 ..... N89-19916 #
CONF-8706364 ..... N89-19795 #
CONF-8804232-1 ..... N89-19405 #
CONF-8808176-1 ..... N89-19572 #
CONF-8808187-1 ..... N89-20011 #
CONF-8809201-3 ..... N89-20014 #

CR-010825 ..... N89-19297 #

CRARP-88-1 ..... N89-19772 #
CRARP-88-2 ..... N89-19773 #
CRARP-88-3 ..... N89-19774 #
CRARP-88-4 ..... N89-19775 #
CRARP-88-5 ..... N89-19776 #
CRARP-88-6 ..... N89-19777 #
CRARP-88-7 ..... N89-19778 #

CSDL-R-2076 ..... N89-19999 #

CUCOMB-3 ..... N89-19391 #

CWP-063R ..... N89-19940 #

DAITC/TR-88/007 ..... N89-20030 #

DCIEM-88-TR-27 ..... N89-19279 #

DDA-EDR-13632 ..... N89-19301 #

DE88-010280 ..... N89-19387 #
DE88-704951 ..... N89-19989 #
DE88-704966 ..... N89-19936 #
DE88-756063 ..... N89-19506 #
DE88-756071 ..... N89-19795 #
DE88-756073 ..... N89-19997 #
DE88-756084 ..... N89-20022 #
DE89-000818 ..... N89-19738 #
DE89-000821 ..... N89-19743 #
DE89-000829 ..... N89-19781 #
DE89-000836 ..... N89-19744 #
DE89-000844 ..... N89-19739 #
DE89-002159 ..... N89-19990 #
DE89-002257 ..... N89-19405 #
DE89-004764 ..... N89-19422 #
DE89-005014 ..... N89-19900 #
DE89-005016 ..... N89-19572 #
DE89-005183 ..... N89-19423 #
DE89-005185 ..... N89-19557 #
DE89-005191 ..... N89-20028 #
DE89-005193 ..... N89-19967 #
DE89-005347 ..... N89-19916 #
DE89-005419 ..... N89-19498 #
DE89-005441 ..... N89-19984 #
DE89-005449 ..... N89-19546 #
DE89-005451 ..... N89-20008 #
DE89-005458 ..... N89-19547 #
DE89-005467 ..... N89-19548 #
DE89-005490 ..... N89-19740 #
DE89-005529 ..... N89-19540 #
DE89-005544 ..... N89-19378 #
DE89-005546 ..... N89-19471 #
DE89-005547 ..... N89-19490 #
DE89-005621 ..... N89-19491 #
DE89-005661 ..... N89-19985 #
DE89-005668 ..... N89-20003 #
DE89-005692 ..... N89-19906 #
DE89-005722 ..... N89-20009 #
DE89-005766 ..... N89-20010 #
DE89-005813 ..... N89-19745 #
DE89-005823 ..... N89-19383 #
DE89-005831 ..... N89-20011 #
DE89-005844 ..... N89-20012 #
DE89-005847 ..... N89-20013 #
DE89-005870 ..... N89-19975 #
DE89-005884 ..... N89-20014 #
DE89-005896 ..... N89-19400 #
DE89-005898 ..... N89-19401 #
DE89-006041 ..... N89-19384 #
DE89-006109 ..... N89-19437 #
DE89-006116 ..... N89-19403 #
DE89-006125 ..... N89-20019 #
DE89-006154 ..... N89-19604 #
DE89-006163 ..... N89-19986 #
DE89-006286 ..... N89-20023 #
DE89-006395 ..... N89-19746 #
DE89-006400 ..... N89-19438 #
DE89-006418 ..... N89-19439 #
DE89-006462 ..... N89-19523 #
DE89-006545 ..... N89-19550 #
DE89-006546 ..... N89-19551 #
DE89-006547 ..... N89-19552 #
DE89-006549 ..... N89-19549 #

DE89-006563 ..... N89-19964 #
DE89-006567 ..... N89-19553 #
DE89-006568 ..... N89-20015 #
DE89-006608 ..... N89-19404 #
DE89-007060 ..... N89-19534 #
DE89-007127 ..... N89-20020 #

DFVLR-FB-88-30 ..... N89-19522 #
DFVLR-FB-88-31 ..... N89-19282 #
DFVLR-FB-88-37 ..... N89-19287 #
DFVLR-FB-88-38 ..... N89-19304 #
DFVLR-FB-88-39 ..... N89-19415 #
DFVLR-FB-88-40 ..... N89-19896 #

DFVLR-MITT-88-22 ..... N89-19742 #
DFVLR-MITT-88-23 ..... N89-19288 #
DFVLR-MITT-88-24 ..... N89-19966 #

DIGEL-78 ..... N89-19898 #
DIGEL-79 ..... N89-19917 #

DODA-AR-005-526 ..... N89-19290 #

DOE/CH-10093/36 ..... N89-19738 #

DOE/ER-04915/3 ..... N89-20023 #
DOE/ER-13451/4 ..... N89-19403 #
DOE/ER-13864/1 ..... N89-19400 #
DOE/ER-45252/T3 ..... N89-19422 #
DOE/ER-45253/3 ..... N89-19401 #
DOE/ER-45307/T1 ..... N89-19437 #
DOE/ER-45320/2 ..... N89-20009 #

DOE/MC-21180/2617 ..... N89-19387 #

DOE/NASA/1005-11 ..... N89-19737* #

DOE/NE-37968/1 ..... N89-19900 #
DOE/NE-37968/5 ..... N89-19572 #

DOE/PC-79678/T1 ..... N89-19990 #
DOE/PC-79931/T3 ..... N89-19745 #

DOT-TSC-FAA-88-6 ..... N89-19229 #

DOT/FAA/AS-89/1 ..... N89-19283 #

DOT/FAA/DS-88/12 ..... N89-19283 #

DOT/FAA/PM-87-22 ..... N89-19473 #
DOT/FAA/PM-87/35 ..... N89-19782 #

DRIC-T-8130 ..... N89-19296 #

DTIC-TR-89/2 ..... N89-20030 #

D6-53196-2-VOL-2 ..... N89-19505* #
D6-53344 ..... N89-19556* #
D180-30083 ..... N89-19366* #

E-2417 ..... N89-19265* #
E-3277 ..... N89-19737* #
E-4311 ..... N89-19371* #
E-4510 ..... N89-19578* #
E-4550-1 ..... N89-19493* #
E-4596 ..... N89-19435* #
E-4622 ..... N89-19965* #
E-4660 ..... N89-19402* #
E-4661 ..... N89-19446* #
E-4677 ..... N89-19305* #

EER58-36198-FR6/8 ..... N89-19420* #

EGG-ES-8093 ..... N89-19369 #

EGG-M-88049 ..... N89-19557 #
EGG-M-88053 ..... N89-19967 #
EGG-M-88094 ..... N89-19423 #
EGG-M-88377 ..... N89-20028 #
EGG-M-881162 ..... N89-19498 #

EOARD-TR-89-03 ..... N89-19752 #

ESA-CR(P)-2542 ..... N89-19447 #
ESA-CR(P)-2588 ..... N89-19494 #
ESA-CR(P)-2591 ..... N89-19477 #
ESA-CR(P)-2592-VOL-2 ..... N89-19478 #
ESA-CR(P)-2601-VOL-1 ..... N89-19530 #
ESA-CR(P)-2601-VOL-2 ..... N89-19531 #
ESA-CR(P)-2632 ..... N89-19359 #
ESA-CR(P)-2661 ..... N89-19320 #
ESA-CR(P)-2666 ..... N89-19766 #
ESA-CR(P)-2667 ..... N89-19361 #
ESA-CR(P)-2670 ..... N89-19362 #
ESA-CR(P)-2673 ..... N89-19285 #
ESA-CR(P)-2674 ..... N89-19286 #
ESA-CR(P)-2677 ..... N89-19895 #
ESA-CR(P)-2681 ..... N89-19495 #
ESA-CR(P)-2684 ..... N89-19443 #
ESA-CR(P)-2685 ..... N89-19370 #
ESA-CR(P)-2688 ..... N89-19482 #
ESA-CR(P)-2689 ..... N89-19360 #
ESA-CR(P)-2692 ..... N89-19444 #
ESA-CR(P)-2693 ..... N89-19816 #
ESA-CR(P)-2698 ..... N89-19363 #
ESA-CR(P)-2699 ..... N89-19483 #
ESA-CR(P)-2703 ..... N89-19496 #
ESA-CR(P)-2704 ..... N89-19364 #

ESD-TR-87-281 ..... N89-19929 #
ESD-TR-88-004 ..... N89-19903 #

ETL-0504 ..... N89-19730 #

ETN-89-93347 ..... N89-19413 #
ETN-89-93463 ..... N89-19987 #
ETN-89-93470 ..... N89-20049 #
ETN-89-93639 ..... N89-19447 #
ETN-89-93640 ..... N89-19494 #
ETN-89-93641 ..... N89-19477 #
ETN-89-93643 ..... N89-19478 #
ETN-89-93645 ..... N89-19530 #
ETN-89-93646 ..... N89-19531 #
ETN-89-93647 ..... N89-19359 #
ETN-89-93655 ..... N89-19605
ETN-89-93670 ..... N89-19296 #
ETN-89-93671 ..... N89-19319 #
ETN-89-93675 ..... N89-19302 #
ETN-89-93681 ..... N89-19894 #
ETN-89-93687 ..... N89-19436 #
ETN-89-93689 ..... N89-19532 #
ETN-89-93690 ..... N89-19303 #
ETN-89-93691 ..... N89-19414 #
ETN-89-93694 ..... N89-19571 #
ETN-89-93698 ..... N89-19382 #
ETN-89-93702 ..... N89-19306 #
ETN-89-93703 ..... N89-19525 #
ETN-89-93704 ..... N89-19307 #
ETN-89-93705 ..... N89-19308 #
ETN-89-93706 ..... N89-19533 #
ETN-89-93711 ..... N89-19793 #
ETN-89-93712 ..... N89-19794 #
ETN-89-93713 ..... N89-19600 #
ETN-89-93714 ..... N89-19601 #
ETN-89-93715 ..... N89-19448 #
ETN-89-93716 ..... N89-19914
ETN-89-93717 ..... N89-19930
ETN-89-93718 ..... N89-19479
ETN-89-93719 ..... N89-19480
ETN-89-93720 ..... N89-19481
ETN-89-93721 ..... N89-19915
ETN-89-93722 ..... N89-19931
ETN-89-93723 ..... N89-19932
ETN-89-93749 ..... N89-19769
ETN-89-93780 ..... N89-20050 #
ETN-89-93782 ..... N89-19526 #
ETN-89-93790 ..... N89-20006 #
ETN-89-93791 ..... N89-20007 #
ETN-89-93794 ..... N89-19991 #
ETN-89-93795 ..... N89-20046 #
ETN-89-93802 ..... N89-20056
ETN-89-93812 ..... N89-19527 #
ETN-89-93838 ..... N89-19941 #
ETN-89-93841 ..... N89-19942 #
ETN-89-93842 ..... N89-19322 #
ETN-89-93843 ..... N89-20054 #
ETN-89-93844 ..... N89-20026 #
ETN-89-93845 ..... N89-19943 #
ETN-89-93846 ..... N89-19944 #
ETN-89-93847 ..... N89-19945 #
ETN-89-93848 ..... N89-19946 #
ETN-89-93849 ..... N89-19933 #
ETN-89-93850 ..... N89-19961 #
ETN-89-93872 ..... N89-19732 #
ETN-89-93873 ..... N89-19733 #
ETN-89-93874 ..... N89-19734 #
ETN-89-93875 ..... N89-19735 #
ETN-89-93879 ..... N89-19898 #
ETN-89-93880 ..... N89-19917 #
ETN-89-93894 ..... N89-19804 #
ETN-89-93896 ..... N89-19934 #
ETN-89-93897 ..... N89-19978 #
ETN-89-93898 ..... N89-19574 #
ETN-89-93899 ..... N89-19602 #
ETN-89-93900 ..... N89-19736 #
ETN-89-93901 ..... N89-19575 #
ETN-89-93902 ..... N89-20038 #
ETN-89-93912 ..... N89-19766 #
ETN-89-93913 ..... N89-19285 #
ETN-89-93917 ..... N89-19443 #
ETN-89-93918 ..... N89-19360 #
ETN-89-93923 ..... N89-19320 #
ETN-89-93925 ..... N89-19361 #
ETN-89-93926 ..... N89-19362 #
ETN-89-93928 ..... N89-19286 #
ETN-89-93931 ..... N89-19895 #
ETN-89-93933 ..... N89-19495 #
ETN-89-93934 ..... N89-19370 #
ETN-89-93935 ..... N89-19482 #
ETN-89-93936 ..... N89-19444 #
ETN-89-93937 ..... N89-19816 #
ETN-89-93939 ..... N89-19363 #
ETN-89-93940 ..... N89-19483 #
ETN-89-93941 ..... N89-19496 #
ETN-89-93942 ..... N89-19364 #
ETN-89-93952 ..... N89-19417 #
ETN-89-93954 ..... N89-19497
ETN-89-93955 ..... N89-19767 #
ETN-89-93959 ..... N89-19947 #
ETN-89-93960 ..... N89-19979 #
ETN-89-93966 ..... N89-19418 #
ETN-89-93967 ..... N89-19992 #
ETN-89-93968 ..... N89-19419 #
ETN-89-93969 ..... N89-19522 #
ETN-89-93970 ..... N89-19282 #
ETN-89-93971 ..... N89-19287 #
ETN-89-93972 ..... N89-19304 #
ETN-89-93973 ..... N89-19415 #
ETN-89-93974 ..... N89-19896 #
ETN-89-93975 ..... N89-19742 #
ETN-89-93976 ..... N89-19288 #
ETN-89-93977 ..... N89-19966 #
ETN-89-93978 ..... N89-19323 #
ETN-89-93979 ..... N89-19329 #
ETN-89-93980 ..... N89-19330 #
ETN-89-93981 ..... N89-19331 #
ETN-89-93982 ..... N89-19790 #
ETN-89-93983 ..... N89-19993 #
ETN-89-93984 ..... N89-19416 #
ETN-89-93987 ..... N89-19747 #
ETN-89-93990 ..... N89-19994 #
ETN-89-93993 ..... N89-19995
ETN-89-93994 ..... N89-19996
ETN-89-93999 ..... N89-19962 #
ETN-89-94000 ..... N89-19948 #
ETN-89-94001 ..... N89-19918 #
ETN-89-94002 ..... N89-19949 #
ETN-89-94003 ..... N89-19950 #
ETN-89-94004 ..... N89-19951 #
ETN-89-94005 ..... N89-19528 #
ETN-89-94006 ..... N89-19603 #
ETN-89-94007 ..... N89-20027 #
ETN-89-94008 ..... N89-19952 #
ETN-89-94009 ..... N89-19963 #
ETN-89-94010 ..... N89-19919 #
ETN-89-94011 ..... N89-19953 #
ETN-89-94012 ..... N89-19920 #
ETN-89-94013 ..... N89-19576 #
ETN-89-94014 ..... N89-19577 #
ETN-89-94096 ..... N89-19297 #

FAA-MS-88-5 ..... N89-19229 #

FNAL/C-88/166 ..... N89-19491 #

FPA-88-2 ..... N89-19992 #

FR-688106 ..... N89-19316* #

GKSS-88/E/32 ..... N89-19417 #

GPO-80-201 ..... N89-19332 #
GPO-84-990 ..... N89-20031 #
GPO-87-608 ..... N89-19325 #

GRL/8802 ..... N89-19542 #

HAC-REF-F4890 ..... N89-19354 #

HMI-B-451 ..... N89-19497

HSER-9247 ..... N89-19299* #

IAE-4477/7 ..... N89-19989 #

IFSI-87-16 ..... N89-19987 #
IFSI-88-3 ..... N89-20049 #

IKU-88.068 ..... N89-19285 #
IKU-88.068 ..... N89-19286 #

ILR-MITT-205 ..... N89-19323 #
ILR-MITT-207 ..... N89-19329 #
ILR-MITT-208 ..... N89-19330 #
ILR-MITT-210 ..... N89-19331 #

IMEC-SP/CCD-255/88-03 ..... N89-19495 #

INPE-4626-PRE/1344 ..... N89-19750 #
INPE-4688-NTE/285 ..... N89-19351 #

IOM/CAEE-002/87(TR) ..... N89-19443 #

IOS-257 ..... N89-19794 #
IOS-258 ..... N89-19793 #

IPP-6/276 ..... N89-19994 #

ISAS-630 ..... N89-19353 #

ISBN-3-88-148240-7 ..... N89-19605
ISBN-9-03-700015-0 ..... N89-19941 #
ISBN-90-9002330-5 ..... N89-19804 #
ISBN-92-835-0488-7 ..... N89-20024 #

ISSN-0065-3715 ..... N89-19789
ISSN-0072-4122 ..... N89-19605
ISSN-0171-1342 ..... N89-19282 #
ISSN-0171-1342 ..... N89-19287 #
ISSN-0171-1342 ..... N89-19304 #
ISSN-0171-1342 ..... N89-19415 #
ISSN-0171-1342 ..... N89-19522 #
ISSN-0171-1342 ..... N89-19896 #
ISSN-0175-8349 ..... N89-19497
ISSN-0176-0777 ..... N89-19767 #
ISSN-0176-7739 ..... N89-19288 #
ISSN-0176-7739 ..... N89-19742 #
ISSN-0176-7739 ..... N89-19966 #
ISSN-0280-1078 ..... N89-19278 #
ISSN-0285-6808 ..... N89-19353 #
ISSN-0303-4003 ..... N89-19418 #
ISSN-0303-4003 ..... N89-19419 #
ISSN-0303-4003 ..... N89-19992 #
ISSN-0344-9629 ..... N89-19417 #
ISSN-0366-0885 ..... N89-19947 #
ISSN-0366-0885 ..... N89-19979 #
ISSN-0436-1199 ..... N89-19527 #
ISSN-0920-2358 ..... N89-19933 #
ISSN-0920-2358 ..... N89-19961 #
ISSN-0920-8577 ..... N89-19322 #
ISSN-0920-8577 ..... N89-19528 #
ISSN-0920-8577 ..... N89-19576 #
ISSN-0920-8577 ..... N89-19577 #
ISSN-0920-8577 ..... N89-19603 #
ISSN-0920-8577 ..... N89-19918 #
ISSN-0920-8577 ..... N89-19919 #
ISSN-0920-8577 ..... N89-19920 #
ISSN-0920-8577 ..... N89-19942 #
ISSN-0920-8577 ..... N89-19943 #
ISSN-0920-8577 ..... N89-19944 #
ISSN-0920-8577 ..... N89-19945 #
ISSN-0920-8577 ..... N89-19946 #
ISSN-0920-8577 ..... N89-19948 #
ISSN-0920-8577 ..... N89-19949 #
ISSN-0920-8577 ..... N89-19950 #
ISSN-0920-8577 ..... N89-19951 #
ISSN-0920-8577 ..... N89-19952 #
ISSN-0920-8577 ..... N89-19953 #
ISSN-0920-8577 ..... N89-19962 #
ISSN-0920-8577 ..... N89-19963 #
ISSN-0920-8577 ..... N89-20026 #
ISSN-0920-8577 ..... N89-20027 #
ISSN-0920-8577 ..... N89-20054 #

JAERI-M-88-173 ..... N89-19506 #

JINR-R-2-88-132 ..... N89-19936 #

JPL-TDA-PR-42-96 ..... N89-19451* #

JPRS-JST-88-020 ..... N89-19924 #

JPRS-UEE-88-005 ..... N89-19485 #

JUEL-2202 ..... N89-19947 #
JUEL-2203 ..... N89-19979 #

K/ETAC-80 ..... N89-19523 #

KAI-R-1 ..... N89-19779* #

KEK-87-29 ..... N89-19795 #
KEK-88-2 ..... N89-19997 #

KFK-4409 ..... N89-19418 #
KFK-4433 ..... N89-19992 #
KFK-4449 ..... N89-19419 #

KTH-AERO-REPT-57 ..... N89-19278 #

L-16322 ..... N89-19231* #
L-16482 ..... N89-19309* #
L-16483 ..... N89-19232* #
L-16504 ..... N89-19899* #
L-16506 ..... N89-19579* #
L-16513 ..... N89-19580* #
L-16526 ..... N89-19499* #
L-16532-PT-1 ..... N89-19234* #
L-16532-PT-2 ..... N89-19247* #
L-16538 ..... N89-19529* #
L-16547 ..... N89-19230* #
L-16549 ..... N89-19385* #

LA-TR-89-3 ..... N89-19986 #

LA-UR-88-3301 ..... N89-19984 #
LA-UR-88-4030 ..... N89-19546 #
LA-UR-88-4038 ..... N89-20008 #
LA-UR-88-4114 ..... N89-19547 #
LA-UR-88-4200 ..... N89-19548 #
LA-UR-89-19 ..... N89-19549 #
LA-UR-89-40 ..... N89-19552 #
LA-UR-89-48 ..... N89-19551 #
LA-UR-89-49 ..... N89-19550 #

LA-10966-MS ..... N89-19484 #
LA-11082-MS ..... N89-19922 #
LA-11228-MS ..... N89-19980 #
LA-11382-MS ..... N89-19553 #
LA-11395-MS ..... N89-19984 #
LA-11473-MS ..... N89-20015 #

LBL-25323 ..... N89-19404 #
LBL-26337 ..... N89-20020 #

LG88ER0053 ..... N89-19289* #

LMSC-HEC-TR-F225968 ..... N89-19367* #

MATRA-NT/139/1939 ..... N89-19447 #
MATRA-NT/2113/139-VOL-2 ..... N89-19478 #

MDC-K0171 ..... N89-19509 #

ME-TSPC-TR-87-13 ..... N89-19503* #

MMP-1-IS-02-3302-FR ..... N89-19895 #

MPE-PREPRINT-108 ..... N89-20056
MPE-PREPRINT-127 ..... N89-19995
MPE-PREPRINT-128 ..... N89-19996

MPIS-4/1988 ..... N89-19527 #

NAE-AN-53 ..... N89-19267 #

NAS 1.15:4091 ..... N89-19749* #
NAS 1.15:4095 ..... N89-19899* #
NAS 1.15:4096 ..... N89-19231* #
NAS 1.15:4104 ..... N89-19529* #
NAS 1.15:4106 ..... N89-19578* #
NAS 1.15:87030 ..... N89-19265* #
NAS 1.15:87652 ..... N89-19892* #
NAS 1.15:88846 ..... N89-19737* #
NAS 1.15:89073 ..... N89-19266* #
NAS 1.15:100709 ..... N89-19976* #
NAS 1.15:100720 ..... N89-19729* #
NAS 1.15:101287 ..... N89-19321* #
NAS 1.15:101288 ..... N89-19789* #
NAS 1.15:101476 ..... N89-19435* #
NAS 1.15:101486 ..... N89-19965* #
NAS 1.15:101507 ..... N89-19589* #
NAS 1.15:101539 ..... N89-19783* #
NAS 1.15:101954 ..... N89-19371* #
NAS 1.15:101962 ..... N89-19402* #
NAS 1.15:101963 ..... N89-19446* #
NAS 1.15:101978 ..... N89-19305* #
NAS 1.15:101981 ..... N89-19493* #
NAS 1.15:102144 ..... N89-19326* #
NAS 1.26:4225 ..... N89-19545* #
NAS 1.26:4226 ..... N89-19316* #
NAS 1.26:166079 ..... N89-19779* #
NAS 1.26:172117 ..... N89-19809* #
NAS 1.26:172118-VOL-1 ..... N89-20058* #
NAS 1.26:172118-VOL-2 ..... N89-20073* #
NAS 1.26:174786 ..... N89-19299* #
NAS 1.26:174967 ..... N89-19583* #
NAS 1.26:175003 ..... N89-19300* #
NAS 1.26:175096 ..... N89-19289* #
NAS 1.26:178217 ..... N89-19505* #
NAS 1.26:178280 ..... N89-19780* #
NAS 1.26:179161 ..... N89-19555* #
NAS 1.26:179454 ..... N89-19556* #
NAS 1.26:179525 ..... N89-19421* #
NAS 1.26:182238 ..... N89-19973* #
NAS 1.26:182243 ..... N89-19449* #
NAS 1.26:182256 ..... N89-19442* #
NAS 1.26:182820 ..... N89-19539* #
NAS 1.26:183584 ..... N89-19366* #
NAS 1.26:183594 ..... N89-19365*
NAS 1.26:183595 ..... N89-19367* #
NAS 1.26:183596 ..... N89-19420* #
NAS 1.26:184688 ..... N89-19502* #
NAS 1.26:184705 ..... N89-20040* #
NAS 1.26:184706 ..... N89-20041* #
NAS 1.26:184714 ..... N89-19324* #
NAS 1.26:184728 ..... N89-19352* #
NAS 1.26:184730 ..... N89-19808* #
NAS 1.26:184753 ..... N89-19807* #
NAS 1.26:184756 ..... N89-19503* #
NAS 1.26:184775-APP-1 ..... N89-19581* #
NAS 1.26:184789 ..... N89-19504* #
NAS 1.26:184796-APP-2 ..... N89-19582* #
NAS 1.26:184812 ..... N89-19451* #
NAS 1.26:184823 ..... N89-19764* #
NAS 1.26:184826 ..... N89-20051* #
NAS 1.26:184893 ..... N89-19599* #
NAS 1.55:3019 ..... N89-19817* #
NAS 1.55:3022-PT-1 ..... N89-19234* #
NAS 1.55:3022-PT-2 ..... N89-19247* #
NAS 1.55:3028 ..... N89-19230* #
NAS 1.60:2820 ..... N89-19406* #
NAS 1.60:2868 ..... N89-19579* #
NAS 1.60:2885 ..... N89-19309* #
NAS 1.60:2894 ..... N89-19499* #
NAS 1.60:2895 ..... N89-19232* #
NAS 1.60:2897 ..... N89-19580* #
NAS 1.60:2906 ..... N89-19385* #

NASA-CP-3019 ..... N89-19817* #
NASA-CP-3022-PT-1 ..... N89-19234* #
NASA-CP-3022-PT-2 ..... N89-19247* #
NASA-CP-3028 ..... N89-19230* #

NASA-CR-4225 ..... N89-19545* #
NASA-CR-4226 ..... N89-19316* #
NASA-CR-166079 ..... N89-19779* #
NASA-CR-172117 ..... N89-19809* #
NASA-CR-172118-VOL-1 ..... N89-20058* #
NASA-CR-172118-VOL-2 ..... N89-20073* #
NASA-CR-174786 ..... N89-19299* #
NASA-CR-174967 ..... N89-19583* #
NASA-CR-175003 ..... N89-19300* #
NASA-CR-175096 ..... N89-19289* #
NASA-CR-178217 ..... N89-19505* #
NASA-CR-178280 ..... N89-19780* #
NASA-CR-179161 ..... N89-19555* #
NASA-CR-179454 ..... N89-19556* #
NASA-CR-179525 ..... N89-19421* #
NASA-CR-182238 ..... N89-19973* #
NASA-CR-182243 ..... N89-19449* #
NASA-CR-182256 ..... N89-19442* #
NASA-CR-182820 ..... N89-19539* #
NASA-CR-183584 ..... N89-19366* #
NASA-CR-183594 ..... N89-19365*
NASA-CR-183595 ..... N89-19367* #
NASA-CR-183596 ..... N89-19420* #
NASA-CR-184688 ..... N89-19502* #
NASA-CR-184705 ..... N89-20040* #
NASA-CR-184706 ..... N89-20041* #
NASA-CR-184714 ..... N89-19324* #
NASA-CR-184728 ..... N89-19352* #
NASA-CR-184730 ..... N89-19808* #
NASA-CR-184753 ..... N89-19807* #
NASA-CR-184756 ..... N89-19503* #
NASA-CR-184775-APP-1 ..... N89-19581* #
NASA-CR-184789 ..... N89-19504* #
NASA-CR-184796-APP-2 ..... N89-19582* #
NASA-CR-184812 ..... N89-19451* #
NASA-CR-184823 ..... N89-19764* #
NASA-CR-184826 ..... N89-20051* #
NASA-CR-184893 ..... N89-19599* #

NASA-TM-4091 ..... N89-19749* #
NASA-TM-4095 ..... N89-19899* #
NASA-TM-4096 ..... N89-19231* #
NASA-TM-4104 ..... N89-19529* #
NASA-TM-4106 ..... N89-19578* #
NASA-TM-87030 ..... N89-19265* #
NASA-TM-87652 ..... N89-19892* #
NASA-TM-88846 ..... N89-19737* #
NASA-TM-89073 ..... N89-19266* #
NASA-TM-100709 ..... N89-19976* #
NASA-TM-100720 ..... N89-19729* #
NASA-TM-101287 ..... N89-19321* #
NASA-TM-101288 ..... N89-19789* #
NASA-TM-101476 ..... N89-19435* #
NASA-TM-101486 ..... N89-19965* #
NASA-TM-101507 ..... N89-19589* #
NASA-TM-101539 ..... N89-19783* #
NASA-TM-101954 ..... N89-19371* #
NASA-TM-101962 ..... N89-19402* #
NASA-TM-101963 ..... N89-19446* #
NASA-TM-101978 ..... N89-19305* #
NASA-TM-101981 ..... N89-19493* #
NASA-TM-102144 ..... N89-19326* #

NASA-TP-2820 ..... N89-19406* #
NASA-TP-2868 ..... N89-19579* #
NASA-TP-2885 ..... N89-19309* #
NASA-TP-2894 ..... N89-19499* #
NASA-TP-2895 ..... N89-19232* #
NASA-TP-2897 ..... N89-19580* #
NASA-TP-2906 ..... N89-19385* #

NATC-TM-88-46-SY ..... N89-19298 #

NATICK-TR-88/003 ..... N89-19811 #
NATICK-TR-88/045 ..... N89-19812 #
NATICK-TR-88/048 ..... N89-19813 #

NOAA-TM-NWS-CR-88 ..... N89-19771 #

NOSC-TR-1244 ..... N89-19284 #

NPRDC-TN-89-6 ..... N89-19797 #

NPS55-88-010 ..... N89-19958 #

NRC-29459 ..... N89-19267 #

NRL-MR-6365 ..... N89-19538 #

NSWC-TR-87-89 ..... N89-19276 #

NWRA-CR-88-R031 ..... N89-19765 #

ORNL/TM-10976 ..... N89-19906 #

PB88-210836 ..... N89-19771 #

PH-288 ..... N89-19450

PME-FM-86-2 ..... N89-19521 #

PNR90472 ..... N89-19302 #
PNR90483 ..... N89-19894 #
PNR90492 ..... N89-19436 #
PNR90495 ..... N89-19532 #
PNR90496 ..... N89-19303 #
PNR90499 ..... N89-19414 #
PNR90503 ..... N89-19413 #
PNR90510 ..... N89-19571 #
PNR90522 ..... N89-19382 #
PNR90530 ..... N89-19306 #
PNR90534 ..... N89-19525 #
PNR90537 ..... N89-19307 #
PNR90540 ..... N89-19308 #
PNR90542 ..... N89-19533 #

PREPRINT-1134 ..... N89-19526 #

R-343 ..... N89-19477 #

R/D-5491-EN-01-F ..... N89-19593 #
R/D-5574-EE-01 ..... N89-19488 #

R/D/REPO/8801 ..... N89-19496 #

RAE-TM-FM-6 ..... N89-19319 #

RDA-TR-144200-002 ..... N89-19368 #

REPT-AQ-ES-576/88 ..... N89-19444 #

REPT-B090 ..... N89-19530 #
REPT-B091 ..... N89-19531 #

REPT-18 ..... N89-20050 #
REPT-36-6008480 ..... N89-19393 #
REPT-77 ..... N89-19957 #
REPT-85/535800 ..... N89-19297 #
REPT-88-N4-173 ..... N89-19993 #
REPT-88-04 ..... N89-19942 #
REPT-88-05 ..... N89-19322 #
REPT-88-06 ..... N89-20054 #
REPT-88-07 ..... N89-20026 #
REPT-88-08 ..... N89-19943 #
REPT-88-09 ..... N89-19944 #
REPT-88-10 ..... N89-19945 #
REPT-88-11 ..... N89-19946 #
REPT-88-12 ..... N89-19933 #
REPT-88-13 ..... N89-19961 #
REPT-88-14 ..... N89-19962 #
REPT-88-16 ..... N89-19948 #
REPT-88-17 ..... N89-19918 #
REPT-88-18 ..... N89-19949 #
REPT-88-19 ..... N89-19950 #
REPT-88-21 ..... N89-19951 #
REPT-88-22 ..... N89-19528 #
REPT-88-23 ..... N89-19603 #
REPT-88-26 ..... N89-20027 #
REPT-88-28 ..... N89-19952 #
REPT-88-40 ..... N89-19963 #
REPT-88-41 ..... N89-19919 #
REPT-88-42 ..... N89-19953 #
REPT-88-44 ..... N89-19920 #
REPT-88-45 ..... N89-19576 #
REPT-88-46 ..... N89-19577 #
REPT-88-011 ..... N89-19914
REPT-88-013 ..... N89-19930
REPT-88-015 ..... N89-19479
REPT-88-022 ..... N89-19480
REPT-88-023 ..... N89-19481
REPT-88-025 ..... N89-19915
REPT-88-028 ..... N89-19931
REPT-88-029 ..... N89-19932
REPT-89B0005 ..... N89-19976* #
REPT-89B00065 ..... N89-19729* #
REPT-1013-CA/TS ..... N89-19285 #
REPT-2021 ..... N89-19735 #
REPT-7313/88 ..... N89-19488 #

RRK-88-20 ..... N89-20022 #

RSRE-87011 ..... N89-19921 #

S-HRG-100-579-PT-2 ..... N89-20031 #
S-HRG-100-750 ..... N89-19325 #

S-585 ..... N89-19617* #

SAND-88-2251C ..... N89-19916 #
SAND-88-2506 ..... N89-19534 #
SAND-88-7028 ..... N89-19746 #
SAND-88-7032 ..... N89-19740 #

SC5485.FR ..... N89-19492 #

SD-TR-88-85 ..... N89-19764* #
SD-TR-88-108 ..... N89-19476 #

SDL-88-2513-27F/76 ..... N89-19545* #

SERI/SP-253-3383 ..... N89-19744 #

SERI/STR-211-3374 ..... N89-19739 #
SERI/STR-217-3320 ..... N89-19781 #
SERI/STR-217-3370 ..... N89-19743 #

SPI-13-14-VOL-1 ..... N89-20004 #

SR-1 ..... N89-19394 #
SR-2 ..... N89-19765 #
SR-4 ..... N89-19354 #

SU-SOL-88-17 ..... N89-19908 #
SU-SOL-88-19 ..... N89-19912 #
SU-SOL-88-20 ..... N89-19913 #

SWRI-17-7958-840 ..... N89-19441 #

TL-SEAL-2-87 ..... N89-19555* #

TR-1 ..... N89-19398 #
TR-7 ..... N89-19389 #
TR-19 ..... N89-19396 #
TR-20 ..... N89-19397 #
TR-29 ..... N89-19998 #
TR-259 ..... N89-19560 #
TR-410 ..... N89-19959 #
TR-505 ..... N89-19929 #
TR-0088(3940-05)-1 ..... N89-19764* #
TR-0088(3945-04)-1 ..... N89-19476 #

TRITA-FPT-051 ..... N89-19278 #

TUHH-TRI-ESA-1987 ..... N89-19370 #

UCLA-ENG-88-09 ..... N89-19598 #

UCRL-21135 ..... N89-19378 #
UCRL-21138 ..... N89-19490 #
UCRL-21140 ..... N89-19471 #
UCRL-100040 ..... N89-19604 #

UDRI-TR-88-45 ..... N89-19544 #
UDRI-TR-88-89 ..... N89-19981 #

UIC-EECS-88-07-15-PT-A ..... N89-19467 #

UILU-ENG-88-2250 ..... N89-19901 #
UILU-ENG-88-2257 ..... N89-19904 #

ULRF-446/CAR ..... N89-19761 #

UNC/OR/TR-88/3 ..... N89-19955 #

USAAEFA-84-33 ..... N89-19295 #

USAFOEHL-88-140EH0087JNA ..... N89-19317 #

USAFSAM-TP-88-10 ..... N89-19796 #

USARIEM-M2-89 ..... N89-19800 #
USARIEM-M39-88 ..... N89-19799 #

UVA/525673/MAE88/102 ..... N89-19333 #

VPI-E-88-30 ..... N89-19434 #

VPI-ESM-352-277-1 ..... N89-19584 #

VPI/EE-SATCOM-82-2 ..... N89-19472 #

WTHD-188 ..... N89-19941 #

YMD/EF/0175 ..... N89-19361 #

☆ U.S. GOVERNMENT PRINTING OFFICE: 1989— 241-445/00103

FEDERAL REGIONAL DEPOSITORY LIBRARIES

ALABAMA

AUBURN UNIV. AT MONTGOMERY LIBRARY
Documents Department
Montgomery, AL 36193
(205) 271-9650

UNIV. OF ALABAMA LIBRARY
Documents Dept.-Box S
University, AL 35486
(205) 348-6046

ARIZONA

DEPT. OF LIBRARY, ARCHIVES AND PUBLIC RECORDS
Third Floor—State Cap.
1700 West Washington
Phoenix, AZ 85007
(602) 255-4121

UNIVERSITY OF ARIZONA LIB.
Government Documents Dept.
Tucson, AZ 85721
(602) 621-6433

ARKANSAS

ARKANSAS STATE LIBRARY
One Capitol Mall
Little Rock, AR 72201
(501) 371-2326

CALIFORNIA

CALIFORNIA STATE LIBRARY
Govt. Publications Section
P.O. Box 2037
Sacramento, CA 95809
(916) 324-4863

COLORADO

UNIV OF COLORADO LIB.
Government Pub. Division
Campus Box 184
Boulder, CO 80309
(303) 492-8834

DENVER PUBLIC LIBRARY
Govt. Pub. Department
1357 Broadway
Denver, CO 80203
(303) 571-2131

CONNECTICUT

CONNECTICUT STATE LIBRARY
Government Documents Unit
231 Capitol Avenue
Hartford, CT 06106
(203) 566-7029

FLORIDA

UNIV. OF FLORIDA LIBRARIES
Library West
Documents Department
Gainesville, FL 32611
(904) 392-0367

GEORGIA

UNIV. OF GEORGIA LIBRARIES
Government Reference Dept.
Athens, GA 30602
(404) 542-8949

HAWAII

UNIV. OF HAWAII LIBRARY
Govt. Documents Collection
2550 The Mall
Honolulu, HI 96822
(808) 948-8230

IDAHO

UNIV. OF IDAHO LIBRARY
Documents Section
Moscow, ID 83843
(208) 885-6344

ILLINOIS

ILLINOIS STATE LIBRARY
Information Services Branch
Centennial Building
Springfield, IL 62756
(217) 782-5185

INDIANA

INDIANA STATE LIBRARY
Serials Documents Section
140 North Senate Avenue
Indianapolis, IN 46204
(317) 232-3686

IOWA

UNIV. OF IOWA LIBRARIES
Govt. Documents Department
Iowa City, IA 52242
(319) 353-3318

KANSAS

UNIVERSITY OF KANSAS
Doc. Collect—Spencer Lib.
Lawrence, KS 66045-2800
(913) 864-4662

KENTUCKY

UNIV. OF KENTUCKY LIBRARIES
Govt. Pub. Department
Lexington, KY 40506-0039
(606) 257-3139

LOUISIANA

LOUISIANA STATE UNIVERSITY
Middleton Library
Govt. Docs. Dept.
Baton Rouge, LA 70803
(504) 388-2570

LOUISIANA TECHNICAL UNIV. LIBRARY
Documents Department
Ruston, LA 71272-0046
(318) 257-4962

MAINE

UNIVERSITY OF MAINE
Raymond H. Fogler Library
Tri-State Regional Documents Depository
Orono, ME 04469
(207) 581-1680

MARYLAND

UNIVERSITY OF MARYLAND
McKeldin Lib.—Doc. Div.
College Park, MD 20742
(301) 454-3034

MASSACHUSETTS

BOSTON PUBLIC LIBRARY
Government Docs. Dept.
Boston, MA 02117
(617) 536-5400 ext.226

MICHIGAN

DETROIT PUBLIC LIBRARY
Sociology Department
5201 Woodward Avenue
Detroit, MI 48202-4093
(313) 833-1409

MICHIGAN STATE LIBRARY
P.O. Box 30007
Lansing, MI 48909
(517) 373-1593

MINNESOTA

UNIVERSITY OF MINNESOTA
Government Pubs. Division
409 Wilson Library
309 19th Avenue South
Minneapolis, MN 55455
(612) 373-7870

MISSISSIPPI

UNIV. OF MISSISSIPPI LIB.
Documents Department
University, MS 38677
(601) 232-5857

MONTANA

UNIV. OF MONTANA
Mansfield Library
Documents Division
Missoula, MT 59812
(406) 243-6700

NEBRASKA

UNIVERSITY OF NEBRASKA - LINCOLN
Love Library
Documents Department
Lincoln, NE 68588-0410
(402) 472-2562

NEVADA

UNIVERSITY OF NEVADA LIB.
Govt. Pub. Department
Reno, NV 89557-0044
(702) 784-6579

NEW JERSEY

NEWARK PUBLIC LIBRARY
5 Washington Street
Newark, NJ 07101-0630
(201) 733-7812

NEW MEXICO

UNIVERSITY OF NEW MEXICO
Zimmerman Library
Government Pub. Dept.
Albuquerque, NM 87131
(505) 277-5441

NEW MEXICO STATE LIBRARY
Reference Department
325 Don Gaspar Avenue
Santa Fe, NM 87503
(505) 827-3826

NEW YORK

NEW YORK STATE LIBRARY
Empire State Plaza
Albany, NY 12230
(518) 474-5563

NORTH CAROLINA

UNIVERSITY OF NORTH CAROLINA AT CHAPEL HILL
Davis Library
BA/SS Documents Division
Chapel Hill, NC 27515
(919) 962-1151

NORTH DAKOTA

UNIVERSITY OF NORTH DAKOTA
Chester Fritz Library
Documents Department
Grand Forks, ND 58202
(701) 777-4629
In cooperation with North Dakota State Univ. Library

OHIO

STATE LIBRARY OF OHIO
Documents Department
65 South Front Street
Columbus, OH 43266-0334
(614) 462-7051

OKLAHOMA

OKLAHOMA DEPT. OF LIB.
Government Documents
200 NE 18th Street
Oklahoma City, OK 73105
(405) 521-2502, ext. 252

OKLAHOMA STATE UNIV. LIB.
Documents Department
Stillwater, OK 74078
(405) 624-6546

OREGON

PORTLAND STATE UNIV. LIB.
Documents Department
P.O. Box 1151
Portland, OR 97207
(503) 229-3673

PENNSYLVANIA

STATE LIBRARY OF PENN.
Government Pub. Section
P.O. Box 1601
Harrisburg, PA 17105
(717) 787-3752

TEXAS

TEXAS STATE LIBRARY
Public Services Department
P.O. Box 12927—Cap. Sta.
Austin, TX 78711
(512) 475-2996

TEXAS TECH. UNIV. LIBRARY
Govt. Documents Department
Lubbock, TX 79409
(806) 742-2268

UTAH

UTAH STATE UNIVERSITY
Merrill Library, U.M.C. 30
Logan, UT 84322
(801) 750-2682

VIRGINIA

UNIVERSITY OF VIRGINIA
Alderman Lib.—Public Doc.
Charlottesville, VA 22903-2498
(804) 924-3133

WASHINGTON

WASHINGTON STATE LIBRARY
Documents Section
Olympia, WA 98504
(206) 753-4027

WEST VIRGINIA

WEST VIRGINIA UNIV. LIB.
Documents Department
Morgantown, WV 26506-6069
(304) 293-3640

WISCONSIN

MILWAUKEE PUBLIC LIBRARY
814 West Wisconsin Avenue
Milwaukee, WI 53233
(414) 278-3065

ST. HIST LIB. OF WISCONSIN
Government Pub. Section
816 State Street
Madison, WI 53706
(608) 262-4347

WYOMING

WYOMING STATE LIBRARY
Supreme Ct. & Library Bld.
Cheyenne, WY 82002
(307) 777-5919

National Aeronautics and
Space Administration
Code NTT-4
Washington, D.C.
20546

Official Business

Penalty for Private Use, $300

SPECIAL FOURTH-CLASS RATE
POSTAGE & FEES PAID
NASA
PERMIT No. G 27

NASA

POSTMASTER: If Undeliverable (Section 158
Postal Manual) Do Not Return